Handbook of Anti-Gravity Research

A Collection of Research Papers and Patents Related to the Modification of Gravity

Handbook of Anti-Gravity Research

Handbook of Anti-Gravity Research

A Collection of Research Papers and Patents
Related to the Modification of Gravity

This book was set in the LaTeXprogramming language by the editor.

Version 1, October 2018

This handbook was created with the purpose of encouraging the advancement of research on anti-gravity

Contents

Research on Achieving Thrust by EM Inertia Manipulation - *H. Brito*

Specially Conditioned EM Radiation Research with Transmitting Toroid Antennas - *H. D. Froning Jr. and G. W. Hathaway*

An Experimental Investigation of the Physical Effects in a Dynamic Magnetic System - *V. V. Roshchin and S. M. Godin*

Rapid Spacetime Transport and Machian Mass Fluctuations: Theory and Experiment - *J. Woodward and T. Mahood*

Global Monopoles and the Bondi-Forward Mechanism - *C. Van Den Broeck*

Induction and Amplifications of Non-Newtonian Gravitational Fields - *M. Tajmar and C. J. de Matos*

Towards the Control of Matter with Gravity - *D. Burton et al.*

Rapid Spacetime Transport and Machian Mass Fluctuations: Theory and Experiment - *J. Cameron*

Fabrication of Large Bulk Ceramic Superconductor Disks for Gravity Modification Experiments and Performance of YBCO Disks Under e.m. Field Excitation - *R. Koczor and D. Noever*

Large Scale Sakharov Condition - *D. Noever and C. Bremner*

Breakthrough propulsion physics research program - *M. G. Millis*

Measurement of Repulsive Quantum Vacuum Forces - *J. Hammer et al.*

Search for Effects of Electric Potentials on Charged Particle Clocks - *H. I. Ringermacher*

Tests of Mach's Principle with a Mechanical Oscillator - *J. G. Cramer et al.*

Superluminal but Causal Wave Propagation - *M. Mojahedi, K. Malloy, and R. Chiao*

Geometrodynamics, Inertia and the Quantum Vacuum - *B. Haisch and A. Rueda*

Interplay between gravity and quintessence: a set of new GR solutions - *A. D. Chernin, D. I. Santiago, A. S. Silbergleit*

Classical analogous of quantum cosmological perfect fluid models - *A.B. Batista, J.C. Fabris, S.V.B. Gonçalves, J. Tossa*

Gravity and antigravity in a brane world with metastable gravitons - *Ruth Gregory a, V. A. Rubakov, S. M. Sibiryakov*

The ac magnetic response in type-II superconductors - *Y. Enomotoy and K. Okadaz*

Exploration Of Anomalous Gravity Effects by Magnetized High-Tc Superconducting Oxides - *G. A. Robertson and R. Litchford*

The Other Side of Gravity and Geometry: Antigravity and Anticurvature - *M. I. Wanas*

Impulse Gravity Generator Based on Charged $YBa_2Cu_3O_{7-y}$ Superconductor with Composite Crystal Structure - *E. Podkletnov1, G. Modanese*

On the Mechanism for a Gravity Effect using Type II Superconductors - *G. A. Robertson*

Stan Deyo: Stream of Consciousness - *S. Deyo*

Negative Gravitational Mass in a Superfluid Bose-Einstein Condensate - *Fran de Aquino*

Gravitational Interaction between Photons and Unification of All the Fundamental Interactions - *Fran de Aquino*

Searching for the Gravific Photons - *Fran de Aquino*

The Gravitational Spacecraft - *Fran de Aquino*

Possibility of Control of the Gravitational Mass by Means of Extra-Low Frequencies Radiation - *Fran de Aquino*

Gravity Control by Means of Modified Electromagnetic Radiationt- *Fran de Aquino*

Correlation Between Gravitational and Inertial Mass: Theory and Experimental Test - *Fran de Aquino*

Gravity Control produced by a Thermoionic Current through the Air at Very Low Pressure - *Fran de Aquino*

Gravity Control by means of Electromagnetic Field through Gas or Plasma at Ultra-Low Pressure - *Fran de Aquino*

The Gravitational Mass at the Superconducting State - *Fran de Aquino*

A Gravitational Shielding Based on ZnS:Ag Phosphor - *Fran de Aquino*

A Possibility of Gravity Control in Luminescent Materials - *Fran de Aquino*

Possiblility of Control of the Gravitational Mass by means of Extra-Low Frequencies Radiation - *Fran de Aquino*

Repulsive Gravitational Force Field - *Fran de Aquino*

Gravitational Holographic Teleportation - *Fran de Aquino*

Bose-Einstein Condensate and Gravitational Shielding - *Fran de Aquino*

Gravitational Shockwave Weapons - *Fran de Aquino*

Negative Gravitational Mass in a Superfluid Bose-Einstein Condensate - *Fran de Aquino*

Controlling the Gravitational Mass of a Metallic Lamina, and the Gravity Acceleration Above It - *Fran de Aquino*

Quantum Controller of Gravity - *Fran de Aquino*

Quantum Gravitational Shielding - *Fran de Aquino*

New Gravitational Effects from Rotating Masses - *Fran de Aquino*

The Bipolar Linear Momentum Transported by the Electromagnetic Waves: Origin of the Gravitational Interaction - *Fran de Aquino*

Gravity Control by Means of Electromagnetic Field Through Gas or Plasma at Ultra-Low Pressure- *Fran de Aquino*

Further Readings

Introduction

Anti-gravity (also known as non-gravitational field) is an idea of creating a place or object that is free from the force of gravity. It does not refer to the lack of weight under gravity experienced in free fall or orbit, or to balancing the force of gravity with some other force, such as electromagnetism or aerodynamic lift. Anti-gravity is a recurring concept in science fiction, particularly in the context of spacecraft propulsion. Examples are the gravity blocking substance "Cavorite" in H. G. Wells' The First Men in the Moon and the Spindizzy machines in James Blish's Cities in Flight.

In Newton's law of universal gravitation, gravity was an external force transmitted by unknown means. In the 20th century, Newton's model was replaced by general relativity where gravity is not a force but the result of the geometry of spacetime. Under general relativity, anti-gravity is impossible except under contrived circumstances.[1][2][3] Quantum physicists have postulated the existence of gravitons, massless elementary particles that transmit gravitational force, but the possibility of creating or destroying these is unclear.

"Anti-gravity" is often used colloquially to refer to devices that look as if they reverse gravity even though they operate through other means, such as lifters, which fly in the air by moving air with electromagnetic fields.

Source: Wikepedia (https://en.wikipedia.org/wiki/Anti-gravity).

Who's Who in Antigravity

By Tim Ventura, January 27th, 2004 [tventura6@comcast.net]

Please note: the following list is as comprehensive as possible, but due to the nature of Antigravity research, such a list cannot possibly encompass the scope of work being done on these concepts around the world. Therefore, this list may not contain references to all relevant information, but does attempt to be as comprehensive as possible.

Mach's Principle: Offcenter-rotators, inertial-thrusters, or piezo-devices. These devices attempt to "pull themselves up by the bootstraps" to overcome gravity mechanically.
→ Dr. James F. Woodward, Piezo-Electric Transducers
→ Robert Cook, Cook Inertial Propulsion Device
→ Paul March (Lockheed), Indy-experiments with Woodward's research
→ James Cox, Offcenter-Rotator Device

ELF-Grav Shielding: Low-Frequency EM-waves block gravitons from interacting with mass, creating a shield from gravity and inertia.
→ Prof. Fran De Aquino, Brazilian inventor (possibly working with Braz. Military)
→ Steve Burns, M.A. Nuclear Physics, Designer of De Aquino's device
→ Martin Tajmar, Presenting ELF-Replication attempt at STAIF 2005.

Mass-Fluctuation: Utilizing EM-waves to create mass fluctations simulates "negative mass" which has been proposed to generate an Antigravity Effect.
→ William Alek, built Gravimetric Mass Fluctuation Prototype

Biefield-Brown: High-voltages are used to create an asymmetrical-capacitance, which Puthoff & Sakarov have proposed creates forward directional thrust by interacting with quantum-foam.
→ TT Brown, Built a varied collection of disk-shaped BB-Effect rotators.
→ Dr. Alfred Biefeld, experimental colleague of TT Brown.
→ RL Talley, experiments showed non-conservative force from spark discharge.
→ Dr's. Haisch, Rueda, and Puthoff, Quantum-Foam theory
→ Jean-Louis Naudin, Conducted open-source experimental validation.
→ Tim Ventura, Enhancement of BB-Effect via Ultraviolet Preionization
→ Saviour, Demonstrated inertial anomalies related to angular momentum
→ Alexander DeSeversky, Early pioneer of the Ion-Wind thrust component.
→ Russell Anderson, builder of world's largest BB-Effect devices.

Superconductive Grav-Shield: A rotating superconductor or gas-plasma creates a shield around the test device that blocks inertia and mass, similar to the ELF shield above.
→ Dr. Eugene Podkletnov, Claims 2% to 9% decrease in weight due to SC-shielding

→ Dr. Ning Li, Claims to have replicated rotating SC grav-shield
→ John Schnurer, Popular experimental replication claim (invalidated, 1998)
→ Pete Skeggs, Inventor responsible for collating Podkletnov's early work.
→ Dr. Ning Wu, Theoretical prediction suggests phase-transition causes effect.
→ Tony Robertson, Scientist in NASA 2001 Podkletnov Rotation Experiment
→ Ron Koczor, Scientist in NASA 2001 Podkletnov Rotation Experiment.

Superconductive HFGW: The Gertsenshtein Effect allows a high-frequency interaction between Electromagnetism and Gravitation that creates powerful Gravitational-Waves, capable of exerting tons of force.
→ Dr. Eugene Podkletnov, Experimental claim for hundreds of pounds of force from new force-beam apparatus (smashing brick, warping metal, etc.). This is from a pulse-discharge HFGW apparatus (2 MV Marx Discharge).
→ Dr. Ning Li, Claims to be generating continuous-duty 11-kilowatt AC-Gravity beam from RF components on Type-II SC (push/pull effect, high output).
→ Dr. David Maker, unGauged GR theory supporting Podkletnov's results.
→ Dr. Ning Wu, Gauge GR theory supporting Podkletnov's results.
→ Dr. Bob Baker, designer of nanoscale high-frequency grav-wave experiment.
→ Tony Robertson, proposes nanoscale Type-II SC defect creating grav-waves.
→ Gary Stephenson, proposes Gerstenshtein Effect responsible for Force-Beam.
→ Paul Murad, organizer for STAIF conference & chief scientific review head.

Bismuth/ Element 115: A poorly understood mechanism claimed to be the result of reverse-engineering UFO's that somehow translates high-voltage electricity into a propulsive gravity-wave. More recently it has been suggested that Bismuth and Mercury have unique nuclear shell interactions with gravitational force.
→ Bob Lazar, Claims Element 115 decay cycle releases propulsive gravity-waves.
→ John Dering, Claims that Bismuth is an enhancer for gravito-electric effects.

Gyroscopic-Precession: A variation on Mach's Principle in which a force applied horizontally creates an upward thrust in a rotating gyroscope. Includes NMR Antigravity, a nanoscale-variation of Gyroscopic precession in which EM-radiation is used to generate Nuclear Magnetic Resonance and create a precessional force against gravity for the entire test-object.
→ Dr. Eric Laithwaite, Demonstration of precession for British Royal Society.
→ Bruce DePalma, Independent experimentation with precession force thrust.
→ Dr. Richard Hoagland, Proposes NMR version of precession experiments.

Lenz-Law: A series of variations on the common electromagnetic inductive-force in which an Antigravity craft is repelled from the Earth's surface using a macro-scale variant of Lenz's Law.

→ Boyd Bushman, Proposes high-frequency Lenz Levitation aircraft.
→ Bill Butler, Proposal for Lenz-Levitation circa 1992.

GeoMagnetic Levitation: A high-energy, low-efficiency device that generates upward and directional thrust by applying a very high-strength magnetic field to repel against the Earth's natural magnetic field.
→ Bill Butler, Experimenting with high-amplitude magnetic field levitation.
→ Howe Wachspress, inventor working with H.A. magnetic levitation.
→ Mark Goldes, supporter of Butler's research & owner of Wachspress' patent.

Rotating Magnetic Field Device: A broad category of Antigravity device in which a series of high-speed rotating electromagnetic fields are used to warp-space and generate a pure, high-efficiency, and sometimes overunity Antigravity Effect. May be related to Magnus-Effect propulsion or Rotating Superconductive Antigravity.
→ John Searl, British inventor of SEG & IGV Antigravity devices.
→ Dr. Paul Brown, performed successful independent 1986 SEG replication.
→ John Thomas, American affiliate for SEG research (DISC Corp).
→ Russell Anderson, leading Applied-Electrogravitics 2005 SEG replication.
→ Saviour, created 2003 Magnus-Effect levitation replication.
→ Marcus Hollingshead, Rotating fields are applied to stationary core for AG thrust.
→ Sergei Godin, Built Russian SEG replication w/ gear-roller enhancements.
→ Vladimir Roschin, Assistant to Godin for 1992 & 2005 Russian SEG replications.
→ Harold Aspden, discoverer of a virtual magnetic inertia in rotating fields.

Hutchison-Effect: A poorly understood high-voltage/high-frequency Antigravity mechanism capable of lifting hundreds of pounds of weight, but lacking the repeatability for close scientific scrutiny and easy replication. This is an aspect of scalar-technology, and may be also called "scalar-antigravity" or "Bearden Antigravity".
→ John Hutchison, Canadian inventor & tinkerer – inventor of H-Effect.
→ Boyd Bushman, Claims to have seen Lockheed experimental confirmation
→ Rex Webb, Claims to have an optical-assembly for replicating H-Effect.
→ Ted Gagnon, Developed theoretical predictions & tests for H-Effect.

Poynting Vector Propulsion: A real, workable reactionless-drive based on classical electrodynamics principles, tested to generate pounds of thrust. Scalability for this system is unknown – early prototypes are unstable.
→ Jean-Louis Naudin, created 1999 prototype "Poynting swing" experiment.
→ John Dering, Participated in 2000 Poynting-vector thrust replication.
→ Dr. Tom Bearden, Theoretical design for Poynting-ventor propulsor.

Einstein's UFT Effect: An engineering-level approach to AG based on tensor analysis from Einstein's 1929+ Unified Field Theory. In practical form, it translates into rotating RF wave devices utilizing mercury (Nazi Bell, SARA Wheel, Philadelphia Experiment).
→ John Dering, SARA physicist predicting Einstein's UFT as explanation for the Nazi Bell technology. Dering performed independent validation of UFT anomalous Effects at SARA under funding from ISSO in 2000.
→ Dr. James Corum, PhD EE suggesting Einstein's UFT as explanation for Nazi Antigravity research and Philadelphia Experiment. Corum performed replication of Allied radar-invisibility in 1994 to validate the Philadelphia Experiment physics.
→ Dr. Walther Gerlach, WW-II German physicist involved with Nazi UFT experiments.
→ Dr. Nikola Tesla, PhD EE reportedly involved with Allied UFT research during WW-II (creator of mirage effect).
→ Dr. Albert Einstein, reportedly involved with Allied UFT research for mirage effect, assigned to Navy on Philadelphia Experiment during 1943.

Casimir Force & ZPE: A variety of proposed Antigravity devices have come from work relating to Zero-Point energy from Quantum Mechanics. These remain highly-speculative & subject to further investigation.
→ Dr. Hal Puthoff: Proposing a "polarized vacuum" theory.
→ Dr. Andreas Sakharov, 1960's Russian theory (precursor to PV theory)
→ Dr. Bernard Haisch, Proposing a Quantum Foam virtual-particle theory.
→ Dr. Alfonse Rueda, Co-Author with Haisch of Quantum-Foam theory.
→ Dr. Paul Laviolette, Proposing SubQuantum Kinetics theory predicting Podkletnov force-beam experiment.
→ Dr. Ning Li, Proposing Quantum Cooper-Pair theory predicting Podkletnov experiment.

Torsion Fields: Initially predicted by Einstein's Unified Field Theory, a number of Russian scientists spent considerable research into a modified abstract of these ideas from 1960-onward, due to Einstein's prediction that Torsion Fields can "unbend" the gravitational curvature of space in a local area.
→ Albert Einstein, predicted a torsion-tensor as a component of 1929+ UFT.
→ Alexander Frolov, publisher of "New Energy Technologies" Magazine in Moscow, has categorized a vast number of Russian researchers experimenting with Torsion Fields from the 1960's onward.
→ Dr. N.A. Kosyrev: Spin Field proposal with energy implications.
→ Dr's Nachalov/Parkhomov/Sokolov, Russian researchers in torsion-field mechanics.
→ A.E. Akimov, G. I. Shipov, Spin-Field Proposal reportedly similar to theories supported by Jack Sarfatti.
→ A. A. Shpilman, Torsion Field investigation.

Electromagnetic Plenum Effect: Modified Air-Cushion concept proposing to contain ions between vehicle and ground to create surface-effect levitation. Recirculation of charged air in plenum increases lift efficiency for surface-effect transport.
→ Bill Butler, 1992 experiments with ion-containment levitation systems.

→ Tim Ventura, Conducted 2003 BB-Effect / Bernoulli plenum levitation experiment.

Coanda-Effect Levitation: Aerodynamic Effect often confused with Antigravity designed to create low-pressure area to create lift over conventional lifting surface. Variants include the high-efficiency vortex-thruster technology & well-known AvroCar Air Force Prototype. The Vortex Thruster showed promise at lift efficiencies up to 10x compared to helicopter (4 tons per square meter).

→ Andreas Epp: Developed WW-II mechanical Coanda-disk for Germany.
→ Viktor Schaumberger: Developed WW-II "Repulsine" Coanda-thruster.
→ Dr. Mikhail Goldshtik: Developed HE Vortex Thruster at U. of Texas in 1997.
→ Tim Ventura, Developed self-compressing Vortex-Thruster in 2003.
→ Terry Day, Developed box-style high-intensity vortex (tornado) generator.
→ AvroCar, 1960's era military prototype for Coanda surface-effect levitation.
→ Bob Iannini, Developed box-style high-intensity vortex (tornado) generator.
→ Dr. Paul Moller, inventor of the Moller SkyCar, 1990's-era updated AvroCar.

Alt-Energy Systems: The following are a few of the more well-known pursuits of high-output mobile electrical generation proposed for use in Antigravity technologies.

→ Dr. Paul Brown, proposing stimulated decay nuclear batteries.
→ Patrick Herda, CEO of Paul Brown's Nuclear Solutions company.
→ Michael McDonnough, founder of Betavoltaic, proposing micronuclear power-supplies based on LENR & plasma-fusion.
→ Arie DeGiess, invented micro-scale plasma-fusion generator for AG systems.
→ Dr. Ronald Mills, Founder of Blacklight Power, proposing plasma hydrino-reaction suitable for onboard AG power.
→ Jim Henry, Armor Systems International, inventor of microscale steam-turbine for Stanford/DARPA battle armor project. Proposing same for onboard AG power.
→ John Dering, proposing laser-stimulated nuclear-isomer decay "throttleable" nuclear powerplants.

Boundary Layer Reduction & Stealth: The application of the Biefeld-Brown effect for the reduction of air-compression in aircraft due to the boundary-layer condition. Various testing has also suggested that this is a potential method for generating aircraft radar-insibility.

→ Dr. Paul Laviolette, Proposed BB-Effect stealth-enhancements for the B2.
→ Dr. James Corum, demonstrated naval stealth replication for the Philadelphia Experiment and proposed plasma-shielding through radar absorption to confirm Laviolette's claim.
→ Jean-Louis Naudin, demonstrated boundary-layer reduction via the Biefeld-Brown Effect in dielectric fluids.
→ John Dering, described 1960's RF-plasma experiments by Northrop leading to "cold-plasma" boundary-layer reduction for aircraft performance.

Relativity Theory: This theory has been investigated by many with regard to applications for space-travel. The following is a highly-truncated list of research pertaining to Antigravity.
→ Miguel Alcubierre, a 1960's era warp-drive concept from within general relativity allowing "folded space" to create FTL travel and a new method of propulsion. (The Warp Drive in Star Trek is based on Alcubierre's work).
→ Dr. Jack Sarfatti, independently derived a post-Einsteinian theory similar to UFT that he claims supports UFO & AG technologies.
→ Dr. David Maker, author of an ungauged theory of general relativity supporting Podkletnov's force-beam claims.
→ Dr. Ning Wu, author of a gauge-theory of Relativity supporting Podkletnov's research.

Government Interest: A variety of organizations have conducted limited investigation into Antigravity technologies. The following is a truncated list of recent known investigations. Please note that none of these investigations has involved a full-scale organizational commitment to research.

→ Naval Research Labs, Conducted internal 2003 investigation of Lifter & Biefeld-Brown Effect technologies.

→ NASA, conducted a variety of exploratory investigations into Biefeld-Brown Effect technologies from 1980-onward, resulting in several related patents in 2001. NASA also has a variety of employees working off-the-clock with the open-source community, and attempted a replication of the Podkletnov rotating disk apparatus in 2001.

→ Los Alamos National Labs, has been very actively conducting internet-research for AG related information. Additionally, they reportedly conducted an internal replication of Lifter technology in October 2003.
→ US Air Force, has no current official interest in AG technologies, but does show interest in staying current with latest research. Additionally, the Air Force has financed studies of Biefeld-Brown Technology dating back to the 1950's.

→ Oak Ridge National Labs, published 2001 research findings to demonstrate that they have actively pursued energy-related research based on open-source community work over the last decade.

→ Defense Intelligence Agency, has no official interest in AG technologies, but does show interest in staying current with latest research.
→ United States Army, Aviation and Missile Command financed Dr. Ning Li's 2002 AC-Gravity experiments.

→ Japanese Government, financed educational replication of Lifter experiment for students in 2002. Results included testing of a 25-foot Lifter involving several hundred thousand dollars in equipment investment.

→ Brazilian Army R&D, published a 2001 paper describing socio-economic impact of gravity-control. Brazilian military has also reportedly been closely scrutinizing AG research by Dr. Fran De Aquino.

→ British Government, Reportedly financing research by Marcus Hollinshead, in addition to maintaining interest in recently-defunct BAE Greenglow project.

Patents

List of patents:

1. Triangular Spacecraft (US20060145019A1) - John St. Clair
2. Photon Spacecraft (US20060144035A1) - John St. Clair
3. Method and Apparatus for Generating a Secondary Gravitational Force Field (US3626605) - H. Wallace

US 20060145019A1

(19) **United States**

(12) **Patent Application Publication** (10) **Pub. No.: US 2006/0145019 A1**

St. Clair (43) **Pub. Date: Jul. 6, 2006**

(54) **TRIANGULAR SPACECRAFT**

(76) Inventor: **John Quincy St. Clair**, San Juan, PR (US)

Correspondence Address:
JOHN ST. CLAIR
52 KINGS COURT, 4A
SAN JUAN, PR 00911 (US)

(21) Appl. No.: **11/017,093**

(22) Filed: **Dec. 20, 2004**

Publication Classification

(51) **Int. Cl.**
B64G 1/40 (2006.01)

(52) **U.S. Cl.** **244/171.5**

(57) **ABSTRACT**

A spacecraft having a triangular hull with vertical electrostatic line charges on each corner that produce a horizontal electric field parallel to the sides of the hull. This field, interacting with a plane wave emitted by antennas on the side of the hull, generates a force per volume combining both lift and propulsion.

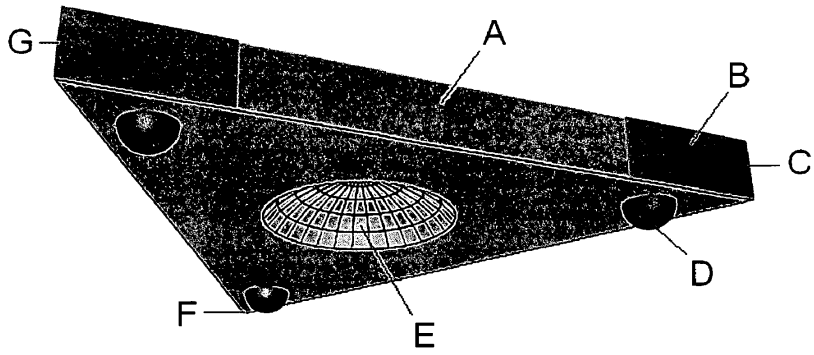

Figure 1

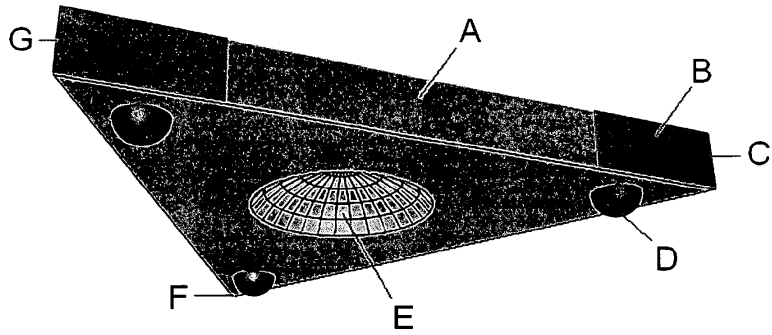

Figure 2

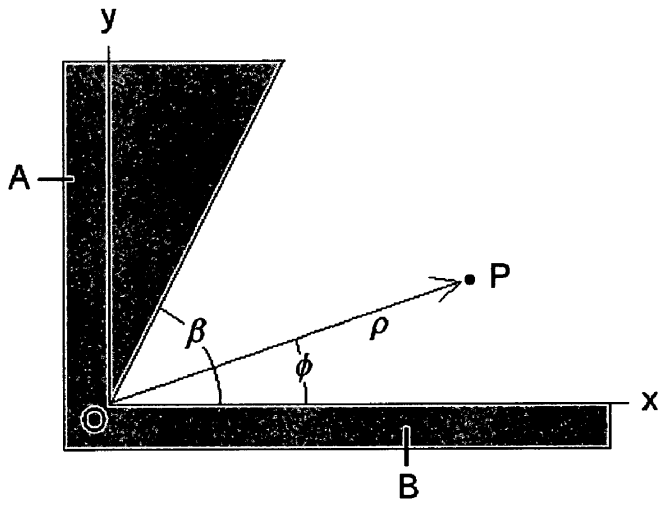

Figure 3

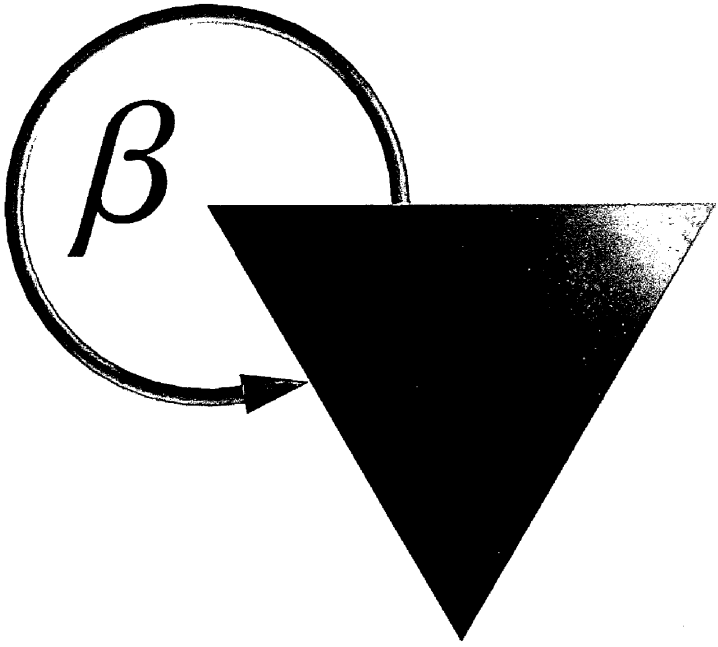

Figure 4

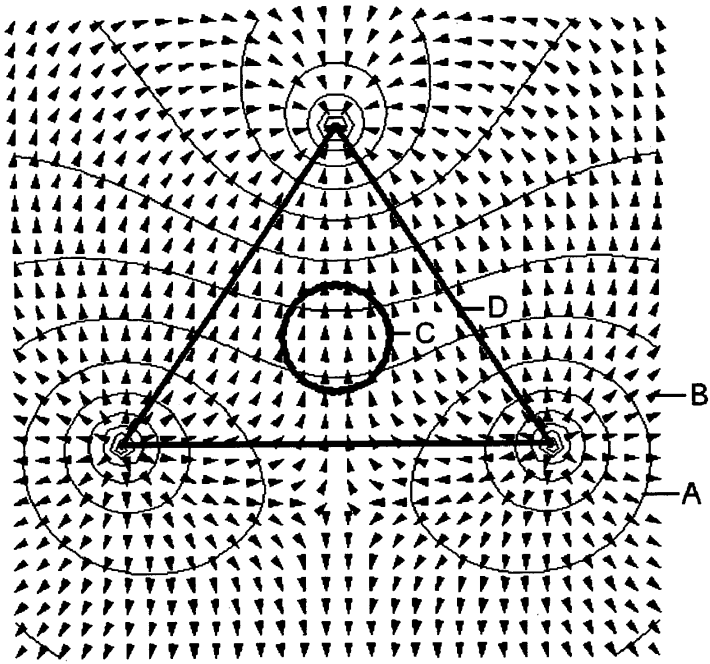

Figure 5

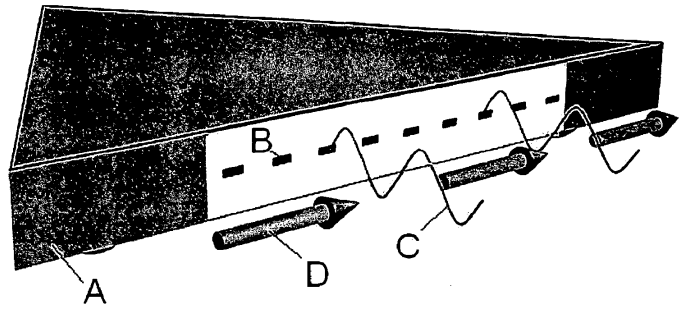

Figure 6

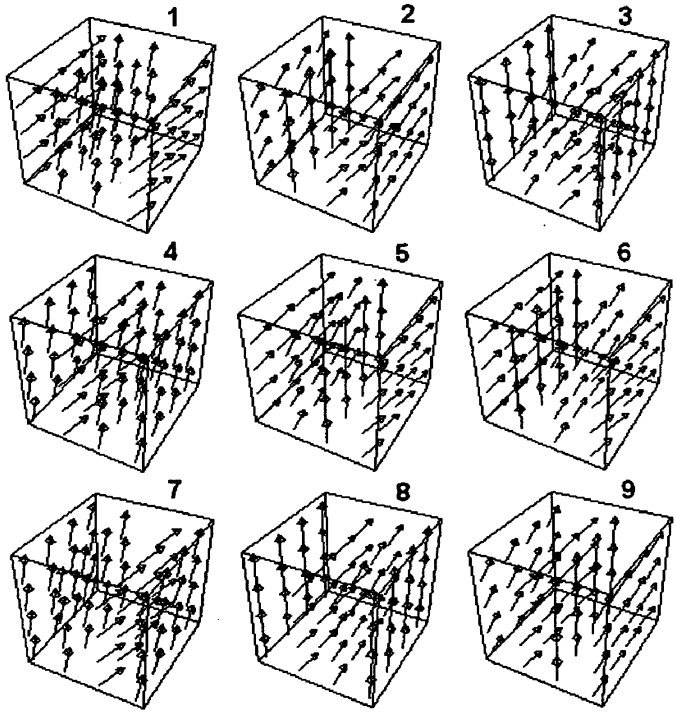

Figure 7

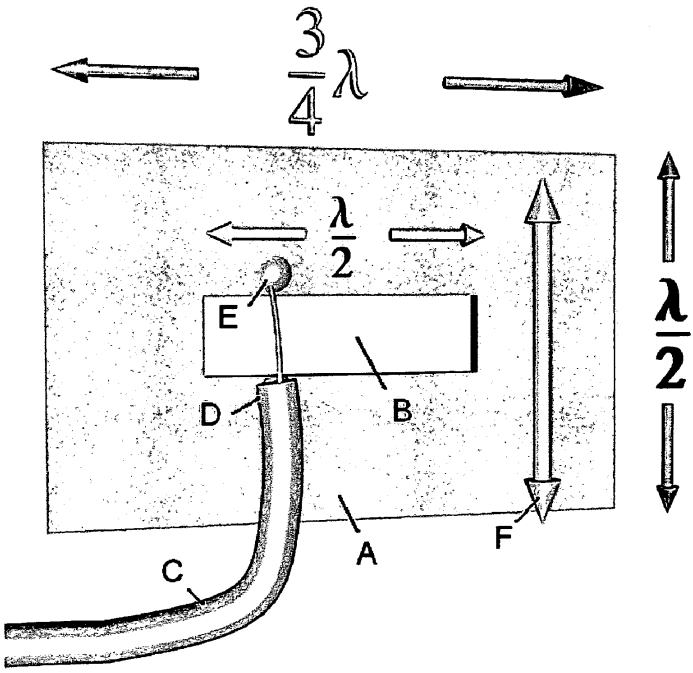

TRIANGULAR SPACECRAFT

BRIEF SUMMARY OF THE INVENTION

[0001] This invention is a spacecraft having a triangular hull with vertical electrostatic line charges on each corner. The line charges create a horizontal electric field that, together with a plane wave emitted by antennas on the side of the hull, generates a force per volume providing a unique combination of both lift and propulsion.

BACKGROUND OF THE INVENTION

[0002] Referring to **FIG. 1**, the spacecraft has a hull in the shape of an equilateral triangle. A parabolic antenna (E) is centrally located in the bottom of the hull. An array of horizontal slot antennas is located along the side of the hull (A). Each back corner (F,G) has a corner conducting plate which is charged to a positive voltage +V. The forward corner (C) has a conducting plate charged to a negative voltage −V. A motion control hemisphere (D) is located on the bottom surface in each of the three corners.

[0003] Referring to **FIG. 2**, two planes (A,B) intersect at the origin O at an opening angle β. Each plane (x,y) is charged to a voltage V. The potential at point P is determined in polar coordinates {ρφ}. The Laplace equation for the potential Φ in polar coordinates is given by:

$$\frac{1}{\rho}\frac{\partial}{\partial\rho}\left(\rho\frac{\partial\Phi}{\partial\rho}\right)+\frac{1}{\rho^2}\frac{\partial^2\Phi}{\partial\phi^2}=0$$

Using a separation of variables solution, the potential is given as the product of two functions:

$$\Phi(\rho,\phi)=R(\rho)\Psi(\phi)$$

which when substituted into the Laplace equation becomes:

$$\frac{\rho}{R}\frac{d}{d\rho}\left(\rho\frac{dR}{d\rho}\right)+\frac{1}{\Psi}\frac{d^2\Psi}{d\phi^2}=0$$

Since the two terns are separately functions of ρ and φ respectively, each one has to be constant with the sum of the constants equal to zero:

$$\frac{\rho}{R}\frac{d}{d\rho}\left(\rho\frac{dR}{d\rho}\right)=\nu^2\quad\frac{1}{\Psi}\frac{d^2\Psi}{d\phi^2}=-\nu^2$$

These two equations have solutions:

$$R(\rho)=a\rho^{\nu+b\rho-\nu}$$

$$\psi(\phi)=A\cos(\nu\phi)+B\sin(\nu\phi)$$

The azimuthal angle φ is restricted to a value in the range 0≦φ≦β. The boundary condition is that the potential Φ is equal to V for any radius ρ when φ=0 and φ=β. This means that v has to be an integer value of π so that the sine function is zero:

$$\sin(\nu\beta)=\sin\left(\frac{n\pi}{\beta}\beta\right)=\sin(m\pi)=0\quad m=1,2\ldots$$

which in turn means that the coefficient A of the cosine term has to be zero in the solution above. Choosing b=0 makes the general solution for the potential equal to:

$$\Phi(\rho,\phi)=V+\sum_{m=1}^{\infty}a_m\rho^{m\pi/\beta}\sin(m\pi\phi/\beta)$$

which shows that when the angle is zero, the sine is zero and the potential is V. If the angle is β, then there is a multiple of π such that the sine is zero again.

[0004] Because the series involves positive powers of the radius, for small enough ρ, only the first term $m=1$ in the series is important. Thus around ρ=0, the potential is approximately

$$\Phi(\rho,\phi)\approx V+a_1\rho^{\pi/\beta}\sin(\pi\phi/\beta)$$

[0005] The electric field component is the negative gradient of the potential:

$$E_\phi(\rho,\phi)=-\frac{1}{\rho}\frac{\partial\Phi}{\partial\phi}=-\frac{\pi a_1}{\beta}\rho^{(\pi/\beta)-1}\cos(\pi\phi/\beta)$$

The surface charge distribution σ at φ=0 and φ=β is equal to the electric field perpendicular to the surface times the permittivity of space ϵ_0:

$$\sigma(\rho)=\varepsilon_0E_\phi(\rho,0)=-\frac{\varepsilon_0\pi a_1}{\beta}\rho^{\frac{\pi}{\beta}-1}$$

Notice that if angle of intersection β is less than π, then the equation says that there is a very small radius to a positive power which means little charge density accumulation.

[0006] Referring to **FIG. 3**, the value of β, in the case of the triangular hull, is equal to 360° less 60° for a total of 300° or:

$$\beta=\frac{300}{180}\pi=\frac{5}{3}\pi$$

$$\rho^{\frac{\pi}{\frac{5}{3}\pi}-1}=\frac{1}{\rho^{\frac{2}{5}}}$$

which says that there is a charge density singularity to the two fifths power for small radius. Thus, the corner plates on the hull create a huge line charge density along the sharp vertical corner edge. The equation for the potential of a line charge density is given as:

$$\Phi(x,y)=-\frac{\lambda}{2\pi\varepsilon_0}\mathrm{Ln}((x-x_0)^2+(y-y_0)^2)$$

where λ is the charge per unit length in the vertical z-direction, and x_0 and y_0 are the location of the line charge in the xy-plane.

[0007] Referring to **FIG. 4**, the triangular hull (D) is plotted together with the potential contours (A) and the electric field arrows (B) created by the three corner line charges. The line charges are perpendicular to the paper. Notice that the electric field arrows are parallel crossing the center parabolic antenna (C). The electric field is also parallel to the sides (D) of the triangle.

[0008] Referring to **FIG. 5**, along the side of the triangle (A), an array (B) of horizontal slot antennas emit electromagnetic waves that have a vertically polarized electric E field (C). These traveling waves interact with the electric field (D) produced by the line charges on the corners of the triangle.

[0009] Using differential forms mathematics, this combination of fields is represented by the Hodge star of the differential of the wedge product of the two fields. The antenna electromagnetic field is a combination of a traveling magnetic field B_w, and electric field E_w. The stationary field E created by the line charges is perpendicular to the traveling wave.

$$*d(E \wedge (B_w + E_w \wedge dt))\frac{\varepsilon}{c} = \frac{\text{force}}{\text{volume}}$$

where ϵ is the linear capacitance of space and c is the speed of light. Thus there is a force per volume around the hull.

[0010] This combination of fields produces a spacetime curvature as determined by Einstein's General Theory of Relativity. The traveling electric field has an amplitude in the vertical z-direction and travels in the x-direction

$$E_{w=Ez}\cos(x-t)$$

The Faraday electromagnetic tensor contains all the electric and magnetic fields in all the {x,y,z} directions. The first row and first column contain the two electric fields

$$F^{\alpha}_{\beta} = \begin{array}{c|cccc} & t & x & y & z \\ \hline t & 0 & E_x & 0 & E_z\cos(x-t) \\ x & E_x & 0 & 0 & 0 \\ y & 0 & 0 & 0 & 0 \\ z & E_z\cos(x-t) & 0 & 0 & 0 \end{array}$$

The stress exerted on spacetime occurs in the xx, yy and zz-direction as calculated from the stress-energy tensor T of gravitational physics

$$4\pi T^{\mu\nu} = F^{\mu\alpha}F^{\mu}_{\alpha} - \frac{1}{4}g^{\mu\nu}F_{\alpha\beta}F^{\alpha\beta}$$

where g is the metric tensor for Cartesian space

$$g_{\alpha\beta} = \begin{array}{c|cccc} & t & x & y & z \\ \hline t & -1 & 0 & 0 & 0 \\ x & 0 & 1 & 0 & 0 \\ y & 0 & 0 & 1 & 0 \\ z & 0 & 0 & 0 & 1 \end{array}$$

where the diagonal components are the coefficients of the elementary spacetime length ds squared

$$(ds)^2 = -(dt)^2 + (dx)^2 + (dy)^2 + (dz)^2$$

The calculation produces three stresses T^{xx},T^{yy} and T^{zz} in their respective {x,y,z} directions.

[0011] Referring to **FIG. 6**, these three stresses are plotted together as a **3**D vector field animated over time in nine frames. The graphs show that there is a lift force as depicted by the vertical arrows as well as a force of propulsion as shown by the interspersed horizontal arrows. With the passage of time, these vectors exchange places with each other so that the lift becomes the propulsion and vice versa, creating a wavy stress-energy field around the hull.

SUMMARY OF THE INVENTION

[0012] This invention is a spacecraft with a triangular hull having charged flat plates on the vertical corners of the three sides. The two rear corners are charged to a potential V. The forward corner is charged to a potential −V. The 60° angle on the corner creates a line charge density singularity that produces a huge horizontal electric field pointing from the back to the front of the craft which is also parallel to the sides of the triangle. An array of horizontal slot antennas located on the sides of the triangular hull produce an electromagnetic wave with the electric field polarized in the vertical direction. This combination of fields produces a spacetime force in both the vertical and horizontal directions such that the spacecraft receives a lift force and a force of propulsion.

A BRIEF DESCRIPTION OF THE DRAWINGS

[0013] **FIG. 1**. Perspective view of triangular spacecraft.

[0014] **FIG. 2**. Drawing of the intersection of two charged plates in order to calculate the charge density in the corner.

[0015] **FIG. 3**. Perspective view of the corner angle β for the equilateral triangle.

[0016] **FIG. 4**. Planar **2**D graph showing the electric field produced by three line charges on the corners of the triangular hull.

[0017] **FIG. 5**. Perspective view of electric field produced by the linear charge interacting with the traveling electromagnetic wave produced by the slot antenna.

[0018] **FIG. 6**. **3**D vector animation of the lift and thrust force generated by the fields.

[0019] **FIG. 7**. Perspective view of slot antenna.

DETAILED DESCRIPTION OF THE INVENTION

[0020] Referring to **FIG. 7**, the antenna (A) is made out of sheet copper in which a rectangular horizontal slot (B) has been notched out using a die press and sheet metal fixture. A coaxial cable from the amplifier and frequency generator is attached across the slot by soldering the outer cable (D) to one side of the slot and the inner cable (E) to the other side of the slot. This creates the positive and negative charges across the gap which forms the vertical electric field (F) which radiates out perpendicularly to the copper sheet.

[0021] Although the invention has been described with reference to specific embodiments, such as a particular antenna system, those skilled in the art will appreciate that many modifications and variations are possible without departing from the teachings of the invention. All such modifications and variations are intended to be encompassed within the scope of the following claims.

1. A spacecraft comprised of the following components:

(a) a triangular hull in the form of an equilateral triangle;

(b) two copper plates attached on opposite vertical sides at each of the three corners of the hull (**1***a*) such that a sharp vertical edge is formed where they come together;

(c) an electrostatic generator used to charge the back two copper-cladded corners (**1***b*) to a high positive voltage, and the third forward copper-cladded corner to a high negative voltage;

(d) a horizontal slot antenna array mounted-on the sides of the hull; and

(e) a frequency generator, antenna and coaxial cables to drive the antenna array (**1***d*).

2. To create, by claims (**1***a*, **1***b*, **1***c*), an intense vertical line charge at the corners (**1***b*) and a horizontal electric field that that is parallel to the sides of the hull (**1***a*);

3. To create, by claims (**1***d*,**1***e*), an electromagnetic wave with a vertically polarized electric field traveling outward from the side of the hull (**1***a*); and

4. To create, by claims (**2**,**3**), an interaction of the electrostatic field (**2**) with the electromagnetic wave (**3**) such that a combined spacetime curvature pressure is generated on the hull in the upward and forward direction to produce lift and propulsion respectively.

* * * * *

US 20060144035A1

(19) **United States**

(12) **Patent Application Publication** (10) **Pub. No.: US 2006/0144035 A1**

St. Clair (43) **Pub. Date: Jul. 6, 2006**

(54) **PHOTON SPACECRAFT**

(76) Inventor: **John Quincy St. Clair**, San Juan, PR (US)

Correspondence Address:
JOHN ST. CLAIR
52 KINGS COURT, 4A
SAN JUAN, PR 00911 (US)

(21) Appl. No.: **11/027,969**

(22) Filed: **Jan. 3, 2005**

Publication Classification

(51) **Int. Cl.**
F03H 1/00 (2006.01)

(52) **U.S. Cl.** **60/203.1**; 60/204

(57) **ABSTRACT**

A spacecraft propulsion system utilizing photon particles to create negative energy over the hull in order to generate a lift force on the hull.

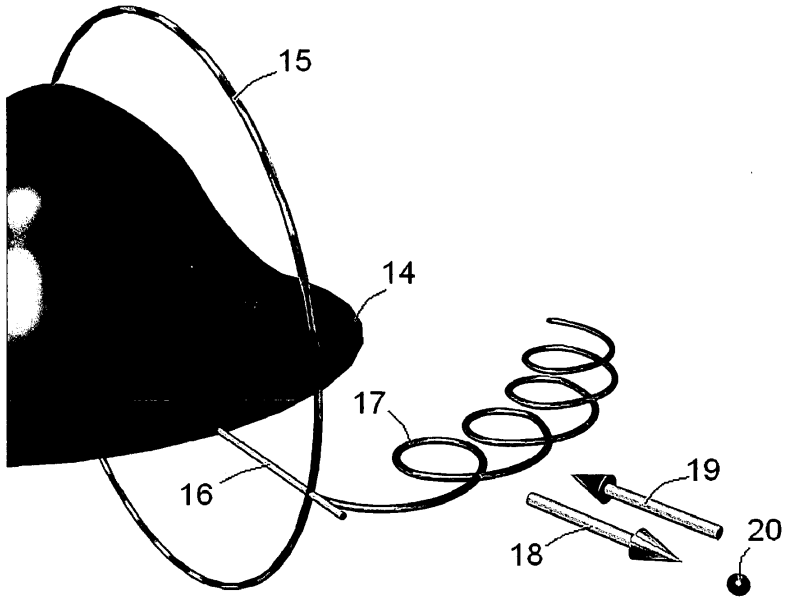

Figure 1

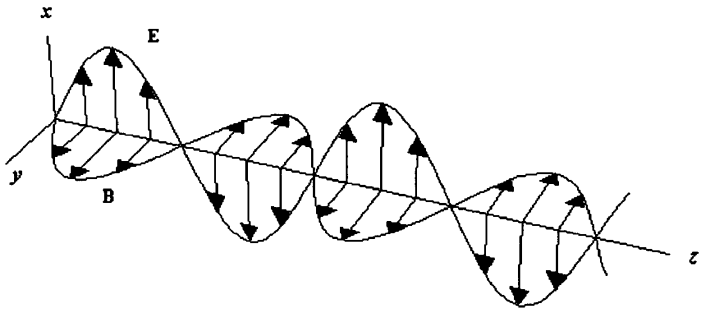

Figure 2

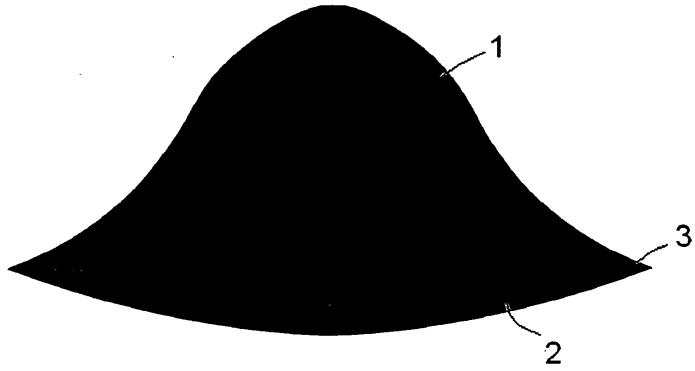

Figure 3

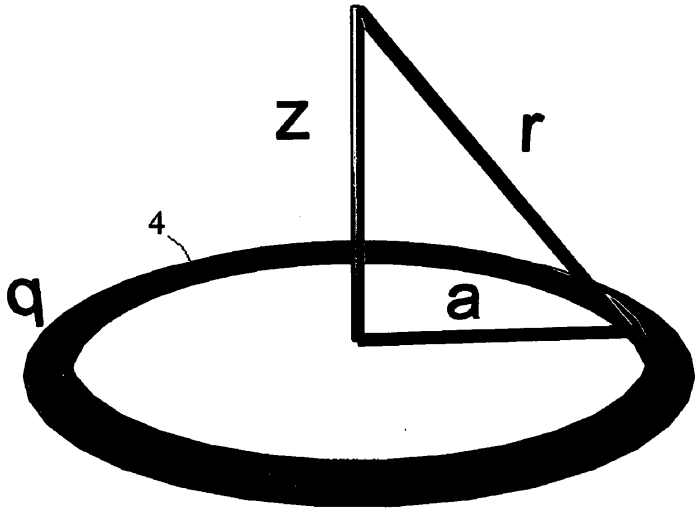

Figure 4

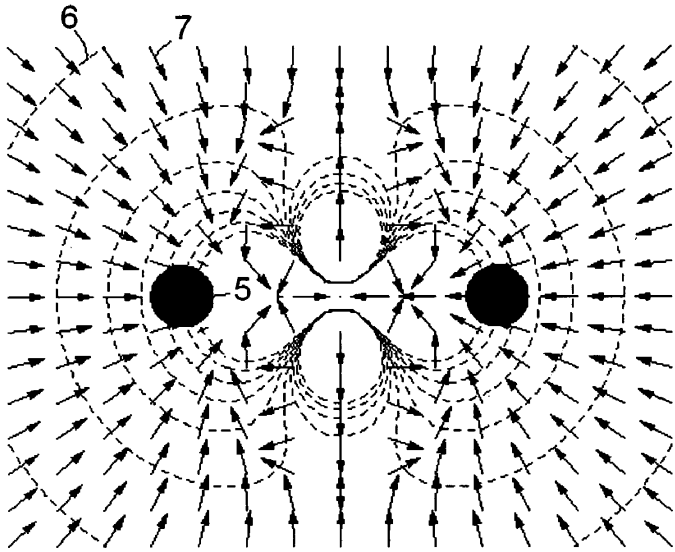

Figure 5

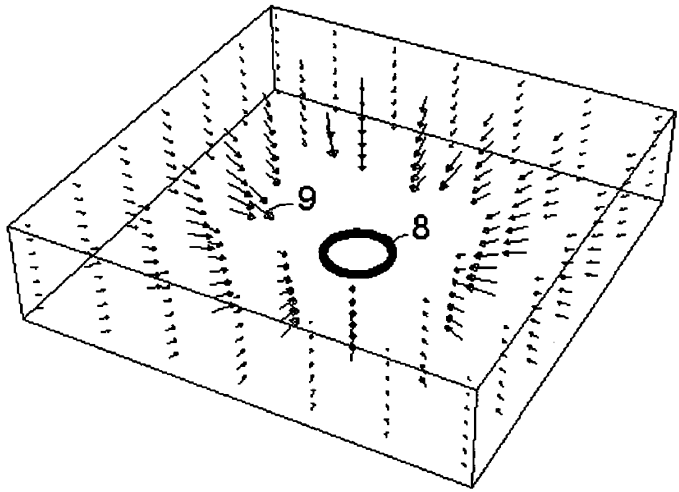

Figure 6

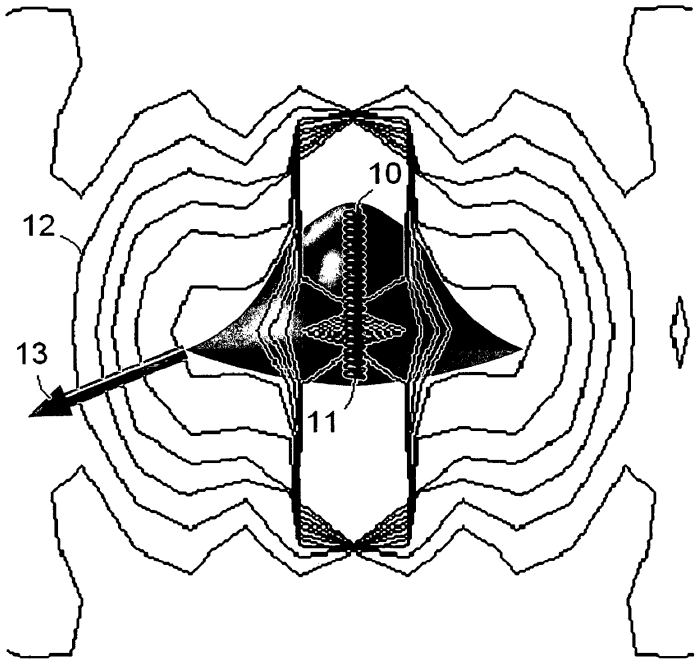

Figure 7

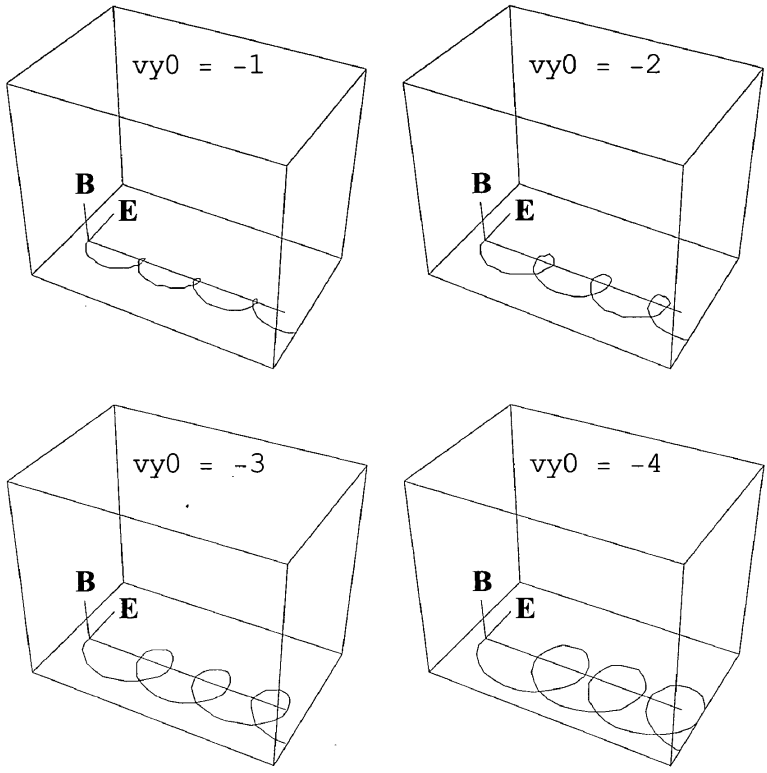

Figure 8

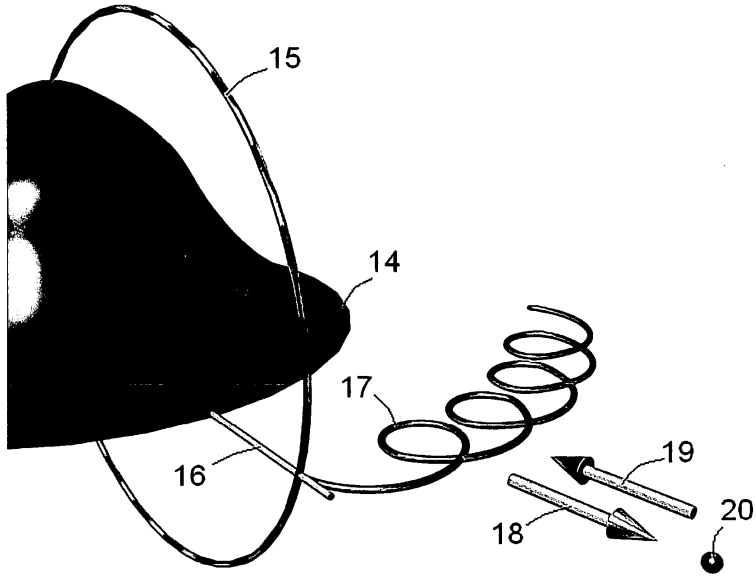

Figure 9

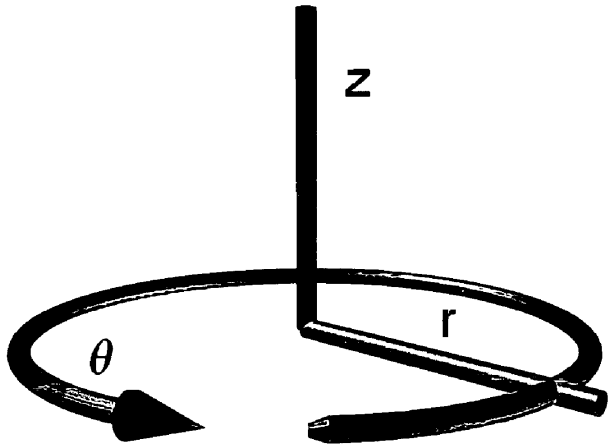

PHOTON SPACECRAFT

BRIEF SUMMARY OF THE INVENTION

[0001] This invention is a spacecraft propulsion system that employs photon particles to generate a field of negative energy in order to produce lift on the hull.

BACKGROUND OF THE INVENTION

[0002] Referring to **FIG. 1**, an electromagnetic wave traveling in the z-direction consists of an electric E field vibrating in the x-direction and a magnetic flux density B field vibrating at right angles in the horizontal y-direction. The energy-stress-momentum of this photon can be analyzed using Einstein's General Theory of Relativity and the Faraday F tensor. The Faraday tensor is a 4×4 matrix containing the electromagnetic wave components as shown here in general where c is the speed of light

$$F_{\beta}^{\alpha} = \begin{array}{c|cccc} & t & x & y & z \\ t & 0 & \frac{E_x}{c} & \frac{E_y}{c} & \frac{E_z}{c} \\ x & \frac{E_x}{c} & 0 & B_z & -B_y \\ y & \frac{E_y}{c} & -B_z & 0 & B_x \\ z & \frac{E_z}{c} & B_y & -B_x & 0 \end{array}$$

For this particular photon, this tensor is

$$F_{\beta}^{\alpha} = \begin{array}{c|cccc} & t & x & y & z \\ t & 0 & \frac{E_x}{c} & 0 & 0 \\ x & \frac{E_x}{c} & 0 & 0 & -B_y \\ y & 0 & 0 & 0 & 0 \\ z & 0 & B_y & 0 & 0 \end{array}$$

[0003] The elemental spacetime length ds squared is equal to sum of the squares of the Cartesian elemental lengths

$$(ds)^2=-(dt)^2+(dx)^2+(dy)^2+(dz)^2$$

The coefficients of this equation, {−1,1,1,1} are the diagonal components of the g metric tensor

$$g_{\alpha\beta} = \begin{array}{c|cccc} & t & x & y & z \\ t & -1 & 0 & 0 & 0 \\ x & 0 & 1 & 0 & 0 \\ y & 0 & 0 & 1 & 0 \\ z & 0 & 0 & 0 & 1 \end{array}$$

The stress-energy-momentum tensor T can then be calculated for the photon using the Faraday tensor and the g metric tensor in the following equation from gravitation physics

$$4\pi T^{\mu\nu} = F^{\mu\alpha}F_{\alpha}^{\nu} - \frac{1}{4}g^{\mu\nu}F_{\alpha\beta}F^{\alpha\beta}$$

The stress-energy-momentum tensor indicates the curvature of space due to the application of electromagnetic fields, mass, angular momentum and charge. The mass of the Earth, for example, generates a negative curvature of spacetime such that objects fall toward the mass. The T tensor, which is also a 4×4 matrix, contains the momentum or flux terms in the first row and first column. The normal pressure stress is located along the diagonal. The shearing stresses are located off the diagonal. The energy term is in the upper left corner as depicted here,

$$T^{\mu\nu} = \begin{array}{c|cccc} & t & x & y & z \\ t & \text{energy} & flux_x & flux_y & flux_z \\ x & -flux_x & pressure_x & shear_{xy} & shear_{xz} \\ y & -flux_y & shear_{yx} & pressure_y & shear_{yz} \\ z & -flux_z & shear_{zx} & shear_{zy} & pressure_z \end{array}$$

[0004] Since $B^2=E^2/c^2$, the stress-energy-momentum tensor for the photon is therefore

$$T_{\nu}^{\mu} = \begin{array}{c|cccc} & t & x & y & z \\ t & \frac{-E^2}{c^2} & 0 & 0 & \frac{+E^2}{c^2} \\ x & 0 & 0 & 0 & 0 \\ y & 0 & 0 & 0 & 0 \\ z & \frac{-E^2}{c^2} & 0 & 0 & \frac{+E^2}{c^2} \end{array}$$

This remarkable result shows that the photon is actually a negative energy particle (top left corner) which is pushed along by a positive pressure wave (lower right corner). The particle has a positive flux (upper right corner) in the z-direction, as well as a balancing negative flux in the lower left corner so that the overall momentum of the universe remains the same. All four components cancel and we see the photon as a massless particle moving at the speed of light.

[0005] Thus the key idea behind this invention is that it is possible to cancel out the pressure term and leave a stationary vibrating electromagnetic field of negative energy over the hull of the spacecraft. The importance of negative energy is that it is a prerequisite to generating wormholes between space and hyperspace.

[0006] Hyperspace consists of the those co-dimensions which have different physics constants such as a low speed of light. The existence of hyperspace, which has a white misty look, is not a well-known scientific concept. Experiments with our magnetic vortex wormhole generators, hyperspace torque generator, full body levitation using Chi Kung breathing, arm levitation by spinning the co-gravitational K field, full body teleportation through hyperspace a distance of 100 meters using a pulsed gravitational wave, jumping into hyperspace, having a plate of toast enfold off the breakfast table and disappear into thin air, walking through walls and doors out-of-dimension, looking into other dimensions, remote viewing through subspace to distances of 100,000 light years, and other electromagnetic experiments carried out by co-researchers, have shown us the reality and existence of hyperspace.

[0007] Referring to **FIG. 2**, the spacecraft consists of an upper (**1**) and lower (**2**) hull attached by ceramic insulators

to a circular ring (**3**). The ring provides support and is attached to an outer sharp-edged rim which is electrostatically charged to a potential −V. The purpose of the charged rim is to generate a radial electric E field around the vehicle.

[**0008**] Referring to **FIG. 3**, the radius of the ring (**4**) is equal to a. The distance from a point on the ring to the z-axis is r. The potential on the z-axis is therefore the charge divided by the distance,

$$potZ = \frac{q}{\sqrt{a^2 + r^2}}$$

This potential is expanded as a series in terms of inverse radius r

$$potZout = \frac{35qa^8}{128r^9} - \frac{5qa^6}{16r^7} + \frac{2qa^4}{8r^5} - \frac{qa^2}{2r^3} + \frac{q}{r}$$

The potential outside the ring can be written in terms of the Legendre polynomials P

$$Vout = \sum_{n=0}^{s} \left(\frac{a}{r}\right)^{n+1} A[n] LegendreP[n, \mathrm{Cos}(\theta)]$$

where s is the number of terms in the expansion. By equating the known particular solution potZout on the z-axis with the general Vout solution, the coefficients A[n] are found to be

$$A(0) = \frac{q}{a}$$
$$A(1) = 0$$
$$A(2) = \frac{-q}{2a}$$
$$A(3) = 0$$

which are substituted back into the Vout equation to get the potential outside the ring.

[**0009**] Referring to **FIG. 4**, the potential (dotted lines **6**) looking at a slice through the ring (**5**) is shown together with the electric E field. The negative gradient of the potential is the electric field (**7**) shown by the direction of the arrows. The importance of this diagram is that the electric field points in the radial direction toward the negatively charged ring. The force on an electron is the electron charge times the electric field

$$F = q_e E_r = -|q_e|(-|E_r|) = +F$$

Because the electron charge is negative and the radial field points in the negative direction toward the ring, the force on the electron is positive. Thus the electron moves away from the ring in the positive radial direction. A 3-dimensional plot of the ring (**8**) and the electric field (**9**) is shown in **FIG. 5**.

[**0010**] The stress-energy-momentum generated by a radial electric field is calculated using the Faraday F tensor

$$F_\alpha^\beta = \begin{vmatrix} 0 & E_r & 0 & 0 \\ E_r & 0 & 0 & 0 \\ 0 & 0 & 0 & 0 \\ 0 & 0 & 0 & 0 \end{vmatrix}$$

The g metric tensor has to be given in spherical coordinates {r,θ,φ}

$$g_{\alpha\beta} = \begin{vmatrix} -1 & 0 & 0 & 0 \\ 0 & 1 & 0 & 0 \\ 0 & 0 & r^2 & 0 \\ 0 & 0 & 0 & r^2 \sin(\theta)^2 \end{vmatrix}$$

where θ is the angle from the vertical to the radius r. The stress tensor T^{rr} along the radial direction is

$$T^{rr} = \frac{E_r^2}{8\pi c^2}$$

which shows that the pressure is negative along the radial line equal to the square of the radial electric field divided by the square of the speed of light. Because the field is squared, it doesn't matter that the electric field points in the negative direction. The square makes it positive, but the overall curvature pressure is negative. Thus this negative pressure cancels out the positive pressure propelling the photon along. The second key idea of the invention is how to generate this photon moving in the radial direction.

[**0011**] It has been known for a long time in physics that an electron moving in a circular path will emit photons in a process known by the German word Bremsstrahlung which is translated as "breaking radiation." There are several types of radiation such as classical Bremsstrahlung involving a charged particle making a collision with another charged or uncharged particle in which photons are emitted. The quantum mechanical Bremsstrahlung involves the sudden appearance or disappearance of a charged particle which also emits radiation. In space, having a field of wormholes in which the electrons are spiraling down into hyperspace would result in the emission of photons by the quantum mechanical method. Also, in the atmosphere, having collisions with air molecules results in emission of photons in the classical way.

[**0012**] In order to get the electrons to spiral around and emit photons, a crossed electromagnetic field is used as shown by the following equation

$$F = q(E_r + v_r \times B_\theta)$$

where the velocity v is in the positive radial direction due to the force of the electric field. The velocity crossed with a magnetic flux density B field in the θ-direction makes the electron move sideways back and forth in a wiggling motion.

[**0013**] Referring to **FIG. 6**, a direct current solenoid (**10**), represented by multiple current loops, running vertically

through the center of the hull, generates a magnetic field that curves around the outside of the hull, as shown by contour lines (**12**). The north pole (**11**) is at the bottom of the hull. A radial arrow (**13**) from the electrostatically-charged rim is perpendicular to the magnetic field lines. The cross product in the force equation becomes the electron radial velocity times the magnetic field $v_r B_\theta$.

[**0014**] Referring to **FIG. 7**, the electric field is in the y-direction and the magnetic field is in the z-direction. The flat looping path in the x-direction is the motion of the electron. The electron, which has a negative charge, starts to move in the direction opposite to that of the electric field. In this particular diagram, the electron acquires a velocity in the negative y-direction. Then a sideways force in the x-direction is produced due to the cross product of the velocity with the magnetic field times the negative charge

$$-q(-v_y \times B_z) = +F_x$$

Depending on the magnitude of the velocity, various size loops can be produced.

[**0015**] In terms of the hull coordinates, because the flat loop is in the plane of the electric field which points in the radial direction, the electron emits light in the radial direction. This condition means that the negative radial pressure created by the electric field cancels the radial pressure of the photon. Thus the photon becomes a stationary vibrating quantum of negative energy. This has the appearance of a luminescent light source. The stress tensor for this condition is therefore

$$T_\mu^\nu = \begin{vmatrix} -\frac{E^2}{c^2} & 0 & 0 & \frac{E^2}{c^2} \\ 0 & 0 & 0 & 0 \\ 0 & 0 & 0 & 0 \\ -\frac{E^2}{c^2} & 0 & 0 & 0 \end{vmatrix} = -\frac{E^2}{c^2} \text{residual negative energy}$$

[**0016**] residual negative energy

which leaves a residual negative energy per photon.

[**0017**] Referring to **FIG. 8**, the negatively charged rim (**14**) produces a radial electric field (**16**) that crosses the magnetic B field (**15**) of the solenoid. Electrons emitted by the charged rim then encounter this crossed field which makes them spiral (**17**) around the hull. Because of the tight loop, the electron emits Bremsstahlung radiation in the radial direction (**18**). The positive pressure field of the photon, which is directed in the radial direction, is canceled by the negative pressure field (**19**) created by the electric field. Because the photon energy is negative, a stationary vibrating electromagnetic quantum of negative energy (**20**) surrounds the hull.

[**0018**] This negative energy and the pressure stress created by the electromagnetic fields open up wormholes between space and hyperspace. The potential head is positive from hyperspace into space because the energy of hyperspace is more positive than the negative energy field. The low-density hyperspace energy fills the hull and its surrounding space with a white misty hyperspace energy which makes the spacecraft lighter in mass, and therefore lighter in weight within a gravitational field. The actual physics is more complicated still because the electrons find that the resistance of hyperspace is lower than the resistance of space. Thus they spiral down the wormholes which results in a sudden disappearance of charge. The quantum mechanical effect of this is to radiate even more photons which in turn produce even more negative energy.

[**0019**] The lift on the hull is generated by the radial electric field. In cylindrical coordinates, the g metric tensor is

$$g_{\alpha\beta} = \begin{vmatrix} -1 & 0 & 0 & 0 \\ 0 & 1 & 0 & 0 \\ 0 & 0 & r^2 & 0 \\ 0 & 0 & 0 & 1 \end{vmatrix}$$

Using this metric tensor, the pressure stress in the vertical direction T^{zz} is

$$T^{zz} = \frac{E^2}{8\pi c^2}$$

which is a positive curvature over the hull. The mass of Earth produces a negative curvature in which objects fall toward the mass. By counteracting this negative curvature with a more than positive curvature, lift is developed on the spacecraft. Because the negative energy lowers the effective mass of the vehicle, the acceleration is large with a modest electric field. Moreover, in our dimension, the speed of light is 299792458 meters per second. Hyperspace energy has a speed of light equal to one meter per second. Thus the stress is amplified by a factor of

$$A = \left(\frac{299792458 m/s}{1 m/s}\right)^2 \approx 9 \cdot 10^{16}$$

Because electromagnetic fields are relativistic, motion in a low-velocity-of-light energy field amplifies their strength.

SUMMARY OF THE INVENTION

[**0020**] It is the object of this invention to create a spacecraft propulsion system that produces wormholes between space and hyperspace using negative energy in order to generate lift on the hull. It was discovered in the Riemannian curvature calculations of gravitation physics that negative energy is required to keep open the throat of the wormhole. From experiments with the magnetic vortex wormhole generator, it is known that the proper combination of electromagnetic fields, together with this negative energy, can create a wormhole through which smoke can be blown into hyperspace.

[**0021**] Referring to **FIG. 9**, the directions of force, velocity, and electromagnetic fields are referred to in the cylindrical coordinate system $\{r,\theta,z\}$. An electrostatically charged sharp-edged ring in the θ-direction around the hull of the spacecraft produces a radial electric field. A vertical solenoid in the z-direction through the center of the hull

produces a magnetic field which is perpendicular at the rim to the electric field. With the current in the solenoid flowing in the clockwise (−θ) direction, using the right-hand rule, the magnetic field points in the upward z-direction outside the rim. Because the rim is charged to a negative voltage, the electric field points toward the hull in the negative radial (−r) direction. Electrons emitted by the rim travel outward (+v) because the charge on the electron is negative which, together with the negative electric field, produces a positive radial force. The radial force on the electron causes it to acquire a velocity which interacts with the magnetic field. The cross product of the velocity (+v) with the positive (+B) magnetic field produces a sideways force on the electron in the negative θ-direction. However, because the charge on the electron is negative, the force is

$$F=-q\{v,0,0\}\times\{0,0,B_z\}=\{0,qB_z,v_r,0\}$$

which is positive in the θ-direction. It is this sideways force that produces a flat spiraling or looping motion whereby the electron emits photons, known in German as Bremsstahlung radiation, in the radial direction. The photon, which is actually a quantum of negative energy, has a positive radial pressure which propels it along. Because the radial electric field produces a negative pressure in the radial direction, the two opposite fields cancel in the radial direction to form a residual stationary vibrating negative energy. Thus the hull becomes surrounded by negative energy which, together with the pressure stresses created by the electric field, generates wormholes between space and hyperspace.

[0022] The gravitational potential between hyperspace and space is positive because the hyperspace energy is more positive than the negative energy around the hull. Thus the low-density, low-speed-of-light hyperspace energy flows through the wormhole and fills the hull. This has the effect of reducing the effective mass of the hull. Because the electric field generates a positive pressure over the hull in the vertical z-direction, there is an upward force on the vehicle due to the pressure times the hull area. Since the vehicle has a low mass, there is a modest upward acceleration on the spacecraft equal to the force divided by mass.

A BRIEF DESCRIPTION OF THE DRAWINGS

[0023] **FIG. 1**. Perspective view of an electromagnetic wave.

[0024] **FIG. 2**. Perspective view of spacecraft.

[0025] **FIG. 3**. Perspective view of charged ring.

[0026] **FIG. 4**. Planar plot of the radial electric field produced by charged ring.

[0027] **FIG. 5**. Perspective view of radial electric field around ring.

[0028] **FIG. 6**. Planar view of magnetic flux density field contour lines.

[0029] **FIG. 7**. Perspective view of electron motion in crossed electric and magnetic fields.

[0030] **FIG. 8**. Perspective view of production of negative energy around hull.

[0031] **FIG. 9**. Perspective view of cylindrical coordinate system {r,θ,z}.

DETAILED DESCRIPTION OF THE INVENTION

[0032] 1. The hull is made from a single sheet of aluminum which has been stretched to its yield point by hydraulic cylinders. An upper and lower die is CNC machined to the profile of the hull. The soft sheet is then clamped in the die where it takes on the smooth shape of the hull without any wrinkles. The hull is extremely rigid after forming and does not require any structural reinforcements.

[0033] 2. A section of the aluminum ring is made in a 3D computer graphics program. The model is stored as a stereolithography file (*.stl). The computer model is then sent via Internet e-mail to the stl server who prints the part in an ultraviolet light-cured polymer. The part is returned the next day by Express Mail. Using a rubber blanket mold to create several ring sections, the entire ring is assembled together in another wooden mold box having thin circular laminate-coated particulate wall boards on either side of the ring. Then a liquid rubber mold is poured on top of the ring and allowed to harden overnight at room temperature. Since the rubber mold is flexible, the ring can be extracted fairly easily. This ring model is then sent to the foundry where it is cast in aluminum using the lost wax process in which a wax mold evaporates out of the sand casting. We are also experimenting with non-magnetic copper casting metals containing beryllium having good conductivity.

[0034] 3. A 11.5 cm plastic pipe is mounted on a rotating fixture driven slowly by a microcontoller, stepper motor, and power electronics board. Using a large diameter insulated wire, such as a 17 AWG with a wire diameter of 0.127 cm, the wire is wound slowly on the pipe and expoxied so that the windings don't come loose. The solenoid is then mounted vertically in the hull supported by the support ring and driven by a current generator located nearby on the test rig.

[0035] 4. The ring is driven by a high voltage electrostatic generator similar to the night vision scope high voltage power supplies. The ring charge is isolated from the hull by ceramic insulators.

I claim:

1. A spacecraft propulsion system comprising the components:

an aluminum horizontal circular structural support ring;

an aluminum hull in the shape of a high dome on top and shallow dome on the bottom attached to the circular support ring using ceramic insulators;

an electrostatically negatively-charged sharp-edged circular ring, preferably of non-magnetic aluminum or copper, attached with ceramic insulators to the outside of the support ring;

a solenoid mounted through the center of the hull in the vertical direction and attached to the center of the support ring;

an electrostatic high-voltage generator to drive the outer electrostatic ring; and

a direct high-current generator to drive the solenoid.

2. The method of claim 1, wherein a negative radial electric field is generated around the hull by placing a negative potential on the sharp-edged electrostatic ring using the electrostatic generator.

3. The method of claim 1, wherein the current-driven solenoid generates a vertical magnetic field around the hull with the north pole of the solenoid facing down through the bottom of the hull which causes the magnetic flux density field to point up outside the rim.

4. The method of claim 1, wherein electrons are emitted radially by the sharp edge of the charged ring.

5. The methods of claims **2**, **3** and **4**, wherein the crossed electromagnetic fields cause the electrons to spiral around in flat loops during which photons are emitted in the radial direction.

6. The methods of claims **2** and **5**, wherein the negative radial pressure created by the electric field cancels the positive radial pressure of the photon to leave a residual quantum of negative energy per photon around the hull.

7. The methods of claims **2** and **6**, wherein the pressure stress created by the electric field, and the negative energy combine to form wormholes between space and hyperspace.

8. The method of claim 7, wherein low-density hyperspace energy of a higher gravitational potential flows through the wormholes to fill the hull and surrounding space around the hull with the effect of reducing the effective mass of the spacecraft.

9. The method of claim 2, wherein the electric field generates a positive pressure in the vertical direction over the hull which together with the hull surface area, generates an upward lift force on the hull.

10. The method of claim 6, wherein the negative energy, having a low light speed, amplifies the strength of the electromagnetic fields and pressure stress fields.

11. The methods of claims **4** and **7**, wherein the electrons spiral down the low resistance wormholes into hyperspace such as to create a sudden disappearance of electrical charge which quantum mechanically causes a large emission of additional photons.

* * * * *

Dec. 14, 1971 H. W. WALLACE 3,626,605

METHOD AND APPARATUS FOR GENERATING A SECONDARY GRAVITATIONAL FORCE FIELD

Filed Nov. 4, 1968 6 Sheets-Sheet 1

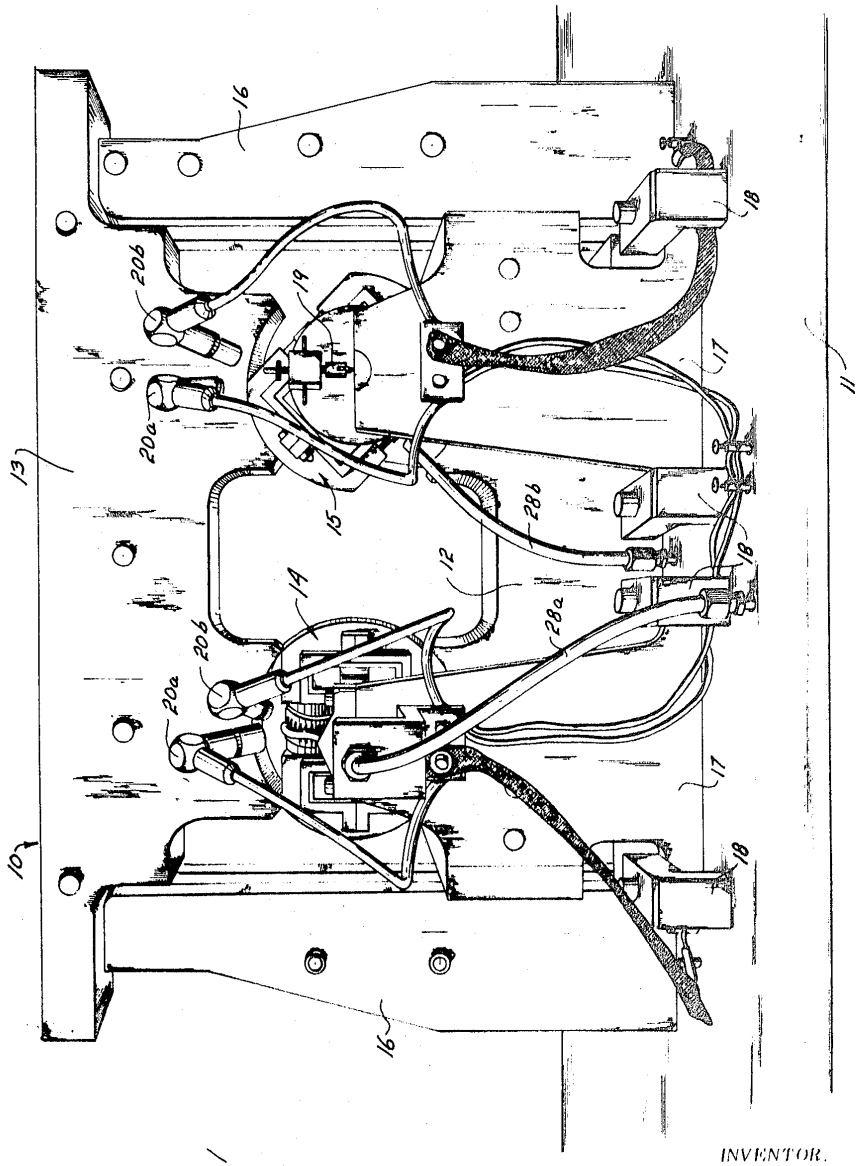

FIG-1

INVENTOR.
HENRY W. WALLACE
BY
Symmes Maddock & Dechnes
ATTORNEY

Dec. 14, 1971 H. W. WALLACE 3,626,605

METHOD AND APPARATUS FOR GENERATING A SECONDARY GRAVITATIONAL FORCE FIELD

Filed Nov. 4, 1968 6 Sheets-Sheet 2

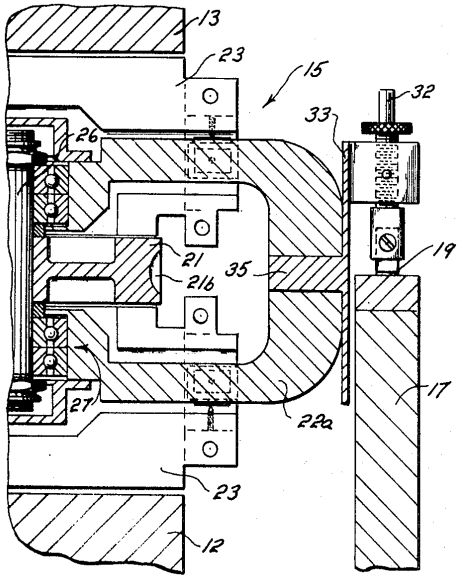

FIG -3A

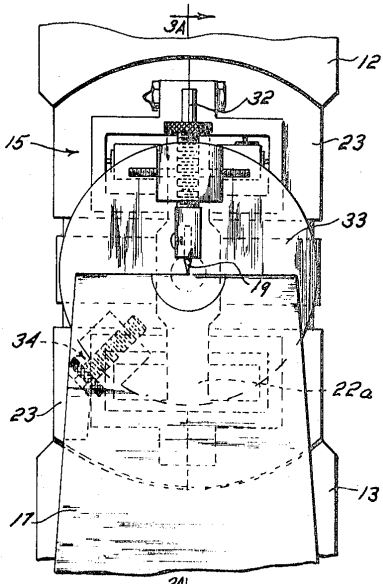

FIG-3B

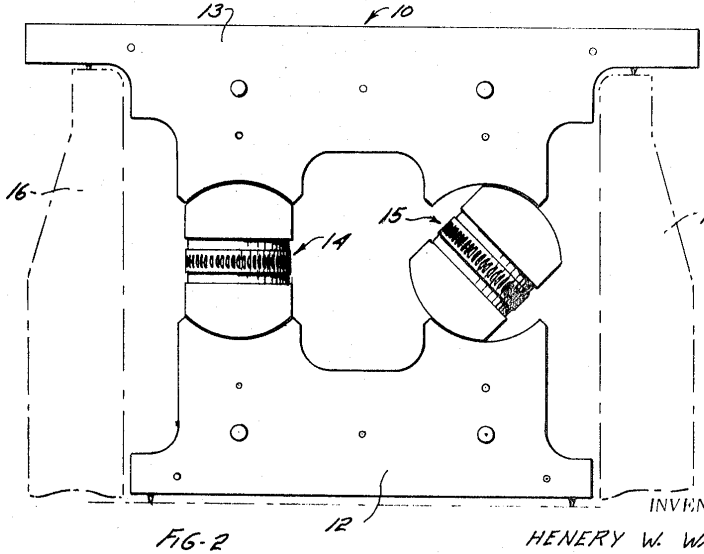

FIG-2

INVENTOR.
HENERY W. WALLACE
BY
Symmestvedt & Lechner
ATTORNEYS

Dec. 14, 1971 H. W. WALLACE 3,626,605

METHOD AND APPARATUS FOR GENERATING A SECONDARY GRAVITATIONAL FORCE FIELD

Filed Nov. 4, 1968 6 Sheets-Sheet 3

FIG. 3

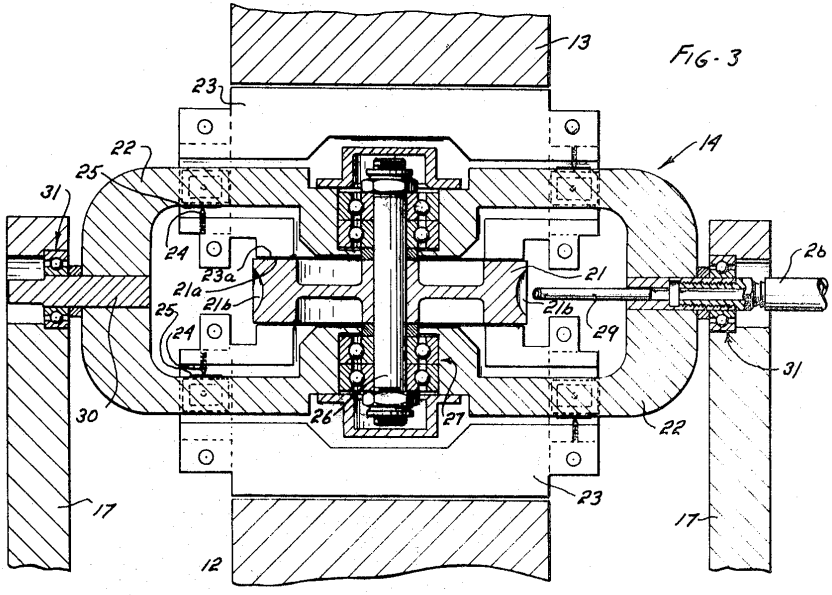

FIG. 4

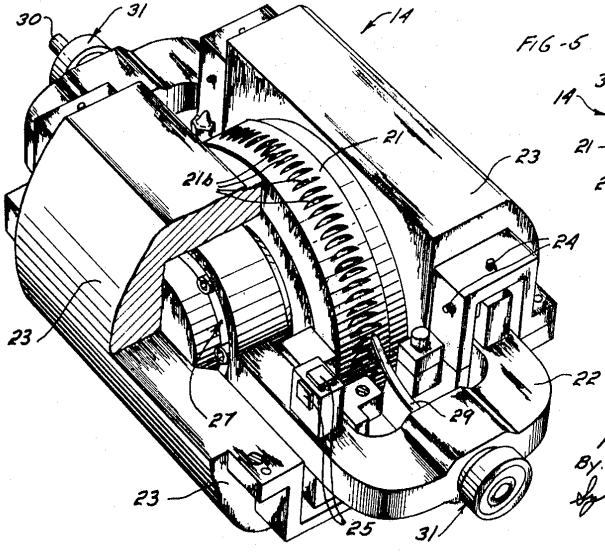

FIG. 5

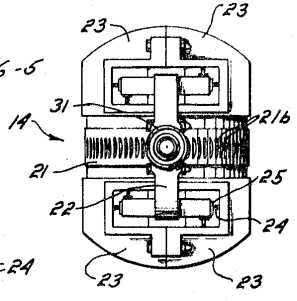

INVENTOR.
HENRY W. WALLACE
By.
Lyon, Lyon & Lechner
ATTORNEYS

Dec. 14, 1971 H. W. WALLACE 3,626,605

METHOD AND APPARATUS FOR GENERATING A SECONDARY GRAVITATIONAL FORCE FIELD

Filed Nov. 4, 1968 6 Sheets-Sheet 4

FIG-6

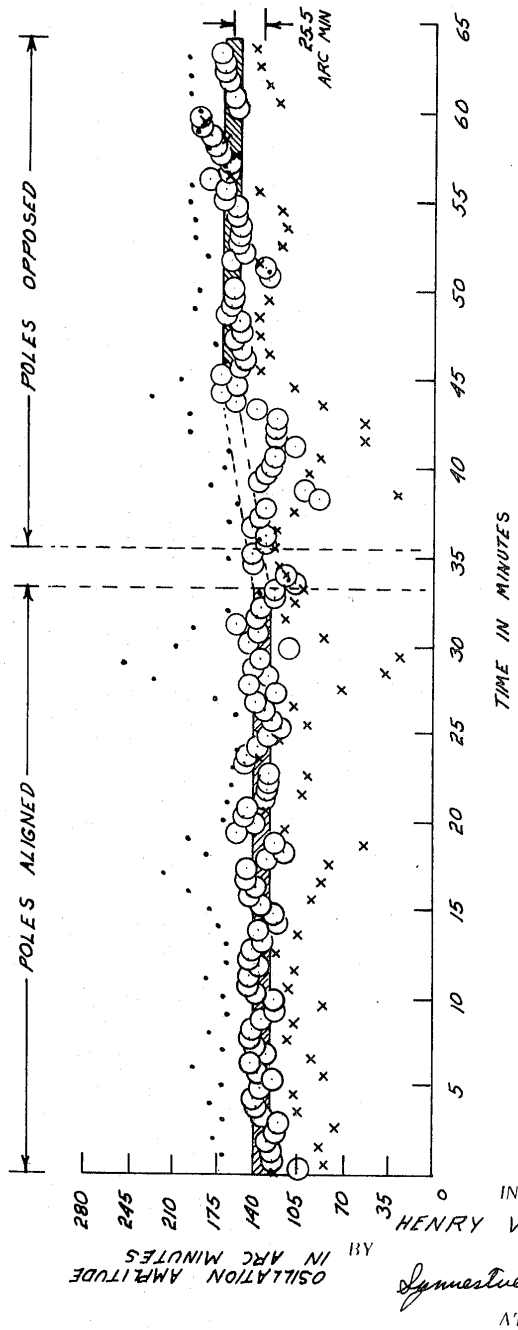

INVENTOR.
HENRY W. WALLACE
BY
Synnestvedt & Lechner
ATTORNEYS

Dec. 14, 1971 H. W. WALLACE 3,626,605

METHOD AND APPARATUS FOR GENERATING A SECONDARY GRAVITATIONAL FORCE FIELD

Filed Nov. 4, 1968 6 Sheets-Sheet 5

FIG-7

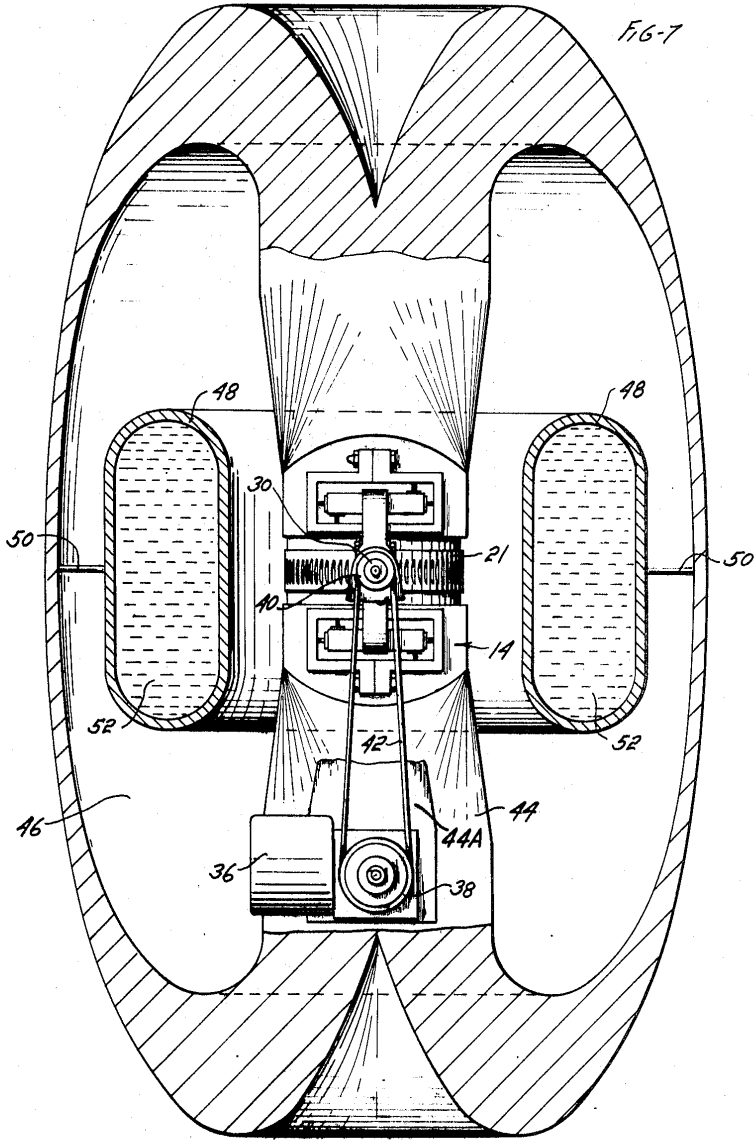

INVENTOR.
HENRY W. WALLACE
BY
Dynes, Quelle & Lechner
ATTORNEYS

Dec. 14, 1971 H. W. WALLACE 3,626,605

METHOD AND APPARATUS FOR GENERATING A SECONDARY GRAVITATIONAL FORCE FIELD

Filed Nov. 4, 1968 6 Sheets-Sheet 6

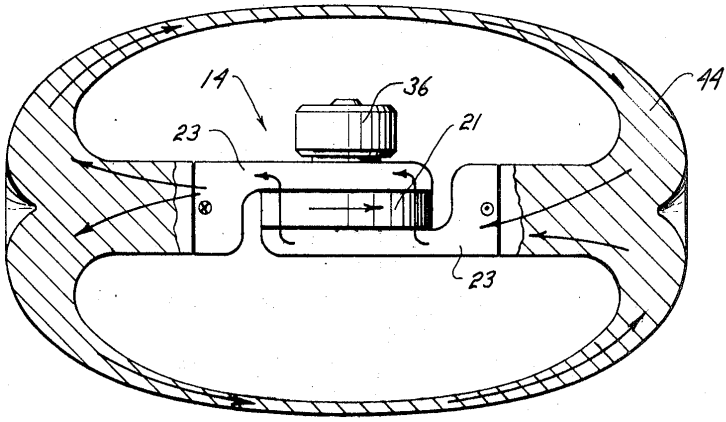

FIG. 7A

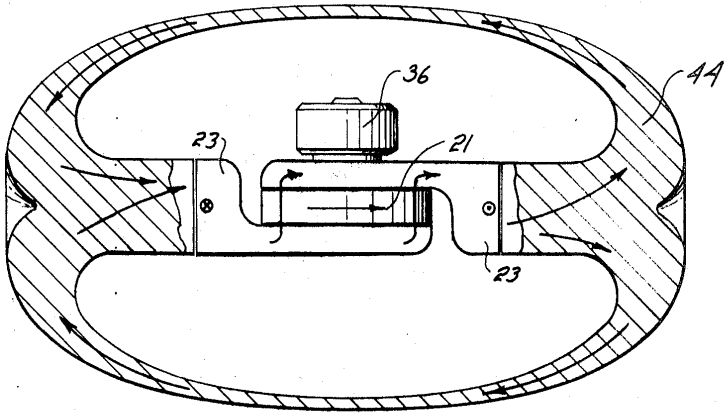

FIG. 7B

INVENTOR.
HENRY W. WALLACE
BY
Synnestvedt & Lechner
ATTORNEY

United States Patent Office 3,626,605
Patented Dec. 14, 1971

3,626,605

METHOD AND APPARATUS FOR GENERATING A SECONDARY GRAVITATIONAL FORCE FIELD

Henry Wm. Wallace, Ardmore, Pa.
(803 Cherry Lane, Laurel, Miss. 39440)

Filed Nov. 4, 1968, Ser. No. 773,051
Int. Cl. G09b 23/06
U.S. Cl. 35—19 10 Claims

ABSTRACT OF THE DISCLOSURE

Apparatus and method for generating a time variant non-electromagnetic force field due to the dynamic interaction of relatively moving bodies and for transforming such force fields into energy for doing useful work.

The method of generating such time variant force fields including the steps of juxtaposing in field series relationship a stationary member of spin nuclei material, and a member capable of assuming relative motion with respect to said stationary member also characterized by spin nuclei material; initiating relative motion by rotation of said one member with respect to the other, which rotational motion may occur both about an axis within the plane of said other member and about an axis perpendicular thereto; whereby the rotational motion of said one member about the axis perpendicular to the plane of said other member results in the dual interaction of the angular momentum property of said one member with inertial space and also with respect to the angular momentum property of said other member thereby resulting in a dynamic interaction field arising through gravitational coupling which dynamic interaction field is further characterized by its nonelectromagnetic nature and its mass-proximity and relative motion dependency; the rotation of said one member about the axis within the plane of said other member further resulting in an undulation of the dynamic interaction field within said other member which in turn gives rise to a secondary time-variant gravitational field in the surrounding space.

The present invention relates to an apparatus and method for generating a time-variant force field due to the relative motion of moving bodies; which force field exhibits itself in the form of an induced secondary gravitational force. As such, this invention constitutes a continuation-in-part of an application filed Nov. 4, 1968 by the same inventor, entitled Method and Apparatus for Generating a Dynamic Force Field and bearing Ser. No. 773,116.

In the practice of the present invention it has been found that when bodies composed of certain material are placed in relative motion with respect to one another there is generated an energy field therein not heretofore observed. This field is not electromagnetic in nature; being by theoretical prediction related to the gravitational coupling of relatively moving bodies.

The initial evidence indicates that this nonelectromagnetic field is generated as a result of the relative motion of bodies constituted of elements whose nuclei are characterized by half integral "spin" values, the spin of the nuclei being associated with the net angular momentum of the nucleons thereof. The nucleons in turn comprise the elemental particles of the nucleus; i.e., the neutrons and protons. For purposes of the present invention the field, generated by the relative motion of materials characterized by a half integral spin value, is referred to as a "kinemassic" force field.

It will be appreciated that relative motion occurs on various levels, i.e., there may be relative motion of discrete bodies as well as of the constituents thereof including, on a subatomic level, the nucleons of the nucleus. The kinemassic force field under consideration is a result of such relative motion, being a function of the dynamic interaction of two relatively moving bodies including the elemental particles thereof. The value of the kinemassic force field created, by reason of the dynamic interaction of the bodies experiencing relative motion, is the algebraic sum of the fields created by reason of the dynamic interaction of both elementary particles and of the discrete bodies.

For a closed system comprising only a stationary body, the kinemassic force, due to the dynamic interaction of the subatomic particles therein, is zero because of the random distribution of spin orientations of the respective particles. Polarization of the spin components so as to align a majority thereof in a preferred direction establishes a flux field aligned with the spin axes of the elementary particles. The present invention is in part comprised of an apparatus for polarizing its spin nuclei material, while additional means are provided to induce an alternating or undulating effect in the kinemassic field so generated.

Accordingly, a primary object of the present invention concerns the provision of means for generating a time-variant kinemassic field within a permeable field body due to the dynamic interaction of relatively moving bodies and the relative rotation of said generating means with respect to the permeable field body.

The kinemassic force field finds theoretical support in the laws of physics, being substantiated by the generalized theory of relativity. According to the general theory of relativity three exists not only a static gravitational field but also a dynamic component thereof due to the gravitational coupling of relatively moving bodies.

This theory proposes that two spinning bodies will exert force on each other. Heretofore the theoretical predictions have never been experimentally substantiated; however, as early as 1896, experiments were conducted in an effort to detect predicted centrifugal forces on stationary bodies placed near large, rapidly rotating masses. The results of these early experiments were inconclusive, and little else in the nature of this type of work is known to have been conducted.

It is therefore another object of the present invention to set forth an operative technique for generating a measurable time-variant force field due to the gravitational coupling of relatively moving bodies.

In carrying out the present invention, means are provided to enable the relative rotational motion of a first member with respect to a stationary member positioned in close proximity thereto; the construction of one embodiment of the first member being such as to enable portions thereof to assume rotational motion about an axis perpendicular to the plane of said stationary member. The effect of the rotation of said member about the axis perpendicular to the plane of the stationary member is to establish a kinemassic force field in the nature of that referred to in the aforementioned copending application of the same inventor. The rotation of said member about the axis lying within the plane of said stationary member results in an undulation of the dynamic interaction field within said field members which in turn induces a secondary time-variant gravitational field in the surrounding space.

Accordingly, another more specific object of the present invention concerns a method of generating a non-electromagnetic force field due to the dynamic interaction of relatively moving bodies and for utilizing such force field to further generate a secondary gravitational field.

The foregoing objects and features of novelty which characterize the present invention, as well as other objects

of the invention, are pointed out with particularity in the claims annexed to and forming a part of the present specification. For a better understanding of the invention, its advantages and specific objects allied with its use, reference should be made to the accompanying drawings and descriptive matter in which there is illustrated and described a preferred embodiment of the invention.

In the drawings:

FIG. 1 shows an overall view of equipment constructed in accordance with the principles of the present invention, including means to demonstrate the effect of a time-variant kinemassic force field;

FIG. 2 is an isolation schematic of apparatus components comprising the time-variant kinemassic field circuit of FIG. 1;

FIGS. 3, 3A, 3B, 4 and 5 show the details of construction of the generator and detector assemblies of FIGS. 1 and 2;

FIG. 6 represents measured changes in operating characteristics of the apparatus of FIGS. 1 and 2 demonstrating the time-variant nature of the kinemassic force field so produced; and

FIGS. 7, 7A and 7B are sectioned views of various embodiments of the present invention for demonstrating the time-variant nature of the kinemassic force field as used in establishing a secondary gravitational component.

Before getting into a detailed discussion of the apparatus and the steps involved in the practice of the present invention, it should be helpful to an understanding if the present invention of consideration is first given to certain defining characteristics thereof, many of which bear an analogous relationship to electromagnetic field theory.

A first feature is that the kinemassic field is vectorial in nature. The direction of the field vector is a function of the geometry in which the relative motion between mass particles takes place.

The second significant property of the kinemassic field relates the field strength to the nature of the material in the field. This property may be thought of as the kinemassic permeability by analogy to the concept of permeability in magnetic field theory. The field strength is apparently a function of the density of the spin nuclei material comprising the field circuit members. Whereas the permeability in magnetic field theory is a function of the density of unpaired electrons, the kinemassic permeability is a function of the density of spin nuclei and the measure of magnitude of their half integral spin values. As a consequence of this latter property, the field may be directed and confined by interposing into it denser portions of desired configuration. For example, the field may be in large measure confined to a closed loop of dense material starting and terminating adjacent a system wherein relative motion between masses is occurring.

A further property of the kinemassic force field relates field strength to the relative spacing between two masses in relative motion with respect to one another. Thus, the strength of the resultant field is a function of the proximity of the relatively moving bodies such that relative motion occurring between two masses which are closely adjacent will result in the generation of a field stronger than that created when the same two relatively moving bodies are spaced farther apart.

As mentioned above, a material consideration in generating the kinemassic force field concerns the use of spin nuclei material. By spin nuclei material is meant materials in nature which exhibit a nuclear external angular momentum. This includes both the intrinsic spin of the unpaired nucleon as well as that due to the orbital motion of these nucleons.

Since the dynamic interaction field arising through gravitational coupling is a function of both the mass and proximity of two relatively moving bodies, then the resultant force field is predictably maximized within the nucleus of an atom due to the relatively high densities of the nucleons plus the fact that the nucleons possess both intrinsic and orbital components of angular momentum. Such force fields may in fact account for a significant portion of the nuclear binding force found in all of nature.

It has been found that for certain materials, namely those characterized by a half integral spin value, the external component of angular momentum thereof will be accompanied by a force due to the dynamic interaction of the nucleons.

This is the so-called kinemassic force which on a submacroscopic basis exhibits itself as a field dipole moment aligned with the external angular momentum vector. These moments are of sufficient magnitude that they interact with adjacent, or near adjacent, spin nuclei field dipole moments of neighboring atoms.

This latter feature gives rise to a further analogy to electromagnetic field theory in that the interaction of adjacent spin nuclei field dipole moments gives rise to nuclear domain-like structures within matter containing a sufficient portion of spin nuclei material.

Although certain analogies exist between the kinemassic force field and electromagnetic field theory, it should be remembered that the kinemassic force is essentially non-responsive to or affected by electromagnetic force phenomena. This latter condition further substantiates the ability of the kinemassic field to penetrate through and extend outward beyond the ambient electromagnetic field established by the moving electrons in the atomic structure surrounding the respective spin nuclei.

As in electromagnetic field theory, in an unpolarized sample the external components of angular momentum of the nuclei to be subjected to a kinemassic force field are originally randomly oriented such that the material exhibits no residual kinemassic field of its own. However, establishing the necessary criteria for such a force field effects a polarization of the spin components of adjacent nuclei in a preferred direction thereby resulting in a force field which may be represented in terms of kinemassic field flux lines normal to the direction of spin.

The fact that spin nuclei material exhibits external kinemassic forces suggests that these forces should exhibit themselves on a macroscopic basis and thus be detectable, when arranged in a manner similar to that for demonstrating the Barnett effect when dealing with electromagnetic phenomena.

In the Barnett effect a long iron cylinder, when rotated at high speed about its longitudinal axis, was found to develop a measurable component of magnetization, the value of which was found to be proportional to the angular speed. The effect was attributed to the influence of the impressed rotation upon the revolving electronic systems due to the mass property of the unpaired electrons within the atoms.

In an apparatus constructed in accordance with the foregoing principles it was found that a rotating member such as a wheel composed of spin nuclei material exhibits a kinemassic force field. The interaction of the spin nuclei angular momentum with inertial space causes the spin nuclei axes of the respective nuclei of the material being spun to tend to reorient parallel with the axis of the rotating member. This results in the nuclear polarization of the spin nuclei material. With sufficient polarization, an appreciable field of summed dipole moments emanates from the wheel rim flange surfaces to form a secondary dynamic interaction with the dipole moments of spin nuclei contained within the facing surface of a stationary body positioned immediately adjacent the rotating member.

When the stationary body, composed of suitable spin nuclei material, is connected in spatial series with the rotating member, a circuitous form of kinemassic field

is created; the flux of which is primarily restricted to the field circuit.

If now means are provided to periodically reverse the direction of rotation of the wheel with respect to the facing surfaces of the stationary body positioned in immediate proximity thereto, then the resultant time-varying kinemassic field generates or induces an accompanying time-varying secondary gravitational field in the space immediately surrounding. That is to say, if the time-varying kinemassic field is made to undulate typically sinusoidally, there will be induced an accompanying undulating secondary gravitational field which is phase-related to the kinemassic field. In this repsect the induced secondary gravitational field is generated in a manner analogous to electromagnetic induction theory.

By properly configuring the undulating kinemassic field, the resultant secondary gravitational field may be essentially restrained to or confined within an enclosed space. Although numerous specific geometric configurations may be proposed, the necessary conditions are established in the preferred embodiment of the present invention by enclosing the kinemassic field generating apparatus, including the rotational members and at least a portion of the stationary member thereof, within an enclosure, the material portions of which obey the rules concerning kniemassic permeability.

The kinemassic field when so configured, will shield the enclosed space both with respect to the secondary gravitational field induced therein and with respect to the ambient gravitational field caused by the earth and other cosmic bodies, existing externally of the shielded space. The undulating kinemassic field, which gives rise to the enclosed secondary undulating gravitational field, is effective in reducing the quantity of flux lines within the space surrounded by the undulating kinemassic field contributed by the ambient gravitational field, thus reducing the mutual force of gravitational attraction acting between this structure and the earth or other cosmic bodies dependent upon their relative contribution to the local gravitational flux density.

It is well known that nature opposes heterogeneous field flux densities. If the normal local flux density contributed by the earth and the other cosmic bodies within the space occupied by and surrounded by the undulating kinemassic field permeable structure were added to by the forcibly enclosed flux of the induced secondary undulating gravitational field, this increased flux density would be in opposition to nature. Although the induced secondary undulating gravitational field would cause an undulating variation of the cosmic or primary gravitational field flux lines of force to penetrate within the kinemassic field permeable structure, if this undulation were sinusoidal, for example, the RMS or 0.707 value of peak reduction in mutual gravitational attraction would apply.

Means for increasing the relative magnitude of the undulating kinemassic field is effected by positioning a mass circuit within the induced secondary field space. The mass circuit in linking with the undulating kinemassic field circuit results in an increase in the kinemassic field and in the same sense effectively intensifies the primary gravitational field shielding. A partial parallel can be found in electromagnetic field theory, where it is known that a shorted secondary turn enhances iron saturation.

The mass circuit located in the induced secondary field space need not be comprised of material having a spin nuclei characteristic; rather, it is more important that this mass circuit have high mass density. A further desirable characteristic of this mass circuit is that it have a capability for mass flow with respect to the undulating kinemassic field structure. Mercury has the desired combination of properties and while other materials may be used, mercury is the most effective thus far known.

As indicated above, the effective result of generating a secondary undulating gravitational field within the space enclosed by the undulating kinemassic field is a relative reduction in apparent weight of the kinemassic field permeable structure, with respect to its apparent weight without such an undulating kinemassic field. The explanation of this phenomenon may be readily conceived as caused by the generation of a field force vector antiparallel in direction to the local gravitational field force vector. If the shielding is sufficiently effective to reduce the density of gravitational field flux lines within the shielded space to the equivalent of the ambient flux line density, there will be no net local distortion of the gravitational field flux line pattern in the space occupied by the kinemassic field permeable material or the space enclosed by the kinemassic field configuration. Without distortion of the local flux line pattern the two bodies cease to mutually attract and, in effect, become weightless, one with respect to the other.

Although similar in result, the technique for effecting the state of weightlessness in the present invention differs from conventional apparatus for achieving such a state of weightlessness. The latter, in general, utilize the force of radial acceleration to effectively "balance" the gravitational forces acting on a body.

The relative magnitude of the undulating kinemassic force field and the kinemassic permeability characterizing the associated structure are both influential in determining the effective shielding of the kinemassic field permeable structure. If the shielding is sufficiently effective so as to reduce the primary gravitational field flux line density within the enclosed space to less than that of the ambient, the distortion of the local gravitational field flux line pattern of reduced flux density would result in the antiparallel field force vector magnitudes exceeding that force of the kinemassic field body's initial weight, i.e., the effective weight of the kinemassic field permeable structure absent the generated undulating kinemassic field. This condition would effectively endow the kinemassic field structure with a negative weight characteristic. As a consequence, the two bodies, that is the kinemassic field body and the earth or other cosmic body, would experience relative motion separating one another along the local primary gravitational field flux lines unless acted upon by other forces.

The hardware required to generate and sustain such an undulating kinemassic field is in part comprised of components which continue to retain a "non-field-energized" weight during the period of field generation. Therefore, the ambient gravitational field flux line pattern within the structure will simultaneously experience zones of both reduced and increased densities. It is the average density of all the zones that determines the magnitude of the antiparallel field force vecor in its opposition to the ambient gravitational field force vector. Bodies located within the shielded space enclosed by the undulating kinemassic field will lose their weight with respect to the body earth in direct proportion to the reduction of ambient gravitaional field flux lines which are common to it and the body earth.

As a consequence of the above, the shielding which results in a reduction of mutual attraction between bodies screened by the shielding effected by the undulating kinemassic force field does not violate the principle of equivalence. Thus, two free bodies of different masses, located within the shielded space, will fall within this space toward or away from earth with equal accelerations. Also, the force of mutual gravitational attraction of two or more bodies located within the shielded space will be unaffected by the various degrees of shielding although their free-fall acceleration toward one another will be effected.

Having now further defined the substantiating theory giving rise to the kinemassic forces operative in the present invention, reference is now made to the aforementioned drawings depicting in general an apparatus embodying the defining characteristics outlined above.

From the foregoing discussion, it will be appreciated that both for the purpose of detecting the kinemassic field forces operative in the present invention, and for trans-

forming such forces into energy for doing useful work, several basic apparatus elements are necessary. First, apparatus is needed to enable masses to be placed in relative motion to one another; which relative motion may occur in two mutually orthogonal directions. In order to maximize field strength the apparatus should be capable of generating high velocities between the particles in relative motion. Furthermore, the apparatus should be configured so that the proximity of the particles which are in relative motion is maximized. The necessity of using relatively dense material comprising half integral spin nuclei for the field circuit portion of the apparatus has already been stressed. These and other features are discussed in greater detail below in explanation of the drawings depicting an implementation of the invention.

In considering the drawings, reference will first be made to the general arrangement of components shown in FIGS. 1 and 2. As viewed in FIG. 1, the equipment is mounted upon a stationary base comprising a horizontal structural element **11** which rests upon poured concrete, precast concrete pilings not shown, or other suitable structurally rigid material. It should be made clear at the outset, that the stationary base although not a critical element in its present form nevertheless serves an important function in the subject invention. Thus, the stationary base acts as a stabilized support member for mounting the equipment and, perhaps more significantly, the horizontal portion thereof is of such material that it tends to localize the kinemassic force field to the kinemassic force field generating apparatus proper. This latter feature is discussed in more detail below. The surface uniformity of the horizontal structural element **11** also facilitates the alignment of equipment components. In the reduction to practice embodiment of the present invention a layer of shock absorbing material, not shown, was interposed between the stationary base and the floor.

Shown mounted on the horizontal structural element **11** is the kinemassic force field generating apparatus indicated generally as **10**, the lower portion of which is referred to as the lower mass member **12**. The lower mass member **12** is not to be confusingly associated with the mass circuit mentioned above as being positioned in the space experiencing the secondary gravitational field. The nature and specific identity of the latter mentioned mass circuit will be more fully explained in connection with the explanation of FIG. 7.

An upper mass member **13** is positioned in mirrored relationship with respect to member **12** and separated somewhat to provide two air gaps therebetween. The lower and upper mass members **12** and **13** function as field circuit members in relationship to a generator **14** and a detector **15** positioned with respective one's of said two gaps. The spatial relationship of the generator **14**, the detector **15** and the mass members **12** and **13** is such as to form a kinemassic force field series circuit.

All of the material members of the field circuit are comprised of half integral spin material. For example, the major portion of the generator **14**, the detector **15**, as well as the upper and lower mass members **13** and **12** are formed of a particular brass alloy containing 89% copper of which both isotopes provide a three-halves proton spin, 10% zinc, and 1% lead as well as traces of tin and nickel. The zinc possesses one spin nuclei isotope which is 4.11% in abundance and likewise the lead also contains one spin nuclei isotope which is 22.6% in abundance. In order to gain an estimate of apparatus size, the upper mass member **13** has an overall length of 56 centimeters and a mass of 43 kilograms.

It will be seen that, by far, the constituents of the mass members are such as satify the criteria of half integral spin nuclei material for those apparatus parts associated with the field and the use of non-spin nuclei material for those parts where it is desired to inhibit the field. Accordingly, all support or structural members, such as the horizontal structural element **11**, consist of steel. The iron and carbon nuclei of these structural members are classed as no-spin nuclei and thus represent high relative reluctance to the kinemassic field. Supports **16** are provided to accommodate the suspension of the upper mass member **13**. The supports **16** are of steel the same as the horizontal support element **11**. The high relative reluctance of steel to the kinemassic field minimizes the field flux loss created in the field series circuit of mass members **12** and **13**, the generator **14** and the detector **15**. The loss of field strength is further minimized by employing high-reluctance isolation bridges at the point of contact between the lower and upper mass members **12** and **13**, and the structural support members **11** and **16**.

Shunt losses within the apparatus are in general minimized by employing the technique of minimum mass contact; the use of low field permeability material at the isolation bridges or structural connections; and avoiding bulk mass proximity of non-field generating components.

A number of techniques were devolped for optimizing the isolation bridge units including carboloy cones and spherical spacers. As is depicted more clearly in FIGS. 3, 4 and 5, the structural connection unit ultimately utilized consisted of a hardened 60° steel cone mounted within a set screw and bearing against a hardened steel platen. The contact diameter of the cone against the platen measured approximately 0.007 inch and was loaded within elastic limits. Adjustment is made by means of turning the set screw within a mated, threaded hole.

FIG. 2 is presented in rather diagrammatic form; however, the diagrammatic configuration emphasizes that it consists of a rotatable member corresponding to the generator **14** of FIG. 1 which is "sandwiched" between a pair of generally U-shaped members corresponding to the lower and upper mass members **12** and **13** of FIG. 1. The wheel of generator **14** is mounted for rotation about an axis lying in the plane of the drawing. The generator assembly is also shown as being mounted for rotation about an axis perpendicular to the plane of the drawing; however, the generator assembly may alternatively be oriented to rotate in the plane of the drawing. When member **14** is rotated rapidly with respect to the U-shaped members **12** and **13**, a kinemassic field is generated which is normal to the plane defined by the rotating member and within the plane of the drawing. As such, it may be represented in the drawing of FIG. 2, as taking a generally counter-clockwise direction with respect to the field series circuit members.

Referring once more to FIG. 1, it is seen that support for the generator unit **14** is provided by way of a support assembly **17**, also fabricated of steel components. The support assembly **17** is in turn clamped to the horizontal structural element **11** by way of bracket assemblies **18**.

The detector **15** is of similar configuration to the generator assembly **14**, the exception being that the detector assembly is mounted for limited rotation about the axis normal to the plane of the paper. The limited rotational capability is effected by a knife-edge mounting **19** more clearly discernible in FIGS. 3A and 3B. As will become more readily apparent from the discussion of the operation of the embodiment of FIG. 1 which follows, the knife-edge mounting enables a slow sinusoidal oscillation of the detector assembly about its knife-edge axis.

A pair of light-emitting and light-sensing elements **20***a* and **20***b* respectively are shown in FIG. 1 in operative relationship to the generator and detector assemblies **14** and **15**. The function of the light-generating and-sensing members **20***a* and **20***b* is to measure the rate of spin of the generator and detector wheels respectively. For this purpose every other quadrant on the rim surface is painted black. Accordingly, light directed at the rim of the wheel will be reflected by the unpainted quadrants into light-sensing cells associated with a rate-sensing circuit of conventional design. Since the rate-measuring circuit forms no part of the present invention it has not

been depicted in the actual drawing nor is it the subject of further explanation.

Compressed air or nitrogen is used to drive the generator and detector wheels. In this respect the compressed gas is directed against turbine buckets **21***b* cut in the rim of the wheel **21** of both the generator and detector assemblies and such buckets are more readily discernible in FIGS. 3, 4 and 5. The compressed gas is supplied to the generator and detector assemblies by way of air supply lines **28***a* and **28***b*.

FIGS. 3, 4 and 5 present details of the generator and detector assemblies of FIGS. 1 and 2. In particular, these figures disclose the relationship between a freely rotatable wheel **21**, a bearing frame **22**, and a pair of pole pieces **23**. The bearing frame **22** is of structural steel, and functions to spatially orient the three generator parts without shunting the generated field potential as well as to maintain this orientation against the force moment stresses of precession.

Positioning of the generator wheel **21** with respect to the cooperative faces of the pole pieces **23** is effected by way of the bearing frame upon which the generator wheel is mounted. In this respect the high-reluctance isolation bridges mentioned with respect to FIGS. 1 and 2 are herein shown as set screws **24** which are adjustably positioned to cooperate with hardened steel platens **25**. The set screws **24** are mounted on the pole pieces **23** and are adjustably positioned with respect to steel platens **25** cemented to the bearing frame **22** so as to facilitate the centering of the generator wheel **21** with respect to the interface surfaces **23***a* of the pole pieces **23**.

In the implementation of the present invention the air gap formed between the generator wheel rim flanges and the stationary pole pieces **23** was adjusted to a light-rub relationship when the wheel was slowly rotated; as such this separation was calculated to be 0.001 centimeter for a wheel spin rate of 28,000 revolutions per minute due to the resulting hoop tension. In the drawing of FIG. 3 the spacing between the pole pieces **23** and the generator wheel rim flange has been greatly exaggerated to indicate that in fact such a spacing does exist.

The generator wheel **21** utilized in the implementation of the present invention has a 8.60 centimeter diameter and an axial rim dimension of 1.88 centimeters. The rim flange surfaces **21***a* which are those field emanating areas closely adjacent the surfaces **23***a* of the pole pieces **23**, are each 29.6 square centimeters. The rim portion of the wheel has a volume of 55.7 cubic centimeters neglecting the rim turbine slots **21***b*.

The generator wheel **21** and an associated mounting shaft **26** are mounted on the bearing frame **22** by means of enclosed double sets of matched high speed bearings **27**.

Shaft members **30** carry suitable bearing members **31** for rotatably mounting the generator assembly will respect to a second axis. The support assembly **17** of FIG. 1 is partially represented in FIG. 3, and as noted above provides the mounting means for positioning the generator assembly **14** with respect to the lower and upper mass members **12** and **13**.

Reference is now made to FIGS. 3A and 3B which disclose a portion of the detector **15** of FIG. **1** including the knife-edge mounting **19** of FIG. 1. Adjusting means **32** are shown connected to the bearing frame **22***a* of the detector assembly **15** by means of a disc-like member **33**. Attached to the lower portion of the disc **33**, and depicted in the end view of the detector assembly of FIG. 3B, is shown a second adjusting member **34**, which in combination with equivalent members **32** and **34** mounted on the other end of the detector assembly, provide means for symmetrically aligning the detector assembly within the gap provided by the lower and upper mass members **12** and **13**. This further means that the knife-edge assembly is mounted so that the knife-edge axis is coincident with the geometric axis of the detector assembly. At the same time, the center of mass of the detector assembly is located below the geometric center of the detector assembly thereby providing a righting moment to the assembly due to the asymmetry of the mass center with respect to the knife-edge axis. The adjusting means **32** is shown as bearing against the support assembly **17**, thereby, in combination with the knife-edge mounting at either end of the detector assembly, providing an effective four point suspension for symmetrically positioning the detector assembly **15** within the end poles of the upper and lower mass members.

In FIGS. 1, 2 and 3 the detector assembly **15** is shown in three different positions. As will become apparent from the discussion of the operation of the subject system which follows, the facility to so reposition the detector assembly is necessary to demonstrate its operative capabilities. Accordingly, the bearing frame **22***a* is rotatably mounted with respect to the disc **33** by means of a bearing surface interfacing the frame **22***a* with the shaft **35**, the latter being affixed to the face of the disc **33**.

Proceeding now to an explanation of the operation of the embodiment of the invention thus far disclosed, it will be appreciated that in accordance with the theory of operation of the present apparatus when the generator wheel is made to spin at rates upwards of 10 to 20 thousand revolutions per minute, effective polarization of spin nuclei within the wheel structure gradually occurs. This polarization gradually gives rise to domain-like structures which continue to grow so as to extend their field dipole moment across the interface separating the rim **21** from the pole pieces **23**. Secondary dynamic interaction of gravitational coupling increases the field flux lines around the kinemassic force generating assembly, thus resulting in ever increasing total nuclear polarization of half integral spin nuclei.

The non-electromagnetic forces so generated within the subject apparatus are primarily channeled through the high-kinemassic permeability material defining the series field circuit of the apparatus. The fact that the high speed rotatable wheels of both the generator and detector assemblies are capable of being positioned in a series aiding or series opposing relationship, facilitates the determination of the effective influence of the energies generated in one on the other.

The detector, when carefully balanced on its knife-edges as shown in FIGS. 3A and 3B, exhibits an oscillation period of 11 seconds. When the wheels are energized a stiffening action is induced due to the reaction of the compressed gas impingement against the wheel bucket **21***b*, since the jet nozzle is fixed with respect to the apparatus base. This results in a reduction of the oscillation period to approximately 6 seconds. A light image not shown is directed against the mirrored face of the knife-edge **19** and reflected onto a calibrated wall screen. Measurements were taken with the apparatus so operative, which measurements established the oscillatory extremes of the reflected light beam for a pole-aligned relationship of the spinning generator and detector wheels. The results of one such set of measurements are recorded in FIG. 6. Therein, the *x*'s and dots represent extremes in deviation while the larger circles represent the mean thereof. The mean was in turn used to establish a null line to be compared with a similar null line derived from poles-opposed orientation of the generator and detector wheels. As a result, a displacement from equilibrium of approximately 13 arc minutes is shown.

In order to maximize the shift of the null line, the field circuit polar relationship of the generator and detector poles was reversed every 30 or 40 minutes from a relation of poles aligned, to poles opposed, to poles aligned. An average null shift of 26 arc minutes is indicated in FIG. 6. That the interaction between generator and detector was in fact accountable for the recorded results was demonstratively supported when the upper mass member was raised so as to create two air gaps one centimeter

in length respectively. Predictably, the disruption to the field circuit continuity resulted in the failure of the apparatus to register a shift in the null lines upon reversal of the poles.

Reference is now made to FIG. 7 which discloses an apparatus constructed in accordance with the principles of the present invention for generating a time-variant secondary gravitational field. This apparatus is a mere modification of the apparatus of FIGS. 1 and 2 wherein one detector assembly **15** has been removed and supplementary means are provided to mechanically implement the rotation of the generator assembly **14** about the axis perpendicular to the plane of the paper. These supplementary means are in the nature of an auxiliary motor **36** having a drive pulley **38** adapted to spin the generator assembly **14** about an axis normal to the plane of the drawing and coincident with that of the shaft **30**. The shaft **30** carries a pulley **40** which is driven by the motor and pulley assembly **36–38** by way of a conventional drive belt **42**. The wheel **21** of the generator assembly **14** is driven in the manner outlined above, namely by means of a source of compressed air not shown.

The supporting assembly depicted in FIG. 7 in partially sectioned form as member **44**, is in reality the equivalent of the series mass circuit of FIGS. 1 and 2, inverted or turned inside out so as to form a shield for the kinemassic field generating apparatus. Included as part of the supporting assembly is member **44A** which is provided to position the generator assembly **14** in the discontinuity formed in the mass circuit. The kinemassic field generated within the apparatus of FIG. 7 upon energization of the wheel **21** is directed in an enveloping fashion about its generator, being confined in general to the shell. The cross sectional thickness of the shell along equipotential lines must be equal in order to ensure a homogeneous field within the structure. If now the spin rate of the wheel **21** is made to vary, or if the generator assembly **14** is made to rotate about the axis defined by the shaft **30**, a time-variant secondary gravitational field is induced in the toroidal space **46**.

The secondary gravitational field undulates in a sinusoidal manner with the undulating kinemassic field confined to the series mass circuit. Since the kinemassic field in the dense mass circuit **44** has been restricted through permeability, into an enveloping shell about the generator **14**, it follows that the induced undulating secondary gravitational field is likewise restricted primarily to the enclosure **46** as the flux lines of both fields must interlink. In accordance with analogous electromagnetic field theory, the kinemassic field flux lines and the secondary gravitational field flux lines interlink in such manner that, as the kinemassic field alternates, these interlinking loops decay and build up in alternate vector directions in proper phase relation.

A hollow ring member **48** is positioned within the toroidal space **46** and supported thereby a series of fine steel wire spokes **50** secured to the ring and the outer portion of the inverted core housing **44** preferably along points of equipotential of the kinemassic field. Within the hollow ring **48** is contained a dense fluid such as mercury depicted in FIG. 7 generally as member **52**. Alternatively, the ring-fluid combination may take the form of a single solid mass. In the latter event the mass circuit would be supported on bearings facilitating its rotation about an axis common to the axis of the generator wheel **21** in order to permit mass flow or rotation of the mass circuit under the influence of the alternating secondary gravitational field. The shielding effected by the design considerations of the toroidal shell **44** with respect to the primary gravitational field reduces the inertial parameter of mass acceleration within the toroidal space **46** in proportion to the ambient gravitational shielding effect. With reduced inertia there will be an appreciable rotational flow displacement of the mass circuit **48–52** for each half cycle of the induced secondary gravitational field, thereby further strengthening the coupling effected between the effective field forces i.e., the primary gravitational field, the kinemassic field and the secondary gravitational field.

Consider now that the apparatus of FIG. 7 is energized such that the wheel **21** spins about its axis creating a uniformly distributed kinemassic field throughout the entire field circuit referred to generally as that encompassed within the inverted core housing **44**. As the generator assembly **14** is energized to rotate about the axis passing through shaft **30**, a uniformly distributed alternating kinemassic field is established throughout the field circuit.

The presence of the undulating kinemassic field produces a shielding effect within the inverted housing effectively restricting the induced secondary gravitational field while at the same time tending to shield or force out the flux due to the ambient gravitational field. As the spin rates of the wheel and the generator assembly about their respective axes are increased, there results a stronger undulating kinemassic force field of higher frequency. The spin rates may be so varied that a mean gravitatinal flux line density within the apparatus of FIG. 7 exists which is equivalent to the primary gravitational flux line density i.e., that due to the earth and other cosmic bodies. This condition establishes a state of weightlessness or zero gravitational force of attraction with respect to other masses such as earth, for that particular value of gravitational field gradient.

If the spin rates of the wheel and the generator assembly are further increased there results a "bowing-out" or spreading of the gravitational flux lines within the immediate proximity of the apparatus of FIG. 7 so as to result in a lesser local flux line density, thus resulting in the propulsion of the apparatus along the local gravitational field lines of force in a direction diametrically opposed to the local gravitational field force vector.

Because of the nature of the interaction of the primary gravitational field, the secondary gravitational field and the kinemassic field, the secondary gravitational field forces will continue to act upon the apparatus as it passes into lesser gravitational field gradients; however, it will do so with diminishing magnitudes until the local gravitational flux line density about the apparatus of FIG. 7 is no longer effectively diminished thereby. The energy required to propel a vehicle powered by an engine, such as is described above, is accounted for by way of the gravitational field potential energy gained by such a vehicle as it passes to areas of lesser gravitational field intensities. Energy input into this engine would appear as the product of torque and rotational values about the spin axes of both the wheel and the generator assembly, and especially about the latter axis which is responsible for alternating the kinemassic field and thereby generating the secondary gravitational component.

As was mentioned above in explanation of the embodiment of FIGS. 1 and 2, the wheel **21** and the generator assembly **14** are mounted so as to be rotatable in mutually orthogonal directions. It was further mentioned that such orthogonal rotation is not an absolute necessity, it being only necessary that relative motion be established between the wheel **21** and the stationary pole pieces **23**. The generator assembly is made to rotate thereby effecting an undulation in the kinemassic field flux in the associated mass circuit. FIG. 7A and 7B disclose a variation of the apparatus of FIG. 7 which satisfies the basic requirements outlined above while at the same time providing certain advantages not available in the aforementioned structure.

In this respect FIGS. 7A and 7B disclose an embodiment wherein the spin axis of the equivalent wheel structure **21** and the generator assembly **14** are concentric thereby eliminating precessional forces present in the embodiment of FIG. 7 due to the rotation of the respective members about the two mutually orthogonal axes. The absence of precessional forces permits a close tolerance to

be established between the cooperating faces of the wheel structure **21**, the pole pieces **23** and the mass circuit **44**.

The embodiment of FIGS. 7A and 7B is also to be preferred to that of FIG. 7 in that the design of the generator assembly of the former permits the energization of the independently rotatable members **21** and **23** by means of a single motor **36** differentially geared so as to effect the rotation of the wheel **21** at a speed far in excess of that of the generator assembly, and as indicated, in a reverse direction thereto.

Also indicated in the embodiment of FIGS. 7A and 7B is the orientation of the flux within the mass circuit, the latter being constructed preferredly of bismuth. It should be understood that the direction of flux within the mass circuit reverses with each reverseal in orientation of the equivalent pole pieces **23** due to the rotation of the generator assembly **14**.

It will be apparent from the foregoing description that there has been provided an apparatus for generating time-variant kinemassic forces due to the dynamic interaction of relatively moving bodies. Although in its disclosed application, the time-variant kinemassic force has been described in relation to its function of generating a secondary gravitational force, it should be readily apparent that other equally basic applications of these forces are contemplated.

Thus, in addition to providing an effective propulsion technique, the principles of the present invention may be utilized for the purpose of generating localized areas of gravitational shielding for housing medical patients for which such weight reductions would be beneficial. In addition, the principles may be adapted to laboratory use, as for example the analysis of the effects of a sustained reduction of "*g*" value upon astronauts and for specialized manufacturing techniques.

While in accordance with the provisions of the statutes there has been illustrated and described the best form of the invention known, it will be apparent to those skilled in the art that changes may be made in the apparatus described without departing from the spirit of the invention as set forth in the appended claims, and that in some cases, certain features of the invention may be used to advantage without a corresponding use of other features.

Having now described the invention, what is claimed as new and for which it is desired to secure Letters Patent is:

1. An apparatus for establishing a time-variant kinemassic force field resulting from the relative motion of moving bodies, comprising a generator assembly independent portions of which are mounted to assume relative rotational motion about at least a single axis located within said generator assembly, a mass circuit of dense material of discontinuous configuration, means for positioning said generator assembly within said mass circuit discontinuity, and means for initiating independent relative rotational motion of said generator assembly portions whereby an undulating kinemassic force field is established within said mass circuit.

2. Apparatus according to claim **1** further characterized in that said mass circuit and said relatively moving portions are comprised of spin nuclei material.

3. An apparatus according to claim **1** wherein said mass circuit is further characterized by first and second U-shaped members positioned in mirrored relationship with respect to each other and displaced somewhat so as to form two gaps therebetween, one of said gaps corresponding to said mass circuit discontinuity and being adapted to receive said generator assembly and the other said gap being adapted to receive a detector assembly.

4. Apparatus constructed in accordance with claim **1** wherein said mass circuit is further characterized by a shell of generally toroidal configuration having a cylindrical central portion within which is located said mass circuit discontinuity.

5. An apparatus constructed in accordance with claim **2** wherein said generator assembly mounted within said mass circuit discontinuity further comprises a rotatable member, a frame, means for mounting said rotatable member on said frame, pole pieces mounted on said frame on either side of said rotatable member, each pole piece presenting a generally circular face in close proximity to but spaced from a face of said rotatable member, means for effecting the rotation of said rotatable member about a first axis, and means for rotating said frame about a second axis oriented perpendicular to said first axis.

6. Apparatus constructed in accordance with claim **4** and further characterized by a dense mass ring mounted within the walls of said shell structure by mounting means establishing small area contact between said mass ring and said shell structure.

7. An apparatus constructed in accordance with claim **6** wherein said dense mass ring is further comprised of a hollow shell housing a liquid metal of suitable density.

8. Apparatus according to claim **6** wherein said dense mass ring has as its axis the axis of revolution defining the surface of said shell.

9. Apparatus constructed according to claim **3** wherein said shell is further characterized as being of equal cross sectional area normal to the kinemassic field lines of force.

10. A method of generating a time-variant kinemassic force field including the steps of:

juxtaposing in field series relationship a first member comprised of spin nuclei material of half integral spin value and a second member similarly constituted, portions of said first member being adapted to assume relative rotational motion about at least a single axis;

initiating the independent rotation of said first member about at least a single axis whereby an undulating kinemassic force field is established therein;

and so configuring said second member as to confine said undulating kinemassic force field thereto whereby a time-variant secondary gravitational force field is induced in the surrounding space.

No references cited

HARLAND S. SKOGQUIST, Primary Examiner

UNITED STATES PATENT OFFICE
CERTIFICATE OF CORRECTION

Patent No. 3,626,605 Dated December 14, 1971

Inventor(s) Henry W. Wallace

It is certified that error appears in the above-identified patent and that said Letters Patent are hereby corrected as shown below:

IN THE SPECIFICATION

Column 1, lines 19 to 42, should appear as a part of the "Abstract of the Disclosure".

Column 2, line 31, "three" should read --there--.

Column 3, line 31, "if" should read --of--.

Column 3, line 32, "of" should read --if--.

Column 7, line 51, "with" should read --within--.

Column 8, line 73, "rate-sensing" should read --rate-measuring-

Column 11, line 10, "one" should read --the--.

Column 13, line 15, "reverseal" should read --reversal--.

Signed and sealed this 5th day of September 1972.

(SEAL)
Attest:

EDWARD M.FLETCHER,JR.
Attesting Officer

ROBERT GOTTSCHALK
Commissioner of Patents

FORM PO-1050 (10-69)

USCOMM-DC 60376-P69
* U.S. GOVERNMENT PRINTING OFFICE : 1969 O—366-334

Research Papers

List of research papers:

1. "Outside the Box" Space and Terrestrial Transportation and Energy Technologies for the 21st Century
2. Some Observations on Avoiding Pitfalls in Developing Future Flight Systems
3. An Experimental Investigation of the Physical Effects in a Dynamic Magnetic System
4. Antimatter Production at a Potential Boundary
5. Gravity Modification by High-Temperature Superconductors
6. A Proposed Experimental Assessment of a Possible Propellantless Propulsion System
7. Research on Achieving Thrust by EM Inertia Manipulation
8. Specially Conditioned EM Radiation Research with Transmitting Toroid Antennas
9. An Experimental Investigation of the Physical Effects in a Dynamic Magnetic System
10. Rapid Spacetime Transport and Machian Mass Fluctuations: Theory and Experiment
11. Global Monopoles and the Bondi-Forward Mechanism
12. induction and Amplifications of Non-Newtonian Gravitational Fields
13. Towards the Control of Matter wth Gravity

14. Rapid Spacetime Transport and Machian Mass Fluctuations: Theory and Experiment

15. Fabrication of Large Bulk Ceramic Superconductor Disks for Gravity Modification Experiments and Performance of YBCO Disks Under e.m. Field Excitation

16. Large Scale Sakharov Condition

17. Breakthrough propulsion physics research program

18. Measurement of Repulsive Quantum Vacuum Forces

19. Search for Effects of Electric Potentials on Charged Particle Clocks

20. Tests of Mach's Principle with a Mechanical Oscillator

21. Superluminal but Causal Wave Propagation

22. Geometrodynamics, Inertia and the Quantum Vacuum

23. Interplay between gravity and quintessence: a set of new GR solutions

24. Classical analogous of quantum cosmological perfect fluid models

25. Gravity and antigravity in a brane world with metastable gravitons

26. The ac magnetic response in type-II superconductors

27. Exploration Of Anomalous Gravity Effects by Magnetized High-Tc Superconducting Oxides

28. The Other Side of Gravity and Geometry: Antigravity and Anticurvature

29. Impulse Gravity Generator Based on Charged Y Ba2Cu3O7y Superconductor with Composite Crystal

30. On the Mechanism for a Gravity Effect using Type II Superconductors - Glen A. Robertson

31. Negative Gravitational Mass in a Superfluid Bose-Einstein Condensate

32. Stan Deyo: Stream of Consciousness

33. Searching for the Gravific Photons

34. Gravitational Interaction between Photons and Unification of All the Fundamental Interactions

35. The Gravitational Spacecraft

36. Possibility of Control of the Gravitational Mass by means of Extra-Low Freqencies Radiation

37. Correlation Between Gravitational and Inertial Mass: Theory and Experimental Test

38. Gravity Control by Means of Modified Electromagnetic Radiation

39. Gravity Control produced by a Thermoionic Current through the Air at Very Low Pressure

40. Gravity Control by means of Electromagnetic Field through Gas or Plasma at Ultra-Low Pressure

41. The Gravitational Mass at the Superconducting State

42. A Gravitational Shielding Based on ZnS: Ag Phosphor

43. A Possibility of Gravity Control in Luminescent Materials

44. Repulsive Gravitational Force Field

45. Gravitational Holographic Teleportation

46. Bose-Einstein Condensate and Gravitational Shielding

47. Gravitational Shockwave Weapons

48. Negative Gravitational Mass in a Superfluid Bose-Einstein Condensate

49. Controlling the Gravitational Mass of a Metallic Lamina, and the Gravity Acceleration Above It.

50. Quantum Controller of Gravity

51. Quantum Gravitational Shielding

52. New Gravitational Effects from Rotating Masses

53. The Bipolar Linear Momentum Transported by the Electromagnetic Waves: Origin of the Gravitational Interaction

54. Gravity Control by Means of Electromagnetic Field Through Gas or Plasma at Ultra-Low Pressure

A02-14241

AIAA-2002-1131
"Outside the Box" Space and Terrestrial Transportation and Energy Technologies for the 21st Century

Theodore C. Loder, III
Institute for the Study of Earth, Oceans and Space
University of New Hampshire
Morse Hall
Durham, NH 03824

40th AIAA Aerospace Sciences Meeting and Exhibit
14-17 January 2002
Reno, Nevada

AIAA-2002-1131

"OUTSIDE THE BOX" SPACE AND TERRESTRIAL TRANSPORTATION AND ENERGY TECHNOLOGIES FOR THE 21ST CENTURY

Theodore C. Loder, III[1]
Institute for the Study of Earth, Oceans and Space
University of New Hampshire
Durham, NH 03824

Abstract

This paper reviews the development of antigravity research in the US and notes how research activity seemed to disappear by the mid 1950s. It then addresses recently reported scientific findings and witness testimonies - that show us that this research and technology is alive and well and very advanced. The revelations of findings in this area will alter dramatically our 20th century view of physics and technology and must be considered in planning for both energy and transportation needs in the 21st century.

Historical Background

Townsend Brown's Technology of Electrogravitics[1]

In the mid 1920's Townsend Brown[2] discovered that electric charge and gravitational mass are coupled. He found that when he charged a capacitor to a high voltage, it had a tendency to move toward its positive pole. This became known as the Biefeld-Brown effect. His findings were opposed by conventional minded physicists of his time.

The Pearl Harbor Demonstration. Around 1953, Brown conducted a demonstration for military top brass. He flew a pair of 3-foot diameter discs around a 50-foot course tethered to a central pole. Energized with 150,000 volts and emitting ions from their leading edge, they attained speeds of several hundred miles per hour. The subject was thereafter classified.

Project Winterhaven. Brown submitted a proposal to the Pentagon for the development of a Mach 3 disc shaped electrogravitic fighter craft. Drawings of its basic design are shown in one of his patents. They are essentially large-scale versions of his tethered test discs.

Review of Issues From the 1950s

Once Brown's findings became well known, some scientists began to openly speak about the flying technology of UFOs, which had been observed extensively since the 1940s. None other than Professor Hermann Oberth, considered by some to be one of the fathers of the space age, who later worked in the US with Wernher von Braun, the Army Ballistic Missile Agency and NASA, stated the following in 1954:[3]

"It is my thesis that flying saucers are real and that they are space ships from another solar system." Perhaps of more interest to our present discussion on propulsion, he then stated that: "They are flying by the means of artificial fields of gravity... They produce high-tension electric charges in order to push the air out of their paths, so it does not start glowing, and strong magnetic fields to influence the ionized air at higher altitudes. First, this would explain their luminosity... Secondly, it would explain the noiselessness of UFO flight..." We now know that he was fundamentally correct in his assessment.

In 1956, a British research company, Aviation Studies (International) Ltd. published a classified report on Electrogravitics Systems examining various aspects of gravity control. They summarized the pioneering work of Townsend Brown and then described the use of electrogravitic thrust as follows:

"The essence of electrogravitics thrust is the use of a very strong positive charge on one side of the vehicle and a negative on the other. The core of the motor is a condenser and the ability of the condenser to hold its charge (the K-number) is the yardstick of performance. With air as 1, current dielectrical materials can yield 6

and use of barium aluminate can raise this considerably, barium titanium oxide (a baked ceramic) can offer 6,000 and there is a promise of 30,000, which would be sufficient for supersonic speed."[4]

In one of their conclusions, based on Brown's work, they suggested that: "Electrostatic energy sufficient to produce a Mach 3 fighter is possible with megavolt energies and a k of over 10,000."[5]

In spite of Brown's solid research, they later stated that, "One of the difficulties in 1954 and 1955 was to get aviation to take electrogravitics seriously. The name alone was enough to put people off."[6] It seems that is as true today as it was in the 1950s.

A report by another British company, Gravity Rand, Ltd. in 1956, agrees with this assessment and states: "To assert electrogravitics is nonsense is as unreal as to say it is practically extant. Management should be careful of men in their employ with a closed mind or even partially closed mind on the subject."[7]

However, a trade press magazine, The Aviation Report, made a numerous references to antigravity projects and listed many of the companies pursuing research in this area. Quotes from The Aviation Report listed in the Aviation Studies (International) Ltd. report[8] are suggestive of what was going on behind the scenes.

In 1954 they predicted that: "... progress has been slow. But indications are now that the Pentagon is ready to sponsor a range of devices to help further knowledge."... "Tentative targets now being set anticipate that the first disk should be complete before 1960 and it would take the whole of the 'sixties to develop it properly, even though some combat things might be available ten years from now." (Aviation Report 12 October 1954)[9]

During this time period many of the major defense and technology companies were cited as either having research projects or activities in this new field. For example: "Companies studying the implications of gravitics are said, in a new statement, to include Glenn Martin, Convair, Sperry-Rand, and Sikorsky, Bell, Lear Inc. and Clark Electronics. Other companies who have previously evinced interest include Lockheed, Douglas and Hiller." (Aviation Report 9 December 1955)[10].

Others of these reports mention: AT&T, General Electric, as well as Curtiss-Wright, Boeing and North American as having groups studying electrogravitics.

During the same time period, the Gravity Rand report notes that: "Already companies are specializing in evolution of particular components of an electogravitics disk."[11]

However, in the area of predictions, the Aviation Report stated the following based on an extrapolation of technology development: "Thus this century will be divided into two parts – almost to the day. The first half belonged to the Wright Brothers who foresaw nearly all the basic issues in which gravity was the bitter foe. In part of the second half, gravity will be the great provider. Electrical energy, rather irrelevant for propulsion in the first half becomes a kind of catalyst to motion in the second half of the century." (Aviation Report 7 September 1954).[12]

Looking back it is easy to say that they missed the mark. Did they really miss it by a half a century? Reading through these reports it is quite obvious that there was much interest in antigravity among a number of very high profile companies, as well as in the Department of Defense. What happened to this interest and why was it all downplayed during the following four plus decades? After all, T. Brown had shown that there is a demonstrable connection between high voltage fields and gravity. Why has it taken until the 1990s for more than just a few scientists to look at these results and publish on them in the open literature? A review of recent statements by former military personnel and civilians connected to covert projects begins to shed light on research activity in these areas over the last half century. And it appears that there had been significant breakthroughs during this time period, well shielded from both the scientific and public eye.

Recent Scientific Developments

In this section we consider developments in the antigravity field since the late 1980s and why the confluence of scientific findings and the testimony of witnesses associated with the military and covert groups indicates that a gravity solution with technological implications has been found.

Although general relativity has not been able to explain Brown's electrogravitic observations, or any other antigravity phenomenon, the recent physics methodology of quantum electrodynamics (QED), appears to offer the theoretical framework to explain electrogravitic coupling. Recent papers by members of the Institute for Advanced Study Alpha Foundation are putting a solid theoretical foundation onto the antigravity effects within the theory of electrodynamics and include papers by Evans[13] and Anastasozki et al.[14]

Earlier in a breakthrough paper in 1994, Alcubierre showed that superluminal space travel is, in principle, physically possible and will not violate the tenants of the theory of relativity[15]. Puthoff[16] later analyzed these findings in light of the present SETI (Search for Extraterrestrial Intelligence) paradigms that insist that we could not be visited by extraterrestrial civilizations because of the speed-of-light limitations dictated by the general relativity theory. He suggests that superluminal travel is indeed possible. This leads to reduced-time interstellar travel and the possibility of extraterrestrial visitation, which our limited understanding of physics and scientific arrogance has "forbidden" in some sectors for most of the 20th century.

The second aspect of these physics findings deals with the zero point or vacuum state energy shown by the Casimir effect, which predicts that two metal plates close together attract each other due to imbalance in the quantum fluctuations. The implications of this zero point or vacuum state energy are tremendous and are described in several papers by Puthoff[17] starting during the late 1980s. A detailed bibliography on this and similar topics is available on the WWWeb.[18] Bearden[19] and colleagues have also written extensively on the theoretical physics of zero point energy and additionally have described various technological means of extracting this energy (for example see the recent paper by Anastasozki et al.[20]). A theoretical book on zero point energy by Bearden will soon be available.[21] There is significant evidence that scientists since Tesla have known about this energy, but that its existence and potential use has been discouraged and indeed suppressed over the past half century or more. [22].

The coupling of the electrogravitic phenomena observations and the zero point energy findings are leading to a new understanding of both the nature of matter and of gravity. This is just now being discussed in scientific journals (though some evidence suggests that it has been understood for decades within the black project covert community). The question that is being addressed is: what keeps the universe running? Or more specifically, where do electrons get their energy to keep spinning around atoms? As electrons change state they absorb or release energy, and where does it come from? The simplistic answer is that it is coming from the vacuum state. Puthoff[23] describes the process as follows: "I discovered that you can consider the electron as continually radiating away its energy as predicted by classical theory, but SIMULTANEOUSLY ABSORBING a COMPENSATING AMOUNT of energy from the ever-present sea of zero-point energy in which the atom is immersed. An equilibrium between these two processes leads to the correct values for the parameters that define the lowest energy, or ground-state orbit (see "Why atoms don't collapse," NEW SCIENTIST, July 1987). Thus there is a DYNAMIC EQUILIBRIUM in which the zero-point energy stabilizes the electron in a set ground-state orbit. It seems that the very stability of matter itself appears to depend on an underlying sea of electromagnetic zero-point energy."

Furthermore, it appears that it is the spinning of electrons that provides inertia and mass to atoms. These theories, linking electron spin, zero point energy, mass, and inertia have been presented in a number of recent papers, such as those by Haisch[24] and colleagues and provide us with a possible explanation of the Biefield-Brown effect. It appears that an intense voltage field creates an electromagnetic barrier that blocks the atomic structure of an atom from interacting with the zero point field. This slows down the electrons, reducing their gyroscopic effect, and thus reducing atomic mass and inertia, making them easier to move around.

Evidence of Extensive Antigravity Technology

The B-2 Advanced Technology Bomber

In 1993, LaViolette wrote a paper[25] discussing the B-2 bomber and speculating on its probable antigravity propulsion system, based on a solid understanding of electrogravitics,[26] the aircraft's design and the materials used in its manufacture. It appears that the craft is using a sophisticated form of the antigravity principles first described by T. Brown. Support for this thesis came from the Aviation Week and Space Technology (March 9, 1992), which reported that the B-2 bomber electrostatically charges its leading edge and its exhaust stream. Their information had come from a small group of former black project research scientists and engineers suggesting the B-2 utilizes antigravity technology. This information was supported by Bob Oechsler, an ex-NASA mission specialist who had publicly made a similar claim in 1990. These findings support the contention that there have been major developments in the area of antigravity propulsion which are presently being applied in advanced aircraft.

LaViolette later states the obvious that "the commercial airline industry could dramatically benefit with this technology which would not only substantially increase the miles per gallon fuel efficiency of jet airliners, but would also permit high-speed flight that would dramatically cut flight time."[27]

The Disclosure Project Witnesses

On May 9, 2001 a private organization, "The Disclosure Project"[28] held a press conference at the National Press Club in Washington DC. They presented nearly two dozen witnesses including retired Army, Navy and Air Force personnel, a top FAA official, members of various intelligence organizations including the CIA and NRO, and industry personnel, all of whom who had witnessed UFO events or had inside knowledge of government or industrial activities in this area. They also produced a briefing document[29] for members of the press and Congress and a book[30] which includes the testimony of nearly 70 such witnesses from a pool of hundreds. Although they all spoke of the reality of the UFO phenomena, many also spoke of covert projects dealing with antigravity, zero point energy technologies and development of alien reproduction vehicles (ARVs) by US black project and covert interests. The following excerpted quotes from these witnesses support the above contentions.

Dan Morris[31] is a retired Air Force career Master Sergeant who was involved in the extraterrestrial

projects for many years. After leaving the Air Force, he was recruited into the super-secret National Reconnaissance Organization (NRO), during which time he worked specifically on extraterrestrial-connected operations. He had a cosmic top-secret clearance (38 levels above top secret) which, he states, no U.S. president, to his knowledge, has ever held.

"UFOs are both extraterrestrial and man made. Well, the guys that were doing the UFOs, they weren't sleeping, and Townsend Brown was one of our guys who was almost up with the Germans. So we had a problem. We had to keep Townsend Brown - what he was doing on anti-gravity electromagnetic propulsion secret." He then describes a type of zero point energy device.

"Well, if you have one of these units that's about sixteen inches long and about eight inches high and about ten inches wide, then you don't need to plug into the local electric company. These devices burn nothing. No pollution. It never wears out, because there are no moving parts. What moves are electrons, in the gravity field, in the electronic field, and they turn in opposite directions, okay?"

"Dr. B."[32] (name withheld since he still works in this area) is a scientist and engineer who has worked on top-secret projects almost all his life. Over the years he has directly worked on or had involvement with such projects involving anti-gravity, chemical warfare, secure telemetry and communications, extremely high-energy space based laser systems, and electromagnetic pulse technology.

"Anti-gravity. As a matter of fact, I used to go out to the Hughes in Malibu. They had a big think tank up there. Big anti-gravity projects; I used to talk to them out there. I'd give them ideas, because they bought all my equipment. But the American public will never, never hear about that." . . . "This flying disc has a little plutonium reactor in it, which creates electricity, which drives these anti-gravity plates. We also have the next level of propulsion, it is called virtual field, which are called hydrodynamic waves..."

Captain Bill Uhouse[33] served 10 years in the Marine Corps as a fighter pilot, and four years with the Air Force at Wright-Patterson AFB as a civilian doing flight-testing of exotic experimental aircraft. Later, for the next 30 years, he worked for defense contractors as an engineer of antigravity propulsion systems: on flight simulators for exotic aircraft - and on actual flying discs.

"I don't think any flying disc simulators went into operation until the early 1960s - around 1962 or 1963. The reason why I am saying this is because the simulator wasn't actually functional until around 1958. The simulator that they used was for the extraterrestrial craft they had, which is a 30-meter one that crashed in Kingman, Arizona, back in 1953 or 1952."

"We operated it with six large capacitors that were charged with a million volts each, so there were six million volts in those capacitors." . . . "There weren't any windows. The only way we had any visibility at all was done with cameras or video-type devices." . . ."Over the last 40 years or so, not counting the simulators - I'm talking about actual craft - there are probably two or three-dozen, and various sizes that we built."

"A.H."[34] formally of Boeing Aerospace, is a person who has gained significant information from inside the UFO extraterrestrial groups within our government, military, and civilian companies. He has friends at the NSA, CIA, NASA, JPL, ONI, NRO, Area 51, the Air Force, Northrup, Boeing, and others.

"Most of the craft operate on antigravity and electrogravitic propulsion. We are just about at the conclusion state right now regarding antigravity. I would give it maybe about 15 years and we will have cars that will levitate using this type of technology. We're doing it up at Area 51 right now. That's some of the stuff that my buddy worked on up at Area 51 with Northrup, who lives now in Pahrump, Nevada. We're flying anti-gravity vehicles up there and in Utah right now..."

Lieutenant Colonel Williams[35] entered the Air Force in 1964 and became a rescue helicopter pilot in Vietnam. He has an electrical engineering degree and was in charge of all the construction projects for the Military Air Command. During his time in the military he knew that there was a facility inside of Norton Air Force Base in California that no one was to know about.

"There was one facility at Norton Air Force Base that was close hold - not even the wing commander there could know what was going on. During that time period it was always rumored by the pilots that that was a cover for in fact the location of one UFO craft."

Note that all he knew was of the rumor, however, it is confirmed by the next testimony, which also confirms some of the comments made by Captain Uhouse.

Mark McCandlish[36] is an accomplished aerospace illustrator and has worked for many of the top aerospace corporations in the United States. A colleague, with whom he studied, has been inside a facility at Norton Air Force Base, where he witnessed alien reproduction vehicles, or ARVs, that were fully operational and hovering. He states that the US not only has operational antigravity propulsion devices, but we have had them for many, many years, and they have been developed through the study, in part, of extraterrestrial vehicles over the past fifty years.

A close friend, Brad Sorensen, told him of visiting The Big Hangar, during an air show at Norton Air Force Base on November 12, 1988 and how he had

seen flying saucers in this hangar. "There were three flying saucers floating off the floor—no cables suspended from the ceiling holding them up, no landing gear underneath—just floating, hovering above the floor. He said that the smallest was somewhat bell-shaped. They were all identical in shape and proportion, except that there were three different sizes. They had little exhibits with a videotape running, showing the smallest of the three vehicles sitting out in the desert, presumably over a dry lakebed, some place like Area 51. It showed this vehicle making three little quick, hopping motions; then [it] accelerated straight up and out of sight, completely disappearing from view in just a couple of seconds—no sound, no sonic boom—nothing."

"Well, this craft was what they called the Alien Reproduction Vehicle; it was also nicknamed the Flux Liner. This antigravity propulsion system—this flying saucer—was one of three that were in this hangar at Norton Air Force Base. [Its] synthetic vision system [used] the same kind of technology as the gun slaving system they have in the Apache helicopter: if [the pilot] wants to look behind him, he can pick a view in that direction, and the cameras slew in pairs. [The pilot] has a little screen in front of his helmet, and it gives him an alternating view. He [also] has a little set of glasses that he wears—in fact, you can actually buy a 3-D viewing system for your video camera now that does this same thing—so when he looks around, he has a perfect 3-D view of the outside, but no windows. So, why do they have no windows? Well, it's probably because the voltages that we're talking about [being] used in this system were probably something between, say, half a million and a million volts of electricity." Brad Sorensen stated that at the ARV display, "a three star general said that these vehicles were capable of doing light speed or better."

All of these witness testimonies do not prove the existence of a successful US covert program in antigravity technologies. Only the demonstration of such craft coupled with the accompanying government and technical specification documents would 'prove' this. However, these testimonies coupled with information from other substantial sources such as Nick Cook's new book mentioned below, strongly supports this contention.

The Hunt for Zero Point[37]

Although this very recent book (August, 2001) is not yet available in the US, it contains some of the strongest evidence yet for major efforts and success in the field of antigravity technology. The author, Nick Cook, who for the past 15 years has been the Aviation Editor and Aerospace Consultant for Jane's Defense Weekly, spent the last 10 years collecting information for the book. This included archival research on Nazi Germany's antigravity technology and interviews with top officials at NASA, the Pentagon and secret defense installations. He shows that America has cracked the gravity code and classified the information at the highest security levels. Because antigravity and its allied zero point energy technologies potentially offer the world a future of unlimited, non-polluting energy it has been suppressed because of the "huge economic threat". His findings support those reported by many of the Disclosure Project witnesses cited above.

Antigravity Technology Demonstrations

Although T. Brown reported many of his findings nearly a half century ago, other experimenters have just recently begun to reproduce his work and report it in the open literature and on the WWWeb. For example, Davenport[38] published the results of his work in 1995 supporting the findings of T. Brown. More recently, Transdimensional Technologies[39] in the USA and J. Naudin[40] labs in France have posted on the WWWeb: diagrams, web videos, and data on their versions of antigravity "Lifters" based on an extension of Brown's work. It is a sad commentary on this whole area of research to see that public science is requiring us to demonstrate principles that were demonstrated nearly fifty years ago.

There have also been a number of other demonstrations of "antigravity" phenomena by researchers throughout the world. This includes the work of Brazilian physics professor, Fran De Aquino, and such devices as: the Searl Electrogravity Disc, the Podkletnov Gravity Shield and Project Greenglow, the Zinsser Kineto-baric Field Propulsion and the Woodward Field Thrust Experiments on Piezoelectrics. All of these are described in more detail by Greer and Loder.[41]

Implications of This Research

• Antigravity and zero point energy research and their applications are finally being addressed by some of the open scientific community. This means there will have to be a rewriting of textbooks in this area so our new generation of students can apply this "new knowledge." Its application will lead to major breakthroughs in transportation technologies both earthside and in outer space. The implications are that we have the potential for human exploration of our solar system and beyond, if we have the will, within our lifetimes. It also means that the majority of 20th century space technology will be obsolete and in fact may already be so.

• The zero point or vacuum state energy source is seen as a totally non-polluting energy source, which has the potential to replace all the fossil fuels on this planet. It also will provide the energy needed for long range space flights. This means that fuel cells and solar cells

in common use today for space flight energy applications will only be needed until we transition to these new energy technologies.

• Based on an analysis of trends in antigravity research over the last half-century and the information provided by numerous witnesses, it appears that there is both good and bad news. The good news is that it appears that we (at least covert projects) have already developed the theories of antigravity, and additionally have developed working spacecraft based on these principles. The bad news is that these technologies have been developed for at least several decades, at the public's expense and that human kind has been deprived of these technologies, while continuing to waste energy using less efficient and pollution enhancing technologies.

Supporting this contention is the following quote from Ben Rich, former head of the Lockheed Skunkworks. Just prior to his death, he stated to a small group after a lecture that: "We already have the means to travel among the stars, but these technologies are locked up in black projects and it would take an act of God to ever get them out to benefit humanity..." He further went on to say that, 'anything you can imagine we already know how to do.' Strong words from a knowledgeable deep insider and words that support what a number of the witnesses stated as well.

• As the reality of this knowledge begins to be understood, there will be an outcry among space scientists not on the inside for release of these technologies to allow all of us to explore space. There will be major changes in the way that NASA does its business, though predicting these changes is difficult.

• Not only has space exploration in the public sector suffered, but our planet's environment has suffered as well. Thus as this knowledge begins to sink in there will be an outcry among all concerned citizens on this planet for release of these technologies to allow all of us to reduce and ultimately eliminate global warming and environmental pollution that so threatens our way of life. These technologies will not only affect space travel technologies, but will also have a profound effect on transportation and energy production on the earth's surface.

• In conclusion, we might consider the observation made by Halton Arp[42]:

"We are certainly not at the end of science.
Most probably we are just at the beginning!"

Acknowledgements

I thank the following people for many discussions while preparing and writing this paper including: S. Greer, A. Craddock, T. Bearden, P. LaViolette, M. McCandlish, D. Hamilton, T. Valone, E. Mallove, T. Loder, C. Loder, S. Patel and many of the courageous Disclosure Project witnesses.

References Cited

[1] Quoted from: LaViolette, P. A. 2000. Moving Beyond the First Law and Advanced Field Propulsion Technologies. In T. Loder (ed.), "Outside-the-Box" Technologies, Their Critical Role Concerning Environmental Trends, and the Unnecessary Energy Crisis. Report prepared for The U.S. Senate Environment and Public Works Comm. www.senate.gov/~epw/loder.htm.

[2] Brown, T. T. 1929. How I control gravity. Science and Information Magazine, Aug. 1929. Reprinted in Psychic Observer 37 (1): 66-67.

[3] Oberth, Hermann: "Flying Saucers Come from a Distant World," *The American Weekly*, October 24, 1954.

[4] Aviation Studies (International) Ltd. 1956. Electrogravitics Systems: An examination of electrostatic motion, dynamic counterbary and barycentric control. p. 14. In Valone, T. (ed.), 1994. Electrogravitics Systems: Reports on a new propulsion methodology. Integrity Research Institute, Washington, DC 20005.

[5] Ibid. p. 27.

[6] Ibid. p. 19.

[7] Gravity Rand Ltd. 1956. The Gravitics Situation. p. 54. In Valone, T. (ed.), 1994. Electrogravitics Systems: Reports on a new propulsion methodology. Integrity Research Institute, Washington, DC 20005.

[8] Aviation Studies (International) Ltd. 1956. Electrogravitics Systems: An examination of electrostatic motion, dynamic counterbary and barycentric control. p. 11. In Valone, T. (ed.), 1994. Electrogravitics Systems: Reports on a new propulsion methodology. Integrity Research Institute, Washington, DC 20005.

[9] Ibid. p. 34.

[10] Ibid p. 41.

[11] Gravity Rand Ltd. 1956. The Gravitics Situation. p. 47. In Valone, T. (ed.), 1994. Electrogravitics Systems: Reports on a new propulsion methodology. Integrity Research Institute, Washington, DC 20005.

[12] Aviation Studies (International) Ltd. 1956. Electrogravitics Systems: An examination of electrostatic motion, dynamic counterbary and barycentric control. p. 32. In Valone, T. (ed.), 1994. Electrogravitics Systems: Reports on a new propulsion methodology. Integrity Research Institute, Washington, DC 20005.

[13] Evans, M. W. 2002. The link between the Sachs and O(3) theories of electrodynamics. In Evans, M.W. (ed.), Modern Nonlinear Physics, Pun 2. 2nd ed., Advances in Chemical Physics 19:469-494.

[14] Anastasovski, P.K., T.E. Bearden, C. Ciubotariu, W.T. Coffey, L.B. Crowell, G.J. Evans, M.W. Evans, R. Flower, A. Labounsky, B. Lehnert, M. Mészáros, P.R. Molnár, S. Roy, and J.-P. Vigier. (In Press). Anti

gravity effects in the Sachs theory of electrodynamics Foundations of Physics Letters.

[15] Alcubierre, M. 1994. The Warp Drive: Hyper-fast travel within general relativity. Classical and Quantum Gravity, 11, L73.

[16] Puthoff, H. E. 1996. SETI, The Velocity-of-Light Limitation, and the Alcubierre Warp Drive: An Integrating Overview, Physics Essays 9:156.

[17] Puthoff, H. 1989. Gravity as a Zero-Point Fluctuation Force." Phys. Rev A., 39(5):2333-2342.

Puthoff, H. 1989. Source of Electromagnetic Zero-Point Energy." Phys. Rev A, 40(9):4597-4862.

[18] www.motionsciences.com

[19] See the Tom Bearden web site for an extensive listing and copies of his papers at: www.cheniere.org.

[20] Anastasovski, P.K., T.E. Bearden, C. Ciubotariu, W.T. Coffey, L.B. Crowell, G.J. Evans, M.W. Evans, R. Flower, A. Labounsky, B. Lehnert, M. Mészáros, P.R. Molnár, J.K. Moscicki, S. Roy, and J.P. Vigier. 2001. Explanation of the motionless electromagnetic generator with 0(3) Electrodynamics. Foundations of Physics Letters, 14(1):87-93.

[21] Bearden, T. 2002. Energy from the Vacuum: Concepts and Principles. World Scientific (In Press).

[22] Valone, T. 2000. The Right Time to Develop Future Energy Technologies. in T. Loder (ed.). "Outside-the-Box" Technologies, Their Critical Role Concerning Environmental Trends, and the Unnecessary Energy Crisis. Report prepared for The U.S. Senate Environment and Public Works Comm. www.senate.gov/~epw/loder.htm.

[23] Puthoff, H. 1990. Everything for Nothing. New Scientist, 28 July 1990, pp. 52-55.

[24] Haisch, B., Rueda, A. and Puthoff, H. 1994. Beyond E =mc2 ; A First Glimpse of a Postmodern Physics, in which Mass, Inertia and Gravity Arise from Underlying Electromagnetic Processes. The Sciences, 34:26.

Haisch, B., Rueda, A., and Puthoff, H. 1997. Physics of the Zero-Point Field: Implications for Inertia, Gravitation and Mass. Speculations in Science and Technology, 20:99.

Haisch, B. and Rueda, A. 1998. An Electromagnetic Basis for Inertia and Gravitation: What Are the Implications for 21st Century Physics and Technology? in El-Genk, M. S. (ed.), Space Technology and Applications International Forum-1998, DOE CNF-980103, CP420, p. 1443.

Haisch, B. and Rueda, A. 1999. The Zero-Point Field and the NASA Challenge to Create the Space Drive. Proc. NASA Breakthrough Propulsion Physics Workshop, NASA/CP-1999-208694, p. 55.

[25] LaViolette, P. 1993. The U.S. Antigravity Squadron. p. 82-101. In Valone, T. (ed.), 1994. Electrogravitics Systems: Reports on a new propulsion methodology. Integrity Research Institute, Washington, DC 20005.p.82-101.

[26] LaViolette, P. A. 1992. Electrogravitics: Back to the future. Electric Spacecraft, Issue 4, pp. 23-28.

LaViolette, P. A. 1993. A theory of electrogravitics. Electric Spacecraft, Issue 8, pp. 33-36

[27] LaViolette, P. A. 2000. Moving Beyond the First Law and Advanced Field Propulsion Technologies. in T. Loder (ed.). "Outside-the-Box" Technologies, Their Critical Role Concerning Environmental Trends, and the Unnecessary Energy Crisis. Report prepared for The U.S. Senate Environment and Public Works Comm. www.senate.gov/~epw/loder.htm.

[28] Information available at: www.disclosureproject.org.

[29] Greer, S.M. and T.C. Loder III. 2001. Disclosure Project Briefing Document, 492 pp. Available on CD from: The Disclosure Project, P.O. Box 2365, Charlottesville, VA 22902. Also available from: www.disclosureproject.org.

[30] Greer, S. M. 2001. Disclosure: Military and government witnesses reveal the greatest secrets in modern history. Crossing Point, Inc. Crozet, VA, 573 pp.

[31] Ibid. pp. 357-366.

[32] Ibid. pp. 262-270.

[33] Ibid. pp. 384-387.

[34] Ibid. pp. 391-403.

[35] Ibid. pp. 388-389.

[36] Ibid. pp. 497-510.

[37] Cook, N. 2001. The Hunt for Zero Point. Available from: www.amazon.co.uk.

[38] Deavenport, L. 1995. "T.T. Brown Experiment replicated. Electric Spacecraft Journal. Issue 16. Oct. 1995. (Reprinted in: Valone, T. (ed.), 1994. Electrogravitics Systems: Reports on a new propulsion methodology. Integrity Research Institute, Washington, DC 20005)

[39] Transdimensional Technologies, 906-E Bob Wallace, Ave., Huntsville, AL 35801.

[40] http://jnaudin.free.fr

[41] Greer, S.M. and T.C. Loder III. 2001. Disclosure Project Briefing Document, 492 pp. Available on CD from: The Disclosure Project, P.O. Box 2365, Charlottesville, VA 22902. Also available from: www.disclosureproject.org.

[42] Arp, H. 1998. Seeing Red: Redshifts, Cosmology and Academic Science. Montreal: Aperion. (p. 249).

A97-36388

AIAA 97-3209

Some Observations on Avoiding Pitfalls in Developing Future Flight Systems

Gary L. Bennett
Metaspace Enterprises
Emmett, Idaho; U.S.A.

33rd AIAA/ASME/SAE/ASEEJoint Propulsion Conference & Exhibit
July 6 - 9, 1997 / Seattle, WA

SOME OBSERVATIONS ON AVOIDING PITFALLS IN DEVELOPING FUTURE FLIGHT SYSTEMS

Gary L. Bennett*
5000 Butte Road
Emmett, Idaho 83617-9500

Abstract

A number of programs and concepts have been proposed to achieve breakthrough propulsion. As an cautionary aid to researchers in breakthrough propulsion or other fields of advanced endeavor, case histories of potential pitfalls in scientific research are described. From these case histories some general characteristics of erroneous science are presented. Guidelines for assessing exotic propulsion systems are suggested. The scientific method is discussed and some tools for skeptical thinking are presented. Lessons learned from a recent case of erroneous science are listed.

Introduction

Over the past few years a number of speculative propulsion/transportation ideas have been advanced which, if they can be verified, promise to revolutionize space transportation.[1-4] In addition, a question has been asked and some proposed answers given on the possible propulsion system(s) for unidentified flying objects (UFOs) or "flying saucers", if the existence of UFOs is accepted.[5,6] Researchers at the U.S. Air Force (USAF) Phillips Laboratory have proposed research into "... more advanced ideas ... [such as]... fundamental physics concepts which require basic research and/or substantial development to create some sort of breakthrough. These include vacuum zero point energy, energetic species (i.e. nuclear or electronic metastables), ball lightning, and various 'breakthrough physics' concepts. In addition, a number of new emerging technologies and popular ideas will be followed such as nanotechnology, above unity devices, and cold fusion".[7]

Separately, NASA has recently initiated a "breakthrough propulsion physics" program which "... implies discovering fundamentally new ways to create motion, presumably by manipulating inertia and gravity or by harnessing other interactions of matter, fields and space-time".[8,9]

*Fellow, AIAA

Given the speculative proposals and the interest in developing breakthrough propulsion systems it seems prudent and appropriate to review some of the pitfalls that have befallen other programs in "speculative science" so that similar pitfalls can be avoided in the future. And, given the interest in UFO propulsion, some guidelines to use in assessing the reality of UFOs will also be presented.

This paper will summarize some of the principal areas of "speculative science" in which researchers were led astray and it will then provide an overview of guidelines which, if implemented, can greatly reduce the occurrence of errors in research.

Some Case Histories of Errors in Science

This section will briefly describe several case histories involving errors in science: (1) N rays; (2) Davis and Barnes experiment; (3) polywater; (4) infinite dilution; and (5) cold fusion.

N Rays

In 1903, French physicist René-Prosper Blondlot claimed to have discovered that by heating a filament inside an iron tube containing an aluminum-covered opening one could see faintly illuminated objects better in a darkened room. Some of his early experiments were performed with pieces of paper which were barely illuminated by a glowing calcium sulfide screen or a lamp shining through pinholes. Since the heated filament inside the iron tube improved the viewing, Blondlot concluded that a new type of ray was being produced, a ray which was stopped by the iron but not by the aluminum. He called this new ray an "N ray" to honor the University of Nancy, where he worked.[10]

Blondlot discovered that certain objects could be made to store these N rays. For example, if a brick was wrapped in black paper and exposed to sunlight it would give off N rays when taken back into the darkened laboratory. Blondlot noted that if the brick was held close to one's head it made it easier to see the paper in the darkened room. Holding the brick near the paper had a similar effect.[10]

Blondlot reported that the N rays had some odd effects. For example there was no improvement in the effect of improved illumination if more than one brick was used. Loud noises (such as someone entering the laboratory) could spoil the effect. Heat increased the effect but Blondlot said N rays were not the same as heat. Blondlot also claimed to have found negative N rays, which he called N' rays that could nullify the effect of the N rays. It was necessary to spend some time in the darkened room to see the effect.[10]

Blondlot published a number of papers on N rays. Other scientists also published papers with about half confirming Blondlot's work.[10]

The American physicist R. W. Wood visited Blondlot to witness some of the N ray experiments. Wood watched as Blondlot used a large aluminum prism with a 60° angle to measure the refractive index of the N rays to two or three significant figures.[10]

When Wood questioned Blondlot as to how he could measure the position of the beam to within 0.1 mm when the slits in the Nernst filament were 2-mm wide, Blondlot replied to the effect "That's one of the fascinating things about the N rays. They don't follow the ordinary laws of science that you ordinarily think of".[10]

At Wood's request, Blondlot repeated the experiments; however, unbeknownst to Blondlot in the darkened room, Wood had removed the aluminum prism. Blondlot got the same measurements! Wood subsequently published this result, effectively ending the era of the N rays.[10]

Later some German researchers investigated how Blondlot had been deceived. They observed that in a darkened room it is difficult to see the paper so one is tempted to pass one's hand in front of the paper to see if the paper is being illuminated. The interesting result the German researchers found was that the hand could be "observed" whether it was in front of the paper or behind it. Langmuir has remarked that this "... is the natural thing, because this is a threshold phenomenon. And a threshold phenomenon means that you don't know, *you really don't know*, whether you are seeing it or not. But if you have your hand there, well, of course, you see your hand because you *know* your hand's there and that's just enough to win you over to where you know that you see it. But you know it just as well if the paper happens to be in front of your hand instead of in back of your hand, because you don't know where the paper is but you *do* know where your hand is".[10]

The phenomenon of accepting a false belief and then continuing to defend it in the face of information showing the falsity of the belief is not new. In a landmark study published in 1956 it was stated that "A man with a conviction is a hard man to change. Tell him you disagree and he turns away. Show him facts or figures and he questions your sources. Appeal to logic and he fails to see your point".[11] As this study demonstrated, showing someone unequivocal and undeniable evidence that a person's belief is wrong means "The individual will frequently emerge, not only unshaken, but even more convinced of the truth of his beliefs than ever before. Indeed, he may even show a new fervor about convincing and converting other people to his view".[11]

Davis and Barnes Experiment

Around 1930, two American physicists, Bergen Davis and Arthur Barnes conducted a series of experiments in which electrons from a hot filament were accelerated to match the speed of alpha particles being emitted from a polonium source. By carefully adjusting the voltage used to accelerate the electrons the experimenters claimed that they could cause the electrons to be captured by the alpha particles. The measurements were made in a darkened room by counting the number of scintillations on a zinc sulfide screen with a microscope. To save time, the experiments were focused on the voltages where it was calculated that the peaks should occur according to the Bohr theory. Davis and Barnes claimed to be able to achieve electron capture at each of the energy levels of the Bohr theory of the helium atom with measured accuracies of 0.01 volts.[10]

Irving Langmuir and Willis R. Whitney (then both at the General Electric Research Laboratory in Schenectady, New York) visited the Columbia University laboratory of Davis and Barnes and witnessed some of the experiments. They found that Barnes was not counting for a fixed two minutes as claimed and that he was ruling out some counts arbitrarily. When Langmuir secretly had the technician try a wider range of voltages Barnes got measurements that no longer correlated with the Bohr energy levels. Barnes had an *ad hoc* excuse for every criticism Langmuir raised about the way the experiments were being conducted.[10]

Langmuir, who was to earn the 1932 Nobel Prize in chemistry, subsequently wrote Barnes a 22-page letter giving Barnes all the data obtained by Whitney and himself "... and showing really that the whole approach to the thing was wrong; [Barnes] was counting

hallucinations, which I find is common among people who work with scintillations if they count for too long. Barnes counted for six hours a day and it never fatigued him. Of course it didn't fatigue him, because it was all made up out of his head".[10] The next year Davis and Barnes admitted in a short article in *Physical Review* that they hadn't been able to reproduce the effect. They noted that the scintillations they were measuring were a threshold phenomenon.[10]

Polywater

In the 1960s and early 1970s reports from N. N. Fedyakin of the Kostrama Polytechnical Institute of the former Soviet Union and Boris V. Derjaguin of the Institute of Physical Chemistry of the Academy of Sciences of the former Soviet Union claimed there was a new form of water, later called polywater, that was more dense and viscous than normal water. Polywater, which was claimed to be formed in capillary tubes in an atmosphere nearly saturated with water, reportedly froze at -50 °C and boiled near 300 °C. Infrared spectroscopy showed that polywater produced a spectrum entirely different from normal water. Many papers were published on polywater and several theories were developed.[12]

As part of a study of polywater, Denis L. Rousseau and Sergio Porto, then at the University of Southern California, irradiated a sample of polywater with a laser to obtain a Raman spectrum. The laser turned the polywater into a black char, indicating that it "... was no polymer of water but more likely a carbonaceous material".[12] Whenever negative results like these were obtained, the proponents of polywater would always claim that the samples giving the negative results were contaminated but that their own samples, which showed polywater, were clean. Rousseau later showed that one could obtain the infrared spectrum for polywater from ordinary human sweat. This showed "... that polywater is not water at all but a product of organic contamination in the capillary tubes".[12]

Rousseau subsequently observed that "The polywater episode illustrates the loss of objectivity that can accompany the quest for great new discoveries. The quantities of polywater available were so small that many useful experiments could not be done. Many theories were put forward to describe the structure of polywater without even considering the thermodynamic difficulty of accounting for its very existence. Finally, definitive experiments showing high levels of contamination were done but not accepted, until overwhelming evidence showed that a new polymer of water had not been discovered".[12]

Infinite Dilution

In 1988 Jacques Benveniste of the University of Paris and his collaborators reported that water retained a memory or template of a molecule even when there should be no molecules present. This phenomenon is referred to as "infinite dilution" meaning that a biological effect is produced even when the "... biologically active solution is diluted so many times that no active molecules can be present ..."[12]

After Benveniste's paper was published in *Nature*, John Maddox, the editor of *Nature*, James Randi (a professional magician), and Walter Stewart (an experienced fraud investigator) spent three weeks in Benveniste's laboratory witnessing the experiments. When an elaborate series of double-blind experiments were conducted the biological effect was not measured. This committee of three reported "... that the original experiments were poorly controlled and that no effort had been made to exclude systematic error or observer bias".[12]

Many of the traits reported in the earlier episodes of erroneous science were present with infinite dilution. The effect was weak and independent of the causative agent. The counting was done visually and it was extremely difficult to do. When the control produced results at variance with the experimenters's beliefs the counting was redone. Negative results were overlooked. Sometimes experiments would not work for several months and one investigator seemed to be the best at making the experiments work.[12]

Rousseau has written that "Benveniste and his colleagues were not doing fraudulent work. They observed the effects that they reported. But they so believed in the phenomenon that they could ignore or reinterpret any questionable findings. In replying to the Maddox committee, Benveniste wrote, 'It may be that all of us are wrong in good faith. This is no crime but science as usual and only the future knows.' But, self-delusion is not science as usual".[12]

Cold Fusion

In 1989 two research groups in Utah announced that they had discovered cold fusion by means of simple electrochemical cells. Both research groups used heavy water although their salts were different. The heavy water would split into deuteroxyl ions (OD^-) and deuterons when a current was passed through the cells. What they hoped to achieve was to collect enough deuterons at the palladium cathode to cause them to pack so tightly that they would fuse at room

temperature and release energy, a process normally requiring temperatures on the order of 10^8 °C.[12]

B. Stanley Pons of the University of Utah and Martin Fleischmann of the University of Southampton reported achieving enough cold fusion that the thermal output exceeded the energy input by 4.5 times. To explain away the absence of the neutrons which should have been present at a level sufficient to kill the experimenters they reported that "... the bulk of the energy release is due to a hitherto unknown nuclear process".[12] It was later learned that their electrochemical cell was not a closed system so they did not have a good heat balance. Moreover, their method of calculating the energy release was flawed.[13,14]

David E. Williams, the Thomas Graham Professor of Chemistry at University College London and previously a research group leader at the Harwell Laboratory of the U.K. Atomic Energy Authority responsible for that laboratory's attempts to verify cold fusion, has written about one staunch advocate of cold fusion repeating "... the common assertion that the excess energies associated with the electrolysis of D_2O with a Pd cathode are on the order of tens to hundreds of MJ/cm^3 and hence can only find an explanation in some phenomenon outside the chemistry of the system. In this he displays an ignorance of the experimental measurement and a naive belief in the significance of impressively large numbers. The great majority of experiments measure power; the large numbers are obtained by multiplying an (often small) power by a large time (the duration of the experiment) and dividing by a small volume (that of the Pd cathode). In comparison with the total energy applied to the electrolytic cell, the excesses are much less impressive, on the order of a few percent. More properly, in comparison with the power applied to the cell, the claimed excess power is often also small ...".[15]

Steven Jones of Brigham Young University and his collaborators found evidence of increased neutron production but nothing like the heat output reported by Pons and Fleischmann.[12]

Other researchers were unable to duplicate the experiments of the two Utah groups. The neutron emissions measured by Pons and Fleischmann were inferred from a gamma-ray emission spectrum that was more narrow than the resolution of their detector. The claim that tritium, one product of a deuteron-deuteron fusion reaction, had been found was later discredited when it was learned that tritium was a contaminant in the palladium electrode.[12]

As Rousseau has summarized it, "Cold fusion was doomed from the start when a race to be first took precedence over the desire to be right. Most measurements reporting nuclear effects from cold fusion were barely above the background noise, and extended periods of failed experiments afflicted even Pons's laboratory. The proponents of cold fusion attributed the failure to several causes: differences in the materials, the size of the electrodes, impurities in the electrodes, and low current density. The list goes on.

"Nuclear reactions, however, are very well understood. Any theory offered to account for the reported observations must postulate new nuclear processes that only occur in the palladium electrodes ... The investigators of cold fusion also ignored definitive experiments".[12]

The whole sorry episode of cold fusion, which the co-chair of the Department of Energy Energy Research Advisory Board panel on cold fusion, Professor John R. Huizenga, has termed the "scientific fiasco of the century", has been well documented in Refs. 13,14, 16-18. Suffice it to say that it is not a pretty picture but as Prof. Huizenga stated: "The cold fusion fiasco illustrates once again that the scientific process works by exposing and correcting its own errors".[13]

Despite all these problems the U.S. Air Force has considered studying (as noted earlier) "... a number of new emerging technologies and popular ideas ... such as nanotechnology, above unity devices, and cold fusion".[7] Some USAF personnel apparently foresee using cold fusion for satellite power and for fast acting thrusters for survivability. The payoffs are listed as (1) lower weight; (2) near limitless source of heat; (3) high reliability and operability; and (4) simplicity and robustness. The only technology needs identified were the scaling up of cold fusion and the development of specialized pumps, valves, and nozzles.[7] The fact that no reputable, objective scientist has been able to prove the existence of cold fusion seems to be beside the point! (Even NASA got in the cold fusion act briefly in response to the NASA Administrator's order that no nuclear power sources be flown again on NASA spacecraft. After researchers at Lewis Research Center were unable to make cold fusion work and mission planners at the Jet Propulsion Laboratory showed to the Administrator's satisfaction that there wasn't much sunlight in the outer Solar System he recanted his order against nuclear power although he does want a more sporty -- and possibly unachievable within current funding and schedule limits -- conversion system for the next generation of radioisotope power sources.)

As shown by the original hullabaloo over cold fusion and the more recent NASA activities followed by the proposed USAF program, an unfortunate aspect to bad science such as cold fusion is that it diverts time and funding from real science. Science writer Gary Taubes has written that "What cold fusion had proven, nonetheless, was that the nonexistence of a phenomenon is by no means a fatal impediment to continued research. As long as financial support could be found, the research would continue. And that support might always be found so long as the researchers could obtain positive results. In fact, the few researchers still working in the field would have little incentive to acknowledge negative results as valid, because such recognition would only cut off their funds. It promised to be an endless loop".[14]

Something like this has certainly occurred with thermionic reactor research in the U.S. where hundreds of millions of dollars have been spent yet no long-lived (>5 years), high efficiency (≥10%), high specific power (>5.5 We/kg) in-reactor-core thermionic system has been built in the U.S.[19-21] Still the studies continue, now with a focus on bimodal power/propulsion systems.[22] And despite the investment of over $500 million in today's dollars with no U.S. in-core thermionic reactor being built and meeting the aforementioned goals, General Atomics of San Diego, California was recently awarded a $5.4 million cost-plus-fixed-fee contract by the Defense Special Weapons Agency "... for the research, development, test and evaluation of advanced in-core thermionic technologies to support long duration space missions for national security purposes. Focus is on the advancement of thermionic performance rather than an overall system design improvement *since no specific mission has yet been identified on which to base detailed system requirements*"[emphasis added].[23] Given the end of the Cold War and the lack of military reactor missions coupled with the lack of any real progress in U.S. in-core thermionic research it is doubtful if there will ever be any real military system requirements but contracts will continue to be awarded in an "endless loop". Is this pathological science or pork barrel politics -- or both?

Symptoms of Pathological Science

On 18 December 1953, Nobel-laureate Irving Langmuir gave a colloquium on the subject of what he termed "pathological science", the science of things that aren't so. As Langmuir stated it, "These are cases where there is no dishonesty involved but where people are tricked into false results by a lack of understanding about what human beings can do to themselves in the way of being led astray by subjective effects, wishful thinking or threshold interactions".[10]

Based on his study of the Davis and Barnes experiment, the incident of the N rays and other early mistakes, Langmuir listed six symptoms of pathological science:[10]

- *The maximum effect that is observed is produced by a causative agent of barely detectable intensity, and the magnitude of the effect is substantially independent of the intensity of the cause.*

- *The effect is of a magnitude that remains close to the limit of detectability or, many measurements are necessary because of the very low statistical significance of the results.*

- *There are claims of great accuracy.*

- *Fantastic theories contrary to experience are suggested.*

- *Criticisms are met by* ad hoc *excuses thought up on the spur of the moment.*

- *The ratio of supporters to critics rises up to somewhere near 50% and then falls gradually to oblivion.*

Working with more recent erroneous science such as polywater, infinite dilution and cold fusion, Denis L. Rousseau, at the time a Distinguished Member of the Technical Staff at AT&T Bell Laboratories, condensed Langmuir's six symptoms into two characteristics and added a third, which he believes to be the most important:[12]

1. *The effect being studied is often at the limits of detectability or has a very low statistical significance.*

2. *There is a readiness to disregard prevailing ideas and theories.*

3. *The investigator finds it nearly impossible to do the critical experiments that would determine whether or not the effect is real.*

In looking at the cases of pathological science presented in this paper it is clear that most of them are at the limits of detectability and they often were based on subjective visual observations. The fact that there may be no direct connection between the causative agent (e.g., number of hot bricks supposedly emitting N rays) and the effect (better viewing) is not seen as an impediment to the "new" scientific "discovery". News accounts of the advertised anti-gravity effect also place

the effect at the limits of detectability.[1,2]

Cold fusion represents perhaps the most extreme example of concocting new theories to explain a poorly understood and poorly conducted set of experiments.[13,14] In contrast to the ready belief of the cold fusion proponents in the fantastic new physics invoked to explain their results, the author found it refreshing to hear from several of the original nuclear fission researchers (who were coincidentally meeting in a special 50th anniversary conference at the same time as the cold fusion fiasco erupted) that they were unwilling to accept their experimental results until all other avenues had been explored.[24] Would that other researchers had been as careful!

In none of the examples considered in the previous section did the researchers conduct experiments to determine if their results could be wrong. And in those cases where other researchers came to different conclusions they were criticized for having made mistakes or using bad samples or the wrong procedures.

Carl Sagan has written about people who make extraordinary claims, "The burden of proof is on them, not on those who might be dubious".[25] In short, if someone believes he/she has discovered cold fusion or anti-gravity it is up to him/her to prove it beyond a shadow of doubt. It is not up to the skeptics to disprove it. Unfortunately, as Sagan has observed pseudoscience operates just the opposite from normal science: "Hypotheses are often framed precisely so they are invulnerable to any experiment that offers a prospect of disproof, so even in principle they cannot be invalidated. Practitioners are defensive and wary. Skeptical scrutiny is opposed. When the pseudoscientific hypothesis fails to catch fire with scientists, conspiracies to suppress it are deduced".[26]

As Sagan has so eloquently put it, "I believe that the extraordinary should certainly be pursued. But extraordinary claims require extraordinary evidence".[25] To date the extraordinary evidence has not been reported for cold fusion or anti-gravity.

Guidelines for Assessing Other Exotic Propulsion Systems

One writer has pondered the question of what sort of propulsion system a UFO would have to have to match the reported observations of the motions of so-called flying saucers.[5,6] Even though people have seen strange things in the sky for centuries, the "Age of Confusion" about flying saucers began with the sighting near Mount Rainier by private pilot Kenneth Arnold on 24 June 1947.[27] Following Arnold's claimed sighting there have been thousands of reports of strange craft in the skies.[27,28]

Unfortunately, the sightings remain for the most part anecdotal and the photographs are generally suspect. Supposed artifacts have been shown to be of terrestrial manufacture. In short, while there remain some unexplained episodes, the vast majority of "sightings" are of natural phenomena or they are delusions or hoaxes.[25-28]

Astronomer Alan Hale, who is co-discoverer of Comet Hale-Bopp and director of the Southwest Institute for Space Research, has listed three basic principles as guides he uses in confronting beliefs about UFOs or other paranormal phenomena:[29]

1. *Extraordinary claims require extraordinary evidence.*

As an example of the kind of extraordinary evidence he is seeking, Hale lists "... the actual physical aliens themselves, where I and other trustworthy and competent scientists and individuals can study and communicate with them. I'd like to examine their spacecraft and learn the physical principles under which it operates. I'd like a ride on that spacecraft."[29] And he lists other things he would like to see and investigate directly.

Personally, I would like to see the UFO land on the Mall in Washington, D.C. and be subjected to a complete inspection using all the resources (scientists, engineers, technicians, equipment, etc.) at humanity's disposal. Like Sagan [25,26], I am highly skeptical about these reported aliens in UFOs since they never seem to contact any officials, they never demonstrate or leave any technology we don't already have and they never leave any messages that we don't already know.

2. *The burden of proof is on the positive.*

Hale demands that the one making the claim produce the extraordinary evidence to prove the correctness of the claim, noting that the burden is not on the skeptic to prove that the advocate is wrong. He goes on to state that "... you must prove your case by providing the direct and compelling evidence for it; you can't prove it by eliminating a few token explanations and then crying, 'Well, what else can it be?'"[29]

3. *Occam's Razor: If one is confronted with a series of phenomena for which there exists more than one viable explanation, one should choose the simplest*

explanation which fits all the observed facts.

Hale notes that people can make mistakes in their observations and that most people are not aware of the natural phenomena one can observe in the sky. Many people are not trained to observe what they claim to observe. People can be deceived by their preconceived notions and expectations and some people will create hoaxes. Hale asserts that "Taking all these undeniable facts together, the simplest explanation--to me, anyway--for the UFO phenomenon is that every report is either a hoax or is a mistake of some sort. If this explanation is incorrect, then you have to increase the sphere of undeniable facts; and for this, see points 1) and 2) above".[29]

Another "breakthrough physics" concept being studied is based on the belief that energy can be extracted from the zero-point fluctuations of the vacuum.[7] In searching for the origin of this idea, R. L Park of the American Physical Society wrote that "'The New Energy News' ... credits the idea to physicist Harold E. Puthoff and proclaimed him 'The New Energy News Theorist of the Year.' ... Puthoff's ideas are controversial; but he's accustomed to controversy. In 1972, at the Stanford Research Institute, Puthoff and Russell Targ were promoting psychic spoon-bender Uri Geller; five years later, they published 'Mind Reach,' a book about remote-viewing that inspired the CIA to invest in psychic espionage. Reportedly, Puthoff himself once sent his mind to explore the surface of planet Mercury".[30] Clearly, Hale's principles should be applied to this type of research!

Author's Note: For those not familiar with the *New Energy News*, it has been published by something called the Fusion Information Center which also disseminated information on cold fusion. This publication states that it is interested in "... papers ... covering both theory and practice of energy producing devices and systems such as cold nuclear fusion, rotating N-Machines, Solid-State energy systems, Magnetic over-unity machines, Tapping Space Energy (Zero-Point Energy), gravity control techniques, energetic transmutations (nuclear reactions), and other new energy research".[31] Those interested in some of the activities of Harold Puthoff, Russell Targ and the spoon-bender Uri Geller are encouraged to read *Science, Good, Bad and Bogus* by Martin Gardner.[32]

The Scientific Method

Physicist Alan Cromer has described science as "... the search for a consensus of rational opinion among all competent researchers ... The products of science give empirical proofs of its theories. Mathematics and experimentation provide powerful arguments with which to convince and persuade".[33] Cromer states that "Science is the heretical belief that the truth about the real nature of things is to be found by studying the things themselves".[33] Cromer also notes that the scientific way of thinking is not natural to humans; it is something which has to be learned.[33] Sagan has observed that "Science is a way of thinking much more than it is a body of knowledge".[25]

To study things requires the use of the scientific method. While there is no single absolute detailed process to be followed for all science, the American philosopher Morris R. Cohen has written that "The problem of how to get rid of illusion and see what truly goes on in nature requires that persistent and arduous use of reason which we call scientific method ... Scientific method is a systematic effort to eliminate the poison of error from our common knowledge".[34] In short, science is as much a process as it is an assembly of facts, but it is a process that requires assembling of the relevant facts (quantitative measurements) and the testing of hypotheses. It is a process that any scientist in the field should be able to duplicate in order to check claims of new discoveries.[25,26,29,32-35]

To aid in avoiding pitfalls in developing advanced propulsion (or exploring any new field), Sagan's tools of skeptical thinking are highly recommended:[26]

- *Obtain independent confirmation of the "facts".*
- *"Encourage substantive debate on the evidence by knowledgeable proponents of all points of view."*
- *Give little weight to arguments from authority.*
- *Develop and test more than one hypothesis in a fair and objective manner.*
- *Do not become overly attached to your own hypothesis.*
- *Quantify your observations wherever possible.*
- *Test the entire argument -- "If there's a chain of argument, every link in the chain must work (including the premise)--not just most of them".*
- *Use Occam's Razor -- when two or more hypotheses explain the data equally well, choose the simplest hypothesis.*
- *"Always ask whether the hypothesis can be, at*

least in principle, falsified. Propositions that are untestable, unfalsifiable are not worth much ... You must be able to check assertions out. Inveterate skeptics must be given the chance to follow your reasoning, to duplicate your experiments and see if they get the same result."

A useful guide in conducting scientific research is the National Academy of Sciences publication *On Being a Scientist.*[35]

Lessons Learned

In the concluding chapter of his book, *Cold Fusion: The Scientific Fiasco of the Century*, Professor John R. Huizenga lists 15 lessons from which we all may profit in conducting research. These lessons are [13]

- **Handling far-out ideas and claims**

Far-out ideas and claims should be presented first informally at a meeting of colleagues to address the hard questions. Where the work involves science or technology outside the advocate's main area of expertise the briefings should include experts from those areas. When all questions have been answered and all the experimental checks made one should present the results to other experts outside the laboratory or organization and then submit to the peer-review process.

- **Judging hypotheses**

One should avoid the extreme position of rejecting all previous work in the field just because one has obtained some anomalous result. If a hypothesis requires the belief in several miraculous occurrences then the hypothesis is probably pathological.

- **Premature publication**

Researchers should submit to the full peer review process to avoid being caught later with an unsound paper. Editors and reviewers also have a responsibility to ensure the technical soundness of a paper. Where there is some justifiable need for urgent publication the editor can always put a disclaimer on the paper noting that it has not been peer reviewed. (The author proposed something like this for speculative papers submitted to the annual Intersociety Energy Conversion Conference not only as a caution for other researchers but as a warning to potential investors.)

- **Publication by press conference**

The announcement of a new scientific discovery at a press conference should only be done where it is justified and where there is enough supporting information to back up the claimed discovery. Generally, it is far better and safer to "announce" the discovery through the normal peer review process.

- **Publication of primary data**

Researchers should publish enough of their primary data and experimental procedures to enable other researchers to check their results. If mistakes are later found these should be formally noted in the same publication that carried the original data.

- **Reproducibility in science**

Researchers should publish sufficient information about how they conducted their experiments so that other researchers can check their work. As Huizenga has written, "The foundation of science requires that experimental results must be reproducible. Validation is an integral part of the scientific process".[13]

- **Scientific isolation in research**

Breakthroughs in science generally are made by researchers who are fully knowledgeable in their fields and in contact with other researchers. In contrast, University of Utah officials claimed that the isolation of Pons and Fleischmann from both the traditional centers of fusion research and from nuclear scientists was what led them to make their claimed breakthrough discovery of cold fusion. Unfortunately, when their cold fusion results could not be duplicated by reputable, objective (and skeptical) scientists, cold fusion was dubbed another example of the "Utah Effect" (a term first used in connection with University of Utah Professor Edward Eyring's 1972 mistaken claim of discovering the x-ray laser).[13,14]

- **Control of information**

Researchers must be open with and willing to share their research data and experimental techniques. Free and open communication is central to the scientific process.

- **Secrecy in basic research**

Basic research is best conducted openly with the peer review process. If the research is done in secret the kinds of errors that afflicted so-called cold fusion can occur. Similar problems occurred when the former Strategic Defense Initiative Organization (SDIO) tried to develop a nuclear rocket code-named "Timber Wind" using a technology (particle bed reactor) that

was highly questioned by outside experts. In that case people who had technical concerns about the viability of the concept were either ignored or denied further access to information on the program.[36]

- **Discovery by outsiders**

There seems to be a growing belief that only people who are not experts can make breakthrough discoveries because their minds are not clouded by "official" science. The facts are quite different--it is very rare that a non-expert makes a breakthrough discovery outside his or her field. As Prof. Huizenga has observed, "Most fundamental discoveries are made by persons intimately familiar with their research discipline because they not only know the subject matter of the field but also know the pitfalls and traps and have made many of the obvious mistakes".[13]

- **Lobbying before Congressional committees**

Lobbying before Congressional committees is contrary to the scientific process of peer review and it is particularly dangerous when the advocates are championing something like cold fusion which has not been confirmed. Not only is lobbying for unproven concepts damaging to science it wastes the country's limited research funds. Prof. Huizenga has estimated that "It has taken upwards of some fifty to one hundred million dollars of research time and resources to show that there is no convincing evidence for room temperature fusion".[13] Timber Wind cost the U.S. at least $139 million between Government Fiscal Years 1987 and 1991 largely on the basis of Congressional lobbying.[36] Thermionic reactor research has cost the country on the order of $500 million in today's dollars.[19] These monies could have been better spent on peer-reviewed space technology of more benefit to the country.

- **Funding large initiatives**

Large initiatives should be funded only when there is clear, objective, peer-reviewed evidence in support of the concept.

- **Patents and revenues from basic science**

If the concern is over protecting patent and intellectual property rights, the normal process is to verify the scientific results first, then file the patents and then announce the work. The process of announcing the results first with very limited information and no scientific verification was a key contributor to the cold fusion fiasco.

- **The press and basic science**

The press should explore claims of breakthrough science thoroughly making sure that the public is being given a true picture of what is claimed. The preferred process for publicly reporting new discoveries is to wait until the research paper has been peer reviewed and accepted for publication by a respected journal in the field. Using press conferences before complete scientific papers were accepted contributed to the confusion about and eventually distrust of claims of cold fusion.

- **The scientific process**

Claims of breakthrough discoveries should be made through the usual scientific process of peer review and validation through independent reproduction of the results.

Concluding Remarks

Advanced propulsion research must be continued because of the tremendous payoff it offers to our ability to conduct scientific, exploration, and commercial space missions. However, in our studies of advanced propulsion concepts we should be guided by the scientific method so that we can avoid the types of pitfalls that have ensnared other scientists in what Irving Langmuir has called "pathological science". Physicist Richard P. Feynman said it best in his minority report on the Challenger accident: "For a successful technology, reality must take precedence over public relations, for nature cannot be fooled".[37] Unfortunately, what has often occurred with pseudoscience is that "... for the survival of an unsuccessful technology, public relations must take precedence over reality".[14] If we ignore reality then everyone loses and our research field is damaged.

References

1. "NASA's Fling With Anti-Gravity", *Science*, Vol. 274, p. 183, 11 October 1996.

2. M. Burkey and L. David, "Changing Gravity: A Weighty Issue", *Space News*, p. 15, 11-17 November 1996.

3. J. H. Vance, "A Force Sink in Classically Defined Non-Inertial Space", AIAA paper 92-3781, prepared for the AIAA/SAE/ASME/ASEE 28th Joint Propulsion Conference and Exhibit, held in Nashville, Tennessee, 6-8 July 1992.

4. L. T. Cox, Jr., *Calculation of Resonant Values of Electromagnetic Energy Incident Upon Dielectric Spheres*, PL-TR-93-3002, Phillips Laboratory, Edwards Air Force Base, California, February 1994.

5. P. Murad, "An Electromagnetic Rocket Stellar Drive - Myth or Reality? Electromagnetic Evidence and Relativistic Phenomenon", AIAA paper 95-2602, prepared for the 31st AIAA/ASME/SAE/ASEE Joint Propulsion Conference and Exhibit, held in San Diego, California, 10-12 July 1995.

6. P. Murad, "An Electromagnetic Rocket Stellar Drive - Myth or Reality? Fluid Dynamic Interactions and an Engine Concept", AIAA paper 95-2894, prepared for the 31st AIAA/ASME/SAE/ASEE Joint Propulsion Conference and Exhibit, held in San Diego, California, 10-12 July 1995.

7. F. Mead and G. Olson, "Advanced Concepts for Consideration at Phillips Laboratory Propulsion Directorate", presentation given at the Sixth Advanced Space Propulsion Workshop held at the Jet Propulsion Laboratory, Pasadena, California, 21-23 March 1995.

8. L. David, "Mind Fields", *Final Frontier*, Vol. 10, No. 1, pp. 19-23, January/February 1997.

9. M. G. Millis letter to G. L. Bennett, dated 3 May 1997.

10. I. Langmuir, "Pathological Science", transcribed and edited by R. N. Hall, *Physics Today*, pp. 36-48, October 1989. See also the "Letters" column in the March 1990 and April 1990 issues of *Physics Today*. Langmuir gave this talk on 18 December 1953 at General Electric's Knolls Atomic Power Laboratory.

11. L. Festinger, H. W. Riecken and S. Schachter, *When Prophecy Fails*, University of Minnesota Press, Minneapolis, Minnesota, 1956.

12. D. L. Rousseau, "Case Studies in Pathological Science", *American Scientist*, Vol. 80, pp. 54-63, January-February 1992.

13. J. R. Huizenga, *Cold Fusion: The Scientific Fiasco of the Century*, University of Rochester Press, Rochester, New York, 1992.

14. G. Taubes, *Bad Science, The Short Life and Weird Times of Cold Fusion*, Random House, New York, New York, 1993.

15. D. E. Williams, letter to *Physics Today*, p. 94, March 1994.

16. F. Close, *Too Hot To Handle, The Race for Cold Fusion*, Princeton University Press, Princeton, New Jersey, 1991.

17. N. Hoffman, *A Dialogue on Chemically Induced Nuclear Effects, A Guide for the Perplexed About Cold Fusion*, American Nuclear Society, La Grange Park, Illinois, 1995.

18. Energy Research Advisory Board, *Cold Fusion Research*, DOE/S--0073, DE90 005611, A Report of the Energy Research Advisory Board to the United States Department of Energy, Washington, D.C., November 1989.

19. Anon., "Thermionic Space Nuclear Power, An Option for NASA Missions", General Atomics briefing package, July 1991.

20. Technology Group, "Space Nuclear Reactor Power Systems Report of Technology Group to Program Planning Group", U.S. Department of Energy, Germantown, Maryland, 18 February 1992.

21. R. J. Sovie, "Presentation on Thermionic Technology Status to SP-100 Program Review Group", Dallas, Texas, 19-20 December 1989.

22. E. L. James, W. D. Ramsey and G. J. Talbot, "Thermionic Converters for ISUS", *Proceedings of the Space Technology and Applications International Forum (STAIF-97)*, Part One, pp. 479-484, AIP Conference Proceedings 387 published by the American Institute of Physics, Woodbury, New York. Proceedings of a conference held in Albuquerque, New Mexico, 26-30 January 1997.

23. Department of Defense Contracts News Release No. 194-97 posted on the World Wide Web, 23 April 1997.

24. J. W. Behrens and A. D. Carlson, editors, *50 Years with Nuclear Fission*, 2 volumes, American Nuclear Society, Inc., La Grange Park, Illinois (proceedings of a conference commemorating 50 years with nuclear fission held at the National Academy of Sciences, Washington, D.C. and the National Institute of Standards and Technology, Gaithersburg, Maryland, 25-28 April 1989).

25. C. Sagan, *Broca's Brain, Reflections on the Romance of Science*, Ballantine Books, New York, New York, 1980. Originally published in 1978 by Random House, New York, New York.

26. C. Sagan, *The Demon-Haunted World, Science as*

a Candle in the Dark, Random House, New York, New York, 1995.

27. C. Peebles, *Watch the Skies! A Chronicle of the Flying Saucer Myth*, Smithsonian Institution Press, Washington, D.C. and London, 1994.

28. C. Sagan and T. Page, editors, *UFO's-- A Scientific Debate*, Barnes and Noble Books, New York, New York, 1996. Originally published in 1972 by Cornell University Press, Ithaca, New York.

29. A. Hale, "An Astronomer's Personal Statement on UFOs", *Skeptical Inquirer*, Vol. 21, No. 2, pp. 29-30, March/April 1997.

30. R. L. Park, "What's New for Mar 11, 1994", Internet message sent on 11 March 1994.

31. *New Energy News*, Monthly Newsletter of the Institute for New Energy, Salt Lake City, Utah. February 1994.

32. M. Gardner, *Science, Good, Bad and Bogus*, Prometheus Books, Buffalo, New York, 1989.

33. A. Cromer, *Uncommon Sense, The Heretical Nature of Science*, Oxford University Press, New York and Oxford, 1993.

34. M. R. Cohen, *Reason and Nature, An Essay on the Meaning of Scientific Method*, Dover Publications, Inc., New York, New York, 1978. The first edition of this work was originally published by Harcourt, Brace and Company, New York, in 1931.

35. Committee on the Conduct of Science, *On Being a Scientist*, National Academy of Sciences, National Academy Press, Washington, D.C., 1989.

36. Office of the Inspector General, *The Timber Wind Special Access Program*, Audit Report Number 93-033, Department of Defense, Arlington, Virginia, 16 December 1992.

37. R. P. Feynman, "Appendix F--Personal Observations on Reliability of Shuttle", in *Report of the Presidential Commission on the Space Shuttle Challenger Accident*, Volume II, Washington, D.C., 1986.

Technical Physics Letters, Vol. 26, No. 12, 2000, pp. 1105–1107. Translated from Pis'ma v Zhurnal Tekhnicheskoĭ Fiziki, Vol. 26, No. 24, 2000, pp. 70–75.

An Experimental Investigation of the Physical Effects in a Dynamic Magnetic System

V. V. Roshchin and S. M. Godin

Institute of High Temperatures, Russian Academy of Sciences, Moscow, Russia;
e-mail: rochtchin@mail.ru
e-mail: smgodin@online.ru
Received June 16, 2000

Abstract—It is demonstrated that a magnetic system based on rare-earth magnets is capable of converting various forms of the energy, provided that certain critical operating regime is set. As the critical regime is attained, the experimental setup becomes energetically fully autonomous. This is accompanied by local variations in the total structure weight, a decrease in the surrounding air temperature, and the formation of concentric "magnetic walls" at a distance of up to 15 m from the experimental setup. © *2000 MAIK "Nauka/Interperiodica".*

Introduction. We have experimentally studied the physical effects in a system based on rotating permanent magnets [1]. Below, we describe the technology of manufacture; assembly; and the results of testing this experimental setup, which is referred to as the converter.

Technological description. The converter comprises an immobile stator and a rotor moving around the stator and carrying fixed magnetic rollers. The magnetic system of the working body of the converter has a diameter of about 1 m. The stator and magnetic rollers were manufactured from separate magnetized segments made of rare-earth magnets (REMs) with a residual magnetization of 0.85 T, a coercive force of $[Hc] \sim 600$ kA/m, and a specific magnetic energy of $[W] \sim 150$ J/m^3. The segments were magnetized by a conventional method based on a discharge of a capacitor bank through an inductor coil. Then the magnetized segments were assembled and glued together in a special mounting stage, which provided for the necessary tolerance in positioning the segments and for the removal of magnetic energy. Using this mounting stage, it was possible to glue the elements into the common unit. The stator incorporated REMs with a total weight of 110 kg and the rollers contained 115 kg of the same REM material.

The magnetic system elements were assembled into a single structure on a special platform made of nonmagnetic structural alloys. The platform construction was provided with springs and shock absorbers and allowed the converter setup to move in the vertical direction on three slides. The motion was monitored by an inductive transducer, which allowed changes in the platform weight to be determined in the course of the experiment. The total weight of the platform with the magnetic system in the initial state was 350 kg.

Description of observed effects. The converter was installed in a 2.5-m-high laboratory room using three concrete supports on a ground level. In additional to the ordinary steel-reinforced concrete ceiling blocks, the converter environment featured a usual electrodynamic generator and an electric motor, with a total iron weight of a several dozen kilograms (only these parts could, in principle, introduce distortions into the electromagnetic field pattern observed).

The converter was set to operation by the electric motor. The motor speed was gradually increased until the amperemeter connected in the motor circuit showed zero consumed current and the current direction reversal. This state corresponded to a rotor speed of approximately 550 rpm, but the motion transducer began to indicate a change in the platform weight already at 200 rpm. Then the electric motor was disconnected using an electromagnetic overrunning clutch, and a usual electrodynamic generator was connected instead to the main shaft of the converter via another electromagnetic clutch. On attaining the critical regime (~550 rpm), the rotor exhibited a sharp increase in the rotation speed; this was accompanied by a slow-down in the rate of the current weight variation. At this instant, the first 1 kW load was connected to the system. Immediately upon this connection, the rotation speed began to decrease, while the ΔG value kept increasing, and so on, as depicted in figure.

The system weight variations depend both on the power consumed by the active load (the load consisted of ten ordinary 1-kW heating elements) and on the polarization voltage applied. For the maximum consumed power (7 kW), a change in the total platform weight reached 35% of the initial value in the immobile state (350 kg), which corresponded to 50% of the pure weight of the working body of the converter. An increase in the load power above 7 kW led to a gradual

1063-7850/00/2612-1105$20.00

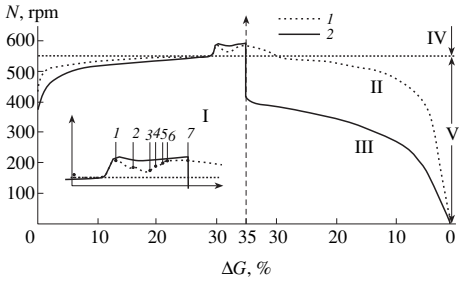

A diagram illustrating various operation regimes of the magnetogravitational converter showing (I) load power (kW) and system weight variation; (II) 7-kW load (high voltage off); (III) 7-kW load (high voltage on); (IV) supercritical regime; (V) subcritical regime (*1*, high voltage off; *2*, high voltage on).

decrease in the rotor speed and, eventually, to the system going out of the self-generation regime and the rotor speed decreasing until the full stop.

The platform weight could be controlled by applying a high-voltage signal to the cellular ring electrodes situated 10 mm above the external roller surface. Upon applying a 20-kV signal (negative polarity on the electrodes), an increase in the load power consumption above 6 kW did not affect the ΔG value even when the rotor speed decreased down to 400 rpm. This was equivalent to "prolongation" of the effect and was accompanied by phenomena of the "remanent induction" type with respect to ΔG. The converter operation in various experimental regimes is illustrated in the figure.

The effect of the system weight variation is reversible with respect to the direction of rotor motion and exhibits certain hysteresis. For the clockwise rotation, the critical regime is observed in the region of 550 rpm and is accompanied by development of the force acting against the gravity vector. For the counterclockwise rotation, the onset of the critical regime is observed at approximately 600 rpm and the extra force coincides in direction with the gravity vector. The onset of the critical regime exhibited a scatter within 50–60 rpm. It should be noted that some other critical resonance regimes may exist which correspond to higher rotor speeds and markedly greater useful load levels. Proceeding from the general theoretical considerations, the output mechanical energy must nonlinearly depend on the internal parameters of the converter magnetic system and the rotor speed, so that the observed effects are likely to be far from optimum. Establishing the maximum output power, maximum weight variation, and the converter energy resource is of considerable theoretical and practical interest.

Besides the phenomena described above, a number of other interesting effects were observed in the system studied. In particular, the converter operation in the dark is accompanied by a corona discharge with a pinkish blue light emission and by the ozone production. The ionization cloud is formed around the stator and rotor, acquiring a toroidal shape. The general corona discharge background is superimposed with a wavy pattern corresponding to the surface of rollers: the zones of increased emission intensity are distributed along the roller height in a manner similar to that observed for the high-voltage microwave induction energy storage in the prebreakdown state. These zones appeared yellowish white, but the emission was not accompanied by sounds characteristic of the arc discharge. We also did not observe any visible erosive damage on the stator and rotor surfaces.

One more effect which was never reported previously is the appearance of vertical "magnetic walls" surrounding the setup. We have detected and measured an anomalous constant magnetic field around the converter. The measurements revealed zones of increased magnetic field strength on the order of 0.05 T arranged coaxially relative to the system center. The direction of the magnetic field vector on the "walls" coincides with that in the rollers. The structure of these magnetic zones resembles the pattern of circular waves on the water surface. No anomalous field is detected by a mobile magnetometer, employing the Hall effect transducer, in the areas between zones. The layers of increased magnetic field strength are propagating with virtually no attenuation to a distance of 15 m from the converter center and then rapidly decayed at the boundary of this 15-m area. Each layer zone is 5–8 cm thick and exhibits sharp boundaries. The layers are spaced by 50–60 cm, the spacing slightly increasing with the distance from the converter center. A stable pattern was also observed at a height of 5 m above the setup (the measurements were conducted in a second-floor room above the laboratory; no tests were performed on a higher level).

Another interesting phenomenon consists in an anomalous temperature drop in the immediate vicinity of the converter. At a general room temperature level in the laboratory +22°C (±2°C), the temperature at the converter surface was 6–8°C lower. Similar temperature variations were detected in the vertical magnetic "walls." The temperature changes in the walls were detected by an ordinary alcohol thermometer with a reading set time of 1.5 min. The temperature variations in the magnetic "walls" can be even sensed by the human body: a hand placed inside the "wall" immediately feels cold. The same pattern was observed at a height of 5 m above the setup in a second-floor room above the laboratory (despite the steel-reinforced concrete blocks separating the rooms).

Discussion of results. All the experimental results described above are very unusual and need some theoretical rationalization. Unfortunately, attempts at interpreting the obtained results within the framework of the

existing physical theories showed that no one of these models can explain the whole set of experimental data.

Recently, Dyatlov [2] attempted to combine the concepts of electricity and gravity by introducing the so-called electrogravitation and magnetic-spin coefficients into the Heaviside gravity equations and the Maxwell field equations. This provides for a relationship between the gravitational and electrical components, as well as between the magnetic and rotational components in a given medium. The assumptions are built around a special model of inhomogeneous physical vacuum, called the vacuum domain model [2]. It is suggested that the extra relationships are absent outside the vacuum domain. Although it is difficult to imagine a long-living vacuum domain, the proposed model provides for a satisfactory explanation (at least on a qualitative phenomenological level) for the appearance of emission, the system weight variations, and the conversion of energy taken from the surrounding medium into the rotational mechanical moment of the rollers. Unfortunately, the theory cannot provide a physical pattern of the observed phenomena.

Conclusion. At present, the works on a developed variant of the converter are in progress at the Glushko "NPE Énergomash" stock company (Moscow). This setup would allow a deeper insight into the physics of observed phenomena. Another aim is the creation of commercial samples for various practical applications.

REFERENCES

1. J. A. Thomas, Jr., in *ANTI-GRAVITY: The Dream Made Reality: The Story of John R. R. Searl* (Direct International Science Consortium, London, 1994), Vol. VI, Iss. 2.
2. V. L. Dyatlov, *Polarization Model Heterogeneous Physical Vacuum* (Inst. Mat., Novosibirsk, 1998).

Translated by P. Pozdeev

A01-34136

AIAA 2001-3361

Antimatter Production at a Potential Boundary

Michael LaPointe
Ohio Aerospace Institute
Cleveland, OH 44135

37th AIAA/ASME/SAE/ASEE Joint Propulsion Conference
Salt Lake City, UT
July 8 – 11, 2001

AIAA 2001-3361

ANTIMATTER PRODUCTION AT A POTENTIAL BOUNDARY

Michael LaPointe*
Ohio Aerospace Institute
Cleveland, OH

ABSTRACT

Current antiproton production techniques rely on high-energy collisions between beam particles and target nuclei to produce particle and antiparticle pairs, but inherently low production and capture efficiencies render these techniques impractical for the cost-effective production of antimatter for space propulsion and other commercial applications. Based on Dirac's theory of the vacuum field, a new antimatter production concept is proposed in which particle-antiparticle pairs are created at the boundary of a steep potential step formed by the suppression of the local vacuum fields. Current antimatter production techniques are reviewed, followed by a description of Dirac's relativistic quantum theory of the vacuum state and corresponding solutions for particle tunneling and reflection from a potential barrier. The use of the Casimir effect to suppress local vacuum fields is presented as a possible technique for generating the sharp potential gradients required for particle-antiparticle pair creation.

INTRODUCTION

Present chemical engines and electric propulsion thrusters are well suited for near-Earth applications and robotic space flight, but advanced propulsion technologies must be developed to enable fast piloted and robotic deep space missions. Of all the known energy sources, none provides more specific energy than the annihilation of matter and antimatter. The energy released per kilogram of combined matter and antimatter is nearly 250 times the specific energy released in nuclear fusion, and over 8 orders of magnitude greater than the specific energy released in chemical combustion.[1] The possibility of producing photon rockets using gamma rays from electron-positron annihilation was investigated over half a century ago,[2] but the efficiency of the engines were curtailed by an inability to collimate the energetic photons. With the experimental discovery of the antiproton in 1955, attention turned to the use of proton-antiproton annihilation as an energy source for spacecraft propulsion. The higher rest mass energy of the proton-antiproton pair yields 1877 MeV per annihilation event, compared with 1.02 MeV released by electron-positron annihilation. Equally important, a significant fraction of the proton-antiproton annihilation energy appears in the kinetic energy of charged particles,[3-5] which may be collimated for direct thrust or used to heat an expellant more effectively than electron-positron gamma radiation. Several antiproton-powered rocket designs have been proposed over the past few decades, ranging from low thrust, high specific impulse pion engines to higher thrust, lower specific impulse solid and gas core thermal rockets.[6-20] Recent modeling efforts have simulated the performance of magnetically confined hydrogen plasma engines heated by charged proton-antiproton annihilation byproducts[21-24] and have investigated antiproton-boosted fission reactions as a driver for an inertial confinement fusion rocket.[25,26]

Although a number of potential antiproton propulsion concepts have been analyzed, their transition from theoretical design to experimental validation and practical use has been constrained by the prohibitive cost of creating and storing the antiprotons. The following section discusses current antiproton production methods, and outlines near-term prospects for efficient antiproton production and storage.

Current Antiproton Production Methods

The two leading facilities for antiproton production and storage are the European Laboratory for Particle Physics (formerly CERN, the Center for European Nuclear Research) in Geneva, and the Fermi National Accelerator Laboratory (FNAL) in the United States. At the

* Senior Research Associate; Member, AIAA

CERN facility, protons are accelerated by a linear accelerator to 50 MeV ($8x10^{-12}$ J), injected into a booster ring and accelerated to 800 MeV, and then sent to a proton synchrotron, where they are further accelerated to 26 GeV. The high-energy protons are then focused into a 2-mm beam and directed into a 3-mm diameter, 11-cm long copper wire target. The relativistic protons collide with the target nuclei, producing a spray of gammas, pions, kaons, and baryons, including antiprotons. On leaving the target, the antiprotons have a peak momentum of 3.5 GeV/c, corresponding to a peak energy of roughly 3 GeV. A short focal length, pulsed magnetic horn is used to capture antiprotons that have momenta within 1.5% of their peak value, at angles up to 50 mrad from the target centerline. The captured antiprotons are sent to a storage ring in bursts of about 10^7 antiprotons every few seconds, and around 10^{11} antiprotons can be accumulated before space charge effects scatter the circulating beam. The antiprotons are sent back to the proton synchrotron, which decelerates them to an energy of 200 MeV, and then to the low energy antiproton ring, where the circulating beam is further decelerated, stochastically cooled, and stored. Similar techniques are used to create antiprotons at FNAL.

During the high-energy collisions, approximately one antiproton is created for every 10^5-10^6 high-energy protons incident on the target. The energy efficiency, defined as the energy released in a proton-antiproton annihilation event (1.88 GeV at rest) divided by the energy required to create an antiproton, is abysmally low. On average, CERN creates 1 antiproton for every $2.5x10^6$ protons; at an average energy of 26 GeV per proton, the corresponding energy efficiency is approximately $3x10^{-8}$. FNAL, which uses a 120 GeV proton beam to strike the target, creates 1 antiproton for every $3.3x10^4$ protons, corresponding to an energy efficiency of around $4x10^{-7}$. Assuming a "wall-plug" efficiency for each accelerator of around 5%, the total antiproton production efficiencies are roughly $1.5x10^{-9}$ for CERN and $2x10^{-8}$ for FNAL. The total annihilation energy contained in 1-mg of antiprotons (roughly $6x10^{20}$ antiprotons) is $1.8x10^{11}$ J; an efficiency of $1.5x10^{-9}$ means that it would take nearly $1.2x10^{20}$ J ($3.3x10^{13}$ kW-hr) to create 1 mg of antiprotons. Assuming a conservative energy cost of $0.05/kW-hr, the estimated production cost is a staggering $\$1.6x10^{11}$ per milligram of antiprotons. Most antimatter propulsion concepts require milligrams to grams of antiprotons, indicating that current antiproton production techniques are inadequate for future spacecraft propulsion applications. However, as discussed by Forward[1] and Schmidt *et al.*,[27] neither CERN nor FNAL were designed as dedicated antiproton production facilities. As such, a number of upgrades to the current facilities could be made to improve antiproton production and storage capabilities. Magnetic fields produced by electric currents flowing through the metal wire targets could be used to keep the spray of antiprotons closer to the target axis, reducing their angular spread. Multiple targets could be employed, with magnetic lenses used to refocus the antiprotons between each section. Angular capture efficiencies could be improved by going to higher beam energies, creating a forward-peaked distribution that allows more antiprotons to be captured. Material lenses could be replaced with current-carrying plasma lenses, which are less likely to absorb the antiprotons and would not need active cooling. Using linear rather than synchrotron accelerators to produce the initial high-energy proton beams could increase the accelerator energy efficiency by an order of magnitude over the current 5%wall plug efficiencies.

Taken together, the potential facility improvements could result in the yearly production and storage of microgram quantities of antiprotons at a potential cost[27] of around $\$6.4x10^6/\mu g$ ($\$6.4x10^9$/mg). While these production numbers and costs are approaching those required for ground testing antimatter propulsion concepts, they are not adequate for antimatter-based propulsion systems. Forward[1,20] calculates that antiproton propulsion becomes cost competitive with chemical propellant systems at an antiproton production cost of approximately $\$10^7$/mg, and antiproton propulsion becomes the most cost effective propulsion source available if the production costs can be lowered to $\$2x10^6$/mg. Because the near term facility modifications outlined above are unlikely to produce the necessary reduction in antiproton production costs, a number of alternative antiproton production techniques have been suggested. Chapline[28] has proposed colliding heavy ion beams, made up of singly charged uranium atoms, to produce up to 10^{18} antiprotons/sec. Unfortunately, the antiprotons will be emitted isotropically and will be very difficult to collect. Equally problematic, the colliding heavy ion beams will produce a significant amount of nuclear debris and radiation, which would have to be safely and efficiently removed from the spray of antiprotons. Cassenti[29] has suggested that the pions generated during the collision of high-energy protons with heavy target nuclei could be redirected toward the target to increase the number of antiprotons and improve the efficiency of current antiproton production techniques. Although promising, the collection and redirection of the pions and antiprotons remains a major challenge to this concept.

Hora[30] proposed the use of a high intensity laser that could generate sufficiently strong electric fields to pro-

duce proton-antiproton pairs from the vacuum, and Crowe[31] separately proposed the use of high intensity lasers to produce electron-positron pairs. At present, however, there are no known lasers that can produce the high intensity electric fields needed for pair production. Forward[1,20] and Haloulakos and Ayotte[32] have investigated the possibility of building and operating an antiproton factory in space, where the proton accelerator could be powered by solar energy. However, the estimated cost to produce and store the antiprotons is still nearly $\$10^9$/mg, which is a factor of 10^2 too high for cost-effective space propulsion applications.[32]

Rather than rely on high-energy proton beam collisions with a stationary target, this paper outlines a new concept that may lead to the more efficient production of antimatter in quantities sufficient for propulsion and other commercial applications. The proposed technique is based upon particle-antiparticle pair production at the steep potential boundary created by the suppression of local vacuum field energies. The premise is based on Dirac's relativistic theory of the vacuum state, which is outlined in the following section. The theory underlying particle-antiparticle pair creation at a potential boundary is discussed, followed by an explanation of the technique proposed to create the required potential step. The paper concludes with an overview of an experimental approach designed to demonstrate the feasibility of this new antimatter production concept.

DIRAC'S THEORY OF THE VACUUM STATE

Dirac was the first to develop a relativistic wave equation that correctly describes the interaction of spin-1/2 particles, such as electrons and protons.[33] Dirac's equation contains both positive and negative energy solutions, the latter identified with the continuum energy of the vacuum state (Fig. 1). As defined by Dirac, the vacuum state is characterized by the absence of all real electrons in positive energy states, but has electrons filling all negative energy states (the "Dirac sea"). Because of the Pauli exclusion principle, real electrons cannot transition into negative energy states since all such states are already occupied; however, an electron in a negative energy state can absorb radiation and transition to a positive energy state, leaving behind a "hole" in the negative energy continuum. The hole behaves like a positive electron and represents the antiparticle of the electron. The creation of an electron and an antielectron (positron) is identified as pair creation and requires a minimum energy of $2m_oc^2$. Pair annihilation occurs when an electron drops back into the (unoccupied) hole, with the resulting transition energy emitted as radiation.

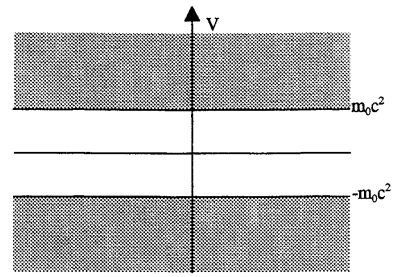

Figure 1. Energy Levels of the Dirac Equation

More generally, in Dirac's theory the vacuum represents a continuum of negative energy states occupied by negative energy particles. Pair creation is the process in which sufficient energy is given to a particle in the negative energy state to raise it to a positive energy state (creating a real particle and leaving behind a hole, or antiparticle); annihilation occurs when the particle falls back into the hole, with the energy carried away as radiation. The vacuum itself should have zero energy, zero mass, and no charge, which is clearly not satisfied by the simple form of the theory. Instead, there are infinitely many negative energy states, which together have an infinitely large negative energy, and, in the case of electrons populating the negative energy continuum, an infinitely large negative charge. These difficulties are removed by renormalizing the zero point of charge and energy in such a way that the vacuum has no mass, energy, or charge. This renormalization process is not pleasing from an aesthetic viewpoint, but it does satisfy the constraint that only departures from the vacuum state are observable and hence relevant.

TUNNELING AND POTENTIAL BARRIERS

Related to Dirac's theory of the vacuum is the quantum mechanical process of particle tunneling in the presence of a steep potential step. An overview of this process is provided by Greiner,[34] the salient features of which are given here.

Consider a spin-1/2 particle (for example, an electron or proton) with energy, E, and momentum, p, traveling along the z-axis (Figure 2). The particle encounters a step potential of magnitude V_0 that rises to full value in a distance equal to the Compton wavelength of the particle, λ_c:

$$\lambda_c = \frac{h}{m_0 c} \tag{1}$$

where h is Planck's constant (6.626×10^{-34} J-s), m_0 is the

particle rest mass, and c is the speed of light.

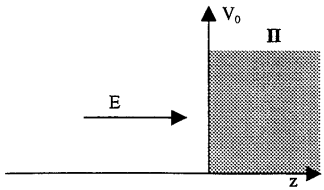

Figure 2. Particle incident on a potential step.

The Dirac equation describing the propagation of the particle in Region I is:

$$i\hbar\frac{\partial\psi}{\partial t}=\left[\frac{\hbar c}{i}\left(\hat{\alpha}_1\frac{\partial}{\partial x^1}+\hat{\alpha}_2\frac{\partial}{\partial x^2}+\hat{\alpha}_3\frac{\partial}{\partial x^3}\right)+\hat{\beta}m_0c^2\right]\psi=H_f\psi \quad (2)$$

where ψ is the particle wave function, $\hbar$ is the reduced Planck constant (h/2π), H_f is the Hamiltonian, and $\hat{\alpha},\hat{\beta}$ are the standard Dirac matrices. Noting that the momentum operator $\vec{p}$ is given by:

$$\vec{p}=\frac{\hbar c}{i}\left(\hat{\alpha}_1\frac{\partial}{\partial x^1}+\hat{\alpha}_2\frac{\partial}{\partial x^2}+\hat{\alpha}_3\frac{\partial}{\partial x^3}\right)=\frac{\hbar}{i}\nabla \quad (3)$$

the Dirac equation can be written in the more compact form:

$$i\hbar\frac{\partial\psi}{\partial t}=\left[c(\hat{\alpha}\cdot\vec{p})+\hat{\beta}m_0c^2\right]\psi=H_f\psi \quad (4)$$

The Hamiltonian for Region I (zero potential) is the total particle energy, E, while in Region II the Hamiltonian becomes (E-V_0). The Dirac equation for a particle wave traveling along the +z direction in Region I is then:

$$\left[c(\hat{\alpha}_3\cdot\vec{p}_1)+\hat{\beta}m_0c^2\right]\psi=(E-V_0)\psi \quad (5)$$

In Region II, the Dirac equation for the traveling particle wave becomes:

$$\left[c(\hat{\alpha}_3\cdot\vec{p}_1)+\hat{\beta}m_0c^2\right]\psi=E\psi \quad (6)$$

The solution for the particle wave function in Region I is:

$$\psi_I=A\begin{pmatrix}1\\0\\\dfrac{p_1c}{E+m_0c^2}\\0\end{pmatrix}\exp\left[\frac{ip_1z}{\hbar}\right] \quad (7)$$

where A is a constant and the particle momentum, p_1c, is given by:

$$p_1c=\sqrt{E^2-m_0^2c^4} \quad (8)$$

At the potential boundary, part of the particle wave will be reflected and part will be transmitted. The reflected wave solution in Region I is:

$$\psi_I^r=B\begin{pmatrix}1\\0\\\dfrac{-p_1c}{E+m_0c^2}\\0\end{pmatrix}\exp\left[\frac{-ip_1z}{\hbar}\right] \quad (9)$$

and the transmitted solution in Region II is:

$$\psi_{II}=D\begin{pmatrix}1\\0\\\dfrac{-p_2c}{V_0-E-m_0c^2}\\0\end{pmatrix}\exp\left[\frac{ip_2z}{\hbar}\right] \quad (10)$$

where again B and D are constants. The particle momentum in Region II is given by:

$$p_2c=\sqrt{(E-V_0)^2-m_0^2c^4} \quad (11)$$

The incident and reflected wave functions must equal the transmitted wave function at the step boundary (z=0):

$$\psi_I\big|_{z=0}+\psi_I^r\big|_{z=0}=\psi_{II}\big|_{z=0} \quad (12)$$

from which the following conditions are obtained for the coefficients A, B and D:

$$A+B=D \quad (13)$$

$$\begin{aligned}A-B&=-D\frac{p_2}{p_1}\left(\frac{E+m_0c^2}{V_0-E-m_0c^2}\right)\\&=-D\sqrt{\frac{(V_0-E+m_0c^2)(E+m_0c^2)}{(V_0-E-m_0c^2)(E-m_0c^2)}}=-D\gamma\end{aligned} \quad (14)$$

where γ is defined as:

$$\gamma=\sqrt{\frac{(V_0-E+m_0c^2)(E+m_0c^2)}{(V_0-E-m_0c^2)(E-m_0c^2)}} \quad (15)$$

Upon rearrangement, Equations 13 and 14 yield:

$$\frac{B}{A}=\left(\frac{1-\gamma}{1+\gamma}\right) \tag{16}$$

Dividing Equation 14 by the coefficient A and substituting Equation 16 for (B/A) yields:

$$\frac{D}{A}=\frac{2}{1-\gamma} \tag{17}$$

The particle current j is defined to be:

$$j(z)=c\psi^{\dagger}(z)\hat{\alpha}\psi(z) \tag{18}$$

where $\psi^{\dagger}(z)$ is the adjoint of $\psi(z)$. The values of $\psi^{\dagger}\hat{\alpha}$ in Region I are:

$$\begin{aligned}
\psi_I^{\dagger}\hat{\alpha}_1 &= A^*\left(0,\frac{p_1c}{E+m_0c^2},0,1\right)\exp\left[\frac{-ip_1z}{\hbar}\right]\\
\psi_I^{\dagger}\hat{\alpha}_2 &= A^*\left(0,-i\frac{p_2c}{E+m_0c^2},0,-i\right)\exp\left[\frac{-ip_1z}{\hbar}\right]\\
\psi_I^{\dagger}\hat{\alpha}_3 &= A^*\left(\frac{p_1c}{E+m_0c^2},0,1,0\right)\exp\left[\frac{-ip_1z}{\hbar}\right]
\end{aligned} \tag{19}$$

from which j_I, the incident particle current in Region I, is:

$$j_I=-AA^*\frac{2p_1c^2}{E+m_0c^2} \tag{20}$$

Similarly, the reflected (j_I^r) and transmitted (j_{II}) particle currents are:

$$j_I^r=-BB^*\frac{2p_1c^2}{E+m_0c^2} \tag{21}$$

$$j_{II}=DD^*\left(\frac{-2p_1c^2}{V_0-E-m_0c^2}\right) \tag{22}$$

Equations 20-22 can now be used to calculate the reflection and transmission coefficients for the particle wave function impacting the potential boundary. Taking the ratio of the reflected current to the incident particle current yields:

$$\frac{|j_I^r|}{|j_I|}=\left|\frac{BB^*\dfrac{2p_1c^2}{E+m_0c^2}}{AA^*\dfrac{2p_1c^2}{E+m_0c^2}}\right|=\left|\frac{BB^*}{AA^*}\right|=\left|\frac{B^2}{A^2}\right|=\frac{(1+\gamma)^2}{(1-\gamma)^2} \tag{23}$$

The ratio of the transmitted current to the incident current is given by:

$$\frac{|j_{II}|}{|j_I|}=\left|\frac{DD^*\dfrac{2p_2c^2}{V_0-E-m_0c^2}}{AA^*\dfrac{2p_1c^2}{E+m_0c^2}}\right|=\left|\frac{DD^*}{AA^*}\right|\gamma$$
$$=\left|\frac{D^2}{A^2}\right|\gamma=\frac{4\gamma}{(1-\gamma)^2} \tag{24}$$

For a potential step $V_0 > (E+m_0c^2)$, the value $\gamma>1$. From Equation 23, this indicates that the reflected particle current exceeds the incident particle current in Region I ($|j_I^r|>|j_{II}|$). It appears that electrons are entering Region I from Region II, but there are no electrons initially present in Region II. This result, known as Klein's Paradox, is most often interpreted as particle-antiparticle pair creation at the potential boundary.

Discussion of Results.

Applying a potential $V_0 > E + m_0c^2$ raises the energy in Region II sufficiently for there to be an overlap between the negative energy continuum ($z>0$) and the positive energy continuum ($z<0$), as shown in Figure 3:

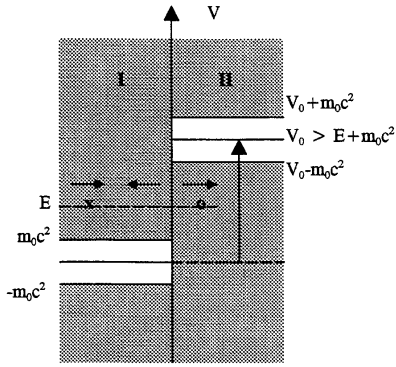

Figure 3. Energy Continuum of the Dirac Equation at a Potential Barrier.[34] (x) = particle, (o) = antiparticle

When $V_0 > E + m_0c^2$, the particles striking the barrier from the left are able to knock additional particles out of the vacuum on the right, leading to an antiparticle current flowing from the left to the right in Region II and a particle current flowing from right to left in Region I. This pair creation is depicted schematically in Figure 3, with the additional particles entering Region I from the right accounting for the increase in return cur-

rent. As noted by Greiner,[34] this process is most readily understood as particle-antiparticle pair creation at the potential barrier and is related to the decay of the vacuum in the presence of supercritical fields. When the potential function V_0 is less than $E + m_0c^2$, the particle momentum in Region II is imaginary (Eq. 11) and the wave solution will be exponentially damped (Eq. 10); all of the incident current is then reflected back into Region I, and no particle current is transmitted into Region II. It is only when $V_0 > E + m_0c^2$ that the momentum in Region II becomes real and the particle wave function in Region II again becomes a traveling wave.

The above derivations may be summarized as follows:

- The Dirac equation is used to represent the evolution of spin-1/2 particle wave functions.
- Dirac's equation permits both positive and negative energy solutions; the negative energy states are filled with virtual particles, which prevent particle transitions from positive energy states to negative energy states via the Pauli exclusion principle.
- Particles will be completely reflected from a potential barrier (V_0) when their energy $E < V_0$; the transmitted particle wavefunction is exponentially damped within the potential barrier.
- For potential steps with $V_0 > E + m_0c^2$, an incident particle will induce pair creation at the potential boundary, resulting in a (real) return particle current and a (real) transmitted antiparticle current.

The question now arises as to whether this effect can actually be applied to the production of antimatter. The potential step must be greater than $E + m_0c^2$, where E is the total particle energy (rest mass plus kinetic), and the potential must rise to its full value over a distance comparable to the Compton wavelength of the particle, $h/(m_0c)$. For an electron, the minimum potential step height is 1.02 MeV (plus the kinetic energy of the electron), and the Compton wavelength is approximately 2.4×10^{-12} m. For a proton, the minimum potential step height is 1876 MeV and the Compton wavelength is approximately 1.3×10^{-16} m. These supercritical potentials are too large to be generated over such short distances using laboratory electric fields, but there may be another option: rather than use externally applied fields to raise the vacuum energy in Region II, it may be possible to use the Casimir effect to lower the vacuum energy in Region I. This concept, shown schematically in Figure 4, may be able to produce the same pair creation effects depicted in Figure 3 without requiring the application of supercritical external fields. A brief discussion of the Casimir effect is provided below, followed by an outline of a possible experimental test of the proposed antimatter production mechanism.

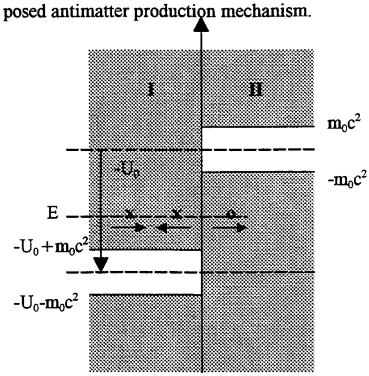

Figure 4. Lowering the vacuum energy via the Casimir effect.

VACUUM FIELDS AND THE CASIMIR EFFECT

Dirac's vacuum is a negative energy continuum populated by particles that prevent positive energy particles from transitioning into the negative energy states. To avoid obvious problems associated with infinite vacuum charges and energies, the vacuum state is renormalized to zero; only deviations from the vacuum state are measurable. As such, the potential step shown in Figure 3 represents an applied field measured with respect to the background vacuum; the energy in Region II has been raised by the applied field such that the negative energy states now overlap the positive energy states in Region I. However, raising the background vacuum in Region II requires a tremendous amount of energy ($V_0 > E + m_0c^2$) over a very small distance, which is clearly beyond present capabilities. Rather than raising the vacuum energy in Region II, it is proposed that the same effect can be generated by suppressing the relative vacuum energy in Region I, as shown in Figure 4. This process can be viewed either as lowering the positive energy states such that they now overlap with the negative energy states in Region II, or the background vacuum in Region I can be renormalized to zero to yield an energy diagram similar to Figure 3. In either instance, a particle wave traveling from Region I into Region II will be described by the same solutions outlined in the section above, leading to particle-antiparticle pair creation at the potential boundary. Unlike Figure 3, pair production is achieved not by raising the potential but by lowering the relative vacuum energy, an effect that might be accomplished through the use of a Casimir cavity.

Before discussing the Casimir effect, it should be noted that Dirac's interpretation of the vacuum as a continuum of negative energy states occupied by negative energy particles, though somewhat dated, is not in disagreement with the current quantum electrodynamic (QED) interpretation of the vacuum as an infinite sea of electromagnetic radiation populated with virtual particle pairs. Because exchange interactions occur in Dirac's theory, virtual electron-positron pairs are continuously created and annihilated in the vacuum; an electron in a bound or free state can fill a virtual hole in the Dirac sea, with a virtual electron taking its place. Renormalization of the vacuum energy and charge is required both in Dirac's original theory and in QED, and as noted by Greiner,[34] the physical content of the Dirac theory forms the basis of current quantum electrodynamics. This is mentioned because the Casimir effect is generally discussed in terms of the QED interpretation of the vacuum state, and it is necessary to point out that both the Dirac and QED vacuum interpretations are complementary.

The Casimir Effect

As in the Dirac theory, the vacuum state in quantum electrodynamics is interpreted to be the state of lowest energy. This lowest energy state is not at rest, but fluctuates with a "zero-point" energy.[35-39] The vacuum fluctuations have measurable effects, including the experimentally observed Lamb-Retherford shift between the *s* and *p* energy levels of the hydrogen atom, and the attractive Casimir force that occurs between closely spaced uncharged conductors. As discussed by Mostepanenko *et al.*,[35] the Casimir effect can be accounted for by assuming the force is a consequence of the separation-dependent vacuum field energy trapped between the conductors. For example, assume that two square conducting plates with side dimensions L, separated by a distance z, are placed in a vacuum. In the QED interpretation, the vacuum is teeming with electromagnetic radiation (although mathematically the vacuum state is renormalized to zero), hence the plates may be considered to constitute a cavity that supports vacuum fluctuation modes with wave numbers down to about z^{-1}. The vacuum energy trapped between the plates is approximately given by:

$$U = \sum_{k=\frac{1}{2}}^{K} \frac{1}{2}\hbar\omega \approx (L^2 z)\int_{z^{-1}}^{K} \hbar c k k^2 dk \cong \frac{1}{4}L^2\hbar c\left[zK^4 - z^{-3}\right] = U_U - U_L \tag{25}$$

where U_U is the upper energy bound, U_L is the lower energy bound, and K represents a high frequency cut-off to make the total energy finite. The negative rate of change of the lower cut-off energy U_L with separation z constitutes a force of attraction, F, per unit area, given by:

$$\frac{F}{A} = -\frac{1}{L^2}\frac{dU_L}{dz} \approx \frac{\hbar c}{z^4} \tag{26}$$

A more careful analysis leads to the exact relationship for the force per unit area between the parallel conducting plates:[39]

$$\frac{F}{A} = \frac{\pi^2}{240}\frac{\hbar c}{z^4} \tag{27}$$

In other words, the vacuum energy density between the plates is lower than the vacuum energy density outside the plates by an amount equal to the right hand side of Equation 27. For reasonable plate sizes and small separation distances, the change in the vacuum energy density can be appreciable. Assuming the plates have length L=0.1 m and are separated by a distance of 1-μm (10^{-6} m), the change in the vacuum energy density is approximately $1.3\text{x}10^{-4}$ J/m^3, corresponding to an inward pressure of $1.3\text{x}10^{-4}$ N/m^2 on the plates. For a separation distance of 0.1-μm (10^{-7} m), the change in the vacuum energy density is equal to 1.3 J/m^3, corresponding to an inward pressure of 1.3 N/m^2. The calculations can be carried down to separation distances that are approximately equal to the cut-off wavelength of the conducting material, at which point the plates can no longer be considered good electromagnetic reflectors.

Equations 26 and 27 demonstrate that the vacuum energy density between the conducting plates is lower than the external vacuum energy density. Multiplying Equation 27 by the plate surface area (L^2) and the separation distance between the plates (z) yields an expression relating the decrease in the vacuum energy between the plates compared to the external vacuum field energy:

$$\Delta E_{VAC} = -\frac{\pi^2}{720}\frac{\hbar c L^2}{z^3} \tag{28}$$

For square plate dimensions of L = 0.1 m and a separation distance of 0.1-μm, the change in vacuum energy is calculated to be $4.3\text{x}10^{-9}$ J, or roughly $2.7\text{x}10^{10}$ eV (27 GeV). The vacuum energy between the plates is thus substantially lower than the vacuum energy external to the plates, or conversely, if the vacuum energy between the plates is renormalized to zero, the vacuum energy external to the plates is substantially higher than the vacuum energy between the plates. By adjusting the plate dimensions and separation distance, it may thus be possible to significantly suppress the vacuum energy in a given region and generate a condition similar to that shown in Figure 4. A particle generated in the suppressed vacuum fields of Region I will see a higher vacuum field energy outside of the plates, and if the relative change in the vacuum energy exceeds $E+m_0c^2$, it may be possible to generate particle-antiparticle pairs

at the vacuum energy step. Because the Dirac solutions hold equally well for electrons or protons, the possibility exists that low energy proton-antiproton pairs might be created at the steep potential boundary created by vacuum field suppression in a Casimir cavity.

Creating a Potential Gradient

The Casimir effect provides an avenue for creating sufficiently large potential steps, but the question arises as to whether these steps can be generated over a distance comparable to the Compton wavelength of the particle. From Equation 1, the Compton wavelength for electrons is 2.42×10^{-12} m, while for protons the Compton wavelength is 1.32×10^{-15} m. Either distance is several orders of magnitude smaller than any realistic plate thickness separating the interior and exterior vacuum fields, hence typical flat plates will not provide a sufficiently steep potential step for pair creation to occur.

A possible solution to this dilemma is to create a suitable potential gradient over a distance larger than the Compton wavelength, such that the required step change in potential occurs over a distance comparable to the Compton wavelength. Assuming the required potential step has magnitude V and the change in vacuum field energy due to the Casimir effect has magnitude ΔE_{vac}, the gradient relation can be expressed:

$$\frac{V}{\lambda_c} \approx \frac{\Delta E_{vac}}{d} \tag{29}$$

where λ_c is the Compton wavelength of the particle and d is the plate thickness, or more properly the thickness of the region over which the change in vacuum field energy occurs. For pair production to occur at the step boundary, the potential V must exceed $E+m_0c^2$, where E is the total energy of the particle (rest mass plus kinetic energy). Assuming the particle kinetic energy at the boundary is small compared to its rest mass energy, the requirement for V becomes:

$$V \geq 2m_0c^2 \tag{30}$$

Inserting Equations 28 and 30 into Equation 29 yields the following expression for the plate area, thickness, and separation as a function of particle mass and Compton wavelength:

$$\frac{2m_0c^2}{\lambda_c} \approx \frac{\pi^2 \hbar c L^2}{720 z^3 d} \tag{31}$$

which reduces to:

$$\frac{L^2}{z^3 d} \approx 4.15 \times 10^{44} \frac{m_0}{\lambda_c} \tag{32}$$

Equation 32 expresses necessary conditions for a flat parallel plate geometry to form a sufficiently steep potential gradient for particle-antiparticle pair production to occur. For electrons, this condition can be written:

$$\frac{L^2}{z^3 d} \approx 1.56 \times 10^{26} (m^{-2}) \tag{33}$$

Assuming a plate separation distance $z = 10^{-7}$ m and a gradient length $d = 10^{-6}$ m, the required plate area, L^2, is around 0.156 m^2; for square plates this corresponds to a side length of approximately 0.4 m. Plates of this size and flatness are well within current manufacturing capabilities, offering some encouragement for experimental verification of the proposed concept. For protons,

$$\frac{L^2}{z^3 d} \approx 5.26 \times 10^{32} (m^{-2}) \tag{34}$$

Using the same plate separation and gradient distances above would require a plate length of 725 m to provide a suitable potential gradient. However, a number of Casimir force experiments have been performed over the past several years with plate separations down to several nanometers, and a reasonable lower limit of 10^{-8} m can be assumed for the plate separation z. The distance over which the potential gradient is formed, d, can also be reduced by locally thinning the plate support structure; a more realistic lower bound on d is thus assumed to be 10^{-9} m. Given these values, the plate size for producing the required potential step for proton-antiproton pair production is around 0.73 m, which is difficult but not impossible to manufacture.

Ideally, the potential gradient would be formed in a region devoid of plate material; this can be accomplished by designing the Casimir plate with a small hole whose diameter is of the same order or smaller than the plate separation distance. Vacuum electromagnetic fields with wavelengths larger than the hole diameter will still be blocked by the cavity, but the potential gradient formed by the plates is now in a material-free region that more faithfully reproduces the assumptions behind Figures 3 and 4. Possible effects due to the fringing of vacuum electromagnetic fields at the hole boundaries remain to be evaluated, but this method appears promising to provide the required potential gradients in a material-free region.

Summary. In summary, it appears possible to produce a Casimir cavity geometry that will provide sufficiently steep potential gradients for particle-antiparticle pair creation. By introducing a small hole in the plate material with a diameter similar to the plate separation distance, a potential step may be created in a material-free region, as depicted in Figure 4. Electron-positron pairs and proton-antiproton pairs can conceivably be gener-

ated using this technique, with significantly less infrastructure and presumably lower cost than current antimatter production methods.

EXPERIMENTAL DESIGN

The following experiment is proposed to evaluate the possibility of producing particle-antiparticle pairs at a potential boundary created within a Casimir cavity. The proposed experiment is a modified version of a similar experiment performed by the author under a prior contract to the NASA Marshall Space Flight Center.[40] In that experiment, flat parallel plates were used to form a Casimir cavity to investigate pair creation, but the plate geometries were not properly designed to generate sharp potential gradients. Based on that effort and the additional analysis in this report, the following experiment is suggested for a proof-of-concept test.

Electron-Positron Production

To investigate the formation of electron-positron pairs, it is proposed that a Casimir cavity be constructed from two flat, square metallic plates, each with an area of 1.61×10^{-2} m^2 ($L = 12.7$ cm). From Equation 33, spacing the plates a distance $z = 10^{-7}$ m apart should provide a suitably steep potential gradient for electron-positron pair creation to occur. To create a material free region for the steep potential step, one plate should include a central hole, drilled perpendicular to the plate boundary, of diameter $d \leq 10^{-7}$ m; vacuum electromagnetic fields with wavelengths larger than d will still be blocked by the cavity, although there may be minor effects on the potential step due to field fringing. On the opposite plate, a small amount of radioactive material can be deposited to act as a source of electrons within the cavity; Ni^{63} is a readily available commercial source, and the kinetic energy of the emitted electrons (0.067 MeV) are sufficiently below the rest mass energy of the electron that Equation 30 remains a viable approximation. Alternatively, the metallic plate can be irradiated to produce subsequent electron emissions within the cavity.

The plate surfaces must be aligned and moved to within 10^{-7} m to form the required potential step, which can be accomplished using commercially available piezoelectric transducers. The close separation distance requires that the surface flatness of the plates not exceed 10^{-8} m, which is a stringent but commercially attainable constraint. The entire system should be mounted in a vacuum system capable of achieving a hard vacuum ($\leq 10^{-8}$ torr), and isolated from vibrations. To evaluate whether the proposed pair production method works, a small target placed outside the central plate hole can be used to intercept any positrons emitted at the potential boundary. The resulting annihilation of the positrons with the target material will produce 0.511-MeV gamma rays that can be measured with a detector located behind the target.

Proton-Antiproton Production

If successful, the experimental arrangement outlined above will demonstrate the basic feasibility of the proposed pair production process. However, for propulsion applications it is desirable to produce antiprotons rather than positrons. As previously discussed, the constraints on plate size, flatness, and separation become significantly more demanding, but remain within the capability of current manufacturing techniques. For proton-antiproton pair production, square plates with areas of 0.526 m^2 ($L = 0.725$ m) would have to be separated by a distance of 10^{-8} m, indicating that the surface flatness of the plates would have to be on the order of angstroms. Larger plate areas would relax this constraint by allowing larger separation distances, and the ability to machine flat surface areas must be traded against the fabrication of larger plate dimensions. The central hole diameter would again be on the order of the plate separation distance to provide a material-free potential step, and the electron source would be replaced with a proton source to provide the particles within the cavity. If this scheme is successful, the antiprotons can be captured upon exiting through the hole in the Casimir plate and stored in portable Penning traps for later use.

CONCLUDING REMARKS

A new concept has been described for creating matter-antimatter particle pairs at a steep potential boundary. The potential step is created using the Casimir effect to suppress the vacuum energy between parallel conducting plates. Preliminary calculations indicate that a sufficiently steep potential gradient can be formed for reasonable plate dimensions and separation distances. A preliminary experimental design is outlined as a proof-of-concept test for the proposed antimatter production scheme. Additional analysis remains to be performed to validate the concept, including an evaluation of material and temperature effects on the plate boundaries, the effect of fringing fields on the potential step at the plate central hole, and the consequences of imperfect parallel plate alignment on the required potential gradient. Nevertheless, based on the preliminary analysis presented in this paper, the proposed concept appears to be a potentially viable alternative to the high-energy antimatter production methods currently in use.

ACKNOWLEDGEMENTS

Funding for this research was provided through NASA SBIR Contract NAS8-98109 during the period April – November 1998.

REFERENCES

1. Forward, R.L., *Antiproton Annihilation Propulsion*, AFRPL-TR-85-034, Forward Unlimited, Oxnard, CA, 1985.

2. Sanger, E., "Zur Theorie der Photoneraketen" ("The Theory of Photon Rockets"), *Ingenieur-Archiv.*, **21**, 1953, pp. 213-226.

3. Morgan, D.L. and Hughes, V.M., "Atomic Processes Involved in Matter-Antimatter Annihilation", *Phys. Rev.*, **D-2** (8), 1979, pp. 1389-1391.

4. Agnew, L.E., Jr., Elioff, T., Fowler, W.G., Lander, R.L., Powell, W.M., Segre, E., Steiner, H.M., White, H.S., Wiegand, C., and Ypsilantis, T., "Antiproton Interactions in Hydrogen and Carbon Below 200 MeV," *Phys. Rev.*, **118** (5), 1960, pp. 1371-1391.

5. Morgan, D.L., *Annihilation of Antiprotons in Heavy Nuclei*, AFRPL TR-86-011, Lawrence Livermore National Laboratory, Livermore, CA, Apr 1986.

6. Massier, P., "The Need for Expanded Exploration of Matter-Antimatter Annihilation for Propulsion Applications," *J. Br. Interplanetary Soc.*, **35** (9), 1982, pp. 387-390.

7. Forward, R.L., "Antimatter Propulsion," *J. Br. Interplanetary Soc.*, **35** (9), 1982, pp. 391-395.

8. Cassenti, B.N., "Design Considerations for Relativistic Antimatter Rockets," *J. Br. Interplanetary Soc.*, **35** (9), 1982, pp. 396-404.

9. Morgan, D.L., "Concepts for the Design of an Antimatter Annihilation Rocket," *J. Br. Interplanetary Soc.*, **35** (9), 1982, pp. 396-404.

10. Cassenti, B.N., "Antimatter Propulsion for OTV Applications," *J. Propulsion and Power*, **1** (2), 1985, pp. 143-149.

11. Vulpetti, G., "Antimatter Propulsion for Space Exploration," *J. Br. Interplanetary Soc.*, **39** (9), 1986, pp. 391-409.

12. Forward, R.L., *Advanced Space Propulsion Study: Antiproton and Beamed Power Propulsion*, AFAL-TR-87-070, Hughes Research Laboratories, Malibu, CA, Oct 1987.

13. Cassenti, B.N., "Energy Transfer in Antiproton Annihilation Rockets," in Antiproton Science and Technology, B.W. Augenstein *et al.*, eds., World Scientific, Singapore, 1988, pp. 574-602.

14. Cassenti, B.N., "Conceptual Designs for Antiproton Propulsion Systems," AIAA Paper No. 89-2333, presented at the 25th Joint Propulsion Conference, Monterey, CA, Jul 10-12, 1989

15. Vulpetti, G., and Pecchioli, M., "Considerations About the Specific Impulse of an Antimatter-Based Thermal Engine", *J. Propulsion and Power*, **5** (5), 1989, pp. 591-595.

16. Howe, S.D., and Metzger, J.D., "Antiproton-Based Propulsion Concepts and Potential Impact on a Manned Mars Mission," *J. Propulsion and Power*, **5** (3), 1989, pp. 295-300.

17. Forward, R.L., *21st Century Space Propulsion Study*, AL-TR-90-030, Forward Unlimited, Malibu, CA, Oct 1990.

18. Tarpley, C., Lewis, M.J., and Kothari, A.P., "Safety Issues is SSTO Spacecraft Powered by Antimatter Rocket Engines," AIAA Paper No. 90-2365, 26th Joint Propulsion Conference, Orlando, FL, Jul 16-18, 1990.

19. Cassenti, B.N., "High Specific Impulse Antimatter Rockets," AIAA Paper No. 91-2548, presented at the 27th Joint Propulsion Conference, Sacramento, CA, June 24-26, 1991.

20. Forward, R.L., and Davis, J., Mirror Matter: Pioneering Antimatter Physics, J. Wiley & Sons, NY, NY, 1988.

21. LaPointe, M.R., Antiproton Annihilation Propulsion Using Magnetically Confined Plasma Engines, Dissertation, U. New Mexico, Dept. Chemical and Nuclear Engineering, Albuquerque, NM, 1989.

22. LaPointe, M.R., "Antiproton Powered Propulsion with Magnetically Confined Plasma Engines", *J. Propulsion and Power*, 7 (5), pp. 749-759.

23. Callas, J.L., *The Application of Monte Carlo Modeling to Matter-Antimatter Annihilation Propulsion Concepts*, JPL D-6830, Jet Propulsion Laboratory, Pasadena, CA, Oct 1989.

24. Huber, F., Antimatterie-Annihilationsantriebe fur Interplanetare Raumfahrtmissionen, Ph.D. Dissertation, Universitat Stuttgart, Institute fur Raumfahrtsysteme, 1994.

25. Lewis, R.A., Newton, R., Smith, G.A., Toothacker, W.S., and Kanzleiter, R.J., "An Antiproton Catalyst for Inertial Confinement Fusion Propulsion," AIAA Paper No. 90-2760, presented at the 26th Joint Propulsion Conference, Orlando, FL, Jul 16-18, 1990.

26. Lewis, R.A., Smith, G.A., Toothacker, W.S., Kanzleiter, R.J., Surratt, M.S., Higman, K.I., and Newton, R.J., "An Antiproton Driver for Inertial Confinement Fusion Propulsion", AIAA Paper No. 91-3618, presented at AIAA/NASA/OAI Conf. on Advanced SEI Technologies, Cleveland, OH, Sep 4-6, 1991.

27. Schmidt, G. R., Gerrish, H. P., Martin, J. J., Smith, G. A., and Meyer, K. J., "Antimatter Requirements and Energy Costs for Near-Term Propulsion Applications", *J. Propulsion and Power*, **16** (5), Sep-Oct 2000, pp. 923-928.

28. Chapline, G. "Antimatter Breeders," *J. Br. Interplanetary Soc.*, **35** (9), pp. 423-424, 1982.

29. Cassenti, B.N., "Concepts for the Efficient Production and Storage of Antimatter," AIAA-93-2031, presented at the 29th Joint Propulsion Conference, Monterey, CA, Jun 28-30, 1993.

30. Hora, H., "Estimates of the Efficient Production of Antihydrogen by Lasers of Very High Intensities," *OptoElectronics*, **5**, 1973, pp. 491-501.

31. Crowe, E.G., "Laser Induced Pair Production as a Matter-Antimatter Source," *J. Br. Interplanetary Soc.*, **36**, 1983, pp. 507-508.

32. Haloulakos, V., and Ayotte, A., "The Prospects for Space-Based Antimatter Production," AIAA Paper 91-1987, presented at the 27th Joint Propulsion Conference, Sacramento, CA, Jun 24-26, 1991.

33. Dirac, P.A.M., Directions in Physics, John Wiley & Sons, New York, NY, 1978, pp. 1-37, 55-70.

34. Greiner, W., Relativistic Quantum Mechanics: Wave Equations, Springer-Verlag, Inc., Berlin, 1994, pp. 261-267.

35. Mostepanenko, V. M. and N. N. Trunov, The Casimir Effect and its Applications, Oxford Science Publications, Clarendon Press, Oxford, 1997.

36. Weinberg, S., The Quantum Theory of Fields, Vol. 1, Cambridge University Press, 1995, pp. 578-593.

37. Forward, R.L., *Mass Modification Experiment Definition Study*, PL-TR-96-3004, Forward Unlimited, Malibu, CA, Feb 1996.

38. Boyer, T.H., "The Classical Vacuum," *Sci. Am.*, **253** (3), Aug 1985, pp. 70-78.

39. Milonni, P.W., The Quantum Vacuum: An Introduction to Quantum Electronics, Academic Press, New York, NY, 1994.

40. LaPointe, M. R., *Antimatter Production at a Potential Boundary*, NASA SBIR Phase I Final Report, Contract NAS8-98109, prepared for the NASA Marshall Space Flight Center, Huntsville, AL, Nov 1998.

A01-34137

AIAA 2001-3363

Gravity Modification by High-Temperature Superconductors

C. Woods
University of Sheffield
Sheffield, UK

S. Cooke
Cooke Computers,
Jersey, British Isles

J. Helme
University of Sheffield
Sheffield, UK

C. Caldwell
Motorola Ltd.
Basingstoke, UK

37th AIAA/ASME/SAE/ASEE
Joint Propulsion Conference and Exhibit
8-11 July 2001
Salt Lake City, Utah

AIAA 2001-3363

GRAVITY MODIFICATION BY HIGH-TEMPERATURE SUPERCONDUCTORS

R.C. Woods, S.G. Cooke*, J. Helme, C.H. Caldwell†

Department of Electronic and Electrical Engineering, University of Sheffield, Mappin Street, Sheffield, S1 3JD, U.K.

ABSTRACT

Claims that the weight of test masses can be changed in non-relativistic experiments have been investigated. Amongst the most prominent reports has been a paper by Podkletnov & Nieminen (Physica C **203** 441, 1992); more recently, Rounds (Proc. NASA Breakthrough Propulsion Phys. Workshop, Cleveland, 297, 1998) used a simpler experimental arrangement. Both of these experiments measure the gravitational field above $YBa_2Cu_3O_{7-\delta}$ (superconducting below $T_c \approx 93K$). Podkletnov & Nieminen specify that the superconductor must be cooled below 70K, magnetically rotated at ~5000 rpm, and simultaneously levitated magnetically using two separate frequency excitations; weight changes of ~1% were reported. Rounds specifies less stringent conditions, mainly that the YBCO is cooled to 77K whilst stationary. The Rounds experiment has been repeated virtually exactly, and the Podkletnov experiment has been investigated by reproducing some of the conditions specified. No measurable gravity modification (within ±0.03%) was observed using the subset of the Podkletnov conditions, (but this does *not* preclude gravity modification arising from the full specified conditions). The Rounds configuration also has not shown any effects reliably ascribable to gravity modification, although there was unusual thermal behaviour.

1. INTRODUCTION

A number of reports recently claimed that the weight of test masses can be changed as a result of using various materials in various configurations and using various excitations. One of the most prominent of these has been that by Podkletnov and Nieminen[1]; as far as the present authors are aware, not only is this the only such paper that has appeared in a peer-reviewed journal, but it is also one of the few that cannot immediately be dismissed as spurious.

The experimental results reported by these authors appear to contradict conventional gravitational theory, because their claims amount to apparent modifications to the gravitational field in a laboratory-based system that – at face value – does not require analysis by General Relativity. This experiment is therefore potentially highly important scientifically because of the enormous technological implications for the design of current transportation vehicles and handling methods for bulk materials if gravity modification (and, in particular, gravitation reduction) were demonstrated to be feasible.

Objections to the Podkletnov and Nieminen experiment have been raised. Podesta and Bull[2] discuss the measurements[1] in terms of buoyancy effects that could be present because of the helium cooling the air surrounding the test weight. Although interesting, the air temperature required to achieve a buoyancy effect of the same magnitude as seen by Podkletnov is 150K which seems to be too low to make this a likely explanation. Unnikrishnan[3] includes a description of static levitation of a large superconducting disk that finds no gravity effect, but is more interesting for its discussion of Podkletnov's claim that the gravitational effects have no dependence on the height above the spinning disk, which appears extremely strange at first sight. This, along with Podkletnov's claims to have seen increases as well as reductions in test mass weight, confirms that the effect claimed must be "Gravity modification" rather than passive "Gravitational shielding".

Pokeltnov's report[1] was therefore selected for particular attention and experimental testing in the present work, along with a subsequent and broadly similar (though smaller) effect reported by Rounds[4]

* Present address: Cooke Computers, Jersey, British Isles.

† Present address: Motorola Ltd., Basingstoke, U.K..

using a much simplified experimental arrangement. The experiment due to Rounds[4] has been repeated virtually exactly, and that due to Podkletnov[1] (experimentally much more challenging) has been investigated by examining some (although not yet all) of the conditions reported as necessary for demonstrating gravity modification.

Both of these experiments have in common that they require the gravitational field to be measured above the high-temperature superconductor $YBa_2Cu_3O_{7-\delta}$ (which is superconducting below the critical temperature $T_c \approx 93$K). In the Podkletnov arrangement, the superconductor (in the form of a multiphase circular disk having a minimum diameter 10cm) must be cooled below 70K, and magnetically rotated at high speed (e.g., 5000 rpm) and simultaneously levitated magnetically using two separate frequency excitations; weight changes (in a test mass) of the order of 1% were reported. In the Rounds arrangement, the conditions are much less stringent and mainly require the YBCO to be cooled to 77K in a stationary magnetic field.

1.1 Other claims of gravity modification

Reiss[5] has reported work on the weight of a PTFE capsule containing pellets of various materials including 2212 BSCCO high-T_c superconductor when the capsule is immersed in liquid nitrogen. All of Reiss's measurements showed the apparent weight rising with immersion time to some final figure after about 5 minutes. This rise is a result of the thermal contraction of the holder (giving a steadily reducing buoyancy in the liquid nitrogen) and shows some scatter as well as differences for different materials contained within the holder. However, Reiss's figures indicate that the capsules containing the superconductor have the biggest apparent weight increase (although not markedly bigger). Reiss interprets this in terms of the superconductor gaining weight as the inside of the sample holder cools below his superconductor's critical temperature (~95K). Reiss points out that the variation in the buoyancy drop found for his three non-superconducting materials (alumina, copper and PVC, in order of the lowest to highest drop) does not match variations in their specific heat. However, the variation in buoyancy drop *does* occur in the same order as the thermal expansion of these materials (i.e. alumina has a thermal expansion coefficient smaller than that of copper, which in turn is smaller than that of PVC). The room-temperature expansion coefficient of BSCCO (which shows the largest buoyancy drop) is roughly the same size as that of copper. Reiss's calculations show that the shrinkage of the PTFE capsule should lead to a buoyancy drop three times larger than that seen in any of his experiments; this inconsistency alone throws doubt upon gravity modification having been demonstrated conclusively.

Gravity experiments by Schnurer[6] use a 1" diameter superconducting disk attached to the top of three coils in a triangular arrangement and a metallic test mass is attached to the top of the superconductor. This assembly forms the weight on one end of a balance; the counter weight then sits on digital laboratory scales so that a weight decrease in the superconductor assembly produces an increase in the scales reading. The superconductor assembly is immersed in liquid nitrogen; once it has cooled the scales reading is noted, and power applied to the coils. The scales show an increase proportional to the sample mass. Nitrogen boiling due to the resistive heating by the coils, and possible flexing of the wires supplying the coils, may be possible explanations for these observations.

2. TESTS OF WEIGHT REDUCTION USING ROTATING SUPERCONDUCTORS

2.1 Background

Fully reproducing the Podkletnov conditions[1] is not straightforward. As far as the present authors are aware, no others have demonstrated gravity modification using similar experimental arrangements, though other partial tests[7] have been reported.

The present approach to this experiment was to start by spinning a superconductor at high speed. The basic equipment used in initial tests is illustrated in Fig. 1. A nominal 2" diameter (the die size, not the precise final disk size; where appropriate this is given in mm) granular disk fabricated ten years previously was employed. Although this disk was able to produce significant levitation (~5mm) of a 10g FeCo magnet, it could not levitate a 40g, 1" 0.45T NdFe magnet, nor could it sustainably levitate itself above an array of these magnets. A number of tests where the superconductor was cooled to 77K, spun at up to 5000 rpm, then slowed, and finally tested with a small magnet to ensure that the Meissner effect was still present, never produced any change in the test weight.

2.2 Present Project

In developing this investigation further, it was clear that reproducing the full Podkletnov conditions would take considerable time. Dr. Podkletnov has visited our laboratory to observe our experiments, and has made

some helpful comments based upon his own experience[8]. The strategy adopted was as follows:

- to be limited initially to 3" diameter disks,
- to develop a melt texturing process for disk fabrication (Podkletnov partially melt textured his disks to achieve much greater levitation for the same magnetic flux density),
- to develop a new weight measurement system,
- to use permanent magnets to provide levitation and/or rotating fields, and
- to produce low field, high frequency excitation using a 13.56MHz generator.

These points will be discussed in turn below.

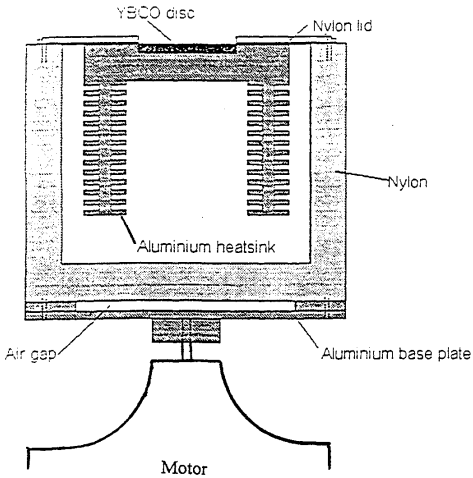

***Fig. 1:** The basic gravity test equipment. The aim was to spin the nitrogen container at high speed, while keeping the superconductor below T_c*

2.2.1 Melt Texturing and Disk Fabrication

Melt texturing has been found to improve YBCO's levitation force significantly for a given field and so was developed to produce disks that could self-levitate above NdFe magnets.

When YBCO is raised above 1008°C it begins to decompose according to the reaction:

$$2YBa_2Cu_3O_6(s) \rightarrow Y_2BaCuO_5(s) + \text{copper/barium rich liquid,}$$

i.e., the high temperature form of the superconducting YBCO phase decomposes to a liquid that is mostly $BaCuO_2$ and solid green phase YBCO. This reaction is partially reversible, i.e. slow cooling back through 1008°C re-forms the 123 (superconducting) phase with inclusions of the 211 (green) phase and solidified copper/barium material. The resulting YBCO is referred to as "melt textured"; essentially the grain boundaries which limit the bulk superconductivity of a granular sample have been reduced as the grains have melted into each other. Most importantly the crystal axes in a melt textured sample tend to be aligned (usually so that the larger *c*-axis is vertical) so that the sample properties are no longer an average of the good in-plane and poor out-of-plane superconductivity exhibited by YBCO.

One step further than melt texturing is top seeded melt texturing. Seeding is carried out using small 123 phase crystals with the yttrium replaced with neodymium or samarium. This substitution produces a material with the same crystal structure (except that the larger rare earths have a tendency to be disordered because their size means that they can partially substitute for barium) but having a higher decomposition temperature. These crystals when placed on the surface of an YBCO pellet above the decomposition temperature can, on cooling, seed the growth of large single domain pseudo-crystals of 123 YBCO (they are not true single crystals because of the 211 and Cu/Ba inclusions).

Practical problems such as liquid flowing out from the pellet above 1008°C can be controlled by adding extra 211 phase to increase the solid content at high temperatures, but precise temperature control, without significant temperature gradients, is necessary. (Temperature gradients lead to different crystallisation rates across the disks, causing disk cracking.)

The aim of this work was to produce 3" disks with an even distribution of reasonably sized, randomly oriented domains across their surface. Although single YBCO domains up to 70mm across have been demonstrated[9], owing to the level of furnace temperature control currently available to the present work the largest single domain produced was approximately 12mm × 12mm. In addition Podkletnov considered inter-grain junctions to be crucial to the gravity effect and we did not want to eliminate grain or domain junctions entirely.

It was found that attempting to distribute Nd123 crystals across the disk surface did not produce the even domain distribution necessary. Not all of the Nd seeds produced large domains and in any case

distributing small seed crystals in a furnace at 1020°C is not an easy process. A disk resulting from multiple top seeding is shown in Fig. 2; it clearly showed visibly uneven crystal distribution, giving a levitation force varying from place to place across the disk.

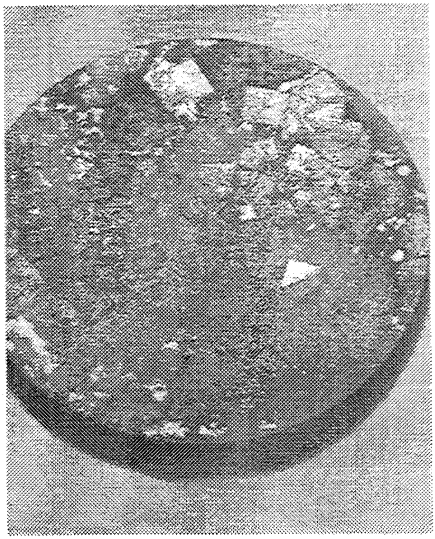

***Fig. 2:** Top seeded 3" disk*

A better disk was produced not by seeding, but by dropping the post-decomposition temperature from the 982°C used for seeded growth to 975°C. This lower temperature produces self-seeding and smaller randomly shaped but evenly distributed domains resulted (Fig. 3). This 110g disk, following oxygenation between 500 and 200°C for a week, could self-levitate above an array of seven NdFe magnets at a height of approximately 15mm, and could levitate a single NdFe magnet plus a further 80g at 2mm above its surface.

As an alternative to homogeneous self-seeding a new process, heterogeneous self-seeding, was tried. This involves including some Nd211 phase in the Y123/211 mix so that the Nd/Y ratio was 2/98. When the disk was raised to 1100°C (above the decomposition temperature of Nd123) and then cooled to 982°C, Nd123 is able to solidify from the 211/liquid mix first. This is because of its higher decomposition temperature and because the neodymium's similar size to barium makes Nd much more soluble than Y in the melt – enhancing diffusion to a growing crystal surface. The Nd123 crystals formed in this way then act as seeds distributed evenly throughout the disk for the Y123 growth. A disk grown by this method (Fig. 4) had levitation characteristics similar to the homogeneously seeded disk; it is expected that further development of this process would lead to still higher levitation forces.

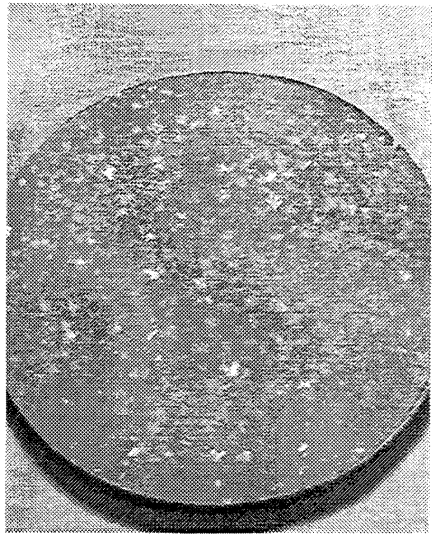

***Fig. 3:** Homogeneously seeded 3" disk*

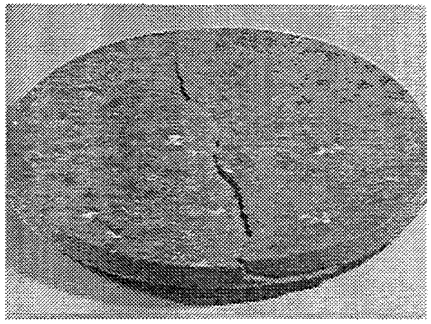

***Fig. 4:** Heterogeneously self-seeded 3" disk. The crystallisation is more evenly distributed with a more random orientation than the top seeded disk*

The chief problem found in this work is that of disk cracking. It was found that any indication of a crack in

the unfired disk that had been compacted in a die from the precursor powders using a fifty tonne hydraulic press would lead to catastrophic cracking during firing. Only one in four disks as-pressed was good enough to be fired (although unfired disks could usually be reground and pressed again). One in two that were fired held together, with or without some evidence of cracking, after melt texturing. The extra shrinkage due to the densification that occurs during melt texturing, plus the uneven crystallisation resulting from temperature gradients, puts a big strain on the mechanical stability of the disk.

One final innovation used during disk manufacture was the use of Saffil fabric (Alumina/Silica fibres pressed into a loose fabric/board) between disk and substrate on firing. This served two purposes; the main one was to ensure that disk could be separated from the substrate post partial melting. Secondly, since both aluminium and silicon chemically poison YBCO, incorporation of the fabric into the lower layer of the disk during melt texturing meant that there was a graduated poisoning of the superconductivity from top to bottom. In effect, the disks were bi-layered as specified by Podkletnov[1].

2.2.2 Experimental Apparatus

A beam balance was designed having the necessary resolution (0.004g or better for a 100g test mass, i.e. 0.004%) using a knife-edge pivot. Damping was essential, and was incorporated using a magnet that induced a Lorentz current in an aluminium plate opposing motion in proportion to velocity. The final design is shown in Fig. 5. The balance counter-mass was adjustable to give sensitivities that ranged from 1mm deflection for 0.02g difference, to 5mm deflection for 0.02g difference. The test mass used was 100g in all the tests undertaken as part of the present work, so that the best resolution obtainable was of the order of 0.004%, certainly sufficient for this application.

The cryostat body was made of aluminium and uses chemically-expanding foam as a thermal insulator. An aluminium heat-exchanger, for thermal coupling of the superconductor to the liquid nitrogen refrigerant, was also used.

Tests on this cryostat assembly showed that although it performed better than previous cryostats (fabricated from nylon) in maintaining superconductivity during static tests, after spinning at 5000 rpm and slowing to rest the superconductor had warmed above T_c (determined using the Meissner effect). Over 20 tests were performed using this cryostat (on the basis that the disk would be superconducting for at least some of the time that it was being spun) with the old 2" YBCO disk and various magnet configurations. No balance deflections were seen that could be definitely ascribed to anything except vibration and so using this configuration a gravity effect larger than 0.02% can be formally ruled out.

Following this work a foil liner was added to the cryostat between the liquid nitrogen refrigerant and the foam insulator to reduce the friction on the nitrogen during acceleration. With this liner in place and using a new partially crystallised 2" disk (an early melt-textured sample that could only levitate the NdFe magnets a few millimetres) the superconductor could be consistently accelerated to a top speed of 6000 rpm, stopped, and then still levitate a magnet afterwards.

In this new configuration 32 full runs were performed using a video camera to record any balance deflections. The kinds of magnet configurations used are illustrated in Fig. 6. In some tests the superconductor was cooled through T_c in the presence of a magnetic field ("field cooling") and in others the superconductor was cooled without a field.

One variation (two NdFe magnets held over the edge of the disk, one with north up and one with north down, and the superconductor field-cooled) seemed to show balance deviations that indicated a very small weight loss during disk acceleration and deceleration. However, the vibration produced by the rotating cryostat was such that rotation alone produced balance deviations as large as any possible gravity effect. The movements were not consistent enough to be ascribed gravity effects, which in this configuration can be formally ruled out down to 0.03%.

2.3 Experimental Results from Rotating Field Tests

The aim of this work was to rotate a levitated three inch disk. However, whilst a levitated cylindrical magnet can be freely rotated about its axis in any orientation, levitated superconducting disks resist rotation in a stationary field. Therefore, the superconductor was fixed in place at the levitation height – 10 to 20mm – above a rotating array of NdFe magnets (Fig. 7). If the superconductor was not fixed in these experiments then it tended to rotate unstably with the rotating magnets. If a container was used that only just contained the superconducting disk, then sometimes the disk was seen to rise out of the position in which it had been lodged and rotate slowly when the magnets were rotating fast.

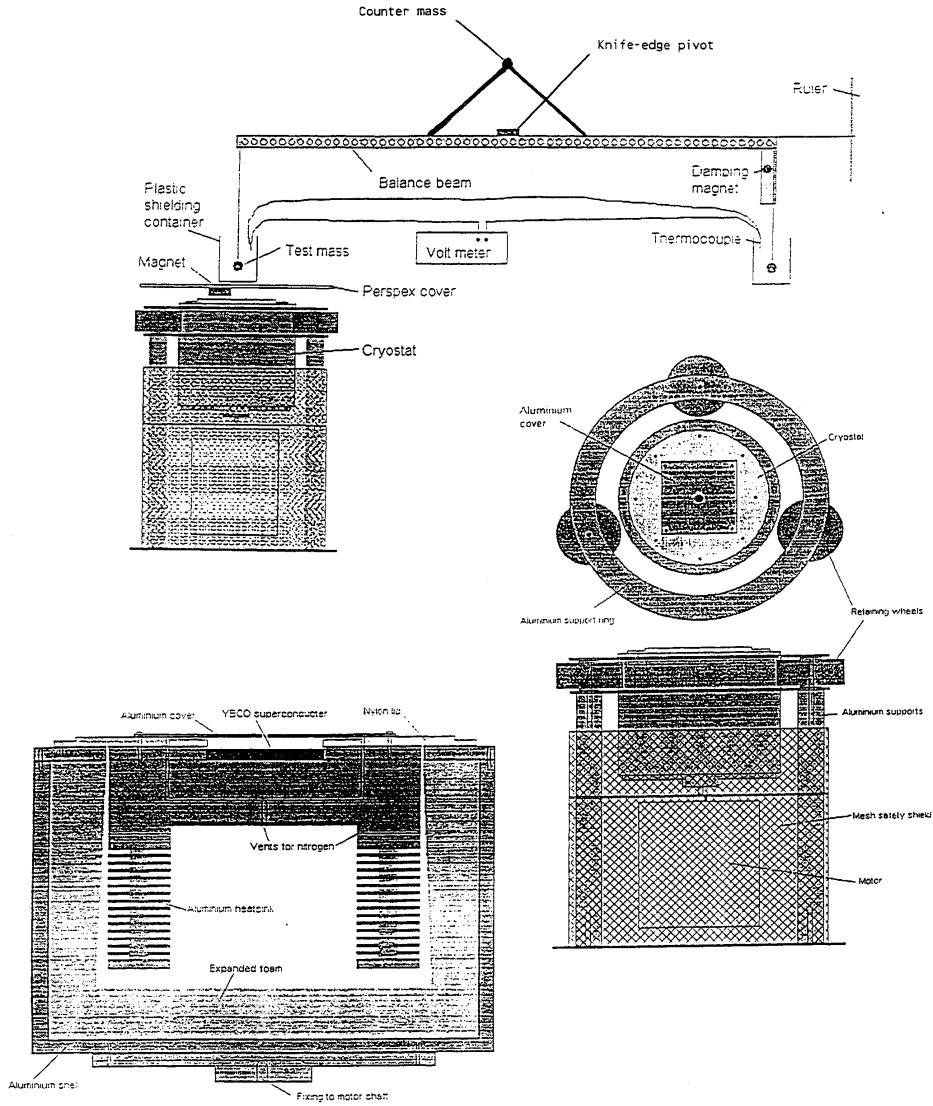

Fig. 5: *The final assembly for the rotating disk tests*

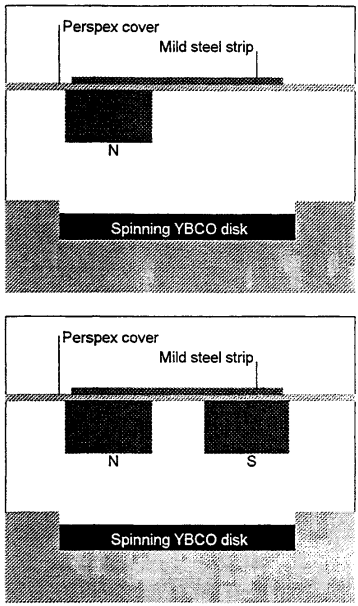

***Fig. 6:** Sample magnet configurations*

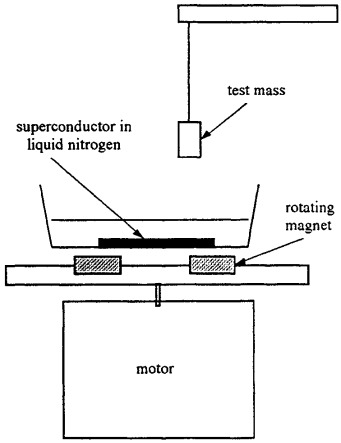

***Fig. 7:** Rotating field apparatus*

If the superconductor was fixed in place and the container was unsecured, then when the magnet rotation speed reached around 2000 rpm the superconductor lifted the whole container with liquid nitrogen, and the container then vibrated violently. This agrees with Podkletnov's observation of his disks rising when rotated[8], but it seems more likely that this is due to Lorentz force rather than a weight loss.

When the superconductor was firmly fixed in position the field linkage between superconductor and magnets meant that at least ~10% more power was required to start the motor turning. If the superconductor was then allowed to warm through T_c with the magnets still rotating below, the motor immediately accelerated, indicating that high rotation speeds do not diminish the torque between superconductor and magnets.

Several magnet arrangements were tried (see Fig. 8). The only noticeable result arising from the different arrangements was that greater variation in the field distribution produced greater rotational stiffness of the superconductor rotating in that field. Both the homogeneously and heterogeneously self-seeded disks discussed in Section 2.2.1 were used with no obvious differences between their behaviour. No balance deflections were seen for magnet rotation speeds of up to 10000 rpm (using three pairs of opposed magnets at this speed is equivalent to a 500Hz levitation field) and a gravitational effect can be ruled out down to 0.01% (these experiments did not require the "see-saw" balance to be moved for each run, giving better resolution).

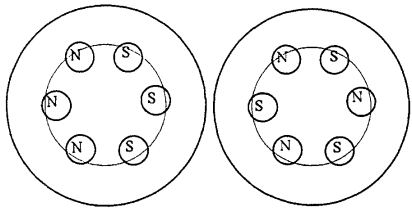

***Fig. 8:** Two different rotating magnet configurations tried during the present work*

A variation on the above was to use four vertical magnets placed around the superconductor (Fig. 9). These magnetically contained the superconductor which was not secured in place mechanically. When the magnets below were rotating at speed the superconductor rotated slowly from the face of one containment magnet to the next. No balance deflections were observed.

Finally, five turns of copper tube were placed around the superconductor and connected through a matching unit to a 13.56MHz r.f. supply. The matching unit was designed for capacitive loads and had very little effect in minimising the reflected power. In fact the generator

instrumentation suggested that for 200W forward power only 2W was absorbed by the load. Nevertheless, significant r.f. radiation was present in the vicinity of the superconductor, evidenced by the fact that the magnetic pick-up coil used for measuring rotation speed developed 3V peak to peak at r.f., swamping the output from the small magnets bonded to the rotating assembly. The r.f. had no other effect on the experiment and a gravity effect could still be ruled out to 0.01%.

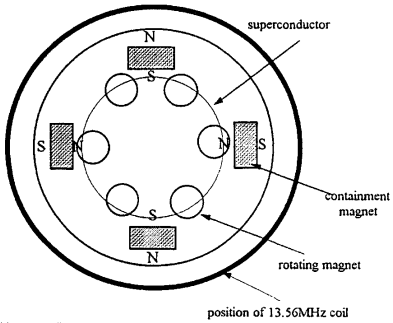

***Fig. 9:** Positioning of containment magnets to prevent the superconductor rotating uncontrollably*

2.4 Discussion

It can be argued that the fact that no effect has been observed in tests such as those described above is that these tests have not fulfilled the specified conditions for a gravity effect. These are:

- A disk with a diameter greater than 100mm
- A disk containing ~ 30% non-superconducting YBCO, preferably organised into two layers
- A disk capable of self-levitation, but still containing large numbers of intergrain junctions
- An a.c. levitation field with a frequency ~10kHz
- A second a.c. excitation field with a frequency of ~1MHz, for disk rotation
- Disk rotation speeds of a few thousand rpm for large (>0.05%) gravity effects (the largest effects (>2%) were reported[1] when the disk was being decelerated at around 3000 rpm).

The difficulties involved in meeting Podkletnov's experimental conditions[1] have already been discussed. In 1999 another team[7] working on reproducing Podkletnov's work followed a broadly similar route to the present work, i.e. using melt textured disks levitated with low frequencies. This group was not able to achieve stable static levitation of large disks at frequencies greater than 600Hz, and with disks that were not melt-textured stable levitation was achieved only with frequencies up to 45Hz. No gravity effects greater than 0.000001% were found.

The present work has investigated melt-texturing technology and produced high quality bi-layer disks with a final diameter of 70mm. There seems no *a priori* reason why this process may not produce larger diameter YBCO samples, particularly if annuli are formed so that larger diameters can be achieved at similar surface areas. An annular sample may also significantly reduce cracking due to shrinkage during the sintering process.

Rotating a melt-textured bi-layer 45mm disk at up to 7500 rpm through small static magnetic fields produced no effects that could be extracted from the system noise. Nor did various arrangements of high quality bi-layer 70mm superconducting disks held at levitation height above magnets rotating at up to 10000 rpm produce any gravity effect. The addition of a small 13.56MHz excitation field did not alter this negative result.

3. ROUNDS'S EXPERIMENT: STATIC SUPERCONDUCTOR

3.1 Introduction

Rounds[4] discussed a series of experiments in which a superconductor in the presence of a permanent magnet and immersed in liquid nitrogen was slowly allowed to warm. Rounds measured the weight of the whole system, reasoning that as the superconductor passed through T_c any weight anomaly associated with the Podkletnov effect would show up as a deviation from the monotonic weight loss as the nitrogen boiled off.

Rounds found deviations from linearity in his weight against time curves for superconducting disks, and less so for copper disks. However, as with the Reiss experiment[5], it is possible to postulate a number of thermal effects that could account for this observation.

Nevertheless, the experiment was interesting and has been repeated. Exactly the same type of superconducting disk and magnet (Edmund Scientific, part numbers CR37-446 and C52-867 respectively) were used, along with a somewhat larger nitrogen container than used by Rounds and also with a thermocouple bonded to the top of the YBCO and copper disks used.

3.2 Results

The results from a typical run with a thermocouple, an YBCO disk and a magnet separated from the YBCO by 10mm of plasticine are shown in Fig. 10, and for a copper sample in Fig. 11. Different ambient conditions along with the larger container meant that our experiments took longer (210s to the prominent inflection in the curve) than those of Rounds[4] (48s) and the initial portion of the weight loss curve shows greater deviation from a straight line. However, the deviation of our weight loss curve from a straight line (Fig. 12) shows behaviour similar to that reported by Rounds, in particular an anomaly at around 20s elapsed time. Unfortunately our results contain too much scatter (probably a result of vibrations in the thermocouple wires) for us to ascribe this anomaly to anything more than noise.

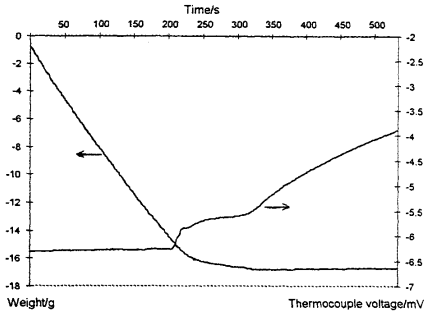

Fig. 10: *The changes in weight of the experimental apparatus as nitrogen boils off in the present work*

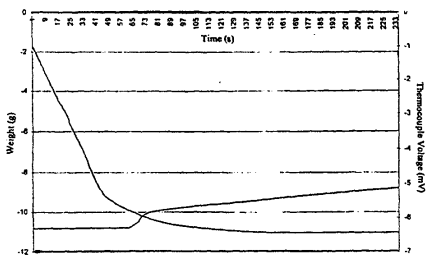

Fig. 11: *As for Fig. 10 except that the YBCO disk has been replaced with a copper disk of the same size*

However, the inclusion of a thermocouple does allow identification of the point at which the superconductor sample's temperature begins to rise. Inspection of Fig. 13 shows this to be after 205s, i.e. at the same time as the inflection in the weight loss curve. This concurrence can be explained by hypothesising that the heat flux into the experimental apparatus prior to 205s produced only nitrogen refrigerant boil-off, but post-205s was also required to raise the superconductor temperature, thus resulting in a slower boil-off rate.

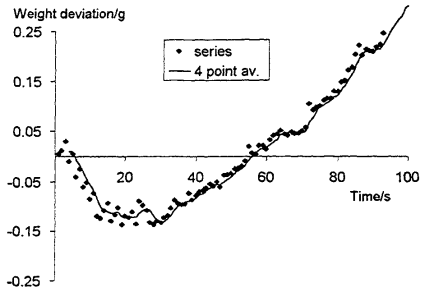

Fig. 12: *The deviation from a straight line of the weight changes in Fig. 10*

After 220s, as shown in Fig. 13, the rate of increase of temperature slowed dramatically, and the temperature effectively paused for a period of 10s at 93–94K. This is, of course, the critical temperature of the superconductor. Thereafter the rate of increase was slow until after 320s when no further liquid nitrogen refrigerant remained. This behaviour was reproducible using the YBCO superconductor sample but no such temperature pause was seen when the superconductor was replaced with a copper disc of similar dimensions.

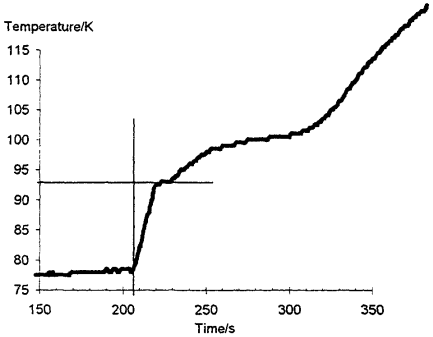

Fig. 13: *Graph of thermocouple temperature vs. time in the Rounds-configuration experiment*

3.3 Discussion

With the superconductor sample (and to a lesser extent the copper sample), the inflection in the weight loss

curve corresponded to the sample starting to warm. A consequence of this (and presumably Rounds's original equipment[4] behaved similarly) is that any anomalies in the weight loss curve before the inflection point occur while the superconductor is at a constant 77K and are therefore most unlikely to be related to modification of gravitation.

Of more interest in the results is the slowing of warming rate at T_c which is reminiscent of a first order phase transition (like, for example, the melting of ice). However, the only first order phase transition reported in high T_c superconductors is flux vortex lattice melting and this has only been observed in small, high quality, flux grown single crystals, not in granular samples like ours[10]. Whilst this is an interesting observation and in need of further investigation, it appears to be a purely thermal effect without any implications for gravity research.

4. CONCLUSIONS

The conclusions from the present work are that the subset of the Podkletnov conditions examined here does not produce gravity modification measurable with our equipment (a resolution of the order of ±0.004%); it remains an open question whether gravity modification can be *repeatably* observed using the full set of Podkletnov conditions. This may, of course, only be a confirmation that not all of the correct and prescribed conditions have been achieved so far and that the present experiments could not be expected to show positive results.

The Rounds configuration also has not shown any effects unequivocally indicating gravity modification. Although some interesting effects have been produced, no effects reliably ascribable to gravity modification have been observed using either experimental arrangement.

From our repetition of the Rounds experiment, it appears likely that Rounds[4] was seeking a gravitational anomaly at an incorrect temperature. There was, however, unusual thermal behaviour in the YBCO results for which as yet there is no adequate explanation. Unusual behaviour around T_c has been found by other authors and it is known that high T_c superconductors with very short coherence lengths can show short-lived superconducting fluctuations up to 15K either side of T_c (the width of the distribution describing these fluctuations is proportional to coherence length). It is not clear that such fluctuations or thermal effects have any relation to any gravity effect.

4.1 Simplified summary of conclusions

Two recent experiments, one in Finland and the other in the U.S.A., have claimed to demonstrate reduction of the earth's gravity in a laboratory. Such observations are potentially of great importance to the future of spaceflight, air travel, and other endeavours in which gravity plays an important part. These experiments are extremely challenging technically and so an exact repetition is difficult; nevertheless, a partial repetition of the specified experimental conditions has been undertaken. No reduction in the earth's gravity has been observed by the present researchers to date. However, this may simply be because the full specified conditions have not yet been met.

5. FURTHER WORK

The next step in this work is to attempt a more complete test of the Podkletnov conditions. Work is already in hand to increase the disk size to 10cm diameter, to construct a magnetic levitation system, to construct rotation coils and to construct a disk braking system. Investigation of the detailed theory of such effects, in our view, should properly follow a repeatable demonstration of the Podkletnov observations beyond reasonable doubt.

6. ACKNOWLEDGEMENTS

It is a pleasure to acknowledge the continued support of Dr. R.A. Evans, BAE Systems, Warton, U.K., under "Project Greenglow".

7. REFERENCES

1 E. Podkletnov & R. Nieminen, Physica C **203** 441 (1992)
2 M. de Podesta & M. Bull, Physica C **253** 199 (1995)
3 C.S. Unnikrishnan, Physica C **266** 133 (1996))
4 F.N. Rounds, Proc. NASA Breakthrough Propulsion Phys. Wkshp., Cleveland 297 (1998)
5 H. Reiss, Proc. 15th Europ. Conf. Thermophys. Prop., Würzburg (1999)
6 J. Schnurer, website url: http://inetarena.com/~noetic/pls/schnurer.html (1997)
7 R. Koczor & D. Noever, AIAA/ASME/SAE/ASEE Joint Propulsion Conference AIAA 99-2147 (1999)
8 E. Podkletnov, private communication (2000)
9 P. Gautier-Picard, X. Chaud, E. Beaugnon, A. Erraud & R. Tournier, Mat. Sci. Eng. **B53** 66 (1998)
10 A. Schilling, R.A. Fisher, N.E. Phillips, U. Welp, D. Dasgupta, W.K. Kwok & G.W. Crabtree, Nature **382** 791 (1996)

A01-34340

AIAA 2001-3653

A PROPOSED EXPERIMENTAL ASSESSMENT OF A POSSIBLE PROPELLANTLESS PROPULSION SYSTEM

D. Goodwin
U.S. Department of Energy
Germantown, Maryland

37th Joint Propulsion Conference
8-11 July 2001
Salt Lake City, Utah

AIAA 2001-3653

Abstract. A proof-of-principal experiment is described for a possible propellantless propulsion system (PPS) concept presented during the Space Technology and Applications International Forum of 2001. A newly available, high power, solid state switch and recent improvements in superconducting magnets, may have made a propellantless propulsion system (PPS) possible. Propulsion may occur during the non-steady state condition of the ramp-up of a very rapidly pulsed, high power magnet. Propulsion would not occur after the first 100 nanoseconds of each pulse, since the magnetic field will have reached steady state. The switch can provide 100 nanosecond ramp-ups at a rate of 0.4 megahertz, and at 9,000 volts and 30 amperes. To produce an asymmetry in the magnetic field, a plate would need to be attached to one end of the magnet. The primary components of such a PPS would be an electrical power supply, the switch, and a low temperature, superconducting magnet, capable of 2,000 amperes per square millimeter. Other applications may include propulsion with significantly reduced thermal and acoustical signatures; and a means to dampen inertia.

Introduction

A proof-of-principal experiment is described for a possible propellantless propulsion system (PPS) concept presented during the Space Technology and Applications International Forum of 2001 (Goodwin, 2001). The effect under investigation for a possible propellantless propulsion system (PPS) is the movement of high power magnets, under certain conditions, during initial power ramp-ups. A newly available, high power, solid state switch, coupled with recent improvements in superconducting magnets, may have made possible a PPS based on this effect. This new concept could be termed "a solid state PPS".

If successful, this type of PPS would meet one of the NASA's Breakthrough Propulsion Physics (BPP) technical challenge #1 for "propulsion methods that eliminate ... the need for propellant"; and may meet BPP technical challenge #2 to "dramatically reduce transit times" (Millis, 2000).

Background

High power magnets are designed to avoid movements since such movements have detrimental effects on the experiments. When movements of the magnets are encountered, the magnets are redesigned to eliminate such movements (e.g., eliminate vibrations). By designing a system to exploit and enhance this Lenz's Law based movement, it may be possible to produce propulsion during the non-steady state conditions of the ramp-ups of very rapidly pulsed magnets.

The propulsion, if any, would only occur during the 100-nanosecond ramp-up of each pulse. After this ramp-up, the magnetic field will have reached steady state and no propulsion would occur. The non-steady, high power pulse might be producing an inertia drive effect, but without the need to mechanically move massive objects (which are limited by the strength of materials and produce only small amounts of propulsion, with supplied power; and, perhaps, no propulsion with on-board power). With sufficient power, it may be possible to accelerate the mass of the plate to 100s of g's.

The time for the magnetic field to reach steady state is related to the pulse duration (100 nanoseconds) and the size of the system (100 feet of wire). Given the size of the system (less than 1,000 feet), the magnetic field reaches steady state in less than 1 microsecond. This

effect, if it exists, is different from magnetic "levitation" or Lenz's Law "jumping rings", both of which require the object to push off (or pull towards) other objects.

Until the recent improvements in technology, the motion produced by pulsed magnets has been an experimental interference. The motion is produced due to the Lenz's Law interaction of a pulsed magnet with an attached component producing an asymmetric magnet field. A large magnet for a particle physics moved about a centimeter every time the upgraded magnet was powered up, due to an attached component from a previous experiment. Since the component was no longer required, it was removed and the motion ceased. A small magnet for a fusion experiment moved several centimeters with the once per second pulses of 2,000 volts and 600 amperes. Since the attached asymmetric component could not be removed, the magnet was allowed to slide back into its original position. In this case, other interactions were discounted because the experiment was located in a laboratory with concrete block walls and with no rebar in the floor.

The form of Lenz's Law for a loop with fixed area is: $V = -A\,(dB/dt)$, where V is the voltage, A is the area of the plate, and B is the magnetic field. In addition to mass penalties and costs, increasing the magnetic field (B) is limited by the physical stresses on the magnet. Superconducting magnets can produce about 10 Tesla magnetic fields for years, but a 100 Tesla field destroys the magnet after about 500 pulses and a 500 Tesla field destroys the magnet after 1 pulse. There are substantial mass penalties and costs associated with increasing the area (A). The newly available switch allows more rapidly varying the magnetic field (dt) without significant mass penalties or costs. Modifying the waveform, by adding more switches and/or modifying the switches, could increase the pulses per second and reduce the size and mass of the system. Further system optimization would be to increase the amperage (superconducting magnets have been run at kiloamps); to modify the waveform of the switch (to provide more of the pulse in the ramp-up and less in the flat-top); and to reduce the size, mass, and complexity of the interfaces between the power supply and the switch and between the switch and the magnet (e.g., reducing the need for transformers and/or using superconducting transformers).

Concept

The primary components of such a PPS would consist of the switches; low temperature, superconducting magnets; and an electrical power supply.

In FY 2000, an IR-100 award was earned by Diversified Technologies of Bedford, MA (http://www.divtecs.com), for the development of a high power solid-state switch. The $6K, 7"X7"X3" switch can provide 100 nanosecond ramp-ups at a rate of 0.4 megahertz (MHz), and at 9,000 volts and 30 amperes. Allowing for the duty cycle of the ramp-ups and ramp-downs, the switch provides an integrated power of about 250 KWe. Compared to previous switches, the new switch is more compact, of lower mass, 10 times more energy efficient (only a 0.2% energy loss), and has 1000s of times higher reliability than vacuum tubes. Since the new switch has a pulse rate 10 times faster than previously available, the mass of the magnet can be reduced by a factor of 10.

Another recent improvement in technology which contributes to the possible enabling of a PPS, is a the low temperature superconductor that has recently become available which operates at 2,000 amperes per square millimeter; i.e., 10,000 times more than a non-superconductor (Barletta, 1999). High temperature superconductors carry 20 times less amperage and would probably not be able to tolerate the magnetic fields and/or the pulsed power.

To produce an asymmetry in the magnetic field for the Lenz's Law interaction, a plate would need to be attached to one end of the magnet. To prevent the energy from the pulse being carried away as induced current, the plate would need to be insulated during the ramp-ups. To prevent oscillations during the ramp-downs, the plate would to be uninsulated until the next ramp-up (by using a voltage-regulated switch with a timer to connect the plate to a drain during the flattop of the pulse and then disconnect the plate from the drain before the next ramp-up).

Experiment

The proof-of-principal laboratory experiment should initially use 1 switch, 1 magnet, and externally supplied power. The experiment could use the commercial-off-the-shelf (COTS)

switch and a commercially available cable for the superconducting magnet. As with the designs for other types of experiments, the cryostats would need to be electromagnetically non-interacting.

Superconducting cable consists on up to 60 superconducting wires in a parallel conductor configuration. Allowing 500 nanoseconds during each power pulse to connect the plate to the drain, drain the plate, and reinsulate the plate, indicates about 2,000 feet of superconducting wire would be required for the propulsion magnet (to convert the electrical energy to propulsion in the remaining 2,000 nanoseconds of the power pulse). Reconfiguring 20 of the wires in the cable to be a series conductor would result in 100 feet of cable being required for the propulsion magnet. This configuration would convert each power pulse from the switch into 20 pulses of the magnet (8 MHz) and allow 20 passes through the magnet to convert each power pulse into propulsion, if the returns can be tuned to increase the ramp-up without producing a flat-top. Only about 5 KWe (2%) of the 250 KWe may be converted to propulsion since the ramp-up is only 4% of the duty cycle and the ramp-up starts at 0% power and increases to 100% rated power (i.e., averages 50% of rated power). As the ramp-up continues to build, the wires would be carrying 300 amperes (20 passes at 50% rated power). If a 2 g acceleration is produced, each pulse of the magnet would result, on average, in 0.6 milliwatt-seconds being converted into 1.2 microns of lateral motion on a supporting surface. With 32 windings and a 1-foot diameter, the magnet would have a height of about 3 feet. The cable would have a mass of about 25 kilograms. The magnet, with the cryostat, would have a mass of $\geq$ 50 kilograms (excluding the plate).

A holdup magnet (without a plate) would be required to allow the unused energy to be returned to the switch with the correct timing for the next power pulse. Reconfiguring the 60 wires in the cable into a series conductor would result in 40 feet of cable being required to return this 2,400 nanoseconds of the power pulse. The holdup magnet would be similar in size and mass to the propulsion magnet. The wires in holdup magnet would only be carrying 30 amperes.

PPS assessment criteria (Millis, 1997) include: "must ... induce a unidirectional acceleration ... be controllable ... sustainable ... be effective enough to propel the vehicle ... satisfy conservation of momentum (and) energy ...can be ... carried ... on the vehicle (and) consistent with empirical observations." (Millis, 1997).

Although the proposed PPS appears consistent with empirical observations and conservation of energy is not an issue, the following tests are required to confirm this and to determine if the other PPS criteria are met:

1. Confirm uni-directional motion (net external force) is produced (e.g., not limited to oscillations).

2. Confirm momentum is conserved without pushing off or pulling toward other objects (voltage regulated switch locked to drain should result in no motion; and locked to insulated mode should result in oscillations).

3. Confirm the system is effective enough to be carried on a vehicle and propel a vehicle (by measuring acceleration produced against power input). Given the potential for high energy efficiency, this type of PPS may be capable of producing near the theoretical maximum conversion of 20 kg/kWh for a 1 g thrust-per-power.

4. Confirm the system is sustainable (by long duration runs). The DOE Office of High Energy and Nuclear Physics is providing funds for the Alpha Magnetic Spectrometer (AMS) to be flown on the International Space Station. Most of the mass of this 7-ton detector is a superconducting magnet, which will operate for 3 years without maintenance. The magnet has 90 km of superconducting cable and an 800-watt cooling system.

Although the proposed PPS appears readily controllable, this could be confirmed by follow-on laboratory experiments with additional switches and magnets.

Demonstration

A sub-orbital demonstration vehicle would require an on-board electrical power supply, such as the 30 KWe "microturbine", commercially available from Capstone Turbine Corporation of Chatsworth, CA (http://www.capstoneturbine.com). Extensive

modifications would be required for this COTS power supply.

To match the microturbine, 6 switches (@ 5 KWe) would be required to convert the 30 KWe into propulsion. By configuring all 60 wires of the propulsion magnet into 3 sets of 20 conductors in series, the same propulsion magnet (and holdup magnet) could be used from the above experiment, if the switches can be tuned to have their ramp-ups build and not produce a flattop. With 2 switches for each set of 20 conductors in series, the propulsion magnet would be carrying 600 amperes, whereas the holdup magnet would be carrying 180 amperes (from the 6 switches). Since the propulsion magnet would still be operating at 8 MHz, a 2 g acceleration (a net of 1 g over gravity) would result in each pulse of the magnet, on average, converting 3.6 milliwatt-seconds into 0.6 microns of vertical motion (for this more massive object moving against gravity).

Given the maximum conversion of energy to propulsion noted above (10 kg per KWH for a 2 g acceleration), the mass of the demonstration vehicle would need to be kept below about 300 kilograms (including about 2 kg of fuel/oxidizer per KWH). Test stand runups could initially be performed with air, and then with an on-board oxidizer (e.g., LOX).

Applications

Possible NASA missions for this type of PPS would include the manned mission to Mars and the interstellar "precursor" probe. If the solid state PPS can provide a continuous acceleration of up to 0.2 g, the transit times for robotic missions would be reduced from years to months and for manned missions from months to weeks. As discussed below, the mass of the reactors/PPS may be only about 20% of the vehicle mass for a 0.2 g acceleration.

For launches within gravitational wells, specific power (KWe/kg) is the critical factor (which requires chemical based power supplies). For transits through the solar system and beyond, specific energy (KWH/kg) is the critical factor (which requires nuclear based power supplies). A space-based reactor with a specific mass of $\leq$ 18 kilograms per KWe and a conversion efficiency of $\leq$ 30% can be available with existing technology in 5 years for units with $\leq$ 0.3 MWe and 10 years for units of $\geq$ 1 MWe (Houts 2001, Lenard 2001, Lipinski 2001, Polk 2001, and Poston 2001).

The solid state PPS, with about a 0.1 MWe reactor, should be suitable for most robotic missions. For example, this sized system would provide more payload, power, and data return capability for such missions as the (precursor) "interstellar probe" to the heliopause at about 200 AU and on into the interstellar medium to about 400 AU (Liewer, 2000). Using the maximum conversion efficiency noted above (100 kg per 0.2 g acceleration), 90 KWe may result in a vehicle mass of up to 9 tons (what a Delta IV heavy can take to an escape orbit) and would use an optimized propulsion magnet. To match the 90 KWe, would require 18 switches (@ 5 KWe), with 6 switches connected to each of the 20 conductors in series, if the switches can be tuned to produce ramp-ups and not a flat-top. The wires in the propulsion magnet would be carrying 1,800 amperes and the wires in the holdup magnet would be carrying 540 amperes. The size and mass of the magnets would be the same as for the experiment and the demonstration. Since the propulsion magnet would still be operating at 8 MHz, a 0.2 g acceleration, would result in each pulse of the magnet, on average, converting 11 milliwatt-seconds into 0.1 microns of motion (for this much more massive object). Scaling from the AMS magnet, $\geq$ 10 watts of cooling would be required for each magnet.

At the maximum conversion efficiency, the solid state PPS, with a 1 MWe power supply, may be able to propel a 100-ton, manned vehicle at 0.2 g for manned missions within the solar system. Reactors can be placed in Earth orbit in a non-critical configuration. All subsequent departures and returns could be to the lunar polar orbit which faces the maximum distance away from the Earth. For launches to and returns from LEO and the polar lunar orbit, the same type of vehicle could be used, except with a chemical based electrical power supply. With the maximum conversion energy to propulsion and fuel/oxidizer consumption per KWH noted above, a vehicle to LEO would require at least 7% of the vehicle mass for fuel/oxidizer. The solid state PPS may also be able to provide substantial maneuver capability for manned and unmanned vehicles. Providing an acceleration of 0.4 g (increasing the mass of the reactors/PPS to 40% of the vehicle mass), would allow for

nuclear powered landers for Mars and most moons.

To convert 1 MWe into propulsion would require 200 switches (@ 5 KWe); i.e., 11 or 12 of the 90 KWe (optimized) propulsion magnets. For the propulsion magnets, the rep rate (8 MHz), size, mass, power conversion per pulse, motion, cooling, and amperes would be the same as described above for the robotic missions. Three holdup magnets would be required (each operating at 2,000 amperes), and with the same size, mass, and cooling as described above.

The NASA BPP interest in PPS is because the potential ISP is in the billions of seconds, as compared to $\leq$ 480 seconds for rockets and $\leq$ 5,000 seconds for ion drives.

The solid state PPS may be able to provide:

1. Substantially reduced thermal signatures for aerospace craft and substantially reduced acoustical signatures for military and commercial aircraft, surface ("electric") ships and submarines (for the protection of the astronauts and the ISS, the AMS magnetic is being designed to minimize stray electromagnetic fields).

2. Cost-effective boost and maneuver for trans-atmospheric vehicles and for orbital vehicles to transfer from one orbit to another (possibly including real time, varying adjustments over each ISS orbit).

3. Commercial supersonic flight.

4. Significantly reduced vibrations and acceleration/deceleration from launch/deorbit.

5. Elimination of the need for tiles.

6. Powered landings.

7. The additional safety of twin engines, either of which may be able to return the vehicle (with a lifting body fuselage for additional safety inside the atmosphere).

With this type of propulsion system, it might be possible to dampen inertia. Using < 20 femtosecond pulses, a 10 g acceleration could be divided into 0.01 angstrom increments, which may allow the biological cells time to recover from each short burst of acceleration. This approach should lend itself to microfabrication. For example, using a 1 megahertz switch (under development by the vendor)), an integrated circuit with 50 million micromagnets would be required to convert 5 KWe to propulsion without inertia. Each micromagnet would have about 5 microns of wire to convert 0.1 nanowatt-seconds per pulse into propulsion. Since the micromagnets would be in series, they would need to fail closed. Since 10 square microns of wire are required for each unit, 10 micromagnets in parallel in each unit would allow the micromagnets to fail closed. By more rapidly varying the magnetic field, such a system may also increase the conversion efficiency of electrical energy to propulsion. The cooling requirements may also be reduced.

Summary/Conclusions

By using very rapidly pulsed magnets, it may be possible to develop a propulsion system that does not rely on propellants. If successful, such a system would substantially reduce the cost of the spacecraft and would reduce the transit times for robotic missions from year to months and for manned missions from months to weeks.

Acknowledgments

The development of the high power, solid state switch and the high performance superconductors were funded, in part, by the U.S. Dept. of Energy, Office of High Energy and Nuclear Physics.

References

Barletta, W., et al. "1999 Accelerator and Fusion Research and Development Research Highlights," published by the Lawrence Berkeley National Laboratory, page 4-14.

Goodwin, D. (DOE), "A Possible Propellantless Propulsion System", in Proceedings of *Space Technology and Applications International Forum* (STAIF-2001), Feb. 13, 2001.

Houts, M. (NASA MSFC, formerly with Los Alamos National Laboratory), et al, "Options for the Development of Space Fission Propulsion Systems" in Proceedings of STAIF-2001, Feb 14, 2001.

Lenard, R. (Sandia National Laboratory), et al, "Evolutionary Strategy for the Use of Nuclear Electric Propulsion in Planetary Exploration", in the Proceedings of STAIF-2001, Feb. 13, 2001.

Liewer, P. (JPL) "Interstellar Probe: Exploring the Interstellar Medium and the Boundaries of the Heliosphere", (http://interstellar.jpl.nasa.gov/), November 17, 2000.

Lipinski, R. (Sandia National Laboratory), et al, "Mass Estimates for Very Small Reactor Cores Fueled by U-235, U-233, and Cm-245" in Proceedings of STAIF-2001, Feb. 13, 2001.

Millis, M., (NASA GRC) "Project Plan for Breakthrough Propulsion Physics" (NASA GRC document TD15-PLN-015), December 4, 2000.

Millis, M., (NASA GRC) "The Challenge to Create The Space Drive", in AIAA Journal of Propulsion and Power, V. 13, N. 5, pp. 577-582, Sept-Oct 97.

Polk, J., (Jet Propulsion Laboratory) "The JPL Advanced Propulsion Concepts Research Program" in the Proceeding of the University of Alabama "Advanced Space Propulsion Workshop", April 3, 2001.

Poston, D. (Los Alamos National Laboratory). "The Heatpipe-Operated Mars Explorer Reactor," in Proceedings of STAIF-2001, Feb. 13, 2001.

A01-34342

AIAA 2001-3656

Research on Achieving Thrust by EM Inertia Manipulation

H. Brito
Instituto Universitario Aeronautico
Cordoba, Argentina

37th AIAA/ASME/SAE/ASEE Joint Propulsion Conference and Exhibit
8 -11 July 2001
Salt Lake City, Utah

AIAA-2001-3656

RESEARCH ON ACHIEVING THRUST BY EM INERTIA MANIPULATION

Hector H. Brito*
Instituto Universitario Aeronautico
Córdoba, Argentina

ABSTRACT

One of the challenges of interstellar travel being to discover a self-contained means of propulsion that requires no propellant, it has already been shown that a solution to the problem does exist, provided the system is endowed with tensor mass properties. The aim of this paper is to discuss a "propellantless" propulsion concept based on electromagnetic fields to modify the inertial properties of the system. Mass tensor properties were found to be replicated in Electromagnetism in connection with the still standing Abraham-Minkowski controversy. An experiment to settle the question has been implemented which consists of mounting the device as a seismic mass atop a mechanical suspension. Results gathered during the 1993 – 1997 period consistently point to a mechanical vibration induced by matter-EM field momentum exchange, as predicted by Minkowski's formulation, after all other sources of vibration were taken into account, or removed when possible. Tests conducted since 1999 on a redesigned experiment aiming at getting rid of most of the identified spurious effects, yield comparatively sharper and clearer evidence of sustained thrusting. However, it must yet be seen as an "anomalous" effect, since the system momentum is not conserved; thus further work remains to be done to confirm these results.

INTRODUCTION

Human interstellar exploration may not be possible without the discovery of a self-contained means of propulsion that requires no propellant.[1] This formally translates into the problem of achieving "jet-less" propulsion of spaceships that can then be seen as closed systems, i.e., without external assistance or mass/energy exchanges with the surrounding medium. It follows from this picture that the 4-Momentum of the system should be conserved. As already shown, a formal solution to the problem does exist, provided the system is endowed with tensor mass properties. This is embodied in the Covariant Propulsion Principle (CPP) which derives from a mass tensor description of the closed system consisting of the rocket driven spaceship and its propellant mass, provided the "solidification" point is other than the system center of mass, within a relativistic covariant formulation.[2]

The mass tensor formulation shows that the propulsion effect is to be related to the deviatoric part of the tensor, which exhibits the particularity of producing a non-vanishing linear momentum in the spaceship comoving Lorentzian frame. This can be seen as the physical signature of a non-diagonal 4-mass tensor. The situation is reminiscent of the concept of static EM field momentum which can develop in the rest frame of a physical arrangement of electric and magnetic sources including polarizable media, as depicted in Fig. 1.

Different theoretical results are possible depending whether Planck's principle of inertia of energy is satisfied or not in the relationship between the Poynting vector (energy flow density) and the electromagnetic momentum density.[3] These different results are basically Abraham's and Minkowski's forms of the EM momentum density, as the three dimensional expression of the so called "Abraham-Minkowski controversy" about the correct Energy-Momentum tensor of EM fields in polarizable media. The controversy, lasting since 1909, strikingly remains as a yet unsolved issue of Physics.[4,5] Supporters on the theoretical aspect split about equally between the two forms, according to literature reviews, while existing experimental evidence does not allow to draw definite conclusions.

* Project Manager, Applied Research Center, Member AIAA.

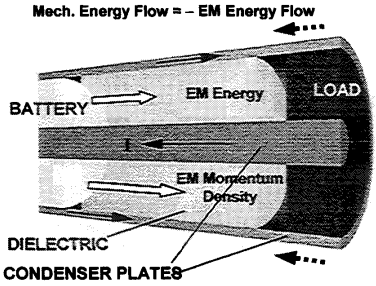

$$\text{EM Momentum Density} \begin{cases} = \text{EM Energy Flow} / c_0^2 \\ = \text{EM Energy Flow} / c^2 \end{cases}$$

Fig. 1 Different determinations of the EM momentum density in the "matter" rest frame with polarizable media.

In the present work, by using Minkowski's formalism,[6-8] a non-vanishing momentum of electromagnetic origin is shown to arise for the particular device depicted in Fig. 1. The whole system would then enjoy tensor mass properties of electromagnetic origin, when viewed as a single particle at rest in the "matter" subsystem frame. It follows that the EM field, given suitable charge and current distributions, can modify the inertial properties of the generating device, giving rise to the possibility of obtaining mechanical impulses on the device, not undergoing any exchange of mass-energy with the surrounding medium, as stated by the CPP. A propulsion concept based upon this kind of inertia manipulation mechanism is subsequently drawn; the experimental setup built to test that concept is discussed, as well as the obtained results and the applied signal processing techniques.

THRUST BY TENSOR MASS "WARPING"

The Relativistic Rocket Approach

A fully covariant reformulation of the relativistic rocket motion has been achieved and the two-particle and one-particle models of the related physical system were analyzed in Ref. 2, together with the effect of a generalized "solidification point" location, w.r.t. the center of mass (c.m.) location. When the whole system (Rocket + Ejecta) is analyzed as a single particle located at the "Rocket" system c.m. (or any "structural" point), a mass tensor is readily found as related to the whole system which reads in geometric notation

$$\mathbf{M} = \left(m_0 + m_E^*\right)\mathbf{I} + \left(\mathbf{p}_E \wedge \mathbf{v}\right) / c_0^2 . \qquad (1)$$

where m_0 and m_E^* represent the masses of the rocket and of the ejecta in the rocket rest frame, $\mathbf{I}$ is the identity 4-tensor, $\mathbf{p}_E$ the 4-momentum of the ejecta and $\mathbf{v}$ the 4-velocity of the "solidification point". For a closed system ($\mathbf{f} = \mathbf{0}$),

$$d\left(\mathbf{M}\cdot\mathbf{v}\right) = \mathbf{0} \quad \Rightarrow \quad \mathbf{M}\cdot d\mathbf{v} = -\,d\mathbf{M}\cdot\mathbf{v}, \qquad (2)$$

thus, the 4-acceleration of the chosen "solidification point" is to be related to the rate of variation of the mass tensor deviator, this being written as

$$m_0\, d\mathbf{v} = -\left(d\mathbf{p}_E \wedge \mathbf{v}\right)\cdot\mathbf{v} / c_0^2 . \qquad (3)$$

Eq. (3) shows that to have zero "Rocket" 4-acceleration for any 4-velocity, ($d\mathbf{p}_E \wedge \mathbf{v}$) must vanish, i.e., the deviatoric part of the mass tensor variation must vanish. It is also shown that this comes out as a necessary condition for vanishing acceleration.

The Covariant Propulsion Principle

Now, to achieve 4-acceleration, anisotropy of the mass tensor must follow at some instant and, as a result, a non-vanishing 3-momentum shows up in the spacecraft comoving Lorentz frame. An elementary algebraic analysis shows that a mass 4-ellipsoid arises as a "geometrical" representation of the mass tensor; a given variation of this tensor, related to a propulsion effect, can be viewed as a mass 4-ellipsoid warping, giving rise to the Covariant Propulsion Principle: *A spaceship undergoes a propulsion effect when the whole system mass 4-ellipsoid warps.*[2]

The C.P.P. furnishes an alternative wording for the Action and Reaction Principle (A.R.P.) which is known to fail in relativistic mechanics even in its weak form; it does not substitute the four-momentum conservation law, but extends its meaning to complex systems when they are represented as pointlike particles which are not collocal with the whole system center of mass. They are both derived concepts which allow, in their domains of validity, for an intuitive representation of the involved propulsion mechanisms. In the same way the A.R.P. allowed for the "mass-spring" analogy as an intuitive model, the C.P.P. allows for the essentially geometrical analogy with the *jétée* motion of the ballet dancer, during which she gets angular acceleration by retracting her extremities onto the gyration axis, i.e., by ***warping its inertia tensor*** in 3-D space. As for the propulsion case, a linear acceleration/deceleration is achieved by ***warping the mass tensor***, which must be defined in

Minkowski's 4-D space. A pictorial representation of the propulsive effect is shown in Figs. 2 and 3, where a mass ellipsoid is assigned to a "Flatland" rocket system.

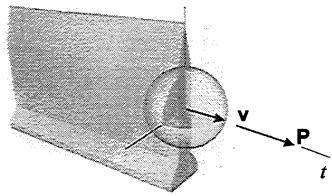

Fig. 2 "Flatland" rocket at rest in its 3-D spacetime and the corresponding mass ellipsoid.

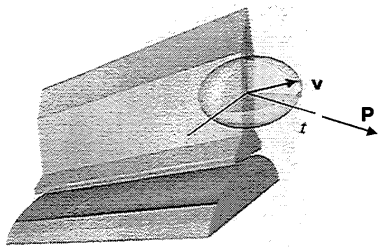

Fig. 3 "Flatland" rocket after acceleration in its 3-D spacetime and the corresponding mass ellipsoid.

Studies about inertia as something that could be manipulated for propulsion purposes are not new, a tentative explanation has already been undertaken on the basis of the relativistic mechanics of extended bodies under electrostatic pressures.[9] However, the C.P.P. allows for a general formulation of the problem, provided a "propulsion field" of 4-momentum $\mathbf{p}_F$ can be ascribed to the whole system, analog to the rocket ejecta subsystem. The system can then be viewed as a single particle located at the "matter" system c.m. (or any "structural" point) so that a mass tensor is readily found as related to the whole system. The 4-acceleration of the chosen "solidification point" now becomes

$$m_0 \, d\mathbf{v} = -\left(d\mathbf{p}_F \wedge \mathbf{v}\right) \cdot \mathbf{v} / c_0^2 \, . \qquad (4)$$

Thus, the 4-thrust on the single particle, in any arbitrary frame, is given by

$$\mathbf{F} = -\frac{d\mathbf{p}_F}{d\tau} \, . \qquad (5)$$

Equation (5) expresses, as expected, the law of conservation of the total system energy-momentum, consistently with Equation (2). The change of the mechanical (matter) momentum exactly balances the change of the propulsion field momentum; momentum is then being exchanged within the whole closed system. The device works as a propulsion field momentum "accumulator" whereas the mechanical momentum that can be drawn from it is, by present Physics paradigms, limited to the propulsion field momentum amount.

ELECTROMAGNETIC MASS TENSOR

Since mass tensor anisotropy means non-vanishing 3-momentum in some convenient frame, question arises about the general existence conditions of momentum of electromagnetic origin in the "matter" comoving frame. A fully covariant formulation of the problem requires to consider the Energy-Momentum tensors for a closed physical system consisting of "matter" and EM fields. By applying the Law of 4-Momentum Conservation to the particles and fields contained in any four-dimensional region of space-time bounded by a closed, three-dimensional surface, the system 4-momentum is found, for closed systems, to be conserved in time. Now, if the observer's frame coincides with the frame where the "matter" is at rest when no EM field is present, the condition for anisotropic mass tensor when the EM field is ON, means that in no case the system 4-momentum aligns with the observer's 4-velocity.[10] These are global consequences of mass tensor anisotropy.

When consideration is given to the locality of the energy-momentum conservation law, the following relationship can be found for the volume integral of the momentum densities[11]

$$\int_V \left(g^{(m)} + g^{(f)}\right) dV = - \int_V x \, div\left(g^{(m)} + g^{(f)}\right) dV . \qquad (6)$$

By introducing the relationship between energy flow and momentum density, and assuming that Plank's principle of inertia of energy does not necessarily hold for the EM energy flux, such as a field of group velocity c of electromagnetic waves propagation exists, Eq. (6) becomes

$$\int_V \left(\boldsymbol{g}^{(m)} + \boldsymbol{g}^{(f)}\right) dV = \int_V \frac{\boldsymbol{x}}{c_0^2}\left[\frac{\partial w}{\partial t} - grad\left(\frac{c_0}{c}\right)^2 \cdot \boldsymbol{s}^{(f)} + \left(\frac{c_0^2}{c^2} - 1\right) div\, \boldsymbol{s}^{(f)}\right] dV, \tag{7}$$

with w standing for the mass-energy density.

Transient Regimes

It can be seen that to obtain non-zero total momentum for specific matter-field configurations, a non-vanishing energy density variation rate is a sufficient condition. It is a sufficient condition for any matter-field configuration, provided Planck's principle of inertia holds within polarizable matter too.

Mass tensor anisotropy, as related to a special frame, can thus arise when net mass-energy fluxes take place within closed systems where Planck's principle of inertia holds everywhere, or, in other words, when the system is under anisotropic non-equilibrium conditions.

Stationary Regimes

Eq. (7) becomes, for stationary regimes and any matter-field configuration

$$\int_V \boldsymbol{g}^{(f)} dV = . \\ -\int_V \boldsymbol{x}\left[grad\left(\frac{1}{c^2}\right)\cdot \boldsymbol{s}^{(f)} + \left(\frac{1}{c^2}\right) div\, \boldsymbol{s}^{(f)}\right] dV \tag{8}$$

The quantity between brackets being $div\, \boldsymbol{g}^{(f)}$, a non-zero LHS is possible provided $\boldsymbol{g}^{(f)}$ is not divergence-free everywhere. This can be achieved for arbitrary matter-field configurations if gradients of EM wave propagation group velocity occur in the integration region, i.e., as assumed for the derivation of Eq. (7), Planck's principle of inertia does not hold within polarizable media, in which case the energy-momentum tensor becomes unsymmetrical. This is the case for the setup shown in Fig. 4, where $div\, \boldsymbol{s}^{(f)} = 0$ everywhere and a non-vanishing total EM momentum can only arise from the RHS first term of Eq. (8). The contributions for the volume integral come from the free surfaces of the dielectric, through which jumps of the velocity of light take place in the direction of the EM energy flux.

For this particular setup, transient regimes do not allow to produce an EM momentum contribution since energy density variation rates distribute symmetrically throughout the setup regions.

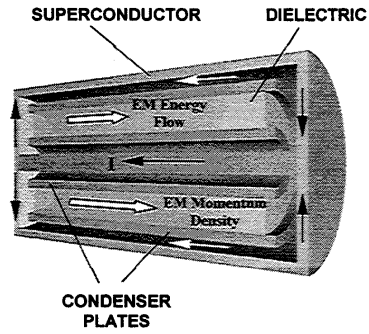

Fig. 4 Stationary regime in the 'matter 'rest frame with polarizable media.

THE ABRAHAM-MINKOWSKI CONNECTION

A non-vanishing EM momentum in the stationary case implies that the whole system Energy-Momentum tensor is unsymmetrical; this is a rather uncomfortable property for a system assumed to be a closed one. Either the assumption that Planck's principle of inertia of energy does not hold everywhere is false, or the system is open and one must consider an extended closed system to which the present one belongs. The first possibility, as far as stationary regimes are considered, completely precludes a closed system to bear a tensor mass; the second possibility leads to the question about what that extended closed system is like. A hint comes from the fact that the "excess" EM momentum behaves as an "external" stress in 4-space. As a conjecture, if ZPF (Zero Point Field) were a physical reality for describing inertia,[12] that "excess" EM momentum could be explained as a form of "directed", anisotropic vacuum fluctuations of EM energy. The sought extended system would then happen to be space-time itself.

The existence conditions are consistent with the use of Minkowski's Energy-Momentum tensor for the EM field.[3] By definition, the Relativistic Mechanics Laws of Conservation are satisfied; the same being true, nevertheless, for Abraham's Energy-Momentum tensor, together with other forms of the electromagnetic Energy-Momentum tensor. This is precisely the still-standing[4,5] Abraham-Minkowski controversy about the form of that Energy-Momentum tensor, specially for low frequency or quasi-stationary fields.[3,13-15] It reduces, basically, to the discrepancy around the mathematical expression of the EM momentum density:

$$\textit{Abraham's claim:} \qquad g^A = \frac{(E \times H)}{c_0^2}, \qquad (9)$$

$$\textit{Minkowski's claim:} \qquad g^M = (D \times B). \qquad (10)$$

The issue is thus highly relevant to "propellantless" propulsion, since the resultant total EM 4-momentum acts exactly as the generic propulsion field $\mathbf{p}_F$ in Eq. (5), so EM inertia manipulation becomes a theoretical possibility. Experiments to definitely settle the question were still missing besides some partialized attempts,[16-19] leading to non conclusive enough results. A positive answer for Minkowski's EM tensor would allow to obtain "jet-less" propulsive effects by EM fields manipulation; furthermore, it could mean an indirect demonstration of the physical reality of ZPF.

A propulsion concept based upon this kind of inertia manipulation mechanism can subsequently be drawn. It basically consists on suitably grouping the sources of electric and magnetic fields within a rigidly connecting device, as depicted in Fig. 4. By doing so, a stationary Minkowski's EM field momentum can develop thanks to the dielectric filled region; by controlling the intensities of these fields, the inertia properties of the system as a whole, when represented by its "matter" part – the device –, are allowed to change so that a conversion of the EM field momentum into mechanical momentum of the device is expected to happen, and reciprocally; again if Minkowski is right. Nevertheless, it must be realized that this device works as an EM momentum "accumulator". The mechanical momentum that can be drawn from, is, in accordance with present Physics paradigms, limited to the "accumulated" EM momentum amount.

ALTERNATE THRUST EXPERIMENTS

Experimental Setup Rationale

An electromagnetic momentum generator (EMMG), based on the schematics of Fig. 5, was engineered up to the "proof of concept" level and an experiment was designed aimed to verify that: a) Minkowski's EM Energy-Momentum tensor does properly describe the electromagnetic field-matter interactions in polarizable media. b) Global EM momentum in the matter rest frame of a closed system is being generated, or, equivalently for such a system, a non scalar 4-mass tensor behaviour is being obtained. c) The experimental thruster is applying mechanical forces on the test stand without expenditure of mass, besides that equivalent to the radiant energy dissipated from the system (e.g., Joule heating), which cannot account for the observed effects.

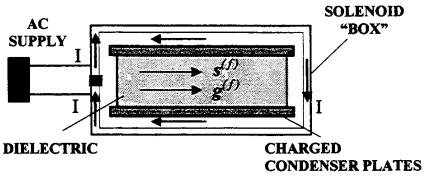

Fig. 5 EM Momentum Generator schematics.

An experimental setup was accordingly built up which consists of mounting the device as a seismic mass atop a mechanical suspension. A supply of 6 A - AC (square wave) to the coils and 4 kV - DC to the capacitors allows for a total EM momentum (Minkowski's formulation) of around 1.E-8 Ns (square wave), by using $BaTiO_3$ ceramic dielectrics. The alleged conversion of Minkowski's EM momentum into mechanical momentum of the EMMG in turn generates forces acting upon this device. By means of a square wave activation of the device at a frequency close to the fundamental frequency of the seismic suspension, the supporting blade of the test fixture can be made to resonate so an amplified upper end displacement response is obtained.

Displacements in the range 10^{-8} - 10^{-7} m were to be expected. Piezoceramic strain transducers were devised to detect this range of displacements, taking into account technological as well as financial constraints. PZTs output voltages proportional to the strain level in a broad dynamic range, achieving sensitivities (seismic and acoustic threshold in controlled environments) up to 10^{-11} m/m.[20] This is two orders of magnitude lower than the expected levels, as related to the sensing fixture shown in Fig. 6. However, the full signal includes ground and environment induced noise as observed in preliminary testing. This microseismic excitation can account for displacements comparable to those expected to be caused by the investigated effect, with a narrow band frequency response centered in the first natural frequency of the sensing fixture.

Another source of unwanted noise is the residual interaction between the coils and the Earth magnetic field, which can account for equally comparable total displacements, albeit with a deterministic distribution in the frequency domain. A third source of noise relates to the magnetic interaction between the moving and the fixed parts of the AC and DC circuits (self magnetic interaction), those belonging to the device atop the resonant blade and to the external power supply

respectively. It was also found to contribute to the displacements on practically the same foot as the formerly two mentioned sources but at twice the coil activation frequency.

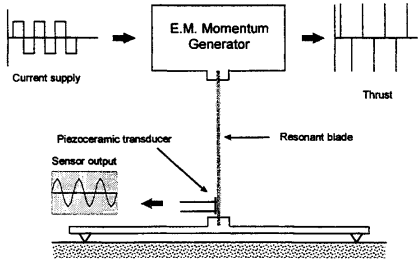

Fig. 6 Micromotion sensing concept.

Other sources of noise have been considered, too, like air motion, electrostatic couplings, sound, radiometric effects, spherics, etc, which can have a degrading effect on the measurements quality, although to a lesser extent than the forementioned sources. The overall estimated effect amounts to -60 dB < S/N < -40 dB at the transducer output and the need for further processing arises. To this aim, the analog transducer output signal is digitalized through a 12 Bit data acquisition board, making it available to PC based storage devices.

Test Implementation and Philosophy

Two series of tests were conducted during the period 1993 - 1997. Only one measurement channel was available along the first series of tests with no vibration isolation provisions. The second test series included, besides the main transducer measurement channel, a dummy seismic fixture with its transducer and measurement channel, a voltage supply measurement channel, and a vibration-free table. In both series data was acquired in 5000 samples sequences at a rate of 500 samples/sec. Power Spectral Density (PSD) using Welch's averaged periodogram method was estimated over a 2048 length frequency interval. The test philosophy was based upon comparison of results in the frequency domain, due to different excitation schemes. These were: A) Ground induced noise. B) Coils ON, capacitors OFF + (A). C) Coils ON, capacitors ON + (A). D) Coils OFF, capacitors ON + (A).

Following modeling and simulation activities, geomagnetic and self-magnetic interaction noises were expected to appear in (B) and (C) as compared to (A), while the influence of the capacitors should appear in (C) as compared to (B) if thrust by inertia manipulation is acting upon the device; no difference was expected to arise beween (D) and (A), since static electric fields alone cannot account for the vibratory behavior of the sensing fixture.

First Test Series

Results corresponding to the first test series are shown in Figs. 7-10 where, as expected, differences can be observed between the (A) and (B) spectra, mainly caused by geomagnetic noise. Differences can also be observed between the (A) and (C) spectra, but there are intriguing differences between the (B) and (C) spectra, while again, as expected, no difference appears between the (A) and (D) spectra.

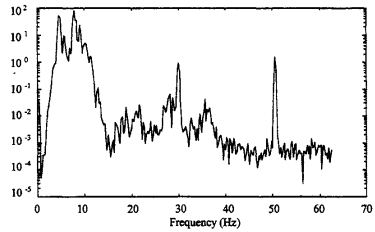

Fig. 7 First test series PSD [V^2/Hz] – Case (A)

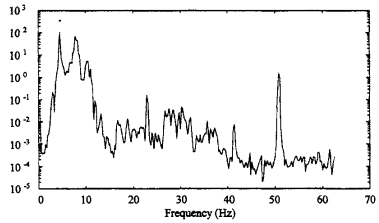

Fig. 8 First test series PSD [V^2/Hz] – Case (B)

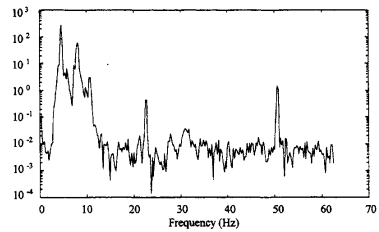

Fig. 9 First test series PSD [V^2/Hz] – Case (C)

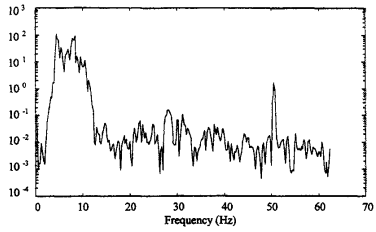

Fig. 10 First test series PSD [V^2/Hz] – Case (D)

Second Test Series

Since a significant amount of ground induced noise was observed during the first test series, a second test series was performed with the improved setup as mentioned before. It was also decided to proceed to intensive signal processing so as to achieve a higher confidence in the EMIM (Electro-Magnetic Inertia Manipulation) effect detection. Data gathered during this second series of tests, was firstly processed to achieve a system identification on the basis of the ground motion excitation only. An ARMA (Auto Regressive Moving Average) model structure was then identified; later, inverse filtering was performed for every output sequence in order to obtain the equivalent ground motion; then, filtering by the vibration isolation fixture led to the reconstruction of the sensing device base motion; finally, optimal filtering (Wiener filter) was performed on the resultant ouput, using the EMMG induced excitation as the "desired" signal.

Raw data exhibit, when transformed to the frequency domain, nearly the same pattern as those of the first test series. However, they show, after processing, a more accurate spectral structure as related to the sought excitation spectrum which consists of equal amplitude odd harmonics of the square wave fundamental frequency, as shown in Fig. 11. Spectrum (A) contains low level residuals induced by the Wiener filter - a sort of numerical artifact - as well as Spectrum(D); Spectrum (B) does not match the "message" spectrum, it better fits that of the geomagnetic noise square wave excitation; Spectrum (C) shows a structure which strongly suggests an alternate impulsive excitation, as it turns out to be when a square wave EM field-matter momenta exchange is present. The figures are representative of around 16 sequences by case. Better detectability can be obtained by means of statistical analysis over the whole ensembles and adaptive noise cancellation procedures, either on the raw output data or on the inverse filtered output data.[21-23]

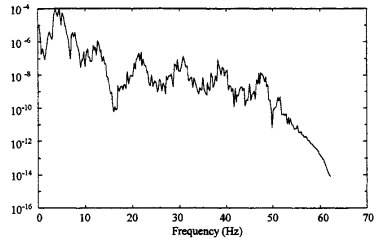

Fig. 11 Second test series PSD [V^2/Hz] – Case (A)

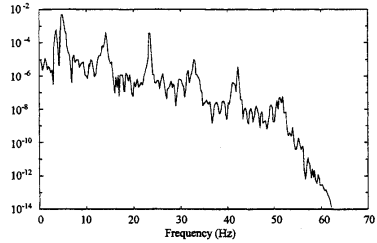

Fig. 12 Second test series PSD [V^2/Hz] – Case (B)

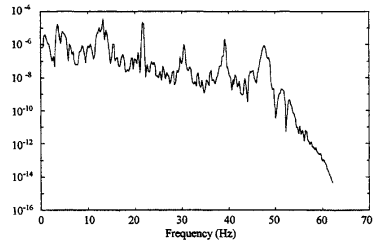

Fig. 13 Second test series PSD [V^2/Hz] – Case (C)

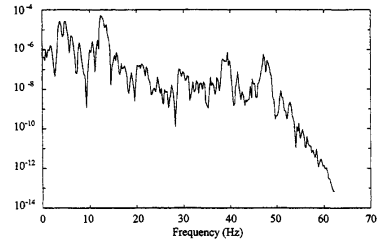

Fig. 14 Second test series PSD [V^2/Hz] – Case (D)

SUSTAINED THRUST EXPERIMENTS

Third Test Series

Notwithstanding the improvements implemented on the second test series, uncertainties still remained which could account for the observed "positive" results, regarding especially to:

a) Geomagnetic influence.
b) Numerical artifacts as in Figs. 11, 14.
c) Colored ground noise centered around the excitation frequency.
d) Air motion (ionic wind).
e) Power supply induced EMI.

In order to get rid of these interfering effects, the experiment was modified during 1999, according to an alternative formulation of the Abraham-Minkowski controversy, this time in terms of force densities. If dispersion is negligible and the medium is allowed to be spatially inhomogeneous and anisotropic, $D_i = \varepsilon_{ik} E_k$, $B_i = \mu_{ik} H_k$. The force densities are given by[3,8]

$$\boldsymbol{f}^M = \rho \boldsymbol{E} + \boldsymbol{j} \times \boldsymbol{B} - \tfrac{1}{2} E_i E_k \nabla \varepsilon_{ik} - \tfrac{1}{2} H_i H_k \nabla \mu_{ik}, \quad (11)$$

$$\boldsymbol{f}^A = \boldsymbol{f}^M - \nabla \cdot (\boldsymbol{DE} - \boldsymbol{ED}) - \nabla \cdot (\boldsymbol{BH} - \boldsymbol{HB}) + \frac{\partial}{\partial t}\left(\boldsymbol{D} \times \boldsymbol{B} - \frac{1}{c_0^2} \boldsymbol{E} \times \boldsymbol{H} \right) . \quad (12)$$

With the isotropic medium approximation Eqs. (11) and (12), reduce to

$$\boldsymbol{f}^M = \rho \boldsymbol{E} + \boldsymbol{j} \times \boldsymbol{B} - \tfrac{1}{2} E^2 \nabla \varepsilon - \tfrac{1}{2} H^2 \nabla \mu , \quad (13)$$

$$\boldsymbol{f}^A = \boldsymbol{f}^M + \frac{\varepsilon_r \mu_r - 1}{c_0^2} \frac{\partial}{\partial t} (\boldsymbol{E} \times \boldsymbol{H}) . \quad (14)$$

These force densities clearly differ inside matter for generic fields; they are however identical for static fields, irrespective of the medium. If harmonic fields are considered, the force densities instantaneous values differ but their averaged values become identical and therefore useless for discriminating between the two formulations. This is the reason Walker&Walker's claim,[18] favoring Abraham's one, is essentially wrong and the experiment remains inconclusive.

The EM inertia manipulation (EMIM) experiment was modified in such a way that both $\boldsymbol{D}$ and $\boldsymbol{B}$ fields were subjected to harmonic evolution. The averaged effect of the total EM force was sought after, so Eq. (13) must be used for its theoretical estimation as applied to the schematics of Fig. 5. This estimation can proceed straighforwardly by neglecting capacitor edge effects, by considering the coils as a conducting "box" bearing a negligible voltage w.r.t. to the capacitor plates and by assuming that the polarization current within the dielectric contributes to the second term of Eq. (13).

As a result, electric self-interaction, represented by the first term of Eq. (13) and magnetic self-interaction represented by the second term of the same equation, simply cancel out. Since non-magnetic matter is involved, contribution to the total EM force acting upon the device comes from the third term. This contribution is non-zero through the boundaries of the dielectric filled volume. Since induced electric fields of magnitude E_i appear on these boundaries yielding an unbalancing effect on the electric field of magnitude E set by the capacitor, the integrated effect does not cancel out in the $\boldsymbol{E} \times \boldsymbol{H}$ direction and can be written as ($\varepsilon_r >> 1$)

$$F = 2 \varepsilon_r \varepsilon_0 E E_i A_L , \quad (15)$$

where A_L represents the lateral open surfaces of the dielectric. Application of the formula for parallel plates capacitor of width d, Lenz's Law and Ampere's Law for an infinite length solenoid of n turns, yields the following expression for the EM instantaneous thrust, as a function of the harmonic voltage $V \sin \omega t$ on the capacitor and the harmonic current $I \sin(\omega t + \phi)$

$$F = -\frac{\varepsilon_r \varpi n I V d}{c_0^2} \left(\frac{1}{2} \sin 2\varpi t \cos\varphi - \sin^2 \varpi t \sin\varphi \right) . \quad (16)$$

The averaged value then results

$$\langle F \rangle = \frac{\varepsilon_r \varpi n I V d}{2 c_0^2} \sin\varphi , \quad (17)$$

with maxima at $\varphi = \pm \pi/2$. The results obtained with Walker&Walker's experiment are consistent with this formulation and can, as the authors readily did, be interpreted in terms of the polarization current contribution to the Lorentz force.

However, Eq. (17) must be seen as a conflicting result if total momentum must be conserved, as stated previously. In fact, the standard treatment of the problem requires the polarization current to be excluded from the magnetic contribution to the Lorentz force, the self-magnetic interaction does not longer cancel out and Eq. (16) must be corrected as follows

$$F = 2\varepsilon_r \varepsilon_0 E E_i A_L - \dot{P} B V_C \ , \qquad (18)$$

where V_C stands for the capacitor volume filled with the dielectric. By adopting the same assumptions as for the derivation of Eq. (16), the second term of Eq. (18) becomes

$$F_{(2)} = -\frac{\varepsilon_r \varpi n I V d}{c_0^2}\left(\frac{1}{2}\sin 2\varpi t \cos\varphi + \cos^2 \varpi t \sin\varphi\right) \qquad (19)$$

so the total "standard" force is

$$F^S = -\frac{\varepsilon_r \varpi n I V d}{c_0^2}\left(\sin 2\varpi t \cos\varphi + \cos 2\varpi t \sin\varphi\right), \qquad (20)$$

and the averaged value goes to zero.

Therefore, the modified EMIM experiment should allow to discriminate between the "standard" and the presently proposed formulation of the averaged EM force. To take advantage of the sensing device characteristics, the voltage supply is reversed at a frequency different from the supply frequency, so the seismic setup is put into vibratory motion if the "proposed" formulation is correct. By detecting this force, the interfering effect (a) becomes averaged out; direct detection also permits to overcome the interfering effect (b) since no Wiener filtering is necessary; if the voltage reversing frequency is different from the setup natural frequencies, the interfering effect (c) becomes less significant and air motion (d) being related to the power supply frequency averages out too. Uncertainties are expected to remain regarding interfering effect (e).

Experiments were performed according to the test philosophy of the preceding test series. A reversing frequency of 30 Hz was chosen. Propulsive effects show up only when the Caps ON – Coils ON condition holds. Furthermore, maxima are obtained for a voltage-current phase shift of nearly 90 degrees, as predicted by the proposed formulation. A comparison of case (C) results with the corresponding simulation results (dotted line) is shown in Fig. 15, where a close agreement is found for the response to the alleged EMIM averaged force at 30 Hz reversing frequency. A comparison between cases (A) and (C) is shown in Fig. 16. Phase shift dependence is shown in Fig. 17, where experimental PSD peak values at 27 Hz are plotted against the voltage-current shift angle.

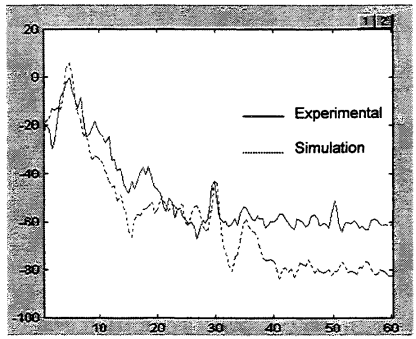

Fig. 15 Third test series PSD [dB] – Case (C) experimental and simulation results.

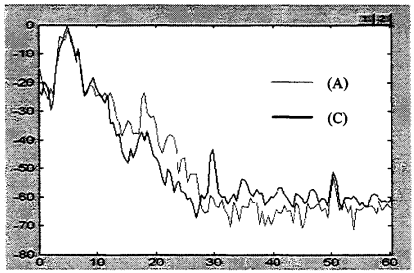

Fig. 16 Third test series PSD [dB] – Cases (A)&(C).

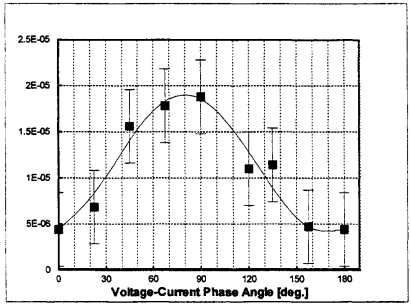

Fig. 17 Third test series average PSD peak values [V^2/Hz] @ 27 Hz, with 90% confidence intervals.

Spreading of the PSD peak values for a given angle was initially thought being due to contributions of magnetic interactions between the capacitor and the coil circuits during non-synchronized voltage reversings and/or between the capacitor circuit and the geomagnetic field. However, order of magnitude estimations show those interactions to be unable to account for the observed deviations. Their source remains unknown, so far, except for fluctuations of ground noise components at the reversing frequency. Nevertheless, a slightly shifted squared sine trend can clearly be seen to emerge from the plotted data.

LAYMAN'S SUMMARY

Either to go to the stars or, more pragmatically, to substantially cut down space transportation costs, new propulsion mechanisms must be found which get rid of propellants and/or conventional external assistance, i.e., the mythical "space drive" must still be invented.

Recent theoretical works show that jetless–sailless–beamless–tetherless propulsion can be achieved by manipulating the spaceship inertia in a way analogous to a dancer who increases her angular velocity by manipulating her body moment of inertia. To do that, an "extended" spaceship including the fields it eventually generates must be considered; a thrust then appears on the "material" spaceship by means of momentum exchange with its "field" complement.

This research has been conducted with the goal of checking whether the electromagnetic field is suitable for the above-mentioned purpose, since it can be shown that a theoretical formalism (Minkowski's) gives credit to that possibility. Experiments were designed and performed which, in an exploratory phase, gave indirect evidence of Minkowski's approach being valid. In a second and ongoing phase, following slight changes of the experiment implementation, direct and clearer evidence of sustained thrust (as it should be for operational propulsion) is being found.

However, the sustained thrust must, in principle, be seen as an "anomalous" effect since the Law of Momentum Conservation seems to be violated. This casts doubts about the validity and/or interpretation of the results and further experimental work, including in-orbit testing, is required to arrive to safer conclusions. If the effect still remains, propellantless propulsion would have been achieved but additional theoretical work will be needed for the full understanding of the underlying physical principles.

CONCLUSIONS

Theoretical as well as experimental research about a propellantless propulsion concept has been presented. On the theoretical side, thrusting without reaction mass or beamed power, seems to be possible by EM inertia manipulation, provided existence conditions hold, as those consistent with Minkowski's Energy-Momentum tensor for the EM field. However, the validity of this formalism is presently arguable under the still-standing Abraham-Minkowski controversy, the main argument being the unsymmetrical nature of that tensor. Experimental elucidation of the controversy was sought after and instrumented around a so called EMIM force-producing device.

Tests performed during the period 1993 - 1997 produced results which after intensive data processing, consistently pointed to a mechanical vibration induced by mass/inertia tensor warping of the device, or matter-electromagnetic field momentum exchange, as predicted by Minkowski's formalism. However, no direct detection of the sought effect has been obtained up to now; the experimental setup overall detectability needs further improvements, jeopardized by several potentially interfering effects.

A third series of tests conducted during 1999 and 2000 on a redesigned experiment to get rid of most of the identified spurious effects, yield comparatively sharper and clearer evidence of EMIM induced effects, albeit in contradiction with null results predicted by the "standard" formulation of global EM forces. Moreover, the results seem to indicate that the system momentum is not conserved, casting severe doubts about their validity; however, a conclusive demonstration that this is absolutely forbidden by the laws of Physics has not yet been provided and future breakthroughs in understanding the nature of inertia and motion may lead to more optimistics prospects. On the other hand, the alternative formulation presented in this paper correctly predicts peer-reviewed experimental results.

Further work still remain to be done to confirm these results, especially from the viewpoint of power supply induced EMI on the measurement channels, sharing the same spectral signature with the pursued effect, which could be overcome by means of Interferometer/Doppler vibrometry techniques. Another noise source was identified as being related to self-magnetic interactions in wiring and windings of power-supply components. Although efforts have already been made to filter out its influence from the experimental data, safer results will be obtained by a substantial increase of power. This will allow to use a reversing voltage frequency close to the fundamental frequency of the sensing device, in

order for the alleged observable effect to show up well over the ground induced noise. In-orbit testing will indeed provide final answers, by simultaneously getting rid of all mentioned interferences.

ACKNOWLEDGMENTS

The author wishes to thank the U.S. Air Force Research Laboratory for supporting the presentation of this work under its Windows-on-Science Program, and to NASA BPP Project for procuring that help. Support from the Argentine National Agency for the Advancement of Science and Technology under Grant PICT-99-10-07107, and "Instituto Universitario Aeronautico" of Cordoba, Argentina, are also gratefully acknowledged.

REFERENCES

[1] Millis, M. G., "Challenge to Create the Space Drive," *Journal. of Propulsion and Power* **5**, 577-582 (1997).

[2] Brito, H. H., "A Propulsion-Mass Tensor Coupling in Relativistic Rockets Motion," in *Proceedings of the Space Technology Applications International Forum (STAIF-98)*, edited by Institute for Space and Nuclear Power Studies, Albuquerque, NM, Part Three, 1998, pp. 1509-1515.

[3] Brevik, I., "Definition of some Energy-Momentum Tensors," *Experiments in Phenomenological Electrodynamics and the Electromagnetic Energy-Momentum Tensor,* PHYSICS REPORT (Review Section of Physics Letters) **52**, No. 3, 1979, p. 139.

[4] Antoci, S., Mihich, L., "A forgotten argument by Gordon uniquely selects Abraham's tensor as the energy-momentum tensor for the electromagnetic field in homogeneous, isotropic matter," *Nuovo Cimento B* **112 B**, 991-1007 (1997).

[5] Johnson, F. S., Cragin, B. L., Hodges, R. R., "Electromagnetic momentum density and the Poynting vector in static fields," *American Jnl. of Physics* **62**, 33-41 (1994).

[6] Jackson, J. D., "Time-Varying Fields, Maxwell's Equations, Conservation Laws," in *Classical Electrodynamics*, 2nd Ed., edited by John Wiley & Sons, Inc., New York, Publisher, 1962, pp. 169-202.

[7] Portis, A. M., "Fuentes del campo electromagnético III - Cantidad de movimiento del campo," in *Campos Electromagnéticos*, Sp. ed., Vol. 2, edited by Ed. Reverté, Barcelona, Publisher, 1985, pp. 469-472.

[8] Eu, B. C., "Statistical foundation of the Minkowski tensor for ponderable media," *Phys. Review A* **33**, 4121-4131 (1986).

[9] Marchal, R., "Sur l'inertie électromagnétique," *Comptes Rendus* **268 A**, 299-301 (1969).

[10] Brito, H. H., "Propellantless Propulsion by Electromagnetic Inertia Manipulation: Theory and Experiment," *AIP Conference Proceedings 458*, American Institute of Physics, New York, 1999, pp. 994-1004.

[11] Furry, W. H., "Examples of Momentum Distributions in the Electromagnetic Field and in Matter," *American Jnl. of Physics* **37**, 621-636 (1969).

[12] Haisch, B., Rueda, A., Puthoff, H. E., "Inertia as a zero-point field Lorentz force,"*Physical Review A* **49**, 678-694 (1994).

[13] Lai, H. M., "Electromagnetic momentum in static fields and the Abraham-Minkowski controversy," *American Jnl. of Physics* **48**, 658-659 (1980).

[14] Brevik, I., "Comment on "Electromagnetic Momentum in Static Fields and the Abraham-Minkowski Controversy"," *Physics Letters* **88 A**, 335-338 (1982).

[15] Lai, H. M., "Reply to "Comment on 'Electromagnetic Momentum in Static Fields and the Abraham-Minkowski Controversy'"," *Physics Letters* **100 A**, 177 (1984).

[16] James, R. P., "Force on Permeable Matter in Time-Varying Fields," *Ph.D Thesis*, Dept. of Electrical Engineering, Stanford University, 1968.

[17] Walker, G. B., Lahoz, D. G., Walker, G., "Measurement of the Abraham Force in Barium Titanate Specimen," *Canadian Jnl. of Physics* **53**, 2577-2586 (1975).

[18] Walker, G. B., Walker, G., "Mechanical forces in a dielectric due to electromagnetic fields," *Canadian Jnl. of Physic* **55**, 2121-2127 (1977).

[19] Lahoz, D. G., Graham, G. M., "Observation of Electromagnetic Angular Momentum within Magnetite," *Physical Review Letters* **42**, 137-1140 (1979).

[20] Forward, R. L., "Picostrain measurements with piezoelectric transducers," *Jnl. of Applied Physics* **51**, 5601-5603 (1980).

[21] Widrow, B. et al, "Adaptive Noise Cancelling:Principles and Applications," *Proceedings of the IEEE*, Vol. 63, No. 12, Dec. 1975, pp. 1692-1716.

[22] Proakis, J. G., Rader, C. M., Ling, F., Nikias, C. L., "Adaptive Filters," in *Advanced Signal Processing*, Macmillian Publishing Company, New York, 1992, pp. 315-399.

[23] "DSP Design and Simulation Using the SIMULINK DSP Blockset," *SIMULINK Technical Computing Brief*, The Mathworks Inc., Natick MA, 1996.

A01-34344

AIAA 2001–3658
Specially Conditioned EM Radiation Research with Transmitting Toroid Antennas

H.D. Froning Jr.
Flight Unlimited
Flagstaff, AZ, USA

G.W. Hathaway
Hathaway Consulting Services
Toronto, ON, Canada

37th AIAA/ASME/SAE/ASEE Joint Propulsion Conference and Exhibit
8-11 July, 2001
Salt Lake City, UTAH

AIAA 2001-3658

SPECIALLY CONDITIONED EM RADIATION RESEARCH WITH TRANSMITTING TOROID ANTENNAS

H. David Froning
Flight Unlimited
5450 Country Club Dr.
Flagstaff, AZ 86004, U.S.A.

George Hathaway
Hathaway Consulting Services
39 Kendal Ave.
Toronto, ON/M5R IL5, Canada

Abstract

Experimental work to: (a) determine em field characteristics associated with em radiation created by alternating current flowing through toroidal coils at resonant frequencies, and (b) determine if the specially conditioned em fields associated with such radiation could cause a discernable gravity modification, is described. This experimental work was the result of collaboration between Flight Unlimited (FU) and Hathaway Consulting Services (HCS), performed at the laboratories of HCS in Toronto, Canada during a test period in 1998 and during a test period in 2000. Tested toroid configurations included: circular toroids with differing diameters and winding densities; and asymmetrical toroids for focusing em radiation into narrower and more intense beams. The toroid configurations and the AC power and instrumentation systems available at HCS limited the experimental work to the relatively low radio frequencies (400 kHz to 110 MHZ) of the electromagnetic spectrum.

INTRODUCTION

Just as airflight was not revolutionized until propeller propulsion was superceded by a new mode of impulsion (jet propulsion), so spaceflight may not be revolutionized until jet propulsion is superceded by a new mode of impulsion (field propulsion). Field propulsion would develop thrust by actions and reactions of fields instead of by combustion and expulsion of mass. And field actions and reactions that would greatly reduce propellant (the major portion of rocketship mass) and engine thrust requirements would be those that would reduce the resistance of gravity and inertia to ship acceleration.

One conceivable way of reducing the resistance of gravity and inertia is by accomplishment of a favorable coupling between those fields which underlie electromagnetism and gravity. But no significant coupling of ordinary em fields with those that give rise to gravity may be achievable because their essence is completely dissimilar. Yang (1) notes that "nonabelian" fields which probably give rise to gravity are of more intricate topology and higher internal symmetry than the "abelian U(1)" fields that underlie ordinary electromagnetism. In this respect, Barrett (2, 3) has identified two ways of transforming ordinary em fields into specially conditioned em fields of nonabelian form and higher than U(1) symmetry. One identified way of creating such fields is modulating the polarization of em wave energy emitted from microwave or laser transmitters. Such polarization modulation creates em fields of nonabelian form and SU(2) symmetry within beams of radiated power that can be focused into very narrow beams of very high energy density. Thus an experiment to detect possible gravity modifications within narrow polarization modulated laser beams has been submitted to the NASA Breakthrough Propulsion Physics (BPP) program. This experiment is described in (4).

Another way of transforming ordinary em fields into specially conditioned em fields of nonabelian form and SU(2) symmetry is with toroidal coils through which alternating current is flowing at resonant frequencies. Barrett (3) shows that such specially conditioned em radiation includes - not only electric and magnetic field energy - but A Vector potential field energy as well. Barrett predicts that A Vector field intensity maximizes at discreet resonant frequencies. Thus, if an A Vector potential field underlies the essence of gravitation, gravity modification might be possible in the vicinity of toroids transmitting at such frequencies.

Fabrication and testing costs were significant for polarization modulated laser beams. However, they were found to be relatively modest for toroidal coils

configured for operation in the lower (radio-frequency) range of the em spectrum. Thus a cooperation between Hathaway Consulting Services (HCS) and Flight Unlimited (FU) was established to: test Barrett's hypotheses as to specially conditioned em radiation emitted from toroidal coils; and to determine if gravity modification could occur within such radiation. Probability of gravity modification by radio frequency radiation from inexpensive toroids was deemed to be very low. But it was hoped that the tests would reveal interesting electromagnetic phenomenon and extend our knowledge of electromagnetics.

TRANSMITTING TOROID ANTENNAS

EM wave propagation by transmitting toroid antennas has been examined by various investigators for more than a decade. Examples are U.S. Patent No. 4,751,515 awarded to Corum for an "electrically small, efficient electromagnetic structure that may be used as an antenna or waveguide probe" and U.S. Patent No. 5,442,369 awarded to Van Voorhies et al. for an antenna that "has windings that are contra wound in segments on a toroid form and that have opposed currents on selected segments". In this respect, Barrett (4) has shown that specially conditioned em fields of SU(2) symmetry and nonabelian form can be created by transmitting toroid antennas - as in Figure 1.

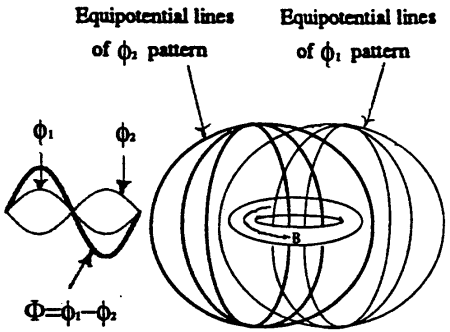

Fig. 1 – A Vector Potential Patterns

The magnetic and electric fields which encompass a transmitting toroid are accompanied by A Vector potential fields, and the alternating current flow produces overlapping A Vector potential patterns which encircle the toroid ring, as shown in Figure 1. These A Vector patterns combine into "phase factor" waves which represent disturbances in A Vector potential. The maximum disturbance in A Vector potential occurs as phase factor wave intensity peaks at the resonant frequencies where A Vector potential patterns are exactly out-of-phase, and a predicted pattern of these disturbances is shown in Figure 2.

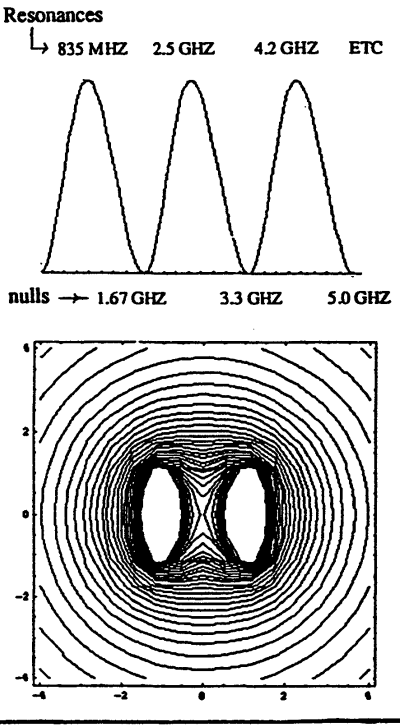

Fig. 2 – "Phase Factor" Wave Patterns

Resonant frequencies are determined by the shape and dimensions of the toroid, and by the propagating direction and speed of the alternating electric current thru its windings. And, if an A Vector potential field underlies the essence of gravitation, the probability of gravity modification in the toroid vicinity would be highest at resonant frequencies.

INITIAL TOROID EXPERIMENTS

Initial experimental work involved: (a) fabrication of transmitting toroid antennas that, according to (4), should emanate specially conditioned em radiation; and testing of the toroids at low power levels at the laboratories of HCS in Toronto. The general goals of this initial work, which was performed on March 6 and 7 during 1998, were: perfection of techniques for fabricating toroidal coils, detection of resonant phenomenon indicative of A Vector potential resonances with such coils; and identification of problems associated with operating toroidal coils over wide frequency ranges and at significant power levels.

Most of the goals of the initial work were achieved. Toroid antennas with conventional and caduceus windings were successfully fabricated, and although no instrumentation (such as Josephson Junction arrays) were available for directly detecting A Vector fields, measured resonances (reversals in phase and amplification of signal strength) were in good agreement, as indicated in Figure 3, with Barrett's predictions predicated on occurrence of A Vector fields. Heat generated by current flow within the relatively thin windings of the toroids and their relatively fragile styrofoam interiors limited input power to less than 100 watts in the initial experiments. This identified the need for thicker wires and stronger structures for higher toroid power and temperature.

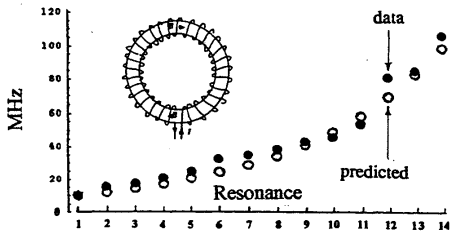

Fig. 3 – Correlation of Theory and Experiment

FOLLOW-ON TOROID EXPERIMENTS

Because results of the initial toroid experiments were somewhat encouraging, it was decided to have a follow-on experimental program, which included toroids configured for much higher power levels, at HCS between June 9 and June 15, 2000. It included: (a) signal phase/amplitude tests to precisely determine the resonant frequency characteristics of each different transmitting toroid configuration; (b) magnetic field measurements to map em field intensity in the vicinity of each toroid; (c) propagation characteristics of toroid radiation; and (d) limited gravitometer testing to search for a gravitational disturbance at a one location near one of the transmitting toroids.

Toroid Configurations Tested

To our knowledge, transmitting toroid antennas built and tested by most other investigators have been designed for communication purposes - with wires loosely wound (widely separated) around the toroid's ring in order to maximize far field intensity and range. By contrast, our tested toroids were "tightly wound" to maximize near-field intensity for possible gravity modification - not far field range for communication. Our tested toroids were "contra-wound" in a caduceus pattern to allow 2 types of modulation. One, in which current flowed in opposite directions in crossing wires, resulted in an "opposing" or "bucking" mode which caused opposing magnetic fields that cancel themselves along the toroid ring centerline. The other, in which current flowed in the same direction - resulted in an "adding" mode. Figure 4 shows the 4 different toroid configurations that were tested during the follow-on experimental program.

The loosely-wound toroid (upper left) was built for comparing its near-field intensity with that of the tightly wound toroid (lower left). Both toroids had similar cross sections (approximately 4.0 cm) and the same outer diameters (21cm) and wire size (No. 20). The greater winding density of the tightly wound toroid (350/333 inner/outer turns vs 26/25 inner/outer turns) resulted in greater near-field intensity for a given input power. The toroid in the upper right was configured with a larger outer diameter (31 cm.) than the lower left one and No. 20 wire size but its cross-section is the same. The larger diameter resulted in more windings (398/384 inner/outer turns of No. 14 wire). And the "tear drop" shaped toroid (lower right) was configured to focus radiation into more intense and elongated beams. Its length, breadth and thickness was 26.5, 18.0, 2.5 cm. It had a hole diameter of 7.3 cm; and 95/88 inner/outer turns of No. 14 wire. And, because of their stronger structure (hard maple wood) and larger wire diameter, the tear drop and larger diameter toroids could withstand the heating associated with 1.0 KW of radiated em power.

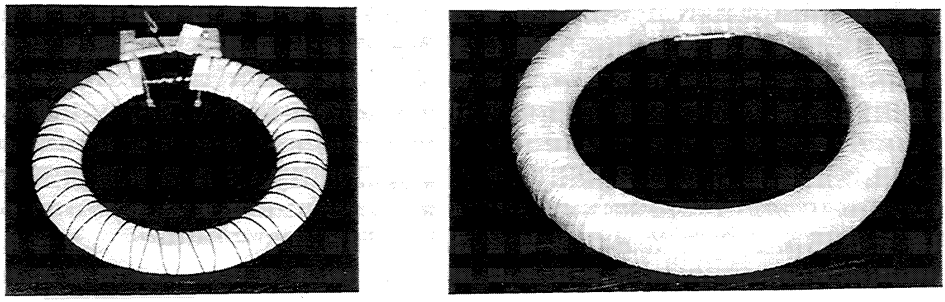

Fig. 4 – Toroid Configurations Tested

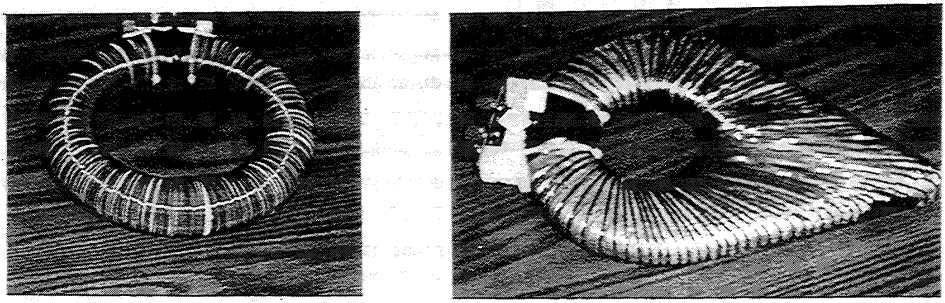

As in the first test series, resonant conditions (revealed by reversal in signal phase and rise in signal amplitude) were searched for at all ac frequencies between 400 KHZ and 110 MHZ. This was done for each toroid configuration for current opposing and current adding modes of operation. Equipment used for the resonance sweeps was an HP 4193 vector impedance analyzer. Figure 5 shows part of the test set-up for detecting resonant modes for each toroid configuration and each operating mode.

Although resonances were detected throughout almost the entire 400 KHZ to 110 MHZ frequency spectrum available at HCS, toroid radiation of significant power was only achievable in the 1.0 to 20 MHZ range. Resonant frequencies selected for measuring field characteristics of each toroid were therefore within this range. Selected resonant frequencies for the large diameter toroid were 2.36 and 17.30 MHZ for current-adding and current-opposing modes of operation, while those for the medium diameter toroid were 2.36 and 18.30 MHZ. Selected resonant frequencies for the tear drop toroid was 5.66 and 3.94 MHZ for current-adding and current-opposing, while the current-opposing, resonant frequency selected for the loosely wound toroid was 19.70 MHZ.

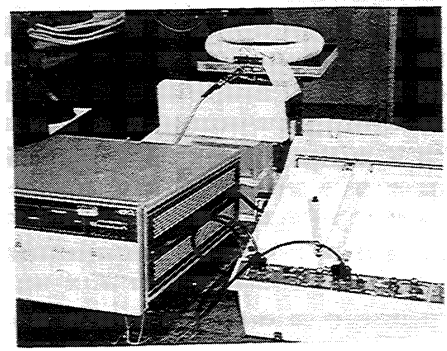

Fig. 5 – Resonance Sweep Set-Up

Toroid Field Intensity Measurements

Magnetic field intensity was measured out to 50 cm from each toroid center, and along the upper and lower surface of each toroid as well. For an applied power of 10W, the magnetic field component of each toroid's radiation was measured by a small magnetic pick-up coil shown in Figure 6, which converted the actual magnetic field intensity into an equivalent electric field strength (in micro volts per meter).

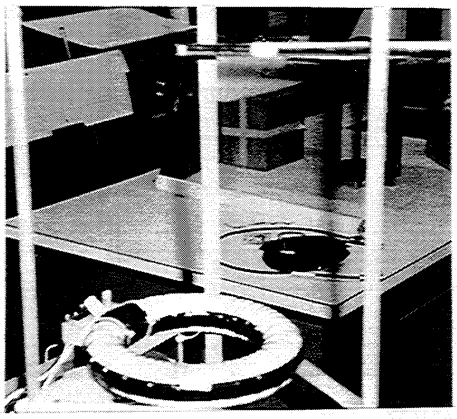

Fig. 6 – Magnetic Field Probe

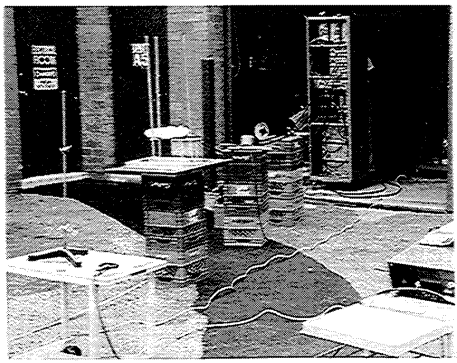

Fig. 7 –Toroid Range Test Set-Up

Variation of the large diameter toroid's field strength with range (out to 10 meters) was measured with various types of antennas outside the HCS facility with the test set up as indicated in Figure 7. Data consistent with expected near-field signal strength variation with range was measured when the toroid was radiating in a current-adding resonant mode at 1.20 MHZ. But measurements in a current-opposing resonant mode were anomalous - in that no significant signal strength variation with range was detected.

Search For Gravity Modification

Final toroid testing activity was searching for gravitational field modifications within the specially conditioned em field regions surrounding toroids radiating at resonant frequencies. Gravitational disturbances were searched for with a "Prospector Model 420" gravitometer, manufactured by W. Sodin Ltd, which is capable of detecting changes as small as one-millionth of one percent of ambient gravity. This gravitometer's stainless steel shell and aluminum base does not provide complete magnetic field shielding. But its dewar-enclosed, all-quartz mechanical balance system is not influenced by ordinary em emissions. Unfortunately, preceding test activities took longer than expected, leaving time to search for gravity modification for only one of the toroids (the large diameter one) at only one location with respect to the gravitometer. The limited time remaining also required a very rapid toroid/gravitometer set up. This was achieved by the positioning shown in Figure 8.

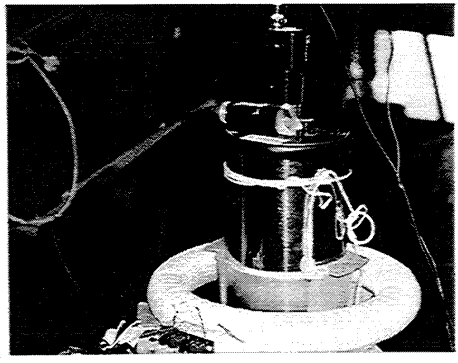

Fig. 8 – Toroid/Gravitometer Set-Up

TOROID TESTING RESULTS

Resonant frequencies between 400 KHZ and 110 MHZ were obtained for each toroid. And, for the purposes of mapping magnetic field intensity in each toroid's vicinity, one resonant frequency was selected for each operating mode for each toroid. Field intensity out to 10 m from the large diameter toroid was also measured together with the influences of magnetically shielded structures on its field intensity. Finally, the effect of large diameter toroid field intensity on gravity modification was explored. The results of these efforts are summarized in the following sections.

Toroid Resonance Determination

Resonant frequencies for current-adding and current-opposing operating modes were obtained for each toroid. Figures 9 and 10 show examples of the resonances obtained for the large diameter and tear-drop toroids throughout the 400 KHZ-110 MHZ radio frequency spectrum available at HCS.

Toroid Field Patterns

Magnetic field intensity variation with radial distance for the 3 circular toroids was similar with intensity maximizing near the inner surface of each toroid's ring. And, as would be expected, intensity diminished rapidly with increasing distance above and outside each toroid. Figure 11a and 11b show no definite trend with respect to the influence of toroid diameter. Higher magnetic field intensity is achieved by the smaller diameter toroid in a current-opposing mode of operation while higher magnetic field intensity is achieved by the larger diameter toroid in a current-aiding mode. Figure 11c shows a definite trend - with increased windings over a given toroid geometry resulting in increased magnetic field intensity.

Significant focusing of the electromagnetic energy radiated from the asymmetrical "tear drop" toroid was accomplished. Figure 11d shows that magnetic field intensity is enormously greater at given distances forward of the center of the toroid's hole than for the same distances aft of the hole center. Figure 9d also shows a top and front view of the tear drop toroid field pattern for a given magnetic field intensity. It is seen that more electromagnetic energy is focused into the forward direction than into the aft or side directions and that the toroids flattened shape (its reduced thickness) causes less radiation to be dissipated in directions transverse to the toroid plane.

One interesting discovery was formation, in the circumferential direction, of standing em waves along the upper and lower surfaces of transmitting toroids. No standing wave measurements were made on the loosely wound toroid. However, numbers of magnetic field peaks and nodes measured circumferentially on the top and bottom surfaces of the other circular toroids were 8 for the medium diameter toroid and 10 for the large diameter one. And at least 6 magnetic field peaks and nodes were measured on the top and bottom surface of the tear drop toroid.

Attenuation of Toroid Field Intensity

Field strength attenuation with range from the center of the large diameter toroid is shown in Figure 12. It was about as expected when radiating at a resonant frequency of 1.2 MHZ in a current adding mode of operation, with a steep signal drop (greater than $(1/r)^3$ out to about 1.0 meter and with an expected near-field $(1/r)^2$ variation between 3 and 10 meters from the toroid. But measurements made with the toroid radiating at a resonant frequency of 17.3 MHZ in a current opposing mode indicated no significant variation in signal strength at distances 3 to 10 meters from the toroid. After continual measurements and re-measurements with various types of antennas, we have no definitive explanation for lack of signal strength reduction with increasing range - other than the possibility of operating slightly off resonance and a significant drop in signal strength.

Additional anomalous behavior may also have been observed for the large-diameter toroid - in that almost identical signal strength was measured at a given location and distance from the toroid when radiating in free space and when radiating from within a magnetically shielded (mu metal) enclosure. These results are considered inconclusive because stray signals were detected from power supply leads which were outside the shielded enclosure. Since measured signals were almost identical for both shielded and un-shielded conditions, and since it is unlikely that almost all of the measured free space signal was from the power supply leads, it is conceivable that some of the toroid's em wave energy was propagated through the magnetically shielded mu metal walls.

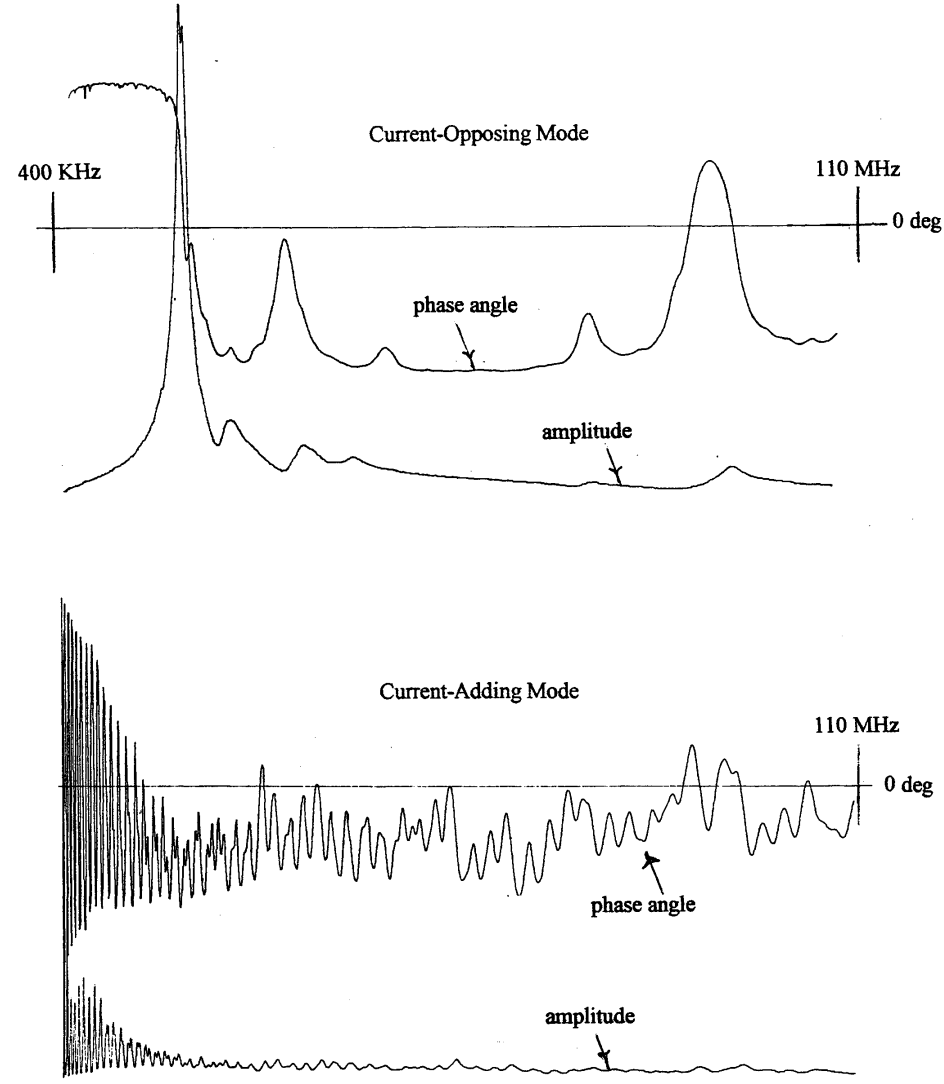

Fig. 9 – Resonances for Large Diameter Toroid

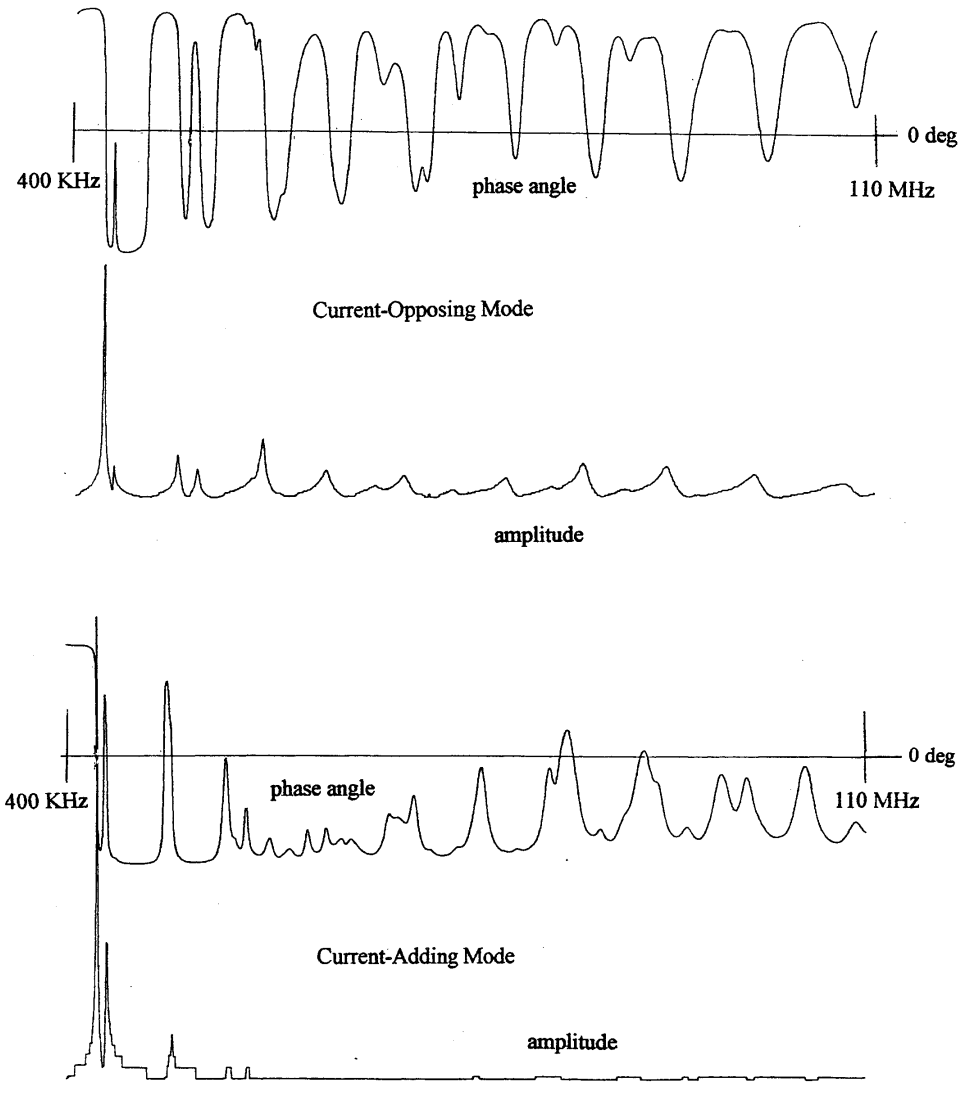

Fig. 10 – Resonances for "Tear-Drop" Toroid

Fig. 11 – Magnetic Field Patterns in Toroid Vicinity

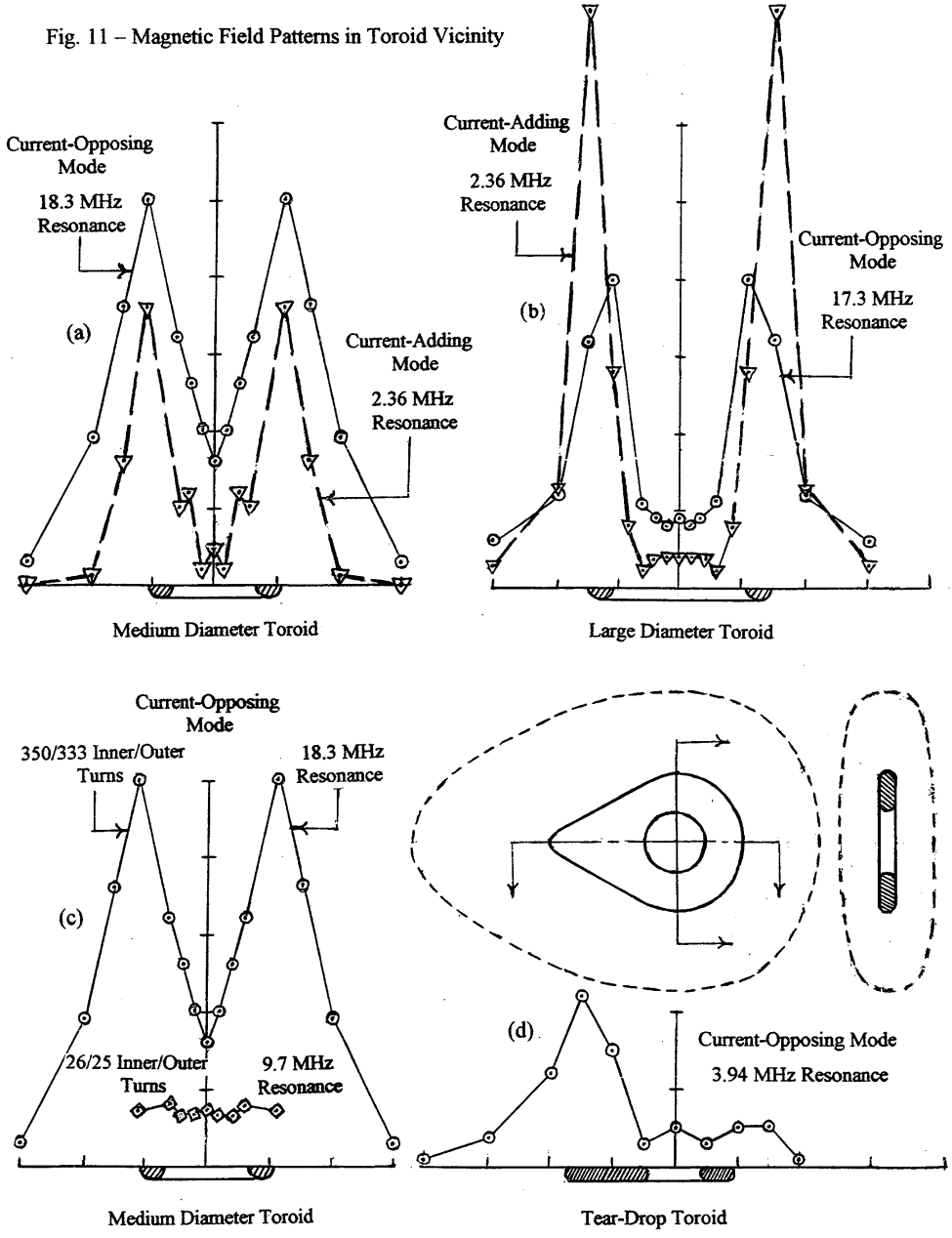

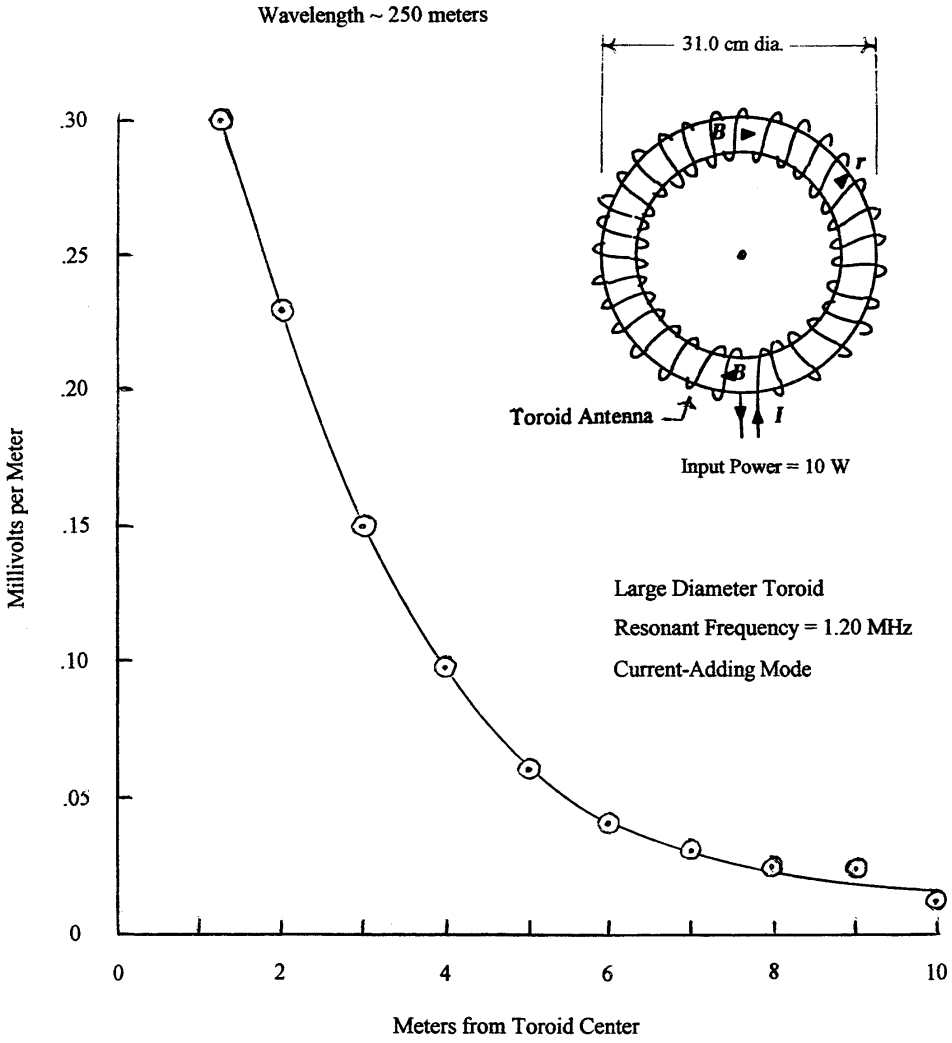

Fig. 12 - Attenuation of Toroid Signal with Range

Search for Gravity Modification

The possibility of gravity modification in the vicinity of transmitting toroid antennas was briefly investigated by use of the Prospector 420 gravitometer and the large diameter toroid radiating up to 0.5 KW of average power at the resonant frequencies associated with current-aiding and current-opposing operation modes. For these powers and operating modes, no discernable gravity modification was detected for the single toroid/gravitometer positioning that time allowed.

As previously mentioned, time limitations required a rapid toroid/gravitometer test set-up which resulted in the gravitational mass being located in a magnetic field region whose intensity was subsequently found to be much less than magnetic field intensity existing in other locations. For the current opposing mode of operation, measured magnetic field intensity at the gravitometer test mass location was only about 15 percent of the maximum intensity measured near the toroids inner diameter. And toroid magnetic field intensity at the gravitometer test mass location was only about 2 percent of the maximum measured magnetic field intensity for the current-adding mode.

One conceivable reason for non-discernable gravity modification is, of course, 5 to 50 times less em field intensity at the single location probed by the gravitometer, as compared to locations of maximum intensity. But another reason could be dissimilarity in field topologies associated with toroid em emanations and gravity. And still another reason could be enormous possible differences in the frequencies and wavelengths characterizing gravitational fields and those that characterize electromagnetic fields created by transmitting toroid antennas.

SUMMARY AND CONCLUSIONS

Although interesting phenomenon are associated with em fields created by alternating current flowing at resonant frequencies through toroid coils, no discernable gravity modification (caused by coupling of these fields with those of gravity) was detected.

Interesting electromagnetic phenomenon were: (a) standing em waves along toroid surfaces; (b) em wave energy focused into more intense beams by asymmetrical toroid shapes; and (c) possibly, em wave propagation through magnetically shielded enclosures.

There might have been increased probability of detecting a discernable gravity modification if there had been time for gravitometer measurements in regions where toroid field strength was much greater.

The possibility of anomalous wave propagation should be confirmed or refuted by re-testing the large diameter toroid within a magnetically shielded structure that encloses both the toroid and its power leads.

Zero gravity modification within the radio frequency em fields surrounding transmitting toroid antennas should be confirmed by a gravitometer search throughout the entire vicinity of the large diameter toroid.

ACKNOWLEDGMENTS

This experimental work was motivated by theoretical work by Dr. Terence Barrett with respect to specially conditioned em fields created by transmitting toroid antennas. Dr. Barrett also contributed useful suggestions as to recommended toroid configurations and test procedures. The most recent experimental work was conducted with the considerable assistance of Mr. Blair Cleveland, who was intimately involved in every aspect of the test preparations conduction and data gathering portions of this work.

REFERENCES

(1) Yang, C.N., "Gauge Theory", McGraw-Hill Encyclopedia of Physics, 2nd Edition, p483, (1993)

(2) Barrett, T.W., "Electromagnetic Phenomenon not Explained by Maxwell's Equations", Essays on Formal Aspects of Electromagnetic Theory, p6, World Scientific Publ. Co., (1993)

(3) Barrett, T.W., " Toroid Antenna as Conditioner of Electromagnetic Fields into (Low Energy) Gauge Fields", Proceedings of the: Progress in Electromegnetic Research Symposium 1998, (PIERS '98) 13-17 July, Nantes, France (1998)

(4) Froning, H.D., Barrett, T.W., "Theoretical and Experimental Investigations of Gravity Modification by Specially Conditioned EM Radiation", Space Technology and Applications International Forum 2000, Editor: Mohamed S. El-Genk, Published by the American Institute of Physics (2000)

A01-34345

AIAA 2001-3660

An Experimental Investigation of the Physical Effects in a Dynamic Magnetic System

V. Roschin and S. Godin
Institute for High Temperatures
Russian Academy of Science
Moscow, Russia

37th AIAA/ASME/SAE/ASEE
Joint Propulsion Conference and Exhibit
8-11 July 2001
Salt Lake City, Utah

AIAA # 2001-3660

AN EXPERIMENTAL INVESTIGATION OF THE PHYSICAL EFFECTS IN A DYNAMIC MAGNETIC SYSTEM.

Vladimir Roschin, E-mail: rochtchin@mail.ru
Sergei Godin, E-mail: smgodin@online.ru
Institute for High Temperatures, Russian Academy of Science
Izhorskaya st. 13/19, Moscow 127412, Russia

Abstract

In the current paper the results of experimental research of magnetic-gravity effects are presented. Anomalous magnetic and thermal changes within a radius of 15 meters from the researched device were measured as well.
PACS: 41.20.-q; 44.60.+k; 76.50.+q

Introduction

We have experimentally studied the physical effects in a system based on rotating permanent magnets [1]. Below we describe the technology of manufacture, assembly, and the results of testing this experimental setup, which is referred to as the converter.

Received effects:

- Generation of mechanical energy in a self-governing mode of operations;
- Change of weight of the converter;
- Formation of a local magnetic and temperature fields as concentric cylinders around converter.

Description of the Experimental Setup

The basic difficulty arises in choosing the materials and maintaining the necessary magnetic pattern ("imprinting") on the plate and roller surfaces. To simplify the technology we decided to use a one-ring design with one-ring plate (stator) and one set of rollers (rotor). It is obvious, that it was necessary to strengthen the rollers on a rotor by the bearings and balance the rollers well. In the suggested design, air bearings were used which provided the minimum losses due to friction.

From the available description [1] it was not clear how it is possible to make and magnetize the stator with a diameter of about one meter. In order to make the stator from separate magnetized segments executed with rare earth magnets with the residual induction of 1T, the segments were magnetized in a usual way by discharging a capacitor-battery energizer through a coil. Afterwards the segments were assembled and glued together in a special iron armature, which reduced magnetic energy.

To manufacture the stator 110 kg of rare earth magnets were used. To manufacture the rotor 115 kg of that material was used. High-frequency field magnetization was not applied. It was decided to replace imprinting technology described in [1] with cross-magnetic inserts having a flux vector directed at 90 degrees to the primary magnetization vector of the stator and rollers. For these cross-inserts the modified rare earth magnets with residual magnetization of 1.2 T and coercive force a little bit greater than in a base material were used. Fig.1 and Fig.2 show the joint arrangement of stator 1 and rotor, made up of rollers 2, and a way of their mutual gearing or sprocketing by means of cross magnetic inserts 19. Between the stator and roller surfaces air gap δ of 1 mm is maintained.

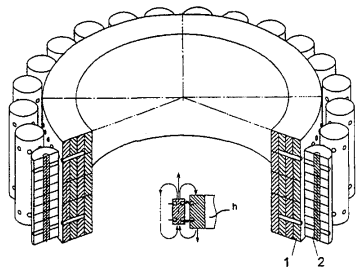

Fig. 1. Variant of one-ring converter.

No layered structure was used except a continuous copper foil of 0.8 mm thickness, in which the stator and rollers was wrapped up. This foil had a direct electrical contact to magnets of the stator and rollers. Distance between the inserts in rollers is equal to distance between the inserts on the stator. In other words $t_1 = t_2$ on a Fig.2.

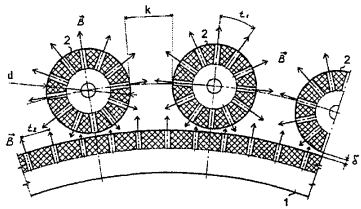

Fig.2. Sprocket effect of magnetic stator and roller inserts.

The ratio of parameters of the stator 1 and the rotor 2 on Fig.2 is chosen so that the relation of stator diameter D to the roller diameter d is an integer equal to or greater than 12. Choosing such ratio allowed us to achieve a resonant mode between elements of a working body of the device.

The elements of magnetic system were assembled in a uniform design on an aluminum platform. Fig.3 displays the general view of the platform with the one-ring converter. This platform was supplied with springs, shock absorbers and had a possibility of moving vertically on three supports. The possible vertical displacement was 10mm and the induction meter 14 was used for measuring this displacement. Thus, the instantaneous change of platform weight was defined during the experiment in real time. Gross weight of the platform with magnetic system in an initial condition was 350 kg.

The stator 1 was mounted motionlessly and the rollers 2 were assembled on a mobile common rotor - separator 3, which is connected with the basic shaft 4 of the converter. Through this shaft the rotary moment was transferred. The basic shaft by the means of friction muff 5 was connected to a starting engine 6, which accelerated rotor of the converter up to a mode of self-sustained rotation. An ordinary DC electrodynamics generator 7 also was connected to the basic shaft as a main loading of the converter. Adjacent to the rotor, electromagnetic inductors 8 with open cores 9 were located.

The magnetic rollers 2 crossed the open cores of inductors and closed the magnetic flux circuit through electromagnetic inductors 8, inducing an electromotive force in them, which acted directly on an auxiliary active load 10 - a set of incandescent lamps with total active power of 1 kW. The electromagnetic inductors 8 were equipped with an electrical drive 11 on supports 12. Driven coils were used for smooth stabilization of the rotor rpm. The speed of the rotor also could be adjusted by changing the main loading 10.

To study influence of high voltage on characteristics of the converter, a system for radial electrical polarization was mounted. On a periphery of rotor the ring electrodes 13 were set between the electromagnetic inductors 8 and had an air gap of 10 mm with the rollers 2. The electrodes are connected to a high-voltage source; the positive potential was connected to the stator, and the negative - to the polarization electrodes. The polarizing voltage was adjusted in a range of 0-20 kV. In the experiments, a constant value of 20 kV was used.

In case of emergency braking, a friction disk from the ordinary car braking system was mounted on a basic shaft of the rotor. The electrodynamics generator 7 was connected to an ordinary passive resistive load through a set of switches guaranteeing a step connection to the load from 1 kW to 10 kW - a set of ten ordinary electric water heaters.

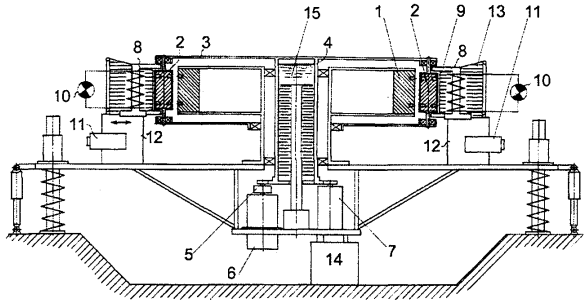

Fig.3. The general view of the converter and its platform.

Converter under testing had in its inner core the oil friction generator of thermal energy 15 intended for directing a superfluous power (more than 10 kW) into the thermo-exchange contour. But since the real output power of the converter in experiment has not exceeded 7 kW, the oil friction thermal generator was not used.

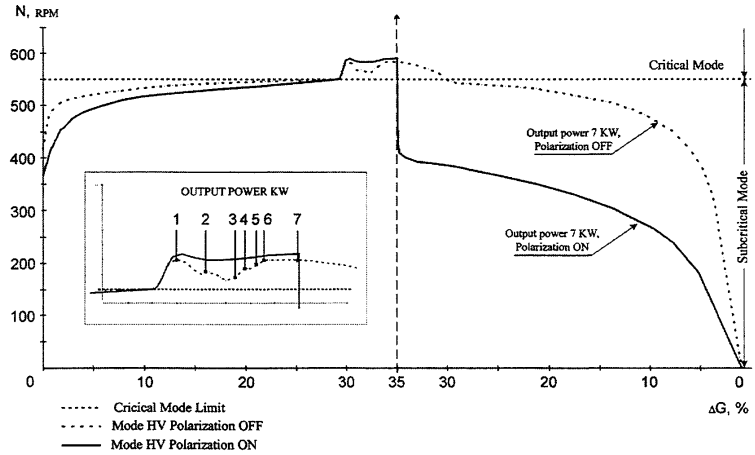

Fig.4. A diagram illustrating various operation regimes of the converter, -G, +G changes in weight of the platform vs. rpm

Experimental results

The magnetic converter was mounted in a laboratory room on three concrete supports at a ground level. The ceiling height of lab room was 3 meter. A common working area of the laboratory was about 100 sq. meters. Besides a presence of an iron-concrete ceiling in the immediate proximity from the magnetic system there was a generator and electric motor, which contained tens of kilos of iron and could potentially deform the field structures.

The device was started by the electric motor, which accelerated rpm of the rotor. The revolutions were smoothly increased up to the moment the ammeter included in a circuit of the electric motor begin to show zero or a negative value of consumed current. The negative value indicated a presence of back current. This back current was detected at approximately 550 rpm under clockwise rotation. The displacement meter 14 starts to detect the change in weight of the whole installation at 200 rpm. Afterwards, the electric motor is completely disconnected by the electromagnetic muff and an ordinary electrodynamics generator is connected to the switchable 10 kW resistive load. The converter rotor continues self-accelerating and approaches the critical regime of 550 rpm when the weight of the whole installation quickly changes.

In addition to dependence on a speed of rotation, the common weight of device depends from output power on the load and from applied polarizing voltage as well. As seen on Fig.4, under maximum output power is equal to 6-7 kW the change of weight ΔG of the whole platform (total weight is about 350 kg), reaches 35 % of the weight in an initial condition G_i. Applying a load of more than 7 kW results in a gradual decrease of rotation speed and an exit from self-sustained mode (right sides of the curves on Fig.4 for a 7 kW loading).

The net weight G_n of the platform can be controlled by applying high voltage to polarization ring electrodes located at a distance of 10 mm from external surfaces of the rollers. Under a high 20 kV voltage (electrodes have a negative polarity) the increase of tapped power of the basic generator more than 6 kW does not influence ΔG if rotation speed is kept above 400 rpm. "Tightening" of this effect is observed as well as the effect of hysteresis on ΔG at rotation of a rotor on a clockwise and counter-clockwise (a kind of "residual induction"). The experimental diagrams given on Fig.4 illustrate the +G and –G changes in weight of the converter vs. rotor rpm. The effect of a local change of the platform weight is reversible, relative to the direction of rotor revolution, and has the same hysteresis. A clockwise rotation causes the critical regime to occur in area of 550 rpm and a propulsion force against the direction of gravitation vector is created. Correspondingly, a counter-clockwise rotation causes the critical mode to occur the in area of 600 rpm and a force in the direction of gravitation vector is created.

The difference in approach to a critical regime of 50 - 60 rpm was observed. It is necessary to mention that the most interesting region are situated above the critical area of 550 rpm, but due to of a number of circumstances the implementation of such research was not possible. Probably, there are also other resonant modes appropriate to higher rpm of a rotor and to the significant levels of useful loading and weight changing. Proceeding from the theoretical assumptions, the dependence of tapped mechanical energy from the parameters of magnetic system of the converter and rpm of a rotor has a non-linear character and the received effects are not optimum. From this point of view, the revealing of a maximal output power, of maximal change of weight and converter resource represents a large practical and scientific interest. In tested sample of the converter the using of higher rpm was inadmissible because of unsufficient mechanical durability of the magnetic system, which has been stuck together from separate pieces.

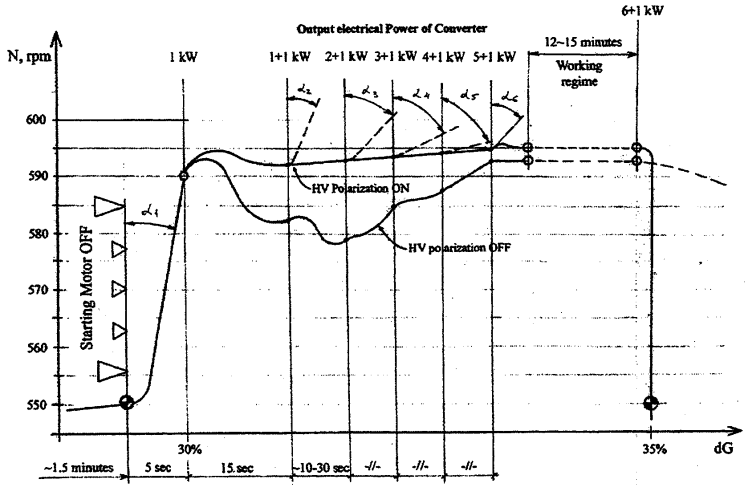

Fig.5 Diagrams of rotor accelerating and loading of the converter.

On Fig.5 the dependence of total weight of whole installation and its output power directed into active loading from rpm of a rotor of the converter is explained in detail. The diagrams are constructed for a case of HV polarization ON (top diagram) and HV polarization OFF (bottom diagram). The time from starting of the engine up to a mode of self-sustaining of the converter at the rotation of a rotor clockwise approximately is equal 1.5 minutes. Power of starting DC engine was about of 2 kW and reduction on a shaft of the converter was equal 1/10. At achievement of a critical mode (550 rpm.) the change of gross weight of a platform already achieves +/-30% from $\mathbf{G}_i$. Under transition to resonant mode the revolutions with the large acceleration have increases up to 590 rpm and weight has changes up to + /-35% from $\mathbf{G}_i$. This point on the diagram begins at once after a critical point (inclination of a curve α_1). At achievement of 590 rpm the first stage of active loading 1 kW is connected to the electrodynamics generator. The revolutions have a sharply reducing and ΔG also is changing. As soon as the revolutions begin to grow again, the second switchable loading is connected and rotor rpm are stabilized at a level of 590-595 rpm. ΔG continues to change. The increasing of switchable loading occurs by steps on 1 kW up to total power of 6 kW. All intervals are equal approximately of 10-30 sec. Afterwards the short-term increasing of revolutions and then the full stabilization of the 6 kW output during of 12-15 min was observed.

More than 50 launches of the converter with an absolute repeatability within three months were carried out. It is necessary to note that revolutions will grow with acceleration shown on Fig.5 by angles $\alpha_1 \ldots \alpha_5$, if do not switch on the next step of loading to the genera-

tor at rpm increasing. For returning to a previous rpm mode it is necessary to switch on a twice more loading.

The words above concern a mode with switched ON a high voltage polarization of 20 kV, "plus" is on a grounded stator. Without polarization voltage (lower curve on Fig.5) the diagram is approximately the same, but is well indicated the more soft character of a loading and faster changing of weight of a platform due to decreasing of rpm.

Other interesting effect is corona discharges, which was observed at the work of the converter in a dark room. At this, around the converter rotor a blue-pink glowing luminescence and a characteristic ozone smell were noticed. On Fig.6 the cloud of ionization covers area of the stator and rotor and is having accordingly a toroidal form.

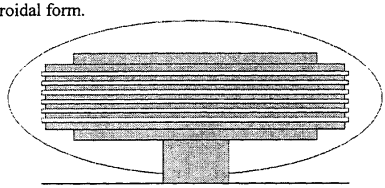

Fig.6. Corona discharges around the converter.

On a background of luminescence glowing on the roller surfaces, we distinguished a separate «wave picture». A number of more vigorous strips of discharges around the rollers were observed. These discharges were of a white-yellow color but the characteristic sound for arc discharges was not audible. There were not noticed any erosive damages by arc discharges on surfaces of the stator and the rollers as well.

One more effect previously not mentioned anywhere was observed - the vertical concentric magnetic "walls" around the installation. We noticed and measured a permanent magnetic field around the converter within a radius of 15 meters. For this magnetic field measurement a Russian made magnetometer F4354/1 was used. Magnetometer had a Hall-effect sensor in a copper shielding. The zones of increased intensity of a magnetic flux 0.05 T, located concentrically from the center of the installation were detected. The direction of the magnetic field vector in these walls coincided with direction of magnetic field vector of rollers. The structure of these zones was like the Bessel function of zero order of two arguments. No any magnetic fields were registered between these zones by portable magnetometer. The layers of increased intensity were distributed practically without losses up to a distance of about 15 meters from a center of the converter and had a quick decreasing at a border of this zone. The thickness of each layer was approximately of 5 - 6 cm the border of each layer was very sharp. The distance between layers was about of 50 - 80 cm where the upper value is seen when moving from center of the converter. A stable picture of this field was observed as well as at a height of 6 m above the installation (on the second floor above the lab). Above the second floor, measurements were not carried out. The similar picture was observed and outside of a room of laboratory, directly in the street, on the ground. The concentric walls were strictly vertical and no had appreciable distortions. The Fig.7 illustrates the schematic placing of the converter in a room of laboratory and arrangement of concentric magnetic and thermal fields around the installation.

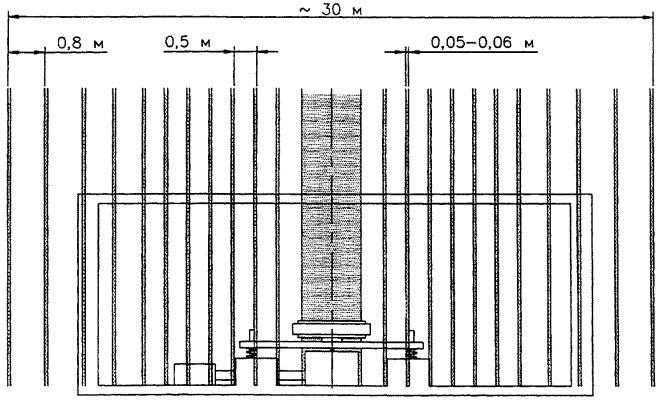

Fig.7. Schematic placing of the converter and field patterns in lab room.

An anomalous decrease of temperature in a vicinity of the converter was also found. While the common temperature background in laboratory was + 22°C (±2°C) the stable fall of temperature of 6-8°C was noticed. The same phenomenon was observed in concentric vertical magnetic walls as well as. The measurements of temperature inside the magnetic walls were carried out by an ordinary alcohol thermometer with an inertia of indication about 1.5 min. Inside the magnetic walls the temperature changes can even be distinctly observed by hand. When the hand is placed into this magnetic wall the cold is felt at once. A similar thermal picture was observed at height above the installation, i.e. on a second floor of the laboratory as well as despite the steel-reinforced concrete blocks of a ceiling and also on an open air outside of the laboratory.

Concentric magnetic walls and accompanied thermal effects begin to appear approximately from 200 rpm and have a linearly increasing with speeding up of revolutions up to a critical regime. The measurements above 600 rpm were not made because of fear of destruction of magnetic system. On Fig.8 the curve of intensity of magnetic field in mT and change of temperature in Celsius degrees due to rpm changing is represented.

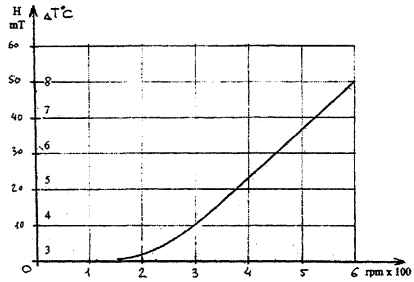

Fig.8. The dependence of intensity of magnetic field and changes of temperature vs. rotor rpm of the converter.

Discussion

All the results we obtained are extremely unusual and require some theoretical explanation. Some theoretical approaches and phenomenological descriptions can be found in our book [2]. Unfortunately, interpretation of these results within the framework of conventional physical theory cannot explain all observed phenomena especially the change of weight. We can interpret change of weight as a local change of gravitation or as some propulsion force like a propeller work in air. Only a role of a propeller the magnetic system is playing, and a role of air - the quantum environment - ether filled with a "dark matter and energy". Direct experiment, which would has confirming the presence of a propulsion force was not performed, but in any case both interpretations of the weight change do not correspond to the modern physics paradigm.

In conclusion we would like to emphasize that issues of biological influence and especially effects of unknown radiation around of the converter were not considered at all. Our own experience allows us to do only cautious assumption that the short-term stay (dozen minutes) in a working zone of the converter with fixed output power of 6 kW remains without observed consequences for exposed persons.

Bibliography

1. J. A. Thomas, Jr., ANTI-GRAVITY: the Dream Made Reality: the Story of John R. Searl (Direct International Science Consortium, London, 1994), Vol.VI, Iss.2.

2. V.F. Zolotarev, V.V. Roschin, S.M. Godin. About the structure of space-time and some interactions. (The theory and original experiments with extraction of an internal atomic energy). Moscow, 'Prest', 2000, 309p. with illustrations. (in Russian).

A01-34536

AIAA 2001-3907

Rapid Spacetime Transport and Machian Mass Fluctuations: Theory and Experiment

J. Woodward and T. Mahood
California State University
Fullerton, CA

P. March
Lockheed Martin Space Operations
Houston, TX

37th AIAA/ASME/SAE/ASEE
Joint Propulsion Conference and Exhibit
8-11 July 2001
Salt Lake City, Utah

AIAA 2001-3907

RAPID SPACETIME TRANSPORT AND MACHIAN MASS FLUCTUATIONS: THEORY AND EXPERIMENT

James F. Woodward,* Thomas L. Mahood,* and Paul March†

ABSTRACT

The various schemes for achieving rapid spacetime transport currently in circulation are briefly reviewed, and then the methods based on Machian mass fluctuations are considered. Results of experimental work designed to detect a negative-definite Machian mass fluctuation expected on the basis of simple theory are then reported. They suggest that such mass fluctuations may in fact occur and have sufficient magnitude to be engineerable into practical devices.

INTRODUCTION

It is a commonplace that although rockets may serve to cover interplanetary distances, however inefficiently, when interstellar voyages in some reasonable fraction of a human lifetime are considered, conventional rocketry comes up seriously wanting. The fundamental problem, simply put, is: How does one accelerate a reasonable payload to some significant fraction of the speed of light in short order without having to lug idiotically large amounts of propellant along to push off of? Only a moment's reflection is required to see that, short of creating "wormhole" spacetime shortcuts with "exotic matter", there are two distinct, but related ways to tackle this problem. One is to reduce the mass of the payload. The other is to find some means of producing an accelerating force on the payload without lugging along all the propellant required by rockets. Conventional approaches of considerable ingenuity have been devised in both cases. But they still fall far short of the technical requirements for serious interstellar travel. The question then is, do the laws of physics allow the invention of unconventional spacecraft – starships – equal to interstellar voyages?

In the matter of payload reduction, ideally one would want to render the mass of a ship and its contents as nearly equal to zero as possible. Were that possible, only minute forces would be needed to accelerate the ship to near lightspeed. Is this possible? To answer this question we must understand the cause of the inertial properties of matter; that is, why things push back on us when we try to accelerate them.

At the moment three putative causes of inertia are advocated. There are those who simply assert that inertia is an innate property of matter that is independent of all external circumstances. Others believe that inertia results from the local action of quantum mechanical "zero point" fluctuations of the electromagnetic field (and perhaps other non-gravitational fields) on things that are accelerated. And some are convinced that inertial reaction forces are caused by the gravitational action of chiefly distant matter in the universe. If inertia is an inalterable, innate property of matter, then the only way to reduce the mass of a ship is to find and collect some "exotic" matter (with negative mass) to offset the positive mass of the payload. Such material, naturally occurring, has yet to be discovered in nature.

Compelling reasons exist to set aside the electromagnetic "zero point" fluctuations explanation of inertia.[1,2] But even were that not the case, it seems exceedingly unlikely that any means could ever be found to suppress zero point fluctuations over the volume of a starship (thereby supposedly rendering it essentially inertialess). The Casimir effect, often cited in connection with these arguments, does point up the fundamental problem here. It is the low frequency part of the vacuum fluctuation spectrum that is suppressed by material objects in close proximity that produces this effect. But, alas, it is the high frequency part of the fluctuation spectrum that is chiefly responsible for the induction of the vast bulk of inertia in this scheme. (We note here that Lorentz invariance requires that the spectral energy density of the vacuum fluctuations increase with the cube of the frequency thereof.)

Taking inertial forces to be due to the gravitational action of chiefly distant matter in the universe – as is the case in general relativity theory – leads to two possible approaches. One is to find some means of "shielding" the bulk of the starship from the action of the gravity field of the distant matter. This might be done either passively by finding a "gravity insulator" – H.G. Wells' cavorite that is – or actively by devising some apparatus that generates a gravity field that can

* California State University, Fullerton, CA 92634; email: jwoodward@fullerton.edu
† Lockheed-Martin Space Operations, 2400 NASA Rd. 1, MS: C18, Houston, TX 77058-3799

be used to "null" the gravity field produced by distant matter. Cavorite, like naturally occurring "exotic" matter, remains to be discovered. Several active methods have been explored – notably spinning superconducting disks in suitable electromagnetic fields – so far to no avail. One troubling aspect of these schemes is that they do not follow from the widely accepted form of the laws of physics. And they usually lead to violations of fundamental conservation laws. The second approach consists of finding a way, within the structure of accepted physical laws, to transiently induce a reduced mass state, perhaps fleetingly even an "exotic" mass state, in normal matter by some technically feasible means. This may sound quite implausible, but it turns out that there may be a way to do this. We discuss this, along with some experimental results, below.

Turning to the issue of generating accelerating forces, we see that the fundamental problem, irrespective of the propulsion system being considered, is how to push off of the distant matter in the universe. In conventional rocket propulsion systems, this is achieved by using propellant as an intermediary. That is, when we push on propellant, the gravitational action of the chiefly distant matter in the universe causes the propellant to push back on us, causing an accelerating force on us. Since the prodigious propellant payload is the chief impediment to interstellar voyages, one might want to devise a propulsion scheme that involves, ideally at least, no lugged propellant whatsoever. In conventional systems this requirement translates to either "harvesting" propellant locally as one goes along, using beamed energy from home with "sails", or finding a way to couple locally to cosmic fields of one sort or another. None of these seem very realistic at present.

Alas, the strictly propellantless "breakthrough" schemes appear even less realistic than the conventional proposals, for they all seem to violate some fundamental, well-tested physical principle. Usually, but not always, it is the conservation of momentum that bites the vacuum. The best known of these schemes involves the aforementioned spinning superconducting disks. In these circumstances, however, the action of the disks is not interpreted as shielding or attenuating the gravitational field of other objects. Rather, it is regarded as generating a directed "gravity or inertia-like" field analogous to the "gravitomagnetic" field generated by spinning objects that is predicted by general relativity, but magnified in intensity by many orders of magnitude. This putative force does not act on the generating apparatus *per se*. But aimed at distant matter in the direction one wants to go, it acts on the distant matter and a mutual force is established that accelerates the spacecraft. No violation of momentum conservation is necessarily involved here. But there is no compelling reason to believe that when electric charge carriers form Cooper pairs (as they do in the superconducting state), no matter how they are acted upon by external electro-magnetic fields, they acquire the magical ability to create from nothing the gargantuan "inertialike" fields claimed.

Another strictly propellantless propulsion scheme is based on the observation that electromagnetic circuits can be arranged so that they appear to generate self-forces – that is, forces appear in one part of the circuit that seem not to be cancelled by equal and opposite forces anywhere else in the circuit. Perhaps the best example of this type of scheme is the "Slepian" approach advocated by Dering, Corum, and several of their associates.[3] The issue of "hidden momentum" in electrical circuits has a long history. Suffice it to say that the generation of a net force in an isolated electrical circuit capable of accelerating a spacecraft is a very dubious proposition. To be relativistically (and empirically) correct, the laws of electrodynamics must be invariant under the group of infinitesimal Lorentz transformations. This invariance insures that energy and momentum are conserved in isolated systems. Aside from the obvious violation of the conservation of momentum involved in the Slepian scheme, simple physical common sense suggests that it is not reasonable. Accelerations take place with respect to the distant matter in the universe. The likelihood that one could produce accelerations without coupling to that matter in any way is, on its face, pretty preposterous. Well, unless the quantum vacuum couples to the distant matter and can be acted upon in some way by the local electromagnetic fields. But that is not what is claimed in "Slepian" systems.

Should it prove possible to produce transient variations in the masses of material objects, another means of propulsion may be achievable. Here some local mass is used as a propellant. But instead of simply ejecting the matter once and for all, after it has been "ejected" one operates on it to reduce its mass so that it can be recovered without canceling the momentum imparted to the craft when it was earlier ejected. It may then be ejected again in its normal state, and the mass-reduced recovery repeated. And this cycle may be repeated over and over again, *ad nauseam*. This may sound like having one's cake and eating it too. But when we keep in mind that the gravity/inertia field couples the craft (and recycled propellant) to the distant matter in the universe, it is apparent that such a scheme merely amounts to producing a directed momentum flux in the gravitational/inertial field by the local manipulations matter. One may object that the propagating "momenergy" in the gravitational field produced by any reasonable concentration of local matter is so ridiculously small that even were such a scheme in principle possible, surely it would be utterly

impractical. But one ignores, in this view, the fact that inertial reaction forces are gravitational actions too. *They are enormous and instantaneous.* So there is hope, should it prove possible to induce a transient mass-reduced state in some propellant without violating the laws of physics.

THEORY

When inertial reaction forces are viewed as arising from the action of a locally Lorentz-invariant field (as they actually are), one finds that objects subjected to accelerations by external forces undergo changes in their restmasses during the accelerations.[4, 5, 6, 7] This is a consequence of the four-vector nature of the reaction forces – and the fields producing them – and the four-dimensionality of the divergence operator that is applied to the four-field strength to obtain an expression for the local charge density. To see how this works, consider an object accelerated by an external force. An (equal and opposite) inertial reaction force arises in the object owing to the action of the local "inertial" field on it.[8, 9] The field strength experienced by the object is just the inertial reaction four-force divided by the mass of the object. To get the local source density of this field we apply the four-dimensional generalization of Gauss's divergence theorem. Taking account of the fact that the field is irrotational (so the three-force can be expressed as the gradient of a scalar potential) and translating charges into charge densities (as is customary in constructing field equations), this yields:

$$\nabla^2\phi - (\phi/\rho_o c^2)(\partial^2 E_o/\partial t^2) - (\phi/\rho_o c^2)^2(\partial E_o/\partial t)^2 = 4\pi G\rho_o, \qquad (1)$$

where ϕ is the scalar potential of the inertial field, ρ_o the local restmass density, c the vacuum speed of light, E_o the local rest-energy density ($=\rho_o c^2$), and G Newton's universal gravitational constant.

To transform this equation into a field equation of standard form we need merely note that inertial reaction forces are gravitational forces (Mach's principle) and that since this is true, in this approximation we have that $\phi = c^2$ and the rest energy density E_o can be written as $E_o = \rho_o\phi$ [$= \rho_o c^2$]. Using this expression for E_o in Equation (1) and rearranging we obtain:

$$\nabla.\phi - (1/c^2)(\partial^2\phi/\partial t^2) = \Box\phi = 4\pi G\rho_o + (\phi/\rho_o c^2)(\partial^2\rho_o/\partial t^2) - (\phi/\rho_o c^2)^2(\partial\rho_o/\partial t)^2 - c^{-4}(\partial\phi/\partial t)^2, \qquad (2)$$

the inhomogeneous relativistically invariant wave equation for the scalar gravitational potential. Note the transient matter source terms on the RHS of Equation (2). *If real*, they may make rapid spacetime transport technically feasible.

If we ignore $-c^{-4}(\partial\phi/\partial t)^2$ since it is always minuscule given its c^{-4} coefficient (not compensated for by any factor of ϕ in the numerator, as in the other terms), and extract a factor $4\pi G$, we may write the total, time-dependent matter density as:

$$\rho(t) \approx \rho_o + (1/4\pi G)[(\phi/\rho_o c^2)(\partial^2\rho_o/\partial t^2) - (\phi/\rho_o c^2)^2(\partial\rho_o/\partial t)^2]. \qquad (3)$$

The first time-dependent term – $(1/4\pi G)[(\phi/\rho_o c^2)(\partial^2\rho_o/\partial t^2)]$ – can be both positive and negative when ρ_o undergoes periodic fluctuations. When effects arising from this term are convolved with a second periodic force in an object, this restmass fluctuation can lead to the production of stationary forces.[10, 11, 7] One merely pushes on an object made more massive by this mass fluctuation, and then pulls it back when it is in a mass-reduced state to achieve a net accelerating force. For this reason we call this the "impulse engine" term in Equations (2) and (3). The second time-dependent term, unlike the first, is always negative, because the negative sign of the term is unaffected by the sign of ρ_o since it appears exclusively in quadratic factors: $-(1/4\pi G)[(\phi/\rho_o c^2)^2(\partial\rho_o/\partial t)^2]$. This term, if it can be made large, holds out the possibility of the transient formation of "exotic" matter – matter with negative mass – the material needed to achieve the most extreme types of rapid spacetime transport by the warping of spacetime. We resist the temptation to assign this term a romantic label, calling it merely the "negative mass" term in Equations (2) and (3).

As with the impulse engine term, when mass fluctuations driven by the negative mass term in some object are convolved with a second periodic force, stationary forces can be produced. So both the impulse engine and negative mass effect terms hold out the promise of realizable propellantless propulsion. *Note that the transient mass terms in Equation (3) are enormous in comparison with, for example, the mass changes that occur from simply changing the energy content of some region in space-time. This is a consequence of the transient terms being "magnified" by the factor* $(\phi/\rho_o c^2)$ *coefficients where, as a consequence of Mach's principle,* $\phi/c^2 \approx 1$, *rather than being a very small number as one might otherwise expect when* ϕ *has a value of the scale normally assumed (that is,* $<< c^2$).

The stationary forces that result from both of these terms depend on the relative phase of the driven mass fluctuation and the second applied force. Their periodicities, as a function of the relative phase, how-

ever, are not the same because for a driven periodic fluctuation in ρ_o, the resulting contributions from the impulse engine term have the same periodicity as the driving signal, but the negative mass term varies at twice the frequency of the driving signal because the time derivative of the driving signal is squared. Were the negative mass term much smaller than the impulse engine term, as simple calculations can lead one to believe, this would not be a matter of much moment. But, in fact, the negative mass term is comparable to the impulse engine term, as can be seen by inserting the *ansatz* $\rho_o = \rho cos(\omega t)$ into Equation (2) and computing the resulting expressions for the impulse engine and negative mass terms. This procedure does not yield an exact solution of this non-linear equation. But it does reveal that the amplitudes of the two factors in the square brackets are the same, to factors of order unity at any rate. Thus, should Machian mass fluctuations actually occur, one should be prepared to see evidence of the negative mass term in any system sensitive enough to detect the impulse engine term.

Before turning to a discussion of experiments designed to test for the presence of the mass fluctuations just described, we mention general considerations that should inform experiments. We ask first, where might one expect to see the sort of mass fluctuations predicted by Equation (2) above? Since this equation follows from the consideration of the action of an accelerating force on matter, plainly some material must be present that is accelerated. The fact that the transient terms in Equation (2) both involve derivatives of the local rest matter density, ρ_o, indicates that the local *rest* energy density, E_o [$=\rho_o/c^2$], must also be changing. Evidently, the largest Machian mass fluctuation effects are to be expected in materials where, viewed at the microscopic level, the application of external electromagnetic fields produce large accelerations accompanied by rapid changes in stored internal energy. Thus, for example, if mass fluctuations are to be driven in dielectric mater-ials in capacitors, then one will want to use material with the highest possible dielectric con-stant. In particular, ferroelectric substances. It is worth noting, nonetheless, that if the vacuum can be truly regarded as a polar-izable substance, then one may expect to drive mass fluctuations in the vacuum itself. And should such fluctuations be convolved with an appropriate periodic force, stationary forces like those expected in material media should be producible. Such forces, however, would be minuscule in comparison with those pro-duced in materials with large dielectric constants. An experiment designed to test for mass fluctuations in the vacuum would make a good test of the reality of the "polarizable vacuum" model of GRT that has recently been elaborated by Puthoff.[12]

EXPERIMENT

Results of experiments designed to detect Machian mass fluctuations have already been reported.[4, 5, 11, 13, 7] We report here current results of the ongoing experimental program underway at California State University, Fullerton (CSUF). For the past several years that program was focused on the detection of stationary forces in stacks of lead-zirconium-titanate [PZT] crystals driven with voltage signals of several hundred volts at several tens of kHz using sensitive torsion pendula, started by JFW and TLM in the course of TLM's graduate work. (See refs. 7, 13, and especially 14 for the details of this work.) Since fall 2000 the focus of this work has changed to an updated version of early experimental tests of mass fluctuations by looking for the effect as a weight fluctuation with force transducers.[4, 5] *Approaching experimental detection of any mass fluctuation effect in this way has the great merit that only the mass fluctuation* per se *is detected (as a weight fluctuation), so all issues relating to the production of stationary forces by signals of several frequencies and phases are set aside (unless such forces are inadvertently produced by convolution of harmonics of the fundamental signal with mass fluctuations driven thereby that might affect weight determinations).*

The search we are conducting for Machian mass/weight fluctuations, for the moment at least, utilizes PZT stacks like that shown in Figure 1. This PZT stack consists of ten crystal disks, 1.91 cm in diameter made of EDO Ceramics EC-65 material

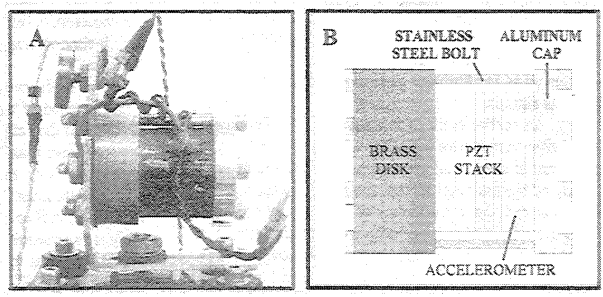

Figure 1: A. A picture of the device mounted on the force transducer. The thermisor and accelerometer connection are at the top center-left. B. A schematic diagram of the device showing the arrangement of the crystals and accelerometer in the PZT stack.

epoxied together along with suitable electrodes between the crystals. The stack is clamped by six machine screws between an aluminum cap and a 0.95 cm thick brass disk. The pair of crystal disks closest to the brass disk are 0.31 cm thick, whereas all but two of the crystal disks at the other end of the stack are 0.15 cm thick. Thinner disks, with higher stored energy for a given applied voltage to the stack, are used in the part of the stack near the aluminum cap where the largest accelerations, and thus predicted effects, are expected. Two of the crystal disks are very thin, being only 0.03 cm thick. This pair of crystals was placed between the two pairs of 0.15 cm thick crystals closest to the aluminum cap and independently wired so that they could be used as an accelerometer to monitor the behavior of this part of the PZT stack.

An aluminum mounting bracket is attached to the brass disk as shown in Figure 1. Note the thin rubber pad that isolates the bracket from the brass disk. This was included to suppress the transmission of vibration from the stack assembly to the weight sensors used. This pad, however, contributes significantly to improved performance of the stack. It also suppresses the flow of heat into the bracket. The temperature of the stack assembly is monitored with a thermistor glued onto a small aluminum ear that is also attached (without a rubber pad) to the brass disk. (This aluminum ear also carries a bimetallic strip thermometer used in earlier work.)

Two different weight detection systems were developed for the work we report here. The chief system employed a Unimeasure U-80 position sensor configured as a load cell. (See Figure 2.) This type of weigh system has been used extensively by one of us (JFW) in earlier work, and the chief results reported here were obtained with this system. The second weight detection system, still under development at the time of this writing, utilizes optical detection of displacements driven in a cantilevered beam to detect any weight fluctuations. (The optical/cantilevered beam technique was suggested by John Cramer.) Both weigh systems were enclosed in clear acrylic containers that were pumped down to vacua typically of 10 to 20 microns so as to eliminate several potential sources of spurious signals.

In earlier work of this sort, arrays of capacitors, rather than stacks of PZTs, were driven by a voltage signal at about half the mechanical resonance frequency of the load cell so that the mass fluctuation excited at the power frequency of the applied voltage signal would produce a periodic weight fluctuation that would be resonance amplified by mechanical properties of the load cell.[4,5] Since the resonance frequency of the load cell was typically about 100 Hz, and the magnitude of the mass fluctuation scales with the square of the frequency of the voltage signal, only minuscule weight fluctuations could be driven at the 100 Hz frequency, and mechanical resonance amplification and signal averaging were essential to see any effect at all. Nonetheless, this seemed the only path to

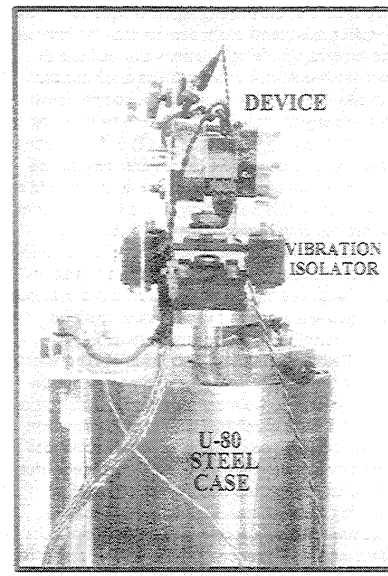

Figure 2: The device mounted on the U-80 (located in the steel shielding case) via a vibration isolator made from several layers of plastic and neoprene rubber. An accelerometer is affixed to the bottom of the aluminum stage that the isolator is bolted to. The stage is stabilized against lateral motion by tensioned fine steel wires.

detection of the mass fluctuation effect open at that time, for the presence and significance of the negative mass term in Equations (2) and (3) above was not then appreciated. Confined to the impulse engine term, which time-averages to zero, no other approach seems feasible.

In the present experiments, the cantilevered beam method of weight detection is problematical because of the rather large mass of the suspended device (more than 100 grams). In order to get sufficient sensitivity, the mechanical resonance frequency of the beam must be made rather low (less than ten Hz). This makes it difficult to detect a short, transient weight fluctuation. The situation with the U-80 load cell is better, as its mechanical resonance frequency is several tens of Hz – out of the range of low frequency acoustic and seismic noise sources. Moreover, this higher resonance frequency makes it possible to follow transient weight fluctuations with durations in the 100

to 200 millisecond range. This is especially important as, since the early work was done, the importance of the negative mass term in Equations (2) and (3) has come to light. Because the effect of this term is always to reduce the mass of the object in which it is excited (being negative definite), a stationary time-averaged mass shift arising from this effect can be produced by a voltage signal of much higher frequency than the mechanical resonance frequency of the load cell. Indeed, this effect can be optimized by driving the PZT stack at one of *its* mechanical resonance frequencies (typically about 75 kHz in devices like that in Figure 1). *Since the time-average of this effect during an applied power interval will lead to a stationary weight reduction, one may simply observe any weight change directly should it be large enough.* Impulse engine term effects, by themselves, do *not* lead to such stationary weight shifts since they time-average to zero.

Mass fluctuations arising from the negative mass term, in real circumstances, if present at all, may be much smaller than ideal considerations suggest. So, should one want to excite a mechanical oscillation of the weigh system near its resonant frequency to bring out a small effect, one need only pulse the high frequency voltage signal delivered to the PZT stack at some suitable low frequency. This procedure, however, proved unnecessary, as with reasonable signal averaging an effect of the sort sought could be obtained. Instead, the frequency of the applied voltage signal was swept through a predetermined range of values to allow for the fact that changing conditions in the PZT stack might cause the frequency of peak effect to change from test to test.

The experimental protocol actually followed was to take data during an interval of several seconds. During the first and last parts of this interval no appreciable voltage signal was applied to the device being weighed. For several seconds between these quiescent periods the voltage signal was applied to the device. By frequency modulation of the signal generator used, the frequency was swept from 70 to 78 kHz during this interval. This frequency interval was chosen because it includes the fundamental mechanical resonance frequency of the PZT stack where the effect sought was expected. Even though a surprisingly large weight fluctuation near the resonance was found, because of a rather poor signal to noise ratio in the weigh signal, we found it necessary to average the data for typically 50 to 100 or more of these data cycles together in order to extract a clear, statistically significant signal.

Aside from the weigh systems *per se*, other components of the apparatus used in this experiment, indicated in Figure 3, are: a power amplifier (a DBX 150 Watt linear amplifier), a 5-to-1 toroidal stepup and isolation transformer (TRANS), voltage and current sense resistors in the high voltage secondary transformer circuit so that the voltage and current signals could be multiplied (4 QUAD MULT.) to get the instantaneous power delivered to the PZT stack, and a rectification and filtering circuit (POWER METER) so that the power could be read as a voltage in real time. Additional instrumentation allows measurement of acceleration of the PZT stack by the embedded accelerometer and the temperature of the device was recorded with the aforementioned thermistor.

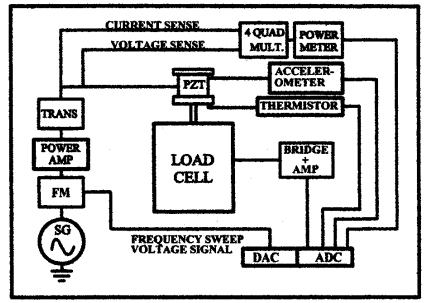

Figure 3: A schematic diagram of the chief electronic circuits used in this experiment. The DAC and ADC are computer controlled.

While the chief parts of the associated circuitry and instrumentation are displayed schematically in Figure 3, several other signal detection features are not displayed. For example, a Picoscope AD212 was also used to monitor various signals at various times. Its software provides FFT power spectrum display capability that is quite helpful for analyzing harmonics present in those signals. Toward the end of the acquisition of data for this paper it became clear that more detailed know-ledge of the thermal behavior of the device than that provided by the thermistor was desirable, so two types of non-contact infrared (IR) detection – one a simple thermo-couple device and the other an IR imaging camera – were introduced. A thermocouple vacuum gauge was used to monitor the vacuum in the vacuum vessels. Operation of the system and data acquisition and processing is computer controlled via a Canetics PCDMA data acquisition board. Data acquisition and post-acquisition data processing is done with software written specifically for that task (adapted from software used in earlier experiments).

The core apparatus in use in the load cell version of this experiment is shown in Figure 2. The weight transducer is located in the 1 cm thick steel shielding case visible in the figure. The load cell vacuum chamber is a small box about 22 cm on a side 26 cm high made of 3 cm thick acrylic plastic (not shown in Figure 2). As in earlier realizations of

experiments using the U-80 load cell, *with sufficient averaging of data from individual cycles*, a mass (or weight) shift of a few milligrams could be resolved – assuming that the static calibration of the load cell with a one gram mass is applicable to signals registered in conditions where high frequency vibration is present in the PZT stack. This last assumption is open to question, for the manufacturer of the U-80 stipulates that the sensitivity of the Hall probe used changes unpredictably in the presence of significant vibration with frequencies above 1 kHz.

The obvious way to deal with this potential problem is to mount the PZT device on the weigh stage of the U-80 with high frequency vibration isolation. (Low frequency isolation is neither needed nor desirable. Indeed, hard coupling at low frequencies is required to make the weight measurements that are the objective of this experiment.) This was done in the earlier phase of this experiment by progressively introducing more and more vibration isolation components. Changes in the weight response of the U-80 disappeared before the isolator configuration seen in Figure 2 was implemented. That is, the isolator shown constitutes over-kill. Nonetheless, to be certain that appreciable high frequency vibration was not communicated to the U-80, an accelerometer (made with thin chips of PZT material) was affixed to the bottom of the weigh stage, and the weight signal was scrutinized with the Pico-scope run in power spectrum mode. Both the accelerometer signals and the power spectrum analysis of the weight signal confirmed that no significant high frequency vibration was present in the U-80 during the operation of the PZT device.

RESULTS

The chief result of this experiment is displayed in Figure 4. It shows the average of several hundred cycles of data taken in a variety of different circumstances. The data displayed is "net" data. While the actual data were being acquired, "null" data where the power to the device in each cycle was manually shut off as soon as the power was automatically activated. The average of the null data has been subtract-ed from the raw data average. In each cycle data was taken for a period of 14 "seconds" at a rate of 50 acquisitions per "second". In fact one "second" was 0.65 actual seconds, the shift having been made by the adjustment of a delay loop in the data acquisition program. Power was not applied to the device until four "seconds" into each cycle. When power was turned on, the frequency of the applied sinusoidal signal was swept from 70 kHz to 78 kHz during the ensuing six "seconds". After the power was switched off, data continued to be taken for an additional four "seconds". Three channels of data in addition to the weight sensor were acquired. One channel recorded the rectified and filtered (10 millisecond time-constant) power signal. This is displayed with the weight signal in panel A of Figure 4. Another channel recorded the rectified and filtered signal from the accelerometer embedded in the PZT stack; and yet another channel recorded the temperature measured by the thermistor epoxied to the aluminum ear bolted to the back of the brass disk on which the PZT stack was mounted. The data from these channels are displayed with the weight signal in panel B of Figure 4.

Simple inspection of Figure 4 reveals that a pronounced weight decrease occurs near 74 kHz. The magnitude of the decrease, about 60 ADC counts, corresponds to roughly 0.1 gram for a peak applied power of about 105 Watts. This is nearly the fluctuation expected on the basis of a naïve, ideal calculation based on Equation (3) above (within a factor of three or so). Note that the weight fluctuation is correlated to spikes in the power and accelerometer traces that signal the occurrence of resonant behavior in the PZT stack. Moreover, the temperature trace recorded by the thermistor shows an inflection in the heating rate that also correlates to the weight shift at 74 kHz.

The thermistor, of course, does not promptly measure the temperature of the PZT stack. Heat evolved in the PZT stack as power is applied is localized in the end of the stack where, by design, the maximum activity is induced – as can be seen in the far infrared (7.5 to 13.3 micron) image of the device

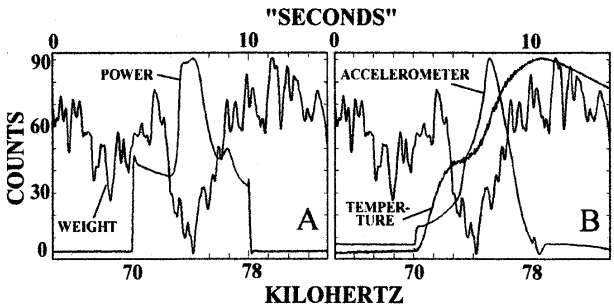

Figure 4: The weight fluctuation in the device shown in Figures 1 and 2 was swept with a sinusoidal signal. The weight is recorded in ADC counts, 66 counts scaling to 0.1 gram. The power trace shown in panel A peaks at 105 Watts. The corresponding thermistor (temperature) and accelerometer traces shown in panel B were not absolutely calibrated.

during power application presented in Figure 5 (taken with an Indigo Alpha Microbolometer camera). Prompt heating of the thermistor, evidently, is produced by vibration driven by the activated PZT stack. And the inflection in the thermistor trace shows that this vibration at the thermistor drops dramatically just before and during the onset of the power and accelerometer resonances.

This device and several others like it were actually designed to behave in this way, though they are so cranky that the preload on the PZT stack and the operating temperature must be "just so" to get them to work as intended. Indeed, the device used to obtain the data displayed showed such crankiness. When optimal operating conditions were not present, the inflection in the thermistor trace was markedly diminished. So thermistor trace inflection was used as a selection criterion for the inclusion of cycle data in the averaged result. (Roughly one cycle in four was rejected using the thermistor trace inflection criterion. The cycle rejection rate improved [decreased] with knowledge of the operation of the system during the course of data acquisition.)

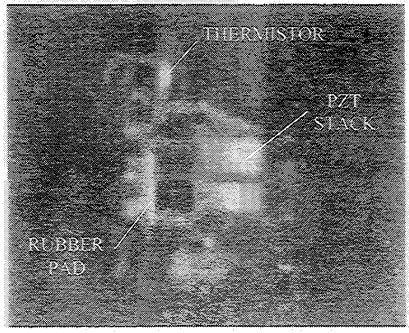

Figure 5: A far infrared image of the device during a power cycle. As expected, the bulk of the energy is delivered to the end of the PZT stack near the aluminum cap. Note too the prompt heating of the thermistor and rubber pads. The temperature rise in the stack during a power cycle is about 5 degrees Celsius.

One may ask: Is the weight fluctuation correlated with the power, thermistor, and accelerometer events is real, or just a statistical fluke? Inasmuch as the number of cycles averaged is about 250, and taking into consideration the weight trace away from the fluctuation, it seems quite plain that the correlated weight fluctuation is *most unlikely* to be a mere statistical fluke. More elaborate statistical analyses of the data are possible. For example, a formal error can be obtained by selective suppression of parts of the data and computing the mean and standard deviation of the spread of the resulting weight fluctuations. This, however, doesn't really shed more light on the significance of the result contained in Figure 4. Given that a weight fluctuation of the sort expected is seen in Figure 4, the question then is: Is the observed weight fluctuation caused by a real Machian effect? Or is it the consequence of the operation of some spurious signal source? Keeping in mind that, "extraordinary claims require extraordinary evidence," we turn now to the tests we have conducted to see if the signal in Figure 4 can be claimed to be real.

SPURIOUS SIGNALS AND CHECK PROTOCOLS

If we assume that the weight fluctuation signal in Figure 4 is *not* due to the predicted Machian effect, then, evidently, it must be a consequence of either the electromagnetic signals present during activation of the device or the mechanical vibration induced by those signals, for no other possibilities worth considering exist. Of these two classes of potential spurious signals, those due to electromagnetic effects are much easier to deal with. All one has to do is recreate the electromagnetic signals without driving the electromechanical response in the PZT stack to test for their effects. This is easily done by shorting out the PZT stack while applying the same voltage signal to another, similar device wired into the circuit far from the weigh system. This way all of the currents and voltages in the device can be emulated, but the electromechanical response that purportedly produces the effect is not excited. Figure 6 displays the results of

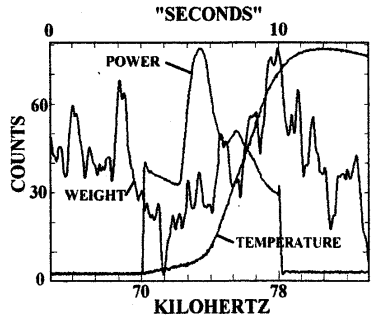

Figure 6: The averages of the current and voltage emulation weight traces. Note the absence of any weight fluctuation correlated with the peak of the power resonance.

this test. Very obviously, no weight fluctuation of the sort seen in Figure 4 is present, so the effect seen cannot be attributed to this source. A small systematic

effect is seen in Figure 6 however. It is caused by the heating of the power leads to the device. (This heating effect is not seen in Figure 4 because data for two lead configurations were averaged together to cancel it out.)

The fact that the current and voltage emulation test does not *exactly* replicate all of the conditions present in the actual data runs makes possible the elimination of another potential source of spurious signals. When the device is actually run, one of the power leads is "hot" while the other is at ground potential. In emulation runs either both leads are hot, or both are not. A moment's reflection should convince one that the "both not" configuration more nearly approximates actual running conditions. Nonetheless, emulations were done in both configurations, and averaged together in Figure 6 because there was no significant difference in the results for the two configurations. In the "hot" configuration, however, since the entire device is (periodically) driven to high voltage, dielectrics in proximity to the device (the vacuum case in particular) will be polarized by the electric field. Since the field may be expected to have large gradients, these polarization charges might interact with the field, and thus the device. Roughly half of the data averaged in Figure 6 being for the "hot" configuration, it shows that no such effects are present.

Other tests of electromagnetic effects were carried out; notably, static magnetic fields of a few Gauss were applied to the system during its operation. No detectable effect was found in any of these tests that would lead one to suspect the effect seen in Figure 6 to be spurious. Mechanical vibration, the other leading candidate for spurious effects, was dealt with chiefly by aggressive vibration suppression and careful monitoring of vibration in the U-80 transducer. In addition, a test involving a unique signature of the negative mass effect was carried out. Note that the negative mass term in Equation (3) above depends on the square of the time derivative of the matter density. Thus, it also depends on the square of the energy density, and ultimately the square of the applied power (and their time derivatives). Normal effects driven by mechanical vibrations, however, may be expected to scale linearly with the applied power.

Although simple in principle, this test is difficult to carry out in practice for several reasons, chiefly secular evolutionary changes in the system during the extensive data runs needed to get even plausible results. Nevertheless, we present results of such a test in Figure 7. They cannot be claimed to be compelling, especially given the noise in the low power weight trace. Moreover, the differences in the power curves for the two power levels casts further doubt on simple comparisons of the two responses. But notwithstanding theses caveats, the predicted power scaling appears to be present.

So far we have considered voltage and current emulation, the induction of electric dipoles in surrounding media, static magnetic fields, the vibration measurements of the mounting stage accelerometer, and the power scaling behavior of the system. And all results are consistent with a real Machian mass fluctuation as the cause of the signals in Figures 4 and 7. It would seem that but a few potential sources of spurious results remain to be considered. Perhaps the most important of these are corona and sonic wind. Both of these depend strongly on the density of the air in which the device is run. So they may be explored by noting any change in the behavior of the system as the pressure in the vacuum vessel is changed. To insure that these effects were not responsible for the signals seen, the device was run at atmospheric pressure, 150 microns, and the normal operating pressure of roughly

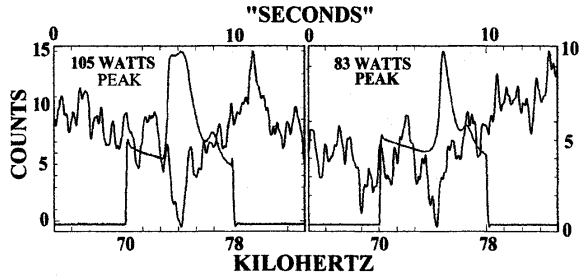

Figure 7: The weight fluctuations recorded for two different power levels. Note that whereas the ratio of the powers is 1.27, the ratio of the weight fluctuations is about 1.6, suggesting that the weight fluctuation scales with the square of the applied power.

15 microns. No noticeable change in behavior with pressure was observed, allowing us to set aside these possible sources of signals. (Nonetheless, the device was operated at the pump limit of about 15 microns except during these tests.)

In light of the results of the tests we report here, perhaps the most important test remaining is the replication of the main result using a completely different weigh system – in particular, a system like the cantilevered beam mentioned above. Time has not permitted us to complete such a test by the time of this writing. But we hope to have one done shortly.

CONCLUSION:

As noted above, the Saganism that extraordinary claims require extraordinary evidence is certainly true. Extraordinarity, however, like beauty, is in some measure in the eye of the beholder. So whether the evidence we present here rises to that level is a matter of individual judgment. Our judgment is that the evidence suggests that a real effect is present; although, being quite cranky, it is far more difficult to produce and manipulate than we would like. Partly, perhaps, these difficulties can be attributed to the very modest effort involved. Greater effort, we think, is warranted.

But where, beyond further confirmation and exploration of the effects reported here, does one go from here? Well, from the point of view of rapid spacetime transport two issues seem to be the most important. First, can the effects reported here be scaled to useful levels? A mass fluctuation of a tenth of a gram or so is only of laboratory interest. It is worth noting that the negative mass term effect, everything else held constant, scales with the square of the frequency and with the square of the power. So, in principle, very large mass fluctuation effects should be producible with only relatively modest power levels. We hasten to add that there are subtleties to the production of this effect that are not yet fully explored. For example, generation of the effect seems to depend quite critically on the production of higher harmonics in the PZT stacks, for sinking a lot of power into a stack at a mechanical resonance of the stack is not, itself, sufficient to yield an effect. The details of the processes that lead to large mass fluctuations need to be studied and *understood* in some detail before serious engineering is undertaken.

Second, from the point of view of propellantless propulsion, the creation of impulse engines requires that objects with induced mass fluctuations be acted upon by another periodic force to extract a stationary force. In the torsion pendulum experiments that preceded those sketched here, two of us (JFW and TLM) were only able to produce minuscule forces many orders of magnitude smaller than those expected on the basis of naïve calculations. Likely this can in part be attributed to subtleties involving the yet to be explored details of the production of mass fluctuations in real non-linear systems. These details will have to be sorted out before the dream of propellantless propulsion can be fully realized.

In this regard we note that it may be worth exploring systems other than simple stacks of PZT crystals driven with complex voltage waveforms (like those already investigated by TLM and JFW). For instance, one might expect to see impulse engine effects in the system described by Corum, *et al.* where a sinusoidal voltage is applied to a circuit with an inductor and capacitor in series.[3] The inductor is arranged so that the periodic magnetic field it generates permeates the dielectric between the plates of the capacitor, orthogonal to the electric field therein. Taken as a strictly electromagnetic system, the conservation principles mentioned at the outset of this paper require that any forces produced in the dielectric be balanced by equal and opposite forces elsewhere in the circuit. So there is no reason to expect to see strictly electromagnetic propulsive forces in this type of system.

But note that if Machian mass fluctuations actually occur, then the acceleration of the charge carriers that comprise the displacement current in the dielectric in the capacitor, driven by the periodic electric field, will induce a mass fluctuation at the power frequency of the voltage frequency – that is, at twice the frequency of the applied voltage signal. Now consider the action of the magnetic field. The motion of the displacement current charge carriers will interact with the period magnetic field to yield a force on the charge carriers via the magnetic part of the Lorentz force: $(q/c)(\boldsymbol{v} \times \boldsymbol{B})$. Since the velocity of the charge carriers, $\boldsymbol{v}$, and the magnetic field, $\boldsymbol{B}$, are both periodic with a frequency equal to the applied voltage frequency, their cross product will yield a force with twice this frequency -- that is, the frequency of the mass fluctuation putatively being driven by the action of the electric field in the dielectric. Should the relative phase of the mass fluctuation and the magnetic part of the Lorentz force be auspicious, a stationary force should result.

Such a force, if present, is a result of the mass fluctuation that arises from the inertial coupling of the constituents of the dielectric to the rest of the universe. It is not due to a local violation of the conservation of momentum in a purely electrodynamical system. It is worth remarking that a stationary force in a system of this sort may be expected even if the "substance" between the plates of the capacitor is the vacuum. If the charged particle pair production in the vacuum of quantum lore actually takes place, the pairs should experience the same effects as material dielectric media. So exploration of this sort of arrangement of circuit elements has scientific value (as a test of the "polarizable vacuum" conjecture), as well as potential technological implications.

Finally, we note that the nearly 0.1 gm mass shift that seems to have taken place in the PZT stack approaches a percent of the total mass of the PZT material (about 40 gm), and this with an applied power on the order of 100 Watts. If this effect is real, and should no physical mechanism operate that enjoins true negative total mass states, then it seems that we may be able to actually generate, however fleetingly, truly exotic matter. Should this prove possible, the most extreme sorts of rapid spacetime transport may be

feasible. Experiments designed to probe these possibilities, however, should be undertaken with some care.

ACKNOWLEDGEMENT:

The work now in progress at CSUF has profited significantly from important contributions of others. They have contributed in several veins. Kirk Goodall helped with the construction of parts of the apparatus, participated in many discussions about the experiment, and did some of the testing of various systems. Probing questions and comments from John Cramer, Michael Dornheim, Edward Harris, and Graham O'Neil, among others, have made us think carefully about several important aspects of Machian mass fluctuations and their application to rapid space-time transport. And the careful critiques of colleagues at CSUF, especially Ronald Crowley and Stephen Goode have been essential. Indeed, those critiques are largely responsible for the appreciation of the significance of the negative mass term in Equations (1) and (2) that underlies the work reported here.

REFERENCES:

1. Woodward, J.F. and Mahood, T.L. (1999), "What is the Cause of Inertia?," *Foundations of Physics* **29**, 899 – 930.
2. Woodward, J.F. (2001), "Gravity, Inertia, and Quantum Vacuum Zero Point Fields," *Foundations of Physics* **31**, 819 – 835.
3. Corum, J.F., Dering, J.P., Pesavento, P., and Donne, A. (1999), "EM Stress-Tensor Space Drive," *Space Technology and Applications International Forum-1999* (ed. M.S. El-Genk, AIP Press, 1999), pp. 1027-1032.
4. Woodward, J.F. (1990), "A New Experimental Approach to Mach's Principle and Relativistic Gravitation," *Foundations of Physics Letters* **3**, 497 – 506.
5. Woodward, J.F. (1991), "Measurements of a Machian Transient Mass Fluctuation," *Foundations of Physics Letters* **4**, 407 – 423.
6. Woodward, J.F. (1995), "Making the Universe Safe for Historians: Time Travel and the Laws of Physcis," *Foundations of Physics Letters* **8**, 1 – 39.
7. Mahood, T.L. (1999), "A Torsion Pendulum Investigation of Transient Machian Effects," California State University, Fullerton masters thesis, available at http://www.serve.com/mahood/thesis.pdf.
8. Sciama, D. (1953), "On the Origin of Inertia," *Monthly Notices of the Royal Astronomical Society* **113**, 34 – 42.
9. Sciama, D.W. (1964), "The Physical Structure of General Relativity," *Reviews of Modern Physics* **36**, 463 – 469.
10. Woodward, J.F. (1992), "A Stationary Apparent Weight Shift from a Transient Machian Mass Fluctuation," *Foundations of Physics Letters* **5**, 425 – 442.
11. Woodward, J.F. (1996), "A Laboratory Test of Mach's Principle and Strong-Field Relativistic Gravity," *Foundations of Physics Letters* **9**, 247 – 293.
12. Puthoff, H. E. (1999), "Polarizable-Vacuum representation of general relativity," available at http://xxx.lanl.gov/abs/gr-qc/9909037.
13. Woodward, J.F. (2000), "Mass Fluctuations, Stationary Forces, and Propellantless Propulsion," *Space Technology and Applications International Forum 2000* (American Institute of Physics/Springer Verlag, New York, 2000), pp. 1018 – 1025.
14. Woodward, J.F. and Mahood, T.L. (2000), "Mach's Principle, Mass Fluctuations, and Rapid Spacetime Transport," unpublished conference paper available at: http://chaos.fullerton.edu/jimw/staif2000.pdf.

AIAA 2001-3910

Global Monopoles and the Bondi-Forward Mechanism

C. Van Den Broeck
The Pennsylvania State University
University Park, PA

37th AIAA/ASME/SAE/ASEE
Joint Propulsion Conference and Exhibit
8-11 July 2001
Salt Lake City, Utah

GLOBAL MONOPOLES AND THE BONDI–FORWARD MECHANISM

Chris Van Den Broeck
Department of Physics, The Pennsylvania State University, 104 Davey Laboratory, University Park, PA 16802, USA
e-mail: vdbroeck@gravity.phys.psu.edu

Abstract. Based on work by Bondi, Forward considered the possibility of using putative negative masses for a propellantless propulsion mechanism. Recent advances in the study of black holes in the presence of fields may provide an explicit mechanism to mimick the effects of negative mass without the need to invoke exotic quantum effects, or to postulate the existence of matter with negative mass in the classical domain. We evaluate the feasibility of using such objects in a Bondi–Forward type propulsion mechanism.

1. Introduction

Bondi[1] was the first to consider the effects of putative negative masses within classical general relativity. As pointed out by Forward[2], negative mass could be used to create a propellantless propulsion mechanism.

The underlying principle can most easily be understood in Newtonian mechanics. Consider a point particle 1 with gravitational mass $m > 0$ and a particle 2 with mass $-m$, both moving along the x–axis of a Cartesian coordinate system. Let $\bar{e}_x$ be the unit vector pointing in the positive x–direction, and suppose that initially $x_2 < x_1$, where x_1 and x_2 are the coordinates of particle 1 and particle 2, respectively. Particle 2 exerts a force on particle 1 equal to

$$\bar{F}_1 = -\frac{G(-m)m}{(x_1 - x_2)^2}\bar{e}_x = \frac{Gm^2}{(x_1 - x_2)^2}\bar{e}_x, \qquad (1)$$

while particle 1 exerts a force on particle 2 given by

$$\bar{F}_2 = \frac{Gm(-m)}{(x_1 - x_2)^2}\bar{e}_x = -\frac{Gm^2}{(x_1 - x_2)^2}\bar{e}_x. \qquad (2)$$

Note that the forces are equal in magnitude but have opposite direction, in accordance with Newton's third law. To get the accelerations, we now have to divide the forces by the respective *inertial* masses. We will assume these to be equal to the gravitational masses, including the sign. To fully understand why this is a reasonable assumption, one would have to take recourse to general relativity[1]; we will also come back to this issue in Section 3. Dividing $\bar{F}_1$ by m and $\bar{F}_2$ by $-m$, we find the accelerations for particle 1 and particle 2 to be

$$\bar{a}_1 = \bar{a}_2 = \frac{Gm}{(x_1 - x_2)^2}\bar{e}_x. \qquad (3)$$

This means that both particles will undergo an acceleration *in the same direction*, and this acceleration will persist until the relativistic regime is reached. (Note that in this special case the magnitudes of the accelerations are also equal to each other; this is just because we chose the absolute values of the masses to be the same.) Again taking into account the signs of the masses, it will be clear that both the (Newtonian) total momentum and total kinetic energy are conserved. (In fact, in this case both are identically zero for all times.)

Negative masses have never been observed in Nature, although it is generally assumed that quantum field theory effects can give rise to negative energy densities (a very readable introduction can be found in Visser's book[3]). In this paper, we will describe a possible mechanism to *mimick* the effects of negative mass, starting from purely classical physics. Our tools will be general relativity, together with the classical theory of the weak and strong nuclear interactions.

As it is well–known, black holes can carry an electric charge, and when a charged particle is moving in such a spacetime, it will feel the effect of both the charge Q of the hole and its mass M. Since energy is stored in the electric field generated by the charge Q, it will contribute to the curvature of spacetime in the vicinity of the hole. Because of the fact that in general relativity, the gravitational force is a result of the curvature of spacetime, this contribution will make it seem as if the hole has a mass different from M. Consequently, even the motion of an *uncharged* particle in such a spacetime will be different from what it would have been if the hole had only carried a mass M, and no charge. In particular, the particle will appear to be moving in the gravitational field of a mass that is *smaller* than M.

It is a generic feature of general relativity that objects appear to have a mass that is smaller than their actual mass content (see e.g. Wald[4]). Consider the example of a spherical, non–rotating star. According to Birkhoff's theorem, the geometry outside the star is that of Schwarzschild spacetime, with some characteristic mass $\tilde{M}$. This is the mass outside observers will *perceive* the star to have, for example by releasing test particles and observing their motion. As it turns out, $\tilde{M}$ will always be slightly smaller than the 'proper' mass content M of the star (i.e., the mass that went into the star when it formed). If we define $\Delta M = M - \tilde{M}$, then $E_B = \Delta M\, c^2$ may be interpreted as the gravitational binding energy.

It needs to be stressed that the latter is merely a

heuristic statement, since gravitational binding energy has no general definition. Even so, one could ask the following question: Can a self–gravitating object be so strongly bound that its apparent mass is negative (i.e., can the contribution to the mass due to binding energy be larger than the proper mass content)? Preliminary investigations seem to point towards a positive answer. The purpose of this paper is to describe under what circumstances this could come about, and to evaluate its relevance for the Bondi–Forward (BF) propulsion mechanism.

The paper is structured as follows. In the next Section, we will introduce solutions to Einstein gravity in the presence of additional, non–gravitational fields, which for all practical purposes have a negative gravitational mass, even though the energy stored in the fields, as well as any proper mass that may be present, are positive. In Section 3, we first of all evaluate to what extent the objects described may be considered realistic, or physically acceptable, and we consider the problems that may be expected when incorporating them in BF propulsion. Conclusions are presented in Section 4. Although we will assume that the reader has some knowledge of basic relativistic physics, we will review the theory of the Higgs field and its coupling to gravity in the Appendix, as it will be the basis for the more promising class of objects discussed in Section 3.

Throughout this note we will use units such that $G = c = \hbar = 1$, unless stated otherwise. The signature of spacetime metrics is chosen to be $(-,+,+,+)$.

2. Black holes with negative mass

The fact that in the presence of fields, black holes can appear to have negative mass has been known for quite some time; it is apparent in the solutions discovered by Barriola and Vilenkin[5]. Recently, two classes of black holes with negative effective mass were studied in detail. In what follows, we will talk about proper mass and proper charge; for definiteness, let us first define these rigorously. The spacetimes we will consider all have a metric of the form

$$ds^2 = -\sigma^2 N dt^2 + N^{-1} dr^2 + r^2(d\theta^2 + \sin^2\theta\, d\phi^2), \quad (4)$$

where σ and N are functions of r. Define $u(r) = r^2 N(r)$ and expand this function near $r = 0$:

$$u = Q^2 - 2Mr + \ldots. \quad (5)$$

By definition, Q is the proper charge and M the proper mass. This definition is motivated by the fact that in the case of a charged black hole, Q and M are indeed the amounts of charge and mass that end up in the hole as it is formed. These should be distinguished from the *effective* charge and mass, which are the values measured by an outside observer, e.g. using test particles.

So far we have only talked about black holes carrying the electric charge associated to electromagnetism. However, holes can also have proper charges associated to the weak and strong nuclear forces. Just like electromagnetism, these interactions are described by *gauge theories*, which are characterized by some internal group of invariances, or *symmetries*. (In the case of electromagnetism, this is the invariance of the electric and magnetic fields when adding to the vector potential the gradient of an arbitrary smooth function.) The symmetry group inherent in electromagnetism is called $U(1)$, and those of the weak and strong interactions are $SU(2)$ and $SU(3)$, respectively. The weak interaction is somewhat special, in that its symmetry is broken in Nature, presumably by interaction with the yet to be discovered Higgs field. For an elementary introduction into the physics involved, we refer the reader to the textbook by Aitchison and Hey[6].

Zotov[7] studied the appearance of black holes with negative effective mass in the context of *unbroken* $SU(2)$ gauge theory, called *Yang–Mills theory*. Although this model is not realized in Nature, it can be considered as a useful 'toy model' for the full $SU(3)$ theory describing the strong interaction. It is generally believed that the qualitative features of solutions of Yang–Mills theory coupled to gravity will usually carry over to $SU(3)$. Zotov's black holes have a proper mass, and also a proper charge. The latter is not the familiar charge of electromagnetism, but its $SU(2)$ equivalent. Numerical results suggest that Yang–Mills theory admits black hole like solutions with negative effective mass but positive proper mass. However, the solutions studied by Zotov do not have an event horizon; their singularities are naked. Although a proof is lacking, it is generally assumed that this cannot happen in Nature (this is the famous *Cosmic Censorship Conjecture*[8]), so we will not discuss these solutions any further.

Instead, we turn to the slightly earlier work of Nucamendi and Sudarsky[9]. They studied black hole solutions with an event horizon, arising from a model with three scalar fields having a broken *global* $O(3)$ symmetry. Here 'global' merely means that, unlike gauge symmetries, the transformations under which the theory is invariant are not allowed to depend on the position in spacetime. The broken $O(3)$ theory should be a good model for the Higgs interaction. It is assumed that there exists more than one Higgs. The way they interact among themselves will involve a global symmetry, which needs to be broken itself in order to break the $SU(2)$ symmetry of the weak interaction. The breaking occurs when the Higgs particles form a *condensate*, meaning that the Higgs fields acquire a non–zero vacuum expectation value.

A peculiar feature of the solutions presented by Nucamendi and Sudarsky is that they carry neither proper mass nor proper charge. Instead, they are 'topological defects', usually called *global monopoles*. A useful picture is that of a field which has been tied into a knot.

The energy stored in such a 'knotted' field can give rise to a spacetime geometry which is similar to that of a black hole with an event horizon. (Note that the term 'topological defect' refers to the gauge field itself, *not* the topology of the spacetime it gives rise to.) Henceforth, we will refer to the particular solutions found by Nucamendi and Sudarsky as *NS monopoles*.

In general, the equations describing the interaction between the fields and gravity in the model of Nucamendi and Sudarsky are too complex to solve analytically. As a consequence, the spacetime metrics for black hole like solutions can usually not be written in closed form. However, at large distances, NS monopoles have a metric that looks like

$$ds^2 \simeq -\left(1-\frac{2\tilde{M}}{r}\right)dt^2+\left(1-\frac{2\tilde{M}}{r}\right)^{-1}dr^2 +(1-\alpha)\,r^2(d\theta^2+\sin^2\theta\,d\phi^2), \qquad (6)$$

where $\alpha = 8\pi\eta^2$, with η the magnitude of the Higgs field condensate. The equations of motion for uncharged test particles with positive mass moving in the vicinity of the monopole are given by the geodesic equation. A particle that is initially at rest at sufficiently large distances will be subject to a radial proper acceleration

$$a_r \simeq \frac{-\tilde{M}}{r^2-2\tilde{M}r}. \qquad (7)$$

As numerical results show, it is possible to have solutions with $\tilde{M} < 0$, so that $a_r > 0$: The central object is repelling the particle. For all practical purposes, the global monopole behaves as an object with negative mass.

It is worth pointing out that although the monopole behaves as if it carries negative mass/energy, all of the energy conditions of general relativity are satisfied because of the way the fields couple to gravity[10]. Therefore, no observer will ever measure negative energy density in this spacetime; the monopole indeed only *mimicks* the effect.

Note that the metric (6) is not asymptotically flat: In the limit $r \to \infty$, one does not retrieve the usual uncurved (or Minkowski) spacetime. Rather, the geometry is 'asymptotically flat up to a deficit angle'. This means that if we were to measure the surface area of a sphere with very large radius R centered on the black hole, we would not find the usual value of $4\pi R^2$, but rather $4\pi(1-\alpha)R^2$. We will come back to this important fact in the next section.

3. Global monopoles and the BF mechanism

Although the NS monopoles satisfy most of the criteria to be physically acceptable solutions of the broken $O(3)$ theory coupled to gravity, it is not known how they could be created in Nature. The relevant literature is very recent, and it deals only with static solutions, so that at this time it would be inappropriate to speculate on how global monopoles with negative effective mass might come about. This makes it impossible to assess how much energy is needed to generate these objects. As we mentioned, the proper mass is zero; all energy is stored in the fields. In general relativity there is no generic scheme to compute the energy stored in a particular fields configuration, especially for solutions that are not asymptotically flat.

The failure of the metric (6) to be asymptotically flat is a possibly problematic feature from a physical point of view. The deficit angle will create tidal stresses. As we mentioned in the previous section, the magnitude of α is determined by the magnitude of the Higgs field condensate. The magnitude of the stresses on a compact object of fixed size will depend on distance; even though the metric is not asymptotically flat globally, it still approaches flatness locally. A good analogy is to consider the surface of a cone. The spheres of radius R we talked about in the previous section are now circles on the cone in a plane perpendicular to the cone's axis. R should be interpreted as the distance of a circle from the apex of the cone, so that their circumference is $2\pi(1-\beta)R$, with $2\pi\beta$ some deficit angle. But now consider a disk of radius ρ stuck on the surface of the cone. If the disk is close to the apex, its surface area will be smaller than $\pi\rho^2$. However, as one slides the disk away from the apex while keeping ρ fixed, the curvature of the cone's surface becomes less noticeable and the area of the disk will tend to $\pi\rho^2$ asymptotically. Similarly, in the spacetime (6), a spherical object with radius ρ will have a volume smaller than $4\pi\rho^3/3$ when close to the central singularity, but as it is moved away from it while keeping ρ fixed, the volume *will* tend to that value.

The magnitude of the Higgs condensate is expected to be $\eta \simeq 250\ \mathrm{MeV/m}^3$; in units where $G = c = \hbar = 1$, this becomes $\eta \simeq 5\times 10^{-126}$, so that the deficit angle $4\pi\alpha = 32\pi^2\eta^2$ will be of no consequence in the regime where the approximation (6) is valid.

NS monopoles have two characteristic length scales associated to them: The radius of the event horizon r_h, and the monopole's 'core radius' r_c. The latter is completely fixed by the mass the Higgs bosons themselves acquire due to symmetry breaking. Different NS monopole solutions are characterized by different values of r_h. Negative effective masses occur when $r_h \ll r_c$, so that for these solutions the metric (6) is a good approximation for $r \gg r_c$. In units where $G = c = \hbar = 1$, one has $r_c = 1/(\sqrt{2}m_H)$. Although the Higgs mass is as yet unknown, it is generally assumed to be approximately $m_H \simeq 200$ GeV. In SI units, this gives $r_c \sim 10^{-35}$ m. For all practical purposes, the monopole can be considered as a point particle.

The smallness of the core radius raises an important question. So far, we have been discussing purely classical

field theory, both on the gravitational and on the Higgs side. However, r_c is comparable to the Planck length. This means that realistic NS monopoles are not only essentially quantum mechanical objects; quantum gravity effects can be expected to influence their structure in a major way. As yet, no quantum gravity theory has been verified either experimentally or observationally, so that it is impossible to say what these effects will do to the monopole. However, although the Higgs mass is a parameter in the Standard Model of elementary particle physics, it is not generally considered to be a fixed constant of Nature. This is because it is not only determined by the coupling strength of the Higgs self-interaction, but also by the magnitude of the Higgs condensate. The latter is expected to be a consequence of the particular conditions that existed shortly after the Big Bang[11]. It is not unimaginable that its value could be changed locally, although any statement as to how this could be done would again be pure speculation. For now, I will confine myself to saying that it is justifiable to continue the discussion on the basis of the qualitative results from the classical theory.

Without going through the full numerical computation for the spacetime geometry, from looking at the evolution equations in the paper by Nucamendi and Sudarsky[9] one can immediately tell that if $\alpha \simeq 0$, the effective mass will also be exceedingly small. Nevertheless, one can think of schemes to use NS monopoles for BF propulsion. For instance, consider a very large number of them contained in a spherical shell of positive mass. Using Newtonian arguments again, the spherical shell will not influence the effectively negative mass inside; as it is well-known, such a shell acts like the gravitational equivalent of a Faraday cage. On the other hand, negative mass particles will repel both each other and the surrounding shell. One can therefore conceive of a thin, spherical, positive mass shell filled homogeneously with negative mass. If the amount of negative mass inside is much larger in absolute value than the mass of the shell, the net gravitational field outside will be that of a negative point mass. Still using Newtonian arguments, for an amount of negative mass in the order of, say, a large asteroid mass ($M \sim -10^{20}$ kg), the outward pressure on the spherical shell will be comparable to the inward pressure felt by the matter in a positive mass asteroid (this is of course assuming the dimensions are comparable). Close to the shell, the repulsive gravitational force will be the same in magnitude as the (attractive) force caused by an asteroid with the same (positive) mass and dimensions. This will then be the force acting on a positive 'payload' mass placed close to the shell.

A possible implementation of the BF mechanism would consist of a container of NS monopoles together with a positive payload mass, which would act as the positive mass particle in the system. Now a new question arises: Although we know that the container will repell the payload, can we be sure that the payload will attract the container? Phrased differently, is the inertial mass of NS monopoles equal to the negative effective mass? Recall from the Introduction that it was precisely the fact that we divided the force on the particle with negative gravitational mass by $-m$ that led to an acceleration in the same direction as that of the positive mass particle. The inherent assumption was the equality of graviational and inertial mass. So far, we have tacitly assumed that this equality holds for NS monopoles. Are we justified in doing so?

When computing the inertial mass of e.g. a proton, the binding energy of its quarks due to the strong nuclear interaction needs to be taken into account to arrive at the correct result. Similarly, if the negative effective mass of NS monopoles is to be understood as a consequence of gravitational binding energy (cf. the example of the spherical non-rotating star), then one expects a positive answer.

Since gravitational binding energy is but a heuristic concept, a more fruitful way of looking at the problem is to consider the metric caused by an isolated payload mass. Supposing the payload mass is spherically symmetric, the metric of the geometry outside will be Schwarzschild. If the negative mass container is sufficiently far away, it can be considered as a point particle. Alternatively, one could look at the motion of just a single NS monopole, which for all practical purposes should behave as a test particle in the technical sense: A point particle with negligible mass. It is reasonable to assume that a single monopole will move on a geodesic, and that this will also be approximately true for a container of macroscopic extent. Since the geodesic equation is insensitive to the mass of the point particle of which it describes the motion, in that case a monopole, and a negative mass container, would certainly be attracted by the payload.

The geodesic equation can be derived from Einstein's equations by considering the motion of an extended body in curved spacetime and taking the limit where its spatial extent goes to zero. The derivation is subtle, as was made clear most recently by the work of Mino, Sasaki and Tanaka[12], and Quinn and Wald[13]. In the case of a small and light NS monopole superposed on a curved background, the analysis will be extremely complicated, partly because of the internal structure of an monopole, and especially because of the fact that the spacetime geometry is not asymptotically flat. A direct proof that NS monopoles will move on geodesics can be expected to be very difficult.

Because of its importance for the BF mechanism, the issue of inertia calls for further investigation. To evaluate the inertial mass rigorously, one needs a detailed study of the behavior of NS monopoles in a dynamical situation. One possibility would be to construct a binary solution of two NS monopoles connected by a

'strut'. Such constructions have been carried out for binary black hole solutions (a recent reference is Letelier and Oliveira[14]). If NS monopoles have negative inertial mass as well as negative effective mass, what we would expect for a monopole pair is that the connecting strut would tend to be stretched. Alternatively, one could consider perturbations of the NS monopole metric with non–zero momentum and study the recoil effects, as has been done by Andrade and Price[15] for ordinary black holes.

Assuming that the system composed of the negative mass container and the payload mass can not go superluminal, it is easy to guess what will happen as it approaches relativistic speeds. The neutral positive matter can only radiate gravitationally. Since the Higgs interaction is much stronger than the gravitational one, the NS monopoles inside the shell will start radiating 'Higgs field waves' before the positive matter loses energy through gravitational wave emission. The Higgs radiation will carry off positive energy: The positive energy stored in the fields composing the monopoles. The strength of those fields then diminishes, and the effective negative mass becomes less negative *even though positive energy is being radiated away.* We reiterate that although the monopoles generate a repulsive gravitational force indistinguishable from that of negative mass, the true energy density is positive everywhere.

4. Summary and conclusions

We have described a possible implementation of the Bondi–Forward propulsion mechanism on the basis of global monopoles arising in a spontaneously broken $O(3)$ Higgs model coupled to gravity. Clearly, there are several open problems, each of them crucial to the relevance of NS monopoles in the context of the BF scheme.

The typical length scale of a monopole with negative effective mass is the core radius, which is determined by the Higgs mass and turns out to be of the order of the Planck scale. In that case, the classical description is inappropriate, and a description in terms of quantum gravity is called for. Since no quantum gravity theory has ever been tested, it is impossible to say at this point how this will effect the properties of the monopole. However, the Higgs mass depends both on the coupling strength of the Higgs self–interaction and the magnitude of the condensate. Both are parameters in the Higgs potential (see the Appendix), and standard lore[11] has it that this potential is dynamically generated by whatever physics goes on at very high energies. Consequently, it is possible that these parameters can be changed in a physical process, but the theoretical framework to even conceive of a mechanism to bring this about is not yet in place.

So far, the study of solutions to the theory of the Higgs coupled to gravity has been confined to static ones. As a result, no physical mechanism is known in which NS monopoles might be created. Since these objects do not have a proper mass or charge, this makes it hard to even estimate how much energy would be involved.

The most pressing problem is the question whether NS monopoles with negative effective mass also have negative inertial mass. One would expect a positive answer, but this should not be taken for granted. We have indicated a number of ways in which it could be tested computationally. It seems unrealistic to hope for a direct proof that the motion of NS monopoles is approximately geodesic, but we have proposed other schemes which have already been worked out for less exotic objects.

It will be clear that a full evaluation of the possibility of using NS monopoles to implement the BF mechanism would require a protracted effort on the theory side. Even then, it seems unlikely that a definite statement could be made on the basis of what we currently know about high energy physics. But at least there is some hope; even though negative mass presumably does not exist in its 'pure' form, Nature may have given us a loophole.

Appendix

It is generally assumed that the breaking of the $SU(2)$ gauge symmetry of the electroweak interaction is a consequence of the breaking of a *global* symmetry associated with the dynamics of the Higgs fields. Nucamendi and Sudarsky considered a theory with three Higgs fields ϕ^a, $a = 1, 2, 3$, interacting with each other according to a potential

$$V(\phi^a) = V(\phi^1, \phi^2, \phi^3) = \frac{\lambda}{4}(\phi^2 - \eta^2)^2, \qquad (8)$$

where ϕ^2 is shorthand for $\sum_{a=1}^{3} \phi^a \phi^a$. Note that if one would set e.g. ϕ^3 to zero and consider only ϕ^1 and ϕ^2, a diagram of the potential versus ϕ^1, ϕ^2 would resemble a Mexican hat. Indeed, $V(\phi^a)$ then has a local maximum at the origin of the (ϕ^1, ϕ^2)–plane given by $V(0,0,0) = (\lambda/4)\,\eta^4$ (the top of the 'hat'). As one moves away from the origin, the potential decreases until the valley defined by $\phi^2 = \eta^2$ is reached, where $V = 0$ (the rim of the hat). Moving still further away from the origin, V increases without bound.

What cosmologists generally expect to have happened during the early phases of the Universe can be very roughly described as follows. Shortly after the Big Bang, when the temperature of the Universe was still very high, η was equal to zero, so that the potential had a unique minimum at the origin and increased without bound as one moved away from the origin. The equilibrium value for the classical fields ϕ^a was then $\phi^a = 0$ for $a = 1, 2, 3$, since the potential is then at its minimum, $V = 0$. As the Universe cooled down, η increased and the potential formed a 'bump' near the origin, leading to the Mexican hat shape. The values $\phi^a = 0$ now corresponded to an

unstable equilibrium point: The top of the 'hat'. Consequently, the fields ϕ^a acquired non–zero values throughout spacetime, namely values that minimized the new potential. But note that for $\eta \neq 0$, (8) does not have a unique minimum; all values of ϕ^a for which $\phi^2 = \eta^2$ are a minimum of the potential. Which minimum the fields ended up in was determined by the small perturbations causing the field configuration to be pushed away from the unstable equilibrium point, and may be considered arbitrary for all practical purposes. The situation is comparable to that of a pencil balanced on its tip: The pencil could fall in any direction. This process is called *spontaneous symmetry breaking*. The result is that the classical values of the Higgs fields are no longer zero; in the jargon one says that the particles associated to the fields have formed a *condensate* ϕ^a such that $\phi^2 = \eta^2$. η is the magnitude of the condensate; presumably it is determined by the specific conditions existing in the early Universe, together with the dynamics of the as yet unknown high–energy physics driving the symmetry breaking. The terminology stems from a very analogous process in condensed matter physics, the Meissner effect, which is responsible for superfluidity and superconductivity.

In a curved spacetime, the field equations governing the classical dynamics of the Higgs fields are given by

$$\nabla_\mu \nabla^\mu \phi^a = \frac{\partial V}{\partial \phi^a}, \tag{9}$$

where the ∇_μ ($\mu = 0, \ldots, 3$) are the covariant derivatives associated to the metric; in flat spacetime these would simply be the partial derivatives with respect to the coordinates. (Raising and lowering of indices is done using the metric and its inverse, and as always summation over repeated indices is implied.) Using the expression for the potential (8), the field equations (9) can be written in more detail as

$$\nabla_\mu \nabla^\mu \phi^a + \lambda \eta^2 \phi^a - \lambda \phi^2 \phi^a = 0. \tag{10}$$

As usual, the prefactor of the term that is linear in the fields and carries no derivatives gives us the square of the mass[7], so that the Higgs mass is equal to $m_H = (\lambda \eta^2)^{\frac{1}{2}}$. Apart from that, there is a cubic interaction of the Higgs among themselves, with coupling strength λ.

The presence of the fields affects the geometry of spacetime through the Einstein equations,

$$R^{\mu\nu} - \frac{1}{2} g^{\mu\nu} R = 8\pi T^{\mu\nu}. \tag{11}$$

Here $R^{\mu\nu}$ is a tensor formed from the metric $g_{\mu\nu}$ and its first and second derivatives, $R = R^{\mu\nu} g_{\mu\nu}$, and $T^{\mu\nu}$ is the stress–energy tensor of the Higgs fields. One has

$$T^{\mu\nu} = \nabla^\mu \phi^b \nabla^\nu \phi^b - g^{\mu\nu} \left[\frac{1}{2} (\nabla^\kappa \phi^b)(\nabla_\kappa \phi^b) + V(\phi^a) \right], \tag{12}$$

where summation over the indices b is assumed. For derivations we refer to Aitchison and Hey[7] and Hawking and Ellis[10].

To solve the equations (9) and (11), Nucamendi and Sudarsky started with the ansatz

$$\phi^a = \eta f(r) \frac{x^a}{r} \tag{13}$$

for the fields, and

$$ds^2 = -\left(1 - \frac{2m(r)}{r}\right) e^{-2\delta(r)} dt^2 + \left(1 - \frac{2m(r)}{r}\right)^{-1} dr^2 + (1-\alpha)\, r^2 (d\theta^2 + \sin^2\theta\, d\phi^2) \tag{14}$$

for the spacetime metric. The x^a are spatial asymptotic Cartesian coordinates, obtained from (r, θ, ϕ) in the same way as Cartesian coordinates in Euclidean space. The functions $f(r)$, $m(r)$, and $\delta(r)$ are to be obtained from the field equations (9) and the Einstein equations (11), with suitable boundary conditions. We note in passing that (14) is indeed of the form (4).

The natural boundary condition for f as $r \to \infty$ is $f(r) \to 1$, since one wants the Higgs fields (13) to tend to a minimum of the potential, i.e., $\phi^2 \to \eta^2$. As was shown by Barriola and Vilenkin[5], the asymptotic behavior (6) then leads to a globally well–defined solution for both the fields and the metric (apart from a central singularity). However, in numerically solving (9) and (11), Nucamendi and Sudarsky found it more convenient to impose boundary conditions at the origin $r = 0$:

$$\begin{aligned} f(0) &= 0, \\ m(0) &= 0, \\ \frac{\partial m}{\partial r}(0) &= -\frac{\alpha}{2(1-\alpha)}. \end{aligned} \tag{15}$$

The fact that one needs $f \to 1$ as $r \to \infty$ then imposes a unique value for $\partial f / \partial r$ at $r = 0$, which can only be determined by a 'shooting method': Different values are tried out until a consistent solution for fields and metric is obtained. For more details, the reader is encouraged to read the original paper[9].

Using the conditions (15), it is easy to convince oneself that the proper mass and charge of an NS monopole as defined by the expansion (5) are indeed zero. The function $u(r)$ is

$$u = r^2 \left(1 - \frac{2m(r)}{r}\right) = -2m(r)\, r + r^2. \tag{16}$$

Near $r = 0$ there is no zeroth order term in r, so $Q = 0$, and since $m(0) = 0$ the first order term vanishes as well, which gives $M = 0$.

Acknowledgement

It is a pleasure to thank Jorge Pullin for very helpful discussions.

---

[1] H. Bondi, Review of Modern Physics **29** (1957) 423–428
[2] R.L. Forward, Journal of Propulsion and Power **6** (1990) 28–37
[3] M. Visser, *Lorentzian Wormholes*, American Institute of Physics, Woodbury, New York, 1995
[4] R.M. Wald, *General Relativity*, University of Chicago Press, Chigaco, 1984
[5] M. Barriola and A. Vilenkin, Physical Review Letters **63** (1989) 341
[6] I.J.R. Aitchison and A.J.G. Hey, *Gauge Theories in Particle Physics*, 2nd ed., Institute of Physics Publishing, London, 1989
[7] M.Y. Zotov, unpublished; LANL preprint gr-qc/0011065
[8] R. Penrose, in *General Relativity, and Einstein Centenary Survey*, Eds. S.W. Hawking and W. Israel, Cambridge University Press, Cambridge, 1979
[9] U. Nucamendi and D. Sudarsky, Classical and Quantum Gravity **17** (2000) 4051–4058
[10] S.W. Hawking and G.F.R. Ellis, *The large scale structure of spacetime*, Cambridge University Press, Cambridge, 1973
[11] An excellent overview of current ideas in cosmology is *COSMO–99: Proceedings of the Third International Workshop on Particle Physics and the Early Universe*, Eds. U. Cotti, R. Jeannerot, G. Senjanović, and A. Smirnov, World Scientific, London, 2000
[12] Y. Mino, M. Sasaki, and T. Tanaka, Physical Review D **55** (1997) 3457–3476
[13] T.C. Quinn and R.M. Wald, Physical Review D **56** (1997) 3381–3394
[14] P.S. Letelier and S.R. Oliveira, Classical and Quantum Gravity **15** (1998) 421–433
[15] Z. Andrade and R. Price, Physical Review D **56** (1997) 6336–6350

A01-34540

AIAA 2001-3911

Induction and Amplifications of Non-Newtonian Gravitational Fields

M. Tajmar
Austrian Research Centers Seibersdorf
Austria

and C.J. de Matos
ESA-ESTEC
The Netherlands

37th AIAA/ASME/SAE/ASEE Joint Propulsion Conference and Exhibit
8-11 July 2001
Salt Lake City, Utah, USA

AIAA 2001-3911

Induction and Amplification of Non-Newtonian Gravitational Fields

M. Tajmar*
Austrian Research Centers Seibersdorf, A-2444 Seibersdorf, Austria

C. J. de Matos†
ESA-ESTEC, Directorate of Scientific Programmes, PO Box 299, NL-2200 AG Noordwijk, The Netherlands

One obtains a Maxwell-like structure of gravitation by applying the weak-field approximation to the well accepted theory of general relativity or by extending Newton's laws to time-dependent systems. This splits gravity in two parts, namely a gravitoelectric and gravitomagnetic (or cogravitational) one. Both solutions differ usually only in the definition of the speed of propagation, the lorentz force law and the expression of the gravitomagnetic potential energy. However, only by extending Newton's laws we obtain a set of Maxwell-like equations which are perfectly isomorphic to electromagnetism. Applying this theory to explain the measured advance of the mercury perihelion we obtain exactly the same prediction as starting from general relativity theory. This is not possible using the weak-field approximation approach. Due to the obtained similar structure between gravitation and electromagnetism, one can express one field by the other one using a coupling constant depending on the mass to charge ratio of the field source. This leads to equations e.g. of how to obtain non-Newtonian gravitational fields by time-varying magnetic fields. Unfortunately the coupling constant is so small that using present day technology engineering applications for gravitation using electromagnetic fields are very difficult. Calculations of induced gravitational fields using state-of-the-art fusion plasmas reach only accelerator threshold values for laboratory testing. Possible amplification mechanisms are mentioned in the literature and need to be explored. We review work by Henry Wallace suggesting a very high gravitomagnetic susceptibility of nuclear half-spin material as well as coupling of charge and mass as shown by e.g. torque pendulum experiments. The possibility of using the principle of equivalence in the weak field approximation to induce non-Newtonian gravitational fields and the influence of electric charge on the free fall of bodies are also investigated, leading to some additional experimental recommendations.

1. Introduction

The control and modification of gravitational fields is a dream pursued by propulsion engineers and physicists around the world. NASA's Breakthrough Propulsion Physics Project is funding exploratory research in this area to stimulate possible breakthroughs in physics that could drastically lower costs for access to space[1]. Although not commonly known, Einstein's well accepted general relativity theory, which describes gravitation in our macroscopic world, allows induction phenomena of non-Newtonian gravitational fields similar to Faraday induction in electromagnetic fields by moving heavy masses at high velocities.

The basis for such phenomena are even dating back before general relativity theory when Oliver Heaviside[2] in 1893 investigated how energy is propagated in a gravitational field. Since energy propagation in electromagnetic fields is defined by the Poynting vector – a vector product between electric and magnetic fields – Heaviside proposed a gravitational analogue to the magnetic field. Moreover he postulated that this energy must also be propagating at the speed of light. Another approach to the magnetic part of gravity is to start from Newtonian gravity and add the necessary components to conserve momentum and energy[3]. This leads to the same magnetic component and a finite speed of propagation, the speed of light.

Heaviside's gravitomagnetic fields are hidden in Einstein's Tensor equations. Alternatively, general relativity theory can be written as linear perturbations of Minkowski spacetime. Forward[4] was the first to show that these perturbations can be rearranged to assemble a Maxwell-type structure which splits gravitation into a gravitoelectric (classical Newtonian gravitation) and a gravitomagnetic (Heaviside's prediction) field. The magnetic effects in gravitation are more commonly known as the Lense-Thirring or frame dragging effect describing precision forces of rotating masses orbiting each other. NASA's mission Gravity Probe B will look for experimental evidence of this effect. Similar to electrodynamics, a variation in gravitomagnetic fields induces a gravitoelectric (non-Newtonian) field and hence provides the possibility to modify gravitation.

* Research Scientist, Space Propulsion,
Phone: +43-50550-3142, Fax: +43-50550-3366,
E-mail: martin.tajmar@arcs.ac.at
† Staff Member, Science Management
Communication Division,
Phone: +31-71-565 3460, Fax: +31-71-565 4101,
E-mail: clovis.de.matos@esa.int

Since both gravitation and electromagnetism have the same source, the particle, the authors recently published a paper evaluating coupling constants between both fields[5] based on the charge-to-mass ratio of the source particle. This paper will review the coupling between gravitation and electromagnetism and point out the limits of present day technology and the expected order of magnitude of non-Newtonian gravitational fields that can be created by this method. Possible amplification mechanism such as ferro-gravitomagnetism and more speculative work published in the literature will be reviewed.

The principle of equivalence in the limit of weak gravitational fields (the gravitational Larmor theorem) will be explored and a possible new effect (the gravitomagnetic Barnett effect) recently suggested by the authors is discussed[6]. However the direct detection of this effect is pending on the possibility to have materials with high gravitomagnetic susceptibility. Nevertheless we show that the principle of equivalence in the weak field approximation together with the gravitational Poynting vector associated with induced non Newtonian gravitational fields (through angular acceleration) account properly for the conservation of energy in the case of cylindrical mass with angular acceleration. This is an encouraging result regarding the possible detection of macroscopic non-Newtonian gravitational fields induced through the angular acceleration of the cylinder in the region located outside the rotating cylinder. The detection of these non-Newtonian gravitational fields outside the cylinder would represent an indirect evidence of the existence of the gravitomagnetic Barnett effect.

Finally the free fall of a massive cylinder carrying electric charge is studied. It is shown that in order to comply with the law of conservation of energy, and with the equivalence principle, the acceleration with which the cylinder will fall depends on its electric charge, its mass and its length.

If the last two effects exposed above are experimentally detected, a technology that can control the free fall of bodies with mass in the laboratory is at hand. If the result is negative, a better empirical understanding of Einstein's general relativity theory in the limit of weak gravitational fields and when extended to electrically charged bodies, would have been achieved, which is a significant scientific result as well.

2. Maxwell Structure of General Relativity Theory

Einstein's field equation[7] is given by

$$R_{\alpha\beta} - \frac{1}{2} g_{\alpha\beta} R = \frac{8\pi G}{c^4} T_{\alpha\beta} \qquad (1)$$

During the linearization process, the following limitations are applied:

1. all motions are much slower than the speed of light to neglect special relativity
2. the kinetic or potential energy of all bodies being considered is much smaller than their mass energy to neglect space curvature effects
3. the gravitational fields are always weak enough so that superposition is valid
4. the distance between objects is not so large that we have to take retardation into account

We therefore approximate the metric by

$$g_{\alpha\beta} \equiv \eta_{\alpha\beta} + h_{\alpha\beta} \qquad (2)$$

where the greek indices $\alpha, \beta = 0, 1, 2, 3$ and $\eta_{\alpha\beta} = (+1, -1, -1, -1)$ is the flat spacetime metric tensor, and $|h_{\alpha\beta}| << 1$ is the perturbation to the flat metric. By proper substitutions and after some lengthy calculations[5] (the reader is referred to the literature for details), we obtain a Maxwell structure of gravitation which is very similar to electromagnetics and only differs due to the fact that masses attract each other and similar charges repel:

$$\begin{aligned}
&div\,\vec{E} = \frac{\rho}{\varepsilon_0} && div\,\vec{g} = -\frac{\rho_m}{\varepsilon_g} \\
&div\,\vec{B} = 0 && div\,\vec{B}_g = 0 \\
&rot\,\vec{E} = -\frac{\partial \vec{B}}{\partial t} && rot\,\vec{g} = -\frac{\partial \vec{B}_g}{\partial t} \\
&rot\,\vec{B} = \mu_0 \rho \vec{v} + \frac{1}{c^2}\frac{\partial \vec{E}}{\partial t} && rot\,\vec{B}_g = -\mu_g \rho_m \vec{v} + \frac{1}{c^2}\frac{\partial \vec{g}}{\partial t}
\end{aligned} \qquad (3)$$

Maxwell Equation (Electromagnetism) | Maxwell-Einstein Equation (Gravitation)

where $\vec{g}$ is the gravitoelectric (or Newtonian gravitational) field and $\vec{B}_g$ the gravitomagnetic field. The gravitational permittivity ε_g and gravitomagnetic permeability η_g is defined as:

$$\varepsilon_g = \frac{1}{4\pi G} = 1.19 \times 10^9 \frac{\mathrm{kg \cdot s^2}}{\mathrm{m^3}} \qquad (4)$$

$$\mu_g = \frac{4\pi G}{c^2} = 9.31 \times 10^{-27} \frac{\mathrm{m}}{\mathrm{kg}} \qquad (5)$$

by assuming that gravitation propagates at the speed of light c. Although not unusual, this assumption turns out to be very important. Only if gravity propagates at c the Maxwell-Einstein equations match the ones obtained from adding necessary terms to Newtonian gravity to conserve momentum and energy[3].

Moreover, the authors could show that with this set of equations, the advance of the Mercury perihelion – one of the most successful tests of general relativity – can be calculated giving the exact prediction than without linearization[8]. This is a very surprising result because the advance of Mercury's perihelion is attributed to a space curvature in general relativity (Schwarzschild metric) which we neglected in our linearization process. The assumption of c as the speed of gravity propagation also implies that the Lorentz force law and the gravitomagnetic potential energy differ from their electromagnetic counterparts by a factor of four[8]. Therefore some authors[4] use $c/2$ as the speed of gravity propagation to get a gravity Lorentz force law similar to electromagnetics.

The Einstein-Maxwell equations allow to clearly see the gravitomagnetic component of gravitation and the possibility to induce non-Newtonian gravitational fields. Their close relation to electrodynamics allow to transform electromagnetic calculations into their gravitational counterparts[9].

3. Coupling of Electromagnetism and Gravitation in General Relativity

By comparing gravitation and electromagnetism in Equation (3), we see that both fields are coupled by the e/m ratio of the field source and we can write:

$$\begin{aligned} \vec{g} &= \kappa \cdot \vec{E} \\ \vec{B}_g &= \kappa \cdot \vec{B} \end{aligned} \tag{6}$$

using the coupling coefficient κ

$$\kappa = -\frac{m}{e}\frac{\mu_g}{\mu_0} = -\frac{m}{e}\frac{\varepsilon_0}{\varepsilon_g} = -7.41\text{x}10^{-21}\cdot\frac{m}{e} \tag{7}$$

Obviously, this coefficient is very small and gravitational effects associated with electromagnetism have never been detected so far[10]. By combining Equation (6) with Equation (3), we see how both fields can induce each other:

$$\begin{aligned} rot\,\vec{E} &= -\frac{1}{\kappa}\frac{\partial \vec{B}_g}{\partial t} \\ rot\,\vec{B} &= \frac{e}{m}\mu_0\rho_m\vec{v} + \frac{1}{\kappa}\frac{1}{c^2}\frac{\partial \vec{g}}{\partial t} \end{aligned} \tag{8}$$

Coupled Maxwell-Einstein Equations
(Gravitation→Electromagnetism)

$$\begin{aligned} rot\,\vec{g} &= -\kappa\frac{\partial \vec{B}}{\partial t} \\ rot\,\vec{B}_g &= -\frac{m}{e}\mu_g\rho\vec{v} - \kappa\frac{1}{c^2}\frac{\partial \vec{E}}{\partial t} \end{aligned} \tag{9}$$

Coupled Maxwell-Einstein Equations
(Electromagnetism→Gravitation)

For an electron in a vacuum environment κ=4.22x10^{-32} kg/C. For example, let us consider an infinitely long coil as shown in Figure 1.

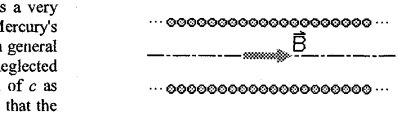

Figure 1 Magnetic Field Induced in a Coil

The magnetic field induced in the center line is then

$$B = \mu_0 In \tag{10}$$

where I is the current and n is the number of coil wounds per length unit. For a current of 10,000 Ampére and 1,000 wounds per meter, the magnetic field would be B=12.56 T which is state of the art. The corresponding gravitomagnetic field is then B_g=5.3x10^{-31} s^{-1}. Even using a coil with 100,000 wounds to induce an electric field, the amplitude of the resulting gravitational field would only be in the order of g=10^{-26} ms^{-2}. This is much too small to be detected by any accelerometers having measurement thresholds of 10^{-9} ms^{-2}. By using heavy ions in a plasma instead of electrons we can increase the m/e ratio by 6 orders of magnitude, however, the magnetic fields to contain such a plasma transmitting a similar current of 10,000 Ampére are out of reach.

Nevertheless, although the induced gravitational fields are very small, in principle it is possible to create non-Newtonian gravitational fields along the same principles as we are used to in electromagnetism.

4. Amplification Mechanisms

Since all these electromagnetic-gravitational phenomena are so small, how can we amplify the coupling coefficient in order to obtain measurable non-Newtonian fields?

4.1 Gravitation-Magnetism

Similar to para-, dia-, and ferro-magnetism, the angular and spin momentums from free electrons in material media could be used to obtain a gravitomagnetic relative permeability μ_{gr} which increases the gravitomagnetic field $\vec{B}_g$. Since an alignment of magnetic moments causes also an alignement of gravitomagnetic moments, the gravitomagnetic susceptibility will be the same as the magnetic susceptibility in a magnetized material[5]

$$\chi_g = \chi \tag{11}$$

For our example of the coil in Figure 1, a ferromagnetic core would accordingly increase the gravitomagnetic field and induced non-Newtonian gravitational field by three orders of magnitude. Although significant, the resulting fields are still too low to be detected.

4.2 Coupling of Charge and Mass

All our discussions up to now are based on a coupling at the source particle by the e/m ratio. However, an additional coupling between charge and mass of the source itself might exist and provide a significant amplification mechanism.

Well accepted peer-review journals like Nature and Foundations of Physics featured articles on this topic describing experiments that suggest a coupling between charge and mass in combination with rotation (or acceleration, movement in general).

Dr. Erwin Saxl published an article[11] reporting a period change of a torque pendulum if the pendulum was charged. A positive charge caused the pendulum to rotate slower than when it was charged negatively, Figure 3 shows his observations with a small asymmetry of the period change between positive and negative potentials applied to the pendulum. The period is expressed by

$$T = \text{Constant} \cdot \sqrt{\frac{m}{g}} \qquad (12)$$

where m is the mass of the pendulum and g the Earth's gravitational acceleration. Assuming that g is not changed (it is highly improbable that the whole Earth is affected), Saxl's measurement can be interpreted as a change of the pendulum's mass by applying an electric potential to it.

Prof. James Woodward from the University of California reported experiments of accelerating masses that, on the other hand, charged up according to their mass and speed of rotation. His experiments were done both for rotating masses[12] as well as for linear accelerated test bodies[13]. Published in the Foundations of Physics and General Relativity and Gravitation, he suggested a broader conservation principle including mass, charge and energy. Results of a test body hitting a target and inducing a charge are shown in Figure 4. His results follow

$$q' \equiv \text{Constant} \cdot m \cdot a \qquad (11)$$

where q' is the induced charge, m the test mass and a the acceleration (from rotation or calculated from the impact velocity).

Hence, both Saxl and Woodward experimentally reasoned a relationship between charge, mass and acceleration. A combination of all these factors to reduce/increase the weight of a body is described in a patent by Yamashita and Toyama[14]. A cylinder was rotated and charged using a Van der Graff generator. During operation the weight of the rotating cylinder was monitored on a scale. The setup is shown in Figure 5. If the cylinder was charged positively, a positive change of weight up to 4 grams at top speed was indicated. The same charge negative produced a reduction of weight of about 11 grams (out of 1300 grams total weight). This is an asymmetry similar to the one mentioned by Saxl[11]. Also the relationship between charge, rotation and mass is similar to Saxl and Woodward. The experimentors note that the weight changed according to the speed of the cylinder ruling out electrostatic forces, and that it did not depend on the orientation of rotation ruling out magnetic forces. The reported change of weight (below 1 %) is significant and indicates a very high order of magnitude effect.

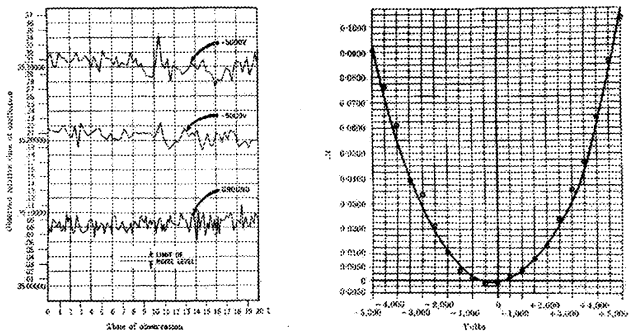

Figure 3 Change of Torque Pendulum Period vs. Applied Potential[11]

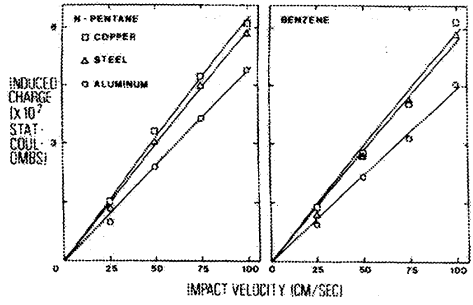

Figure 4 Charged Induced by Body Hitting Target[13]

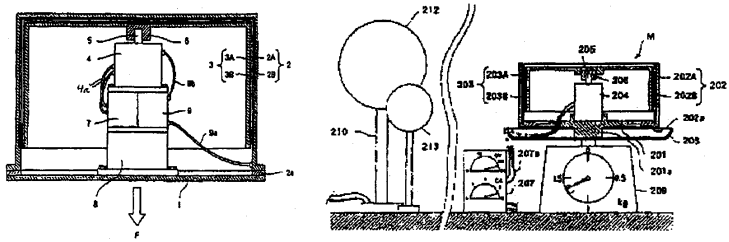

Figure 5 Setup of Charged Rotating Cylinder on Scale[14]

4.3 Alignment of Nuclear Spins

Henry Wallace, an engineer from General Electric, holds three patents on a method to produce a macroscopic gravitomagnetic and gravitational field by aligning nuclear spins due to rotation[15-17]. He claims that if materials with a net nuclear half-spin (one neutron more than protons in the nucleus) are rotated, this nuclear spin is aligned and produces a macroscopic gravitational effect. This is in fact similar to the Barnett effect where a metal rod is rotated and magnetisation of the material is observed. However, macroscopic magnetism in electromagnetism is caused by spin alignment of electrons, nuclear magnetism plays a very minor role due to the much higher mass of a proton or neutron compared to the electron. In a gravitational context the difference in mass is no major drawback anymore and nuclear magnetism should be on the same order of magnitude than electron magnetism. Usually, very low temperatures in the order of nano Kelvin are required to align nuclear spins, simple rotation would be much more easy.

The contribution of neutron spins to gravitomagnetic fields is theoretically on the order of ferromagnetism[5]. However, since Wallace claims to have measured at least the induction of nuclear spin alignment in a rotating detector material – by what he thinks a gravitomagnetic field, possible unknown amplification mechanisms (quantum gravity, nuclear strong force interaction) could cause much higher order of magnitude effects.

His setup is shown in Figure 6. A generator assembly (test mass rotating in 2 axis) is mounted on the left side and a detector assembly (similar to generator) is mounted on the right side with the possibility of rotation in the plane of the paper. A laser is monitoring the oscillations of this detector assembly. If both are rotated in the same orientation and counter wise, the laser detected a difference (Figure 7) which Wallace attributed to a force field. Since it only depended on the nuclear spin (e.g. Iron did not work but is a strong ferromagnetic material), Wallace ruled out magnetism as the origin of the force. In a different setup he showed that the field generated could constructively reduce the vibrational degrees of freedom of the crystal structure resulting in a change of its electrical properties (Figure 8).

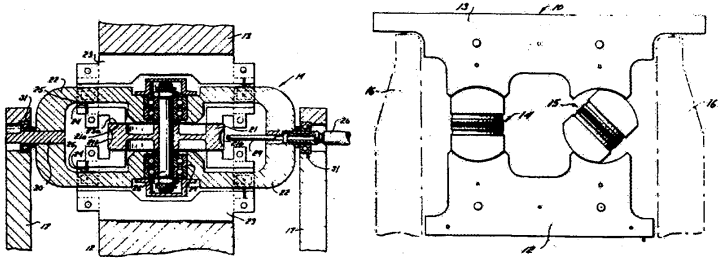

Figure 6 Setup of Rotating Test Mass (2 Axis) and Generator (Left) and Detector (Right) Position[15]

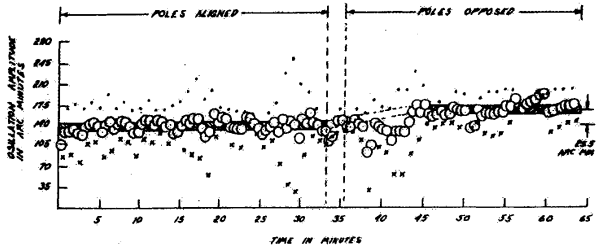

Figure 7 Oscillations of Detector Assembly[15]

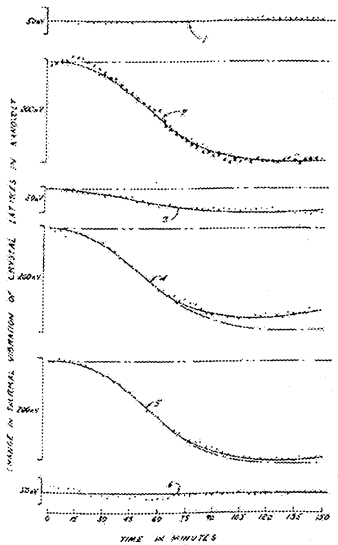

Figure 8 Change in Thermal Vibration of Crystal Lattices[15]

Hence, there is quite some experimental evidence for an amplification mechanism through nuclear magnetism to generate non-Newtonian gravitational fields using effects predicted by general relativity theory.

5. Principle of Equivalence and High-Order of Magnitude Non-Newtonian Gravitation

We explored the limits of inducing non-Newtonian gravitation using general relativity theory as well as looking at possible and speculative amplification mechanisms. Let us go back to the foundation of gravitation itself and explore the principle of equivalence in the limit of weak gravitational fields.

Einstein based his thoughts of gravitation on a famous Gedankenexperiment explaining the principle of equivalence: An observer can not distinguish between being inside a falling elevator or in a uniform gravitational field. Based on this equivalence, he developed the geometrical structure of general relativity. In the limit of weak gravitational fields, this simple Gedankenexperiment however is not complete as it covers only gravitoelectric fields and not the magnetic component of gravitation. According to the Larmor theorem of electromagnetics, a magnetic field can be replaced locally by a rotating reference frame with the Lamor frequency

$$\omega_L = \frac{1}{2}\frac{e}{m}B \tag{14}$$

The same argument applies for gravitation and a rotating reference frame rotating with the Lamor frequency can replace a gravitomagnetic field

$$\omega_{Lg} = -B_g \tag{15}$$

independent of the particle mass. The principle of equivalence[18] for weak gravitational fields (neglecting space curvature) also called gravitational Larmor theorem (GLT) should then be:

An observer can not distinguish between a uniformly accelerated ($\vec{v}$) reference frame rotating with the gravitational Larmor frequency (ω_{Lg}) and a reference frame at rest in a corresponding gravitational field ($\vec{\gamma} = -\dot{\vec{v}}$, $\omega_{Lg} = -\vec{B}_g$).

But what happens if the speed of rotation of the elevator changes? According to the GLT, this would correspond to a change of a gravitomagnetic field flux and therefore induce a non-Newtonian gravitational component according to the gravitational Faraday law:

$$\varepsilon_g = \oint_\Gamma \vec{\gamma}\cdot d\vec{l} = -\frac{d\phi_{gm}}{dt} = -\frac{d}{dt}\iint_\Sigma \vec{B}_g \cdot d\vec{\sigma} \tag{16}$$
$$= \frac{d}{dt}\iint_\Sigma \vec{\Omega}\cdot d\vec{\sigma}$$

where $\vec{\gamma}$ is the non-Newtonian gravitational field, Γ and Σ are respectively the contour and surface of integration, ϕ_{gm} is the gravitomagnetic flux, $\vec{B}_g$ is the gravitomagnetic field, and $\vec{\Omega}$ is the angular velocity of the reference frame. If the observer measures this additional gravitational field the principle of equivalence holds and he can not distinguish between the elevator and the gravitational field. If he does not observe this effect, the gravitational Larmor theorem is not valid, as a weak field approximation to Einstein's general relativity theory. We will show later that these "induced" non-Newtonian gravitational fields contribute to account for the mechanical energy absorbed (dissipated) by a rotating body during the phase of angular acceleration (deceleration).

Suppose the gravitational Larmor theorem holds, every rotation corresponds to a gravitomagnetic field, which is many orders of magnitude higher than the gravitomagnetic field responsible for the precession forces in the classical Lense-Thirring effect.

5.1 Gravitomagnetic Barnett Effect

The authors discussed such rotational effect described as the gravitational Barnett effect[6]. In 1915 Barnett[19] observed that a body of any substance set into rotation becomes the seat of a uniform intrinsic magnetic field parallel to the axis of rotation, and proportional to the angular velocity. If the substance is magnetic, magnetization results, otherwise not. This physical phenomenon is referred to as *magnetization by rotation* or as the *Barnett effect*.

If a mechanical momentum with angular velocity Ω is applied to a substance, it will create a force on the elementary gyrostats (electrons orbiting the nucleus) trying to align them. This is equivalent to the effect of a magnetic field in this substance B_{equi} and we can write:

$$B_{equi} = -\frac{1}{g_l}\frac{2m}{e}\Omega \tag{17}$$

where g_l is the Landé factor for obtaining the correct gyromagnetic ratio. We can now apply the same argument to the gravitational case and postolate an equivalent gravitomagnetic field $B_{g\ equi}$ which counteracts the mechanical momentum:

$$B_{g\,equi} = -\frac{2}{g}\Omega \tag{18}$$

For an electron, g_r=2 and we see that physical rotation is indeed equivalent to a gravitomagnetic field. From Equation (18) we can compute the gravitomagnetization acquired by the rotating material:

$$\vec{M}_g = \frac{\chi_g}{\mu_{0g}} \vec{B}_{g\,equi} = -\frac{\chi_g}{\mu_{0g}} \frac{2}{g} \vec{\Omega} \tag{19}$$

where χ_g is the garvitomagnetic susceptibility. Taking into account the coupling between gravitation and electromagnetism presented above we can demonstrate the general result:

$$\vec{M}_g = -\frac{\chi}{\mu_0} \frac{2}{g} \left(\frac{m}{e}\right)^2 \vec{\Omega} \tag{20}$$

where χ is the magnetic susceptibility of the material[6]. This indicates that the gravitomagnetic moment associated with the substance will be extremely small. Therefore we can not use this gravitomagnetic moment to induce macroscopic non-Newtonian gravitational fields. However we can show, following our discussion on the equivalence principle, that if the field of rotation in Equation (18) can not be distinguished from gravitomagnetism, it must be a real field which we can use to induce non-Newtonian gravitational fields. The detection of such fields would represent an indirect proof of the existence of the gravitomagnetic Barnett effect.

5.2 Gravitational Poynting Vector and Gravitational Larmor Theorem in Rotating Bodies with Angular Acceleration

The gravitational Poynting vector, defined as the vectorial product between the gravitational and the gravitomagnetic fields, $\vec{S}_g = \frac{c^2}{4\pi G} \vec{\gamma} \times \vec{B}_g$, provides a mechanism for the transfer of gravitational energy to a system of falling objects (we will consider in the following a cylindrical mass m, with radius a and length l). It has been shown[20] that using the gravitational Poynting vector, the rate at which the kinetic energy of a falling body increases is completely accounted by the influx of gravitational field energy into the body. Applying the gravitational Larmor Theorem (GLT) to a body with angular acceleration. We get that a time varying angular velocity flux will be associated with a non-Newtonian gravitational field proportional to the tangential acceleration. The gravitational electromotive force produced in a gyrogravitomagnetic experiment can be calculated using the gravitational Faraday induction law as given in Equ (16). Together with the GLT expressed through Equation (15) we get

$$\varepsilon_g = \frac{d}{dt} \iint_{\Sigma} \vec{\Omega} \cdot d\vec{\sigma} \tag{21}$$

The induced non-Newtonian gravitational field associated with this gravitational electromotive force is at the surface of the cylinder is:

$$\oint_{\Gamma} \vec{\gamma} \cdot d\vec{l} = \frac{d}{dt} \iint_{\Sigma} \vec{\Omega} \cdot d\vec{\sigma} \tag{22}$$

$$\vec{\gamma}_\theta = \frac{1}{2} a\dot{\Omega}\, \hat{e}_\theta \tag{23}$$

From this non-Newtonian gravitational field and the gravitomagnetic field produced by the rotating mass current, we can compute a gravitational poynting vector

$$\vec{S}_{g\Omega} = \frac{c^2}{4\pi G} \vec{\gamma}_\theta \times \vec{B}_{g\Omega} = \frac{1}{4\pi} \left(\frac{a}{a+\ell}\right) \Omega\dot{\Omega} m\, \hat{n} \tag{24}$$

which will also provide an energy transfer mechanism to explain how massive bodies acquire rotational kinetic energy when mechanical forces are applied on them[21]. The rate at which the rotational kinetic energy of a body increases (or decreases) due to the application of external mechanical forces on that body, is completely accounted by the influx (out-flux) of gravitational energy into (outward) the body.

$$\left.\frac{dU}{dt}\right|_{\Omega} = S_{g\Omega}(2\pi a^2 + 2\pi a\ell) = \frac{d}{dt}\left(\frac{1}{2} I\Omega^2\right) \tag{25}$$

where I, is the moment of inertia of the cylinder. This demonstrates the validity of the gravitational Larmor theorem, and shows how the transfer of mechanical work to a body can be interpreted as a flux of gravitational energy associated with non-Newtonian gravitational fields produced by time varying angular velocities. This is an encouraging result regarding the possible detection of macroscopic non-Newtonian gravitational fields induced through the angular acceleration of the cylinder in the region located outside the rotating cylinder. The non-Newtonian gravitational field outside the cylinder is given by:

$$\gamma = \frac{1}{2} \frac{a^2}{r} \dot{\Omega} \tag{26}$$

where $r > a$ is the distance from the cylinder's longitudinal axis. For $r \le a$ we have, $\gamma = 0.5 \times a\dot{\Omega}$. For the following values of r=1 m, a=0.1 m, $\dot{\Omega} = 200$ Hz/s, γ will have the value of 1 ms^{-2}. We recommend that experiments shall be performed with the aim of evaluating Equation (26).

Is it possible to use fluxes of radiated electromagnetic energy to counteract the effect of absorbed fluxes of gravitational energy? That is a question Saxl, Woodward and Yamashita tried to evaluate empirically. These empirical approaches shall be complemented in the following by a

theoretical analysis of the net energy flow associated with the free fall of an electrically charged cylindrical mass.

5.3 Free Fall of a Cylindrical Mass Electrically Charged

A cylindrical mass electrically charged in free fall must comply with the law of conservation of energy and with the principle of equivalence[22]. During the free fall the cylindrical mass will absorb gravitational energy, which is described by the following gravitational Poynting vector:

$$\vec{S}_g = \frac{c^2}{4\pi G}\vec{\gamma}\times\vec{B}_g = \frac{mv\gamma}{2\pi a\ell}\hat{n}_{in} \qquad (27)$$

where v is the speed of the cylinder while it is falling, γ is the Earth gravitational field, m, a, l are respectively the mass, length and radius of the cylinder and $\hat{n}_{in}$ is a unit vector orthogonal to the surface of the cylinder and Poynting inwards. The cylinder due to its electric charge will also radiate electromagnetic energy according to the following electromagnetic Poynting vector:

$$\vec{S}_{em} = \frac{1}{\mu_0}\vec{B}\times\vec{E} = \frac{\mu_0}{8\pi^2}\frac{Q^2 v\dot{v}}{a\ell(a+\ell)}\hat{n}_{out} \qquad (28)$$

where Q is the electric charge carried by the cylinder, μ_0 is the magnetic permeability of vacuum and $\hat{n}_{out}$ is a unit vector orthogonal to the surface of the cylinder and Poynting outwards. The principle of equivalence states that if the cylinder is at rest with respect to a reference frame which is uniformly accelerating upwards (with respect to the laboratory) with acceleration $\dot{\vec{v}} = \gamma\hat{e}_z$, the cylinder will radiate (with respect to the laboratory) according to the following Poynting vector:

$$\vec{S}_{em} = \frac{1}{\mu_0}\vec{B}\times\vec{E} = \frac{\mu_0}{8\pi^2}\frac{Q^2 v\gamma}{a\ell(a+\ell)}\hat{n}_{out} \qquad (29)$$

Therefore to comply with the principle of equivalence, we shall take in Equation (28) $\dot{v} = \gamma$ [23].

The sum of both energy fluxes in Equations (27) and (29) must comply with the law of conservation of energy. Therefore the Sum of gravitational incoming flux and the radiated electromagnetic energy flux must be equal to the rate at which the kinetic energy of the body varies in time.

$$S_{em}\left(2\pi a^2 + 2\pi a\ell\right) + S_g\, 2\pi a\ell = \frac{d}{dt}\left(\frac{1}{2}mv^2\right) \qquad (30)$$

From Equation (30) we deduce that the acceleration with which the electrically charged cylindrical mass will fall is:

$$\dot{v} = \gamma\left(1 - \frac{\mu_0}{4\pi}\frac{Q^2}{m\ell}\right) \qquad (31)$$

Equation (31) shows that the free fall of an electrically charged body would violate the law of Galilean free fall, because the acceleration of fall would depend on the electric charge, size and mass of the falling body. The fact that the acceleration of fall depends on the square of the electric charge rules out the possibility to explain with the present analysis, the observations of Saxl and Yamashita, regarding the increase of mass for positively charged bodies and the decrease of mass for negatively charged bodies. Notice that following the rational which leads to equation (31), the phenomenon described by this equation should happen either in a reference frame at rest in an external gravitational field or inside a uniformly accelerated reference frame, therefore we are not able to use this phenomenon to distinguish between both situations. Consequently equation (31) do not violate the principle of equivalence. To test equation (31) we propose to measure the time of fall of charged cylindrical capacitors, and compare it with the time of fall of similar uncharged capacitors. For m=10 grams, l=10 cm, Q=100 C, we will have $\dot{v} = 0$. For these values the cylinder would not be able to fall! However to avoid disruption currents for such a high value of electric charge is a technological challenge.

Conclusion

In the present work we did an extensive review of possible "classical ways" to induce non-Newtonian gravitational fields from electromagnetic phenomena or by using the principle of equivalence in the limit of weak gravitational fields. If the experiments performed by Saxl, Yamashita, Woodward and Wallace were reproducible this would represent a breakthrough in the possibility to control gravitational phenomena at the laboratory scale. The understanding of the principle of equivalence for electrically charged bodies and in the limit of weak gravitational fields is crucial to evaluate respectively:

- the possibility of directly convert gravitational energy into electromagnetic energy during the free fall of an electrically charged body.
- the possibility of inducing non-Newtonian gravitational fields through the angular acceleration we might communicate to solid bodies.

The experimental confirmation of such phenomena would be a dramatic step forward in the technological control of free fall. The non detection of the presented phenomena could lead to a better

empirical understanding of Einstein's general relativity theory in the limit of weak gravitational fields and when extended to electrically charged bodies, which is a significant scientific result as well. These experiments could also contribute to decide which approach to weak gravity is the correct one, i.e. linearized general relativity or the extension of Newton's laws to time dependent systems.

References

[1]Millis, M., "Breakthrough Propulsion Physics Research Program", NASA TM 107381, Lewis Research Center, 1997

[2]Heaviside, O., "A Gravitational and Electromagnetic Analogy", *The Electrician*, **31**, 1893, pp. 281-282 and 359

[3]Jefimenko, O.D., "Causality, Electromagnetic Induction and Gravitation," Electret Scientific Company, 1992

[4]Forward, R.L. "General Relativity for the Experimentalist", *Proceedings of the IRE*, **49**, 1961, pp. 892-586

[5]Tajmar, M., and de Matos, C.J., "Coupling of Electromagnetism and Gravitation in the Weak Field Approximation," *Journal of Theoretics*, **3**(1), 2001

[6]De Matos, C.J., and Tajmar, M., "Gravitomagnetic Barnett Effect", *Indian Journal of Physics*, 2001, submitted

[7]Misner, C.W., Thorne, K.S., and Wheeler, J.A., "Gravitation", W.H.Freeman, San Francisco, 1973

[8]De Matos, C.J., and Tajmar, M., "Advance of Mercury Perihelion Explained by Cogravity", Proceedings of the Spanish Relativity Meeting, 2000

[9]Forward, R.L., "Guidelines to Antigravity", *American Journal of Physics*, **31**, 1963, pp. 166-170

[10]Braginski, V.B., Caves, C.M., Thorne, K.S., "Laboratory Experiments to Test Relativity Gravity", Physical Review D, **15**(5), 1977, pp. 2047-2068

[11]Saxl, E.J., "An Electrically Charged Torque Pendulum", *Nature*, **203**, 1964, pp. 136-138

[12]Woodward, J.F., "Electrogravitational Induction and Rotation", *Foundations of Physics*, **12**(5), 1982, pp. 467-479

[13]Woodward, J.F., "An Experimental Reexamination of Faradayan Electrogravitational Induction", *General Relativity and Gravitation*, **12**, 1980, pp. 1055-1067

[14]Yamashita, H., and Toyama, T., "Machine for Acceleration in a Gravitational Field", European Patent EP 0 486 243 A2, 1982

[15]Wallace, H.W., "Method and Apparatus for Generating a Secondary Gravitational Force Field", US Patent 3.626.605, 1971

[16]Wallace, H.W., "Method and Apparatus for Generating a Dynamic Force Field", US Patent 3.626.606, 1971

[17]Wallace, H.W., "Heat Pump", US Patent 3.823.570, 1974

[18]Mashhoon, B., "Gravitoelectromagnetism", Los Alamos Archive, gr-qc/0011014, 2000

[19]Barnett, S.J., "Magnetization by Rotation", *Physical Review*, **4**(4), 1915

[20]Krumm, P., Bedford, D., "The Gravitational Poynting Vector and Energy Transfer", American Journal of Physics, **55**(4), 1987, pp. 362-363

[21]De Matos, C. J., Tajmar, M., "Gravitational Poynting Vector, Gravitational Larmor Theorem and Rotational Kinetic Energy", submitted to Los Alamos Archive, 2001

[22]De Matos, C. J., Tajmar, M., "Free Fall of a Cylindrical Mass Electrically Charged", submitted to Los Alamos Archive, 2001

[23]Soker, N., "Radiation from an Accelerated Charge and the Principle of Equivalence", NASA Breakthrough Propulsion Physics Workshop Proceedings, NASA / CP – 1999-208694, 1999, pp. 427-440

A01-34541

AIAA 2001-3912

TOWARDS THE CONTROL OF MATTER WITH GRAVITY

Dr D Burton, Dr S Clark, Prof T Dereli, Dr J Gratus
Mr W Johnson, Prof R W Tucker, Dr C Wang

Department of Physics,
Lancaster University,
Lancaster LA1 4YB, UK

37th Aerospace Sciences Meeting and Exhibit
8-11 July 2001
Salt Lake City, Utah

AIAA 2001-3912

TOWARDS THE CONTROL OF MATTER WITH GRAVITY

Dr D Burton, Dr S Clark, Prof T Dereli, Dr J Gratus
Mr W Johnston, Prof R W Tucker, Dr C Wang

Department of Physics, Lancaster University, Lancaster LA1 4YB, UK

d.burton@lancaster.ac.uk, t.dereli@lancaster.ac.uk, j.gratus@lancaster.ac.uk
robin.tucker@lancaster.ac.uk, c.wang@lancaster.ac.uk

Abstract

This article summarises some of the current activities of the gravitational research group above. After surveying the role of gauge fields as carriers of the basic forces in physics and the momentum conservation constraints placed on current propulsion technology a number of alternative strategies, under active investigation, are briefly discussed. The essential theme is the detection of hitherto undetected components of gravitation that may have implications for the motion of matter. Such components include gravito-magnetic fields and radiation modes as well as new scalar interactions resulting from various proposals for the unification of gravitation with the other basic forces. Experiments are suggested that may shed light on the existence of novel gravitational interactions. These include the detection of transient gravitational fields by means of orbiting Cosserat antennae and the effects of torsional forces on the perihelion shift of planets.

1 Forces and Physics

The effective exploration of interplanetary systems and beyond demands advances in propulsion technology. Our visionaries tell us that the pace of development will be interrupted by sudden advances analogous to the past discoveries of manned flight and reciprocating combustion, gas turbine and rocket engines. Besides "technological breakthroughs" there is also a hope that new "conceptual breakthroughs" in the foundations of physics will offer new perspectives as guides in the search for new technologies. Harnessing the power of the electromagnetic field had to wait for Faraday and Maxwell and the development of nuclear power sprang from an understanding of the quantum nature of matter and the relativistic structure of space-time. History teaches one that major developments in science and engineering are not always predictable within the context of the prevailing wisdom of the time.

Modern physics continues to power technology on many fronts. Much of this development springs from the quantum nature of matter and radiation. By contrast gravitation defies a unique and consistent quantum formulation. Its most elegant formulation is in terms of the classical geometrical properties of space-time and it is related to the other interactions in nature at the level of classical physics. Here classical fields are the primary structures and matter is modelled as "crystallised field energy". Such concentrations of energy owe their existence to the basic quantum laws of nature but classical laws are often adequate to describe the interactions of such matter with fields on a macroscopic level. These interactions depend on a small number of physical attributes such as inertial mass and interaction strengths ("charges") that enter into the classical field equations. These are expressed as tensor equations on a dynamic space-time in general. Thus electromagnetic fields couple to electric charge, nuclear force fields to colour charge, the forces responsible for radioactivity to weak-hypercharge and the mass-energy of all fields to gravity. The significance of different force fields in any particular situation is in large measure determined by the relative sizes of these couplings. This follows since most basic laws follow remarkable mathematical similarities. See Figure 1. They are all associated with symmetries of mathematical patterns (Lie groups) with field

Interaction	Mediating Quanta	Lie Group	Connection	Dynamics
Electromagnetic: Electric charge	QED: Photon	U(1)	$\mathbf{A}_6$	$\mathbf{F} = d\,\mathbf{A}_6$ $d \star \mathbf{F} = \mathbf{J}[\Phi, \mathbf{A}_6]$
Electroweak: Hypercharge	QAD: W and Z Bosons	SU(2) × U(1)	$\mathbf{A}_4$	$\mathbf{F} = d\,\mathbf{A}_4 + [\mathbf{A}_4, \mathbf{A}_4]$ $D \star \mathbf{F} = \mathbf{J}[\Phi, \mathbf{A}_4]$
Strong: Colourcharge	QCD: Gluons	SU(3)	$\mathbf{A}_3$	$\mathbf{F} = d\,\mathbf{A}_3 + [\mathbf{A}_3, \mathbf{A}_3]$ $D \star \mathbf{F} = \mathbf{J}[\Phi, \mathbf{A}_3]$
Gravity: Mass-energy and spin	QG: Graviton	Spin(3,1)	$\mathbf{A}_5$	$\mathbf{F} = d\,\mathbf{A}_5 + [\mathbf{A}_5, \mathbf{A}_5]$ $E[g, \mathbf{A}_5] = T[g, \Phi, \mathbf{A}_6, \mathbf{A}_5, \mathbf{A}_3, \mathbf{A}_4]$

Figure 1: *This table classifies the known force fields in terms of their attributes. Each can be associated with a mathematical symmetry (Lie group) that determines how the fields interact with themselves, other force fields and matter at each event in space-time. The precise coupling to matter is determined by different kinds of charge. Thus electrically charged particles couple to the electromagnetic field, colour charged particles to the chromodynamic nuclear field and weak-hypercharged particles to the electro-weak fields responsible for radioactive decay. At the quantum level these fields are mediated by field quanta; photons, gluons and W-Z bosons respectively. All matter and fields with mass-energy couple to gravity. It is expected that the quanta of gravitational waves (gravitons) will be responsible for a theory of quantum gravity. The dynamics of all these fields have many similarities (they arise from "connections associated with Lie groups") although gravitation occupies a unique position in classical physics since it is intimately related to the structure of space and time itself.*

strengths defined in terms of directions ("connections") in collections of mathematical structures at each event in space-time. The gravitational field is similarly determined by a field strength associated with a Lie group although according to Einstein its field equation breaks the mould set by the other force fields in nature. This difference is accentuated by the recognition that relativistic gravitation may be formulated in terms of space-time geometry, an idea that has had profound implications for cosmogony and cosmology.

1.1 Propulsion Constraints

Given a propulsion unit, its effectiveness can usually be gauged from the laws of *classical* physics. In most cases forces on matter are prescribed and Newtonian dynamics is in principle adequate to describe the subsequent motion. For propulsion in the vicinity of the earth the earth's gravitational field (along with lift and drag of the air) is omni-present and propulsion forces are derived from the rate of change of momentum between "fuel" and "propelled system". If propellant is to be ejected as radiation or systems achieve speeds that are an appreciable fraction of the speed of light c, Newtonian dynamics is inadequate and must be replaced by the more accurate relativistic equations of motion.

A great deal can be learnt about the demands of enhanced propulsion proposals by elementary considerations based on well established physical principles[1]. It is inconceivable that the constraints imposed by such principles will require dramatic refinement by future scientific developments.

It is useful to distinguish between propulsion systems that must operate in the vicinity of the earth's surface and those in which Newtonian gravitational fields are negligible. With current technology expensive multi-stage chemical propellants are required to place structures into earth orbit and beyond. For a single propulsion system of mass $M(t)$ and speed $V(t)$ at time t, lifting vertically off the surface of a non-rotating earth with zero initial velocity and ejecting mass at a speed u_0 relative to the propelled system, $V(t)$ is given by

$$V(t) = -u_0 \log \frac{M(0)}{M(t)} - gt \qquad (1)$$

in a region where the acceleration due to gravity g may be considered constant. If the rate of mass ejection is constant one may eliminate the burn time $t = t_b$ given the specific thrust ratio $\mathcal{R} = 1 + \frac{\mathcal{A}}{g}$ where $\mathcal{A}$ is the initial acceleration of the system at lift off. Then

$$\frac{V(t_b)}{V_{esc}} = \frac{u_0}{V_{esc}} \left\{ \log \frac{M(t_b)}{M(0)} + \frac{1}{\mathcal{R}} \left(1 - \frac{M(t_b)}{M(0)} \right) \right\}$$

where V_{esc} is the escape velocity for the earth. Figure 2 shows $V(t_b)/V_{esc}$ versus $M(t_b)/M(0)$ for three values of u_0/V_{esc} appropriate for chemical propellants for both $\mathcal{R} = 1$ and $\mathcal{R} = 2$. These

estimates set a benchmark for any new terrestrial propulsion system that claims to improve current multi-staging and chemical propellant technology.

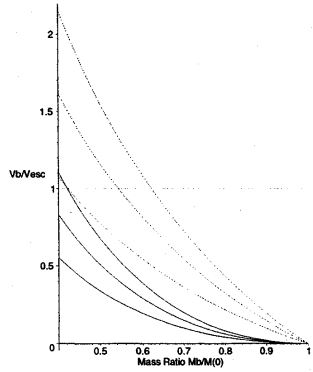

Figure 2: These plots indicate the mass ratio $M(t_b)/M(0)$ required to reach a non-relativistic speed V_b in the presence of the earth's (uniform) gravitational field. V_{esc} is the escape velocity for the earth. The upper three (dotted) curves correspond to a specific thrust parameter $\mathcal{R} = 2$. The lower three (full) curves correspond to $\mathcal{R} = 1$. In each triplet the ejection speed is chosen to vary according to three typical chemical propellants.

1.2 Relativistic Rockets

In an extra-terrestrial environment where Newtonian gravitational fields are negligible the system dynamics are different. To accommodate relativistic mass-energy ejection one has from consideration of rectilinear relativistic impulse dynamics in an inertial frame:

$$\lim_{\Delta t \mapsto 0} \frac{p_{t+\Delta t} - p_t}{\Delta t} = 0 \tag{2}$$

where the 4-momenta of the composite system are respectively

$$p_t = \Pi(V,\, M), \tag{3}$$

and

$$p_{t+\Delta t} =$$

$$\Pi(V + dV, M + dM) + \Pi\left(\frac{V + dV - u_0}{1 - \frac{u_0(V+dV)}{c^2}},\, dm\right) \tag{4}$$

for

$$\Pi(V, M) = \frac{M}{\left(1 - \frac{V^2}{c^2}\right)^{1/2}}[c,\, V, 0, 0]. \tag{5}$$

Taking the limit in (2) and eliminating dm yields:

$$\frac{1}{M(t)}\frac{dM(t)}{dt} = -\frac{dV(t)}{dt}\frac{1}{u_0(1 - \frac{V^2}{c^2})} \tag{6}$$

where $V(t)$ is the speed of the system relative to an inertial frame with clock time t. Here u_0 is the mass-energy ejection speed relative to the system at any ejection event. If the initial speed of the system is $V(0)$ in the inertial frame and u_0 is constant then at any time $t > 0$ where mass-energy ejection continues it follows that:

$$\frac{V(t)}{c} = \frac{1 - \alpha\mu(t)^\lambda}{1 + \alpha\mu(t)^\lambda} \tag{7}$$

where $\alpha = \left(1 - \frac{V(0)}{c}\right)/\left(1 + \frac{V(0)}{c}\right)$, $\mu(t) = M(t)/M(0)$, $\lambda = 2u_0/c$. This reduces to (1) for $g = 0$ when $c \mapsto \infty$. For chemical propellants with $u_0 \simeq 10$ km/sec, $M(t) \simeq 1$ ton and for a final speed $V(t) \simeq c/2$ this implies $M(0) \simeq 10^{7000}$ tons! In Figure 3, V/c is plotted against the mass ratio μ for any t for $V(0) = 0$ and varying values of u_0/c.

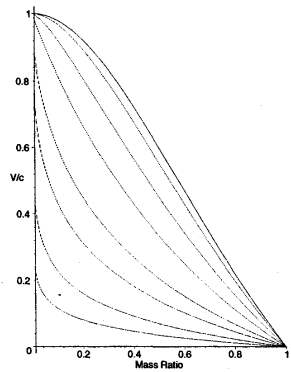

Figure 3: These plots indicate the mass-energy ratio $M(t)/M(0)$ required to reach a relativistic speed ratio V/c in the absence of any gravitational field. Each curve has a definite ejection speed ratio u_0/c relative to the propulsion system. These are 1/20,1/10,1/5,3/10,1/2,7/10 and 9/10 in order starting from the bottom of the plot. The advantage of relativistic mass-energy ejection is apparent from these curves.

The advantages of high speed ejection $u_0 \mapsto c$ over non-relativistic mass ejection are apparent in this picture. To establish propulsion efficiency in such cases one needs to know how the ejection

mass ratio μ varies with proper time τ (i.e.the time measured by an on board clock). This permits one to integrate equation (7) for the motion of the system. Even for on-board robots a consideration of non-destructive proper accelerations is clearly desirable. Writing $\mu(\tau) = \exp(-\rho(\tau))$ the rectilinear relativistic equations of motion (2) of the system become:

$$\frac{dx(\tau)}{d\tau} = c \sinh \frac{\lambda\rho(\tau)}{2} \tag{8}$$

$$\frac{dt(\tau)}{d\tau} = \cosh \frac{\lambda\rho(\tau)}{2}. \tag{9}$$

The second equation (9) relates the on-board passage of time measured by τ to a clock fixed in the inertial frame measuring t. An attractive solution can be found that gives the propulsion system a constant proper acceleration $\mathcal{A}$:

$$x(\tau) = \frac{c^2}{\mathcal{A}} \left\{ \cosh \frac{\mathcal{A}}{c}\tau - 1 \right\} \tag{10}$$

$$t(\tau) = \frac{c}{\mathcal{A}} \sinh \frac{\mathcal{A}}{c}\tau. \tag{11}$$

To achieve such a uniform proper acceleration the proper mass ejection rate is required to satisfy

$$\frac{d\rho(\tau)}{d\tau} = \frac{\mathcal{A}}{u_0}. \tag{12}$$

If a "photon" rocket ($u_0 = c$) could be produced to achieve an on-board mass-energy ejection system with $\mathcal{A} = g$ (9.8 m/sec/sec) for an interval of time τ_b then $\mu(\tau_b) = \exp(-\frac{g\tau_b}{c})$. One readily finds that $M(0) = M(\tau_b)\exp(\kappa)$ if τ_b is taken as κ years. These considerations have powerful implications given the scales of space and time compared to those of human existence. For a round trip to a neighbouring star by such a photon rocket with $\kappa \simeq 9$ one has $\exp(9) \simeq 8000$. Even a mass ratio on this scale in a compact unit raises severe issues of heat dissipation.

2 Alternative Strategies

An alternative approach is to restrict mass-energy ejection mechanisms to local control programmes and seek dynamical propulsion in terms of interactions between ambient fields and their associated charges. Thus the system may be regarded as spending most of its time "coasting" or "surfing" in space. Standard "coasting" in a gravitational field is often referred to as "free-fall" and the motion of some point in the system under such conditions can be used as a reference of zero proper acceleration. It would be a rare occurrence for space travel to be based entirely on free fall in an ambient gravitational field. Departure from such motion is often associated with non-gravitational forces. Like any surfer or swimmer, adjusting body configuration to the environment can optimise transport. Such manoeuvering require a local expenditure of energy. However it may be possible to mine this energy from the environment itself. A natural source in the solar system is the sun itself or power transmitted by microwave from orbiting space-stations. When these sources are not available recourse to other fields including the gravitational field itself may be necessary. Thus it is important to understand the interaction of fields and gravity with matter, particularly if the latter has an extended structure that can respond to the geometry of space-time.

2.1 Gravicraft

To illustrate a "swimming" mechanism one may explore the concept of the gravicraft. In 1968 Beletsky and Givertz [2, 3, 4] introduced this notion, powered by actively controlling the dimensions of an extended body in orbit. Effective rates of orbital elevation above the earth demanded eccentric orbits and tethered structures on the order of several thousand kilometers in extent. Similar systems [5, 6, 7, 8] have been proposed to enhance maneuverability without the intervention of chemical propellants and offer an attractive means of cargo transfer between orbiting stations and energy generation. However, most theoretical estimates of the transfer speed between orbits have remained disappointingly low despite the obvious advantages of relying on environmental energy sources such as solar radiation and gravitational tidal forces*. Gravicraft motion relies on its coupling to the tidal component of a gravitational field. For static gravitational fields the spatial dimension of a gravicraft is determined by the scale over which the field varies. We have recently devised[9] a new method of gravicraft propulsion by actively varying its instantaneous moment of inertia in a quasi-circular orbit. A primitive craft is composed of two massive bodies connected via a light tether whose length can vary between l_{max} and l_{min} by the use of powered winches inside the bodies. By varying the moment of inertia of such a rotating system it is possible to transfer energy between the spin and orbital angular momentum of the craft. If the cycle of tether length variation is chosen appropriately it is possible for the entire structure to gain lift in the gravitational field. In

*Another attractive feature of gravicraft structures controlled by tethers in the ionosphere is their potential for generating power from ambient magnetic fields. In 1996 NASA used a conducting tether connected to the space shuttle in order to generate electricity.

the static field of a spherical mass M an estimate of the average rate of height gain at radius r is given by:

$$\dot{r} = \frac{3(GM)^{1/2}}{4\pi\, r^{5/2}}(l^2_{max} - l^2_{min}) \qquad (13)$$

where G is the Newtonian gravitational coupling constant. For a gravicraft in low earth orbit with a tether length varying between 50 and 10 km this yields $\dot{r} \simeq 300m/hr$ and if its mass is 10^3 kg it expends about 425 watts. This ascension rate is an order of magnitude greater than any previous gravicraft mechanism known to the authors. Although primitive, such a mechanism illustrates how one can in principle manoeuver matter in an ambient gravitational field by exploiting its interaction with the field gradient. It also shows that the smallness of G demands a significant sustained gradient field for this mechanism to offer a viable means of long term propulsion. It may however offer a viable means to transport cargo between space-stations in distinct orbits by taking energy from the sun.

2.2 Gravito-electromagnetism

Several authors have noticed that a subset of the Einstein equations when perturbed about flat spacetime can be written in a form that looks remarkably similar to Maxwell's equations with the Newtonian gravitational field corresponding to the *gravito-electric* field and mass-currents playing the role of electric currents. Since the laws of electromagnetism are well studied and understood this analogy has proved quite fruitful in the *gravito-electromagnetic* context particularly in astrophysical applications. Extended "astrophysical jet-structures" are now thought to have their origin in *gravito-electromagnetic* forces.

In[10] we have considered the *most useful way* to define the *gravito-electromagnetic* fields in terms of the perturbed components of the space-time metric. Different choices are often responsible for the location of odd factors of 4 that permeate the *gravito-electromagnetic* equations compared with the Maxwell equations. Such choices also have implications for the form of the induced *gravito-electromagnetic* Lorentz force (and torque) in terms of the *gravito-electromagnetic* fields that enter into the equation for the motion of a massive point (spinning) particle. By analogy with the covariant laws of electromagnetism in space-time *gravito-electromagnetic* potentials and fields are then defined to emulate electromagnetic gauge transformations under substitutions belonging to the gauge symmetry group of perturbative gravitation. These definitions have the advantage that on a flat background, with the aid of a covariantly constant time-like vector field, a *subset* of the linearised gravitational field equations can be written in a form that is *fully analogous to Maxwell's equations* (without awkward factors of 4 and extraneous tensor fields). It is shown how the remaining equations in the perturbed gravitational system restrict the time dependence of solutions to these equations and thereby prohibit the existence of propagating vector fields. The induced *gravito-electromagnetic* Lorentz force on a test particle is evaluated by geodesic perturbation in terms of these fields together with the torque on a small gyroscope. It is concluded that the analogy of perturbative gravity to Maxwell's description of electromagnetism can be valuable for (quasi-) stationary gravitational phenomena but that the analogy has its limitations. The relevance of this work for propulsion is that the equation of motion for any massive particle with velocity $\mathbf{v}$ in a pure *gravito-electromagnetic* field $(\mathcal{E}, \mathcal{B})$ takes the form

$$\frac{d\mathbf{v}}{dt} = \frac{1}{4}\mathcal{E} + \mathbf{v} \times \mathcal{B} \qquad (14)$$

in close correspondence with the Lorentz force on electrically charged particles in the electromagnetic field $(\mathbf{E}, \mathbf{B})$. In the static field of the earth the term $\mathcal{E}/4$ is responsible for the Newtonian gravitational acceleration field. The accompanying gravito-magnetic force determined by $\mathcal{B}$ on mass currents has to date escaped detection, but along with propagating gravitational waves is thought to exist. A gyroscope in such a field with velocity $\mathbf{v}$ is predicted to precess at a rate $(\frac{3}{4}\mathbf{v} \times \mathcal{E} - \mathcal{B})/2$ independent of its spin. In 2002 the NASA satellite Gravity Probe B will be launched to measure this effect. Although such *gravito-electromagnetic* forces and torques are small in a terrestrial environment they can be made to accumulate and their detection could herald a new avenue of gravitational precision technology. In addition to the $\mathcal{E}$ and $\mathcal{B}$ *gravito-electromagnetic* fields the equations of Einsteinian gravitation involve a second degree symmetric tensor $\mathbf{\Sigma}$ that has no electromagnetic analogue. The *gravito-electromagnetic* fields couple to this tensor and produce non-Maxwellian terms in the *gravito-electromagnetic* force and torque equations. This suggests that the equations of motion for massive spinning particles in gravitational fields deserve closer scrutiny.

2.3 Orbiting Cosserat Detectors

We have begun an intensive study of the behaviour of slender visco-elastic structures in space.

Such structures can be used to convert tidal gravitational fields into heat and hence extract energy from gravitational fields.

They are also being studied with a view to using them as antennae for the detection of gravitational radiation. The orbital dynamics of slender loop structures, several km in length, are ideally suited to analysis by the simple theory of *Cosserat rods* [11]. Such a description offers a clean conceptual separation of the vibrations induced by bending, shear, twist and extension and the coupling between eigen-modes due to tidal accelerations can be reliably estimated in terms of the constitutive properties of each structure.

The proposal is to use (several) orbiting Cosserat structures in order to detect gravitationally induced displacement correlations from among unwanted sonic signals in the system. Each continuum structure can be tuned to the entire acceleration field of a gravitational wave and resonant response to circumferential excitations tuned to optimise power absorption from continuous or pulsed gravitational excitations. Different topologies (e.g. open spirals) yield alternative broadband non-resonant responses.

The detection of gravitational signals in the 1 Hz region would provide vital information about stochastic backgrounds in the early Universe and the relevance of super-massive black holes to the processes that lead to processes in the centre of galaxies. Such information can only enhance our understanding of the interaction of gravity and matter and test the predictions of many proposed generalisations of Einstein's description of gravitation.

2.4 Scalar Fields and Mass Generation

In section (1) it was stated that the structure of the basic interactions was related to a pattern of symmetry groups. For gravity the symmetry group of relevance encodes the invariance of the speed of light in space-time and the behaviour of particles with mass and intrinsic spin. One of the great advances in recent years has been the recognition that all these symmetries arise as approximations from a description of extended structures in higher dimensions and that space-time is a classical approximation to a more general quantum description that unites all the fields shown in Figure 1. Although this picture is incomplete there are indications that Einstein's original description of pure gravitation may need supplementing with additional fields. In particular, remnants of a higher symmetry group may persist on scales accessible to experiment. In this regime additional scalar fields seem inevitable. The role of such scalar fields can modify the short range behaviour of gravitation. It is therefore of importance to explore whether such fields can be detected experimentally and assess their significance on the behaviour of other matter.

One approach is to examine the manner in which residual symmetries for gravity are broken. We have recently shown [12] that the breakdown of local Weyl symmetry in a theory of gravity can be accommodated in the context of the standard model of particle interactions. A natural setting for this mechanism is a space-time geometry described by a connection with dynamical torsion and a metric that is not covariantly constant. Together with a scalar field such a connection encodes new gravitational interactions that can be reformulated in terms of the standard description of Einsteinian gravity. The emergence of space-time torsion, dependent on the gradient of the dynamic scalar field, is responsible for the appearance of the so-called *improved stress-energy tensor*. In the broken phase in which electro-weak phenomenology is discussed the theory gives rise to a Higgs particle with mass M_η and a new electrically neutral vector boson with mass M_Q such that

$$\frac{M_\eta^2}{M_Q^2} = \frac{8\lambda v^2}{\gamma}$$

in terms of the couplings in the theory. It is of interest to note that a number of grand unified models predict a new neutral vector boson and experimental data are now detailed enough to check for its existence. It appears that such data are better described if the presence of such a boson is assumed. The theory above has been analysed in a broken phase in which normal gravitation (based on metric perturbations about Minkowski space-time) is negligible. The mass generation mechanism has been connected with a component of non-Einsteinian gravitation associated with the Weyl connection Q. This forms part of the natural space-time geometry determined from an action principle and may be expected to give rise to new kinds of force on matter. If the neutral boson described by the excitation of the Weyl potential Q in Minkowski space-time can be observed in current electro-weak data it may signal that a new component of gravitation can influence phenomenology at energies well above the Planck scale.

2.5 Scalar Fields and Torsion Forces

In the scalar-tensor theory of gravitation formulated by Brans and Dicke[13], the motion of a test particle was originally assumed to be a "Levi-

Civita geodesic" associated with the metric derived from the Brans-Dicke field equations (even though the scalar field could vary in space-time). Later Dirac in [15] showed that in a Weyl invariant generalisation it was more natural to generate the motion of a test particle from a Weyl invariant action principle and that such a motion in general differed from a Brans-Dicke Levi-Civita geodesic. Although Dirac was concerned with the identification of electromagnetism with aspects of Weyl geometry even for neutral test particles it turns out that test particles would follow "auto-parallels" of a connection with torsion. We have shown[16] that the theory of Brans and Dicke[13] can be reformulated as a field theory on a space-time with dynamic torsion determined by the gradient of the Brans-Dicke scalar field Φ. Of course no new physics *of the fields* can arise from such a reformulation, although it does clarify certain issues relating to the conformal structure of the theory and its couplings to matter with intrinsic spin. However, the behaviour of spin-less *particles* in such a geometry with torsion depends on the choice made from two possible alternatives. One may assert that their histories are *either* geodesics associated with auto-parallels of the Levi-Civita connection *or* the auto-parallels of the non-Riemannian connection with torsion. Since one may find a spherically symmetric, static solution to the Brans-Dicke theory (in either formulation), it is possible to compare these alternatives for the history of Mercury about the Sun by regarding it as a spin-less test particle as in General Relativity.

To summarise the relevant equations of motion the language of covariant differentiation is appropriate. Differentiation involves a limiting procedure in which objects are compared at the same point. In ordinary calculus space has an "affine vector space structure" and there is a natural parallelism which permits vectors at different points to be transported to common points for comparison. Gravitation is formulated on a more general manifold. A manifold does not in general have a vector space structure and such a "natural parallelism" is absent. A new structure† called a "space-time connection", ∇ , is required to transport vectors from one point in the manifold to another, along an arbitrary curve.

The equation for a time-like auto-parallel is

$$\nabla_{\dot C}\,\dot C = 0$$

where the 4-velocity $\dot C$ is normalised with respect to the space-time metric $\mathbf{g}$:

$$\mathbf{g}(\dot C, \dot C) = -c^2. \tag{15}$$

By expressing ∇ in terms of the Levi-Civita connection $\tilde\nabla$ with $\tilde V = g(V,-)$ for any vector V one may write this as

$$\widetilde{\hat\nabla_{\dot C}\dot C} = -\frac{1}{2\Phi} i_{\dot C}(d\Phi \wedge \tilde{\dot C})$$

(the operator $i_{\dot C}$ denotes contraction of the 2-form with the vector $\dot C$) and interpret the right hand side as a torsion acceleration field analogous to the Lorentz force on electrically charged particles. Note however that the torsion force produces the same acceleration on all massive test particles. If $\dot C$ is parameterised in terms of proper time τ in any coordinates $x^\mu(\tau)$, the above is:

$$\frac{d}{d\tau}\left(\Phi^{1/2}\frac{dx^\mu}{d\tau}\right) + \Phi^{1/2}\left\{{\mu \atop \nu\lambda}\right\}\frac{dx^\nu}{d\tau}\frac{dx^\lambda}{d\tau}$$

$$= -g^{\mu\nu}\frac{\partial_\nu\Phi}{2\Phi^{1/2}}. \tag{16}$$

To illustrate the effects of this equation of motion we have recomputed[17] the classical shift in the perihelion rate of Mercury's orbit about the Sun in terms of a static spherically symmetric solution of the vacuum Brans-Dicke field equations [13]. Taking into account that the speed of Mercury is non-relativistic and that its Newtonian orbit is much larger than the Schwarzschild radius $r_s = 2GM/c^2$ of the Sun, one finds the perihelion shift per revolution Δ of the orbit:

$$\Delta = \frac{3\omega+5}{3\omega+6}\,\delta_\omega \tag{17}$$

where $\delta_\omega = 3\lambda_\omega\pi$, $\lambda_\omega = r_s/\hat r_0$ and ω is the Brans-Dicke coupling parameter. Using the Kepler period

$$\hat T = 2\pi(\hat r_0^3/(1-\hat\epsilon^2)GM)^{1/2},$$

the shift δ_ω may be expressed in terms of $\hat T$ and $\hat\epsilon$. This may be compared with the result based on the assumption that Mercury's orbit follows from a geodesic of the torsion-free Levi-Civita connection. In this case one finds

$$\Delta = \frac{3\omega+4}{3\omega+6}\,\delta \tag{18}$$

†Consider a curve C with tangent vector $\dot C$ and an arbitrary vector field X . An affine connection at a point p in space-time is a map that takes the pair $(\dot C, X)$ to a new vector $\nabla_{\dot C}X$ at p, which is linear in $\dot C$, and satisfies

$$\nabla_{\dot C}(X+Y) = \nabla_{\dot C}X + \nabla_{\dot C}Y$$

$$\nabla_{\dot C}(\phi X) = \dot C(\phi)X + \phi\nabla_{\dot C}X$$

for all scalar fields ϕ and vector fields X, Y. Due to the $\dot C$ linearity $(\nabla X)_p$ is a (1,1) tensor at p with $(\nabla X)_p(\dot C, \alpha_p) = \alpha_p(\nabla_{\dot C}X)$ for all covectors α_p at p. It is called the covariant differential of X at p.

where $\delta = 3\lambda\pi$ (with $\lambda = r_s/r_0$) is the perihelion shift per revolution of the orbit based on the Schwarzschild solution for the metric in General Relativity.

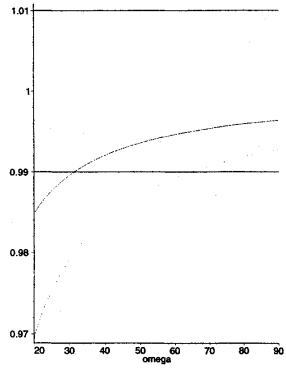

Figure 4: Behaviour of Δ/δ as a function of the Brans-Dicke coupling parameter ω. The full curve corresponds to a precession rate of Mercury's orbit under both metric and torsional acceleration. The lower dotted line corresponds to the original prediction of the Brans-Dicke theory. The experimental observations are consistent with Δ/δ lying between the full horizontal lines centered on $\Delta/\delta = 1$

Given the prominent role played by the motion of test particles in many astrophysical phenomena and the possibility of new gravitational interactions mediated by scalar fields we feel that, with the enhanced technology now available to modern space science, the possible relevance of scalar field induced space-time torsion should not be ignored. Should the departure of spin-less particles from Levi-Civita geodesic motion be detected in some purely gravitational environment it would indicate that matter has additional "gravitational charge" in addition to its mass and to its electromagnetic, weak and strong couplings to other fields in nature.

3 Summary

This article summarises some of the current activities of the gravitational research group above. Having surveyed the role of gauge fields as carriers of the basic forces in physics and the momentum conservation constraints placed on current propulsion technology a number of alternative strategies, under active investigation, have been briefly discussed. The essential theme is the detection of hitherto undetected components of gravitation that may have implications for the motion of matter. Such components include expected configurations of Einsteinian gravitation (including gravito-magnetic and radiation modes) as well as new scalar interactions resulting from various proposals for the unification of gravitation with the other basic forces. It would be premature to rank these strategies in terms of potential for the advancement of propulsion technology. International efforts are well advanced for the detection of gravitational radiation and the STEP experiment[18] is expected to place firm experimental bounds on the foundations of General Relativity. We have suggested above that there are also less expensive experiments that may also shed light on the existence of novel gravitational fields and that if scalar field gravitational interactions with matter can be detected they may offer unsuspected avenues for development.

4 Acknowledgement

The authors are grateful to BAe-Systems for the support of this research and to Dr R Evans (BAe-Systems UK) for stimulating discussions.

References

[1] W Rindler, Introduction to Special Relativity, Clarendon Press, Oxford,

[2] V V Beletsky, M E Givertz, *On the motion of a Pulsating Dumbbell in the Gravitational Field*, Kosmicheskie Issledovaniya **6** 304-306 (1968) (in Russian)

[3] V V Beletsky, Essays on Motions of Space Bodies, Moscow, Nauka 1997 (in Russian)

[4] V V Beletsky, E M Levein, Dynamics of Space Tether Systems, Advances in the Astronautical Sciences, Vol 83, American Astronautical Society Publications 1993

[5] NASA/AIAA/PSN International Conference on Tethers, Arlington, VA. USA. 1986 , Advances in the Astronautical Sciences, Vol 62, American Astronautical Society Publications 1986. Eds. P M Bainum et al.

[6] S Kalantzis, V J Modi, A K Misra, S Pradhan, *Dynamics and Control of Multibody Tethered Systems*, Acta Astronautica **42** (9) 503-517 (1998)

[7] K Kumar, K D Kumar, *Variable Attitude Maneuver via Tethers for a 'Drifting' Twin Satellite System in Elliptic Orbits*, Acta Astronautica **45** (3) 135-142 (1999)

[8] J Ashenberg, E C Lorenzini, *Active Gravity-Gradient Stabilization of a Satellite in Elliptic Orbits*, Acta Astronautica **45** (10) 619-627

[9] J Gratus, R W Tucker. An Improved Method of Gravicraft Propulsion, Submitted for Publ. 2000.

[10] S Clark, R W Tucker Gauge Symmetry and Gravito-electromagnetism Class. Quantum Grav. **17** 4125-4157 (2000)

[11] R Tucker, C Wang, A Cosserat Detector for Dynamic Geometry, International Conference on Geometrical Methods in Continuum Mechanics, University of Torino, 2000.

[12] T Dereli, R W Tucker, A Broken Gauge Approach to Gravitational Mass and Charge, Lancaster University Preprint, Submitted for Publ. 2000.

[13] C H Brans, R Dicke, Phys.Rev. **124** 925 (1961)

[14] A Einstein, L Infeld, B Hoffmann, Ann. Math. **39** 65 (1938)

[15] P A M Dirac, Proc. Roy. Soc **A333** 403 (1973)

[16] T Dereli, R W Tucker, Phys. Letts **110** 206 (1982)

[17] T Dereli, R W Tucker, On the Detection of Scalar Field Induced Spacetime Torsion, gr-qc/0104050.

[18] R Reinhard, Y Jafry,R Laurance, STEP-A Satellite Test of the Equivalence Principle, ESA Journal-European Space Agency 17: (3) 251-263 (1993)

A01-34542

AIAA 2001-3913
An Asymmetric Gravitational Wave Propulsion System

J. Cameron
Huntsville, AL

Joint Propulsion Conference
8-11 July 2001
Salt Lake City, Utah

AIAA 2001-4335

AN ASYMMETRIC GRAVITATIONAL WAVE PROPULSION SYSTEM

Jeffery A. Cameron, member, Chief Scientist
Transdimensional Technologies, Inc., Huntsville, Alabama 35801

Abstract

Gravitational wave radiation is generated by the quadrapole moment of matter that is in motion. An analytical model is constructed to investigate the radiation pattern and radiated power of a single resonant vibrator cylinder, as compared to that of a phased linear array. The linear array is then evaluated in terms of phase relationship in order to create an asymmetry in the radiated pattern and hence a directional force. This is compared to the force of a solar sail in the earth orbital plane.

Introduction

Einstein[1] derived the weak-field solution of the gravitational wave in accordance with the general and special theories of relativity. This paper uses this scientific background to describe a revolutionary new approach to propulsion. Programmable laser diodes in conjunction with semiconductor materials will be used to generate a highly directional transverse wave gravitational wave (TWGW) radiator. This asymmetric TWGW radiator will create a directional force through the center of mass of the radiating system, thus forming a propellantless propulsion system.

Theoretical work indicates the ability to generate gravitational wave radiation through the quadrapole moment of matter under stress and strain. The radiation pattern is symmetric about the center of mass, and the direction of the pattern is at right angles to the stress and strain vector. The radiation pattern looks like a torus. The radiated power is very small (10^{-29}) watts); however, when a linear sequence of radiators is put together and their patterns are allowed to superimpose, the total radiated power can approach kilowatts. The asymmetry of the radiated pattern is produced by adjusting the phase of the radiators. The resulting power imbalance will produce a force through the center of mass of the radiators. In order to accomplish this task, high peak power laser diodes will be used to photo-accoustically drive thin-film resonators. It becomes imperative to understand the energy flow between the laser diode driving the resonator and the result in gravitational radiation from the radiator.

Theory

In order to establish an analytical background consider the following. Let $\eta_{\mu\nu}$ be a Lorentz metric, then the Riemannian metric is expressed as

$$g_{\mu\nu} = \eta_{\mu\nu}\sqrt{K}h_{\mu\nu} \tag{1}$$

as a first approximation under the weak-field assumptions, K is Einstein's constant. The potential of the field can be expressed as

$$\phi_{\mu\nu} = h_{\mu\nu} - \frac{1}{2}\eta_{\mu\nu}h \tag{2}$$

resulting in the form for 4-space

$$\Box\phi^{\alpha\beta} = 2\sqrt{K}T^{\alpha\beta} \tag{3}$$

with retarded potential solutions of the form

$$\phi^{\mu\nu}(x) = (\sqrt{K}/2\pi\int T^{\mu\nu}(x^{t}, x^{0}) \tag{4}$$

This form will enable the definition of the energy-momentum complex of the gravitational field in order to evaluate the radiation energy and directivity of the gravitational wave.

The Poynting vector of the gravitational wave can be expressed as

$$U_o^l = \frac{1}{8}(-2\phi^{\rho\sigma,l}\phi_{\rho\sigma,o} + \phi^{,l}\phi_{,o}) \tag{5}$$

The derivatives of the potential fields ϕ with respect to time and space coordinates are expressed by the second and third derivatives of the mass tensor,

$$mc^2 \equiv \iiint T^{00}(x', x_G^0)d^3x' \tag{6}$$

momentum tensor,

$$cP^K = \delta_0 x^{K'} \iiint T'^{00}(x', x_G^0) d^3x' \qquad (7)$$

and the quadruple moment tensor,

$$I^{iK} = x^i x^{K'} \iiint T_{00}(x', x_G^0) d^3x' \qquad (8)$$

The derivative forms for the potential fields are substituted into the expression for the Poynting vector, thus giving the expression for the radiated energy per unit time, or power, within a solid angle $d\Omega$, as follows

$$P_o^t = U_o^t d\sigma_t = \frac{1}{8}\left(\frac{\sqrt{K}}{4\pi}\right)^2 f(\theta, \phi, x_G^o) d\Omega \qquad (9)$$

Here the factor

$$f(\theta, \phi, x_G^o) \qquad (10)$$

represents the directivity of the gravitational wave radiator.

Of particular interest for this paper is the resonance vibrator, conceptually similar to what Weber[2,3,4] used as a gravitational wave detector. The resonance vibrator is a cylinder (Figure 1), which is placed under stress and strain.

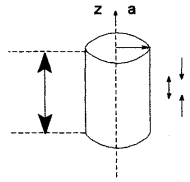

Figure 1: Resonant Vibrator Cylinder

At this point assume the following dynamic variables:

$$\text{Displacement } \varepsilon = A_1 \sin\left(\frac{\omega}{V_s}\right) \cos wt \qquad (11a)$$

$$\text{Particle velocity } v = \frac{d\xi}{dt} = -V_p \sin\left(\frac{\omega}{V_s}\right) z \sin \omega t \qquad (11b)$$

$$\text{Strain } \varepsilon = = \frac{d\xi}{dz} = \frac{V_p}{V_s} \cos\left(\frac{\omega}{V_s}\right) z \cos wt \qquad (11c)$$

$$V_p = A_1 \omega \qquad V_2 = \left(\frac{B_s}{\rho}\right)^{\frac{1}{2}} \qquad (11d)$$

$B_s \rightarrow$ Young's Modulus

The directivity can now be expressed as follows (Figure 2).

$$f \sim \sin^4 \theta \qquad (12)$$

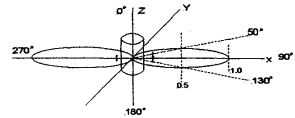

Figure 2: Resonant Vibrator/Gravitational Wave Radiation

The pattern resembles a torus or "donut" mode.

It can be seen that the maximum radiation occurs in the plane perpendicular to the vibrating z axis (Figure 2).

Consider a linear array of resonant vibrators (Figure 3).

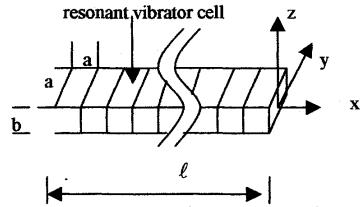

Figure 3: Resonant Vibrator Linear Array

Let high peak power laser radiation from laser diodes be injected along the z axis to induce acoustic stress in the material (Figure 4).

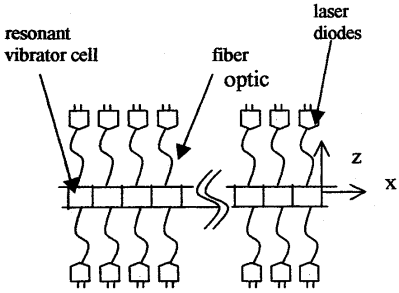

Figure 4: Laser Diodes and Linear Array

The stresses will generate a weak gravitational wave along the x axis. The gravitational wave generated from a number of "cells" along the x axis can be added in phase. The resultant gravitational "beam" along the x axis is extremely intensified compared to a single resonant vibrator "cell." The linear arrangement will be referred to as a traveling wave (TW)gravitational wave (GW) radiator, or TWGW radiator.

The directivity of the TWGW radiator can be expressed as (Figure 5).

$$f \approx \left(\frac{\sin\left(\frac{\pi\omega}{V_s}(1-\cos\Theta)\right)}{\left(\frac{\pi\omega}{V_s}\right)(1-\cos\Theta)}\right)^2 \cos^4\Theta \qquad (13)$$

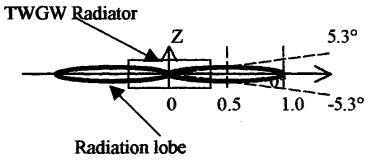

Figure 5: TWGW Radiator Symmetric Radiation Pattern

The graphical result of Figure 5 is based on the geometry of Figure 3 and the constants as follows.

Material: Quartz

$b = 3x10^{-5} m$

$a = 3x10^{-3} m$

$\ell = 0.3m$

$\omega = 6.28x10^{12}\, radian/\sec$

(*resonant frequency*)

$V_S = 5x10^3 m/\sec$ (*wave speed*)

$\rho_o = 2650 kg/m^3$ (*density*)

As can be seen in Figure 5, the TWGW radiation is very directional. This brings to question what type of power levels could be estimated. To begin, consider the single resonant vibrator cell (Figures 2 and 3). The radiated power can be estimated by the following expression.

$$P_{RV} = (5.7x10^{-2}) G\rho_o^2\pi^2 a^4 e_m^2 V_s \left(\frac{V_s}{C}\right)^5 \qquad (14)$$

Where

$$G = 6.67x10^{-11}\frac{Nt\cdot m^2}{kg}$$

(Gravitational Constant)

$\varepsilon_M = 4x10^{-3}$ (Strain)

Then

$$P_{RV} = 2.14x10^{-29} watt \qquad (15)$$

As anticipated, this is a very small number. However, for the TWGW radiator, the radiated power can be estimated by the following expression.

$$P_{TW} = (7x10^{-5}) G\rho_o^2 a^2 \ell^2 e_m^2 V_s \left(\frac{V_s}{C}\right)^5 \left(\frac{b\omega}{V_s}\right)^6 \Omega \text{ W} \qquad (16)$$

here

$\Omega(\pm 5.3^\circ) = 2.7x10^{-2} sr$

(Solid angle of the radiation)

Then

$$P_{TW} = 1.66x10^3 watt \qquad (17)$$

This shows how important the phase relationships between individual resonant vibrators are!

At this point it is important to realize that the radiated gravitational wave carries energy and momentum with it. This is expressed as

$$P = \frac{\varepsilon}{C} = \frac{\underline{P}t}{C} \tag{18}$$

Where $\underline{P}$ is the radiated power, t is time, ε is the energy of the gravitational wave, and P is the momentum.

The resulting reaction force on the TWGW structure is expressed as

$$F = \frac{P}{t} = \frac{\underline{P}}{C} \tag{19}$$

Referring to Figure 5, it can be seen that the radiation pattern is symmetric about the center of the TWGW structure. Therefore any reaction force is balanced! However, consider a variation in the phasing of the laser diodes (Figure 4), where the lobes become asymmetric (Figure 6).

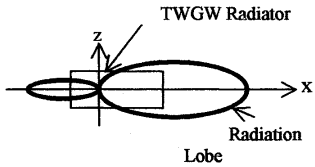

Figure 6: TWGW Radiator Asymmetric Radiation Pattern

This can be accomplished by pulse timing, variation in pulse rate, laser diode intensity, alternate materials, and geometry. Here there is a net force in the direction of the least intense gravitational wave (Figure 7).

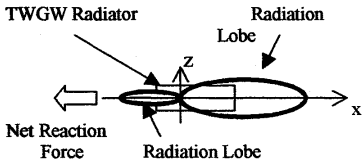

Figure 7: Reaction Force for Asymmetric Radiator TWGW

The reaction force is expressed as

$$F_{net} = F_{RL1} - F_{RL2} = \frac{\underline{P}_{RL1} - \underline{P}_{RL2}}{C} \tag{20}$$

As an example, let $\underline{P}_{RL1}$ = 500 watt and $\underline{P}_{RL2}$ = 3.5 x 10^3 watt, then

The net force, although small, raises the possibility of a propellantless propulsion concept, utilizing current technologies.

$$F_{net} = 10 x 10^{-6} Nt \tag{21}$$

Further Investigations

Mathematical analysis indicates that gravitational wave propulsion is possible. Further investigation will entail the following objectives.

1) Investigate the efficiency of converting laser light into acoustic stress within TWGW generating material candidates. The acoustic stresses are responsible for generating the quadrapole moment needed to give rise to TWGW radiation. It will be imperative to address questions on how material uniformity, temperature, geometry, laser pulse width, repetition rate, and wavelength will impact performance.

2) Investigate phasing techniques of the TWGW elements in order to create various asymmetries in the radiating pattern. The directivity and intensity of the TWGW radiator is key to the success of generating a net propulsive force. How energy and momentum transports are affected by individual radiator phasing are of utmost importance. The question of whether harmonics distribute energy into other "modes" or are negligible must be considered.

The TWGW system must be analytically modeled as part of the above investigations. The results will lead to study of a test article that will be used to demonstrate the use of the gravitational wave Poynting vector imbalance as a means of generating a propulsive force through the center of mass of the TWGW system. Conceptually a scale version of the system could provide propellantless propulsion into the outer regions of the solar system and/or orbital transfer missions.

Space Flight Application

An interesting example is a comparison of the TWGW system to that of a solar sail at the earth orbital plane. Let the TWGW system be 1000 meters in length. The resulting net propulsive force would be about 61 Nt. For a square solar sail with a perfect reflectivity experiencing a solar flux of 1.3×10^3 watts/m^2, the required area would be around 1.4×10^7 m^2 for a force of 61 Nt. This is a perimeter length of approximately 3.7×10^3m and must be normal to the solar disk to experience the maximum momentum transfer. Also, as the sail increases its distance from the solar disk, the intercepted flux decreases with the square of the distance. The TWGW system is not dependent on the solar disk for operation.

Conclusion

An analytical model has been created to investigate the nature of the radiated TWGW pattern with respect to phase relationships between individual "cell" radiators. Future models will investigate the magnitude of side lobes or harmonics to determine whether asymmetries cause less than desirable effects. These results will be used for evaluation of the generation of a net propulsive force.

References

[1] Einstein, A., *Naherungsweise Integration der Feldgleichunger der Gravitation* (Berlin Sitzungsberichte, 1916), pp. 688-696.

[2] Weber, J., *Physics Review,* 117, 1960, p. 306.

[3] Weber, J. *General Relativity and Gravitational Waves* (Interscience, New York, 1961).

[4] Weber, J., *Physics Review Letters,* 22, 1969, p. 1320.

Acknowledgements

The author wishes to express sincere thanks to Remigius Shatas and Robert Asprey of 2C Computing, Huntsville, Alabama for their encouragement and support.

A99-31034

AIAA 99-2147

Fabrication of Large Bulk Ceramic Superconductor Disks for Gravity Modification Experiments and Performance of YBCO Disks Under e.m. Field Excitation

R. Koczor and D. Noever
NASA Marshall
Huntsville, AL

35th AIAA/ASME/SAE/ASEE Joint Propulsion Conference and Exhibit
20–24 June 1999
Los Angeles, California

AIAA-99-2147

ABSTRACT

We have previously reported on investigations pertaining to the measurements of gravitational field changes in the vicinity of a large rotating Type II superconducting disk. Published reports indicate that test masses have been observed to lose up to 2% of their weight when in the vicinity of such rotating disks. We have produced 30 cm (nominal) diameter disks using $YBa_2Cu_3O_{7-x}$ and BiSCCO. In addition we have performed tests on the interactions between smaller YBCO disks and AC levitation fields and RF fields, using a sensitive gravimeter to monitor and record the local gravity field above the superconductors. We have not yet duplicated the reported experimental protocols, including rotation and levitation of a large two-layered YBCO disk. Static disk experiments to date have uncovered no measurable and repeatable gravity effect for the conditions tested to within the sensitivity of the gravimeter (which has a noise level on the order of 10 nano-G or less).

FABRICATION OF LARGE BULK CERAMIC SUPERCONDUCTOR DISKS FOR GRAVITY MODIFICATION EXPERIMENTS AND PERFORMANCE OF YBCO DISKS UNDER EM FIELD EXCITATION

Ronald J. Koczor, NASA, Marshall Space Flight Center, AL,
David A. Noever, NASA, Marshall Space Flight Center, AL

Background

Attempts to unify theories of gravity with the other forces of nature have a long and checkered history. Some of the greatest minds the world of physics has known have believed that the connection is there. Clearly at the astronomical scale, gravity and electromagnetics interact through the mechanism of gravitational warping of space around massive bodies. Nonetheless, all credible attempts to experimentally demonstrate that connection on a laboratory scale have remained elusive. It is clear that if a manipulative method is found to treat gravity, extensive changes would occur in our everyday life, just as our lives changed once electromagnetism was understood.

In 1992, E. Podkletnov and researchers at the University of Tampere, Finland, reported [1] demonstration of what he termed "gravity shielding." The experiment consisted of spinning a Type 2 superconductor (yttrium, barium, copper oxide, YBCO) in the presence of electromagnetic levitation and rotation fields and measuring weight changes in test masses suspended above the spinning disk. The effect reported was small, varying from tenths of a percent to as much as 2% of the test mass' weight. A subsequent paper was distributed giving more details of the experiment. [2]

While this is a small effect, it can be recalled that some of the most telling and seminal experiments in electromagnetics in the early 19th century were similarly of small magnitude. Their value was in demonstrating the basic phenomenon; useful amplifications and extensions came from others, once the basic idea had been demonstrated and accepted.

In 1997 researchers at the Marshall Space Flight Center, Huntsville, Alabama, and colleagues began to investigate the Podkletnov experiment. The goal was to understand various phenomena related to the experiment and to replicate it. Marshall has a historical connection to the YBCO material, having been intimately involved in the first fabrication and characterization experiments over a decade ago.

While there is general information available about to experimental set up, several critical

details are unclear. However, as we have reported, [3,4,5] progress is being made and our understanding of bulk ceramic superconductors and their interactions with various electromagnetic fields grows. Also, a significant step forward in the measurement of small changes in gravity fields was made with the application of a highly sensitive and stable gravimeter to the experiment. This gravimeter is capable of measuring changes in the local gravity field as small as 5×10^{-9} G. In this paper we will discuss our progress in fabricating large bulk superconductors and various preliminary experiments to understand how these materials interact with AC fields levitation.

Large Bulk YBCO and BiSCCO Disks

The central component in the Podkletnov experiments is a composite structure annular disk of YBCO superconductor. The YBCO material normally exhibits a superconducting transition temperature of around 94K, making it an exciting superconducting material since it is useable with liquid nitrogen cooling. Podkletnov fabricated a dual layered disk, having one layer of YBCO that became superconducting around 94K and another layer that became superconducting around 60K. It is his belief that this composite structure is a mandatory feature to see the effect. Our results to date do not dispute that assertion.

While the ceramic superconductors offer much potential, their well-known characteristics have led present day research with YBCO from bulk to thin film configurations. There are no published reports of fabrication of large bulk ceramic superconductors, in part due to the enormous challenges facing anyone who attempts to fabricate them. Since it is central to our goals, we undertook to fabricate such a disk. Working with colleagues at the University of Alabama in Huntsville and at Martin Technologies, Inc. (also of Huntsville), and after much trial and error, we succeeded in fabricating several single layer YBCO disks (on the order of 30 cm in diameter and ranging in thickness from 0.5 to 1 cm). Recently with our colleagues at Tomorrowtools, Huntsville, we fabricated as 32 cm diameter annular disk made from BiSCCO (bismuth, strontium, calcium, copper, oxide) superconducting material with a nominal superconducting transition temperature between 100 and 110 K . Figure 1 shows the YBCO disk (left) and the BiSCCO disk (right) fabricated at Marshall.

Successful fabrication of such large superconductors resulted from attention to 3 process steps, material selection, mechanical pressing, and thermal processing. Details of the process are being reviewed for patent applicability and so cannot yet be discussed. However, the process results in disks having excellent mechanical structure and moderate superconductive performance as expected from sintered bulk materials. Characterization of the resulting disks indicates transition temperatures for YBCO in the 92K to 94K range and critical currents on the order of 20 to 100 amps/cm^2. The BiSCCO disk is presently undergoing characterization and results are not available.

Fabrication of the YBCO disk used pre-processed YBCO superconducting powders; The process used for the BiSCCO disk was based upon the sol-gel process prepared with precurser nitrates in an autoignition process. Subsequent pressing and heat treating created the correct BiSCCO superconducting formulation.

Only one em field test was run using these large disks, as we are presently completing their characterization. This test involved a preliminary attempt to induce radio frequency energy into the disk and measure any resultant gravity field changes. This test is reported below. Other experiments have been underway using smaller, commercially available YBCO disks to characterize their interactions with various electromagnetic fields. These experiments are also reported below.

Small Disk Interactions with AC Levitation Fields

One series of tests was run to determine how the superconductors react to alternating current, AC, levitation fields. It is generally known that these materials react differently to AC fields than DC. And, again, while much information is available for thin films and very small bulk samples, we believe these tests are the first reported for large pieces.

The experiments were performed using two commercially available melt-textured crystal seeded YBCO disks. One was a single layer disk having a diameter of about 13 cm and a thickness of about 1 cm. The other disk was a 10 cm diameter two layer disk. The levitation field was generated by a 3 solenoid assembly driven by Elgar model 1001SL variable voltage, variable frequency power supplies with a Model 9023 variable frequency oscillator for frequency control. These supplies are capable of generating up to 30 amps from 50 Hz to 4500Hz. Magnetic field characteristics were measured using an F.W. Bell model 9500 gaussmeter. The experimental protocol was to cool the superconductor, place it over the solenoids and turn on the field.

Results show that the 13 cm diameter single layered disk levitated with an 860g field at 45 Hz, 750g at 300 Hz, and 650g at 600 Hz. Levitation was

not achieved at higher frequencies due to the inductive reactance of the solenoids and the subsequent current limitations in them. Another test revealed that the 10 cm two-layer disk levitated with 600 g at 45 Hz.

Given these data and the fact that a sintered 30 cm disk will be both heavier and have lower critical current than the melt textured disks above, we expect significantly stronger fields will be required to levitate the large disks. On the other hand, the coils had small field cross sections Larger field cross sections as well as stronger fields will assist levitation.

For one series of tests, we placed the levitating disk approximately 1 meter below the gravimeter. The disk and levitation fields were in a Faraday cage with the gravimeter above and outside the cage. Tests without the disk in place demonstrated that the gravimeter reading was not influenced by the levitation fields. For this test a 45 Hz field was applied to the disk using the 3-solenoid system described above for levitation while the gravimeter was recording. Figure 2 gives the results for one run using the 10 cm two layered disk. Each division on the vertical scale is 10 nano-G; each division on the horizontal scale is 72 seconds in elapsed time. In all cases reported here, the gravimeter is set for a 2 second sample integration time. The results of this test show no evidence of any effect of the levitating disk on the gravimeter above the noise level of the gravimeter. Other frequencies were run with similar results. At higher frequencies, fields were applied even though they were insufficient to levitate the disk. In some cases changes in the gravity reading are seen; however, they are all on the order of a 100 nano-Gs or less and are not repeatable.

Figure 3 (having the same scale as Figure 2) exhibits data from a run in which the 10 cm composite structure disk was exposed to 9 pulses of 45 Hz field. For this test field intensity was 1100 gauss and the disk did levitate with each pulse. Pulse rate was one pulse per minute with a 50% duty cycle. As can be seen, there is no significant change visible the in gravimeter reading during the experiment although there are minor transients that may be related to the pulses. The experimental setup was as described above.

It has been suggested that when a superconductor transitions from normal to super conducting mode, a possible transient gravity signal is produced. Figure 4 exhibits data from a run in which gravimeter readings were taken during cooldown of the 2 layer disk using the experimental setup described above. The figure shows where the liquid nitrogen was first poured and when rapid boiling of the liquid stopped. A small magnet levitated when placed over the disk at the cessation of boiling, indicating that the disk was superconducting.

In summary, no conditions were found in which excitation of a small YBCO disk by a low frequency levitation signal produced repeatable changes in the gravimeter reading.

Large YBCO disk RF Field Interactions

A series of experiments was run to characterize the effects of megahertz-range rf on a 30 cm YBCO disk. The experiments used a tunable rf generator and amplifier capable of 100 watts output between 1 and 100 MHz. Most tests focused on the 3 to 20 MHz range. Rf was applied through a 12 turn coil wound toroidally around one section of the disk. An impedance matching network was used to maintain a constant load to the amplifier.

Initial tests demonstrated that the gravimeter was susceptible to the rf. This susceptibility manifested itself in lockup of the gravimeter data system at high rf levels (25 watts or more). This susceptibility was eliminated using standard rf shielding procedures on the gravimeter and by enclosing the YBCO disk and rf coil in a grounded Faraday cage.

Figure 5 is representative of these tests. In this case a series of four 3.5 MHz, 100 watt pulses were applied to the disk while it was superconducting. As can be seen, there are changes in the gravimeter reading appearing to coincide with the pulses, having amplitudes on the order of 10 nano-G.

Other tests performed include application of rf during cooldown of the disk and measurement of the gravity field with various rf frequencies applied. These data are presently being evaluated and will be reported later. In general, there are more repeatable and consistent gravimeter variations observed with the rf excitation than with the low frequency AC levitation excitation. However, all changes seen to date are less than 100 nano-G in amplitude.

Summary

We have succeeded in manufacturing large (30 cm diameter) superconducting disks using the YBCO and BiSCCO materials. These disks, weighing between 3 and 4 Kg, depending on thickness, are being used to investigate reported interactions between em fields and the local gravity field.

The reported interactions occur in an experimental protocol that we have not yet duplicated. Our initial attempts are to individually

characterize possible interactions under static (non-rotating) conditions. We have completed these initial characterizations, data is being analyzed, and preliminary results were reported here.

All observed interactions were on the order of nano-Gs and considerable care is being taken to assure that these observations are not artifacts of the experimental set up or interactions between the em fields and the gravimeter.

We are currently developing experimental hardware to test the large disks now being routinely fabricated. We expect to achieve levitation of the 30 cm disks under em field excitation later this year, with rotation soon to follow. Further experiments are also underway to optimize disk fabrication for increased critical current and mechanical stability and to develop a process to fabricate a two layered 30 cm disk.

The authors wish to acknowledge the indefatigable support provided by Tony Robertson, of MSFC's Space Transportation Directorate, Rick Roberson, of Tomorrowtools, Inc., Robert Hiser, of Maartin Technologies, Greg Jerman, of the MSFC Engineering Directorate, and Charles Sisk of the MSFC Science Directorate. We also wish to acknowledge and thank Ning Li and her colleagues at the University of Alabama in Huntsville, for their participation in the formative stages of this investigation.

References

1. "A possibility of gravitational force shielding by Bulk $YBa_2Cu_3O_{7-x}$ superconductor" E. Podkletnov and R. Nieminen, Physica C 203 (1992) 441-444.
2. "Weak gravitational shielding properties of composite bulk $YBa_2Cu_3O_{7-x}$ superconductor below 70K under an e.m. field" E. Podkletnov, MSU-chem-95-cond-mat/9701074 5 Feb 1997 preprint.
3. "Static test for a gravitational force coupled to type II YBCO superconductors," N. Li, et al, Physica C 281 (1997) 260-267.
4. "Superconductor-mediated Modifications of gravity? AC motor experiments with bulk YBCO disks in rotating magnetic fields," D. Noever, R. Koczor, AIAA 98-3139, Proceedings, 1998 AIAA/AASME/SAE/ASEE Joint Propulsion Conference, Cleveland, OH, July 13-15, 1998.
5. "Granular superconductors and gravity," D. Noever, R. Koczor, NASA/CP1999-208694, NASA Breakthrough Propulsion Physics Workshop Proceedings, August 12-14, 1998, Lewis Research Center, Cleveland, OH.

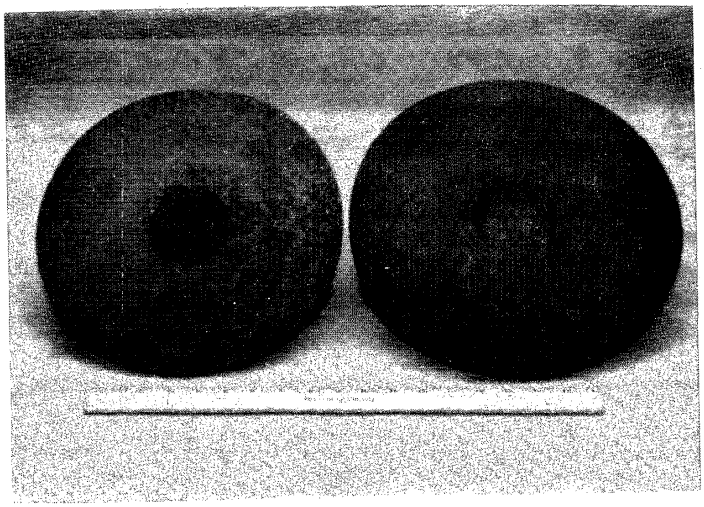

Figure 1 30 cm YBCO superconducting disk (left) and 32 cm BiSCCO superconducting disk (right) fabricated at NASA/MSFC.

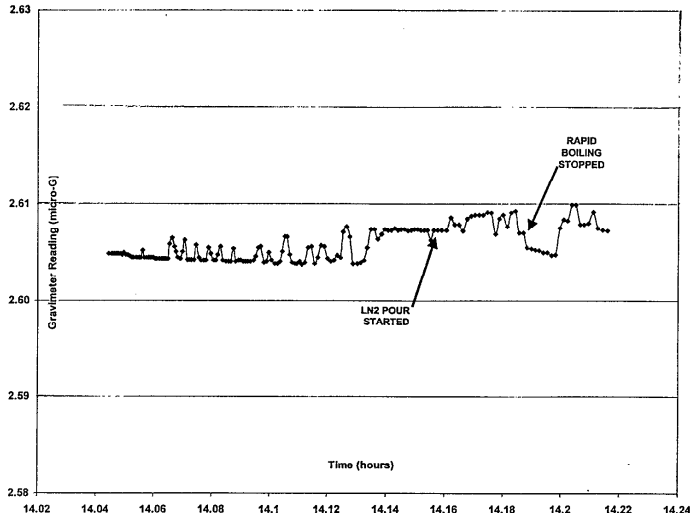

Figure 4 Gravimeter reading during cool down of a 10 cm YBCO superconducting disk.

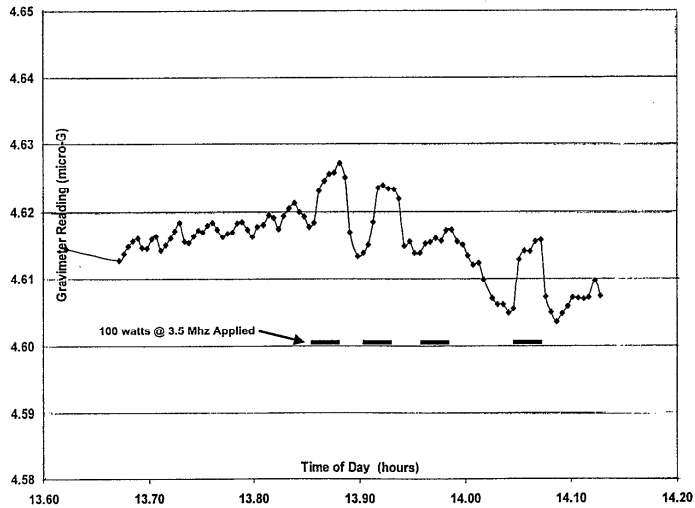

Figure 5 Gravimeter reading during rf excitation of a 30 cm YBCO superconducting disk.

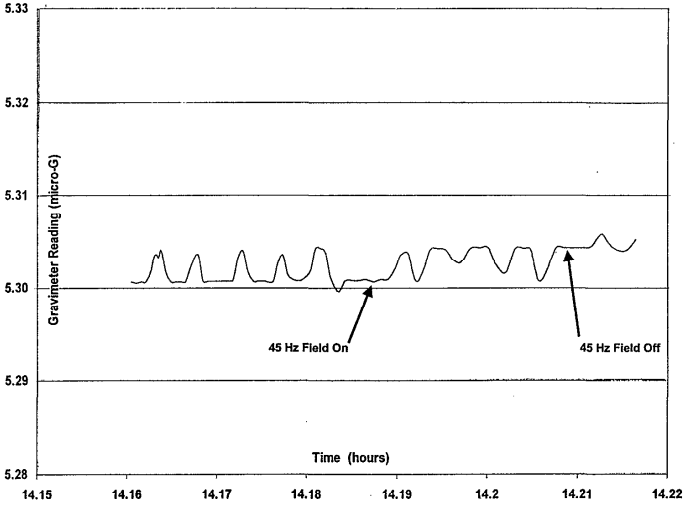

Figure 2 Gravimeter reading with 600 gauss, 45 Hz levitation field applied to a 10 cm YBCO superconducting disk.

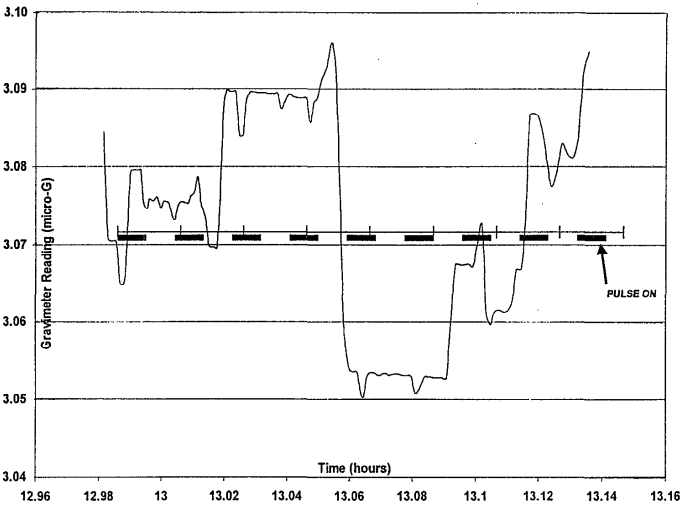

Figure 3 Gravimeter reading with 9 pulses of 1100 gauss, 45 Hz levitation field applied to 10 cm YBCO superconducting disk.

A99-31033

AIAA 99-2146

Large Scale Sakharov Condition

D. Noever and C. Bremner
NASA Marshall Space Flight Center
Huntsville, AL

35th AIAA/ASME/SAE/ASEE Joint Propulsion Conference and Exhibit
20–24 June 1999
Los Angeles, California

AIAA-99-2146

ABSTRACT

Recent far-reaching theoretical results have used the quantum vacuum noise as a fundamental electromagnetic radiation field to derive a frequency (ω) -dependent version of Newton's gravitational coupling term, $G(\omega)$. This paper reconciles the cutoff frequency with the observed cosmological constant, then briefly puts forward a realizable laboratory test case in the 10-100 MHz frequency range. One analogy is drawn between the classical vacuum energy experiments with attraction between two closely spaced plates (Casimir cavity) and the arbitrarily dense material boundaries possible in Bose condensates, such as irradiation at MHz frequencies of superfluid helium or superconductors.

LARGE-SCALE SAKHAROV CONDITION

David Noever and Christopher Bremner

NASA Marshall Space Flight Center, Space Sciences Laboratory, Mail Code: ES76, Huntsville, AL 35812

Theoretical Background

Zel'dovich [1] first suggested that gravitational interactions could lead to a small disturbance in the (non-zero) quantum fluctuations of the vacuum and thus give rise to a finite value of Einstein's cosmological constant in agreement with astrophysical data. Using dimensional analysis and the suggestion by Zel'dovich, Sakharov [2] derived a value for Newton's gravitational constant, G, in only one free parameter, frequency, ω:

$$G \sim c^5/h \int \omega \, d\omega \sim 1/\int \omega \, d\omega$$

where c is the speed of light and h is the Planck constant. The free parameter in frequency when integrated over all values from zero to high frequencies, must contain the usual integration cutoff value (Planck frequency on observable electromagnetic phenomenon).

Puthoff [3] and others [4-5] have extended Sakharov's condition in a relativistically consistent model to determine constants of proportionality. His model derives an acceleration term in first order expansion (in flat space-time), then equates inertial and gravitational mass (by the equivalence principle) to make contact with the gravitational constant, G, directly as:

$$G=(\pi c^5/h\omega_c^2) \sim 1/\int \omega \, d\omega$$

which is the Sakharov condition [2,3]. This paper revisits the meaning of the cutoff frequency, ω_c, for radiation interactions, of which the quantum vacuum [6-10] and Planck frequency are only the leading terms, and for which linear combinations of forces can introduce other plausible frequencies. One purpose of this reexamination is whether the resulting gravitational coupling constant, G, can be reconciled with the anticipated energy density of the universe [11] without resorting to extreme space-time curvature and thus yield enough critical density to contain the expansion of the universe. Finally we particularize the case to the high density fluctuations possible in Bose condensates [12], a potential experimental test case for how the effects of vacuum noise might manifest observably.

One far-reaching consequence of the vacuum energy model is the attractive force of gravity becomes reducible to the radiative interaction between oscillating charges, e.g. the zero point field (ZPF) applied to subatomic charges. Mass and inertia arise from the fundamentally electromagnetic ZPF oscillations.

This random background gives the usual quantum mechanical energy spectrum from particle-field effects:

$$\rho(\omega)\, d\omega \sim \omega^3\, d\omega,$$

a very important dimensional relationship, since the third power in frequency avoids anomalous Doppler shifts from velocity boosts, or stated alternatively is the correct spectra for a Lorentzian (non-accelerated) invariant radiation field [13].

More specifically, the energy spectrum [3] can be written as:

$$\rho(\omega)\, d\omega = [\omega^2/\pi^2c^3]\,[h\omega/2]d\omega$$
$$= h\omega^3/2\pi^2c^3\, d\omega \sim \omega^3\, d\omega$$

which is an expression in the first parenthesis of the density of the normal modes and in the second parenthesis of the average energy per mode. When this energy density is integrated over all frequencies, the ω^3 divergence produces well-known infinities in the integration limit of high frequencies, thus an assumed cutoff frequency (appropriate to experimental observation limits at the Planck frequency), is usually introduced:

$$\omega_p = (c^5/hG)^{1/2}$$

For mass, m, moving in an accelerated reference frame, $g = -a = Gm/r^2$, the resulting energy spectrum includes a gravitational spectral shift [3],

$$\Delta\rho'(\omega)\, d\omega = h\omega/2\pi^2c^5\,[Gm/r^2]^2 d\omega \sim 1/r^4\, d\omega$$

a kind of short-range ($1/r^4$) gravitational energy shift, but electromagnetic in origin when zero point fluctuations are included. (N.B. To account for equal gravitational mass effects in neutrons and protons, the ZPF oscillations must involve subatomic charges, or 'parton' effects. The assumption derives from high-frequency interactions of ZPF wherein these subatomic particles are asymptotically free to oscillate as independent or free particles as quantum noise].

A further far-reaching consequence [3] is mass itself becomes interpretable as a dependent quantity derived from a damped (with decay constant, Γ) oscillation driven by random ZPF:

$$m = \Gamma c^3/G = 2h\,\Gamma/\pi^2c^3 \int \omega\, d\omega,$$

with the only two free parameters, the damping factor Γ, and again the frequency, ω. The internal kinetic energy of the system contributes to the effective mass.

This leads to an overall average spectral density, written in terms of mass as:

$$\Delta\rho'(\omega) = m^2c^5\omega/2h\omega_c^4r^4$$

for the electromagnetic field distribution near ($1/r^4$) to the mass, m, which in detail is half electric and half magnetic.

One additionally attractive feature is the correspondence between this derivation and the view of gravity as a dynamical scale-invariance-breaking model (e..g symmetry breaking near the Planck mass energy [14]). A final result includes the force calculation between two ZPF radiation oscillators, of the correct form yielding Newton's average force law:

$$\langle F\rangle = -Gm^2/r^2$$

Thus, for a Newtonian force to first order in a flat space-time, Sakharov [2] could be credited for proposing gravity as not a fundamentally separate force and Puthoff [3] and co-workers [4-5] applied the vacuum electromagnetic field to equate gravity to a long-range radiation force (e.g. van der Waals-like force). Higher order oscillatory gravity modes vary as $(\sin[\omega_o/\omega_c])^2$.

To first order, a weak G coupling constant, $G \sim (\pi c^5/h\omega_c^2)$, appears for high frequency cutoffs at the Planck scale. A corollary in analogy to electromagnetic shielding by ordinary matter can be rationalized as the problem of frequency mismatch at high Planck frequencies, e.g. ZPF cannot be fundamentally shielded. In other words, frequency mismatch precludes gravity shielding by matter.

The purpose here is to revisit the only free parameter, the frequency cutoff, more in the spirit of a mass resonant frequency. The motivation for this approach can be summarized as: 1) the generality of other complementary radiation effects without relying on ZPF alone (e.g. other isotropic, homogeneous radiation sources); 2) the weak coupling constant, G, yields a vastly smaller than observed size of the universe (e.g. too small cosmological constant) when the Planck frequency is used as a cutoff value; and (3) the particle mass, $m = \Gamma c^3/G$, can be viewed as a renormalized or 'dressed' mass with a resonant interaction potential that is frequency dependent in its coupling constant, G, and with 'bare' mass that is large, $m_o \sim (m_p^2/m)$, where the experimentally unobservable, $m_p = (hc/G)^{1/2}$ is the Planck mass.

In particular, why this large 'bare' mass does not generate a large gravitational field is not a unique anomaly in the Sakharov

derivation, since similarly large vacuum point energies are common to field theories. The important point is that the derivation $G(\omega)$ is general however to any isotropic radition field with the Lorentz-invariant energy spectra [$\rho(\omega) \sim\omega^3$], thus the candidates for the cutoff frequency of the particular radiation source can be interpreted as a Planck scale only if the rest mass, m_o, is not composed of many terms, rather than just the ZPF leading term. Since the ZPF is akin to a van der Waals force [3-5], polarizability (in charge and mass) must be considered, but without also excluding any number of linear combinations that might have alternative cutoff frequencies, ω_c, or damping terms, Γ, 'ala particle physics interpretations for resonant masses during renormalization. In other words, once a gravitational energy spectrum, $\rho(\omega)$, is postulated that is Lorentzian invariant, many fundamental sizes (or corresponding frequency values) are smeared (or dressed) by any number of characteristic frequencies between zero and the high frequency electromagnetic (Planck) cutoff, ω_p. Quite simply, is the expression, $\omega_c = \omega_P$ a requirement for all radiation sources?

Many types of particle oscillations may satisfy the general requirements of a Sakharov condition, each having a characteristic mass (and energy) as in calculating the mass of any fundamental particle at its resonant frequency (including underlying partial charges or dense bosons). This brings the calculation to a consideration of the high density fluctuations characteristic of a Bose condensate [15-19]. While the high density variation may intrinsically be of interest, the exploration has more to do with reconciling the ZPF interpretation of the Sakharov condition with the observed cosmological constant [14].

A 'top-down' view of calculating the cutoff frequency imposes the self-consistency test for the cosmological constant, Λ, from the outset. To calculate, Λ, for ZPF, the total frequency-integrated energy density of the universe must be included:

$$\rho(E)=\int \rho(E)\, dE = h\omega_c^4/8\pi^2c^3$$

which must have a mass equivalent, contribute to the universe's curvature, and thus have a fundamental relation to the critical density to contain the expansion of the universe [14-15]. The mass-equivalent ZPF to reach the universe's critical density [15], $\rho \sim 10^{-29}$ g cm^{-3} would necessarily limit the cutoff frequency for gravity to the value, $\omega_c < 7\times10^7$ s^{-1}, or between 10-100 MHz.

A higher frequency greatly overshoots the cosmological constant, Λ, and induces extreme curvature in the universe. This problem has been cited frequently and stated most bluntly as either ZPF or the cosmological constant requires revision. The relevance here arises from similarly large positive coupling terms in quantum gravity [15], which also generate a local gravitational instability for typical upper limits on the cosmological constant, $\Lambda/8\pi G < 10^{12}$ cm^{-4}.

Rather than to dwell on the inconsistencies that plague attempts to reconcile quantum gravity, we particularize the problem to a case where the restriction to Planck scale becomes less clear, namely the high density fluctuations and universal scaling introduced in a Bose condensate. A Bose condensate, such as superfluid helium or superconductors [15-19], becomes of potential interest, mainly because of its arbitrarily dense boundaries and the classic Casimir experiment [20-22] which allows such dense material boundaries (two closely spaced conducting plates), if available, to modulate the background quantum fluctuation of ZPF. In other words, the matter-ZPF interaction becomes measurable by the observed attraction between two material boundaries. What dense boundaries might generate in Bose condensates remains a subject of greate interest.

The significant case to investigate is whether Casimir-like interactions [20-22] will not only couple to ZPF radiation at a scale comparable to the quantum noise (or other radiation field), but also alter the value imposed by the Sakharov condition for G. It remains an open question whether this potential coupling interaction shares, as in ordinary critical phenomenon, the density correlation function, Φ, that is both independent of the coupling strength (or universal in renormalization) and consistent with the observed average energy density of the visible universe.

Thus the purpose here has been to restate the Sakharov condition in the gravitational coupling constant, G, based on its only free parameter, a frequency cutoff, ω_c. Any potential relevance arises from similarly large values for the positive coupling term in quantum gravity, which generate conditions for a local

gravitational instability for typical upper limits on the cosmological constant, $\Lambda/8\pi G<10^{12}$ cm^{-4}.

To restate the Sakharov condition, matter in the vacuum provides boundaries for reduced 'Casimir-like' modes available for otherwise isotropic radiation from quantum fluctuations (broad spectral noise). That this view reproduces Einstein gravity has been examined, including the full relativistic derivation [4-5]. The details of the appropriate mass, however, remain buried in the kinetic energy of general internal particle ('parton') motion [3]. Any appeal to a specific parton representation is limited only by essentially free particles with high-frequency interactions, including underlying partial charges or dense bosons. The basis of considering arbitrarily high density fluctuations in Bose condensate in analogy to the ZPF-Casimir experiment remains both an empirical and theoretical case to examine. There exist laboratory scale cases [15-19] where resonant radiation in the required 10-100 MHz range appear to produce anomalous effects for such Bose condensates as superconductors, but further work to confirm these results would be needed. In other contexts, these effects have been discussed as the Schiff-Barnhill effect for superconductors interacting with a gravitational field [23], but for the static rest mass rather than an effective mass in a conduction band.

Experimental Propositions

J. Weber [24,25] proposed the use of a superconducting Bose condensate for gravity wave detection, principally because of its potentially higher signal-to-noise ratio in carrying electrical signals upon length dilations in a relativistic framework for gravity waves travelling near the speed of light. W. Weber and Hickman [26] derived an experimentally testable relation based on torquing of a charged capacitor parallel to a gravity field, with

$$\tau=2E_g/\pi\,[\alpha/(1-\alpha)^{1/2}],$$

where the capacitor will rotate relative to the gravity vector, for $\alpha=2GM/rc^2$, r is Schwarzschild radial coordinate [$dR=dr(1-\alpha)^{1/2}$], E_g is dependent on the capacitor charge and geometry of the plates, $E_g=Q^2d/[2\varepsilon WL(1-\alpha)^{1/2}]$, for a plate separation, d, and radial dimensions, W and L, charge Q, and ε the permittivity of free space. For plate separations of 2 mm on Earth, the maximum torque is approximately $\tau=10^{-12}$ Nm, when charged to 2/3 dielectric breakdown. While not entirely promising for detection of such low torques, the large separation (2 mm) distance between capacitative plates naturally prompts generalization to the classic Casimir force [21] experiments only recently confirmed experimentally [20]. In particular, we rewrite the torque values to include the frequency terms derived with the Sakharov condition [$G=(\pi c^5/\hbar\omega_c^2)$]:

$$\alpha=2\,M\,\pi c^3/\hbar\omega_c^2 r$$

The appeal of this formulation is that a frequency dependent torque is derived, which further makes contact with proposals to modulate the Casimir capacitative plates for continuous extraction of energy [27]. This result requires further investigation experimentally, particularly to compare with previous reports for anomalies in AC-tuned electrical capacitors [28].

References

[1] Zel'dovich, Ya. B. JETP Letters, 6, 345, 1967.

[2] Sakharov, A. Vacuum quantum fluctuations in Curved Space and the Theory of Gravitation, Sov. Phys. Doklady, 12, 1968, 1040-1041.

[3] Puthoff, H. E. (1989) Gravity as a zero-point-fluctuation force, Physical Review A, 39(5):2333-2342, March 1, 1989.

[4] Haisch, B., Rueda, A., and Puthoff, H. E. (1994) Inertia as a Zero-Point Field Lorentz Force, Physical Review A, 49:678-694.

[5] Haisch, B.. A. Rueda, H.E. Puthoff, "Inertia as a Zero-Point Field Force" Physical Review A 4 9, Nr 2, 678 (1994).

[6] Ambjørn, J. and Wolfram, S. (1983) Properties of the Vacuum, 1. Mechanical and Thermodynamic, and Properties of the Vacuum, 2. Electrodynamic, Annals of Physics,

[7] AmbjØrn, J. and Wolfram, S. (1983) Properties of the Vacuum. I. Mechanical and Thermodynamic, Annals of Physics, 147:1-32.

[8] Fulcher et al., "The Decay of the Vacuum," Sci. Am., vol. 241, p. 150, Dec. 1979

[9] Puthoff, H.E. "Source of Vacuum Electromagnetic Zero-Point Energy" Physical Review A 4 0, 4857 Nov 1 (1989); Errata and Comments,Physical Review A 4 1, March

1(1990); Physical Review A 4 4, 3382, 3385 (1991).
[10] Senitzky, I. R.,"Radiation-Reaction and Vacuum Field Effects in Heisenberg - Picture Quantum Electrodynamics," Phys. Rev. Lett. 31(15), 955 (1973). As pointed out by Puthoff [3} the relativistic results for the Sakharov condition have so far been encouraging, while the consequences for nuclear interactions in all coordinate frames have not been fully explored.
[11] da Costa, L. N., Freudling, W., Wegner, G., Giovanelli, R., Haynes, M. P., and Salzer, J. J. (1996) The Mass Distribution in the Nearby Universe, Astrophysical Journal Letters, 468: L5-L8 and Plate L1
[12] Modanese, G. (1996) Theoretical analysis of a reported weak gravitational shielding effect, Europhy. Lett., 35(6):413-418.
[13] Shupe, M.A. The Lorentz-invariant vacuum media, Am. J. Phys. 53, 122 (1985). A cautionary note is that lower frequency cutoffs can violate Lorentzian invariance, thus allowing a moving detector to reveal absolute motion by recording Doppler-shifted frequencies. Standard methods might treat such effects like the cancellation of terms that remove anomalous ZPF infinities from field theories, but these topics remain to be explored.
[14] Zee, A.Phys. Rev. Lett., 42,417 (1979); Phys. Rev. D. 23, 858, (1981).
[15] Torr, D. G. and Li. N. (1993) Gravitoelectric-Electric Coupling vVia Superconductivity, Foundations of Physics Letters, 6(4):371-383.
[16]Unnikrishnan, C. S. (1996) Does a superconductor shield gravity?, Physica C, 266:133-137.
[17] Podkletnov, E. and Nieminen, R. (1992) A Possibility of Gravitational Force Shielding by Bulk $YBa_2Cu_3O_{7-x}$ Superconductor, Physica C, C203:441-444.
[18]Li, N. and Torr, D. G. (1992) Gravitational effects on the magnetic attenuation of superconductors, Physical Review B, 46(9):5489-5494. A simple consequence of the Sakharov condition, $G=(\pi c^5/h\omega_c^2)\sim 1/\int \omega\, d\omega$, can be written for the gravitomagnetic permeability as:
$\mu_g=4\pi G/c^2=4\pi^2c^3/(h\int_o^{\infty}\omega d\omega)\sim 1/\int \omega\, d\omega$
which suggest that the same frequency resonance implied by the ZPF derivation will share similar consequences for vector gravity effects. See also, DeWitt, B.S. Superconductors and Gravitational Drag, Phys. Rev. Lett. 16, 1092 (1966).
[19] Li, N., Noever, D., Robertson, T., Koczor, R., and Brantley, W. (1997) Static Test for a Gravitational Force Coupled to Type II YBCO Superconductors, Physica C, 55, 287.
[20] Lamoreaux, S. K. (1997) Demonstration of the Casimir Force in the 0.6 to 6 μm Range, Phys. Rev. Letters, 78:5-8.
[21] Milonni, P.W. et al., "Radiation pressure from the vacuum: Physical interpretation of the Casimir force", Phys. Rev. A, Vol. 38, No. 3, 1621 August 1988.
[22] Milonni, P. W. (1994) The Quantum Vacuum, Academic Press, San Diego, CA.
[23] Schiff, L.I. and Barnhill, M.V. Bull. Am. Phys. Soc. 11, 96, (1966) and refn. 18.
[24]Weber, J. (1960), Detection and Generation of Gravitational Waves, Physical Review, 117(1):306-313.
[25]Weber, J. (1966) Gravitational Shielding and Absorption, The Physical Review (The American Physical Society), 146(4):935-937.
[26] Weber, W. and Hickman, H. (1997)A possible interaction between gravity and the electric field, Spec. Science Tech. 20, 133-136
[27]Forward, R.L."Extracting electrical energy from the vacuum by cohesion of charged foliated conductors" Phys. Rev. B, Vol. 30, No. 4, 1700 August 1994
[28]Woodward, J. F. (1992) A Stationary Apparent Weight Shift From a Transient Machian Mass Fluctuation, Foundations of Physics Letters, 5:425-442.

Breakthrough propulsion physics research program

Marc G. Millis

Citation: AIP Conference Proceedings **387**, 1297 (1997); doi: 10.1063/1.51939
View online: http://dx.doi.org/10.1063/1.51939
View Table of Contents: http://aip.scitation.org/toc/apc/387/1
Published by the American Institute of Physics

BREAKTHROUGH PROPULSION PHYSICS RESEARCH PROGRAM

Marc G. Millis
NASA Lewis Research Center
21000 Brookpark Rd., Cleveland, OH 44135
(216) 977-7535
marc.millis@lerc.nasa.gov

Abstract

In 1996, a team of government, university and industry researchers proposed a program to seek the ultimate breakthroughs in space transportation: propulsion that requires no propellant mass, propulsion that can approach and, if possible, circumvent light speed, and breakthrough methods of energy production to power such devices. This Breakthrough Propulsion Physics program, managed by Lewis Research Center, is one part of a comprehensive, long range Advanced Space Transportation Plan managed by Marshall Space Flight Center. Because the breakthrough goals are beyond existing science, a main emphasis of this program is to establish metrics and ground rules to produce near-term credible progress toward these incredible possibilities. An introduction to the emerging scientific possibilities from which such solutions can be sought is also presented.

INTRODUCTION

In 1996, Marshall Space Flight Center (MSFC) was tasked to formulate a comprehensive strategic plan for developing space propulsion technology for the next 25 years. This "Advanced Space Transportation Plan" spans the nearer-term launcher technologies all the way through seeking the breakthroughs that could revolutionize space travel and enable interstellar voyages.

New theories and phenomena have emerged in recent scientific literature that have reawakened consideration that such breakthroughs may be achievable. To establish a program to address these visionary possibilities, a "Product Definition Team" of researchers was assembled. This team, led by NASA Lewis Research Center, consisted of 19 individuals from various NASA Centers, other government laboratories, industries, and academia (listed in acknowledgments section). Most team members are part of an existing informal network that had already recognized the potential of the emerging science and had conducted preparatory research on how to apply these prospects to the goal of creating revolutionary propulsion.

To anchor the program in real and tangible terms, the team configured the program to produce near-term, credible, and measurable progress toward determining how and if such breakthroughs can be achieved -- credible progress to incredible possibilities. There is no guarantee that the desired breakthroughs are achievable, but it is possible to produce progress toward a goal without first proving it is achievable. This paper introduces how this program aims to answer these challenges as well as giving a brief introduction to the emerging physics which reawakened interest in these visionary ambitions.

SPECIFYING GOALS AND SCOPE

To focus the program, the first step is to specify what breakthroughs are genuinely required to revolutionize space travel. A NASA precedent for systematically seeking revolutionary capabilities is the "Horizon Mission Methodology" (Anderson 1996). This method forces paradigm shifts beyond extrapolations of existing technologies by using *impossible* hypothetical mission goals to solicit new solutions. By setting impossible goals, the common practice of limiting visions to extrapolations of existing solutions is prevented. The "impossible" goal used in this exercise is to enable practical interstellar travel. Three major barriers exist to practical interstellar travel; propellant mass, trip time, and propulsion energy. To conquer these hurdles the following three propulsion breakthroughs are sought. These are the goals of the Breakthrough Propulsion Physics program:

CONF 970115

(1) Eliminate or dramatically reduce the need for rocket propellant. This implies discovering fundamentally new ways to create motion, presumably by manipulating inertia, gravity, or by any other interactions between matter, fields, and spacetime.
(2) Dramatically reduce trip time to make deep space travel practical. This implies discovering a means to move a vehicle at or near the actual maximum speed limit for motion through space or through the motion of spacetime itself. If possible, this means circumventing the light speed limit.
(3) Discover fundamentally new on-board energy production methods to power propulsion devices. This third goal is included in the program since the first two breakthroughs could require breakthroughs in energy generation to power them, and since the physics underlying the propulsion goals is closely linked to energy physics.

The scope of this program only covers seeking the genuinely needed breakthroughs rather than seeking refinements to existing solutions. As such, existing concepts that are based on firmly established science, such as light sails, magnetic sails, beamed energy, nuclear rockets, and antimatter rockets, are not part of this program. These concepts are being explored in other programs.

SCIENTIFIC FOUNDATIONS

New possibilities have emerged in recent scientific literature that have reawakened interest toward conquering the goals described above. These include theories that suggest that gravity and inertia are electromagnetic side effects of vacuum fluctuations (Haisch 1994 and Puthoff 1989), anomalous experimental evidence suggesting a possible gravity altering affect from spinning superconductors (Podkletnov 1992), theories suggesting that faster-than-light transport may be possible using wormholes (Morris 1988) or using warp drives (Alcubierre 1994), and a theory suggesting that sonoluminescence is evidence of extracting virtual photons from vacuum fluctuation energy (Eberlein 1996). These are in addition to older theories about creating propulsive effects without rockets (Bondi 1957 and Forward 1963).

In addition, there have been workshops (Bennett 1995, Evans 1990, and Landis 1990), recent surveys (Cravens 1990, Forward 1990, and Mead 1989), suggested research approaches (Cramer 1994, Forward 1984 and 1996, and Millis 1996), and even some exploratory experiments (Millis 1995, Schlicher 1995, and Talley 1991) on this subject. And recently, a non-profit society, the Interstellar Propulsion Society, was established to provide a collaborative forum to accelerate advancements toward these goals (Hujsak 1995).

PROGRAM CHALLENGES

Since the scientific principles do not yet exist from which to engineer the technological solutions to these challenges, new scientific principles are sought. Seeking such visionary and application-focused physics is not a usual activity for aerospace institutions, so this program faces both the technical challenge of discovering the desired breakthroughs and the programmatic challenges of how to conduct this work. To answer these challenges, the program will develop the research solicitation and selection criteria and the metrics for quantifying progress to meet the technical and programmatic challenges.

The technical challenges include: (1) focusing emerging theories and experiments to answer NASA's propulsion needs, (2) finding the shortest path to developing the breakthroughs amidst several, divergent and competing approaches, and (3) balancing the imagination and vision necessary to point the way to breakthroughs with the credible, systematic rigor necessary to make genuine progress.

The programmatic challenges include: (1) advocating such long range research amidst dwindling resources and stiff competition from nearer-term, more conservative programs, (2) creating confidence that research funded today will lead to the necessary breakthroughs, (3) selecting the most promising research tasks from the large number of divergent and competing approaches, and (4) conducting meaningful and credible research economically

PROGRAM PRIORITIES

To simultaneously focus emerging sciences toward answering the needs of space travel and to provide a programmatic tool for measuring progress and relevance, this program will develop prioritization criteria suitable for breakthrough-seeking research. These criteria help potential researchers to focus their work, and provide NASA with the means to quantify the relative benefit of competing research proposals. Examples of these criteria, which are still evolving, are presented below:

- APPLICABILITY: Research proposals that directly address a propulsive effect are given preference over those addressing basic science or supporting technologies.
- EMPIRICISM: Research proposals for experimental tests are given preference over proposals for analytical or theoretical work. Empiricism is considered to be a more direct indication of physical phenomena and experimental hardware is considered to be closer to becoming technology than pure theory.
- TARGETED GAIN: Research proposals that address large potential improvements in propulsive abilities are given preference over those of lesser potential improvements. This comparison can only be made between concepts that are of similar developmental maturity. Targeted gains include reducing trip time, reducing non-payload vehicle mass, reducing energy requirements, and reducing development cost.
- ACHIEVABILITY: Research proposals whose subjects are closer to becoming a working device are given preference over longer range developments. This comparison can only be made between concepts that are of similar propulsive ability.
- IMPACT: The more likely the research results will be used by others, the higher it is ranked.

Another criteria to be used is a "Traceability Tree." This tree is the reverse of a fault tree (a common tool used in accident risk assessments). Instead of branching out all the ways that a given accident can occur, the Traceability Tree branches out the conceivable paths to reach a propulsion breakthrough, Figure 1. This tool provides a means to measure how a given research task is linked to the end goals of discovering a propulsion breakthrough.

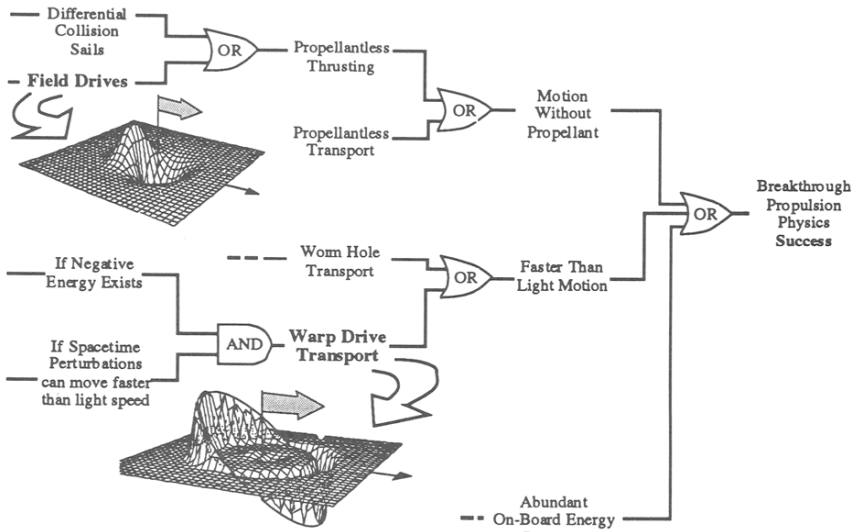

FIGURE 1. Illustrative Example of a Traceability Tree.

Another philosophy behind the NASA program is to support multiple small tasks rather than a single, larger task. Since the search for breakthrough propulsion physics is at an early stage, there are a large number of divergent and competing approaches. It is still too soon to tell which approaches will provide the shortest path to success. To cover the bases, a diverse program of multiple, small, and short-term projects is preferred.

To balance vision and imagination with credible systematic rigor, the NASA program is open to perspectives that go beyond or appear to contradict conventional theory, with the conditions that (1) the perspectives must be completely consistent with credible empirical evidence, (2) the utility of the alternate perspective must be clearly delineated, and (3) the make-or-break issues must be clearly identified to suggest the next-step research objectives.

There is another facet to this "beyond conventionalism." Institutions such as NASA routinely get numerous unsolicited submissions from individuals who claim to have a breakthrough device or theory. Frequently these submissions are too poorly conceived or incomplete, or too complex to be easily evaluated. To distribute this workload to other credible organizations and to keep an open mind to the possibility that one of these maverick inventors may have actually made a breakthrough, the following approach is suggested. Any individual who thinks they have a breakthrough device or theory is strongly advised to collaborate with a university or other educational institute to conduct a credible test of their claim. The university can propose the test as an educational student project, where the students will learn first-hand about the scientific method and how to apply systematic rigor and open-mindedness in conducting a credible test of an incredible claim. In such collaborations it is suggested that the inventors retain full intellectual property rights to their devices or theories, and that the universities make the proposal and receive all the funds to conduct the student projects. With this procedure, if the device or theory works, then supporting evidence would be established in a credible fashion and the originator would retain the intellectual property rights. If the device or theory does not work, then at least the students would have had a meaningful educational experience, and the concept's originator can work on another idea.

MEASURING PROGRESS

One of the challenges to this program is to demonstrate that research conducted today is making measurable progress directly toward the long-range targeted breakthroughs. The traceability tree and selection criteria presented earlier provides a means to demonstrate that a given research approach is linked to the end goals, but another metric is needed to quantify that progress is being made. To provide this measure, a more explicit version of the Scientific Method is used for measuring the level of advancement of a given scientific approach, similar to the way that the "Technology Readiness Levels" (Hord 1985) are used for quantifying technological progress. A draft of these scientific readiness levels is below:

- **Pre-Science**: Suggests a correlation between a desired effect and an existing knowledge base, or reports observations of unexplained anomalous effect.
- **Scientific Method Level 1, Problem Formulation**: Defines a problem specifically enough to identify the established knowledge base and the remaining knowledge gaps. A "problem" is an explicit statement of a desired goal (e.g. the 3 Breakthrough Propulsion Physics program goals) or explicit observations of an anomalous effect which cannot be explained using the established knowledge base.
- **Scientific Method Level 2, Data Collection**: Compiles relevant information to address a specific problem by experiment, observation, or mathematical proof.
- **Scientific Method Level 3, Hypothesis**: Suggests a mathematical representation of an effect or the relation between physical phenomena.
- **Scientific Method Level 4, Test Hypothesis**: Empirically tests a hypothesis by comparison to observable phenomena or by experiment.
- **Technology Readiness Level 1, Basic Principles Observed and Reported**: Equivalent to established science, where an effect has been observed, confirmed, and modeled sufficiently to produce a mathematical description of its operation.
- **Technology Readiness Level 2, Conceptual Application Designed.**
- **Technology Readiness Level 3, Conceptual Design Tested Analytically or Experimentally.**

STATUS AND DIRECTION

A government steering group containing members from various NASA centers, DOD and DOE laboratories has been established to develop the research solicitation and selection criteria to meet the programmatic and technical challenges. These criteria are to be in place by mid 1997, in time for the next program milestone; a kick-off workshop. The invitation-only workshop will examine the relevant emerging physics and will produce a list of next-step research tasks. If the workshop successfully demonstrates that promising and affordable approaches exist, funding may be granted to begin conducting the step-by-step research that may eventually lead to the breakthroughs.

CONCLUSIONS

New theories and laboratory-scale effects have emerged that provide new approaches to seeking propulsion breakthroughs. To align these emerging possibilities toward answering the propulsion needs of NASA, a research program has been established that focuses on producing near term and credible progress that is traceable to the breakthrough goals.

Acknowledgments

Special thanks is owed to the Product Definition Team who helped shape this program: Team Leader; Marc G. Millis, NASA Lewis Research Center: Team Members: Dana Andrews, Boeing Defense and Space Group; Gregory Benford, University of California, Irvine; Leo Bitteker, Los Alamos National Labs; John Brandenburg, Research Support Instruments; Brice Cassenti, United Technologies Research Center; John Cramer, University of Washington, Seattle; Robert Forward, Forward Unlimited; Robert Frisbee, NASA Jet Propulsion Lab; V.E. Haloulakos, McDonnell Douglas Aerospace; Alan Holt, NASA Johnson Space Flight Center; Joe Howell, NASA Marshall Space Flight Center; Jonathan Hujsak, Interstellar Propulsion Society; Jordin Kare, Lawrence Livermore National Labs; Gregory Matloff, New York University; Franklin Mead Jr., Phillips Labs, Edwards Air Force Base; Gary Polansky, Sandia National Labs; Jag Singh, NASA Langley Research Center; Gerald Smith, Pennsylvania State University; and to the Lewis Research Center volunteers; Michael Binder, Gustav Fralick, Joseph Hemminger, Geoffrey Landis, Gary S. Williamson, Jeffrey Wilson, and Edward Zampino.

References

Alcubierre, M. (1994) "The Warp Drive: Hyper-fast Travel Within General Relativity," *Classical and Quantum Gravity*, 11:L73-L77.

Anderson, J. L. (1996) "Leaps of the Imagination: Interstellar Flight and the Horizon Mission Methodology," *Journal of the British Interplanetary Society*, 49:15-20.

Bennett, G., R. L. Forward, and R. Frisbee (1995) "Report on the NASA/JPL Workshop on Advanced Quantum/Relativity Theory Propulsion," AIAA 95-2599, *31st AIAA/ASME/SAE/ASEE Joint Propulsion Conference*.

Bondi, H. (1957) "Negative Mass in General Relativity," *Reviews of Modern Physics*, 29:423-428.

Cramer, J., R. L. Forward, M. Morris, M. Visser, G. Benford, and G. Landis (1994) "Natural Wormholes as Gravitational Lenses," *Physical Review D*, 15 March 1995:3124-3127.

Cravens D. L. (1990) "Electric Propulsion Study," Report # AL-TR-89-040, Air Force Astronautics Lab (AFSC), Edwards AFB, CA

Eberlein, C. (1996) "Theory of Quantum Radiation Observed as Sonoluminescence," *Phys Rev A*, 53:2772-2787.

Evans, R. A., ed. (1990) *BAe University Round Table on Gravitational Research*, Report on Meeting held in Preston UK, March 26-27, 1990, Report # FBS 007, British Aerospace Limited, Preston, Lancashire, UK.

Forward, R. L. (1963) "Guidelines to Antigravity," *American Journal of Physics*, 31:166-170.

Forward, R. L. (1984) "Extracting Electrical Energy from the Vacuum by Cohesion of Charged Foliated Conductors," *Physical Review B*, 15 AUG 1984 :1700-1702.

Forward, R. L. (1990) "21st Century Space Propulsion Study," Report # AL-TR-90-030, Air Force Astronautics Lab (AFSC), Edwards AFB, CA.

Forward, R. L. (1996) "Mass Modification Experiment Definition Study," Report # PL-TR-96-3004, Phillips Lab, Edwards AFB, CA

Foster, R. N. (1986) *Innovation; The Attacker's Advantage*, Summit Books.

Haisch, B., A. Rueda, and H. E. Puthoff (1994) "Inertia as a Zero-Point Field Lorentz Force," *Physical Review A*, 49:678-694.

Hord, R. M. (1985) *CRC Handbook of Space Technology: Status and Projections*, CRC Press, Inc. Boca Raton, FL.

Hujsak, J. T. and E. Hujsak (1995) "Interstellar Propulsion Society," Internet address: http://www.tyrian.com/IPS/.

Landis, G. L., ed. (1990) "Vision-21: Space Travel for the Next Millennium," Proceedings, NASA Lewis Research Center, April 3-4 1990, NASA CP 10059, NASA Lewis Research Center.

Mead, F. Jr. (1989) "Exotic Concepts for Future Propulsion and Space Travel," *Advanced Propulsion Concepts, 1989 JPM Specialist Session*, (JANNAF), CPIA Publication 528:93-99.

Millis, M. G. and G. S. Williamson (1995) "Experimental Results of Hooper's Gravity-Electromagnetic Coupling Concept," NASA TM 106963, Lewis Research Center.

Millis, M. G. (1996) "The Challenge to Create the Space Drive," NASA TM 107289, Lewis Research Center.

Morris, M. and K. Thorne (1988) "Wormholes in Spacetime and Their Use for Interstellar Travel: A Tool for Teaching General Relativity," *American Journal of Physics*, 56:395-412.

Podkletnov, E. and R. Nieminen (1992) "A Possibility of Gravitational Force Shielding by Bulk $YBa_2 Cu_3 O_{7-x}$ Superconductor" *Physica*, C203:441-444.

Puthoff, H. E. (1989) "Gravity as a Zero-Point-Fluctuation Force," *Phys Rev A*, 39:2333-2342.

Schlicher R. L., A. W. Biggs, and W. J. Tedeschi (1995) "Mechanical Propulsion From Unsymmetrical Magnetic Induction Fields," AIAA 95-2643, *31st AIAA/ASME/SAE/ASEE Joint Propulsion Conference*.

Talley, R. L. (1991) "Twenty First Century Propulsion Concept," Report # PL-TR-91-3009, Phillips Laboratory, Air Force Systems Command, Edwards AFB, CA.

A01-34134

AIAA 2001-~~4092~~ 3359

Measurement of Repulsive Quantum Vacuum Forces

J. Maclay
Quantum Fields LLC
Richland Center WI

J. Hammer and Rod Clark
MEMS Optical
Huntsville, AL

M. George and L. Sanderson
University of Alabama
Huntsville, AL

R. Ilic
Cornell University
Ithaca, NY

Q. Leonard
University of Wisconsin at Madison
Stoughton, WI

37th Joint Propulsion Meeting
8-11 July 2001
Salt Lake City, Nevada

AIAA-2001-4092

MEASUREMENT OF REPULSIVE QUANTUM VACUUM FORCES

Jordan Maclay, Principal Scientist, Member, Quantum Fields LLC, Richland Center WI 53581
Jay Hammer, Senior Engineer, MEMS Optical Inc., 205 Import Circle, Huntsville AL 35806
Michael A. George, Assoc. Professor, Lelon Sanderson, Research Assistant, Department of Chemistry, University of Alabama at Huntsville, Huntsville, AL 35899
Rob Ilic, Research Assistant, Department of Applied Physics, Cornell University, 212 Clark Hall, Ithaca NY 14853
Quinn Leonard, Laboratory Manager, Univ.of Wisc.-Madison, Center for NanoTechnology, Stoughton, WI 53558
Rod Clark, President, MEMS Optical Inc., 205 Import Circle, Huntsville AL 35806

ABSTRACT

Quantum electrodynamics predicts that empty space (the quantum vacuum) contains a large amount of energy that corresponds to the lowest energy state (energy >0) of the electromagnetic field. Surfaces in the vacuum can experience forces that arise from the disturbance in the vacuum energy. The presence of attractive "Casimir" forces between uncharged, parallel, metal plates has been accurately verified in the last several years. Theoretical calculations have suggested the presence of repulsive vacuum forces for certain geometrical configurations. Here we describe an experiment in progress that is designed to determine if repulsive vacuum forces exist. In the experiment we measure the force exerted on a 200 um diameter metallized sphere mounted on an Atomic Force Microscope (AFM) that is placed very close to an array of gold microcavities. Observing a repulsive force on the sphere would verify the existence of repulsive forces. The ability to create attractive and repulsive vacuum forces by means of the geometry of the surfaces may permit the construction of devices that use ubiquitous vacuum energy in ways that assist with the space travel mission of NASA.

INTRODUCTION

Understanding the nature of vacuum forces and vacuum energy and how to manipulate this energy to obtain desired forces is a prerequisite to using these ubiquitous natural resources in any space application[1]. The theory for vacuum forces and quantum vacuum energy comes from Quantum Electrodynamics (QED), the theory of the interaction of matter and light[2]. **The role of the quantum vacuum is pervasive in modern physics. For example, it is involved in the calculation of atomic energy levels, the magnetic moment of the electron, the mass of elementary particles, spontaneous emission, dispersion forces between molecules, the large-scale structure of space-time.**

The experiment discussed in this paper is part of a three-year effort to begin to build, step by step, the knowledge base necessary for vacuum engineering. Our objective is to develop theoretical models of elementary systems that utilized vacuum forces and energy, to understand how these models behave, and then to explore some of these models experimentally. Since the critical dimensions required for these devices are typically micron to submicron, the experimental research utilizes microfabrication technology, and the methods developed for MicroElectro-Mechanical Systems (MEMS).

In space applications the application of vacuum energy systems might be power generation, propulsion itself, or the manipulation of the metric of space-time itself by the creation of regions of positive and negative energy density[3]. It is too early to determine if such developments are possible or to be able to clearly determine the role of vacuum energy in future space applications. If we can develop technologies for space travel that utilize vacuum energy, it is very convenient since this energy is pervasive throughout the universe.

Fifty years ago, Casimir predicted that the modifications to the vacuum energy arising from the presence of two uncharged, parallel, metal plates would cause the plates to attract each other. This attractive Casimir force varies as the inverse fourth power of the separation. At a separation of 10 nm the force/area is about 1 atm. In 1997 the prediction of Casimir was verified for the first time. In 1998 precision measurements corroborated the predictions of an attractive vacuum force between neutral parallel plates to an accuracy of several percent. **In March 2001, scientists at Lucent Technology used attractive parallel plate vacuum forces (Casimir forces) to actuate a MEMS torsion device[4]. Other MEMS devices using vacuum energy have been proposed. [5]**

Recent calculations have indicated that forces due to the quantum vacuum predicted by QED depend very strongly on the geometry of surfaces. For certain rectangular metal cavities, QED predicts the existence of repulsive forces on the walls of the cavity[6]. **In this paper we describe the current status of the first experiment specifically designed to measure repulsive forces due to modifications in vacuum energy density achieved by using metal surfaces.** The vacuum force is measured by means of an Atomic Force Microscope using a 200 um diameter metallized ball placed on the end of a calibrated cantilever. Our model suggests that a repulsive force on the ball would be observed when it approaches within 10's of nanometers from the top of an array of rectangular cavities, each of which is 100nm across and 1 um deep, patterned in gold using x-ray photolithography (Figure 2). For small separations between the surface of the sphere and the top of the cavity array, we are approximating an array of closed cavities, which, according to a QED calculation, exhibit repulsive forces. **The force between the sphere and the cavity array is modeled numerically, with heuristic approximations, to be compared to the measured force. It is important to note that no rigorous method has yet been developed to calculate the vacuum force between any two non-planar conducting surfaces using QED.** Only the parallel plate problem has been solved. Indeed there is some disagreement that a repulsive Casimir force should ever be present between two separate bodies[7]. Measurement of repulsive forces between separate conducting bodies may be expected to stimulate new developments in QED.

If our experiment verifies the existence of repulsive vacuum forces, then it may be possible to utilize repulsive forces as well as attractive vacuum forces in microelectro-mechanical systems (MEMS). The existence of attractive and repulsive Casimir forces might permit the development of a variety of novel MEMS devices of potential use to NASA.

Quantum Electrodynamics (QED), Vacuum Energy and Casimir Forces

Quantum Electrodynamics (QED), the theory of the interaction of electromagnetic fields and matter, has made predictions of atomic energy levels and electron magnetic moments that have been verified to 1 part in 10^{12}, which makes QED the most precisely verified theory in science[8,9]. In order to achieve this accuracy, QED predictions have to include the interaction of matter with "empty space" or, more accurately, the quantum vacuum[10].

Some predictions of QED are less enthusiastically received by the physics community than others. One of the confounding predictions of QED is an energy density in empty space that is many orders of magnitude greater that the energy density of matter itself[11]. For years this feature of QED was dismissed as of no physical significance. However, observable forces can result when surfaces are present that alter this vacuum energy density. About 50 years ago, Phillips Laboratory physicist H.G.B. Casimir predicted the presence of an attractive quantum vacuum force between neutral, parallel, metal plates[12]. In the last three years, experiments have accurately confirmed this prediction of QED for the first time, verifying the existence of attractive vacuum forces between conductive surfaces[13,14,4]. The parallel plate Casimir force goes as the inverse fourth power of the separation between the plates. At a separation of 100 nm the predicted force/area is equivalent to about 10^{-4} atm.; at 10 nm it is about 1 atm.

BACKGROUND

Since most aerospace researchers do not have backgrounds in quantum systems, we provide a brief background to motivate our study. It is certainly not obvious that there should be any energy at all in empty space, much less a very large amount! Nor is obvious why there should be forces due to the vacuum fluctuations. The evidence for this theoretical conclusion lies in numerous well verified experiments on atomic energy levels, the magnetic moment of the electron, the behavior of liquid helium, and the scattering of elementary particles[15].

Vacuum energy is a consequence of the quantum nature of the electromagnetic field, which is composed of photons. A photon of frequency ω has energy $\hbar\omega$, where $\hbar$ is Planck's constant. **The quantum vacuum can be interpreted as the lowest energy state (or ground state) of the electromagnetic (EM) field that occurs when all charges and currents have been removed, and the temperature has been reduced to absolute zero. In this state no ordinary photons are present. Nevertheless, because the electromagnetic field is a quantum system, like an atom, which has internal motion even at absolute zero, the energy of the ground state of the EM field is NOT zero.** Although the average value of the electric field $\langle E \rangle$ vanishes in the ground state, the Root Mean Square (RMS) of the field $\langle E^2 \rangle$ is **not** zero. Similarly the

RMS of the ground state magnetic field $\langle B^2 \rangle$ is not zero. Therefore the electromagnetic energy in the ground state, which from classical electrodynamics is proportional to $\langle E^2 \rangle + \langle B^2 \rangle$, is not zero. **A detailed theoretical calculation tells us that the electromagnetic energy in each mode of oscillation with frequency ω is $\frac{1}{2}\hbar\omega$, which equals one half of the amount of energy that would be present if a single "real" photon of that mode were present.** Adding up $\frac{1}{2}\hbar\omega$ for all possible modes of the electromagnetic field gives a very large number for the vacuum energy E_0 in the quantum vacuum:

$$E_o = \tfrac{1}{2}\sum_i \hbar\omega_i \qquad (0.1)$$

The resulting vacuum energy E_0 is infinity unless a high frequency limit is used.

Inserting surfaces into the vacuum causes the modes of the EM field to change. This change in the modes that are present occurs since the electromagnetic field must meet the appropriate boundary conditions at each surface[16]. **Surfaces alter the modes of oscillation and therefore the surfaces alter the energy density corresponding to the lowest state of the EM field.** In actual practice, the modes with frequencies above the plasma frequency do not appear to be significantly affected by the metal surfaces since the metal becomes transparent to radiation above this frequency. In order to avoid dealing with infinite quantities, the usual approach is to compute the finite change in the energy of the vacuum ΔE_0 due to the presence of the surfaces[17]:

$$\Delta E_0\left[\begin{matrix}change\cdot in\cdot vacuum\cdot\\ energy\cdot due\cdot to\cdot surfaces\end{matrix}\right] = E_0\left[\begin{matrix}energy\cdot in\cdot\\ empty\cdot space\end{matrix}\right] - E_S\left[\begin{matrix}energy\cdot in\cdot space\cdot\\ with\cdot surfaces\end{matrix}\right] \qquad (0.2)$$

where the definition of each term is given in brackets. This equation can be expressed as a sum over the corresponding modes:

$$\Delta E_0(due\cdot to\cdot surfaces) = \frac{1}{2}\sum_n^{\substack{empty\\ space}} \hbar\omega_n - \frac{1}{2}\sum_i^{\substack{surfaces\\ present}} \hbar\omega'_i \qquad (0.3)$$

The quantity ΔE_0, which is the change in the vacuum energy due to the presence of the surfaces, can be computed for various geometries. The forces F due to the quantum vacuum are obtained by computing the change in the vacuum energy for a small change in the geometry. For example, consider a hollow conducting rectangular cavity with sides a_1, a_2, a_3. Let $en(a_1, a_2, a_3)$ be the change in the vacuum energy due to the cavity, then the force F_1 on the side perpendicular to a_1 is:

$$F_1 = -\frac{\partial en}{\partial a_1} \qquad (0.4)$$

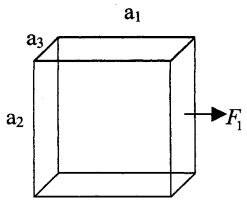

Figure 1. Geometry of rectangular cavity.

Equation (0.4) also represents the conservation of energy when the wall perpendicular to a_1 is moved infinitesimally[18]:

$$\delta en = -F_1\delta a_1 \qquad (0.5)$$

Thus if we can calculate the vacuum energy as a function of the dimensions of the cavity we can compute derivatives which give the forces on the surfaces. For uncharged parallel plates with a large area A, very close to each other, this equation predicts an attractive or negative force between the plates:

$$F_{att} = -\frac{\pi^2}{240}\frac{\hbar c}{d^4}A \qquad (0.6)$$

This force is called the parallel plate Casimir force, which was measured in three different experiments in the last three years[13,14,4]. The Casimir force has only been computed and measured for this very large parallel plate geometry.

QED makes some unexpected predictions about Casimir forces in other geometries that have never been verified. For conductive rectangular cavities, the vacuum forces on a given face can be repulsive (positive), attractive (negative), or zero depending on the ratio of the sides[6]. **We are particularly interested in measuring these repulsive Casimir forces. Verifying the existence of such forces would have important implications in quantum electrodynamics and would be an important step to utilizing Casimir forces in a variety of MEMS devices.**

DESCRIPTION OF THE EXPERIMENT

Atomic Force Microscope

It is not practical to directly measure the force on one wall of a submicron metallic cavity. Hence another approach is needed. We chose to use an Atomic Force Microscope (AFM), which can provide a very sensitive measure of forces into the piconewton range (10^{-12} Newton). The AFM employs a 300 um long micromachined silicon nitride cantilever with a 200 um metallized sphere on the end that can be used to probe the vacuum energy density in the neighborhood of a rectangular micromachined cavity with no top surface[19] (Figure 2). When the sphere experiences a force, the cantilever is deflected. The deflection of the sphere is measured by shining a laser diode onto the reflective surface of the cantilever. The reflected light is collected in a photodiode that is divided into two adjacent regions. As the spot of light moves during a deflection, the ratio of current from the two regions changes, giving a sensitive quantitative measure of the cantilever deflection. It is possible to measure deflections of several nanometers in this manner. The cantilever is calibrated by determining the cantilever deflection for a known electrostatic force. The high precision of this experiment is made possible by the use of a Molecular Imaging AFM system that was specially developed at the University of Alabama at Huntsville for vacuum operation. With the very small distance (much less than the mean free path of the molecules) between the sphere and cavity, gas molecules can become effectively trapped, taking hours to remove under vacuum. For the most reliable measurements it is necessary to remove the trapped molecules and operate at a sufficiently low vacuum. Trapped molecules may result in a squeeze film damping force because the cantilever is always vibrating slightly.

The AFM stage was connected to a vacuum flange with the necessary feedthroughs. The sample is mounted and aligned when the AFM is in air (Figure 3a). Then the AFM is inserted into the vacuum chamber and the flange bolted in place using copper gaskets (Figure 3b). The vacuum without the AFM is 10^{-8} torr; inserting the AFM reduces the vacuum to about 10^{-4} torr. The system is pumped with a turbo molecular pump and an ion pump. The AFM is housed in a clean room environment.

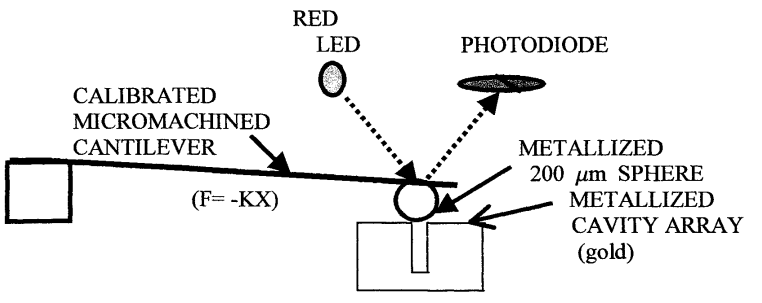

Figure 2. Schematic of Atomic Force Microscope measurement of the vacuum force between a metallized sphere on a cantilever and a rectangular cavity etched in gold (not to scale).

The force constant of the AFM cantilever is measured by using electrostatic forces. A know potential is applied between the test surface and the cantilever, and the deflection of the cantilever due to this potential is measured. The corresponding force is calculated using a finite element classical electrodynamic calculation. The system was tested by making measurements on the attractive Casimir force between the metallized sphere and a flat gold region and comparing these results to know values.

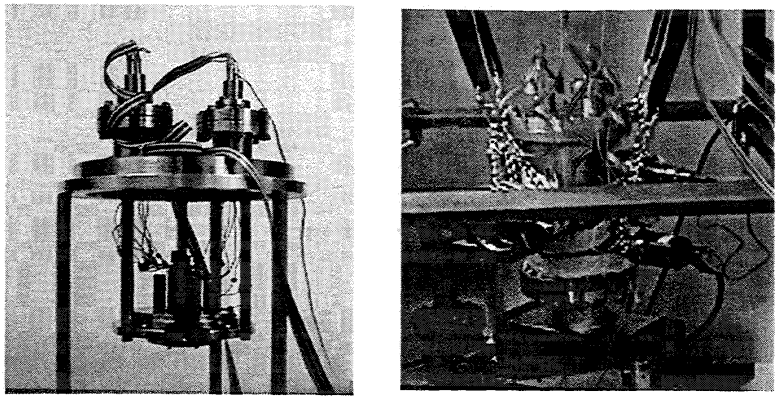

Figure 3. (a) shows the AFM stage below the vacuum flange, connected to the vacuum feedthroughs above. (b) shows the AFM mounted inside a small, stainless steel, vacuum chamber supported by elastic cords to reduce vibration.

Cavity Design

Numerical computations were done of the change in the vacuum energy and vacuum forces for a variety of rectangular cavities using QED methods[1,6]. The goal was to determine a cavity geometry that 1) would yield a large, detectable, repulsive force, 2) the repulsive force would change slowly with distance, and 3) that could be fabricated. The second requirement was deemed advisable to insure that the repulsive vacuum force would not vary too rapidly as the distance between the sphere and the opening of an etched rectangular cavity changed. The final cavity design selected was 0.1 um x 100 um x 1 um (width x length x depth), with walls that are 0.1 um thick.

Wisconsin Center for X-Ray Lithography. The cavity arrays fabricated are 100um x 100 um square, with cavity walls 0.5 um deep, with thickness t between 250 and 300 nm thick, and cavity widths w between 125 and 150 nm. Calibration surfaces for the AFM were also included in the design. The overall test pattern design is shown in Figure 4, and a portion of one of the cavity arrays closest to the target design is show in Figure 5.

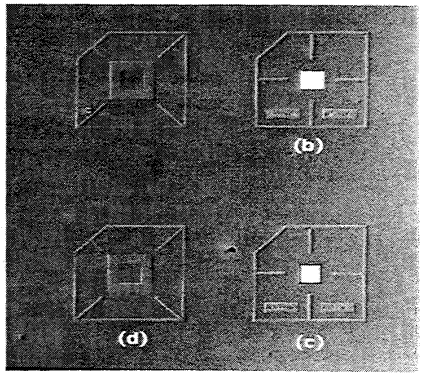

Figure 4. A SEM photograph of a portion of the test die, showing two 500 um square calibration patterns on the left, and two 500 um square cavity array regions on the right side. The center of each calibration pattern is a flat gold surface at the same level as the bottom of the cavities, surrounded by a gold surface at the level of the top of the array. The white regions on the right are the 100 x 100 um cavity arrays. The rectangular regions below the arrays indicate the nominal cavity width and wall thickness (50 x).

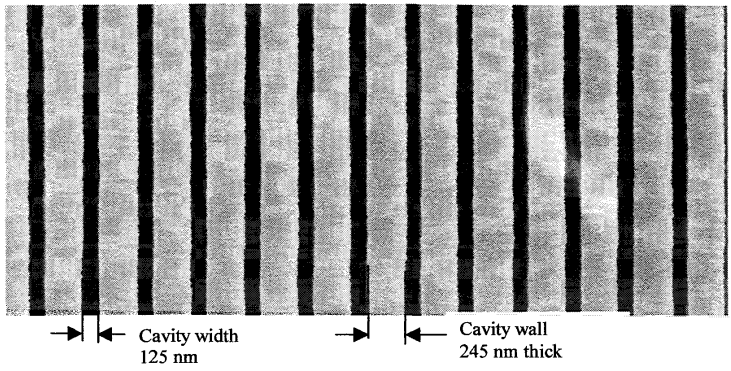

Figure 5. SEM photograph of portion of the gold cavity array. Each cavity is actually100 um long. The entire array is 100 um wide (magnification 37,000; 15kV).

Theoretical Modeling

As mentioned previously, no QED method has been developed to compute the vacuum forces between separate conducting surfaces. There is no theoretical model for such a configuration of two separate surfaces in the literature; no QED calculation of Casimir forces have been done except for planar or slightly rough planar surfaces. Hence we developed a heuristic model in which we assume the force on the sphere arises from two effects: 1) the attractive force due to the proximity of the sphere to the flat top surfaces of the cavity walls (parallel plate attractive Casimir force Eq 1.6), and 2) the repulsive forces on the sphere due to the cavity. The geometry of the experiment is shown in Figure 4.

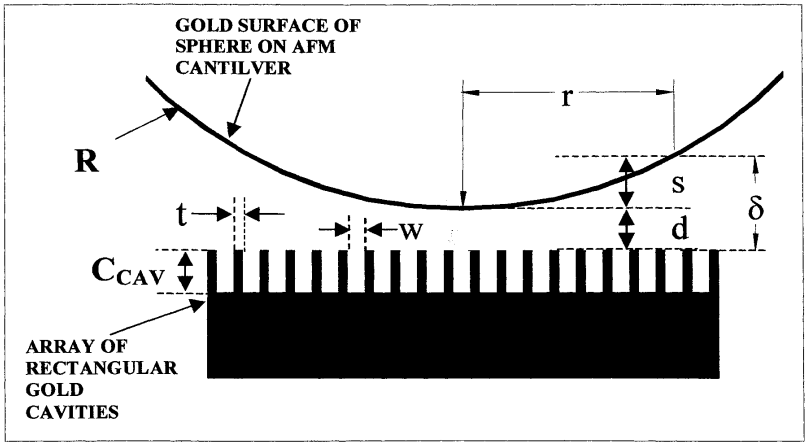

Figure 6. Distance definitions, illustrating actual cavity depth (C_{CAV}), individual cavity width (w), cavity wall thickness (t), separation distance (d), local sag (s), and local separation distance (δ).

The sphere has radius R. The closest point or tangent point of the sphere is located a distance d above the tops of the cavities. The local separation distance is $\delta = d + s$, where s is the local sag of the spherical surface. The quantity δ can be given as a function of r, the horizontal distance from the tangent point of the sphere. The expression for the attractive Casimir force Eq. 0.6 is actually derived for an infinite parallel plate geometry in which the lateral dimensions of the plates are much bigger than the spacing between the plates. Since this condition is not met for spacing d>t (width of cavity wall), we applied a correction factor to the attractive force, obtaining the expression for the attractive force:

$$F_{att}(r) = \frac{\pi^2}{240}\frac{\hbar c}{\delta(r)^4} A_w \left(\frac{t}{t+\delta(r)}\right) \qquad 0.7$$

where we used the local separation distance $\delta(r)$,. t is the thickness of the cavity wall, and A_w is the area of the tops of the cavity walls. The QED calculation of the repulsive Casimir force was for a closed, rectangular metallic box. Therefore we need a method to correct for the experimental geometry in which there is a gap at the top of the box. For the repulsive cavity force, we used the computed force for a closed cavity of width "w" with a depth equal to the actual depth (C_{CAV}), and multiplied it by an approximate correction factor K(r) suggested by theoretical analysis[20]:

$$K(r) = \left(\frac{C_{CAV}}{C_{CAV}+\delta(r)}\right)^3 \left(\frac{w}{w+\delta(r)}\right) \qquad 0.8$$

Eqs. 0.7 and 0.8 predict that both forces decay rapidly as the separation distance is increased. Rather than sum over individual cavities, we used an effective pressure distribution, which is an area-weighted combination of the cavity force and wall force. This provides a pressure distribution $p(r)$ over the surface of the sphere, where r is the radial coordinate. This pressure distribution depends on the geometry, including the separation distance, d.

To obtain the total force on the sphere, we integrated the pressure $p(r)$ on the bottom of the sphere due to the sum of the forces, i.e.,

$$F = \int_0^{R/2} 2\pi r p(r) dr \qquad 0.9$$

Figure 7 shows a plot of the force F as a function of the separation d for a cavity array with 1) the target dimensions, namely w= 0.1 um wide with t=0.1 um thick sidewalls and 1.0 um deep, and 2) the best actual cavity dimensions fabricated, namely w=0.125 um wide cavities with t=0.250 um sidewalls, 0.5 um deep.

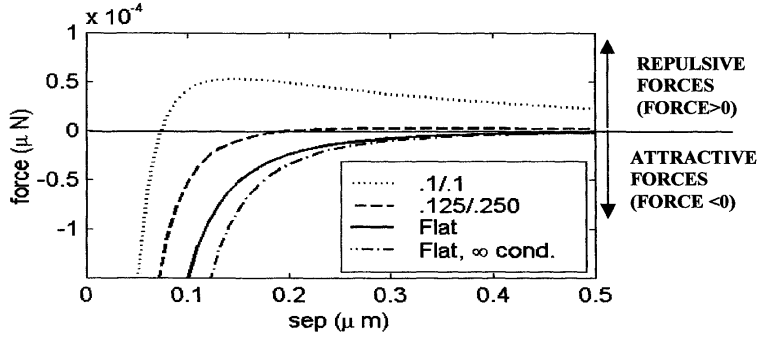

Figure 7. Force vs. distance d for a 100 um square cavity array with 1) the target dimensions, cavity width w = 0.1 um, wall thickness t=0.1 um, depth Ccav = 1.0 um deep; 2) the best fabricated cavity, width w=0.125 um, thickness 0.250, depth 0.5 um deep. The two uppermost curves show the force for the sphere above the cavity arrays. The solid curve shows the attractive force for a flat surface, with no cavities. Conductivity corrections are included. The sphere diameter is 210 um.

Also shown for comparison, is the calculated force (labeled Flat in the figure) for the case of a sphere over a flat surface, i.e. with no cavities at all in the gold. The known correction factors for finite conductivity for the force between parallel plates were used except for the curve labeled infinite conductivity. For the lack of any other theory, the same conductivity correction factors were applied to the cavity geometry.

For the parallel plate case, the force is always negative or attractive, and the force decreases rapidly (Eq 1.7 integrated over the hemisphere, or approximately as $-1/\delta^4$) with the separation δ. The component with upward curvature in the cavity array curve is due to the repulsive force (Eq 1.8 integrated over the hemisphere, which goes approximately as $1/\delta^3$). Because of the more rapid inverse variation of the attractive force, the attractive force dominates at very small separations d, going to zero more rapidly than the attractive force. Hence the repulsive force dominates at larger separations, above about 0.1 um. From QED we expect that smaller cavities would give larger repulsive forces; and thinner walls give smaller attractive forces. The predictions of the model show this desired behavior, and the model calculations appear to go smoothly into these known curves for flat surfaces. It appears that the repulsive force is on the edge of detectability for the cavities fabricated.

CONCLUSIONS

Quantum electrodynamics, which has made predictions which have been verified to 1 part in 10^{12}, predicts the existence of a large, ubiquitous, zero-point vacuum energy density in empty space. The question arises: Can we make use of this energy in some way to facilitate space travel, such as energy generation, propulsion, or creation of wormholes? It is too early to determine if such developments are possible or to be able to clearly determine the role of vacuum energy in future space applications. Our investigation begins with what we do know about vacuum energy, and extends those boundaries. We know that QED predicts that as a consequence of this energy, an attractive force will exist between uncharged, parallel, metal plates. In the last few years, accurate measurements have confirmed the existence of this force. QED also predicts the existence of repulsive forces in small rectangular metal boxes in which one dimension is much less than at least one of the other two dimensions. Although no one has done a rigorous calculation, it appears probable, based on theory, that a repulsive force should exist between two separate surfaces that closely approximate such a closed box. Vacuum forces that are repulsive because of the geometry have never been observed.

We have designed an experiment to measure repulsive vacuum forces. A model has been developed to predict the vacuum force on a metallized sphere attached to a cantilever on an AFM when the sphere is brought to within nanometer distances of an array of gold cavities. An AFM that operates in vacuum at 10^{-4} torr has been constructed to perform the experiment. Based on our model calculations, it appears we should be able to measure repulsive vacuum forces using the AFM, provided the cavities have small enough dimensions. Based on our model calculations (Figure 7) the cavities fabricated to date (125 nm width, 245 nm wall thickness) have dimensions that may be too large to provide a clear indication of a repulsive force. We need to utilize cavities with dimensions of approximately 100 nm width, 100 nm wall thickness in order to have a clear indication of repulsive forces. The University of Wisconsin Center for NanoTechnology is currently upgrading one of its synchrotron exposure systems in order to provide features of this size.

If we can obtain repulsive as well as attractive vacuum forces by a suitable choice of geometry, we are one step closer to being able to design a variety of novel MEMS devices using vacuum energy that could assist in attaining some of the NASA objectives for space travel.

Acknowledgements: GJM would like to thank Marc Millis and the NASA Breakthrough Propulsion Physics Program, MEMS Optical Inc., and Quantum Fields LLC for their support of this program, and Robert Forward, Peter Milonni, Carlos Villarreal, Gabriel Barton, and Michael Serry for helpful conversations. MG and LS would like to thank Molecular Imaging Inc. for their support development of a vacuum AFM. We would like to thank Hui Liu for taking SEM photographs and Jeff Meyer for assistance with microfabrication.

---

[1] J. Maclay, "A Design Manual for Micromachines using Casimir Forces: Preliminary Consideration," **PROCEEDINGS of STAIF-00** (Space Technology and Applications International Forum-2000, Albuquerque, NM, January, 1999), edited by M.S. El-Genk, AIP Conference Proceedings, American Institute of Physics, New York 2000. Published in hardcopy and CD-ROM by AIP.

[2] P. Milonni, *The Quantum Vacuum* (Academic Press, San Diego, CA, 1994).
[3] M. Visser, pp 81-87, *Lorentzian Wormholes: From Einstein to Hawking,* (American Institute of Physics, New York, 1996).
[4] Chan H B, Aksyuk V A, Kleiman R N, Bishop D J, and Capasso F, Quantum mechanical actuation of microelectromechanical systems by the Casimir force Science **291**, 1941-44 (2001).
[5] M. Serry, D. Walliser, J. Maclay, "The anharmonic Casimir oscillator (ACO)- the Casimir effect in a model microelectromechanical system," J. Microelectromechanical Systems **4**, 193-205 (1995).
[6] J. Maclay, "Analysis of zero-point electromagnetic energy and Casimir forces in conducting rectangular cavities," Phys. Rev. A, 61, 052110(2000)
[7] G. Barton, "Perturbative Casimir energies of dispersive spheres, cubes, and cylinders," J. Phys. A.: Mathematical and General **34,** 4083-114 (2001). Also personal communication from Dr. Barton, Boston 6/01.
[8] R. Van Dyck, Jr., P. Schwinberg, and H. Dehmelt, Phys Rev. Lett. **59**, 26 (1987).
[9] P. Milonni, p. 108, The *Quantum Vacuum* (Academic Press, San Diego, CA, 1994).
[10] J. Bjorken, and S. Drell, *Relativistic Quantum Fields*, McGraw-Hill, New York (1965)
[11] C. Misner, K. Thorne, J. Wheeler, p. 1203, *Gravitation*, W.H.Freeman, SanFrancisco (1973).
[12] [30] E.Elizalde and A.Romero, "Essentials of the Casimir effect and its computation," Am. J. Phys. **59**, 711-719 (1991). Also see reference 2, p.54.
[13] S. Lamoroux., " Measurement of the Casimir force between conducting plates," Physics Review Letters, **78**, 5-8 (1997).
[14] Mohideen, U., Anushree, Roy, "Precision Measurement of the Casimir Force from 0.1 to 0.9 micron", Physical Review Letters, **81**, 4549 (1998).
[15] See ref 2 for a discussion. Also it should be mentioned that these phenomena can be interpreted in an equivalent way in which we postulate that the effects are due to the fluctuational energy in the atoms involved in these experiments.
[16] J.D. Jackson, *Classical Electrodynamics*, Wiley, New York (1962)
[17] P. Plunian, B. Muller, W. Greiner, "The Casimir Effect," Physics Reports (Review Section of Physics Letters) **134**, 2&3, pp. 87-193 (1986).
[18] L. Brown, and J. Maclay, "Vacuum Stress between Conducting Plates: an image solution," Phys. Rev. **184**, 1272-1279 (1969). We assume absolute zero temperature.
[19] J. Maclay, R. Ilic, M. Serry, P. Neuzil, "Use of AFM (Atomic Force Microscope) Methods to Measure Variations in Vacuum Energy Density and Vacuum Forces in Microfabricated Structures," NASA Breakthrough Propulsion Workshop, Cleveland, Ohio, May, 1997.
[20] D.Deutsch and P. Candelas, "Boundary effects in quantum field theory," Phy. Rev. D **20**, 3063-3080 (1979).

A01-34535

AIAA 2001-3906
Search for Effects of Electric Potentials on Charged Particle Clocks

Harry I. Ringermacher
KRONOTRAN Enterprises LLC
Delanson, NY

Mark S. Conradi and Caleb D. Browning
Washington University
St. Louis, MO

Brice N. Cassenti
United Technologies Research Center
East Hartford, CT

37th AIAA/ASME/SAE/ASEE Joint Propulsion Conference and Exhibit
8-11 July, 2001
Salt Lake City, Utah

AIAA-2001-3906

SEARCH FOR EFFECTS OF ELECTRIC POTENTIALS ON CHARGED PARTICLE CLOCKS

Harry I. Ringermacher*
Mark S. Conradi and Caleb D. Browning †
Brice N. Cassenti‡

ABSTRACT

Results of experiment to confirm a theory that links classical electromagnetism with the geometry of space-time will be described. The theory, based on the introduction of a Torsion tensor into Einstein's equations and following the approach of E. Schrödinger, predicts effects on clocks attached to charged particles, subject to intense electric fields, analogous to the effects on clocks in a gravitational field. We show that in order to interpret this theory, one must re-interpret all clock changes – both gravitational and electromagnetic – as arising from changes in potential energy and not merely potential. The clock is provided naturally by proton spins in hydrogen atoms subject to Nuclear Magnetic Resonance trials. No frequency change of clocks was observed to a resolution of 6×10^{-9}. A new "Clock Principle" was postulated to explain the null result. There are two possible implications of the experiments: (a) The Clock Principle is invalid and, in fact, no metric theory incorporating electromagnetism is possible; (b) The Clock Principle is valid and it follows that negative rest mass cannot exist.

INTRODUCTION

The goal of the present work is to investigate an electromagnetic alternative to exotic physics for the purpose of coupling matter to space-time. Electromagnetic forces have distinct advantages. They are 10^{40} times stronger than gravity. They can be manipulated at will. Resources to create intense fields of virtually any geometry are readily available. However, there is currently no accepted theory linking electrodynamics directly with the geometry of space-time other than to curve it via extremely high energy densities. The mainstream approach taken is "bottom up", attempting to unite all forces in the context of quantum gauge field theory which has to-date been successful in unifying the weak and electromagnetic forces and describing the strong force in what is known as "the standard model". Gravity and therefore space-time geometry remains isolated from the internal geometry of gauge theory. If such a theory could be found and even its simplest predictions tested and verified, then there would be hope that electromagnetic coupling to space and time might be possible. This could lead to new interpretations and possibly new effects in gravitation and electromagnetism.

The experiments described in this work measure the predictions of a theory[1], linking space-time geometry and electrodynamics. This is grounded upon E. Schrödinger's later works on gravitation theory[2]. In his work, Schrödinger attempted to link electromagnetism to geometry through a non-symmetric affine connection (Torsion tensor). He failed at the attempt, primarily because of an error of oversight. The theory upon which the present work is based corrects this error[3], resulting in the definition of a new type of affine connection – an electrodynamic connection – that precisely matches Schrödinger's concepts.

THEORY

We describe a simplified theory and shall only write the new field equations and their solutions for the present case. The theory is summarized in the BPP final report*. The governing equations are:

$$G_{\mu\nu} = -\frac{\kappa}{2} u^{\sigma} (F_{\nu\sigma;\mu} + F_{\mu\sigma;\nu}) \qquad (1)$$

$$F^{\mu\tau}_{\ ;\tau} = 0 \quad ; \quad F_{\mu\nu;\sigma} + F_{\nu\sigma;\mu} + F_{\sigma\mu;\nu} = 0 \qquad (2)$$

$G_{\mu\nu}$ is the Einstein tensor. $F_{\mu\nu}$ is the Maxwell electromagnetic field tensor. u^{λ} is the test particle 4-velocity and $\kappa = -e/mc2$, the charge/mass ratio of the test particle. Greek indices range from 0, the time index, to 1,2,3, the space indices. Equation (1) is the modified Einstein equation including Electrodynamic Torsion. Equations (2) are the usual covariant Maxwell equations. Selecting a metric for an appropriate geometry results in a set of solvable differential

* KRONOTRAN Enterprises LLC, Delanson, NY 12053
† Washington University, St. Louis, MO 63130
‡ United Technologies Research Center, E. Hartford, CT 06108

* General Electric Corp. R&D Center, Schenectady, NY 12301

equations coupling the metric and electromagnetic field variables.

Ideal Experiment

The theory predicts that a particle of charge e, and mass m, immersed in a suitable electric field but unshielded and supported will see, in its rest frame, a time differing from the proper time of an external observer arising from the electrostatic potential at its location. In general, from the theory, the time shift in a clock interval is related to the potential difference between two points:

$$\frac{d\tau_2}{d\tau_1} = 1 + 2\kappa(\varphi_2 - \varphi_1) \tag{3}$$

This equation is exactly analogous to that for the gravitational red shift.

One possible clock for such a test is Nuclear Magnetic Resonance. A proton placed in an intense electric field within a radio-frequency transverse field "H_1" coil aligned orthogonally to a uniform magnetic field, H_0, is resonant at the Larmor frequency, $\omega = \gamma H_0$, where the gyromagnetic ratio, γ, for the proton spin is proportional to e/m. We thus have a natural clock. From eq. (3) we expect the proton's clock frequency to depend on its relative positions r_1 and r_2:

$$\omega(r_2) = \omega(r_1)\left[1 + 2\kappa(\varphi_2 - \varphi_1)\right] \tag{4}$$

The Larmor field distribution is then given by

$$H(r_2) = H(r_1)\left[1 + 2\kappa(\varphi_2 - \varphi_1)\right] \tag{5}$$

From this it is straightforward to calculate the NMR lineshape and shift that will result when the electric field is turned on as compared to the field off. Under ideal circumstances, for a supported proton in a 8T magnetic field with a 5kV/cm electric field, a line shift and broadening of approximately five parts per million is expected. The expected NMR lines are modeled in the "Experiments" section.

Present Approach

In practice it is experimentally difficult to "support" a charged particle. Generally, this can be accomplished electromagnetically, but then, by definition, the electric field and force at the particle location must vanish since the charge does not accelerate. The approach we have chosen uses the proton in a hydrogen atom. It is supported electromagnetically. The consequences of this approach will be the main subject of the conclusions of this work. A detailed description of the three experiments performed follows.

EXPERIMENTS

Three experiments were performed: A temporally and spatially constant potential applied to the proton in the hydrogen atom; A time-varying but spatially constant potential applied to the proton in the hydrogen atom; A hydrogen atom physically displaced through an intense electric field.

Experiment 1 – Constant potential

A 354 MHz, 8.4 Tesla NMR system was chosen for the experiments. This magnet has a field homogeneity of 0.1 ppm or about 35 Hz, more than sufficient to resolve small effects. The proton sample was Benzene. The initial experiment was a simple free induction decay (FID) with the E-field on vs. off. The sample was enclosed in a 2mm thick aluminum can (Fig. 1) placed at high potential. Thus the E-field will vanish in the interior of the can at the sample but there will remain a constant potential. The voltage terminal (sample chamber) could be set + or – with respect to ground and the NMR FID was monitored.

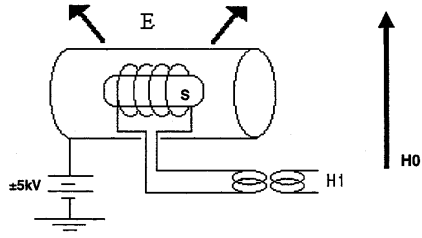

Figure 1. NMR "can" arrangement. External magnetic field, H0, is perpendicular to the radio frequency field, H1, applied through a coil wrapped around the proton sample, S. The 5kV electric field is applied outside the can leaving a constant 5kV potential inside.

A field homogeneity of 10 ppb was achieved for the 8.4T field, sufficient to resolve the smallest predicted effects. The observed line shift, was $\Delta\nu/\nu \le 0 \pm 1.0\text{x}10^{-9}$, consistent with a null prediction of both classical E&M and the present theory. The null result is consistent with both classical theory and the present one.

Experiment 2 - Time-varying potential

The second experiment, a time-varying potential applied to the proton in the hydrogen atom, was initially expected to produce an effect. However, it was found during the course of this program that this theory was also invariant under a pure time-varying potential[5], a result consistent with the classical "Lorentz gauge condition" which is the relativistic generalization of the Coulomb gauge condition. That is, it states that the potential is also arbitrary to an additive time-derivative of a scalar. Thus, a null result was also expected and was observed. A "spin-echo" experiment was performed to observe any phase shift introduced by the time varying electric field. Extreme care was taken to calibrate the system to ensure that any small phase shift could be identified and that stray currents would not affect the data. Upon application of a 5KV step-function (20 ms risetime) between the aluminum can and ground in both turn-on and turn-off modes, the observed shift in the NMR line was $\Delta\nu/\nu \leq 0 \pm 1.0 \times 10^{-11}$.

Experiment 3 - Physical displacement of Hydrogen atom through high electric field

For the third and final experiment, hydrogen in benzene at room temperature was gravity-flowed between two electrodes, an upper one at ground potential and a lower one at +5000 V, both situated in the NMR coil in the external 8.4T magnetic field while NMR was performed with the electric field on and off. The electrodes were copper discs placed in the 3mm I.D. of glass tubing and connected to a high voltage source through glass/epoxy seals. The electrode spacing was 1.0 cm giving an average electric field of 5000V/cm. The 2-turn NMR coil diameter was 1.5 cm ensuring that the HV region was inside the coil. The coil was untuned to avoid radiation damping since the signal was already very large. Figure 2 shows the NMR coil system arrangement and a photo of the open chamber.

An NMR FID experiment was performed with and without flow. A 20-30 ms T_2 was obtained by careful adjustment of the B-field shim coils. The NMR line and effects of flow without the presence of an E-field were modeled. The T_2 value gives a line width of approximately 17 Hz ($\Delta f = 1/\pi T_2$). Figure 3 shows the measured NMR line with voltage off as a function of flow velocity through the coil varying from 3 cm/s to 50 cm/s. Since the FID has a time constant of 20-30 ms, the proton must stay in the H1 field at least this long in order to contribute a significant time-shift signal arising from the maximum 5kV potential change. This corresponds to a flow speed of 15-30 cm/s, the mid-range of the chosen flows. Note that the measured shift with zero volts is approximately 10 Hz, from 0 to 50 cm/s flow rate, in approximate agreement with the theoretical calculation, Figure 3. Figure 4 shows the predicted lines for a maximum potential of 5000 Volts. The shift is at least ten times that for zero volts.

For the flow experiment, the NMR line was obtained for voltage off, voltage on, and a dummy voltage on (voltage on but HV cable disconnected). The probe voltage was discharged when the dummy experiment was performed. Figure 5 shows data for flows of 0, 3, 6, 12, 25 and 50 cm/s with the voltage applied .

We note in Figure 5 that there is no change in the line positions greater than the FFT resolution of $\pm$ 2 Hz corresponding approximately to a line shift of $\Delta\nu/\nu \leq 0 \pm 6.0 \times 10^{-9}$, at least a hundred times smaller than the predicted shift of Figure 4. Figure 3 is therefore representative of the results with applied field as well.

When the experiment was completed, the probe was disassembled and carefully inspected to ensure that all voltage connections were secure.

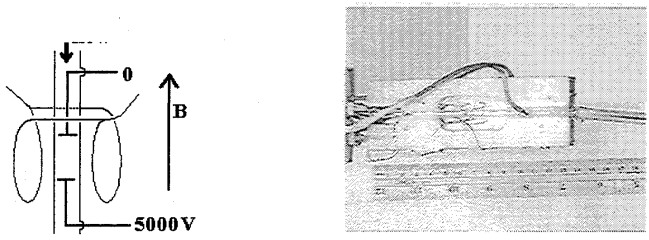

Figure 2. Diagram and photo of NMR coil and flow arrangement for E-field experiment

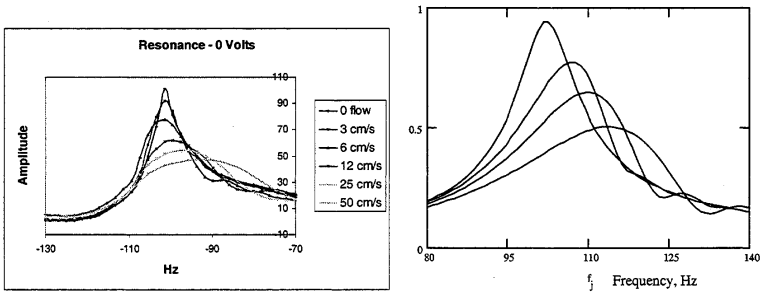

Figure 3. Measured NMR lines (left) and calculated (0,12,25,50 cm/s) for zero E-field and flows from 0 - 50 cm/s.

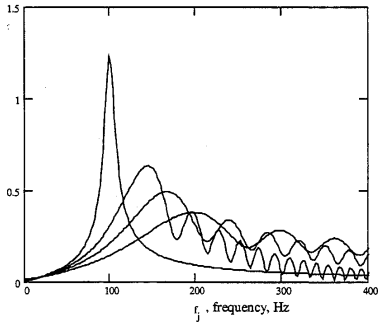

Figure 4. Calculated NMR lines for 5000V/cm E-field for flows of 0, 12, 25 and 50 cm/s.

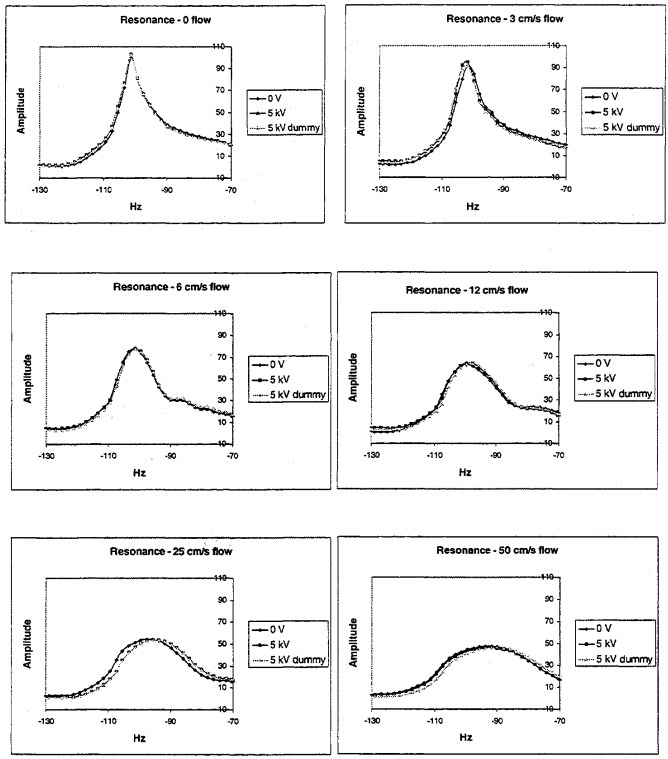

Figure 5. Measured variation in NMR line at 0, 6, 25 and 50 cm/s flow with applied voltage.

CONCLUSIONS

Experimental Conclusions

All three experiments showed null results. The first experiment, constant potential applied to the proton in the hydrogen atom, produced a null result as expected and explained earlier. The second experiment, a time-varying potential applied to the proton in the hydrogen atom, also produced a null result as expected and explained. From the second experiment we have learned that the present theory is relativistically Gauge Invariant in the context of Maxwell's equations – as it should be.

The third experiment, physical displacement of a proton in a hydrogen atom through an electric field, was expected to produce a frequency shift of 5ppm in the NMR line. No change was observed to high precision. This could be explained as follows. When a hydrogen atom is placed in an electric field, classically, only one effect is produced – an induced dipole moment of the atom resulting from the stretching of the electron orbital. Otherwise, no work is done on the hydrogen atom (except for the exceedingly small amount involved in stretching) since the work done on the proton is cancelled by the opposite work done on the electron(due to its negative charge) in the electric field. Furthermore, it is straightforward to show[4] that no work is actually done on the proton itself since the electric

force on it is precisely balanced by an opposing force, in the field direction, from the electron.

Implied Conclusions

If we substitute potential energy change and therefore work done rather than simple potential in the metric, then the fact that no work is done on the proton because of the electron's influence can explain the null result. We now discuss the relation of work to the metric.

Relation of the Metric to the Lagrangian and Work Done

Let $\tilde{L}$ be defined as the specific Lagrangian or Lagrangian per unit rest energy,

$$\tilde{L} = \frac{(T-V)}{mc^2} \tag{6}$$

where T, V and m are the kinetic energy, potential energy and rest mass of the test particle respectively.

Suppose we are at rest at some height z in a gravitational field, so that $T=0$ and $V=mgz$, then $\tilde{L} = gz/c^2$. We have shown for weak fields and nonrelativistic speeds that the proper time element can be written in terms of the Specific Lagrangian and coordinate time element as:

$$d\tau = \sqrt{1-2\tilde{L}}\, dt \tag{7}$$

This describes the behavior of clocks. Consider two positions in the gravitational field z_1 and $z_2 = z_1 + h$. Assume a proper time interval $d\tau_1$ at z_1 and $d\tau_2$ at z_2. Then, for weak fields:

$$\frac{d\tau_2}{d\tau_1} = 1 - \frac{gh}{c^2} \tag{8}$$

We can rewrite this in terms of potential energy and Lagrangian rather than potential;

$$\frac{d\tau_2}{d\tau_1} = 1 - \frac{mgh}{mc^2} = 1 - (\tilde{L}_2 - \tilde{L}_1) = 1 - \Delta\tilde{L} \tag{9}$$

In general, a variation in the Specific Lagrangian results in a change in the clock rate. Referring more concisely to the metric for a single particle, p, we may express the Lagrangian change more clearly in terms of the net conservative work, W_c, done on p.

$$\Delta\tilde{L}_p = 1 - \frac{(\Delta T - \Delta V)}{m_p c^2} = \frac{\Delta T_p + W_c}{m_p c^2} \tag{10}$$

The weak-field, non-relativistic, metric for a given particle, p, acted upon by forces and hence net conservative work, W_{cp}, done upon it by all other particles in the field is given by

$$d\tau_p^{\,2} = \left(1 - \frac{2W_{cp}}{mc^2}\right) c^2 dt_p^{\,2} - dx_p^{\,2} - dy_p^{\,2} - dz_p^{\,2}, \tag{11}$$

We have rewritten the metric in this way because potential is not well-defined except through potential energy and work, where it is defined as work per unit mass in gravitation and work per unit charge in electromagnetism.

The Clock Principle

In the previous section we found a simple Lagrangian formulation that places gravitation on an equal footing with our theory in regards to changes in the temporal portion of the metric. The Lagrangian formulation deals with kinetic and potential energy changes. Clocks raised in a gravitational field are at rest in the two positions and can be slowly moved between them. Thus the Lagrangian becomes simply the negative change of potential energy(work done on) of the clock, moved from the lower position to the upper. However, we must be careful and can no longer use the word "clock" loosely. When we refer to "clock" henceforth, we mean the *mechanism of the clock*. Thus we mean that work is performed on the *mechanism*. Clearly all clock mechanisms are driven by energy changes. What is not as obvious is that the mechanism of any clock must reflect the proper time variations in a gravitational field. For example, the mass-spring mechanism of a simple clock must somehow change with different heights in a gravitational field. Similarly, a pendulum clock must exhibit changes in its mechanism. Even an atomic clock is subject to this consideration. This brings us to the ***first clock postulate***:

1) Every clock has a mechanism which must be held accountable for observed changes in its measurement of time.

We shall now examine the relationship between work and changes in clock time in a gravitational field. We use the notation "nc" to mean nonconservative and "c" for conservative forces.

Einstein Rocket -- Equivalence Principle for clock changes in a Gravitational Field

We shall employ the famous Einstein rocket "gedanken-experiment" to demonstrate our concepts. Consider a rocket lifting a mass, m, by a stiff wire in a gravitational field. Let us suppose that we adjust its thrust to precisely oppose the graviational pull on the mass. The rocket-mass system is now balanced and hovers, for example, at the surface of the earth. An arbitrarily small external force, $\bar{\varepsilon}$, may now raise the system to a height, h. This is shown in Figure 7. The force $\bar{\varepsilon}$ does no work on the system since it can be made arbitrarily small. However, upon rising a height h, due to the infinitesimal assistance of the guiding force, the rocket does work on the mass m. The potential energy of the mass is V_1 at the surface and V_2 at height h.

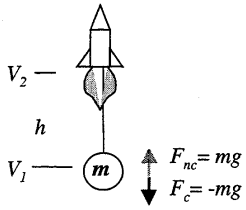

Figure 7. Balanced force configuration of a rocket-mass system

In this situation, the nonconservative force is that of the rocket. This is equal and opposite to gravity. We make the following definitions:

$$z_2 - z_1 = h \quad ; \quad d\bar{s} = dz\hat{k} \quad ; \quad \bar{g} = -g\hat{k} \tag{12}$$

Then the non-conservative work performed on the mass m by the rocket is

$$W_{nc} = \int_{z_1}^{z_2} \bar{F}_{nc} \cdot d\bar{s} = mgh \tag{13}$$

and the conservative work done on m by gravity, opposing the rocket is:

$$W_c = -mgh = -(V_2 - V_1) = -\Delta V \tag{14}$$

Einstein rocket replaced by negative mass

Let us now reconsider the rocket of Figure 7. We can replace the rocket by negative mass equal in magnitude to the lower positive mass (Fig. 8). Earth's gravity repels negative mass and thus an amount $(-m)$ will precisely balance the force of attraction on m, a situation equivalent to the rocket.

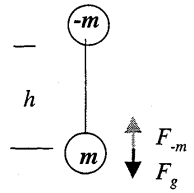

Figure 8. Balanced force configuration for rocket replaced by negative mass

We evaluate the work done in this situation. There are two forces acting on m, $\bar{F}_g$ and $\bar{F}_{-m}$. This time *both* forces are conservative. The total work done on the mass m is zero because there is no change in the kinetic energy, since $\bar{F}_{-m} = -\bar{F}_g$.

$$W_{total} = \int \bar{F}_g \cdot d\bar{s} + \int \bar{F}_{-m} \cdot d\bar{s} = \Delta T = 0 \tag{15}$$

However, now the total work done on m is conservative since, unlike with the rocket, there are no non-conservative forces acting. The rigid wire transmits the conservative force from $-m$. Thus we find:

$$W_c = W_g + W_{-m} = 0 \tag{16}$$

This model of a massive neutral dipole is exactly equivalent to an electric neutral dipole such as the proton and electron of a hydrogen atom in an electric field. In the latter case, the two forces acting on the proton, the external electric field and the opposing force of the electron are both conservative. The total conservative work on the proton is zero when the atom is moved a distance h through a known potential difference. That is precisely our experiment. There was no clock change observed.

This leads us to the ***second and third Clock Postulates***:

2) External conservative work done on a clock mechanism is responsible for changes in its rate when the motion of the clock can be neglected.

3) When the clock is not at rest, the change in its rate arises more generally from the change in the Specific Lagrangian for the mechanism.

The third postulate takes into account the change when there is kinetic energy present.

These postulates reconcile the observations and considerations of the present experiment with those observed for gravity. Therefore one should not expect to see a clock change in the imagined massive dipole

experiment since there was no net conservative work done on m.

Inconsistency between General Relativity and existence of a neutral mass dipole

Now consider a clock on the mass *m* attached to the rocket. The mass *m* might itself be part of a clock mechanism. Upon reaching height *h*, the clock will change. But the mass *m* cannot distinguish between the pull of the rocket on the wire from that of the negative mass. In the case of the negative mass , the Clock Principle states that since no net conservative work is done on *m* , no clock change should be observed. So, there is a conflict here. It follows that:

Since we assume GR to be true, either the Clock Principle is false or a mass dipole cannot exist as the analogue of a charge dipole. Thus, if the clock principle is true, negative mass cannot exist. If the clock principle is false, then work and energy change are not related in general to time change. It follows that a metric theory of forces other than gravitation cannot be constructed.

Clock Conclusions

It is generally agreed that in order for a clock to indicate the passage of time, energy change in the mechanism is required. Thus, it appears that space is coupled to time through energy. When a clock is raised in a gravitational field, external work is performed on the mechanism. This permits a time change. If $W_c = 0$ so that applied forces opposing conservative forces are also conservative, then there will be no observed clock change.

We have shown that if the clock principle is correct then ***negative mass cannot exist***. This does not preclude the existence of negative energy since the general energy-momentum relation has two roots,

$$E = \pm\sqrt{p^2c^2 + m^2c^4}$$

of which the positive root, in the rest frame of a particle of mass m (p=0), is the famous Einstein energy-mass relation.

ACKNOWLEDGEMENTS

This work was supported by the NASA Glenn Research Center under Contract NAS3-00094. We wish to thank Marc Millis for having the daring and fortitude to envision and create the BPP program and support this effort as part of it. We would like to thank Prof. Larry Mead for supportive discussions revolving around this new view of General Relativity. We also wish to thank Dan Leopold for his advice and support of the experiment.

REFERENCES

1. Harry I. Ringermacher and Brice N. Cassenti , *Search for Effects of an Electrostatic Potential on Clocks in the Frame of Reference of a Charged Particle*, Breakthrough Propulsion Physics Workshop, (NASA Lewis Research Center, Cleveland, August 12-14, 1997, NASA publ. CP-208694 , 1999, Millis & Williamson, ed).
2. E. Schrödinger, *Space-Time Structure*, (Cambridge University Press, 1986).
3. H. I. Ringermacher, *Classical and Quantum Grav.*, **11**, 2383 (1994).
4. NASA-GRC final report, Contract NAS3-00094.
5. "Mathematica" was used to test for invariance of the Modified Einstein equations in this theory under a purely time-dependent potential in g_{00}. The solutions to the equations were found to be invariant under an additive time-dependent potential.

A01-34537

AIAA 2001-3908

Tests of Mach's Principle with a Mechanical Oscillator

John G. Cramer, Damon P. Cassissi, and Curran W. Fey
Department of Physics, Box 351560
University of Washington
Seattle, WA 98195-1560

Joint Propulsion Conference
BPP Session Breakout
9-11 July, 2001
Salt Lake City, Utah

AIAA-2001-3908

Tests of Mach's Principle with a Mechanical Oscillator*

John G. Cramer†, Damon P. Cassissi, and Curran W. Fey
Department of Physics, Box 351560, University of Washington,, Seattle, WA 98195-1560, USA

Abstract

James F. Woodward has made a prediction, based on Sciama's formulation of Mach's Principle in the framework of general relativity, that in the presence of energy flow the inertial mass of an object may undergo sizable variations, changing as the 2nd time derivative of the energy. We describe an attempt to observe the predicted effect for a charging capacitor, using a technique that does not require a reactionless force or any local violation of Newton's 3rd law of motion. We attempt to observe the effect of the mass variation on a driven harmonic oscillator with the charging capacitor as the oscillating mass. Positive and negative phase shifts in the oscillator motion with respect to the driving force are predicted to result from appropriately programmed inertial mass variations. The phase shift is constant, so that data may be accumulated over a very large number of oscillation cycles to insure high precision in the phase shift determination. We report on the predicted effect and the design and implementation of the measurement apparatus. At this time, however, we will *not* report on observations of the presence or absence of the Woodward effect.

Introduction

This is a status report on a new experiment to test a prediction based on general relativity and Mach's Principle, which has been supported by the Breakthrough Propulsion Program of NASA.

Einstein's Principle of Equivalence, a cornerstone of general relativity, asserts the exact universal identity of inertial mass and gravitational mass. However, the origins of inertia and its connection to gravitational mass remain obscure. Mach's Principle, the idea that inertia originates in the gravitational interaction of massive objects with the distant matter of the universe, is an attempt to unify gravitational and inertial mass, but it is not a part of general relativity. Dennis Sciama [1,2] attempted to improve this situation by showing that, for sufficiently symmetric and homogeneous universes, the gravitational interaction of massive objects with distant matter leads to an acceleration-dependent force, i.e., inertia.

James F. Woodward [3,4] extended Sciama's calculations by introducing energy flow (e.g., the energy flowing to a charging capacitor) into the gravitating system. He demonstrated that the equations acquire extra transient contributions in Sciama's inertia term that are proportional to 1/G (Newton's gravitational constant) and therefore are quite large. The implications of this work are: (a) that it may be possible to modify inertia, and (b) that it may be possible to demonstrate the validity of Mach's Principle with a tabletop experiment.

Woodward and his students [4-7] have attempted to observe the predicted inertia-variation effect by accelerating a mass-varying object so that it produces a reactionless force. To illustrate this, assume that an inertia-varying test mass is accelerated to the right when it has low inertia and to the left when it has high inertia. In this circumstance, it is argued, the reaction forces of the two accelerations are unequal and one might expect the net reactionless force to "row" the system to the right. Woodward's group reports [7] using a sensitive torsion balance to observed small reactionless forces at magnitudes that are near the limits of their sensitivity and about five orders of

* Supported in part by the National Aeronautics and Space Administration.

† *E-mail address:* cramer@phys.washington.edu

magnitude smaller than the predicted effect (see the calculations below.)

Unfortunately, this scheme for observing the predicted inertia variation appears to be at odds with the relativistically invariant form of Newton's 2nd law of motion:

$$\vec{F} = d\vec{p}/dt = m\, d\vec{v}/dt + \vec{v}\, dm/dt \qquad (1)$$

Since the inertial mass **m** of the test body is expected to vary with time, the last term of Eqn. (1) cannot be ignored. It is not surprising, in view of Newton's 3rd law of motion, that for any closed cycle of acceleration and variation of the inertial mass around a central value, the force contribution from the **v dm/dt** term is found to precisely cancel the supposed "reactionless force" arising from the **m dv/dt** term, leading to a net force of zero for the overall system.

From this simple calculation, it appears that reactionless force searches are ***not*** good tests of the proposed effect. There remains the question of whether the Woodward inertia variation is indeed present in a system with energy flow. We have found, as will be described below, that a mechanical oscillator, driven at resonance, with its mass programmed to vary at the drive frequency, shows sensitive variations in drive-to-response phase and amplitude, depending on the relative phase between the mass variation and the oscillator drive.

Theory

Woodward has shown [5] that the relativistically invariant wave equation, in the simplest approximation and expressed as a function of an overall scalar gravitational potential ϕ, has the form:

$$\nabla.\phi - (1/c^2)(\partial^2\phi/\partial t^2) = \Box\phi = 4\pi G\rho_o + (\phi/\rho_o c^2)(\partial^2\rho_o/\partial t^2) - (\phi/\rho_o c^2)^2(\partial\rho_o/\partial t)^2 \qquad (2)$$

where G is Newton's gravitational constant, ρ_o the rest mass density, and c the speed of light. This field equation is obtained only if one assumes, as suggested by Mach's Principle, that the local energy density of matter is equal to the matter density times ϕ. Since Mach's Principle demands that $\phi = c^2$ when measured locally, this constraint is equivalent to asserting that $E = mc^2$. Additional terms would be present in this equation were it not for the fact that, as a consequence of Mach's principle in this approximation, $\phi = c^2$.

In writing Eqn. (2), Woodward neglects a term of the form $c^{-4}(\partial\phi/\partial t)^2$ because it is always small, given its c^{-4} coefficient that is not compensated for by any factor of ϕ in the numerator. Combining the last three terms of Eqn. (2) into an effective mass density $\rho(t)$ and solving for this quantity gives the time-dependent effective mass density as:

$$\rho(t) \approx \rho_o + (1/4\pi G)[(\phi/\rho_o c^2)(\partial^2\rho_o/\partial t^2)] - (1/4\pi G)[(\phi/\rho_o c^2)^2(\partial\rho_o/\partial t)^2]. \qquad (3)$$

The second term in Eqn. (3) has the form $(1/4\pi G)[(\phi/\rho_o c^2)(\partial^2\rho_o/\partial t^2)]$. This time-dependent fluctuation in the inertial mass can be both positive and negative when ρ_o undergoes periodic time variations, e.g., when a varying flow of mass-energy is present. This is the inertia-varying term of interest.

In the present work we will ignore the last time-dependent or "wormhole" term, which has the form $-(1/4\pi G)[(\phi/\rho_o c^2)^2(\partial\rho_o/\partial t)^2]$. This mass term is always negative or zero and for sinusoidal variations is about 0.1% or less of the other terms.

If a capacitance **C** is driven by a voltage source with time dependent potential $\mathbf{V(t) = V_0 Sin(\omega t)}$, then the energy in the capacitor, assuming dissipative and inductive effects can be neglected, is $\mathbf{U(t) = \tfrac{1}{2}C\,V(t)^2 = \tfrac{1}{2}C\,V_0^2 Sin^2(wt)}$. The second time derivative of this stored energy divided by $\mathbf{c^2}$ (to convert it to a mass) is $\mathbf{d^2U/dt^2 = C\,V_0^2\,\omega^2\,Cos(2\omega t)/c^2}$. This is the $(\partial^2\rho_o/\partial t^2)$ factor in Woodward's Eqn. (3). The corresponding time dependent variation in inertial mass, assuming that $\phi = c^2$, is then:

$$\mathbf{dm(t) = 1/(4\pi\rho_o G\,c^2)\,C\,V_0^2\,\omega^2\,Cos(2\omega t).} \qquad (4)$$

We will use this form for the variation in inertial mass in the analysis that follows.

To give this prediction a scale, let us assume that c=2.998×10^8 m/s, G=6.672×10^{-11} m^3/kg s^2, ρ_0=2,000 kg/m^3, C=9.3×10^{-9} F, V_0=2,000 V, and ω=2π×1,000 Hz. With these values, we find that:

$$\mathbf{dm(t) = 9.7\ mg \times Cos(2\pi \times 2{,}000\ Hz \times t).} \qquad (5)$$

In other words, under these conditions, which should be realizable in the experiment described here, the inertial mass of the capacitance is predicted to vary by about ±10 milligrams at *twice* the capacitor charging frequency, or 2,000 Hz. If the mass of the capacitor and its holder were about 1 g, this would represent a mass variation of about ±1%. Such a mass variation would have large observable consequences. However,

we note that Woodward [4] has made arguments involving mobile charges to explain why the actual variation in the inertial mass may be orders of magnitude smaller than that predicted by simple calculations and more consistent with his reported observation of very small reactionless forces.

It is also of interest to consider the maximum current flow that is necessary to charge the capacitor in the manner assumed above. The charge on the capacitor is **q=C V(t)**, so the charging current is **i(t) =C dV/dt = C V_0 ωCos(ωt) = 116 mA × Cos(ωt)** for the specified conditions. It turns out that a high voltage power supply/amplifier capable of delivering an audio-frequency peak current of a few hundred milliamps at a few kilovolts is very expensive (~$14,000) and represent the most costly component required for the present test of the Woodward effect.

A Driven Mass-Varying Oscillator

We test for the presence of the Woodward effect by using the capacitor as the mass in a system that forms a driven mechanical mass-and-spring oscillator with an undriven resonant frequency of ω_o. Such an oscillator is shown schematically in Fig. 1

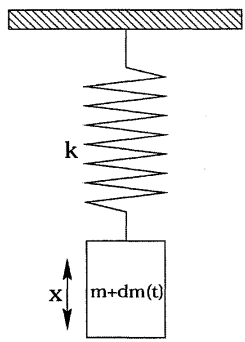

Figure 1. Schematic mass-and-spring mechanical oscillator with time varying mass **m+dm(t)** and restoring-force spring constant **k**. The system is assumed to have a dissipative damping force of **–b dx/dt**.

The oscillator is driven at its resonant frequency $\omega_d=(\omega_0^2 - b/2m)^{1/2}$ with a voice coil actuator and audio amplifier. At the same time, we charge the capacitor sinusoidally, using approximately the parameters specified above, at a frequency of $\omega_d/2$ so that, in the presence of the Woodward effect, the capacitor's inertial mass should vary at frequency ω_d.

The inhomogeneous non-linear differential equation describing such a system is:

$$F_d Cos[\omega_d t] = kx(t) + [b + \mu'(t)]x'(t) + [m + \mu(t)]x''(t), \quad (6)$$

where **x(t)** is the motion of the capacitor, $\mathbf{F_d}$ is the magnitude of the driving force, ω_d is the angular frequency of the driving force, **k** is the Hooke's law restoring force constant, **b** is the damping constant representing dissipative forces in the system, **m** is the average mass of the capacitor and associated structure, and **μ(t)** is the time-dependent mass variation due to the Woodward effect. Note that the **μ'(t)x'(t)** term in Eqn. (6) arises from the **v dm/dt** term in Eqn. (1).

We can replace the spring constant **k** with $\mathbf{m}\ \omega_o^2$ and replace **μ(t)** with $\mu_0 Cos(\omega_d t + \phi_m)$, which assumes that we have arranged the mass variation to be at the same frequency as the driving force but shifted in phase by ϕ_m. With these substitutions, Eqn. (6) becomes:

$$F_d Cos(\omega_d t) = m\omega_0^2 x(t) + [b - \mu_0 \omega_d Sin(\omega_d t + \varphi_m)]x'(t) + [m + \mu_0 Cos(\omega_d t + \varphi_m)]x''(t) \quad (7)$$

This non-linear differential equation has no analytic solutions and must be solved numerically. Fig. 2 shows the results of such numerical solutions of Eqn. (7), assuming that $\mathbf{F_d/m}$=0.01, **b/m**=0.01, and $\mu_0/\mathbf{m}$=0.001. The latter assumption represents only about 10% of the predicted 10 mg mass variation.

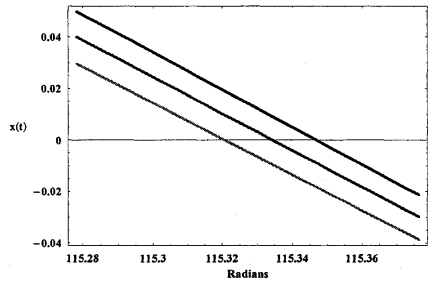

Figure 2. Response phase shifts of the system to variable mass. The central line is the system response with μ_0=0. The other two lines represent μ_0=0.001 with $\phi_m = -\pi/2$ (low), and $\phi_m = +\pi/2$ (high). The phase shifts shown are about ±0.04 radians=±2.3 degrees.

We find that when the mass variation has a relative phase of $\pm\pi/2$ with respect to the driving force, it causes a positive or negative phase shift in the response motion by shifts, using the values listed above, of several degrees. Other phases near 0 or π can cause an increase or decrease in the amplitude of oscillation. The experiment we have constructed is designed in an attempt to observe these phase-shift effects.

Experimental Apparatus

Fig. 2 below shows a top view of the mechanical oscillator arrangement, which we call the "Mach Guitar". The barium titanate capacitor test mass is suspended between pairs of tensioned wires, with the tension adjusted so that the resonant vibration frequency for vertical oscillations is about 1-2 kHz.

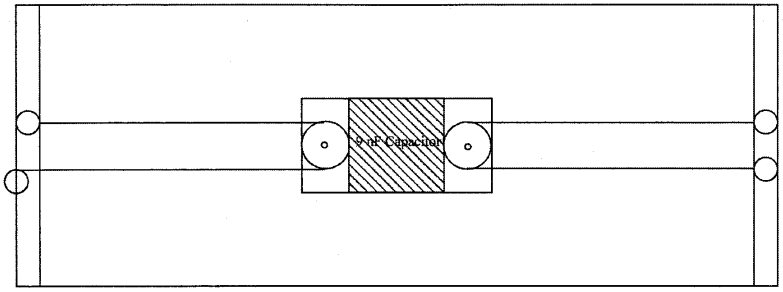

Figure 2 Top view of "Mach Guitar" arrangement. The capacitor is suspended between pairs of tensioned wires that provide the restoring force for the mechanical oscillator. Capacitor drive voltage is supplied through the wires.

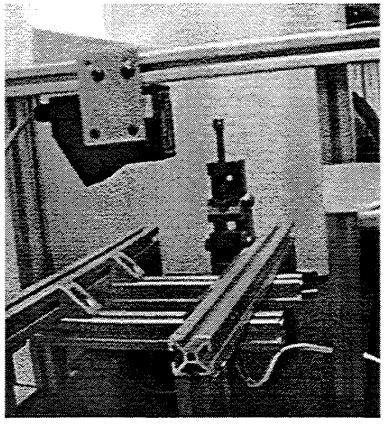

Figure 3 Laser-optics table with oscillator removed, showing voice-coil drive (below) and laser position monitor (above).

Electrical connections for the capacitor drive voltage are supplied through the tensioned wire pairs. The capacitor and its support structure have a net mass of about 1 g.

The restoring force provided by the tensioned wire pairs is $\mathbf{F=-(8T/L)x}$, where **T** is the tension in a given wire, **L** is the overall length, from bridge to bridge, of the system, and **x** is the vertical displacement of the capacitor. Therefore, neglecting the mass of the wire, the resonant frequency of the oscillator is $\omega_o=(8T/mL)^{1/2}$. If **m**=1 g, **L**=0.5 m and $\omega_0=2\pi \times 1000$ Hz, then the required tension is 553 lb. This tension can be reached with 13 gauge steel wire.

Fig. 3 shows a view of the laser-optics table (with oscillator removed) that is the foundation of the experiment. A pre-drilled aluminum laser-optics base plate supports the general-purpose aluminum beam structures, on which are mounted (below) the voice-coil drive (a modified audio speaker) for the mechanical oscillator, and (above) the laser position-measuring device shown in Fig. 4.

The Mach Guitar is mounted on the laser-optics base, which provides "bridges" to support for the wires

and their tensioning mechanism. Electrical connections to the capacitance are made through the support wires. Below the oscillator is an audio speaker, which drives the oscillator through a light spring. Above the oscillator is a commercial laser position detector, which measures the vertical position of the capacitor's upper surface by electronic triangulation. The laser position sensor is shown in Fig. 4

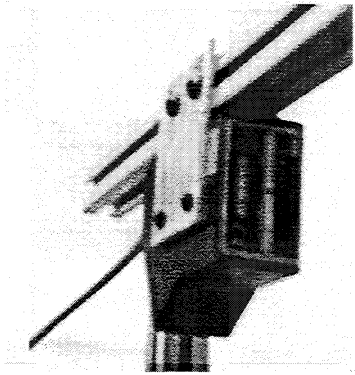

Fig. 4 Laser position measurement device.

The mass-varying object used in the measurements is a low-loss and low-mechanical-movement barium titanate capacitor with a capacitance of about 9 nF and a voltage rating of 3 kV. This oscillator mass is suspended between pairs of 13 gauge steel wires (0.25 m long on each side) that have been tensioned to about 500 lb to provide a system resonant frequency of about 1000 Hz.

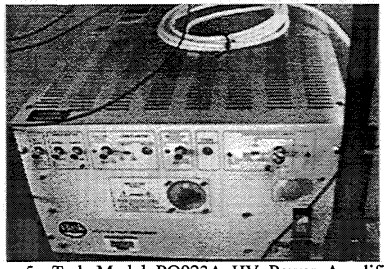

Fig. 5 Trek Model PO923A HV Power Amplifier, used for driving the capacitor at 2 kV and 400 mA.

As previously mentioned, the most challenging problem presented by the present experiment is driving the capacitor to high voltages at audio frequencies. The reason is that all high-voltage amplifiers driving capacitive loads are severely limited by the charging current that they must deliver. We have selected a Trek Model PO923A High Voltage Power Amplifier, shown in Fig. 5, as the capacitor driver. It can drive at voltages up to 2 kV with a peak charging current of up to 400 mA.

The Mach's Principle test employs a Pentium-2 850 MHz computer system with a Windows 98 operating system for experiment control, using control software based on LabView. It consists .of controls for the mechanical oscillator driver and the capacitance driver, a data collection system that records the drive signal and the position measurements, a data recording and retrieval system, and analysis software for processing the data and extracting the phase information of interest.

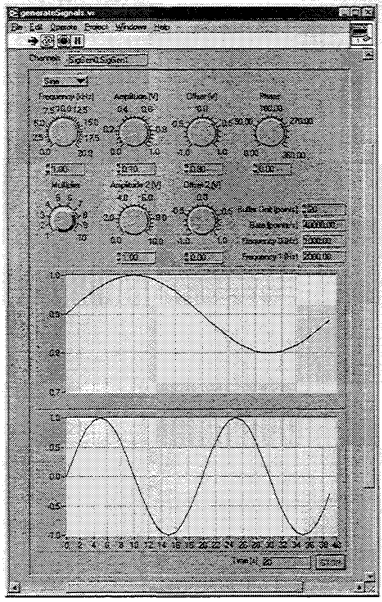

Figure 6. LabView control panel and display for system drivers.

The LabView control panel and display for the experiment is shown in Fig. 6 above. The system generates sine waves with adjustable phases and amplitudes at two frequencies, normally set to differ by a factor of two. The low frequency signal provides the input to the high voltage amplifier that drives the capacitor. The high frequency provides input to an audio amplifier connected to a voice coil that drives the mechanical oscillator.

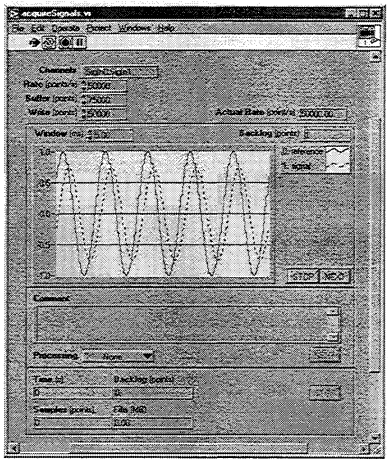

Figure 7. LabView data acquisition and display.

Figure 7 shows the LabView panel for the data collection system. The system samples the mechanical drive voltage and the capacitor position measurement of the mechanical oscillator as separate data streams. These are sampled for real-time display and also recorded on the system hard disk. These data streams can be read back and re-analyzed. The data are analyzed by integration over a long time period to extract the relative phase of the drive and response signals for a given setting of the capacitor drive phase with respect to the mechanical driver.

The processed quantity that will be accumulated in the analysis is the cosine of the relative phase between the driving signal **D(t)** and the mechanical response signal **R(t)**. There are a variety of ways of extracting this signal, but the one we will use initially is:

$$Cos(\varphi) = \frac{\int_0^T [D(t)+R(t)]^2\,dt - \int_0^T [D(t)-R(t)]^2\,dt}{4\sqrt{\int_0^T D(t)^2 dt \times \int_0^T R(t)^2 dt}} \qquad (8)$$

Here **T** is an arbitrary integration time that increases as data is collected and the running integrals are accumulated. The values of **Cos(ϕ)**, which is near 0 because ϕ is approximately $\pi/2$ on resonance, will be compared for the two most extreme settings of the phase of the capacitor drive, which should produce phase shifts like those shown in Fig. 2. We estimate that with a data collection cycle of a few hours, **Cos(ϕ)** can be determined to an accuracy of a few parts in 10^5. This should enable us to determine the shift in ϕ to similar accuracy, providing a fairly stringent test of the presence or absence of the Woodward mass variation.

Experiment Status

The experiment is presently being reconfigured on the laser-optic table. The initial cantilever arrangement is being replaced with the new "Mach guitar" mechanical oscillator system described above.

The previous mechanical oscillator, which used a capacitor mass suspended at the free end of an aluminum cantilever, was tested and found to present three serious problems for the experiment: (1) its resonant frequency was fixed by the length and mass of the cantilever and was not easily adjustable, (2) The cantilever mass dominated that of the capacitor, greatly reducing the magnitude of the predicted effect and (3) it was not capable of achieving resonant frequencies above a few hundred Hz. Since the size of the predicted mass-variation effect increases as ω_0^2, this was a serious limitation. However, initial experience with this cantilever oscillator provided valuable experience in operating and testing the position measuring device and the data collection system.

The new Mach Guitar oscillator provides significant improvements over the cantilever in reduced mass and increased operating frequencies, and it offers the additional advantage that it is easily tunable through simple adjustments of the wire tension.

We expect to begin data collection with the new configuration in the next few weeks.

Conclusion

The test of Mach's principle and the Woodward effect described above is not yet completed, but it shows promise of providing an independent test of the predictions that does not depend on the possibility of a reactionless force. The experiment in the present configuration is not as sensitive as the torsion-balance measurements recently reported by Woodward [7]. However, since it is not based on a reactionless force, it may not need that sensitivity.

If the Woodward Effect is observed, it will have important implications for general relativity and cosmology, for validating Mach's Principle, for control of inertia, and possibly for propulsion. If the Woodward Effect is not observed at the sensitivity limit of the experiment, this will also be worth knowing.

Acknowledgements

The authors are grateful to Marc G. Millis and the NASA Breakthrough Propulsion Program for providing encouragement and funding for the present experiment. We thank James F. Woodward for providing the very high quality barium titanate capacitors used in the experiment, along with much useful advice.

Bibliography

[1] D. Sciama, "On the Origin of Inertia," *Monthly Notices of the Royal Astronomical Society* **113**, 34–42 (1953).

[2] D. Sciama, "The Physical Structure of General Relativity," *Reviews of Modern Physics* **36**, 463–469 (1964).

[3] Woodward, J.F., "A New Experimental Approach to Mach's Principle and Relativistic Gravitation," *Foundations of Physics Letters* **3**, 497 – 506 (1990).

[4] James F. Woodward, "Measurements of a Machian Transient Mass Fluctuation," *Foundations of Physics Letters* **4**, 407–423 (1991).

[5] James F. Woodward ,"A Stationary Apparent Weight Shift from a Transient Machian Mass Fluctuation," *Foundations of Physics Letters* **5**, 425–442 (1992).

[6] James F. Woodward, "A Laboratory Test of Mach's Principle and Strong-Field Relativistic Gravity," *Foundations of Physics Letters* **9**, 247 – 293 (1996).

[7] James F. Woodward, "Mass Fluctuations, Stationary Forces, and Propellantless Propulsion," *Space Technology and Applications International Forum 2000* (American Institute of Physics/Springer Verlag, New York, 2000), pp. 1018 – 1025 (2000).

A01-34538

AIAA 2001-3909

Superluminal but Causal Wave Propagation

M. Mojahedi and K. Malloy
University of New Mexico
Albuquerque, New Mexico

R. Chiao
University of California at Berkeley
Berkeley, California

37th AIAA/ASME/SAE/ASEE
Joint Propulsion Conference and Exhibit
8-11 July 2001
Salt Lake City, Utah

AIAA-2001-3909

SUPERLUMINAL BUT CAUSAL WAVE PROPAGATION

Mohammad Mojahedi, Kevin J. Malloy
Center for High Technology Materials, Department of Electrical and Computer Engineering, University of New Mexico, 1313 Goddard SE, Albuquerque NM, 87106, (email: mojahed@chtm.unm.edu).
Raymond Chiao
Department of Physics, University of California at Berkeley, Berkeley, CA 94720.

Abstract: A series of experiments in recent years have shown that under carefully designed circumstances the group velocity, or even more surprisingly the energy velocity can exceed the speed of light in vacuum or become negative (abnormal velocities). These abnormal results have led some researchers to question the validity of special relativity, or at least cast doubt on the relevance of these principles to the aforementioned experiments. In this work, experiments with single electromagnetic pulses measured in the time domain and experiments in the frequency domain are described. It is seen that while these experiments verify the aforementioned abnormal velocities, they are not in contradiction with the principles of special relativity (Einstein causality). In this regard, the important concept of "front" or "Sommerfeld forerunner" is reintroduced, and it is argued that the only physical velocity required to obey the Einstein causality is the "front velocity."

I. Introduction

The fact that the group velocity of an electromagnetic wave packet (pulse) can exceed the speed of light in vacuum (become superluminal) has been demonstrated in many experiments using single photons[1,2], at optical frequencies[3], and using microwaves[4-10]. As a starting point, an interested reader may consult the review by Chiao and the references therein[11]. Despite one's initial impression, the superluminal group or even energy velocities (defined as the ratio of the Poynting vector to the stored electromagnetic energy) are not at odds with the requirements of relativistic causality (Einstein causality), and indeed it can be shown that they must exist as the natural consequence of the Kramers-Kronig relations, which in themselves are a statement of the system linearity and causality[12-15].

The point that in the regions of anomalous dispersion, group velocity can become superluminal was first considered by Sommerfeld and his student Brillouin[16]. In their studies, they examined a sinusoidally modulated step-function propagating through a medium with Lorentzian dispersion. They identified five different velocities: phase, group, energy, Sommerfeld forerunner ("front[†]") and Brillouin forerunner velocities[‡]. However, with the passage of time, and for reasons unknown to the authors, while the first three velocity terms have received much attention in both undergraduate and graduate books, the latter two have not enjoyed the same status. This is even more surprising since, among the above velocities, it is only the

[†] To be more rigorous the term "front" refers to the onset of Sommerfeld forerunner propagation.
[‡] To be complete one has to add the term "signal velocity" defined as the velocity of the half maximum point to the list. However, by their own admission such a definition is arbitrary[16] and as discussed in Ref. 4 can become superluminal.

velocity of the "front" that must satisfy the requirements of Einstein causality under all circumstances. In other words, it is rather a naïve understanding of Einstein causality to equate the group velocity with the velocity of information transfer under all circumstances, particularly when one is concerned with the propagation of "attenuated traveling waves[§]."

Our objective here is to discuss the phenomenon of superluminal and negative group and energy velocities, which generically is referred to as the abnormal velocities. In Sec. II a time-domain experiment used to detect the superluminal group velocities in the case of a one dimensional photonic crystal (1DPC) is described. Section III discusses a frequency-domain experiment used to demonstrate the same superluminal phenomenon. The case of superluminal or negative group and energy velocities for an inverted medium (medium with gain) or in the case of medium with negative index of refraction is considered in Sec. IV. Section V is intended to put the reader's mind at ease by providing some general arguments on why the abnormal velocities discussed in the previous sections are not in contradiction with the requirements of special relativity. Section VI is our condensed attempt is addressing the issue of superluminality in the limit of very weak light (very few photons). Our final remarks and a discussion for the general public can be found in Sec. VII.

II. Time-domain Experiment

Consider the problem of electromagnetic wave propagation through a periodic structure. Figure 1 shows an experimental setup used to detect the superluminal group velocity for a microwave wave packet tunneling through a 1DPC. A backward wave oscillator (BWO) was used to generate the pulse, and a mode converter (MC) was used to convert the TM_{01} mode of the BWO to a TE_{11}. The pulse was then radiated via a conical horn

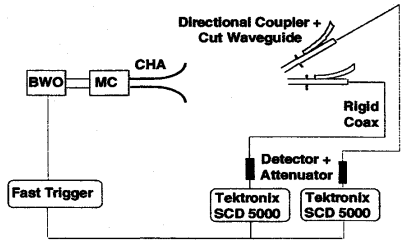

Fig. 1: Time-domain experimental setup

antenna (CHA). The frequency output of the source was tuned to the mid-gap frequency of the 1DPC at 9.68 GHz (FWHM of 100 MHz) and was detected by two HP 8470-B, Schottky diode detector (provided in pairs). The CHA radiation intensity was sampled along two distinct directions (paths), referred to as "side" and "center". A series of microwave pulses were fired in order to measure and then remove the time difference between the two paths due to the differences in cable lengths, internal detection of the oscilloscopes (Tektronix SCD 5000) and other incompatibilities. This measured time difference was electronically compensated such that the peaks corresponding to the pulses traveling through the "center" path and "side" path in the absence of the 1DPC arrived at the same time. At this point, the 1DPC was inserted along the "center" path and series of single pulse were fired. Figure 2 shows the result. It is seen that the peak of the wave packet propagating along the "center" path and tunneling through the 1DPC arrives (440 ± 20) ps earlier than the accompanying pulse propagating through free-space along the "side" path. This

[§] We have used the term "attenuated traveling waves" in the same sense as in Ref. (17), although, sometimes the term evanescent is used to signify the same thing.

advancement in time for the tunneling pulse can easily be translated to a measure of the pulse group velocity, indicating that the tunneling wave packet propagated with a

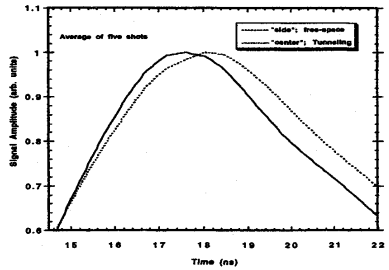

Fig. 2: Superluminal propagation for the tunneling pulse

group velocity $(2.38 \pm 0.15)\,c$.

Furthermore, the traditional view of pulse propagation through a region with high attenuation (regions of anomalous dispersion) held that the extreme

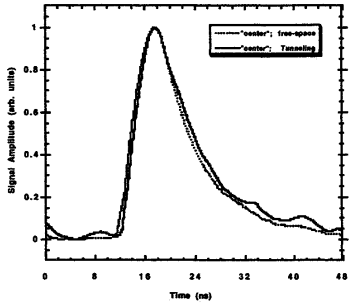

Fig. 3: A measure of the pulse broadening due to tunneling through the 1DPC. The two pulses have propagated along the same path ("center"); one in the free-space and the other through the 1DPC.

attenuation, coupled with the dispersion, would distort the signal to such an extent that the originally well defined wave packet and its peak would not be recognizable upon the emergence from such a medium[17 16]. Figure 3 shows that in contrast to this common belief, the tunneling wave packet of Fig. (2) suffered minimal dispersion such that the FWHM of the pulse after tunneling was only increased by 1.5%. In obtaining this figure the tunneling wave packet was manually moved to later times as to make the comparison between the two pulses easier. A full description of the above experiment can be found in Ref. 4.

III. Frequency-Domain Experiment

In the last section the feasibility of measuring superluminal group velocities directly in time-domain was discussed. This abnormal behavior can also be demonstrated in frequency-domain. Figure 4 shows the

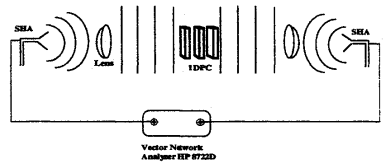

Fig. 4: Frequency-domain experimental setup

free-space setup used to detect the superluminal group velocities in frequency-domain. The setup consists of two K-band standard horn antennas (SHA) configured a transmitter and receiver and connected to ports 1 and 2 of an HP 8722D vector network analyzer (VNA). The radiated quasi-continuous waves are collimated using two microwave lenses and the setup is enclosed in a anechoic chamber to reduce stray signals.

The essence of the approach is to measure *accurately* and *reliably* the transmission phase associated with the 1DPC. Once this quantity is measured, the group delay (τ_g) and group velocity (V_g) can be calculated according to

$$\tau_g = -\partial\phi/\partial\omega, \tag{1}$$

$$\frac{v_g}{c} = \frac{L_{pc}}{c\,\tau_g} = \frac{-L_{pc}}{c\,(\partial\phi/\partial\omega)}, \tag{2}$$

where ϕ is the transmission phase, and L_{pc} is the physical length of the 1DPC.

Fortunately, recent advances in non-coaxial (free-space) calibration techniques for VNA such as the "Thru-Line-Reflect" (TRL) technique[18, 19] make it possible to measured the transmission coefficient accurately and reliably. After calibrating the system (without the 1DPC), a reference plane of unit magnitude for transmission magnitude and zero phase for ϕ is established midway between the two SHAs. At this point, the 1DPC is inserted and the receiver horn is moved back exactly by a length equal to the thickness of the 1DPC (L_{pc}).

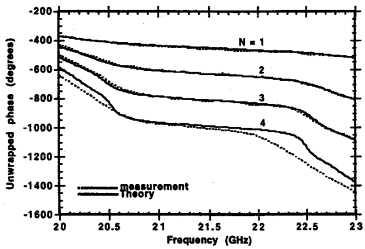

Fig 5: The unwrapped transmission phase for the 1DPC with various number of Eccostock® dielectric slabs.

Figure 5 is the calculated (solid line) and measured (dotted line) unwrapped phase for a 1DPC with four, three, two and one dielectric slabs (the spacer is always air). The theoretical calculations are based on the diagonalization of the one period matrix, and are presented in Ref. 5.

According to Eqs. (1) and (2), to ascertain the group delay and group velocity the data presented in Fig. 5 must be differentiated. However, differentiating noisy data amplifies the noise and may lead to spurious effects. To avoid the arbitrariness associated with smoothing, a best nonlinear least square fit of the experimental phase data is obtained. The parameters used in fitting the experimental data all match the actual variables very well and for the sake of brevity are not given here, but can be found in Ref. 5.

Figure 6 shows the result of the least square fit to the phase data of Fig. 5 together

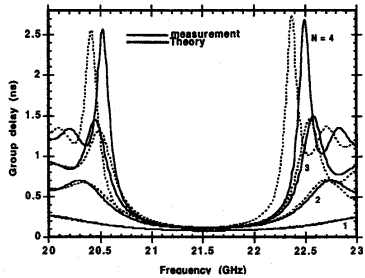

Fig. 6: Measured and calculated group delay for the 1DPC. The parameters used to obtain the fitted curves (measurement) and the calculated curves (theory) are given in Ref 5.

with Eq. (1), in order to determine the group delay in a 1DPC with one, two, three, and four dielectric slabs. Consequently, the normalized group velocity given by Eq. (2)

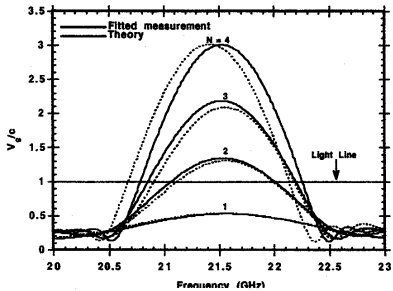

Fig. 7. Normalized group velocity for the 1DPC. The dotted curves are the measured results obtained from the fitted curves in Fig. 6 and Eq. 2. The solid curves are theoretically calculated.

can be obtained from the Fig. 6 and is shown in Fig. 7. Along with the velocities derived from the fit (dotted curves), the theoretical group velocities calculated from the measured values of thicknesses and indices are also shown (solid curves). As Fig. 7

indicates, in the case of $N=4$ and $N=3$, a maximum superluminal group velocities 3 and 2.1 times c is observed. The results depicted in this figure can be interpreted in the following way. If one is to construct a pulse entirely composed of the frequency components for which the superluminal behavior is predicted, then the pulse is expected to propagate with group velocity exceeding c, similar to the situation discussed in the Sec. II.

IV. Abnormal Velocities in Inverted Medium and Medium with Negative Index

The circumstances under which the group or even energy velocity is abnormal are not limited to the evanescent wave propagation discussed so far. In this section three situations are described which exhibit the aforementioned abnormal behavior.

First, for an inverted medium (medium with gain) described by a Lorentz-Lorenz dispersion, the index of refraction is given by

$$n(\omega)=\left(1-\frac{\omega_p^2}{\omega_0^2-\omega^2-i\gamma\omega}\right)^{1/2} \qquad (3)$$

where ω_0 is the resonance frequency, γ is a small damping factor, and ω_p is the effective plasma frequency. Note that a negative sign precedes the second term under the square root due to the population inversion of the medium. A plot of the index of refraction for both the inverted and non-inverted medium is shown in Fig. 8. From the figure it is clear that for an inverted medium, in the limit of very low frequencies, the index is less than one implying that the phase velocity is superluminal. More importantly, at the low frequencies, the group velocity given by

$$V_g(0)=\frac{c}{\left[n(\omega)+\omega\, dn/d\omega\right]_{\omega\to 0}}= \frac{c}{n(0)}=V_p(0)>c \qquad (4)$$

is also superluminal. Under these circumstances the energy velocity (V_e), given by the ratio of Poynting vector (S), to the stored energy density (u), is also equal to the phase and group velocity and exceeds the speed of light in vacuum.

$$V_e=\frac{S}{u}=\frac{c}{n(0)}=V_p(0)>c \qquad (5)$$

The equivalence of the above three

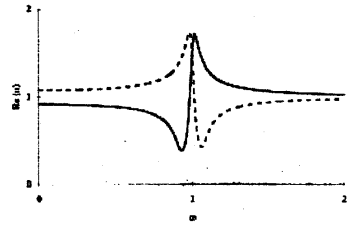

Fig. 8: The real part of the index of refraction for an inverted medium (solid curve) and non-inverted medium (dashed curve.)

velocities is merely a statement of the fact that in the limit of low frequencies the medium is transparent and dispersion-free[13].

Second, it is also possible to observe

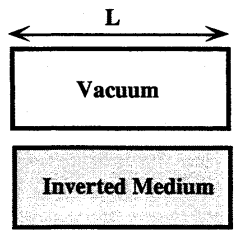

Fig. 9: Two cells of equal length containing inverted medium and vacuum.

negative group velocities for electromagnetic (EM) pulses tuned slightly away from a gain line of an inverted

medium[14, 20-22]. The physical meaning of a negative group velocity can be explained as the following. Consider two cells of physical length L containing an inverted medium and vacuum as shown in Fig. 9. The time difference between two well behaved identical EM pulses propagating through the lower (inverted) and the upper cell (vacuum) is given by

$$\Delta t = \tau_g - t_{vac} = \frac{L}{V_g} - \frac{L}{c} = \frac{L}{c}\left(n_g - 1\right) \quad (6)$$

where n_g is the group index. From the above equation it is clear that if the group index is zero the time difference between the two pulses is given by the negative of L/c In other words, when one of the EM pulses is at the exit face of the lower cell the other pulse is about to enter the upper vacuum cell. Stating this point differently, if one only considers a single cell containing the inverted medium, for a negative group index, the peak of the transmitted wave packet leaves the cell prior to the peak of the incoming wave packet entering the medium. It must be pointed out that as shown by Landauer[23-25] it is naïve to regard the peak of the outgoing pulse as the causal response of the medium to the peak of the incident pulse. The theoretical prediction by one of the authors[22] regarding the feasibility of detecting negative group velocity was recently verified in an experiment by Wang[26] in which the inverted medium was a cell containing cesium vapor.

Finally, let us consider a situation for which the medium effective index is a negative value. A point worth emphasizing is the fact that for these media it is the effective index and not the actual material index which is negative. In other words, the wavelength of the incident wave is many times larger than the physical size of the components comprising the media, allowing one to characterize the over all response of the media in terms of an effective index.

The first theoretical work in this area was done by Veselago[27, 28], and the more

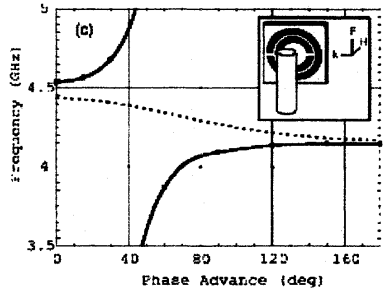

Fig. 10: The dispersion curves for a medium with negative effective index

recent interest in the subject was re-ignited by the work of Pendry[29, 30] and Smith et. al.[31, 32], which demonstrated the possibility of manufacturing these media at microwave frequencies. Figure 10, shows the dispersion relation for a negative index medium, borrowed from Ref. 32. From the figure it is clear that for a certain frequency range, the derivative of the curve depicted in Fig. 10, (i.e. the group velocity) is negative. Even more surprising is the fact that the energy velocity, given by Eq. (7), is also negative, since in these media both permittivity and permeability are negative parameters.

$$V_e \propto \frac{\vec{E} \times \vec{H}}{\varepsilon \left|\vec{E}\right|^2 + \mu \left|\vec{H}\right|^2} \quad (7)$$

The presence of negative group and energy velocities for the above media can be understood in the following manner. The negative index medium, considered by Smith et. al.[31], is in essence a distributed LRC transmission line that its response can be approximated by a lumped LRC circuit. The inset in Fig. 11 is a typical LRC circuit that exhibits negative group delay in the

region of maximum attenuation**. Once again, if one is to construct an EM pulse

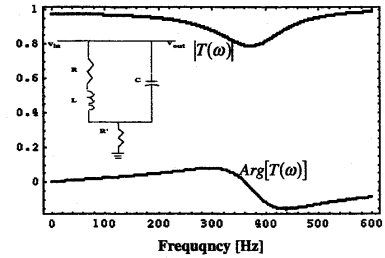

Fig. 11: Transmission magnitude and phase for the LRC circuit shown in the inset.

mostly composed of frequency components having negative group delays, it is expected that the group and energy velocities for this EM pulse to be negative. We currently are pursuing the detection of the aforementioned abnormal velocities in the negative index media. We end this section by pointing out that in addition to negative velocities, the negative index medium has many other interesting properties such as inverted Doppler shift, Cherenkov radiation, and Snell's law.

V. Superluminal Velocities and Einstein Causality

In so far we have discussed situations for which the phase, group, and energy velocities are abnormal (superluminal or negative). The reader may begin to wonder whether or not these abnormal velocities are in contradiction with the requirements of relativistic causality. The short answer to this question is that under no circumstances the so-called "front velocity" may exceed the speed of light in vacuum, and in fact under all circumstances the "front velocity" is exactly luminal. In other words, the requirement of Einstein causality that no "signal" (information) can be transmitted superluminally is satisfied in all cases, since the "front velocity' is always luminal. This means that the presence of the genuine information should not be associated with the pulse maximum, half maximum, or the envelope, but indeed is contained within the singularities (points of non-analyticity) of the pulse. Because of the important role played by the "front" in satisfying the requirements of special relativity, let us briefly discuss some of the most general ideas associated with this concept. The interested reader may consult the Ref. (4) for more detailed analysis.

The essential point to remember is the fact that any *physically realizable* signal is restrictively time-limited. In other words, any electromagnetic signal created and later propagated through free-space or a 1DPC must be generated at a point in time and space. One can then always point to a time prior to which the signal did not exist. This point in time, or more precisely the transient "turn on times," are points of non-analyticity for which the amplitude of the pulse or its first or higher derivative are discontinuous.

The importance of these points of non-analyticity becomes clear when considering the following. While the future behavior of a truly analytical signal such as a Gaussian wave packet can be completely predicted by means such as a Taylor expansion (or a Laurent expansion for functions that are holomorphic in an annular region), the presence or arrival of the singularities do not yield themselves to such an extrapolation. Moreover, as discussed in the above, no *physically realizable* signal can be presented by an *entire function*†† hence, any communication of information must involve the transmission of the "front". To summarize, there is no more information

** In obtaining Fig. 11, in contrast to the curves depicted in Fig. 5, a time dependency of $e^{-i\omega t}$ in place of $e^{j\omega t}$ was used. In other word, the group delay has the opposite sign of that shown in Eq. (1).

†† An *entire function* is the one that is analytical everywhere in the complex domain.

in a pulse peak or envelope that is not already contained within the earliest parts of the signal.

The mathematical proof that no signal (information) may be detected sooner than $t_0 = x/c$ can be seen via contour integration of an expression such as Eq. (8). Equation (8) describes the field at the position x and time t for a wave packet impinging at normal incident on a medium characterized by an index of refraction, n, [33].

$$u(x,t) = \int_{-\infty}^{+\infty} \frac{2}{1+n(\omega)} A(\omega) e^{ik(\omega)x - i\omega t} d\omega, \quad (8)$$

$$A(\omega) = \frac{1}{2\pi} \int_{-\infty}^{+\infty} u(x=0,t)\, e^{i\omega t} d\omega. \quad (9)$$

Transforming the integral in Eq. (8) into the complex domain and closing the contour over the upper-half-plan, along with requiring that the medium characterized by n to be causal, and that the incident wave packet has a "front," are sufficient conditions to show that the value of the integral is identically zero for $t \le t_0 = x/c$ or equally for velocities, $V = x/t > c$. The condition that the medium characterized by n is causal, means that for this medium the effect cannot proceed the cause. Mathematically this is expressed as $G(\tau) = 0$ for $\tau < 0$, where $G(\tau)$ is the susceptibility kernel given by

$$G(\tau) = \frac{1}{2\pi} \int_{-\infty}^{+\infty} [\varepsilon(\omega)/\varepsilon_0 - 1] e^{-i\omega\tau} d\omega. \quad (10)$$

For times immediately after t_0, ($t >\approx t_0$) the earliest part of the signal known as the Sommerfeld forerunner or precursor can be detected. The frequency of oscillation and the field amplitude for the Sommerfeld forerunner are discussed by Mojahedi et. al.[4,34]. To summarize those results, the frequency of oscillation is given by

$$\omega_s = \sqrt{G'(0)} \Big/ \sqrt{2\left(\frac{t}{t_0} - 1\right)}, \quad (11)$$

where $G'(0)$ is the time derivative of the susceptibility kernel[33] evaluated at $t = 0$. Furthermore, for the incident wave packet proportional to t^m (m is an integer) the Sommerfeld forerunner is described by a Bessel function of order m according to

$$u(x,t) \approx a\left(\frac{t-t_0}{\gamma}\right)^{m/2} J_m\left(2\sqrt{\gamma(t-t_0)}\right); \quad (12)$$

$$\gamma = \frac{G'(0)\, t_0}{2}; \qquad for\ t > t_0.$$

From the above discussion it is clear that, for a given medium if the quantity $G'(0)$ is known, the calculation of the Sommerfeld forerunner frequency of

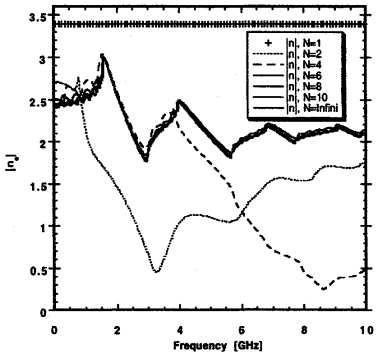

Fig. 12: Effective index for a 1DPC. The structure parameters are: $d_i = 1.76$ cm, $d_j = 1.33$ cm, $n_i = 1$, $n_j = 3.40$

oscillation and functional form is straightforward. In other words, if one is capable of calculating $\varepsilon(\omega)/\varepsilon_0 - 1 = n^2 - 1$ for a 1DPC, undersized waveguide, or any other photonic barrier used in the superluminal experiments, then one can perform the inverse Fourier transform and the differentiation operation to obtain $G'(0)$. For example, let us consider the case of

1DPC used in the experiments discussed in Sections. II and III.

At the normal incidence the dispersion relation (K *vs.* ω) can be obtained from

$$\cos(K\Lambda) = \cos\left(\frac{\omega n_i d_i}{c}\right)\cos\left(\frac{\omega n_j d_j}{c}\right) - \frac{1}{2}\left(R + R^{-1}\right)\sin\left(\frac{\omega n_i d_i}{c}\right) \sin\left(\frac{\omega n_j d_j}{c}\right), \quad (13)$$

where R is the ratio of the indices given by $R = n_i/n_j$, Λ is the one-period length $\Lambda = d_i + d_j$, and K is the Bloch wave vector. The above equation can be used to solve for the real and imaginary parts of the Bloch wave vector, and Eqs. (14)-(16), below, can in turn be used to transform the photonic crystal spatial dispersion [Eq. (13)] to a more manageable temporal dispersion

$$\mathrm{Re}(n_e) = n_e' = \frac{c}{\omega}\mathrm{Re}[K(\omega)], \quad (14)$$

$$\mathrm{Im}(n_e) = n_e'' = \frac{c}{\omega}\mathrm{Im}[K(\omega)], \quad (15)$$

$$|n_e| = \left[(n_e')^2 + (n_e'')^2\right]^{1/2} = \frac{c}{\omega}|K(\omega)|. \quad (16)$$

The results are shown in Fig. (12) which displays our first attempt in obtaining an effective index for a 1DPC, with 1, 2, 3,..., and infinite number of dielectric slabs. The next step is to perform the Fourier transform indicated by Eq. (10), followed by the differential operation evaluated at time equal to zero. Having obtained the quantity $G'(0)$, the frequency of oscillation and the functional form of the Sommerfeld forerunner in a 1DPC can be arrived at with the help of Eqs. (11) and (12).

VI. Superluminal Propagation and Quantum Noise in the Limit of Very Weak Pulse.

The question of superluminality in the limit of very weak pulse (one or few photons) was considered in a recent work[35]. For the sake of brevity, we refer the interested reader to Ref. 36 for a complete and detailed analysis of the situation. Here, we suffice to mention that according to Aharonov et. al.[36] in the limit of few photons, signal must be exponentially large in order to distinguish it from the quantum noise. In other words, the signal-to-noise ratio becomes vanishingly small. In Ref. 36 this assertion is investigated and it is seen that if the condition stated by Aharonov et. al. is replaced by a weaker condition, the signal-to-noise ratio can exceed unity even for one photon pulse. It is worth mentioning that the original experiment by Chiao and Steinberg[2], although involved the detection of single photon, but the results were interpreted in terms of statistics of many photons.

VII. Concluding Remarks: A Discussion for General Public

A simple yet interesting description of superluminal propagation can be found at weblink: http://www.abqjournal.com/scitech/180964scitech11-19-00.htm. This article, written by John Fleck, the science writer for Albuquerque Journal, tries to explain our newly published paper in *Physical Review E* to the general public. To use Fleck's analogy, consider two dragsters competing against each other, driving the same exact cars and traveling the same exact distances. However, whereas one of the dragsters travels through air (or vacuum) with the maximum allowable speed, the other driver travels through a series of barriers normally thought to slow his car. The question is then the following: What does the referee at the end line observe? The answer depends on the referee's detection equipment. If the referee is well equipped with the most sensitive and expensive detection systems he or she will observe that the front bumpers of the two cars arrive at the finishing line at

exactly the same instance. The referee will also observe that the bulk (the main body, the cockpit and the driver) of the dragster's car that tunneled through the barriers reaches the end line sooner than his challenger. If the race is decided by arrival of the cars' main body or if the referee is not equipped with the most sensitive detection apparatus, he or she will call the race for the tunneling dragster.

Bibliography

1 A. M. Steinberg and R. Y. Chiao, Physical Review a **51**, 3525-3528 (1995).

2 A. M. Steinberg, P. G. Kwiat, and R. Y. Chiao, Physical Review Letters **71**, 708-711 (1993).

3 C. Spielmann, R. Szipocs, A. Stingl, *et al.*, Physical Review Letters **73**, 2308-2311 (1994).

4 M. Mojahedi, E. Schamiloglu, F. Hegeler, *et al.*, Physical Review E **62**, 5758-5766 (2000).

5 M. Mojahedi, E. Schamiloglu, K. Agi, *et al.*, Ieee Journal of Quantum Electronics **36**, 418-424 (2000).

6 A. Ranfagni, P. Fabeni, G. P. Pazzi, *et al.*, Physical Review E **48**, 1453-1460 (1993).

7 A. Ranfagni, D. Mugnai, P. Fabeni, *et al.*, Applied Physics Letters **58**, 774-776 (1991).

8 D. Mugnai, A. Ranfagni, and L. Ronchi, Physics Letters a **247**, 281-286 (1998).

9 A. Enders and G. Nimtz, Physical Review B **47**, 9605-9609 (1993).

10 A. Enders and G. Nimtz, Journal De Physique I **2**, 1693-1698 (1992).

11 R. Y. Chiao and A. M. Steinberg, Progress in Optics **37**, 345-405 (1997).

12 E. L. Bolda, R. Y. Chiao, and J. C. Garrison, Physical Review A **48**, 3890-3894 (1993).

13 R. Y. Chiao, Physical Review a **48**, R34-R37 (1993).

14 E. L. Bolda, J. C. Garrison, and R. Y. Chiao, Physical Review a **49**, 2938-2947 (1994).

15 R. Y. Chiao and J. Boyce, Physical Review Letters **73**, 3383-3386 (1994).

16 L. Brillouin, *Wave propagation and group velocity* (Academic Press, New York,, 1960).

17 L. D. Landau, E. M. Lifshittz, and L. P. Pitaevski, *Electrodynamics of continuous media* (Pergamon, Oxford [Oxfordshire] ; New York, 1984).

18 (Hewlett Packard, 1997), p. 1-60.

19 (Hewlett Packard, 1992), p. 1-24.

20 R. Y. Chiao, A. E. Kozhekin, and G. Kurizki, Physical Review Letters **77**, 1254-1257 (1996).

21 A. M. Steinberg and R. Y. Chiao, Physical Review a **49**, 2071-2075 (1994).

22 R. Y. Chiao, *Amazing light : a volume dedicated to Charles Hard Townes on his 80th birthday* (Springer, New York, 1996).

23 T. Martin and R. Landauer, Physical Review a **45**, 2611-2617 (1992).

24 M. Buttiker and R. Landauer, Physica Scripta **32**, 429-434 (1985).

25 R. Landauer, Nature **365**, 692-693 (1993).

26 L. J. Wang, A. Kuzmich, and A. Dogariu, Nature ; **406**, 277-279 (2000).

27 V. G. Veselago, Soviet Physics-Solid State **8**, 2854-2856 (1967).

28 V. G. Veselago, Soviet Physics USPEKHI **10**, 509-514 (1968).

29 J. B. Pendry, A. J. Holden, D. J. Robbins, *et al.*, Ieee Transactions On Microwave Theory and Techniques **47**, 2075-2084 (1999).

30 J. B. Pendry, Physical Review Letters **85**, 3966-3969 (2000).

31 D. R. Smith, W. J. Padilla, D. C. Vier, *et al.*, Physical Review Letters **84**, 4184-4187 (2000).

32 R. A. Shelby, D. R. Smith, and S. Schultz, Science **292**, 77-79 (2001).

33 J. D. Jackson, *Classical electrodynamics* (Wiley, New York, 1998).

34 M. Mojahedi, in *EECE* (University of New Mexico, Albuquerque, 1999).

35 B. Segev, P. W. Milonni, J. F. Babb, *et al.*, Physical Review a **62**, 022114-1-15 (2000).

36 Y. Aharonov, B. Reznik, and A. Stern, Physical Review Letters **81**, 2190-2193 (1998).

A01-34135

AIAA 2001-3360
Geometrodynamics, Inertia and the Quantum Vacuum

Bernard Haisch
California Institute for Physics and Astrophysics
366 Cambridge Ave., Palo Alto, CA 94306

Alfonso Rueda
Department of Electrical Engineering, ECS Building
California State University, 1250 Bellflower Blvd.
Long Beach, California 90840

37th AIAA/ASME/SAE/ASEE Joint Propulsion Conference and Exhibit
8-11 July 2001
Salt Lake City, Utah

AIAA 2001-3360

Geometrodynamics, Inertia and the Quantum Vacuum

Bernard Haisch

California Institute for Physics and Astrophysics, 366 Cambridge Ave., Palo Alto, CA 94306
<www.calphysics.org>
Associate Fellow, AIAA — *haisch@calphysics.org*

Alfonso Rueda
Department of Electrical Engineering, ECS Building
California State University, 1250 Bellflower Blvd., Long Beach, California 90840
arueda@csulb.edu

(*Presented at the AIAA/ASME/SAE/ASEE Joint Propulsion Conference, Salt Lake City, July 8–11, 2001*)

ABSTRACT

Why does **F** equal **ma** in Newton's equation of motion? How does a gravitational field produce a force? Why are inertial mass and gravitational mass the same? It appears that all three of these seemingly axiomatic foundational questions have an answer involving an identical physical process: interaction between the electromagnetic quantum vacuum and the fundamental charged particles (quarks and electrons) constituting matter. All three of these effects and equalities can be traced back to the appearance of a specific asymmetry in the otherwise uniform and isotropic electromagnetic quantum vacuum. This asymmetry gives rise to a non-zero Poynting vector from the perspective of an accelerating object. We call the resulting energy-momentum flux the *Rindler flux*. The key insight is that the asymmetry in an accelerating reference frame in flat spacetime is identical to that in a stationary reference frame (one that is not falling) in curved spacetime. Therefore the same Rindler flux that creates inertial reaction forces also creates weight. All of this is consistent with the conceptualizaton and formalism of general relativity. What this view adds to physics is insight into a specific physical process creating identical inertial and gravitational forces from which springs the weak principle of equivalence. What this view hints at in terms of advanced propulsion technology is the possibility that by locally modifying either the electromagnetic quantum vacuum and/or its interaction with matter, inertial and gravitational forces could be modified.

INTRODUCTION

Why does **F** equal **ma** in Newton's equation of motion, $\mathbf{F} = m\mathbf{a}$?
How does a gravitational field produce a force?
Why are inertial mass and gravitational mass the same?

These are questions that are usually thought to be more appropriate for philosophers than for physicists, since the apparent facts of nature addressed in these questions are generally regarded as axiomatic.[1] If one assumes that one plus one equals two, plus a limited number of additional axioms, one can develop a self-consistent system of mathematics, but one has to start with such assumptions. In the realm of geometry, the discovery of non-Euclidean geometry in the 19th century taught us that other, non-intuitive assumptions are possible, and indeed, Riemannian geometry became the basis for physics in Einstein's general relativity (GR). Alternate foundational assumptions can lead to new insights.

Since 1991 we have been engaged in investigations involving the nature of inertia based on the foundational assumption that the electromagnetic quantum vacuum, also called the zero-point field or zero-point

fluctuations, is a real and underlying universal sea of energy capable of interacting with matter, and that this interaction may be described using the techniques of stochastic electrodynamics (SED).[2] Following a successful multiyear NASA-funded investigation at Lockheed Martin and California State University at Long Beach, the privately-funded California Institute for Physics and Astrophysics (CIPA) was established in 1999 specifically to study the electromagnetic quantum vacuum and its effects. A group of five postdoctoral fellows with expertise in quantum electrodynamics, superstring and M-brane theory, general relativity, plasma physics and Casimir effects are engaged in theoretical efforts to come to a deeper understanding of foundational questions in physics and to examine the possible nature and degree of electromagnetic quantum vacuum–matter interactions both within and beyond the SED approximations. CIPA has also funded projects by experts at several universities directed toward the general goal of explaining the origin of inertia and certain aspects of gravitation and other relevant physical and astrophysical effects as due to the electromagnetic quantum vacuum.

It appears that all three of the seemingly axiomatic foundational questions posed above have an answer involving an identical physical process: interaction between the electromagnetic quantum vacuum and the fundamental charged particles (quarks and electrons) constituting matter. All three of these effects and equalities can be traced back to the appearance of a specific asymmetry in the otherwise uniform and isotropic electromagnetic quantum vacuum. The key insight is that the asymmetry in an accelerating reference frame in flat spacetime is identical to that in a stationary reference frame in curved spacetime.

It was shown by Unruh [3] and by Davies [4] that a uniformly-accelerating detector will experience a Planckian-like heat bath whose apparent "temperature" is a result of quantum vacuum radiation. A tiny fraction of the (enormous) electromagnetic quantum vacuum energy can emerge as real radiation under the appropriate conditions. The theoretical prediction of Unruh-Davies radiation is now generally accepted and SLAC physicist P. Chen has recently proposed an experiment to detect and measure it.[5] Rueda and Haisch (hereafter RH) [6] analyzed a related process and found that as perceived by an accelerating object, an energy and momentum flux of radiation emerges from the electromagnetic quantum vacuum and that the strength of this momentum flux is such that the radiation pressure force on the accelerating object is proportional to acceleration. Owing to its origin in an accelerating reference frame customarily called the *Rindler frame*, and to the relation of this flux to the existence of a *Rindler event horizon*, we call this flux of energy and momentum that emerges out of the electromagnetic quantum vacuum upon acceleration the *Rindler flux*.

If the Rindler flux is allowed to electromagnetically interact with matter, mainly but perhaps not exclusively at the level of quarks and electrons, a reaction force is produced that can be interpreted as the origin of Newton's $\mathbf{F} = m\mathbf{a}$. In this view, which we call the *quantum vacuum inertia hypothesis*, matter resists acceleration not because of some innate property of inertia, but rather because the quantum vacuum fields provide an acceleration-dependent drag force. In future attempts we and coworkers intend to examine the possible contributions of other components of the quantum vacuum besides the electromagnetic. (This is relevant to the issue of possible neutrino mass, which could not be due to the electromagnetic quantum vacuum, but might possibly be due to the vacuum fields of the weak interaction.)

GR declares that gravity can be interpreted as spacetime curvature. Wheeler coined the term geometrodynamics to describe this: the dynamics of objects subject to gravity is determined by the geometry of four-dimensional spacetime. What geometrodynamics actually specifies is the family of geodesics — the shortest four-dimensional distances between two points in spacetime — in the presence of a gravitating body. Freely-falling objects and light rays follow geodesics. However when an object is prevented from following a geodetic trajectory, a force is experienced: the well-known force called weight. Where does this force come from? Or put another way, how does a gravitational field exert a force on a non freely-falling, fixed, object, such as an observer standing on a scale on the Earth's surface? *This proves to be the identical physical process as described in the quantum vacuum inertia hypothesis, due to a non-zero Rindler flux.*

In the SED approximation, the electromagnetic quantum vacuum is represented as propagating electromagnetic waves.[7,8] These should follow geodesics. It can be shown that propagation along curved geodesics creates the identical electromagnetic Rindler flux with respect to a stationary fixed object as is the case for an

accelerating object.[9] This is perfectly consistent with Einstein's fundamental assumption of the equivalence of gravitation and acceleration. An object fixed above a gravitating body will perceive the electromagnetic quantum vacuum to be accelerating past it, which is of course the same as the perception of the object when it is doing the accelerating through the quantum vacuum. Thus in the case of gravity, it would be the electromagnetic Rindler flux acting upon a fixed object that creates the force known as weight, thereby answering the second question. The answer to the third question then immediately follows. Since the same flux would be seen by either a fixed object in a gravitational field or an accelerating object in free space, the force that is felt would be the same, hence the parameters we traditionally call inertial and gravitational mass must be the same. This would explain the physical origin of the weak principle of equivalence.

All of this is consistent with the mathematics of GR. What this view adds to physics is insight into a specific physical process creating identical inertial and gravitational forces. What this view hints at in terms of advanced propulsion technology is the possibility that by locally modifying either the quantum vacuum fields and/or their interaction with matter, inertial and gravitational forces could be modified and possibly one day freely controlled.

THE ELECTROMAGNETIC QUANTUM VACUUM

The quantization of the electromagnetic field in terms of quantum-mechanical operators may be found in various standard textbooks, e.g. Loudon [10]: "The electromagnetic field is now quantized by the association of a quantum-mechanical harmonic oscillator with each mode $\mathbf{k}$ of the radiation field." This can be understood as follows: Application of the Heisenberg uncertainty relation to a harmonic oscillator requires that its ground state have a non-zero energy of $h\nu/2$. This reflects the fact that quantum mechanically a particle cannot simultaneously be exactly at the bottom of its potential well and have exactly zero momentum. There exists the same $h\nu/2$ zero-point energy expression for each mode of the electromagnetic field as for a mechanical oscillator. (Formally, mode decomposition yields that each mode can be mathematically made into a harmonic oscillator in the sense that the same differential equation is obeyed as for a mechanical oscillator.)

Summing up the energy over the modes for all frequencies, directions, and polarization states, one arrives at a zero-point energy density for the electromagnetic fluctuations, and this is the origin of the electromagnetic quantum vacuum. An energy of $h\nu/2$ per mode of the field characterizes the fluctuations of the quantized radiation field in quantum field theory. In the semi-classical representation of SED the quantum vacuum is represented by propagating electromagnetic plane waves, $\mathbf{E}^{zp}$ and $\mathbf{B}^{zp}$, of random phase having this average energy, $h\nu/2$, in each mode.

The volumetric density of modes between frequencies ν and $\nu + d\nu$ is given by the density of states function $N_\nu d\nu = (8\pi\nu^2/c^3)d\nu$. Each state has a minimum $h\nu/2$ of energy, and using this density of states function and this minimum energy — that we call the zero-point energy — per state one gets the spectral energy density of the electromagnetic quantum vacuum:

$$\rho(\nu)d\nu = \frac{8\pi\nu^2}{c^3}\frac{h\nu}{2}d\nu. \tag{1}$$

Writing this zero-point radiation together with ordinary blackbody radiation, the energy density is:

$$\rho(\nu,T)d\nu = \frac{8\pi\nu^2}{c^3}\left(\frac{h\nu}{e^{h\nu/kT}-1}+\frac{h\nu}{2}\right)d\nu. \tag{2}$$

The first term (outside the parentheses) represents the mode density, and the terms inside the parentheses are the average energy per mode of thermal radiation at temperature T plus the zero-point energy, $h\nu/2$, which has no temperature dependence. Take away all thermal energy by formally letting T go to zero, and one is still left with the zero-point term. The laws of quantum mechanics as applied to electromagnetic

radiation force the existence of a background sea of electromagnetic zero-point energy that is traditionally called the electromagnetic quantum vacuum.

The spectral energy density of eqn. (1) was thought to be no more than a spatially uniform constant offset that cancels out when considering energy fluxes, but it was discovered in the mid-1970's that the quantum vacuum acquires special characteristics when viewed from an accelerating frame. Just as there is an event horizon for a black hole, there is an analogous event horizon for an accelerating reference frame. Similar to radiation from evaporating black holes proposed by Hawking [11], Unruh [3] and Davies [4] determined that a Planck-like radiation component will arise out of the quantum vacuum in a uniformly-accelerating coordinate system having constant proper acceleration a (where $|\mathbf{a}| = a$) with what amounts to an effective "temperature"

$$T_a = \frac{\hbar a}{2\pi c k}. \tag{3}$$

This "temperature" characterizing Unruh-Davies radiation does not originate in emission from particles undergoing thermal motions. [a] As discussed by Davies, Dray and Manogue [12]:

> One of the most curious properties to be discussed in recent years is the prediction that an observer who accelerates in the conventional quantum vacuum of Minkowski space will perceive a bath of radiation, while an inertial observer of course perceives nothing. In the case of linear acceleration, for which there exists an extensive literature, the response of a model particle detector mimics the effect of its being immersed in a bath of thermal radiation (the so-called Unruh effect).

This "heat bath" is a quantum phenomenon. The "temperature" is negligible for most accelerations. Only in the extremely large gravitational fields of black holes or in high-energy particle collisions can this become significant. Recently, P. Chen at the Stanford Linear Accelerator Center has proposed using an ultra high intensity laser to accelerate electrons violently enough to directly detect Unruh-Davies radiation.[5]

Unruh and Davies treated the electromagnetic quantum vacuum as a scalar field. If a true vectorial approach is considered there appear additional terms beyond the quasi-thermal Unruh-Davies component. For the case of no true external thermal radiation ($T = 0$) but including the acceleration effect (T_a), eqn. (1) becomes

$$\rho(\nu, T_a)d\nu = \frac{8\pi\nu^2}{c^3}\left[1 + \left(\frac{a}{2\pi c\nu}\right)^2\right]\left[\frac{h\nu}{2} + \frac{h\nu}{e^{h\nu/kT_a} - 1}\right]d\nu, \tag{4}$$

where the acceleration-dependent pseudo-Planckian Unruh-Davies component is placed after the $h\nu/2$ term to indicate that except for extreme accelerations (e.g. particle collisions at high energies) this term is negligibly small. While these additional acceleration-dependent terms do not show any spatial asymmetry in the expression for the spectral energy density, certain asymmetries do appear when the momentum flux of this radiation is calculated, resulting in a non-zero Rindler flux.[6] This asymmetry appears to be the process underlying inertial and gravitational forces.

ORIGIN OF THE INERTIAL REACTION FORCE

Newton's third law states that if an agent applies a force to a point on an object, at that point there arises an equal and opposite reaction force back upon the agent. In the case of a fixed object the equal and opposite reaction force can be traced to interatomic forces in the neighborhood of the point of contact which act to resist compression, and these in turn can be traced to electromagnetic interactions involving orbital electrons of adjacent atoms or molecules, etc.

[a] There is likely to be a deep connection between the fact that the spectrum that arises in this fashion due to acceleration and the ordinary blackbody spectrum have identical form.

Now a similar experience of an equal and opposite reaction force arises when a non-fixed object is forced to accelerate. Why does acceleration create such a reaction force? We suggest that this equal and opposite reaction force also has an underlying cause which is at least partially electromagnetic, and specifically may be due to the scattering of electromagnetic quantum vacuum radiation. RH demonstrated that from the point of view of the pushing agent there exists a net flux (Poynting vector) of quantum vacuum radiation transiting the accelerating object in a direction opposite to the acceleration: the Rindler flux.[6] Interaction of this flux with the quarks and electrons constituting a material object would create a back reaction force that can be interpreted as inertia. One simply needs to assume that there is some dimensionless efficiency factor, $\eta(\omega)$, that in the case of particles corresponds to whatever the interaction process is (e.g. dipole scattering). In the case of elementary particles we suspect that $\eta(\omega)$ contains one or more resonances — and in the Appendix discuss why these resonances likely involve Compton frequencies of relevant particles forming a composite particle or object — but this is not a necessary assumption.

The RH approach relies on making transformations of the $\mathbf{E}^{zp}$ and $\mathbf{B}^{zp}$ from a stationary to a uniformly-accelerating coordinate system (see, for example, §11.10 of Jackson for the relevant transformations [13]). In a stationary or uniformly-moving frame the $\mathbf{E}^{zp}$ and $\mathbf{B}^{zp}$ constitute an isotropic radiation pattern. In a uniformly-accelerating frame the radiation pattern acquires asymmetries. There appears a non-zero Poynting vector in any accelerating frame, and therefore a non-zero Rindler flux which carries a net flux of electromagnetic momentum. The scattering of this momentum flux generates a reaction force, $\mathbf{F}_r$, proportional to the acceleration. RH found an invariant scalar with the dimension of mass quantifying the inertial resistance force of opposition per unit of acceleration resulting from this process. We interpret this scalar as the inertial mass,

$$m_i = \frac{V_0}{c^2} \int \eta(\nu) \rho_{zp}(\nu)\, d\nu, \tag{5}$$

where ρ_{zp} is the well known spectral energy density of the electromagnetic quantum vacuum of eqn. (1). In other words, the amount of electromagnetic zero point energy instantaneously transiting through an object of volume V_0 and interacting with the quarks, electrons and all charges in that object is what constitutes the inertial mass of that object in this view. It is change in the momentum of the radiation field that creates the resistance to acceleration usually attributed to the inertia of an object.

Indeed, not only does the ordinary form of Newton's second law, $\mathbf{F} = m_i \mathbf{a}$, emerge from this analysis, but one can also obtain the relativistic form of the second law: [6]

$$\mathcal{F} = \frac{d\mathcal{P}}{d\tau} = \frac{d}{d\tau}(\gamma_\tau m_i c,\ \mathbf{p}\ ). \tag{6}$$

The origin of inertia, in this picture, becomes remarkably intuitive. Any material object resists acceleration because the acceleration produces a perceived flux of radiation in the opposite direction that scatters within the object and thereby pushes against the accelerating agent. Inertia in the present model appears as a kind of acceleration-dependent electromagnetic quantum vacuum drag force acting upon electromagnetically-interacting elementary particles. The relativistic law for "mass" transformation involving the Lorentz factor γ — that is, the formula describing how the *inertia* of a body has been calculated to change according to an observer's relative motion — is automatically satisfied in this view, because the correct relativistic form of the reaction force is derived, as shown in eqn. (6).

ORIGIN OF WEIGHT AND THE WEAK EQUIVALENCE PRINCIPLE

Einstein introduced the *local Lorentz invariance* (LLI) principle in order to pass from special relativity to GR. It is possible to use this principle immediately to extend the results of the quantum vacuum inertia hypothesis to gravitation (details discussed in two forthcoming papers [9]).

The idea behind the LLI principle is embodied in the Einstein elevator thought experiment. He proposed that a freely-falling elevator in a gravitational field is equivalent to one that is not accelerating and is far

from any gravitating body. Physics experiments would yield the same results in either elevator, and therefore a freely-falling coordinate frame in a gravitational field is the same as an inertial Lorentz frame. (This is rigorously only true for a "small elevator" since a gravitational field around a planet, say, must be radial, hence there are inevitably tidal forces which would not be the case for an ideal acceleration.) The device Einstein used to develop general relativity was to invoke an infinite set of such freely falling frames. In each such frame, the laws of physics are those of special relativity. The additional features of general relativity emerge by comparing the properties of measurements made in freely-falling Lorentz frames "dropped" one after the other.

This appraoch of Einstein is both elegant and powerful. The LLI principle immediately tells us that an object accelerating through the electromagnetic quantum vacuum is equivalent to an object held fixed in a gravitational field while the electromagnetic quantum vacuum is effectively accelerating (falling) past it. The prediction of GR that light rays deviate from straight-line propagation in the presence of a gravitating body — which Eddington measured in 1919 thereby validating GR — translates into acceleration (falling) of the electromagnetic quantum vacuum. An object accelerating through the electromagnetic quantum vacuum experiences a Rindler flux which causes the inertia reaction force. A fixed object past which the electromagnetic quantum vacuum is accelerating, following the laws of GR, experiences the same Rindler flux and the resulting force is what we call weight. That is why $m_g = m_i$ and is the basis of the weak equivalence principle.

CONCLUSIONS

Geometrodynamics is an elegant theoretical structure, but there is a very fundamental physics question that geometrodynamics has never satisfactorily addressed. If an object is forced to deviate from its natural geodesic motion, a reaction force arises, i.e. the weight of an object. Where does the reaction force that is weight come from? That same force would also be the enforcer of geodesic motion for freely falling objects. GR specifies the metric of spacetime from which geodesics can be calculated, but is there a physical mechanism to keep freely-falling objects from straying from their proper geodesics? Geometrodynamics does not provide a physical mechanism for this. It can only claim that deviations of an object from its proper geodesic motion results in an inertial reaction force. This is true but uninformative. The quantum vacuum inertia hypothesis provides a physical process generating inertia and weight.

Quantum physics predicts the existence of an underlying sea of zero-point energy at every point in the universe. This is different from the cosmic microwave background and is also referred to as the electromagnetic quantum vacuum since it is the lowest state of otherwise empty space. This sea of energy fills all of space and is absolutely the same everywhere as perceived from a constant velocity reference frame. But viewed from an accelerating reference frame, the radiation pattern of the energy becomes minutely distorted: a tiny directional flow is experienced by an accelerating object or observer, the Rindler flux. Importantly, the force resulting from that energy-momentum flow turns out to be proportional to the acceleration. When this energy-momentum flow — that arises automatically when any object accelerates — interacts with the fundamental particles constituting matter (quarks and electrons) a force arises in the direction opposite to the acceleration. This process can be interpreted as the origin of inertia, i.e. as the basis of Newton's second law of mechanics: $\mathbf{F} = m\mathbf{a}$ (and its relativistic extension).[6]

It has now been discovered that exactly the same distortion of the radiation pattern occurs in geometrodynamics when the metric is non-Minkowskian.[9] The curved spacetime geodesics of geometrodynamics affect the zero-point energy in the same way as light rays (because the zero-point energy is also a mode of electromagnetic radiation). The gravitational force causing weight and the reaction force causing inertia originate in an identical interaction with a distortion in the radiation of the zero-point energy field. Both are a kind of radiation pressure originating in the electromagnetic quantum vacuum. The underlying distortion of the radiation pattern is due to an event horizon-like effect and is related to Unruh-Davies radiation and Hawking radiation.

What the quantum vacuum inertia hypothesis accomplishes is to identify the physical process which is the enforcer of geometrodynamics or general relativity. The quantum vacuum inertia hypothesis appears

to provide a link between light propagation along geodesics and mechanics of material objects. Moreover, since the distortion of the zero-point energy radiation pattern is the same whether due to acceleration or being held stationary in a gravitational field, this explains a centuries old puzzle: why inertial mass and gravitational mass are the same: both are due to the same non-zero Rindler flux. This gives us a deeper insight into Einstein's principle of equivalence.

APPENDIX: INERTIA AND THE DE BROGLIE WAVELENGTH

Four-momentum is defined as

$$\mathbf{P} = \left(\frac{E}{c}, \quad \mathbf{p}\right) = (\gamma m_0 c, \quad \mathbf{p}) = (\gamma m_0 c, \quad \gamma m_0 \mathbf{v}), \tag{A1}$$

where $|\mathbf{P}| = m_0 c$ and $E = \gamma m_0 c^2$. The Einstein-de Broglie relation defines the Compton frequency $h\nu_C = m_o c^2$ for an object of rest mass m_0, and if we make the de Broglie assumption that the momentum-wave number relation for light also characterizes matter then $\mathbf{p} = \hbar \mathbf{k}_B$ where $\mathbf{k}_B = 2\pi(\lambda_{B,1}^{-1}, \lambda_{B,2}^{-1}, \lambda_{B,3}^{-1})$. We thus write

$$\frac{\mathbf{P}}{\hbar} = \left(\frac{2\pi\gamma\nu_C}{c}, \mathbf{k}_B\right) = 2\pi\left(\frac{\gamma}{\lambda_C}, \frac{1}{\lambda_{B,1}}, \frac{1}{\lambda_{B,2}}, \frac{1}{\lambda_{B,3}}\right) \tag{A2}$$

and from this obtain the relationship

$$\lambda_B = \frac{c}{\gamma v}\lambda_C \tag{A3}$$

between the Compton wavelength, λ_C, and the de Broglie wavelength, λ_B. For a stationary object λ_B is infinite, and the de Broglie wavelength decreases in inverse proportion to the momentum.

Eqn. (5) is very suggestive that quantum vacuum-elementary particle interaction involves a resonance at the Compton frequency. De Broglie proposed that an elementary particle is associated with a localized wave whose frequency is the Compton frequency. As summarized by Hunter [14]: "...what we regard as the (inertial) mass of the particle is, according to de Broglie's proposal, simply the vibrational energy (divided by c^2) of a localized oscillating field (most likely the electromagnetic field). From this standpoint inertial mass is not an elementary property of a particle, but rather a property derived from the localized oscillation of the (electromagnetic) field. De Broglie described this equivalence between mass and the energy of oscillational motion...as *'une grande loi de la Nature'* (a great law of nature)."

This perspective is consistent with the proposition that inertial mass, m_i, may be a coupling parameter between electromagnetically interacting particles and the quantum vacuum. Although De Broglie assumed that his wave at the Compton frequency originates in the particle itself (due to some intrinsic oscillation or circulation of charge perhaps) there is an alternative interpretation discussed in some detail by de la Peña and Cetto that a particle "is tuned to a wave originating in the high-frequency modes of the zero-point background field."[8] The de Broglie oscillation would thus be due to a resonant interaction with the quantum vacuum, presumably the same resonance that is responsible for creating a contribution to inertial mass as in eqn. (5). In other words, the electromagnetic quantum vacuum would be driving this ν_C oscillation.

We therefore suggest that an elementary charge driven to oscillate at the Compton frequency, ν_C, by the quantum vacuum may be the physical basis of the $\eta(\nu)$ scattering parameter in eqn. (5). For the case of the electron, this would imply that $\eta(\nu)$ is a sharply-peaked resonance at the frequency, expressed in terms of energy, $h\nu_C = 512$ keV. The inertial mass of the electron would physically be the reaction force due to resonance scattering of the electromagnetic quantum vacuum radiation, the Rindler flux, at that frequency.

This leads to a surprising corollary. It has been shown that as viewed from a laboratory frame, a standing wave at the Compton frequency in the electron frame transforms into a traveling wave having the de Broglie wavelength for a moving electron.[8,14,15,16] The wave nature of the moving electron (as measured in the Davisson-Germer experiment, for example) would be basically due to Doppler shifts associated with its Einstein-de Broglie resonance at the Compton frequency. A simplified heuristic model shows this, and

a detailed treatment showing the same result may be found in de la Peña and Cetto [8]. Represent a quantum vacuum-like driving force field as two waves having the Compton frequency $\omega_C = 2\pi\nu_C$ travelling in equal and opposite directions, $\pm\hat{x}$. The amplitude of the combined oppositely-moving waves acting upon an electron will be

$$\phi = \phi_+ + \phi_- = 2\cos\omega_C t \cos k_C x. \qquad (A4)$$

But now assume an electron is moving with velocity v in the $+x$-direction. The wave responsible for driving the resonant oscillation impinging on the electron from the front will be the wave seen in the laboratory frame to have frequency $\omega_- = \gamma\omega_C(1 - v/c)$, i.e. it is the wave below the Compton frequency in the laboratory that for the electron is Doppler shifted up to the ω_C resonance. Similarly the zero-point wave responsible for driving the electron resonant oscillation impinging on the electron from the rear will have a laboratory frequency $\omega_+ = \gamma\omega_C(1 + v/c)$ which is Doppler shifted down to ω_C for the electron. The same transformations apply to the wave numbers, k_+ and k_-. The Lorentz invariance of the electromagnetic quantum vacuum spectrum ensures that regardless of the electron's (unaccelerated) motion the up- and down-shifting of the laboratory-frame spectral energy density will always yield a standing wave in the electron's frame.

It can be shown [8,15] that the superposition of these two oppositely-moving, Doppler-shifted waves is

$$\phi' = \phi'_+ + \phi'_- = 2\cos(\gamma\omega_C t - k_B x)\cos(\omega_B t - \gamma k_C x). \qquad (A5)$$

Observe that for fixed x, the rapidly oscillating "carrier" of frequency $\gamma\omega_C$ is modulated by the slowly varying envelope function in frequency ω_B. And *vice versa* observe that at a given t the "carrier" in space appears to have a relatively large wave number γk_C which is modulated by the envelope of much smaller wave number k_B. Hence both timewise at a fixed point in space and spacewise at a given time, there appears a carrier that is modulated by a much broader wave of dimension corresponding to the de Broglie time $t_B = 2\pi/\omega_B$, or equivalently, the de Broglie wavelength $\lambda_B = 2\pi/k_B$.

This result may be generalized to include quantum vacuum radiation from all other directions, as may be found in the monograph of de la Peña and Cetto [8]. They conclude by stating: "The foregoing discussion assigns a physical meaning to de Broglie's wave: it is the *modulation* of the wave formed by the Lorentz-transformed, Doppler-shifted superposition of the whole set of random stationary electromagnetic waves of frequency ω_C with which the electron interacts selectively."

Another way of looking at the spatial modulation is in terms of the wave function: the spatial modulation of eqn. (A5) is exactly the $e^{ipx/\hbar}$ wave function of a freely moving particle satisfying the Schrödinger equation. The same argument has been made by Hunter [14]. In such a view the quantum wave function of a moving free particle becomes a "beat frequency" produced by the relative motion of the observer with respect to the particle and its oscillating charge.

It thus appears that a simple model of a particle as an electromagentic quantum vacuum-driven oscillating charge with a resonance at its Compton frequency may simultaneously offer insight into the nature of inertial mass, i.e. into rest inertial mass and its relativistic extension, the Einstein-de Broglie formula and into its associated wave function involving the de Broglie wavelength of a moving particle. If the de Broglie oscillation is indeed driven by the electromagnetic quantum vacuum, then it is a form of Schrödinger's *zitterbewegung*. Moreover there is a substantial literature attempting to associate spin with *zitterbewegung* tracing back to the work of Schrödinger [17]; see for example Huang [18] and Barut and Zanghi [19].

REFERENCES

1] M. Jammer, Concepts of Mass in Contemporary Physics and Philosopy, Princeton Univ. Press (2000)
[2] B. Haisch, A. Rueda, and H. E. Puthoff, Phys. Rev. A **49** 678 (HRP) (1994)

[3] W. G. Unruh, Phys. Rev. D, **14** 870 (1976)
[4] P. C. W. Davies, J. Phys. A, **8** 609 (1975)
[5] P. Chen, reported at American Astronomical Society meeting, June 6, 2000.
[6] A. Rueda and B. Haisch, Found. Phys. **28** 1057 (1998); A. Rueda and B. Haisch, Phys. Lett. A **240** 115 (1998)
[7] T. H. Boyer, Phys. Rev. D, **11** 790 (1975)
[8] L. de la Peña, and A. M. Cetto, The Quantum Vacuum: An Introduction to Stochastic Electrodynamics, Kluwer Acad. Publ. (1996)
[9] A. Rueda, B. Haisch and R. Tung, in prep. (2001); R. Tung, B. Haisch and A. Rueda, in prep. (2001)
[10] R. Loudon, The Quantum Theory of Light (2nd ed.) Clarendon Press, Oxford (1983)
[11] S. Hawking, Nature, **248** 30 (1974)
[12] P. C. W. Davies, T. Dray, and C. A. Manogue, Phys. Rev. D **53** 4382 (1996)
[13] J. D. Jackson, Classical Electrodynamics (3rd ed.) (1999)
[14] G. Hunter, in The Present Status of the Quantum Theory of Light, S. Jeffers et al. (eds.), (Kluwer Acad. Publ.), chap. 12 (1996)
[15] A. F. Kracklauer, Physics Essays **5** 226 (1992); for a formal derivation and further illuminating discussion see Chap. 12 of [4]
[16] B. Haisch and A. Rueda, Phys. Lett. A, **268**, 224 (2000)
[17] E. Schrödinger, Sitz. Ber. Preuss. Akad. Wiss. Phys.-Math. Kl, **24**, 4318 (1930)
[18] K. Huang, Am. J. Phys. **20** 479 (1952)
[19] A. O. Barut and N. Zanghi, Phys. Rev. Lett. **52** 209 (1984)

18 February 2002

PHYSICS LETTERS A

ELSEVIER

Physics Letters A 294 (2002) 79–83

www.elsevier.com/locate/pla

Interplay between gravity and quintessence: a set of new GR solutions

Arthur D. Chernin [a,b,c], David I. Santiago [d,*], Alexander S. Silbergleit [e]

[a] *Sternberg Astronomical Institute, Moscow University, Moscow, 119899, Russia*
[b] *Astronomy Division, Oulu University, Oulu, 90401, Finland*
[c] *Tuorla Observatory, University of Turku, Piikkiö, 21 500, Finland*
[d] *Department of Physics, Stanford University, Stanford, CA 94305-4060, USA*
[e] *Gravity Probe B, W.W. Hansen Experimental Physics Laboratory, Stanford University, Stanford, CA 94305-4085, USA*

Received 15 June 2001; received in revised form 21 August 2001; accepted 8 October 2001

Communicated by P.R. Holland

Abstract

A set of new exact analytical general relativity (GR) solutions with time-dependent and spatially inhomogeneous quintessence demonstrate (1) a static non-empty space–time with a horizon-type singular surface; (2) time-dependent spatially homogeneous 'spheres' which are completely different in geometry from the Friedmann isotropic models; (3) infinitely strong anti-gravity at a 'true' singularity where the density is infinitely large. It is also found that (4) the GR solutions allow for an extreme 'density-free' form of energy that can generate regular space–time geometries.

PACS: 98.80.Cq; 04.25.Dm; 04.60.-m

1. Introduction

The idea of quintessence (Q) as a dynamic, time-dependent and spatially inhomogeneous energy with negative pressure-to-density ratio ($p = wp$, $-1 < w < 0$) [1] provides new 'degrees of freedom' in cosmology [1,2] and extends the variety of modern field models to include extreme forms of energy [1,3]. It may also stimulate a better understanding of the fundamental problem of interplay between gravity and the known field theories (for a review of this problem, see [4]).

The equation of state with $w = -1$ represents vacuum-type quintessence (VQ) which is phenomenologically described by the cosmological constant [5]; VQ is known to induce the dynamic effect of cosmological acceleration, if its density is positive. Recent data on the brightness of distant SN Ia [6] (as well as the evidence coming from the cosmic age, large scale structure, and cosmic microwave background anisotropy combined with the cluster dynamics) most probably indicate that the observed cosmological expansion is indeed accelerating if the universe is homogeneous. The physical reason for the cosmic acceleration may generally be attributed not only to VQ, but to

* Corresponding author.
E-mail address: david@small.stanford.edu (D.I. Santiago).

0375-9601/02/$ – see front matter
PII: S0375-9601(01)00672-7

any form of Q with $w < -1/3$, $\rho > 0$ or $w > -1/3$, $\rho < 0$, as seen from the Friedmann equations. In the original paper [1], positive energy for Q is preferred; in contrast with that, the whole range $-\infty < \rho < +\infty$ is considered below, for completeness and to examine whether any restrictions on the sign of energy could come from GR, if $w = \text{const}$. Note that the 'inertial energy dominance condition', $\rho + p > 0$, which is not met in the basic case of VQ, $w = -1$, is not satisfied also for some other forms of energy discussed below.

The special case $w = -1/3$ represents the only form of energy (with the linear equation of state) that can generate gravity with zero acceleration or deceleration effect in a homogeneous and isotropic universe, regardless the sign of the energy density. Gravity of this origin reveals itself only in the curvature of the four-dimensional space–time, it has no Newtonian analogs (unlike all other forms of Q, including VQ), and its nature is completely due to general relativity (GR) physics. Historically, Q with $w = -1/3$ was the first energy component that appeared in GR cosmology: in the Einstein static cosmological solution of 1917 the dynamic balance of anti-gravity of the cosmological constant and gravity of pressure-free matter gives rise to an effective equation of state with $w = -1/3$. This special type of Q with $w = -1/3$ may be called *Einstein quintessence* (EQ).

In the present Letter, some special properties of gravity produced by EQ, as well as by other extreme forms of Q in static and time-dependent, spatially homogeneous and inhomogeneous space–times are studied by means of a set of new exact analytical GR solutions. The metric of the solutions has 3D spherical symmetry,

$$ds^2 = A(r,t)\,dt^2 - B(r,t)\,d\Omega^2 - C(r,t)\,dr^2; \qquad (1)$$

the components of the metric tensor $A(r,t)$, $B(r,t)$, $C(r,t)$ are functions of the radial coordinate r and time t, and $d\Omega^2 = \sin^2\theta\,d\varphi^2 + d\theta^2$.

Four major new results are reported in the Letter. (1) The interplay between gravity and Q is capable of creating a static non-empty space–time with a horizon-type singular surface. (2) This interplay is also revealed in the formation of time-dependent spatially homogeneous 'spheres' which are completely different from the Friedmann isotropic models and have no analogs in Newtonian gravity. (3) Q can induce infinitely strong anti-gravity at a 'true' singularity where the density is infinitely large. (4) GR allows for an extreme 'density-free' form of energy that can generate regular space–time geometries. We use units with $G = c = 1$.

2. Solution S±

All 'static' (no dependence on t in the metric coefficients (1)) solutions to Einstein's equations (see, for instance, [7]) with EQ equation of state ($w = -1/3$) are given by

$$B(r) = r^2, \qquad C = \frac{r^4}{a^2}\frac{(A')^2}{A},$$
$$8\pi\rho = \frac{3a^2}{r^5}\frac{A}{(A')^2}\left(\frac{A''}{A'} + \frac{2}{r}\right), \qquad (2)$$

where $A(r)$ is determined from a quadratic equation

$$kA^2 + \frac{2}{a^2}A + b + \frac{1}{r^2} = 0, \qquad (3)$$

with three arbitrary constants k, b and $a^2 > 0$. For $k \neq 0$ the two (S±) solutions thus are

$$A(r) = \frac{1}{ka^2}\left[-1 \pm \sqrt{K(r)}\right],$$
$$C(r) = \frac{-1 \mp \sqrt{K(r)}}{(br^2+1)K(r)}, \qquad (4)$$

$$8\pi\rho(r) = -\frac{3(1-ka^4b)}{ka^4}\left[-1 \pm \sqrt{K(r)}\right],$$
$$K(r) = 1 - ka^4\left(b + 1/r^2\right). \qquad (5)$$

To describe the parameter cases, it is convenient to introduce $q = 1 - ka^4b$, so that $K(r) = q - ka^4/r^2$. Evidently, $\sqrt{K(r)}$ should be positive at least for some interval of r, which leads to the following:

(A) For $q \leqslant 0$, $k > 0$ there are no (physical) solutions.

(B) For $q < 0$, $k < 0$ we have 'interior' solutions, $r^2 \leqslant ka^4/q$; S+ does not have an event horizon for $q < -1/2$, its horizon coincides with the boundary $r^2 = 2|k|a^4$ for $q = -1/2$, there is a horizon inside the space–time for $-1/2 < q < 0$; apparently, S− always has no horizon.

(C) For $q = 0$, $\rho = 0$, $k < 0$ S+ is the Schwarzschild exterior solution, S− is not physical because it is also Schwarzschild but with a negative central mass.

(D) For $q > 0$, $k < 0$ both solutions are 'global' (space–time extends to any r), S+ has a horizon.

(E) For $q > 0$, $k > 0$ both are 'exterior' solutions, $r^2 \geqslant ka^4/q$, S+ has no horizon for $0 < q < 1/2$, its horizon coincides with the boundary $r^2 = 2ka^4$ for $q = 1/2$, there is a horizon inside the space–time for $q > 1/2$.

Note that whenever $r = 0$ is within the space–time, solutions S± have there a true (non-coordinate) singularity: both the Ricci curvature and the density are infinite at $r = 0$. For S− this is a naked singularity, with no horizon around it. Note also that in the limit $k \to 0$ S+ goes to the solution S-1, which is obtained from Eq. (3) with $k = 0$ and is discussed immediately below, while S− is singular.

3. Solution S-1

If $k = 0$ in Eq. (3), we have a particular solution for EQ of an especially simple form:

$$A(r) = A_0\left(1 - \frac{1}{\alpha r^2}\right), \qquad B(r) = r^2,$$
$$C(r) = \frac{2}{\alpha r^2}\left(1 - \frac{1}{\alpha r^2}\right)^{-1}, \tag{6}$$

$$8\pi\rho = \frac{3}{2}\alpha\left(\frac{1}{\alpha r^2} - 1\right), \tag{7}$$

where $\alpha = -b$ and $A_0 = a^2\alpha/2$. To keep the proper signature of the metric as $r \to \infty$, we require $A_0 > 0$, so that $\alpha > 0$; without loss of generality, we set $A_0 = 1$, i.e., $a^2 = 2/\alpha = -2/b > 0$. Let us discuss this solution in more detail, setting, for simplicity, $\alpha = 1$.

(A) The space–time of the solution S-1 has a horizon at $r = 1$ where the components of the metric tensor $g_{00} = A(r)$ and $g_{11} = -C(r)$ change their signs. The horizon separates (or connects) a static spatially inhomogeneous exterior space (E-space) at $r > 1$ and a 'hidden' interior object (I-object) at $r < 1$. These two regions are similar to R- and T-regions, respectively, as described by Novikov [8] for the Schwarzschild solution. The true singularity with the infinite Ricci curvature and density is at $r = 0$. The density in S-1 may be regarded as consisting of two components with the same equation of state: one is uniform and negative, $8\pi\rho_- = -3/2 < 0$, the other is non-uniform ('isothermal' law) and positive, $8\pi\rho_+(r) = 3/2r^2 > 0$. The first one dominates the E-space, and the other one dominates the I-object; the total density changes its sign at the horizon.

(B) The 'energy equation' introduced for the metric of Eq. (1) by Lemaître (see Ref. [5]) may be used to find an analog of the Newtonian gravitational potential as one of the physical characteristics of gravity produced by EQ in S-l. The equation has a form of energy conservation relation, $(1/2)(dB^{1/2}/dt)^2 - m(r,t)/r = E$, where $E = C^{-1}(dB^{1/2}/dr)^2 - 1$ and $m(r,t)$ is the Newtonian analog of gravitating mass. In S-1, the Newtonian mass proves to be $m(r) = (3/4) \times r[1 - (1/3)r^2]$, and the Newtonian potential $u(r) = -m/r = -(3/4)[1 - (1/3)r^2]$ describes 'the Newtonian component' of gravity produced by EQ in S-1. The potential u is finite at the true singularity ($u(0) = -3/4$) (unlike that in the Schwarzschild solution) and goes to $+\infty$ at spatial infinity where the density becomes constant (see below). On the singular surface, $m(1) = 1/2$, and so $2|u(1)| = 1$ (like that in the Schwarzschild solution).

(C) EQ gravity in S-1 is not reduced to Newtonian gravity completely; in particular, the dynamic effect of acceleration is essentially different in S-1 from what may be produced by the Newtonian potential u. The total accelerating effect can be evaluated in terms of the effective potential, $U(r)$, which may be derived using the fact that S-1 describes EQ in a state of hydrostatic equilibrium: its pressure and self-gravity are balanced in the E-space. The pressure gradient produces radial acceleration $F_p = -(dp/dr)(\rho + p)^{-1} = [8\pi(r^3 - r)]^{-1}$, which is positive. So the gravity acceleration is $F = -F_p = -[8\pi(r^3 - r)]^{-1}$; it is negative, and therefore gravity is attracting. The effective gravitational potential responsible for this attraction is $U = (1/2)\ln[r^2/(r^2 - 1)]$.

(D) S-1 can be rewritten in the E-space as

$$ds^2 = \tanh^2\left(\chi/\sqrt{2}\right)dt^2 - \cosh^2\left(\chi/\sqrt{2}\right)d\Omega^2 - d\chi^2, \tag{8}$$

$$8\pi\rho = -\frac{3}{2}\tanh\left(\chi/\sqrt{2}\right), \tag{9}$$

with the new spatial coordinate χ related to r by $r = \cosh(\chi/\sqrt{2})$; its range is from zero to infinity. The density decreases monotonically from zero at $\chi = 0$

to $-3/2$ at $\chi = \infty$. This form of S-1 may possibly be considered both in relation to and independently of the I-object. In the limit $r \to \infty$, where the density is spatially homogeneous, the metric of S-1 takes the form $ds^2 = dt^2 - r^2\,d\Omega^2 - 2r^{-2}\,dr^2$, or $ds^2 = dt^2 - \exp(\sqrt{2}\chi)\,d\Omega^2 - d\chi^2$. Since the general static solution for EQ in the homogeneous and isotropic 3-space has the form $ds^2 = dt^2 - r^2\,d\Omega^2 - (1 - kr^2/a_0^2)^{-1}\,dr^2$, $8\pi\rho = -24\pi\rho = 3k/a_0^2$ ($k = 1, 0, -1$ is the sign of 3-curvature, a_0 is an arbitrary scalling constant), one can see that the metric of Eqs. (2), (4) reduces to the isotropic metric with $k = -1$ and $a_0 = 1/2$ in the limit $r \to \infty$. For comparison: $k = 1$, $a_0 = 1$ in the Einstein static solution.

(E) Since $A(r)$ and $C(r)$ in S-1 change their signs at the singular surface, the signature of the metric of the I-object is $(---+)$. This means that the coordinate r becomes time-like, and the coordinate t becomes space-like inside the I-object. The same is true for the Schwarzschild space–time [8]. Because of that, the density of the I-object depends only on the time-like coordinate, thus it is spatially homogeneous. However, in contrast with the Schwarzschild space–time, a formal replacement of g_{00} with g_{11} and vice versa, which transforms the signature of the I-object to the 'ordinary' type $(+---)$, does not work for S-1, because the metric resulting from Eqs. (2) after this transformation is not a solution to the GR equations.

4. Solution S-2

GR equations for the same metric of Eq. (1) allow for the following time-dependent particular solution

$$A(t) = \frac{1}{4}\bigl(n^2 - 4\bigr) = \text{const} > 0,$$
$$B(t) = t^2, \qquad C(t) = t^n, \tag{10}$$

$$8\pi\rho = \frac{n(n+4)}{n^2-4}\,\frac{1}{t^2}, \qquad p = w\rho,$$
$$n = -\frac{4w}{1+w} = \text{const}. \tag{11}$$

The parameter range of this solution apparently consists of two parts: $n > 2$ $(-1 < w < -1/3)$ and $n < -2$ ($|w| > 1$; this is not Q as defined above). Note that both VQ ($w = -1$) and EQ ($w = -1/3$) are outside this range.

(A) The most striking feature of this solution (S-2) is that A, C and even B do not depend on r, and are functions of the time only. One may see here a similarity to the I-object of S-1 whose metric also depends on the time-like coordinate only. A closer similarity may be recognized with the 'T-sphere' found by Ruban [9] for pressure-free matter and the same S-2 symmetry of 3-space with $B = B(t)$. The density and pressure are spatially homogeneous (functions of the time only) in both the S-2 and Ruban's T-sphere. Time t varies in S-2 from $-\infty$ to $+\infty$, and the density varies from zero at $t \to \pm\infty$ to infinity in the (true) singularity $t = 0$ which has the same character as that in homogeneous and isotropic cosmological models. However, there are no coordinate transformations that could reduce S-2 and Ruban's T-sphere to the FRW metric with the isotropic 3-space.

(B) Unlike the Friedmann solutions, gravity in S-2 and Ruban's T-sphere does not have any Newtonian analogs. Rather, the space–time of this special type has common features with anisotropic spatially homogeneous cosmological models (cf. [9]).

(C) The pressure, $p = -n^2/[8\pi(n^2-4)t^2]$, is negative in S-2, while the density may be either positive or negative. The density is positive if w is in 'the Q range' $-1 < w < -1/3$ ($n > 2$). (Note that in the isotropic 3-space Q with w in this range produces positive acceleration, see Section 1.) The density is also positive for $w > 1$ (i.e., $-4 < n < 2$), but it is negative when $w < -1$ ($n < -4$).

(D) The density turns to zero for $w = \infty$ ($n = -4$). This case describes a form of energy with $\rho = 0$, $p < 0$, which is perhaps the most extreme form of Q. As we see, GR does not exclude the equation of state with $w = \infty$, and gives a regular solution for it, $A(r) = 3$, $B(r) = t^2$, $C = t^{-4}$. 'Density-free' energy may also be in a state of hydrostatic equilibrium (see below).

5. Solution S-3

A power law particular static solution, which is a counterpart to S-2, is also allowed by the GR equations for the metric of Eq. (1):

$$A(r) = r^n, \qquad B(r) = r^2,$$
$$C(r) = \frac{1}{4}\bigl(4 + 4n - n^2\bigr) = \text{const} > 0, \tag{12}$$

$$8\pi\rho = \frac{n(4-n)}{4+4n-n^2}\frac{1}{r^2}, \qquad p = w\rho,$$
$$n = \frac{4w}{1+w}. \tag{13}$$

The parameter range here looks even more peculiar: $-2(\sqrt{2}-1) < n < 2(\sqrt{2}+1)$, which corresponds to the two intervals for the values of w, $w > -(\sqrt{2}-1)/(\sqrt{2}+1) > -1/3$ and $w < -1$. Neither VQ nor EQ are within this range, and the solution relates to Q only when $-(\sqrt{2}-1)/(\sqrt{2}+1) < w < 0$.

(A) Similar to S-1 and S-2, solution S-3 depends on one coordinate only, and the true singularity of all the three solutions is at the origin of this coordinate. The positive component of density in S-1, and the total densities in S-2 and S-3 follow the inverse square law. Both S-1 and S-3 describe Q in a state of hydrostatic equilibrium.

(B) The pressure, $p = n^2/[8\pi(4+4n-n^2)r^2]$, is positive in S-3 for any $n \neq 0$. At $n = 0$ the pressure and density are both identically zero. In this case, $A = 1$, $C = 1$, and the metric of S-3 turns to the Lorentz metric of empty space–time. The density in S-3 is positive for $0 < n < 4$ and negative otherwise.

(C) The density vanishes also for $n = 4$, $w = \pm\infty$. This is the 'density-free' ($\rho = 0$, $p > 0$) form of energy, and S-3 (same as S-2 above) gives a regular metric for this case: $A = 1$, $B(r) = r^2$, $C(r) = r^4$. The fact that this form of energy is in the state of hydrostatic equilibrium shows that 'density-free' energy has its inertial mass (per unit volume) $\rho_i = p$ which is equal to its passive gravitational mass, and that the active mass density is positive.

(D) For $n \neq 0$, the sign of the active gravitating mass depends on the sign of n. If n is positive, the mass is positive; but if n is negative (and thus w is negative), the active mass is negative also. In terms of Newtonian physics, the negative mass produces a positive acceleration, which goes to infinity as $r \to 0$, and so anti-gravity is infinitely strong at the singularity. Whether it is capable, under these conditions, of producing 'auto-emission' of particles from the singularity (where the density is infinite), and/or enhance quantum evaporation of particles from the singularity, should be discussed separately.

(E) S-3 describes hydrostatic equilibrium of not only Q with negative w, but also, for instance, of ultra-relativistic fluid ($w = 1/3$, $n = 1$, $C = 7/4$) and of Zeldovich ultra-stiff fluid ($w = 1$, $n = 2$, $C = 2$).

References

[1] R.R. Caldwell, R. Dave, P.J. Steinhard, Phys. Rev. Lett. 80 (1998) 1582.

[2] R.R. Caldwell, R. Dave, P.J. Steinhard, Appl. Space Sci. 261 (1998) 303;
L. Wang, P.J. Steinhard, Astrophys. J. 508 (1998) 483;
C.-P. Ma, R.R. Caldwell, P. Bode, L. Wang, Astrophys. J. 521 (1999) L1;
A.R. Cooray, D. Huterer, Astrophys. J. 513 (1999) L95;
J.S. Alcaniz, J.A.S. Lima, Astron. Astrophys. 349 (1999) 729;
I.S. Zlatev, P.J. Steinhard, Phys. Lett. B 459 (1999) 570;
L. Hui, Astrophys. J. 519 (1999) L9;
I. Zlatev, L. Wang, P.J. Steinhard, Phys. Rev. Lett. 82 (1999) 896;
P.J.E. Peebles, A. Vilenkin, Phys. Rev. D 590 (1999) 811;
M. Giovannini, Phys. Rev. D 601 (1999) 277;
L. Wang, R.R. Caldwell, J.P. Ostriker, P.J. Steinhard, Astrophys. J. 550 (2000) 17;
G. Efstathiou, MN RAS 310 (2000) 842;
P.P. González-Díaz, Phys. Lett. B 481 (2000) 353;
J.D. Barrow, R. Bean, J. Magueijo, MN RAS 316 (2000) L41.

[3] S.M. Carroll, Phys. Rev. Lett. 81 (1998) 3067;
S.M. Barr, Phys. Lett. B 454 (1999) 92;
R.S. Kalyana, Phys. Lett. B 457 (1999) 268;
Ch. Kolda, D.H. Lyth, Phys. Lett. B 459 (1999) 570;
P. Binétruy, Phys. Rev. D 600 (1999) 80;
R. Horvat, Mod. Phys. Lett. A 14 (1999) 2245;
T. Chiba, Phys. Rev. D 601 (1999) 4634;
P.H. Brax, J. Martin, Phys. Lett. B 468 (1999) 40;
A.B. Kaganovich, Nucl. Phys. B Proc. Suppl. 87 (1999) 496;
O. Bertolami, P.J. Martins, Phys. Rev. D 610 (2000) 7;
Y. Nomura, T. Watari, T. Yanagida, Phys. Lett. B 484 (2000) 103;
S.C.C. Ng, Phys. Lett. B 485 (2000) 1;
I.G. Dynmikova, Phys. Lett. B 472 (2000) 33;
A. Hebecker, C. Wetterich, Phys. Rev. Lett. 85 (2000) 3339;
N. Arkani-Hamed, L.J. Hall, C. Colda, H. Murayama, Phys. Rev. Lett. 85 (2000) 4434;
C. Armendariz-Picon, V. Mukhanov, P.J. Steinhard, Phys. Rev. Lett. 85 (2000) 4438.

[4] S. Weinberg, Rev. Mod. Phys. 61 (1989) 1.

[5] G. Lemaître, Rev. Mod. Phys. 21 (1949) 357;
E.B. Gliner, JETP 22 (1966) 378;
E.B. Gliner, Sov. Phys. Dokl. 6 (1970) 559.

[6] A.G. Riess et al., Astron. J. 116 (1998) 1009;
S. Perlmuter et al., Astrophys. J. 517 (1999) 565;
J. Cohn, astro-ph/9807128;
S. Carol, astro-ph/0004075.

[7] L.D. Landau, E.M. Lifshitz, The Classical Field Theory, Pergamon Press, London, 1959.

[8] I.D. Novikov, Comm. Sternberg Astron. Inst. 132 (1963) 43.

[9] V.A. Ruban, JETP 29 (1969) 1027.

7 May 2001

PHYSICS LETTERS A

ELSEVIER

Physics Letters A 283 (2001) 62–70

www.elsevier.nl/locate/pla

Classical analogous of quantum cosmological perfect fluid models

A.B. Batista, J.C. Fabris *, S.V.B. Gonçalves, J. Tossa [1]

Departamento de Física, Universidade Federal do Espírito Santo, 29060-900, Vitória, Espírito Santo, Brazil

Received 16 January 2001; received in revised form 15 March 2001; accepted 26 March 2001
Communicated by P.R. Holland

Abstract

Quantization in the minisuperspace of a gravity system coupled to a perfect fluid, leads to a solvable model which implies singularity free solutions through the construction of a superposition of the wavefunctions. We show that such models are equivalent to a classical system where, besides the perfect fluid, a repulsive fluid with an equation of state $p_Q = \rho_Q$ is present. This leads to speculate on the true nature of this quantization procedure. A perturbative analysis of the classical system reveals the condition for the stability of the classical system in terms of the existence of an anti-gravity phase. © 2001 Elsevier Science B.V. All rights reserved.

PACS: 04.20.Cv; 04.20.Me

The existence of an initial singularity is one of the major drawbacks of the so-called standard cosmological model. It is a general belief that such problem can be solved through the employment of a quantum theory of gravity. Indeed, near the singularity sub-Planckian scales are reached and a classical description of the Universe under this situation is not appropriate. However, there is no consistent quantum theory of gravity until now, and in this sense the problem of the initial singularity remains of actuality. On the other hand, it is possible to construct a quantum model for the Universe as a whole, through the Wheeler–DeWitt equation, based in the ADM decomposition of the gravity sector, which leads to a Hamiltonian formulation of general relativity, from which a canonical quantization procedure can be applied. This gives birth to quantum cosmology [1,2].

Quantum cosmology is not free from problems. First, it can be applied only to geometries where a foliation is possible. Moreover, the Hamiltonian formalism leads to a breakdown of general covariance, and the notion of time is lost [3]. There are some recent proposals by which this notion of time can be recovered. One of these proposals is based in the coupling of the gravity sector to a perfect fluid. Using the Schutz's formulation of a perfect fluid [4], a quantization procedure is possible. The canonical momentum associated with the perfect fluid appears linearly in the Wheeler–DeWitt equation, permitting to rewrite this equation in the form of a Schrödinger equation and a time coordinate associated with the matter field can be identified.

Solutions based on this approach reveal that a superposition of the wavefunctions which are solu-

* Corresponding author.
E-mail addresses: brasil@cce.ufes.br (A.B. Batista), fabris@cce.ufes.br (J.C. Fabris), sergio@cce.ufes.br (S.V.B. Gonçalves), jtoss@syfed.bj.refer.org (J. Tossa).
[1] Permanent address: IMSP, Université Nationale du Bénin, Porto Novo, Benin.

PII: S0375-9601(01)00229-8

tions of the resulting Schrödinger equation leads to a singularity-free Universe [5–8]. The behaviour of the scale factor may be determined in two different ways: calculating the expectation value of the scale factor, in the spirit of the many worlds' interpretation of quantum mechanics; evaluating the Bohmian trajectories in the ontological formulation of quantum mechanics. The results are essentially the same in both approaches and the scale factor display a bounce, the singularity never being reached. It must be noted that even if the two procedures are technically equivalent, they are conceptually very different from each other; there are claims that from the conceptual point of view only the ontological formalism can be consistently applied to quantum cosmology [2].

The existence of a bounce indicates that there is a repulsive effect, of quantum origin, when the scale factor approaches the singularity. In this Letter we study more in detail such scenario. It is shown that the quantum scenario can be reproduced exactly by a very simple classical model where a repulsive fluid is added to the normal perfect fluid. It is surprising that the repulsive fluid is always the same, given by a stiff matter equation of state $p_Q = \rho_Q$, independently of the content of the normal fluid. The existence of this classical analogous of the quantum model leads us to ask questions on the true nature of the quantization in this case. Under which conditions the features of a quantum system can be exactly reproduced by a classical system? Our analysis is restricted to a perfect fluid coupled to gravity system, where the notion of time is recovered. But we sketch some considerations on other situations where gravity is coupled to matter fields.

The existence of a classical analogous of the quantum model allows us to perform a perturbative analysis establishing under which conditions the repulsive phase near singularity may be stable or not. In fact, when the mechanism responsible for the avoidance of the singularity implies the violation of the strong energy condition only, we can expect this configuration to be stable; but, our analysis suggests that the quantum effects are due to a real anti-gravity phase, which can lead to instabilities under certain conditions.

In the perfect fluid formulation developed by Schutz, the degrees of freedom associated with the fluid are given by five scalar potentials in terms of which the four velocity is written:

$$u_\mu = \frac{1}{\mu}(\phi_{,\nu} + \zeta\beta_{,\nu} + \theta S_{,\nu}), \tag{1}$$

where μ is the specific enthalpy. The four velocity is subjected to the condition

$$u^\nu u_\nu = 1 \tag{2}$$

what enables us to express the specific enthalpy in terms of the other five potentials. From now on, we work in natural units, for which $G = c = \hbar = 1$. The action is then given by

$$S = \int_M d^4x\,\sqrt{-g}R + 2\int_{\partial M} d^3x\,\sqrt{h}h_{ij}K^{ij} + \int_M d^4x\,\sqrt{-g}p, \tag{3}$$

where h_{ij} is the metric on the spatial section, K_{ij} is the extrinsic curvature and p is the pressure of ordinary matter. Action (3) is apparently non-covariant because of the pressure term. But, in fact, the constraints intrinsic to this formalism permit to recover the covariance.

We will consider from now on the Robertson–Walker flat geometry (the spatial section must be compact in order to be consistent with the boundary conditions)

$$ds^2 = N^2\,dt^2 - a(t)^2 h_{ij}\,dx^i\,dx^j. \tag{4}$$

We assume a barotropic equation of state $p = \alpha\rho$. Analyzing the conjugate momentum, and eliminating non-physical degrees of freedom, we can reduce action (3) to [6]

$$S = \int \left\{\dot{a}\,p_a + \dot{\phi}\,p_\phi + \dot{S}\,p_S - NH\right\}, \tag{5}$$

where

$$H = -\frac{p_a^2}{24a} + p_\phi^{\alpha+1}a^{-3\alpha}e^S. \tag{6}$$

There are three cases which will interest us here: $\alpha = -1$, $\alpha = 1/3$ and $\alpha = 0$. The dynamical vacuum ($\alpha = -1$) has been studied in [6], the radiative fluid ($\alpha = 1/3$) in [5,8,9], while the dust case ($\alpha = 0$) was treated in [7].

Following the Schutz formalism for the description of perfect fluid, and specializing it to a dust fluid, with

$p = 0$, we obtain the following Lagrangian:

$$L = \dot{a}\,p_a + \dot{\phi}\,p_\phi - N\,H, \tag{7}$$

where ϕ is the dust variable, with p_ϕ being its conjugate momentum, and H is the Hamiltonian

$$H = -\frac{p_a^2}{24a} + e^S p_\phi. \tag{8}$$

Classically, this system admits, for the flat case, the well-known dust solution $a \propto t^{2/3}$, where t is the proper time, or equivalently $a \propto \eta^2$, where η is the conformal time.

Now, we perform the canonical transformation

$$\tau = p_S e^{-S} p_\phi^{-1}, \qquad \pi_\tau = p_\phi e^S, \tag{9}$$

reducing the Lagrangian to the form

$$H = -\frac{p_a^2}{24a} + p_\tau. \tag{10}$$

Imposing the quantization rules

$$p_a \to -i\frac{\partial}{\partial a}, \qquad p_\tau \to -i\frac{\partial}{\partial \tau}, \tag{11}$$

and considering that the Hamiltonian becomes an operator which acts on the wavefunction annihilating it,

$$\tilde{H}\Psi = 0, \tag{12}$$

we obtain the following partial differential equation governing the behaviour of the wavefunction:

$$\frac{1}{24}\frac{\partial^2\Psi}{\partial a^2} - i a\frac{\partial\Psi}{\partial\tau} = 0. \tag{13}$$

The fact that the conjugate momentum p_τ associated to the dust fluid variable appears linearly in the Hamiltonian, implies that the Wheeler–DeWitt equation in the minisuperspace assumes a form similar to the Schrödinger equation with τ playing the role of time. It is possible to show, through the canonical transformations, that in this cases it is the cosmic time. Performing the redefinitions [10]

$$a = \frac{R}{\sqrt{12}}, \qquad \tau = \frac{t}{\sqrt{12}}, \tag{14}$$

we end up with the equation

$$\frac{1}{2}\frac{\partial^2\Psi}{\partial R^2} = i\,R\frac{\partial\Psi}{\partial t}. \tag{15}$$

We solve Eq. (15) using the method of separation of variables. It leads to the following decomposition of $\Psi(R,t)$:

$$\Psi(R,t) = \xi(R)e^{iEt}, \tag{16}$$

where E is a (positive) constant, and $\xi(R)$ obeys the equation

$$\xi'' + 2RE\xi = 0. \tag{17}$$

The prime means derivative with respect to R. The solution for (17) is under the form of Bessel functions:

$$\xi(R) = \sqrt{R}\big(c_1 J_{1/3}\big(\beta R^{3/2}\big) + c_2 J_{-1/3}\big(\beta R^{3/2}\big)\big), \tag{18}$$

with $\beta = \sqrt{8E/9}$. The condition for the Hamiltonian operator to be self-adjoint leads to two possible boundary conditions:

$$\xi(0) = 0 \quad \text{or} \quad \xi'(0) = 0. \tag{19}$$

The final results is insensitive to which boundary condition we employ. Hence, we will work with the first one, but all results are essentially recovered if the second condition is used.

The general solution is a superposition of (18). In order to have analytical expressions, we will use the following superposition:

$$\Psi(R,t) = \sqrt{R}\int_0^\infty \beta^{4/3} e^{-\gamma\beta} e^{i(9/8)\beta^2 t} \times J_{1/3}\big(\beta R^{3/2}\big)\,d\beta, \tag{20}$$

where γ is a kind of "Gaussian factor" determining the rapidity the wavefunction goes to zero as β increases. Its solution is [11]

$$\Psi(R,t) = \frac{R}{(2A)^{4/3}} e^{-R^3/4A}, \tag{21}$$

where $A = \gamma - i(9/8)t$.

It may be asked which predictions such model makes for the behaviour of the scale factor. Using the many worlds' interpretation, this mounts to evaluate the expectation value of the scale factor. It must be stressed that essentially the same result is achieved by calculating the Bohmian trajectories [2]. The measure employed in the expression is imposed again by the self-adjoint condition, and the expression for the

expectation value reads

$$\sqrt{12}\langle a(t)\rangle = \langle R\rangle = \frac{\int_0^\infty R^2\Psi(R,t)^*\Psi(R,t)\,dR}{\int_0^\infty R\Psi(R,t)^*\Psi(R,t)\,dR}. \quad (22)$$

Using (21), the expectation value for the scale factor can be calculated and the final result is

$$\langle a(t)\rangle = \frac{1}{\sqrt{12}}\left(\frac{2}{\gamma}\right)^{1/3}\frac{\Gamma(5/3)}{\Gamma(4/3)}\left(\gamma^2+\frac{81}{64}t^2\right)^{1/3}. \quad (23)$$

The parameter t can be identified as the cosmic time due to the canonical transformations employed before. Notice that the classical behaviour is recovered for $t\to\infty$. But, in general, the quantum model predicts a non-singular model exhibiting a bounce: when the singularity is approached, quantum effects leads to a repulsive effect, which leads to a regular transition from a contracting to an expanding phase.

A dynamical vacuum and a radiative fluid can be analyzed through the same lines as before. These problem were treated in [5,6,8] and we just present the final results.

The dynamical vacuum is realized through the equation of state $p=-\rho$. Using again the Schutz formalism for this particular case, we rewrite the Hamiltonian (6), with $\alpha=-1$, as

$$H = -\frac{p_a^2}{24a} + a^3 p_T \quad (24)$$

through the canonical transformations $p_T = e^S$ and $T=-e^{-S}p_S$ [6]. Since p_T appears linearly in the Hamiltonian, it can be identified with a time variable as before, in this case in the gauge $dt = dT/a^3$, where t is the cosmic time [6]. Finding the solutions of the corresponding Wheeler–DeWitt equation, evaluating the expectation value of the scale factor, it results

$$\langle a(T)\rangle = \frac{\Gamma(4/3)}{\Gamma(7/6)}\left[\frac{64\gamma^2+9T^2}{8\gamma}\right]^{1/6}. \quad (25)$$

Asymptotically the classical solution for a cosmological constant is recovered if we choose, in the classical equations of motion, the time gauge $N=a^{-3}$ (the identification of the time coordinates can be justified rigorously [6] using the canonical transformations). In terms of the proper time, the solution (25) can be rewritten as

$$\langle a(t)\rangle = \frac{\Gamma(4/3)}{\Gamma(7/6)}\sqrt{8\gamma}\times\left\{\cosh\left[\frac{3}{\sqrt{8\gamma}}\left(\frac{\Gamma(4/3)}{\Gamma(7/6)}\right)^3 t\right]\right\}^{1/3}. \quad (26)$$

For the radiative case, Hamiltonian (6) reads [5,9], for $\alpha=1/3$ and after the canonical transformations $T = p_S e^{-S}p_\phi^{-4/3}$ and $p_T = p_\phi^{4/3}e^S$,

$$H = -\frac{p_a^2}{24a} + \frac{p_T}{a}. \quad (27)$$

Again, the conjugate momentum associated to the matter variable appears linearly and consequently we can identify this matter variable with a time variable in the gauge $dt = a\,d\eta$, with is justified through the canonical transformation as in the preceding cases. Hence this time variable is the conformal time. The wavefunctions can be determined through the Green's function method. Fixing the wavefunction at $t=0$ as [9]

$$\Psi(a) = \left(\frac{8\sigma_1}{\pi}\right)^{1/4} e^{-(\sigma_1+i\sigma_2)a^2} \quad (28)$$

and using the harmonic oscillator Green's function, integrable expression can be obtained [5,9]. The scale factor expectation value is given by

$$\langle a(\eta)\rangle = \frac{1}{12}\sqrt{\frac{2}{\pi\sigma_1}}\sqrt{\sigma_1^2\eta^2+(6-\sigma_2\eta)^2}, \quad (29)$$

where η is the conformal time, σ_1 and σ_2 being real parameters. Again, this solution represents a non-singular eternal Universe which coincides asymptotically with the classical radiative solution $a\propto\eta$.

It must be stressed that in all cases, the classical behaviour is recovered for large values of the proper time. Also, all solutions are singularity-free, with a bounce. Near the bounce repulsive effects appear which, in the ontological formulation, are connected with the quantum potential which corrects the classical equations of motion.

A general feature of the quantum models developed previously is the appearance of a repulsive phase for small values of the scale factor, leading to the avoidance of the singularity. In [12], it was shown that a repulsive gravity single fluid model can lead

to consistent cosmological models if the curvature is negative; however, its stability is not assured in the absence of ordinary (attractive) matter. Another way of implementing a repulsive phase in classical cosmology is to consider two fluids, one that acts attractively, and the other that acts repulsively. In this case, we may have consistent solutions with flat spatial section. It is desirable that the repulsive fluid dominates for small values of the scale factor, whereas the attractive fluid dominates for large values of the scale factor. Hence, in the general, considering just the flat spatial section, we may obtain possible consistent models from

$$\left(\frac{\dot{a}}{a}\right)^2 = 8\pi G(\rho_M - \rho_Q) = \frac{C_1}{a^m} - \frac{C_2}{a^n}, \tag{30}$$

where $p_M = \alpha_M \rho_M$, $p_Q = \alpha_Q \rho_Q$, $m = 3(1+\alpha_M)$ and $n = 3(1+\alpha_Q)$. The subscripts M and Q stand for "normal" matter component and for "quantum" repulsive component.

Ordinarily, normal matter may be a cosmological constant, dust or a radiative fluid, corresponding to $\alpha_M = -1, 0, 1/3$, respectively. Since it is desirable that the repulsive component dominates at small values of a, then $\alpha_Q > 1/3$. We choose then a repulsive stiff matter fluid $\alpha_Q = 1$, what leads to $n = 6$. Hence, we will solve Eq. (30) with $n = 6$ and $m = 0$, 3 and 4. The solutions are the following:

$\alpha_M = -1,\ \alpha_Q = 1$:

$$a(t) = \left(\frac{C_2}{C_1}\right)^{1/6} \cosh^{1/3} 3\sqrt{C_1}t, \tag{31}$$

$\alpha_M = 0,\ \alpha_Q = 1$:

$$a(t) = \left(\frac{C_2}{C_1}\right)^{1/3} \left[\frac{9}{4}\frac{C_1^2}{C_2}t^2 + 1\right]^{1/3}, \tag{32}$$

$\alpha_M = 1/3,\ \alpha_Q = 1$:

$$a(\eta) = \sqrt{\frac{C_2}{C_1}}\left[\frac{C_1^2}{C_2}(\eta - \eta_0)^2 + 1\right]^{1/2}. \tag{33}$$

The comparison of the above solutions with those obtained through the construction of a superposition of the wavefunctions resulting from the Wheeler–DeWitt equation in the minisuperspace with only the ordinary perfect fluid, reveals that they are the same provided that C_1 and C_2 are suitable functions of the parameters of the wavepackets. For the dust case, for example, we can fix

$$C_1 = \frac{1}{12^{3/2}}\frac{9}{8}\frac{1}{\gamma}\left(\frac{\Gamma(5/3)}{\Gamma(4/3)}\right)^3,$$

$$C_2 = \frac{1}{12^3}\frac{9}{4}\left(\frac{\Gamma(5/3)}{\Gamma(4/3)}\right)^6. \tag{34}$$

For the other cases, the expressions for these constants are quite similar. But notice that, in the radiative case, we have introduced a phase η_0, which can be zero only if σ_2 is also zero. Hence, wavepackets constructed from a quantum model where, besides the scale factor, there is a perfect fluid matter degree of freedom (which leads to a time coordinate) are equivalent to a classical model where gravity is coupled to the same perfect fluid plus a repulsive fluid with a stiff matter equation of state $p_Q = \rho_Q$. It is really surprising that the repulsive fluid, in the classical model, is the same irrespective of the normal fluid employed in the quantum model.

The question of reproducing the classical equations of motion from the quantum ones appears already in the ordinary quantum mechanics, and they are expressed in the so-called Ehrenfest's theorem. According to this theorem, the center of the wavepacket may follow a classical trajectory under certain conditions. Explicitly, taking the expectation values of the Heisenberg's equations for the position and momentum operators for a particle of mass m in a potential $V(\vec{r})$, we find [13]

$$\langle \dot{\vec{r}} \rangle = \frac{\vec{p}}{m}, \tag{35}$$

$$\langle \dot{\vec{p}} \rangle = -\langle \nabla V(\vec{r}) \rangle. \tag{36}$$

These relations coincide with the classical one only if $\langle \nabla V(\vec{r}) \rangle = \nabla V(\langle \vec{r} \rangle)$. This happens only for very special forms of the potential, the harmonic oscillator being an example. Only in these special cases, we may say that the center of the wavepacket follows a classical trajectory.

However, the situation discussed here is somehow different from that analyzed in the Ehrenfest's theorem. In fact the expectation value of the scale factor of a quantum model derived from gravity and a perfect fluid of attractive nature is reproduced by a classical model where another fluid, of repulsive nature, appears. This seems somehow mysterious.

Some insights into what is happening in this case may come from the employment of the ontological interpretation of quantum mechanics. In this case, the problem of time is solved in any situation (not only when a matter field is present). In fact, the ontological interpretation predicts that the system follows a real trajectory given by the equations

$$p_q = S_{,q}, \tag{37}$$

where the subscript q designates one of the degrees of freedom of the system, and S is the phase of the wavefunction, which is written as $\Psi = Re^{iS}$, R and S being real functions. The equation of motion (37) is governed not only by a classical potential V but also by a quantum potential $V_Q = \nabla^2 R/R$.

These considerations suggest that the quantum potential has, at least in the case of the quantization of perfect fluid systems, a very clear behaviour which can be classically reproduced by a repulsive stiff matter fluid. However, we must stress that even in this case we must find first the wavefunction, through the Wheeler–DeWitt equation, determining than its phase, from which the Bohmian trajectories is computed. In the quantum models studied previously, it is not possible, in principle, to identify a classical and quantum potential in terms of the scale factor from the beginning. Moreover, even if this would be possible, the classical analogous we have determined are completely independent of the Wheeler–DeWitt equation.

We may obtain more informations on the meaning of this classical analogous of a quantum system by studying the dispersion of the wavepacket. We will treat again the dust case where the wavepacket is given by (21). The calculation is standard and we obtain the following expression for the dispersion of the wavepacket:

$$\begin{aligned}\Delta a(t) &= \left[\left\langle a^2(t)\right\rangle - \left\langle a(t)^2\right\rangle\right]^{1/2} \\ &= \frac{1}{\sqrt{12}}\left(\frac{2}{\gamma}\right)^{1/3}\left[\frac{\Gamma(2)}{\Gamma(4/3)} - \frac{\Gamma(5/3)^2}{\Gamma(4/3)^2}\right]^{1/2} \\ &\quad\times\left(\gamma^2 + \frac{81}{64}t^2\right)^{1/3}. \end{aligned}\tag{38}$$

Hence, the wavepacket disperse as time evolves; its minimal dispersion is reached in the origin $t = 0$, exactly where the classical and quantum behaviours (both with just the dust fluid) do not coincide. Notice that the ratio of $\Delta a(t)$ to $\langle a(t)\rangle$ is constant, and as the wavepacket becomes more localized, the scale factor approaches the singularity. A localized wavepacket means a small value for γ. Notice that as γ becomes small, the coefficient C_2 becomes negligible compared with C_1 (Eqs. (34)), and the two-fluid model tends to approach the one fluid model.

The situation described above is very similar to what happens with a free particle in ordinary quantum mechanics: the wavepacket has its minimum width at origin and disperse as time evolves. In this case the question of the classical limit is somehow subtle. If an ensemble of classical particles, with some initial dispersion in their velocities, is settled in the origin, their trajectories do not reproduce the possible results of measurement of the free quantum particle initially; as time evolves, the dispersion of the wavepacket tends to coincide with the dispersion of the trajectories of the classical particles. This does not mean that notion of classical trajectory is recovered [13,14].

In quantum cosmology, however, the scenario is more complex. In this case, we may use the many worlds' interpretation [15] or the ontological interpretation [16] of quantum mechanics. In any case, the notion of trajectory is recovered. In this sense, the above results indicate that, for large values of time, the quantum trajectory coincides with the corresponding classical trajectory with suitable initial conditions, while near the origin these trajectories do not coincide. But, our analogous model, with two fluids, reproduce the quantum trajectory even in the vicinity of the origin, keeping the asymptotical agreement untouched.

Since we have a classical analogous of the bounce models determined through the Wheeler–DeWitt equation, we can investigate if the repulsive effect leading to the avoidance of the singularity may spoil the stability of the model. First of all we define what we understand here by instability. A cosmological model is considered unstable if the perturbative variables diverge when all background quantities are finite. Here, we will consider a weaker condition: the model is unstable if the perturbed quantities takes very large values in comparison with the background quantities, even if they are not divergent. This is due to the fact that, if this happens, the hypothesis of homogeneity and isotropy, employed in the definition of the background, are compromised.

Let us consider our non-singular classical system. It can be written as

$$R_{\mu\nu} = 8\pi G\left[\overset{M}{T}_{\mu\nu} - \frac{1}{2}g_{\mu\nu}\overset{M}{T}\right] - 8\pi G\left[\overset{Q}{T}_{\mu\nu} - \frac{1}{2}g_{\mu\nu}\overset{Q}{T}\right], \tag{39}$$

$$\overset{M}{T}{}^{\mu\nu}{}_{;\mu} = 0, \tag{40}$$

$$\overset{Q}{T}{}^{\mu\nu}{}_{;\mu} = 0. \tag{41}$$

We perturb these equations in the usual way, introducing the quantities

$$g_{\mu\nu} = \overset{0}{g}_{\mu\nu} + h_{\mu\nu}, \qquad \rho_M = \overset{0}{\rho}_M + \delta\rho_M,$$
$$\rho_Q = \overset{0}{\rho}_Q + \delta\rho_Q.$$

The computation of the perturbed equations is quite standard [17], and we just present the final equations, at linear level:

$$\ddot{h} + 2\frac{\dot{a}}{a}\dot{h} = \frac{1}{\alpha_M - \alpha_Q} \times \left[-(1+3\alpha_M)\left(2\frac{\ddot{a}}{a} + (1+3\alpha_Q)\frac{\dot{a}^2}{a^2}\right)\Delta_M + (1+3\alpha_Q)\left(2\frac{\ddot{a}}{a} + (1+3\alpha_M)\frac{\dot{a}^2}{a^2}\right)\Delta_Q \right], \tag{42}$$

$$\dot{\Delta}_M + (1+\alpha_M)\left(\Psi - \frac{\dot{h}}{2}\right) = 0, \tag{43}$$

$$(1+\alpha_M)\left[\dot{\Psi} + (2-3\alpha_M)\frac{\dot{a}}{a}\Psi\right] - \frac{n^2}{a^2}\alpha_M\Delta_M = 0, \tag{44}$$

$$\dot{\Delta}_Q + (1+\alpha_Q)\left(\theta - \frac{\dot{h}}{2}\right) = 0, \tag{45}$$

$$(1+\alpha_Q)\left[\dot{\theta} + (2-3\alpha_Q)\frac{\dot{a}}{a}\theta\right] - \frac{n^2}{a^2}\alpha_Q\Delta_Q = 0. \tag{46}$$

In these expressions, we have used the following definitions: $h = h_{kk}/a^2$, $\Delta_M = \delta\rho_M/\rho_M$, $\Delta_Q = \delta\rho_Q/\delta\rho$, $\Psi = \delta u^i_M$, $\theta = \delta u^i_Q$, where δu^i_M and δu^i_Q are the perturbations on the four velocity of the normal and repulsive fluid, respectively.

The perturbed equations presented above do not seem to admit analytical solutions for the background solutions (31)–(33). Hence, we are obliged to perform a numerical integration. In Figs. 1, 2 and 3 we display the evolution of density perturbations for the exotic fluid for the cosmological constant, dust and radiative cases, respectively, in the long wavelength limit $n \to 0$. The other perturbed quantities exhibits essentially the same features.

Fig. 1. Behaviour of $\Delta_Q(t)$ for $n = 0$ with cosmological constant.

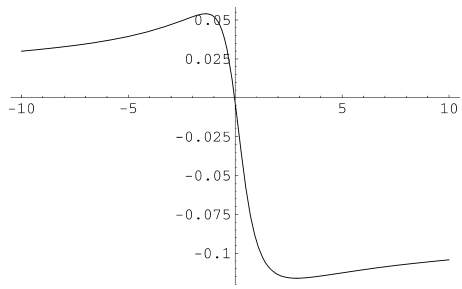

Fig. 2. Behaviour of $\Delta_Q(t)$ for $n = 0$ with a dust fluid.

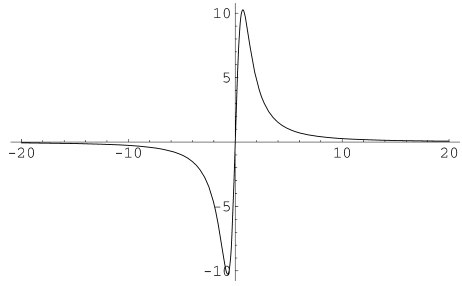

Fig. 3. Behaviour of $\Delta_Q(t)$ for $n = 0$ with a radiative fluid.

From the numerical study performed we can expose the following conclusions. When the cosmological constant is coupled to the repulsive fluid, the bounce model is unstable. Approaching the minimum of the scale factor (which in all three cases occurs in the origin), the perturbations diverge. However, when the dust or radiative fluid is coupled to the repulsive fluid, the perturbations behave regularly during all the evolution of the Universe. Hence, these models are stable. The different behaviours for the cosmological constant and the other cases may be easily understood. Indeed, in [12] a stability study was performed for the same repulsive fluid (represented there by a free scalar field); the curvature was taken to be negative. Instabilities were found in the absence of ordinary matter. In the present cosmological constant case, as it happens also in [12], the perturbation of ordinary matter decouples completely and the metric perturbation is coupled only to the perturbation of the repulsive fluid. In contrast, for the radiative and dust cases all perturbed variables are coupled. More important, in the present cosmological constant case, and in the model studied in [12], the energy conditions are violated during all the evolution of the Universe, while for the dust and radiative cases studied here, this violation occurs only near the bounce. The violation of the energy conditions leads to a repulsive gravity effect which contributes to a very fast growing of perturbations. If it occurs for all times, this lead to divergence.

In spite of the fact that we display the results for $n = 0$ only, for other values of n the features are very similar. For very large values of n, the perturbations exhibit strong oscillations, and they become divergent near the minimum of the scale factor for the cosmological constant case. Of course, we have studied the stability of the classical analogous of the quantum model. But, this study leads to some insights to what happens in the original framework. Indeed, the considerations made above about the expectation value of the scale factor and the dispersion of the wavepacket permits to take seriously the classical perturbative study as indication of the behaviour of the quantum model, mainly if we take the point of view that in quantum cosmology the notion of trajectory is essential. The only important drawback concerns the fact that a complete quantum perturbation should take into account excitations of degrees of freedom that were frozen in the minisuperspace approach. Other important point is what we mean by "near the bounce", where instabilities may appear. In fact, we consider it as the region where the quantum effects are dominant and all energy conditions are violated.

The main point of the present work is that the quantum model, derived from the Wheeler–DeWitt equation for gravity plus perfect fluid through the Schutz's formalism, has a classical analogous. In this classical analogous system, the perfect fluid is coupled to another perfect fluid, with a fixed equation of state $p_Q = \rho_Q$ which appears with a "wrong" sign for the gravitational coupling. The existence of this classical analogous for all equations of state of the normal fluid studied in this work, rises doubts about the true quantum nature of the original quantum cosmological scenario. It is not clear to us how to solve these doubts for the moment. But, the existence of a classical system reproducing different quantum models may indicate that the quantization of a gravity system in the minisuperspace may be not a real quantization and a more careful analysis of this problem is deserved.

In the analysis performed previously, it has been considered a specific superposition of the solutions of the Wheeler–DeWitt equation. Since these solutions are not square integrable, a superposition of them is in fact a necessity in those models. It can be argued that other types of superpositions are possible which may not be in agreement with the classical analogous treated here; all the richness of the original quantum model would not be reproduced by the classical model. However, the superposition procedure must agree with physical requirements as, for example, the localization of the wavepacket, what is the case of the preceding examples. We may guess that other possible superpositions, satisfying the same physical requirements, will lead to essentially the same results. These comments can also be applied to the question of the boundary conditions. Perhaps, the choice of other boundary conditions could lead to different scenarios. But, the boundary conditions used here are motivated by physical requirements, like the regularity of the wavefunction and the self-adjointness of the Hamiltonian operator. We may guess that any physically reasonable boundary condition would lead to similar scenarios to those presented here.

A perturbative study was performed in the classical model. It can happens that a bounce model, where the avoidance of the singularity is obtained through an

anti-gravity phase, may not be a stable model. We have verified that when the normal fluid decouples from the other perturbed equations, in such a way that the metric perturbation are coupled to the repulsive fluid only, the background model is unstable. Otherwise, we can obtain stable singularity-free models with an anti-gravity phase.

We must stress that the classical analogous model reveals that the "quantum effects" exhibit an anti-gravity behaviour. That is, the singularity is avoided with conditions much more stronger than the simple violation of the strong energy condition, as it happens in many others singularity-free models [18]. It must also be emphasized that all considerations have been done for a perfect fluid quantum model. It should be important to verify if the correspondence found here remains when gravity are coupled to matter fields. In [19] the case of a free scalar field was analyzed. However, a free scalar field is equivalent to stiff matter. Consequently, the classical analogous (if still valid for this case) would contain two kinds of stiff matter, an attractive one and a repulsive one. Perhaps, the strange behaviour found in [19], with the quantum phase being recovered for large values of the scale factor, is due to this fact. This specific case deserves to be analyzed carefully.

Acknowledgements

We have benefited of many enlightfull discussions with N. Pinto-Neto and Nivaldo Lemos. A.B.B., J.C.F. and S.V.B.G. thank CNPq (Brazil) for financial support. J.T. thanks CAPES (Brazil) for financial support and the Department of Physics of the Universidade Federal do Espírito Santo for hospitality.

References

[1] J.A. Halliwell, in: S. Coleman, J.B. Hartle, T. Piran, S. Weinberg (Eds.), Quantum Cosmology and Baby Universes, World Scientific, Singapore, 1991.
[2] N. Pinto Neto, in: M. Novello (Ed.), Cosmology and Gravitation II, 1996, p. 229.
[3] C.J. Isham, gr-qc/9210011.
[4] B.F. Schutz, Phys. Rev. D 2 (1970) 2762;
B.F. Schutz, Phys. Rev. D 4 (1971) 3559.
[5] N.A. Lemos, J. Math. Phys. 37 (1996) 1449.
[6] F.G. Alvarenga, N.A. Lemos, Gen. Rel. Grav. 30 (1998) 681.
[7] M.J. Gotay, J. Demaret, Phys. Rev. D 28 (1983) 2402.
[8] J. Acacio de Barros, N. Pinto-Neto, M.A. Sagioro-Leal, Phys. Lett. A 241 (1998) 229.
[9] V.G. Lapchinskii, V.A. Rubakov, Theor. Math. Phys. 33 (1977) 1076.
[10] F.G. Alvarenga, N.A. Lemos, Gen. Rel. Grav. 31 (1999) 1743.
[11] I.S. Gradshteyn, I.M. Rizhik, Tables of Integrals, Series and Products, Academic Press, New York, 1980.
[12] A.B. Batista, J.C. Fabris, S.V.B. Gonçalves, gr-qc/0009040, to appear in Class. Quantum Grav.
[13] C. Cohen-Tannoudji, B. Diu, F. Laloë, Quantum Mechanics, Vol. 1, Wiley, 1977.
[14] A. Messiah, Quantum Mechanics, Vol. 1, North-Holland, Amsterdam, 1961.
[15] F.J. Tipler, Phys. Rep. 137 (1986) 231.
[16] P.R. Holland, The Quantum Theory of Motion, Cambridge University Press, Cambridge, 1993.
[17] S. Weinberg, Gravitation and Cosmology, Wiley, New York, 1972.
[18] C.P. Constantinidis, J.C. Fabris, R.G. Furtado, M. Picco, Phys. Rev. D 61 (2000) 043503.
[19] R. Colistete Jr., J.C. Fabris, N. Pinto Neto, Phys. Rev. D 57 (1998) 4707.

ELSEVIER

14 September 2000

Physics Letters B 489 (2000) 203–206

PHYSICS LETTERS B

www.elsevier.nl/locate/npe

Gravity and antigravity in a brane world with metastable gravitons

Ruth Gregory [a], Valery A. Rubakov [b], Sergei M. Sibiryakov [b]

[a] *Centre for Particle Theory, Durham University, South Road, Durham, DH1 3LE, UK*
[b] *Institute for Nuclear Research of the Russian Academy of Sciences, 60th October Anniversary prospect, 7a, Moscow 117312, Russia*

Received 26 July 2000; accepted 11 August 2000
Editor: P.V. Landshoff

Abstract

In the framework of a five-dimensional three-brane model with quasi-localized gravitons we evaluate metric perturbations induced on the positive tension brane by matter residing thereon. We find that at intermediate distances, the effective four-dimensional theory coincides, up to small corrections, with General Relativity. This is in accord with Csaki, Erlich and Hollowood and in contrast to Dvali, Gabadadze and Porrati. We show, however, that at ultra-large distances this effective four-dimensional theory becomes dramatically different: conventional tensor gravity changes into scalar anti-gravity. © 2000 Published by Elsevier Science B.V.

The papers by Dvali, Gabadadze and Porrati, [1], and Csaki, Erlich and Hollowood, [2], address the issue of whether four-dimensional gravity is phenomenologically acceptable in a class of brane models with infinite extra dimensions in which the five-dimensional gravitons have a metastable 'bound state', rather than a genuine zero mode. A model of this sort has been proposed in Refs. [3,4] and is a variation of the Randall–Sundrum (RS) scenario for a non-compact fifth dimension [5]. The construction with metastable gravitons has been put in a more general setting in Refs. [1,6]. It has been argued in Ref. [1] that models with metastable gravitons are not viable: from the four-dimensional point of view, gravitons are effectively massive and hence appear to suffer from a van Dam–Veltman–Zakharov [7] discontinuity in the propagator in the massless limit. In particular, it has been claimed [1] that the prediction for the deflection of light by massive bodies would be considerably different from that of General Relativity. The issue has recently been analyzed in more detail in Ref. [2], where explicit calculations of four dimensional gravity have been performed along the lines of Garriga and Tanaka [8], and Giddings, Katz and Randall [9]. The outcome of that analysis is that four-dimensional gravity has been claimed to be in fact Einsteinian, despite the peculiarity of apparently massive gravitons.

In this letter we also apply the Garriga–Tanaka (GT) technique to obtain effective four-dimensional gravity at the linearized level, considering as an example the model of Refs. [3,4]. We find that at intermediate distances (which should extend from microscopic to very large scales in a phenomenologically acceptable model) four dimensional gravity is

E-mail address: r.h.w.gregory@durham.ac.uk (R. Gregory).

0370-2693/00/$ - see front matter © 2000 Published by Elsevier Science B.V.
PII: S0370-2693(00)00917-5

indeed Einsteinian, in accord with Ref. [2] and in contrast to Ref. [1]. However, at ultra-large scales we find a new phenomenon: four-dimensional gravity changes dramatically, becoming *scalar anti-gravity* rather than tensor gravity. This may or may not signal an internal inconsistency of the models under discussion.

To recapitulate, the set up of Refs. [3,4] is as follows. The model has five dimensions and contains one brane with tension $\sigma > 0$ and two branes with equal tensions $-\sigma/2$ placed at equal distances to the right and to the left of the positive tension brane in the fifth direction. There is a reflection symmetry, $z \to -z$, which enables one to consider explicitly only the region to the right of the positive tension brane (hereafter z denotes the fifth coordinate). Conventional matter resides on the central positive tension brane. The bulk cosmological constant between the branes, Λ, is negative, whereas it is equal to zero to the right of the negative tension brane. With appropriately tuned Λ, there exists a solution to the five-dimensional Einstein equations for which both positive and negative tension branes are at rest at $z = 0$ and $z = z_c$ respectively, z_c being an arbitrary constant. The metric of this solution is

$$ds^2 = a^2(z)\eta_{\mu\nu}dx^\mu dx^\nu - dz^2 \tag{1}$$

where

$$a(z) = \begin{cases} e^{-kz}, & 0 < z < z_c \\ e^{-kz_c} \equiv a_-, & z > z_c \end{cases} \tag{2}$$

The constant k is related to σ and Λ. The four-dimensional hypersurfaces $z = const.$ are flat, the five-dimensional space-time is flat to the right of the negative-tension brane and anti-de Sitter between the branes. The spacetime to the left of the positive tension brane is a mirror image of this set-up.

This background has two different length scales, k^{-1} and

$$r_c = k^{-1}e^{3kz_c} \tag{3}$$

These are assumed to be well separated, $r_c \gg k^{-1}$. It has been argued in Ref. [4] that the extra dimension 'opens up' both at short distances, $r \ll k^{-1}$ and ultra-long ones, $r \gg r_c$.

To find the four-dimensional gravity experienced by matter residing on the positive tension brane, we follow GT and consider a Gaussian–Normal (GN) gauge

$$g_{zz} = -1 \quad g_{z\mu} = 0 \tag{4}$$

In the bulk, one can further restrict the gauge to be transverse-tracefree (TTF)

$$h^\mu_\mu = h^\mu_{\nu,\mu} = 0 \tag{5}$$

Hereafter $h_{\mu\nu}$ are metric perturbations; indices are raised and lowered by the four-dimensional Minkowski metric. The linearized Einstein equations in the bulk take one and the same simple form for all components of $h_{\mu\nu}$,

$$\begin{cases} h'' - 4k^2 h - \dfrac{1}{a^2}\Box^{(4)}h = 0, & 0 < z < z_c \\ h'' - \dfrac{1}{a_-^2}\Box^{(4)}h = 0, & z > z_c \end{cases} \tag{6}$$

It is convenient, however, to formulate the junction conditions on the positive tension brane in the local GN frame. In this frame, metric perturbations $\bar{h}_{\mu\nu}$ are not transverse-tracefree, so the two sets of perturbations are related in the bulk between the two branes by a five-dimensional gauge transformation preserving (4),

$$\bar{h}_{\mu\nu} = h_{\mu\nu} + \frac{1}{k}\hat{\xi}^5_{,\mu\nu} - 2ka^2\eta_{\mu\nu}\hat{\xi}^5 + a^2(\xi_{\mu,\nu} + \xi_{\nu,\mu}) \tag{7}$$

where $\xi_\mu(x)$ and $\hat{\xi}^5(x)$ are the gauge parameters. Notice that if ξ^5 is not zero, there is a 'shift' in the location of the wall relative to an observer at infinity, i.e. the wall appears bent to such an observer (as discussed in [8,9]). Physically, this simply represents the fact that the wall GN frame is constructed by integrating normal geodesics from the wall, and in the presence of matter these geodesics will be distorted, thereby altering the proper distance between the wall and infinity. In fact, one finds a similar 'bending' of the equatorial plane in the Schwarzschild spacetime if one tries to impose a local GN frame away from the horizon.

In the presence of additional matter on the positive tension brane with energy momentum $T_{\mu\nu}$, the junction conditions on this brane read

$$\bar{h}'_{\mu\nu} + 2k\bar{h}_{\mu\nu} = 8\pi G_5\left(T_{\mu\nu} - \tfrac{1}{3}\eta_{\mu\nu}T^{\lambda}_{\lambda}\right) \tag{8}$$

where G_5 is the five-dimensional gravitational constant. The solution to Eqs. (5)–(8) has been obtained by Garriga and Tanaka. They found that $\hat{\xi}^5$ obeys

$$\Box^{(4)}\hat{\xi}^5 = -\frac{4\pi}{3}G_5 T^{\lambda}_{\lambda} \tag{9}$$

We will need the expression for the induced metric on the positive tension brane. Up to terms that can be gauged away on this brane, the induced metric is [8]

$$\bar{h}_{\mu\nu}(z=0) = h^{(m)}_{\mu\nu} - 2k\eta_{\mu\nu}\hat{\xi}^5 \tag{10}$$

where

$$h^{(m)}_{\mu\nu} = 16\pi G_5 \int dx'\, G_R^{(5)}(x,x';z=z'=0) \times\left(T_{\mu\nu} - \tfrac{1}{3}\eta_{\mu\nu}T^{\lambda}_{\lambda}\right)(x') \tag{11}$$

Here $G_R^{(5)}$ is the retarded Green's function of Eq. (6) with appropriate (source-free) junction conditions on the two branes. This Green's function is mirror-symmetric and obeys

$$\left[\partial_z^2 - 4k^2\theta(z_c - z) - \frac{1}{a^2}\Box^{(4)} + 4k\delta(z) - 2k\delta(z - z_c)\right]G_R^{(5)}(x,x';z,z') = \delta(x-x')\,\delta(z-z') \tag{12}$$

Let us consider the case of the static source first. It has been found in Ref. [4] that for $k^{-1} \ll r \ll r_c$, the leading behavior of the static Green's function (given by $\int dt\, G_R^{(5)}(z=z'=0)$) is the same as in the RS model (up to small corrections), and corresponds to a $1/r$ potential. Hence, at intermediate distances the analysis is identical to GT, and the induced metric is the same as in the linearized four-dimensional General Relativity. This is in accord with Ref. [2].

On the other hand, it follows from Ref. [4] that at ultra-large distances, $r \gg r_c$, the contribution (11) behaves like $1/r^2$ (the fifth dimension 'opens up'). There remains, however, the second term in Eq. (10). Since Eq. (9) has a four-dimensional form, this term gives rise to a $1/r$ potential (missed in Ref. [4]) even at ultra-large distances. For a point-like static source of unit mass, the corresponding gravitational potential is

$$V(r) \equiv \tfrac{1}{2}\bar{h}_{00}(r) = +\tfrac{1}{3}G_4\frac{1}{r} \tag{13}$$

where $G_4 = kG_5$ is the four-dimensional Newton's constant entering also into the conventional Newton's law at intermediate distances. We see that at $r \gg r_c$, four-dimensional gravity is induced by the trace of energy-momentum tensor and has a repulsive $1/r$ potential. At ultra-large distances tensor gravity changes to scalar anti-gravity.

Likewise, the four-dimensional gravitational waves emitted by non-static sources are conventional tensor ones at intermediate distances and transform into scalar waves at ultra-large distances (the relevant distance scale being different from r_c due to relativistic effects, see Ref. [4]). Indeed, the first term in Eq. (10) dissipates [4], whereas the second term survives, again due to the four-dimensional structure of Eq. (9).

These two cases illustrate the general property of Eq. (10): the first term becomes irrelevant at ultra-large distances (the physical reason being the metastability of the five-dimensional graviton bound state), so the four-dimensional gravity (in effect, anti-gravity) is entirely due to the second, scalar term.

This bizarre feature of models with a metastable graviton bound state obviously deserves further investigation. In particular, it will be interesting to identify the four-dimensional massless scalar mode, which is present at ultra-large distances, among the free sourceless perturbations. This mode is unlikely to be the radion [10,11], studied in this model in Ref. [3]: the radion would show up at intermediate distances, as well as at ultra-large ones[1]; furthermore, the experience [13] with models where the distance between the branes is stabilized [14] suggests that the

[1] The radion presumably couples exponentially weakly to the matter on the positive tension brane, as it does [3,8] in the two-brane model of Randall and Sundrum [12]. This may be the reason why the radion effects have not been revealed by the analyses made in Ref. [2] and this note.

massless four-dimensional mode parametrized by $\hat{\xi}^5$ exists even if the radion is made massive.

More importantly, one would like to understand whether anti-gravity at ultra-large distances is a signal of an intrinsic inconsistency of this class of models, or simply a signal that physics is intrinsically five-dimensional at these scales. In four dimensions, scalar antigravity requires either negative kinetic and gradient energy or a ghost. Whether or not a similar feature is inherent in models with extra dimensions remains an open question. If it is, there still would remain a possibility that fields with negative energy might be acceptable, as their effect might show up at ultra-large distances only.

We note finally, that anti-gravity may not be a special feature of models with quasi-localized gravitons. It is also possible that this phenomenon may be present in models of the type suggested by Kogan et. al. [15], where some Kaluza–Klein graviton excitations are extremely light. The same question about internal consistency then would apply to these models as well.

Acknowledgements

We would like to thank Sergei Dubovsky, Dmitry Gorbunov, Maxim Libanov and Sergei Troitsky for useful discussions. We are indebted to C. Csaki, J. Erlich and T. J. Hollowood for sending their paper [2] prior to publication. R.G. was supported in part by the Royal Society, and V.R. and S.S. by the Russian Foundation for Basic Research, grant 990218410.

References

[1] G. Dvali, G. Gabadadze, M. Porrati, Metastable gravitons and infinite volume extra dimensions, hep-th/0002190.
[2] C. Csaki, J. Erlich, T.J. Hollowood, Graviton propagators, brane bending and bending of light in theories with quasi-localized gravity, hep-th/0003020.
[3] C. Charmousis, R. Gregory, V.A. Rubakov, Wave function of the radion in a brane world, hep-th/9912160.
[4] R. Gregory, V.A. Rubakov, S.M. Sibiryakov, Opening up extra dimensions at ultra-large scales, hep-th/0002072.
[5] L. Randall, R. Sundrum, Phys. Rev. Lett. 83 (1999) 3370, hep-th/9905221. Phys. Rev. Lett. 83 (1999) 4690, hep-th/9906064.
[6] C. Csaki, J. Erlich, T.J. Hollowood, Quasi-localization of gravity by resonant modes, hep-th/0002161.
[7] H. van Dam, M. Veltman, Nucl. Phys. B 22 (1970) 397; V.I. Zakharov, JETP Lett. 12 (1970) 312.
[8] J. Garriga, T. Tanaka, Gravity in the brane-world, hep-th/9911055.
[9] S.B. Giddings, E. Katz, L. Randall, Linearized Gravity in Brane Backgrounds, hep-th/0002091.
[10] C. Csaki, M. Graesser, L. Randall, J. Terning, Cosmology of brane models with radion stabilization, hep-ph/9911406.
[11] W.D. Goldberger, M.B. Wise, Phenomenology of a stabilized modulus, hep-ph/9911457.
[12] L. Randall, R. Sundrum, Phys. Rev. Lett. 83 (1999) 3370.
[13] T. Tanaka, X. Montes, Gravity in the brane-world for two-branes model with stabilized modulus, hep-th/0001092.
[14] W.D. Goldberger, M.B. Wise, Phys. Rev. Lett. 83 (1999) 4922.
[15] I.I. Kogan, S. Mouslopoulos, A. Papazoglou, G.G. Ross, J. Santiago, A three three-brane universe: New phenomenology for the new millennium? hep-ph/9912552.

The ac magnetic response in type-II superconductors

1996 J. Phys.: Condens. Matter 8 L445

(http://iopscience.iop.org/0953-8984/8/33/002)

J. Phys.: Condens. Matter **8** (1996) L445–L453. Printed in the UK

LETTER TO THE EDITOR

The ac magnetic response in type-II superconductors

Yoshihisa Enomoto† and Kazuma Okada‡

† Department of Physics, Nagoya Institute of Technology, Gokiso, Nagoya 466, Japan
‡ Department of Applied Physics, Nagoya University, Nagoya 464-01, Japan

Received 13 May 1996, in final form 1 July 1996

Abstract. The ac response of type-II superconductors to an alternating magnetic field is numerically studied on the basis of the time-dependent Ginzburg–Landau equations. We examine the temperature dependence of the ac susceptibility associated with a small ac magnetic field in the absence of a bias dc field. It is shown that with increasing temperature the in-phase component of the fundamental susceptibility exhibits a step-like change from a negative constant value to zero, while the out-of-phase component of the fundamental susceptibility and the third-harmonic component have a peak at a certain temperature near the superconducting transition temperature. These results are in qualitative agreement with those of recent experiments on high-T_c superconductors.

Magnetization measurements using alternating fields have been widely employed in the study of type-II superconductors [1]. This is because in these experiments the effective time window can be easily changed by varying the frequency of the applied ac field. Thus, the study of the ac magnetic response of type-II superconductors provides direct information on flux dynamics in these materials. Recently, several authors have measured the ac susceptibility in high-T_c materials as functions of various physical parameters such as temperature, and the frequency and amplitude of the applied ac field [2–5].

Various models have been proposed to explain experimental data for the ac susceptibility of type-II superconductors, and especially of high-T_c materials [6–12]. Although these models have partially succeeded in explaining the ac magnetic response of type-II superconductors, they are at rather macroscopic and/or phenomenological levels, and thus are still incomplete. In this letter, to complement the previous study, we attack the above problem by using a different type of approach, that is, the numerical approach of the time-dependent Ginzburg–Landau (TDGL) equations [13, 14]. The main advantage offered by this computer simulation study is the ability to visualize the dynamical processes of magnetization and thus to directly obtain information on the dynamics of the magnetic flux structure without making any of the *ad hoc* electrodynamical assumptions used in previous models (e.g., the field dependence of the critical current in the critical state model). Here, performing numerical calculation of the TDGL equations, we examine the ac magnetic response of type-II superconductors to a small alternating magnetic field in the absence of the steady bias field. In particular, we discuss the temperature dependence of the ac susceptibility with the amplitude and frequency of the ac field being fixed.

The TDGL equations are composed of two partial differential ones for the complex order parameter $\psi(\boldsymbol{r}, t)$ and the vector potential $\boldsymbol{A}(\boldsymbol{r}, t)$ at time t and position $\boldsymbol{r}$ [13–15]:

$$\frac{\hbar^2}{2mD}\left(\frac{\partial}{\partial t} + \mathrm{i}\frac{e\phi}{\hbar}\right)\psi = -\frac{\delta F}{\delta \psi^*} + f(\boldsymbol{r}, t) \tag{1}$$

0953-8984/96/330445+09$19.50

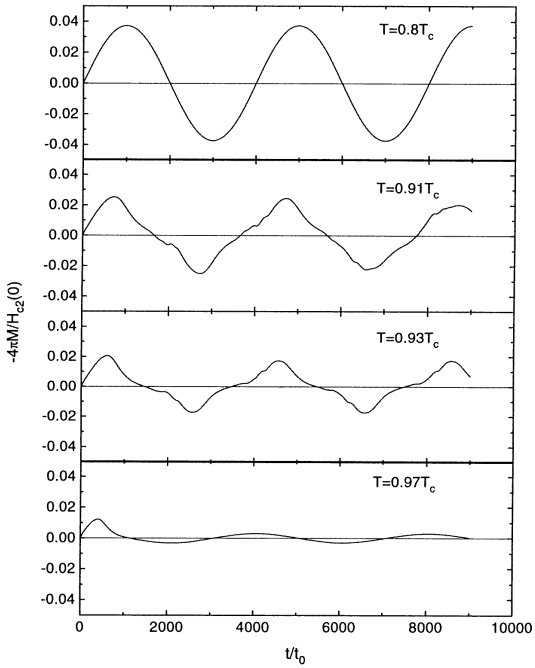

Figure 1. Time variation of the magnetization $M(t)$ for $T/T_c = 0.8$, 0.91, 0.93, and 0.97.

$$\sigma\left(\frac{1}{c}\frac{\partial \boldsymbol{A}}{\partial t} + \boldsymbol{\nabla}\phi\right) = -\frac{\delta F}{\delta \boldsymbol{A}} \tag{2}$$

with the covariant time derivative $(\partial/\partial t + \mathrm{i}e\phi/\hbar)$ and a scalar potential ϕ, where ψ^* denotes the complex conjugate of ψ. These equations are invariant under the local U(1) gauge transformation for ψ, $\boldsymbol{A}$, and ϕ. Here, D and σ are the diffusion constant and the conductivity, associated with the normal phase, respectively, and they have the relation [16]

$$\sigma = \frac{c^2\xi^2}{48\pi\lambda^2}\frac{1}{D} \tag{3}$$

with the coherence length ξ and the magnetic penetration depth λ. The last term of the r.h.s. of equation (1), $f(\boldsymbol{r}, t)$, denotes the thermal noise with zero mean, i.e. $\langle\langle f\rangle\rangle = 0$, and the correlation

$$\langle\langle f^*(\boldsymbol{r}', t')f(\boldsymbol{r}, t)\rangle\rangle = 12\xi_0^{-4}t_0k_BT\left(\frac{H_c(0)^2}{8\pi}\right)^{-1}\delta(\boldsymbol{r}' - \boldsymbol{r})\delta(t' - t) \tag{4}$$

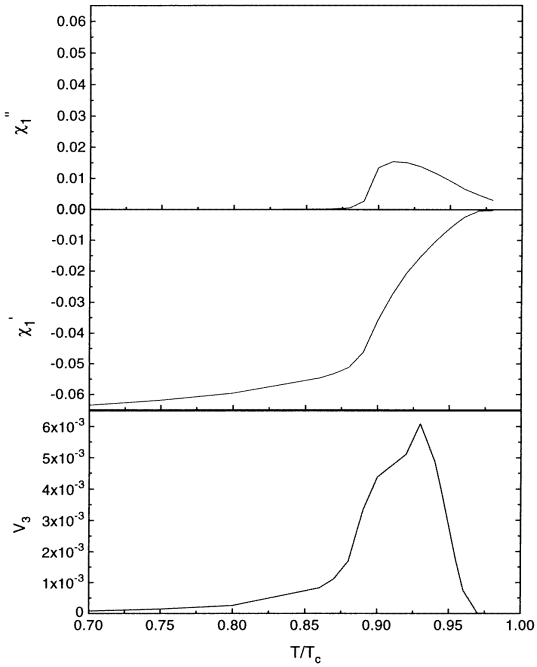

Figure 2. Temperature dependences of χ_1', χ_1'', and V_3.

where $\langle\langle\cdots\rangle\rangle$ denotes the ensemble average, ξ_0 is the coherence length at zero temperature, and $t_0 \equiv \pi\hbar/(96k_BT_c)$ with the superconducting transition temperature T_c at zero field. The Ginzburg–Landau (GL) free-energy functional $F[\psi, \boldsymbol{A}]$ is given by

$$F = \int \mathrm{d}\boldsymbol{r} \left[\frac{1}{2m}|\boldsymbol{D}\psi|^2 + \alpha(T)|\psi|^2 + \frac{\beta}{2}|\psi|^4 + \frac{1}{8\pi}(\boldsymbol{\nabla}\times\boldsymbol{A})^2\right] \tag{5}$$

with the covariant derivative $\boldsymbol{D} \equiv -\mathrm{i}\boldsymbol{\nabla} - (e/c)\boldsymbol{A}$ and the local magnetic flux density $\boldsymbol{b}(\boldsymbol{r}, t) \equiv \boldsymbol{\nabla}\times\boldsymbol{A}$. Under the assumption that $\alpha(T) = \alpha(0)(T/T_c - 1)$, and $\alpha(0)$ and β are positive constants in equation (5), the upper and lower critical fields are given by $H_{c2}(T)/H_{c2}(0) = 1 - T/T_c$ and $H_{c1}(T)/H_{c2}(0) = (\ln\kappa/(2\kappa^2))(1 - T/T_c)$, respectively, with the GL parameter κ. The other notation is conventional [16]. These equations are supplemented with boundary conditions, $\boldsymbol{D}\psi|_n = 0$ and $\boldsymbol{\nabla}\times\boldsymbol{A}|_s = \boldsymbol{H}_e$, where the index n denotes the normal direction on the sample boundary and the index s denotes the sample boundary with an applied magnetic field $\boldsymbol{H}_e$.

We here consider a type-II superconductor in the x–y plane with a size $L_x \times L_y$. The

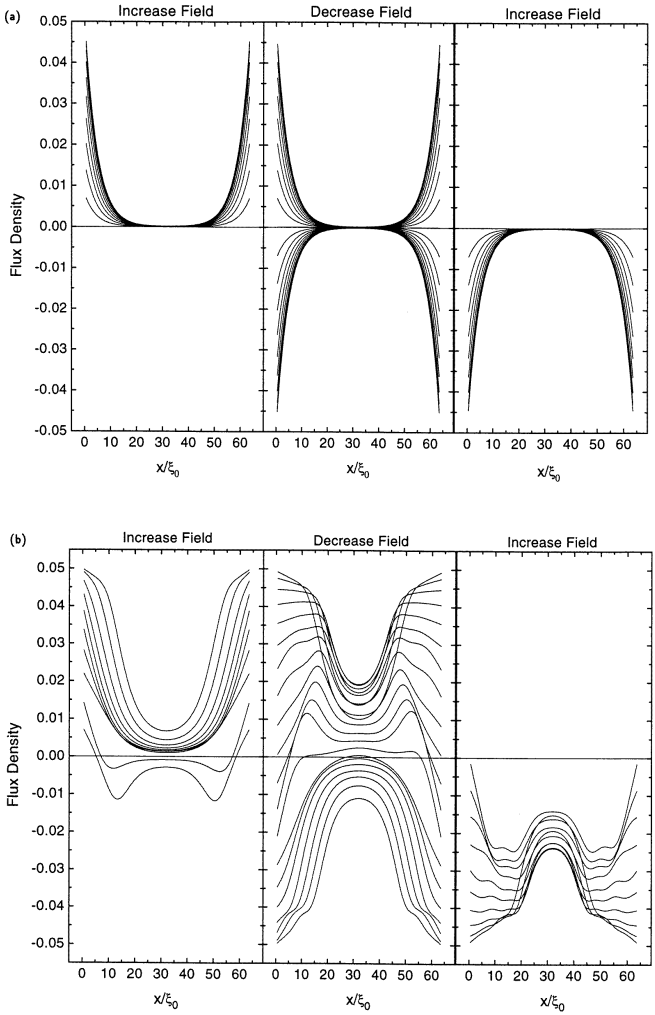

Figure 3. See facing page.

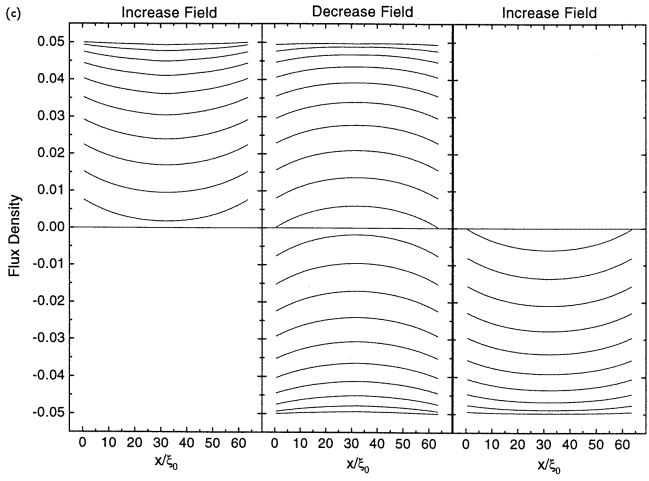

Figure 3. (Continued) Time variations of profiles of the z-component of the local magnetic flux density, b_z, in units of $H_{c2}(0)$ along the x-axis at $y = 32\xi_0$ for $T/T_c = 0.8$ (a), 0.91 (b), and 0.97 (c). Time goes from the left-hand column to the right-hand one for one cycle of the ac field.

sample is assumed to be infinite in the z-direction, and the problem is reduced to two dimensions neglecting all derivatives along z. The external ac magnetic field is applied to the sample as $\boldsymbol{H}_e = H(t)\hat{\boldsymbol{z}}$ with $H(t) = H_{ac}\sin\omega t$ where H_{ac} and ω denote the amplitude and angular frequency of the ac field, respectively, and $\hat{\boldsymbol{z}}$ is the unit vector along the z-axis. In actual simulations the TDGL equations are transformed into the dimensionless discretized equations on a two-dimensional lattice by introducing link variables for the vector potential and the gauge fixing such that the scalar potential is set to zero. Since these procedures are the same as those in references [13, 14], we will not discuss the numerical procedures any further.

In the following simulations, we set $L_x = L_y = 64\xi_0$ and $\kappa = 2$. The amplitude and frequency of the ac field are fixed to be $H_{ac} = 0.05H_{c2}(0)$ and $\omega t_0/2\pi = 0.25 \times 10^{-3}$ (that is, the period of the ac field is $4000t_0$), respectively. We also take the lattice spacing and time step for numerical calculations to be $0.5\xi_0$ and $0.0125t_0$, respectively. These values are chosen for the computational reason of obtaining efficient results within our computer availability. As the initial state we choose the zero-field-cooling state.

In figure 1 the magnetization, $M(t)$, of the sample is plotted against time for various values of temperature. The magnetization $M(t)$ is defined as $4\pi M(t) = \langle B\rangle(t) - H(t)$, where the magnetic induction $\langle B\rangle(t)$ is obtained from the sample average of the z-component, $b_z(\boldsymbol{r}, t)$, of the local magnetic flux density $\boldsymbol{b}(\boldsymbol{r}, t)$. At $T = 0.8T_c$, the magnetization is sinusoidal in nature, according to the external ac field $H_{ac}\sin\omega t$. With increasing temperature, the magnetization deviates from the sinusoidal character with a

decrease of its magnitude, and simultaneously a phase-shift phenomenon occurs in the t–$M(t)$ curve. Further increase of temperature results in the large degree of phase shift. Indeed, at $T = 0.97T_c$, the magnetization becomes almost zero at times when the applied ac field is maximum (minimum). Note that even for no bulk pinning case, the phase-shift phenomena take place due to the sample boundary effect, as has been discussed in our previous work [17].

To give details of the ac magnetic response of the system, we study the ac susceptibility defined by the Fourier transformation of the magnetization $M(t)$:

$$M(t) = H_{ac} \sum_{n=1}^{\infty} (\chi_n' \sin n\omega t - \chi_n'' \cos n\omega t) \tag{6}$$

where χ_n' and χ_n'' ($n = 1, 2, \ldots$) denote the in-phase and out-of-phase components of the nth-harmonic susceptibility, respectively, with the nth harmonics $V_n \equiv \sqrt{\chi_n'^2 + \chi_n''^2}$. In calculating the ac susceptibility, simulation data during the first period have been discarded to avoid transient effects. In the present case we have numerically checked that only odd harmonics are generated [8]. In figure 2, χ_1', χ_1'', and V_3 are plotted as functions of temperature; they have been often measured experimentally. It is shown that with increasing temperature, χ_1' exhibits a step-like change from a negative constant value ($=-1/(4\pi)$ theoretically [6]) to zero, while χ_1'' initially rises from zero, goes through a maximum at $0.91T_c$ (called the peak temperature, denoted by T_p), and then returns to a small value near T_c. Note that $H_{c1}(T_p) \simeq 0.008 < H_{ac} = 0.05 < H_{c2}(T_p) = 0.09$ for $T_p = 0.91T_c$ in units of $H_{c2}(0)$. The third harmonic V_3 is also found to have a similar temperature dependence to χ_1'' with the peak temperature $T_p = 0.93T_c$. These results are qualitatively consistent with those of recent experiments on high-T_c superconductors [2–5]. At present it is unclear whether the slight difference between the peak temperature estimated from χ_1'' and that from V_3 is physically meaningful or not.

Now we relate the above macroscopic behaviour of the system to the spatio-temporal structure of the local magnetic flux. In figures 3(a)–3(c) the time evolution of the profile of the local magnetic flux density b_z along the x-axis is shown at $y = 32\xi_0$ for a complete cycle of the ac field for $T/T_c = 0.8$ (a), 0.91 (b), and 0.97 (c), respectively. In figure 4 the time evolution of the profile of the y-component of the current density is shown along the x-axis at $y = 32\xi_0$ for $T = 0.91T_c$ during one half of the period of the ac field, as well as b_z. The current density is given by $(c/4\pi)\boldsymbol{\nabla} \times \boldsymbol{\nabla} \times \boldsymbol{A}$ in units of $j_0 \equiv cH_{c2}(0)/(4\pi\xi_0)$. No definite magnetic vortex structures are observed in figures 3(a)–3(c). It is also found that the step in χ_1' is due to the transition from near-perfect screening (figure 3(a)) to complete penetration ($\langle B \rangle(t) \simeq H(t)$) of the ac field impinging into the whole sample (figure 3(c)). Moreover, we have numerically checked that the smallest temperature at which penetrating magnetic flux (current) reaches to the centre of the sample is $0.90T_c$ in the present case. Thus, the peak in χ_1'' (and maybe the peak in V_3) corresponds to the first penetration of the flux (current) to the centre of the sample (figure 3(b) and figure 4). Although such an interpretation has been already proposed by several authors [7, 9, 10], this is the first simulation study to discuss the ac magnetic response of type-II superconductors from the point of view of the local magnetic flux dynamics without making any of the *ad hoc* electrodynamical assumptions used in previous models. Finally, we remark that the magnetic relaxation phenomenon can be seen in figure 3(b) and figure 4. Indeed, even when the external field changes to a decreasing stage from the initial ramp-up phase, the magnetic flux near the centre of the sample still increases for a while. An importance of this relaxation behaviour has recently been pointed out as one of possible causes for the frequency dependence of the ac susceptibility [3, 12]. Such magnetic relaxation effects on the ac susceptibility will be

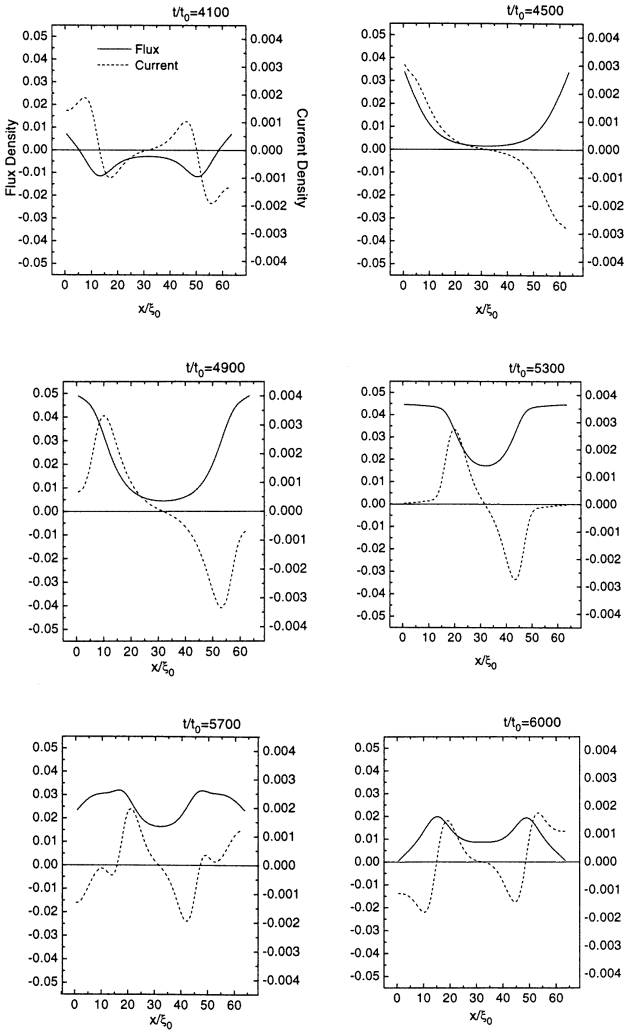

Figure 4. Time variations of profiles of the y-component of the current density (dashed lines) in units of $j_0 = cH_{c2}(0)/(4\pi\xi_0)$ along the x-axis at $y = 32\xi_0$ for $T/T_c = 0.91$ during one half of the period of the ac field. Profiles of b_z are also shown for comparison, as solid lines.

discussed elsewhere.

In conclusion, we have studied the ac magnetic response of type-II superconductors to the alternating magnetic field on the basis of numerical calculation of the TDGL equations. In particular, the temperature dependence of the ac susceptibility in the absence of the dc field with the amplitude and frequency of the ac field being fixed has been discussed. We have found a step-like change in χ_1', and a peak in χ_1'' and also in the third harmonic V_3 at a certain temperature near T_c. These results are in qualitative agreement with recent experimental data on high-T_c superconductors. Moreover, we have briefly discussed the relationship between these macroscopic behaviours of the system and the spatio-temporal behaviour of the local magnetic flux.

However, we should mention that there can be a big distance between simulations and experiments. This is because there are the following faults in the present model. Firstly, in real systems the ac response is strongly affected by pinning and thermal fluctuations, which are not in the model. Secondly, we have neglected the z-dependence of the problem. The present results, therefore, apply only to films, not bulk materials where the entanglement of flux lines may be important. These points will be discussed in future work.

Nevertheless, the present approach based on computer simulations of TDGL equations has been found to be potentially rich for throwing novel light on the problem studied here. For instance, the present model is applicable for discussing the validity of assumptions used in macroscopic and/or phenomenological models. Since the present study is still in a primitive stage, detailed simulations are now under way to allow discussion of a quantitative comparison of simulation results with theoretical results and experimental data obtained by not only the ac method but also the Hall probe method [18]. Moreover, many interesting problems still remain open, such as the dependence of the ac response on various physical parameters (e.g., the amplitude and frequency of the ac field, the dc field, bulk pinning and the sample geometry), and also the universal behaviour of the ac susceptibility. These problems are also now under consideration.

The authors are grateful to Professor S Maekawa for a number of valuable discussions.

References

[1] For a review, see
Hein R A, Francavilla T L and Liebenberg D H (ed) 1991 *Magnetic Susceptibility of Superconductors and Other Spin Systems* (New York: Plenum)
[2] Ghatak S K, Mitra A and Sen D 1992 *Phys. Rev.* B **45** 951
[3] Wolfus Y, Abulafia Y, Klein L, Larkin V A, Shaulov A, Yeshurun Y, Konczykowski M and Feigel'man M 1994 *Physica* C **224** 213
[4] Ding S Y, Wang G Q, Yao X X, Peng H T, Peng Q Y and Zhou S H 1995 *Phys. Rev.* B **51** 9107
[5] Kumaraswamy B V, Lal R and Narlikar A V 1996 *Phys. Rev.* B **53** 6759
[6] Bean C P 1964 *Rev. Mod. Phys.* **36** 31
[7] Chen D X, Nogues J and Rao K V 1989 *Cryogenics* **29** 800
[8] Ji L, Sohn R H, Spalding G C, Lobb C J and Tinkham M 1989 *Phys. Rev.* B **40** 10 936
[9] Geshkenbein V B, Vinokur V M and Fehrenbaher R 1991 *Phys. Rev.* B **43** 3748
[10] van der Beek C J, Geshkenbein V B and Vinokur V M 1993 *Phys. Rev.* B **48** 3393
[11] Shatz S, Shaulov A and Yeshurun Y 1993 *Phys. Rev.* B **48** 13 871
[12] Prozorov R, Shaulov A, Wolfus Y and Yeshurun Y 1995 *Phys. Rev.* B **52** 12 541
[13] For a review, see
Enomoto Y, Kato R and Maekawa S 1993 *Studies of High Temperature Superconductors* vol 11, ed A V Narlikar (New York: Nova Science) p 309
[14] Fram H, Ullah S and Dorsey A T 1991 *Phys. Rev. Lett.* **66** 3067
Liu F, Mondello M and Goldenfeld N 1991 *Phys. Rev. Lett.* **66** 3071

Kato R, Enomoto Y and Maekawa S 1991 *Phys. Rev.* B **44** 6916; 1993 *Phys. Rev.* B **47** 8016
[15] Schmid A 1969 *Phys. Rev.* **180** 527
[16] Tinkham M 1975 *Introduction to Superconductivity* (New York: McGraw-Hill)
[17] Enomoto Y, Ishikawa Y and Maekawa S 1996 *Physica* C **263** 21
[18] Zeldov E, Majer D, Konczykowski M, Larkin A I, Vinokur V M, Geshkenbein V B, Chikumoto N and Shtrikman H 1995 *Europhys. Lett.* **30** 367

A01-34138

AIAA 2001-3364
Exploration Of Anomalous Gravity Effects by Magnetized High-T_c Superconducting Oxides

Glen A. Robertson and Ron Litchford
NASA Marshall Space Flight Center
Huntsville, AL

Bryan Thompson
TMET
Winchester, TN

Dr. Randall Peters
Mercer University
Macon, GA

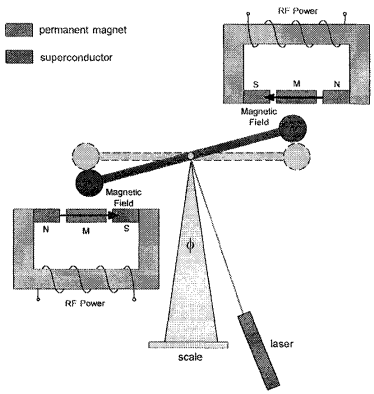

37th AIAA/ASME/SAE/ASEE JPC Conference and Exhibit
8-11 July 2001
Salt Lake City, Utah

A IAA 2001-3364

EXPLORATION OF ANOMALOUS GRAVITY EFFECTS BY MAGNETIZED HIGH-T_C SUPERCONDUCTING OXIDES

Glen A. Robertson* and Ron Litchford†
NASA Marshall Space Flight Center
Huntsville, AL

Bryan Thompson‡
TMET
Winchester, TN

Dr. Randall Peters¶
Mercer University
Macon, GA

ABSTRACT

Driven by the knowledge that mass-ejection from a rocket engine is a major drawback in the exploration of space, investigations of fringe effects (or abnormalities) in known science and dealing with mass reduction was undertaken. This research, then examines the possible connection between gravity and electro-magnetic affects on the Type II, YBCO superconductor, as reported by the Russian scientist, Eugene Podkletnov. It is suggested that the quantum fluctuations of the electrons across the multitude of superconductor grain boundaries in a properly prepared Type II; superconductors may produce a measurable force on the vacuum that could counteract the effect of gravity, an acceleratory force. Within known physicists, the driving phenomena appears to relate to both the Maxwell Stress Tensor as derived by Oliver Heaviside and Woodward's transient mass theory. As a means of improving this understanding, a simplified laboratory experiment has been constructed using a modified–automated commercial Cavendish balance. The larger lead masses used in this balance was replaced by a system to EM modulate a superconductor. Tests results were inconclusive because at both room temperature and at liquid nitrogen temperatures the application of the electromagnetic (EM) or rf energy resulted in an upward climb in the data.

* Research Scientist; Propulsion Research Center
† Project Scientist; Advanced Space Transportation Program Office
‡ Research Engineer
¶ Research Consultant; Department of Physics and Earth Science

INTRODUCTION

Engineers working in the aerospace fields dealing with rocket engine technology quickly learn that mass-ejection is a major drawback in the exploration of space. Using current rocket technology a trip to the next star would easy consume the mass-energy equivalent of a planet in order to arrive within a reasonable lifetime with reasonable hardware and expendables for the journey. Technologies like nuclear fission and fusion offer some hope, but still will not support the "Star Trek" vision of space exploration. Therefore, the NASA Propulsion Research Center at the Marshall Space Flight Center in response to the propulsion challenges specified by the NASA Breakthrough Propulsion Physics (BPP)** project, specially to investigations fringe effects or abnormalities in known science and dealing with mass reduction, proposed to explore the recently report observation of anomalous gravitation behavior in experiments using high temperature superconductor.

The thesis of this research is to see if there is a possibility to circumvent the rocket equation without violating physical laws and to produce valid experimental data that can be used to show credible validation of these effects. The intend here is then to examining the possible connection between gravity and electro-magnetic affects on the Type II, YBCO superconductor, as reported by the Russian scientist, Eugene Podkletnov and provide a rigorous, independent, empirical conformation (or refutation) of the effect.

It has been suggested that the quantum fluctuations (or electromagnetic nature) of the electrons across the multitude of small superconductor grains, called Josephson junctions, in properly prepared sintered Type II, superconductors

** Lead by the NASA Glen Research Center

may produce a measurable force on the vacuum (i.e., space vacuum) that could counteract the acceleratory force of gravity.

The experiment that was proposed utilizes a commercially available torsion balance called a Cavendish balance, which is commonly used by physics students to measure the value of the gravitational constant. The extent of the experiment is not to measure the gravitational constant, but to measure the change in the dynamic angle induced on a torsion beam as a result of the attraction between the beam masses and external test masses (i.e., superconductor). In theory, the values of the calculated dynamic angles between two tests should be different if the masses are of different weight values. Assuming that the characteristics of the balance do not change between tests, the difference between the two dynamic angles can be used to correlate the mass change. Whereby, if a change is detected between a superconductor and an electro-magnetically radiated superconductor, one can deduce that there is a possibility that an interaction with the vacuum had occurred.

The research conducted here is but a first step in the possible application of a theory into an applicable engineering space drive model, which can then be used to design a purely massless propulsion system for interplanetary applications.

A successful or null test would however, not indicate the full benefit of the phenomena nor that it is truly a physical effect. Whereby, further testing would need to be conducted to validate the results and to devise the true nature and applicability to a space propulsion system.

BACKGROUND

A number of anomalous gravitational effects (or acceleratory forces) have been reported in the scientific literature during recent years, but there has been no independent confirmation with regard to any of these claims. One such experiments was reported by the Russian scientist, Eugene Podkletnov, in which he reported anomalous weight loss (0.05–2.1%) for a variety of test masses suspended above a rotating YBCO[#], type-II superconductor.[1,2] Further experiments using simplified apparatus without rotation have reported transients of up to 5% weight loss.[3,4] Still, a great deal of skepticism continues to be expressed, mainly due to uncertainties associated with experimental technique. Other researchers, for example, have yet to duplicate Podkletnov's rotating disk experiments and obtained null results in a set of simplified experiments using a stationary disk.[5]

The technical goal was then to critically test this revolutionary physical claim and provide a rigorous, independent, empirical confirmation (or refutation) of anomalous effects related to the manipulation of gravity by rf-pumped magnetized type-II superconductors. Because the current empirical evidence for gravity modification is anecdotal, our objective was to design, construct, and meticulously implement a discriminating experiment, which would put these observations on a more firm footing within the scientific community. Our approach is unique in that we advocate the construction of an extremely sensitive torsion balance with which to measure gravity modification effects by rf-pumped type-II superconductor test masses.

Three competing theoretical explanations have been proposed to explain these gravitational anomalies: (1) gravity shielding,[1,2] (2) absorption via coupling to a Bose condensate,[3,4] and (3) a gravito-magnetic force.[5-9, 18] To date, however, there has been no definitive corroboration between any of these theories and empirical observations. Therefore, it is clear that carefully designed and meticulously executed experiments are needed to explore these anomalies and to convincingly demonstrate the alleged effects. However, validation of a new theory is in itself a long and mischievous task. This is more so when you have to consider the nature of electrons at the atomic scale.

In light of the granular nature of a sintered YBCO superconductor disk, one can address the much larger grain interfaces in more macroscopic terms using electric-potentials, displacement currents, and magnetic fields. This is due to the Josephson junction effect at the interface, which is somewhat like an AC capacitor.

A search of the literature has produced several experiments using capacitors to interact with the vacuum to cause a force; 1) the Trouton and Noble (T-N) experiment[21], 2) the Biefield-Brown (B-B) experiment[10], 3) the Graham and Lahoz (Heaviside) experiment[20], and 4) the Woodward (Transient Mass) experiment[17].

ENGINEERING APPLICATION OF QUANTUM VACUUM

As aerospace engineers we deal more with the technology development of machines that have proven to work within the physical boundaries of known physical laws, which govern the rocket equations. Speculative theories can only lead to

[#] Yttrium, Barium, Copper, and Oxygen.

misunderstanding and lost paths. Therefore, space propulsive systems are designed to overcome gravitational forces by the application of time varying the mass of a vehicle, i.e., the exhausting of onboard mass at high velocities. What seems to be lost in this rational is that as the propellant becomes smaller with higher and higher exhaust velocities, as in the case of a laser or photon drive, the mass approaches a more quantum state. The logical next step would then be to connect propulsion to the quantum vacuum through acceleratory forces, i.e., gravity.

Long ago internationally renowned physicists hypothesized that gravity is an induced effect associated with zero point fluctuations (ZPF) of the quantum vacuum.[13-14] Zeldovich first suggested that gravitational interactions could lead to a small disturbance in the non-zero quantum fluctuations of the vacuum and thus give rise to a finite value of Einstein's cosmological constant.[13] Sakharov later derived a value for Newton's gravitational constant G using frequency ω as the only free parameter.[14]

$$G = c^5/h \int \omega d\omega \qquad (1)$$

where c is the speed of light and h is the Plank constant. The integral is carried out over all frequencies using the Plank frequency on observable electromagnetic phenomena ($\omega_p \sim 10^{-33}$ cm) as a cutoff value.

Using this hypothesis as a basis, Puthoff has further extended Sakharov's condition in a relativistically consistent manner.[15] As a result of this work, it is possible to envision the attractive force of gravity in terms of the radiative interaction between oscillating charges. That is, the zero point field applied to subatomic particles. From this standpoint, it is plausible that MHz frequency irradiation of superconductors rich in Josephson junction sites, as occurred in Podkletnov's experiments, could lead to a gravity modification effect through quantum ZPF interaction.

Scientific evidence continues to mount in favor of a frequency dependent interpretation of gravity as an induced effect associated with the zero point fluctuations of the vacuum. Accelerating theoretical progress combined with the anomalous gravity modification effects observed in experiments with irradiated Type II superconductors leads one to strongly suspect a deep physical connection.

THE PODKLETNOV EXPERIMENTS

Podkletnov's gravity modification experiments were conducted in the early 1990's. Nevertheless, skepticism persists, especially since the experiments have not been adequately documented and repeated. Podkletnov reports the use of fairly large superconductor disks, 10 and 12 inches in diameter and approximately ½ inches thick, which were magnetically levitated and magnetically rotated in the presence of an rf electromagnetic field. Samples placed over the rotating disk initially demonstrated a weight loss of 0.2–0.5%. When the rotation speed was slowly reduced, the shielding effect became considerably higher and reached a maximum reduction of 1.9–2.1%.

Of what is known of the YBCO superconductor disk used in these experiments, it seems certain that a large number of superconductor-oxide Josephson junctions exist within the disk. These types of Josephson junctions, when conversed by an ac current, emit electromagnetic waves in the rf frequency range, and when radiated at rf frequencies, generate an ac current. In a general sense, Josephson junctions are very small capacitors with the electrodes composed of superconductor material and the dielectric composed of an oxide layer.[12] The junction is modeled as shown in figure 1, where the superconductors (SC) are small sintered grains (noting that one or both of the grains could be a normal conductor), *rf* is the rf energy applied, JJ is the Josephson junction site, and i is the induced or applied current.

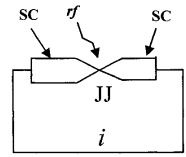

Figure 1. SC Josephson Junction Model.

A superconductor with a structure of sintered grains would have many flux pinning sites around which Josephson junction sites exist. Flux pinning is a well-known phenomenon associated with type-II superconductors (like YBCO) where magnetic flux penetrates the superconductor and is held in place by self-generated super-currents. Flux pinning results from any spatial inhomogeneity of the material, such as impurities, grain boundaries, voids, etc. where the magnetic flux can become trapped. To be most effective, these inhomogeneities must be on the scale of the order of the penetration depth or the coherence length, i.e. ~10.6 to 10.5 cm, rather than on the atomic scale where inhomogeneity causes electronic scattering which limits the mean free path.[12]

The Josephson junction sites at the grain boundaries would generally not produce flux pinning due to the resistive nature of the boundary. The exceptions might be under very high static magnetic field conditions. Radiation of the sites with rf energy would allow current flows, but could cause the flux to vibrate and jump from one site to another depending on the frequency.

Experiments conducted on both sintered and melt textured YBCO superconductors for the purpose of magnetic flux compression have shown that the rapidly moving flux with a millisecond rise time to approximately 1 kilogauss penetrates the superconductor with little (<35 gauss) compression of the field. [Ψ] This would indicate that a magnetic field could easily move through the body of a sintered superconductor to produce currents within the grain structure. Contradictory to this, it has also been shown during tests to repeat the Podkletnov experiment that an AC magnetic field will levitate a sintered (12 inch) disk.[++]

Podkletnov's experiment used both AC magnetic fields and rf energy. It would therefore seem that Podkletnov has produced a device to enhance the production of rf energy and rf energy to enhance the production of superconductor currents. These reinforcing phenomena should lead to high electron densities in the superconductor disk, focused at the Josephson junction sites and generated at the junction frequency.

It is then suggested here that the quantum fluctuations of the electrons across the multitude of Josephson junctions in properly prepared Type II, superconductors may produce a measurable force on the vacuum that could counteract the effect of gravity.

OTHER RELATED EXPERIMENTS

The capacitive like nature of the Josephson junction would make one wonder if other experiments have been conducted using capacitors to affect the vacuum. Research of the literature indicates that experiments using capacitors as a coupling mechanism to the quantum vacuum is not a new idea. In 1904, Trouton and Noble (T-N) reported that a mechanical force could be detected from a charged capacitor, which was free to rotate[21]. And in 1929, Townsend Brown reported translational motion using the now famous Biefield-Brown (B-B) effect, which utilizes capacitors with extremely high electrical potentials (>70 kV)[10]. To the author's knowledge, no one has report a successful duplication of the B-B experiment.[11] However in 1998, Cornille, Naudin, and Szames reported a successful duplication of the T-N experiment also using voltages near 70 kV.[22]

Trying to connect these two experiments to Podkletnov's experiment is somewhat deceptive as only statically charged capacitors with no magnetic fields were used. One could speculate that the leakage current across the dielectric medium could occur at some (low) frequency associate with the atomic electron energy states. Also, stray magnetic fields could have been present; at the least, the magnetic field of the earth was. From a more physical sense, the time varying magnetic fields in the Podkletnov experiment would have created time varying high electrical potentials in the superconductor.

In more recent times, Graham and Lahoz (in 1980) reported the use of a coaxial capacitor to produce rotational motion from the vacuum by setting up a non-vanishing Poynting vector, as Maxwell and Poynting foresaw and predicted by Heaviside's[**] time variation of Maxwell's equations.[20] Further, Woodward has recently done some very interesting work with capacitors, both theoretically and experimentally to validate the notion of a transient mass effect.[17] These two experiments do have similarity to the Josephson junction and a further clarification follows.

Heaviside Force

Oliver Heaviside in 1886 obtained an express from the divergence of the Maxwell stress tensor, which is a vector with units of force density (N/m^3), and therefore implies momentum transfer. Corum names this the Heaviside force f_H and gives it in vector form as

$$f_H = \frac{\partial(DxB)}{\partial t}, \qquad (2)$$

where D is the electric displacement and B is the magnetic induction[19].

Corum goes on to present a space-drive that was first presented in an essay by Joseph Slepian in 1949. In the essay, Slepian models the space-drive by employing an rf source to drive two solenoids and a parallel-plate capacitor electrically wired in series. The rf energy was directed between the plates and perpendicular to the electric field of the plates. In this arrangement, the current passing through the coils must also cross the capacitor. This is shown in figure 2.

[Ψ] Conducted by the first two authors.

[++] This work is being conducted under a NASA SBIR Phase II.

[**] Referred to as the Heaviside Force by Corum[19].

In the Slepian model, one may say that the current can only cross the capacitor in the presence of an rf field. This is the case for a superconductor Josephson junction. In fact, Slepian space-drive model is a crude approximation of a Josephson junction and is only a short stretch to the junction model of figure 1.

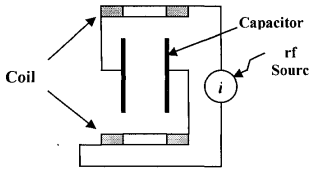

Figure 2. Slepian Space Drive Model.

Transient Mass Shifts

Woodward has come up with an equation for a transient mass shift (TMS) derived from Mach's Principle (Woodward, 1991). Woodward presented the transient mass shift ∂m_0 in general terms as:

$$\partial m_0 = \frac{\beta \omega P_0}{2\pi G \rho_0 c^2}, \qquad (3)$$

where ∂m_0 is the transient mass; β is the ratio ϕ / c^2 (ϕ is the gravitational potential due to all the matter of the universe) and is approximately 1 and unitless; ω is the frequency of the driving voltage into the capacitors in radians per second; P_0 is the power applied to the capacitors in Watts; G is the gravitational constant = 6.673 x 10-11 N m2/kg2; ρ_0 is the density of the capacitors; and c is the velocity of light = 2.9979 x 108 m/s.

A connection between Woodward's transient mass and Podkletnov's gravity modification experiment was presented in a previous paper.[16] In the paper, a model of the Josephson junction, transient mass relationship was given similar to figure 3.

As with figure 1, figure 3 presents a two-grain Josephson junction where one grain is a normal conductor NC and the other is superconductive SC. The current has been represented as a function $f(i)$ due to the uncertainty of this mechanism (i.e., time varying fields and rotation). The prospective is that electron charges e formed in the normal conductor. The application of the rf energy at the appropriate frequency allows the flow of electron to cross the junction as pairs $2e$. Noting the reverse effect is also possible.

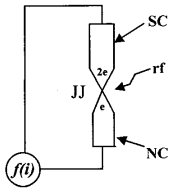

Figure 3. Josephson Junction TMS Model.

As cited in the previous paper, Woodward's TMS formula has commonality with Modanese's anomalous coupling theory (ACT)[3,4] and Woodward's capacitor experiment has commonality with the layered superconductor disk of Podkletnov's second experiment where the top part was a superconductor and the bottom portion a normal conductor. The TMS formula derives a mass fluctuation from a time-varying energy density. The ACT suggests that the essential ingredient for the gravity phenomenon is the presence of strong variations or fluctuations of the Cooper pair density (a time- varying energy density). Woodward's experiment used a small array of capacitors whose energy density was varied by an applied 11 kHz signal. When these are vibrated up and down at the correct frequency so that they are going up when their mass is minimum and going down when their mass is maximum, then a small, constant, mass-force change is possible. Podkletnov's superconductor disk contained many Josephson junctions, which were radiated with a 3-4 MHz signal. At the layered interface, the Cooper pairs are moving upward, while the electron pair separations are moving downward.

These commonalties allow for ease in rewriting the transient mass shift equation in terms of a superconductor mass shift ∂m_{sc} as

$$\partial m_{sc} = \frac{\beta f_{jj} P_{ij}}{G \rho_{sc} c^2}, \qquad (4)$$

where f_{jj} is the resonance frequency (in Hz) of the superconductor Josephson junctions, P_{jj} the effective combined power (in watts) of all the junctions, and ρ_{sc} is the density of the superconductor. Equation 4 then represents the mass change of the superconductor.

EXPERIMENTAL APPROACH

Repeating the original Podkletnov experiment has been a major undertaking within the Marshall Space Flight Center for several years. Confusion over

the original experimental design and the ability to produce the large superconductors have been the major problems. Given these problems a much simpler experimental approach was devised to investigate the possible gravity connection. This approach has not been without problems.

The approach involved the replacement of the large (~1 kg) lead masses in a commercially available computerized torsion or Cavendish balance with a system that magnetically modulates an YBCO superconductor. A sketch of the proposed experiment is given in figure 4.

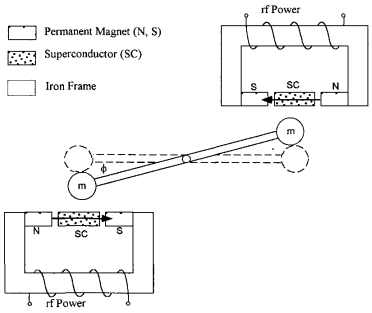

Figure 4. Sketch of the Cavendish balance experiment.

The measurement of the gravitation constant G (6.67×10^{-11} N·m^2/kg^2) using a Cavendish balance is a simple experiment, which is routinely performed by beginning physics students. Using Newton's universal law of gravitation, it is possible to express the angular displacement ϕ of the beam in terms of directly measurable quantities

$$\phi = \frac{2GMml}{R^2\kappa} \tag{5}$$

where M is the test mass, m is the mass attached to each end of the beam, l is the separation length of the beam mounted masses, R is the distance from the center of each test mass to the center of each beam mounted mass, and κ is the torsion constant of the fiber supporting the beam (not shown).

Corrections

The use of the Cavendish balance as supplied with the large lead masses requires several corrections. Such as a correction for the gravitational torque on the beam and the cross torque between the opposite masses. These corrections are easily approximated and are applied to the smaller masses. Other corrections such as the variations in R can be averaged out over many data points.

In this experiment, the spherical large lead masses are being replaced by a much larger mass that is more like a rectangular box. Such a shape makes the calculation of these corrections much more complicated without extensive testing. The simple solution is to look at the things that are measurable versus those that are not and see how these change from one condition to the other. Equation 5 is then rewritten as,

$$k_c\left(\frac{M}{R^2}\right) = \left(\frac{\kappa}{2Gml}\right)\phi \tag{6}$$

where k_c is the correction to m the small mass.

Equation 6 can then be used in the formulation of a percent mass change $M\%$ even though the left side of the equation is unknown. For example, a percent mass change $M\%$ between a non-modulated superconductor mass M_1 and a modulated superconductor mass M_2 is just the ratio of the angular displacements ϕ_1 and ϕ_2, given by

$$M\% = \frac{M_2}{M_1} = \frac{\phi_2}{\phi_1} \tag{7}$$

where the angular displacements are measurable.

Sensitivity

Equation 6 also is true for two different tests using two different mass weights. The change in the measured angular displacement of the torsion fiber will then be directly proportional to the change in the test mass. For example, the change in angular displacement $d\phi$ associated with an effective change in the test masses dM is given by

$$\frac{d\phi}{dM} = K_c G \tag{8}$$

The sensitivity of the device is therefore dependent on the magnitude of

$$K_c = \left(\frac{k_c}{R^2}\right)\frac{2ml}{\kappa}. \tag{9}$$

$$K_c = \left(\frac{1}{R^2}\right)\left(\frac{2T^2}{l\pi^2}\right) \tag{10}$$

which is independent of the smaller mass and any correction to it as long as the period T is measurable.

Based on the published characteristics of the as delivered Cavendish balance a numerical estimate for the sensitivity was determined to be

$$\frac{d\phi}{dM} = 0.3 \text{ microradians / gram} \tag{11}$$

for T = 120 sec, l = 30 cm, and R = 4.6 cm.

The commercially available Cavendish balance was chosen because it contained a computerized electronic detector known as a symmetric differential capacitive (SDC) control unit** to electronically measure the position of the beam as it rotates. The SDC is easily capable of measuring a displacement angle of 1 micro-radian. Therefore for a 0.5% weight change of a 300-gram superconductor, a displacement angle of 1.5 micro-radians would be detectable.

Testing has shown that the calculated displacement angle varies not with M but with M/R^2. This is due to the uneven mass density of the superconductor containment system or modulator that will be described later. That is, as the mass of the superconductor (or test mass) changes, the average density displacement of the modulator also changes, which in turn shifts the position of the modulators center of mass. This makes the determination of the percent mass change or equation 7 more difficult to determine. However, since we are only concerned at this point with seeing a change in the relationship between tests, the sensitivity to $1/R^2$ in equation 9 is a plus. In the general sense, the sensitivity as given in equation 11 is enhanced by the square of the difference in the shifted R values as a result of the test mass weight change.

Test Apparatus

In order to operate the balance in the hand-off operation inside a liquid nitrogen cyro-tank, the balance was fitted into a structure and the motion of the large masses was automated using a National Instruments, nuDrive (model 4SX-411) stepper motor controller and a National Instrument's rack (PXI-1010 Chassis) mounted computer (PXI-8156B) using Labview 5.1 software written specifically for this operation. The modified balance is shown in figure 5.

The large masses were replaced by a system, referred to as the modulator, which was required to modulate the superconductor sample with electromagnetic (EM) or rf energy. The modulator was composed of a superconductor, permanent magnets, an iron frame, a kHz coil, and an MHz antenna. Electrodes were placed adjacent to the superconductor to detect the hall current induced in the superconductor. A magnetic shield (1006 steel) was added due to an attraction problem with the balance's aluminum beam. A picture of the modified balance with the modulators is shown in figure 6 and a sketch of the modulator is shown in figure 7.

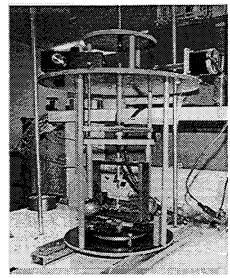

Figure 5. Automated Cavendish Balance.

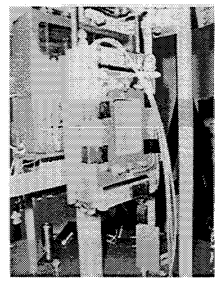

Figure 6. Modulator & Balance.

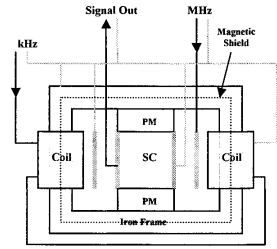

Figure 7. Sketch of Modulator.

The iron frame forms a magnetic circuit that directs the field through the superconductor and parallel to the balance's beam. The placement of the coil around the iron frame induces a time varying kHz field in the static field. The MHz antenna is placed near the coils also inducing a time varying field in the static field. The effect of these time varying fields

** The SDC is an invention of Dr. Randall Peters; Research Consultant.

were measured perpendicular to the static field.

The purpose of the static magnetic field produced by the permanent magnets was to induce currents in the superconductor about pinned flux sights and possibly the weaker holes about the grains, which would be much higher than that seen by the AC levitated superconductor in the Podkletnov experiment. The kHz modulation field would then act to break the pinning sites freeing the pinning currents to move according to the motion of the magnetic field in the superconductor material. In theory, the radiated MHz field reduces the resistance of the Josephson junction between the grain boundaries and to allow resistiveless passage of the currents throughout the superconductor.

The configuration of the superconductor then determines the mode of operation. That is, if the superconductor is composed entirely of sintered grains, the Heaviside force at the Josephson junction sights will dominate any gravity effect. On the other hand, if a non-superconducting, conductive layer is placed on the outward side of the sintered superconductor away from the balance; the electron motion across the boundary will produce a mass transit effect.

Instabilities

Several months were spent after the initial completion of the automated balance in determining and eliminating instabilities caused by the automation mechanism. The major mechanical problem was caused by the support apparatus, which would bend downward (ah gravity) as the modulator moved through the zero position. This allowed the spur gear to hit the support structure. Repositioning of the gear only made it hit other structures. The problem was fixed by grinding the top and bottom of the spur gear at an angle.

Placement of the drive motor also presented a problem. Due to the lack of support perpendicular to the balance beam, lead to the introduction of vibration. Placement of the motor such that the shaft rotation was in the plane of the modulator's motion and adding support structures provided a major reduction in the induced vibrations.

The deduction of these problems and the resulting fix thereof was hindered by the enclosure of the spur gear and the fact that some of the vibrations could only be detected by the analysis of the data. A data run was typically done overnight to allow the balance to stabilize. Three to five data cycles were typically required before stabilization occurred. One data cycle of about 35 minutes was required to get one dynamic angle measurement.

The only problem to arise during cooling in liquid nitrogen was with the electrical connections. Cooling below 170C caused intermittent signal disturbances. This was fixed by insulating the connections exposed to the liquid nitrogen temperatures.

TESTS RESULTS

Only one type of superconductor sample has been tested. It was composed of two layers; one of YBCO and one of PrBCO (Pr – Praseodymium). The substitution of Pr for Y was done to cause the layer to be a conductor with similar crystal structure to the YBCO. This sample was fabricated by the same manufacture producing the samples for the repeat of the Pokletnov experiment under a NASA SBIR phase II. Tests were conducted at room temperature and at liquid nitrogen (-196 C) temperature.

The YBCO superconductor only required < -180 C to become superconductive. The type K thermocouples used in the experiments flat lined between –186 C and –188 C in liquid nitrogen. Therefore to insure that the superconductor was in a superconductive state, tests were not conducted until a temperature < -186 C was optioned. The following graphs (figure 8 – 12) represent a data set using the same torsion wire. The numbers across the bottom (x – axis) of each chart refers to the number of cycles from which each dynamic angle was calculated. The sequence is in order of time from start to finish of a data run. Each dynamic angle (or cycle) depended on the period of the torsion beam, but typically was between 30 and 40 minutes. The voltage value on the left (y -axis) of each chart refers to the calculated dynamic angle. The values have been left in its voltage value because the conversion factor for the control unit was stable between tests.

The results of the superconductor tests are base lined against a copper (Cu) sample.

No-Modulation

The results of the room temperature and the liquid nitrogen (i.e., superconductive) tests for the non-modulated or static magnetic field cases are shown in figure 8 and figure 9, respectfully.

As seen in the room temperature tests of figure 8, the calculated dynamic angles between the varying weighted masses increased with decrease mass weight due to the non-uniform density of the modulator (i.e., $1/R^2$). Additional tests were conducted using other weights composed of fiberglass epoxy, aluminum, and lead, which showed the same result.

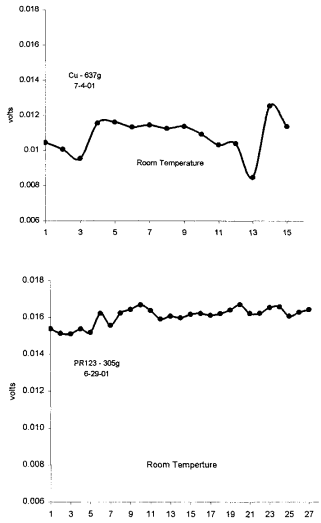

Figure 8: Dynamic Angle of copper sample (Cu) and superconductor sample (PR123) at room temperatures.

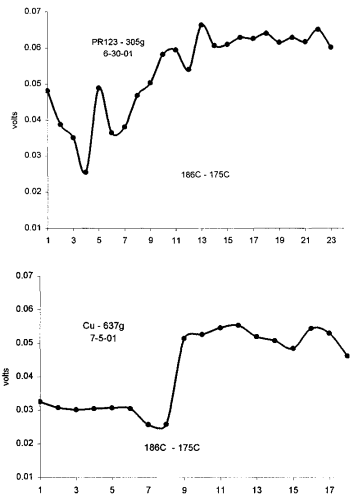

Figure 9: Dynamic Angle of copper sample (Cu) and superconductor sample (PR123) from superconductive temperatures to non-superconductive temperature.

In the liquid nitrogen tests of figure 9, the tests were started when the superconductor was at superconductive temperatures and allow to warm-up over night. As shown, at the non-superconductive temperature of – 175 C there is a noticeable change in the values of the dynamic angles. (Approximately 0.06 v for the superconductor sample and 0.05 for the copper sample.) Earlier tests down to –170 C with the original lead masses in the balance, also show good results in the calculation of the gravitational constant, which changed by less than 2% from the room temperature value.

Instabilities noted at the beginning of the liquid nitrogen test of the superconductor sample warranted a repeat at the lower temperature. This was conducted immediately following the first test as not to disturb the balance. Figure 10 shows the data from the repeated run.

Figures 9 and 10 then show that the superconductor and the copper samples produced similar results at the lower temperatures.

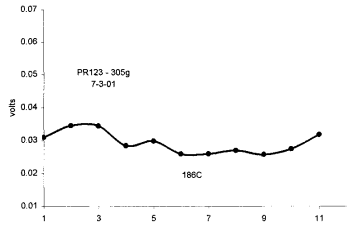

Figure 10: Dynamic Angle of the superconductor sample (PR123) at superconductive temperatures.

EM Modulation

EM modulation tests were conducted at room temperatures and at liquid nitrogen temperatures for only the superconductor. These tests are shown in figure 11 and figure 12. The room temperature tests of figure 11 shows the effect of the MHz and kHz frequencies separately. In the liquid nitrogen test shown in figure 12, both the MHz and KHz frequencies are used together.

In both cases, the calculated dynamic angle increased over time. In the liquid nitrogen tests, the first two data points are with no EM modulation. This was done to detect a change before the boil off of the liquid nitrogen due to the rf heating of the iron frame, which was partially submerged in the liquid nitrogen. Rapid boil off reduced the superconductive

run time from approximately six hours with no EM modulation down to two hours with EM modulation.

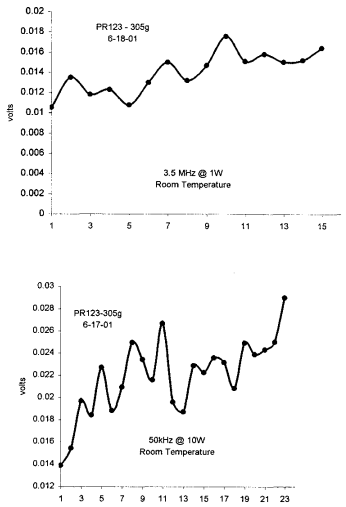

Figure 11: Dynamic Angle of the superconductor sample (PR123) at room temperatures with EM energy applied.

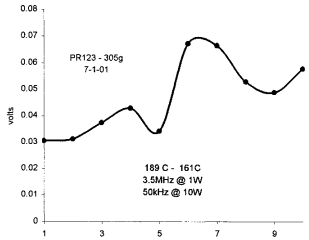

Figure 12: Dynamic Angle of the superconductor sample (PR123) at superconductive temperatures with EM energy applied.

CONCLUSIONS AND RECOMMENDATIONS

To summarize, we note that these exploratory experiments have been carried out in an attempt to quantify the effects of EM energy on a superconductor. The general conclusion is that the results of these tests gave a null result. That is, no conclusion at this time can be made to the EM effects on the superconductor. This conclusion is reached based on the increasing dynamic angle over time in both the room temperature and liquid nitrogen temperature tests.

Further, it is concluded that the balance is sensitive to mass changes at room temperature and down to approximately -175 C but not when the temperature is < -186. This conclusion was reached based on the similarities in the data for both the copper and superconductor samples in figure 9. However because no time varying temperature data was taken on these tests, further testing is required to pin point the actual shift point between –175 C and – 186 C.

If a temperature at which the superconductor becomes superconductive and within the sensitivity of the balance is determined, it is recommended that non-EM modulated tests on the masses reported here and on a non-layered superconductor be conducted. Regardless of the results, a redesign of the balance is recommended to eliminate the EM modulation effects on the balance control unit and to reduce the heating effect of the modulator.

REFERANCES

[1.] E. Podkletnov and R. Niemen, :"A Possibility of Gravitational Force Shielding by Bulk $YBa_2Cu_3O_{7-X}$ Superconductor," Physica C, Vol. 203, 1992, pp. 441 - 444.

[2.] E. E. Podkletnov, "Weak gravitation shielding properties of composite bulk $YBa_2Cu_3O_{7-x}$ superconductor below 70K under e.m. field," cond-mat/9701074 v3, 16 Sept. 1997.

[3.] G. Mandanese, *Europhys Lett.,* Vol. 35, 1996, p. 413; *Phys. Rev. D*, Vol. 54, 1996, p. 5002.

[4.] Modanese, Giovanni, "On the theoretical interpretation of E. Podkletnov's experiment," LANL gr-qc/9612022, Presented for the World Congress of the International Astronautical Federation, 1997, nr. IAA-97-4.1.07.

[5.] N. Li, D. Noever, T. Robertson, R. Koczor, and W. Brantley, "Static Test for a Gravitational Force Coupled to Type-II YBCO Superconductors," *Physica C*, Vol. 281, 1997, pp. 260-267.

[6.] N. Li and D. G. Torr, *Phys. Rev. D*, Vol. 43, 1990, p. 457.

[7.] N. Li and D. G. Torr, "Gravitational effects on the magnetic attenuation of superconductors," *Phys. Rev. B*, Vol. 46, 1992, p. 5489.

[8.] D. G. Torr and N. Li, "Gravito-Electric Coupling Via Superconductivity," *Found. Phys. Lett.,* Vol. 6, 1993, p. 371.

[9.] C. S. Unnikrishnan, "Does a superconductor shield gravity," *Physica C*, Vol. 266, 1996, pp. 371-383.

[10.] T. T. Brown, "How I control gravitation," *Science & Invention Magazine*, 1929.

[11.] R. L. Talley, "Twenty-First Century Propulsion Concept", Phillips Laboratory (Propulsion Directorate), Air Force Systems Command, Final Report No. PL-TR-91-3009, Project 3058, 1991.

[12.] M. Tinkham and G. McKay, *Introduction to Superconductivity*, McGraw-Hill, Inc., 1996.

[13.] Ya. B. Zeldovich, *JETP Letters*, Vol. 6, 1967. p. 345.

[14.] A. Sakharov, "Vacuum quantum fluctuations in curved space and the theory of gravitation, *Sov. Phys. Doklady*, Vol. 12, 1968, pp. 1040-1041.

[15.] H. E. Puthoff, "Gravity as a zero-point-fluctuation force," *Physical Review A*, Vol. 39, No. 5, pp. 2333-2342, 1989.

[16.] Glen A. Robertson, "Search for a Correlation Between Josephson Junctions and Gravity," Space Technology and Applications International Forum - 2000, pp. 1026-1031.

[17.] J. F. Woodward, "Mach's Principle of Weight Reduction = Propellantless Propulsion," *Foundation of Physics Letters*, Vol. 9, No. 3, 1996, pg. 247 – 293.

[18.] Agop, A., C. Gh. Buzea, and P. Nica, "Local Gravitoelectromagnetic Effects on a Superconductor," Physica C, 339, pp. 120-128, 2000.

[19.] Corum, James F., John P. Dering, Philip Pesavento, and Alexana Donne, ""EM Stress-Tensor Space Drive," "Space Technology and Applications International Forum 1999," American Institute of Physics, AIP Conference Proceedings 458. (The papers on BPP topics are in pages 875-937 and 954-1059.)

[20.] G. M Graham and D. G. Lahoz, "Observation of static electromagnetic angular momentum *in vacuo*," Nature Vol. 285, pg 154-155, May 1980.

[21.] F. T. Trouton and H. R. Noble, "The mechanical forces acting on a charged condenser moving through space," Philosophical Transactions of the Royal Society of London, 202A, 1904, pp. 165-181.

[22.] Patrick Cornille, Jean-Louis Naudin, and Alexandre Szames, "Stimulated Forces Demonstrated: Why the Trouton-Noble Experiment Failed and How to Make it Succeed," Space Technology and Applications International Forum – 1999, pp. 1005-1013.

Hindawi Publishing Corporation
Advances in High Energy Physics
Volume 2012, Article ID 752613, 10 pages
doi:10.1155/2012/752613

Research Article

The Other Side of Gravity and Geometry: Antigravity and Anticurvature

M. I. Wanas[1, 2, 3]

[1] *Astronomy Department, Faculty of Science, Cairo University, Giza 12613, Egypt*
[2] *Center for Theoretical Physics (CTP), The British University in Egypt (BUE), El Sherouk City 11837, Egypt*
[3] *Egyptian Relativity Group (ERG), Cairo University, Giza, Egypt*

Correspondence should be addressed to M. I. Wanas, mamdouh.wanas@bue.edu.eg

Received 8 July 2012; Accepted 20 August 2012

Academic Editor: Joseph Formaggio

Gravity is one of the four known fundamental interactions used to study and interpret physical phenomenae. It governs diverse phenomenae, especially those connected with large-scale structures. From more than one decade, existing gravity theories have suffered from some problems, when confronting their predictions with the results of some experiments and observations. This situation has led to many suggestions, none of which is final, so far. Here, we show that the assumption of existence of another side of gravity, a repulsive gravity or antigravity, together with its attractive side, may give a satisfactory solution to gravity problems. We caught here two pieces of evidence for the existence of antigravity in nature. The first is on the laboratory scale, the COW experiment, and the second is on the cosmic scale, SN type Ia observation. On the other hand, we show how gravity theories can predict antigravity, using a new defined geometric object called Parameterized anticurvature. This shows clearly how Einstein's geometrization philosophy can solve recent gravity problems in a satisfactory and easy way. Also, it may throw some light on the mystery of physical nature of "Dark Energy."

1. Introduction

Nowadays, it is well known that most of the phenomenae in the Universe can be interpreted successfully using one or more of the following interactions:

(1) *gravity;*

(2) *electromagnetism;*

(3) *weak force;*

(4) *strong force.*

Although gravity is the most popular among the above-mentioned interactions, one can say that we are now living in an electromagnetic civilization. Most of the tools and equipments of modern civilization depend on electromagnetism. This is mainly due to our deep understanding of the electromagnetic interaction compared with other interactions. However, there are some pieces of evidence forcing one to claim that ancient civilization has been a gravitational one. Among these pieces of evidence, a "null one," that is, the ignorance of mankind, in that civilization, of any interaction but gravity. Unfortunately, there are no documents found, so far, supporting the above-mentioned claim.

In contrast to other interactions, gravity is the long-range force that cannot be shielded. It affects many, if not all, processes, activities, and phenomenae, starting from biological processes within biological systems, passing through human activities (e.g., lifting liquids, flights, rockets, etc.), ending with the stability of large-scale systems (e.g., atmosphere of the Earth and planets, solar system, stars, galaxies, and the Universe itself). A better understanding of gravity would certainly give a signal for the beginning of a new era of civilization.

Gravity, as we experience on the Earth's surface and in the solar and similar systems, is associated with an attraction force. Theoretical physicists take this "*fact*" into consideration when constructing gravity theories. Newton has succeeded to quantify this attractive force using his law of universal gravity. Einstein, in the context of his theory of General Relativity (GR), has interpreted gravity as a geometric property, *space-time curvature*. It has been shown that, using Einstein's point of view, one can interpret more physical phenomenae than using Newton's one.

Although GR is the most acceptable theory for gravity, so far, it suffers from several problems, especially those connected with recent observations. None of the existing theories of gravity, including GR, can interpret the results of the following observations, for instance

(1) supernova type Ia observation [1];

(2) the rotation velocities of stars in spiral galaxies [2];

(3) pioneer 10, 11 velocity observation, "*Pioneer Anomaly*" [3];

(4) the mass discrepancy in clusters of galaxies [4].

Such observations indicate that our understanding of gravity is not complete enough. It seems that there is something missing in the theories describing gravity. Such theories should be modified or replaced by others, that take into account the *missing factors*, if any. Many authors have tried to tackle such problems, suggesting different solutions. The most famous candidate used is "*Dark Energy*" (cf. [5–8]), an exotic term implying the existence of an unknown force, most likely repulsive.

Assuming that *attraction* is one side of gravity and *repulsion* is its other side, many of the recent gravity problems can be analyzed, understood, and solved. This paper discusses briefly some experimental and observational pieces of evidence, also theoretical predictions, for the existence of the other side of gravity, the *repulsive* side. This may illuminate the road towards a more satisfactory theory for gravity and a better understanding of this interaction. Pieces of evidences for attractive gravity are popular and do not need any sophisticated equipments to discover. In contrast, lines of evidence for *repulsive* gravity are not so obvious and need sophisticated technology to be explored. In what follows, we are going to discuss, briefly, two of these lines of evidence. The first evidence is on the very large scale, the cosmic scale, while the second evidence is on the laboratory scale.

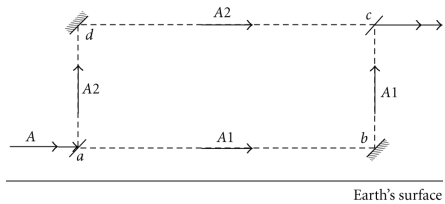

Figure 1: COW Neutron Interferometer.

2. Observational and Experimental Evidence for Repulsive Gravity

The first evidence emerged from the analysis of the results of Supernovae type Ia observation [1]. These observations need space telescopes and equipments and would not have been carried out without the use of such sophisticated space technology. The objects associated with this type of Supernovae are considered to be standard candles, which can be used to measure long distances in the Universe with high accuracy. On the other hand, radial velocities of such objects can be easily obtained as a result of measurements of their red shifts. Knowing distances and velocities, one can get the rate of expansion of our Universe, using Hubble's relation. It has been shown [1] that the Universe is in a phase, with an accelerating expansion rate. This result is in contradiction with all accepted theories of gravity, including GR (with vanishing cosmological constant). The increasing rate of expansion indicates very clearly that there is a large scale *repulsive force* driving the expansion of the Universe.

The second evidence comes from a sophisticated experiment which has been suggested and carried out from more than three decades ago, in an Earth's laboratory. This experiment is known in the literature as the "COW" experiment. It has been suggested by Colella, Overhauser, and Werner in 1974 and carried out many times starting from 1975 to 1997 [9–13]. The results of this experiment indicate clearly that there is a real discrepancy with existing theories. Before discussing this discrepancy, we give a simple account on the experiment.

The experiment studies quantum interference of thermal neutrons moving in the Earth's gravitational field. A neutron interferometer is used for this purpose (see Figure 1). A beam of thermal neutrons A is split into two beams $A1$, $A2$ at the point a. The beam $A1$ is reflected at b, while $A2$ is reflected at d. The two reflected beams $A1$ and $A2$ interfere at the point c of the interferometer.

Assuming that the path lengths $ab = dc$, $ad = bc$ and that the trajectory of the neutrons is affected by the Earth's gravitational potential, a phase difference between the two beams $A1$ and $A2$ is expected. This is due to the difference in the Earth's gravitational potential affecting the paths ab and dc, (since ab is more close to the Earth's surface than dc). Using the interference pattern, one can measure the phase difference, and consequently the difference in the Earth's gravitational potential.

The theories used for calculating the phase shift have been quantum mechanics and Newton's theory of gravitation (The Earth's gravitational field is a weak field. Newton's theory of gravitation is a limiting case of GR in the weak field regime. So both theories will give about the same prediction) . It has been found that the experimental results are lower than theoretical predictions by eight parts in one thousand (0.008), while the sensitivity of

the interferometer used is one part in one thousand (0.001). Consequently, there is a real discrepancy between the results of this experiment and theoretical predictions [9].

Now, the results of this experiment show clearly that the Earth gravitational potential measured is different from that predicted by Newton theory of gravity (or by GR), even in the weak field regime. The absolute value (measured) of this potential is less than the corresponding value predicted by known theories of gravity! One probable interpretation is that there is a *repulsive force* reducing the value of the potential, predicted by theories that take into consideration attraction only.

The above two lines of evidence give a probable indication that there is a *repulsive force* affecting trajectories of particles, whether long range (photons in the cosmos) or short range (neutrons in the laboratory). Now, we have two possible approaches for interpreting the above evidence. The first is that they can be considered as indicators for the existence of a new interaction, fifth force, different from those given in the introduction. The second is that one, or more, of the four known interactions is not well understood. The first possibility has been extensively examined (cf. [14, 15]). So, let us examine the second one. Weak and strong interactions can be easily ruled out, since they are of very short range (the order of one Fermi). Also, the electromagnetic interaction can be excluded since the two pieces of evidence considered concern trajectories of electrically neutral particles (photons or neutrons). Thus, we are left with the gravitational interaction only. Deep examination of this interaction may lead to a better understanding of gravity.

If we assume that gravity has two sides as mentioned above. The first is the side that is well known on the Earth's surface and in the solar and similar systems, the side connected with *attraction*. The second is the side connected with *repulsion* which is not so obvious in the solar system. Then, two important questions emerge as follows.

(i) What geometric object (Assuming the geometrization philosophy (very successful in dealing with gravity) is being applied) is responsible for repulsion?

(ii) Why repulsion is so small, compared with attraction, in some systems while it is relativity large in others?

In what follows we are going to discuss two theoretical (geometric) features predicting, very naturally, the existence of repulsive gravity. This will give possible answers to the above-mentioned questions and, consequently, a convincing theoretical interpretation for accelerating expansion of the Universe and for the discrepancy in the COW experiment.

3. Geometric Predictions of Repulsive Gravity

In the last decade, many attempts have been done suggesting new theories, or modifying the existing theories, of gravity in order to account for the accelerating expansion of the Universe and the repulsive force driving it. These attempts can be classified into two classes: physical and geometrical. The physical class includes suggestions about the existence of types of peculiar matter, having certain equations of state, filling the Universe (e.g., Chapling gas [16], phantom [17], etc.). The geometrical class comprises geometric suggestions to solve the problem (e.g., increasing the number of space-time dimensions [18], increasing the order of the curvature scalar R in the lagrangian, $f(R)$ theories [19], the use of geometries with non-vanishing torsion [20], the increase of order of torsion (T) in the lagrangian, $f(T)$ theories [21], etc.). None of the above-mentioned attempts could explain, satisfactorily, the repulsive features of gravity. If one of these attempts is accepted as an interpretation for accelerating

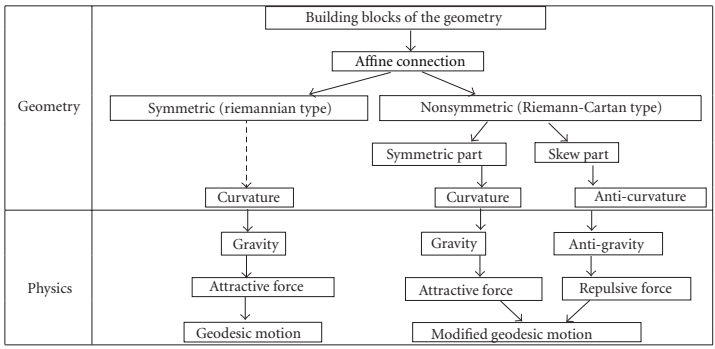

Figure 2: Geometrization of physics using geometries of Riemann and of Riemann-Cartan type.

expansion of the Universe, it cannot account for the discrepancy of the COW experiment, discussed above.

In what follows we are going to give a brief account on an attempt, belonging to the geometric class, that can give a convincing interpretation for both large-scale and laboratory scale problems as those given in the above Section. This attempt also gives *two* geometric properties for the existence of *repulsive* gravity, and convincing answers to the two questions, raised at the end of Section 2.

Before reviewing the attempt, we are going to give a brief idea, as simple as possible, about the underlying geometry of this attempt. The geometric structure used is called the "Parameterized Absolute Parallelism" (PAP) geometry [22]. In 4-dimensions, the structure of a PAP space is defined completely by a tetrad vector field. The general linear connection characterizing this space is written as (we are using starred symbol, to characterize an object belonging to the PAP-geometry, while the same symbol, unstarred, is used for AP objects ($b = 1$))

$$\overset{*}{\Gamma}{}^{\alpha}_{\cdot\,\beta\sigma} = \left\{ \begin{matrix} \alpha \\ \beta\sigma \end{matrix} \right\} + b\Upsilon^{\alpha}_{\cdot\,\beta\sigma}, \tag{3.1}$$

where $\left\{ \begin{matrix} \alpha \\ \beta\sigma \end{matrix} \right\}$ is the ordinary Christoffel symbol of the Riemannian space (used to construct GR), $\Upsilon^{\alpha}_{\cdot\,\beta\sigma}$ is a third order nonsymmetric tensor, called contortion, defined in the PAP-space, and b is a dimensionless parameter whose importance will be discussed later. An important feature of the PAP-space is that it is more general than both Riemannian and conventional Absolute Parallelism (AP) spaces in the sense that

(i) for $b = 0$ the PAP-space covers all the Riemannian structure, without any need for a vanishing contortion;

(ii) for $b = 1$ the PAP-space reduces to the conventional AP space.

Among other things, these features facilitate comparison between a theory constructed in the PAP-space and the results of any other theory constructed in the AP space or in the Riemannian one, including GR.

The antisymmetric part of the parameterized linear connection (3.1) is called the torsion $\overset{*}{\Lambda}{}^{\alpha}_{\cdot\,\beta\sigma}$ of the connection:

$$\overset{*}{\Lambda}{}^{\alpha}_{\cdot\,\beta\sigma} = b\Lambda^{\alpha}_{\cdot\,\beta\sigma}, \tag{3.2}$$

where $\Lambda^{\alpha}_{\cdot\,\beta\sigma}$ is the torsion of the AP space. The PAP curvature tensor is defined by the fourth order tensor [20] given by

$$\overset{*}{B}{}^{\alpha}{}_{\mu\nu\sigma} \overset{\text{def.}}{=} R^{\alpha}_{\mu\nu\sigma} + b\,\overset{*}{Q}{}^{\alpha}_{\mu\nu\sigma} \neq 0, \tag{3.3}$$

where

$$R^{\alpha}_{\mu\nu\sigma} \overset{\text{def.}}{=} \left\{ \begin{matrix} \alpha \\ \mu\sigma \end{matrix} \right\}_{,\nu} - \left\{ \begin{matrix} \alpha \\ \mu\nu \end{matrix} \right\}_{,\sigma} + \left\{ \begin{matrix} \alpha \\ \epsilon\nu \end{matrix} \right\} \left\{ \begin{matrix} \epsilon \\ \mu\sigma \end{matrix} \right\} - \left\{ \begin{matrix} \alpha \\ \epsilon\sigma \end{matrix} \right\} \left\{ \begin{matrix} \epsilon \\ \mu\nu \end{matrix} \right\} \tag{3.4}$$

is the Riemann-Christoffel curvature tensor and

$$\overset{*}{Q}{}^{\alpha}_{\cdot\,\mu\nu\sigma} \overset{\text{def.}}{=} \underset{+\,-|\,\nu}{\Upsilon^{\alpha}_{\cdot\,\mu\,\sigma}} - \Upsilon^{\alpha}_{\cdot\,\mu\nu|^{\sigma}_{+}} + b\left[\Upsilon^{\epsilon}_{\cdot\,\mu\nu}\Upsilon^{\alpha}_{\cdot\,\epsilon\sigma} - \Upsilon^{\epsilon}_{\cdot\,\mu\sigma}\Upsilon^{\alpha}_{\cdot\,\epsilon\nu}\right], \tag{3.5}$$

is a tensor of type $(1,3)$, purely made of $\Upsilon^{\alpha}_{\cdot\,\beta\sigma}$.

The curvature (3.3) is, in general, nonvanishing. Consequently, the PAP-space is of the Riemann-Cartan type, that is having simultaneously non-vanishing torsion (3.2) and curvature (3.3).

Now, the two geometric properties predicting the existence of antigravity, and consequent repulsive force, are given below.

(1) Since the PAP geometry covers, at least the domains of both Riemannian and AP-geometries as limiting cases, we are going to use the advantages and properties of these two limiting cases to discuss relation (3.3). The tensor $R^{\alpha}_{\cdot\,\beta\sigma\delta}$, in Riemannian geometry, measures the curvature of the space, that is, the deviation of the space from being flat. It is completely made of Christoffel symbols. Its vanishing is a necessary and sufficient condition for the space to be flat. Einstein's idea has been to use this tensor as a measure of the gravitational field of the system.

Let us now examine the curvature in the case of the AP space. It can be written, using (3.3) with $b = 1$, as

$$B^{\alpha}_{\cdot\,\beta\sigma\delta} = R^{\alpha}_{\cdot\,\beta\sigma\delta} + Q^{\alpha}_{\cdot\,\beta\sigma\delta} \equiv 0, \tag{3.6}$$

where $Q^{\alpha}_{\cdot\,\beta\sigma\delta}$ is the limiting case of $\overset{*}{Q}{}^{\alpha}_{\cdot\,\beta\sigma\delta}$ for $b = 1$. It is to be considered that neither $R^{\alpha}_{\cdot\,\beta\sigma\delta}$ nor $Q^{\alpha}_{\cdot\,\beta\sigma\delta}$ vanishes, while their sum, that is, the curvature $B^{\alpha}_{\cdot\,\beta\sigma\delta}$ of the AP space, vanishes identically. This implies an interesting property, that is, the non-vanishing tensors $R^{\alpha}_{\cdot\,\beta\sigma\delta}$ and $Q^{\alpha}_{\cdot\,\beta\sigma\delta}$ compensate (balance) each other in such a way that the total curvature of the space is zero. This compensation gives rise to the flatness of the AP space. Now, as $R^{\alpha}_{\cdot\,\beta\sigma\delta}$ measures

the curvature of the space, $Q^{\alpha}_{\cdot\,\beta\sigma\delta}$ represents the additive inverse of this curvature. For this reason, we call $Q^{\alpha}_{\cdot\,\beta\sigma\delta}$ the "*anticurvature*" tensor [23], and consequently the tensor defined by (3.5) is the "*parameterized anticurvature*" tensor.

An interesting physical result can now be obtained. Einstein has used curvature $R^{\alpha}_{\cdot\,\beta\sigma\delta}$ as a geometric object representing gravity, in his theory of GR. Similarly, we can use the *anticurvature* $Q^{\alpha}_{\cdot\,\beta\sigma\delta}$ as a geometric object representing *antigravity*, in any suggested theory. But, the complete balance between $R^{\alpha}_{\cdot\,\beta\sigma\delta}$ and $Q^{\alpha}_{\cdot\,\beta\sigma\delta}$ gives rise to a flat space, that is, balance of the two (basic features) sides of gravity. Observationally, this is not the case, at least in the solar and similar systems, in which gravity dominates over antigravity, that is, curvature dominates over anticurvature. Thus, one needs a certain parameter, to be adjusted, in order to fine tune the ratio between the curvature and anticurvature in any theory dealing with both sides of gravity. This is ready and clarifies the importance of the parameter b, which appears in (3.5), in the PAP-geometry. The presence of this parameter in (3.3) makes the PAP-curvature non-vanishing (in general $b \neq 1$).

This represents the first geometric feature which shows how antigravity can be predicted in the context of the geometrization philosophy. It gives the first geometric feature predicting the existence of *antigravity*, on theoretical basis.

(2) In the context of the geometrization philosophy, path equations in any appropriate geometry are used to represent trajectories of test particles. For example, the geodesic equation, of Riemannian geometry, is used as equation of motion of a test particle (e.g., planet) in the solar system, in the context of GR. Now, for the PAP-geometry, the path equation can be written in the following form [20]:

$$\frac{d^2x^{\mu}}{d\tau^2} + \left\{ \begin{matrix} \mu \\ \alpha\beta \end{matrix} \right\} \frac{dx^{\alpha}}{d\tau}\frac{dx^{\beta}}{d\tau} = -b\Lambda^{\cdot\cdot\,\mu}_{(\alpha\beta)\cdot}\frac{dx^{\alpha}}{d\tau}\frac{dx^{\beta}}{d\tau}, \tag{3.7}$$

where τ is the parameter characterizing the path. If $b = 0$, (3.7) reduces to the ordinary geodesic of Riemannian geometry. Equation (3.7) can be considered as a geodesic equation modified by a torsion term. For any field theory written in the PAP-geometry, (3.7) can be used as an equation of motion of a neutral test particle moving in the field, in the domain of this theory.

In order to understand (3.7), physically, let us analyze it using Newton's terminology. The first term of (3.7) can be considered as the generalized acceleration of a test particle. The other two terms can be viewed as representing two forces driving the motion of this test particle. On one hand, the first force is related to the Christoffel symbols $\left\{ \begin{matrix} \alpha \\ \beta\sigma \end{matrix} \right\}$, which is the only geometric object forming the curvature $R^{\alpha}_{\cdot\,\beta\sigma\delta}$. This force is the gravity force, since it is connected with the curvature of the space time. On the other hand, the second force is connected with the torsion (or contortion (There are some relations between torsion and contortion [24] in such a way that the vanishing of one is a necessary and sufficient condition for the vanishing of the other. So, in principle, any function of the contortion can be easily written in terms of the torsion and vice versa.)) of space-time. Since the contortion (or torsion) is the only ingredient forming the anticurvature $Q^{\alpha}_{\cdot\,\beta\sigma\delta}$, then by similarity, we can call this force the "*antigravity force*". So, this equation can be written in the following block equation:

$$\text{Acceleration} + \text{Gravity force} = \text{Antigravity force}. \tag{3.8}$$

Consequently, a complete balance between gravity and antigravity forces would result in the vanishing of acceleration.

In order to explore the quantitative nature of these two forces, let us examine the consequences of linearizing (3.7). It has been shown [25] that the potential ϕ resulting from the existence of the two forces (two sides of gravity) is given by

$$\phi = \phi_N - b\phi_N. \tag{3.9}$$

The first term, on the R.H.S., is the Newtonian potential due to gravity and the second term is the potential due to antigravity, written in terms of ϕ_N, for simplicity. Recalling the classical relation between potential and force, and knowing that $b \geq 0$ appear in due course as will, then we can easily conclude that as gravity force is attractive, antigravity force is necessarily repulsive (due to the negative sign on the R.H.S. of (3.9)).

Now, we come to the dimensionless parameter b of (3.7). As stated above, the function of this parameter is to adjust a certain ratio between *gravity* and *antigravity* (i.e., between attraction and repulsion) in a certain system. This parameter can be decomposed as follows [23]:

$$b = \frac{n}{2}\alpha\gamma = \frac{\text{antigravity}}{\text{gravity}}, \tag{3.10}$$

where n is a natural number taking the values $0, 1, 2, \ldots$ for particles with quantum spin $0, 1/2, 1, \ldots$, respectively; α is the fine structure constant (~1/137) and γ is a dimensionless parameter depending on the size of the system under consideration, to be fixed by experiment or observation. The vanishing of b switches off antigravity in any system and reduces any suggested theory, constructed in the PAP-geometry, to a conventional gravity theory (e.g., orthodox GR). Also, in this case (3.7) reduces to the geodesic equation, in which attraction is the only force affecting the trajectory of any test particle.

The discussion given above represents the second geometric feature which shows the quantity and quality of the repulsive force predicted in the context of the geometrization philosophy.

From the discussion given in (1) and (2), one can outlines the main features of a geometric theory predicting and dealing with the two sides of gravity. Applying such theory, a satisfactory interpretation can be achieved to the discrepancy in the COW experiment [26] and for the accelerating expansion of the Universe [27]. The values of the parameter γ are found to be of order unity for the Earth's system and which more greater than unity for the Universe.

For the two questions raised at the end of the previous Section, we have now the following answers.

(1) For the first question: *the geometric object responsible for repulsion is the anticurvature tensor* (3.5) *(or the torsion tensor) of the background geometry characterizing the field.*

(2) For the second question: *the strength of the repulsive force depends on the value of the parameter γ which characterizes the size of the system under consideration.*

4. Concluding Remarks

(1) Two main philosophies are used in the 20th century, to solve the emerged physical problems, *quantization* and *geometrization*.

(2) Gravity problems are successfully solved using the geometrization philosophy, not the quantization one.

(3) The two main objects characterizing any geometry are curvature and torsion (giving rise to anticurvature).

(4) Einstein has used the curvature in constructing the theory of General Relativity, solving the problems of attractive gravity in the Solar and comparative systems, in the context of the geometrization philosophy.

(5) Some experiments and recent observations give strong evidence for the existence of repulsive gravity together with the attractive one.

(6) In the present paper it is shown that using both *curvature* and *the parameterized anticurvature*, one can account for both sides of gravity, attraction and repulsion, and consequently give a satisfactory interpretation for accelerating expansion of the Universe and the discrepancy of COW experiment.

(7) The modified geodesic equation (3.7), in its linearized form, shows clearly that the force resulting from the torsion term (R.H.S. of (3.7)) is a repulsive force (see (3.9)).

The schematic diagram shown in Figure 2 summarizes the advantages of using a complete geometry, that is, a geometry with simultaneously non-vanishing curvature and torsion, in constructing field theories for gravity. The left-hand branch of this diagram gives the geometrization scheme to be used to construct GR (attractive gravity only). The right-hand branch gives a geometrization scheme to be used to construct a theory for both sides of gravity.

References

[1] J. L. Tonry, B. P. Schmidt, B. Barris et al., "Cosmological results from high-z supernovae," *Astrophysical Journal Letters*, vol. 594, no. 1 I, pp. 1–24, 2003.

[2] E. Battaner and E. Florido, "The rotation curve of spiral galaxies and its cosmological implications," *Fundamentals of Cosmic Physics*, vol. 21, pp. 1–154, 2000.

[3] S. G. Turyshev and V. T. Toth, "The pioneer anomaly," *Living Reviews in Relativity*, vol. 13, no. 4, pp. 9–175, 2010.

[4] P. Salucci, A. Lapi, C. Tonini, G. Gentile, I. Yegorova, and U. Klein, "The universal rotation curve of spiral galaxies—II. The dark matter distribution out to the virial radius," *Monthly Notices of the Royal Astronomical Society*, vol. 378, p. 41, 2007.

[5] A. F. Heavens, T. D. Kitching, and L. Verde, "On model selection forecasting, dark energy and modified gravity," *Monthly Notices of the Royal Astronomical Society*, vol. 380, no. 3, pp. 1029–1035, 2007.

[6] L. M. Krauss, K. Jones-Smith, and D. Huterer, "Dark energy, a cosmological constant, and type la supernovae," *New Journal of Physics*, vol. 9, article no. 141, 2007.

[7] J. S. Alcaniz, "Dark energy and some alternatives: a brief overview," *Brazilian Journal of Physics*, vol. 36, no. 4 A, pp. 1109–1117, 2006.

[8] C. Marinoni and A. Buzzi, "A geometric measure of dark energy with pairs of galaxies," *Nature*, vol. 468, no. 7323, pp. 539–541, 2010.

[9] R. Colella, A. W. Overhauser, and S. A. Werner, "Observation of gravitationally induced quantum interference," *Physical Review Letters*, vol. 34, no. 23, pp. 1472–1474, 1975.

[10] J. L. Staudenmann, S. A. Werner, R. Colella, and A. W. Overhauser, "Gravity and inertia in quantum mechanics," *Physical Review A*, vol. 21, no. 5, pp. 1419–1438, 1980.
[11] S. A. Werner, H. Kaiser, M. Arif, and R. Clothier, "Neutron interference induced by gravity: new results and interpretations," *Physica B+C*, vol. 151, no. 1-2, pp. 22–35, 1988.
[12] M. Arif, M. S. Dewey, G. L. Greene, D. Jacobson, and S. Werner, "X-ray determination of the elastic deformation of a perfect crystal neutron interferometer: implications for gravitational phase shift experiments," *Physics Letters A*, vol. 184, no. 2, pp. 154–158, 1994.
[13] K. C. Littrell, B. E. Allman, and S. A. Werner, "Two-wavelength-difference measurement of gravitationally induced quantum interference phases," *Physical Review A*, vol. 56, no. 3, pp. 1767–1780, 1997.
[14] E. Fischbach and C. Talmadge, "Six years of the fifth force," *Nature*, vol. 356, no. 6366, pp. 207–215, 1992.
[15] J. Bovy and G. R. Farrar, "Connection between a possible fifth force and the direct detection of dark matter," *Physical Review Letters*, vol. 102, no. 10, Article ID 101301, 2009.
[16] N. Bili, G. B. Tupper, and R. D. Viollier, "Unification of dark matter and dark energy: the inhomogeneous Chaplygin gas," vol. 535, no. 1-4, pp. 17–21, 2002.
[17] J. Cepa, "Constraints on the cosmic equation of state: age conflict versus phantom energy Age-redshift relations in an accelerated universe," *Astronomy and Astrophysics*, vol. 422, no. 3, pp. 831–839, 2004.
[18] C. P. Burgess, "Supersymmetric large extra dimensions and the cosmological constant: an update," *Annals of Physics*, vol. 313, no. 2, pp. 383–401, 2004.
[19] A. De Felice and S. Tsujikawa, "f(R) theories," *Living Reviews in Relativity*, vol. 13, p. 3, 2010.
[20] M. I. Wanas, "Absolute parallelism geometry: developments, applications and problems," *Studii Si Cercetari Stiintifice. Seria Matematica*, no. 10, pp. 297–309, 2001.
[21] R. Myrzakulov, "Accelerating universe from *F(T)* gravity," *European Physical Journal C*, vol. 71, no. 9, pp. 1–8, 2011.
[22] M. I. Wanas, "Parameterized absolute parallelism: a geometry for physical applications," *Turkish Journal of Physics*, vol. 24, no. 3, pp. 473–488, 2000.
[23] M. I. Wanas, "The geometric origin of dark energy," in *Proceedings of the 4th International Workshop on The Dark Side of the Universe (DSU'08)*, vol. 115, pp. 218–223, AIP, Cairo, Egypt, June 2008.
[24] K. Hayashi and T. Shirafuji, "New general relativity," *Physical Review D*, vol. 19, no. 12, pp. 3524–3553, 1979.
[25] M. I. Wanas, "Motion of spinning particles in gravitational fields," *Astrophysics and Space Science*, vol. 258, no. 1-2, pp. 237–248, 1998.
[26] M. I. Wanas, M. Melek, and M. E. Kahil, "Quantum interference of thermal neutrons and spin-torsion interaction," *Gravitation and Cosmology*, vol. 6, pp. 319–322, 2000.
[27] M. I. Wanas, "The accelerating expansion of the universe and torsion energy," *International Journal of Modern Physics A*, vol. 22, no. 31, pp. 5709–5716, 2007.

Impulse Gravity Generator Based on Charged $YBa_2Cu_3O_{7-y}$ Superconductor with Composite Crystal Structure

Evgeny Podkletnov[1], Giovanni Modanese[2]

[1] *Moscow Chemical Scientific Research Centre*
113452 Moscow - Russia
E-mail: epodkletnov@hotmail.com

[2] *California Institute for Physics and Astrophysics*
366 Cambridge Ave., Palo Alto, CA 94306
and
University of Bolzano – Industrial Engineering
Via Sernesi 1, 39100 Bolzano, Italy
E-mail: giovanni.modanese@unibz.it

Abstract

The detection of apparent anomalous forces in the vicinity of high-T_c superconductors under non equilibrium conditions has stimulated an experimental research in which the operating parameters of the experiment have been pushed to values higher than those employed in previous attempts. The results confirm the existence of an unexpected physical interaction. An apparatus has been constructed and tested in which the superconductor is subjected to peak currents in excess of 10^4 A, surface potentials in excess of 1 MV, trapped magnetic field up to 1 T, and temperature down to 40 K. In order to produce the required currents a high voltage discharge technique has been employed. Discharges originating from a superconducting ceramic electrode are accompanied by the emission of radiation which propagates in a focused beam without noticeable attenuation through different materials and exerts a short repulsive force on small movable objects along the propagation axis. Within the measurement error (5 to 7 %) the impulse is proportional to the mass of the objects and independent on their composition. It therefore resembles a gravitational impulse. The observed phenomenon appears to be absolutely new and unprecedented in the literature. It cannot be understood in the framework of general relativity. A theory is proposed which combines a quantum gravity approach with anomalous vacuum fluctuations.

Contents

1 Introduction

Experiments showing possible anomalous forces between high-T_c ceramic superconductors under non equilibrium conditions and test objects have been reported by several investigators since 1992 [1, 2, 3, 4, 5]. The observed phenomenology was difficult to explain and has been attributed to a so called "gravity modification", because the reported effects mimic well the properties of the gravitational interaction, although their nature has never been clearly understood. In fact several alternative explanations of these results have been proposed [6, 7, 8, 9, 42] in the attempt to bring the observed anomalies into the realm of known effects.

Because of the great importance of any possible technical application of the reported effects, research activities have started in many laboratories since the first observation of the phenomenon [1]. Our recent research work focused on the improvement of the structure of the high-T_c ceramic superconductors which have demonstrated capabilities of creating anomalous forces. Moreover a high-voltage discharge apparatus has been designed and constructed in order to easily reach those non equilibrium electromagnetic conditions that seem required to produce the force effects in HTCs.

The results described in this report should be regarded as preliminary. An improved version of the experiment is currently being planned. Nevertheless, the body of results, as well as the complexity of the experimental procedures and of the theoretical interpretation are such that a detailed description and diffusion could not be further delayed. All measurements were done by E. Podkletnov in Moscow, while G. Modanese provided theoretical advice.

2 Experimental

2.1 General description of the installation

The initial variant of the experimental set-up was based on a high-voltage generator placed in a closed cylinder chamber with a controlled gas atmosphere, as shown in Fig. 1. Two metal spheres inside the chamber were supported by hollow ceramic insulators and had electrical connections that allowed to organize a discharge between them, with voltage

up to 500 kV. One of the spheres had a thin superconducting coating of $YBa_2Cu_3O_{7-y}$ obtained by plasma spraying using a "Plasmatech 3000S" installation. This sphere could be charged to high voltage using a high voltage generator similar to that of Van de Graaf. The second sphere could be moved along the axis of the chamber, the distance between the spheres varying from 250 to 2000 mm. Spheres with a diameter from 250 to 500 mm were used in the experiment. It was possible to fill the chamber with helium vapours or to create rough vacuum using a rotary pump. The walls of the chamber were made of non-conducting plastic composite material, with a big quartz glass window along one of the walls which allowed to observe the shape, the trajectory and the colour of the discharge. In order to protect the environment and the computer network from static electricity and powerful electromagnetic pulses, the chamber could be shielded by a Faraday cage with cell dimensions of 2.0×2.0 cm and a rubber-plastic film material absorbing ultra high frequency (UHF) radiation.

The superconducting sphere was kept at a temperature between 40 and 80 K, which was achieved by injecting liquid helium or liquid nitrogen through a quartz tube inside the volume of the superconducting sphere before the charging began. The inside volume of the chamber was evacuated or filled with helium in order to avoid the condensation of moisture and different gases on the superconducting sphere. The temperature of the superconductor was measured using a standard thermocouple for low temperature measurements and was typically around 55-60 K. Given the good heat conductivity of the superconductor, we estimated that the temperature difference in the ceramic did not exceed 1 K.

An improved variant of the discharge chamber is shown in Fig. 2. The charged electrode was changed to a toroid attached to a metal plate and a superconducting emitter which had the shape of a disk with round corners. The non-superconducting part of the emitter was fixed to a metal plate using metal Indium or Wood's metal, the superconducting part of the emitter faced the opposite electrode. The second electrode was a metal toroid of smaller diameter, connected to a target. The target was a metal disk with the diameter of 100 mm and the height of 15 mm. The target was attached to a metal plate welded to the toroid.

This improved design of the generator was able to create a well-formed discharge between the emitter and the target, still the trajectory was not always repeatable and it was difficult to maintain constant values of current and voltage. The chamber was also not rigid enough to obtain high vacuum and some moisture was condensing on the emitter, damaging the superconducting material and affecting the discharge characteristics. The large distance between the electrodes also caused considerable dissipation of energy during discharge. In order to improve the efficiency of operation, the measuring system and the reproducibility of the discharge, an entirely new design of the vacuum chamber and the charging system was created.

The final variant of the discharge chamber is presented in Fig. 3 (the apparatus is shown in a vertical position though actually it is situated parallel to the floor). This set-up allowed to reduce the dimensions of the installation and to increase the efficiency of the process. The chamber has the form of a cylinder with the approximate diameter of 1 m and the length of 1.5 m and is made of quartz glass. The chamber has two connecting sections with flanges which allow to change the emitter easily. The design permits to

create high vacuum inside or to fill the whole volume with any gas that is required. The distance of the discharge has been decreased considerably giving the possibility to reduce energy dissipation and to organize the discharge in a better way. The distance between the electrodes can vary from 0.15 to 0.40 m in order to find the optimum length for each type of the emitter.

The discharge can be concentrated on a smaller target area using a big solenoid with the diameter of 1.05 m that is wound around the chamber using copper wire with the diameter of 0.5 cm. The magnetic flux density is 0.9 T. A small solenoid is also wound around the emitter (Fig. 3) so that the magnetic field can be frozen inside a superconductor when it is cooled down below the critical temperature.

The refrigeration system for the superconducting emitter provides a sufficient amount of liquid nitrogen or liquid helium for the long-term operation and the losses of gas due to evaporation are minimized because of the high vacuum inside the chamber and thus of a better thermal insulation.

A photodiode is placed on the transparent wall of the chamber and is connected to an oscilloscope, in order to provide information on the light parameters of the discharge. Given the low pressure and the high applied voltage, emission of X-rays from the metallic electrode cannot be excluded, but the short duration of the discharge makes their detection difficult. Use of a Geiger counter and of X-rays sensitive photographic plates did not yield any clear signature of X-rays.

A precise measurement of the voltage of the discharge is achieved using a capacitive sensor that is connected to an oscilloscope with a memory option as shown in the upper part of Fig. 3. Electrical current measurements are carried out using a Rogowski belt, which is a single loop of a coaxial cable placed around the target electrode and connected to the oscilloscope.

The old fashioned Van de Graaf generator used in the previous stage of this work was replaced by a high voltage pulse generator as shown in Fig. 4. This pulse generator is executed according to the scheme of Arkadjev-Marx and consists of twenty capacitors (25 nF each) connected in parallel and charged to a voltage up to 50-100 kV using a high voltage transformer and a diode bridge. The capacitors are separated by resistive elements of about 100 $k\Omega$. The scheme allows to charge the capacitors up to the needed voltage and then to change the connection from a parallel to a serial one. The required voltage is achieved by changing the length of the air gap between the contact spheres C and D. A syncro pulse is then sent to the contacts C and D which causes an overall discharge and serial connection of the capacitors and provides a powerful impulse up to 2 MV which is sent to the discharge chamber. The use of such an impulse generator allows for a precisely controlled voltage, much shorter charging time and good reproducibility of the process.

2.2 Superconducting emitter, fabrication methods

The superconducting emitter has the shape of a disk with the diameter of 80-120 mm and the thickness of 7-15 mm. This disk consists of two layers: a superconducting layer with chemical composition $YBa_2Cu_3O_{7-y}$ (containing small amounts of Ce and Ag) and

a normal conducting layer with chemical composition $Y_{1-x}Re_xBa_2Cu_3O_{7-y}$, where Re represents Ce, Pr, Sm, Pm, Tb or other rare earth elements. The materials of both layers were synthesized using a solid state reaction under low oxygen pressure (stage 1), then the powder was subjected to a melt texture growth (MTG) procedure (stage 2). Dense material after MTG was crushed, ground and put through sieves in order to separate the particles with the required size. A bi-layered disk was prepared by powder compaction in a stainless steel die and sintering using seeded oxygen controlled melt texture growth (OCMTG) (stage 3). For the emitters with the diameter of 120 mm usual sintering was applied instead of seeded OCMTG (stage 4). After mechanical treatment the ceramic emitter was attached to the surface of the cooling tank in the discharge chamber using Indium based alloy.

Stage 1 - Micron-size powders of Y_2O_3 and CuO, $BaCO_3$ were mixed in alcohol for 2 hours, then dried and put in zirconia boats in a tube furnace for heat treatment. The mixture of powders was heated to 830 ^oC and kept at this temperature for 8 hours at oxygen partial pressure of $2.7 \cdot 10^2$ Pa (or 2-4 $mBar$) according to [10, 11]. The material of the normal conducting layer was sintered in a similar way.

Stage 2 - Micron-size powder of $YBa_2Cu_3O_x$ was pressed into pellets using a metal die and low pressure. The pellets were heated in air to 1050 ^oC (100 ^oC per hour) then cooled to 1010 ^oC (10 ^oC per hour) then cooled to 960 ^oC (2 ^oC per hour) then cooled to room temperature (100 ^oC per hour) according to a standard MTG technique [12, 13]. The quantity of 211 phase during heating was considerably reduced and the temperature was changed correspondingly. $ReBa_2Cu_3O_{7-x}$ was also prepared using MTG, but the temperature was slightly changed according to the properties of the corresponding rare earth oxide.

Stage 3 - Bulk material after MTG processing was crushed and ground in a ball mill. The particles with the size less than 30 μm were used for both layers of the ceramic disk. The particles were mixed with polyvinyl alcohol binder. The material of the first layer was put into a die, flattened and then the material of the second layer was placed over it. The disk was formed using a pressure of 50 MPa. The single crystal seeds of $Sm123$ (about 1 mm^3) were placed on the surface of the bi-layered disk so that the distance between them was about 15 mm and the disk was subjected to a OCMTG treatment in 1% oxygen atmosphere. The growth kinetics of YBCO superconductor were controlled during isothermal melt texturing. A modified melt texturing process was applied, where instead of slow cooling following melting, isothermal hold was employed in the temperature range where the growth is isotropic. By this modification, the time required to texture the disk was reduced to 7 hours which is about 10 times faster than a typical slow cooling melt texturing process. The crystallization depth was controlled by applying the corresponding temperature and time parameters. Cubic $Sm123$ seeds were obtained using the nucleation and growth procedure as described in [16, 17]. A thin layer of the material was removed from the top surface of the disk to a depth of 0.3 mm and the edges of the upper surface were rounded using diamond tools.

Stage 4 - For the emitters with the diameter of 120 mm it is technically difficult to apply seeded MTG method, therefore normal sintering was carried out. Bulk material after MTG processing (after stage 2) was crushed and sieved and the following size particles

were used for both layers of the ceramic disk, the amount is given in weight percent:

500-400 μm	50-60%
120-60 μm	25-35%
< 20 μm	15-25%

The particles were mixed according to the ratio listed above using polyvinyl alcohol as a binder. The material of the first layer was put into a die, flattened and the material of the second layer was placed over it. The disk was formed using the pressure of 120 MPa and sintered in oxygen at 930 ^oC for 12 hours followed by slow cooling down to room temperature. The edges of the upper surface were rounded using diamond tools.

X-ray diffraction, transition temperature, electrical conductivity and critical current density were measured for both layers of various emitters using standard techniques.

2.3 Organization of the discharge and measurements of the effect.

The discharge chamber is evacuated to 1.0 Pa using first a rotary pump and then a cryogenic pump. When this level of vacuum is reached, liquid nitrogen is pumped into a tank inside the chamber that contacts the superconducting emitter. Simultaneously a current is sent to the solenoid that is wound around the emitter, in order to create a magnetic flux inside the superconducting ceramic disk. When the temperature of the disk falls below the transition temperature (usually 90 K) the solenoid is switched off. The experiment can be carried out at liquid nitrogen temperatures or at liquid helium temperatures. If low temperatures are required, the tank is filled with liquid helium and in that case the temperature of the emitter reaches 40-50 K.

The high voltage pulse generator is switched on and the capacitors are charged to the required voltage. It takes about 120 s to charge the capacitors. A syncro pulse is sent to a pair of small metal spheres marked as C and D in Fig. 5. A discharge with voltage up to 2 MV occurs between the emitter and the target. Half a second before the discharge, a short pulse of direct current is sent for 1 s to the big solenoid that is wound around the chamber, in order to concentrate the discharge and to direct it to the same area on the target electrode. This pulse lasts for only 1 s not to cause the overheating of the big solenoid.

The effects are measured along the projection of the axis line which connects the center of the emitter with the center of the target. Laser pointers were used to define the projection of the axis line and impulse sensitive devices were situated at the distance of 6 m and 150 m from the installation (in another building across the area).

Normal pendulums were used to measure the pulses of gravity radiation coming from the emitter. The pendulums consisted of spheres of different materials hanging on cotton strings inside glass cylinders under vacuum. One end of the string was fixed to the upper cap of the cylinder, the other one was connected to a sphere. The spheres had typically a diameter from 10 to 25 mm and had a small pointer in the bottom part. A ruler was placed in the bottom part of the cylinder, 2 mm lower than the pointer. The deflection

was observed visually using a ruler inside the cylinder (Fig. 5). The length of the string was typically 800 mm, though we also used a string 500 mm long. Various materials were used as spheres in the pendulum: metal, glass, ceramics, wood, rubber, plastic. The tests were carried out when the installation was covered with a Faraday cage and UHF radiation absorbing material and also without them. The installation was separated from the impulse measuring devices situated 6 m away by a brick wall of 0.3 m thickness and a list of steel with the dimensions 1 $m \times 1.2$ $m \times 0.025$ m. The measuring systems that were situated 150 m away were additionally shielded by a brick wall of 0.8 m thickness.

In order to define some other characteristics of the gravity impulse - in particular its frequency spectrum - a condenser microphone was placed along the impact line just after the glass cylinders. The microphone was connected to a computer and placed in a plastic spherical box filled with porous rubber. The microphone was first oriented with a membrane facing the direction of the discharge, then it was turned 22.5 degrees to the left, then 45 degrees to the left, then 67.5 degrees and finally 90 degrees. Several discharges were recorded in all these positions at equal discharge voltage.

3 Results

Several unexpected phenomena were observed during the experiments. The discharge in the installation corresponding to the initial set-up (Fig. 1) at room temperature in the voltage range from 100 kV to 450 kV was similar to a discharge with non-coated metal spheres and consisted of a single spark between the closest points on the spheres. When the superconductor coated sphere was cooled down below the transition temperature, the shape of the discharge changed in such a way that it did not form a direct spark between two spheres, but the sparks appeared from many points on the superconducting sphere and then moved to the corresponding electrode. When the voltage was over 500 kV the discharge at the initial stage had a tendency to cause some glow with the shape of a hemisphere. This glow separated from the sphere and then broke into multiple sparks which combined into more narrow bundle and finally hit the surface of the target electrode.

Repeated discharges at high voltages caused damage to the superconducting coating and partial separation of the ceramic material from the metal sphere, as the refrigeration system was not efficient enough. Also the direction of the discharge was not always repeatable. The experiments were continued with the improved variant of the installation as shown in Fig. 2 and then with the final variant of the installation as shown in Fig. 3. This new configuration allowed to increase the reproducibility of the discharge and the superconducting emitter was not damaged with high voltage. With voltage lower than 400 kV the discharge had the shape of a spark but when the voltage was increased to 500 kV the front of the moving discharge became flat with diameter corresponding to that of the emitter. This flat glowing discharge separated from the emitter and moved to the target electrode with great speed. The whole time of the discharge as defined by the photo diode was between 10^{-5} and 10^{-4} s. The peak value of the current at the discharge for the maximum voltage ($2 \cdot 10^6$ V) is of the order of 10^4 A.

It was found that high voltages discharges organized through the superconducting

Table 1: Emitter N. 2. Influence of high voltage discharges on the deflection of the pendulum. Experimental data are the average of 12 measurements. The standard deviation of the single data is between 5 and 7 %.

Voltage (kV)	Δl (mm)	Δh (mm)	Estimated ΔE ($J \cdot 10^{-4}$)
500	56.5	2.0	3.6
750	91.3	5.2	9.5
1000	110.4	7.7	13.9
1250	123.0	9.5	17.3
1500	131.6	10.9	19.8
1750	137.6	11.9	21.7
2000	142.0	12.7	23.1

emitter kept at the temperature of 50-70 K were accompanied by a very short pulse of radiation coming from the superconductor and propagating along the axis line connecting the center of the emitter and the center of the target electrode in the same direction as the discharge. The radiation appeared to penetrate through different bodies without any noticeable loss of energy. It acted on small interposed mobile objects like a repulsive force field, with a force proportional to the mass of the objects. As the properties of this radiation are similar to the properties of the gravity force, the observed phenomenon was called a gravity impulse.

In order to investigate the interaction of this gravity impulse with various materials, several tests were carried out, with pendulums and microphones, as described in the experimental part. The deflection of the pendulum was observed visually (see Fig. 5) and the corresponding Δl value was measured as a function of the discharge voltage. The correlation between the discharge voltage and the corresponding deflection of the pendulum as measured for two different emitters is listed in Tables 1, 2. Each value of Δl that is given in the table represents the average figure calculated from 12 discharges. A rubber sphere with a weight of 18.5 grams was used as material of the pendulum for the data listed in Tables 1, 2. The deflection caused an alteration in the potential energy of the pendulum which was proportional to Δh as shown in the table. A graphic illustration of this dependence for two different emitters is given in Fig. 6.

Both emitters, N. 1 and N. 2, were manufactured using the same OCMTG technology, but the thickness of the superconducting layer was equal to 4 mm for the emitter N. 1 and 8 mm for the emitter N. 2. Emitter N. 2 could be magnetized to a much higher value. The thickness of the normal conducting layer has a smaller influence on the force of the gravity impulse, but for better results the thickness should be bigger than 5 mm.

It was found that the force of the impact on pendulums made of different materials does not depend on the material but is only proportional to the mass of the sample. Pendulums of different mass demonstrated equal deflection at constant voltage. This was proved by a large number of measurements using spherical samples of different mass and

Table 2: Same for Emitter N. 1.

Voltage (kV)	Δl (mm)	Δh (mm)	Estimated ΔE ($J \cdot 10^{-4}$)
500	40.0	1.0	1.8
750	70.9	3.2	5.7
1000	85.3	4.6	8.3
1250	94.6	5.6	10.2
1500	100.8	6.4	11.6
1750	104.7	6.9	12.5
2000	107.1	7.2	13.1

diameter. The range of the employed test masses was between 10 and 50 grams. It was also found that there exist certain deviations in the force of the gravity impulse within the area of the projection of the emitter. These deviations (up to 12-15% max) were found to be connected with the inhomogenities of the emitter material and various imperfections of the crystals of the ceramic superconductor, and with the thickness of the interface between superconducting and normal conducting layers.

Measurements of the impulse taken at close distance (3-6 m) from the installation and at the distance of 150 m gave identical results, within the experimental errors. As these two points of measurements were separated by a thick brick wall and by air, it is possible to admit that the gravity impulse was not absorbed by the media, or the losses were negligible.

The force "beam" obtained with the latest experimental set-up does not appear to diverge and its borders are clear-cut. However, considerable efforts were necessary in order to concentrate the radiation and reach a good reproducibility. As mentioned above, the direction emission always coincides with the direction of the discharge. In the initial experiments (with the Van den Graaf generator), the direction of the beam varied, depending on the direction of the discharge, as the sparks moved to different points on the superconducting sphere. Later it was found that the magnetic field created by the solenoid wound around the chamber is able to concentrate the discharge and to direct it to the same area on the superconducting electrode.

The bi-layered emitters used in this experiment were mainly of two types. The first one was obtained after Stage 3 and had a structure typical for multiple-domain levitators with well crystallized and oriented grains of the superconducting layer. The second type was made by the material obtained after Stage 4 and consisted of densely packed non oriented polycrystalline structure in both layers. The superconducting layer in both types of emitters consisted of $YBa_2Cu_3O_{7-y}$ orthorhombic superconductor with lattice parameters $a = 3.89\mathring{A}$, $b = 11.69\mathring{A}$, $c = 3.82\mathring{A}$. The addition of small amounts of CeO_2 led to an improvement in the magnetic flux pinning properties of the Y123 compound. The emitter obtained by seeded MTG process had a superconducting layer with a maximum trapped field of 0.5 T at 77 K and a critical current density in excess of $5 \cdot 10^4$ A/cm^2. The transition temperature varied from 87 to 90 K with a transition width of about 2 degrees. The normal conducting layer had crystal lattice parameters close to those of the super-

conductor: $a = 3.88\mathring{A}$, $b = 11.79\mathring{A}$, $c = 3.82\mathring{A}$. Both layers demonstrated high electrical conductivity (over 1.5 Sm) at room temperature and the $Y_{1-x}Re_xBa_2Cu_3O_{7-y}$ layer was a normal conductor above 20 K.

In general the emitters obtained by seeded OCMTG were much more efficient than the sintered bi-layered emitters and allowed to obtain a much stronger radiation impulse, contained by the projection of the emitter. The sintered bi-layered emitters had much lower values of the trapped magnetic field and this yielded bigger energy dissipation and a weaker gravity impulse. The only advantage of the sintered emitters is that a weak impulse effect is always present, probably because the diffusion between the layers is limited. The emitters with oriented crystal structure (after seeded MTG) can be easily spoiled if the interface thickness between the two layers reaches a certain value, therefore the temperature and time parameters should be monitored carefully in order to limit the interaction between the two layers. It was found that the seeded crystal growth should be stopped before it reaches the interface region.

It was also found that the gravity impulse was to some extent proportional to the magnetic field inside the superconductor, which was created using a small solenoid during cooling down to liquid nitrogen temperature. Therefore, at recent stages of the experiment the solenoid was replaced by a powerful permanent NdFeB magnet (50 MOe) with a diameter corresponding to the diameter of the emitter and a thickness of 20 mm. This disk-shaped magnet was attached with one surface to the cooling tank and with another surface to the ceramic emitter.

The response recorded by the microphone has the typical behavior of an ideal pulse filtered by the impulse response of a physical low pass system with a bandwidth of about 16 kHz, attributed to the microphone (Fig. 7). In spite of the filtering, the relative energy of the pulses can be measured as a function of the angle of the normal to the diaphragm respect to the axis of propagation of the force.

Relative pulse amplitude with energies averaged over four pulses per angle are shown in Fig. 8 and are in agreement with a possible manifestation of a vector force acting directly on the membrane. No signal has been detected outside the impact region.

4 Discussion

(a) Capacitance of the emitter. Current at the discharge.

High voltage discharges like those described in Sections 2, 3 are well known in the literature. They do not require pre-ionisation, provided the electric field between the electrodes is sufficient to cause avalanche ionisation. However, the presence of a superconducting electrode causes some difference in the form and colour of the crown and of the sparkle, with respect to discharges between normal electrodes.

We recall that for the maximum voltage ($2 \cdot 10^6$ V) the peak value of the current is of the order of 10^4 A, and the duration of the discharge varies between 10^{-5} and 10^{-4} s. This implies a total negative charge Q on the emitter, just before the discharge, up to 0.1 C. The associated electrostatic energy is $U = QV/2 \sim 10^5$ J.

If the emitter was made of a normal conductor, its capacitance could be at most $10^{-10}\ F$ (for an estimate one can consider the capacitance of a sphere, namely $C \sim 10^{-10} \cdot R$ in SI units, where R is the radius). The above value for Q implies a much higher effective capacitance, of the order of $10^{-7}\ F$.

During the discharge an intense super-current flows from the superconducting electrode towards the ionised gas. After the superconducting charge carriers leave the negative electrode, pairs are broken and electrons are captured by the helium ions which are striking the electrode. We thus have a peculiar kind of superconductor-normal junction. Another junction is that between the superconducting emitter and the normal metallic plate.

From the theoretical point of view, these junctions can be described by Ginzburg-Landau models without specific reference to the microscopic theory. A typical time scale for the time-dependent Ginzburg-Landau equation in YBCO is of the order of $10^{-8}\ s$ [42], much smaller than the discharge time. This suggests that a quasi-stationary approximation could be adequate. The situation is however complicated by the following circumstances:

(1) In anisotropic materials like HTCs the Ginzburg-Landau equation involves an order parameter with non-trivial symmetry and the pairs are thought to possess intrinsic angular momentum.

(2) The transport current is very intense. In type-II superconductors, transport currents are associated to non-reversible displacement of flux lines, and this effect in turn depends strongly on the pinning properties of the material.

(3) The emitter is subjected to a strong external magnetic field during the discharge.

More efforts are therefore necessary, both on the experimental and theoretical side, for a complete understanding of the state of the superconducting emitter during the discharge.

(b) Evidence of the gravitational-like nature of the effect.

The gravitational-like nature of the effect is best demonstrated by its independence on the mass and composition of the targets (see Section 3). We are aware, of course, that gravitational interactions of this kind are absolutely unusual (see Sections 4.1, 4.3). For this reason, several details of the experimental apparatus were designed with the explicit purpose of reducing spurious effects like mechanical and acoustic vibrations much below the magnitude order of the observed anomalous forces.

Indirect evidence for a gravitational effect comes from the fact that any kind of electromagnetic shielding is ineffective. Note that if one can explain in some way the anomalous generation of a gravitational field in the superconductor, its undisturbed propagation follows as a well-known property of gravity (see Section 4.2). Indirect support for the gravitational hypothesis also comes from the partial similarity of this apparatus to that employed by Podkletnov for the stationary weak gravitational shielding experiment [1].

If the effect is truly gravitational, then the acceleration of any test body on which the impulse acts should be in principle independent on the mass of the body. Suppose that l is the length of a detection pendulum and g is the local gravitational acceleration. Let d be the half-amplitude of the oscillation. Let t be the duration of the impulse, and F its strength. F has the dimensions of an acceleration (m/s^2) and can be compared with g.

One easily computes that the product of the strength of the impulse by its duration is

$$Ft = \sqrt{2gl[1 - \sqrt{1 - (d/l)^2}]} \tag{1}$$

If $d \ll l$, this formula can be simplified, and we have approximately $Ft \sim \sqrt{(g/l)}d = 2\pi d/T$, where T is the period of the pendulum. With the data of Table 1, taking $t = 10^{-4}$ s, one finds $F \sim 10^3 g$.

Here, however, we encounter a conceptual difficulty. Suppose to place on the trajectory of the beam a very massive pendulum (say, 10^3 Kg). If the effect is gravitational, then the acceleration of a test mass should not depend on its mass. However, it is clear that in order to give this mass the same oscillation amplitude of the small masses employed in the experiment, a huge energy amount is necessary, which cannot be provided by the device. Therefore the effect would seem to violate the equivalence principle. Considering the back-reaction is probably necessary, namely the fact that the test mass exerts a reaction on the source of the impulse. This reaction is negligible as long as we use small test masses.

(c) Anomalous features of the observed "radiation".

Independently from any interpretation, the abnormal character of this radiation appears immediately clear. It appears to propagate through walls and metal plates without noticeable absorption, but this is not due to a weak coupling with matter, because the radiation acts with significant strength on the test masses free to move. Furthermore, this radiation conveys an impulse which is certainly not related to the carried energy by the usual dispersion relation $E = p/c$. A corresponding energy transfer to the test masses is not in fact observed (unless one admits perfect reflection, which seems however very unlikely).

The denomination "radiation" is actually unsuitable, and one could possibly envisage an unknown quasi-static force field. In this way one could explain why an impulse is transmitted to the test masses. However, it is hard to understand how such a field could be so well focused.

4.1 A possible theoretical explanation. Basic concepts.

The following Sections contain an informal introduction to a theoretical model originally developed by one of the authors [18, 19, 20, 21, 22] in order to explain the weak gravitational shielding effect by HTC superconductors [1, 2]. We suggest that this theory may be a starting point for the explanation of the impulsive gravitational-like forces described in the present paper.

The quantum properties of the gravitational field play an essential role in this model. These properties are not adequately known yet, therefore the proposed model is still in a preliminary development phase and its predictive capabilities are quite limited. Its primary merit is to envisage a new dynamic mechanism which could account for the effect. However, a full theory which justifies the model does not exist so far. This should be, in fact, a theory of the interaction between gravity (including its quantum aspects), and a particular state of matter - that of a HTC superconductor - which in turn is not completely known.

The glossary below [1] collects some keywords and their equivalent, also for a better orientation in the cited works.

(a) Weakness of the standard coupling with gravity. Anomalous coupling.

The standard coupling of matter to gravity is obtained from the Einstein equations by including the material part of the system into the energy-impulse tensor. Since the coupling constant is G/c^4, very large amounts of matter/energy, or at least large densities, are always necessary in order to obtain gravitational effects of some importance. This holds also at the quantum level, in weak field approximation. It is possible to quantize the gravitational field by introducing quantum fluctuations with respect to a classical background, and then calculate the graviton emission probabilities associated to transitions in atomic systems. These always turn out to be extremely small, still because of the weakness of the coupling.

What we proved in our cited works is that a peculiar "anomalous" coupling mechanism exists, between gravity and matter in a macroscopic quantum state. In this state matter is described by a collective wave function. Also in this state the energy-impulse of matter couples to the gravitational field in the standard way prescribed by the equivalence principle. However, the new idea is that besides this standard coupling there is another effect, due to the interference of the Lagrangian L of coherent matter with the "natural" vacuum energy term $\Lambda/8\pi G$ which is present in the Einstein equations. The two quantities have in fact the same tensorial form but possibly different sign, and it turns out that their interference can lead to a dramatic enhancement of vacuum fluctuations.

(b) Contribution of a quantum condensate to the vacuum energy density.

It is well known that the "natural" vacuum energy, or cosmological term, is very small. Until recently, it was thought to be exactly null. The most recent observations give a value different from zero, but in any case very tiny [23, 47], of the order of 0.1 J/m^3. This is usually supposed to be relevant at cosmological level, in determining the curvature and expansion rate of the universe on very large scales.

The observed value can be regarded as the residual of a complex interplay, in a still unknown high energy sector of particle physics, between positive and negative vacuum energy densities. According to [24], the observed residual should also be scale-dependent and this dependence could appear most clearly at length scales corresponding to the mass of the lightest particles like neutrinos or unidentified scalars.

[1] *Cosmological term = vacuum energy density*: see (b).

Lagrangian L = action density. Minimization of the action of a system gives its dynamical equations.

Quantum condensate in a superconductor: ensemble of the Cooper pairs, with collective wave function ψ_{GL} (also called an "order parameter") supposed to obey the Ginzburg-Landau (GL) equation. In the non-relativistic limit, the Lagrangian density of the condensate is just the opposite of the GL free energy density.

Zero-modes of the Einstein action = gravitational dipolar fluctuations: see (c).

Critical region: region of the condensate with positive Lagrangian density. According to the GL theory, it can only exist for constant solutions of the GL equation or in the neighbourhood of a local relative maximum of the Cooper pair density $|\psi_{GL}|^2$. See (f).

Noise source = density matrix: a formal way to express the fact that inside a critical region the gravitational field undergoes strong dipolar fluctuations and therefore takes on at random values h_i^2 with probability ξ_i. See (h), (i).

In certain conditions, the action density of a Bose condensate in condensed matter can be greater than the cosmological term, but it is nonetheless very small. Its effect on the local space curvature is absolutely negligible.

(c) The gravitational zero modes and the polarization of the gravitational vacuum.

Why so do we think that the interference of these two terms, which are in any case very small, can lead to some observable gravitational effect? Because we proved the existence of gravitational field configurations in vacuum, for which the value of the pure Einstein action (without the cosmological term) is exactly null, like for flat space. We called these configurations "zero modes of the Einstein action". At the quantum level, where fluctuations are admitted with respect to flat space, they are free to grow unrestrained. In a certain sense, the quantum space-time is unstable and has a natural tendency not to stay in the flat state, but to fall into these configurations, with a definite probability. They are virtual configurations, in the sense that they are permitted in the Feynman integral describing the quantum theory. In the Feynman integral all the possible configurations are admitted - not only those satisfying the field equations - each weighed with probability equal to the exponential of its action divided by $\hbar$. All these configurations (fluctuations) take part in defining the state of the system.

The zero-modes of the Einstein action are in all the same as fields produced by mass dipoles. In nature, mass dipoles do not exist as real sources. Nevertheless, the dipolar fluctuations mathematically have such a form. Being vacuum fluctuations, they are invariant under translations and Lorentz transformations, they are homogeneously allocated in space and at all length scales. That is, the dipolar fluctuations correspond to the fields produced by dipoles of various sizes, distributed in a uniform way. They can only show their presence if, in some way, their homogeneity and uniformity are broken. We are in presence of an analogue of the vacuum polarization in quantum electrodynamics. In that case, virtual couples of electrons/positrons pop up in the vacuum, and then quickly annihilate, generating uniform fluctuations. It is well known that these virtual processes must be taken into account, because they affect, for instance, the bare charge of the particles and their couplings. However, quantum corrections are, as a rule, very small in quantum electrodynamics.

It is important to be aware that the gravitational dipolar fluctuations we are talking about are neither the ordinary fluctuations of perturbation theory nor the well known "spacetime foam" fluctuations, which appear in quantum gravity at very short distances. Their nature is completely different. Although their intensity can be very large, they have null action, thanks to the compensation of positive and negative curvature between adjacent zones of space-time. The dipolar fluctuations are not zero-modes of the Lagrangian, but of the action. Their existence is possible thanks to the fact that the gravitational Lagrangian is not defined positive, unlike the Lagrangian of electromagnetic and gauge fields.

(d) The vacuum energy cuts the gravitational zero-modes to a certain level.

Let us go back to the cosmological term. One finds that it is related to the dipolar fluctuations, because it sets an upper limit on their amplitude. The contribution of a

dipolar fluctuation to the cosmological term is typically of the form [21]

$$\Delta S = \Lambda \tau M r^2 Q \tag{2}$$

where natural units are used ($\hbar = c = 1$); τ is the duration of the fluctuation, M is the order of magnitude of the virtual +/- masses, r their distance and Q is an adimensional function which depends on the detailed form of the dipole. If $\Delta S \gg 1$, then the fluctuation is suppressed.

With an electromagnetic analogy (not to be pushed too far) we could then say that the cosmological term sets the gravitational polarizability of free space. One expects that in a full non-perturbative theory of quantum gravity the bare value of the gravitational constant G should be renormalized by this effect. However, as long as the cosmological term is uniform in space and time, there are no observable consequences. On the other hand, if the vacuum energy density changes locally, this can have observable effects. In particular, if there are positive local contributions which subtract from the natural density, the result can be a local increase in the gravitational polarizability.

(e) The anomalous coupling is only active when the condensate is in certain particular states.

Our model can also explain why only certain superconductors in certain conditions show evidence of anomalous coupling with the gravitational field. The key point is not simply the presence of a quantum condensate, nor the density of this condensate. In fact, if this was the case, anomalous gravitational effects would be observed also with low temperature superconductors, or with superfluids. But even in the static Podkletnov experiment, only in certain conditions observable effects are obtained, and their intensity is variable.

Therefore the presence of the condensate is not sufficient to cause the effect. What are the necessary conditions? The anomalous contribution to the cosmological term is given by the Lagrangian density of the condensate, according to the following equations. Consider a scalar field ϕ interacting with gravity (we use units $\hbar = c = 1$; SI units will be restored in eq. (12)). The interaction action is obtained from the energy-momentum tensor:

$$L = \frac{1}{2}(\partial_\alpha \phi \partial^\alpha \phi - m^2 |\phi|^2) \tag{3}$$

$$T_{\mu\nu} = \Pi_\mu \partial_\nu \phi - g_{\mu\nu} L = \partial_\mu \phi^* \partial_\nu \phi - g_{\mu\nu} L \tag{4}$$

$$S_{interaction} = \frac{1}{2} \int d^4x \sqrt{g(x)} T^{\mu\nu}(x) h_{\mu\nu}(x) \tag{5}$$

To lowest order in $h_{\mu\nu}$ the interaction action can be rewritten as

$$S_{interaction} = \frac{1}{2} \int d^4x \, (h_{\mu\nu} \partial^\mu \phi^* \partial^\nu \phi - \mathrm{Tr} h L) \tag{6}$$

On the other hand, the cosmological term is (still to lowest order in $h_{\mu\nu}$ and expanding $\sqrt{g} = 1 + \frac{1}{2}\mathrm{Tr}h + ...$)

$$S_\Lambda = \frac{\Lambda}{8\pi G} \int d^4x \left(1 + \frac{1}{2}\mathrm{Tr}h\right) \tag{7}$$

Therefore the sum of the two terms can be rewritten as

$$S_{interaction} + S_\Lambda = \frac{1}{2}\int d^4x h_{\mu\nu}\partial^\mu\phi^*\partial^\nu\phi + \frac{1}{2}\int d^4x \mathrm{Tr}h\left(\frac{\Lambda}{8\pi G} - L\right) \tag{8}$$

We see that to leading order the coupling of gravity to ϕ gives a typical source term $(h_{\mu\nu}\partial^\mu\phi^*\partial^\nu\phi)$ and subtracts from Λ the local density $8\pi GL(x)$. This separation is arbitrary, but useful and reasonable if the Lagrangian density is such to affect locally the "natural" cosmological term and change the spectrum of gravitational vacuum fluctuations corresponding to virtual mass densities *much larger than the real density of* ϕ.

For example, suppose that ϕ represents a condensate with the density of ordinary matter ($\sim 1\ g/cm^3$). At the scale $r \sim 10^{-4}\ cm$, $\tau \sim 10^{-4}\ s$, with the observed value of Λ, the upper bound on the virtual source density is $\sim 10^{17}\ g/cm^3$, which is much larger than the real density. If L is comparable to $\Lambda/8\pi G$ in some region, an inhomogeneity in the cut-off mechanism of the dipolar fluctuations will follow, and this effect could exceed by far the effects of the coupling $(h_{\mu\nu}\partial^\mu\phi^*\partial^\nu\phi)$ to real matter.

The value of the Lagrangian depends on the state the condensate is in, and more exactly on the macroscopic wave function ψ_{GL} of the Cooper pairs. The problem of finding the wave function in given experimental conditions is still open. From the wave function one can compute the Lagrangian, and then the local contribution of the superconductor to the vacuum energy, and its ability to produce anomalous gravitational coupling.

(f) L subtracts from Λ only where the density $|\psi_{GL}|^2$ has a local maximum.

The Lagrangian L in eq. (3) is the Klein-Gordon Lagrangian which describes a relativistic free scalar field. In order to relate it, in the low energy limit, to the Ginzburg-Landau (GL) free energy of superconductors [25] one makes the standard transformation

$$\psi_{KG}(\mathbf{x}) = e^{imt}\phi(x) \tag{9}$$

where m is the Cooper pair mass. Then one turns to the GL wave function by re-normalizing ψ_{KG} as follows

$$\psi_{KG}(\mathbf{x}) = \sqrt{m}\psi_{GL}(\mathbf{x}) \tag{10}$$

This normalization corresponds to the standard relation $|\psi_{GL}(\mathbf{x})|^2 = \rho(\mathbf{x})$, where ρ is the density of Cooper pairs. Finally, the free Lagrangian is generalized by adding a quadratic and a quartic interaction term and the minimal electromagnetic coupling. In this way one finds

$$L = -\frac{1}{2m}|-i\nabla\psi + 2e\mathbf{A}\psi|^2 - \alpha\psi^*\psi - \frac{1}{2}\beta(\psi^*\psi)^2 \tag{11}$$

This is the Lagrangian density to be inserted into eq. (8) as contribution to the vacuum energy density. It is the opposite of the GL free energy density [**?**], as expected. For wave functions which satisfy the wave equation derived from (11), the expression of L simplifies to

$$L = -\frac{1}{2m}\left[\hbar^2(\nabla\rho)^2 + \hbar^2\rho\nabla^2\rho - m\beta\rho^2\right] \tag{12}$$

where $\hbar$ has been re-introduced to allow for a better numerical estimate.

We recall [26] that the α and β coefficients depend on the absolute temperature T. The coefficient β is always positive and approximately constant near T_c; α is negative for $T < T_c$ and near T_c behaves like $const.(T - T_c)$. The ratio between α and β is given by the relation $n_p = -\alpha/\beta$, where n_p is the average density of pairs in the material. Finally, β is linked to the value of the Ginzburg-Landau parameter $\kappa = \lambda/\xi$ by the relation $\kappa^2 = m^2\beta/(2\mu_0\hbar^2e^2)$. Two further important points which should be taken into account are (i) the boundary conditions on ψ_{GL} at the superconductor/ normal conductor and superconductor/ionized gas interfaces; (ii) the intrinsic anisotropy of HTC materials, which actually also affects the form of the GL free energy.

The relative importance in eq. (12) of the terms with the gradients and the term proportional to β depends on the length scale at which the variations of ψ_{GL} can occur. If, as usual for Type II and HTC superconductors, this scale is of the order of 10^{-8} m or less, the terms with the gradient dominate.

It is straightforward to check that the sign of L is negative, except for two types of configurations:

(1) For the constant solutions of the Ginzburg-Landau equation in the absence of external field, namely $\rho(\mathbf{x}) = n_p$. The corresponding constant Lagrangian density is $L_1 = \frac{1}{2}\beta n_p^2$.

(2) For regions of the condensate where $\rho\nabla^2\rho$ is negative and greater, in absolute value, than $(\nabla\rho)^2$. It is straightforward to check that these are regions located around local density maximums, or more generally about lines and surfaces where the first partial derivatives of ρ are zero and the second derivatives are negative or null. The Lagrangian density at a maximum is $L_2 \sim \frac{1}{2m}\rho|\rho''|$. If the maximum is sharp, L can be much larger than for constant solutions. Configurations of this kind are characteristic of solutions of the Ginzburg-Landau equation with strong magnetic flux penetration [27].

Now we make some numerical estimates of L. Assuming for YBCO $\rho \sim 10^{27}m^{-3}$, $\xi \sim 10^{-9}$ m, $\kappa \sim 10^2$, we obtain for the configurations (1) and (2) densities $L_1 \sim 10^4 J/m^3$ and $L_2 \sim 10^7 J/m^3$, respectively. With reference to our experiment we must explain, on the basis of these figures, why anomalous coupling at the emitter takes place, but only at the moment of the discharge and in presence of strong magnetic flux penetration.

We remind that the vacuum energy density acts as cut-off for the dipolars fluctuations, so that their maximum amplitude A is inversely proportional to Λ. Therefore in presence of a local contribution by the superconductor we have

$$A \propto \frac{1}{|\Lambda/8\pi G - L|} \tag{13}$$

So an amplification of the fluctuations is possible when L has the same sign as Λ. From the experimental observations it is clear that a negative value of L does not give the necessary conditions. In fact, in that case anomalous coupling would be observed every time there are strong density gradients in the superconducting material - which occurs almost always. From this we obtain a first piece of information about the value of Λ at atomic scale (otherwise unknown): it must be positive. $\Lambda/8\pi G$ must furthermore be much larger than L_1, because a constant density does not give observable anomalous effects

either. In conclusion, $\Lambda/8\pi G$ must be larger than L_2, and the amplitude A of the dipolar fluctuations increases as the local value of L approaches it from below. [2]

This can happen in presence of strong magnetic flux penetration (Point 2 above), but that requisite is not sufficient: the presence of a strong transport current is also necessary. In fact, with strong flux penetration, the density ρ is depressed. The current appears like a means to obtain at once a large ρ and a large value of ρ'' in correspondence of the maximums. Indeed, in inhomogeneous materials like HTCs, a very intense transport current inevitably forces a large density in certain regions. In the case of the weak gravitational shielding [1] the transport current is mostly due to the accelerated rotation of the disk [28]. In the present case it is due to the discharge.

(g) The anomalous coupling inside the condensate modifies the field also outside.

Summarizing, we can say that in particular conditions a quantum condensate is able to modify locally the cosmological term of the gravitational action. In turn, the cosmological term fixes the cut level of the dipolar fluctuations, and so the local gravitational vacuum polarizability. Therefore an anomalous coupling of the condensate with the gravitational field is observed. This coupling can be abnormally strong, due to the large amplitude of the vacuum fluctuations. It is a kind of coupling that completely eludes the standard form and so is not proportional, through the G/c^4 constant, to the energy-impulse content of the condensate.

The next question is: how is the gravitational field modified inside the condensate and in its neighbourhood? In other words, let us suppose that the gravitational field displays a much higher level of dipolar fluctuations in some regions of the condensate. What is the consequence for the global behaviour of the field? For instance, with reference to the static experiment, why is there a noticeable reduction of the terrestrial field above the disc? We can say that in that case there is a big gravitational source - the earth - producing a uniform field in the region of interest, according to the usual classical field equations. Into these equations, however, we must also introduce a kind of "random source" located in the condensate. This affects the field also outside.

(h) The modified field equation contains an arbitrary constant.

We have proposed to introduce into the gravitational field equations a term representing a random source located in the condensate. This procedure has some intrinsic arbitrariness. The intensity of the source is arbitrary, too, and cannot be obtained from the ratio between the energy density of the condensate and the "natural" vacuum energy density. In fact, it is true that this ratio allows us to determine the maximum amplitude of the dipolar fluctuations. However, the probability of these fluctuations, and so their weight with respect to the external configurations, is still an unknown element of the theory. We know that certain field configurations give a null contribution to the pure Einstein

[2] The density L_2 can be compared with that obtainable for an electromagnetic field alone - which can also be regarded as "coherent matter" in this context. The electromagnetic energy density is proportional to $(\mathbf{E}^2 + \mathbf{B}^2)$, but the action density is proportional to $(\mathbf{E}^2 - \mathbf{B}^2)$, therefore only an electrostatic field has the right sign. But even with a field strength of $3 \cdot 10^6\ V/m$, one obtains a density of $100\ J/m^3$, definitely lower.

action and can grow up without limit, and we can determine the cut-off amplitude due to the intervention of the cosmological term; however, the probability that these fluctuations really happen is a feature of the quantum theory, which is not known yet. In principle, it would be possible to write a functional integral containing all the involved fields, the test masses etc., evaluate it and obtain everything. In practice, what we can do with such an integral is only a weak field expansion about the minimum of the action.

In conclusion, if we represent the gravitational fluctuations in the quantum condensate as a random source, the intensity of this source must be inserted as a parameter which is fixed "a posteriori" from the experimental data. This should not be unexpected. The experimental observations described in this work are absolutely new and unprecedented. They inform us about a sector of the theory which is otherwise unknown. The validity of our model consists of suggesting a new interaction process, while avoiding contradictions with known facts, and while giving the freedom to fix a new coupling constant.

(i) The modified field equation must be able to describe the observed phenomenology.

After modelling the effect of the fluctuations on the external field (for instance, as random source with a certain strength), we are able to verify the consistency and correctness of the procedure by calculating this field and comparing the result to the data - not only as intensity but also as shape. For instance, we know that in the static experiment a "shielding cylinder" was observed which extended far above the superconducting disc and showed net borders, without diffraction. Obtaining this characteristic from the field equations modified by the anomalous coupling is all but trivial. The observed field configuration is furthermore clearly not conservative. (This can be understood remembering that there is a source term in the equation.) Nonetheless, we succeeded in [20] in obtaining a result of this kind (see also [29]).

(j) Euclidean and Lorentzian formulation of the anomalous coupling and of the modified action.

From the technical point of view, the general program outlined above has been implemented in the Euclidean (or imaginary-time) version of quantum gravity [18, 19, 20], and more recently in the standard Lorentzian version [21].

The occurrence of the dipolar fluctuations and the cut-off role of the vacuum energy density are most clearly and safely exhibited in the Lorentzian formalism. On the other hand, the Euclidean formulation is reliable and more suitable for perturbative calculations of the modified field equations.

The Lorentzian formulation is indispensable for the latest developments (calculation of the low-energy limit of L and determination of its sign as a function of ρ).

4.2 Possible interpretation of the gravitational-like impulse at the discharge

We focus now our attention on the new, puzzling effects described in the experimental part of this paper, and partially analysed at the beginning of this Section. We cannot offer any

quantitative interpretation of these effects yet, so we shall limit ourselves to an hypothesis based on our previous work on the static effect.

(a) From the static to the transient effect: the virtual dipoles emit virtual radiation.

We have seen that the observed impulse can neither be described as a real radiation, nor as a quasi-static field. These are the two types of field configurations which are predicted by any classical theory.

However, we also saw that the weak gravitational shielding effect can be explained introducing the concept of anomalous dipolar quantum fluctuations induced by the condensate. These fluctuations locally increase to observable levels the gravitational vacuum polarizability.

In the transient case, the virtual dipolar fields are rapidly varying in time, because the critical conditions in the quantum condensate are produced only for a short time at the discharge. Therefore it is natural to expect that in this case the formation of virtual dipoles is accompanied by the emission of virtual dipolar radiation.

(b) In quantum mechanics every interaction is equivalent to an exchange of virtual radiation.

Let us recall the concept of "virtual radiation" as intermediate state of a quantum process. In quantum mechanics, every interaction is thought to take place through the exchange of virtual particles - photons, gauge bosons, gravitons. This is especially clear in scattering processes, but also the static interaction potential can be written as an integral over time and four-momentum of the propagator of a mediating virtual particle [30]. In this integral, all values of energy-momentum are included, not only the "on-shell" values satisfying the condition $E = p/c$ which is typical of real photons and gravitons. This is possible just because the mediating particles are virtual, i.e. so short-living that the Heisenberg principle allows for a large indetermination in their energy. In fact, the static force obtained as a sum of virtual processes is very different from the effect of a collection of free photons or gravitons.

It is also possible to compute along these lines the quantum corrections to the classical force. To this end, one includes in the sum some less probable processes, involving the exchange of several mediating particles at the same time, or the creation-annihilation of virtual pairs, and so on.

(c) The impulse at the discharge is made of off-shell gravitons.

In order to explain the weak gravitational shielding effect we hypothesised an anomalous strong quantum correction to the field of the earth. In the transient case, on the other hand, all the emitted "radiation" should be regarded as a quantum effect. The observed impulsive force could be the effect of virtual processes in which:

1. The intense supercurrent flowing across the superconducting cathode produces critical gravitational regions, with strong dipolar vacuum fluctuations. The necessary conditions are those discussed in Section (4.1-f).

2. These fluctuations emit a beam of virtual off-shell gravitons with $E \ll p/c$. The direction of the beam is sharply defined by momentum conservation. Whatever the exact microscopic mechanism, the momentum carried by the virtual radiation can only originate from that of the Cooper pairs entering the critical regions, i.e. from the momentum of the supercurrent. This is in agreement with the fact that if the impact direction of the discharge changes (like in the earlier set-up, see 3), also the direction of the emitted radiation changes.

3. When the beam hits a mobile target, it conveys an impulse to this target. Like for usual gravitational forces (which can also be interpretated as graviton exchange, as mentioned), interposed bodies do not affect transmission.

4.3 Known effects which could be connected to the observed phenomenon.

The following concepts are often quoted to explain anomalous gravitational effects. So we summarise them quickly, even though in our case they do not fit to the observed phenomenology.

We recall that several alternative theories were proposed, in the last decades, in the attempt to "explain" and give a physical basis to spacetime and vacuum. Every one of these, to be credible, must first of all reproduce the known results of general relativity and quantum field theory. Notable examples are theories of "induced" gravity according to Sakharov's idea [31], and string theory. It is not easy to judge if anyone of these theories can also predict, in addition, unusual effects in the presence of superconductors. Some are not developed enough to give a definite answer. Many have been proposed recently, still their authors did not envisage any anomalous coupling to matter in a macroscopic quantum state. In general, if the coupling of gravity to matter conforms to the classical Einstein equations, then the intensity of any generated gravitational field will depend only on the energy-momentum of the source multiplied by G/c^4, so there is no chance for anomalous effects. A notable exception could be torsion theory, which predicts a coupling to quantum spin not allowed in the Einstein equations; however, as we shall see below, there are strict experimental limits on the coupling of matter to torsion. Another possibility is to consider strong quantum effects, as done in Section 4.2; in that case, we chose to start from the standard form of the classical theory.

(a) The gravitomagnetic field

Could the observed anomalous forces be due to the fact that the superconductor produces during the discharge a strong gravitomagnetic field? It is well known from general relativity that the gravitational field contains components of magnetic type, called the gravitomagnetic field. These components have the property to be produced by moving objects and to act on objects in movement. It is possible to write the Einstein field equations in weak field approximation in a form very similar to that of Maxwell equations. The important difference, with respect to the Maxwell equations for electromagnetism, is that gravitomagnetic effects are suppressed by factors $1/c$ or $1/c^2$. So they are always very small with respect to "gravitoelectric" effects - those which have a Newtonian limit. See for instance [32, 33]; in these references an analysis of the Maxwell equations for

gravity and also of the "Gravity Probe B gyroscope experiment" for detecting the Earth's gravitomagnetic field is given.

In certain conditions the gravitomagnetic field can be repulsive. In neutrons stars it can produce a gravitational analogue of the Meissner effect. As one would expect, however, the "gravitational Meissner effect" is exceedingly weak: for instance, it has been computed that in a neutron star with a density of the order of 10^{14} g/cm^3, the London penetration depth is ca. 12 km [34]. In the 1970s experiments were done to detect possible weight decreases of a rotor while it was rotating at very high speed [35], but conclusive results were never obtained.

(b) Gravitomagnetism and quantum spin

The aspects of the theory of quantum gravity concerning the spin are summarized, for instance, in [36]. In previous work [37] O'Connell examined the implications arising from the fact that spin contributions to the gravitational potential are as large as the spin-independent contributions for interparticle separations of the order of Compton length and also that such spin-dependent forces could be repulsive for certain spin orientations. An analysis was also carried out of the possibility of measuring gravitational spin-dependent forces in the laboratory [38]. An idea of one such experiment, as proposed in [39], is to observe a breaking of the equilibrium of a polarized body, hanging in the gravitational field, when its polarized state is destroyed. This effect, if present, is predicted to be extremely small. (See also the results by Ritter et al. [40].) Claims like those by Wallace of "antigravity" forces produced by spin orientation in nuclei [41] appear as totally unreliable today.

(c) The works by Ning Li and Torr

In a series of articles Ning Li and Torr [6] calculated the gravitomagnetic field which would be produced by a superconductor containing circulating supercorrents. According to them, in this case also the movement of the ions, which produce a current of mass, has particular importance. Also the fact that spin alignment is present would be very important. The alignment of the spin of the lattice ions would be a source of gravitomagnetic field. The objections to this model are of two types. First, the total spin amount that is possible to obtain in normal condensed matter is always very small, also in presence of alignment. Therefore, given the weak coupling with the gravitomagnetic field, one does not understand how it could reach detectable intensity. Another objection is of more technical nature. Ning Li and Torr use the Maxwell equations for gravity, which hold in weak field approximation. However, when they find that some terms of these equations "explode", they keep this result even if it is inconsistent with the initial approximation.

Previously to the first Podkletnov experiment [1] and without reference to it, Ning Li and Torr determined another consequence of their model [7]. Not only the alignment of the spin of the lattice ions would produce a gravitomagnetic field, but in the presence of an outside applied time-dependent vector potential, this would be converted into a perceptible gravitoelectric field. Such a conversion is necessary, if one wants to apply this theory to the weak gravitational shielding, because in that case the test bodies are at rest, and so they would not respond to a gravitomagnetic field. However, this is in contrast with the

short-lived permanence of the effect also after all the outside fields are turned off. At last, we notice that Ning Li and Torr never published a work in which they try to interpret the phenomenology of the effect in terms of their model nor to explain why it is observed only with certain types of superconductors.

(d) Other models connected to gravitomagnetism

There have been proposals of alternative interpretations of gravitomagnetism in connection with the Mach principle [45]. In this context, the gravitomagnetic phenomena would achieve a greater importance. Still with reference to a Machian theory, Woodard claims to have experimentally obtained some transient fluctuations in the inertial mass of a capacitor [46]. However we will not be concerned here with these approaches, which to a large extent remained at a subjective level.

Recently Ummarino [42] tried to establish a link between the Podkletnov effect and the gravitomagnetic and gravitoelectric field, following a more standard approach, connected with the Ginzburg-Landau theory for superconductors.

(e) Theories with torsion

We now come to the theories of gravity with torsion. Could the observed phenomenology, not understandable in general relativity, be related to the existence of a torsion field? Let us first recall how the concept of torsion was born: from the idea of considering the connection (which in the metric formalism is simply a quantity derived from the metric and is symmetric with respect to a couple of indexes) like an independent quantity, with its own dynamics and, generally, not symmetric. Torsion theory is an extension of general relativity, which was investigated in great detail in the past. It is necessary in fact in order to introduce the interaction of the gravitational field with the quantum spin, and allows to connect general relativity to the usual gauge theories. After admitting the possibility of the existence of torsion, its features (for instance, its propagation), do not descend from first principles or from the geometrical structure of the theory, but from the form of the various possible terms in the action and from coupling constants fixed on the basis of experimental observations. Over the years a large amount of experimental data have been accumulated, which place strong limits on the couplings.

A picture of the current situation is for instance presented by Carroll and Field [43]. What is concluded is that the possible existence of the torsion can be of interest at the level of gravitational interactions at very short distances (Planck scale), but not at the level of laboratory experiments.

In their work Carroll and Field discuss possible actions for torsion and its interaction with matter fields like those of the standard model of particle physics. They construct a free Lagrangian from powers and derivatives of the torsion, and couple it "minimally" to matter through the covariant derivative. They find that there is only a small range of models possible without placing arbitrary restrictions on the dynamics. In these models only a single mode interacts with matter, either a massive scalar or a massive spin-1 field, and each mode is parameterised by two constants with the dimension of mass. They concentrate on the scalar theory, which is related to several proposals found in the literature and discuss what regions of parameter space are excluded by laboratory and astrophysical

data. Carroll and Field find that a reasonable expectation would be for each of the two mass parameters to be of the order of the Planck scale; such a choice is a safe distance away from the regions excluded by experiment. They conclude that, while there are reasons to expect that the torsion degrees of freedom exist as propagating fields, there is no reason to expect any observable signature from torsion.

Other "not orthodox" points of view are represented in literature [44]. But even though theories of torsion exist since a long time, no attempts to explain the phenomenology of the Podkletnov effect were ever presented.

(f) The value of G and the measurements at short distances

The fundamental characteristics of the gravitational interaction keep on being a very alive and interesting research field. We do not mean by this the consequences of gravity on the structure of the universe, and so the applications of general relativity to black holes, astrophysics etc.; we mean the basic features of the force, including the issue whether general relativity is an adequate and complete description of it. We recall that only two predictions of general relativity have not been verified yet, namely the existence of gravitational waves and of gravitomagnetic fields. There are furthermore several current experiments to detect possible violations of the equivalence principle. Up to now no contradiction has ever been observed with respect to the predictions of general relativity [47].

The precision with which the value of G is known is clearly unsatisfactory compared to the precision with which the other fundamental physical constants are known. This is also due to the fact that while the definition of the other fundamental constants relies on microscopic experiments performed with high precision devices, for the G constant it is necessary to use more or less sophisticated versions of the Cavendish experiment. In particular, we do not know the behaviour of gravity at short distances (millimeters or less). According to Gillies [48], in the second half of 1900 more measurements of G were made than ever before. Some discrepancies were observed in recent times with respect to the best official value fixed in 1982.

The value of G has been called into question by new measurements from respected research teams in Germany, New Zealand, and Russia [49]. The new values disagree wildly. For example, a team from the German Institute of Standards obtained a value for G that is 0.6% larger than the accepted value; a group from the University of Wuppertal in Germany found a value that is 0.06% lower and one at the Measurement Standards Laboratory of New Zealand measured a value that is 0.1% lower. The Russian group found a space and time variation of G of up to 0.7%. The collection of these new results suggests that the uncertainty in G could be much larger than originally thought. This controversy has spurred several efforts to make a more reliable measurement of G.

A recent theoretical prediction suggests that gravity penetrates extra, compact dimensions so that the gravitational inverse square law must be modified at short ranges (less than 1 mm). Arkani-Hamed, Dimopoulos, and Dvali [50], have offered this as an explanation of the hierarchy problem. A team at the university of Washington is doing new measurements in order to check this, but results are negative up to now [51].

(g) The anomalous acceleration of the Pioneer and scalar-tensor theories

Let us now pass from the shortest distances at which it is possible to observe gravitational interactions in the laboratory, to the largest. Surprising results were obtained recently by the observation of the motion of the Pioneer space probes [53]. Direct measurements are possible thanks to the radio signals transmitted by the spacecrafts, which give precise information about their position, speed and acceleration. From the analysis of the data a residual acceleration was found, not explainable through the usual orbit tracking models. Some proposals for a theoretical explanation of the phenomenon were presented. One of these [54] calls for the existence, in addition to Einstein's gravitational field, of a scalar field which, supposed it has certain properties, could lead to the observed effect. This field could also be responsible for the rotation anomalies observed in the galaxies, because it gives a modification of the behaviour of gravity at large distances. The cited model belongs in practice to a wide group of extensions of the standard theory of gravitation [52], which originate from the Brans-Dicke model and in more recent times refer to string theory and to the so-called dilaton field.

(h) Gravitational anomalies at solar eclipses

There is a long history of claims of possible anomalous changes of gravity during sun eclipses. These would be different from tidal changes, which are well known and calculable with precision, and could show that some kind of shielding of the solar attraction by the moon exists, at the moment when it steps in between the earth and the sun. The data, however, are quite contradictory [55].

The original experiments by Allais, in which the change of the oscillation period of a pendulum was observed, seemed to imply a decrease in g of about 1/100 of the solar gravity. The consequence would be an apparent increase of the terrestrial attraction of about one part in a million. During the eclipse of 2000 a net of observers with pendulums and gravimeters was organised by initiative of the NASA, in order to observe possible changes; the definitive results are not available yet. A work was published in 2000 by a Chinese team, with reference to the eclipse of 1997 [56], in which data measured with a high precision gravimeter are reported. Also in this case, some anomalies were observed at the eclipse, but with features very different from those reported before. There is a noticeable decrease of the terrestrial attraction, that is, an apparent anti-screening of the solar gravity. The shielding factor is much smaller than the one declared by Allais, and the time sequence rather strange, with maxima at the beginning and the end of the darkness period.

It is important to remember that other experiments clearly exclude any shielding of gravitation of the so-called "Majorana" type (these phenomena were first investigate by Majorana at the beginning of 1900) [57]. Besides, one would expect a possible shielding effect by the moon to have an analogue for artificial satellites, namely a shielding of solar gravity when the satellite enters the shadow of the earth. Anomalies of this type were actually reported [58], though they are very difficult to confirm, because the irregularities which affects the motion of the artificial satellites are numerous, especially when they are close to the surface of the earth.

(i) Weak gravitational shielding by superconductors

In this variegated field of investigations on possible gravitational anomalies, the work by E. Podkletnov stands out, originally appeared in 1992 [1], then in improved version in 1995 [2]. It describes possible gravitational anomalies caused by HTC superconductors. The observed anomalies reached a maximum of about 2% of g, in transient situations, and 0.3-0.5% of g in almost stationary form. These anomalies were produced by means of discs with multiple layers, rotating at high speed, in very particular conditions, which still have not been completely duplicated. A NASA team already produced a first simplified reproduction of the experiment in 1997 [3], and a new version should start giving some data this year. Besides the remarkable experimental difficulties, the results are puzzling under the theoretical point of view. In fact, the strength of the anomalies is very large with respect to what has been previously observed, and no sufficiently complete theory exists, which can explain this kind of phenomena (see Section 4.1). Here in fact both gravitation is called into play, of which a complete quantum theory does not exist, and typically quantum phenomena (behaviour of the macroscopic wave functions in superconductors). Furthermore, not conventional superconductors are involved, but HTC superconductors, for which several issues are still unsettled, like the pairing mechanism etc.

(j) Terahertz radiation emission by HTC superconductors

A new type of terahertz radiation was discovered by Japanese scientists by irradiating HTC superconductive films with femtosecond laser pulses [59, 60]. The radiation mechanism is thought to be connected with the ultrafast supercurrent modulation by the laser pulses, which induces nonequilibrium superconductivity. The principal design of the experimental installation has some common features with our gravity impulse generator and the behavior of the superconducting crystallized materials might have a similar origin.

5 Conclusions

The experimental apparatus has shown that an impulse of gravitational-like force freely propagating through different physical media can be generated by a dual layered YBCO HTSC under pulsed electric current. The impulse propagates parallel to the direction of the discharge and orthogonal to the surface of the HTSC. The intensity of the impulse has been found to increase with increasing discharge energy, and to depend on the chemical composition and structure of the HTSC and on its internal magnetic state. In a typical measurement, the mechanical energy imparted by the impulse to a pendulum of mass 18.5 g was between $4 \cdot 10^{-4}$ J and $23 \cdot 10^{-4}$ J (Table 1).

From the theoretical point of view, we understand the effect as the result of an anomalous interaction between a special class of gravitational vacuum fluctuations and the macroscopic wave function of the superconductor. This interaction is locally activated when the product of the pairs density ρ and its second derivative ρ'' is sufficiently large. The sign of ρ'' must furthermore be positive. These conditions can be satisfied in the presence of intense transport current and magnetic flux penetration.

Attempts of scientists to control gravity have been present for a long time and in the future these efforts will almost certainly become more prominent. Albert Einstein spent the

last years of his life trying to integrate gravity with the other laws of physics and the entire scientific community remains intrigued with the problem of gravity ever since. However, since our knowledge of gravity is poor in comparison to that of the other fundamental forces, we are unable to control it in any fundamental way. We are therefore left with the option of carrying out experiments based on new theories, on scientific intuition and careful analysis of previous results. This work indicates that a kind of artificial gravity can be generated using the unique properties of superconducting ceramic materials and a combination of electric and magnetic forces.

Acknowledgment - G.M. was supported in part by the California Institute for Physics and Astrophysics via grant CIPA-MG7099.

References

[1] E. Podkletnov and R. Nieminen, *A Possibility of Gravitational Force Shielding by Bulk $YBa_2Cu_3O_{7-x}$ Superconductor*, Physica C Vol. 203 p. 441 (1992).

[2] E. Podkletnov, *Weak Gravitational Shielding Properties of Composite Bulk $YBa_2Cu_3O_{7-x}$ Superconductor Below 70 K Under EM Field*, LANL Physics Preprint Server, preprint cond-mat/9701074, January 1997. Available on the net: http://www.gravity.org/msu.html.

[3] N. Li, D. Noever, T. Robertson, R. Koczor and W. Brantley, *Static Test for a Gravitational Force Coupled to Type II YBCO Superconductors*, Physica C 281, 260-267. R. Koczor and D. Noever, *Fabrication of Large Bulk Ceramic Superconductor Disks for Gravity Modification Experiments and Performance of YBCO Disks Under e.m. Field Excitation*, NASA Marshall, Huntsville, AL, AIAA 99-2147, 35th AIAA/ASME/SAE/ASEE Joint Propulsion Conference, 20-24 June 1999, Los Angeles, CA.

[4] Frederic N. Rounds, *Anomalous Weight Behavior in $YBa_2Cu_3O_{7-x}$ Compounds at Low Temperature*, NASA Ames Research Center. Preprint physics/9705043.

[5] Harald Reiss, *A Possible Interaction Between Gravity and High Temperature Superconductivity-By a Materials Property*, Submitted to the 15th. European Conf. Thermophys. Properties, Wrzburg, Germany, Sept. 5-9, 1999.

[6] Ning Li and D. Torr, *Effects of a gravitomagnetic field on pure superconductors*, Phys. Rev. D 43 (1991) 457; *Gravitational effects on the magnetic attenuation of superconductors*, Phys. Rev. B 64 (1992) 5489.

[7] Ning Li and D. Torr, *Gravitoelectric-electric coupling via superconductivity*, Found. Phys. Lett. 6 (1993) 371.

[8] G. Fontana, *A possibility of emission of high frequency gravitational radiation from junctions between d-wave and s-wave superconductors*, report cond-mat/9812070;

Gravitational radiation and its application to space travel, in CP504, Space Technology and Applications International Forum-2000, edited by M.S. El-Genk, AiP, p. 1085.

[9] M. Agop, C. Gh. Buzea and P. Nica, *Gravitational shielding in an electromagnetic field. Local gravitoelectromagnetic effects on a superconductor*, Physica C: Superconductivity, 339 (2) (2000) pp. 120-128

[10] U. Balachandran, R.B. Poeppel, J.E. Emerson, S.A. Johnson, M.T. Lanagan, C.A. Youngdahl, Donglu Shi, K.C. Goretta, N.G. Eror, *Synthesis of Phase-Pure Orthorhombic $YBa_2Cu_3O_{7-x}$ under Low Oxygen Pressure*, Materials Letters 8 (1989) 454-456.

[11] T.B. Lindemer, F.A. Washburn, C.S. MacDougall, O.B. Cavin, *Synthesis of Y-Ba-Cu-O superconductors in subatmospheric oxygen*, Physica C 174 (1991) 135-143.

[12] M. Murakami, *Processing of bulk YBaCuO*, Supercond. Sci. Technol. vol. 5, pp 185-203, 1992.

[13] S. Nariki, N. Sakai and M. Murakami, *Fabrication of large melt-textured Gd-Ba-Cu-O superconductor with Ag addition*, Physica C: Superconductivity, 341-348 (1-4) (2000) pp. 2409-2412.

[14] M. Muralidhar, S. Koishikawa, M.R. Koblischka and M. Murakami, *Study of superconducting properties of OCMG processed (Nd, Eu, Gd)-Ba-Cu-O with Pr doping*, Physica C: Superconductivity, 314 (3-4) (1999) pp. 277-284.

[15] S.I. Yoo, N. Sakai, T. Higuchi and M. Murakami, *Melt processing for obtaining $NdBa_2Cu_3O_y$ superconductors with high Tc and large Jc*, Appl. Phys. Lett. 65 (1994) pp. 633-635.

[16] V.R. Todt, X.F. Zhang and D.J. Miller, *Nucleation and growth of single- and multiple-domain $YBa_2Cu_3O_{7-x}$ Levitators: Influence of Seed Crystallofraphy*, IEEE Trans. on Appl. Super., vol. 7(2), pp. 1801-1804, June 1997.

[17] Chan-Joong Kim, Young A. Jee, Gye-Won Hong, Tae-Hyun Sung, Young-Hee Han, Sang-Chul Han, Sang-Joon Kim, W. Bieger, G. Fuchs, *Effects of the seed dimension on the top surface growth mode and the magnetic properties of top-seeded melt growth processed YBCO superconductors*, Physica C 331 (2000) pp. 274-284.

[18] G. Modanese, *Theoretical analysis of a reported weak gravitational shielding effect*, Europhys. Lett. 35 (1996) 413-418.

[19] G. Modanese, *Role of a "local" cosmological constant in euclidean quantum gravity*, Phys. Rev. D 54 (1996) 5002.

[20] G. Modanese, *Tunneling of a massless scalar field through a 3D gaussian barrier*, J. Math. Phys. 40 (1999) 3300.

[21] G. Modanese, *Virtual dipoles and large fluctuations in quantum gravity*, Phys. Lett. B 460 (1999) 276; *Large "dipolar" fluctuations in quantum gravity*, Nucl. Phys. B 588 (2000) 419-435; *Paradox of virtual dipoles in the Einstein action*, Phys. Rev. D 62 (2000) 087502;

[22] G. Modanese, *The dipolar zero-modes of Einstein action: An informal summary with some new issues*, in Proceedings of the Vigier III Symp. (Aug. 21-25, 2000, U. California Berkeley), Kluwer Acad. Press.

[23] A.G. Riess et al., Astronom. J. 116 (1998) 1009; S. Perlmutter et al., Astrophys. J. 517 (1999) 565.

[24] I.L. Shapiro and J. Solà, *On the scaling behavior of the cosmological constant and the possible existence of new forces and new light degrees of freedom*, Phys. Lett. **B 475** (2000) 236; *Scaling behavior of the cosmological constant: interface between quantum field theory and cosmology*, report UAB-FT-490, hep-th/0012227.

[25] G. Modanese, *Local contribution of a quantum condensate to the vacuum energy density*, report gr-qc/0107073.

[26] J. Waldram, "Superconductivity of metals and cuprates", IoP, London, 1996.

[27] D.R. Tilley and J. Tilley, "Superfluidity and superconductivity", IoP, Bristol, 1990.

[28] G. Modanese, *The London field in bulk layered superconductors*, report cond-mat/9909441.

[29] G. Modanese, *Gravitational anomalies by HTC superconductors: a 1999 theoretical status report*, report physics/9901011.

[30] For the gravitational case: G. Modanese, *Potential energy in quantum gravity*, Nucl. Phys. B 434 (1995) 697. For the other cases: K. Symanzik, Comm. Math. Phys. 16 (1970) 48.

[31] For a recent account and references see C. Barcelo, S. Liberati and M. Visser, *Analog gravity from field theory normal modes?*, report gr-qc/0104001.

[32] B. Mashhoon, H. Young Paik and C. Will, *Detection of the gravitomagnetic field using an orbiting superconducting gradiometer; theoretical principles*, Phys. Rev. D 39, 2825 (1989).

[33] I. Ciufolini and J. Wheeler, "Gravitation and Inertia", Princeton Series in Physics, Princeton university press, 1995, Cap. 6.

[34] R.P. Lano, *Gravitational Meissner effect*, report U.ofIowa 96-4, March 1996.

[35] H. Hayasaka and S. Takeuchi, Phys. Rev. Lett. 63 (1989) 2701.

[36] B. M. Barker and R. F. O'Connell, *The gravitational interaction: spin, rotation and quantum effects - A review*, Gen. Rel. Grav. 11 (1979) 149.

[37] R. F. O'Connell, Phys. Lett. A 32 (1970) 402.

[38] R. F. O'Connell and S. N. Rasband, Nature Phys. Sci. 232 (1971) 193.

[39] A. Peres, Phys. Rev. D 18 (1978) 2739. See also Y. N. Obukhov, *Spin, gravity, and inertia*, report gr-qc/0012102.

[40] R. C. Ritter, L. I. Winkler, and G. T. Gillies, *Search for anomalous spin-dependent forces with a polarized-mass torsion pendulum*, Phys. Rev. Lett. 70 (1993) 701.

[41] H. Wallace, *Method and apparatus for generating a secondary gravitational force field*, US Patent N. 3626605 (1971).

[42] G. A. Ummarino, *Possible alterations of the gravitational field in a superconductor*, report cond-mat/0010399.

[43] S. M. Carroll and G. B. Field, *Consequences of propagating torsion in connection-dynamic theories of gravity*, Phys. Rev. D 50 (1994) 3867.

[44] A. Ye. Akimov and V. Ya. Tarasenko, *Models of polarization states of the physical vacuum and torsion fields*, Izd. Vuzov. Fizika, 1992, Nov. 3, pp. 13-23. See also on the Web: http://www.amasci.com/freenrg/tors/doc17.html.

[45] K. Nordtvedt, Int. J. Theor. Phys. 27 (1988) 1395.

[46] J. F. Woodward, *Laboratory test of Mach's principle and strong-field relativistic gravity*, Found. Phys. Lett. 9 (1996) 247, and references.

[47] D.E. Groom et al. (Particle Data Group), *Review of particle physics*, Eur. Phys. J. **C 15** (2000); http://pdg.lbl.gov.

[48] G. T. Gillies, *The Newtonian gravitational constant: recent measurements and related studies*, Rep. Prog. Phys. 60 (1997) 151-225.

[49] W. Michaelis, H. Haars, and R. Augustin, Metrologia 32, 267 (1995). M. Fitzgerald and T. R. Armstrong, IEEE Trans. on Inst. and Meas. 44, 494 (1995). H. Walesch, H. Meyer, H. Piehl, and J. Schurr, IEEE Trans. on Inst. and Meas. 44, 491 (1995). V.P. Izmailov, O.V. Karagioz, V.A. Kuznetsov, V.N. Mel'nikov, and A.E. Roslyakov, Measurement Techniques 36, 1065 (1993).

[50] N. Arkani-Hamed, S. Dimopoulos, G. Dvali, *The Hierarchy Problem and New Dimensions at a Millimeter*, Phys.Lett. B429 (1998) 263-272.

[51] C.D. Hoyle, U. Schmidt, B.R. Heckel, E.G. Adelberger, J.H. Gundlach, D.J. Kapner, and H.E. Swanson, *Submillimeter Tests of the Gravitational Inverse-Square Law: A Search for "Large" Extra Dimensions*, Phys. Rev. Lett. (to be published).

[52] D. La and P. J. Steinhardt, Phys. Rev. Lett. 62 (1989) 376 for status and references on scalar-tensor gravitational theories. See also S. Calchi Novati, S. Capozziello and G. Lambiase, *Newtonian limit of induced gravity*, report astro-ph/0005104.

[53] J.D. Anderson at al., Phys. Rev. Lett. 81 (1998) 2858; *Study of the anomalous acceleration of Pioneer 10 and 11*, report gr-qc/0104064.

[54] J.P. Mbelek and M. Lachieze-Rey, report gr-qc/9910105.

[55] T. Kuusela, *New measurements with a torsion pendulum during the solar eclipse*, General Relativity and Gravitation, 4, 543-550, 1992. D. C. Mishra, M. B. S. Vyaghreswara Rao, *Temporal variation in gravity field during solar eclipse on 24 October 1995*, Current Science, 72(11), 782-783, 1997. L. A. Savrov, *Experiment with paraconic pendulums during the November 3, 1994 solar eclipse in Brazil*, Measurement Techniques, 40 (6), 511-516, 1997. And references.

[56] Qian-shen Wang et al., *Precise measurement of gravity variations during a total solar eclipse*, Phys. Rev. D 62 (2000) 041101. C.S. Unnikrishnan, A. K. Mohapatra, G.T. Gillies, *Anomalous gravity data during the 1997 total solar eclipse do not support the hypothesis of gravitational shielding*, Phys. Rev. D 63 (2001) 062002.

[57] *New limits on the gravitational Majorana screening from the Zurich G experiment*, C.S. Unnikrishnan, G.T. Gillies, Phys. Rev. D61 (2000) 101101

[58] T. Van Flandern, *Possible new properties of gravity*, Astrophys. Space Sci. 244 (1996) 249, and ref.s.

[59] M. Tonouchi, M. Tani, Z. Wang, K. Sakai, N. Wada, M. Hangyo, *Novel Terahertz Radiation from Flux-Trapped* $YBa_2Cu_3O_{7-\delta}$ *thin Films Excited by Femtosecond Laser Pulses*, Jpn. J. Appl. Phys. Vol. 36 (1997) pp. L93-L95.

[60] M. Hangyo, S. Tomozawa, Y. Murakami, M. Tonouchi, M. Tani, Z. Wang, K. Sakai, S. Nakashima, *Terahertz radiation from superconducting* $YBa_2Cu_3O_{7-\delta}$ *thin films excited by femtosecond optical pulses*, Appl. Phys. Lett. 69 (14), (1996), pp. 2122-2124

Figure Captions

Fig.1 Initial setup of the impulse gravity generator.

Fig.2 Improved variant of the impulse gravity generator.

Fig.3 Discharge chamber of the impulse gravity generator.

Fig.4 Arkadjev-Marx high-voltage pulse generator.

Fig.5 Pendulum in a glass cylinder under vacuum. (The actual cylinder is wide enough to allow a complete oscillation.)

Fig.6 Correlation between the voltage discharge and the deflection of the pendulum.

Fig.7 Impulse recorded by the microphone at a 67 deg. impact angle. Time scale is sampling periods at $f_s = 44.1\ kHz$. There is a 50 Hz noise due to power grid. The signal is unfiltered.

Fig.8. Relative pulse impulse versus impact angle.

This figure "figure1and2.jpg" is available in "jpg" format from:

http://arXiv.org/ps/physics/0108005


This figure "figure3.jpg" is available in "jpg" format from:
http://arXiv.org/ps/physics/0108005

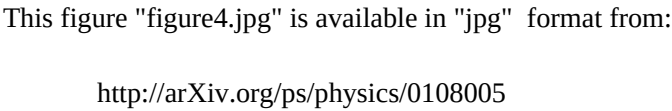
This figure "figure4.jpg" is available in "jpg" format from:
http://arXiv.org/ps/physics/0108005


This figure "figure5.jpg" is available in "jpg" format from:
http://arXiv.org/ps/physics/0108005

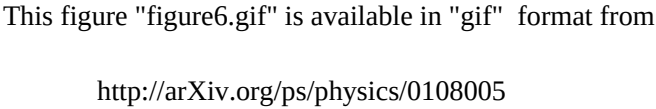
This figure "figure6.gif" is available in "gif" format from:
http://arXiv.org/ps/physics/0108005

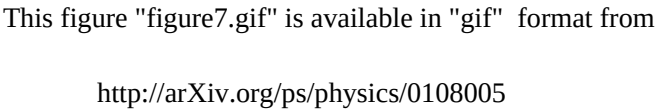
This figure "figure7.gif" is available in "gif" format from:
http://arXiv.org/ps/physics/0108005


This figure "figure8.gif" is available in "gif" format from:
http://arXiv.org/ps/physics/0108005

On the Mechanism for a Gravity Effect using Type II Superconductors

Glen A. Robertson
Advanced Systems and Technology Office, NASA-Marshall Space Flight Center, Huntsville, Alabama 35812

ABSTRACT

In this paper, we formulate a percent mass change equation based on Woodward's transient mass shift and the Cavendish balance equations applied to superconductor Josephson junctions. A correction to the transient mass shift equation is presented due to the emission of the mass energy from the superconductor. The percentage of mass change predicted by the equation was estimated against the maximum percent mass change reported by Podkletnov in his gravity shielding experiments. An experiment is then discussed, which could shed light on the transient mass shift near superconductor and verify the corrected gravitational potential.

INTRODUCTION

Eugene Podkletnov has reported that a gravity shielding effect was seen above a YBCO superconductor being rotated by a magnetic field and irradiated by RF energy.[1] The mechanism for this phenomenon is as debatable as the test itself. Independent of Podkletnov and about the same time, Torr and Li published several papers on the possible connection between gravity and superconductors.[2-4] These papers suggest that the gravity mechanism arise from the spin of the lattice ions aligned by an applied magnetic field. In 1995, Becker a student of Torr, showed mathematically that a significant size gravito-magnetic field could exist along with a magnetic field whenever there is flux pinning or other forms of flux trapping in a type II superconductor.[5] Modanese, a close contact to Podkletnov, has presented a theoretical model from Podkletnov's experimental results.[6]. The model, which is based on the "anomalous" coupling between Bose condensate and the gravitational field, suggests that the essential ingredient for the shielding is the presence of strong variations or fluctuations of the Cooper pair density in the disk.

The behavior of the Bose condensate of Cooper pairs within superconducting materials in an external gravitational field has been the subject of some study in the past.[7] M. Casas, etal, recently suggested that Cooper pairs lead to Bose condensation at temperatures substantially greater than those of the BCS theory of superconductivity.[8] In an unpublished paper presented to the author for review, Noever and Bremner suggest such a connection by indicating that superconductors could modulate the background quantum ZPF.[9] Stirniman presents a related historical overview leading up to gravity's relationship to the superconductor.[10] Other papers have even suggested a connection between gravity and electrons.[11,12]

In this paper, it is suggested that a combination of flux pinning and Cooper pair fluctuating across Josephson junctions produce a mass change about the superconductor. An equation for the mass energy produced across the Josephson junctions and an equation for the percentage of mass change is derived from Woodward's transient mass shift equation.[13] A correction to the gravitational potential Woodward used in the equation is presented. The correction implies the emission of mass energy from the superconductor. The percentage of mass change predicted by this equation was estimated against the maximum percent mass change reported by Podkletnov in his gravity shielding experiments. An experiment is then discussed, which could shed light on the transient mass shift near superconductor and verify the corrected gravitational potential.

BACKGROUND

Of what is known of the type II, YBCO superconductor disk used in the Podkletnov experiments; it seems certain that a large number of superconductor-oxide-superconductor Josephson junctions exist within the disk. In the general sense, Josephson junctions are very small capacitors with the electrodes composed of superconductor material and the dielectric composed of an oxide layer.[14, pg. 196-286] Unlike normal capacitors, Josephson junctions exhibit a unique property. They radiate RF energy when traversed by a current and generate a current when radiated with RF energy. This would indicate a fluctuation of energy across the junction.

With this in mind, it must be noted that the procedure for making the superconductor disk, including the pressing and sintering of varying size SC grains, produces a structure having many flux pinning sites around which exist the Josephson junctions. Flux pinning is a well-known phenomenon associated with Type II superconductors where magnetic flux is trapped inside a superconductor. Flux pinning results from any spatial inhomogeneity of the material, such as impurities, grain boundaries, voids, etc. To be most effective, these inhomogeneities must be on the scale of the order of the penetration depth or the coherence length, i.e. $\sim 10^{-6}$ to 10^{-5} cm, rather than on the atomic scale where inhomogeneity causes electronic scattering which limits the mean free path.[14, pg. 166] This so happens to be in the range of the size superconductor powders used to make Podkletnov's disks.

In order for the magnetic flux to remain trapped, a current loop forms around the holes created by the superconductor particles. It would therefore seem that Podkletnov has produced a device that allows flux pinning to enhance the production of RF energy and RF energy to enhance the production of superconductor currents. These reinforcing phenomena should lead to high electron densities or super currents in the superconductor disk. These currents are focused between the superconductor particles, which are Josephson junction sites.

TRANSIENT MASS SHIFT

During a review of current literature for clues on the connection between mass energy and superconductors, it was found that Woodward, who has done some very interesting work with capacitors, both theoretically and experimentally, has come up with an equation for a transient mass shift derive from Mach's Principle.[13] Mach's Principle explains inertia – the tendency of an object to resist acceleration – by the sum of the gravitational attractions of all objects in the universe. Woodward presented the transient mass shift dm_0 as

$$\partial m_0 = \frac{\beta w P_0}{2\pi G \rho_0 c^2} \qquad (1)$$

Where dm_0 is the transient mass shift; β is the ratio ϕ / c^2 (ϕ is the gravitational potential due to all the matter of the universe) and is approximately 1 and unitless; w is the frequency of the driving voltage into the capacitors in radians per second; P_0 is the power applied to the capacitors in ergs/s (10^7 ergs/s = 1 Watt); G is the gravitational constant = 6.67×10^{-8} dyne cm^2/gm^2; ρ_0 is the density of the capacitors; and c is the velocity of light in cm / s = 300×10^8 cm/s.

A Cavendish balance, which is routinely used to measure the gravitational constant G allows for the expression of G in terms of measurable quantities, which are

$$G = \phi \frac{b^2 l}{8M}\left(\frac{2\pi}{T}\right)^2 \tag{2}$$

Where M is the test mass (superconductor), b is the distance between the center of a known mass m and the test mass M, l is the separation distance of the masses m on a torsion bar, T is the period of the damped harmonic motion of the torsion bar, and ϕ is the angular displacement of the torsion bar caused by the motion of the test masses. Note that the result is independent of the value of m and can be written in the following simplified form

$$\phi = T_C GM \tag{3}$$

Where $T_C = (8/b^2 l)(T/2\pi)^2$ is a proportionality constant associated with the torsion balance characteristics.

If perceptible transient mass shift could be demonstrated with a Cavendish balance, the change in the measured angular displacement of the torsion fiber will be directly proportional to the test mass change, assuming the gravitational constant is unaltered. For example, the change in angular displacement $d\phi$ associated with an effective change in test mass dM due to gravitational modification is given by

$$\partial\phi = T_C G \partial M \tag{4}$$

By combining equations 4 with equation 1, the change $d\phi$ in the angular displacement ϕ due to a mass change dM can be expressed in engineering terms as

$$\partial\phi = \frac{T_C \beta f_i P_i}{\rho_0 c^2} \tag{6}$$

Where f_i is the frequency (in Hz) of the effective input power P_i (in watts).

By setting equation 3 equal to equation 4 through the constant $T_C G$, a relationship between the two angular displacements and the masses can be made. From this relationship, a percent change in mass can be expressed by

$$M\% = \frac{\partial M}{M} * 100 = \frac{\partial\phi}{\phi} * 100 \tag{7}$$

Using $d\phi$ as defined by equation 6 and ϕ as defined by equation 3, the percent change in mass can be expressed as

$$M\% = \left[\frac{\beta f_i P_i}{GM\rho_0 c^2}\right] * 100 \tag{8}$$

In the Podkletnov experiments, the percent change in mass of an object placed above the superconductor disk was maximized at 2%. Assuming the same for equation 8, then $M\rho_0$ is on the order of 10^{12} kg^2/m^3 with $f_i = 10^6$ Hz and $P_i = 100$ watts. Then it is easily seen that this equation does not make much sense if $M\rho_0$ is that of a typical mass and mass density of a YBCO superconductor ($M \sim 2$ kg and $\rho_0 \sim 50$ kg/m3). Therefore, what are these quantities? It is argued that the mass change is due to electrons, which somehow affects the total mass. It is then stated that in the superconductor ρ_0 is the density of the superconductor (given by ρ_{sc}) and M is the mass of the electrons (given by M_e) involved in the phenomena given by

$$M_e = \frac{I_{ij}\overrightarrow{A_{ij}}}{f_{ij}\left(\frac{q_e}{m_e}\right)} \tag{9}$$

Where I_{jj} is the current per area associated with the superconductor Josephson junctions, A_{jj} is the sum of the magnitudes of the normal vector to the cross sectional area of the Josephson junctions, f_{jj} is the Josephson junction frequency, and q_e/m_e is the ratio of charge to mass of an electron (= 1.759×10^{11} coulombs/kg). By incorporating equation 9 into equation 8, then for a superconductor with Josephson junction sites, equation 8 is rewritten as

$$M_{sc}\% = \left[\frac{\beta f_i f_{jj} P_i \left(\frac{q_e}{m_e} \right)}{G I_{jj} A_{jj} \rho_{sc} c^2} \right] * 100 \qquad (10)$$

Given the analysis, from which equation 10 was derived, the transient mass shift expression in equation 1 is modified for the superconductor to produce an energy E_{sc} equation as

$$\partial m_e c^2 = E_{sc} = \frac{\beta f_i P_i}{G \rho_{sc}} \qquad (11)$$

Where E_{sc} is the energy released during the mass change of the superconductor. Letting $f_i = 10^6$ Hz, $P_i = 100$ watts, $\rho_{sc} = 48$ kg/m^3, $G = 6.673 \times 10^{-11}$ N m^2/kg^2, the mass energy radiated by the motion of the electrons across the Josephson junctions is about 10^{16} Joules. Noting that 1 Watt = 1 Joule/s, then the emitted power P_{sc} associated with the mass energy E_{sc} emission can be expressed as

$$P_{sc} = f_{jj} * E_{sc} = \left(\frac{\beta}{G} \right) \left(f_i P_i \right) \left(\frac{f_{jj}}{\rho_{sc}} \right) \qquad (12)$$

The frequency f_{jj} of the electrons fluctuating across the Josephson junctions is used. Since, the mass energy is being created at this frequency. Letting $f_i = f_{jj}$, the Power P_{sc} emitted is about 10^{22} Watts. How can 100-Watts input produce 10^{22}-Watts output? It is argued that the gravitational potential ϕ about the superconductor is changed due to the emission of the mass energy (E_{sc}). This change results in a change (Δ) in the dimensionless constant β, expressed as

$$\Delta\beta = \left(\frac{\phi + \partial\phi}{c^2} \right) = \frac{\alpha}{c^2} \qquad (13)$$

Where α is defined as the new gravitational potential due to the emission of mass energy E_{sc} from the superconductor. Redefining β in equation 10 with $\Delta\beta$ in equation 13 and regrouping the terms, equation 10 can be simplified in terms of the power input and the superconductor properties as

$$M_{sc}\% = \gamma_k * [f_i P_i] * \left[\frac{\alpha f_{jj}}{I_c A_{jj} \rho_{sc}} \right] * 100 \qquad (14)$$

Where $\gamma_k = (q_e/m_e)/(Gc^4)$. Now an approximation of the percent mass change in terms of input power and the superconductor can be made. The estimation is presented in figure 1 where $\alpha = .03$, $q_e/m_e = 1.7588 \times 10^{11}$ C/kg, G = 6.673 x 10-11 N m^2/kg^2, $c = 2.9979 \times 10^8$ m/s, $f_i = f_{jj} = 10^6$ Hz, $\rho_{sc} = 48$ kg/m^3, and $I_{jj} = 10^3$ amps/cm^2, $A_{jj} = 0.001$ cm^2. The term α was chosen to make $P_{sc} \sim 100$ Watts and the magnitude A_{jj} of the Josephson junction cross-sectional area was chosen to make the 2% mass change fall at 100 watts.

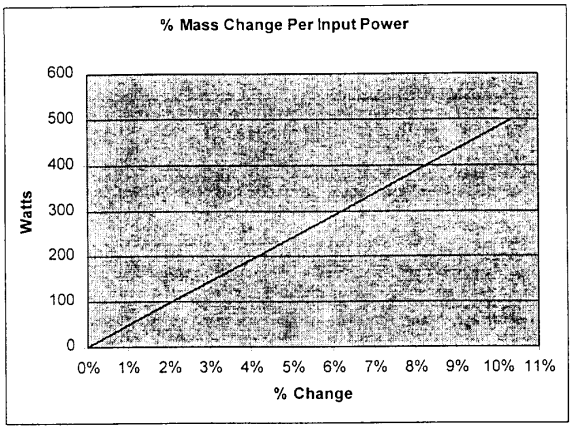

Figure 1

TESTING FOR A TRANSIENT MASS SHIFT

The corrected gravitational potential α can be perceived as the only unknown in equation 14. However, the values for I_{jj} and A_{jj} were chosen to fit the predetermined notion of Podkletnov's experiment. With this in mind, the ratio $\alpha/(I_{jj} A_{jj})$ is the real term in question with respect to a transient mass shift about a superconductor as just changing one of these terms without changing the others could implies an energy loss or gain. Reproduction of the YBCO disk used in Podkletnov's experiments should lead to reasonable values for I_{jj} and A_{jj}. In addition, the direction of the vector sum of the magnitude of A_{jj} should be predominately in the plane perpendicular to the direction of the pressuring force applied to make the disk. The pressing plane used to make Podkletnov's disks was in the plane of rotation, which is perpendicular to the effective force seen on the test masses. Given this assumption the pointing vector associated with the Josephson junctions would be in an upward or downward direction. Due to the two-layer arrangement of the disk and the fact that no change in mass was seen for a mass placed below the disk, it is argued that it is upward. Also worth mentioning is that I_{jj} was chosen for this estimate as the critical current density of small grain YBCO superconductors produced by the author. It may very well be that I_{jj} is the current density across the junction and not the critical current of the superconductor grains.

Utilizing the previous equations, the ratio $\alpha/(I_{jj} A_{jj})$ can be defined in measurable terms as

$$\frac{\alpha}{I_{jj} A_{jj}} = \frac{1}{\gamma_k} * \left[\frac{\rho_{sc}}{f_i f_{jj} P_i} \right] \frac{\partial \phi}{\phi} \qquad (15)$$

Where $d\phi/\phi$ can be experimentally derived using a properly designed Cavendish balance. Figure 2 shows the effect on the transient mass shift changes with the ratio $\alpha/(I_c A_{jj})$ (= 0.003, 0.03 & 0.3). As seen, percent mass change is very sensitive to this ratio.

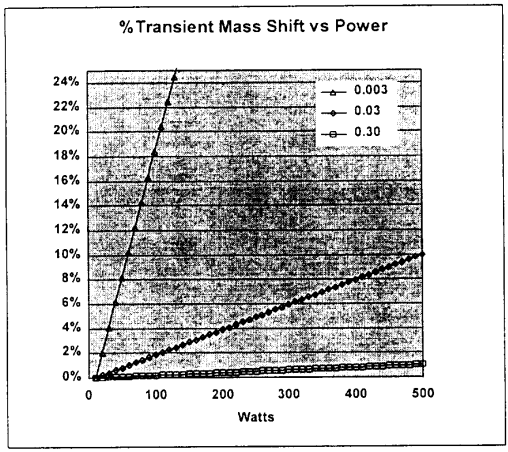

Figure 2

Such an experiment would utilize properly constructed high-Tc oxide superconductors containing multiple Josephson junction sites between superconductor grains. The fabrication of the superconductor would be such that the pressing force was applied perpendicular to the applied magnetic field. This will insure alignment of the Josephson junction predominately in the plane of the magnetic field. Cooper pair super-currents would then be induced across the many Josephson junction sites that are distributed about the flux pinning vortices and modulated by the RF input. A sketch of the proposed experiment is given in Fig. 3. As shown, U-shaped permanent magnets with poles of high field, rare-earth permanent magnets are arranged such that the magnetic field is through a high-T_c oxide superconductor like YBCO. The RF coils are shown for representation. The actual configuration may vary dependent on the frequency required.

From equation 4, an estimate the sensitivity to a transient mass change can be made by making reasonable assumptions for the various balance parameters. Based on the published characteristics of commercially available Cavendish balances, where T = 120 sec; l = 30 cm; b = 3 cm a numerical estimate for the sensitivity is given as

$$\frac{\partial \phi}{\partial M} = 0.7 \text{ microradians / gram} \tag{5}$$

Thus, the sensitivity of a Cavendish balance to small transient mass change effects is generally somewhat limited, and successful detection of these effects will require painstaking efforts in the design and fabrication of the instrument. It will be necessary to push every parameter toward its extreme values in order to achieve the highest possible sensitivity. For example, for a 500 gram superconductor test mass, where the density of the YBCO ceramic is approximately 4.8 gram/cm^3, then a 1% change in effective mass (dM = 5 grams) due to transient mass change effects would yield a torsional displacement of $d\phi$ = 3.5 microradians. This is within the established sensitivity of state-of-the-art torsional displacement transducers, which can easily resolve displacements of less than 1 microradian. Such a Cavendish balance is commercially available from Tel-Atomic.

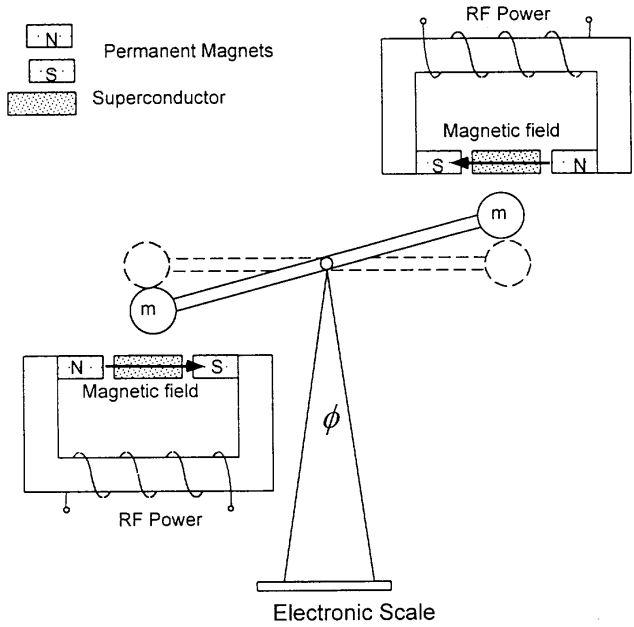

Figure 3

CONCLUSION

Much of the material presented in this paper is clearly hypothetical. The equations are a first order approximation that needs further refinement. For example, the corrected gravitation potential α may also involve an efficiency of the power inputted into the superconductor or the conversion of the power to currents across the Josephson junctions. Although, should a transient mass shift be seen by the described experiment. It would provide the necessary foundation for further work in this area.

This research was supported in part by NASA's Advanced Space Transportation Research, Breakthrough Propulsion Physics. The author wishes to thank R. Litchford for help in the sensitivity analysis of the Cavendish balance and R. Koczor, W. Brantley, and J. Cole for helpful discussions.

References

1. Podkletnov, E. and Nieminen, R. , "A Possibility of Gravitational Force Shielding by Bulk Yba2Cu3O7-x Superconductor," Physica C, C203, 441-444, 1992 and Podkletnov, E. E., "Weak gravitation shielding properties of composite bulk YBa_2Cu_3O_{7-x} superconductor below 70 K under e.m. field," Published on the web at http://xxx.lanl.gov/abs/cond-mat/9701074/
2. N. Li and D. G. Torr, "Gravitational effects on the magnetic attenuation of superconductors," *Phys. Rev. B*, Vol. 46, 1992, p. 5489.
3. N. Li and D. G. Torr, *Phys. Rev. D*, Vol. 43, 1990, p. 457.
4. D. G. Torr and N. Li, "Gravito-Electric Coupling Via Superconductivity," *Found. Phys. Lett.*, Vol. 6, 1993, p. 371
5. Robert Becker, Paul Smith, and Heffrey Bertrand, "Proposal for the Experimental Detection of Gravitomagnetism in the Terrestrial Laboratory," September 1995, Published on the web at http://www.inetarena.com/~noetic/pls/RBecker/Gmexp2.htm
6. Giovanni Modanese, "On the theoretical interpretation of E. Podkletnov's experiment," LANL gr-qc/9612022, Presented for the World Congress of the International Astronautical Federation, 1997, nr. IAA-97-4.1.07. and G. Modanese, "Gravitational Anomalies by HTC superconductors: a 1999 Theoretical Status Report," Published on the web at http://www.gravity.org/nat.htm
7. D. K. Ross, J. Phys. A 16, 1331, 1983, J. Anandan, Class. Q. Grav. 11, A23, 1994 and references.
8. M. Casas, Rigo, A., de Llano, M.,Rojo, O., Solis, M. A., "Bose-Eistein condensation with a BCS model interaction," Physics Letters A, Vol. 245, pg. 55-61, 1998.
9. David Noever, and Bremner, Christopher, "Large-Scale Sakharov Condition," Not published.
10. Robert Stirniman, "The Wallace Inventions, Spin Aligned Nuclei, the Gravitomagnetic Field, and the Tampere 'Gravity-Shielding" Experiment: Is There a Connection?" Published on the web at http://www.padrak.com/agn/WALLACE.html
11. Cornille Patrick, "Electrostatic Pendulum Experiment which Pumps Energy from the Ether, Published on the web at http://members.aol.com/overunity/elecpexp/elecpexp.html
12. Nils Rognerud, "On the Electromagnetic Nature of Gravity," Published on the web at http://www.best.com/~rognerud/html/axioms.html
13. "James F. Woodward: Mach's Principle Weight Reduction = Propellantless Propulsion," (A summary from Foundation of Physics Letters, Vol. 9, No. 3, (1996), pg. 247 – 293. Published on the web at http://www.inetarena.com/~noetic/pls/woodward.html
14. Tinkham, Michael and Gordan McKay, "Introduction to Superconductivity," McGraw-Hill, Inc., pg. 196-286, 1996.
15. "Physicists Condense Supercooled Atoms, Forming New State of Matter," Encarta Yearbook, August 1995. Published on the web at http://encarta.one.microsoft.com/enarta

Stan Deyo: Stream of Consciousness

SPIN & ANTIGRAVITY EFFECTS IN TOROIDAL COILS

Written By Stan Deyo, May 2005 (Compiled by Tim Ventura)

The inductor core was square-sectioned and hollow.... the coils were coaxial and only one turn deep. The first coil was wound with a right twist while the other coil was wound with a left twist. The result formed an "X" pattern where the two coils overlaid. The inductor core had an air gap in it.

Two other flat wire coils were placed at opposite sides of the main coils and then bent over the toroid to form the field navigation mechanism. All power was pulsed DC and the 30 foot diameter coils made a field reach out about 800 feet in diameter.

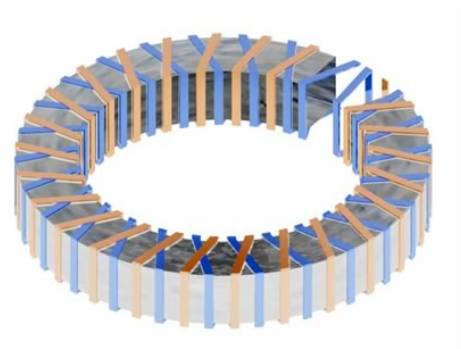

Two other flat wire coils were placed at opposite sides of the main coils and then bent over the toroid to form the field navigation mechanism. All power was pulsed DC and the 30 foot diameter coils made a field reach out about 800 feet in diameter.

I was shown the toroidal field coils of the joint scientific group that discovered it back in the late fifties. They used flat wire in their two coils. They were positioned differently to the Telos experiment though.

The inductor core was square-sectioned and hollow.... the coils were coaxial and only one turn deep. The first coil was wound with a right twist while the other coil was wound with a left twist. The result formed an "X" pattern where the two coils overlaid. The inductor core had an air gap in it.

Two other flat wire coils were placed at opposite sides of the main coils and then bent over the toroid to form the field navigation mechanism. All power was pulsed DC and the 30 foot diameter coils made a field reach out about 800 feet in diameter.

As for the Lazarus project, I am aware of the research although I can't recall hearing the project name. The energy source was from infrared frequencies which were converted to electric charge using a triboluminescent oxide that reacts in the infrared range. This substance releases electrons when exposed to the infrared range of radiation. It is a way to convert nuclear energies (spin, translation and radiation) directly into moving electrons.

Space/time can be altered by putting mass inside a dynamic EM field created by two pulsed, DC, toroidal coils which act as a "flux capacitor" (Faraday's dream). A charge capacitor by definition can be static (qq'/s); however as flux is a function of current which is moving or dynamic charge, the flux capacitor has to be a dynamic circuit which stores the energy (qq's/t). To do this, the current must be added into a chase-tail circuit whereby the layers of the field stack one upon the other to form a field in motion. The currents flow in one direction in each coil but are separated by a timing/vector factor so that they do not interfere with each other. The coils are wrapped of flat bar about 6 inches wide by

1/2 inch thick. they are then wrapped at ninety angles to each other and the current is pulsed first one then the other. The timing of the pulses allows the current to create an apparently perfect inductor with zero resistance (although it is not truly zero since it does radiate energy).

Inside this field in a small craft of about 30-feet diameter, one will experience a peculiar distortion of space/time. This occurs when the field inside the craft is "pumped up" so that the energy density of the space inside the field is much greater than that of normal space here on the Earth's surface. The higher the energy density the more time is dilated so that time in the field occurs at a slower rate to that outside the field. If the energy density is lowered then the converse is true.

An hour in the field of higher density might be a few days outside the field. This is because time is measured as a ratio of lengths. Time has no real dimension when comparing energy density states. It becomes relativistic... a ratio. We compare distances travelled (whether linear, curved or angular) to establish "time" units. A second can be related to distances travelled by a pendulum, a vibrating crystal or even a decaying atomic structure - but they are all relative distances when one compares them as time. When your watch crystal has vibrated "n" times it has covered "x" distance. While it has covered that distance something else has covered another distance (whether it be as atomic structures spinning or in the movement of larger or macro-atomic structures). If one says he has travelled 1 mile in 1 second then he is comparing the change of his energy state and position to the distance the crystal has vibrated while he travelled..... Time is a pure ratio of lengths in the relativistic mass-length-time (mlt) system.

One can theoretically transcend the "light barrier" by using asymmetric propulsion concepts. The barrier only exists (like the sound barrier) when one uses symmetric or Newtonian propulsion systems to "push" through an environment. The linear form of the Michelson-Morley experiment was performed many times and in the later tests a rotational version of the experiment proved the existence of an aether 'fluid'. I explain the error in the linear version of their experiment in my book, "The Cosmic Conspiracy." It was a simple mistake. However, until one learns the concept of asymmetric acceleration through a fluid or a field, one cannot hope to engineer a hyper-light velocity system.

Lorentz and Fitzgerald created a transform factor after wrongly interpreting the results of the linear Michelson-Morley experiment. Their transform was to bring the apparently observed limit velocity into the Newtonian world. Einstein used their transform to derive E=MC^2. This can be shown using basic algebra as I have done in an appendix to my aforementioned book. Using this transform creates an artificial barrier ahead of any object shoving its way through a mass. They did not allow for asymmetric propulsion...

To travel faster than the speed of sound in our atmosphere without creating a sonic boom, one only needs to propel one's craft creating a reduced pressure zone ahead of the craft so that it never pushes the air ahead of it. As hard as this is to believe, the bumblebee, one species of the salmon and a human playing with a garden hose in wet sand or a bucket of water all use asymmetric propulsion. It is totally opposite to all standard thrust-reaction methods of propulsion. It generates motion by entrainment. Where one uses a continuos column of energy pushed in the opposite direction to the intended direction of travel, asymmetric propulsion uses a pulsed thin film pushed ahead in the intended direction of travel. Where one shoves its way ahead, the other is accepted into a lower pressure area....

Think about this... if one pulses a thin film of energy ahead and then accepts a portion of the wake of that pulse into the side of the craft so that its energy can supplement the energy of the next pulse, then one can achieve huge speeds with increasingly less energy required from the prime mover of the craft. It is a totally radical approach to propulsion but it works better than Roddenberry could have hoped for... The field does create a warp around the craft and it does allow for speeds way beyond "C".... way beyond.

In one of his UFO research books, Major Keyhoe mentioned the name of a mystery man in the government who seemed to be in the middle of all the US testing of the "new" antigravity" craft. Major Keyhoe overheard the man's last name as, "Lorenzo".

For years people have assumed there was a mystery man named "Lorenzo".... but those of us inside the propulsion program have laughed at this misconception. You see, the name Keyhoe overhead was not "Lorenzo". It was "Lorentz-O". That is what the original dynamic plasma saucercraft made by Americans was named. This is because the hot, air plasma that moved out, around and back through the saucercraft was accelerated by the Lorentz Force generated by current in the toroidal field coils. The Lorentz-O was the charged, doughnut-shaped, plasma flow around the craft that looked like a glowing smoke ring.

You can see the Lorentz Force in action using a glass of salt water, a copper or aluminum strip bent into a cylinder, a nail and a DC current source of 20 amps or so (like an electric arc welder) and a strong permanent magnet. Place the cylinder of metal in the glass of salt water. Connect one side of the DC source to this cylinder. Place the strong magnet near the side of the glass but not in the water. Connect the nail to the other lead.

CAUTION: the water will heat up rapidly. It will start to ionize and spin bubbles relative to the magnet. This is a crude low-temperature plasma experiment - but it will produce hot water almost explosively and should executed with great care.

I used a large speaker magnet with a hole in it. I then used a quartz tube which fit through the hole. This was as close as I could make the example to the original design of the plasma-dynamic saucer craft that our group developed in the black project. With this configuration the water will spin around inside the tube like a hot tornado.

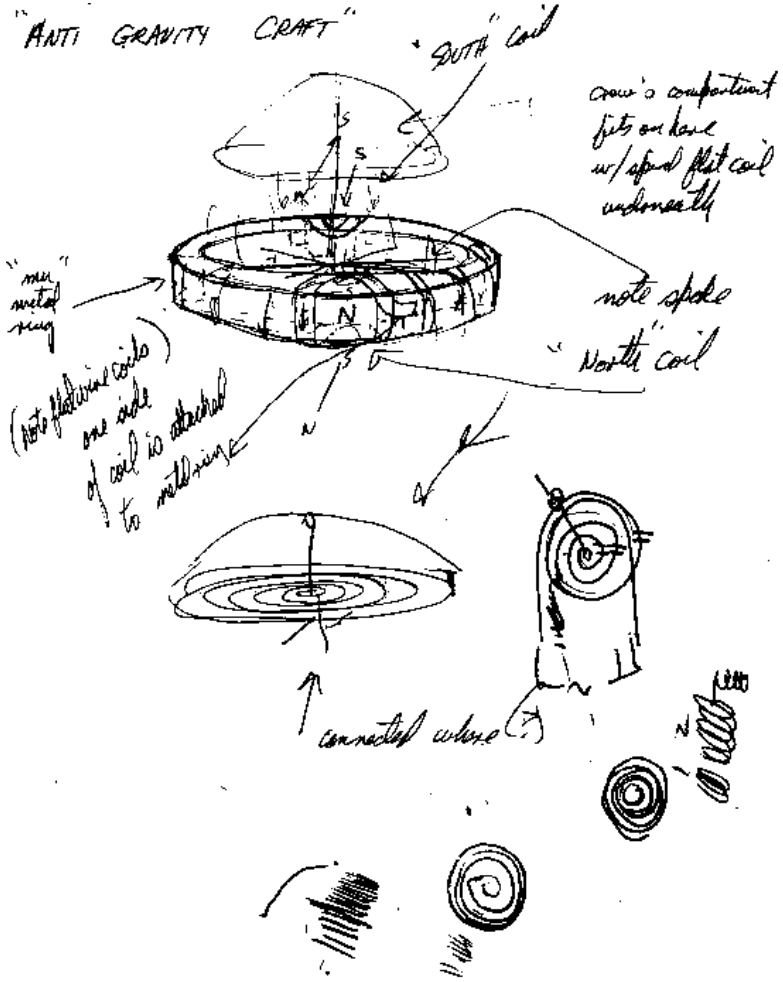

Theory Drawing of electro-gravitic craft I saw in assembly area

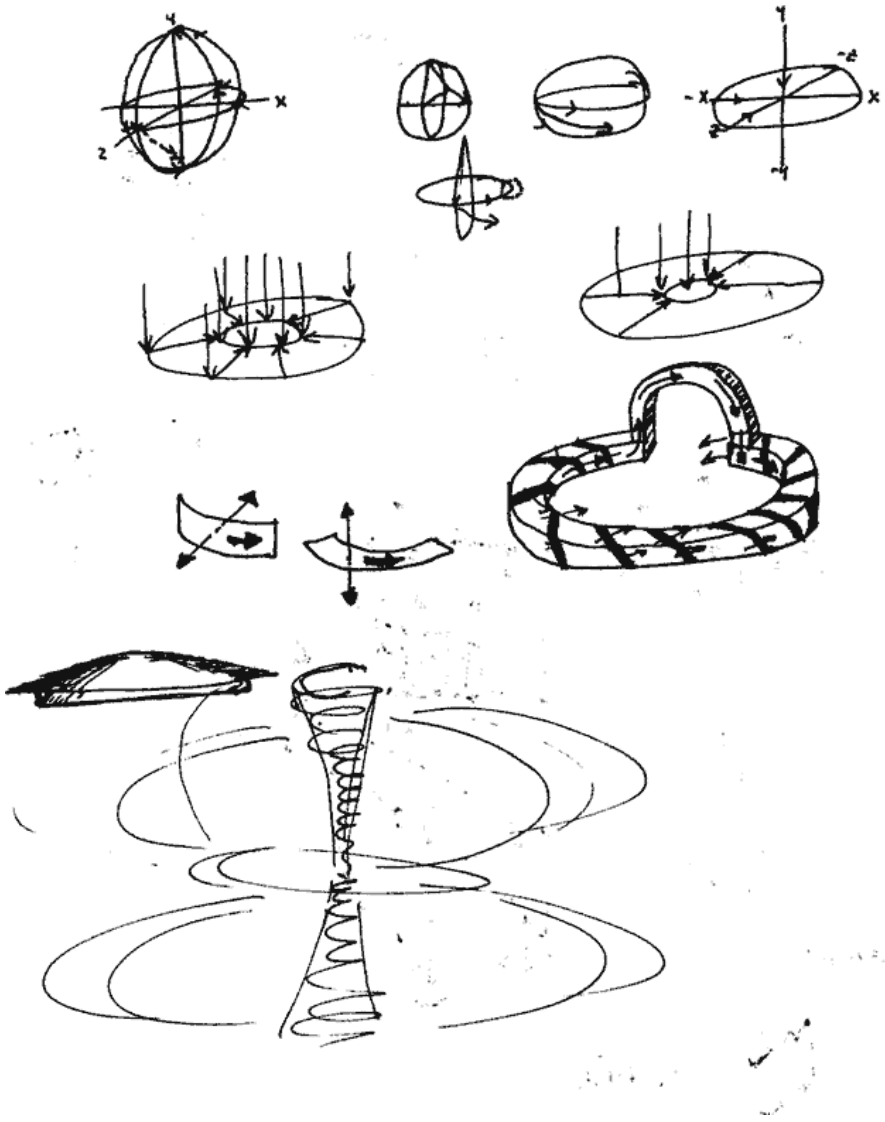

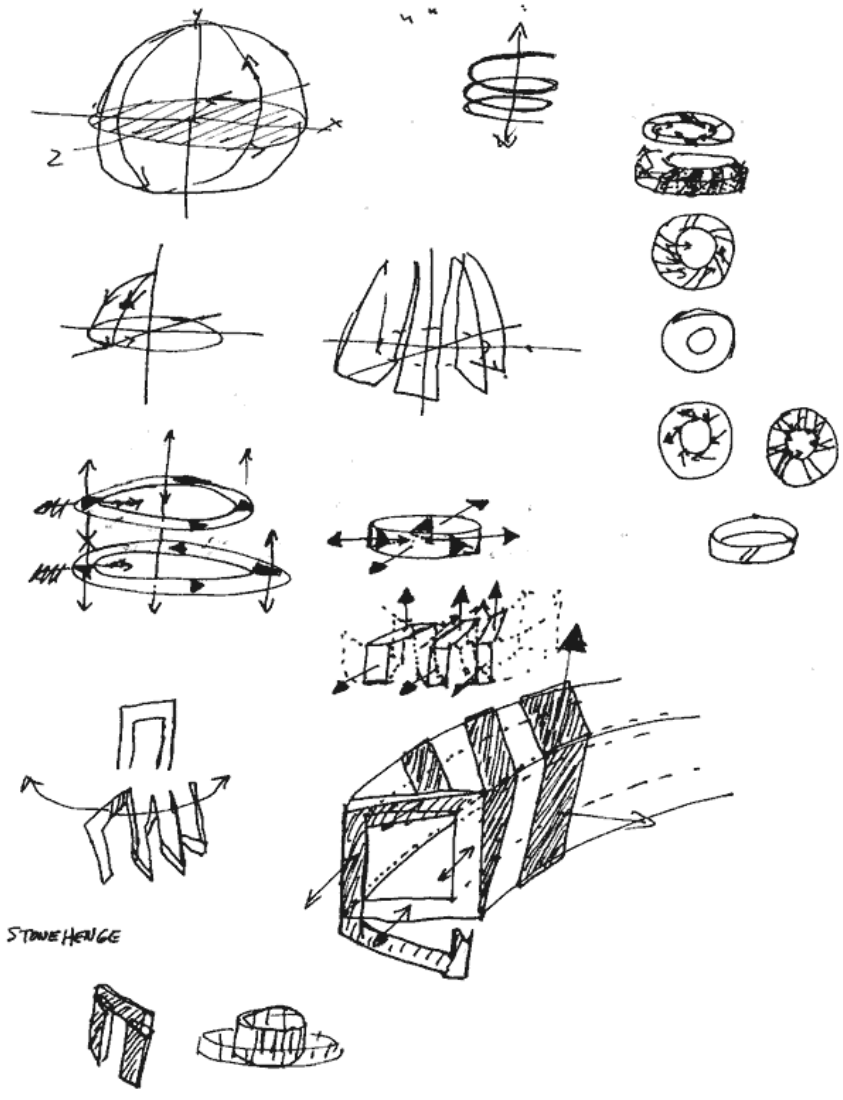
STONEHENGE

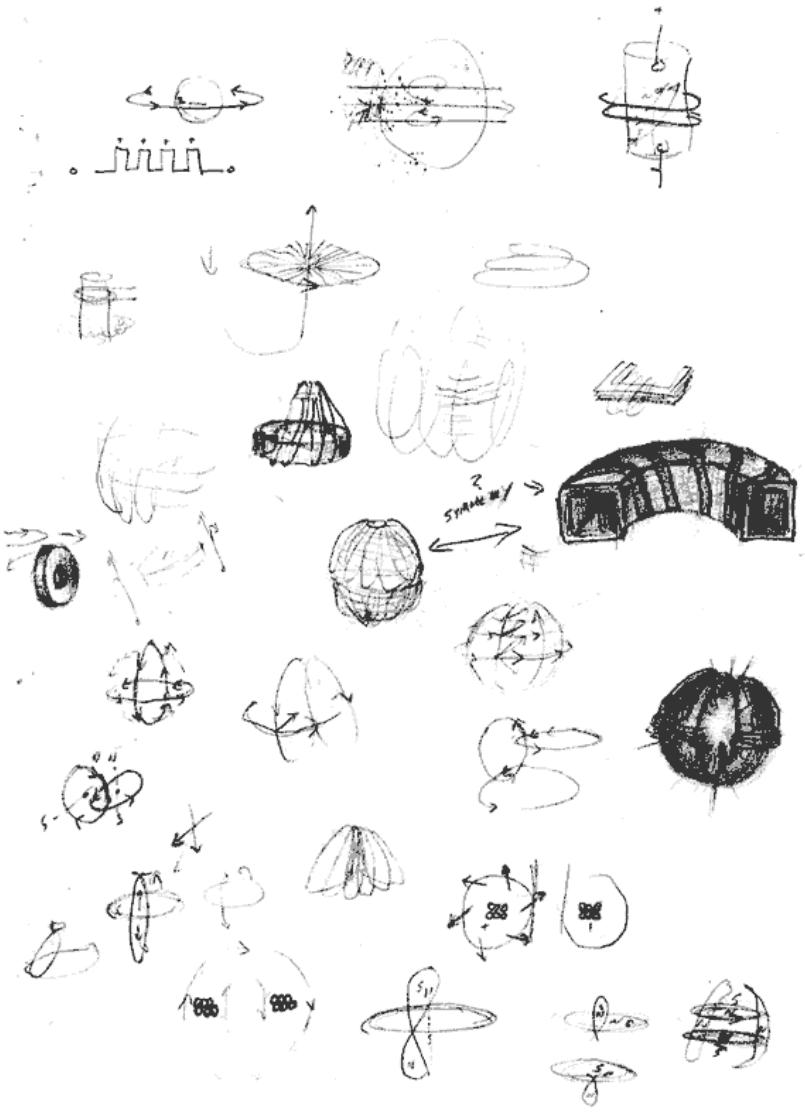

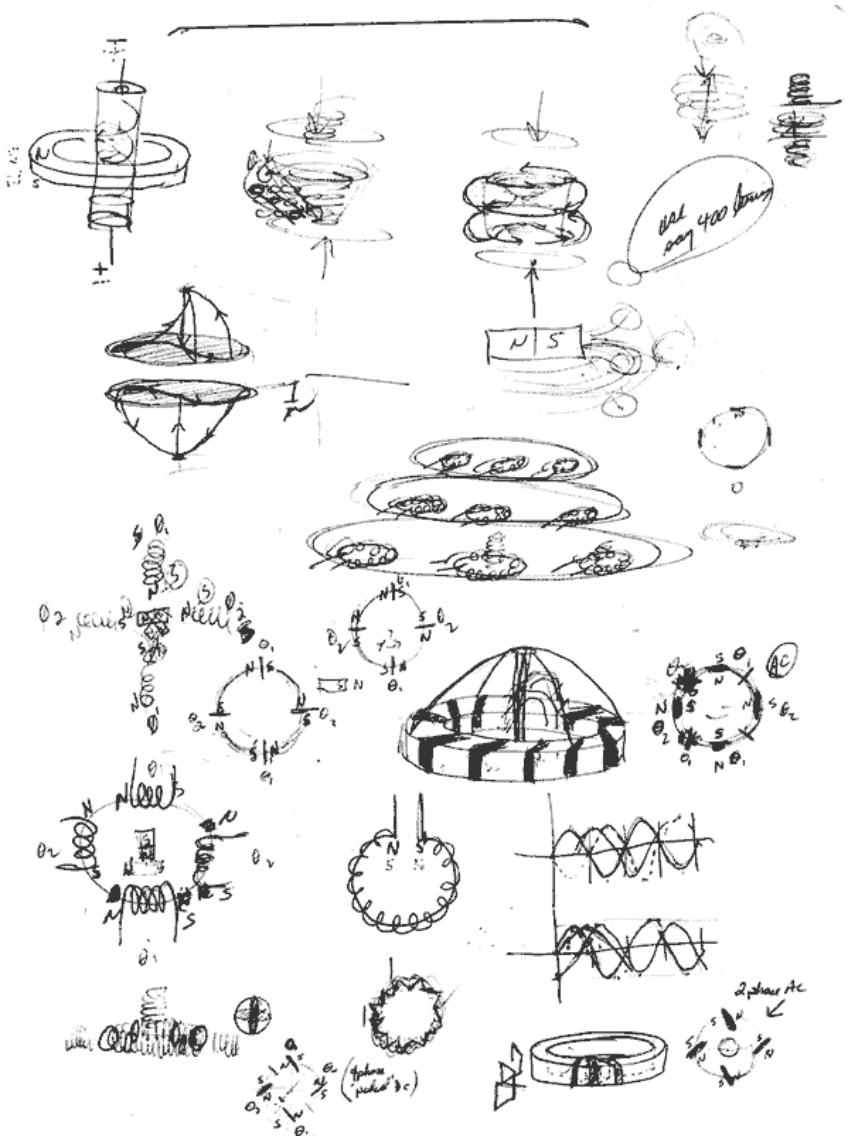
N S
2 phase AC

Negative Gravitational Mass in a Superfluid Bose-Einstein Condensate

Fran De Aquino
Professor Emeritus of Physics, Maranhao State University, UEMA.
Titular Researcher (R) of National Institute for Space Research, INPE

Newton's 2nd law of motion tells us that objects accelerate in the same direction as the applied force. However, recently it was shown experimentally that a Superfluid Bose-Einstein Condensate (BEC) accelerates in the *opposite direction* of the applied force, due to the inertial mass of the BEC becoming *negative* at the specifics conditions of the mentioned experiment. Here we show that is not the inertial mass but the *gravitational mass* of the BEC that becomes *negative*, due to the electromagnetic energy absorbed from the trap and the Raman beams used in the experimental set-up. This finding can be highly relevant to the gravitation theory.

Key words: Negative Gravitational Mass, Bose-Einstein Condensates, Superfluids.

1. Introduction

A recent paper described an experiment that shows a Superfluid Bose-Einstein Condensate (BEC) with *negative* mass, and accelerating in the *opposite direction* of an applied force [1]. The experiment starts with a BEC of approximately 10^5 ^{87}Rb atoms confined in a cigar-shaped trap oriented along the x-axis of a far-detuned crossed dipole trap. Using an adiabatic loading procedure, the BEC is initially prepared such that it occupies the lowest minimum of the lower spin-orbit coupled (SOC) BEC. By suddenly switching off one of the two dipole *trap beams*, the condensate is allowed to spread out along the x-axis. Then, the BEC is imaged in-situ for expansion times of 0, 10 and 14 ms. In the negative x-direction, the BEC encounters an essentially parabolic dispersion, while in the positive x-direction, it enters a *negative mass* region. This leads to a marked asymmetry in the expansion.

Obviously, *negative mass* does not mean *anti-matter*. Anti-matter is simply matter which has the opposite electric charge from normal matter, whereas negative mass means more exactly *negative gravitational mass*. If one particle had ordinary positive gravitational mass, and one had *negative* gravitational mass, then the gravitational force between the masses would be *repulsive* differently of in the case of two positive gravitational masses where the force would be of attraction.

In this article, we show that is not the inertial mass but the *gravitational mass* of the BEC that becomes *negative*, due to the electromagnetic energy absorbed from the trap and the Raman beams used in the experimental set-up. The consequences of this finding can be highly relevant to the gravitation theory.

2. Theory

Some years ago I wrote a paper [2] where a correlation between gravitational mass and inertial mass was obtained. In the paper I pointed out that the relationship between gravitational mass, m_g, and *rest* inertial mass, m_{i0}, is given by

$$\chi = \frac{m_g}{m_{i0}} = \left\{1 - 2\left[\sqrt{1+\left(\frac{Un_r}{m_{i0}c^2}\right)^2} - 1\right]\right\} \qquad (1)$$

where U is *the electromagnetic energy absorbed or emitted by the particle;* $n_r = c/v$ is the index of refraction of the particle; c is the speed of light.

Equation (1) can be rewritten as follows

$$\chi = \frac{m_g}{m_{i0}} = \left\{1 - 2\left[\sqrt{1+\left(\frac{W}{\rho c\ v}\right)^2} - 1\right]\right\} \qquad (2)$$

where ρ is the matter density, v is the velocity of radiation through the particle, and W is the density of absorbed electromagnetic energy. Substitution of the well-known relation $W = 4D/v$ into Eq. (2) yields

$$\chi = \frac{m_g}{m_{i0}} = \left\{1 - 2\left[\sqrt{1+\left(\frac{4D}{\rho c v^2}\right)^2} - 1\right]\right\} \qquad (3)$$

where D is the power density of the radiation *absorbed* by the particle.

In order to apply the Eq. (3) to the BEC previously mentioned, we start calculating the *rest* inertial mass of the BEC, which is given by

$$m_{i0(BEC)} \cong 1\times10^5\left(86.909187\times1.66\times10^{-27}\,kg\right) =$$

$$= 1.4\times10^{-20}\,kg$$

Assuming that the average radius of the BEC is approximately 40 μm (See reference [1]), then we can calculate the density of the BEC, i.e.,

$$\rho_{BEC} = \frac{m_{i0(BEC)}}{V_{BEC}} = \frac{1.4\times10^{-20}kg}{\frac{4}{3}\pi\left(40\times10^{-6}m\right)^3} \cong 5.2\times10^{-8}\,kg.m^{-3}$$

Substitution of the values of ρ_{BEC} into Eq. (3) gives

$$\chi_{BEC} = \frac{m_{g(BEC)}}{m_{i0(BEC)}} = \left\{1 - 2\left[\sqrt{1+0.065\frac{D^2}{v_{BEC}^4}} - 1\right]\right\} \qquad (4)$$

The variable D, in Eq. (4), refers now to the total power density of the radiation *absorbed* by the BEC (from t*he trap and the Raman beams*, used in the experimental set-up of reference [1]). According to the authors of the experiment the power of the Raman beams are of approximately 3mW (2.9 *m*W in one of the two beams,3.3 *m*W in the other), focused to a beam waist of 120 microns ($60\mu m$ radius); the absorption coefficient is $1E_R/2.5E_R = 0.4$. Thus, we can write that

$$D = \frac{P_{abs}}{S_{BEC}} = \frac{0.4P_{beams}}{4\pi\left(60\times10^{-6}m\right)^2} =$$

$$= \frac{0.4\times\left(2.9mW + 3.3mW\right)}{4\pi\left(60\times10^{-6}m\right)^2} \cong 5.4\times10^4\,W.m^{-2} \qquad (5)$$

Substitution of this value into Eq. (4) gives

$$m_{g(BEC)} = \left\{1 - 2\left[\sqrt{1+\frac{1.8\times10^8}{v_{BEC}^4}} - 1\right]\right\} m_{i0(BEC)} \qquad (6)$$

Note that, for $v_{BEC} < 109.5m.s^{-1}$ the *gravitational mass* of the BEC ($m_{g(BEC)}$) becomes *negative*. Lene Hau et al., [3] showed that light speed through a BEC reduces to values much smaller than $100m.s^{-1}$.

Consequently, we can conclude that it is the *gravitational mass* of the BEC of ^{87}Rb atoms that becomes *negative* and not its inertial mass.

Also it was deduced in the reference [2] a generalized expression for the Newton's 2nd law of motion, which shows that the expression for *inertial forces* is given by

$$\vec{F} = m_g\vec{a} \qquad (7)$$

The presence of m_g in this equation shows that the inertial forces have origin in the *gravitational interaction* between the particle and the others particles of the Universe, just as *Mach's principle* predicts. In this way, the new equation expresses the incorporation of the Mach's principle into Gravitation Theory, and reveals that the inertial effects upon a body can be strongly reduced by means of the decreasing of its gravitational mass. Note that only when m_g reduces to m_{i0} is that we have the well-know expression ($\vec{F} = m_i\vec{a}$) of the Newton's law.

Taking Eq. (6) for an arbitrary value of $v_{BEC} < 109.5m.s^{-1}$, we obtain $m_{g(BEC)} = -Km_{i0(BEC)}$, where K is a positive number. Substitution of this equation into Eq. (7) yields

$$\vec{F}_{BEC} = -Km_{i0(BEC)}\vec{a} \qquad (8)$$

The sign $(-)$ in this expression reveals clearly why the BEC accelerates in the *opposite direction* of the *applied force*, i.e.,

$$\vec{F}_{BEC} = -\vec{F}_{BEC} = Km_{i0(BEC)}\vec{a} \qquad (9)$$

Recently it was created a BEC with 2.506×10^{17} ^{23}**Na** atoms [4]. The inertial mass of this BEC is

$$m_{i0(BEC)} = 2.506\times10^{17}(23)\left(1.66\times10^{-27}\right) = 3.8\times10^{-9}\,kg$$

The number of atoms/cm^3, as showed in reference [4], is $n_0 = 2.742\times10^{6}\,cm^{-3} = 2.742\times10^{22}\,m^{-3}$. Thus, the density of the BEC is given by

$$\rho = (23)\left(1.66\times10^{-27}\right)2.742\times10^{22} = 1.04\times10^{-3}\,kg.m^{-3}$$

Substitution of these values into Eq. (3) gives

$$m_{g(BEC)} = \left\{1-2\left[\sqrt{1+1.6\times10^{-10}\frac{D^2}{v_{BEC}^4}}-1\right]\right\}m_{i0(BEC)} \quad (10)$$

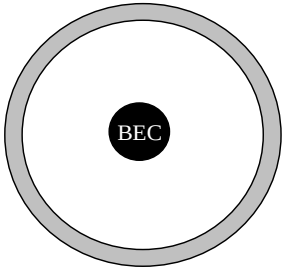

Fig. 1 – A BEC inside a hollow sphere.

Now consider the system showed in Fig.1. Inside the hollow sphere, whose *gravitational* mass is $m_{g(sphere)} \cong m_{i0(sphere)}$, there is a BEC whose *gravitational* mass is given by Eq. (10). Thus, the *total gravitational* mass of the system, $m_{g(SYS)}$, is given by

$$m_{g(SYS)} = m_{g(sphere)} + m_{g(BEC)} =$$

$$\cong m_{i0(sphere)} + \left\{1-2\left[\sqrt{1+1.6\times10^{-10}\frac{D^2}{v_{BEC}^4}}-1\right]\right\}m_{i0(BEC)} \quad (11)$$

In 2001 Lene Hau et al., have shown that the light speed through a BEC could have values very close to *zero*. Therefore, v_{BEC} with these magnitudes are not unusual. This shows that the value of $m_{g(SYS)}$, given Eq. (11), can be strongly reduced even the value of D be small, for example, of the order of $1W/m^2$.

Then, consider a system in which the inertial mass of the hollow sphere is $m_{i0(sphere)} = 10{,}000\,kg$; $m_{i0(BEC)} = 3.8\times10^{-9}\,kg$; $D \cong 1W/m^2$ and $v_{BEC} = 10^{-9}\,m.s^{-1}$ *, then the gravitational mass of the system will have the following value:

$$m_{g(SYS)} = m_{i0(sphere)} - 2.5\times10^{13}\,m_{i0(BEC)} =$$

$$= -8.5\times10^{4}\,kg \quad (12)$$

Thus, if this system is subjected to a gravity acceleration $\vec{g} = 9.8\,m.s^{-1}$, as shown in Fig.2, then its weight force will be given by $\vec{P} = \left|m_{g(SYS)}\right|\vec{g} = 8.5\times10^{4}\,\vec{g}$, $\left(P = 8.3\times10^{5}\,N\right)$. This value is greater than the thrust of the fighter aircraft F-22 Raptor (fifth-generation), which reaches 160,000N.

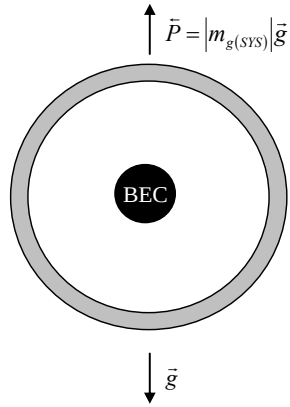

Fig. 2 – The system sphere-BEC, with *negative* gravitational mass ($m_{g(SYS)} < 0$), in a gravitational field.

It is important to note that, in spite the light speed reach values very close to zero through the BEC in the Lene Hau experiments, the number of atoms in the BEC, in this case is very small $\left(10^5 - 10^6\,atoms\right)$ in comparison with the 2.506×10^{17} atoms of the BEC of ^{23}**Na,** here mentioned. Consequently, the weight force, acting on the BEC in the case of the Lene Hau experiments is approximately 10^{-12} times smaller than in the case of the BEC of Na atoms.

* With this velocity the light beam would travel about $0.1mm$ in a day.

References

[1] M.A. Khamehchi *et al*. (2017). *Negative-Mass Hydrodynamics in a Spin-Orbit–Coupled Bose-Einstein Condensate. Phys. Rev. Lett*. 118 (15): 155301; doi: 10.1103/PhysRevLett.118.155301
Available at: https://arxiv.org/abs/1612.04055

[2] De Aquino, F. (2010) *Mathematical Foundations of the Relativistic Theory of Quantum Gravity*, Pacific Journal of Science and Technology, **11** (1), pp. 173-232.
Available at: https://hal.archives-ouvertes.fr/hal-01128520

[3] Hau, L.V, et al., (1999) *Light Speed Reduction to 17 Meters per Second in an Ultracold Atomic Gas*, Nature 397, 594-598.

[4] Pei-Lin You (2016) *Bose–Einstein condensation in a vapor of sodium atoms in an electric field*, Physica B, **491**, 84-92.

Searching for the Gravific Photons

Fran De Aquino

It was show that the linear *momentum* transported by electromagnetic waves has a *negative* component, in such way that, when a radiation incides on a surface, it is exerted a pressure on opposite direction to the direction of propagation of the radiation. In addition, it was predicted the existence of photons in which the *negative* component of the *momentum* is greater than the positive one. These photons were called attractive photons or *gravific photons*. Here, we show how to produce and to detect this type of photons.

Key words: Gravity, Gravitation, Electromagnetic Waves, Radiation Pressure.

1. Introduction

Electromagnetic waves transport energy as well as linear *momentum*. Then, if this *momentum* is absorbed by a surface, pressure is exerted on the surface. In a previous paper [1] we shown that this pressure has a *negative* component (*opposite to the direction of propagation of the photons*) due to the existence of the negative linear *momentum* transported by the photons. Then, it was predicted the existence of photons in which the *negative* component of the *momentum* is greater than the positive one. These photons were called *gravific photons*[1] and is expected that they have frequencies greater than $10^{28}\,Hz$. In addition, it was shown that the limit between the spectrum of the gravific photons and the gamma ray spectrum is defined by a characteristic frequency, $2f_g \approx 10^{28} Hz$ (See Fig. 1).

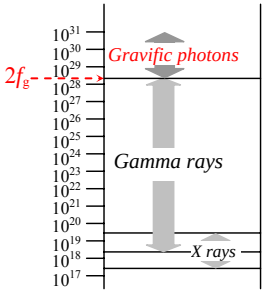

Fig. 1 – The *Gravific Photons* Spectrum (above $2f_g \approx 10^{28} Hz$).

Here, we show how to produce and to detect gravific photons. We start with the well-know process of production of *neutral pions* (Mesons π^0), by means of the collision of high-speed protons. i.e.,

$$p + p \rightarrow p + p + \pi^0 \qquad (1)$$

Neutral pions decay with a much shorter lifetime of 8.4×10^{-17} seconds, producing 2 gamma rays.

$$\pi^0 \rightarrow \gamma + \gamma \qquad (2)$$

When the velocities of the protons are *ultra-relativistic* the energy of the neutral pion, E_{π^0}, is given by [2]

$$E_{\pi^0} = \left(\frac{E_{proton}}{m_{i0(proton)}}\right)^2 m_{\pi^0} c^2 \qquad (3)$$

Neutral pions have rest inertial mass, m_{π^0} equal to $264 m_e$. Thus, the frequency of the gamma rays is

$$f = \frac{1}{2h}\left(\frac{E_{proton}}{m_{i0(proton)}}\right)^2 m_{\pi^0} c^2 \cong$$

$$\cong 1.6\times10^{22}\left(\frac{E_{proton}}{m_{i0(proton)}c^2}\right)^2 \qquad (4)$$

Note that, if $E_{proton} > 10^3 m_{i0(proton)} c^2$, then the produced gamma rays will have frequency $> 10^{28} Hz$. Therefore, by means of collision of *ultra-relativistic* protons it is possible to produce Gravific Photons $\left(f > 2f_g \approx 10^{28} Hz\right)$ [2]. In the system shown in Fig. 2, when the Gravific Photons strike on a plate, it is exerted a pressure on opposite direction to the direction of propagation of the radiation. By measuring the pressure on the plate it is then possible to confirm the existence of the Gravific Photons.

---

[1] *Gravific* Radiation is electromagnetic radiation and cannot be confused with *gravitational* radiation or *gravitational* waves, which are *ripples* on the space-time (predicted by the Einstein Theory).

[2] At the *Large Hadron Collider* (LHC) the protons each have an energy of 6.5 TeV, giving a total collision energy of 13 TeV. At this energy the protons move at about 0.999999990 *c*. Then the frequency of the gamma rays produced by the disintegration of the neutral pions can reach about 10^{30}Hz.

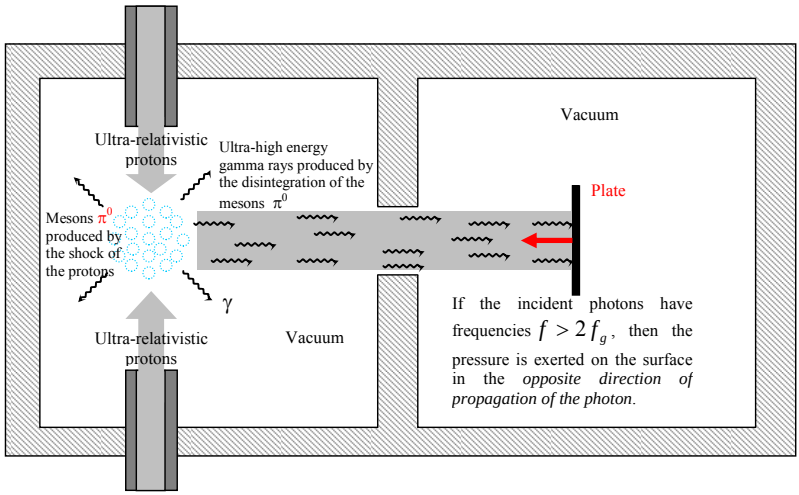

$$p + p \rightarrow p + p + \pi^0$$
$$\hookrightarrow \gamma + \gamma$$

Fig. 2 – If the photons have frequencies $f > 2f_g$ the resultant *momentum* transported by the photon is *negative*. If this *momentum* is absorbed by a surface, pressure is exerted on the surface, in the *opposite direction of propagation of the photon*. This special type of photon is denominated of *attractive photon or Gravific Photons*.

References

[1] De Aquino, F. (2014) *The Bipolar Linear Momentum transported by the Electromagnetic Waves: Origin of the Gravitational Interaction* : https://hal.archives-ouvertes.fr/hal-01077208 ; http://vixra.org/abs/1402.0022

[2] Boldt, E. (1969) *Cosmic Rays Photons*, chap. 4, p.49, in Lectures in High-Energy Astrophysics, STID, NASA, Washington, DC.

Gravitational Interaction between Photons and Unification of All the Fundamental Interactions

Fran De Aquino

Recently, it has been reported an experiment where a very weak laser beam passes through a dense cloud of *ultracold rubidium atoms*. Under these circumstances, it was observed that the photons bound together in pairs or triplets, suggesting an unexpected *attractive* interaction between them. Here, it is shown that mentioned interaction can be related to the *gravitational interaction*, and that this possibility permits the formulation of a solid approach for the *unification* of all the fundamental forces of the Universe.

Key words: Interaction Gravitational, Casimir Force, Interaction between Photons.

1. Introduction

In a paper recently published in *Science* [1], researchers have reported that when they have put a very weak laser beam through a dense cloud of *ultracold rubidium atoms* (as a *quantum* nonlinear medium), the photons bound together in pairs or triplets, suggesting an unexpected *attractive* interaction between them.

Here, it is shown that mentioned interaction is related to the *gravitational interaction*, and that this possibility permits the formulation of a solid theory for the *unification* of all the fundamental forces of the Universe.

2. Theory

I have show in the *Mathematical Foundations of the Relativistic Theory of Quantum Gravity* [2] that, by combination of Gravitation and the *Uncertainty principle* it is possible to derive the expression for the *Casimir force*. The starting point is the expression of correlation between gravitational mass m_g and *rest* inertial mass, $m_{i0,}$ obtained in the mentioned paper, i.e.,

$$\chi = \frac{m_g}{m_{i0}} = \left\{ 1 - 2\left[\sqrt{1 + \left(\frac{p}{m_{i0} c} \right)^2} - 1 \right] \right\} \qquad (1)$$

where p is the variation in the particle's *kinetic momentum*; c is the light speed.

Thus, an uncertainty Δm_{i0} in m_{i0} produces an uncertainty Δp in p and therefore an uncertainty Δm_g in m_g, which according to Eq.(1) , is given by

$$\Delta m_g = \Delta m_{i0} - 2\left[\sqrt{1 + \left(\frac{\Delta p}{\Delta m_{i0} c} \right)^2} - 1 \right] \Delta m_{i0} \qquad (2)$$

From the uncertainty principle for position and momentum, we know that the product of the uncertainties of the simultaneously measurable values of the corresponding position and momentum components are at least of the magnitude order of $\hbar$, i.e.,

$$\Delta p \Delta r \sim \hbar$$

Substitution of $\Delta p \sim \hbar / \Delta r$ into (2) yields

$$\Delta m_g = \Delta m_i - 2\left[\sqrt{1 + \left(\frac{\hbar / \Delta m_i c}{\Delta r} \right)^2} - 1 \right] \Delta m_i \qquad (3)$$

Therefore if

$$\Delta r << \frac{\hbar}{\Delta m_i c} \qquad (4)$$

Then the expression (3) reduces to:

$$\Delta m_g \cong -\frac{2\hbar}{\Delta r c} \qquad (5)$$

Note that, Δm_g does not depend on m_g .

Consequently, an uncertainty ΔF in the gravitational force $F = -G m_g m'_g / r^2$, will be given by

$$\Delta F = -G \frac{\Delta m_g \Delta m'_g}{(\Delta r)^2} = \\ = -\left[\frac{2}{\pi (\Delta r)^2} \right] \frac{hc}{(\Delta r)^2} \left(\frac{G\hbar}{c^3} \right) \qquad (6)$$

The amount $\left(G\hbar / c^3 \right)^{1/2} = 1.61 \times 10^{-35} m$ is called the *Planck length*, l_{planck} ,(the length scale on which quantum fluctuations of the metric of the space time are expected to be of order unity).

Thus, we can write the expression of ΔF as follows

$$\Delta F = -\left(\frac{2}{\pi}\right)\frac{hc}{(\Delta r)^4} l_{planck}^2 = \\ = -\left(\frac{\pi}{480}\right)\frac{hc}{(\Delta r)^4}\left[\left(\frac{960}{\pi^2}\right) l_{planck}^2\right] = \\ = -\left(\frac{\pi A_0}{480}\right)\frac{hc}{(\Delta r)^4} \qquad (7)$$

or

$$F_0 = -\left(\frac{\pi A_0}{480}\right)\frac{hc}{r^4} \qquad (8)$$

which is the expression of the *Casimir force* for $A = A_0 = (960/\pi^2) l_{planck}^2$.

Now, multiplying Eq. (8) (the expression of F_0) by n^2 we obtain

$$F = n^2 F_0 = -\left(\frac{\pi n^2 A_0}{480}\right)\frac{hc}{r^4} = -\left(\frac{\pi A}{480}\right)\frac{hc}{r^4} \qquad (9)$$

This is the general expression of the *Casimir force*.

We can then conclude that *the Casimir effect* is just a *gravitational* effect related to the *uncertainty principle*. In this context, the nature of the Casimir *force* is clearly gravitational as shown in the derivation of Eq. (9), which expresses, in turn, the intensity of the gravitational force *in the case of very small scale* (r very small) [*].

Now consider the discovery reported recently in *Science* [1]. When the researchers have put a very weak laser beam through a dense cloud of *ultracold rubidium atoms* [†], the photons bound together in pairs or triplets, suggesting an unexpected *attractive* interaction between them. Now, we will show that the nature of this interaction is *gravitational*.

According mentioned in the paper, the length of the cloud of ultracold rubidium atoms were of approximately $130\mu m$ (along the propagation direction), while the transverse extent of the probe beam waist had about $4.5\mu m$. Therefore, the distances r between the photons of the cloud were very small. As we have already seen, at very small scale, the *gravitational interaction* cannot be trated via usual Newton's equation of gravitation. In this case, Eq. (9) must be used. Thus, assuming $A \approx \lambda^2 = (c/f)^2 \cong 10^{-13} m^2$, and substituting this value into Eq. (9), we obtain:

$$F \approx 10^{-40}/r^4 \qquad (10)$$

Using the above equation, and considering the dimensions of the mentioned cloud $(130\mu m \times 4.5\mu m)$, we can calculate the intensity of the *gravitational force* between two photons of the cloud, when the distance r between them were, for example, of the order of $1\mu m$, i.e.,

$$F \approx 10^{-16} N \qquad (11)$$

The intensity of this gravitational force is highly significative. Compare for example, with the *Coulombian attractive force* between an *electron and a proton*, separated by *the same distance* ($r \approx 1\mu m$), which is given by

$$F_c = \frac{e^2}{4\pi\varepsilon_0 r^2} \cong \frac{10^{-28}}{r^2} \approx 10^{-16} N \qquad (12)$$

The *Coulombian repulsive force* between *two protons* in an atomic *nucleus*, considering that, $r_{proton} = 1.4 \times 10^{-15} m$, and that the distance between them is $r = 4 \times 10^{-15} m$ [4], is given by

$$F_c = \frac{e^2}{4\pi\varepsilon_0 r^2} \cong 14N \qquad (13)$$

This enormous repulsive force *must be overcomed* by the intense *attractive nuclear force* (*strong* nuclear force).

Now consider Eq. (9), where we put $A = \pi r_{proton}^2 \cong 6 \times 10^{-30} m^2$ and $r = 4 \times 10^{-15} m$, then the result is

---

[*] The Casimir force is only significative when the value of r is very small (*microcosm scale*).

[†] The velocities of the photons through the cloud of *ultracold rubidium atoms* are strongly reduced. This is the reason for the laser to pass through the mentioned cloud. Lene Hau et al., [3] showed that light speed through a cloud of *ultracold rubidium atoms* reduces to values much smaller than $100 m.s^{-1}$.

$$F = -\left(\frac{\pi A}{480}\right)\frac{hc}{r^4} \cong 30N \qquad (14)$$

Comparing Eq. (14) with Eq. (13), we can conclude that the *attractive gravitational force* ($30N$) is sufficient to overcome the *repulsive* Coulombian force expressed by Eq. (13).

These results lead us to formulate the following question: What is the true nature of the "strong nuclear force"? Is it *gravitational* as shown above?

This possibility is reinforced by the derivation the *Coupling Constants for the Fundamental Forces* that we will make hereafter, starting from Eq. (9).

It is known that the *weak* force, F_W, which is related to the *strong* force, F_S, by means of the following expression:

$$\frac{F_W}{F_S} = \frac{\alpha_W}{\alpha_S} \qquad (15)$$

where α_W is the *weak force coupling constant*, and α_S is the *strong force coupling constant* [‡].

Assuming that $F_S = F$, where F is given by Eq. (9), then Eq.(15) can be rewritten as follows

$$F_W = \left(\frac{\alpha_W}{\alpha_S}\right)\left(\frac{\pi A}{480}\right)\frac{hc}{r^4} \qquad (16)$$

At $r \cong 3\times10^{-18}\,m$ (*0.1% of the diameter of a proton*), the weak interaction has a strength of a similar magnitude to electromagnetic force, $F_E = e^2/4\pi\varepsilon_0 r^2$ [5]. Thus, making $F_W = F_E$, and substituting the above mentioned value of r, we obtain

$$\frac{\alpha_W}{\alpha_S} = \frac{480r^2e^2}{4\pi^2\varepsilon_0 Ahc} = \frac{480r^2e^2}{4\pi^3\varepsilon_0 r_p^2 hc} \approx 3\times10^{-7} \qquad (17)$$

This is the same value mentioned in the literature for α_W/α_S [6].

Now, considering that $F_W/F_E = \alpha_W/\alpha_E$, where α_E is the *electromagnetic* force *coupling constant*, then we can write that

$$F_W = \left(\frac{\alpha_W}{\alpha_E}\right)\frac{e^2}{4\pi\varepsilon_0 r^2} \qquad (18)$$

At the maximum range of the weak interaction, $r_{\max}$, we have the minimum value of the weak force, $F_W^{\min}$, which can be expressed by Eq. (16) or Eq. (18) as follows

$$F_W^{\min} = \left(\frac{\alpha_W}{\alpha_S}\right)\left(\frac{\pi A}{480}\right)\frac{hc}{r_{\max}^4} \qquad (19)$$

$$F_W^{\min} = \left(\frac{\alpha_W}{\alpha_E}\right)\frac{e^2}{4\pi\varepsilon_0 r_{\max}^2} \qquad (20)$$

By comparing these equations, we obtain

$$\left(\frac{\alpha_W}{\alpha_S}\right)\left(\frac{\pi A}{480}\right)\frac{hc}{r_{\max}^2} = \left(\frac{\alpha_W}{\alpha_E}\right)\frac{e^2}{4\pi\varepsilon_0} \qquad (21)$$

or

$$\frac{\alpha_S}{\alpha_E} = \frac{4\pi^2 A\varepsilon_0 hc}{480e^2 r_{\max}^2} = \frac{4\pi^3 r_p^2 \varepsilon_0 hc}{480e^2 r_{\max}^2} =$$

$$= \left(\frac{4\pi\varepsilon_0 \hbar c}{e^2}\right)\left(\frac{2\pi^3 r_p^2}{480 r_{\max}^2}\right) \qquad (22)$$

Experimental data, describing the strong force between nucleons is consistent with a strong force coupling constant of about 1 [6]. Thus, making $\alpha_S = 1$ (*strong force coupling constant*) in Eq. (22), we obtain

$$\alpha_E = \left(\frac{e^2}{4\pi\varepsilon_0 \hbar c}\right)\left(\frac{480 r_{\max}^2}{2\pi^3 r_p^2}\right) \qquad (23)$$

The maximum range of the weak interaction, $r_{\max}$, is of the order of $10^{-16}\,m$ [7]. Equation above shows that, for $r_{\max} \cong 5\times10^{-16}\,m$ the term

[‡] Similarly, the weak force is related to the electromagnetic force, F_E, by means of the expression: $F_W/F_E = \alpha_W/\alpha_E$; and the strong force is related to the electromagnetic force, by means of the expression: $F_S/F_E = \alpha_W/\alpha_E$; and the gravitational force, F_G, is related to the electromagnetic force, by means of the expression: $F_G/F_E = \alpha_G/\alpha_E$.

$$\left(\frac{480r_{\max}^2}{2\pi^3 r_p^2}\right)\cong 1 \qquad (24)$$

Consequently, Eq. (23) reduces to

$$\alpha_E = \frac{e^2}{4\pi\varepsilon_0\hbar c}\cong\frac{1}{137} \qquad (25)$$

this is the expression of the *electromagnetic force coupling constant*.

Multiplying α_W/α_S (given by Eq. (17)) by α_S/α_E (given by Eq. (22)), we get

$$\frac{\alpha_W}{\alpha_E}=\left(\frac{480r^2e^2}{4\pi^3\varepsilon_0 r_p^2 hc}\right)\left(\frac{4\pi\varepsilon_0\hbar c}{e^2}\right)\left(\frac{2\pi^3 r_p^2}{480r_{\max}^2}\right)$$

whence we obtain

$$\alpha_W=\left(\frac{480r^2e^2}{4\pi^3\varepsilon_0 r_p^2 hc}\right)\left(\frac{4\pi\varepsilon_0\hbar c}{e^2}\right)\left(\frac{2\pi^3 r_p^2}{480r_{\max}^2}\right)\alpha_E =$$

$$=\left(\frac{480r^2e^2}{4\pi^3\varepsilon_0 r_p^2 hc}\right)\left(\frac{2\pi^3 r_p^2}{480r_{\max}^2}\right)\cong$$

$$\cong\left(\frac{r^2e^2}{2\varepsilon_0 r_{\max}^2 hc}\right)\cong 3\times10^{-7} \qquad (26)$$

Now, we will obtain the *gravitational force coupling constant*, α_G, starting of the fact that the *strong* force, F_G, is related to the *electromagnetic* force, F_E, by means of the following expression:

$$\frac{F_G}{F_E}=\frac{\alpha_G}{\alpha_E} \qquad (27)$$

Then, we can write that

$$\alpha_G=\alpha_E\left(\frac{F_G}{F_E}\right)=\alpha_E\left(\frac{Gm_p^2}{\frac{e^2}{4\pi\varepsilon_0}}\right)\cong 5.9\times10^{-39} \qquad (28)$$

The relative strength of interactions varies with distance [8]. Here, starting from the fact that *the strong nuclear force* and the *weak nuclear force* are *gravitational forces* expressed by Eq. (9), we have showed that, at the range of about 10^{-15} m ($r_{\max}\cong 5\times10^{-16}\,m$), the *strong force*($\alpha_S=1$) is approximately 137 *times as strong* as electromagnetic force ($\alpha_E=1/137$), about *a million times as strong* as the weak force ($\alpha_W\cong 3\times10^{-7}$), and about 10^{38} *times as strong as* gravitation($\alpha_G\cong 5.9\times10^{-39}$). All these values are in strong accordance with the values widely mentioned in the literature [9, 10], given below

$$\alpha_S = 1$$
$$\alpha_E = 1/137$$
$$\alpha_W \approx 3\times10^{-7}$$
$$\alpha_G \cong 5.9\times10^{-39}$$

Finally, we complete the *unification* of the Fundamental Forces of the Universe, by deriving from Eq. (9) the equations of the *Coulombian Force* and of the *Newtonian Force*.

Consider two electric charges q_1 and q_2 separated by a distance r. If we define the *area* A in Eq. (9) by means of the following expression

$$A=\sqrt{A_1A_2}=\sqrt{k_e\left(\frac{q_1}{e}\right)^2 r^2\times k_e\left(\frac{q_2}{e}\right)^2 r^2}=$$
$$=k_e\left(\frac{q_1q_2}{e^2}\right)r^2 \qquad (29)$$

where k_e is a constant to be determined, and $e=1.6\times10^{-19}C$, then Eq. (9) can rewritten as follows

$$F=\frac{\pi\hbar c k_e q_1q_2}{480e^2r^2}=\frac{1}{4\pi\varepsilon_0}\left(\frac{4\pi^2 hck_e\varepsilon_0}{480e^2}\right)\frac{q_1q_2}{r^2} \qquad (30)$$

Note that, the term in brackets is equal to 1 for $k_e=120e^2/\pi^2 hc\varepsilon_0\cong 0.1769$. In this case, Eq. (30) reduces to

$$F = \frac{1}{4\pi\varepsilon_0}\frac{q_1 q_2}{r^2} \qquad (31)$$

which is the expression of the *Coulombian Force*.

In a similar way, we can derive the expression of the *Newtonian Force* for two particles with masses m_1 and m_2 respectively, separated by a distance r. First we define the area A in Eq. (9) by means of the following expression

$$A = \sqrt{A_1 A_2} = \sqrt{k_g\left(\frac{m_1}{m_0}\right)^2 r^2 \times k_g\left(\frac{m_2}{m_0}\right)^2 r^2} = \\ = k_g\left(\frac{m_1 m_2}{m_0^2}\right) r^2 \qquad (32)$$

where k_g is a constant to be determined, and m_0, is a *minimum* value of mass that will be calculated hereafter. Then substitution of Eq. (32) into Eq. (9) yields

$$F = \frac{\pi\hbar c k_g m_1 m_2}{480 m_0^2 r^2} = G\left(\frac{2\pi^2\hbar c k_g}{480 G m_0^2}\right)\frac{m_1 m_2}{r^2} \qquad (33)$$

The term in brackets is equal to 1 for

$$\frac{k_g}{m_0^2} = \left(\frac{60}{\pi^2}\right)\left(\frac{4G}{\hbar c}\right) \qquad (34)$$

Equation (34) can be rewritten as follows

$$\frac{k_g}{m_0^2} = \frac{\left(\frac{60}{\pi^2}\right)}{\left(\sqrt{\frac{\hbar c}{4G}}\right)^2} \qquad (35)$$

where $\sqrt{\hbar c/4G} = 1.08\times10^{-8}\,kg$.

Equation (35) shows that, the term $\left(60/\pi^2\right)$ is a *pure number* such as k_g, and the term $\sqrt{\hbar c/4G}$ is expressed in *kg* such as m_0, then we can conclude that

$$k_g = \frac{60}{\pi^2} \qquad (36)$$

and

$$m_0 = \sqrt{\frac{\hbar c}{4G}} \qquad (37)$$

This expression it was first derivated by Hawking (1971) [11], and it is known as *Hawking mass limit*. Starting from the principle that the gravitational collapse is a process essentially classic, Hawking have concluded that black-holes could not exist with radius less than the *Planck length* $\left(\sqrt{G\hbar/c^3}\right)$ (limit for which *quantum* fluctuations in the metric of the spacetime are considered of the order of 1). In this way, the *minimum* radius of Schwarzschild, $r_S = 2Gm_0/c^2$, would have this value and, to this radius would correspond to a *minimum* value of mass m_0, given by

$$m_0 = \frac{r_S c^2}{2G} = \frac{c^2\sqrt{G\hbar/c^3}}{2G} = \sqrt{\frac{\hbar c}{4G}} \qquad (38)$$

This would be, obviously, the *smaller* mass value for any *macroscopic* gravitational systems (black-holes, etc).

Now, just substitute Eq. (36) and Eq. (37) into Eq.(33), in order to obtain the expression of the *Newtonian Force*.

$$F = G\frac{m_1 m_2}{r^2} \qquad (39)$$

The derivation of the Equations (31) and (39) via Eq. (9), shows clearly the *unification* of the Fundamental Forces of the Universe, i.e. shows that the *nature* of all the fundamental interactions is *Gravitational*.

Starting from Eq. (15), which expresses the correlation between F_W e F_S, i.e.,

$$\frac{F_W}{F_S} = \frac{\alpha_W}{\alpha_S}$$

we can write that

$$\frac{F_W}{F_S} = \frac{\alpha_W\left[\left(\frac{\pi A}{480}\right)\frac{hc}{r^4}\right]}{\alpha_S\left[\left(\frac{\pi A}{480}\right)\frac{hc}{r^4}\right]} \qquad (40)$$

whence we obtain

$$F_W = \alpha_W\left(\frac{\pi A}{480}\right)\frac{hc}{r^4} \qquad (41)$$

$$F_S = \alpha_S\left(\frac{\pi A}{480}\right)\frac{hc}{r^4} \qquad (42)$$

In addition, since

$$\frac{F_W}{F_E}=\frac{\alpha_W}{\alpha_E} \qquad \text{and} \qquad \frac{F_W}{F_G}=\frac{\alpha_W}{\alpha_G}$$

we get

$$F_E=\left(\frac{\alpha_E}{\alpha_W}\right)F_W=\alpha_E\left(\frac{\pi A}{480}\right)\frac{hc}{r^4} \qquad (43)$$

$$F_G=\left(\frac{\alpha_G}{\alpha_W}\right)F_W=\alpha_G\left(\frac{\pi A}{480}\right)\frac{hc}{r^4} \qquad (44)$$

Before 10^{-43} seconds after the Big Bang the forces F_S, F_W, F_E and F_G *become equal in strength, unifying themselves into a single force*, F_U, i.e.,

$$F_U=\alpha_S\left(\frac{\pi A}{480}\right)\frac{hc}{r^4}=\alpha_W\left(\frac{\pi A}{480}\right)\frac{hc}{r^4}= \\ =\alpha_E\left(\frac{\pi A}{480}\right)\frac{hc}{r^4}=\alpha_G\left(\frac{\pi A}{480}\right)\frac{hc}{r^4} \qquad (45)$$

where $\alpha_S=\alpha_W=\alpha_E=\alpha_G$.

Since $\alpha_S=1$, we then conclude that

$$F_U=\left(\frac{\pi A}{480}\right)\frac{hc}{r^4} \qquad (46)$$

Under these conditions, the energy U_U of a system of two particles with masses m_1 and m_2, separated by a distance r, is given by

$$U_U=F_U r=\left(\frac{\pi A}{480}\right)\frac{hc}{r^3} \qquad (47)$$

Since, $A=k_g\left(m_1m_2/m_0^2\right)/r^2$ where $k_g=60/\pi^2$, (See Eqs. (32) and (36)). Then, Eq. (47) can be rewritten as follows

$$U_U=\left(\frac{m_1m_2}{m_0^2}\right)\frac{hc}{8\pi\, r} \qquad (48)$$

Assuming that, in the mentioned conditions (at *the beginning of the Universe*), $m_1=m_2=m_0$, and that the *total mass* of the Universe, $M_{Univ}\cong 10^{54}kg$ [§], at this epoch, it was formed by a number $N=M_{Univ}/m_0\cong 10^{62}$ of particles with mass m_0 and radius r_0, compressed into the volume of the Initial Universe, $V_{Univ}=\frac{4}{3}\pi r_{Univ}^3$, where $r_{Univ}\cong 10^{-14}m$, then we can write that

$$N\left(\tfrac{4}{3}\pi r_0^3\right)\approx \tfrac{4}{3}\pi r_{Univ}^3 \qquad (49)$$

where we get

$$r_0\approx\frac{r_{Univ}}{\sqrt[3]{N}}\cong 10^{-35}m \qquad (50)$$

Therefore, we can assume that the distances r among the particles it was of the order of the Planck length, $l_{Planck}=\sqrt{G\hbar/c^3}\cong 1.6\times10^{-35}m$ [**].

Substitution of $m_1=m_2=m_0$ and $r\cong l_{Planck}$ into Eq. (48) gives

$$U_U\cong\frac{1}{4}\sqrt{\frac{\hbar c^5}{G}}\cong\frac{1}{4}E_p\cong 3\times10^{18}GeV \qquad (51)$$

where $E_p=\sqrt{\hbar c^5/G}\cong 1.22\times10^{19}GeV$ is the called *Planck Energy*

Note that the energy U_U is *above*, but *very close to*, the energy level of the *Total Unification Energy* Λ_{Total} [††] (the energy level above which the *electromagnetic force*, *weak force*, *strong force* and the *gravitational force* become *equal in strength* and unified in a single force)., i.e., $U_U\gtrsim\Lambda_{Total}$. Thus, as $U_U\cong 1/4E_p$, we write that

$$\Lambda_{Total}\lesssim U_U\cong 3\times10^{18}GeV$$

Therefore, the *Total Unification Energy*, Λ_{Total} is about 300 times greater than the called *Grand Unification Energy*, $\Lambda_{GUT}\cong 1\times10^{16}GeV$ [‡‡].

---

§ $M_{Univ}=c^3/2GH_0\cong 10^{54}kg$ [12]. H_0 is the Hubble constant.

** The unification of the electromagnetic *force*, *weak force*, and *strong force* with the gravitational force is generally assumed to be close to the *Planck Scale*.

†† Above Λ_{Total}, as showed in Eq. (45) and (47). Very close to Λ_{Total} because the unification of the 3 fundamental forces with the gravitational force requires that Λ_{Total} has a value *close to* the *Planck Energy*.

‡‡ The *grand unification energy* Λ_{GUT}, is the energy level above which, it is believed, the *electromagnetic force*, *weak force*, and *strong force* become *equal in strength* and unified in a single force.

3. Conclusion

The theoretical results here obtained are in surprisingly good conformity with the experimental and theoretical data accepted currently, and form a solid unified theory for all the fundamental forces of the Universe.

References

[1] Liang, Qi-Yu, et al., (2018) *Observation of three-photon bound states in a quantum nonlinear medium*, Science, Vol. 359, **6377**, pp. 783-786.

[2] De Aquino, F. (2010) *Mathematical Foundations of the Relativistic Theory of Quantum Gravity*, Pacific Journal of Science and Technology, **11** (1), pp. 173-232.

[3] Hau, L.V, et al., (1999) *Light Speed Reduction to 17 Meters per Second in an Ultracold Atomic Gas*, Nature 397, 594-598.

[4] Halliday, D. and Resnick, R. (1968) *Physics*, J. Willey & Sons, Portuguese Version, Ed. USP, p.718.

[5] HyperPhysics. Georgia State University. http://hyperphysics.phy-astr.gsu.edu/hbase/Forces/funfor.html

[6] *Coupling Constants for the Fundamental Forces*. (2011) HyperPhysics. Georgia State University. http://hyperphysics.phy-astr.gsu.edu/hbase/Forces/couple.html

[7] S. B.,Treiman, (1959)*The Weak Interactions*, Scientific American.

[8] Strassler, M. (2013). *The Strengths of the Known Forces*. Available at: https://profmattstrassler.com/articles-and-posts/particle-physics-basics/the-known-forces-of-nature/the-strength-of-the-known-forces/

[9] Rohlf, J.W.(1994) *Modern Physics from a to Z0*,Wiley.

[10] *Coupling Constants for the Fundamental Forces*. (2011) HyperPhysics. Georgia State University. http://hyperphysics.phy-astr.gsu.edu/hbase/Forces/couple.html

[11] Hawking, S.W (1971) *Gravitationally Collapsed Objects of Very low Mass. MNRAS*., **152**, 75-78.

[12] Kragh, H. (1999). *Cosmology and Controversy: The Historical Development of Two Theories of the Universe*: Princeton University Press.

The Gravitational Spacecraft

Fran De Aquino
Maranhao State University, Physics Department, S.Luis/MA, Brazil.

There is an electromagnetic factor of correlation between gravitational mass and inertial mass, which in specific electromagnetic conditions, can be reduced, made negative and increased in numerical value. This means that gravitational forces can be reduced, inverted and intensified by means of electromagnetic fields. Such control of the gravitational interaction can have a lot of practical applications. For example, a new concept of spacecraft and aerospace flight arises from the possibility of the electromagnetic control of the gravitational mass. The novel spacecraft called Gravitational Spacecraft possibly will change the paradigm of space flight and transportation in general. Here, its operation principles and flight possibilities, it will be described. Also it will be shown that other devices based on gravity control, such as the Gravitational Motor and the Quantum Transceivers, can be used in the spacecraft, respectively, for Energy Generation and Telecommunications.

Key words: Gravity, Gravity Control, Quantum Devices.

CONTENTS

1. Introduction

The discovery of the correlation between gravitational mass and inertial mass [1] has shown that the gravity can be *reduced*, *nullified* and *inverted*. Starting from this discovery several ways were proposed in order to obtain experimentally the local gravity control [2]. Consequently, new concepts of spacecraft and aerospace flight have arisen. This novel spacecraft, called Gravitational Spacecraft, can be equipped with other devices also based on gravity control, such as the Gravitational Motor and the Quantum Transceiver that can be used, respectively, for energy generation and telecommunications. Based on the theoretical background which led to the gravity control, the operation principles of the Gravitational Spacecraft and of the devices above mentioned, will be described in this work.

2. Gravitational Shielding

The contemporary greatest challenge of the Theoretical Physics was to prove that, Gravity is a *quantum* phenomenon. Since the General Relativity describes gravity as related to the curvature of the space-time then, the quantization of the gravity implies the quantization of the proper space-time. Until the end of the century XX, several attempts to quantify gravity were accomplished. However, all of them resulted fruitless [3, 4].

In the beginning of this century, it has been clearly noticed that there was something unsatisfactory about the whole notion of quantization and that the quantization process had many ambiguities. Then, a new approach has been proposed starting from the generalization of the *action function*[*]. The result has been the derivation of a theoretical background, which finally led to the so-sought quantization of the gravity and of the space-time. Published under the title: "*Mathematical Foundations of the Relativistic Theory of Quantum Gravity*"[†], this theory predicts a consistent *unification* of Gravity with Electromagnetism. It shows that the *strong* equivalence principle is reaffirmed and, consequently Einstein's equations are preserved. In fact, Einstein's equations can be deduced directly from the *Relativistic Theory of Quantum Gravity*. This shows, therefore, that the General Relativity is a particularization of this new theory, just as the Newton's theory is a particular case from the General Relativity. Besides, it was deduced from the new theory an important correlation between the *gravitational mass* and the *inertial mass*, which shows that the gravitational mass of a particle can be *decreased* and even made *negative*, independently of its inertial mass, i.e., while the gravitational mass is

[*] The formulation of the *action* in Classical Mechanics extends to the Quantum Mechanics and it has been the basis for the development of the *Strings Theory*.
[†] http://arxiv.org/abs/physics/0212033

progressively reduced, the inertial mass does not vary. This is highly relevant because it means that the weight of a body can also be reduced and even inverted in certain circumstances, since Newton's gravity law defines the weight P of a body as the product of its *gravitational mass* m_g by the local gravity acceleration g, i.e.,

$$P = m_g g \qquad (1)$$

It arises from the mentioned law that the gravity acceleration (or simply the gravity) produced by a body with gravitational mass M_g is given by

$$g = \frac{GM_g}{r^2} \qquad (2)$$

The physical property of mass has two distinct aspects: *gravitational mass* m_g and *inertial mass* m_i. The gravitational mass produces and responds to gravitational fields. It supplies the mass factors in Newton's famous inverse-square law of gravity $\left(F = GM_g m_g / r^2\right)$. The inertial mass is the mass factor in *Newton's 2nd Law of Motion* $\left(F = m_i a\right)$. These two masses are not equivalent but correlated by means of the following factor [1]:

$$\frac{m_g}{m_{i0}} = \left\{1 - 2\left[\sqrt{1 + \left(\frac{\Delta p}{m_{i0} c}\right)^2} - 1\right]\right\} \qquad (3)$$

Where m_{i0} is the *rest* inertial mass and Δp is the variation in the particle's *kinetic momentum*; c is the speed of light.

This equation shows that only for $\Delta p = 0$ the gravitational mass is equal to the inertial mass. Instances in which Δp is produced by *electromagnetic radiation*, Eq. (3) can be rewritten as follows:

$$\frac{m_g}{m_{i0}} = \left\{1 - 2\left[\sqrt{1 + \left(\frac{n_r^2 D}{\rho\, c^3}\right)^2} - 1\right]\right\} \qquad (4)$$

Where n_r is the *refraction index* of the particle; D is the power density of the electromagnetic radiation absorbed by the particle; and ρ its density of inertial mass.

It was shown [1] that there is an additional effect of *gravitational shielding* produced by a substance whose gravitational mass was reduced or made negative. This effect shows that just *above the substance* the gravity acceleration g_1 will be reduced at the same proportion $\chi = m_g / m_{i0}$, i.e., $g_1 = \chi\, g$, (g is the gravity acceleration *bellow* the substance).

Equation (4) shows, for example, that, in the case of a gas at ultra-low pressure (*very low density of inertial mass*), the *gravitational mass* of the gas can be strongly reduced or made negative by means of the incidence of electromagnetic radiation with power density relatively low.

Thus, it is possible to use this effect in order to produce gravitational shieldings and, thus, *to control the local gravity*.

The *Gravity Control Cells* (GCC) shown in the article "*Gravity Control by means of Electromagnetic*

Field through Gas or Plasma at Ultra-Low Pressure"[‡], are devices designed on the basis, of this effect, and usually are chambers containing gas or plasma at ultra-low pressure. Therefore, when an oscillating electromagnetic field is applied upon the gas its gravitational mass will be reduced and, consequently, the gravity *above* the mentioned GCC will also be reduced at the same proportion.

It was also shown that it is possible to make a gravitational shielding even with the chamber filled with *Air* at one atmosphere. In this case, the *electric conductivity of the air* must be strongly increased in order to reduce the intensity of the electromagnetic field or the power density of the applied radiation.

This is easily obtained by *ionizing the air* in the local where we want to build the gravitational shielding. There are several manners of ionizing the air. One of them is by means of ionizing radiation produced by a radioactive source of low intensity, for example, by using the radioactive element *Americium* (Am-241). The Americium is widely used as air ionizer in smoke detectors. Inside the detectors, there is just a little amount of americium 241 (about of 1/5000 grams) in the form of AmO_2. Its cost is very low (about of US$ 1500 per gram). The dominant radiation is composed of alpha particles. Alpha particles cannot cross a paper sheet and are also blocked by some centimeters of air. The Americium used in the smoke detectors can only be dangerous if inhaled.

The Relativistic Theory of Quantum Gravity also shows the existence of a *generalized equation for the inertial forces* which has the following form

$$F_i = M_g a \qquad (5)$$

This expression means a *new law for the Inertia*. Further on, it will be shown that it *incorporates the Mach's principle* to Gravitation theory [5].

Equation (3) tell us that the gravitational mass is only equal to the inertial mass when $\Delta p = 0$. Therefore, we can easily conclude that only in this particular situation the new expression of F_i reduces to $F_i = m_i a$, which is the expression for Newton's 2nd Law of Motion. Consequently, this Newton's law is just a particular case from the new law expressed by the Eq. (5), which clearly shows how *the local inertial forces are correlated to the gravitational interaction of the local system with the distribution of cosmic masses* (via m_g) and thus, *incorporates* definitively *the Mach's principle* to the Gravity theory.

The Mach's principle postulates that: "*The local inertial forces would be produced by the gravitational interaction of the local system with the distribution of cosmic masses*". However, in spite of the several attempts carried out, this principle had not yet been incorporated to the Gravitation theory. Also Einstein had carried out several attempts. The *ad hoc* introduction of the cosmological

[‡] http://arxiv.org/abs/physics/0701091

term in his gravitation equations has been one of these attempts.

With the advent of equation (5), *the origin of the inertia* - that was considered the most obscure point of the particles' theory and field theory – becomes now evident.

In addition, this equation also reveals that, if the gravitational mass of a body is very close to zero or if there is around the body a *gravitational shielding* which reduces closely down to zero the *gravity accelerations due to the rest of the Universe*, then the intensities of the inertial forces that act on the body become also very close to zero.

This conclusion is highly relevant because it shows that, under these conditions, the spacecraft could describe, with great velocities, unusual trajectories (such as curves in right angles, abrupt inversion of direction, etc.) without inertial impacts on the occupants of the spacecraft. Obviously, out of the above-mentioned condition, the spacecraft and the crew would be destroyed due to the strong presence of the inertia.

When we make a sharp curve with our car we are pushed towards a direction contrary to that of the motion of the car. This happens due to existence of *the inertial forces*. However, if our car is involved by a *gravitational shielding*, which reduces strongly the gravitational interaction of the car (and everything that is inside the car) with the rest of the Universe, then in accordance with the Mach's principle, the local inertial forces would also be strongly reduced and, consequently, we would not feel anything during the maneuvers of the car.

3. Gravitational Motor: Free Energy

It is known that the energy of the gravitational field of the Earth can be converted into rotational kinetic energy and electric energy. In fact, this is exactly what takes place in hydroelectric plants. However, the construction these hydroelectric plants have a high cost of construction and can only be built, obviously, where there are rivers.

The gravity control by means of any of the processes mentioned in the article: "*Gravity Control by means of Electromagnetic Field through Gas or Plasma at Ultra-Low Pressure*" allows the inversion of the weight of any body, practically at any place. Consequently, the conversion of the gravitational energy into rotational mechanical energy can also be carried out at any place.

In Fig. (1), we show a schematic diagram of a *Gravitational Motor*. The first *Gravity Control Cell* (GCC1) changes the local gravity from g to $g' = -ng$, propelling the left side of the rotor in a direction contrary to the motion of the right side. The second GCC changes the gravity back again to g i.e., from $g' = -ng$ to g, in such a way that the gravitational change occurs just on the region indicated in Fig.1. Thus, a *torque* T given by

$$T = (-F' + F)r = \left[-(m_g/2)g' + (m_g/2)g\right]r =$$

$$= (n+1)\tfrac{1}{2} m_g g r$$

Is applied on the rotor of gravitational mass m_g, making the rotor spin with angular velocity ω.

The average *power*, P, of the motor is $P = T\omega$. However, $-g' + g = \omega^2 r$. Thus, we have

$$P = \tfrac{1}{2} m_i \sqrt{(n+1)^3 g^3 r} \qquad (6)$$

Consider a cylindrical rotor of iron $(\rho = 7800 Kg.m^{-3})$ with height $h = 0.5m$, radius $r = R/3 = 0.0545m$ and inertial mass $m_i = \rho\pi R^2 h = 327.05kg$. By adjusting the GCC 1 in order to obtain $\chi_{air(1)} = m_{g(air)}/m_{i(air)} = -n = -19$ and, since $g = 9.81 m.s^{-2}$, then Eq. (6) gives

$$P \cong 2.19 \times 10^5 \, watts \cong 219 \;\; KW \cong 294 HP$$

This shows that this small motor can be used, for example, to substitute the conventional motors used in the cars. It can also be coupled to an electric generator in order to produce *electric energy*. The conversion of the rotational mechanical energy into electric energy is not a problem since it is a problem technologically resolved several decades ago. Electric generators are usually produced by the industries and they are commercially available, so that it is enough to couple a gravitational motor to an electric generator for we obtaining electric energy. In this case, just a gravitational motor with the power above mentioned it would be enough to supply the need of electric energy of, for example, at least 20 residences. Finally, it can substitute the conventional motors of the same power, with the great advantage of *not needing of fuel for its opera*tion. What means that the gravitational motors can produce energy practically free.

It is easy to see that gravitational motors of this kind can be designed for powers needs of just some watts up to millions of kilowatts.

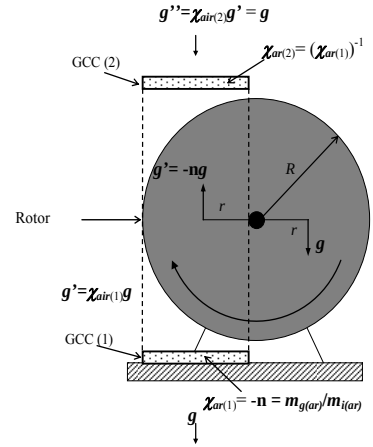

Fig. 1 – Gravitational Motor - The first *Gravity Control Cell* (GCC1) changes the local gravity from g to $g' = -ng$, propelling the left side of the rotor in contrary direction to the motion of the right side. The second GCC changes the gravity back again to g i.e., from $g' = -ng$ to g, in such a way that the gravitational change occurs just on the region shown in figure above.

4. The Gravitational Spacecraft

Consider a metallic sphere with radius r_s in the terrestrial atmosphere. If the external surface of the sphere is recovered with a radioactive substance (for example, containing Americium 241) then the air in the space close to the surface of the sphere will be strongly ionized by the radiation emitted from the radioactive element and, consequently, the electric conductivity of the air close to sphere will become strongly increased.

By applying to the sphere an electric potential of low frequency V_{rms}, in order to produce an electric field E_{rms} starting from the surface of the sphere, then very close to the surface, the intensity of the electric field will be $E_{rms} = V_{rms}/r_s$ and, in agreement with Eq. (4), the *gravitational mass* of the *Air* in this region will be expressed by

$$m_{g(air)} = \left\{1 - 2\left[\sqrt{1 + \frac{\mu_0}{4c^2}\left(\frac{\sigma_{air}}{4\pi f}\right)^3 \frac{V_{rms}^4}{r_s^4 \rho_{air}^2}} - 1\right]\right\} m_{0(air)} \qquad (7)$$

Therefore we will have

$$\chi_{air} = \frac{m_{g(air)}}{m_{0(air)}} = \left\{1 - 2\left[\sqrt{1 + \frac{\mu_0}{4c^2}\left(\frac{\sigma_{air}}{4\pi f}\right)^3 \frac{V_{rms}^4}{r_s^4 \rho_{air}^2}} - 1\right]\right\} \qquad (8)$$

The gravity accelerations acting on the sphere, due to the rest of the Universe (See Fig. 2), will be given by

$$g_i' = \chi_{air} g_i \qquad i = 1,2,\ldots,n$$

Note that by varying V_{rms} or the frequency f, we can easily to *reduce and control* χ_{air}. Consequently, we can also control the intensities of the gravity accelerations g_i' in order to produce a *controllable gravitational shielding* around the sphere.

Thus, the *gravitational forces* acting on the sphere, due to the rest of the Universe, will be given by

$$F_{gi} = M_g g_i' = M_g (\chi_{air} g_i)$$

where M_g is the gravitational mass of the sphere.

The gravitational shielding around of the sphere reduces both the gravity accelerations acting on the sphere, due to the rest of the Universe, and the gravity acceleration produced by the gravitational mass M_g of the own sphere. That is, if inside the shielding the gravity produced by the sphere is $g = -GM_g/r^2$, then, *out of* the shielding it becomes $g' = \chi_{air} g$. Thus, $g' = \chi_{air}\left(-GM_g/r^2\right) = -G\left(\chi_{air} M_g\right)/r^2 = -Gm_g/r^2$, where

$$m_g = \chi_{air} M_g$$

Therefore, *for the Universe out of the shielding* the gravitational mass of the sphere is m_g and not M_g. In these circumstances, the *inertial forces* acting on the sphere, in agreement with the *new law for inertia*, expressed by Eq. (5), will be given by

$$F_{ii} = m_g a_i \qquad (9)$$

Thus, these forces will be almost null when m_g becomes almost null by means of the action of the gravitational shielding. This means that, in these circumstances, the sphere practically loses its *inertial properties*. This effect leads to *a new concept of spacecraft and aerospatial flight*. The spherical form of the spacecraft is just *one* form that the Gravitational Spacecraft can have, since the gravitational shielding can also be obtained with other formats.

An important aspect to be observed is that it is possible to control the gravitational mass of the spacecraft, $M_{g(spacecraf)}$, simply by controlling the gravitational mass of a body *inside* the spacecraft. For instance, consider a parallel plate capacitor inside the spacecraft. The gravitational mass of the *dielectric* between the plates of the capacitor can be controlled by means of the ELF electromagnetic field through it. Under these circumstances, the *total* gravitational mass of the spacecraft will be given by

$$M_{g(spacecraf)}^{total} = M_{g(spacecraf)} + m_g = \\ = M_{i0} + \chi_{dielectric} m_{i0} \qquad (10)$$

where M_{i0} is the rest inertial mass of the spacecraft(without the dielectric) and m_{i0} is the rest inertial mass of the dielectric; $\chi_{dielectric} = m_g / m_{i0}$, where m_g is the gravitational mass of the dielectric. By decreasing the value of $\chi_{dielectric}$, the gravitational mass of the spacecraft decreases. It was shown, that the value of χ can be negative. Thus, when $\chi_{dielectric} \cong -M_{i0}/m_{i0}$, the *gravitational mass of the spacecraft gets very close to zero*. When $\chi_{dielectric} < -M_{i0}/m_{i0}$, the gravitational mass of the spacecraft becomes negative.

Therefore, *for an observer out of the spacecraft*, the gravitational mass of the spacecraft is $M_{g(spacecraf)} = M_{i0} + \chi_{dielectric} m_{i0}$, and not $M_{i0} + m_{i0}$.

Another important aspect to be observed is that we can *control the gravity inside the spacecraft*, in order to produce, for example, a gravity acceleration equal to the Earth's gravity $\left(g = 9.81 m.s^{-2}\right)$. This will be very useful in the case of space flight, and can be easily obtained by putting in the ceiling of the spacecraft the system shown in Fig. 3. This system has three GCC with nuclei of ionized air (or air at low pressure). Above these GCC there is a massive block with mass M_g.

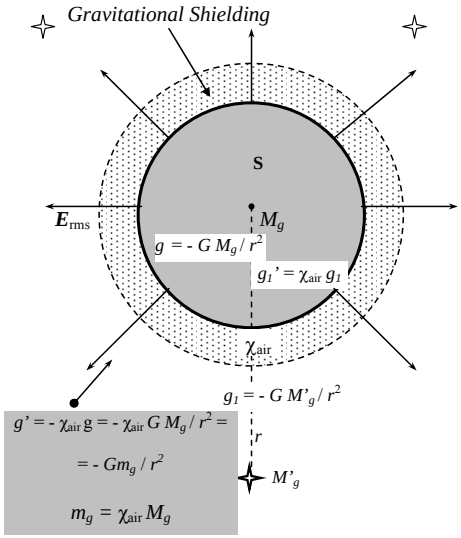

Fig.2- The gravitational shielding reduces the *gravity accelerations* ($\boldsymbol{g_1'}$) acting on the sphere (due to the rest of the Universe) and also reduces the gravity acceleration that the sphere produces upon all the particles of the Universe ($\boldsymbol{g'}$). For the Universe, the gravitational mass of the sphere will be $m_g = \chi_{air} M_g$.

As we have shown [2], a gravitational *repulsion* is established between the mass M_g and any positive gravitational mass below the mentioned system. This means that the particles in this region will stay subjected to a gravity acceleration a_b, given by

$$\vec{a}_b \cong \left(\chi_{air}\right)^3 \vec{g}_M \cong -\left(\chi_{air}\right)^3 G \frac{M_g}{r_0^2} \hat{\mu} \qquad (11)$$

If the Air inside the GCCs is sufficiently ionized, in such way that $\sigma_{air} \cong 10^3 S.m^{-1}$, and if $f = 1\ Hz$, $\rho_{air} \cong 1\ kg.m^{-3}$, $V_{rms} \cong 10\ KV$ and $d = 1\ cm$ then the Eq.8 shows that inside the GCCs we will have

$$\chi_{air} = \frac{m_{g(air)}}{m_{i0(air)}} = \left\{1 - 2\left[\sqrt{1 + \frac{\mu_0}{4c^2}\left(\frac{\sigma_{air}}{4\pi f}\right)^3 \frac{V_{rms}^4}{d^4 \rho_{air}^2}} - 1\right]\right\} \cong -10^3$$

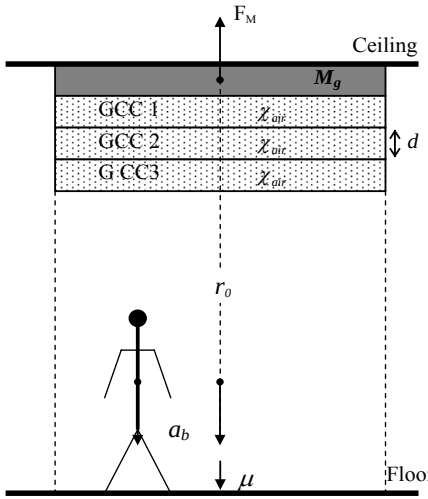

$$\vec{a}_b \cong (\chi_{air})^3 \vec{g}_M \cong -(\chi_{air})^3 G \frac{M_g}{r_0^2} \hat{\mu}$$

Fig.3 – If the Air inside the GCC is sufficiently ionized, in such way that $\sigma_{air} \cong 10^3 S.m^{-1}$ and if $f = 1\ Hz$; $d = 1cm$; $\rho_{air} \cong 1\ kgm^{-3}$ and $V_{rms} \cong 10\ KV$ then Eq. 8 shows that inside the CCGs we will have $\chi_{air} \cong -10^3$. Therefore, for $M_g \cong M_i \cong 100kg$ and $r_o \cong 1m$ the gravity acceleration inside the spacecraft will be directed from the ceiling to the floor of the spacecraft and its intensity will be $a_b \approx 10 m.s^{-2}$.

Therefore the equation (11) gives

$$a_b \approx +10^9 G \frac{M_g}{r_0^2} \qquad (12)$$

For $M_g \cong M_i \cong 100kg$ and $r_0 \cong 1m$ (See Fig.3), the gravity inside the spacecraft will be directed from the ceiling to the floor and its intensity will have the following value

$$a_b \approx 10 m.s^{-2} \qquad (13)$$

Therefore, an interstellar travel in a gravitational spacecraft will be particularly comfortable, since we can travel during all the time subjected to the gravity which we are accustomed to here in the Earth.

We can also use the system shown in Fig. 3 as a thruster in order to propel the spacecraft. Note that the gravitational repulsion that occurs between the block with mass M_g and any particle after the GCCs *does not depend on* of the place where the system is working. Thus, this *Gravitational Thruster* can propel the gravitational spacecraft in *any direction*. Moreover, it can work in the terrestrial atmosphere as well as in the cosmic space. In this case, the energy that produces the propulsion is obviously the *gravitational energy*, which is always present in any point of the Universe.

The schematic diagram in Fig. 4 shows in details the operation of the Gravitational Thruster. A gas of any type injected into the chamber beyond the GCCs acquires an acceleration a_{gas}, as shown in Fig.4, the intensity of which, as we have seen, is given by

$$a_{gas} = (\chi_{gas})^3 g_M \cong -(\chi_{gas})^3 G \frac{M_g}{r_0^2} \qquad (14)$$

Thus, if inside of the GCCs, $\chi_{gas} \cong -10^9$ then the equation above gives

$$a_{gas} \cong +10^{27} G \frac{M_g}{r_0^2} \qquad (15)$$

For $M_g \cong M_i \cong 10kg$, $r_0 \cong 1m$ we have $a_{gas} \cong 6.6 \times 10^{17} m.s^{-2}$. With this enormous acceleration the particles of the gas reach velocities close to the speed of the light in just a few nanoseconds. Thus, if the emission rate of the gas is $dm_{gas}/dt \cong 10^{-3} kg/s \cong 4000 litres/hour$, then the trust produced by the gravitational thruster will be

$$F = v_{gas}\frac{dm_{gas}}{dt} \cong c\frac{dm_{gas}}{dt} \cong 10^5\, N \qquad (16)$$

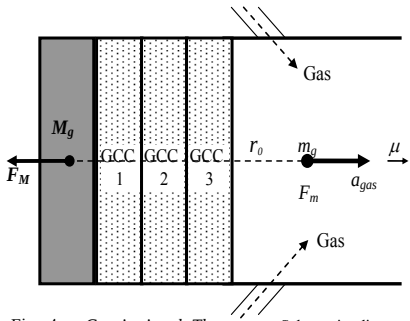

Fig. 4 – *Gravitational Thruster* – Schematic diagram showing the operation of the Gravitational Thruster. Note that in the case of very strong χ_{air}, for example $\chi_{air} \cong -10^9$, the gravity accelerations upon the boxes of the second and third GCCs become very strong. Obviously, the walls of the mentioned boxes cannot to stand the enormous pressures. However, it is possible to build a similar system [2] with 3 or more GCCs, *without material boxes*. Consider for example, a surface with several radioactive sources (Am-241, for example). The *alpha* particles emitted from the Am-241 cannot reach besides 10cm of air. Due to the trajectory of the alpha particles, three or more successive layers of air, with different electrical conductivities σ_1, σ_2 and σ_3, will be established in the ionized region. It is easy to see that the gravitational shielding effect produced by these three layers is similar to the effect produced by the 3 GCCs above.

It is easy to see that the gravitational thrusters are able to produce strong trusts (similarly to the produced by the powerful thrusters of the modern aircrafts) *just by consuming the injected gas for its operation*.

It is important to note that, if F is the thrust produced by the gravitational thruster then, in agreement with Eq. (5), the spacecraft acquires an acceleration $a_{spacecraft}$, expressed by the following equation

$$a_{spacecraft} = \frac{F}{M_{g(spacecraft)}} = \frac{F}{\chi_{out} M_{i(spacecraft)}} \qquad (17)$$

Where χ_{out}, given by Eq. (8), is the factor of gravitational shielding which depends on the external medium where the spacecraft is placed. By adjusting the shielding for $\chi_{out} = 0.01$ and if $M_{spacecraft} = 10^4\, Kg$ then for a thrust $F \cong 10^5\, N$, the acceleration of the spacecraft will be

$$a_{spacecraft} = 1000 m.s^{-2} \qquad (18)$$

With this acceleration, in just at 1(one) day, the velocity of the spacecraft will be close to the speed of light. However it is easy to see that χ_{out} can still be much more reduced and, consequently, the thrust much more increased so that it is possible to increase up to 1 million times the acceleration of the spacecraft.

It is important to note that, the inertial effects upon the spacecraft will be reduced by $\chi_{out} = M_g / M_i \cong 0.01$. Then, in spite of its effective acceleration to be $a = 1000 m.s^{-2}$, the effects for the crew of the spacecraft will be equivalents to an acceleration of only

$$a' = \frac{M_g}{M_i} a \approx 10 m.s^{-1}$$

This is the magnitude of the acceleration on the passengers in a contemporary commercial jet.

Then, it is noticed that the gravitational spacecrafts can be subjected to enormous *accelerations* (or *decelerations*) without imposing any harmful impacts whatsoever on the spacecrafts or its crew.

We can also use the system shown in Fig. 3, as a *lifter*, inclusively within the spacecraft, in order to lift peoples or things into the spacecraft as shown in Fig. 5. Just using two GCCs, the gravitational acceleration produced below the GCCs will be

$$\vec{a}_g = (\chi_{air})^2 g_M \cong -(\chi_{air})^2 G M_g / r_0^2 \, \hat{\mu} \qquad (19)$$

Note that, in this case, if χ_{air} is *negative*, the acceleration $\vec{a}_g$ will have a direction *contrary* to the versor $\hat{\mu}$, i.e., the body will be *attracted* in the direction of the GCCs, as shown in Fig.5. In practice, this will occur when the air inside the GCCs is sufficiently ionized, in such a way that $\sigma_{air} \cong 10^3 S.m^{-1}$. Thus, if the internal thickness of the GCCs is now $d = 1\ mm$ and if $f = 1\ Hz$; $\rho_{air} \cong 1\ kg.m^{-3}$ and $V_{rms} \cong 10\ KV$, we will then have $\chi_{air} \cong -10^5$. Therefore, for $M_g \cong M_i \cong 100kg$ and, for example, $r_0 \cong 10m$ the gravitational acceleration acting on the body will be $a_b \approx 0.6 m.s^{-2}$. It is obvious that this value can be easily increased or decreased, simply by varying the voltage V_{rms}. Thus, by means of this *Gravitational Lifter,* we can lift or lower persons or materials with great versatility of operation.

It was shown [1] that, when the gravitational mass of a particle is reduced into the range, $+0.159M_i$ to $-0.159M_i$, it becomes imaginary, i.e., its masses (gravitational and inertial) becomes imaginary. Consequently, the particle disappears from our ordinary Universe, i.e., it becomes *invisible* for us. This is therefore a manner of to obtain the transitory invisibility of persons, animals, spacecraft, etc. However, the factor $\chi = M_{g(imaginary)} / M_{i(imaginary)}$ remains real because

$$\chi = \frac{M_{g(imaginary)}}{M_{i(imaginary)}} = \frac{M_g i}{M_i i} = \frac{M_g}{M_i} = real$$

Thus, if the gravitational mass of the particle is reduced by means of the absorption of an amount of electromagnetic energy U, for example, then we have

$$\chi = \frac{M_g}{M_i} = \left\{1 - 2\left[\sqrt{1 + \left(U/m_{i0}c^2\right)^2} - 1\right]\right\}$$

This shows that the energy U *continues acting* on the particle turned imaginary. In practice this means that *electromagnetic fields act on imaginary particles*. Therefore, the internal electromagnetic field of a GCC remains acting upon the particles inside the GCC even when their gravitational masses are in the range $+0.159M_i$ to $-0.159M_i$, turning them *imaginaries.* This is very important because it means that the GCCs of a gravitational spacecraft remain working even when the spacecraft becomes imaginary.

Under these conditions, the gravity accelerations acting on the imaginary spacecraft, due to the rest of the Universe will be, as we have see, given by

$$g_i' = \chi \, g_i \qquad i = 1,2,...,n$$

Where $\chi = M_{g(imaginary)} / M_{i(imaginary)}$ and $g_i = -Gm_{gi(imaginary)} / r_i^2$. Thus, the gravitational forces acting on the spacecraft will be given by

$$F_{gi} = M_{g(imaginary)} g_i' =$$
$$= M_{g(imaginary)} \left(-\chi G m_{gj(imaginary)} / r_j^2\right) =$$
$$= M_g i \left(-\chi G m_{gi} i / r_i^2\right) = +\chi G M_g m_{gi} / r_i^2 . \quad (20)$$

Note that these forces are *real*. By calling that, the *Mach's principle* says that the *inertial effects* upon a particle are consequence of the gravitational interaction of the particle with the rest

of the Universe. Then we can conclude that the inertial forces acting on the spacecraft in imaginary state are also *real*. Therefore, it can travel in the imaginary space-time using the gravitational thrusters.

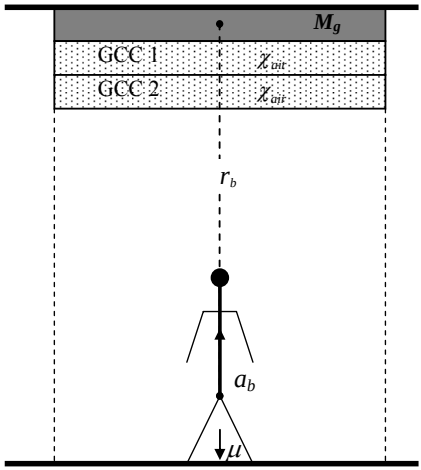

$$\vec{a}_b \cong (\chi_{air})^2 \vec{g}_M \cong -(\chi_{air})^2 G \frac{M_g}{r_b^2} \hat{\mu}$$

Fig.5 – *The Gravitational Lifter* – If the air inside the GCCs is sufficiently ionized, in such way that $\sigma_{air} \cong 10^3 S.m^{-1}$ and the internal thickness of the GCCs is now $d = 1\ mm$ then, if $f = 1\ Hz$; $\rho_{air} \cong 1\ kg.m^{-3}$ and $V_{rms} \cong 10\ KV$, we have $\chi_{air} \cong -10^5$. Therefore, for $M_g \cong M_i \cong 100kg$ and $r_0 \cong 10m$ the gravity acceleration acting on the body will be $a_b \approx 0.6m.s^{-2}$.

It was also shown [1] that *imaginary particles* can have *infinity velocity* in the imaginary space-time. Therefore, this is also the upper limit of velocity for the gravitational spacecrafts traveling in the imaginary space-time. On the other hand, the travel in the imaginary space-time can be very safe, because there will not be any material body in the trajectory of the spacecraft.

It is easy to show that the gravitational forces between two thin layers of air (with masses m_{g1} and m_{g2}) around the spacecraft, are expressed by

$$\vec{F}_{12} = -\vec{F}_{21} = -(\chi_{air})^2 G \frac{m_{i1} m_{i2}}{r^2} \hat{\mu} \qquad (21)$$

Note that these forces can be strongly increased by increasing the value of χ_{air}. In these circumstances, the air around the spacecraft would be strongly compressed upon the external surface of the spacecraft creating an atmosphere around it. This can be particularly useful in order to minimize the *friction* between the spacecraft and the atmosphere of the planet in the case of very high speed movements of the spacecraft. With the atmosphere around the spacecraft the friction will occur between the atmosphere of the spacecraft and the atmosphere of the planet. In this way, the friction will be minimum and the spacecraft could travel at very high speeds without overheating.

However, in order for this to occur, it is necessary to put the gravitational shielding in another position as shown in Fig.2. Thus, the values of χ_{airB} and χ_{airA} will be independent (See Fig.6). Thus, while inside the gravitational shielding, the value of χ_{airB} is put close to zero, in order to strongly reduce the gravitational mass of the spacecraft (inner part of the shielding), the value of χ_{airA} must be reduced to about -10^8 in order to strongly increase the gravitational attraction between the air molecules around the spacecraft. Thus, by

substituting $\chi_{airA} \cong -10^8$ intoEq.21, we get

$$\vec{F}_{12} = -\vec{F}_{21} = -10^{16} G \frac{m_{i1} m_{i2}}{r^2} \hat{\mu} \qquad (22)$$

If, $m_{i1} \cong m_{i2} = \rho_{air} V_1 \cong \rho_{air} V_2 \cong 10^{-8} kg$ and $r = 10^{-3} m$ then Eq. 22 gives

$$\vec{F}_{12} = -\vec{F}_{21} \cong -10^{-4} N \qquad (23)$$

These forces are much more intense than the *inter-atomic forces* (the forces that unite the atoms and molecules) the intensities of which are of the order of $1 - 1000 \times 10^{-8} N$. Consequently, the air around the spacecraft will be strongly compressed upon the surface of the spacecraft and thus will produce a crust of air which will accompany the spacecraft during its displacement and will protect it from the friction with the atmosphere of the planet.

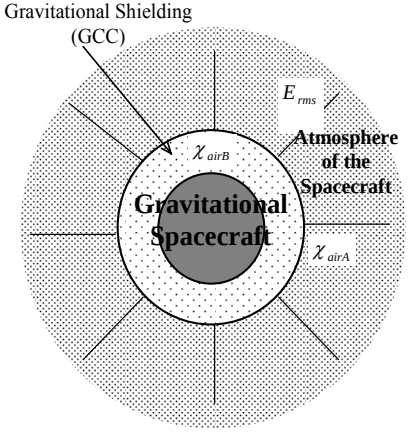

Fig. 6 – *Artificial atmosphere* around the gravitational spacecraft - while inside the gravitational shielding the value of χ_{airB} is putted close to zero, in order to strongly reduces the gravitational mass of the spacecraft (inner part of the shielding), the value of χ_{airA} must be reduced for about -10^8 in order to strongly increase the gravitational attraction between the air molecules around the spacecraft.

5. **The Imaginary Space-time**

The speed of light in free space is, as we know, about of 300.000 km/s. The speeds of the fastest modern airplanes of the present time do not reach 2 km/s and the speed of rockets do not surpass 20 km/s. This shows how much our aircraft and rockets are slow when compared with the speed of light.

The star nearest to the Earth (excluding the Sun obviously) is the Alpha of Centaur, which is about of *4 light-years* distant from the Earth (Approximately 37.8 trillions of kilometers). Traveling at a speed about 100 times greater than the maximum speed of our faster spacecrafts, we would take about 600 years to reach Alpha of Centaur. Then imagine how many years we would take to leave our own galaxy. In fact, it is not difficult to see that our spacecrafts are very slow, even for travels in our own solar system.

One of the fundamental characteristics of the gravitational spacecraft, as we already saw, is its capability to acquire enormous accelerations without submitting the crew to any discomfort.

Impelled by gravitational thrusters gravitational spacecrafts can acquire accelerations until $10^8 m.s^{-2}$ or more. This means that these spacecrafts can reach speeds very close to the speed of light in just a few seconds. These gigantic accelerations can be unconceivable for a layman, however they are common in our Universe. For example, when we submit an electron to an electric field

of just $1\ Volt/m$ it acquires an acceleration a, given by

$$a = \frac{eE}{m_e} = \frac{\left(1.6\times10^{-19}C\right)\left(1\ V/m\right)}{9.11\times10^{-31}} \cong 10^{11} m.s^{-2}$$

As we see, this acceleration is about 100 times greater than that acquired by the gravitational spacecraft previously mentioned.

By using the gravitational shieldings it is possible to reduce the inertial effects upon the spacecraft. As we have shown, they are reduced by the factor $\chi_{out} = M_g / M_i$. Thus, if the inertial mass of the spacecraft is $M_i = 10.000kg$ and, by means of the gravitational shielding effect the gravitational mass of the spacecraft is reduced to $M_g \approx 10^{-8} M_i$ then , in spite of the effective acceleration to be gigantic, for example, $a \approx 10^9 m.s^{-2}$, the effects for the crew of the spacecraft would be *equivalents to* an acceleration a' of only

$$a' = \frac{M_g}{M_i} a = \left(10^{-8}\right)\left(10^9\right) \approx 10 m.s^{-2}$$

This acceleration is similar to that which the passengers of a contemporary commercial jet are subjected.

Therefore the crew of the gravitational spacecraft would be comfortable while the spacecraft would reach speeds close to the speed of light in few seconds. However to travel at such velocities in the Universe may note be practical. Take for example, Alpha of Centaur (4 light-years far from the Earth): a round trip to it would last about eight years. Trips beyond that star could take then several decades, and this obviously is impracticable. Besides, to travel at such a speed would be very dangerous, because a shock with other celestial bodies would be inevitable. However, as we showed [1] there is a possibility of a spacecraft travel *quickly* far beyond our galaxy without the risk of being destroyed by a sudden shock with some celestial body. The solution is the gravitational spacecraft travel through the *Imaginary* or *Complex Space-time.*

It was shown [1] that it is possible to carry out a transition to the *Imaginary space-time* or *Imaginary Universe*. It is enough that the body has its *gravitational mass* reduced to a value in the range of $+0.159M_i$ to $-0.159M_i$. In these circumstances, the masses of the body (gravitational and inertial) become *imaginaries* and, so does the body. (Fig.7). Consequently, the body disappears from our ordinary space-time and appears in the imaginary space-time. In other words, it becomes *invisible* for an observer at the real Universe. Therefore, this is a way to get temporary *invisibility* of human beings, animals, spacecrafts, etc.

Thus, a spacecraft can leave our Universe and appear in the Imaginary Universe, where it can travel at any speed since in the Imaginary Universe *there is no speed limit for the gravitational spacecraft*, as it occurs in our Universe, where the particles cannot surpass the light speed. In this way, as the gravitational spacecraft is propelled by the gravitational thrusters, it can attain accelerations up to $10^9 m.s^{-2}$, then after one day of trip with this acceleration, it can

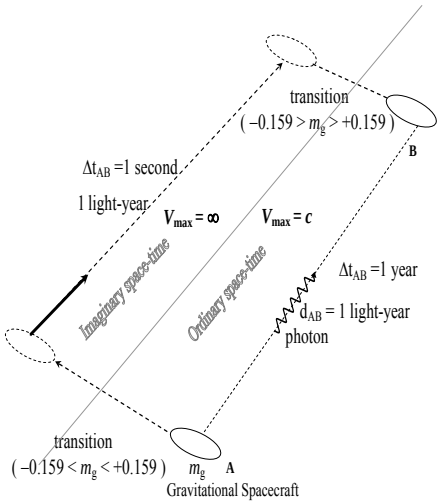

Fig. 7 – Travel in the *Imaginary* Space-time.

reach velocities $V \approx 10^{14}\, m.s^{-1}$ (about 1 million times the speed of light). With this velocity, after 1 month of trip the spacecraft would have traveled about $10^{21}\, m$. In order to have idea of this distance, it is enough to remind that the diameter of our Universe (visible Universe) is of the order of $10^{26}\, m$.

Due to the extremely low density of the imaginary bodies, the collision between them cannot have the same consequences of the collision between the dense real bodies.

Thus for a gravitational spacecraft in imaginary state the problem of the collision doesn't exist in high-speed. Consequently, the gravitational spacecraft can transit freely in the imaginary Universe and, in this way reach easily any point of our real Universe once they can make the transition back to our Universe by only increasing the gravitational mass of the spacecraft in such way that it leaves the range of $+0.159 M_i$ to $-0.159 M_i$. Thus the spacecraft can reappear in our Universe near its target.

The return trip would be done in similar way. That is to say, the spacecraft would transit in the imaginary Universe back to the departure place where would reappear in our Universe and it would make the approach flight to the wanted point. Thus, trips through our Universe that would delay millions of years, at speeds close to the speed of light, could be done in just a few *months* in the imaginary Universe.

What will an observer see when in the imaginary space-time? It will see light, bodies, planets, stars, etc., everything formed by imaginary photons, imaginary atoms, imaginary protons, imaginary neutrons and imaginary electrons. That is to say, the observer will find an Universe similar to ours, just formed by particles with imaginary masses. The term *imaginary* adopted from the Mathematics, as we already saw, gives the false impression that these masses do not exist. In order to avoid this misunderstanding we researched the true nature of that new mass type and matter.

The existence of imaginary mass associated to the *neutrino* is well-known. Although its imaginary mass is not physically observable, its square is. This amount is found experimentally to be negative. Recently, it was shown [1] that *quanta* of imaginary mass exist associated to the *photons, electrons, neutrons,* and

protons, and that these imaginary masses would have psychic properties (elementary capability of "choice"). Thus, the true nature of this new kind of mass and matter shall be psychic and, therefore we should not use the term *imaginary* any longer. Consequently from the above exposed we can conclude that the gravitational spacecraft penetrates in the *Psychic Universe* and not in an "imaginary" Universe.

In this Universe, the matter would be, obviously composed by psychic molecules and psychic atoms formed by psychic neutrons, psychic protons and psychic electrons. i.e., the matter would have psychic mass and consequently it would be *subtle*, much less dense than the matter of our *real* Universe.

Thus, from a quantum viewpoint, the psychic particles are similar to the material particles, so that we can use the Quantum Mechanics to describe the psychic particles. In this case, by analogy to the material particles, a particle with psychic mass m_Ψ will be described by the following expressions:

$$\vec{p}_\psi = \hbar \vec{k}_\psi$$
$$E_\psi = \hbar \omega_\psi$$

Where $\vec{p}_\psi = m_\Psi \vec{V}$ is the *momentum* carried by the wave and E_ψ its energy; $\left|\vec{k}_\psi\right| = 2\pi/\lambda_\psi$ is the *propagation number* and $\lambda_\psi = h/m_\Psi V$ the *wavelength* and $\omega_\psi = 2\pi f_\psi$ its cyclic *frequency*.

The variable quantity that characterizes DeBroglie's waves is called *Wave Function*, usually indicated by Ψ. The wave function associated to a material particle describes the dynamic state of the particle: its value at a particular point x, y, z, t is related to the probability of finding the particle in that place and instant. Although Ψ does not have a physical interpretation, its square Ψ^2 (or $\Psi\,\Psi^*$) calculated for a particular point x, y, z, t is *proportional to the probability of experimentally finding the particle in that place and instant*.

Since Ψ^2 is proportional to the probability P of finding the particle described by Ψ, the integral of Ψ^2 on the *whole space* must be finite – inasmuch as the particle is someplace. Therefore, if

$$\int_{-\infty}^{+\infty} \Psi^2 d\mathrm{V} = 0$$

The interpretation is that the particle does not exist. Conversely, if

$$\int_{-\infty}^{+\infty} \Psi^2 d\mathrm{V} = \infty$$

the particle will be everywhere simultaneously.

The wave function Ψ corresponds, as we know, to the displacement y of the undulatory motion of a rope. However, Ψ as opposed to y, is not a measurable quantity and can, hence, being a *complex* quantity. For this reason, it is admitted that Ψ is described in the x-direction by

$$\Psi = Be^{-(2\pi\, i/h)(Et-px)}$$

This equation is the mathematical description of the wave associated with a free material particle, with total energy E and *momentum* p, moving in the direction $+x$.

As concerns the psychic particle, the variable quantity characterizing psyche waves will also

be called wave function, denoted by Ψ_Ψ (to distinguish it from the material particle wave function), and, by analogy with equation of Ψ, expressed by:

$$\Psi_\Psi = \Psi_0 e^{-(2\pi\, i/h)(E_\Psi t - p_\Psi x)}$$

If an experiment involves a large number of identical particles, all described by the same wave function Ψ , the *real* density of mass ρ of these particles in x, y, z, t is proportional to the corresponding value Ψ^2 (Ψ^2 is known as *density of probability*. If Ψ is *complex* then $\Psi^2 = \Psi\Psi^*$. Thus, $\rho \propto \Psi^2 = \Psi.\Psi^*$). Similarly, in the case of psychic particles, the *density of psychic mass*, ρ_Ψ, in x, y, z, will be expressed by $\rho_\Psi \propto \Psi_\Psi^2 = \Psi_\Psi \Psi_\Psi^*$. It is known that Ψ_Ψ^2 is always *real* and *positive* while $\rho_\Psi = m_\Psi / V$ is an *imaginary* quantity. Thus, as the *modulus* of an imaginary number is always real and positive, we can transform the proportion $\rho_\Psi \propto \Psi_\Psi^2$, in equality in the following form:

$$\Psi_\Psi^2 = k|\rho_\Psi|$$

Where k is a *proportionality constant* (real and positive) to be determined.

In Quantum Mechanics we have studied the *Superposition Principle*, which affirms that, if a particle (or system of particles) is in a *dynamic state* represented by a wave function Ψ_1 and may also be in another dynamic state described by Ψ_2 then, the general dynamic state of the particle may be described by Ψ, where Ψ is a linear combination (superposition) of Ψ_1 and Ψ_2, i.e.,

$$\Psi = c_1\Psi_1 + c_2\Psi_2$$

The C*omplex constants* c_1 e c_2 respectively express the percentage of dynamic state, represented by Ψ_1 e Ψ_2 in the formation of the general dynamic state described by Ψ.

In the case of psychic particles (psychic bodies, consciousness, etc.), by analogy, if $\Psi_{\Psi 1}$, $\Psi_{\Psi 2}$,..., $\Psi_{\Psi n}$ refer to the different dynamic states the psychic particle takes, then its general dynamic state may be described by the wave function Ψ_Ψ , given by:

$$\Psi_\Psi = c_1\Psi_{\Psi 1} + c_2\Psi_{\Psi 2} + ... + c_n\Psi_{\Psi n}$$

The state of superposition of wave functions is, therefore, common for both psychic and material particles. In the case of material particles, it can be verified, for instance, when an electron changes from one orbit to another. Before effecting the transition to another energy level, the electron carries out "virtual transitions" [6]. A kind of *relationship* with other electrons before performing the real transition. During this relationship period, its wave function remains "*scattered*" by *a wide region of the space* [7] thus superposing the wave functions of the other electrons. In this relationship the electrons *mutually* influence each other, with the possibility of *intertwining* their wave functions[§]. When this happens, there occurs the so-called *Phase Relationship* according to quantum-mechanics concept.

In the electrons "virtual" transition mentioned before, the "listing" of all the possibilities of the electrons is described, as we know, by *Schrödinger's wave equation.*

[§] Since the electrons are simultaneously waves and particles, their wave aspects will interfere with each other; besides superposition, there is also the possibility of occurrence of *intertwining* of their wave functions.

Otherwise, it is general for material particles. By analogy, in the case of psychic particles, we may say that the "listing" of all the possibilities of the psyches involved in the relationship will be described by *Schrödinger's equation* – for psychic case, i.e.,

$$\nabla^2 \Psi_\Psi + \frac{p_\Psi^2}{\hbar^2} \Psi_\Psi = 0$$

Because the wave functions are capable of intertwining themselves, the quantum systems may "penetrate" each other, thus establishing an internal relationship where all of them are affected by the relationship, no longer being isolated systems but becoming an integrated part of a larger system. This type of internal relationship, which exists only in quantum systems, was called *Relational Holism* [8].

We have used the Quantum Mechanics in order to describe the foundations of the Psychic Universe which the Gravitational Spacecrafts will find, and that influences us daily. These foundations recently discovered – particularly the *Psychic Interaction*, show us that a rigorous description of the Universe cannot to exclude the psychic energy and the psychic particles. This verification makes evident the need of to redefine the Psychology with basis on the quantum foundations recently discovered. This has been made in the article: "*Physical Foundations of Quantum Psychology*"[**] [9], recently published, where it is shown that the Psychic Interaction leads us to understand the Psychic Universe and the extraordinary relationship that the human consciousnesses establish among themselves and with the Ordinary Universe. Besides, we have shown that the Psychic Interaction postulates a new model for the evolution theory, in which the evolution is interpreted not only as a biological fact, but mainly as *psychic* fact. Therefore, is not only the mankind that evolves in the Earth's planet, but all the ecosystem of the Earth.

[**] http://htpprints.yorku.ca/archive/00000297

6. Past and Future

It was shown [1,9] that the *collapse* of the *psychic* wave function must suddenly also express in reality (*real* space-time) all the possibilities described by it. This is, therefore, *a point of decision* in which there occurs the compelling need of *realization* of the *psychic form*. We have seen that the *materialization* of the psychic form, in the real space-time, occurs when it contains enough *psychic mass* for the total materialization[††] of the psychic form (*Materialization Condition*). When this happens, all the psychic energy contained in the psychic form is transformed in real energy in the real space-time. Thus, in the psychic space-time just the *holographic* register of the psychic form, which gives origin to that fact, survives, since the psychic energy deforms the *metric* of the psychic space-time[‡‡], producing the

[††] By this we mean not only materialization proper but also the movement of matter to realize its psychic content (including radiation).

[‡‡] As shown in *General Theory of Relativity* the energy modifies the metric of the space-time (deforming the space-time).

holographic register. Thus, the past survive in the psychic space-time just in the form of holographic register. That is to say, all that have occurred in the past is holographically registered in the *psychic space-time*. Further ahead, it will be seen that this register can be accessed by an observer in the *psychic* space-time as well as by an observer in the *real* space-time.

A psychic form is intensified by means of a continuous addition of psychic mass. Thus, when it acquires sufficiently psychic mass, its realization occurs in the real space-time. Thus the future is going being built in the present. By means of our current thoughts we shape the psychic forms that will go (or will not) take place in the future. Consequently, those psychic forms are continually being holographically registered in the *psychic space-time* and, just as the holographic registrations of the *past* these future registration can also be accessed by the *psychic* space-time as well as by the *real* space-time.

The access to the holographic registration of the past doesn't allow, obviously, the modification of the past. This is not possible because there would be a clear violation of the *principle of causality* that says that the causes should precede the effects. However, the psychic forms that are being shaped now in order to manifest themselves in the future, can be modified before they manifest themselves. Thus, the access to the registration of those psychic forms becomes highly relevant for our present life, since we can avoid the manifestation of many unpleasant facts in the future.

Since both registrations are in the *psychic* space-time, then the access to their information only occur by means of the interaction with another psychic body, for example, our *consciousness* or a *psychic observer* (body totally formed by psychic mass). We have seen that, if the gravitational mass of a body is reduced to within the range $+0.159M_i$ to $-0.159M_i$, its gravitational and inertial masses become *imaginaries* (*psychics*) and, therefore, the body becomes a *psychic body*. Thus, a *real observer* can also become in a *psychic observer*. In this way, a gravitational spacecraft can transform all its inertial mass into psychic mass, and thus carry out a transition to the psychic space-time and become a psychic spacecraft. In these circumstances, an observer inside the spacecraft also will have its mass transformed into psychic mass, and, therefore, the observer also will be transformed into a psychic observer. What will this observer see when it penetrates the psychic Universe? According to the *Correspondence principle*, all that exists in the real Universe must have the correspondent in the psychic Universe and vice-versa. This principle reminds us that we live in more than one world. At the present time, we live in the real Universe, but we can also live in the psychic Universe. Therefore, the psychic observer will see the psychic bodies and their correspondents in the real Universe. Thus, a pilot of a gravitational spacecraft, in travel through the psychic space-time, won't have difficulty to spot the spacecraft in its trips through the Universe.

The fact of the psychic forms manifest themselves in the real space-time exactly at its images and likeness, it indicates that real forms (forms in the real space-time) are prior to all reflective *images* of psychic forms of the past. Thus, the real space-time is a mirror of the psychic space-time. Consequently, any register in the psychic space-time will have a correspondent image in the real space-time. This means that it is possible that we find in the real space-time the *image* of the holographic register existing in the psychic space-time, corresponding to our *past*. Similarly, every psychic form that is being shaped in the psychic space-time will have reflective image in the real space-time. Thus, the *image* of the holographic register of our future (existing in the psychic space-time) can also be found in the *real* space-time.

Each image of the holographic register of our future will be obviously correlated to a future epoch in the temporal coordinate of the space-time. In the same way, each image of the holographic registration of our past will be correlated to a passed time in the temporal coordinate of the referred space-time. Thus, in order to access the mentioned registrations we should accomplish trips to the past or future in the real space-time. This is possible now, with the advent of the gravitational spacecrafts because they allow us to reach speeds close to the speed of light. Thus, by varying the gravitational mass of the spacecraft for *negative* or *positive* we can go respectively to the *past* or *future* [1].

If the gravitational mass of a particle is *positive*, then t is always *positive* and given by

$$t = +t_0 \Big/ \sqrt{1 - V^2/c^2}$$

This leads to the well-known relativistic prediction that the particle goes to the *future* if $V \to c$. However, if the gravitational mass of the particle is negative, then t is also *negative* and, therefore, given by

$$t = -t_0 \Big/ \sqrt{1 - V^2/c^2}$$

In this case, the prevision is that the particle goes to the *past* if $V \to c$. In this way, *negative gravitational mass* is the necessary condition to the particle to go to the *past*.

Since the acceleration of a spacecraft with gravitational mass m_g, is given by $a = F/m_g$, where F is the thrust of its thrusters, then the more we reduce the value of m_g the bigger the acceleration of the spacecraft will be. However, since the value of m_g cannot be reduced to the range $+0.159M_i$ to $-0.159M_i$ because the spacecraft would become a psychic body, and it needs to remain in the real space-time in order to access the past or the future in the real space-time, then, the ideal values for the spacecraft to operate with safety would be $\pm 0.2m_i$. Let us consider a gravitational spacecraft whose inertial mass is $m_i = 10.000kg$. If its gravitational mass was made *negative* and equal to $m_g = -0.2m_i = -2000kg$ and, at this instant the thrust produced by the

thrusters of the spacecraft was $F = 10^5 N$ then, the spacecraft would acquire acceleration $a = F/m_g = 50 ms^{-2}$ and, after $t = 30 days = 2.5 \times 10^6 s$, the speed of the spacecraft would be $v = 1.2 \times 10^8 m.s^{-1} = 0.4c$. Therefore, right after that the spacecraft returned to the Earth, its crew would find the Earth in the *past* (due to the *negative* gravitational mass of the spacecraft) at a time $t = -t_0 / \sqrt{1 - V^2/c^2}$; t_0 is the time measured by an observer at rest on the Earth. Thus, if $t_0 = 2009$ AD, the time interval $\Delta t = t - t_0$ would be expressed by

$$\Delta t = t - t_0 = -t_0 \left(\frac{1}{\sqrt{1 - V^2/c^2}} - 1 \right) = -t_0 \left(\frac{1}{\sqrt{1 - 0.16}} - 1 \right) \cong$$

$$\cong -0.091 t_0 \cong -183 years$$

That is, the spacecraft would be in the year 1826 AD. On the other hand, if the gravitational mass of the spacecraft would have become positive $m_g = +0.2 m_i = +2000 kg$, instead of negative, then the spacecraft would be in the future at $\Delta t = +183\ years$ from 2009. That is, it would be in the year 2192 AD.

7. Instantaneous Interestelar Communications

Consider a cylindrical GCC (GCC antenna) as shown in Fig.8. The *gravitational mass* of the *air* inside the GCC is

$$m_{g(air)} = \left\{ 1 - 2 \left[\sqrt{1 + \frac{\sigma_{(air)} B^4}{4 \pi f \mu \rho_{(air)}^2 c^2}} - 1 \right] \right\} m_{i(air)} \quad (24)$$

Where $\sigma_{(ar)}$ is the electric conductivity of the ionized air inside the GCC and $\rho_{(ar)}$ is its density; f is the frequency of the magnetic field.

By varying B one can vary $m_{g(air)}$ and consequently to vary the gravitational field generated by $m_{g(air)}$, producing then *Gravitational Radiation*. Then a GCC can work as a *Gravitational Antenna*.

Apparently, Newton's theory of gravity had no gravitational waves because, if a gravitational field changed in some way, that change would have taken place *instantaneously* everywhere in space, and one can think that there is not a wave in this case. However, we have already seen that the gravitational interaction can be repulsive, besides

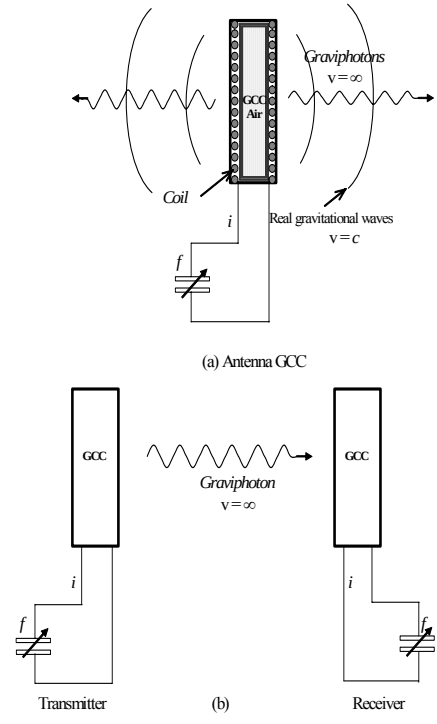

Fig. 8 – Transmitter and Receiver of *Virtual* Gravitational Radiation.

attractive. Thus, as with electromagnetic interaction, the gravitational interaction must be produced by the exchange of "virtual" *quanta of* spin 1 and mass null, i.e., the *gravitational* "virtual" *quanta* (*graviphoton*) must have spin 1 and not 2. Consequently, the fact that a change in a gravitational field reaches *instantaneously* every point in space occurs simply due to the speed of the *graviphoton* to be *infinite*. It is known that there is no speed limit for "*virtual*" photons. On the other hand, the *electromagnetic quanta* ("virtual" photons) can not communicate the *electromagnetic interaction* to an infinite distance.

Thus, there are *two types* of gravitational radiation: the *real* and *virtual*, which is constituted of graviphotons; the *real* gravitational waves are ripples in the space-time generated by *gravitational field* changes. According to Einstein's theory of gravity the velocity of propagation of these waves is equal to the speed of light [10].

Unlike the electromagnetic waves the *real* gravitational waves have low interaction with matter and consequently low scattering. Therefore *real* gravitational waves are suitable as a means of transmitting information. However, when the distance between transmitter and receiver is too large, for example of the order of magnitude of several light-years, the transmission of information by means of gravitational waves becomes impracticable due to the long time necessary to receive the information. On the other hand, there is no delay during the transmissions by means of *virtual* gravitational radiation. In addition, the scattering of this radiation is null. Therefore the *virtual* gravitational radiation is very suitable as a means of transmitting information at any distances, including astronomical distances.

As concerns detection of the *virtual* gravitational radiation from GCC antenna, there are many options. Due to *Resonance Principle* a similar GCC antenna (receiver) *tuned at the same frequency* can absorb energy from an incident *virtual* gravitational radiation (See Fig.8 (b)). Consequently, the gravitational mass of the air inside the GCC receiver will vary such as the gravitational mass of the air inside the GCC transmitter. This will induce a magnetic field similar to the magnetic field of the GCC transmitter and therefore the current through the coil inside the GCC receiver will have the same characteristics of the current through the coil inside the GCC transmitter. However, the *volume* and *pressure* of the air inside the two GCCs must be exactly the same; also the *type* and the *quantity of atoms* in the air inside the two GCCs must be exactly the same. Thus, the GCC antennas are simple but they are not easy to build.

Note that a GCC antenna radiates *graviphotons* and *gravitational waves* simultaneously (Fig. 8 (a)). Thus, it is not only a gravitational antenna: it is a *Quantum Gravitational Antenna* because it can also emit and detect gravitational "virtual" *quanta* (graviphotons), which, in turn, can transmit information *instantaneously* from any

distance in the Universe *without* scattering.

Due to the difficulty to build two similar GCC antennas and, considering that the electric current in the receiver antenna can be detectable even if the gravitational mass of the nuclei of the antennas are not *strongly* reduced, then we propose to replace the gas at the nuclei of the antennas by a thin *dielectric lamina*. When the *virtual* gravitational radiation strikes upon the dielectric lamina, its gravitational mass varies similarly to the gravitational mass of the dielectric lamina of the transmitter antenna, inducing an electromagnetic field (E, B) similar to the transmitter antenna. Thus, the electric current in the receiver antenna will have the same characteristics of the current in the transmitter antenna. In this way, it is then possible to build two similar antennas whose nuclei have the same volumes and the same types and quantities of atoms.

Note that the Quantum Gravitational Antennas can also be used to transmit *electric power*. It is easy to see that the Transmitter and Receiver can work with strong voltages and electric currents. This means that strong electric power can be transmitted among Quantum Gravitational Antennas. This obviously solves the problem of *wireless* electric power transmission. Thus, we can conclude that the spacecrafts *do not necessarily need* to have a system for generation of electric energy inside them. Since the electric energy to be used in the spacecraft can be *instantaneously transmitted* from *any point of the Universe*, by means of the above mentioned systems of transmission and reception of "virtual" gravitational waves.

8. Origin of Gravity and Genesis of the Gravitational Energy

It was shown [1] that the "virtual" *quanta* of the *gravitational interaction* must have spin 1 and not 2, and that they are "virtual" photons (*graviphotons*) with *zero mass* outside the *coherent* matter. Inside the coherent matter the graviphotons mass is *non-zero*. Therefore, the gravitational forces are also *gauge* forces, because they are yielded by the exchange of "virtual" *quanta* of spin 1, such as the electromagnetic forces and the weak and strong nuclear forces.

Thus, the gravitational forces are produced by the exchanging of "virtual" photons (Fig.9). Consequently, this is precisely the *origin of the gravity*.

Newton's theory of gravity does not explain *why* objects attract one another; it simply models this observation. Also Einstein's theory does not explain the origin of gravity. Einstein's theory of gravity only describes gravity with more precision than Newton's theory does.

Besides, there is nothing in both theories explaining the *origin of the energy* that produces the gravitational forces. Earth's gravity attracts all objects on the surface of our planet. This has been going on for over 4.5 billions years, yet no known energy source is being converted to support this tremendous ongoing energy expenditure. Also is the enormous

continuous energy expended by Earth's gravitational field for maintaining the Moon in its orbit - millennium after millennium. In spite of the ongoing energy expended by Earth's gravitational field to hold objects down on surface and the Moon in orbit, why the energy of the field never diminishes in strength or drains its energy source? Is this energy expenditure balanced by a conversion of energy from an unknown energy source?

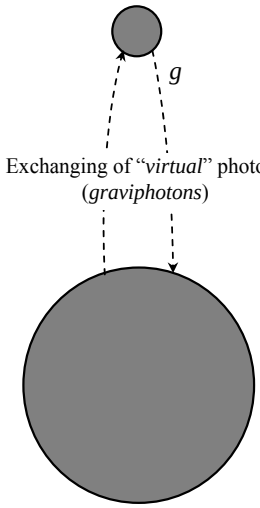

Fig. 9 – *Origin of Gravity*: The gravitational forces are produced by the exchanging of "virtual" photons (*graviphotons*).

The energy W necessary to support the effort expended by the gravitational forces F is well-known and given by

$$W = \int_{\infty}^{r} F dr = -G \frac{M_g m_g}{r}$$

According to the *Principle of Energy Conservation*, the spending of this energy must be compensated by a conversion of another type of energy.

The Uncertainty Principle tells us that, due to the occurrence of exchange of *graviphotons* in a time interval $\Delta t < \hbar/\Delta E$ (where ΔE is the energy of the graviphoton), the energy variation ΔE cannot be detected in the system $M_g - m_g$. Since the total energy W is the sum of the energy of the n graviphotons, i.e., $W = \Delta E_1 + \Delta E_2 + ... + \Delta E_n$, then the energy W *cannot be detected as well*. However, as we know it can be converted into another type of energy, for example, in rotational kinetic energy, as in the hydroelectric plants, or in the *Gravitational Motor*, as shown in this work.

It is known that a *quantum* of energy $\Delta E = hf$, which varies during a time interval $\Delta t = 1/f = \lambda/c < \hbar/\Delta E$ (wave period) cannot be experimentally detected. This is an *imaginary* photon or a "*virtual*" photon. Thus, the graviphotons are *imaginary* photons, i.e., the energies ΔE_i of the graviphotons are imaginaries energies and therefore the energy $W = \Delta E_1 + \Delta E_2 + ... + \Delta E_n$ is also an *imaginary* energy. Consequently, it belongs to the *imaginary space-time*.

It was shown [1] that, imaginary energy is equal to *psychic energy*. Consequently, the *imaginary space-time* is, in fact, the *psychic space-time*, which contains the Supreme Consciousness. Since the Supreme Consciousness has *infinite* psychic mass [1], then the *psychic space-time* contains *infinite psychic energy*. This is highly relevant, because it confers to the *Psychic Universe* the characteristic of *unlimited source of energy.* Thus, as the origin of the gravitational energy it is correlated to the psychic

energy, then the spending of gravitational energy can be supplied *indefinitely* by the Psychic Universe.

This can be easily confirmed by the fact that, in spite of the enormous amount of energy expended by Earth's gravitational field to hold objects down on the surface of the planet and maintain the Moon in its orbit, the energy of Earth's gravitational field never diminishes in strength or drains its energy source.

Acknowledgement

The author would like to thank Dr. *Getúlio Marques Martins* (COPPE – UFRJ, Rio de Janeiro-Brasil) for revising the manuscript.

APPENDIX A: The Simplest Method to Control the Gravity

In this Appendix we show the simplest method to control the gravity.

Consider a body with mass density ρ and the following electric characteristics: $\mu_r, \varepsilon_r, \sigma$ (relative permeability, relative permittivity and electric conductivity, respectively). Through this body, passes an electric current I, which is the sum of a sinusoidal current $i_{osc} = i_0 \sin \omega t$ and the DC current I_{DC}, i.e., $I = I_{DC} + i_0 \sin \omega t$; $\omega = 2\pi f$. If $i_0 << I_{DC}$ then $I \cong I_{DC}$. Thus, the current I varies with the frequency f, but the variation of its intensity is quite small in comparison with I_{DC}, i.e., I will be practically constant (Fig. A1). This is of fundamental importance for maintaining the value of the gravitational mass of the body, m_g, sufficiently stable during all the time.

The *gravitational mass* of the *body* is given by [1]

$$m_g = \left\{1 - 2\left[\sqrt{1 + \left(\frac{n_r U}{m_{i0} c^2}\right)^2} - 1\right]\right\} m_{i0} \qquad (A1)$$

where U, is the electromagnetic energy absorbed by the body and n_r is the index of refraction of the body.

Equation (A1) can also be rewritten in the following form

$$\frac{m_g}{m_{i0}} = \left\{1 - 2\left[\sqrt{1 + \left(\frac{n_r W}{\rho\, c^2}\right)^2} - 1\right]\right\} \qquad (A2)$$

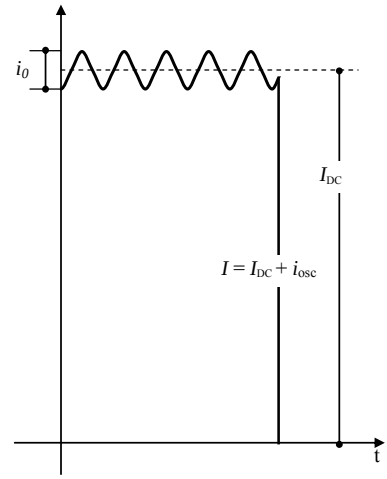

Fig. A1 - The electric current I varies with frequency f. But the variation of I is quite small in comparison with I_{DC} due to $i_o << I_{DC}$. In this way, we can consider $I \cong I_{DC}$.

where, $W = U/V$ is the *density of electromagnetic energy* and $\rho = m_{i0}/\mathrm{V}$ is the density of inertial mass.

The *instantaneous values* of the density of electromagnetic energy in an *electromagnetic* field can be deduced from Maxwell's equations and has the following expression

$$W = \tfrac{1}{2}\varepsilon E^2 + \tfrac{1}{2}\mu H^2 \qquad (A3)$$

where $E = E_m \sin \omega t$ and $H = H \sin \omega t$ are the *instantaneous values* of the electric field and the magnetic field respectively.

It is known that $B = \mu H$, $E/B = \omega/k_r$ [11] and

$$v = \frac{dz}{dt} = \frac{\omega}{\kappa_r} = \frac{c}{\sqrt{\frac{\varepsilon_r \mu_r}{2}\left(\sqrt{1+(\sigma/\omega\varepsilon)^2}+1\right)}} \quad (A4)$$

where k_r is the real part of the *propagation vector* $\vec{k}$ (also called *phase constant*); $k = |\vec{k}| = k_r + ik_i$; ε , μ and σ, are the electromagnetic characteristics of the medium in which the incident (or emitted) radiation is propagating($\varepsilon = \varepsilon_r \varepsilon_0 ; \varepsilon_0 = 8.854\times10^{-12} F/m$; $\mu = \mu_r \mu_0$ where $\mu_0 = 4\pi\times10^{-7} H/m$). It is known that for *free-space* $\sigma = 0$ and $\varepsilon_r = \mu_r = 1$. Then Eq. (A4) gives

$$v = c$$

From (A4), we see that the *index of refraction* $n_r = c/v$ is given by

$$n_r = \frac{c}{v} = \sqrt{\frac{\varepsilon_r \mu_r}{2}\left(\sqrt{1+(\sigma/\omega\varepsilon)^2}+1\right)} \quad (A5)$$

Equation (A4) shows that $\omega/\kappa_r = v$. Thus, $E/B = \omega/k_r = v$, i.e.,

$$E = vB = v\mu H \quad (A6)$$

Then, Eq. (A3) can be rewritten in the following form:

$$W = \tfrac{1}{2}\left(\varepsilon v^2 \mu\right)\mu H^2 + \tfrac{1}{2}\mu H^2 \quad (A7)$$

For $\sigma << \omega\varepsilon$, Eq. (A4) reduces to

$$v = \frac{c}{\sqrt{\varepsilon_r \mu_r}}$$

Then, Eq. (A7) gives

$$W = \tfrac{1}{2}\left[\varepsilon\left(\frac{c^2}{\varepsilon_r \mu_r}\right)\mu\right]\mu H^2 + \tfrac{1}{2}\mu H^2 = \mu H^2$$

This equation can be rewritten in the following forms:

$$W = \frac{B^2}{\mu} \quad (A8)$$

or

$$W = \varepsilon\, E^2 \quad (A9)$$

For $\sigma >> \omega\varepsilon$, Eq. (A4) gives

$$v = \sqrt{\frac{2\omega}{\mu\sigma}} \quad (A10)$$

Then, from Eq. (A7) we get

$$W = \tfrac{1}{2}\left[\varepsilon\left(\frac{2\omega}{\mu\sigma}\right)\mu\right]\mu H^2 + \tfrac{1}{2}\mu H^2 = \left(\frac{\omega\varepsilon}{\sigma}\right)\mu H^2 + \tfrac{1}{2}\mu H^2 \cong$$
$$\cong \tfrac{1}{2}\mu H^2 \quad (A11)$$

Since $E = vB = v\mu H$, we can rewrite (A11) in the following forms:

$$W \cong \frac{B^2}{2\mu} \quad (A12)$$

or

$$W \cong \left(\frac{\sigma}{4\omega}\right)E^2 \quad (A13)$$

By comparing equations (A8) (A9) (A12) and (A13), we can see that Eq. (A13) shows that the best way to obtain a strong value of W *in practice* is by applying an *Extra Low-Frequency* (ELF) *electric field* $(w = 2\pi f << 1Hz)$ through a *medium with high electrical conductivity*.

Substitution of Eq. (A13) into Eq. (A2), gives

$$m_g = \left\{1-2\left[\sqrt{1+\frac{\mu}{4c^2}\left(\frac{\sigma}{4\pi f}\right)^3\frac{E^4}{\rho^2}}-1\right]\right\}m_{i0} =$$
$$= \left\{1-2\left[\sqrt{1+\left(\frac{\mu_0}{256\pi^3 c^2}\right)\left(\frac{\mu_r \sigma^3}{\rho^2 f^3}\right)E^4}-1\right]\right\}m_{i0} =$$
$$= \left\{1-2\left[\sqrt{1+1.758\times10^{-27}\left(\frac{\mu_r \sigma^3}{\rho^2 f^3}\right)E^4}-1\right]\right\}m_{i0} \quad (A14)$$

Note that $E = E_m \sin\omega t$. The average value for E^2 is equal to $\frac{1}{2}E_m^2$ because

E varies sinusoidaly (E_m is the maximum value for E). On the other hand, $E_{rms} = E_m/\sqrt{2}$. Consequently we can change E^4 by E_{rms}^4, and the equation above can be rewritten as follows

$$m_g = \left\{1 - 2\left[\sqrt{1 + 1.758\times10^{-27}\left(\frac{\mu_r\sigma^3}{\rho^2 f^3}\right)E_{rms}^4} - 1\right]\right\}m_{i0}$$

Substitution of the well-known equation of the *Ohm's vectorial Law*: $j = \sigma E$ into (A14), we get

$$m_g = \left\{1 - 2\left[\sqrt{1 + 1.758\times10^{-27}\frac{\mu_r j_{rms}^4}{\sigma\rho^2 f^3}} - 1\right]\right\}m_{i0} \quad (A15)$$

where $j_{rms} = j/\sqrt{2}$.

Consider a 15 cm square *Aluminum thin foil* of *10.5 microns thickness* with the following characteristics: $\mu = 1$; $\sigma = 3.82\times10^7\, S.m^{-1}$; $\rho = 2700\, Kg.m^{-3}$. Then, (A15) gives

$$m_g = \left\{1 - 2\left[\sqrt{1 + 6.313\times10^{-42}\frac{j_{rms}^4}{f^3}} - 1\right]\right\}m_{i0} \quad (A16)$$

Now, consider that the ELF electric current $I = I_{DC} + i_0 \sin\omega t$, $(i_0 << I_{DC})$ passes through that Aluminum foil. Then, the current density is

$$j_{rms} = \frac{I_{rms}}{S} \cong \frac{I_{DC}}{S} \quad (A17)$$

where

$$S = 0.15m\left(10.5\times10^{-6}\, m\right) = 1.57\times10^{-6}\, m^2$$

If the ELF electric current has frequency $f = 2\mu Hz = 2\times10^{-6}\, Hz$, then, the gravitational mass of the aluminum foil, given by (A16), is expressed by

$$m_g = \left\{1 - 2\left[\sqrt{1 + 7.89\times10^{-25}\frac{I_{DC}^4}{S^4}} - 1\right]\right\}m_{i0} =$$

$$= \left\{1 - 2\left[\sqrt{1 + 0.13 I_{DC}^4} - 1\right]\right\}m_{i0} \quad (A18)$$

Then,

$$\chi = \frac{m_g}{m_{i0}} \cong \left\{1 - 2\left[\sqrt{1 + 0.13 I_{DC}^4} - 1\right]\right\} \quad (A19)$$

For $I_{DC} = 2.2A$, the equation above gives

$$\chi = \left(\frac{m_g}{m_{i0}}\right) \cong -1 \quad (A20)$$

This means that *the gravitational shielding* produced by the aluminum foil can change the gravity acceleration *above* the foil down to

$$g' = \chi\, g \cong -1g \quad (A21)$$

Under these conditions, the Aluminum foil works basically as a Gravity Control Cell (GCC).

In order to check these theoretical predictions, we suggest an experimental set-up shown in Fig.A2.

A 15cm square Aluminum foil of *10.5 microns thickness* with the following composition: Al 98.02%; Fe 0.80%; Si 0.70%; Mn 0.10%; Cu 0.10%; Zn 0.10%; Ti 0.08%; Mg 0.05%; Cr 0.05%, and with the following characteristics: $\mu = 1$; $\sigma = 3.82\times10^7\, S.m^{-1}$; $\rho = 2700 Kg.m^{-3}$, is fixed on a 17 cm square *Foam Board* [§§] plate of 6mm thickness as shown in Fig.A3. This device (the simplest

[§§] *Foam board* is a very strong, *lightweight* (density: 24.03 kg.m^{-3}) and easily cut material used for the mounting of photographic prints, as backing in picture framing, in 3D design, and in painting. It consists of three layers — an inner layer of polystyrene clad with outer facing of either white clay coated paper or brown Kraft paper.

Gravity Control Cell GCC) is placed on a pan balance shown in Fig.A2.

Above the Aluminum foil, a *sample* (any type of material, any mass) connected to a dynamometer will check the decrease of the *local gravity acceleration* upon the sample $(g' = \chi\ g)$, due to the gravitational shielding produced by the decreasing of gravitational mass of the Aluminum foil $(\chi = m_g / m_{i0})$. Initially, the sample lies 5 cm above the Aluminum foil. As shown in Fig.A2, the board with the dynamometer can be displaced up to few meters in height. Thus, the initial distance between the Aluminum foil and the sample can be increased in order to check the reach of the gravitational shielding produced by the Aluminum foil.

In order to generate the ELF electric current of $f = 2\mu Hz$, we can use the widely-known Function Generator HP3325A (Op.002 High Voltage Output) that can generate sinusoidal voltages with *extremely-low* frequencies down to $f = 1\times10^{-6} Hz$ and amplitude up to 20V ($40V_{pp}$ into 500Ω load). The maximum output current is $0.08A_{pp}$; output impedance <2Ω at ELF .

Figure A4 (a) shows the equivalent electric circuit for the experimental set-up. The electromotive forces are: ε_1 (HP3325A) and ε_2 (*12V* DC Battery).The values of the *resistors* are : $R_1 = 500\Omega - 2W$; $r_{i1} < 2\Omega$; $R_2 = 4\Omega - 40W$; $r_{i2} < 0.1\Omega$; $R_p = 2.5\times10^{-3}\Omega$; *Rheostat* ($0 \le R \le 10\Omega$ - 90W). The *coupling transformer* has the following characteristics: air core with diameter $\phi = 10mm$; area $S = \pi\phi^2/4 = 7.8\times10^{-5} m^2$; wire#12AWG; $N_1 = N_2 = N = 20$; $l = 42mm$; $L_1 = L_2 = L = \mu_0 N^2 (S/l) = 9.3\times10^{-7} H$ .Thus, we get

$$Z_1 = \sqrt{(R_1 + r_{i1})^2 + (\omega L)^2} \cong 50\Omega$$

and

$$Z_2 = \sqrt{(R_2 + r_{i2} + R_p + R)^2 + (\omega L)^2}$$

For $R = 0$ we get $Z_2 = Z_2^{\min} \cong 4\Omega$; for $R = 10\Omega$ the result is $Z_2 = Z_2^{\max} \cong 14\Omega$. Thus,

$$Z_{1,total}^{\min} = Z_1 + Z_{1,reflected}^{\min} = Z_1 + Z_2^{\min}\left(\frac{N_1}{N_2}\right)^2 \cong 50\Omega$$

$$Z_{1,total}^{\max} = Z_1 + Z_{1,reflected}^{\max} = Z_1 + Z_2^{\max}\left(\frac{N_1}{N_2}\right)^2 \cong 51\Omega$$

The maxima *rms* currents have the following values:

$$I_1^{\max} = \tfrac{1}{\sqrt{2}}\, 40V_{pp} \big/ Z_{1,total}^{\min} = 56mA$$

(The maximum output current of the Function Generator HP3325A (Op.002 High Voltage Output) is $80mA_{pp} \cong 56.5mA_{rms}$);

$$I_2^{\max} = \frac{\varepsilon_2}{Z_2^{\min}} = 3A$$

and

$$I_3^{\max} = I_2^{\max} + I_1^{\max} \cong 3A$$

The new expression for the *inertial forces*, (Eq.5) $\vec{F}_i = M_g \vec{a}$, shows that the inertial forces are proportional to *gravitational mass*. Only in the particular case of $m_g = m_{i0}$, the expression above reduces to the well-known Newtonian expression $\vec{F}_i = m_{i0}\vec{a}$. The equivalence between gravitational and inertial forces $(\vec{F}_i \equiv \vec{F}_g)$ [1] shows then that a balance measures the *gravitational mass* subjected to

acceleration $a = g$. Here, the decrease in the *gravitational mass* of the Aluminum foil will be measured by a pan balance with the following characteristics: range 0-200g; readability 0.01g.

The mass of the Foam Board plate is: $\cong 4.17g$, the mass of the Aluminum foil is: $\cong 0.64g$, the total mass of the ends and the electric wires of connection is $\cong 5g$. Thus, *initially* the balance will show $\cong 9.81g$. According to (A18), when the electric current through the Aluminum foil (resistance $r_p^* = l/\sigma S = 2.5\times10^{-3}\Omega$) reaches the value $I_3 \cong 2.2A$, we will get $m_{g(Al)} \cong -m_{i0(Al)}$. Under these circumstances, the balance will show:

$$9.81g - 0.64g - 0.64g \cong 8.53g$$

and the gravity acceleration g' *above* the Aluminum foil, becomes $g' = \chi\ g \cong -1g$.

It was shown [1] that, when the gravitational mass of a particle is reduced to the gravitational mass ranging between $+0.159M_i$ to $-0.159M_i$, it becomes *imaginary*, i.e., the gravitational and the inertial masses of the particle become *imaginary*. Consequently, the particle *disappears* from our ordinary space-time. This phenomenon can be observed in the proposed experiment, i.e., *the Aluminum foil will disappear* when its gravitational mass becomes smaller than $+0.159M_i$. It will become visible again, only when its gravitational mass becomes smaller than $-0.159M_i$, or when it becomes greater than $+0.159M_i$.

Equation (A18) shows that the gravitational mass of the Aluminum foil, $m_{g(Al)}$, goes *close to zero* when $I_3 \cong 1.76A$. Consequently, the gravity acceleration *above* the Aluminum foil also goes close to zero since $g' = \chi\ g = m_{g(Al)}/m_{i0(Al)}$. Under these circumstances, the Aluminum foil remains *invisible*.

Now consider a rigid Aluminum wire # 14 AWG. The area of its cross section is

$$S = \pi\left(1.628\times10^{-3}\,m\right)^2/4 = 2.08\times10^{-6}\,m^2$$

If an ELF electric current with frequency $f = 2\mu Hz = 2\times10^{-6}\,Hz$ passes through this wire, its gravitational mass, given by (A16), will be expressed by

$$m_g = \left\{1-2\left[\sqrt{1+6.313\times10^{-42}\frac{j_{rms}^4}{f^3}}-1\right]\right\}m_{i0} =$$
$$= \left\{1-2\left[\sqrt{1+7.89\times10^{-25}\frac{I_{DC}^4}{S^4}}-1\right]\right\}m_{i0} =$$
$$= \left\{1-2\left[\sqrt{1+0.13I_{DC}^4}-1\right]\right\}m_{i0} \qquad (A22)$$

For $I_{DC} \cong 3A$ the equation above gives

$$m_g \cong -3.8m_{i0}$$

Note that we can replace the Aluminum foil for this wire in the experimental set-up shown in Fig.A2. It is important also to note that an ELF electric current that passes through a wire - which makes a spherical form, as shown in Fig A5 - reduces the gravitational mass of the wire (Eq.

A22), and the gravity *inside sphere* at the same proportion, $\chi=m_g/m_0$, (Gravitational Shielding Effect). In this case, that effect can be checked by means of the Experimental set-up 2 (Fig.A6). Note that the spherical form can be transformed into an ellipsoidal form or a disc in order to coat, for example, a Gravitational Spacecraft. It is also possible to coat with a wire several forms, such as cylinders, cones, cubes, etc.

The circuit shown in Fig.A4 (a) can be modified in order to produce a new type of Gravitational Shielding, as shown in Fig.A4 (b). In this case, the Gravitational Shielding will be produced in the Aluminum plate, with thickness h, of the parallel plate capacitor connected in the point P of the circuit (See Fig.A4 (b)). Note that, in this circuit, the Aluminum foil (resistance R_p) (Fig.A4(a)) has been replaced by a Copper wire # 14 AWG with *1cm* length ($l=1cm$) in order to produce a resistance $R_\phi=5.21\times10^{-5}\Omega$. Thus, the voltage in the point P of the circuit will have the maximum value $V_p^{\max}=1.1\times10^{-4}V$ when the resistance of the rheostat is null$(R=0)$ and the minimum value $V_p^{\min}=4.03\times10^{-5}V$ when $R=10\Omega$. In this way, the voltage V_p(with frequency $f=2\mu Hz$) applied on the capacitor will produce an electric field E_p with intensity $E_p=V_p/h$ through the Aluminum plate of thickness $h=3mm$. It is important to note that *this plate cannot be connected to ground* (earth), in other words, cannot be grounded, because, in this case, the electric field through it will be *null* [***].

According to Eq. A14, when $E_p^{\max}=V_p^{\max}/h=0.036\,V/m$, $f=2\mu Hz$ and $\sigma_{Al}=3.82\times10^7\,S/m$, $\rho_{Al}=2700\ kg/m^3$ (Aluminum), we get

$$\chi=\frac{m_{(Al)}}{m_{i(Al)}}\cong-0.9$$

Under these conditions, the maximum *current density* through the plate with thickness h will be given by $j^{\max}=\sigma_{Al}E_p^{\max}=1.4\times10^6\,A/m^2$ (It is well-known that the maximum current density supported by the Aluminum is $\approx10^8\,A/m^2$).

Since the area of the plate is $A=(0.2)^2=4\times10^{-2}m^2$, then the maximum current is $i^{\max}=j^{\max}A=56kA$. Despite this enormous current, the maximum dissipated power will be just $P^{\max}=\left(i^{\max}\right)^2R_{plate}=6.2W$, because the resistance of the plate is very small, i.e., $R_{plate}=h/\sigma_{Al}\,A\cong2\times10^{-9}\Omega$.

Note that the area A of the plate (where the Gravitational Shielding takes place) can have several geometrical configurations. For example, it can be the area of the external surface of an ellipsoid, sphere, etc. Thus, it can be the area of the external surface of a Gravitational Spacecraft. In this case, if $A\cong100m^2$, for example, the maximum dissipated

[***] When the voltage V_p is applied on the capacitor, the charge distribution in the dielectric induces positive and negative charges, respectively on opposite sides of the Aluminum plate with thickness *h*. If the plate is not connected to the ground (Earth) this charge distribution produces an electric field $E_p=V_p/h$ through the plate. However, if the plate is connected to the ground, the negative charges (electrons) escapes for the ground and the positive charges are redistributed along the entire surface of the Aluminum plate making *null* the electric field through it.

power will be $P^{\max} \cong 15.4kW$, i.e., approximately $154W/m^2$.

All of these systems work with Extra-Low Frequencies $(f << 10^{-3} Hz)$. Now, we show that, by simply changing *the geometry of the surface of the Aluminum foil*, it is possible to increase the working frequency f up to more than *1Hz*.

Consider the Aluminum foil, now with several semi-spheres stamped on its surface, as shown in Fig. A7 . The semi-spheres have radius $r_0 = 0.9\ mm$, and are joined one to another. The Aluminum foil is now coated by an insulation layer with relative permittivity ε_r and dielectric strength k. A voltage source is connected to the Aluminum foil in order to provide a voltage V_0 (rms) with frequency f. Thus, the electric potential V at a distance r, in the interval from r_0 to a, is given by

$$V = \frac{1}{4\pi\varepsilon_r\varepsilon_0}\frac{q}{r} \qquad (A23)$$

In the interval $a < r \le b$ the electric potential is

$$V = \frac{1}{4\pi\varepsilon_0}\frac{q}{r} \qquad (A24)$$

since for the air we have $\varepsilon_r \cong 1$.

Thus, on the surface of the metallic spheres $(r = r_0)$ we get

$$V_0 = \frac{1}{4\pi\varepsilon_r\varepsilon_0}\frac{q}{r_0} \qquad (A25)$$

Consequently, the electric field is

$$E_0 = \frac{1}{4\pi\varepsilon_r\varepsilon_0}\frac{q}{r_0^2} \qquad (A26)$$

By comparing (A26) with (A25), we obtain

$$E_0 = \frac{V_0}{r_0} \qquad (A27)$$

The electric potential V_b at $r = b$ is

$$V_b = \frac{1}{4\pi\varepsilon_0}\frac{q}{b} = \frac{\varepsilon_r V_0 r_0}{b} \qquad (A28)$$

Consequently, the electric field E_b is given by

$$E_b = \frac{1}{4\pi\varepsilon_0}\frac{q}{b^2} = \frac{\varepsilon_r V_0 r_0}{b^2} \qquad (A29)$$

From $r = r_0$ up to $r = b = a + d$ *the electric field is approximately constant* (See Fig. A7). Along the distance d it will be called E_{air}. For $r > a + d$, the electric field stops being constant. Thus, the intensity of the electric field at $r = b = a + d$ is approximately equal to E_0, i.e., $E_b \cong E_0$. Then, we can write that

$$\frac{\varepsilon_r V_0 r_0}{b^2} \cong \frac{V_0}{r_0} \qquad (A30)$$

whence we get

$$b \cong r_0\sqrt{\varepsilon_r} \qquad (A31)$$

Since the intensity of the electric field through the air, E_{air}, is $E_{air} \cong E_b \cong E_0$, then, we can write that

$$E_{air} = \frac{1}{4\pi\varepsilon_0}\frac{q}{b^2} = \frac{\varepsilon_r V_0 r_0}{b^2} \qquad (A32)$$

Note that, ε_r refers to the *relative permittivity of the insulation layer, which is covering the Aluminum foil*.

If the intensity of this field is greater than the dielectric strength of the air $(3\times10^6 V/m)$ there will occur the well-known *Corona effect*. Here, this effect is necessary in order to increase the electric conductivity of the air at this region (layer with thickness *d*). Thus, we will assume

$$E_{air}^{\min} = \frac{\varepsilon_r V_0^{\min} r_0}{b^2} = \frac{V_0^{\min}}{r_0} = 3\times10^6 V/m$$

and

$$E_{air}^{\max} = \frac{\varepsilon_r V_0^{\max} r_0}{b^2} = \frac{V_0^{\max}}{r_0} = 1\times10^7 V/m \qquad (A33)$$

The electric field $E_{air}^{\min} \le E_{air} \le E_{air}^{\max}$ will

produce an *electrons flux* in a direction and an *ions flux* in an opposite direction. From the viewpoint of electric current, the ions flux can be considered as an "electrons" flux at the same direction of the real electrons flux. Thus, the current density through the air, j_{air}, will be the *double* of the current density expressed by the well-known equation of Langmuir-Child

$$j=\frac{4}{9}\varepsilon_r\varepsilon_0\sqrt{\frac{2e}{m_e}}\frac{V^{\frac{3}{2}}}{d^2}=\alpha\frac{V^{\frac{3}{2}}}{d^2}=2.33\times10^{-6}\frac{V^{\frac{3}{2}}}{d^2} \qquad (A34)$$

where $\varepsilon_r\cong1$ for the *air*; $\alpha=2.33\times10^{-6}$ is the called *Child's constant*.

Thus, we have

$$j_{air}=2\alpha\frac{V^{\frac{3}{2}}}{d^2} \qquad (A35)$$

where d, in this case, is the thickness of the air layer where the electric field is approximately constant and V is the voltage drop given by

$$V=V_a-V_b=\frac{1}{4\pi\varepsilon_0}\frac{q}{a}-\frac{1}{4\pi\varepsilon_0}\frac{q}{b}=$$

$$=V_0r_0\varepsilon_r\left(\frac{b-a}{ab}\right)=\left(\frac{\varepsilon_r r_0 d}{ab}\right)V_0 \qquad (A36)$$

By substituting (A36) into (A35), we get

$$j_{air}=\frac{2\alpha}{d^2}\left(\frac{\varepsilon_r r_0 dV_0}{ab}\right)^{\frac{3}{2}}=\frac{2\alpha}{d^{\frac{1}{2}}}\left(\frac{\varepsilon_r r_0 V_0}{b^2}\right)^{\frac{3}{2}}\left(\frac{b}{a}\right)^{\frac{3}{2}}=$$

$$=\frac{2\alpha}{d^{\frac{1}{2}}}E_{air}^{\frac{3}{2}}\left(\frac{b}{a}\right)^{\frac{3}{2}} \qquad (A37)$$

According to the equation of the *Ohm's vectorial Law*: $j=\sigma E$, we can write that

$$\sigma_{air}=\frac{j_{air}}{E_{air}} \qquad (A38)$$

Substitution of (A37) into (A38) yields

$$\sigma_{air}=2\alpha\left(\frac{E_{air}}{d}\right)^{\frac{1}{2}}\left(\frac{b}{a}\right)^{\frac{3}{2}} \qquad (A39)$$

If the insulation layer has thickness $\Delta=0.6\ mm$, $\varepsilon_r\cong3.5$ (1-60Hz), $k=17kV/mm$ (Acrylic sheet 1.5mm thickness), and the semi-spheres stamped on the metallic surface have $r_0=0.9\ mm$ (See Fig.A7) then $a=r_0+\Delta=1.5\ mm.$ Thus, we obtain from Eq. (A33) that

$$V_0^{\min}=2.7kV$$
$$V_0^{\max}=9kV \qquad (A40)$$

From equation (A31), we obtain the following value for b:

$$b=r_0\sqrt{\varepsilon_r}=1.68\times10^{-3}m \qquad (A41)$$

Since $b=a+d$ we get

$$d=1.8\times10^{-4}m$$

Substitution of a, b, d and A(32) into (A39) produces

$$\sigma_{air}=4.117\times10^{-4}E_{air}^{\frac{1}{2}}=1.375\times10^{-2}V_0^{\frac{1}{2}}$$

Substitution of σ_{air}, $E_{air}(rms)$ and $\rho_{air}=1.2\ kg.m^{-3}$ into (A14) gives

$$\frac{m_{g(air)}}{m_{i0(air)}}=\left\{1-2\left[\sqrt{1+1.758\times10^{-27}\frac{\sigma_{air}^3E_{air}^4}{\rho_{air}^2f^3}}-1\right]\right\}=$$

$$=\left\{1-2\left[\sqrt{1+4.923\times10^{-21}\frac{V_0^{5.5}}{f^3}}-1\right]\right\} \qquad (A42)$$

For $V_0=V_0^{\max}=9kV$ and $f=2Hz$, the result is

$$\frac{m_{g(air)}}{m_{i0(air)}}\cong-1.2$$

Note that, by increasing V_0 the values of E_{air} and σ_{air} are increased. Thus, as show (A42), there are two ways for decrease the value of $m_{g(air)}$: increasing the value of V_0 or decreasing the value of f.

Since $E_0^{\max} = 10^7 V/m = 10kV/mm$ and $\Delta = 0.6\ mm$ then the dielectric strength of the insulation must be $\geq 16.7kV/mm$. As mentioned above, the dielectric strength of the acrylic is $17kV/mm$.

It is important to note that, due to the strong value of E_{air} (Eq. A37) the *drift velocity* v_d, $(v_d = j_{air}/ne = \sigma_{air}E_{air}/ne)$ of the free charges inside the ionized air put them at a distance $x = v_d/t = 2fv_d \cong 0.4m$, which is much greater than the distance $d = 1.8\times10^{-4}m$. Consequently, the number n of free charges decreases strongly inside the air layer of thickness d [†††], except, obviously, in a thin layer, very close to the dielectric, where the number of free charges remains sufficiently increased, to maintain the air conductivity with $\sigma_{air} \cong 1.1S/m$ (Eq. A39).

The thickness h of this thin air layer close to the dielectric can be easily evaluated starting from the charge distribution in the neighborhood of the dielectric, and of the repulsion forces established among them. The result is $h = \sqrt{0.06e/4\pi\varepsilon_0 E} \cong 4\times10^{-9}m$. This is, therefore, the thickness of the *Air* Gravitational Shielding. If the area of this Gravitational Shielding is equal to the area of a format A4 sheet of paper, i.e., $A = 0.20\times0.291 = 0.0582m^2$, we obtain the following value for the resistance R_{air} of the Gravitational Shielding: $R_{air} = h/\sigma_{air}\ A \cong 6\times10^{-8}\Omega$. Since the maximum electrical current through this air layer is $i^{\max} = j^{\max}A \cong 400kA$, then the maximum power radiated from the Gravitational Shielding is $P_{air}^{\max} = R_{air}\left(i_{air}^{\max}\right)^2 \cong 10kW$. This means that a very strong light will be radiated from this type of Gravitational Shielding. Note that this device can also be used as a lamp, which will be much more efficient than conventional lamps.

Coating a ceiling with this lighting system enables the entire area of ceiling to produce light. This is a form of lighting very different from those usually known.

Note that the value $P_{air}^{\max} \cong 10kW$, defines the power of the transformer shown in Fig.A10. Thus, the maximum current in the secondary is $i_s^{\max} = 9kV/10kW = 0.9A$.

Above the Gravitational Shielding, σ_{air} is reduced to the normal value of conductivity of the atmospheric air $\left(\approx 10^{-14}S/m\right)$. Thus, the power radiated from this region is

$$P_{air}^{\max} = (d-h)\left(i_{air}^{\max}\right)^2/\sigma_{air}\ A = \\ = (d-h)A\sigma_{air}\left(E_{air}^{\max}\right)^2 \cong 10^{-4}W$$

Now, we will describe a method to coat the Aluminum semi-spheres with acrylic in the necessary dimension $(\Delta = a - r_0)$. First, take an Aluminum plate with $21cm\times29.1cm$ (A4 format). By means of a convenient process, several semi-spheres can be stamped on its surface. The semi-spheres have radius $r_0 = 0.9\ mm$, and are joined one to another. Next, take an acrylic sheet (A4 format) with 1.5mm thickness (See Fig.A8 (a)). Put a heater below the Aluminum plate in order to heat the Aluminum (Fig.A8 (b)). When the Aluminum is

[†††] Reducing therefore the conductivity, σ_{air}, to the normal value of the conductivity of atmospheric air.

sufficiently heated up, the acrylic sheet and the Aluminum plate are pressed, one against the other, as shown in Fig. A8 (c). The two D devices shown in this figure are used in order to impede that the press compresses the acrylic and the aluminum to a distance shorter than $y + a$. After some seconds, remove the press and the heater. The device is ready to be subjected to a voltage V_0 with frequency f, as shown in Fig.A9. Note that, in this case, the balance is not necessary, because *the substance that produces the gravitational shielding* is an *air layer* with thickness d *above* the acrylic sheet. This is, therefore, more a type of Gravity Control Cell (GCC) with *external gravitational shielding*.

It is important to note that this GCC can be made very thin and as flexible as a fabric. Thus, it can be used to produce *anti- gravity clothes*. These clothes can be extremely useful, for example, to walk on the surface of high gravity planets.

Figure A11 shows some geometrical forms that can be stamped on a metallic surface in order to produce a Gravitational Shielding effect, similar to the produced by the *semi-spherical form*.

An obvious evolution from the semi-spherical form is the *semi-cylindrical* form shown in Fig. A11 (b); Fig.A11(c) shows *concentric metallic rings* stamped on the metallic surface, an evolution from Fig.A11 (b). These geometrical forms produce the same effect as the semi-spherical form, shown in Fig.A11 (a). By using concentric metallic rings, it is possible to build *Gravitational Shieldings* around bodies or spacecrafts with several formats (spheres, ellipsoids, etc); Fig. A11 (d) shows a Gravitational Shielding around a Spacecraft with *ellipsoidal form*.

The previously mentioned Gravitational Shielding, produced on a thin layer of ionized air, has a *behavior different from* the Gravitational Shielding produced on a *rigid substance*. When the gravitational masses of the air molecules, inside the shielding, are reduced to within the range $+0.159m_i < m_g < -0.159m_i$, they go to the *imaginary space-time*, as previously shown in this article. However, the electric field E_{air} stays at the real space-time. Consequently, the molecules return immediately to the real space-time in order to return soon after to the *imaginary* space-time, due to the action of the electric field E_{air}.

In the case of the Gravitational Shielding produced on a *solid substance*, when the molecules of the substance go to the *imaginary* space-time, *the electric field that produces the effect, also goes to the imaginary space-time together with them*, since in this case, the substance of the Gravitational Shielding is rigidly connected to the metal that produces the electric field. (See Fig. A12 (b)). This is the fundamental difference between the *non-solid* and *solid* Gravitational Shieldings.

Now, consider a Gravitational Spacecraft that is able to produce an *Air* Gravitational Shielding and also a *Solid* Gravitational Shielding, as

shown in Fig. A13 (a) [‡‡‡]. Assuming that the intensity of the electric field, E_{air}, necessary to reduce the gravitational mass of the *air molecules* to within the range $+0.159m_i < m_g < -0.159m_i$, *is much smaller* than the intensity of the electric field, E_{rs}, necessary to reduce the gravitational mass of the *solid substance* to within the range $+0.159m_i < m_g < -0.159m_i$, then we conclude that the Gravitational Shielding made of ionized air goes to the imaginary space-time *before* the Gravitational Shielding made of *solid substance*. When this occurs the spacecraft does not go to the imaginary space-time together with the Gravitational Shielding of air, because the air molecules are not rigidly connected to the spacecraft. Thus, while the air molecules go into the imaginary space-time, the spacecraft stays in the *real space-time*, and remains subjected to the effects of the Gravitational Shielding around it, since the shielding does not stop to work, due to its extremely short permanence at the imaginary space-time. Under these circumstances, the gravitational mass of the Gravitational Shielding can be reduced to $m_g \cong 0$. For example, $m_g \cong 10^{-4} kg$. Thus, if the *inertial mass* of the Gravitational Shielding is $m_{i0} \cong 1kg$, then $\chi = m_g / m_{i0} \cong 10^{-4}$. As we have seen, this means that *the inertial effects on the spacecraft* will be reduced by $\chi \cong 10^{-4}$. Then, in spite of the effective acceleration of the spacecraft be, for example, $a = 10^5 m.s^{-2}$, the effects on the crew of the spacecraft will be equivalent to an acceleration of only

$$a' = \frac{m_g}{m_{i0}} a = \chi \ a \approx 10 m.s^{-1}$$

This is the magnitude of the acceleration upon the passengers in a contemporary commercial jet.

Then, it is noticed that Gravitational Spacecrafts can be subjected to enormous *accelerations* (or *decelerations*) without imposing any harmful impacts whatsoever on the spacecrafts or its crew.

Now, imagine that the intensity of the electric field that produces the Gravitational Shielding around the spacecraft is *increased* up to reaching the value E_{rs} that reduces the gravitational mass of the *solid* Gravitational Shielding to within the range $+0.159m_i < m_g < -0.159m_i$. Under these circumstances, the *solid* Gravitational Shielding goes to the imaginary space-time and, since it is rigidly connected to the spacecraft, also the spacecraft goes to the imaginary space-time together with the Gravitational Shielding. Thus, the spacecraft can travel within the

---

[‡‡‡] The *solid* Gravitational Shielding can also be obtained by means of *an ELF electric current through a metallic lamina* placed *between the semi-spheres and the Gravitational Shielding of Air* (See Fig.A13 (a)). The gravitational mass of the solid Gravitational Shielding will be controlled just by means of the intensity of the ELF electric current. Recently, it was discovered that Carbon nanotubes (CNTs) can be added to *Alumina* (Al_2O_3) to convert it into a good electrical conductor. It was found that the electrical conductivity increased up to 3375 S/m at 77°C in samples that were 15% nanotubes by volume [12]. It is known that the density of α-Alumina is $3.98 \times 10^3 kg.m^{-3}$ and that it can withstand 10-20 KV/mm. Thus, these values show that the Alumina-CNT can be used to make a *solid* Gravitational Shielding.

imaginary space-time and make use of the Gravitational Shielding around it.

As we have already seen, the maximum velocity of propagation of the interactions in the imaginary space-time is *infinite* (in the real space-time this limit is equal to the light velocity c). This means that *there are no limits for the velocity of the spacecraft in the imaginary space-time*. Thus, the acceleration of the spacecraft can reach, for example, $a = 10^9\, m.s^{-2}$, which leads the spacecraft to attain velocities $V \approx 10^{14}\, m.s^{-1}$ (about 1 million times the speed of light) after one day of trip. With this velocity, after 1 month of trip the spacecraft would have traveled about $10^{21}\, m$. In order to have idea of this distance, it is enough to remind that the diameter of our Universe (visible Universe) is of the order of $10^{26}\, m$.

Due to the extremely low density of the *imaginary* bodies, the collision between them cannot have the same consequences of the collision between the real bodies.

Thus, *for a Gravitational Spacecraft in imaginary state, the problem of the collision in high-speed doesn't exist.* Consequently, the Gravitational Spacecraft can transit freely in the imaginary Universe and, in this way, reach easily any point of our real Universe once they can make the transition back to our Universe by only increasing the gravitational mass of the Gravitational Shielding of the spacecraft in such way that it leaves the range of $+0.159 M_i$ to $-0.159 M_i$.

The return trip would be done in similar way. That is to say, the spacecraft would transit in the imaginary Universe back to the departure place where would reappear in our Universe. Thus, trips through our Universe that would delay millions of years, at speeds close to the speed of light, could be done in just a few *months* in the imaginary Universe.

In order to produce the acceleration of $a \approx 10^9\, m.s^{-2}$ upon the spacecraft we propose a Gravitational Thruster with 10 GCCs (10 Gravitational Shieldings) of the type with several semi-spheres stamped on the metallic surface, as previously shown, or with the *semi-cylindrical* form shown in Figs. A11 (b) and (c). The 10 GCCs are filled with air at 1 atm and 300K. If the insulation layer is made with *Mica* ($\varepsilon_r \cong 5.4$) and has thickness $\Delta = 0.1\ mm$, and the semi-spheres stamped on the metallic surface have $r_0 = 0.4\ mm$ (See Fig.A7) then $a = r_0 + \Delta = 0.5\ mm$. Thus, we get

$$b = r_0\sqrt{\varepsilon_r} = 9.295\times10^{-4} m$$

and

$$d = b - a = 4.295\times10^{-4} m$$

Then, from Eq. A42 we obtain

$$\chi_{air} = \frac{m_{g(air)}}{m_{i0(air)}} = \left\{1 - 2\left[\sqrt{1 + 1.758\times10^{-27}\frac{\sigma_{air}^3 E_{air}^4}{\rho_{air}^2 f^3}} - 1\right]\right\} =$$

$$= \left\{1 - 2\left[\sqrt{1 + 1.0\times10^{-18}\frac{V_0^{5.5}}{f^3}} - 1\right]\right\}$$

For $V_0 = V_0^{\max} = 15.6 kV$ and $f = 0.12 Hz$, the result is

$$\chi_{air} = \frac{m_{g(air)}}{m_{i0(air)}} \cong -1.6\times10^4$$

Since $E_0^{\max} = V_0^{\max}/r_0$ is now given by $E_0^{\max} = 15.6 kV/0.9 mm = 17.3 kV/mm$ and $\Delta = 0.1\ mm$ then the dielectric strength of the insulation must be $\geq 173 kV/mm$. As

shown in the table below[§§§], *0.1mm - thickness of* Mica *can withstand 17.6 kV* (that is greater than $V_0^{\max} = 15.6kV$), in such way that the dielectric strength is *176 kV/mm*.

The Gravitational Thrusters are positioned at the spacecraft, as shown in Fig. A13 (b). Then, when the spacecraft is in the *intergalactic space*, the gravity acceleration upon the gravitational mass m_{gt} of the bottom of the thruster (See Fig.A13 (c)), is given by [2]

$$\vec{a} \cong (\chi_{air})^{10} \vec{g}_M \cong -(\chi_{air})^{10} G \frac{M_g}{r^2} \hat{\mu}$$

where M_g is the gravitational mass in front of the spacecraft.

For simplicity, let us consider just the effect of a hypothetical volume $V = 10 \times 10^3 \times 10^3 = 10^7 m^3$ of intergalactic matter in front of the spacecraft $(r \cong 30m)$. The average density of matter in the *intergalactic medium (IGM)* is $\rho_{ig} \approx 10^{-26} kg.m^{-3}$)[****]. Thus, for $\chi_{air} \cong -1.6 \times 10^4$ we get

$$a = -\left(-1.6 \times 10^4\right)^{10} \left(6.67 \times 10^{-11}\right) \left(\frac{10^{-19}}{30^2}\right) =$$

$$= -10^9 \, m.s^{-2}$$

In spite of this gigantic acceleration, the inertial effects for the crew of the spacecraft can be strongly reduced if, for example, the gravitational mass of the Gravitational Shielding is reduced down to $m_g \cong 10^{-6} kg$ and its inertial mass is $m_{i0} \cong 100kg$. Then, we get $\chi = m_g / m_{i0} \cong 10^{-8}$. Therefore, *the inertial effects on the spacecraft* will be reduced by $\chi \cong 10^{-8}$, and consequently, the inertial effects on the crew of the spacecraft would be *equivalent to* an acceleration a' of only

$$a' = \frac{m_g}{m_{i0}} a = \left(10^{-8}\right)\left(10^9\right) \approx 10 m.s^{-2}$$

Note that the Gravitational Thrusters in the spacecraft must have a very small diameter (of the order of *millimeters*) since, obviously, the hole through the Gravitational Shielding cannot be large. Thus, these thrusters are in fact, *Micro-Gravitational Thrusters*. As shown in Fig. A13 (b), it is possible to place several micro-gravitational thrusters in the spacecraft. This gives to the Gravitational Spacecraft, several degrees of freedom and shows the enormous superiority of this spacecraft in relation to the contemporaries spacecrafts.

The density of matter in the *intergalactic medium (IGM)* is about 10^{-26} *kg.m*$^{-3}$, which is very less than the density of matter in the *interstellar medium* (~10^{-21} *kg.m*$^{-3}$) that is less than the density of matter in the *interplanetary medium* (~10^{-20} *kg.m*$^{-3}$). The density of matter is enormously

---

[§§§] The *dielectric strength* of some dielectrics can have different values in lower thicknesses. This is, for example, the case of the *Mica*.

Dielectric	*Thickness* (mm)	*Dielectric Strength* (kV/mm)
Mica	0.01 mm	200
Mica	**0.1 mm**	**176**
Mica	1 mm	61

[****] Some theories put the average density of the Universe as the equivalent of *one hydrogen atom per cubic meter* [13,14]. The density of the universe, however, is clearly not uniform. Surrounding and stretching between galaxies, there is rarefied plasma [15] that is thought to possess a cosmic filamentary structure [16] and that is slightly denser than the average density in the universe. This material is called the *intergalactic medium (IGM)* and is mostly ionized hydrogen; i.e. a plasma consisting of equal numbers of electrons and protons. The IGM is thought to exist at a density of 10 to 100 times the average density of the Universe (10 to 100 hydrogen atoms per cubic meter, i.e., $\approx 10^{-26} kg.m^{-3}$).

increased inside the Earth's atmosphere ($1.2 kg.m^{-3}$ near to Earth's surface). Figure A14 shows the gravitational acceleration acquired by a Gravitational Spacecraft, in these media, using Micro-Gravitational thrusters.

In relation to the *Interstellar* and *Interplanetary medium*, the *Intergalactic medium* requires the greatest value of χ_{air} (χ inside the *Micro-Gravitational Thrusters*), i.e., $\chi_{air} \cong -1.6\times10^{4}$. This value strongly decreases when the spacecraft is within the Earth's atmosphere. In this case, it is sufficient only[††††] $\chi_{air} \cong -10$ in order to obtain:

$$a = -(\chi_{air})^{10} G \frac{\rho_{atm} V}{r^2} \cong$$

$$\cong -(-10)^{10}\left(6.67\times10^{-11}\right)\frac{1.2\left(10^{7}\right)}{(20)^{2}} \cong 10^{4}\, m.s^{-2}$$

With this acceleration the Gravitational Spacecraft can reach about *50000 km/h* in a few seconds. Obviously, the Gravitational Shielding of the spacecraft will reduce strongly *the inertial effects upon the crew* of the spacecraft, in such way that the inertial effects of this strong acceleration will not be felt. In addition, the *artificial atmosphere*, which is possible to build around the spacecraft, by means of gravity control technologies shown in this article (See Fig.6) and [2], will protect it from the *heating* produced by the friction with the Earth's atmosphere. Also, the gravity can be controlled inside of the Gravitational Spacecraft in order to maintain a value close to the Earth's gravity as shown in Fig.3.

Finally, it is important to note that a Micro-Gravitational Thruster does not work *outside* a Gravitational Shielding, because, in this case, *the resultant upon the thruster is null* due to the symmetry (See Fig. A15 (a)). Figure A15 (b) shows a micro-gravitational thruster inside a Gravitational Shielding. This thruster has 10 Gravitational Shieldings, in such way that the gravitational acceleration upon the *bottom* of the thruster, due to a gravitational mass M_g *in front* of the thruster, is $a_{10} = \chi_{air}^{10} a_0$ where $a_0 = -G M_g / r^2$ is the gravitational acceleration acting on the front of the micro-gravitational thruster. *In the opposite direction*, the gravitational acceleration upon the bottom of the thruster, produced by a gravitational mass M_g, is

$$a_0' = \chi_s\left(-GM_g / r'^2\right) \cong 0$$

since $\chi_s \cong 0$ due to the Gravitational Shielding around the micro-thruster (See Fig. A15 (b)). Similarly, the acceleration in front of the thruster is

$$a_{10}' = \chi_{air}^{10} a_0' = \left[\chi_{air}^{10}\left(-GM_g / r'^2\right)\right]\chi_s$$

where $\left[\chi_{air}^{10}\left(-GM_g / r'^2\right)\right] < a_{10}$, since $r' > r$. Thus, for $a_{10} \cong 10^{9}\, m.s^{-2}$ and $\chi_s \approx 10^{-8}$ we conclude that $a_{10}' < 10 m.s^{-2}$. This means that $a_{10}' << a_{10}$. Therefore, we can write that the resultant on the micro-thruster can be expressed by means of the following relation

$$R \cong F_{10} = \chi_{air}^{10} F_0$$

[††††] This value is within the range of values of χ ($\chi < -10^{3}$. *See Eq.A15*), which can be produced by means of *ELF electric currents* through metals as *Aluminum*, etc. This means that, in this case, if convenient, we can replace *air* inside the GCCs of the Gravitational Micro-thrusters by metal laminas with *ELF electric currents* through them.

Figure A15 (c) shows a Micro-Gravitational Thruster with *10 Air Gravitational Shieldings* (10 GCCs). Thin Metallic laminas are placed after each *Air* Gravitational Shielding in order to retain the electric field $E_b = V_0/x$, produced by metallic *surface behind* the semi-spheres. The laminas with semi-spheres stamped on its surfaces are connected to the ELF voltage source V_0 and the thin laminas in front of the Air Gravitational Shieldings are grounded. The air inside this Micro-Gravitational Thruster is at 300K, 1atm.

We have seen that the insulation layer of a GCC can be made up of Acrylic, Mica, etc. Now, we will design a GCC using *Water* (*distilled water*, $\varepsilon_{r(H_2O)} = 80$) and Aluminum *semi-cylinders* with radius $r_0 = 1.3mm$. Thus, for $\Delta = 0.6mm$, the new value of a is $a = 1.9mm$. Then, we get

$$b = r_0\sqrt{\varepsilon_{r(H_2O)}} = 11.63\times10^{-3}m \qquad (A43)$$

$$d = b - a = 9.73\times10^{-3}m \qquad (A44)$$

and

$$E_{air} = \frac{1}{4\pi\varepsilon_{r(air)}\varepsilon_0}\frac{q}{b^2} = \varepsilon_{r(H_2O)}\frac{V_0 r_0}{\varepsilon_{r(air)}b^2} = \frac{V_0/r_0}{\varepsilon_{r(air)}} \cong \frac{V_0}{r_0} = 1111.1\ V_0 \qquad (A45)$$

Note that

$$E_{(H_2O)} = \frac{V_0/r_0}{\varepsilon_{r(H_2O)}}$$

and

$$E_{(acrylic)} = \frac{V_0/r_0}{\varepsilon_{r(acrylic)}}$$

Therefore, $E_{(H_2O)}$ and $E_{(acrylic)}$ are much smaller than E_{air}. Note that for $V_0 \le 9kV$ the intensities of $E_{(H_2O)}$ and $E_{(acrylic)}$ are not sufficient to produce the ionization effect, which increases the electrical conductivity. Consequently, the conductivities of the water and the acrylic remain $<< 1\ S.m^{-1}$. In this way, with $E_{(H_2O)}$ and $E_{(acrylic)}$ much smaller than E_{air}, and $\sigma_{(H2O)} << 1$, $\sigma_{(acrylic)} << 1$, the decrease in both the gravitational mass of the acrylic and the gravitational mass of water, according to Eq.A14, is negligible. This means that only in the air layer the decrease in the gravitational mass will be relevant.

Equation A39 gives the electrical conductivity of the air layer, i.e.,

$$\sigma_{air} = 2\alpha\left(\frac{E_{air}}{d}\right)^{\frac{1}{2}}\left(\frac{b}{a}\right)^{\frac{3}{2}} = 0.029V_0^{\frac{1}{2}} \qquad (A46)$$

Note that $b = r_0\sqrt{\varepsilon_{r(H_2O)}}$. Therefore, here the value of b is larger than in the case of the acrylic. Consequently, *the electrical conductivity of the air layer will be larger here than in the case of acrylic.*

Substitution of $\sigma_{(air)}$, E_{air} (*rms*) and $\rho_{air} = 1.2kg.m^{-3}$ into Eq. A14, gives

$$\frac{m_{g(air)}}{m_{i0(air)}} = \left\{1 - 2\left[\sqrt{1 + 4.54\times10^{20}\frac{V_0^{5.5}}{f^3}} - 1\right]\right\} \qquad (A47)$$

For $V_0 = V_0^{\max} = 9kV$ and $f = 2Hz$, the result is

$$\frac{m_{g(air)}}{m_{i0(air)}} \cong -8.4$$

This shows that, by using *water* instead of acrylic, the result is much better.

In order to build the GCC based on the calculations above (See Fig. A16), take an Acrylic plate with *885mm* x *885m* and *2mm* thickness, then paste on it an Aluminum sheet

with *895.2mm* x *885mm* and *0.5mm* thickness(note that two edges of the Aluminum sheet are bent as shown in Figure A16 (b)). Next, take *342* Aluminum yarns with *884mm* length and *2.588mm* diameter (wire # 10 AWG) and insert them side by side on the Aluminum sheet. See in Fig. A16 (b) the detail of fixing of the yarns on the Aluminum sheet. Now, paste acrylic strips (with *13.43mm* height and *2mm* thickness) around the Aluminum/Acrylic, making a box. Put *distilled water* (approximately *1 litter*) inside this box, up to a height of exactly *3.7mm* from the edge of the acrylic base. Afterwards, paste an Acrylic lid (*889mm* x *889mm* and *2mm* thickness) on the box. Note that above the water there is an *air* layer with *885mm* x *885mm* and *7.73mm* thickness (See Fig. A16). This thickness plus the acrylic lid thickness (*2mm*) is equal to $d = b - a = 9.73mm$ where $b = r_0\sqrt{\varepsilon_{r(H_2O)}} = 11.63mm$ and $a = r_0 + \Delta = 1.99mm$, since $r_0 = 1.3mm$, $\varepsilon_{r(H_2O)} = 80$ and $\Delta = 0.6mm$.

Note that the gravitational action of the electric field E_{air}, extends itself only up to the distance d, which, in this GCC, is given by the sum of the Air layer thickness (*7.73mm*) plus the thickness of the Acrylic lid (*2mm*).

Thus, it is ensured the gravitational effect on the air layer while it is practically nullified in the acrylic sheet above the air layer, since $E_{(acrylic)} << E_{air}$ and $\sigma_{(acrylic)} << 1$.

With this GCC, we can carry out an experiment where the *gravitational mass of the air layer* is progressively reduced when the voltage applied to the GCC is increased (or when the frequency is decreased). A precision balance is placed below the GCC in order to measure the mentioned mass decrease for comparison with the values predicted by Eq. A(47). In total, this GCC weighs about *6kg*; the *air layer 7.3grams*. The balance has the following characteristics: *range 0-6kg; readability 0.1g*. Also, in order to prove the *Gravitational Shielding Effect*, we can put a *sample* (connected to a dynamometer) above the GCC in order to check the gravity acceleration in this region.

In order to prove *the exponential effect* produced by the superposition of the Gravitational Shieldings, we can take three similar GCCs and put them one above the other, in such way that above the GCC 1 the gravity acceleration will be $g' = \chi g$; above the GCC2 $g'' = \chi^2 g$, and above the GCC3 $g''' = \chi^3 g$. Where χ is given by Eq. (A47).

It is important to note that the intensity of the electric field through the air *below* the GCC is *much smaller* than the intensity of the electric field through the air layer inside the GCC. In addition, the electrical conductivity of the air below the GCC is much smaller than the conductivity of the air layer inside the GCC. Consequently, the decrease of the gravitational mass of the air below the GCC, according to Eq.A14, is negligible. This means that the GCC1, GCC2 and GCC3 can be simply overlaid, on the experiment proposed above. However, since it is necessary to put samples among them in order to measure the gravity above each GCC, we suggest a spacing of 30cm or more among them.

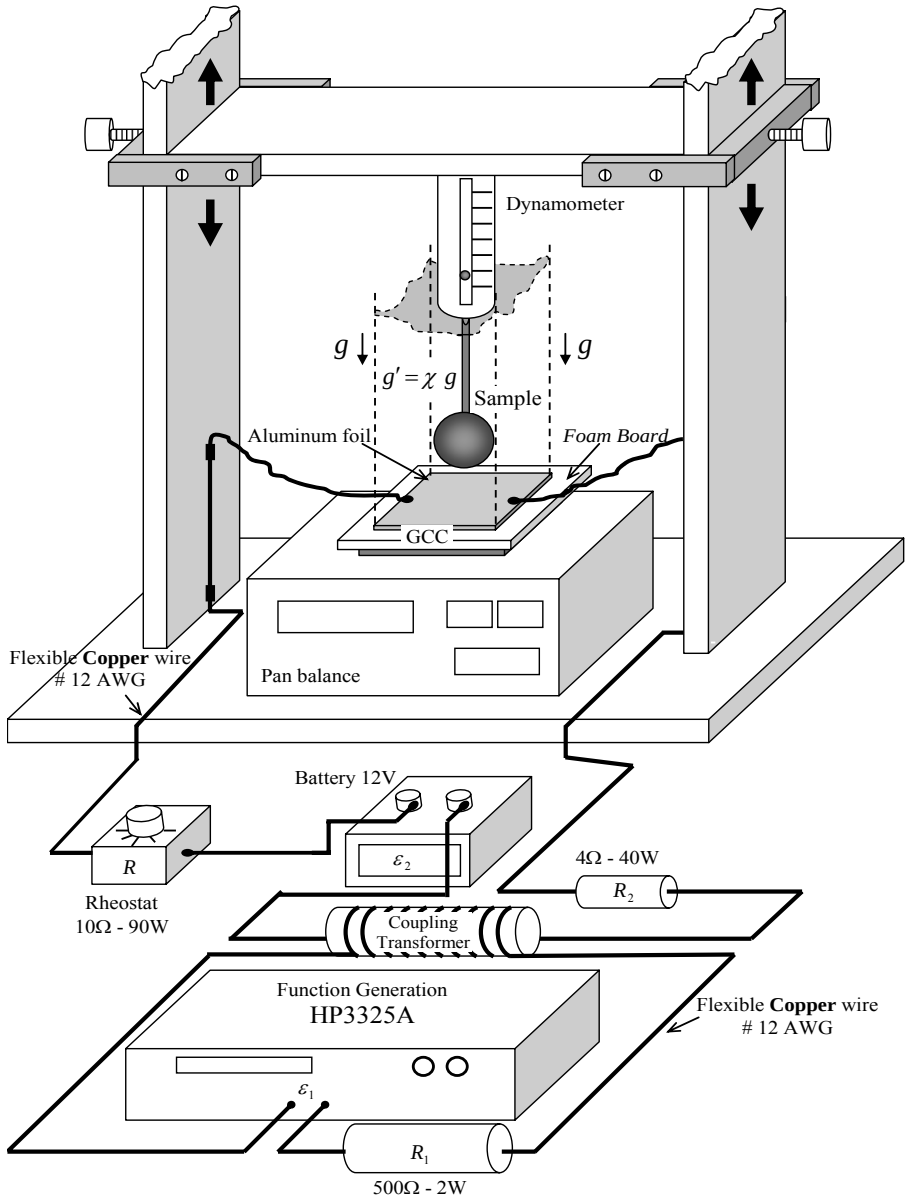

Fig. A2 – Experimental Set-up 1.

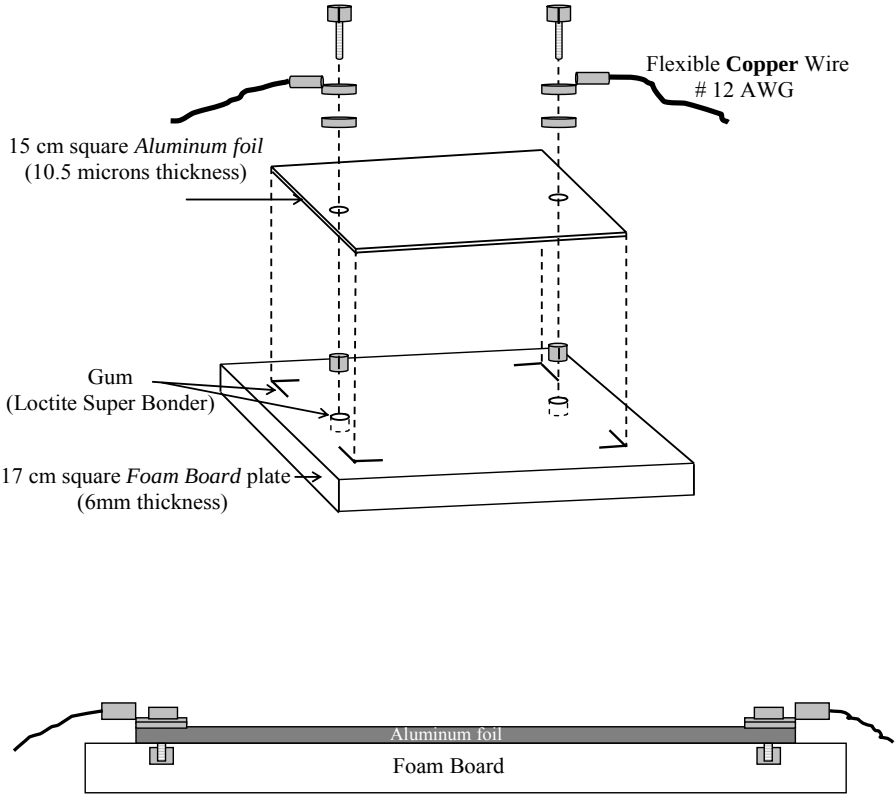

Fig. A3 – The Simplest *Gravity Control Cell* (GCC).

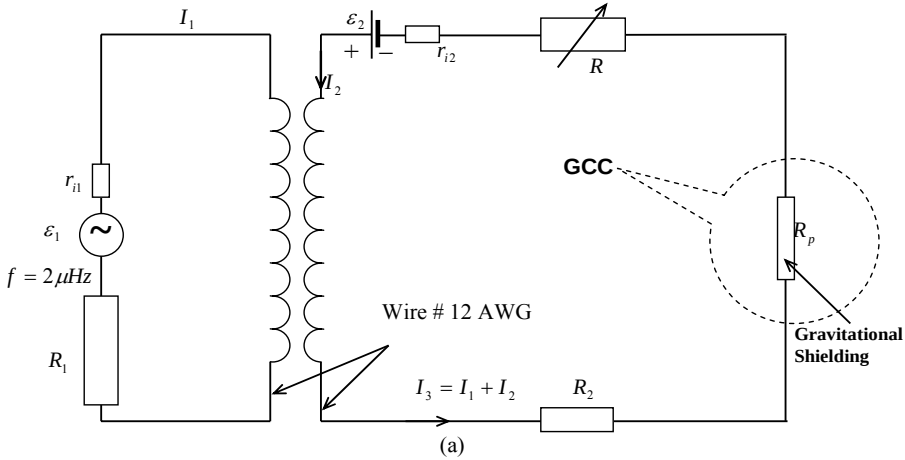

(a)

ε_1 = Function Generator HP3325A(*Option* 002 High Voltage Output)

$r_{i1} < 2\Omega$; $R_1 = 500\Omega - 2\ W$; $\varepsilon_2 = 12V\ DC$; $r_{i2} < 0.1\Omega$ (*Battery*);

$R_2 = 4\Omega - 40W$; $R_p = 2.5\times10^{-3}\Omega$; *Reostat* $= 0 \le R \le 10\Omega - 90W$

$I_1^{\max} = 56mA\ (rms)$; $I_2^{\max} = 3A$; $I_3^{\max} \cong 3A\ (rms)$

Coupling Transformer to isolate the *Function Generator* from the Battery

• Air core 10 - mm diameter; wire #12 AWG; $N_1 = N_2 = 20; l = 42mm$

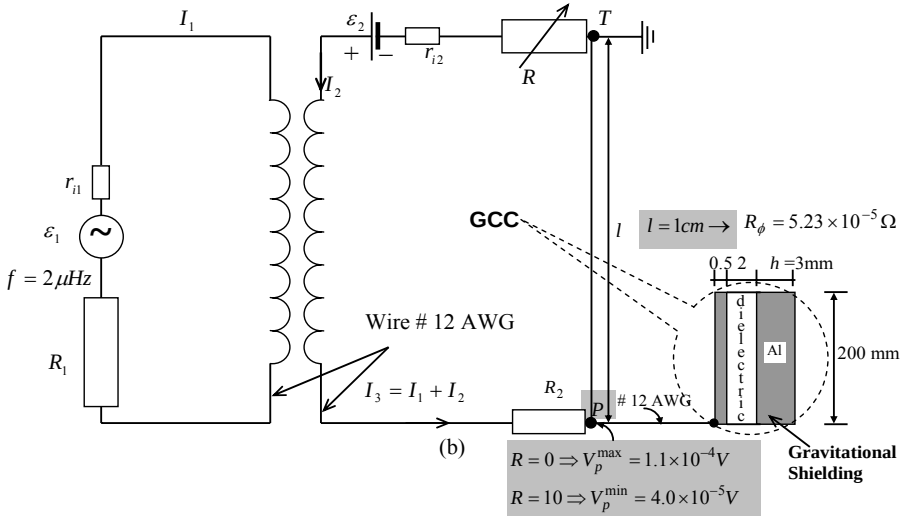

(b)

Fig. A4 – Equivalent Electric Circuits

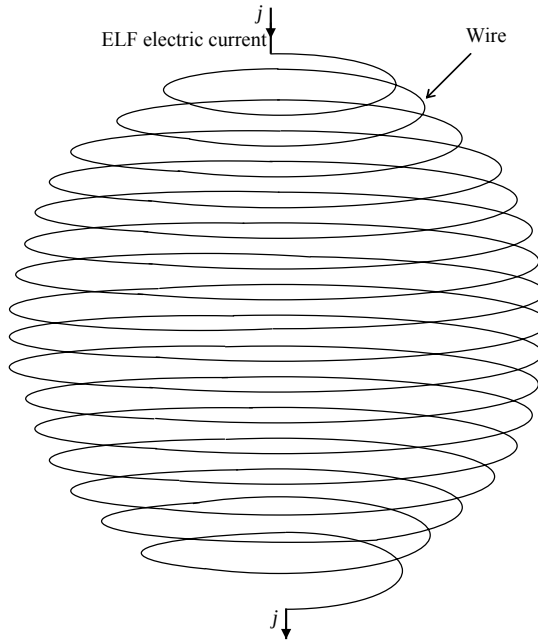

$$m_g = \left\{1 - 2\left[\sqrt{1 + 1.758\times10^{-27}\,\frac{\mu_r j^4}{\sigma\rho^2 f^3}} - 1\right]\right\} m_{i0}$$

Fig. A5 – An ELF electric current through a wire, that makes a spherical form as shown above, reduces the gravitational mass of the wire and the gravity inside sphere at the same proportion $\chi = m_g / m_{i0}$ (Gravitational Shielding Effect). Note that this spherical form can be transformed into an ellipsoidal form or a disc in order to coat, for example, a Gravitational Spacecraft. It is also possible to coat with a wire several forms, such as cylinders, cones, cubes, etc. The characteristics of the wire are expressed by: μ_r, σ, ρ; j is the electric current density and f is the frequency.

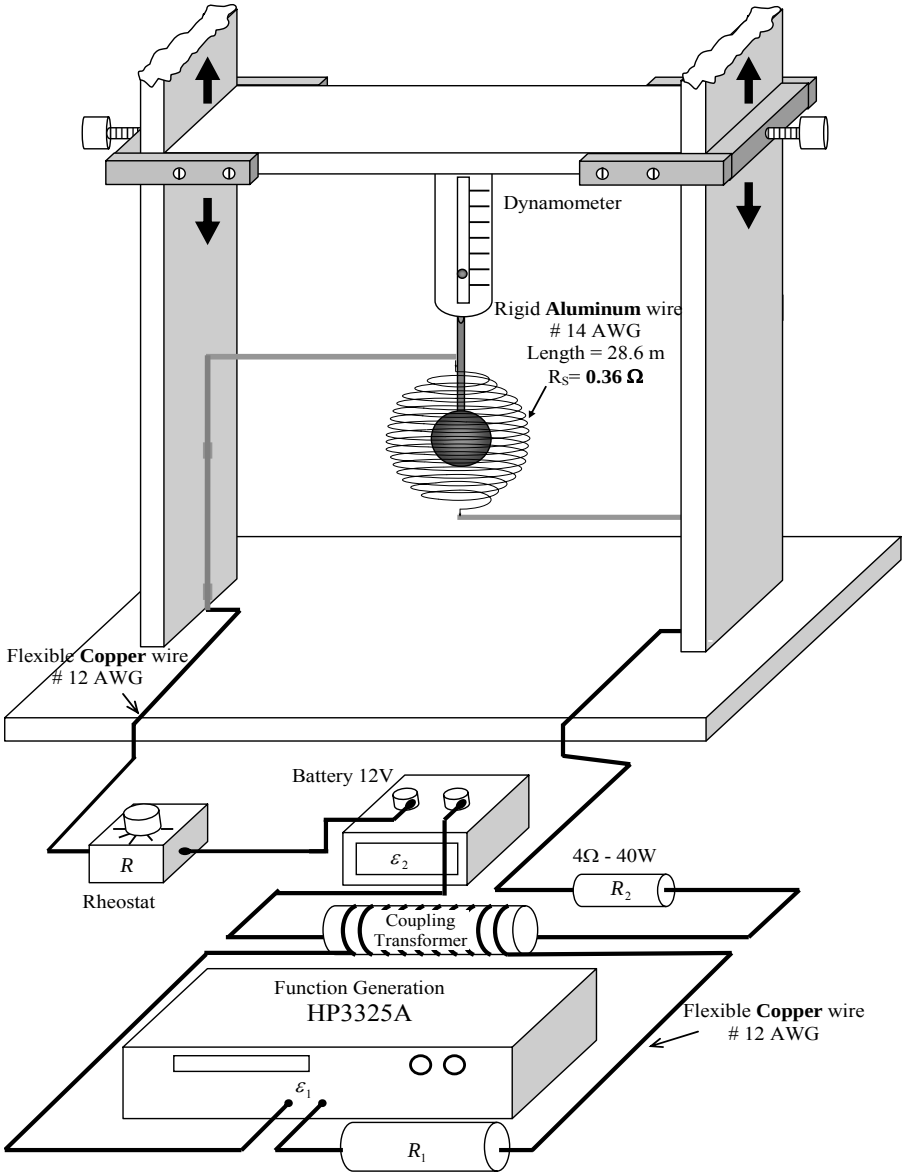

Fig. A6 – Experimental set-up 2.

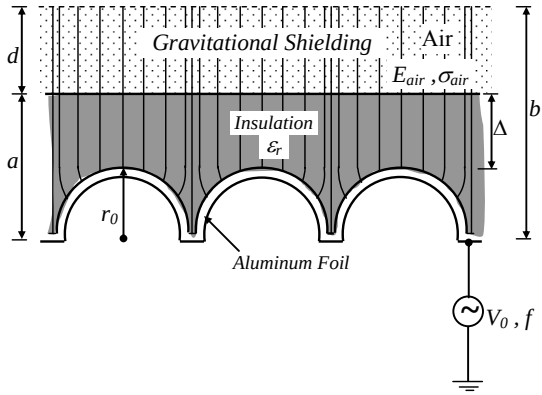

Fig A7 – *Gravitational shielding produced by semi-spheres stamped on the Aluminum foil* - By simply changing the geometry of the surface *of* the Aluminum foil it is possible to increase the working frequency f up to more than *1Hz*.

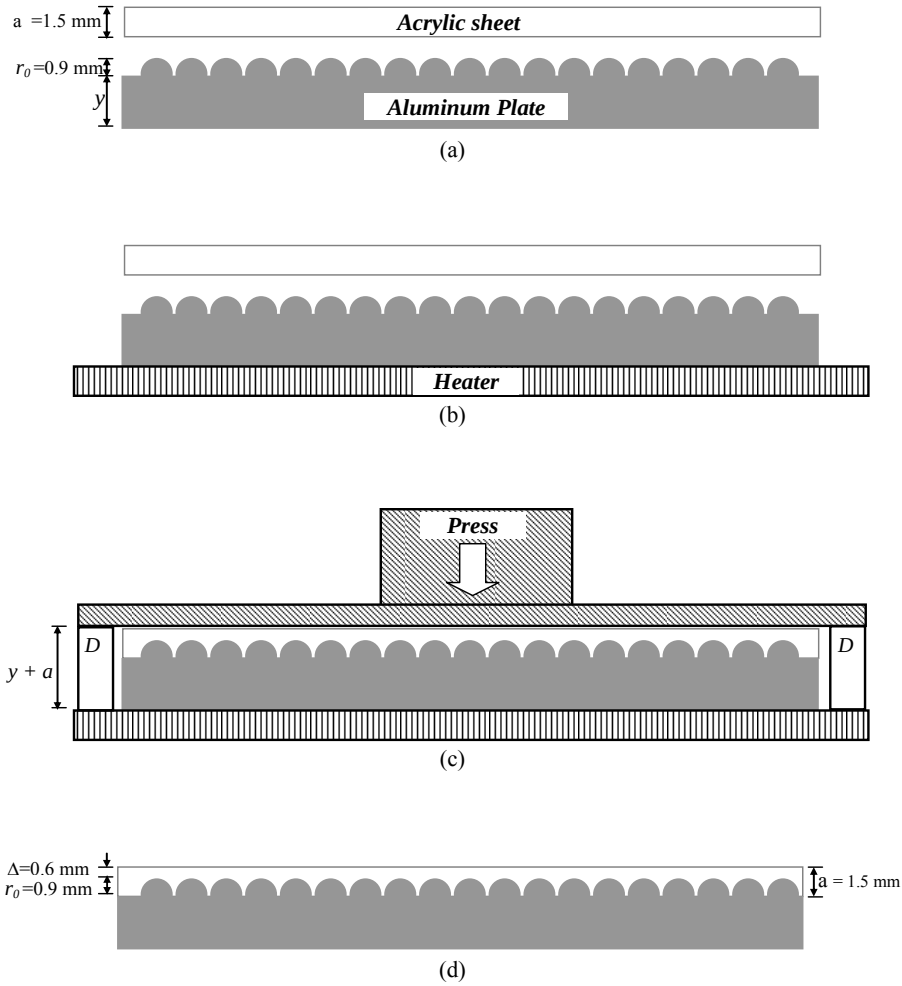

Fig A8 – *Method to coat the Aluminum semi-spheres with acrylic* $(\Delta = a - r_0 = 0.6mm)$. (a)Acrylic sheet (A4 format) with 1.5mm thickness and an Aluminum plate (A4) with several semi-spheres (radius $r_0 = 0.9\ mm$) stamped on its surface. (b)A heater is placed below the Aluminum plate in order to heat the Aluminum. (c)When the Aluminum is sufficiently heated up, the acrylic sheet and the Aluminum plate are pressed, one against the other (The two D devices shown in this figure are used in order to impede that the press compresses the acrylic and the aluminum besides distance $y + a$). (d)After some seconds, the press and the heater are removed, and the device is ready to be used.

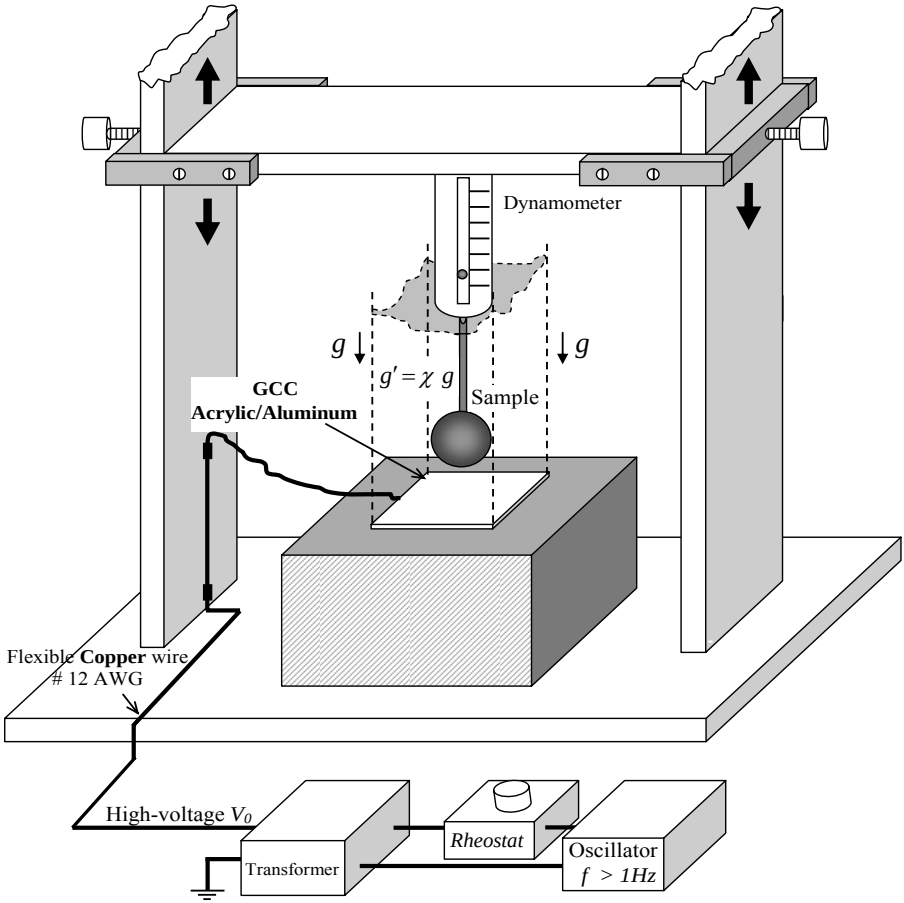

Fig. A9 – *Experimental Set-up using a GCC subjected to high-voltage* V_0 *with frequency* $f > 1Hz$. Note that in this case, the pan balance is not necessary because the substance of the Gravitational Shielding is an *air layer* with thickness d *above* the acrylic sheet. This is therefore, more a type of Gravity Control Cell (GCC) with *external gravitational shielding*.

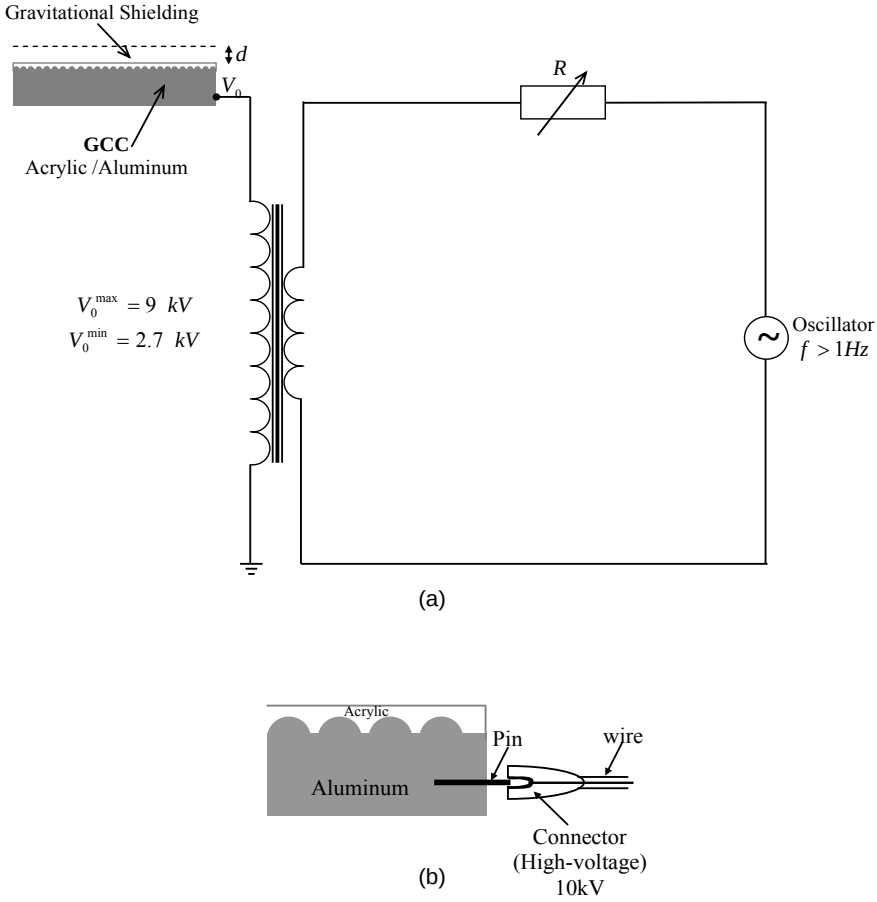

Fig. A10 – (a) *Equivalent Electric Circuit.* (b) Details of the electrical connection with the Aluminum plate. Note that others connection modes (by the top of the device) can produce destructible interference on the electric lines of the E_{air} field.

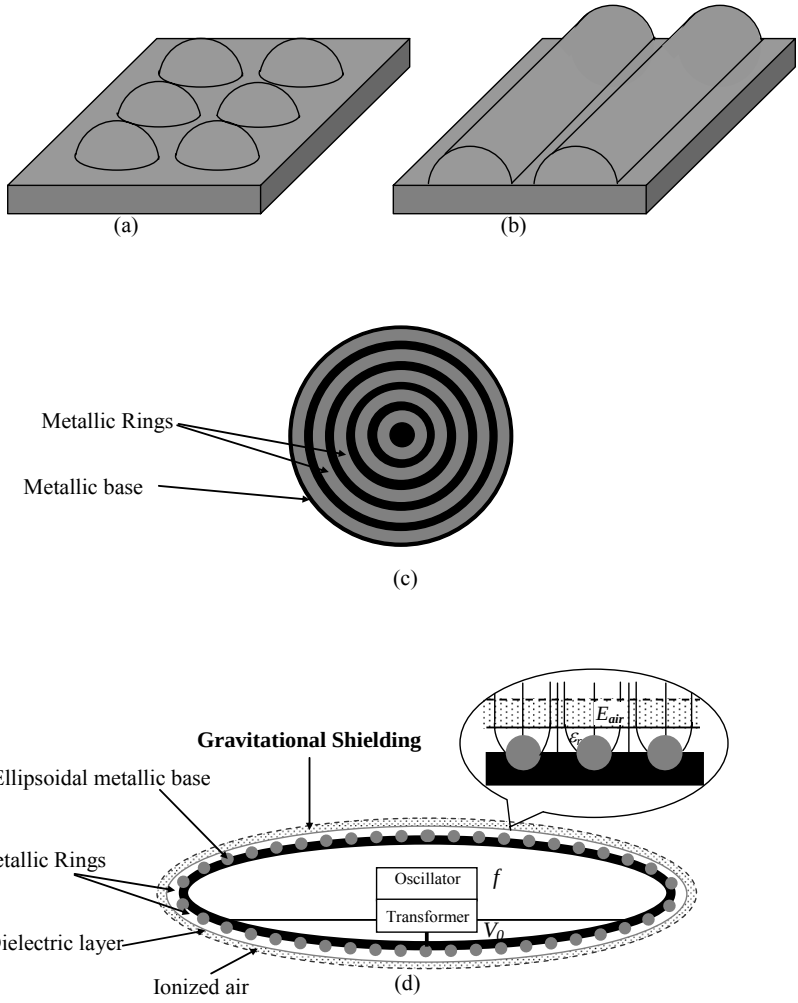

Fig. A11 – *Geometrical forms with similar effects as those produced by the semi-spherical form* – (a) shows the semi-spherical form stamped on the metallic surface; (b) shows the *semi-cylindrical* form (an obvious evolution from the semi-spherical form); (c) shows *concentric metallic rings* stamped on the metallic surface, an evolution from semi-cylindrical form. These geometrical forms produce the same effect as that of the semi-spherical form, shown in Fig.A11 (a). By using concentric metallic rings, it is possible to build *Gravitational Shieldings* around bodies or spacecrafts with several formats (spheres, ellipsoids, etc); (d) shows a Gravitational Shielding around a Spacecraft with *ellipsoidal form*.

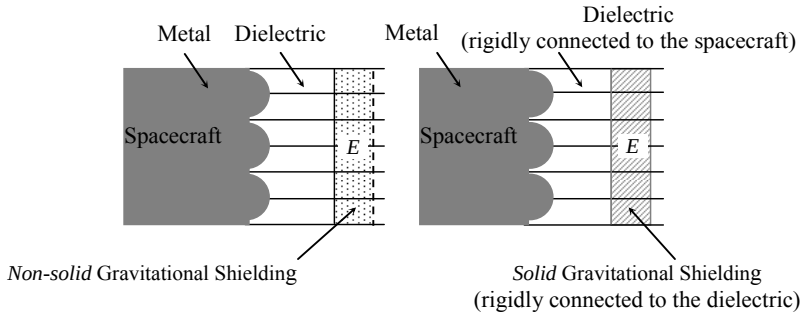

Fig. A12 – *Non-solid and Solid Gravitational Shieldings* - In the case of the Gravitational Shielding produced on a *solid substance* (b), when its molecules go to the *imaginary* space-time, *the electric field that produces the effect also goes to the imaginary space-time together with them*, because in this case, the substance of the Gravitational Shielding is *rigidly connected (by means of the dielectric) to the metal* that produces the electric field. This does not occur in the case of *Air* Gravitational Shielding.

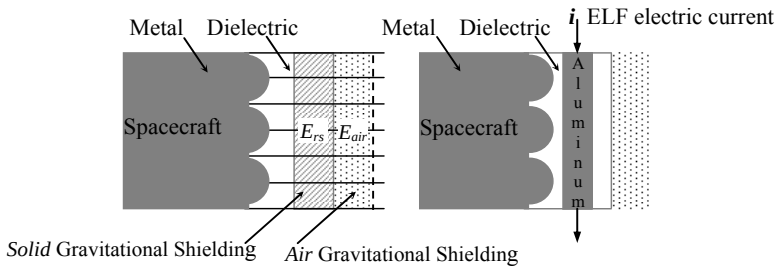

(a)

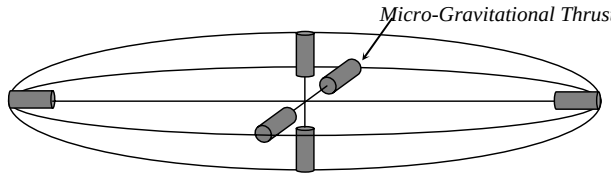

(b)

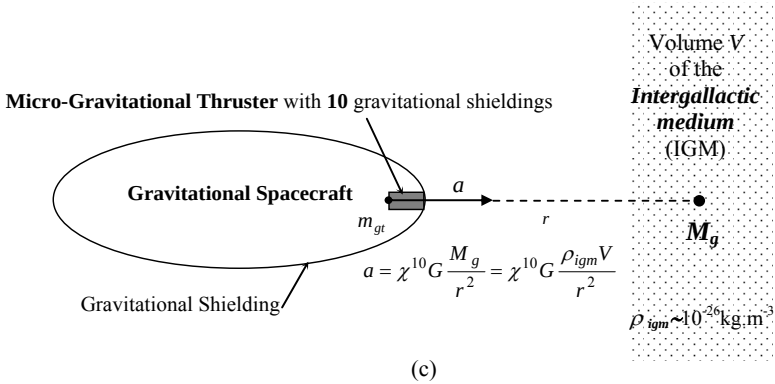

(c)

Fig. A13 – *Double Gravitational Shielding and Micro-thrusters* – (a) Shows a double gravitational shielding that makes possible to decrease the *inertial effects* upon the spacecraft when it is traveling both in the *imaginary* space-time and in the *real* space-time. The *solid* Gravitational Shielding also can be obtained by means of *an ELF electric current through a metallic lamina* placed *between the semi-spheres and the Gravitational Shielding of Air* as shown above. (b) Shows 6 *micro-thrusters* placed inside a Gravitational Spacecraft, in order to propel the spacecraft in the directions x, y and z. Note that the Gravitational Thrusters in the spacecraft must have a very small diameter (of the order of *millimeters*) because the hole through the Gravitational Shielding of the spacecraft cannot be large. Thus, these thrusters are in fact *Micro-thrusters*. (c) Shows a micro-thruster inside a spacecraft, and in front of a volume *V* of the intergalactic medium (IGM). Under these conditions, the spacecraft acquires an acceleration *a* in the direction of the volume *V*.

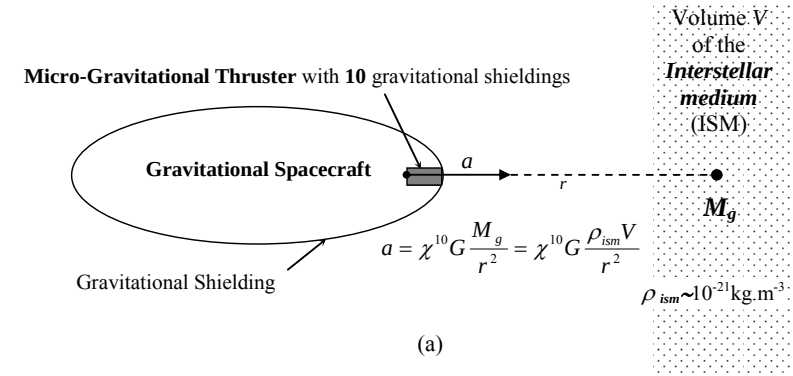

(a)

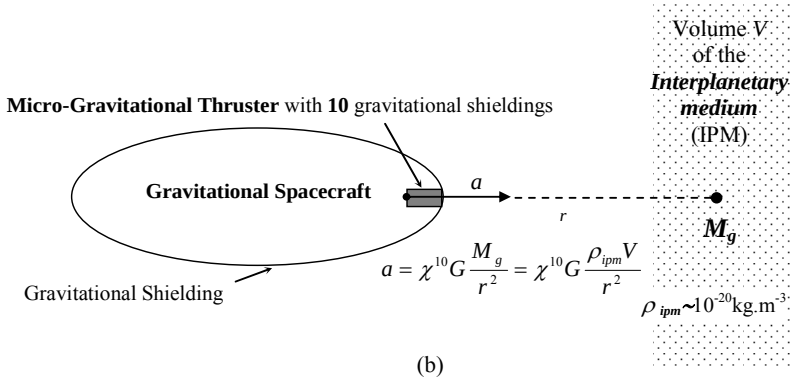

(b)

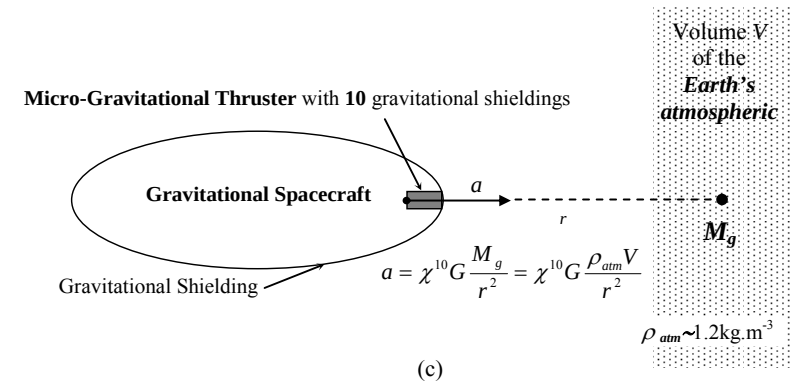

(c)

Fig. A14 – *Gravitational Propulsion using Micro-Gravitational Thruster* – (a) Gravitational acceleration produced by a gravitational mass M_g of the *Interstellar Medium*. The density of the Interstellar Medium is about 10^5 times greater than the density of the *Intergalactic Medium* (b) Gravitational acceleration produced in the *Interplanetary Medium*. (c) Gravitational acceleration produced in the *Earth's atmosphere*. Note that, in this case, ρ_{atm} (*near to the Earth's surface*)is about 10^{26} times greater than the density of the *Intergalactic Medium.*

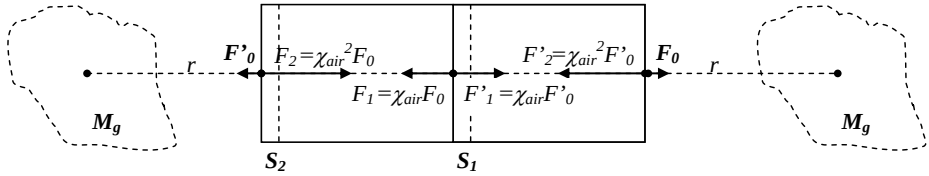

$F'_0 = F_0 \Rightarrow R = (F'_0 - F_2) + (F_1 - F'_1) + (F'_2 - F_0) = 0$

(a)

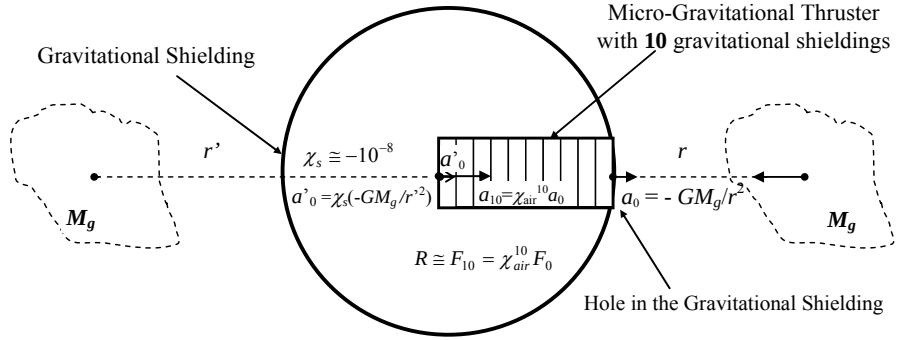

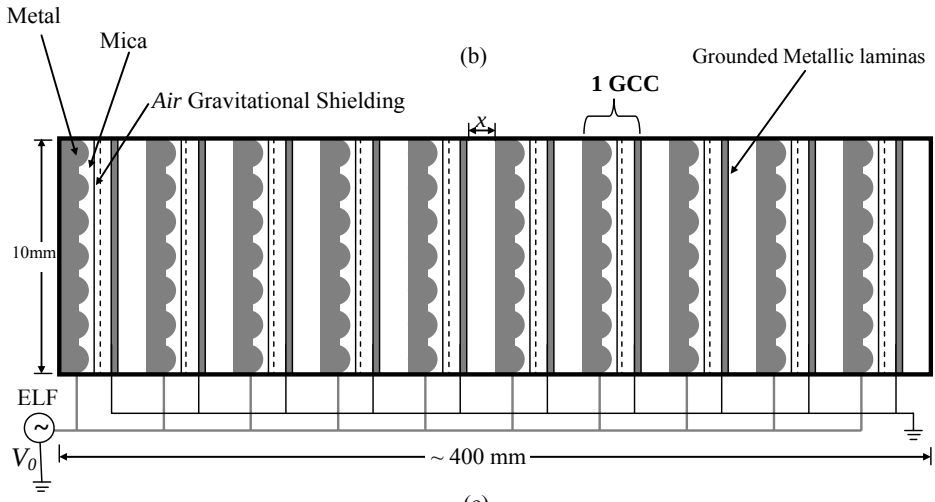

(c)

Fig. A15 – *Dynamics and Structure of the Micro-Gravitational Thrusters* - (a) The Micro-Gravitational Thrusters do not work *outside* the Gravitational Shielding, because, in this case, *the resultant upon the thruster is null* due to the symmetry. (b) The Gravitational Shielding $\left(\chi_s \cong 10^{-8}\right)$ reduces strongly the intensities of the gravitational forces acting on the micro-gravitational thruster, except obviously, through the hole in the gravitational shielding. (c) Micro-Gravitational Thruster with *10 Air Gravitational Shieldings* (10GCCs). The grounded metallic laminas are placed so as to retain the electric field produced by metallic surface behind the semi-spheres.

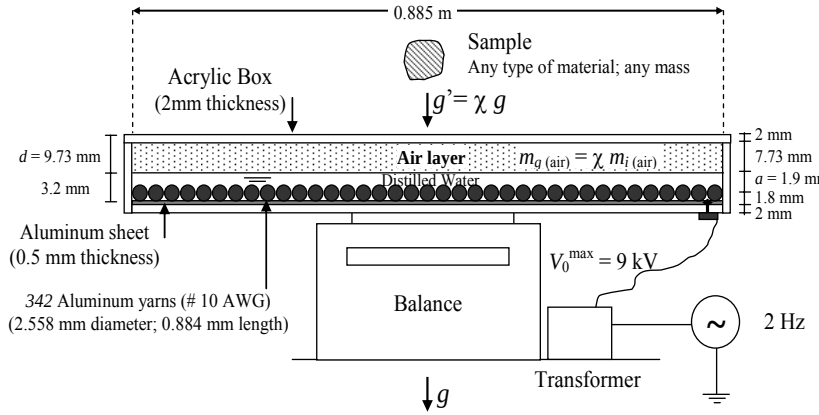

GCC Cross-section Front view

(a)

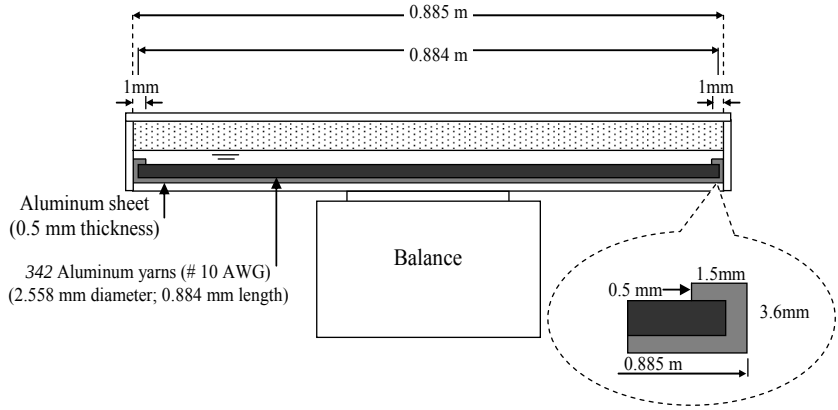

GCC Cross-section Side View

(b)

Fig. A16 – *A GCC using distilled Water*.

In total this GCC weighs about 6kg; the air layer 7.3 grams. The balance has the following characteristics: Range 0 – 6kg; readability 0.1g. The yarns are inserted side by side on the Aluminum sheet. Note the detail of fixing of the yarns on the Aluminum sheet.

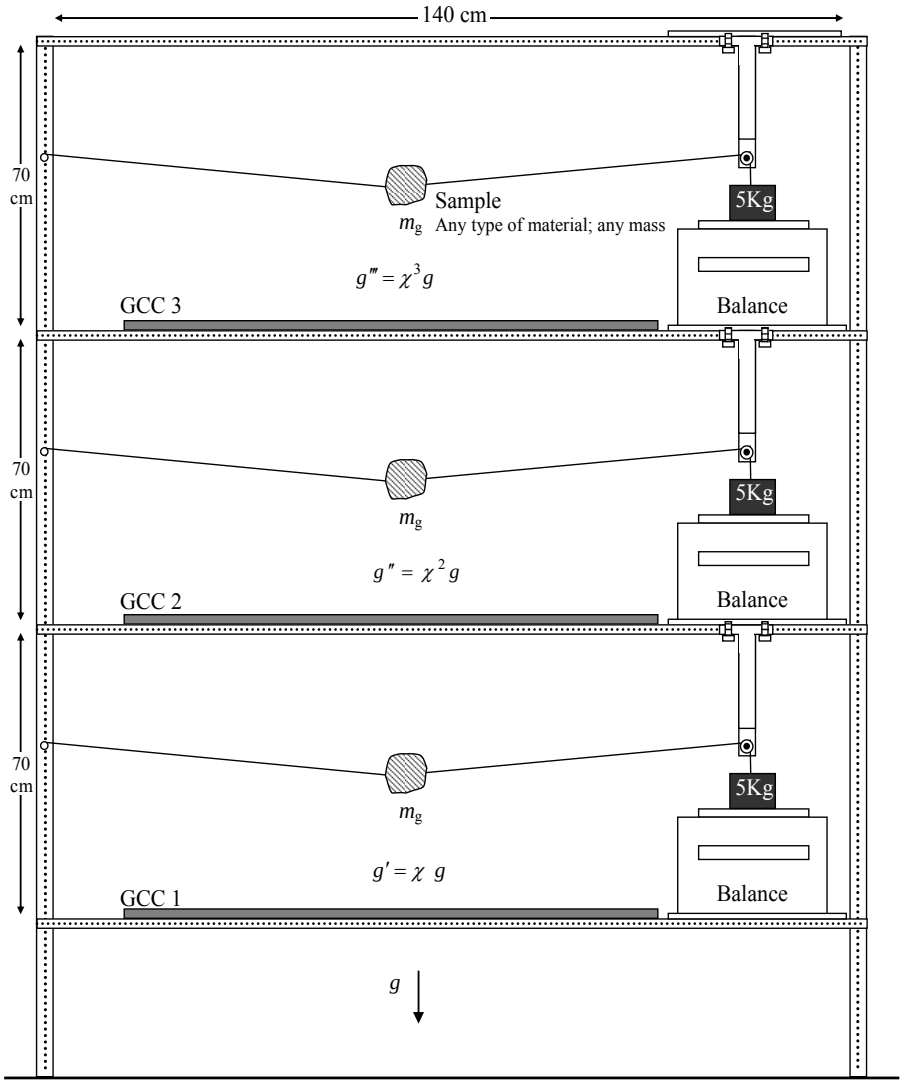

Fig. A17 – *Experimental set-up.* In order to prove *the exponential effect* produced by the superposition of the Gravitational Shieldings, we can take three similar GCCs and put them one above the other, in such way that above the GCC 1 the gravity acceleration will be $g' = \chi\, g$; above the GCC2 $g'' = \chi^2 g$, and above the GCC3 $g''' = \chi^3 g$. Where χ is given by Eq. (A47). The arrangement above has been designed for values of $m_g < 13g$ and χ up to -9 or $m_g < 1kg$ and χ up to -2 .

APPENDIX B: Gravity Control Cells (GCCs) made from *Semiconductor Compounds*.

There are some semiconductors compounds with electrical conductivity between 10^4S/m to 1 S/m, which can have their gravitational mass strongly decreased when subjected to ELF electromagnetic fields.

For instance, the polyvinyl chloride (PVC) compound, called Duracap™ 86103.

It has the following characteristics:

$$\mu_r = 1;\ \varepsilon_r = 3$$
$$\sigma = 3333.3 S/m$$
$$\rho = 1400 kg.m^{-3}$$
$$dieletric\quad strength = 98\, KV/mm$$

Then, according to the following equation below (derived from Eq.A14)

$$m_g = \left\{1 - 2\left[\sqrt{1 + 1.758\times10^{-27}\left(\frac{\mu_r\sigma^3}{\rho^2 f^3}\right)E_{rms}^4} - 1\right]\right\} m_{i0} \qquad (B1)$$

the *gravitational mass*, m_g, of the Duracap™ 86103, when subjected to an electromagnetic field of frequency f, is given by

$$m_g = \left\{1 - 2\left[\sqrt{1 + 3.3\times10^{-23}\frac{E_{rms}^4}{f^3}} - 1\right]\right\} m_{i0} \qquad (B2)$$

Note that, if the electromagnetic field through the Duracap has *extremely-low frequency*, for example, if $f = 2Hz$, and

$$E_{rms} = 9.4\times10^5 V/m \qquad (0.94 kV/mm)$$

Then, its *gravitational mass* will be reduced down to $m_g \cong -1.1 m_{i0}$, reducing in this way, the initial *weight* $(P_0 = m_g g = m_{i0} g)$ of the Duracap down to $-1.1P_0$.

BACKGROUND FOR EXPERIMENTAL

The Duracap™ 86103 is sold under the form of small cubes. Its melting temperature varies from 177ºC to 188ºC. Thus, a 15cm square Duracap plate with 1 mm thickness can be shaped by using a suitable mold, as the shown in Fig.B1.

Figure B2(a) shows the Duracap plate between the Aluminum plates of a parallel plate capacitor. The plates have the following dimensions: 19cm x 15cm x 1mm. They are painted with an insulating varnish spray of high dielectric strength (ISOFILM). They are connected to the secondary of a transformer, which is connected to a Function Generator. The distance between the Aluminum plates is $d = 1mm$. Thus, the electric field through the Duracap is given by

$$E_{rms} = \frac{E_m}{\sqrt{2}} = \frac{V_0}{\varepsilon_r d\sqrt{2}} \qquad (B3)$$

where ε_r is the relative permittivity of the dielectric (Duracap), and V_0 is the amplitude of the wave voltage applied on the capacitor.

In order to generate *ELF wave voltage* of $f = 2Hz$, we can use the widely-known Function Generator HP3325A (Op.002 High Voltage Output) that can generate sinusoidal voltages with *extremely-low* frequencies and amplitude up to *20V* ($40V_{pp}$ into 500Ω load). The maximum output current is $0.08A_{pp}$; output impedance $<2\Omega$ at ELF.

The turns ratio of the transformer (Bosch red coil) is $200:1$. Thus, since the

maximum value of the amplitude of the voltage produced by the Function Generator is $V_p^{\max} = 20\ V$, then the maximum secondary voltage will be $V_s^{\max} = V_0^{\max} = 4kV$. Consequently, Eq. (B3) gives

$$E_{rms}^{\max} = 2.8 \times 10^6 V/m$$

Thus, for $f = 2Hz$, Eq. (B2) gives

$$m_g = -29.5 m_{i0}$$

The *variations on the gravitational mass* of the Duracap plate can be measured by a pan balance with the following characteristics: range 0 – 1.5kg ; readability 0.01g, using the set-up shown in Fig. B2(a).

Figure B2(b) shows the set-up to measure *the gravity acceleration variations above* the Duracap plate (Gravitational Shielding effect). The samples used in this case, can be of several types of material.

Since voltage waves with frequencies very below 1Hz have a very long period, we cannot consider, in practice, their *rms* values. However, we can add a sinusoidal voltage $V_{osc} = V_0 \sin \omega t$ with a DC voltage V_{DC}, by means of the circuit shown in Fig.B3. Thus, we obtain $V = V_{DC} + V_0 \sin \omega t$; $\omega = 2\pi f$. If $V_0 << V_{DC}$ then $V \cong V_{DC}$. Thus, the voltage V varies with the frequency f, but its intensity is approximately equal to V_{DC}, i.e., V will be practically constant. This is of fundamental importance for maintaining the value of the gravitational mass of the body, m_g, sufficiently stable during all the time, in the case of $f << Hz$.

We have shown in this paper that it is possible to control the gravitational mass of a spacecraft, simply by controlling the gravitational mass of a body *inside* the spacecraft (Eq.(10)). This body can be, for example, the *dielectric* between the plates of a capacitor, whose gravitational mass can be easily controlled by means of an ELF electromagnetic field produced between the plates of the capacitor. We will call this type of capacitor of *Capacitor of Gravitational Mass Control* (CGMC).

Figure B 4(a) shows a CGMC placed in the center of the spacecraft. Thus, the gravitational mass of the spacecraft can be controlled simply by varying the gravitational mass of the dielectric of the capacitor by means of an ELF electromagnetic field produced between the plates of the capacitor. Note that the Capacitor of Gravitational Mass Control can have the *spacecraft's own form* as shown in Fig. B 4(b). The dielectric can be, for example, a Duracap plate, as shown in this appendix. In this case, the gravitational mass of the dielectric is expressed by Eq. (B2). Under these circumstances, the *total* gravitational mass of the spacecraft will be given by Eq.(10):

$$M_{g(spacecraf)} = M_{i0} + \chi_{dielectric} m_{i0}$$

where M_{i0} is the rest inertial mass of the spacecraft(without the dielectric) and m_{i0} is the rest inertial mass of the dielectric; $\chi_{dielectric} = m_g / m_{i0}$, where m_g is the gravitational mass of the dielectric. By decreasing the value of $\chi_{dielectric}$, the gravitational mass of the spacecraft decreases. It was shown, that the value of χ can be negative. Thus, for example, when $\chi_{dielectric} \cong -M_{i0}/m_{i0}$, the *gravitational mass of the spacecraft gets very close to zero*. When $\chi_{dielectric} < -M_{i0}/m_{i0}$, the

gravitational mass of the spacecraft becomes negative.

Therefore, *for an observer out of the spacecraft* the gravitational mass of the spacecraft is $M_{g(spacecraft)} = M_{i0} + \chi_{dielectric} m_{i0}$, and not $M_{i0} + m_{i0}$.

Since the dielectric strength of the Duracap is $98kV/mm$, a Duracap plate with *1mm* thickness can withstand up to $98kV$. In this case, the value of $\chi_{dielectric}$ for $f = 2Hz$, according to Eq. (B2), is

$$\chi_{dielectric} = m_g / m_{i0} \cong -10^4$$

Thus, for example, if the inertial mass of the spacecraft is $M_{i0} \cong 10021.0014kg$ and, the inertial mass of the *dielectric* of the *Capacitor of Gravitational Mass Control* is $m_{i0} \cong 1.0021kg$, then the gravitational mass of the spacecraft becomes

$$M_{g(spacecraf)} = M_{i0} + \chi_{dielectric} m_{i0} \cong 10^{-3} kg$$

This value is much smaller than $+0.159 M_{i0}$.

It was shown [1] that, when the gravitational mass of a particle is reduced to values between $+0.159M_i$ and $-0.159M_i$, it becomes *imaginary*, i.e., the gravitational and the inertial masses of the particle become *imaginary*. Consequently, the particle *disappears* from our ordinary space-time.

This means that we cannot reduce the gravitational mass of *the spacecraft* below $+0.159M_i$, *unless we want to make it imaginary*.

Obviously this limits the minimum value of $\chi_{dielectric}$, i.e. $\chi^{\min}_{dielctric} = 0.159$. Consequently, if the gravity acceleration *out of the spacecraft* (in a given direction) is g, then, according to the Gravitational Shielding Principle, the corresponding gravity acceleration upon the crew of the spacecraft can be reduced just down to $0.159g$. In addition, since the Mach's principle says that *the local inertial forces are produced by the gravitational interaction of the local system with the distribution of cosmic masses* then *the inertial effects* upon the crew would be reduced just by $\chi_{dielectric} = 0.159$.

However, there is a way to strongly reduce the inertial effects upon the crew of the spacecraft without making it *imaginary*. As shown in Fig. B4 (c), we can build an *inertial shielding*, with n superimposed CGMCs. In this case, according to the Gravitational Shielding Principle, the gravity upon the crew will be given by $g_n = \chi^n_{dielectric} g$, where g is the gravity acceleration out of the spacecraft (in a given direction) and $\chi_{dielectric} = m_g / m_{i0}$; m_g and m_{i0} are, respectively, the gravitational mass and the inertial mass of the dielectric. Under these conditions the *inertial effects upon the crew* will be reduced by $\chi^n_{dielectric}$.

Thus, for $n = 10$ (*ten* superimposed CGMCs), and $\chi_{dielectric} \cong 0.2$, the *inertial effects upon the crew* will be reduced by $\chi^{10}_{dielectric} \cong 1 \times 10^{-7}$. Therefore, if the maximum thrust produced by the thrusters of the spacecraft is $F = 10^5 N$, then the intensities of the inertial forces upon the crew will not exceed $0.01N$, i.e. they will be practically negligible.

Under these circumstances, the gravitational mass of the spacecraft, for an observer out of the spacecraft, will be just approximately equal to the gravitational mass of the *inertial shielding*, i.e. $M_{g(spacecraft)} \cong M_{g(inertial.shield)}$.

If $M_{g(inertial.shield)} \cong 10^3 kg$, and the thrusters of the spacecraft are able to

produces up to $F = 3 \times 10^5 N$, the spacecraft will acquires an acceleration given by

$$a_{spacecraft} = \frac{F}{M_{g(spacecraft)}} \cong 3 \times 10^2 m.s^{-2}$$

With this acceleration it can reach velocities close to *Mach 10* in some seconds.

The velocity that the spacecraft can reach in the *imaginary* spacetime is much greater than this value, since $M_{g(spacecraft)}$, as we have seen, can be reduced down to $\cong 10^{-3} kg$ or less.

Thus, if the thrusters of the spacecraft are able to produces up to $F = 3 \times 10^5 N$, and $M_{g(spacecraft)} \cong 10^{-3} kg$, the spacecraft will acquires an acceleration given by

$$a_{spacecraft} = \frac{F}{M_{g(spacecraft)}} \cong 3 \times 10^8 m.s^{-2}$$

With this acceleration it can reach velocities close to the light speed in less than 1 second. After 1 month, the velocity of the spacecraft would be about $10^{15} m/s$ (remember that in the *imaginary* spacetime the maximum velocity of propagation of the interactions is *infinity* [1]).

OTHER SEMICONDUCTOR COMPOUNDS

A semiconductor compound, which can have its gravitational mass strongly decreased when subjected to ELF electromagnetic fields is the CoorsTek Pure SiC™ LR CVD *Silicon Carbide*, 99.9995% [‡‡‡‡]. This Low-resistivity (LR) pure Silicon Carbide has electrical conductivity of *5000S/m* at room temperature; $\varepsilon_r = 10.8$; $\rho = 3210 kg.m^{-3}$; dielectric strength >10 KV/mm; maximum working temperature of 1600°C.

Another material is the *Alumina-CNT*, recently discovered [§§§§]. It has electrical conductivity of *3375 S/m* at 77°C in samples that were 15% nanotubes by volume [17]; $\varepsilon_r = 9.8$; $\rho = 3980 kg.m^{-3}$; dielectric strength 10-20KV/mm; maximum working temperature of 1750°C.

The novel *Carbon Nanotubes Aerogels* [*****], called *CNT Aerogels* are also suitable to produce Gravitational Shieldings, mainly due to their very small densities. The electrical conductivity of the *CNT Aerogels* is *70.4S/m* for a density of $\rho = 7.5 kg.m^{-3}$ [18]; $\varepsilon_r \approx 10$. Recently (2010), it was announced the discovered of *Graphene Aerogel* with $\sigma = \sim 1 \times 10^2 S/m$ and $\rho = 10 kg.m^{-3}$ [19] (Aerogels exhibit higher dielectric strength than expected for porous materials).

[‡‡‡‡] www.coorstek.com

[§§§§] Recently, it was discovered that Carbon nanotubes (CNTs) can be added to *Alumina* (Al_2O_3) to convert it into a good electrical conductor.

[*****] In 2007, Mateusz Brying *et al.* working with Prof. Arjun Yodh at the University of Pennsylvania produced the first aerogels made entirely of carbon nanotubes (CNT Aerogels) [20] that, depending on the processing conditions, can have their electrical conductivity ranging as high as 100 S/m.

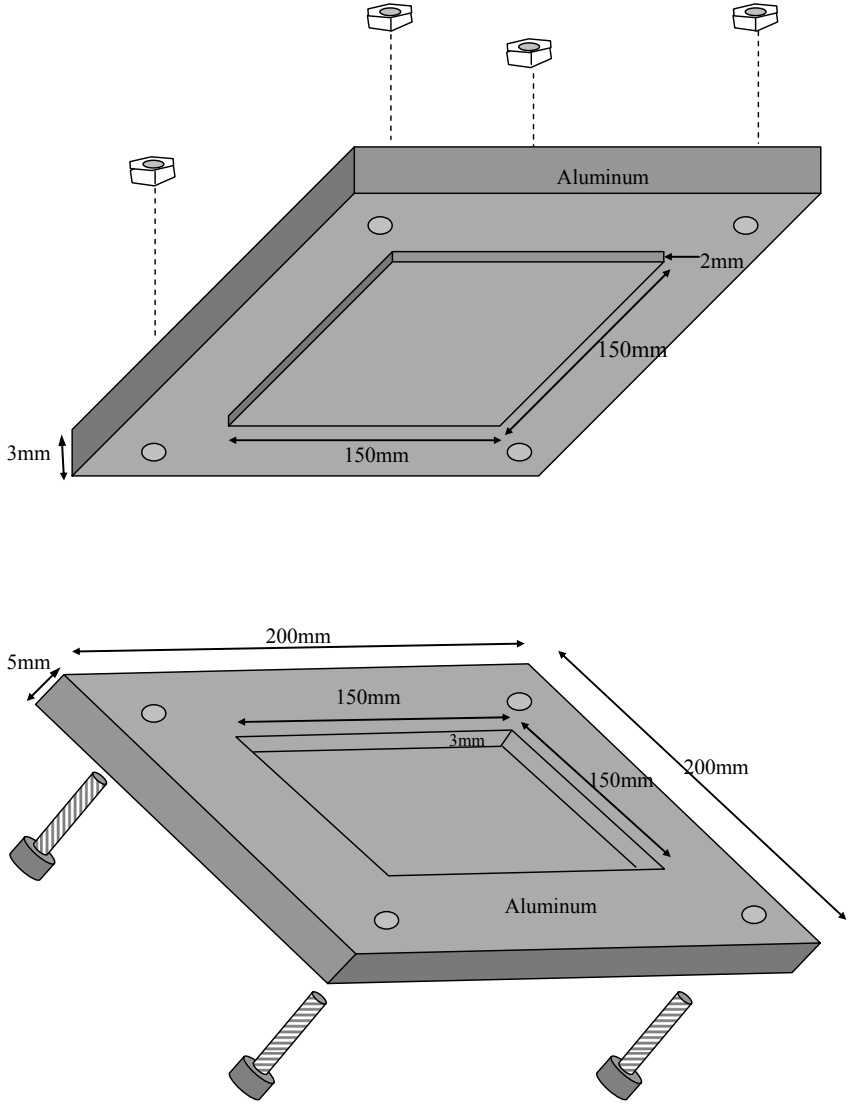

Fig.B1 – Mold design

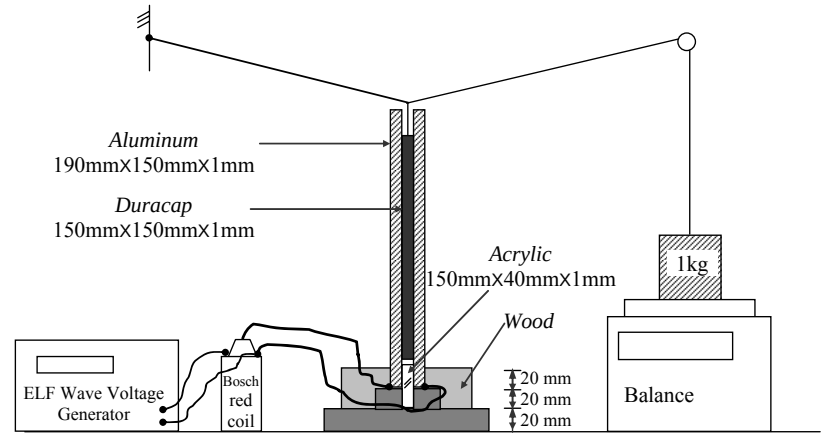

(a)

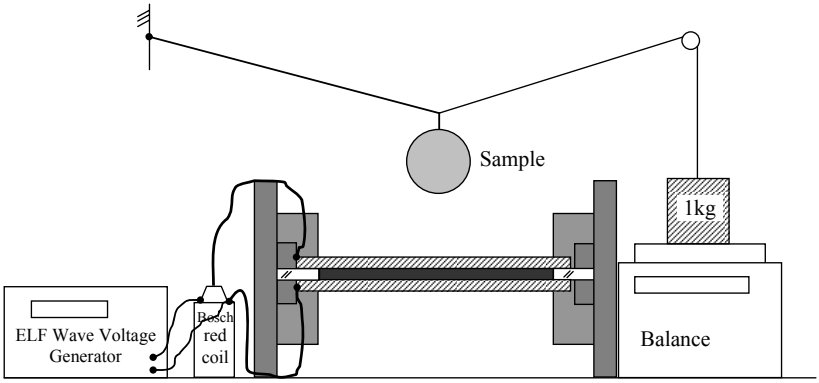

(b)

Fig.B2 – Schematic diagram of the experimental set-up

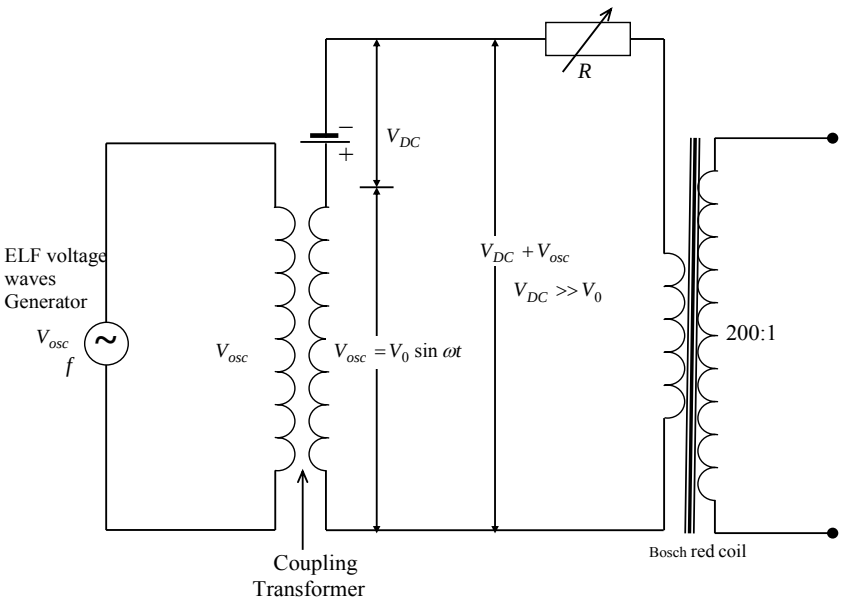

Fig. B3 – Equivalent Electric Circuit

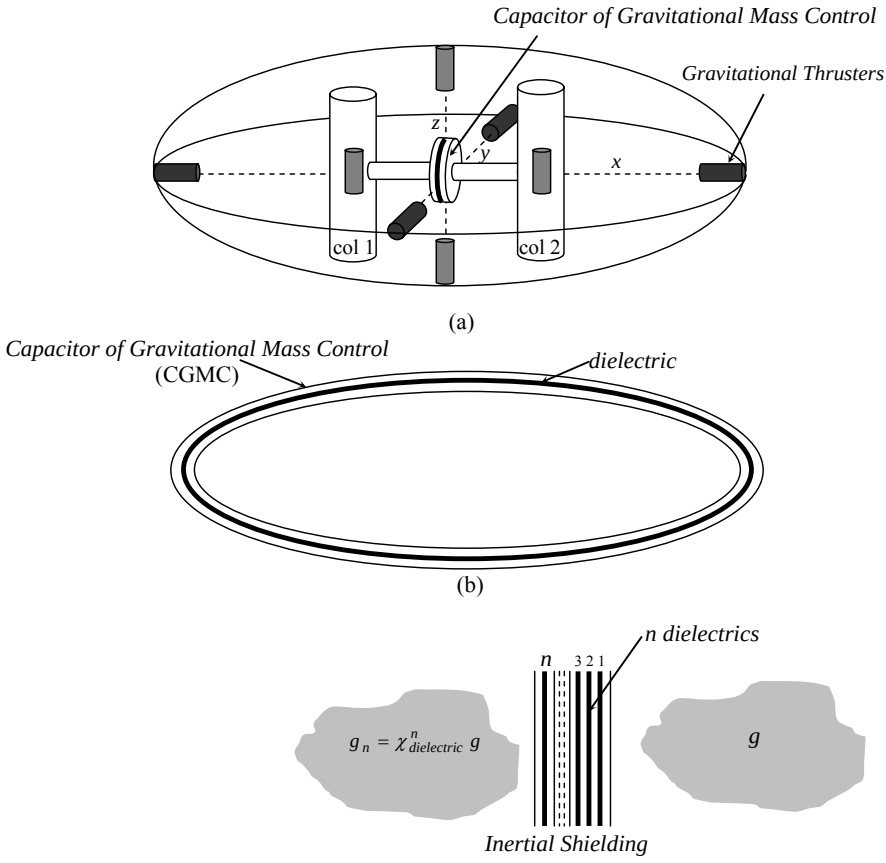

Fig.B4 – Gravitational Propulsion System and *Inertial Shielding* of the Gravitational Spacecraft – (a) eight *gravitational thrusters are* placed inside a Gravitational Spacecraft, in order to propel the spacecraft along the directions x, y and z. Two *gravitational thrusters* are inside the columns 1 and 2, in order to rotate the spacecraft around the y-axis. The functioning of the Gravitational Thrusters is shown in Fig.A14. *The gravitational mass of the spacecraft is controlled by the Capacitor of Gravitational Mass Control* (CGMC). Note that the CGMC can have the *spacecraft's own form*, as shown in (b). In order to strongly reduce the inertial effects upon the crew of the spacecraft, we can build an inertial shielding, with several CGMCs, as shown above (c). In this case, the gravity upon the crew will be given by $g_n = \chi^n_{dielectric}\, g$, where g is the gravity acceleration out of the spacecraft (in a given direction) and $\chi_{dielectric} = m_g / m_{i0}$; m_g and m_{i0} are, respectively, the gravitational mass and the inertial mass of the dielectric. Under these conditions the *inertial effects upon the crew* will be reduced by $\chi^n_{dielectric}$. Thus, for example, if $n = 10$ and $\chi_{dielectric} \cong 0.2$, the inertial effects will be reduced by $\chi^{10}_{dielectric} \cong 1 \times 10^{-7}$. If the maximum thrust produced by the thrusters is $F = 10^5\, N$, then the intensities of the inertial forces upon the crew will not exceed $0.01N$.

APPENDIX C: Longer-Duration Microgravity Environment Produced by *Gravity Control Cells* (GCCs).

The acceleration experienced by an object in a *microgravity* environment, by definition, is one-millionth (10^{-6}) of that experienced at Earth's surface (1g). Consequently, a *microgravity* environment is one where the acceleration induced by gravity has little or no measurable effect. The term *zero-gravity* is, obviously inappropriate since the *quantization of gravity* [1] shows that the gravity can have only discrete values *different of zero* [1, Appendix B].

Only three methods of creating a microgravity environment are currently known: to travel far enough into deep space so as to reduce the effect of gravity by *attenuation*, by *falling*, and by *orbiting* a planet.

The first method is the simplest in conception, but requires traveling an enormous distance, rendering it most impractical with the conventional spacecrafts. The second method, *falling*, is very common but approaches microgravity only when the fall is in a vacuum, as air resistance will provide some resistance to free fall acceleration. Also it is difficult to fall for long enough periods of time. There are also problems which involve avoiding too sudden of a stop at the end. The NASA Lewis Research Center has several drop facilities. One provides a 132 meter drop into a hole in the ground similar to a mine shaft. This drop creates a reduced gravity environment for *5.2 seconds***.** The longest drop time currently available (about *10 seconds*) is at a 490 meter deep vertical mine shaft in Japan that has been converted to a drop facility.

Drop towers are used for experiments that only need a *short duration of microgravity*, or for an initial validation for experiments that will be carried out in longer duration of microgravity.

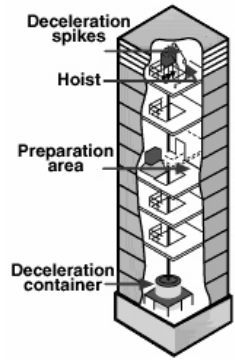

Aircraft can fly in parabolic arcs to achieve period of microgravity of 20 to 25 seconds with g-level of approximately 0.02 g. The airplane climbs rapidly until its nose is about 45-degree angle to the horizon then the engines are cut back. The airplane slows; the plane remains in free fall over the top of the parabola, then it nose-dives to complete the parabola, creating microgravity conditions.

Aircraft parabolic flights give the opportunity to perform medical experiments on human subjects in real microgravity environment. They also offer the possibility of direct intervention by investigators on board the aircraft during and between parabolas. In the mid-1980s, NASA KC-135, a modified Boeing 707,

provided access to microgravity environment. A parabolic flight provided 15 to 20 seconds of 0.01 g or less, followed by a 2-g pull out. On a typical flight, up to 40 parabolic trajectories can be performed. The KC-135 can accommodate up to 21 passengers performing 12 different experiments. In 1993, the Falcon-20 performed its first parabolic flight with microgravity experiment on board. This jet can carry two experimenters and perform up to 3 experiments. Each flight can make up to 4 parabolic trajectories, with each parabola lasting 75 seconds, with 15 to 20 seconds of microgravity at 0.01g or less.

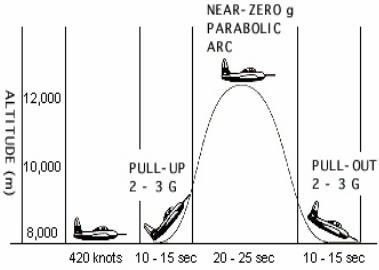

The third method of creating a microgravity environment is *orbiting* a planet. This is the environment commonly experienced in the space shuttle, International Space Station, Mir (no longer in orbit), etc. While this scenario is the most suitable for scientific experimentation and commercial exploitation, it is still quite expensive to operate in, mostly due to launch costs.

A space shuttle provides an ideal laboratory environment to conduct microgravity research. A large panoply of experiments can be carried out in microgravity conditions for up to *17 days*, and scientists can make adjustment to avoid experiment failure and potential loss of data. Unmanned capsules, platforms or satellites, such as the European retrievable carrier Eureka, DLR's retrievable carrier SPAS, or the Russian Photon capsules, the US Space Shuttle (in connection with the European Spacelab laboratory or the US Spacelab module), provide *weeks* or *months* of microgravity.

A space station, maintaining a low earth orbit for several decades, greatly improves access to microgravity environment for up to *several months.*

Thus, microgravity environment can be obtained via different means, providing different duration of microgravity. While *short-duration microgravity environments* can be achieved on Earth with relative easiness, *longer-duration microgravity environments* are too expensive to be obtained.

Here, we propose to use the Gravity Control Cells (GCCs), shown in this work, in order to create *longer-duration microgravity environments*. As we have seen, just above a GCC the gravity can be strongly reduced (*down to* $1\mu g$ or less). In this way, the gravity above a GCC can remain at the

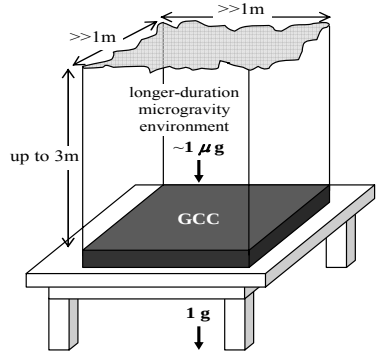

microgravity ranging during a very long time (*several years*). Thus, GCCs can be used in order to create longer-duration microgravity environments on Earth. In addition, due to the cost of the GCCs to be relatively low, also the longer-duration microgravity environments will be produced with low costs.

This possibility appears to be absolutely new and unprecedented in the literature since longer-duration microgravity environments are usually obtained via airplanes, sounding rockets, spacecraft and space station.

It is easy to see that the GCCs can be built with *width* and *length* of until some meters. On the other hand, as the effect of gravity reduction above the GCC can reach up to 3m, we can then conclude that the *longer-duration microgravity environments* produced above the GCCs can have sufficiently large volumes to perform any microgravity experiment on Earth.

The longer-duration microgravity environment produced by a GCC will be a special tool for microgravity research. It will allow to improve and to optimize physical, chemical and biological processes on Earth that are important in science, engineering and also medicine. The reduction of gravitational effects in a microgravity environment shows, for example, that temperature differences in a fluid do not produce convection, buoyancy or sedimentation. The changes in fluid behavior in microgravity lie at the heart of the studies in materials science, combustion and many aspects of space biology and life sciences. Microgravity research holds the promise to develop new materials which can not be made on Earth due to gravity. These new materials shall have properties that are superior to those made on Earth and may be used to:

-increase the speed of future computers,
-improve fiber optics,
-make feasible Room Temperature Superconductors,
-enable medical breakthroughs to cure several diseases (e.g., diabetes).

In a microgravity environment protein crystals can be grown larger and with a purity that is impossible to obtain under gravity of 1g. By analyzing the space-grown crystals it is possible to determine the structure and function of the thousands of proteins used in the human body and in valuable plants and animals. The determination of protein structure represents a huge opportunity for pharmaceutical companies to develop new drugs to fight diseases.

Crystal of HIV protease inhibitor grown in microgravity are significantly larger and of higher quality than any specimens grown under gravity of 1g. This will help in defining the structure of the protein crucial in fighting the AIDS virus.

Protein Crystal Isocitrate Lysase is an enzyme for fungicides. The isocitrate lysase crystals grown in microgravity environments are of larger sizes and fewer structural defects than crystals grown under gravity of 1g. They will lead to more powerful fungicides to treat serious crop diseases such as rice blast, and increase crop output.

Improved crystals of human insulin will help improve treatment for diabetes and *potentially create a cure*.

Anchorage dependent cells attached to a polymer and grown in a bioreactor in microgravity will lead to the production of a protein that is closer in structure and function to the three-dimensional protein living in the body.

Anchorage Dependant Cells
Attached to a Polymer

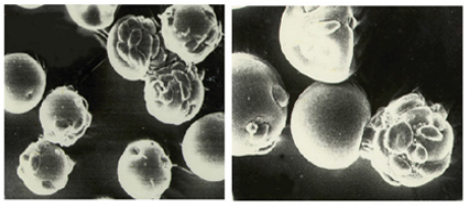

1g μg

This should help reduce or eliminate *transplant rejection* and is therefore critical for organ transplant and for the replacement of damaged bone and tissues. Cells grown on Earth are far from being three-dimensional due to the effect of 1g gravity.

The ZBLAN is a new substance with the potential to revolutionize fiber optics communications. A member of the heavy metal fluoride family of glasses, ZBLAN has promising applications in fiber optics. It can be used in a large array of industries, including manufacture of ultra high purity fiber optics, optical switches for computing, telecommunications, medical surgery and cauterization, temperature monitoring, infrared imaging, fiber-optic lasers, and optical power transmission. A ZBLAN fiber optic cable manufactured in a *microgravity environment* has the potential to carry 100 times the amount of data conveyed by conventional silica-based fibers.

ZBLAN Fiber

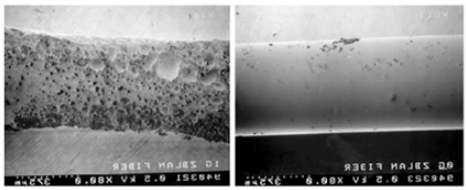

1g μg

In microgravity environment where complications of gravity-driven convection flows are eliminated, we can explore the fundamental processes in fluids of several types more easily and test fundamental theories of three-dimensional laminar, oscillatory and turbulent flow generated by various other forces.

By improving the basics for predicting and controlling the behavior of fluids, we open up possibilities for improving a whole range of industrial processes:

- Civil engineers can design safe buildings in earthquake-prone areas thanks to a better understanding of the fluid-like behavior of soils under stress.

- Materials engineers can benefit from a deeper knowledge of the determination of the structure and properties of a solid metal during its formation and can improve product quality and yield, and, in some cases, lead to the introduction of new products.

- Architects and engineers can design more stable and performing power

plants with the knowledge of the flow characteristics of vapor-liquid mixture.

- Combustion scientists can improve fire safety and fuel efficiency with the knowledge of fluid flow in microgravity.

In microgravity environment, medical researchers can observe the functional changes in cells when the effect of gravity is practically removed. It becomes possible to study fundamental life processes down to the cellular level.

Access to microgravity will provide better opportunities for research, offer repeated testing procedures, and enormously improve the test facilities available for life sciences investigations. This will provide valuable information for medical research and lead to improvements in the health and welfare of the six billion people, which live under the influence of 1g gravity on the Earth's surface.

The utilization of microgravity to develop new and innovative materials, pharmaceuticals and other products is waiting to be explored. Access to microgravity environments currently is limited. Better access, as the produced by GCCs, will help researchers accelerate the experimentation into these new products.

Terrafoam is a rigid, silicate based inorganic foam. It is *nonflammable* and does not five off noxious fumes when in the presence of fire. *It does not conduct heat to any measurable degree* and thus is an outstanding and possible unsurpassed thermal insulator. In addition, it appears to have unique *radiation shielding* capabilities, including an ability to block *alpha*, *beta*, gamma rays). Terrafoam can be constructed to be extremely lightweight. Altering the manufacturing process and the inclusion of other materials can vary the properties of Terrafoam. Properties such as cell structure, tensile strength, bulk density and temperature resistance can be varied to suit specific applications. It self-welds to concrete, aluminum and other metals. The useful variations on the base product are potentially in the thousands. Perhaps the most exciting potential applications for Terrafoam stem from its extraordinary capability as an ultra-lightweight thermal and radioactive shield.

Also, the formation of nanoscale *carbon structures* by electrical arc discharge plasma synthesis has already been investigated in microgravity experiments by NASA. Furthermore, complex plasmas are relevant for processes in which a particle formation is to be prevented, if possible, as, for example, within plasma etching processes for microchip production.

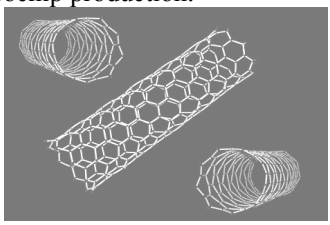

People will benefit from numerous microgravity experiments that can be conducted in Longer-Duration Microgravity Environment Produced by *Gravity Control Cells* (GCCs) on Earth.

APPENDIX D: Antenna with Gravitational Transducer for *Instantaneous Communications* at any distance

It was previously shown in this article that *Quantum Gravitational Antennas* (GCC antennas, Fig.8) can emit and detect *virtual gravitational* radiation. The velocity of this radiation is *infinite*, as we have seen. This means that these quantum antennas can transmit and receive communications *instantaneously* to and from anywhere in the Universe. Here, it is shown how to transmit and receive communications *instantaneously* from any distance in the Universe by utilizing *virtual electromagnetic* (EM) radiation instead of *virtual gravitational* radiation. Starting from the principle that the antennas of usual transceivers (*real* antennas) radiate *real* EM radiation, then we can expect that *imaginary* antennas radiate *imaginary* EM radiation or *virtual* EM radiation. The velocity of this radiation is also *infinite*, in such a way that it can transmit communications *instantaneously* from any distance in the Universe.

It was shown [1] that when the *gravitational mass* of a body is decreased down to the range of $+0.159m_i$ to $-0.159m_i$ (m_i is its inertial mass), the body becomes *imaginary* and goes to an *imaginary* Universe which contains our *real* Universe. Thus, we have the method to convert *real* antennas to *imaginary* antennas.

Now, consider a Gravitational Shielding S, whose gravitational mass is decreased down to the range of $+0.159m_{iS}$ to $-0.159m_{iS}$. By analogy, it becomes imaginary and goes to the imaginary Universe. It is easy to show that, in these circumstances, also a body inside the shielding S becomes imaginary and goes to the imaginary Universe together with the gravitational shielding S. In order to prove it, consider, for example, Fig.D1 where we clearly see that the *Gravitational Shielding Effect* is equivalent to a decrease of $\chi = m_{gS}/m_{iS}$ in the gravitational masses of the bodies A and B, since the *initial* gravitational masses: $m_{gA} \cong m_{iA}$ and $m_{gB} \cong m_{iB}$ become respectively $m_{gA} = \chi m_{iA}$ and $m_{gB} = \chi m_{iB}$, when the gravitational shielding is activated. Thus, when χ becomes less than $+0.159$, both the gravitational masses of S and A become respectively:

$$m_{gS} < +0.159m_{iS}$$

and

$$m_{gA} < +0.159m_{iA}$$

This proves, therefore, that when a Gravitational Shielding S becomes *imaginary*, any particle (including *photons*[‡‡‡‡‡]) inside S, also becomes *imaginary* and goes to the *imaginary*

[‡‡‡‡‡] As shown in the article "*Mathematical Foundations of the Relativistic Theory of Quantum Gravity*", *real* photons become *imaginary* photons or *virtual* photons.

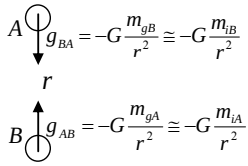

(a)

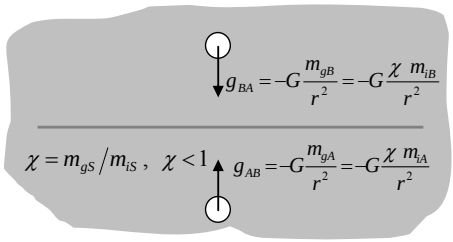

(b)

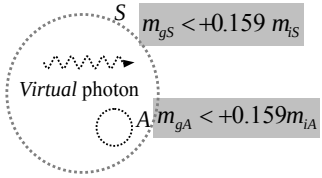

(c)

Fig.D1 – (a) (b) The *Gravitational Shielding Effect* is equivalent to a decrease of $\chi = m_{gS}/m_{iS}$ in the gravitational masses of the bodies A and B. (c) When a Gravitational Shielding S becomes *imaginary*, any particle (including *photons*) inside S, also becomes *imaginary*.

Universe together with the *Gravitational Shielding* S [§§§§§].

Now, consider a transceiver antenna inside a Gravitational Shielding S. When the gravitational mass of S, m_{gS}, is reduced down to the range of $+0.159m_{iS}$ to $-0.159m_{iS}$, the antenna becomes imaginary, and, together with S, it goes to the imaginary Universe. In these circumstances, the *real* photons radiated from the antenna also become imaginary photons or *virtual* photons. Since the velocity of these photons is infinite, they can reach instantaneously the receiving antenna, *if it is also an imaginary antenna in the imaginary Universe*.

Therefore, we can say that the Gravitational Shielding around the antenna works as a *Gravitational* Transducer [******] converting *real* EM energy into *virtual* EM energy.

In practice, we can encapsulate antennas of transceivers with Aluminum cylinders, as shown in Fig.D2(a). By applying an appropriate ELF electric current through the Al cylinders, in order to put the gravitational masses of the cylinders within the range of $+0.159m_{iCyl}$ to $-0.159m_{iCyl}$, we can transform *real* antennas into *imaginary* antennas, making possible *instantaneously communications* at any distance, including astronomical distances.

Figure D2 (b) shows usual transceivers operating with *imaginary* antennas, i.e., real antennas turned into imaginary antennas. It is important to note that the communications between them occur through the *imaginary* space-time. At the end of transmissions, when the Gravitational Transducers are turned off, the antennas reappear in the *real* space-time, i.e., they become *real* antennas again.

[§§§§§] Similarly, the bodies inside a Gravitational Spacecraft become also imaginaries when the Gravitational Spacecraft becomes imaginary.

[******] A *Transducer* is substance or device that converts input energy of one form into output energy of another.

Imagine now cell phones using antennas with gravitational transducers. There will not be any more need of *cell phone signal transmission stations* because the reach of the *virtual* EM radiation is *infinite* (without *scattering*). The new cell phones will transmit and receive communications directly to and from one another. In addition, since the *virtual* EM radiation does not interact with matter, then there will not be any biological effects, as it happens in the case of usual cell phones.

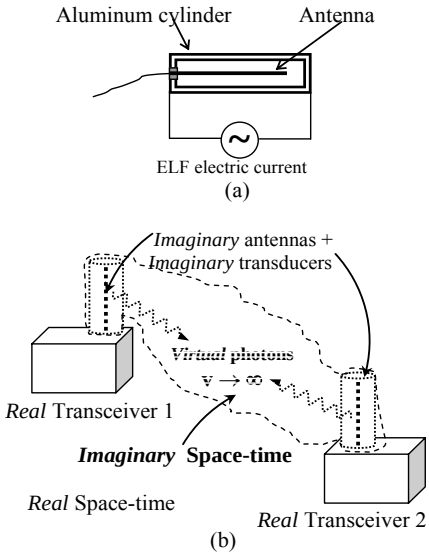

Fig. D2 – (a) Antenna with *Gravitational* Transducer. (b) Transceivers operating with *imaginary* antennas (*instantaneous* communications *at any distance*, including astronomical distances).

Let us now consider the case where a transceiver is *totally* turned into *imaginary* (Fig.D3). In order to convert real antennas into imaginary antennas, we have used the gravitational shielding effect, as we have already seen. Now, it is necessary to put the transceiver *totally* inside a Gravitational Shielding. Then, consider a transceiver X inside the gravitational shielding of a Gravitational Spacecraft. When the spacecraft becomes imaginary, so does the transceiver X. Imagine then, another real transceiver Y with *imaginary* antenna. With their antennas in the imaginary space-time, both transceivers X and Y are able to transmit and receive communications instantaneously between them, by means of *virtual* EM radiation (See Fig. D3(a)). Figure D3(b) shows another possibility: instantaneous communications between two transceivers at *virtual* state.

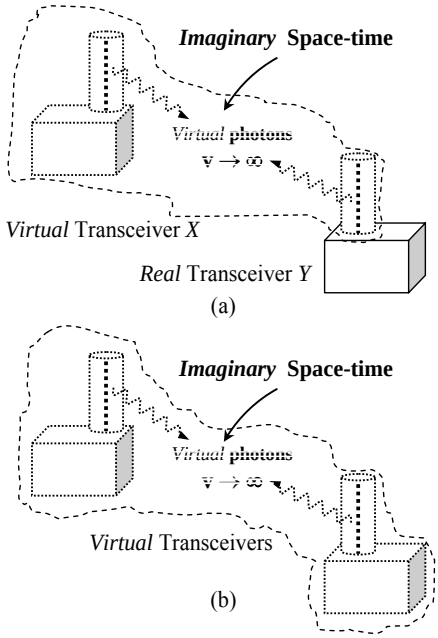

Fig. D3 – (a) Instantaneous communications between the *real* Universe and the *imaginary* Universe.(b) Instantaneous communications between two Virtual Transceivers in the *imaginary* Universe.

References

[1] De Aquino, F.(2010) *Mathematical Foundations of the Relativistic Theory of Quantum Gravity*, Pacific Journal of Science and Technology, **11**(1), June 2010, pp.173-232. Physics/0212033.

[2] De Aquino, F. (2010) *Gravity Control by means of Electromagnetic Field through Gas at Ultra-Low Pressure*, Pacific Journal of Science and Technology, **11**(2) November 2010, pp.178-247, Physics/0701091.

. [3] Isham, C. J. (1975) *Quantum Gravity, in Oxford Symposium,* OUP.

[4] Isham, C.J., (1997) "*Structural Problems Facing Quantum Gravity Theory*'', in M, Francaviglia, G, Longhi, L, Lusanna, and E, Sorace, eds., *Proceedings of the 14th International Conference on General Relativity and Gravitation*, 167-209,(World Scientific, Singapore, 1997).

[5] Mach, E., (1893) *The Science of Mechanics*, London, p.229-38.

[6] Bohm, D. (1951) *Quantum Theory*, Prentice-Hall, N.Y, p.415.

[7] D'Espagnat, B. T*he Question of Quantum Reality*, Scientific American, **241**,128.

[8] Teller, P. *Relational Holism and Quantum Mechanics*, British Journal for the Philosophy of Science, **37**, 71-81.

[9] De Aquino, F. (2008) "*Physical Foundations of Quantum Psychology*", http://htpprints.yorku.ca/archive/00000297

[10] Landau, L. and Lifchitz, E. (1969) *Theorie du Champ*, Ed.MIR, Moscow, Portuguese version (1974) Ed. Hemus, S.Paulo, pp.396-397.

[11] Halliday, D. and Resnick, R. (1968) *Physics,* J. Willey & Sons, Portuguese Version, Ed. USP, p.1118.

[12] Zhan, G.D *et al.* (2003) *Appl. Phys. Lett.* **83,** 1228.

[13] Davidson, K. & Smoot, G. (2008) *Wrinkles in Time*. N. Y: Avon, 158-163.

[14] Silk, Joseph.(1977) *Big Bang*. N.Y, Freeman,299.

[15] Jafelice, L.C. and Opher, R. (1992). *The origin of intergalactic magnetic fields due to extragalactic jets*. RAS. http://adsabs.harvard.edu/cgi-bin/nph-bib query? Bib code = 1992 MNRAS. 257. 135J. Retrieved 2009-06-19.

[16] Wadsley, J., et al. (2002). *The Universe in Hot Gas*. NASA. http://antwrp.gsfc.nasa.gov/apod/ap 020820.html. Retrieved 2009-06-19.

[17] Zhan, G.D *et al.* (2003) *Appl Phys. Lett.* **83,** 1228.

[18] Xianping Lu, Ove Nilsson, Jochen. Fricke, Richard W. Pekala," Thermal and electrical conductivity of monolithic carbon aerogels", *Journal of Applied Physics*, **73**, *2*, 581-584 (Jan 1993).

[19] *Worsley, M.A et al.,* (2010**)** *Synthesis of Graphene Aerogel with High Electrical Conductivity* , *J. Am. Chem. Soc.*, *132* (40), pp 14067–14069.

[20] Bryning, M., Milkie, D., Islam, M., Hough, L., Kikkawa, J. and Yodh, A. (2007), *Carbon Nanotube Aerogels*. AdvancedMaterials,19: 661–664. doi: 10.1002/adma.200601748.

POSSIBILITY OF CONTROL OF THE GRAVITATIONAL MASS BY MEANS OF EXTRA-LOW FREQUENCIES RADIATION

Fran De Aquino*
Physics Department, Maranhao State University, S.Luis/ MA, Brazil.

According to the *weak* form of Einstein's general relativity *equivalence principle*, the gravitational and inertial masses are equivalent. However recent calculations have revealed that they are correlated by an adimensional factor, which is equal to one in absence of radiation only. We have built an experimental system to check this unexpected theoretical result. It verifies the effects of the extra-low frequency (ELF) radiation on the *gravitational mass* of a body. We show that there is a direct correlation between the radiation absorbed by the body and its gravitational mass, independently of the inertial mass.

Introduction

The physical property of mass has two distinct aspects, *gravitational mass* m_g and *inertial mass* m_i . Gravitational mass produces and responds to gravitational fields. It supplies the mass factors in Newton's famous inverse-square law of gravity($F_{12}=Gm_{g1}m_{g2}/r_{12}^2$). Inertial mass is the mass factor in Newton's 2nd Law of Motion ($F=m_i a$**)**. One of the deep mysteries of physics is the correlation between these two aspects of mass. Several experiments[1-6] have been carried out since the century XIX to try to verify the correlation between gravitational mass m_g and inertial mass m_i.

In a recent paper[7] we have shown that the *gravitational mass* and the *inertial mass* are correlated by an adimensional factor, which depends on the incident radiation upon the particle. It was shown that only in the absence of electromagnetic radiation this factor becomes equal to 1 and that, in specific electromagnetic conditions, it can be reduced, nullified or made negative. This means that there is the possibility of control of the gravitational mass by means of the incident radiation.

The general expression of correlation between gravitational mass m_g and inertial mass m_i , is given by

$$m_g = m_i - 2\left\{\sqrt{1+\left\{\frac{U}{m_i c^2}\sqrt{\frac{\varepsilon_r\mu_r}{2}\left(\sqrt{1+(\sigma/\omega\varepsilon)^2}+1\right)}\right\}^2}-1\right\}m_i \quad (1)$$

The electromagnetic characteristics, ε ,μ and σ do not refer to the particle, but to the outside medium around the particle in which the incident radiation is propagating. For an *atom* inside a body , the incident radiation on this atom will be propagating inside the body , and consequently , $\sigma = \sigma_{body}$, $\varepsilon = \varepsilon_{body}$, $\mu = \mu_{body}$. So, if $\omega << \sigma_{body}/\varepsilon_{body}$, equation above reduces to

$$m_g = m_a - 2\left\{\sqrt{1+\left\{\frac{U}{m_a c^2}\sqrt{\frac{c^2\mu_{body}\sigma_{body}}{4\pi f}}\right\}^2}-1\right\}m_a \quad (2)$$

where m_a is the *inertial* mass of the atom .

Thus we see that, *atoms* (or *molecules*)can have their *gravitational masses* strongly reduced by means of extra-low frequency (ELF) radiation.

We have built a system to verify the effects of the ELF radiation on the gravitational mass of a body . In this work we present the experimental set-up and the results obtained.

Experimental

Let us consider the apparatus in figure 1 . The Transformer has the following characteristics:

- Frequency : 60 Hz

* Permanent Address: R.Silva Jardim, 521-centro, 65020-560 S. Luis/MA, Brazil.(E-mail: deaquino@uema.br).

- Power : 11.5kVA
- Number of turns of coil : $n_1 = 12$, $n_2 = 2$
- Coil 1 : copper wire 6 AWG
- Coil 2 : ½ inch diameter copper rod (with insulation paint).
- Core area:502.4cm^2 ;ϕ=10 inch (Steel)
- Maximum input voltage : V_1^{max} = 220 V
- Input impedance : $Z_1 = 4.2\ \Omega$
- Output impedance : $Z_2 < 1\text{m}\ \Omega$ (ELF antenna impedance : 116 mΩ)
- Maximum output voltage with coupled antenna : 34.8V
- Maximum output current with coupled antenna : 300 A

In the system-G the *annealed pure iron* has an electric conductivity $\sigma_i = 1.03\times10^7$S/m, magnetic permeability $\mu_i = 25000\mu_0$ [8],thickness 0.6 mm (to absorb the ELF radiation produced by the antenna).The *iron powder* which encapsulates the ELF antenna has $\sigma_p \approx 10$ S/m ;$\mu_p \approx 75\mu_0$ [9]. The antenna physical length is z_0 = 12 m, see Fig.1c.The power radiated by the antenna can be calculated by the well-known *general* expression, for $z_0 << \lambda$:

$$P = (I_0\,\omega z_0)^2/\ 3\pi\varepsilon v^3\ \{[1+(\sigma/\omega\varepsilon)^2]^{½}+1\} \quad (3)$$

where I_0 is the antenna current amplitude ; $\omega = 2\pi f$; f =60Hz ; $\varepsilon = \varepsilon_p$; $\sigma = \sigma_p$ and v is the wave phase velocity in the *iron powder* (given by Equation1.02 , in reference [1]). The radiation efficiency e = P / P+P_{ohmic} is nearly 100%.

Each atom of the annealed iron toroid absorbs an ELFenergy $U=\eta P_a /f$, where η is a particle-dependent absorption coefficient (the maxima η values occurs, as we know, for the frequencies of the atom's *absorption spectrum*) and P_a is the incident radiation power on the atom ; $P_a=DS_a$ where S_a is the atom's *geometric* cross section and $D=P/S$ the radiation power density on the iron atom (P is the power radiated by the antenna and S is the area of the annealed iron toroid (S = 0.374 m^2,see Fig.1b) . So, we can write :

$$U = \eta S_a(I_0 z_0)^2\omega/3S\varepsilon_i v^3\{[1+(\sigma_i/\omega\varepsilon_i)^2]^{½}+1\} \quad (4)$$

Consequently, according to Eq.(1) , for $\omega << \sigma_i/\varepsilon_i$, the gravitational masses of these iron atoms, under these conditions, will be given by :

$$m_g = m_a - 2\{[1+4.4\times10^{-9}\ I_0^4]^{½}-1\}m_a \quad (5)$$

Equation above shows that the *gravitational masses* (m_g) of the atoms of the annealed pure iron toroid can be *nullified* for I_0 = 129.83A. Above this critical value the gravitational masses becomes negatives (antigravity).

Results and Discussion

Figure 2 presents the results of m_g calculated by means of Eq.5, plotted as a function of current I_0 , for $\mu_i = 25000\mu_0$; $\sigma_i = 1.03\times10^7$ S/m ; $\sigma_p \approx 10$ S/m ; $\mu_p \approx 75\mu_0$; z_0 = 12 m.

The experimental results obtained (see Table1) are plotted on said figure to be compared with those supplied by the theory.

It is important to note that, in practice, when I_0 = 130.01A the gravitational mass of system-G reduces to 5.80kg ; exactly equal to the mass of the *steel toroid* (see fig.1). This occurs due to gravitational mass of the annealed pure iron toroid to become null when I_0 =130.01A (Exactly as predicted by the theory. i.e., the gravitational masses of the atoms of the annealed iron toroid become *null* for I_0 = 129.83A).

Under these circumstances, the toroid doesn't interact gravitationally with the Universe, and consequently , there can be no gravitational interaction between the matter inside the toroid and the rest of the Universe. Therefore, the gravitational mass of system-G reduces to the mass of the *steel toroid* , which is outside the annealed iron toroid.

Conclusion

This experiment (carried out by the author on January 27, 2000)

provides a strong evidence that the general expression of correlation between gravitational mass and inertial mass (Eq.1) is true. So, we can easily conclude that the gravitational forces can be reduced, nullified and inverted by means of electromagnetic radiation .

References

1. Eötvos, R. v. (1890), *Math. Natur. Ber. Ungarn*, **8**,65.
2. Zeeman, P. (1917), *Proc. Ned. Akad. Wet.*, **20**,542.
3. Eötvos, R. v., Pékar, D., Fekete, E. (1922) *Ann. Phys.*, **68**,11.
4. Dicke, R.H. (1963) *Experimental Relativity in "Relativity, Groups and Topology" (Les Houches Lectures)*, p. 185.
5. Roppl, P.G et. al. (1964) *Ann. Phys* (N.Y), **26**,442.
6. Braginskii,V.B, Panov, V.I (1971) *Zh. Eksp. Teor. Fiz*, **61**,873.
7. De Aquino, F.(1999)"Gravitation and Electromagnetism: Correlation and Grand Unification", Los Alamos National Laboratory preprint no.gr-qc/9910036.
8. *Reference Data for Radio Engineers* ,ITT Howard ,W. Sams Co.,1983, p.4-33,Table21,ISB0-672-21218-8.
9. *Standard Handbook for Electrical Engineers*, McGraw-Hill Co, D.G. Fink,H.W.Beaty,1987,p4110,Table 4-50, ISBN 0-07-020975-8 .

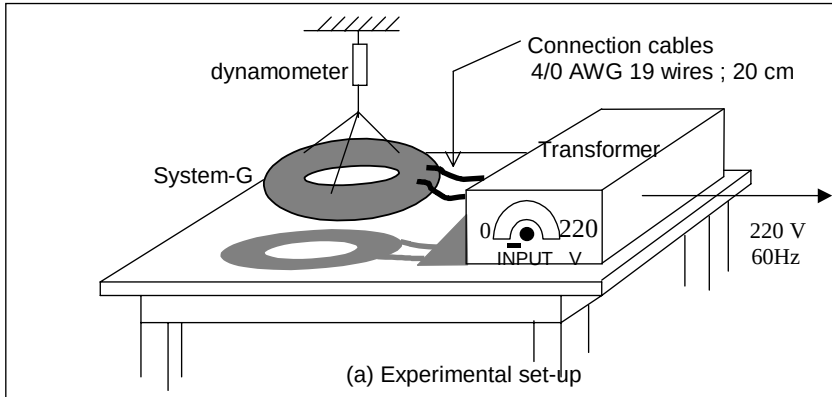

(a) Experimental set-up

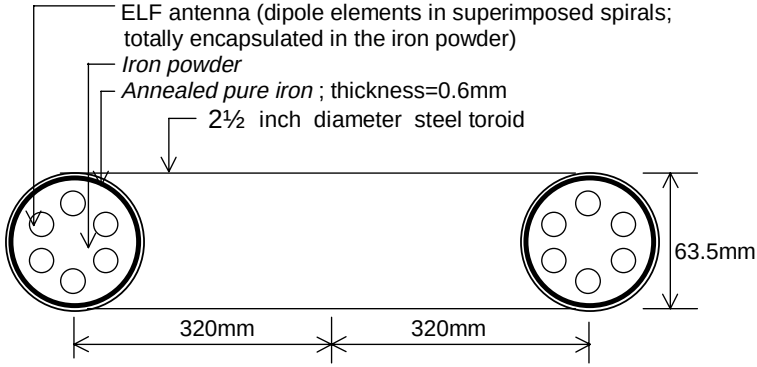

(b) Cross section of the System - G

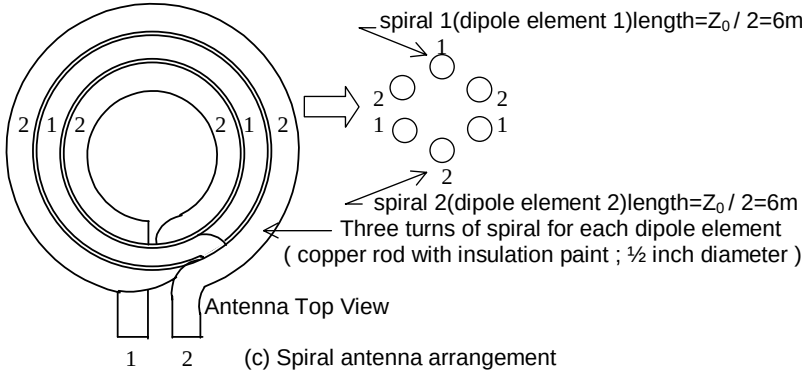

(c) Spiral antenna arrangement

Fig. 1 – Schematic View of the Experimental Apparatus

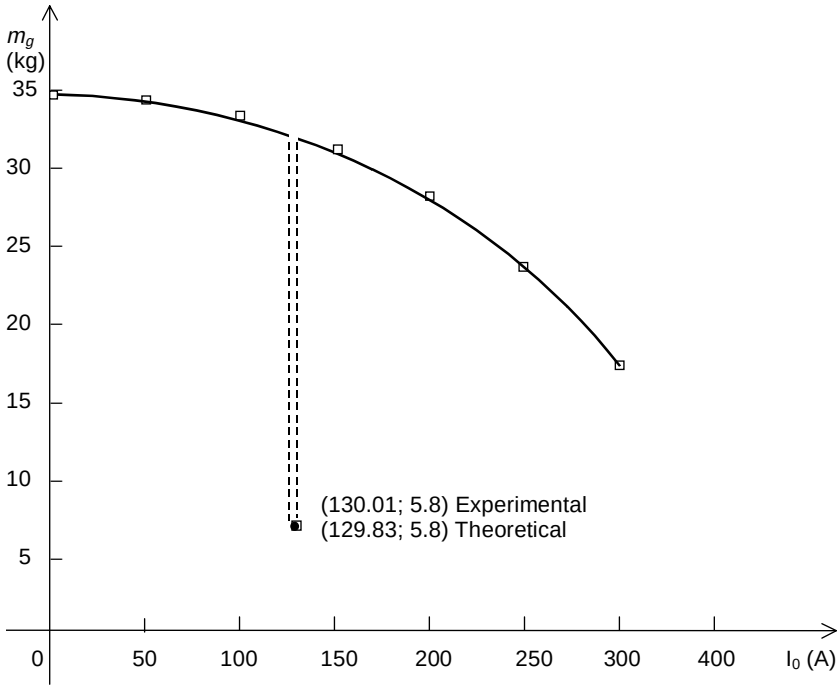

Fig.2 – Comparison between experimental data(□) and theory (solid line).

I_0 (A)	m_g (kg)	
	Theory	Exper.
0	34.85	34.85
50	34.80	34.83
100	34.17	34.26
130.01	5.80	5.80
150	32.14	32.25
200	28.61	28.68
250	23.75	23.80
300	17.68	17.69

Table 1

Correlation Between Gravitational and Inertial Mass: Theory and Experimental Test.

Fran De Aquino
Maranhao State University,
Physics Department,
65058-970 S.Luis/MA, Brazil.

The physical property of mass has two distinct aspects, gravitational mass and inertial mass. The weight of a particle depends on its gravitational mass. According to the weak form of the equivalence principle, the gravitational and inertial masses are equivalent. But, we show here that they are correlated by a dimensionless factor, which can be different of one . The factor depends on the electromagnetic energy absorbed or emitted by the particle and of the index of refraction of the medium around the particle. This theoretical correlation has been experimentally proven by means of a very simple apparatus, presented here.

The *gravitational mass*, m_g , produces and responds to gravitational fields. It supplies the mass factors in Newton's famous inverse-square law of Gravitation $\left(F_{12} = Gm_{g1}m_{g2}/r_{12}^2\right)$. Inertial mass m_i is the mass factor in Newton's 2nd Law of Motion $\left(F = m_i a\right)$.

Several experiments[1-6], have been carried out since Newton to try to establish a correlation between gravitational mass and inertial mass.

Recently J.F.Donoghue and B.R. Holstein[7] have shown that the renormalized mass for temperature $T = 0$ is expressed by $m_r = m + \delta m_0$ where δm_0 is the *temperature-independent mass shift*. In addition, for $T > 0$, mass renormalization leads to the following expressions for inertial and gravitational masses, respectively: $m_i = m + \delta m_0 + \delta m_\beta$; $m_g = m + \delta m_0 - \delta m_\beta$, where δm_β is the *temperature-dependent mass shift* given by $\delta m_\beta = \pi \alpha T^2 / 3m_i$.

This means that a particle's gravitational mass decreases with the increasing temperature and that only in absolute zero $\left(T = 0K\right)$ are gravitational mass and inertial mass equivalent.

The expression of δm_β obtained by Donoghue and Holstein refers solely to thermal radiation. But, δm_β represents also *the inertial mass shift* . It can be seen by repeating the renormalization of the external electromagnetic vertex at finite temperature. On the other hand, it is easy to see that *the inertial mass shift* is related to *inertial Hamiltonian shift* δH . Thus we can obtain the *general expression* of δm_β by means of the *inertial Hamiltonian shift* δH ,i.e.,

$$\delta m_\beta = \frac{\delta H}{c^2} = \frac{c\sqrt{\delta p^2 + m_i^2 c^2} - m_i c^2}{c^2} = \\ = m_i \sqrt{1 + \left(\frac{\delta p}{m_i c}\right)^2} - m_i \qquad [1]$$

where δp is the correspondent particle's *momentum* shift.

Consequently, the general expression of correlation between gravitational and inertial mass can be write in the following form

$$m_g = m_i - 2\delta m_\beta = \left\{1 - 2\left[\sqrt{1 + \left(\frac{\delta p}{m_i c}\right)^2} - 1\right]\right\} m_i \qquad [2]$$

We can look on this change in *momentum* as due to the electromagnetic energy *absorbed* or *emitted* by the particle (absorbed or emitted radiation by the particle and/or *Lorentz's force* upon *charged* particle due to electromagnetic field).

In the case of radiation, according to Quantum Mechanics, we can write

$$\delta p = N\hbar k = N\hbar\omega/(\omega/k) = U/(dz/dt) = \\ = U/v \qquad [3]$$

Where U is *the electromagnetic energy absorbed or emitted by the particle* and v is the velocity of the electromagnetic waves, which can be write as follows

$$v = \frac{c}{\sqrt{\frac{\varepsilon_r\mu_r}{2}\left(\sqrt{1+(\sigma/\omega\varepsilon)^2}+1\right)}} \qquad [4]$$

ε ,μ and σ, are the electromagnetic characteristics of the medium in which the incident (or emitted) radiation is propagating ($\varepsilon = \varepsilon_r\varepsilon_0$ where ε_r is the *relative electric permittivity* and $\varepsilon_0 = 8.854\times10^{-12}F/m$; $\mu = \mu_r\mu_0$ where μ_r is the *relative magnetic permeability* and $\mu_0 = 4\pi\times10^{-7}H/m$). For an *atom* inside a body , the incident(or emitted) radiation on this atom will be propagating inside the body , and consequently , $\sigma = \sigma_{body}$, $\varepsilon = \varepsilon_{body}$, $\mu = \mu_{body}$.

From the Eq.(3) follows that

$$\delta p = \frac{U}{v} = \frac{U}{c}\left(\frac{c}{v}\right) = \frac{U}{c}n_r \qquad [5]$$

where n_r is the *index of refraction*, given by

$$n_r = \frac{c}{v} = \sqrt{\frac{\varepsilon_r\mu_r}{2}\left(\sqrt{1+(\sigma/\omega\varepsilon)^2}+1\right)} \qquad [6]$$

c is the speed in a vacuum and v is the speed in the medium.

By the substitution of Eq.(5) into Eq.(2), we obtain

$$m_g = \left\{1-2\left[\sqrt{1+\left(\frac{U}{m_ic^2}n_r\right)^2}-1\right]\right\}m_i \qquad [7]$$

Recently, L.V. Hau *et al.*,[8] succeeded in reducing the speed of light to 17 m/s by optically inducing a quantum interference in a *Bose-Einstein condensate*. This means an enormous index of refraction ($n_r \approx 10^7$) at ~10^{14}Hz.

Light can be substantially slowed down or frozen completely [9]. If t he speed of light is reduced to <0.1m/s, the Eq.(7) tell us that the gravitational masses of the *atoms* of the Bose-Einstein condensate become *negative*.

If the absorbed (or emitted) radiation is *monochromatic* and has frequency f , we can put $U = nhf$ in Equation(7), where n is the number of incident (or radiated) photons on the particle of mass m_i. Thus we obtain

$$m_g = m_i - 2\left\{\sqrt{1+\left\{\frac{nhf}{m_ic^2}n_r\right\}^2}-1\right\}m \qquad [8]$$

In that case, according to the *Statistical Mechanics*, the calculation of n can be made based on the well-known method of *Distribution Probability* . If all the particles inside the body have the same mass m_i, the result is

$$n = \frac{N}{S}a \qquad [9]$$

where S is the average density of absorbed (or emitted) photons on the body; a is the area of the surface of a particle of mass m_i from the body.

Obviously the power P of the absorbed radiation must be $P = Nhf/\Delta t = Nhf^2$, thus we can write $N = P/hf^2$. Substitution of N into Eq.(9) gives

$$n = \frac{a}{hf^2}\left(\frac{P}{S}\right) = \frac{a}{hf^2}D \qquad [10]$$

where D is the *power density* of the incident(or emitted) radiation. Thus Eq.(8) can be rewritten in the following form:

$$m_g = m_i - 2\left\{\sqrt{1+\left\{\frac{aD}{m_icvf}\right\}^2}-1\right\}m \qquad [11]$$

For $\sigma >> \omega\varepsilon$ Eq.(4) reduces to

$$v = \sqrt{\frac{4\pi f}{\mu\sigma}} \qquad [12]$$

By substitution of Eq.(12) into Eq.(11) we obtain

$$m_g = m_i - 2\left\{\sqrt{1+\left\{\frac{aD}{m_i c}\sqrt{\frac{\mu\sigma}{4\pi f^3}}\right\}^2} - 1\right\}m_i \quad [13]$$

This equation shows clearly that, *atoms* (or *molecules*) can have their *gravitational masses* strongly reduced by means of Extra-Low Frequency (ELF) radiation.

We have built an apparatus to produce ELF radiation (transmitter and antenna) and to check the effects of this radiation upon the gravitational mass of a material surrounding the antenna (see Fig. 1).

The antenna is a *half-wave dipole*, *encapsulated by a iron sphere* (purified iron, 99.95% Fe; $\mu_i = 5{,}000\mu_0$; $\sigma_i = 1.03\times10^7\, S/m$).

The *radiation resistance* of the antenna for a frequency $\omega = 2\pi f$, can be written as follows [10]

$$R_r = \frac{\omega\mu_i\beta_i}{6\pi}\Delta z^2 \quad [14]$$

where Δz is the length of the dipole and

$$\beta_i = \omega\sqrt{\frac{\varepsilon_i\mu_i}{2}\left(\sqrt{1+(\sigma_i/\omega\varepsilon_i)^2}+1\right)} =$$

$$= \frac{\omega}{c}\sqrt{\frac{\varepsilon_{ri}\mu_{ri}}{2}\left(\sqrt{1+(\sigma_i/\omega\varepsilon_i)^2}+1\right)} =$$

$$= \frac{\omega}{c}(n_r) = \frac{\omega}{c}\left(\frac{c}{v_i}\right) = \frac{\omega}{v_i} \quad [15]$$

where v_i is the velocity of the radiation through the iron.

Substituting (15) into (14) gives

$$R_r = \frac{2\pi}{3}\left(\frac{\mu_i}{v_i}\right)(\Delta z f)^2 \quad [16]$$

Note that when the medium surrounding the dipole is *air* and $\omega >> \sigma/\varepsilon$, $\beta \cong \omega\sqrt{\varepsilon_0\mu_0}$, $v \cong c$ and R_r reduces to the well-know expression $R_r \cong (\Delta z\omega)^2/6\pi\varepsilon_0 c^3$.

Here, due to $\sigma_i >> \omega\varepsilon_i$, v_i is given by the Eq.(12). Then Eq.(16) can be rewritten in the following form

$$R_r = (\Delta z)^2\sqrt{\left(\frac{\pi}{9}\right)\sigma_i\mu_i^3 f^3} \quad [17]$$

The *ohmic resistance* of the dipole is [11]

$$R_{ohmic} \cong \frac{\Delta z}{2\pi r_0}R_S \quad [18]$$

where r_0 is the radius of the cross section of the dipole, and R_S is the *surface resistance* ,

$$R_S = \sqrt{\frac{\omega\mu_{dipole}}{2\sigma_{dipole}}} \quad [19]$$

Thus,

$$R_{ohmic} \cong \frac{\Delta z}{r_0}\sqrt{\frac{\mu_{dipole} f}{4\pi\sigma_{dipole}}} \quad [20]$$

Where $\mu_{dipole} = \mu_{copper} \cong \mu_0$ and $\sigma_{dipole} = \sigma_{copper} = 5.8\times10^7\, S/m$.

Let us now consider the apparatus (System H) presented in Fig.1.

The *radiated power* for an *effective* (*rms*) current I is then $P = R_r I^2$ and consequently

$$D = \frac{P}{S} = \frac{(\Delta z I)^2}{S}\sqrt{\left(\frac{\pi}{9}\right)\sigma_i\mu_i^3 f^3} \quad [21]$$

where S is the *effective* area. It can be easily shown that S is the outer area of the iron sphere, i.e., $S = 4\pi r_{outer}^2 = 0.19 m^2$.

The iron surrounding the dipole increases its inductance L. However, for series RLC circuit the *resonance frequency* is $f_r = 1/2\pi\sqrt{LC}$, then when $f = f_r$,

$$X_L - X_C = 2\pi f_r L - \frac{1}{2\pi f_r C} = \sqrt{\frac{L}{C}} - \sqrt{\frac{L}{C}} = 0.$$

Consequently, the impedance of the antenna, Z_{ant}, becomes *purely resistive*, i.e.,

$$Z_{ant} = \sqrt{R_{ant}^2 + (X_L - X_C)^2} = R_{ant} = R_r + R_{ohmic}.$$

For $f = f_r = 9.9 mHz$ the length of the dipole is

$$\Delta z = \lambda/2 = v/2f = \sqrt{\pi/\mu_i\sigma_i f} = 0.070 m = 70 mm.$$

Consequently, the *radiation resistance* R_r, according to Eq.(17), is $R_r = 4.56\mu\Omega$ and the *ohmic resistance*, for $r_0 = 13mm$, according to Eq.(20), is $R_{ohmic} \cong 0.02\mu\Omega$. Thus, $Z_{ant} = R_r + R_{ohmic} = 4.58\mu\Omega$ and the *efficiency* of the antenna is $e = R_r / R_r + R_{ohmic} = 99.56 \quad (99.56\%)$.

The radiation of frequency $f = 9.9mHz$ is totally absorbed by the iron along a critical thickness $\delta = 5z = 5/\sqrt{\pi f \mu_i \sigma_i} \cong 0.11m = 110mm$. Therefore, from the Fig.1 we conclude that the iron sphere will absorb practically all radiation emitted from the dipole. Indeed, the sphere has been designed with this purpose, and in such a manner that all their atoms should be reached by the radiation. In this way, the radiation outside of the sphere is practically negligible.

When the ELF radiation strikes the iron atoms their gravitational masses, m_{gi}, are changed and, according to Eq.(13), become

$$m_{gi} = m_i - 2\left\{\sqrt{1+\frac{\mu_i\sigma_i}{4\pi c^2 f^3}\left(\frac{a_i}{m_i}\right)^2 D^2} - 1\right\}m_i \quad [22]$$

Substitution of (21) into (22) yields

$$m_{gi} = m_i - 2\left\{\sqrt{1+\left(\frac{\mu_i^2\sigma_i}{6cS}\right)^2\left(\frac{a_i}{m_i}\right)^2(\Delta I)^4} - 1\right\}m_i \quad [23]$$

Note that the equation above doesn't depends on f.

Thus, assuming that the radius of the iron atom is $r_{iron} = 1.40\times10^{-10}m$; $a_{iron} = 4\pi r_{iron}^2 = 2.46\times10^{-19}m^2$ and $m_{iron} = 55.85\left(1.66\times10^{-27}kg\right) = 9.27\times10^{-26}kg$ then the Eq.(23) can be rewritten as follows

$$m_{gi} = m_i - 2\left\{\sqrt{1+2.38\times10^{-4}I^4} - 1\right\}m_i \quad [24]$$

The equation above shows that the gravitational masses of the iron atoms can be nullified for $I \cong 8.51A$. Above this critical current, m_{gi} becomes *negative*.

The Table 1 presents the experimental results obtained from the System H for the gravitational mass of the *iron sphere*, $m_{g(iron\ sphere)}$, as a function of the current I, for $m_{iron\ sphere} = 60.50kg$ (*inertial mass* of the iron sphere). The values for $m_{g(iron\ sphere)}$, calculated by means of Eq.(24), are on that Table to be compared with those supplied by the experiment.

REFERENCES

1. Eötvos, R. v. (1890), *Math. Natur. Ber. Ungarn*, **8**,65.
2. Zeeman, P. (1917), *Proc. Ned. Akad. Wet.*, **20**,542.
3. Eötvos, R. v., Pékar, D., Fekete, E. (1922) *Ann. Phys.*, **68**,11.
4. Dicke, R.H. (1963) *Experimental Relativity in "Relativity, Groups and Topology" (Les Houches Lectures)*, p. 185.
5. Roppl, P.G et. al. (1964) *Ann. Phys* (N.Y), **26**,442.
6. Braginskii, V.B, Panov, V.I (1971) *Zh. Eksp. Teor. Fiz*, **61**,873.
7. Donoghue, J.F, Holstein, B.R (1987) *European J. of Physics*, **8**,105.
8. L. V. Hau, S. E. Harris, Z. Dutton, and C. H. Behroozi (1999) *Nature* **397**, 594.
9. M. M. Kash, V. A. Sautenkov, A. S. Zibrov, L. Hollberg, H. Welch, M. D. Lukin, Y. Rostovsev, E. S. Fry, and M. O. Scully, (1999) *Phys. Rev. Lett.* **82**, 5229 ; Z. Dutton, M. Budde, Ch. Slowe, and L. V. Hau, (2001) *Science* 293, 663 ; A. V. Turukhin, V. S. Sudarshanam, M. S. Shahriar, J. A. Musser, B. S. Ham, and P. R. Hemmer, (2002) *Phys. Rev. Lett.* 88, 02360]
10. Stutzman, W.L, Thiele, G.A, *Antenna Theory and Design*. John Wiley & Sons, p.48.
11. Stutzman, W.L, Thiele, G.A, *Antenna Theory and Design*. John Wiley & Sons, p.49.

APPENDIX: A Simple Derivation of the Correlation between Gravitational and Inertial Mass.

In order to obtain the general expression of correlation between m_g and m_i, we will start with the definition of *inertial* Hamiltonian, H_i, and *gravitational* Hamiltonian, H_g, i.e.,

$$H_i = c\sqrt{p_i^2 + m_i^2 c^2} + Q\varphi \qquad [1]$$

$$H_g = c\sqrt{p_g^2 + m_g^2 c^2} + Q\varphi \qquad [2]$$

where m_i and m_g are respectively, the inertial and gravitational *masses at rest* ; p_i is the *inertial momentum* and p_g the *gravitational momentum*; Q is the electric charge and φ is an electromagnetic potential.

A *momentum shift* , δp, on the particle, produces an *inertial Hamiltonian shift*, δH ,given by

$$\delta H = \sqrt{(p_i + \delta p)^2 c^2 + m_i^2 c^4} - \sqrt{p_i^2 c^2 + m_i^2 c^4} \qquad [3]$$

Fundamentally δp is related to *absorption* or *emission* of energy.

In the general case of *absorption* and posterior *emission*, in which the particle acquires a δp at the absorption and another δp at the emission, the *total inertial* Hamiltonian *shift* is

$$\delta H = 2\left(\sqrt{(p_i + \delta p)^2 c^2 + m_i^2 c^4} - \sqrt{p_i^2 c^2 + m_i^2 c^4}\right) \qquad [4]$$

Note that δH is always *positive*.

We now may define the correlation between H_i and H_g as follows

$$H_i = H_g + \delta H \qquad [5]$$

If $\delta H = 0$, $H_i = H_g$, i.e., $m_g = m_i$.

In addition from the Eqs.[1] and [2], we can write:

$$H_i - H_g = \sqrt{p_i^2 c^2 + m_i^2 c^4} - \sqrt{p_g^2 c^2 + m_g^2 c^4} \qquad [6]$$

For a particle at rest, $V = 0$; $p_i = p_g = 0$. Consequently, Eqs.[4] and [6] reduces to

$$\delta H = 2\left(\sqrt{\delta p^2 c^2 + m_i^2 c^4} - m_i c^2\right) \qquad [7]$$

and

$$H_i - H_g = (m_i - m_g)c^2 \qquad [8]$$

Substitution of Eqs[7] and [8] into Eq.[5] yields

$$(m_i - m_g)c^2 = 2\left(\sqrt{\delta p^2 c^2 + m_i^2 c^4} - m_i c^2\right)$$

From this equation we obtain

$$m_g = m_i - 2\left[\sqrt{1 + \left(\frac{\delta p}{m_i c}\right)^2} - 1\right] m_i \qquad [9]$$

This is the general expression of correlation between gravitational and inertial mass.

Note that the term inside the square bracket is always positive. Thus, except for *anti-matter* ($m_i < 0$), the second term on the right hand side of Eq.[9] *is always negative*.

In particular, we can look on the *momentum shift* (δp) as due to absorption or emission of *electromagnetic energy* by the particle (by means of *radiation* and/or by means of *Lorentz's force* upon the *charge* of the particle).

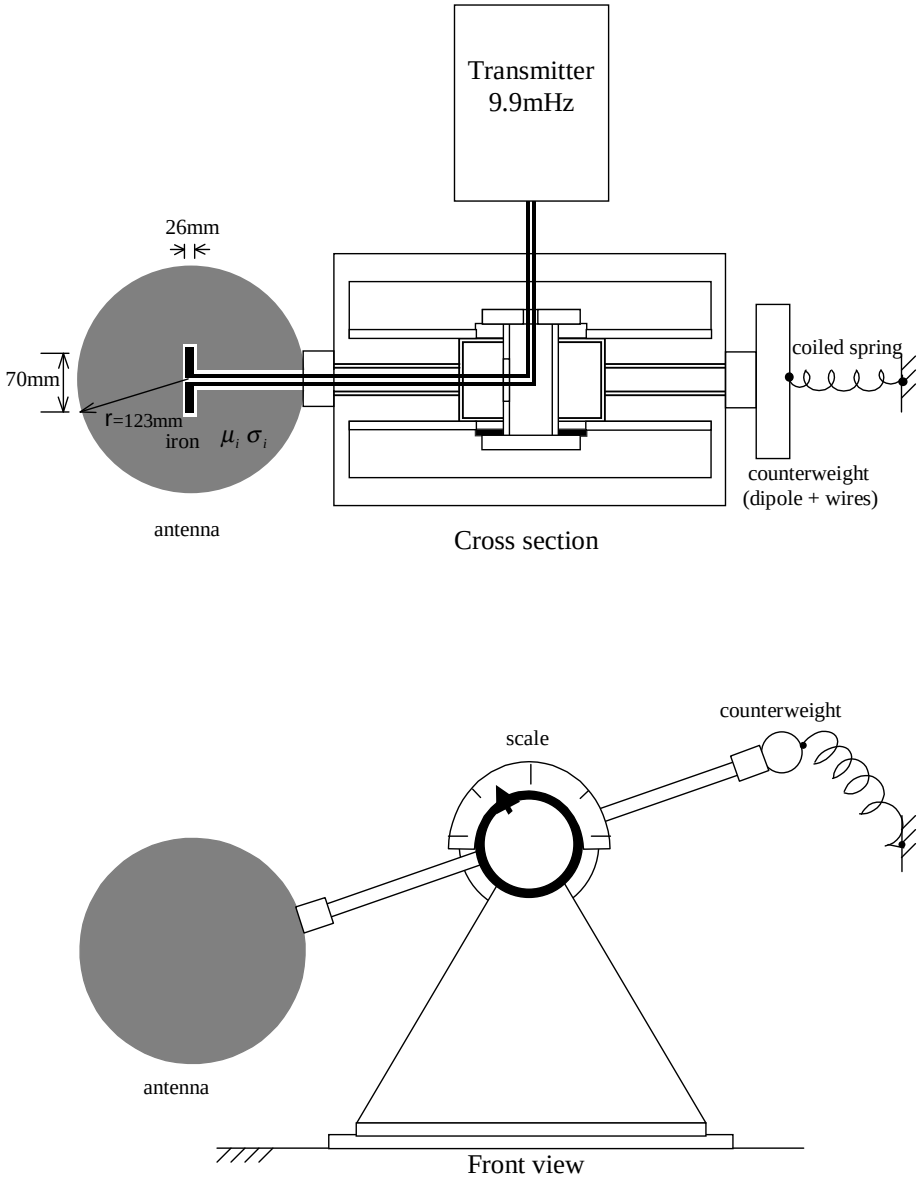

Fig.1 - Schematic diagram of the System H

I (A)	$m_{g(iron\ sphere)}$ (kg)	
	theory	experimental
0.00	60.50	60.5
1.00	60.48	60.(4)
2.00	60.27	60.(3)
3.00	59.34	59.(4)
4.00	56.87	56.(9)
5.00	51.81	51.(9)
6.00	43.09	43.(1)
7.00	29.82	29.(8)
8.00	11.46	11.(5)
8.51	0.0	0.(0)
9.00	-12.16	-12.(1)
10.00	-40.95	-40.(9)

Table 1

Note: The *inertial mass* of the iron sphere is $m_{iron\ sphere} = 60.50kg$

Gravity Control by means of Modified Electromagnetic Radiation

Fran De Aquino
Maranhao State University, Physics Department, S.Luis/MA, Brazil.

Here a new way for gravity control is proposed that uses electromagnetic radiation modified to have a smaller wavelength. It is known that when the velocity of a radiation is reduced its wavelength is also reduced. There are several ways to strongly reduce the velocity of an electromagnetic radiation. Here, it is shown that such a reduction can be done simply by making the radiation cross a conductive foil.

Key words: Modified theories of gravity, Experimental studies of gravity, Electromagnetic wave propagation.
PACS: 04.50.Kd , 04.80.-y, 41.20.Jb, 75.70.-i.

It was shown that the *gravitational mass* m_g and *inertial mass* m_i are correlated by means of the following factor [1]:

$$\frac{m_g}{m_{i0}} = \left\{1 - 2\left[\sqrt{1+\left(\frac{\Delta p}{m_{i0}c}\right)^2} - 1\right]\right\} \qquad (1)$$

where m_{i0} is the *rest* inertial mass of the particle and Δp is the variation in the particle's *kinetic momentum*; c is the speed of light.

When Δp is produced by the absorption of a photon with wavelength λ, it is expressed by $\Delta p = h/\lambda$. In this case, Eq. (1) becomes

$$\frac{m_g}{m_{i0}} = \left\{1 - 2\left[\sqrt{1+\left(\frac{h/m_{i0}c}{\lambda}\right)^2} - 1\right]\right\}$$

$$= \left\{1 - 2\left[\sqrt{1+\left(\frac{\lambda_0}{\lambda}\right)^2} - 1\right]\right\} \qquad (2)$$

where $\lambda_0 = h/m_{i0}c$ is the *De Broglie wavelength* for the particle with *rest* inertial mass m_{i0}.

It is easily seen that m_g cannot be strongly reduced simply by using electromagnetic waves with wavelength λ because λ_0 is very smaller than $10^{-10}\,m$. However, it is known that the wavelength of a radiation can be strongly reduced simply by strongly reducing its velocity.

There are several ways to reduce the velocity of an electromagnetic radiation. For example, by making light cross an *ultra cold atomic gas*, it is possible to reduce its velocity down to *17m/s* [2-7]. Here, it is shown that the velocity of an electromagnetic radiation can be strongly reduced simply by making the radiation cross a conductive foil.

From Electrodynamics we know that when an electromagnetic wave with frequency f and velocity c incides on a material with relative permittivity ε_r, relative magnetic permeability μ_r and electrical conductivity σ, its *velocity is reduced* to $v = c/n_r$ where n_r is the index of refraction of the material, given by [8]

$$n_r = \frac{c}{v} = \sqrt{\frac{\varepsilon_r \mu_r}{2}\left(\sqrt{1+(\sigma/\omega\varepsilon)^2}+1\right)} \qquad (3)$$

If $\sigma >> \omega\varepsilon$, $\omega = 2\pi f$, the Eq. (3) reduces to

$$n_r = \sqrt{\frac{\mu_r \sigma}{4\pi\varepsilon_0 f}} \qquad (4)$$

Thus, the wavelength of the incident radiation becomes

$$\lambda_{\text{mod}} = \frac{v}{f} = \frac{c/f}{n_r} = \frac{\lambda}{n_r} = \sqrt{\frac{4\pi}{\mu f \sigma}} \qquad (5)$$

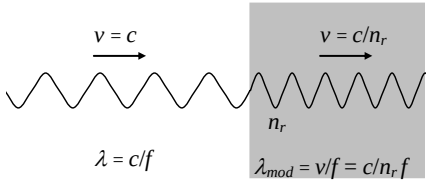

Fig. 1 – *Modified Electromagnetic Wave*. The wavelength of the electromagnetic wave can be strongly reduced, but its frequency remains the same.

Now consider a $1GHz$ ($\lambda \cong 0.3m$) radiation incident on *Aluminum foil* with $\sigma = 3.82\times10^7\,S/m$ and thickness $\xi = 10.5\mu m$. According to Eq. (5), the *modified wavelength* is

$$\lambda_{\mathrm{mod}} = \sqrt{\frac{4\pi}{\mu f \sigma}} = 1.6\times10^{-5} m \qquad (6)$$

Consequently, the wavelength of the $1GHz$ radiation *inside the foil* will be $\lambda_{\mathrm{mod}} = 1.6\times10^{-5} m$ and not $\lambda \cong 0.3m$.

It is known that a radiation with frequency *f*, propagating through a material with electromagnetic characteristics ε, μ and σ, has the amplitudes of its waves decreased in e^{-1}=0.37 (37%), when it passes through a distance *z*, given by

$$z = \frac{1}{\omega\sqrt{\tfrac{1}{2}\varepsilon\mu\left(\sqrt{1+(\sigma/\omega\varepsilon)^2}-1\right)}} \qquad (7)$$

The radiation is totally absorbed at a distance $\delta \cong 5z$ [8].

In the case of the $1GHz$ radiation propagating through the Aluminum foil Eq. (7), gives

$$z = \frac{1}{\sqrt{\pi\mu\sigma f}} = 2.57\times10^{-6} = 2.57\mu m \qquad (8)$$

Since the thickness of the Aluminum foil is $\xi = 10.5\mu m$ then, we can conclude that, practically all the incident $1GHz$ radiation is absorbed by the foil.

If the foil contains n atoms/m^3, then the number of atoms per area unit is $n\xi$. Thus, if the electromagnetic radiation with frequency f incides on an area S of the foil it reaches $nS\xi$ atoms. If it incides on the total area of the foil, S_f, then the total number of atoms reached by the radiation is $N = nS_f\xi$. The number of atoms per unit of volume, n, is given by

$$n = \frac{N_0\rho}{A} \qquad (9)$$

where $N_0 = 6.02\times10^{26} atoms/kmole$ is the Avogadro's number ; ρ is the matter density of the foil (in kg/m^3) and A is the atomic mass. In the case of the *Aluminum* $\left(\rho = 2700kg/m^3, A = 26.98kmole\right)$ the result is

$$n_{Al} = 6.02\times10^{28} atoms/m^3 \qquad (10)$$

The *total number of photons* inciding on the foil is $n_{total\ photons} = P/hf^2$, where P is the power of the radiation flux incident on the foil.

When an electromagnetic wave incides on the Aluminum foil, it strikes on N_f front atoms, where $N_f \cong \left(nS_f\right)\phi_{atom}$. Thus, the wave incides effectively on an area $S = N_f S_a$, where $S_a = \frac{1}{4}\pi\phi^2_{atom}$ is the cross section area of one Aluminum atom. After these collisions, it carries out $n_{collisions}$ with the other atoms of the foil (See Fig.2).

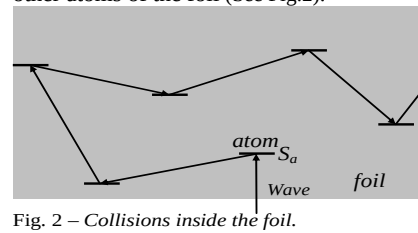

Fig. 2 – *Collisions inside the foil.*

Thus, the total number of collisions in the volume $S\xi$ is

$$N_{collisions} = N_f + n_{collisions} = nS\phi_{atom} + \left(nS\xi - nS\phi_{atom}\right) = nS\xi \qquad (11)$$

The power density, D, of the radiation on the foil can be expressed by

$$D = \frac{P}{S} = \frac{P}{N_f S_a} \qquad (12)$$

The same power density as a function of the power P_0 radiated from the antenna, is given by

$$D = \frac{P_0}{4\pi r^2} \qquad (13)$$

where r is the distance between the antenna and the foil. Comparing equations (12) and (13), we get

$$P = \left(\frac{N_f S_a}{4\pi r^2}\right)P_0 \qquad (14)$$

We can express the *total mean number of collisions in each atom*, n_1, by means of the following equation

$$n_1 = \frac{n_{total\ \ photons}\, N_{collisions}}{N} \qquad (15)$$

Since in each collision is transferred a *momentum* h/λ to the atom, then the *total momentum* transferred to the foil will be $\Delta p = \left(n_1 N\right)h/\lambda$. Therefore, in accordance with Eq. (1), we can write that

$$\frac{m_g}{m_{i0}}=\left\{1-2\left[\sqrt{1+\left[\left(n_1 N\right)\frac{\lambda_0}{\lambda}\right]^2}-1\right]\right\}=$$

$$=\left\{1-2\left[\sqrt{1+\left[n_{total\ photons}N_{collisions}\frac{\lambda_0}{\lambda}\right]^2}-1\right]\right\} \quad (16)$$

Since Eq. (11) gives $N_{collisions}=nS\xi$, we get

$$n_{total\ \ photons}N_{collisions}=\left(\frac{P}{hf^2}\right)\left(nS\xi\right) \quad (17)$$

Substitution of Eq. (17) into Eq. (16) yields

$$\frac{m_g}{m_{i0}}=\left\{1-2\left[\sqrt{1+\left[\left(\frac{P}{hf^2}\right)\left(nS\xi\right)\frac{\lambda_0}{\lambda}\right]^2}-1\right]\right\} \quad (18)$$

Substitution of Eq. (14) into Eq. (18) gives

$$\frac{m_g}{m_{i0}}=\left\{1-2\left[\sqrt{1+\left[\left(\frac{N_f S_a P_0}{4\pi\ r^2 f^2}\right)\left(\frac{nS\xi}{m_{i0}c}\right)\frac{1}{\lambda}\right]^2}-1\right]\right\} \quad (19)$$

Substitution of $N_f\cong\left(nS_f\right)\phi_{atom}$ and $S=N_f S_a$ into Eq. (19) it reduces to

$$\frac{m_g}{m_{i0}}=\left\{1-2\left[\sqrt{1+\left[\left(\frac{n^3 S_f^2 S_a^2\phi_{atom}^2 P_0\xi}{4\pi\ r^2 m_{i0}cf^2}\right)\frac{1}{\lambda}\right]^2}-1\right]\right\} \quad (20)$$

In the case of a 20cm square Aluminum foil, with thickness $\xi=10.5\mu m$, we get $m_{i0}=1.1\times10^{-3}kg$, $S_f=4\times10^{-2}m^2$, $\phi_{atom}\cong10^{-10}m^2$ $S_a\cong10^{-20}m^2$, $n=n_{Al}=6.02\times10^{28}\ atoms/m^3$, Substitution of these values into Eq. (20), gives

$$\frac{m_{g(Al)}}{m_{i0(Al)}}=\left\{1-2\left[\sqrt{1+\left[\left(8.84\times10^{11}\frac{P_0}{r^2 f^2}\right)\frac{1}{\lambda}\right]^2}-1\right]\right\} \quad (21)$$

Thus, if the Aluminum foil is at a distance $r=1m$ from the antenna, and the power radiated from the antenna is $P_0=32W$, and the frequency of the radiation is $f=1GHz$ then Eq.(21) gives

$$\frac{m_{g(Al)}}{m_{i0(Al)}}=\left\{1-2\left[\sqrt{1+\left[\frac{2.8\times10^{-5}}{\lambda}\right]^2}-1\right]\right\} \quad (22)$$

In the case of the Aluminum foil and 1*Ghz* radiation, Eq. (6) shows that $\lambda_{\mathrm{mod}}=1.6\times10^{-5}m$. Thus, by substitution of λ by λ_{mod} into Eq. (22), we get the following expression

$$\frac{m_{g(Al)}}{m_{i0(Al)}}\cong-1 \quad (23)$$

Since $\vec{P}=m_g\vec{g}$ then the result is

$$\vec{P}_{(Al)}=m_{g(Al)}\vec{g}\cong-m_{i0(Al)}\vec{g} \quad (24)$$

This means that, in the mentioned conditions, *the weight force* of the Aluminum foil *is inverted*.

It was shown [1] that there is an additional effect of *Gravitational Shielding* produced by a substance whose gravitational mass was reduced or made negative. This effect shows that just *above the substance* the gravity acceleration g_1 will be reduced at the same ratio $\chi_1=m_g/m_{i0}$, i.e., $g_1=\chi_1 g$, (g is the gravity acceleration *bellow* the substance). This means that above the Aluminum foil the gravity acceleration will be modified according to the following expression

$$g_1=\chi_1 g=\left(\frac{m_{g(Al)}}{m_{i0(Al)}}\right)g \quad (25)$$

where the factor $\chi_1=m_{g(Al)}/m_{i0(Al)}$ will be given Eq. (21).

In order to check the theory presented here, we propose the experimental set-up shown in Fig. 3. The distance between the Aluminum foil and the antenna is $r=1m$. The maximum output power of the 1*GHz* transmitter is 32W CW. A 10g body is placed above Aluminum foil , in order to check the *Gravitational Shielding Effect*. The distance between the Aluminum foil and the 10g body is approximately 10 *cm*. The alternative device to measure the weight variations of the foil and the body (including the *negative* values) uses two balances (200g / 0.01g) as shown in Fig .3.

In order to check the effect of a *second* Gravitational Shielding above the first one(Aluminum foil), we can remove the 10g body, putting in its place a second Aluminum foil, with the same characteristics of the first one. The 10g body can be then placed at a

distance of 10cm above of the second Aluminum foil. Obviously, it must be connected to a third balance.

As shown in a previous paper [9] the gravity above the second Gravitational Shielding, in the case of $\chi_2 = \chi_1$, is given by

$$g_2 = \chi_2 g_1 = \chi_1^2 g \qquad (26)$$

If a third Aluminum foil is placed above the second one, then the gravity above this foil is $g_3 = \chi_3 g_2 = \chi_3 \chi_2 \chi_1 g = \chi_1^3 g$, and so on.

In practice, *Multiple Gravitational Shieldings* can be constructed by inserting N several *parallel* Aluminum foils inside the dielectric of a parallel plate capacitor (See Fig. 4). In this case, the resultant capacity of the capacitor becomes $C_r = C/N = \varepsilon_r \varepsilon_0 S_f / Nd$, where S_f is the area of the Aluminum foils and d the distance between them; ε_r is the relative permeability of the dielectric. By applying a voltage V_{rms} on the plates of the capacitor a current i_{rms} is produced through the Aluminum foils. It is expressed by $i_{rms} = V_{rms} / X_C = 2\pi f C_r V_{rms}$.

Since $j_{rms} = \sigma E_{rms}$ and $j_{rms} = i_{rms} / S_f$ we get $E_{rms} = i_{rms} / S_f \sigma$, which is the oscillating electric field through the Aluminum foils. By substituting this expression into Eq. (20), and considering that $\lambda = \lambda_{\text{mod}} = (4\pi / \mu f \sigma)^{\frac{1}{2}}$ (Eq.6) and $D = P_0 / 4\pi r^2 = n_r E_{rms}^2 / 2\mu_r \mu_0 c$, where $n_r = (\mu_r \sigma / 4\pi \varepsilon_0 f)^{\frac{1}{2}}$ (Eq. 4), we obtain:

$$\chi = \left\{1 - 2\left[\sqrt{1 + \frac{n_{Al}^6 S_a^4 \phi_{atom}^4 i_{rms}^4}{64\pi^2 \rho_{Al}^2 c^2 S_f^2 \sigma_{Al}^2 f^4}} - 1\right]\right\} \qquad (27)$$

Since

$i_{rms} = V_{rms} / X_C = 2\pi f C_r V_{rms} = 2\pi f (\varepsilon_r \varepsilon_0 S_f / Nd) V_{rms}$

Then

$$\frac{i_{rms}}{f} = 2\pi (\varepsilon_r \varepsilon_0 S_f / Nd) V_{rms} \qquad (28)$$

Substitution of this equation into Eq. (27) gives

$$\chi = \left\{1 - 2\left[\sqrt{1 + \frac{\pi^2 n_{Al}^6 S_a^4 \phi_{atom}^4 \varepsilon_r^4 \varepsilon_0^4 S_f^2 V_{rms}^4}{4\rho_{Al}^2 c^2 \sigma_{Al}^2 N^4 d^4}} - 1\right]\right\} \qquad (29)$$

Substitution of the known value of $n_{Al} = 6.02 \times 10^{28} atoms/m^3$, $\phi_{atom} \cong 1 \times 10^{-10} m$, $S_a = \frac{1}{2}\left[4\pi(\phi_{atom}/2)^2\right] = \frac{1}{2}\pi\phi_{atom}^2 \cong 1 \times 10^{-20} m^2$, $\varepsilon_r = 2.1$ (Teflon $24 KV/mm$, Short Time, 1.6 mm [10]), $\rho_{Al} = 2700 kg.m^{-3}$, we get

$$\chi = \left\{1 - 2\left[\sqrt{1 + 1.4 \times 10^{-29} \frac{S_f^2}{N^4}\left(\frac{V_{rms}}{d}\right)^4} - 1\right]\right\} \qquad (30)$$

Note that, based on the equation above, it is possible to create a device for moving very heavy loads such as large monoliths, for example.

Imagine a large monolith on the Earth's surface. If we place below the monolith some sets with *Multiple Gravitational Shieldings* (See Fig.4), the value of the gravity acceleration above each set of Gravitational Shieldings becomes

$$g_R = \chi^\eta g \qquad (31)$$

where η is the number of Gravitational Shieldings in each set.

Since we must have $V_{rms}/d < 24 KV/mm$ (dielectric strength of Teflon) [10] then, for $d = 1.6mm \rightarrow V_{rms} < 38.4 KV$. For $V_{rms} = 37 KV$, $d = 1.6mm$, $S_f = 2.7 m^2$, $N = 2$ and $\eta = 3$ Eq. (30) gives $\chi = -0.36$ and Eq. (31) shows that $g_R = \chi^3 g \cong -0.46 m/s^2$. The sign (-) shows that *the gravity acceleration above the six sets of Gravitational Shieldings* becomes *repulsive* in respect to the Earth. Thus, by controlling the value of χ it is possible to make the total mass of the monolith slightly negative in order to the monolith can float and, in this way, it can be displaced and carried to anywhere with ease.

Considering the dielectric strength of known dielectrics, we can write that $(V_{rms}/d)_{\max} < 200 KV/mm$. Thus, for a single capacitor $(N = 1)$ Eq. (30) gives

$$\chi = \left\{1 - 2\left[\sqrt{1 + \left(<< 2.2 \times 10^4 S_f^2\right)} - 1\right]\right\} \qquad (31)$$

The Gravitational Shielding effect becomes negligible for $\chi < 0.01$ (variation smaller than 1% in the gravitational mass). Thus, considering Eq. (31), we can conclude that *the Gravitational Shielding effect becomes significant only for* $S_f >> 10^{-2} m^2$. Possibly this is why it was not yet detected.

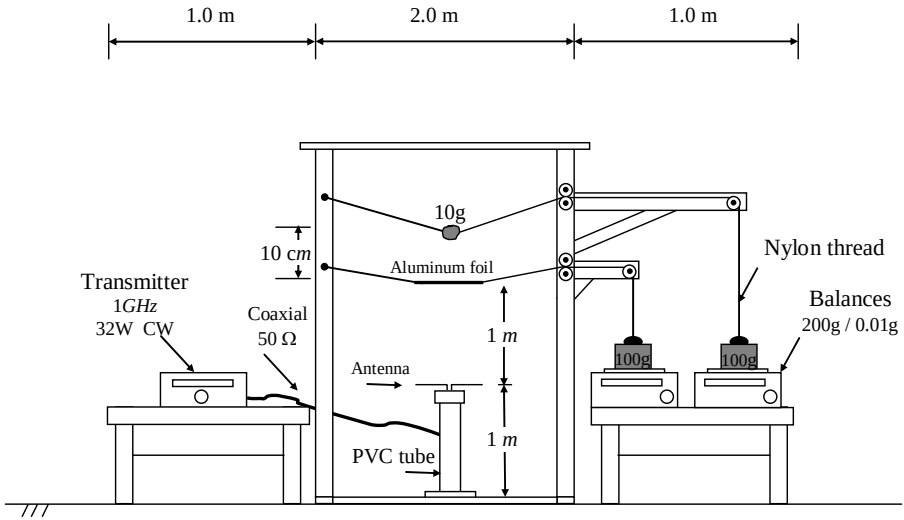

Fig. 3 – Experimental Set-up

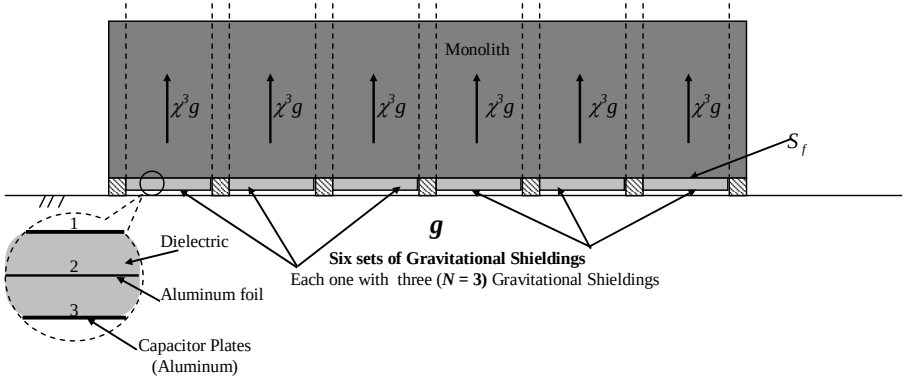

(a)

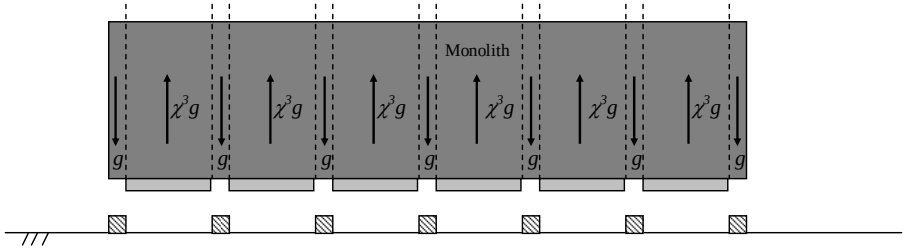

(b)

Fig. 4 – *System with six sets of Gravitational Shieldings for moving very heavy loads.* For $V_{rms} = 37KV$, $d = 1.6mm$, $S_f = 2.7m^2$, $N = 2$ and $\eta = 3$ Eq. (30) gives $\chi = -0.36$ and Eq. (31) shows that $g_R = \chi^3 g \cong -0.46 m/s^2$. The sign (-) shows that *the gravity acceleration above the six sets of Gravitational Shieldings* becomes *repulsive* in respect to the Earth. Thus, by controlling the value of χ it is possible to make the total mass of the monolith slightly negative in order to the monolith can float and, in this way, it can be displaced and carried to anywhere with ease.

References

[1] De Aquino, F. (2010) *Mathematical Foundations of the Relativistic Theory of Quantum Gravity*, Pacific Journal of Science and Technology, **11** (1), pp. 173-232.

[2] Hau, L.V., et al., (1999) Nature, 397, 594-598.

[3] Kash, M. M. et al., (1999) Phys. Rev. Lett. 82, 5229.

[4] Budiker, D. et al., (1999) Phys. Rev. Lett. 83, 1767.

[5] Liu, Ch. et al., (2001) Nature 409, 490.

[6] Dutton, Z., et al., (2001) Science 293, 663.

[7] Turukhin, A. V., et al., (2002) Phys. Rev. Lett. 88, 023602

[8] Quevedo, C. P. (1977) *Eletromagnetismo*, McGraw-Hill, p. 270.

[9] De Aquino, F. (2010) *Gravity Control by means of Electromagnetic Field through Gas at Ultra-Low Pressure*, Pacific Journal of Science and Technology, **11**(2) November 2010, pp.178-247.

[10] Teflon® PTFE, *Properties Handbook*, Du Pont, (7/96) 220313D, USA.

Gravity Control produced by a Thermoionic Current through the Air at Very Low Pressure

Fran De Aquino

Maranhao State University, Physics Department, S.Luis/MA, Brazil.

It was observed that samples hung above a thermoionic current exhibit a weight decrease directly proportional to the intensity of the current. The observed phenomenon appears to be absolutely new and unprecedented in the literature and can not be understood in the framework of the general relativity. It is pointed out the possibility that this unexpected effect is connected with a possible correlation between gravity and electromagnetism.

Key words: Gravity, Gravity Control, Gravitational Motor, Conversion of Gravitational Energy.
PACs: 04.80.-y, 04.80.Cc, 07.30.-t

I. INTRODUCTION

It will be described an experiment in which there has been observed a *strong* decrease in the weight of samples hung above a thermoionic current produced inside a vacuum chamber. The percentage of weight decrease is the same for samples of different masses and chemical compositions. The effect does not seem to diminish with increases in elevation above the current.

This unexpected phenomenon appears to be unprecedented in the literature. On the other hand, the experiment is simple of being performed, and can be easily replicated.

II. EXPERIMENTAL

1. General description of the experimental set-up.

A Fe sample (iron tube with 1.103kg; outer diameter = 100mm; inner diameter = 80mm; height = 50mm) was placed inside a vacuum chamber (at 0.001militorr) and above the oscillating thermoionic current $(f = 60Hz)$ produced by the electrons flow from the cathode to plate as shown in Fig.1. The distance between the cathode and the plate is 10mm (exactly the thickness of the iron tube above the current). The area of the plate is

$$S_{plate} = 2\pi\ bl = \\ = 2\pi(0.050m)(0.030m) = 9.42\times10^{-3}m^2$$

The area of the cathode is

$$S_{cathode} = 2\pi\ al = \\ = 2\pi(0.040m)(0.030m) = 7.56\times10^{-3}m^2$$

Therefore the average area is $S = 8.48\times10^{-3}m^2$.

The cathode, the filament and the plate are made of *tungsten*.

Two piezoelectric sensors for force (S1,S2) are placed as shown in Fig.1, in order to measure the weight of the sample (tube) during the flow of thermoionic current. When the thermoionic current is null the sensor S1 shows the normal weight of the sample. Note that there is a central disk inside the tube to support the sample. Above this disk (very close to the disk) it is the sensor S2. The function of the sensor S2 is to measure the weight of the

sample, in case this weight becomes negative (inversion).

2. Conductivity Measurements.

Atmospheric air conductivity is proportional to both the atmospheric ion concentration η, and the average mobility μ of the air ion population. Molecular ions with μ > 0.5 cm2V-1s-1 are conventionally defined as "small ions" [1]. The unipolar air conductivity σ_{air} can be written as

$$\sigma_{air} = e \int_{0.5cm^2V^{-1}s^{-1}}^{\infty} \eta d\mu \qquad (1)$$

where e is the charge of the electron. Typical surface values of atmospheric air conductivity are $2-100\times10^{-15}\, S.m^{-1}$ [2,3].

The air conductivity between the cathode and the plate is much greater than these values due to the large concentration of free electrons. It can be evaluated by comparing the Gauss' law $(\phi_E = ES = q/\varepsilon_0)$ with $J = \sigma E$, i.e.,

$$J = \frac{i}{S} = \sigma \frac{q}{S\varepsilon_0} = \sigma \frac{(CV)}{S\varepsilon_0} \qquad (2)$$

hence

$$\sigma_{air} = \frac{\varepsilon_0 i}{CV} \qquad (3)$$

where V is the voltage from the anode (plate) to cathode and C is the capacitance of the cylindrical capacitor (cathode/plate) given by

$$C = \frac{2\pi\varepsilon_0 l}{\boldsymbol{ln}(b/a)} \qquad (4)$$

where a and b are the radii of the outer and central electrodes; l is the height of the electrodes(cathode and plate).

Since the Langmuir-Child law states that the *thermoionic current* density is given by

$$J = \frac{4}{9}\varepsilon_0\sqrt{\frac{2e}{m_e}}\frac{V^{\frac{3}{2}}}{d^2} = \alpha\frac{V^{\frac{3}{2}}}{d^2} = 2.33\times10^{-6}\frac{V^{\frac{3}{2}}}{d^2} \qquad (5)$$

where α is the called *Child's constant*.

Then Eq.(3) gives

$$\sigma_{air} = \frac{\varepsilon_0}{CV}(JS) = \left[\frac{\alpha S\, \boldsymbol{ln}(b/a)}{2\pi\, d^2 l}\right]V^{\frac{1}{2}} \qquad (6)$$

As shown in Fig.1, $b = 50mm$; $a = 40mm$ and $l = 30mm$; $S = 8.48\times10^{-3}m^2$. Thus Eq. (6) gives

$$\sigma_{air} = 2.34\times10^{-4}V^{\frac{1}{2}} \qquad (7)$$

3. Pressure, Temperature and Mass Density of the air.

The chamber was sealed and evacuated to about 0.001millitorr using a vacuum pump system (TP-70-2DR oil-free system; wide range vacuum gauge: atmosphere to 10^{-8}torr).

The cathode temperature reach ~2000K at this temperature and 0.001millitorr, the density of the air between the cathode and plate is

$$\rho_{air} \cong 3.1\times10^{-10}\, Kg.m^{-3} \qquad (8)$$

III. RESULTS

We have started with voltage $V_{rms} = 100V$ at $60Hz$. Next, the voltage was progressively increased to $200V$, $300V$, $400V$ and $500V$. Table1 presents the weight behavior of the sample measured by the sensors S1 and S2.

IV. DISCUSSION

The weight behavior of our samples shows strong variations, which apparently can be explained as due to the *thermoionic current*, which flows from the cathode to plate. When this current is removed the effects disappear.

In a previous work [4] we have shown that when an alternating electric current passes through a substance its *gravitational mass* is reduced in accordance with the following expression

$$m_g = \left\{1-2\left[\sqrt{1+\left(i^4\mu/64\pi^3c^2\rho^2S^4f^3\sigma\right)}-1\right]\right\}m_i \quad (9)$$

In this equation i refers to the instantaneous electric current[†] ; $\mu = \mu_r\mu_0$ is the magnetic permeability of the substance; c is the speed of light; ρ , S and σ are respectively the density (kg/m^3), the area of the cross section (m^2) and the electric conductivity (S/m) of the substance; m_i is the *inertial mass* and f the frequency of the electric current (Hz).

It was also shown that there is an additional effect of *gravitational shielding* produced by the substance under these conditions. Above the substance the gravity acceleration g' is reduced at the same ratio $\chi = m_g/m_i$, i.e., $g' = \chi g$.

If the substance is the *air at very low pressure* such as the air between the cathode and the plate of vacuum chamber presented in Fig.1, for example with the following characteristics: relative *magnetic permeability*= $\mu_r \cong 1$; electrical *conductivity* = $\sigma_{air} = 2.34\times10^{-4}V^{\frac{1}{2}}$; *density*= $\rho_{air} \cong 3.1\times10^{-10} kg.m^{-3}$ at 0.001millitorr and ~2000K. Then for $f = 60Hz$ and (9) gives

$$m_{g(air)} = \left\{1-2\left[\sqrt{1+4.26\times10^{-16}V_{max}^{5.5}}-1\right]\right\}m_{i(air)} \quad (10)$$

Therefore, due to the *gravitational shielding effect* produced by the decreasing of $m_{g(air)}$, the gravity acceleration *above* the air between the cathode and the plate will be given by

$$g' = \chi g = \frac{m_{g(air)}}{m_{i(air)}}g = \\ = \left\{1-2\left[\sqrt{1+4.26\times10^{-16}V_{max}^{5.5}}-1\right]\right\}g$$

Consequently, the weight of the sample, P_s , will be given by

$$P_s = m_{gs}g' = m_{is}g' \quad (11)$$

In the case of the Fe sample: $m_{is} = 1.103Kg$. The weight of the sample, measured during the increase of voltage is presented on Table 1. The theoretical values, calculated by means of (10), are also on Table 1 to be compared with those supplied by the experiment.

Afterwards, the iron tube was replaced by similar tubes (same dimensions) with different masses and chemical compositions. The values of the gravity acceleration g' for these samples were the same.

V. CONSEQUENCES

The experimental results point to the possibility of conversion of gravitational energy into mechanical energy and electrical energy. Consider for example the system presented in Fig.3 (a). Basically it is a motor with massive iron rotor and a gravity control cell. This cell is similar to the diode presented in Fig.1 (see Fig.3(b)), it is placed below the rotor in order to become *negative* the acceleration of gravity inside *half* of the rotor $(g' = -ng)$, as showed in Fig.3 (a). Obviously this

[†] It is known that the current is a spectrum in the *Fourier* domain. Here the spectrum has a D.C component, a 60Hz component, a 120Hz component, a 180Hz component, etc. The D.C component does not affect m_g since the effect just occurs for oscillating currents [4]. On the other hand, the effect of the 120Hz component is negligible (in voltage range investigated) in respect to the 60Hz component since the factor $\left(i^4\mu/64\pi^3c^2\rho^2S^4f^3\sigma\right)$ in Eq. (9) is $(120/60)^3$= 8 times smaller than in the case of the 60Hz component. For the 180Hz component the factor is $(180/60)^3$= 27 times smaller than in the case of the 60Hz component. Therefore here we will consider the 60Hz component only.

causes a torque $T=(-F'+F)r$ and the rotor spins with angular velocity ω. The average power, P, of the motor is given by

$$P=T\omega=[(-F'+F)r]\omega \qquad (12)$$

where

$$F'=\tfrac{1}{2}m_g g' \qquad F=\tfrac{1}{2}m_g g$$

and $m_g \cong m_i$ (mass of the rotor). Thus, Eq. (12) gives

$$P=(n+1)\frac{m_i g\omega\, r}{2} \qquad (13)$$

On the other hand, we have that

$$-g'+g=\omega^2 r \qquad (14)$$

Therefore the angular speed of the rotor is given by

$$\omega=\sqrt{\frac{(n+1)g}{r}} \qquad (15)$$

By substituting (15) into (13) we obtain the expression of the average power of the *gravitational motor*, i.e.,

$$P=\tfrac{1}{2}m_i\sqrt{(n+1)^3 g^3 r} \qquad (16)$$

Now consider an electric generator coupling to the gravitational motor in order to produce electric energy. Since $\omega=2\pi f$ then for $f=60Hz$ we have $\omega=120\,\pi rad.s^{-1}=3600\,rpm$. Therefore for $\omega=120\pi rad.s^{-1}$ and $n=788$ $(V_{max}\cong 5.5KV)^{\ddagger}$ the Eq. (15) tell us that we must have

$$r=\frac{(n+1)g}{\omega^2}=0.0545m$$

Since $r=R/3$ and $m_i=\rho\pi R^2 h$ where ρ, R and h are respectively the mass density, the radius and the height of the rotor then for $h=1.0m$ and $\rho=7800Kg.m^{-3}$ (iron) we obtain

$$m_i=654.1kg$$

Then Eq. (16) gives

$$P\cong 5.2\times 10^7\, watts\cong 52MW \qquad (17)$$

This shows that the gravitational motor can be used to yield electric energy at large scale.

VI.CONCLUSION

In the frequency investigated (60Hz), the weight of the samples decrease strongly with the increase of the intensity of the thermoionic current, and, as we have shown, the weight of the samples can even become *negative* (inversion).

The experimental observations described in this work are absolutely new and unprecedented. They tell us about a part of Gravitation Theory which is unknown.

---

‡ Note that, according to Eq.(9), this voltage can be strongly reduced by decreasing the density of the air, ρ, inside the gravity control cell.

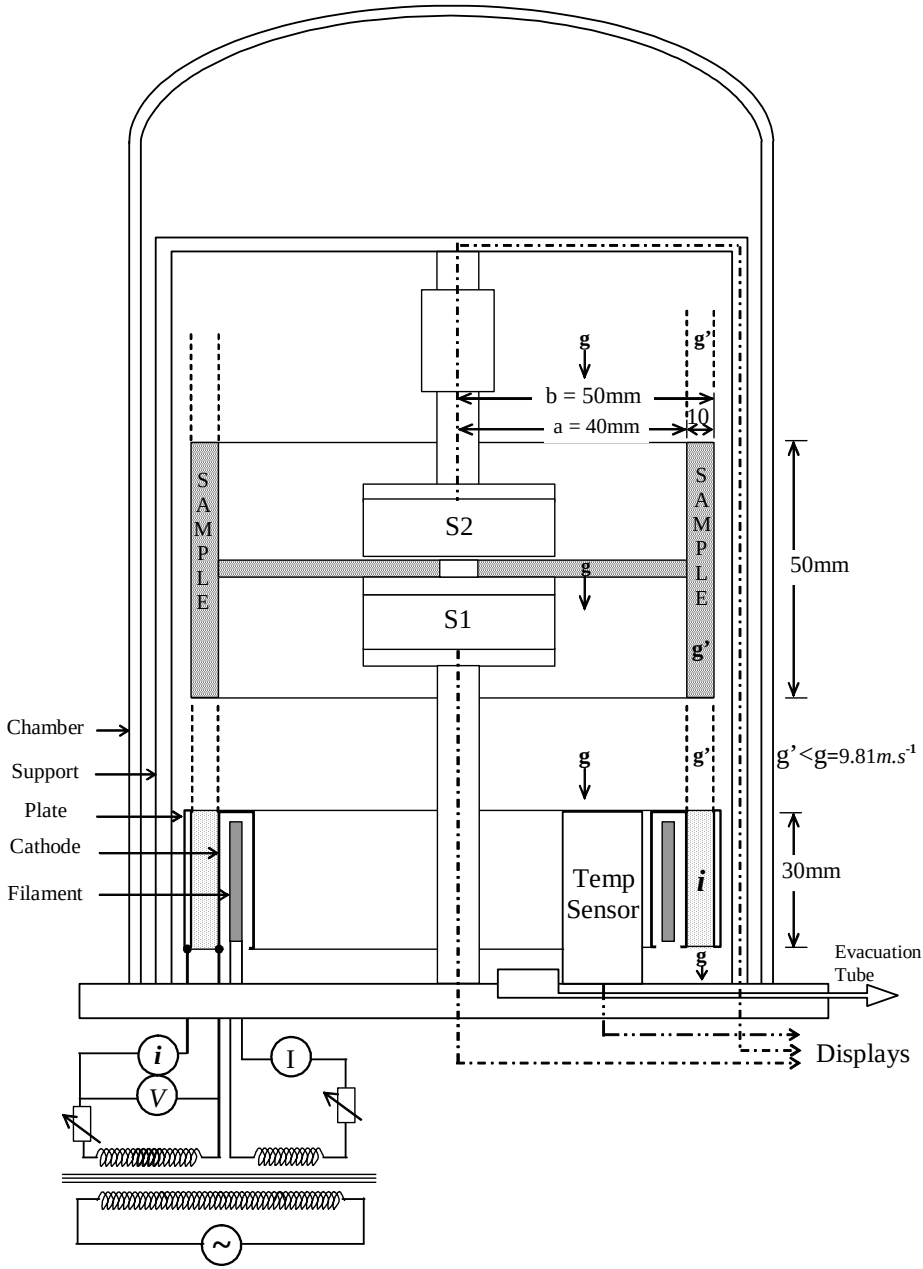

Fig.1- Experimental set-up.

V_{rms} (V)	V_{max} (V)	*Weight*		*g'/g*		Sensor
		Exp (N)	Theo (N)	Exp	Theo	
0	0	10.82	10.82	1	1	S1
100	141.42	10.60	10.71	0.98	0.99	
200	282.84	10.49	10.60	0.97	0.98	
300	424.26	9.30	9.52	0.86	0.88	
400	565.68	4.44	5.19	0.41	0.48	
500	707.11	-7.03	-4.98	-0.65	-0.46	S2

Table 1 - Influence of *thermoionic current* (60Hz) on the weight of the sample. Experimental data are the average of 10 measurements. The standard deviation of the single data is between 3 and 5%.

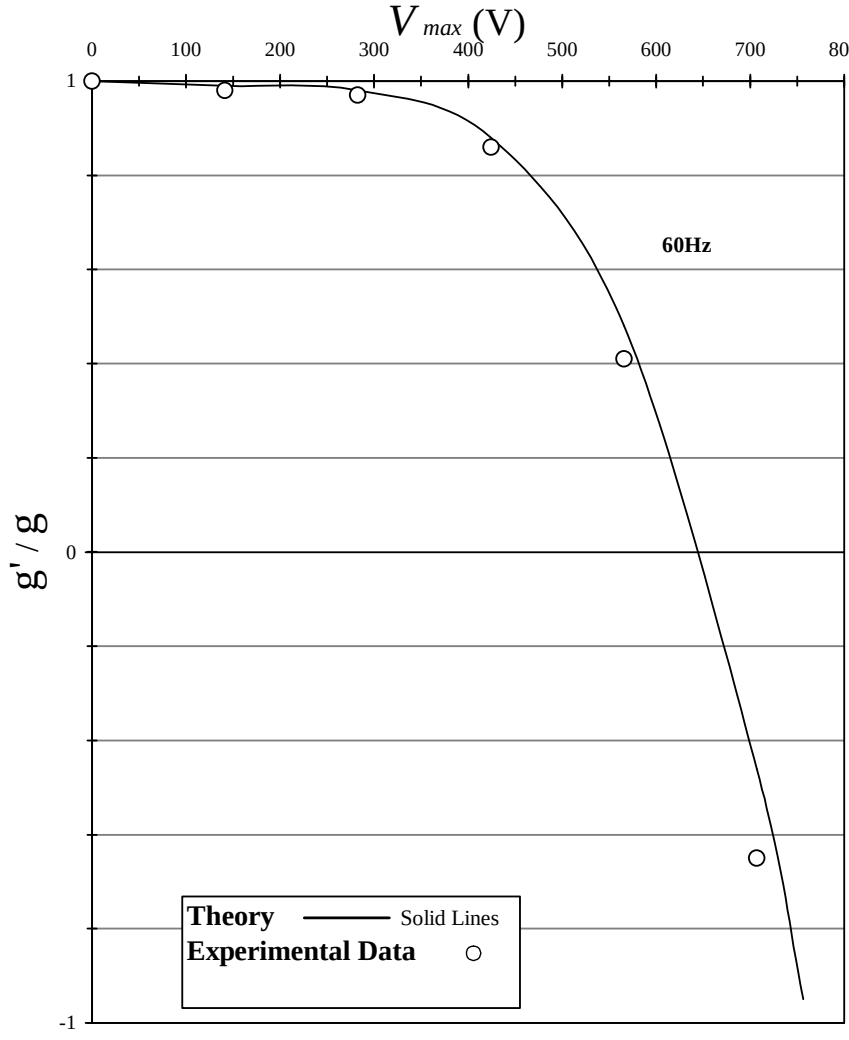

Fig. 2- Distribution of the correlation g'/g as a function of V max.

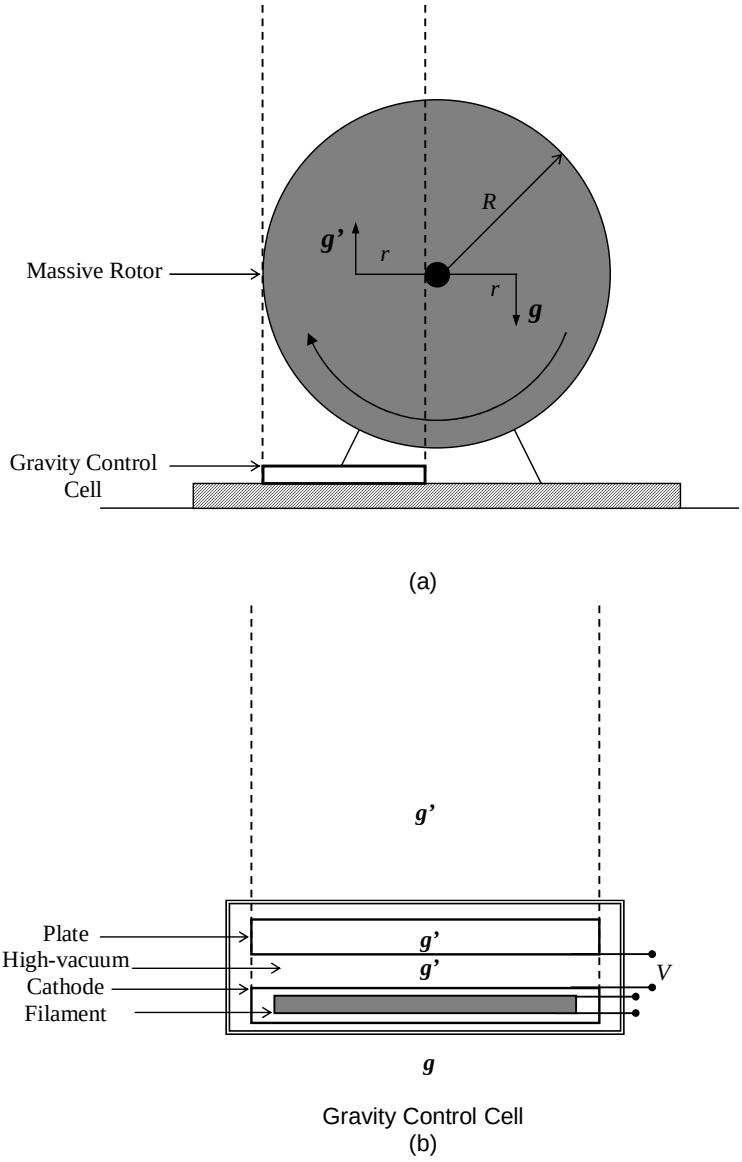

Fig. 3 – The Gravitational Motor

REFERENCES

[1] Hõrrak U., Salm J. and Tammet H., J. (2000) *Geophys. Res*. **105** (D7), 9291-9302

[2] Aplin, K. L. (2000) PhD thesis, The University of Reading, UK

[3] Aplin K. L (2005) *Rev. Sci. Instrum.* **76**, 104501.

[4] De Aquino, F. (2006) *Mathematical Foundations of the Relativistic Theory of Quantum Gravity*, preprint, physics/0212033.

Gravity Control by means of *Electromagnetic Field* through *Gas* or *Plasma* at Ultra-Low Pressure

Fran De Aquino
Maranhao State University, Physics Department, S.Luis/MA, Brazil.

It is shown that the gravity acceleration just above a chamber filled with *gas* or *plasma* at ultra-low pressure can be strongly reduced by applying an Extra Low-Frequency (ELF) electromagnetic field across the gas or the plasma. This Gravitational Shielding Effect is related to recent discovery of *quantum correlation* between gravitational mass and inertial mass. According to the theory samples hung above the gas or the plasma should exhibit a weight decrease when the frequency of the electromagnetic field is decreased or when the intensity of the electromagnetic field is increased. This Gravitational Shielding Effect is unprecedented in the literature and can not be understood in the framework of the General Relativity. From the technical point of view, there are several applications for this discovery; possibly it will change the paradigms of *energy* generation, *transportation* and *telecommunications*.

Key words: Phenomenology of quantum gravity, Experimental Tests of Gravitational Theories, Vacuum Chambers, Plasmas devices. **PACs**: 04.60.Bc, 04.80.Cc, 07.30.Kf, 52.75.-d.

CONTENTS

I. INTRODUCTION

It will be shown that the local gravity acceleration can be controlled by means of a device called Gravity Control Cell (GCC) which is basically a recipient filled with gas or plasma where is applied an *electromagnetic field*. According to the theory samples hung above the gas or plasma should exhibit a weight decrease when the frequency of the electromagnetic field is decreased or when the intensity of the electromagnetic field is increased. The electrical *conductivity* and the *density* of the gas or plasma are also highly relevant in this process.

With a GCC it is possible to convert the gravitational energy into rotational mechanical energy by means of the *Gravitational Motor*. In addition, a new concept of spacecraft (the *Gravitational Spacecraft*) and aerospace flight is presented here based on the possibility of gravity control. We will also see that the gravity control will be very important to *Telecommunication*.

II. THEORY

It was shown [1] that the relativistic *gravitational mass* $M_g = m_g \Big/ \sqrt{1-V^2/c^2}$ and the relativistic *inertial mass* $M_i = m_{i0} \Big/ \sqrt{1-V^2/c^2}$ are *quantized*, and given by $M_g = n_g^2 m_{i0(min)}$, $M_i = n_i^2 m_{i0(min)}$ where n_g and n_i are respectively, the *gravitational quantum number* and the *inertial quantum number* ; $m_{i0(min)} = \pm 3.9 \times 10^{-73} kg$ is the elementary *quantum* of inertial mass. The masses m_g and m_{i0} are correlated by means of the following expression:

$$m_g = m_{i0} - 2\left[\sqrt{1+\left(\frac{\Delta p}{m_i c}\right)^2} - 1\right] m_{i0}. \qquad (1)$$

Where Δp is the *momentum* variation on the particle and m_{i0} is the inertial mass at rest.

In general, the *momentum* variation Δp is expressed by $\Delta p = F\Delta t$ where F is the applied force during a time interval Δt. Note that there is no restriction concerning the *nature* of the force F, i.e., it can be mechanical, electromagnetic, etc.

For example, we can look on the *momentum* variation Δp as due to absorption or emission of *electromagnetic energy* by the particle.

In the case of radiation, Δp can be obtained as follows: It is known that the *radiation pressure*, dP, upon an area $dA = dxdy$ of a volume $dV = dxdydz$ of a particle (the incident radiation normal to the surface dA)is equal to the energy dU absorbed per unit volume (dU/dV).i.e.,

$$dP = \frac{dU}{dV} = \frac{dU}{dxdydz} = \frac{dU}{dAdz} \qquad (2)$$

Substitution of $dz = vdt$ (v is the speed of radiation) into the equation above gives

$$dP = \frac{dU}{dV} = \frac{(dU/dAdt)}{v} = \frac{dD}{v} \qquad (3)$$

Since $dPdA = dF$ we can write:

$$dFdt = \frac{dU}{v} \qquad (4)$$

However we know that $dF = dp/dt$, then

$$dp = \frac{dU}{v} \qquad (5)$$

From this equation it follows that

$$\Delta p = \frac{U}{v}\left(\frac{c}{c}\right) = \frac{U}{c} n_r$$

Substitution into Eq. (1) yields

$$m_g = \left\{1 - 2\left[\sqrt{1+\left(\frac{U}{m_{i0}c^2} n_r\right)^2} - 1\right]\right\} m_{i0} \qquad (6)$$

Where U, is the electromagnetic energy absorbed by the particle; n_r is the index of refraction.

Equation (6) can be rewritten in the following form

$$m_g = \left\{1 - 2\left[\sqrt{1+\left(\frac{W}{\rho\, c^2} n_r\right)^2} - 1\right]\right\} m_{i0} \qquad (7)$$

Where $W = U/V$ is the *density of electromagnetic energy* and $\rho = m_{i0}/\mathrm{V}$ is the density of inertial mass.

The Eq. (7) is the expression of the *quantum correlation* between the *gravitational mass* and the *inertial mass* as a function of the *density of electromagnetic energy*. This is also the expression of correlation between gravitation and electromagnetism.

The density of electromagnetic energy in an *electromagnetic* field can be deduced from Maxwell's equations [2] and has the following expression

$$W = \tfrac{1}{2}\varepsilon\, E^2 + \tfrac{1}{2}\mu H^2 \qquad (8)$$

It is known that $B = \mu H$, $E/B = \omega/k_r$ [3] and

$$v = \frac{dz}{dt} = \frac{\omega}{\kappa_r} = \frac{c}{\sqrt{\frac{\varepsilon_r \mu_r}{2}\left(\sqrt{1+(\sigma/\omega\varepsilon)^2}+1\right)}} \qquad (9)$$

Where k_r is the real part of the *propagation vector* $\vec{k}$ (also called *phase constant* [4]); $k = \left|\vec{k}\right| = k_r + ik_i$; ε, μ and σ, are the electromagnetic characteristics of the medium in which the incident (or emitted) radiation is propagating ($\varepsilon = \varepsilon_r \varepsilon_0$ where ε_r is the *relative dielectric permittivity* and $\varepsilon_0 = 8.854\times10^{-12} F/m$; $\mu = \mu_r \mu_0$ where μ_r is the *relative magnetic permeability* and $\mu_0 = 4\pi\times10^{-7} H/m$; σ is the *electrical conductivity*). It is known that for *free-space* $\sigma = 0$ and $\varepsilon_r = \mu_r = 1$ then Eq. (9) gives

$$v = c \qquad (10)$$

From (9) we see that the *index of refraction* $n_r = c/v$ will be given by

$$n_r = \frac{c}{v} = \sqrt{\frac{\varepsilon_r \mu_r}{2}\left(\sqrt{1+(\sigma/\omega\varepsilon)^2}+1\right)} \qquad (11)$$

Equation (9) shows that $\omega/\kappa_r = v$. Thus, $E/B = \omega/k_r = v$, i.e., $E = vB = v\mu H$. Then, Eq. (8) can be rewritten in the following form:

$$W = \tfrac{1}{2}\left(\varepsilon v^2 \mu\right)\mu H^2 + \tfrac{1}{2}\mu H^2 \qquad (12)$$

For $\sigma << \omega\varepsilon$, Eq. (9) reduces to

$$v = \frac{c}{\sqrt{\varepsilon_r \mu_r}}$$

Then, Eq. (12) gives

$$W = \tfrac{1}{2}\left[\varepsilon\left(\frac{c^2}{\varepsilon_r \mu_r}\right)\mu\right]\mu H^2 + \tfrac{1}{2}\mu H^2 = \mu H^2 \qquad (13)$$

This equation can be rewritten in the following forms:

$$W = \frac{B^2}{\mu} \qquad (14)$$

or

$$W = \varepsilon\, E^2 \qquad (15)$$

For $\sigma >> \omega\varepsilon$, Eq. (9) gives

$$v = \sqrt{\frac{2\omega}{\mu\sigma}} \qquad (16)$$

Then, from Eq. (12) we get

$$W = \tfrac{1}{2}\left[\varepsilon\left(\frac{2\omega}{\mu\sigma}\right)\mu\right]\mu H^2 + \tfrac{1}{2}\mu H^2 = \left(\frac{\omega\varepsilon}{\sigma}\right)\mu H^2 + \tfrac{1}{2}\mu H^2 \cong$$

$$\cong \tfrac{1}{2}\mu H^2 \qquad (17)$$

Since $E = vB = v\mu H$, we can rewrite (17) in the following forms:

$$W \cong \frac{B^2}{2\mu} \qquad (18)$$

or

$$W \cong \left(\frac{\sigma}{4\omega}\right)E^2 \qquad (19)$$

By comparing equations (14) (15) (18) and (19) we see that Eq. (19) shows that the better way to obtain a strong value of W *in practice* is by applying an *Extra Low-Frequency* (ELF) *electric field* $\left(w = 2\pi f << 1Hz\right)$ through a *mean with high electrical conductivity*.

Substitution of Eq. (19) into Eq. (7), gives

$$m_g = \left\{1 - 2\left[\sqrt{1+\frac{\mu}{4c^2}\left(\frac{\sigma}{4\pi f}\right)^3 \frac{E^4}{\rho^2}} - 1\right]\right\} m_{i0} \qquad (20)$$

This equation shows clearly that if an

electrical *conductor mean* has $\rho << 1\ Kg.m^{-3}$ and $\sigma >> 1$, then it is possible obtain strong changes in its gravitational mass, with a relatively small ELF *electric field*. An electrical *conductor mean* with $\rho << 1\ Kg.m^{-3}$ is obviously a *plasma*.

There is a very simple way to test Eq. (20). It is known that inside a fluorescent lamp *lit* there is *low-pressure Mercury plasma.* Consider a 20W T-12 *fluorescent lamp* (80044–F20T12/C50/ECO GE, Ecolux® T12), whose characteristics and dimensions are well-known [5]. At around $T \cong 318.15^0 K$, an optimum mercury vapor pressure of $P = 6\times10^{-3} Torr = 0.8 N.m^{-2}$ is obtained, which is required for maintenance of high luminous efficacy throughout life. Under these conditions, the mass density of the Hg plasma can be calculated by means of the well-known *Equation of State*

$$\rho = \frac{PM_0}{ZRT} \qquad (21)$$

Where $M_0 = 0.2006 kg.mol^{-1}$ is the molecular mass of the Hg; $Z \cong 1$ is the *compressibility factor* for the Hg plasma; $R = 8.314\ joule.mol^{-1}.^0K^{-1}$ is the *gases universal constant*. Thus we get

$$\rho_{Hg\ \ plasma} \cong 6.067\times10^{-5} kg.m^{-3} \qquad (22)$$

The electrical conductivity of the Hg plasma can be deduced from the *continuum form of Ohm's Law* $\vec{j} = \sigma\vec{E}$, since the *operating current* through the lamp and the *current density* are well-known and respectively given by $i = 0.35A$ [5] and $j_{lamp} = i/S = i/\frac{\pi}{4}\phi_{int}^2$, where $\phi_{int} = 36.1mm$ is the inner diameter of the lamp. The voltage drop across the electrodes of the lamp is $57V$ [5] and the distance between them $l = 570mm$. Then the electrical field *along* the lamp E_{lamp} is given by $E_{lamp} = 57V/0.570m = 100\ V.m^{-1}$. Thus, we have

$$\sigma_{Hg\ \ plasma} = \frac{j_{lamp}}{E_{lamp}} = 3.419\ \ S.m^{-1} \qquad (23)$$

Substitution of (22) and (23) into (20) yields

$$\frac{m_{g(Hg\ plasma)}}{m_{i(Hg\ plasma)}} = \left\{1 - 2\left[\sqrt{1 + 1.909\times10^{-17}\frac{E^4}{f^3}} - 1\right]\right\} \qquad (24)$$

Thus, if an *Extra Low-Frequency electric field* E_{ELF} with the following characteristics: $E_{ELF} \approx 100V.m^{-1}$ and $f < 1mHZ$ is applied through the Mercury plasma then a strong *decrease in the gravitational mass of the Hg plasma* will be produced.

It was shown [1] that there is an additional effect of *gravitational shielding* produced by a substance under these conditions. Above the substance the gravity acceleration g_1 is reduced at the same ratio $\chi = m_g/m_{i0}$, i.e., $g_1 = \chi\ g$, (g is the gravity acceleration *under* the *substance*). Therefore, due to the *gravitational shielding effect* produced by the decrease of $m_{g(Hg\ plasma)}$ *in the region where the ELF electric field* E_{ELF} *is applied*, the gravity acceleration just *above* this region will be given by

$$g_1 = \chi_{(Hg\ plasma)} g = \frac{m_{g(Hg\ plasma)}}{m_{i(Hg\ plasma)}} g =$$

$$= \left\{1 - 2\left[\sqrt{1 + 1.909\times10^{-17}\frac{E_{ELF}^4}{f_{ELF}^3}} - 1\right]\right\} g \qquad (25)$$

The trajectories of the electrons/ions through the lamp are determined by the electric field E_{lamp} *along* the lamp. If the ELF electric field *across* the lamp E_{ELF} is much greater than E_{lamp}, the current through the lamp can be interrupted. However, if $E_{ELF} << E_{lamp}$, these trajectories will be only slightly modified. Since here $E_{lamp} = 100\ V.m^{-1}$, then we can arbitrarily choose $E_{ELF}^{max} \cong 33\ V.m^{-1}$. This means that the *maximum* voltage drop, which can be applied across the metallic

plates, placed at distance d, is equal to the outer diameter (max *) of the bulb ϕ_{lamp}^{max} of the 20W T-12 Fluorescent lamp, is given by

$$V_{max} = E_{ELF}^{max}\phi_{lamp}^{max} \cong 1.5\ V$$

Since $\phi_{lamp}^{max} = 40.3mm$ [5].

Substitution of $E_{ELF}^{max} \cong 33\ V.m^{-1}$ into (25) yields

$$g_1 = \chi_{(Hg\ plasma)}g = \frac{m_{g(Hg\ plasma)}}{m_{i(Hg\ plasma)}}g =$$

$$= \left\{1-2\left[\sqrt{1+\frac{2.264\times10^{-11}}{f_{ELF}^3}}-1\right]\right\}g \qquad (26)$$

Note that, for $f < 1mHz = 10^{-3}Hz$, the gravity acceleration can be strongly reduced. These conclusions show that the ELF Voltage Source of the set-up shown in Fig.1 should have the following characteristics:

- Voltage range: 0 – 1.5 V
- Frequency range: 10^{-4}Hz – 10^{-3}Hz

In the experimental arrangement shown in Fig.1, an ELF electric field with intensity $E_{ELF} = V/d$ crosses the fluorescent lamp; V is the voltage drop across the metallic plates of the capacitor and $d = \phi_{lamp}^{max} = 40.3mm$. When the ELF electric field is applied, the gravity acceleration just above the lamp (inside the dotted box) decreases according to (25) and the changes can be measured by means of the system balance/sphere presented on the top of Figure 1.

In Fig. 2 is presented an experimental arrangement with *two* fluorescent lamps in order to test the gravity acceleration above the *second* lamp. Since gravity acceleration above the *first* lamp is given by $\vec{g}_1 = \chi_{1(Hg\ plasma)}\vec{g}$, where

$$\chi_{1(Hg\ plasma)} = \frac{m_{g1(Hg\ plasma)}}{m_{i1(Hg\ plasma)}} =$$

$$= \left\{1-2\left[\sqrt{1+1.909\times10^{-17}\frac{E_{ELF(1)}^4}{f_{ELF(1)}^3}}-1\right]\right\} \qquad (27)$$

Then, above the *second* lamp, the gravity acceleration becomes

$$\vec{g}_2 = \chi_{2(Hg\ plasma)}\vec{g}_1 = \chi_{2(Hg\ plasma)}\chi_{1(Hg\ plasma)}\vec{g} \qquad (28)$$

where

$$\chi_{2(Hg\ plasma)} = \frac{m_{g2(Hg\ plasma)}}{m_{i2(Hg\ plasma)}} =$$

$$= \left\{1-2\left[\sqrt{1+1.909\times10^{-17}\frac{E_{ELF(2)}^4}{f_{ELF(2)}^3}}-1\right]\right\} \qquad (29)$$

Then, results

$$\frac{g_2}{g} = \left\{1-2\left[\sqrt{1+1.909\times10^{-17}\frac{E_{ELF(1)}^4}{f_{ELF(1)}^3}}-1\right]\right\}\times$$

$$\times\left\{1-2\left[\sqrt{1+1.909\times10^{-17}\frac{E_{ELF(2)}^4}{f_{ELF(2)}^3}}-1\right]\right\} \qquad (30)$$

From Eq. (28), we then conclude that if $\chi_{1(Hg\ plasma)} < 0$ and also $\chi_{2(Hg\ plasma)} < 0$, then g_2 will have the *same direction* of g. This way it is possible to intensify several times the gravity in the direction of $\vec{g}$. On the other hand, if $\chi_{1(Hg\ plasma)} < 0$ and $\chi_{2(Hg\ plasma)} > 0$ the direction of $\vec{g}_2$ will be contrary to direction of $\vec{g}$. In this case will be possible to *intensify* and become $\vec{g}_2$ *repulsive* in respect to $\vec{g}$.

If we put a lamp above the *second* lamp, the gravity acceleration above the *third* lamp becomes

$$\vec{g}_3 = \chi_{3(Hg\ plasma)}\vec{g}_2 =$$

$$= \chi_{3(Hg\ plasma)}\chi_{2(Hg\ plasma)}\chi_{1(Hg\ plasma)}\vec{g} \qquad (31)$$

or

* After heating.

$$\frac{g_3}{g}=\left\{1-2\left[\sqrt{1+1.909\times10^{-17}\frac{E_{ELF(1)}^4}{f_{ELF(1)}^3}}-1\right]\right\}\times$$
$$\times\left\{1-2\left[\sqrt{1+1.909\times10^{-17}\frac{E_{ELF(2)}^4}{f_{ELF(2)}^3}}-1\right]\right\}\times$$
$$\times\left\{1-2\left[\sqrt{1+1.909\times10^{-17}\frac{E_{ELF(3)}^4}{f_{ELF(3)}^3}}-1\right]\right\} \qquad (32)$$

If $f_{ELF(1)}=f_{ELF(2)}=f_{ELF(3)}=f$ and

$$E_{ELF(1)}=E_{ELF(2)}=E_{ELF(3)}=V/\phi=$$
$$=V_0\sin\omega t/40.3mm=$$
$$=24.814V_0\sin 2\pi ft.$$

Then, for $t=T/4$ we get

$$E_{ELF(1)}=E_{ELF(2)}=E_{ELF(3)}=24.814V_0.$$

Thus, Eq. (32) gives

$$\frac{g_3}{g}=\left\{1-2\left[\sqrt{1+7.237\times10^{-12}\frac{V_0^4}{f^3}}-1\right]\right\}^3 \qquad (33)$$

For $V_0=1.5V$ and $f=0.2mHz$ $\left(t=T/4=1250s=20.83\text{min}\right)$ the gravity acceleration $\vec{g}_3$ above the *third* lamp will be given by

$$\vec{g}_3=-5.126\vec{g}$$

Above the *second* lamp, the gravity acceleration given by (30), is

$$\vec{g}_2=+2.972\vec{g} \quad .$$

According to (27) the gravity acceleration above the *first* lamp is

$$\vec{g}_1=-1{,}724\vec{g}$$

Note that, by this process an acceleration $\vec{g}$ can be increased several times in the direction of $\vec{g}$ or in the opposite direction.

In the experiment proposed in Fig. 1, we can start with ELF voltage sinusoidal wave of amplitude $V_0=1.0V$ and frequency $1mHz$. Next, the frequency will be progressively decreased down to $0.8mHz$, $0.6mHz$, $0.4mHz$ and $0.2mHz$. Afterwards, the amplitude of the voltage wave must be increased to $V_0=1.5V$ and the frequency decreased in the above mentioned sequence.

Table1 presents the *theoretical* values for g_1 and g_2, calculated respectively by means of (25) and (30).They are also plotted on Figures 5, 6 and 7 as a function of the frequency f_{ELF}.

Now consider a chamber filled with *Air* at $3\times10^{-12}torr$ and 300K as shown in Figure 8 (a). Under these circumstances, the mass density of the *air* inside the chamber, according to Eq. (21) is $\rho_{air}\cong4.94\times10^{-15}kg.m^{-3}$.

If the frequency of the *magnetic* field, B, through the *air* is $f=60Hz$ then $\omega\varepsilon=2\pi f\varepsilon\cong3\times10^{-9}S/m$. Assuming that the electric conductivity of the *air* inside the chamber, $\sigma_{(air)}$ is much less than $\omega\varepsilon$, i.e., $\sigma_{(air)}<<\omega\varepsilon$ (The atmospheric air conductivity is of the order of $2-100\times10^{-15}S.m^{-1}$ [6, 7]) then we can rewritten the Eq. (11) as follows

$$n_{r(air)}\cong\sqrt{\varepsilon_r\mu_r}\cong1 \qquad (34)$$

From Eqs. (7), (14) and (34) we thus obtain

$$m_{g(air)}=\left\{1-2\left[\sqrt{1+\left(\frac{B^2}{\mu_{air}\rho_{air}c^2}n_{r(air)}\right)^2}-1\right]\right\}m_{i(air)}=$$
$$=\left\{1-2\left[\sqrt{1+3.2\times10^6B^4}-1\right]\right\}m_{i(air)} \qquad (35)$$

Therefore, due to the *gravitational shielding effect* produced by the decreasing of $m_{g(air)}$, the gravity acceleration *above* the *air* inside the chamber will be given by

$$g'=\chi_{air}\,g=\frac{m_{g(air)}}{m_{i(air)}}g=$$
$$=\left\{1-2\left[\sqrt{1+3.2\times10^6B^4}-1\right]\right\}g$$

Note that the gravity acceleration above the *air* becomes *negative* for $B>2.5\times10^{-2}T$.

For $B = 0.1T$ the gravity acceleration above the air becomes

$$g' \cong -32.8g$$

Therefore the ultra-low pressure air inside the chamber, such as the Hg plasma inside the fluorescent lamp, works like a Gravitational Shield that in practice, may be used to build *Gravity Control Cells* (GCC) for several practical applications.

Consider for example the GCCs of Plasma presented in Fig.3. The ionization of the plasma can be made of several manners. For example, by means of an electric field between the electrodes (Fig. 3(a)) or by means of a RF signal (Fig. 3(b)). In the first case the ELF electric field and the ionizing electric field can be the same.

Figure 3(c) shows a GCC filled with *air* (at ambient temperature and 1 atm) strongly ionized by means of alpha particles emitted from 36 radioactive ions sources (a very small quantity of *Americium* 241[†]). The radioactive element Americium has a half-life of 432 years, and emits *alpha particles* and low energy gamma rays $(\approx 60KeV)$. In order to shield the *alpha* particles and *gamma* rays emitted from the Americium 241 it is sufficient to encapsulate the GCC with *epoxy*. The alpha particles generated by the americium ionize the oxygen and nitrogen atoms of the air in the *ionization chamber* (See Fig. 3(c)) increasing the *electrical conductivity* of the air inside the chamber. The high-speed alpha particles hit molecules in the air and knock off electrons to form ions, according to the following expressions

$$O_2 + H_e^{++} \rightarrow O_2^+ + e^- + H_e^{++}$$
$$N_2 + H_e^{++} \rightarrow N_2^+ + e^- + H_e^{++}$$

It is known that the electrical conductivity is proportional to both the concentration and the mobility of the *ions* and the *free electrons*, and is expressed by

$$\sigma = \rho_e \mu_e + \rho_i \mu_i$$

Where ρ_e and ρ_i express respectively the concentrations (C/m^3) of electrons and ions; μ_e and μ_i are respectively the mobilities of the electrons and the ions.

In order to calculate the electrical conductivity of the air inside the ionization chamber, we first need to calculate the concentrations ρ_e and ρ_i. We start calculating the *disintegration constant*, λ, for the Am 241 :

$$\lambda = \frac{0.693}{T^{\frac{1}{2}}} = \frac{0.693}{432(3.15 \times 10^7\, s)} = 5.1 \times 10^{-11} s^{-1}$$

Where $T^{\frac{1}{2}} = 432 years$ is the *half-life* of the Am 241.

One *kmole* of an isotope has mass equal to atomic mass of the isotope expressed in kilograms. Therefore, $1g$ of Am 241 has

$$\frac{10^{-3} kg}{241\ \ kg/kmole} = 4.15 \times 10^{-6} kmoles$$

One *kmole* of any isotope contains the Avogadro's number of atoms. Therefore $1g$ of Am 241 has

$$N = 4.15 \times 10^{-6} kmoles \times$$
$$\times 6.025 \times 10^{26}\ atoms/kmole = 2.50 \times 10^{21} atoms$$

Thus, the *activity* [8] of the sample is

[†] The radioactive element *Americium* (Am-241) is widely used in *ionization smoke detectors*. This type of smoke detector is more common because it is inexpensive and better at detecting the smaller amounts of smoke produced by flaming fires. Inside an ionization detector there is a small amount (perhaps 1/5000th of a gram) of americium-241. The Americium is present in oxide form (AmO_2) in the detector. The cost of the AmO_2 is US$ 1,500 per gram. The amount of radiation in a smoke detector is extremely small. It is also predominantly alpha radiation. Alpha radiation cannot penetrate a sheet of paper, and it is blocked by several centimeters of air. The americium in the smoke detector could only pose a danger if inhaled.

$R = \lambda N = 1.3 \times 10^{11}$ disintegrations/s.

However, we will use 36 ionization sources each one with 1/5000th of a gram of Am 241. Therefore we will only use $7.2 \times 10^{-3}\, g$ of Am 241. Thus, R reduces to:

$$R = \lambda N \cong 10^{9} \text{ disintegrations/s}$$

This means that at *one* second, about $10^{9}\, \alpha\ particles$ hit molecules in the air and knock off electrons to form ions O_2^+ and N_2^+ inside the ionization chamber. Assuming that *each* alpha particle yields *one* ion at each $1/10^{9}$ second then the total number of ions produced in one second will be $N_i \cong 10^{18} ions.$ This corresponds to an ions concentration

$$\rho_i = eN_i / V \approx 0.1 / V \quad \left(C/m^3\right)$$

Where V is the volume of the ionization chamber. Obviously, the concentration of electrons will be the same, i.e., $\rho_e = \rho_i$. For $d = 2cm$ and $\phi = 20cm$ (See Fig.3(c)) we obtain

$V = \frac{\pi}{4}(0.20)^2\left(2 \times 10^{-2}\right) = 6.28 \times 10^{-4} m^3$ The n we get:

$$\rho_e = \rho_i \approx 10^{2}\ C/m^3$$

This corresponds to the *minimum* concentration level in the case of *conducting materials*. For these materials, at temperature of 300K, the mobilities μ_e and μ_i vary from 10 up to $100\ m^2V^{-1}s^{-1}$ [9]. Then we can assume that $\mu_e = \mu_i \approx 10\ m^2V^{-1}s^{-1}$. (*minimum* mobility level for conducting materials). Under these conditions, the electrical conductivity of the air inside the ionization chamber is

$$\sigma_{air} = \rho_e\mu_e + \rho_i\mu_i \approx 10^{3} S.m^{-1}$$

At temperature of 300K, the air *density* inside the GCC, is $\rho_{air} = 1.1452 kg.m^{-3}$. Thus, for $d = 2cm$, $\sigma_{air} \approx 10^{3} S.m^{-1}$ and $f = 60Hz$ Eq. (20) gives

$$\chi_{air} = \frac{m_{g(air)}}{m_{i(air)}} =$$

$$= \left\{1 - 2\left[\sqrt{1 + \frac{\mu}{4c^2}\left(\frac{\sigma_{air}}{4\pi f}\right)^3 \frac{V_{rms}^4}{d^4\rho_{air}^2}} - 1\right]\right\} =$$

$$= \left\{1 - 2\left[\sqrt{1 + 3.10 \times 10^{-16} V_{rms}^4} - 1\right]\right\}$$

Note that, for $V_{rms} \cong 7.96KV$, we obtain: $\chi_{(air)} \cong 0$. Therefore, if the voltages range of this GCC is: $0 - 10KV$ then it is possible to reach $\chi_{air} \cong -1$ when $V_{rms} \cong 10KV$.

It is interesting to note that σ_{air} can be strongly increased by increasing the amount of Am 241. For example, by using $0.1g$ of Am 241 the value of R increases to:

$$R = \lambda N \cong 10^{10} \text{ disintegrations/s}$$

This means $N_i \cong 10^{20} ions$ that yield

$$\rho_i = eN_i / V \approx 10 / V \quad \left(C/m^3\right)$$

Then, by reducing, d and ϕ respectively, to 5mm and to 11.5cm, the volume of the ionization chamber reduces to:

$V = \frac{\pi}{4}(0.115)^2\left(5 \times 10^{-3}\right) = 5.19 \times 10^{-5} m^3$

Consequently, we get:

$$\rho_e = \rho_i \approx 10^{5}\ C/m^3$$

Assuming that $\mu_e = \mu_i \approx 10\ m^2V^{-1}s^{-1}$, then the electrical conductivity of the air inside the ionization chamber becomes

$$\sigma_{air} = \rho_e\mu_e + \rho_i\mu_i \approx 10^{6} S.m^{-1}$$

This reduces for $V_{rms} \cong 18.8V$ the voltage necessary to yield $\chi_{(air)} \cong 0$ and reduces

to $V_{rms} \cong 23.5V$ the voltage necessary to reach $\chi_{air} \cong -1$.

If the outer surface of a metallic sphere with radius a is covered with a radioactive element (for example Am 241), then the electrical conductivity of the air (very close to the sphere) can be strongly increased (for example up to $\sigma_{air} \cong 10^6 s.m^{-1}$). By applying a low-frequency electrical potential V_{rms} to the sphere, in order to produce an electric field E_{rms} starting from the outer surface of the sphere, then very close to the sphere the low-frequency electromagnetic field is $E_{rms} = V_{rms}/a$, and according to Eq. (20), the *gravitational mass* of the air in this region expressed by

$$m_{g(air)} = \left\{1-2\left[\sqrt{1+\frac{\mu_0}{4c^2}\left(\frac{\sigma_{air}}{4\pi f}\right)^3 \frac{V_{rms}^4}{a^4\rho_{air}^2}} -1\right]\right\} m_{i0(air)},$$

can be easily reduced, making possible to produce a controlled *Gravitational Shielding* (similar to a GCC) surround the sphere.

This becomes possible to build a spacecraft to work with a gravitational shielding as shown in Fig. 4.

The *gravity accelerations* on the spacecraft (due to the rest of the Universe. See Fig.4) is given by

$$g_i' = \chi_{air} g_i \qquad i = 1, 2, 3 \ldots n$$

Where $\chi_{air} = m_{g(air)}/m_{i0(air)}$. Thus, the *gravitational forces* acting on the spacecraft are given by

$$F_{is} = M_g g_i' = M_g\left(\chi_{air} g_i\right)$$

By reducing the value of χ_{air}, these forces can be reduced.

According to the *Mach's principle*;

"The *local inertial forces* are determined by the *gravitational interactions* of the local system with the distribution of the cosmic masses".

Thus, the local inertia is just the gravitational influence of the rest of matter existing in the Universe. Consequently, if we reduce the gravitational interactions between a spacecraft and the rest of the Universe, then *the inertial properties of the spacecraft* will be also reduced. This effect leads to a new concept of spacecraft and space flight.

Since χ_{air} is given by

$$\chi_{air} = \frac{m_{g(air)}}{m_{i0(air)}} = \left\{1-2\left[\sqrt{1+\frac{\mu_0}{4c^2}\left(\frac{\sigma_{air}}{4\pi f}\right)^3 \frac{V_{rms}^4}{a^4\rho_{air}^2}} -1\right]\right\}$$

Then, for $\sigma_{air} \cong 10^6 s.m^{-1}$, $f = 6Hz$, $a = 5m$, $\rho_{air} \cong 1Kg.m^{-3}$ and $V_{rms} = 3.35KV$ we get

$$\chi_{air} \cong 0$$

Under these conditions, the gravitational forces upon the spacecraft become approximately nulls and consequently, the spacecraft practically *loses its inertial properties.*

Out of the terrestrial atmosphere, the gravity acceleration upon the spacecraft is negligible and therefore the gravitational shielding is not necessary. However, if the spacecraft is in the outer space and we want to use the gravitational shielding then, χ_{air} must be replaced by χ_{vac} where

$$\chi_{vac} = \frac{m_{g(vac)}}{m_{i0(vac)}} = \left\{1-2\left[\sqrt{1+\frac{\mu_0}{4c^2}\left(\frac{\sigma_{vac}}{4\pi f}\right)^3 \frac{V_{rms}^4}{a^4\rho_{vac}^2}} -1\right]\right\}$$

The electrical conductivity of the ionized outer space (very close to the spacecraft) is small; however, its density is remarkably small $\left(<< 10^{-16} Kg.m^{-3}\right)$, in such a manner that the smaller value of the factor $\sigma_{vac}^3/\rho_{vac}^2$ can be easily compensated by the increase of V_{rms}.

It was shown that, when the gravitational mass of a particle is reduced to ranging between $+0.159M_i$ to $-0.159M_i$, it becomes *imaginary* [1], i.e., the gravitational and the inertial masses of the particle become *imaginary*. Consequently, the particle disappears from our ordinary space-time. However, the factor $\chi = M_{g(imaginary)}/M_{i(imaginary)}$ remains *real* because

$$\chi = \frac{M_{g(imaginary)}}{M_{i(imaginary)}} = \frac{M_g i}{M_i i} = \frac{M_g}{M_i} = real$$

Thus, if the gravitational mass of the particle is reduced by means of absorption of an amount of electromagnetic energy U, for example, we have

$$\chi = \frac{M_g}{M_i} = \left\{1 - 2\left[\sqrt{1+\left(U/m_{i0}c^2\right)^2} - 1\right]\right\}$$

This shows that the energy U of the electromagnetic field *remains acting on* the imaginary particle. In practice, this means that *electromagnetic fields act on imaginary particles*. Therefore, the electromagnetic field of a GCC remains acting on the particles inside the GCC even when their gravitational masses reach the gravitational mass ranging between $+0.159M_i$ to $-0.159M_i$ and they become imaginary particles. This is very important because it means that the GCCs of a gravitational spacecraft keep on working when the spacecraft becomes imaginary.

Under these conditions, the gravity accelerations on the *imaginary* spacecraft particle (due to the rest of the imaginary Universe) are given by

$$g'_j = \chi\ g_j \qquad j = 1,2,3,\ldots,n.$$

Where $\chi = M_{g(imaginary)}/M_{i(imaginary)}$ and $g_j = -Gm_{gj(imaginary)}/r_j^2$. Thus, the gravitational forces acting on the spacecraft are given by

$$\begin{aligned} F_{gj} &= M_{g(imaginary)} g'_j = \\ &= M_{g(imaginary)}\left(-\chi G m_{gj(imaginary)}/r_j^2\right) = \\ &= M_g i\left(-\chi G m_{gj} i/r_j^2\right) = +\chi G M_g m_{gj}/r_j^2 . \end{aligned}$$

Note that these forces are *real*. Remind that, the Mach's principle says that the *inertial effects* upon a particle are consequence of the gravitational interaction of the particle with the rest of the Universe. Then we can conclude that the *inertial forces* upon an *imaginary* spacecraft are also *real*. Consequently, it can travel in the imaginary space-time using its thrusters.

It was shown that, *imaginary particles* can have *infinite speed* in the *imaginary space-time* [1] . Therefore, this is also the speed upper limit for the spacecraft in the imaginary space-time.

Since the gravitational spacecraft can use its thrusters after to becoming an imaginary body, then if the thrusters produce a total thrust $F = 1000kN$ and the gravitational mass of the spacecraft is reduced from $M_g = M_i = 10^5 kg$ down to $M_g \cong 10^{-6} kg$, the acceleration of the spacecraft will be, $a = F/M_g \cong 10^{12} m.s^{-2}$. With this acceleration the spacecraft crosses the "visible" Universe ($diameter = d \approx 10^{26} m$) in a time interval $\Delta t = \sqrt{2d/a} \cong 1.4 \times 10^7 m.s^{-1} \cong 5.5\ months$

Since the inertial effects upon the spacecraft are reduced by $M_g/M_i \cong 10^{-11}$ then, in spite of the effective spacecraft acceleration be $a = 10^{12} m.s^{-1}$, the effects for the crew and for the spacecraft will be equivalent to an acceleration a' given by

$$a' = \frac{M_g}{M_i} a \approx 10 m.s^{-1}$$

This is the order of magnitude of the acceleration upon of a commercial jet aircraft.

On the other hand, the travel in the *imaginary* space-time can be very safe, because there won't any material body along the trajectory of the spacecraft.

Now consider the GCCs presented in Fig. 8 (a). Note that below and above the *air* are the bottom and the top of the chamber. Therefore the choice of the material of the chamber is highly relevant. If the chamber is made of steel, for example, and the gravity acceleration below the chamber is g then at the bottom of the chamber, the gravity becomes $g' = \chi_{steel}\, g$; in the air, the gravity is $g'' = \chi_{air} g' = \chi_{air}\chi_{steel} g$. At the top of the chamber, $g''' = \chi_{steel} g'' = (\chi_{steel})^2 \chi_{air} g$. Thus, out of the chamber (close to the top) the gravity acceleration becomes g'''. (See Fig. 8 (a)). However, for the steel at $B < 300T$ and $f = 1\times 10^{-6} Hz$, we have

$$\chi_{steel} = \frac{m_{g(steel)}}{m_{i(steel)}} = \left\{1 - 2\left[\sqrt{1 + \frac{\sigma_{(steel)} B^4}{4\pi f \mu \rho^2_{(steel)} c^2}} - 1\right]\right\} \cong 1$$

Since $\rho_{steel} = 1.1\times 10^6 S.m^{-1}$, $\mu_r = 300$ and $\rho_{(steel)} = 7800 k.m^{-3}$.

Thus, due to $\chi_{steel} \cong 1$ it follows that

$$g''' \cong g'' = \chi_{air}\, g' \cong \chi_{air}\, g$$

If instead of one GCC we have *three* GCC, all with steel box (Fig. 8(b)), then the gravity acceleration above the *second* GCC, g_2 will be given by

$$g_2 \cong \chi_{air} g_1 \cong \chi_{air}\chi_{air} g$$

and the gravity acceleration above the *third* GCC, g_3 will be expressed by

$$g_3 \cong \chi_{air} g'' \cong \chi_{air}{}^3 g$$

III. CONSEQUENCES

These results point to the possibility to convert gravitational energy into rotational mechanical energy. Consider for example the system presented in Fig. 9. Basically it is a motor with massive iron rotor and a box filled with gas or plasma at ultra-low pressure (Gravity Control Cell-GCC) as shown in Fig. 9. The GCC is placed below the rotor in order to become *negative* the acceleration of gravity inside *half* of the rotor $\left(g' = (\chi_{steel})^2 \chi_{air}\, g \cong \chi_{air}\, g = -ng\right)$. Obviously this causes a torque $T = (-F' + F)r$ and the rotor spins with angular velocity ω. The average power, P, of the motor is given by

$$P = T\omega = [(-F' + F)r]\omega \qquad (36)$$

Where

$$F' = \tfrac{1}{2} m_g g' \qquad F = \tfrac{1}{2} m_g g$$

and $m_g \cong m_i$ (mass of the rotor). Thus, Eq. (36) gives

$$P = (n+1)\frac{m_i g \omega\, r}{2} \qquad (37)$$

On the other hand, we have that

$$-g' + g = \omega^2 r \qquad (38)$$

Therefore the angular speed of the rotor is given by

$$\omega = \sqrt{\frac{(n+1)g}{r}} \qquad (39)$$

By substituting (39) into (37) we obtain the expression of the average power of the *gravitational motor*, i.e.,

$$P = \tfrac{1}{2} m_i \sqrt{(n+1)^3 g^3 r} \qquad (40)$$

Now consider an electric generator coupling to the gravitational motor in order to produce electric energy.

Since $\omega = 2\pi f$ then for $f = 60Hz$ we have $\omega = 120\pi rad.s^{-1} = 3600\, rpm$.

Therefore for $\omega = 120\pi rad.s^{-1}$ and $n = 788$ $(B \cong 0.22T)$ the Eq. (40) tell us that we must have

$$r = \frac{(n+1)g}{\omega^2} = 0.0545m$$

Since $r = R/3$ and $m_i = \rho\pi R^2 h$ where ρ, R and h are respectively the mass density, the radius and the height of the rotor then for $h = 0.5m$ and $\rho = 7800 Kg.m^{-3}$ (iron) we obtain

$$m_i = 327.05kg$$

Then Eq. (40) gives

$$P \cong 2.19\times10^{5}\, watts \cong 219\ KW \cong 294 HP \qquad (41)$$

This shows that the *gravitational motor* can be used to yield electric energy at large scale.

The possibility of gravity control leads to a new concept of spacecraft which is presented in Fig. 10. Due to the *Meissner effect*, the magnetic field *B* is expelled from the *superconducting shell*. The Eq. (35) shows that a magnetic field, B, through the *aluminum shell* of the spacecraft reduces its gravitational mass according to the following expression:

$$m_{g(Al)} = \left\{1-2\left[\sqrt{1+\left(\frac{B^2}{\mu c^2 \rho_{(Al)}} n_{r(Al)}\right)^2}-1\right]\right\} m_{i(Al)} \qquad (42)$$

If the frequency of the magnetic field is $f = 10^{-4} Hz$ then we have that $\sigma_{(Al)} >> \omega\varepsilon$ since the electric conductivity of the aluminum is $\sigma_{(Al)} = 3.82\times10^{7}\, S.m^{-1}$. In this case, the Eq. (11) tell us that

$$n_{r(Al)} = \sqrt{\frac{\mu c^2 \sigma_{(Al)}}{4\pi f}} \qquad (43)$$

Substitution of (43) into (42) yields

$$m_{g(Al)} = \left\{1-2\left[\sqrt{1+\frac{\sigma_{(Al)} B^4}{4\pi f \mu \rho_{(Al)}^2 c^2}}-1\right]\right\} m_{i(Al)} \qquad (44)$$

Since the mass density of the Aluminum is $\rho_{(Al)} = 2700\, kg.m^{-3}$ then the Eq. (44) can be rewritten in the following form:

$$\chi_{Al} = \frac{m_{g(Al)}}{m_{i(Al)}} = \left\{1-2\left[\sqrt{1+3.68\times10^{-8} B^4}-1\right]\right\} \qquad (45)$$

In practice it is possible to adjust B in order to become, for example, $\chi_{Al} \cong 10^{-9}$. This occurs to $B \cong 76.3T$. (Novel superconducting magnets are able to produce up to $14.7T$ [10, 11]).

Then the gravity acceleration in any direction *inside* the spacecraft, g_l', will be reduced and given by

$$g_l' = \frac{m_{g(Al)}}{m_{i(Al)}} g_l = \chi_{Al} g_l \cong -10^{-9} g_l \quad l = 1,2,..,n$$

Where g_l is the *externa*l gravity in the direction l. We thus conclude that the gravity acceleration inside the spacecraft becomes negligible if $g_l << 10^{9}\, m.s^{-2}$. This means that the aluminum shell, under these conditions, works like a gravity shielding.

Consequently, the gravitational forces between anyone point inside the spacecraft with gravitational mass, m_{gj}, and another external to the spacecraft (gravitational mass m_{gk}) are given by

$$\vec{F}_j = -\vec{F}_k = -G\frac{m_{gj} m_{gk}}{r_{jk}^2}\hat{\mu}$$

where $m_{gk} \cong m_{ik}$ and $m_{gj} = \chi_{Al} m_{ij}$. Therefore we can rewrite equation above in the following form

$$\vec{F}_j = -\vec{F}_k = -\chi_{Al} G\frac{m_{ij} m_{ik}}{r_{jk}^2}\hat{\mu}$$

Note that when $B = 0$ the *initial gravitational forces* are

$$\vec{F}_j = -\vec{F}_k = -G\frac{m_{ij} m_{ik}}{r_{jk}^2}\hat{\mu}$$

Thus, if $\chi_{Al} \cong -10^{-9}$ then the initial gravitational forces are reduced from 10^9 times and become repulsives.

According to the new expression for the *inertial forces* [1], $\vec{F} = m_g \vec{a}$, we see that these forces have origin in the *gravitational interaction* between a particle and the others of the Universe, just as *Mach's principle* predicts. Hence mentioned expression incorporates the Mach's principle into Gravitation Theory, and furthermore reveals that the inertial effects upon a body can be strongly reduced by means of the decreasing of its gravitational mass.

Consequently, we conclude that if the *gravitational forces* upon the spacecraft are reduced from 10^9 times then also the *inertial forces* upon the

spacecraft will be reduced from 10^9 times when $\chi_{Al} \cong -10^{-9}$. Under these conditions, the inertial effects on the crew would be strongly decreased. Obviously this leads to a new concept of aerospace flight.

Inside the spacecraft the gravitational forces between the dielectric with gravitational mass, M_g and the man (gravitational mass, m_g), when $B = 0$ are

$$\vec{F}_m = -\vec{F}_M = -G\frac{M_g m_g}{r^2}\hat{\mu} \qquad (46)$$

or

$$\vec{F}_m = -G\frac{M_g}{r^2} m_g \hat{\mu} = -m_g g_M \hat{\mu} \qquad (47)$$

$$\vec{F}_M = +G\frac{m_g}{r^2} M_g \hat{\mu} = +M_g g_m \hat{\mu} \qquad (48)$$

If the *superconducting box* under M_g (Fig. 10) is filled with *air* at ultra-low pressure (3×10^{-12} torr, 300K for example) then, when $B \neq 0$, the gravitational mass of the *air* will be reduced according to (35). Consequently, we have

$$g'_M = (\chi_{steel})^2 \chi_{air} g_M \cong \chi_{air} g_M \qquad (49)$$

$$g'_m = (\chi_{steel})^2 \chi_{air} g_m \cong \chi_{air} g_m \qquad (50)$$

Then the forces $\vec{F}_m$ and $\vec{F}_M$ become

$$\vec{F}_m = -m_g(\chi_{air} g_M)\hat{\mu} \qquad (51)$$

$$\vec{F}_M = +M_g(\chi_{air} g_m)\hat{\mu} \qquad (52)$$

Therefore if $\chi_{air} = -n$ we will have

$$\vec{F}_m = +n m_g g_M \hat{\mu} \qquad (53)$$

$$\vec{F}_M = -n M_g g_m \hat{\mu} \qquad (54)$$

Thus, $\vec{F}_m$ and $\vec{F}_M$ become *repulsive*. Consequently, the man inside the spacecraft is subjected to a gravity acceleration given by

$$\vec{a}_{man} = n g_M \hat{\mu} = -\chi_{air} G\frac{M_g}{r^2}\hat{\mu} \qquad (55)$$

Inside the GCC we have,

$$\chi_{air} = \frac{m_{g(air)}}{m_{i(air)}} = \left\{1 - 2\left[\sqrt{1 + \frac{\sigma_{(air)} B^4}{4\pi f \mu \rho^2_{(air)} c^2}} - 1\right]\right\} \qquad (56)$$

By ionizing the air inside the GCC (Fig. 10), for example, by means of a *radioactive* material, it is possible to increase the *air conductivity* inside the GCC up to $\sigma_{(air)} \cong 10^6 S.m^{-1}$. Then for $f = 10\ Hz$; $\rho_{(air)} = 4.94\times10^{-15} kg.m^{-3}$ (Air at 3×10^{-12} torr, 300K) and we obtain

$$\chi_{air} = \left\{2\left[\sqrt{1 + 2.8\times10^{21} B^4} - 1\right] - 1\right\} \qquad (57)$$

For $B = B_{GCC} = 0.1T$ (note that, due to the *Meissner effect*, the magnetic field B_{GCC} stay confined inside the *superconducting box*) the Eq. (57) yields

$$\chi_{air} \cong -10^9$$

Since there is no magnetic field through the *dielectric* presented in Fig.10 then, $M_g \cong M_i$. Therefore if $M_g \cong M_i = 100Kg$ and $r = r_0 \cong 1m$ the gravity acceleration upon the man, according to Eq. (55), is

$$a_{man} \cong 10 m.s^{-1}$$

Consequently it is easy to see that this system is ideal to yield artificial gravity inside the spacecraft in the case of *inter-stellar travel*, when the gravity acceleration out of the spacecraft - due to the Universe - becomes negligible.

The *vertical* displacement of the spacecraft can be produced by means of *Gravitational Thrusters*. A schematic diagram of a Gravitational Thruster is shown in Fig.11. The Gravitational Thrusters can also provide the *horizontal* displacement of the spacecraft.

The concept of Gravitational Thruster results from the theory of the *Gravity Control Battery*, showed in Fig. 8 (b). Note that the number of GCC increases the thrust of the thruster. For example, if the thruster has *three* GCCs then the gravity acceleration upon the gas sprayed inside the thruster will be *repulsive* in respect to M_g (See Fig. 11(a)) and given by

$$a_{gas} = (\chi_{air})^3 (\chi_{steel})^4 g \cong -(\chi_{air})^3 G\frac{M_g}{r_0^2}$$

Thus, if inside the GCCs, $\chi_{air} \cong -10^9$

(See Eq. 56 and 57) then the equation above gives

$$a_{gas} \cong +10^{27} G \frac{M_i}{r_0^2}$$

For $M_i \cong 10kg$, $r_0 \cong 1m$ and $m_{gas} \cong 10^{-12} kg$ the thrust is

$$F = m_{gas} a_{gas} \cong 10^5 N$$

Thus, the Gravitational Thrusters are able to produce strong thrusts.

Note that in the case of very strong χ_{air}, for example $\chi_{air} \cong -10^9$, the gravity accelerations upon the boxes of the second and third GCCs become very strong (Fig.11 (a)). Obviously, the walls of the mentioned boxes cannot to stand the enormous pressures. However, it is possible to build a similar system with 3 or more GCCs, *without material boxes*. Consider for example, a surface with several radioactive sources (Am-241, for example). The *alpha* particles emitted from the Am-241 cannot reach besides 10cm of air. Due to the trajectory of the alpha particles, three or more successive layers of air, with different electrical conductivities σ_1, σ_2 and σ_3, will be established in the ionized region (See Fig.11 (b)). It is easy to see that the gravitational shielding effect produced by these three layers is similar to the effect produced by the 3 GCCs shown in Fig. 11 (a).

It is important to note that if F is force produced by a thruster then the spacecraft acquires acceleration $a_{spacecraft}$ given by [1]

$$a_{spacecraft} = \frac{F}{M_{g(spacecraft)}} = \frac{F}{\chi_{Al} M_{i(inside)} + m_{i(Al)}}$$

Therefore if $\chi_{Al} \cong 10^{-9}$; $M_{i(inside)} = 10^4 Kg$ and $m_{i(Al)} = 100 Kg$ (inertial mass of the aluminum shell) then it will be necessary $F = 10kN$ to produce

$$a_{spacecraft} = 100 m.s^{-2}$$

Note that the concept of Gravitational Thrusters leads directly to the *Gravitational Turbo Motor* concept (See Fig. 12).

Let us now calculate the gravitational forces between two very close *thin* layers of the *air* around the spacecraft. (See Fig. 13).

The gravitational force dF_{12} that dm_{g1} exerts upon dm_{g2}, and the gravitational force dF_{21} that dm_{g2} exerts upon dm_{g1} are given by

$$d\vec{F}_{12} = d\vec{F}_{21} = -G \frac{dm_{g2} dm_{g1}}{r^2} \hat{\mu} \qquad (58)$$

Thus, the gravitational forces between the *air layer* 1, gravitational mass m_{g1}, and the *air layer* 2, gravitational mass m_{g2}, around the spacecraft are

$$\vec{F}_{12} = -\vec{F}_{21} = -\frac{G}{r^2} \int_0^{m_{g1}} \int_0^{m_{g2}} dm_{g1} dm_{g2} \hat{\mu} =$$

$$= -G \frac{m_{g1} m_{g2}}{r^2} \hat{\mu} = -\chi_{air} \chi_{air} G \frac{m_{i1} m_{i2}}{r^2} \hat{\mu} \qquad (59)$$

At 100km altitude the air pressure is $5.691 \times 10^{-3} torr$ and $\rho_{(air)} = 5.998 \times 10^{-6} kg.m^{-3}$ [12]. By ionizing the air surround the spacecraft, for example, by means of an oscillating electric field, E_{osc}, starting from the surface of the spacecraft (See Fig. 13) it is possible to increase the *air conductivity* near the spacecraft up to $\sigma_{(air)} \cong 10^6 S.m^{-1}$. Since $f = 1Hz$ and, in this case $\sigma_{(air)} >> \omega\varepsilon$, then, according to Eq. (11), $n_r = \sqrt{\mu \sigma_{(air)} c^2 / 4\pi f}$. From Eq.(56) we thus obtain

$$\chi_{air} = \frac{m_{g(air)}}{m_{i(air)}} = \left\{ 1 - 2 \left[\sqrt{1 + \frac{\sigma_{(air)} B^4}{4\pi f \mu_0 \rho_{(air)}^2 c^2}} - 1 \right] \right\} \qquad (60)$$

Then for $B = 763T$ the Eq. (60) gives

$$\chi_{air} = \left\{ 1 - 2 \left[\sqrt{1 + \sim 10^4 B^4} - 1 \right] \right\} \cong -10^8 \qquad (61)$$

By substitution of $\chi_{air} \cong -10^8$ into Eq., (59) we get

$$\vec{F}_{12} = -\vec{F}_{21} = -10^{16} G \frac{m_{i1} m_{i2}}{r^2} \hat{\mu} \qquad (62)$$

If $m_{i1} \cong m_{i2} = \rho_{air} \boldsymbol{V}_1 \cong \rho_{air} \boldsymbol{V}_2 \cong 10^{-8} kg$, and $r = 10^{-3} m$ we obtain

$$\vec{F}_{12} = -\vec{F}_{21} \cong -10^{-4} N \qquad (63)$$

These forces are much more intense than the *inter-atomic forces* (the forces which maintain joined atoms, and molecules that make the solids and liquids) whose intensities, according to the Coulomb's law, is of the order of 1-1000×10^{-8}N.

Consequently, the air around the spacecraft will be strongly compressed upon their surface, making an "*air shell*" that will accompany the spacecraft during its displacement and will protect the *aluminum shell* of the direct attrition with the Earth's atmosphere.

In this way, during the flight, the attrition would occur just between the "air shell" and the atmospheric air around her. Thus, the spacecraft would stay free of the thermal effects that would be produced by the direct attrition of the aluminum shell with the Earth's atmosphere.

Another interesting effect produced by the magnetic field B of the spacecraft is the possibility of to lift a body from the surface of the Earth to the spacecraft as shown in Fig. 14. By ionizing the air surround the spacecraft, by means of an oscillating electric field, E_{osc}, the *air conductivity* near the spacecraft can reach, for example, $\sigma_{(air)} \cong 10^6 S.m^{-1}$. Then for $f = 1Hz$; $B = 40.8T$ and $\rho_{(air)} \cong 1.2kg.m^{-3}$ (300K and 1 atm) the Eq. (56) yields

$$\chi_{air} = \left\{1 - 2\left[\sqrt{1 + 4.9 \times 10^{-7} B^4} - 1\right]\right\} \cong -0.1$$

Thus, the weight of the body becomes

$$P_{body} = m_{g(body)} g = \chi_{air} m_{i(body)} g = m_{i(body)} g'$$

Consequently, the body will be lifted on the direction of the spacecraft with acceleration

$$g' = \chi_{air} g \cong +0.98 m.s^{-1}$$

Let us now consider an important aspect of the flight dynamics of a Gravitational Spacecraft.

Before starting the flight, the *gravitational mass of the spacecraft*, M_g, must be strongly reduced, by means of a gravity control system, in order to produce – with a weak thrust $\vec{F}$, a strong acceleration, $\vec{a}$, given by [1]

$$\vec{a} = \frac{\vec{F}}{M_g}$$

In this way, the spacecraft could be strongly accelerated and quickly to reach very high speeds near speed of light.

If the gravity control system of the spacecraft is *suddenly* turned off, the *gravitational mass* of the spacecraft becomes immediately equal to its *inertial mass*, M_i, $\left(M'_g = M_i\right)$ and the velocity $\vec{V}$ becomes equal to $\vec{V}'$. According to the *Momentum* Conservation Principle, we have that

$$M_g V = M'_g V'$$

Supposing that the spacecraft was traveling in space with speed $V \approx c$, and that its gravitational mass it was $M_g = 1Kg$ and $M_i = 10^4 Kg$ then the velocity of the spacecraft is reduced to

$$V' = \frac{M_g}{M'_g} V = \frac{M_g}{M_i} V \approx 10^{-4} c$$

Initially, when the velocity of the spacecraft is $\vec{V}$, its kinetic energy is $E_k = \left(M_g - m_g\right)c^2$. Where $M_g = m_g \Big/ \sqrt{1 - V^2/c^2}$. At the instant in which the gravity control system of the spacecraft is turned off, the kinetic energy becomes $E'_k = \left(M'_g - m'_g\right)c^2$. Where $M'_g = m'_g \Big/ \sqrt{1 - V'^2/c^2}$.

We can rewritten the expressions of E_k and E'_k in the following form

$$E_k = \left(M_g V - m_g V\right)\frac{c^2}{V}$$

$$E'_k = \left(M'_g V' - m'_g V'\right)\frac{c^2}{V'}$$

Substitution of $M_g V = M'_g V' = p$,

$m_g V = p\sqrt{1-V^2/c^2}$ and $m'_g V' = p\sqrt{1-V'^2/c^2}$ into the equations of E_k and E'_k gives

$$E_k = \left(1-\sqrt{1-V^2/c^2}\right)\frac{pc^2}{V}$$

$$E'_k = \left(1-\sqrt{1-V'^2/c^2}\right)\frac{pc^2}{V'}$$

Since $V \approx c$ then follows that

$$E_k \approx pc$$

On the other hand, since $V' << c$ we get

$$E'_k = \left(1-\sqrt{1-V'^2/c^2}\right)\frac{pc^2}{V'} =$$

$$\cong \left(1-\frac{1}{1+\frac{V'^2}{2c^2}+\ldots}\right)\frac{pc^2}{V'} \cong \left(\frac{V'}{2c}\right)pc$$

Therefore we conclude that $E_k >> E'_k$. Consequently, when the gravity control system of the spacecraft is turned off, occurs an *abrupt* decrease in the kinetic energy of the spacecraft, ΔE_k, given by

$$\Delta E_k = E_k - E'_k \approx pc \approx M_g c^2 \approx 10^{17}\,J$$

By comparing the energy ΔE_k with the *inertial energy* of the spacecraft, $E_i = M_i c^2$, we conclude that

$$\Delta E_k \approx \frac{M_g}{M_i} E_i \approx 10^{-4} M_i c^2$$

The energy ΔE_k (several *megatons*) must be released in very short time interval. It is approximately the same amount of energy that would be released in the case of collision of the spacecraft[‡]. However, the situation is very different of a collision (M_g just becomes suddenly equal to M_i), and possibly the energy ΔE_k is converted into a *High Power Electromagnetic Pulse*.

[‡] In this case, the collision of the spacecraft would release $\approx 10^{17}$J (several megatons) and it would be similar to a powerful *kinetic weapon*.

Obviously this electromagnetic pulse (EMP) will induce heavy currents in all electronic equipment that mainly contains semiconducting and conducting materials. This produces immense heat that melts the circuitry inside. As such, *while not being directly responsible for the loss of lives*, these EMP are capable of disabling electric/electronic systems. Therefore, we possibly have a new type of *electromagnetic bomb*. An *electromagnetic bomb* or *E-bomb* is a well-known weapon designed to disable electric/electronic systems on a wide scale with an intense electromagnetic pulse.

Based on the theory of the GCC it is also possible to build a *Gravitational Press* of *ultra-high* pressure as shown in Fig.15.

The chamber 1 and 2 are GCCs with air at 1×10^{-4}torr, 300K $\left(\sigma_{(air)} \approx 10^6\, S.m^{-1};\ \rho_{(air)} = 5\times10^{-8}\, kg.m^{-3}\right)$. Thus, for $f = 10Hz$ and $B = 0.107T$ we have

$$\chi_{air} = \left\{1-2\left[\sqrt{1+\frac{\sigma_{(air)}B^4}{4\pi f\mu_0\rho^2_{(air)}c^2}}-1\right]\right\} \cong -118$$

The gravity acceleration above the air of the chamber 1 is

$$\vec{g}_1 = \chi_{stell}\chi_{air} g\hat{\mu} \cong +1.15\times10^3\,\hat{\mu} \qquad (64)$$

Since, in this case, $\chi_{steel} \cong 1$; $\hat{\mu}$ is an *unitary vector* in the opposite direction of $\vec{g}$.

Above the air of the chamber 2 the gravity acceleration becomes

$$\vec{g}_2 = (\chi_{stell})^2(\chi_{air})^2 g\hat{\mu} \cong -1.4\times10^5\,\hat{\mu} \qquad (65)$$

Therefore the *resultant* force $\vec{R}$ acting on m_2, m_1 and m is

$$\vec{R} = \vec{F}_2 + \vec{F}_1 + \vec{F} = m_2\vec{g}_2 + m_1\vec{g}_1 + m\vec{g} =$$
$$= -1.4\times10^5 m_2\hat{\mu} + 1.15\times10^3 m_1\hat{\mu} - 9.81m\hat{\mu} =$$
$$\cong -1.4\times10^5 m_2\hat{\mu} \qquad (66)$$

where

$$m_2 = \rho_{steel}V_{disk\,2} = \rho_{steel}\left(\frac{\pi}{4}\phi_{inn}^2 H\right) \qquad (67)$$

Thus, for $\rho_{steel} \cong 10^4\, kg.m^{-3}$ we can write that

$$F_2 \cong 10^9\phi_{inn}^2 H$$

For the steel $\tau \cong 10^5\, kg.cm^{-2} = 10^9\, kg.m^{-2}$ consequently we must have $F_2/S_\tau < 10^9\, kg.m^{-2}$ ($S_\tau = \pi\phi_{inn}H$ see Fig.15). This means that

$$\frac{10^9\phi_{inn}^2 H}{\pi\phi_{inn}H} < 10^9\, kg.m^{-2}$$

Then we conclude that

$$\phi_{inn} < 3.1m$$

For $\phi_{inn} = 2m$ and $H = 1m$ the Eq. (67) gives

$$m_2 \cong 3\times10^4\, kg$$

Therefore from the Eq. (66) we obtain

$$R \cong 10^{10}\, N$$

Consequently, in the area $S = 10^{-4}m^2$ of the Gravitational Press, the pressure is

$$p = \frac{R}{S} \cong 10^{14}\, N.m^{-2}$$

This enormous pressure is much greater than the pressure in the center of the Earth ($3.617\times10^{11}\, N.m^{-2}$) [13]. It is near of the gas pressure in the *center of the sun* ($2\times10^{16}\, N.m^{-2}$). Under the action of such intensities new states of matter are created and astrophysical phenomena may be simulated in the lab for the first time, e.g. supernova explosions. Controlled thermonuclear fusion by inertial confinement, fast nuclear ignition for energy gain, novel collective acceleration schemes of particles and the numerous variants of material processing constitute examples of progressive applications of such *Gravitational Press* of ultra-high pressure.

The GCCs can also be applied on generation and detection of *Gravitational Radiation*.

Consider a cylindrical GCC (GCC antenna) as shown in Fig.16 (a). The *gravitational mass* of the *air* inside the GCC is

$$m_{g(air)} = \left\{1 - 2\left[\sqrt{1 + \frac{\sigma_{(air)}B^4}{4\pi f\mu\rho_{(air)}^2 c^2}} - 1\right]\right\} m_{i(air)} \qquad (68)$$

By varying B one can varies $m_{g(air)}$ and consequently to vary the gravitational field generated by $m_{g(air)}$, producing then gravitational radiation. Then a GCC can work like a *Gravitational Antenna*.

Apparently, Newton's theory of gravity had no gravitational waves because, if a gravitational field changed in some way, that change took place *instantaneously* everywhere in space, and one can think that there is not a wave in this case. However, we have already seen that the gravitational interaction can be repulsive, besides attractive. Thus, as with electromagnetic interaction, the gravitational interaction must be produced by the exchange of "virtual" *quanta of* spin 1 and mass null, i.e., the *gravitationa*l "virtual" *quanta* (*graviphoton*) must have spin 1 and not 2. Consequently, the fact of a change in a gravitational field reach *instantaneously* everywhere in space occurs simply due to the speed of the *graviphoton* to be *infinite*. It is known that there is no speed limit for "*virtual*" photons. On the contrary, the *electromagnetic quanta* ("virtual" photons) could not communicate the *electromagnetic interaction* an infinite distance.

Thus, there are *two types* of gravitational radiation: the *real* and *virtual*, which is constituted of graviphotons; the *real* gravitational waves are ripples in the space-time generated by *gravitational field* changes. According to Einstein's theory of gravity the velocity of propagation of these waves is equal to the speed of light (c).

Unlike the electromagnetic waves the *real* gravitational waves have low interaction with matter and consequently low scattering. Therefore *real* gravitational waves are suitable as a means of transmitting information. However, when the distance between transmitter and receiver is too large, for example of the order of magnitude of several light-years, the transmission of information by means of gravitational waves becomes impracticable due to the long time necessary to receive the information. On the other hand, there is no delay during the transmissions by means of *virtual* gravitational radiation. In addition the scattering of this radiation is null. Therefore the *virtual* gravitational radiation is very suitable as a means of transmitting information at any distances including astronomical distances.

As concerns detection of the *virtual* gravitational radiation from GCC antenna, there are many options. Due to *Resonance Principle* a similar GCC antenna (receiver) *tuned at the same frequency* can absorb energy from an incident *virtual* gravitational radiation (See Fig.16 (b)). Consequently, the gravitational mass of the air inside the GCC receiver will vary such as the gravitational mass of the air inside the GCC transmitter. This will induce a magnetic field similar to the magnetic field of the GCC transmitter and therefore the current through the coil inside the GCC receiver will have the same characteristics of the current through the coil inside the GCC transmitter. However, the *volume* and *pressure* of the air inside the two GCCs must be exactly the same; also the *type* and the *quantity of atoms* in the air inside the two GCCs must be exactly the same. Thus, the GCC antennas are simple but they are not easy to build.

Note that a GCC antenna radiates *graviphotons* and *gravitational waves* simultaneously (Fig. 16 (a)). Thus, it is not only a gravitational antenna: it is a *Quantum Gravitational Antenna* because it can also emit and detect gravitational "virtual" *quanta* (graviphotons), which, in turn, can transmit information *instantaneously* from any distance in the Universe *without* scattering.

Due to the difficulty to build two similar GCC antennas and, considering that the electric current in the receiver antenna can be detectable even if the gravitational mass of the nuclei of the antennas are not *strongly* reduced, then we propose to replace the gas at the nuclei of the antennas by a thin *dielectric lamina*. The dielectric lamina with exactly 10^8 atoms (10^3atoms $\times$ 10^3atoms $\times$ 10^2atoms) is placed between the plates (electrodes) as shown in Fig. 17. When the *virtual* gravitational radiation strikes upon the dielectric lamina, its gravitational mass varies similarly to the gravitational mass of the dielectric lamina of the transmitter antenna, inducing an electromagnetic field (E, B) similar to the transmitter antenna. Thus, the electric current in the receiver antenna will have the same characteristics of the current in the transmitter antenna. In this way, it is then possible to build two similar antennas whose nuclei have the same volumes and the same types and quantities of atoms.

Note that the Quantum Gravitational Antennas can also be used to transmit *electric power*. It is easy to see that the Transmitter and Receiver (Fig. 17(a)) can work with strong voltages and electric currents. This means that strong electric power can be transmitted among Quantum Gravitational Antennas. This obviously solves the problem of *wireless* electric power transmission.

The existence of *imaginary masses* has been predicted in a previous work [1]. Here we will propose a method and a device using GCCs for obtaining *images* of *imaginary bodies*.

It was shown that the *inertial* imaginary mass associated to an *electron* is given by

$$m_{ie(ima)} = \frac{2}{\sqrt{3}}\left(\frac{hf}{c^2}\right)i = \frac{2}{\sqrt{3}}m_{ie(real)}\, i \qquad (69)$$

Assuming that the correlation between the gravitational mass and the inertial mass (Eq.6) is the same for both imaginary and real masses then follows that the *gravitational* imaginary mass associated to an *electron* can be written in the following form:

$$m_{ge(ima)} = \left\{1-2\left[\sqrt{1+\left(\frac{U}{m_i c^2}n_r\right)^2}-1\right]\right\}m_{ie(ima)} \qquad (70)$$

Thus, the gravitational *imaginary* mass *associated to matter* can be *reduced*, made

negative and *increased,* just as the gravitational *real* mass.

It was shown that also *photons* have imaginary mass. Therefore, the imaginary mass can be associated or *not* to the matter.

In a general way, the gravitational forces between two gravitational imaginary masses are then given by

$$\vec{F} = -\vec{F} = -G\frac{(iM_g)(im_g)}{r^2}\hat{\mu} = +G\frac{M_g m_g}{r^2}\hat{\mu} \qquad (71)$$

Note that these forces are *real* and *repulsive*.

Now consider a gravitational imaginary mass, $m_{g(ima)} = im_g$, *not associated with matter* (like the gravitational imaginary mass associated to the photons) and another gravitational imaginary mass $M_{g(ima)} = iM_g$ *associated to* a *material* body.

*Any material body has an imaginary mass associated to it, d*ue to the existence of imaginary masses associated to the electrons. We will choose a *quartz crystal* (for the material body with gravitational imaginary mass $M_{g(ima)} = iM_g$) because quartz crystals are widely used to detect forces (piezoelectric effect).

By using GCCs as shown in Fig. 18(b) and Fig.18(c), we can increase the gravitational acceleration, $\vec{a}$, produced by the imaginary mass im_g upon the crystals. Then it becomes

$$a = -\chi_{air}^3 G\frac{m_g}{r^2} \qquad (72)$$

As we have seen, the value of χ_{air} can be increased up to $\chi_{air} \cong -10^9$ (See Eq.57). Note that in this case, the gravitational forces become *attractive*. In addition, if m_g is not small, the gravitational forces between the imaginary body of mass im_g and the crystals can become sufficiently intense to be easily detectable.

Due to the piezoelectric effect, the gravitational force acting on the crystal will produce a voltage proportional to its intensity. Then consider a board with hundreds micro-crystals behind a set of GCCs, as shown in Fig.18(c). By amplifying the voltages generated in each micro-crystal and sending to an appropriated data acquisition system, it will be thus possible to obtain an image of the imaginary body of mass $m_{g(ima)}$ placed in front of the board.

In order to decrease strongly the gravitational effects produced by bodies placed behind the imaginary body of mass im_g, one can put five GCCs making a *Gravitational Shielding* as shown in Fig.18(c). If the GCCs are filled with air at 300K and $3\times10^{-12} torr$. Then $\rho_{air} = 4.94\times10^{-15} kg.m^{-3}$ and $\sigma_{air} \cong 1\times10^{-14} S.m^{-1}$. Thus, for $f = 60Hz$ and $B \cong 0.7T$ the Eq. (56) gives

$$\chi_{air} = \frac{m_{g(air)}}{m_{i(air)}} = \left\{1 - 2\left[\sqrt{1+5B^4} - 1\right]\right\} \cong -10^{-2} \qquad (73)$$

For $\chi_{air} \cong 10^{-2}$ the gravitational shielding presented in Fig.18(c) will reduce any value of g to $\chi_{air}^5 g \cong 10^{-10} g$. This will be sufficiently to reduce strongly the gravitational effects proceeding from both sides of the gravitational shielding.

Another important consequence of the correlation between gravitational mass and inertial mass expressed by Eq. (1) is the possibility of building *Energy Shieldings* around objects in order to protect them from *high-energy particles* and *ultra-intense fluxes of radiation*.

In order to explain that possibility, we start from the new expression [1] for the *momentum* q of a particle with gravitational mass M_g and velocity V, which is given by

$$q = M_g V \qquad (74)$$

where $M_g = m_g \Big/ \sqrt{1 - V^2/c^2}$ and $m_g = \chi\, m_i$ [1]. Thus, we can write

$$\frac{m_g}{\sqrt{1 - V^2/c^2}} = \frac{\chi\ m_i}{\sqrt{1 - V^2/c^2}} \qquad (75)$$

Therefore, we get

$$M_g = \chi M_i \qquad (76)$$

It is known from the Relativistic Mechanics that

$$q = \frac{UV}{c^2} \qquad (77)$$

where U is the *total* energy of the particle. This expression is valid for *any* velocity V of the particle, including $V = c$.

By comparing Eq. (77) with Eq. (74) we obtain

$$U = M_g c^2 \qquad (78)$$

It is a well-known experimental fact that

$$M_i c^2 = hf \qquad (79)$$

Therefore, by substituting Eq. (79) and Eq. (76) into Eq. (74), gives

$$q = \frac{V}{c}\chi\frac{h}{\lambda} \qquad (80)$$

Note that this expression is valid for *any* velocity V of the particle. In the particular case of $V = c$, it reduces to

$$q = \chi\frac{h}{\lambda} \qquad (81)$$

By comparing Eq. (80) with Eq. (77), we obtain

$$U = \chi hf \qquad (82)$$

Note that only for $\chi = 1$ the Eq. (81) and Eq. (82) are reduced to the well=known expressions of DeBroglie $(q = h/\lambda)$ and Einstein $(U = hf)$.

Equations (80) and (82) show for example, that *any* real particle (material particles, real photons, etc) that penetrates a region (with density ρ and electrical conductivity σ), where there is an ELF electric field E, will have its *momentum* q and its energy U reduced by the factor χ, given by

$$\chi = \frac{m_g}{m_i} = \left\{1 - 2\left[\sqrt{1 + \frac{\mu}{4c^2}\left(\frac{\sigma}{4\pi f}\right)^3\frac{E^4}{\rho^2}} - 1\right]\right\} \qquad (83)$$

The remaining amount of *momentum* and *energy*, respectively given by $(1-\chi)\left(\frac{V}{c}\right)\frac{h}{\lambda}$ and $(1-\chi)\,hf$, are *transferred to* the *imaginary* particle associated to the *real* particle[§] (material particles or real photons) that penetrated the mentioned region.

It was previously shown that, when the *gravitational mass* of a particle is reduced to ranging between $+0.159M_i$ to $-0.159M_i$, i.e., when $\chi < 0.159$, it becomes *imaginary* [1], i.e., the gravitational and the inertial masses of the particle become *imaginary*. Consequently, the particle disappears from our ordinary space-time. It goes to the Imaginary Universe. On the other hand, when the gravitational mass of the particle becomes greater than $+0.159M_i$, or less than $-0.159M_i$, i.e., when $\chi > 0.159$, the particle return to our Universe.

Figure 19 (a) clarifies the phenomenon of reduction of the *momentum* for $\chi > 0.159$, and Figure 19 (b) shows the effect in the case of $\chi < 0.159$. In this case, the particles become imaginary and consequently, they go to the *imaginary space-time* when they penetrate the electric field E. However, the electric field E stays at the *real* space-time. Consequently, the particles return immediately to the real space-time in order to return soon after to the *imaginary* space-time, due to the action of the electric field E. Since the particles are moving at a direction, they *appear* and *disappear* while they are crossing the region, up to collide with the plate (See Fig.19) with a *momentum,* $q_m = \chi\left(\frac{V}{c}\right)\frac{h}{\lambda}$, in the case of the *material particle*, and $q_r = \chi\frac{h}{\lambda}$ in the case of the *photon*. Note that by making $\chi \cong 0$, it is possible to block high-energy particles and ultra-intense fluxes of radiation. These *Energy Shieldings* can be built around objects in order to protect them from such particles and radiation.

It is also important to note that the gravity control process described here points to the possibility of obtaining *Controlled Nuclear Fusion* by means of increasing of the intensity of the gravitational interaction between the nuclei. When the gravitational forces $F_G = Gm_g m'_g/r^2$ become greater than the electrical forces $F_E = qq'/4\pi\varepsilon_0 r^2$ between the nuclei, then nuclear fusion reactions can occur.

Note that, according to Eq. (83), the gravitational mass can be strongly increased. Thus, if $E = E_m \sin\omega t$, then the average value for E^2 is equal to $\frac{1}{2}E_m^2$, because E varies sinusoidaly (E_m is the maximum value for E). On the other hand, $E_{rms} = E_m/\sqrt{2}$. Consequently, we can replace

[§] As previously shown, there are *imaginary particles* associated to each *real particle* [1].

E^4 for E_{rms}^4. In addition, as $j = \sigma E$ (*Ohm's vectorial Law*), then Eq. (83) can be rewritten as follows

$$\chi = \frac{m_g}{m_{i0}} = \left\{1 - 2\left[\sqrt{1 + K\frac{\mu_r j_{rms}^4}{\sigma\rho^2 f^3}} - 1\right]\right\} \qquad (84)$$

where $K = 1.758\times10^{-27}$ and $j_{rms} = j/\sqrt{2}$.

Thus, the gravitational force equation can be expressed by

$$F_G = Gm_g m_g'/r^2 = \chi^2 Gm_{i0}m_{i0}'/r^2 =$$
$$= \left\{1 - 2\left[\sqrt{1 + K\frac{\mu_r j_{rms}^4}{\sigma\rho^2 f^3}} - 1\right]\right\}^2 Gm_{i0}m_{i0}'/r^2 \qquad (85)$$

In order to obtain $F_G > F_E$ we must have

$$\left\{1 - 2\left[\sqrt{1 + K\frac{\mu_r j_{rms}^4}{\sigma\rho^2 f^3}} - 1\right]\right\} > \sqrt{\frac{qq'/4\pi\varepsilon_0}{Gm_{i0}m_{i0}'}} \qquad (86)$$

The *carbon fusion* is a set of nuclear fusion reactions that take place in massive stars (at least $8M_{sun}$ at birth). It requires high temperatures ($>5\times10^8 K$) and densities ($>3\times10^9\, kg.m^{-3}$). The principal reactions are:

$$^{12}\mathrm{C} + {}^{12}\mathrm{C} \rightarrow \begin{cases} {}^{23}\mathrm{Na} + \mathrm{p} + 2.24\ \mathrm{MeV} \\ {}^{20}\mathrm{Ne} + \alpha + 4.62\ \mathrm{MeV} \\ {}^{24}\mathrm{Mg} + \gamma + 13.93\ \mathrm{MeV} \end{cases}$$

In the case of Carbon nuclei (^{12}C) of a *thin carbon wire* ($\sigma \cong 4\times10^4 S.m^{-1}$; $\rho = 2.2\times10^3 S.m^{-1}$) Eq. (86) becomes

$$\left\{1 - 2\left[\sqrt{1 + 9.08\times10^{-39}\frac{j_{rms}^4}{f^3}} - 1\right]\right\} > \sqrt{\frac{e^2}{16\pi\varepsilon_0 G m_p^2}}$$

whence we conclude that the condition for the ^{12}C + ^{12}C fusion reactions occur is

$$j_{rms} > 1.7\times10^{18} f^{\frac{3}{4}} \qquad (87)$$

If the electric current through the carbon wire has Extremely-Low Frequency (ELF), for example, if $f = 1\mu Hz$, then the current density, j_{rms}, must have the following value:

$$j_{rms} > 5.4\times10^{13} A.m^{-2} \qquad (88)$$

Since $j_{rms} = i_{rms}/S$ where $S = \pi\phi^2/4$ is the area of the cross section of the wire, we can conclude that, for an *ultra-thin carbon* wire with $10\mu m$-diameter, it is necessary that the current through the wire, i_{rms}, have the following intensity

$$i_{rms} > 4.24\ kA$$

Obviously, this current will *explode* the carbon wire. However, this explosion becomes negligible in comparison with the very strong *gravitational implosion*, which occurs simultaneously due to the enormous increase in intensities of the gravitational forces among the carbon nuclei produced by means of the ELF current through the carbon wire as predicted by Eq. (85). Since, in this case, the gravitational forces among the carbon nuclei become greater than the repulsive electric forces among them the result is the production of ^{12}C + ^{12}C fusion reactions.

Similar reactions can occur by using a *lithium* wire. In addition, it is important to note that j_{rms} is directly proportional to $f^{\frac{3}{4}}$ (Eq. 87). Thus, for example, if $f = 10^{-8} Hz$, the current necessary to produce the nuclear reactions will be $i_{rms} = 130A$.

IV.CONCLUSION

The process described here is clearly the better way in order to control the gravity. This is because the *Gravity Control Cell* in this case is very easy to be built, the cost is low and it works at ambient temperature. The Gravity Control is the starting point for the generation of and detection of *Virtual Gravitational Radiation* (Quantum Gravitational *Transceiver*) also for the construction of the *Gravitational Motor* and the *Gravitational Spacecraft* which includes the system for generation of *artificial gravity* presented in Fig.10 and the *Gravitational Thruster* (Fig.11). While the *Gravitational Transceiver* leads to a new concept in *Telecommunication*, the Gravitational Motor changes the paradigm of *energy conversion* and the Gravitational Spacecraft points to a new concept in *aerospace flight*.

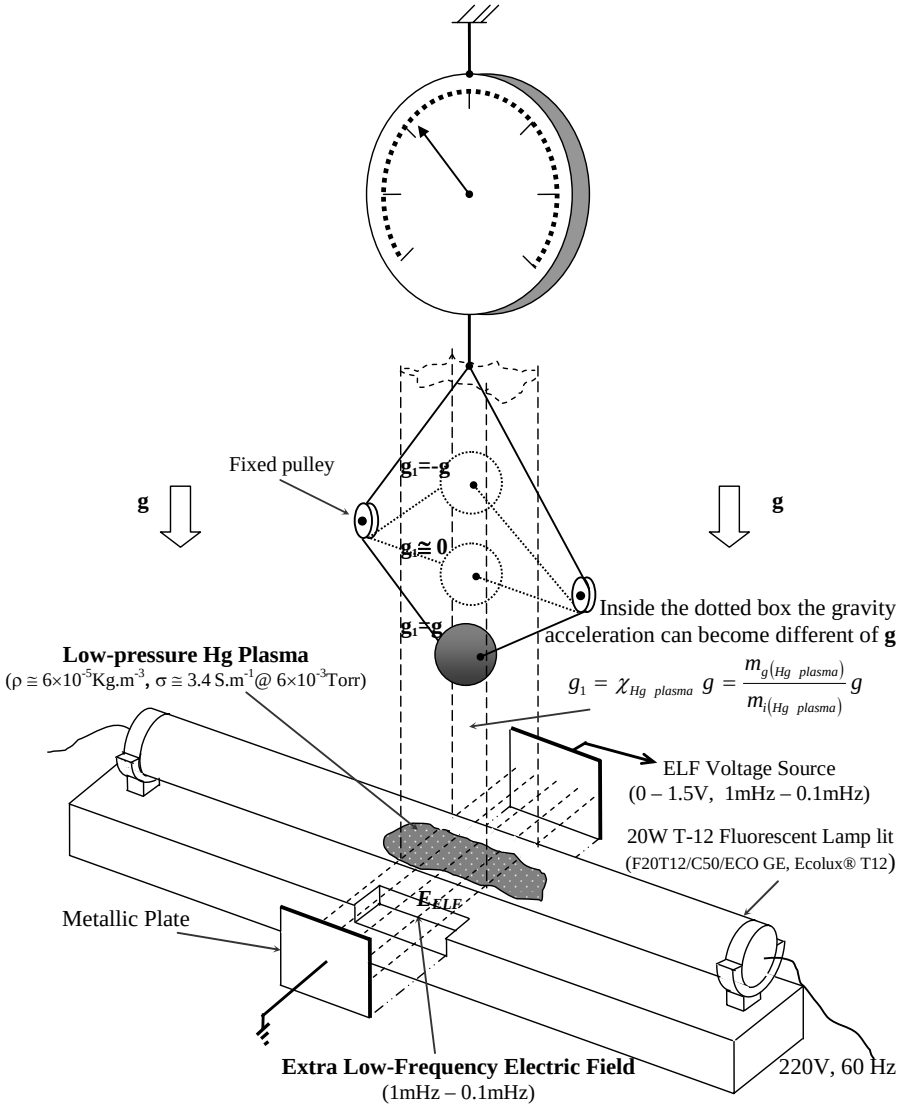

Fig. 1 – Gravitational Shielding Effect by means of an ELF electric field through low- pressure Hg Plasma.

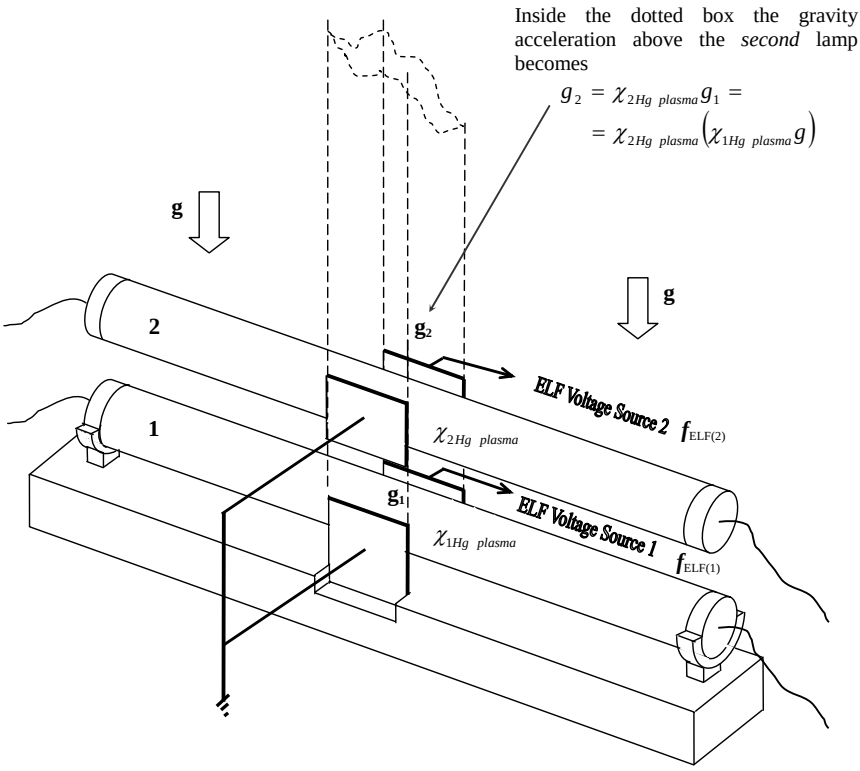

Fig. 2 – Gravity acceleration above a *second* fluorescent lamp.

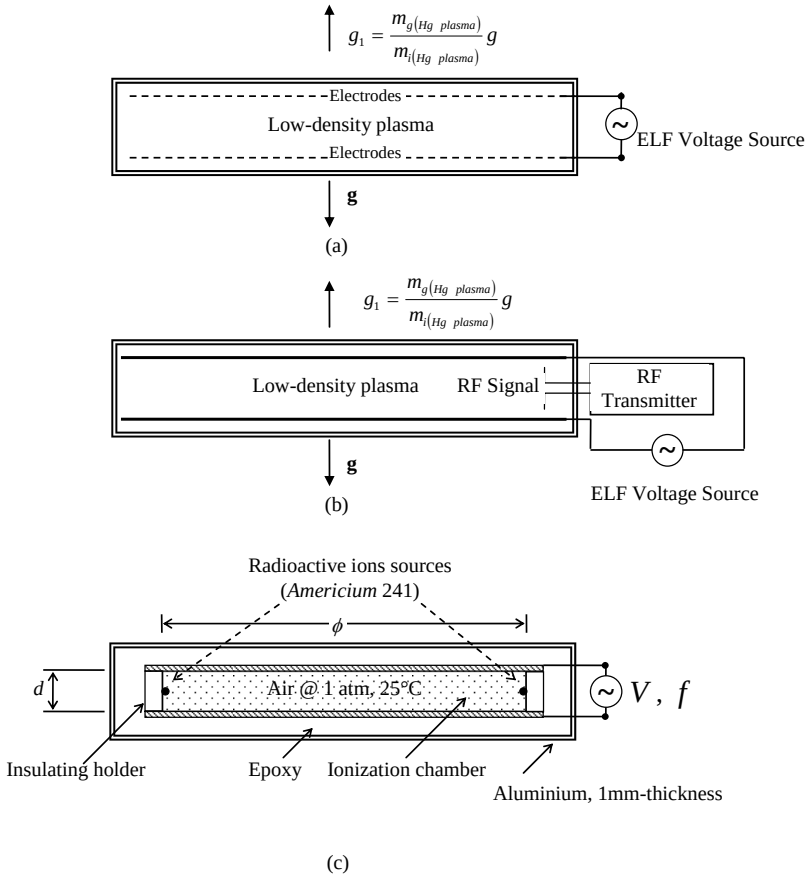

Fig. 3 – *Schematic diagram of Gravity Control Cells (GCCs).*
(a) GCC where the ELF electric field and the ionizing electric field can be the same. (b) GCC where the plasma is ionized by means of a RF signal. (c) GCC filled with *air* (at ambient temperature and 1 atm) strongly ionized by means of alpha particles emitted from radioactive ions sources (Am 241, *half-life* 432 years). Since the electrical conductivity of the ionized air depends on the amount of ions then it can be strongly increased by increasing the amount of Am 241 in the GCC. This GCC has 36 radioactive ions sources each one with $1/5000^{th}$ of gram of Am 241, conveniently positioned around the ionization chamber, in order to obtain $\sigma_{air} \cong 10^3 S.m^{-1}$.

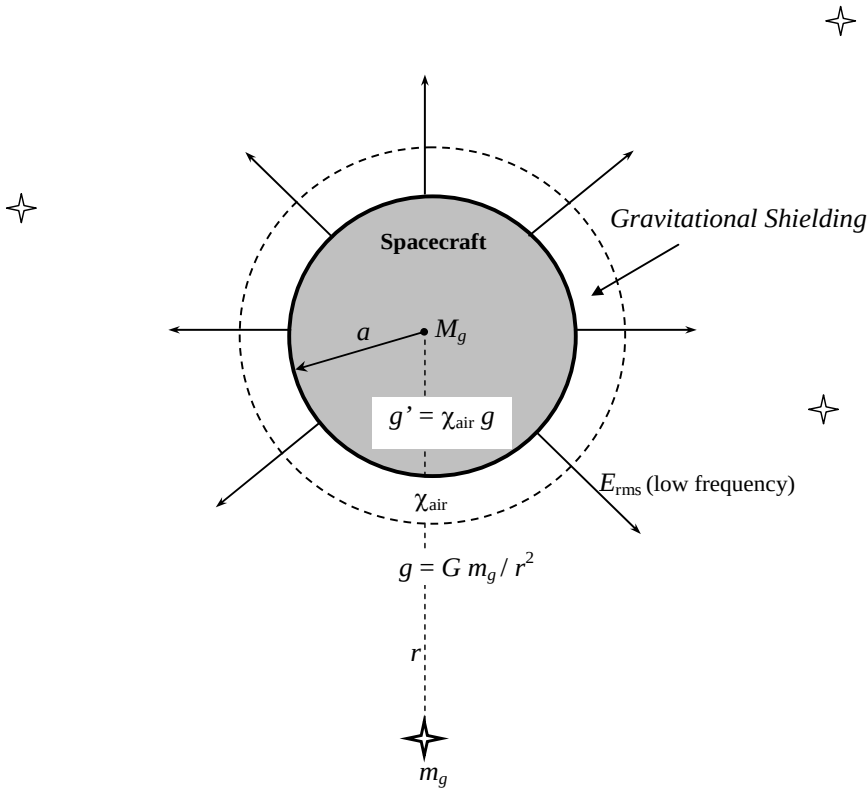

The *gravity accelerations* on the spacecraft (due to the rest of the Universe) can be controlled by means of the *gravitational shielding*, i.e.,

$$g'_i = \chi_{air}\, g_i \qquad i = 1, 2, 3 \ldots n$$

Thus,

$$F_{is} = F_{si} = M_g\, g'_i = M_g\, (\chi_{air}\, g_i)$$

Then the inertial forces acting on the spacecraft (s) can be strongly reduced. According to the *Mach's principle* this effect can reduce *the inertial properties of the spacecraft* and consequently, leads to a new concept of spacecraft and aerospace flight.

Fig. 4 – Gravitational Shielding surround a Spherical Spacecraft.

$V = V_0$ (Volts)	t = T /4		$E_{ELF\,(1)}$ (V/m)	$f_{ELF\,(1)}$ (mHz)	g_1/g		$E_{ELF\,(2)}$ (V/m)	$f_{ELF\,(2)}$ (mHz)	g_2/g	
	(s)	(min)			Exp.	Teo.			Exp.	Teo.
1.0 V	250	**4.17**	24.81	1	-	**0.993**	24.81	1	-	**0.986**
	312.5	**5.21**	24.81	0.8	-	**0.986**	24.81	0.8	-	**0.972**
	416.6	**6.94**	24.81	0.6	-	**0.967**	24.81	0.6	-	**0.935**
	625	**10.42**	24.81	0.4	-	**0.890**	24.81	0.4	-	**0.792**
	1250	**20.83**	24.81	0.2	-	**0.240**	24.81	0.2	-	**0.058**
1.5V	250	**4.17**	37.22	1	-	**0.964**	37.22	1	-	**0.929**
	312.5	**5.21**	37.22	0.8	-	**0.930**	37.22	0.8	-	**0.865**
	416.6	**6.94**	37.22	0.6	-	**0.837**	37.22	0.6	-	**0.700**
	625	**10.42**	37.22	0.4	-	**0,492**	37.22	0.4	-	**0.242**
	1250	**20.83**	37.22	0.2	-	**-1,724**	37.22	0.2	-	**2.972**

Table 1 – Theoretical Results.

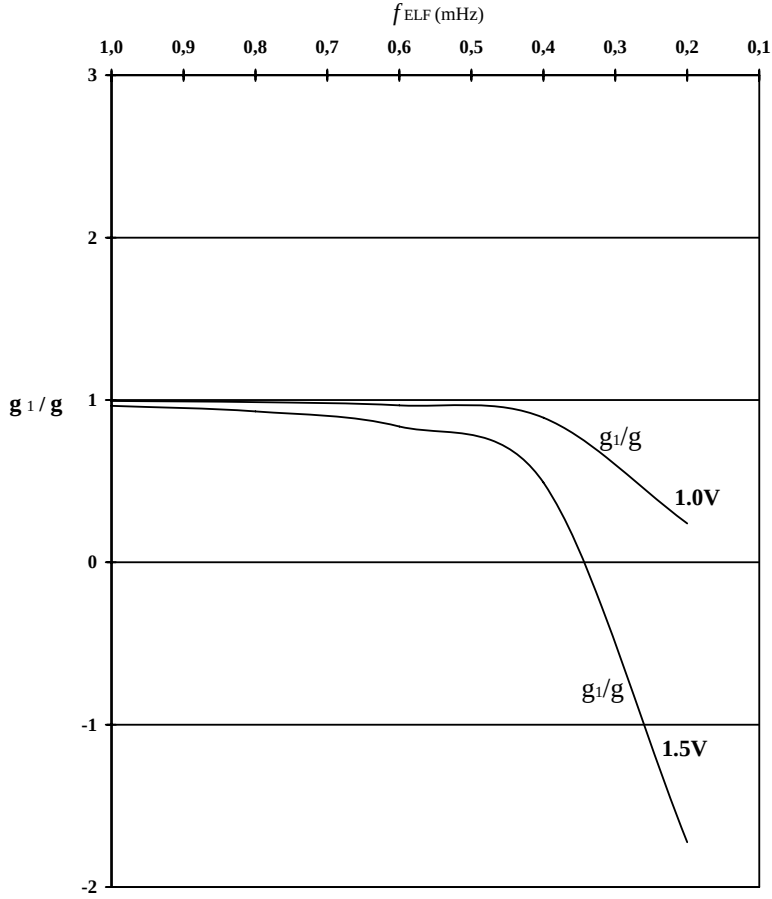

Fig. 5- Distribution of the correlation $\mathbf{g}_1/\mathbf{g}$ as a function of f_{ELF}

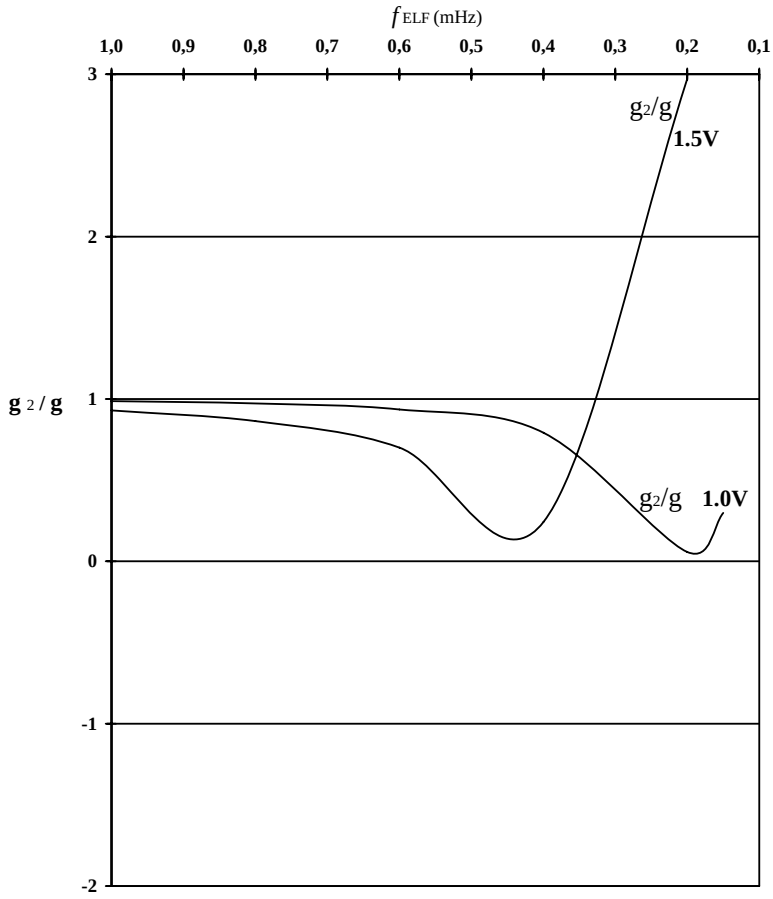

Fig. 6- Distribution of the correlation $\mathbf{g}_2 / \mathbf{g}$ as a function of f_{ELF}

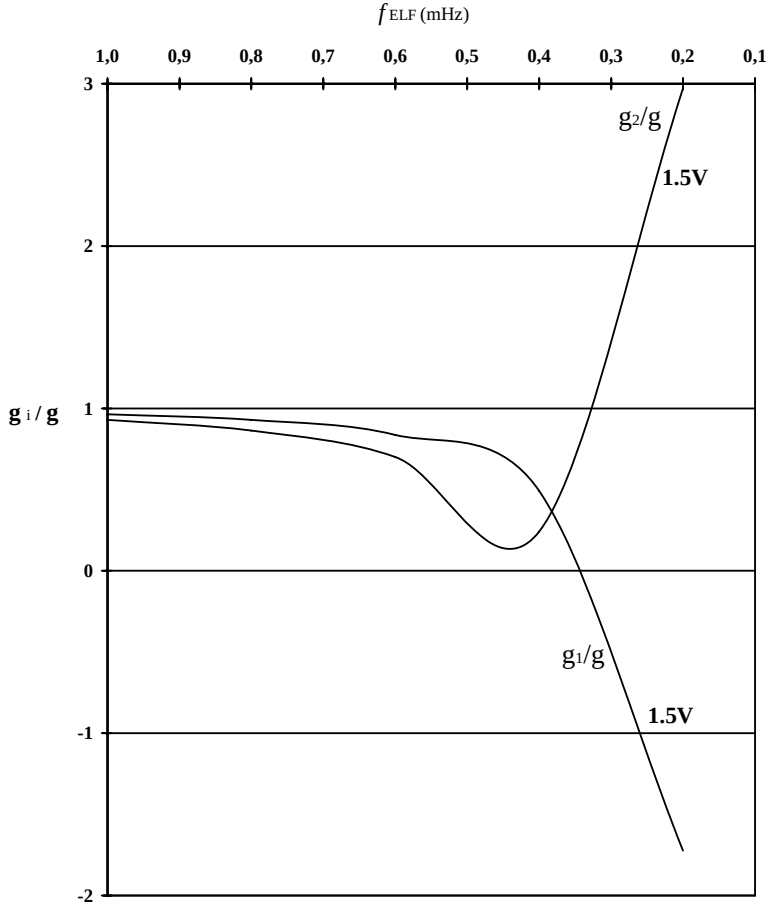

Fig. 7- Distribution of the correlations $\mathbf{g}_i / \mathbf{g}$ as a function of f_{ELF}

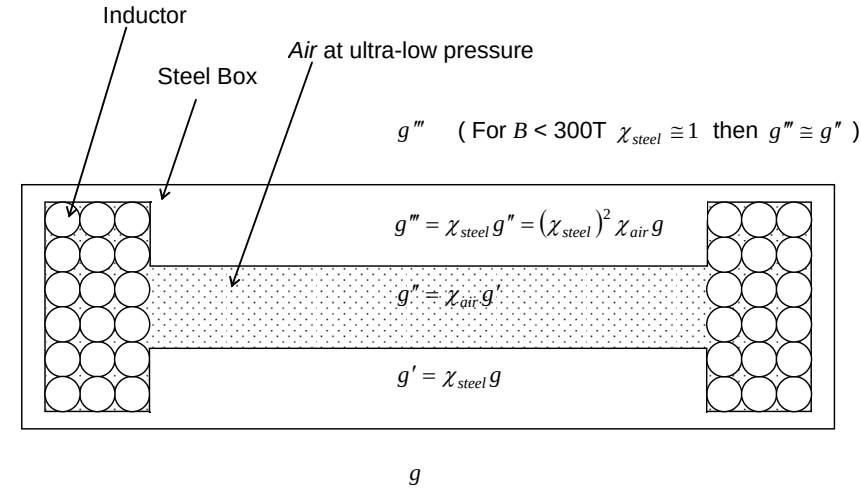

(a)

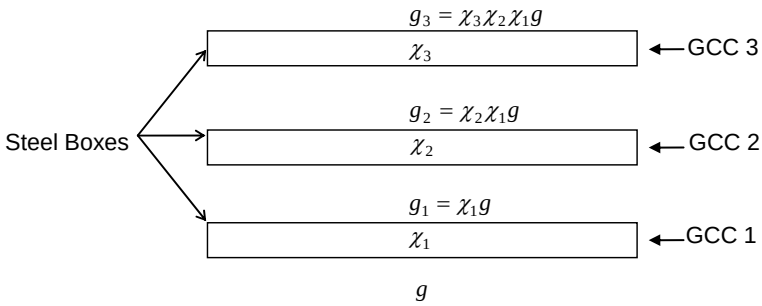

(b)

Fig. 8 – (a) Gravity Control Cell (GCC) filled with *air* at ultra-low pressure.
(b) Gravity Control Battery (Note that if $\chi_1 = \chi_2^{-1} = -1$ then $g'' = g$)

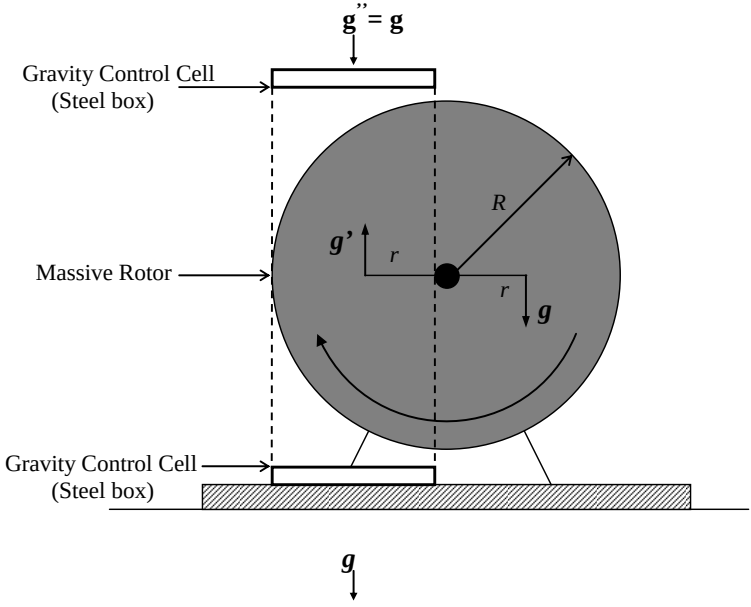

Note that $g' = (\chi_{steel})^2 \chi_{air} g$ and $g'' = (\chi_{steel})^4 (\chi_{air})^2 g$ therefore for $\chi_{steel} \cong 1$ and $\chi_{air(1)} = \chi^{-1}_{air(2)} = -n$ we get $g' \cong -ng$ and $g'' = g$

Fig. 9 – The Gravitational Motor

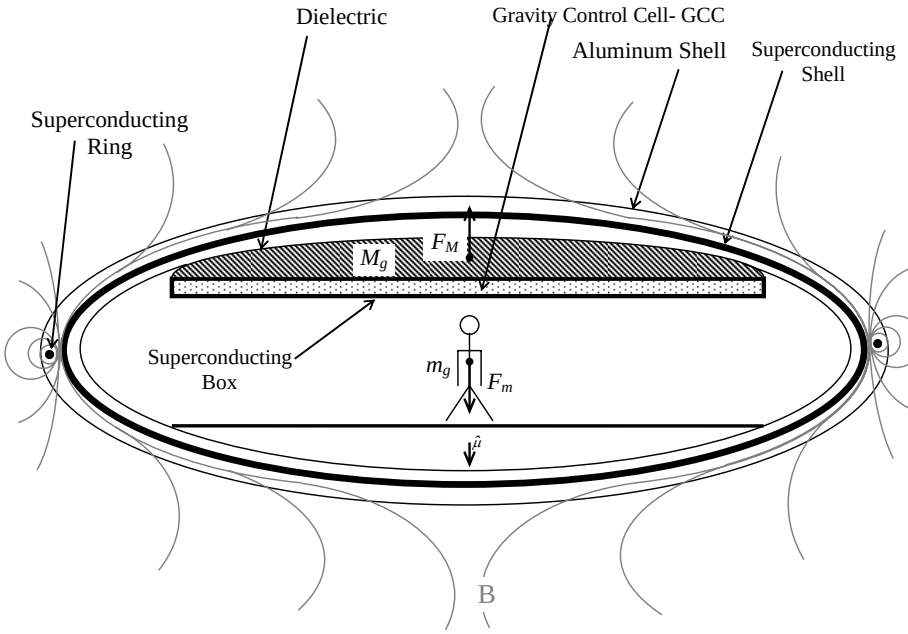

Fig. 10 – The Gravitational Spacecraft – Due to the *Meissner effect*, the magnetic field B is expelled from the *superconducting shell*. Similarly, the magnetic field B_{GCC}, of the GCC stay confined inside the *superconducting box*.

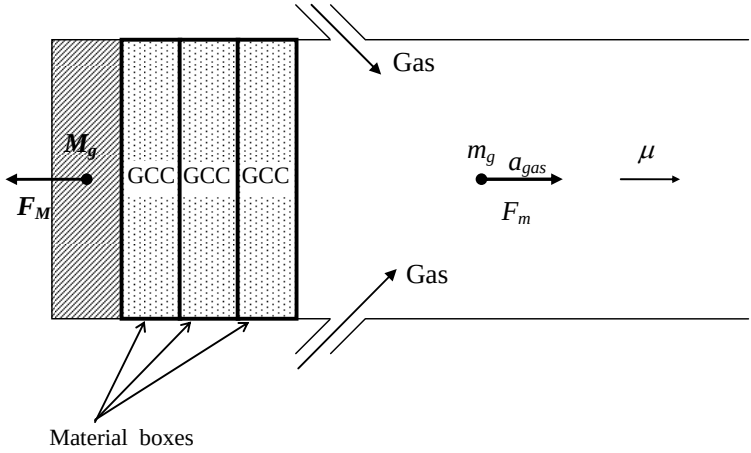

(a)

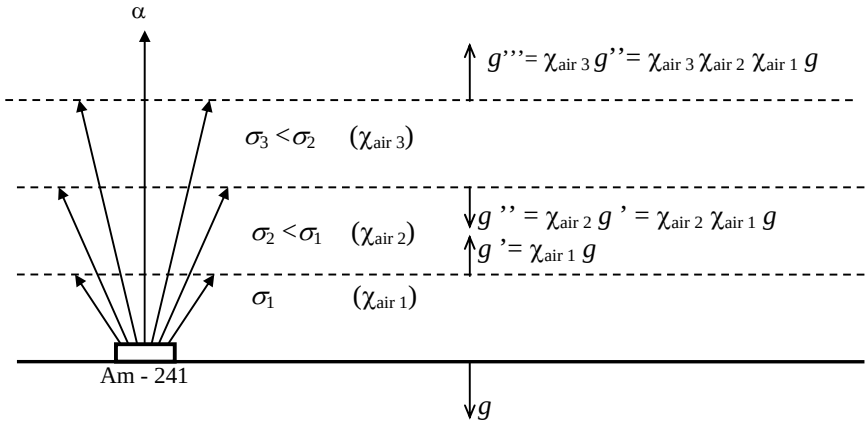

(b)

Fig. 11 – The Gravitational Thruster .
(a) Using material boxes. (b) Without material boxes

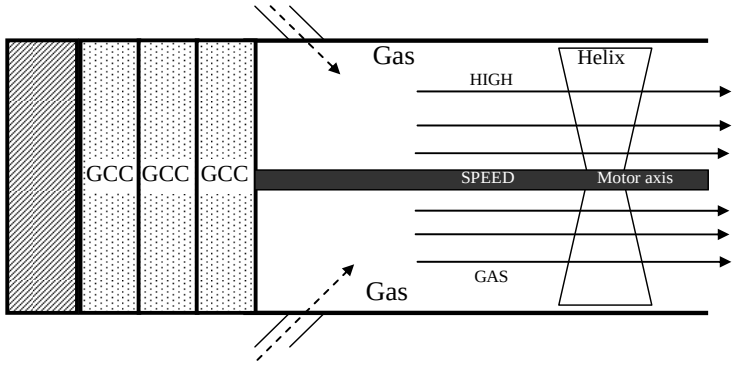

Fig. 12 - The Gravitational Turbo Motor – The gravitationally accelerated gas, by means of the GCCs, propels the helix which movies the motor axis.

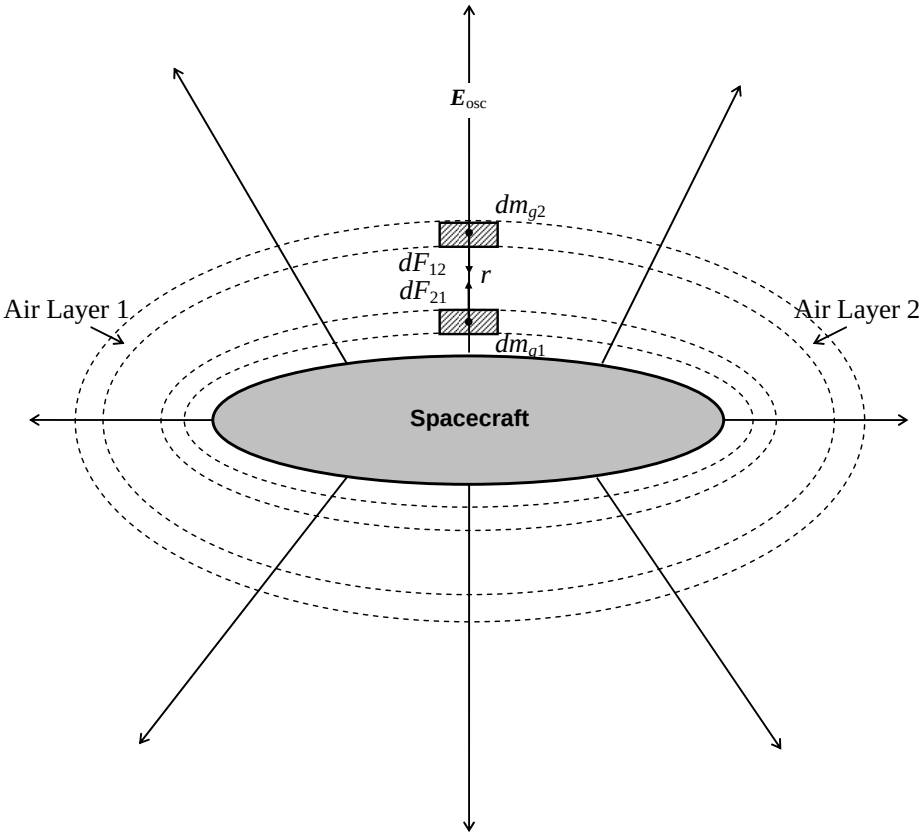

Fig. 13 – Gravitational forces between two layers of the "*air shell*". The electric field $\boldsymbol{E}_{osc}$ provides the *ionization* of the *air*.

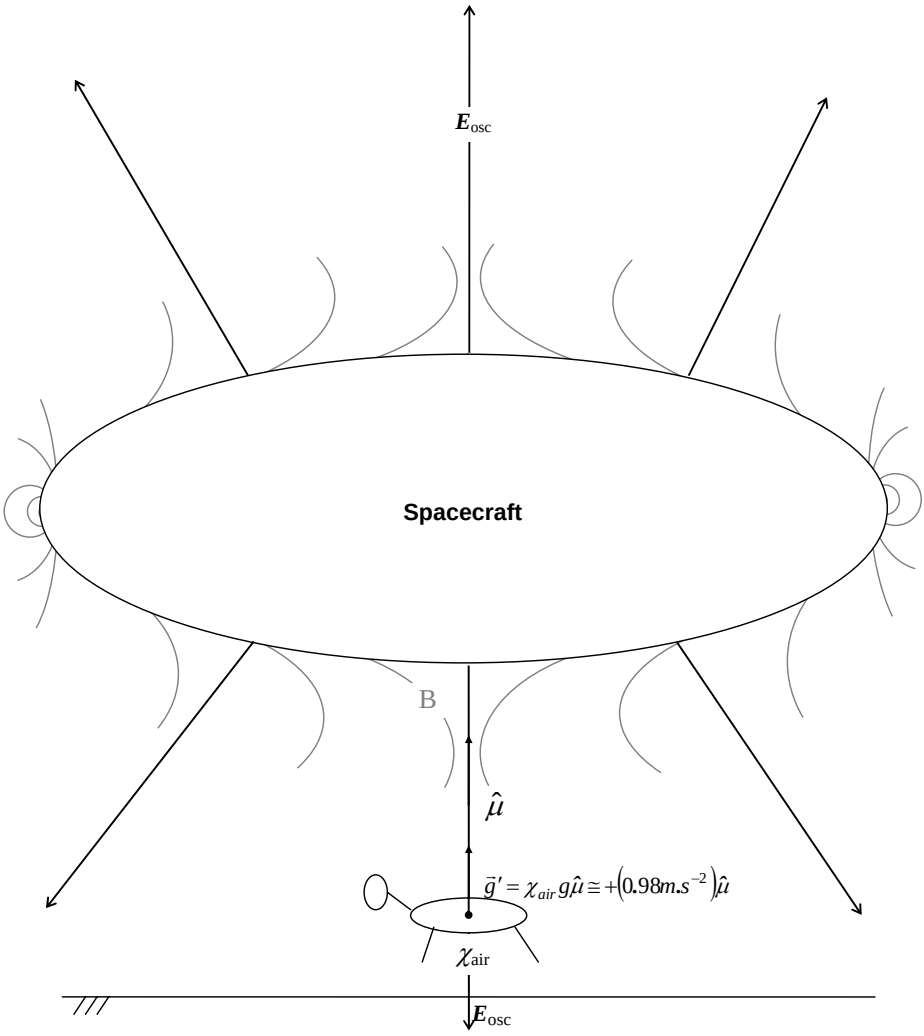

Fig. 14 – The Gravitational Lifter

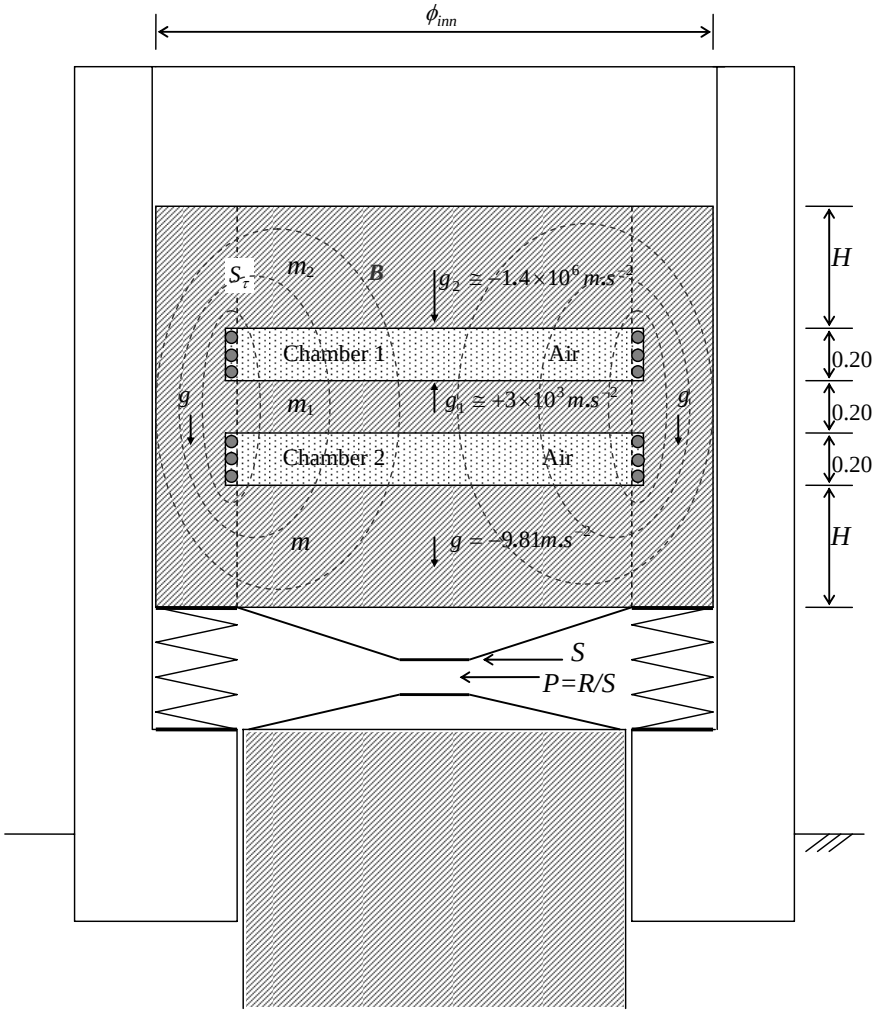

Fig. 15 – *Gravitational Press*

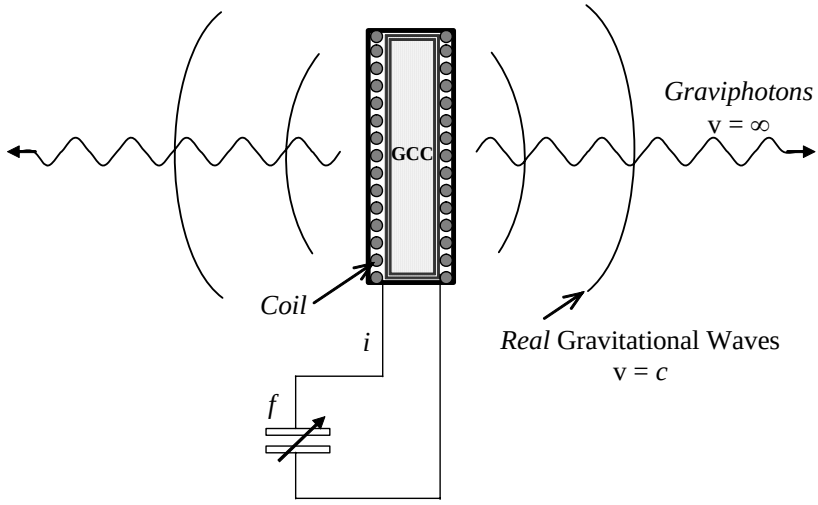

(a) GCC Antenna

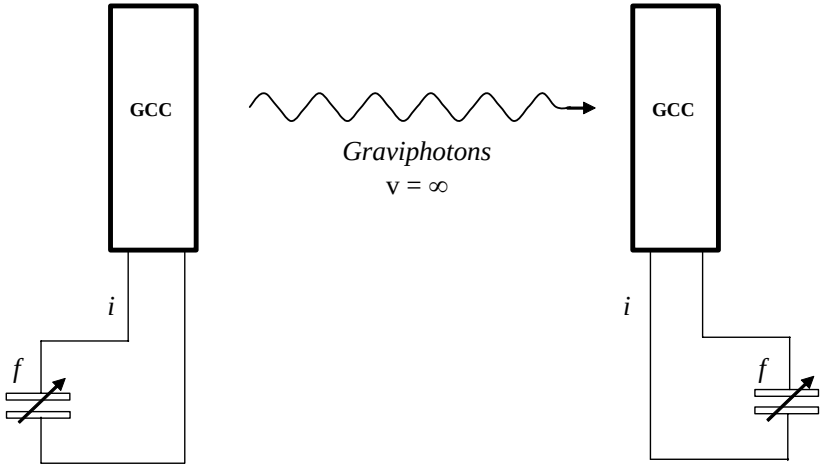

Fig. 16 - Transmitter and Receiver of *Virtual* Gravitational Radiation.

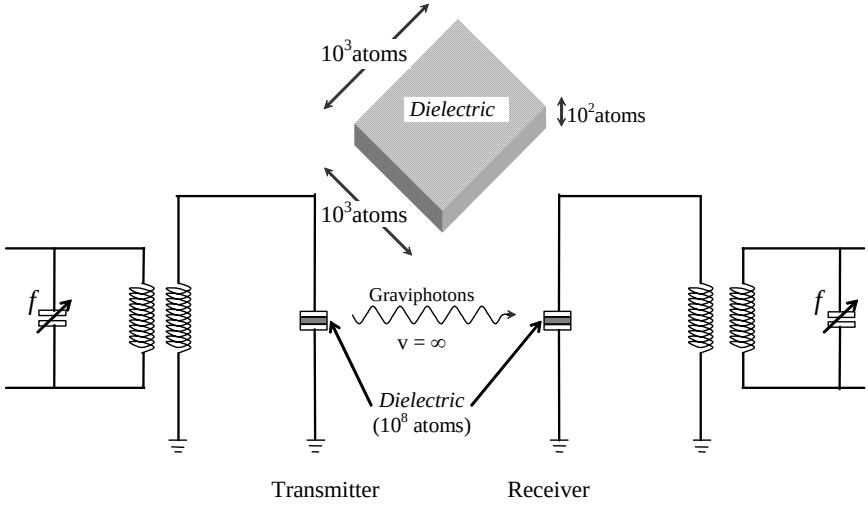

(a)

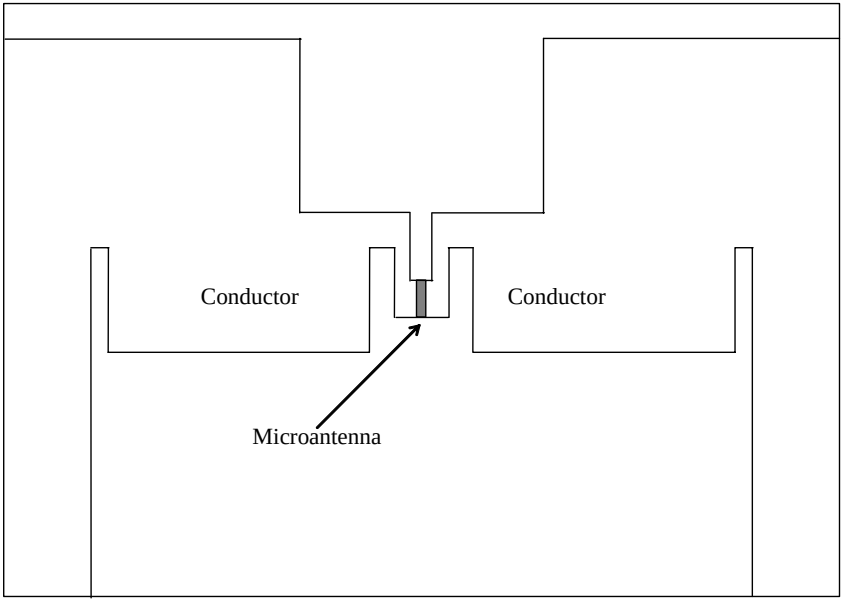

(b)

Fig. 17 – Quantum Gravitational Microantenna

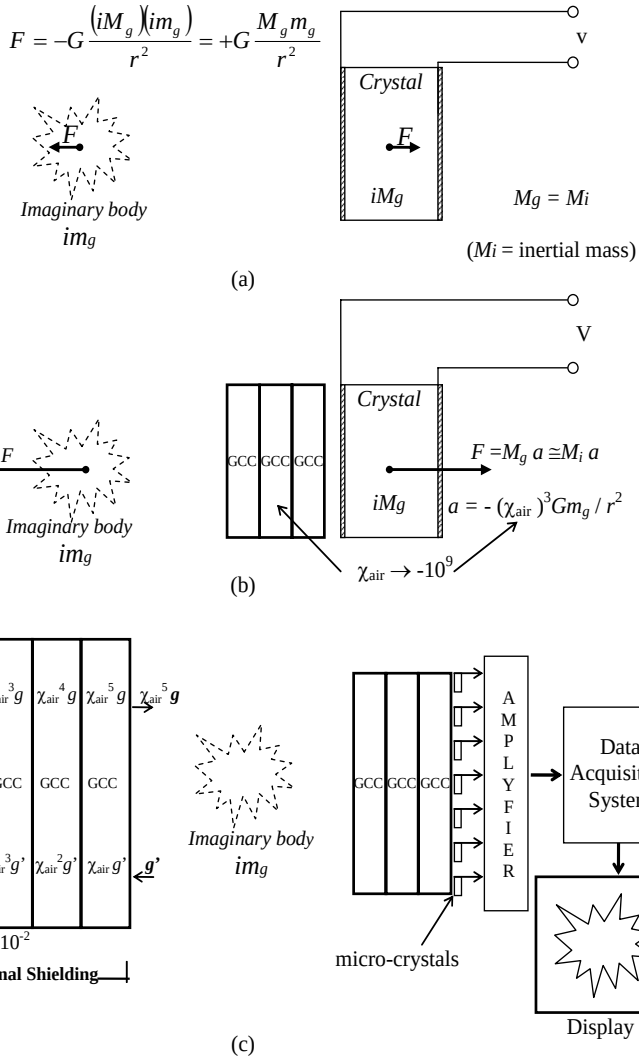

Fig.18 – Method and device using GCCs for obtaining *images* of *imaginary bodies*.

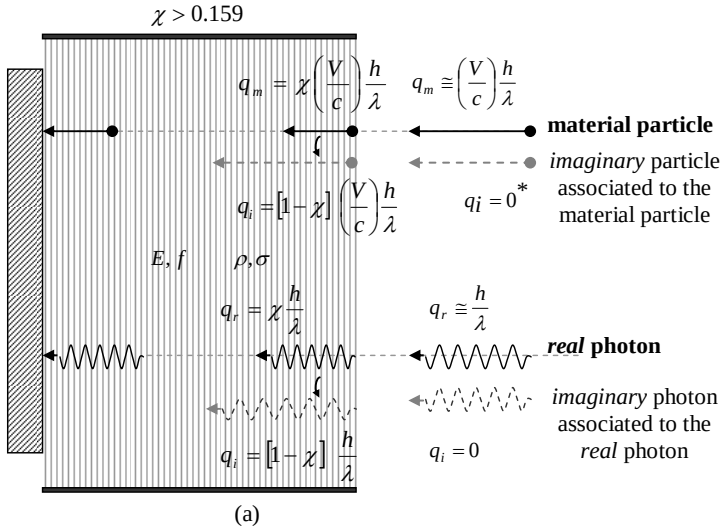

(a)

* There are a type of neutrino, called "ghost" neutrino, predicted by General Relativity, with *zero mass* and *zero momentum*. In spite its *momentum be zero*, it is known that there are wave functions that describe these neutrinos and that prove that really they exist.

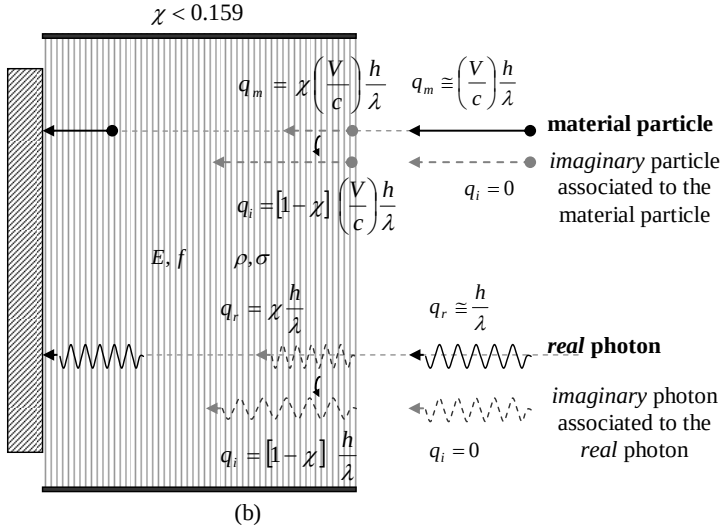

(b)

Fig. 19 – *The phenomenon of reduction of the momentum*. (a) Shows the reduction of *momentum* for $\chi > 0.159$. (b) Shows the effect when $\chi < 0.159$. Note that in both cases, the *material* particles collide with the cowl with the *momentum* $q_m = \chi(V/c)(h/\lambda)$, and the photons with $q_r = \chi\frac{h}{\lambda}$. Therefore, that by making $\chi \cong 0$, it is possible to block high-energy particles and ultra-intense fluxes of radiation.

APPENDIX A: THE SIMPLEST METHOD TO CONTROL THE GRAVITY

In this Appendix we show the simplest method to control the gravity.

Consider a body with mass density ρ and the following electric characteristics: $\mu_r, \varepsilon_r, \sigma$ (relative permeability, relative permittivity and electric conductivity, respectively). Through this body, passes an electric current I, which is the sum of a sinusoidal current $i_{osc} = i_0 \sin \omega t$ and the DC current I_{DC}, i.e., $I = I_{DC} + i_0 \sin \omega t$; $\omega = 2\pi f$. If $i_0 << I_{DC}$ then $I \cong I_{DC}$. Thus, the current I varies with the frequency f, but the variation of its intensity is quite small in comparison with I_{DC}, i.e., I will be practically constant (Fig. 1A). This is of fundamental importance for maintaining the value of the gravitational mass of the body, m_g, sufficiently stable during all the time.

The *gravitational mass* of the *body* is given by [1]

$$m_g = \left\{1 - 2\left[\sqrt{1 + \left(\frac{n_r U}{m_{i0} c^2}\right)^2} - 1\right]\right\} m_{i0} \qquad (A1)$$

where U, is the electromagnetic energy absorbed by the body and n_r is the index of refraction of the body.

Equation (A1) can also be rewritten in the following form

$$\frac{m_g}{m_{i0}} = \left\{1 - 2\left[\sqrt{1 + \left(\frac{n_r W}{\rho\, c^2}\right)^2} - 1\right]\right\} \qquad (A2)$$

where, $W = U/V$ is the *density of electromagnetic energy* and $\rho = m_{i0}/\mathrm{V}$ is the density of inertial mass.

The *instantaneous values* of the density of electromagnetic energy in an *electromagnetic* field can be deduced from Maxwell's equations and has the following expression

$$W = \tfrac{1}{2}\varepsilon E^2 + \tfrac{1}{2}\mu H^2 \qquad (A3)$$

where $E = E_m \sin \omega t$ and $H = H \sin \omega t$ are the *instantaneous values* of the electric field and the magnetic field respectively.

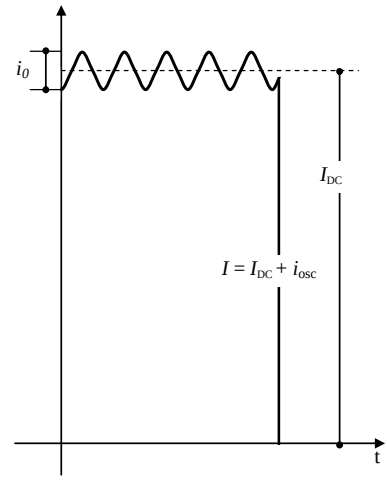

Fig. A1 - The electric current I varies with frequency f. But the variation of I is quite small in comparison with I_{DC} due to $i_o << I_{DC}$. In this way, we can consider $I \cong I_{DC}$.

It is known that $B = \mu H$, $E/B = \omega/k_r$ [11] and

$$v = \frac{dz}{dt} = \frac{\omega}{\kappa_r} = \frac{c}{\sqrt{\frac{\varepsilon_r \mu_r}{2}\left(\sqrt{1 + (\sigma/\omega\varepsilon)^2} + 1\right)}} \qquad (A4)$$

where k_r is the real part of the *propagation vector* $\vec{k}$ (also called *phase constant*); $k = |\vec{k}| = k_r + ik_i$; ε, μ and σ, are the electromagnetic characteristics of the medium in which the incident (or emitted) radiation is propagating($\varepsilon = \varepsilon_r \varepsilon_0$; $\varepsilon_0 = 8.854 \times 10^{-12} F/m$; $\mu = \mu_r \mu_0$ where $\mu_0 = 4\pi \times 10^{-7} H/m$). It is known that for *free-space* $\sigma = 0$ and $\varepsilon_r = \mu_r = 1$. Then Eq. (A4) gives

$$v = c$$

From (A4), we see that the *index of refraction* $n_r = c/v$ is given by

$$n_r = \frac{c}{v} = \sqrt{\frac{\varepsilon_r \mu_r}{2}\left(\sqrt{1 + (\sigma/\omega\varepsilon)^2} + 1\right)} \qquad (A5)$$

Equation (A4) shows that $\omega/\kappa_r = v$. Thus, $E/B = \omega/k_r = v$, i.e.,

$$E = vB = v\mu H \qquad (A6)$$

Then, Eq. (A3) can be rewritten in the following form:

$$W = \tfrac{1}{2}\left(\varepsilon v^2\mu\right)\mu H^2 + \tfrac{1}{2}\mu H^2 \qquad (A7)$$

For $\sigma << \omega\varepsilon$, Eq. (A4) reduces to

$$v = \frac{c}{\sqrt{\varepsilon_r \mu_r}}$$

Then, Eq. (A7) gives

$$W = \tfrac{1}{2}\left[\varepsilon\left(\frac{c^2}{\varepsilon_r\mu_r}\right)\mu\right]\mu H^2 + \tfrac{1}{2}\mu H^2 = \mu H^2$$

This equation can be rewritten in the following forms:

$$W = \frac{B^2}{\mu} \qquad (A8)$$

or

$$W = \varepsilon\ E^2 \qquad (A9)$$

For $\sigma >> \omega\varepsilon$, Eq. (A4) gives

$$v = \sqrt{\frac{2\omega}{\mu\sigma}} \qquad (A10)$$

Then, from Eq. (A7) we get

$$W = \tfrac{1}{2}\left[\varepsilon\left(\frac{2\omega}{\mu\sigma}\right)\mu\right]\mu H^2 + \tfrac{1}{2}\mu H^2 = \left(\frac{\omega\varepsilon}{\sigma}\right)\mu H^2 + \tfrac{1}{2}\mu H^2 \cong$$

$$\cong \tfrac{1}{2}\mu H^2 \qquad (A11)$$

Since $E = vB = v\mu H$, we can rewrite (A11) in the following forms:

$$W \cong \frac{B^2}{2\mu} \qquad (A12)$$

or

$$W \cong \left(\frac{\sigma}{4\omega}\right)E^2 \qquad (A13)$$

By comparing equations (A8) (A9) (A12) and (A13), we can see that Eq. (A13) shows that the best way to obtain a strong value of W *in practice* is by applying an *Extra Low-Frequency* (ELF) *electric field* $\left(w = 2\pi f << 1Hz\right)$ through a *medium with high electrical conductivity*.

Substitution of Eq. (A13) into Eq. (A2), gives

$$m_g = \left\{1 - 2\left[\sqrt{1 + \frac{\mu}{4c^2}\left(\frac{\sigma}{4\pi f}\right)^3\frac{E^4}{\rho^2}} - 1\right]\right\}m_{i0} =$$

$$= \left\{1 - 2\left[\sqrt{1 + \left(\frac{\mu_0}{256\pi^3 c^2}\right)\left(\frac{\mu_r\sigma^3}{\rho^2 f^3}\right)E^4} - 1\right]\right\}m_{i0} =$$

$$= \left\{1 - 2\left[\sqrt{1 + 1.758\times10^{-27}\left(\frac{\mu_r\sigma^3}{\rho^2 f^3}\right)E^4} - 1\right]\right\}m_{i0} \qquad (A14)$$

Note that $E = E_m \sin\omega t$. The average value for E^2 is equal to $\frac{1}{2}E_m^2$ because E varies sinusoidaly (E_m is the maximum value for E). On the other hand, $E_{rms} = E_m/\sqrt{2}$. Consequently, we can change E^4 by E_{rms}^4, and the equation above can be rewritten as follows

$$m_g = \left\{1 - 2\left[\sqrt{1 + 1.758\times10^{-27}\left(\frac{\mu_r\sigma^3}{\rho^2 f^3}\right)E_{rms}^4} - 1\right]\right\}m_{i0}$$

Substitution of the well-known equation of the *Ohm's vectorial Law*: $j = \sigma E$ into (A14), we get

$$m_g = \left\{1 - 2\left[\sqrt{1 + 1.758\times10^{-27}\frac{\mu_r j_{rms}^4}{\sigma\rho^2 f^3}} - 1\right]\right\}m_{i0} \qquad (A15)$$

where $j_{rms} = j/\sqrt{2}$.

Consider a 15 cm square *Aluminum thin foil* of *10.5 microns thickness* with the following characteristics: $\mu_r = 1$; $\sigma = 3.82\times10^7\ S.m^{-1}$; $\rho = 2700\ Kg.m^{-3}$. Then, (A15) gives

$$m_g = \left\{1 - 2\left[\sqrt{1 + 6.313\times10^{-42}\frac{j_{rms}^4}{f^3}} - 1\right]\right\}m_{i0} \qquad (A16)$$

Now, consider that the ELF electric current $I = I_{DC} + i_0 \sin\omega t$, $\left(i_0 << I_{DC}\right)$ passes through that Aluminum foil. Then, the current density is

$$j_{rms} = \frac{I_{rms}}{S} \cong \frac{I_{DC}}{S} \qquad (A17)$$

where

$$S = 0.15m\left(10.5\times10^{-6}\,m\right) = 1.57\times10^{-6}\,m^2$$

If the ELF electric current has frequency $f = 2\mu Hz = 2\times10^{-6}\,Hz$, then, the gravitational mass of the aluminum foil, given by (A16), is expressed by

$$m_g = \left\{1-2\left[\sqrt{1+7.89\times10^{-25}\,\frac{I_{DC}^4}{S^4}}-1\right]\right\}m_{i0} =$$

$$= \left\{1-2\left[\sqrt{1+0.13I_{DC}^4}-1\right]\right\}m_{i0} \qquad (A18)$$

Then,

$$\chi=\frac{m_g}{m_{i0}}\cong\left\{1-2\left[\sqrt{1+0.13I_{DC}^4}-1\right]\right\} \qquad (A19)$$

For $I_{DC}=2.2A$, the equation above gives

$$\chi=\left(\frac{m_g}{m_{i0}}\right)\cong-1 \qquad (A20)$$

This means that *the gravitational shielding* produced by the aluminum foil can change the gravity acceleration *above* the foil down to

$$g'=\chi\ g\cong-1g \qquad (A21)$$

Under these conditions, the Aluminum foil works basically as a Gravity Control Cell (GCC).

In order to check these theoretical predictions, we suggest an experimental set-up shown in Fig.A2.

A 15cm square Aluminum foil of *10.5 microns thickness* with the following composition: Al 98.02%; Fe 0.80%; Si 0.70%; Mn 0.10%; Cu 0.10%; Zn 0.10%; Ti 0.08%; Mg 0.05%; Cr 0.05%, and with the following characteristics: $\mu_t=1$; $\sigma=3.82\times10^7\,S.m^{-1}$; $\rho=2700Kg.m^{-3}$, is fixed on a 17 cm square *Foam Board* [**] plate of 6mm thickness as shown in Fig.A3. This device (the simplest Gravity Control Cell GCC) is placed on a pan balance shown in Fig.A2.

Above the Aluminum foil, a *sample* (any type of material, any mass) connected to a dynamometer will check the decrease of the *local gravity acceleration* upon the sample $\left(g'=\chi\ g\right)$, due to the gravitational shielding produced by the decreasing of gravitational mass of the Aluminum foil $\left(\chi=m_g/m_{i0}\right)$. Initially, the sample lies 5 cm above the Aluminum foil. As shown in Fig.A2, the board with the dynamometer can be displaced up to few meters in height. Thus, the initial distance between the Aluminum foil and the sample can be increased in order to check the reach of the gravitational shielding produced by the Aluminum foil.

In order to generate the ELF electric current of $f=2\mu Hz$, we can use the widely-known Function Generator HP3325A (Op.002 High Voltage Output) that can generate sinusoidal voltages with *extremely-low* frequencies down to $f=1\times10^{-6}Hz$ and amplitude up to 20V ($40V_{pp}$ into 500Ω load). The maximum output current is $0.08A_{pp}$; output impedance <2Ω at ELF.

Figure A4 shows the equivalent electric circuit for the experimental set-up. The electromotive forces are: ε_1 (HP3325A) and ε_2 (*12V* DC Battery).The values of the *resistors* are : $R_1=500\Omega-2W$; $r_{i1}<2\Omega$; $R_2=4\Omega-40W$; $r_{i2}<0.1\Omega$; $R_p=2.5\times10^{-3}\Omega$; *Rheostat* (0≤ *R* ≤10Ω - 90W). The *coupling transformer* has the following characteristics: air core with diameter $\phi=10mm$; area $S=\pi\phi^2/4=7.8\times10^{-5}m^2$; wire#12AWG; $N_1=N_2=N=20$; $l=42mm$; $L_1=L_2=L=\mu_0N^2(S/l)=9.3\times10^{-7}H$ .Thus, we get

$$Z_1=\sqrt{\left(R_1+r_{i1}\right)^2+\left(\omega L\right)^2}\cong501\Omega$$

and

$$Z_2=\sqrt{\left(R_2+r_{i2}+R_p+R\right)^2+\left(\omega L\right)^2}$$

For $R=0$ we get $Z_2=Z_2^{\min}\cong4\Omega$; for $R=10\Omega$ the result is $Z_2=Z_2^{\max}\cong14\Omega$. Thus,

$$Z_{1,total}^{\min}=Z_1+Z_{1,reflected}^{\min}=Z_1+Z_2^{\min}\left(\frac{N_1}{N_2}\right)^2\cong505\Omega$$

$$Z_{1,total}^{\max}=Z_1+Z_{1,reflected}^{\max}=Z_1+Z_2^{\max}\left(\frac{N_1}{N_2}\right)^2\cong515\Omega$$

The maxima *rms* currents have the following values:

$$I_1^{\max}=\tfrac{1}{\sqrt{2}}40V_{pp}\,/\,Z_{1,total}^{\min}=56mA$$

(The maximum output current of the Function Generator HP3325A (Op.002 High Voltage Output) is $80mA_{pp}\cong56.5mA_{rms}$);

$$I_2^{\max}=\frac{\varepsilon_2}{Z_2^{\min}}=3A$$

and

$$I_3^{\max}=I_2^{\max}+I_1^{\max}\cong3A$$

The new expression for the *inertial forces*, (Eq.5) $\vec{F}_i=M_g\vec{a}$, shows that the inertial forces are proportional to *gravitational mass*. Only in the particular case of $m_g=m_{i0}$, the expression above reduces to the well-known Newtonian expression $\vec{F}_i=m_{i0}\vec{a}$. The equivalence

[**] *Foam board* is a very strong, *lightweigh*t (density: 24.03 kg.m^{-3}) and easily cut material used for the mounting of photographic prints, as backing in picture framing, in 3D design, and in painting. It consists of three layers — an inner layer of polystyrene clad with outer facing of either white clay coated paper or brown Kraft paper.

between gravitational and inertial forces $\left(\vec{F}_i \equiv \vec{F}_g\right)$ [1] shows then that a balance measures the *gravitational mass* subjected to acceleration $a = g$. Here, the decrease in the *gravitational mass* of the Aluminum foil will be measured by a pan balance with the following characteristics: range 0-200g; readability 0.01g.

The mass of the Foam Board plate is: $\cong 4.17g$, the mass of the Aluminum foil is: $\cong 0.64g$, the total mass of the ends and the electric wires of connection is $\cong 5g$. Thus, *initially* the balance will show $\cong 9.81g$. According to (A18), when the electric current through the Aluminum foil (resistance $r_p^* = l/\sigma S = 2.5\times10^{-3}\Omega$) reaches the value: $I_3 \cong 2.2A$, we will get $m_{g(Al)} \cong -m_{i0(Al)}$. Under these circumstances, the balance will show:

$$9.81g - 0.64g - 0.64g \cong 8.53g$$

and the gravity acceleration g' *above* the Aluminum foil, becomes $g' = \chi\ g \cong -1g$.

It was shown [1] that, when the gravitational mass of a particle is reduced to the gravitational mass ranging between $+0.159M_i$ to $-0.159M_i$, it becomes *imaginary*, i.e., the gravitational and the inertial masses of the particle become *imaginary*. Consequently, the particle *disappears* from our ordinary space-time. This phenomenon can be observed in the proposed experiment, i.e., *the Aluminum foil will disappear* when its gravitational mass becomes smaller than $+0.159M_i$. It will become visible again, only when its gravitational mass becomes smaller than $-0.159M_i$, or when it becomes greater than $+0.159M_i$.

Equation (A18) shows that the gravitational mass of the Aluminum foil, $m_{g(Al)}$, goes *close to zero* when $I_3 \cong 1.76A$. Consequently, the gravity acceleration *above* the Aluminum foil also goes close to zero since $g' = \chi\ g = m_{g(Al)}/m_{i0(Al)}$. Under these circumstances, the Aluminum foil remains *invisible*.

Now consider a rigid Aluminum wire # 14 AWG. The area of its cross section is

$$S = \pi\left(1.628\times10^{-3}m\right)^2/4 = 2.08\times10^{-6}m^2$$

If an ELF electric current with frequency $f = 2\mu Hz = 2\times10^{-6}Hz$ passes through this wire, its gravitational mass, given by (A16), will be expressed by

$$m_g = \left\{1-2\left[\sqrt{1+6.313\times10^{-42}\frac{j_{rms}^4}{f^3}}-1\right]\right\}m_{i0} =$$

$$= \left\{1-2\left[\sqrt{1+7.89\times10^{-25}\frac{I_{DC}^4}{S^4}}-1\right]\right\}m_{i0} =$$

$$= \left\{1-2\left[\sqrt{1+0.13I_{DC}^4}-1\right]\right\}m_{i0} \qquad (A22)$$

For $I_{DC} \cong 3A$ the equation above gives

$$m_g \cong -3.8m_{i0}$$

Note that we can replace the Aluminum foil for this wire in the experimental set-up shown in Fig.A2. It is important also to note that an ELF electric current that passes through a wire - which makes a spherical form, as shown in Fig A5 - reduces the gravitational mass of the wire (Eq. A22), and the gravity *inside sphere* at the same proportion, $\chi = m_g/m_{i0}$, (Gravitational Shielding Effect). In this case, that effect can be checked by means of the Experimental set-up 2 (Fig.A6). Note that the spherical form can be transformed into an ellipsoidal form or a disc in order to coat, for example, a Gravitational Spacecraft. It is also possible to coat with a wire several forms, such as cylinders, cones, cubes, etc.

The circuit shown in Fig.A4 (a) can be modified in order to produce a new type of Gravitational Shielding, as shown in Fig.A4 (b). In this case, the Gravitational Shielding will be produced in the Aluminum plate, with thickness h, of the parallel plate capacitor connected in the point P of the circuit (See Fig.A4 (b)). Note that, in this circuit, the Aluminum foil (resistance R_p) (Fig.A4(a)) has been replaced by a Copper wire # 14 AWG with *1cm* length ($l = 1cm$) in order to produce a resistance $R_\phi = 5.21\times10^{-5}\Omega$. Thus, the voltage in the point P of the circuit will have the maximum value $V_p^{\max} = 1.1\times10^{-4}V$ when the resistance of the rheostat is null $(R = 0)$ and the minimum value $V_p^{\min} = 4.03\times10^{-5}V$ when $R = 10\Omega$. In this way, the voltage V_p (with frequency $f = 2\mu Hz$) applied on the capacitor will produce an electric field E_p with intensity $E_p = V_p/h$ through the Aluminum plate of thickness $h = 3mm$. It is important to note that *this plate cannot be connected to ground* (earth), in other words, cannot be grounded, because, in

this case, the electric field through it will be *null* [††].

According to Eq. A14, when $E_p^{\max}=V_p^{\max}/h=0.036\,V/m$, $f=2\mu Hz$ and $\sigma_{Al}=3.82\times10^{7}\,S/m$, $\rho_{Al}=2700kg/m^3$ (Aluminum), we get

$$\chi=\frac{m_{(Al)}}{m_{i(Al)}}\cong-0.9$$

Under these conditions, the maximum *current density* through the plate with thickness h will be given by $j^{\max}=\sigma_{Al}E_p^{\max}=1.4\times10^{6}A/m^2$ (It is well-known that the maximum current density supported by the Aluminum is $\approx10^{8}A/m^2$).

Since the area of the plate is $A=(0.2)^2=4\times10^{-2}m^2$, then the maximum current is $i^{\max}=j^{\max}A=56kA$. Despite this enormous current, the maximum dissipated power will be just $P^{\max}=\left(i^{\max}\right)^2R_{plate}=6.2W$, because the resistance of the plate is very small, i.e., $R_{plate}=h/\sigma_{Al}A\cong2\times10^{-9}\Omega$.

Note that the area A of the plate (where the Gravitational Shielding takes place) can have several geometrical configurations. For example, it can be the area of the external surface of an ellipsoid, sphere, etc. Thus, it can be the area of the external surface of a Gravitational Spacecraft. In this case, if $A\cong100m^2$, for example, the maximum dissipated power will be $P^{\max}\cong15.4kW$, i.e., approximately $154W/m^2$.

All of these systems work with Extra-Low Frequencies $\left(f<<10^{-3}Hz\right)$. Now, we show that, by simply changing *the geometry of the surface of the Aluminum foil*, it is possible to increase the working frequency f up to more than *1Hz*.

Consider the Aluminum foil, now with several semi-spheres stamped on its surface, as shown in Fig. A7 . The semi-spheres have radius $r_0=0.9\ mm$, and are joined one to another. The Aluminum foil is now coated by an insulation layer with relative permittivity ε_r and dielectric strength k. A voltage source is connected to the Aluminum foil in order to provide a voltage V_0 (rms) with frequency f. Thus, the electric potential V at a distance r, in the interval from r_0 to a, is given by

$$V=\frac{1}{4\pi\varepsilon_r\varepsilon_0}\frac{q}{r}\qquad(A23)$$

In the interval $a<r\le b$ the electric potential is

$$V=\frac{1}{4\pi\varepsilon_0}\frac{q}{r}\qquad(A24)$$

since for the air we have $\varepsilon_r\cong1$.

Thus, on the surface of the metallic spheres $\left(r=r_0\right)$ we get

$$V_0=\frac{1}{4\pi\varepsilon_r\varepsilon_0}\frac{q}{r_0}\qquad(A25)$$

Consequently, the electric field is

$$E_0=\frac{1}{4\pi\varepsilon_r\varepsilon_0}\frac{q}{r_0^2}\qquad(A26)$$

By comparing (A26) with (A25), we obtain

$$E_0=\frac{V_0}{r_0}\qquad(A27)$$

The electric potential V_b at $r=b$ is

$$V_b=\frac{1}{4\pi\varepsilon_0}\frac{q}{b}=\frac{\varepsilon_rV_0r_0}{b}\qquad(A28)$$

Consequently, the electric field E_b is given by

$$E_b=\frac{1}{4\pi\varepsilon_0}\frac{q}{b^2}=\frac{\varepsilon_rV_0r_0}{b^2}\qquad(A29)$$

From $r=r_0$ up to $r=b=a+d$ *the electric field is approximately constant* (See Fig. A7). Along the distance d it will be called E_{air}. For $r>a+d$, the electric field stops being constant. Thus, the intensity of the electric field at $r=b=a+d$ is approximately equal to E_0, i.e., $E_b\cong E_0$. Then, we can write that

$$\frac{\varepsilon_rV_0r_0}{b^2}\cong\frac{V_0}{r_0}\qquad(A30)$$

whence we get

$$b\cong r_0\sqrt{\varepsilon_r}\qquad(A31)$$

Since the intensity of the electric field through the air, E_{air}, is $E_{air}\cong E_b\cong E_0$, then, we can write that

$$E_{air}=\frac{1}{4\pi\varepsilon_0}\frac{q}{b^2}=\frac{\varepsilon_rV_0r_0}{b^2}\qquad(A32)$$

Note that ε_r refers to the *relative permittivity of*

[††] When the voltage V_p is applied on the capacitor, the charge distribution in the dielectric induces positive and negative charges, respectively on opposite sides of the Aluminum plate with thickness *h*. If the plate is not connected to the ground (Earth) this charge distribution produces an electric field $E_p=V_p/h$ through the plate. However, if the plate is connected to the ground, the negative charges (electrons) escapes for the ground and the positive charges are redistributed along the entire surface of the Aluminum plate making *null* the electric field through it.

the insulation layer, which is covering the Aluminum foil.

If the intensity of this field is greater than the dielectric strength of the air $\left(3\times10^{6}V/m\right)$ there will occur the well-known *Corona effect*. Here, this effect is necessary in order to increase the electric conductivity of the air at this region (layer with thickness *d*). Thus, we will assume

$$E_{air}^{\min}=\frac{\varepsilon_r V_0^{\min} r_0}{b^2}=\frac{V_0^{\min}}{r_0}=3\times10^{6}V/m$$

and

$$E_{air}^{\max}=\frac{\varepsilon_r V_0^{\max} r_0}{b^2}=\frac{V_0^{\max}}{r_0}=1\times10^{7}V/m \quad (A33)$$

The electric field $E_{air}^{\min}\le E_{air}\le E_{air}^{\max}$ will produce an *electrons flux* in a direction and an *ions flux* in an opposite direction. From the viewpoint of electric current, the ions flux can be considered as an "electrons" flux at the same direction of the real electrons flux. Thus, the current density through the air, j_{air}, will be the *double* of the current density expressed by the well-known equation of Langmuir-Child

$$j=\frac{4}{9}\varepsilon_r\varepsilon_0\sqrt{\frac{2e}{m_e}}\frac{V^{\frac{3}{2}}}{d^2}=\alpha\frac{V^{\frac{3}{2}}}{d^2}=2.33\times10^{-6}\frac{V^{\frac{3}{2}}}{d^2} \quad (A34)$$

where $\varepsilon_r\cong1$ for the *air*; $\alpha=2.33\times10^{-6}$ is the called *Child's constant*.

Thus, we have

$$j_{air}=2\alpha\frac{V^{\frac{3}{2}}}{d^2} \quad (A35)$$

where d, in this case, is the thickness of the air layer where the electric field is approximately constant and V is the voltage drop given by

$$V=V_a-V_b=\frac{1}{4\pi\varepsilon_0}\frac{q}{a}-\frac{1}{4\pi\varepsilon_0}\frac{q}{b}=$$

$$=V_0 r_0\varepsilon_r\left(\frac{b-a}{ab}\right)=\left(\frac{\varepsilon_r r_0 d}{ab}\right)V_0 \quad (A36)$$

By substituting (A36) into (A35), we get

$$j_{air}=\frac{2\alpha}{d^2}\left(\frac{\varepsilon_r r_0 d V_0}{ab}\right)^{\frac{3}{2}}=\frac{2\alpha}{d^{\frac{1}{2}}}\left(\frac{\varepsilon_r r_0 V_0}{b^2}\right)^{\frac{3}{2}}\left(\frac{b}{a}\right)^{\frac{3}{2}}=$$

$$=\frac{2\alpha}{d^{\frac{1}{2}}}E_{air}^{\frac{3}{2}}\left(\frac{b}{a}\right)^{\frac{3}{2}} \quad (A37)$$

According to the equation of the *Ohm's vectorial Law*: $j=\sigma E$, we can write that

$$\sigma_{air}=\frac{j_{air}}{E_{air}} \quad (A38)$$

Substitution of (A37) into (A38) yields

$$\sigma_{air}=2\alpha\left(\frac{E_{air}}{d}\right)^{\frac{1}{2}}\left(\frac{b}{a}\right)^{\frac{3}{2}} \quad (A39)$$

If the insulation layer has thickness $\Delta=0.6\ mm$, $\varepsilon_r\cong3.5$ (1- 60Hz), $k=17kV/mm$ (Acrylic sheet 1.5mm thickness), and the semi-spheres stamped on the metallic surface have $r_0=0.9\ mm$ (See Fig.A7) then $a=r_0+\Delta=1.5\ mm$. Thus, we obtain from Eq. (A33) that

$$V_0^{\min}=2.7kV$$

$$V_0^{\max}=9kV \quad (A40)$$

From equation (A31), we obtain the following value for b:

$$b=r_0\sqrt{\varepsilon_r}=1.68\times10^{-3}m \quad (A41)$$

Since $b=a+d$ we get

$$d=1.8\times10^{-4}m$$

Substitution of a, b, d and A(32) into (A39) produces

$$\sigma_{air}=4.117\times10^{-4}E_{air}^{\frac{1}{2}}=1.375\times10^{-2}V_0^{\frac{1}{2}}$$

Substitution of σ_{air}, $E_{air}(rms)$ and $\rho_{air}=1.2\ kg.m^{-3}$ into (A14) gives

$$\frac{m_{g(air)}}{m_{i0(air)}}=\left\{1-2\left[\sqrt{1+1.758\times10^{-27}\frac{\sigma_{air}^3E_{air}^4}{\rho_{air}^2f^3}}-1\right]\right\}=$$

$$=\left\{1-2\left[\sqrt{1+4.923\times10^{-21}\frac{V_0^{5.5}}{f^3}}-1\right]\right\} \quad (A42)$$

For $V_0=V_0^{\max}=9kV$ and $f=2Hz$, the result is

$$\frac{m_{g(air)}}{m_{i0(air)}}\cong-1.2$$

Note that, by increasing V_0, the values of E_{air} and σ_{air} are increased. Thus, as show (A42), there are two ways for decrease the value of $m_{g(air)}$: increasing the value of V_0 or decreasing the value of f.

Since $E_0^{\max}=10^7V/m=10kV/mm$ and $\Delta=0.6\ mm$ then the dielectric strength of the insulation must be $\ge16.7kV/mm$. As mentioned above, the dielectric strength of the acrylic is $17kV/mm$.

It is important to note that, due to the strong value of E_{air} (Eq. A37) the *drift velocity* v_d, $\left(v_d=j_{air}/ne=\sigma_{air}E_{air}/ne\right)$ of the free charges inside the ionized air put them at a

distance $x = v_d / t = 2 f v_d \cong 0.4m$, which is much greater than the distance $d = 1.8 \times 10^{-4} m$. Consequently, the number n of free charges decreases strongly inside the air layer of thickness d [‡‡], except, obviously, in a thin layer, very close to the dielectric, where the number of free charges remains sufficiently increased, to maintain the air conductivity with $\sigma_{air} \cong 1.1 S/m$ (Eq. A39).

The thickness h of this thin air layer close to the dielectric can be easily evaluated starting from the charge distribution in the neighborhood of the dielectric, and of the repulsion forces established among them. The result is $h = \sqrt{0.06e / 4\pi\varepsilon_0 E} \cong 4 \times 10^{-9} m$. This is, therefore, the thickness of the *Air* Gravitational Shielding. If the area of this Gravitational Shielding is equal to the area of a format A4 sheet of paper, i.e., $A = 0.20 \times 0.291 = 0.0582 m^2$, we obtain the following value for the resistance R_{air} of the Gravitational Shielding: $R_{air} = h / \sigma_{air} A \cong 6 \times 10^{8} \Omega$. Since the maximum electrical current through this air layer is $i^{\max} = j^{\max} A \cong 400 kA$, then the maximum power radiated from the Gravitational Shielding is $P_{air}^{\max} = R_{air} \left(i_{air}^{\max} \right)^2 \cong 10 kW$. This means that a very strong light will be radiated from this type of Gravitational Shielding. Note that this device can also be used as a lamp, which will be much more efficient than conventional lamps.

Coating a ceiling with this lighting system enables the entire area of ceiling to produce light. This is a form of lighting very different from those usually known.

Note that the value $P_{air}^{\max} \cong 10 kW$, defines the power of the transformer shown in Fig.A10. Thus, the maximum current in the secondary is $i_s^{\max} = 9 kV / 10 kW = 0.9 A$.

Above the Gravitational Shielding, σ_{air} is reduced to the normal value of conductivity of the atmospheric air $\left(\approx 10^{-14} S/m \right)$. Thus, the power radiated from this region is

$$P_{air}^{\max} = (d - h) \left(i_{air}^{\max} \right)^2 / \sigma_{air} A =$$

$$= (d - h) A \sigma_{air} \left(E_{air}^{\max} \right)^2 \cong 10^{-4} W$$

Now, we will describe a method to coat the Aluminum semi-spheres with acrylic in the necessary dimensions $(\Delta = a - r_0)$, we propose the following method. First, take an Aluminum plate with $21cm \times 29.1cm$ (A4 format). By means of a convenient process, several semi-spheres can be stamped on its surface. The semi-spheres have radius $r_0 = 0.9\ mm$, and are joined one to another. Next, take an acrylic sheet (A4 format) with 1.5mm thickness (See Fig.A8 (a)). Put a heater below the Aluminum plate in order to heat the Aluminum (Fig.A8 (b)). When the Aluminum is sufficiently heated up, the acrylic sheet and the Aluminum plate are pressed, one against the other, as shown in Fig. A8 (c). The two D devices shown in this figure are used in order to impede that the press compresses the acrylic and the aluminum to a distance shorter than $y + a$. After some seconds, remove the press and the heater. The device is ready to be subjected to a voltage V_0 with frequency f, as shown in Fig.A9. Note that, in this case, the balance is not necessary, because *the substance that produces the gravitational shielding* is an *air layer* with thickness d *above* the acrylic sheet. This is, therefore, more a type of Gravity Control Cell (GCC) with *external gravitational shielding*.

It is important to note that this GCC can be made very thin and as flexible as a fabric. Thus, it can be used to produce *anti- gravity clothes*. These clothes can be extremely useful, for example, to walk on the surface of high gravity planets.

Figure A11 shows some geometrical forms that can be stamped on a metallic surface in order to produce a Gravitational Shielding effect, similar to the produced by the *semi-spherical form*.

An obvious evolution from the semi-spherical form is the *semi-cylindrical* form shown in Fig. A11 (b); Fig.A11(c) shows *concentric metallic rings* stamped on the metallic surface, an evolution from Fig.A11 (b). These geometrical forms produce the same effect as the semi-spherical form, shown in Fig.A11 (a). By using concentric metallic rings, it is possible to build *Gravitational Shieldings* around bodies or spacecrafts with several formats (spheres, ellipsoids, etc); Fig. A11 (d) shows a Gravitational Shielding around a Spacecraft with *ellipsoidal form*.

The previously mentioned Gravitational Shielding, produced on a thin layer of ionized air, has a *behavior different from* the Gravitational Shielding produced on a *rigid substance*. When the gravitational masses of the air molecules, inside the shielding, are reduced to within the range $+0.159 m_i < m_g < -0.159 m_i$, they go to the *imaginary space-time*, as previously shown in this article. However, the electric field E_{air} stays at the real space-time. Consequently, the molecules return immediately to the real space-

[‡‡] Reducing therefore, the conductivity σ_{air}, to the normal value of conductivity of the atmospheric air.

time in order to return soon after to the *imaginary* space-time, due to the action of the electric field E_{air}.

In the case of the Gravitational Shielding produced on a *solid substance*, when the molecules of the substance go to the *imaginary* space-time, *the electric field that produces the effect, also goes to the imaginary space-time together with them*, since in this case, the substance of the Gravitational Shielding is rigidly connected to the metal that produces the electric field. (See Fig. A12 (b)). This is the fundamental difference between the *non-solid* and *solid* Gravitational Shieldings.

Now, consider a Gravitational Spacecraft that is able to produce an *Air* Gravitational Shielding and also a *Solid* Gravitational Shielding, as shown in Fig. A13 (a) [§§]. Assuming that the intensity of the electric field, E_{air}, necessary to reduce the gravitational mass of the *air molecules* to within the range $+0.159m_i < m_g < -0.159m_i$, *is much smaller* than the intensity of the electric field, E_{rs}, necessary to reduce the gravitational mass of the *solid substance* to within the range $+0.159m_i < m_g < -0.159m_i$, then we conclude that the Gravitational Shielding made of ionized air goes to the imaginary space-time *before* the Gravitational Shielding made of *solid substance*. When this occurs the spacecraft does not go to the imaginary space-time together with the Gravitational Shielding of air, because the air molecules are not rigidly connected to the spacecraft. Thus, while the air molecules go into the imaginary space-time, the spacecraft stays in the *real space-time*, and remains subjected to the effects of the Gravitational Shielding around it, since the shielding does not stop to work, due to its extremely short permanence at the imaginary space-time. Under these circumstances, the gravitational mass of the Gravitational Shielding can be reduced to $m_g \cong 0$. For example, $m_g \cong 10^{-4} kg$. Thus, if the *inertial mass* of the Gravitational Shielding is $m_{i0} \cong 1kg$, then $\chi = m_g / m_{i0} \cong 10^{-4}$. As we have seen, this means that *the inertial effects on the spacecraft* will be reduced by $\chi \cong 10^{-4}$. Then, in spite of the effective acceleration of the spacecraft be, for example, $a = 10^5 m.s^{-2}$, the effects on the crew of the spacecraft will be equivalent to an acceleration of only

$$a' = \frac{m_g}{m_{i0}} a = \chi \ a \approx 10 m.s^{-1}$$

This is the magnitude of the acceleration upon the passengers in a contemporary commercial jet.

Then, it is noticed that Gravitational Spacecrafts can be subjected to enormous *accelerations* (or *decelerations*) without imposing any harmful impacts whatsoever on the spacecrafts or its crew.

Now, imagine that the intensity of the electric field that produces the Gravitational Shielding around the spacecraft is *increased* up to reaching the value E_{rs} that reduces the gravitational mass of the *solid* Gravitational Shielding to within the range $+0.159m_i < m_g < -0.159m_i$. Under these circumstances, the *solid* Gravitational Shielding goes to the imaginary space-time and, since it is rigidly connected to the spacecraft, also the spacecraft goes to the imaginary space-time together with the Gravitational Shielding. Thus, the spacecraft can travel within the imaginary space-time and make use of the Gravitational Shielding around it.

As we have already seen, the maximum velocity of propagation of the interactions in the imaginary space-time is *infinite* (in the real space-time this limit is equal to the light velocity c). This means that *there are no limits for the velocity of the spacecraft in the imaginary space-time*. Thus, the acceleration of the spacecraft can reach, for example, $a = 10^9 m.s^{-2}$, which leads the spacecraft to attain velocities $V \approx 10^{14} m.s^{-1}$ (about 1 million times the speed of light) after one day of trip. With this velocity, after 1 month of trip the spacecraft would have traveled about $10^{21} m$. In order to have idea of this distance, it is enough to remind that the diameter of our Universe (visible Universe) is of the order of $10^{26} m$.

[§§] The *solid* Gravitational Shielding can also be obtained by means of *an ELF electric current through a metallic lamina* placed *between the semi-spheres and the Gravitational Shielding of Air* (See Fig.A13 (a)). The gravitational mass of the solid Gravitational Shielding will be controlled just by means of the intensity of the ELF electric current. Recently, it was discovered that Carbon nanotubes (CNTs) can be added to *Alumina* (Al_2O_3) to convert it into a good electrical conductor. It was found that the electrical conductivity increased up to 3375 S/m at 77°C in samples that were 15% nanotubes by volume [12]. It is known that the density of α-Alumina is 3.98kg.m^{-3} and that it can withstand 10-20 KV/mm. Thus, these values show that the Alumina-CNT can be used to make a *solid* Gravitational Shielding. In this case, the electric field produced by means of the semi-spheres will be used to control the gravitational mass of the Alumina-CNT.

Due to the extremely low density of the *imaginary* bodies, the collision between them cannot have the same consequences of the collision between the real bodies.

Thus, *for a Gravitational Spacecraft in imaginary state, the problem of the collision in high-speed doesn't exist.* Consequently, the Gravitational Spacecraft can transit freely in the imaginary Universe and, in this way, reach easily any point of our real Universe once they can make the transition back to our Universe by only increasing the gravitational mass of the Gravitational Shielding of the spacecraft in such way that it leaves the range of $+0.159M_i$ to $-0.159M_i$.

The return trip would be done in similar way. That is to say, the spacecraft would transit in the imaginary Universe back to the departure place where would reappear in our Universe. Thus, trips through our Universe that would delay millions of years, at speeds close to the speed of light, could be done in just a few *months* in the imaginary Universe.

In order to produce the acceleration of $a \approx 10^9\, m.s^{-2}$ upon the spacecraft we propose a Gravitational Thruster with 10 GCCs (10 Gravitational Shieldings) of the type with several semi-spheres stamped on the metallic surface, as previously shown, or with the *semi-cylindrical* form shown in Figs. A11 (b) and (c). The 10 GCCs are filled with air at 1 atm and 300K. If the insulation layer is made with *Mica* $(\varepsilon_r \cong 5.4)$ and has thickness $\Delta = 0.1\ mm$, and the semi-spheres stamped on the metallic surface have $r_0 = 0.4\ mm$ (See Fig.A7) then $a = r_0 + \Delta = 0.5\ mm$. Thus, we get

$$b = r_0\sqrt{\varepsilon_r} = 9.295\times10^{-4} m$$

and

$$d = b - a = 4.295\times10^{-4} m$$

Then, from Eq. A42 we obtain

$$\chi_{air} = \frac{m_{g(air)}}{m_{i0(air)}} = \left\{1 - 2\left[\sqrt{1+1.758\times10^{-27}\frac{\sigma_{air}^3 E_{air}^4}{\rho_{air}^2 f^3}} - 1\right]\right\} =$$

$$= \left\{1 - 2\left[\sqrt{1+1.0\times10^{-18}\frac{V_0^{5.5}}{f^3}} - 1\right]\right\}$$

For $V_0 = V_0^{\max} = 15.6kV$ and $f = 0.12Hz$, the result is

$$\chi_{air} = \frac{m_{g(air)}}{m_{i0(air)}} \cong -1.6\times10^4$$

Since $E_0^{\max} = V_0^{\max} / r_0$ is now given by $E_0^{\max} = 15.6kV/0.9mm = 17.3kV/mm$ and $\Delta = 0.1\ mm$ then the dielectric strength of the insulation must be $\geq 173kV/mm$. As shown in the table below[***], *0.1mm - thickness of* Mica *can withstand 17.6 kV* (that is greater than $V_0^{\max} = 15.6kV$), in such way that the dielectric strength is *176 kV/mm*.

The Gravitational Thrusters are positioned at the spacecraft, as shown in Fig. A13 (b). Then, when the spacecraft is in the *intergalactic space*, the gravity acceleration upon the gravitational mass m_{gt} of the bottom of the thruster (See Fig.A13 (c)), is given by [2]

$$\vec{a} \cong (\chi_{air})^{10}\,\vec{g}_M \cong -(\chi_{air})^{10} G\frac{M_g}{r^2}\hat{\mu}$$

where M_g is the gravitational mass in front of the spacecraft.

For simplicity, let us consider just the effect of a hypothetical volume $V = 10\times10^3\times10^3 = 10^7 m^3$ of intergalactic matter in front of the spacecraft $(r \cong 30m)$. The average density of matter in the *intergalactic medium (IGM)* is $\rho_{ig} \approx 10^{-26} kg.m^{-3}$)[†††]. Thus, for $\chi_{air} \cong -1.6\times10^4$ we get

$$a = -\left(-1.6\times10^4\right)^{10}\left(6.67\times10^{-11}\right)\left(\frac{10^{-19}}{30^2}\right) =$$

$$= -10^9\, m.s^{-2}$$

In spite of this gigantic acceleration, the inertial effects for the crew of the spacecraft can be strongly reduced if, for example, the gravitational mass of the Gravitational Shielding is reduced

---

[***] The *dielectric strength* of some dielectrics can have different values in lower thicknesses. This is, for example, the case of the *Mica*.

Dielectric	*Thickness* (mm)	*Dielectric Strength* (kV/mm)
Mica	0.01 mm	200
Mica	**0.1 mm**	**176**
Mica	1 mm	61

[†††] Some theories put the average density of the Universe as the equivalent of *one hydrogen atom per cubic meter* [13,14]. The density of the universe, however, is clearly not uniform. Surrounding and stretching between galaxies, there is a rarefied plasma [15] that is thought to possess a cosmic filamentary structure [16] and that is slightly denser than the average density in the universe. This material is called the *intergalactic medium (IGM)* and is mostly ionized hydrogen; i.e. a plasma consisting of equal numbers of electrons and protons. The IGM is thought to exist at a density of 10 to 100 times the average density of the Universe (10 to 100 hydrogen atoms per cubic meter, i.e., $\approx 10^{-26}\, kg.m^{-3}$).

down to $m_g \cong 10^{-6} kg$ and its inertial mass is $m_{i0} \cong 100kg$. Then, we get $\chi = m_g / m_{i0} \cong 10^{-8}$. Therefore, *the inertial effects on the spacecraft* will be reduced by $\chi \cong 10^{-8}$, and consequently, the inertial effects on the crew of the spacecraft would be *equivalent to* an acceleration a' of only

$$a' = \frac{m_g}{m_{i0}} a = \left(10^{-8}\right)\left(10^{9}\right) \approx 10 m.s^{-2}$$

Note that the Gravitational Thrusters in the spacecraft must have a very small diameter (of the order of *millimeters*) since, obviously, the hole through the Gravitational Shielding cannot be large. Thus, these thrusters are in fact, *Micro-Gravitational Thrusters*. As shown in Fig. A13 (b), it is possible to place several micro-gravitational thrusters in the spacecraft. This gives to the Gravitational Spacecraft, several degrees of freedom and shows the enormous superiority of this spacecraft in relation to the contemporaries spacecrafts.

The density of matter in the *intergalactic medium (IGM)* is about *10 $^{-26}$ kg.m^{-3}* , which is very less than the density of matter in the *interstellar medium* (*~10^{-21} kg.m^{-3}*) that is less than the density of matter in the *interplanetary medium* (*~10^{-20} kg.m^{-3}*). The density of matter is enormously increased inside the Earth's atmosphere (*1.2kg.m^{-3}* near to Earth's surface). Figure A14 shows the gravitational acceleration acquired by a Gravitational Spacecraft, in these media, using Micro-Gravitational thrusters.

In relation to the *Interstellar* and *Interplanetary medium*, the *Intergalactic medium* requires the greatest value of χ_{air} (χ inside the *Micro-Gravitational Thrusters*), i.e., $\chi_{air} \cong -1.6 \times 10^4$. This value strongly decreases when the spacecraft is within the Earth's atmosphere. In this case, it is sufficient only[‡‡‡] $\chi_{air} \cong -10$ in order to obtain:

$$a = -\left(\chi_{air}\right)^{10} G \frac{\rho_{atm} V}{r^2} \cong$$

$$\cong -\left(-10\right)^{10} \left(6.67 \times 10^{-11}\right) \frac{1.2\left(10^7\right)}{\left(20\right)^2} \cong 10^4 m.s^{-2}$$

With this acceleration the Gravitational Spacecraft can reach about *50000 km/h* in a few seconds. Obviously, the Gravitational Shielding of the spacecraft will reduce strongly *the inertial effects upon the crew* of the spacecraft, in such way that the inertial effects of this strong acceleration will not be felt. In addition, the *artificial atmosphere*, which is possible to build around the spacecraft, by means of gravity control technologies shown in this article (See Fig.6) and [2], will protect it from the *heating* produced by the friction with the Earth's atmosphere. Also, the gravity can be controlled inside of the Gravitational Spacecraft in order to maintain a value close to the Earth's gravity as shown in Fig.3.

Finally, it is important to note that a Micro-Gravitational Thruster does not work *outside* a Gravitational Shielding, because, in this case, *the resultant upon the thruster is null* due to the symmetry (See Fig. A15 (a)). Figure A15 (b) shows a micro-gravitational thruster inside a Gravitational Shielding. This thruster has 10 Gravitational Shieldings, in such way that the gravitational acceleration upon the *bottom* of the thruster, due to a gravitational mass M_g *in front* of the thruster, is $a_{10} = \chi_{air}^{10} a_0$ where $a_0 = -G M_g / r^2$ is the gravitational acceleration acting on the front of the micro-gravitational thruster. *In the opposite direction*, the gravitational acceleration upon the bottom of the thruster, produced by a gravitational mass M_g, is

$$a_0' = \chi_s \left(-GM_g / r'^2\right) \cong 0$$

since $\chi_s \cong 0$ due to the Gravitational Shielding around the micro-thruster (See Fig. A15 (b)). Similarly, the acceleration in front of the thruster is

$$a_{10}' = \chi_{air}^{10} a_0' = \left[\chi_{air}^{10}\left(-GM_g / r'^2\right)\right] \chi_s$$

where $\left[\chi_{air}^{10}\left(-GM_g / r'^2\right)\right] < a_{10}$, since $r' > r$. Thus, for $a_{10} \cong 10^9 m.s^{-2}$ and $\chi_s \approx 10^{-8}$ we conclude that $a_{10}' < 10 m.s^{-2}$. This means that $a_{10}' << a_{10}$. Therefore, we can write that the resultant on the micro-thruster can be expressed by means of the following relation

$$R \cong F_{10} = \chi_{air}^{10} F_0$$

Figure A15 (c) shows a Micro-Gravitational Thruster with *10 Air Gravitational Shieldings* (10 GCCs). Thin Metallic laminas are placed after

[‡‡‡] This value is within the range of values of χ $\left(\chi < -10^{3}.\ See\ \ Eq.A15\right)$, which can be produced by means of *ELF electric currents* through metals as *Aluminum*, etc. This means that, in this case, if convenient, we can replace *air* inside the GCCs of the Gravitational Micro-thrusters by metal laminas with *ELF electric currents* through them.

each *Air* Gravitational Shielding in order to retain the electric field $E_b = V_0/x$, produced by metallic *surface behind* the semi-spheres. The laminas with semi-spheres stamped on its surfaces are connected to the ELF voltage source V_0 and the thin laminas in front of the Air Gravitational Shieldings are grounded. The air inside this Micro-Gravitational Thruster is at 300K, 1atm.

We have seen that the insulation layer of a GCC can be made up of Acrylic, Mica, etc. Now, we will design a GCC using *Water* (*distilled water*, $\varepsilon_{r(H_2O)} = 80$) and Aluminum *semi-cylinders* with radius $r_0 = 1.3mm$. Thus, for $\Delta = 0.6mm$, the new value of a is $a = 1.9mm$. Then, we get

$$b = r_0\sqrt{\varepsilon_{r(H_2O)}} = 11.63\times10^{-3}m \qquad (A43)$$

$$d = b - a = 9.73\times10^{-3}m \qquad (A44)$$

and

$$E_{air} = \frac{1}{4\pi\varepsilon_{r(air)}\varepsilon_0}\frac{q}{b^2} =$$

$$= \varepsilon_{r(H_2O)}\frac{V_0 r_0}{\varepsilon_{r(air)} b^2} =$$

$$= \frac{V_0/r_0}{\varepsilon_{r(air)}} \cong \frac{V_0}{r_0} = 11111\ V_0 \qquad (A45)$$

Note that

$$E_{(H_2O)} = \frac{V_0/r_0}{\varepsilon_{r(H_2O)}}$$

and

$$E_{(acrylic)} = \frac{V_0/r_0}{\varepsilon_{r(acrylic)}}$$

Therefore, $E_{(H_2O)}$ and $E_{(acrylic)}$ are much smaller than E_{air}. Note that for $V_0 \le 9kV$ the intensities of $E_{(H_2O)}$ and $E_{(acrylic)}$ are not sufficient to produce the ionization effect, which increases the electrical conductivity. Consequently, the conductivities of the water and the acrylic remain $<< 1\ S.m^{-1}$. In this way, with $E_{(H_2O)}$ and $E_{(acrylic)}$ much smaller than E_{air}, and $\sigma_{(H2O)} << 1$, $\sigma_{(acrylic)} << 1$, the decrease in both the gravitational mass of the acrylic and the gravitational mass of water, according to Eq.A14, is negligible. This means that only in the air layer the decrease in the gravitational mass will be relevant.

Equation A39 gives the electrical conductivity of the air layer, i.e.,

$$\sigma_{air} = 2\alpha\left(\frac{E_{air}}{d}\right)^{\frac{1}{2}}\left(\frac{b}{a}\right)^{\frac{3}{2}} = 0.029V_0^{\frac{1}{2}} \qquad (A46)$$

Note that $b = r_0\sqrt{\varepsilon_{r(H_2O)}}$. Therefore, here the value of b is larger than in the case of the acrylic. Consequently, *the electrical conductivity of the air layer will be larger here than in the case of acrylic.*

Substitution of $\sigma_{(air)}$, E_{air} (*rms*) and $\rho_{air} = 1.2kg.m^{-3}$ into Eq. A14, gives

$$\frac{m_{g(air)}}{m_{i0(air)}} = \left\{1 - 2\left[\sqrt{1 + 4.54\times10^{20}\frac{V_0^{5.5}}{f^3}} - 1\right]\right\} \qquad (A47)$$

For $V_0 = V_0^{\max} = 9kV$ and $f = 2Hz$, the result is

$$\frac{m_{g(air)}}{m_{i0(air)}} \cong -8.4$$

This shows that, by using *water* instead of acrylic, the result is much better.

In order to build the GCC based on the calculations above (See Fig. A16), take an Acrylic plate with *885mm* X *885m* and *2mm* thickness, then paste on it an Aluminum sheet with *895.2mm* X *885mm* and *0.5mm* thickness(note that two edges of the Aluminum sheet are bent as shown in Figure A16 (b)). Next, take *342* Aluminum yarns with *884mm* length and *2.588mm* diameter (wire # 10 AWG) and insert them side by side on the Aluminum sheet. See in Fig. A16 (b) the detail of fixing of the yarns on the Aluminum sheet. Now, paste acrylic strips (with *13.43mm* height and *2mm* thickness) around the Aluminum/Acrylic, making a box. Put *distilled water* (approximately *1 litter*) inside this box, up to a height of exactly *3.7mm* from the edge of the acrylic base. Afterwards, paste an Acrylic lid (*889mm* X *889mm* and *2mm* thickness) on the box. Note that above the water there is an *air* layer with *885mm* X *885mm* and *7.73mm* thickness (See Fig. A16). This thickness plus the acrylic lid thickness (*2mm*) is equal to $d = b - a = 9.73mm$ where $b = r_0\sqrt{\varepsilon_{r(H_2O)}} = 11.63mm$ and $a = r_0 + \Delta = 1.99mm$, since $r_0 = 1.3mm$, $\varepsilon_{r(H_2O)} = 80$ and $\Delta = 0.6mm$.

Note that the gravitational action of the electric field E_{air}, extends itself only up to the distance d, which, in this GCC, is given by the sum of the Air layer thickness (*7.73mm*) plus the thickness of the Acrylic lid (*2mm*).

Thus, it is ensured the gravitational effect on the air layer while it is practically nullified in

the acrylic sheet above the air layer, since $E_{(acrylic)} << E_{air}$ and $\sigma_{(acrylic)} << 1$.

With this GCC, we can carry out an experiment where the *gravitational mass of the air layer* is progressively reduced when the voltage applied to the GCC is increased (or when the frequency is decreased). A precision balance is placed below the GCC in order to measure the mentioned mass decrease for comparison with the values predicted by Eq. A(47). In total, this GCC weighs about *6kg*; the *air layer 7.3grams*. The balance has the following characteristics: *range 0-6kg; readability 0.1g*. Also, in order to prove the *Gravitational Shielding Effect*, we can put a *sample* (connected to a dynamometer) above the GCC in order to check the gravity acceleration in this region.

In order to prove *the exponential effect* produced by the superposition of the Gravitational Shieldings, we can take three similar GCCs and put them one above the other, in such way that above the GCC 1 the gravity acceleration will be $g' = \chi\, g$; above the GCC2 $g'' = \chi^2 g$, and above the GCC3 $g''' = \chi^3 g$. Where χ is given by Eq. (A47).

It is important to note that the intensity of the electric field through the air *below* the GCC is *much smaller* than the intensity of the electric field through the air layer inside the GCC. In addition, the electrical conductivity of the air below the GCC is much smaller than the conductivity of the air layer inside the GCC. Consequently, the decrease of the gravitational mass of the air below the GCC, according to Eq.A14, is negligible. This means that the GCC1, GCC2 and GCC3 can be simply overlaid, on the experiment proposed above. However, since it is necessary to put samples among them in order to measure the gravity above each GCC, we suggest a spacing of 30cm or more among them.

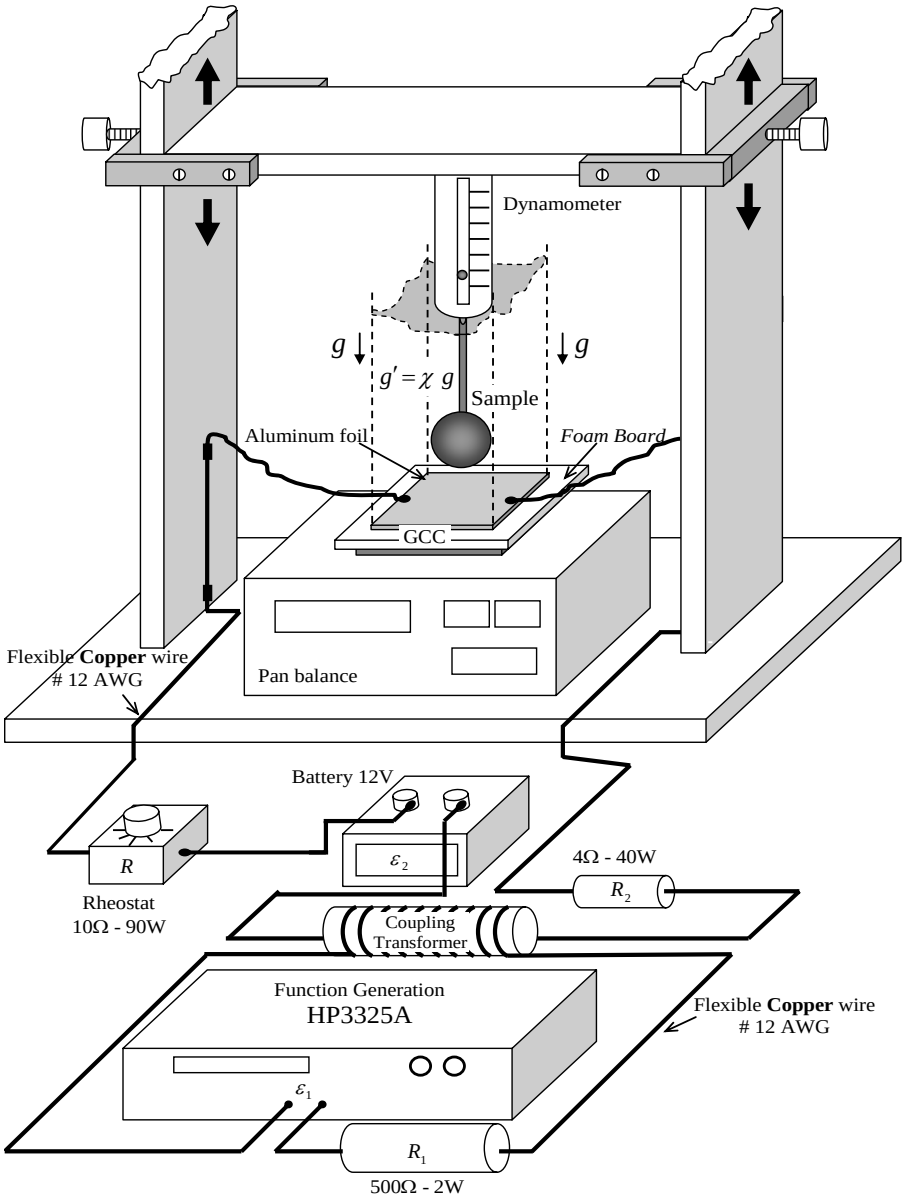

Figure A2 – Experimental Set-up 1.

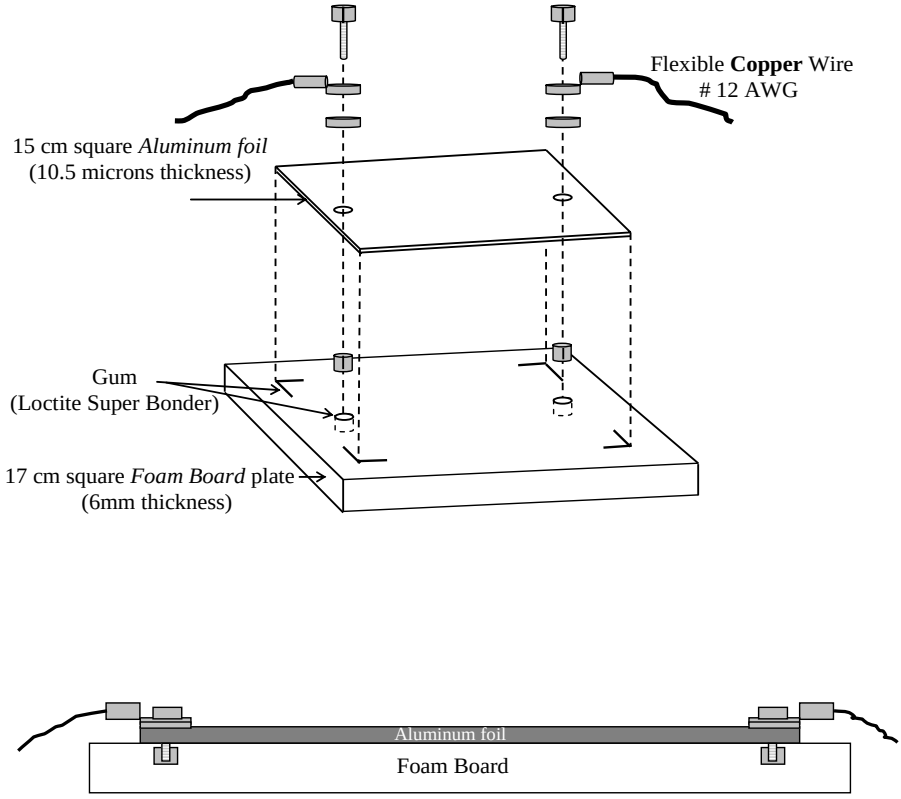

Figure A3 – The Simplest *Gravity Control Cell* (GCC).

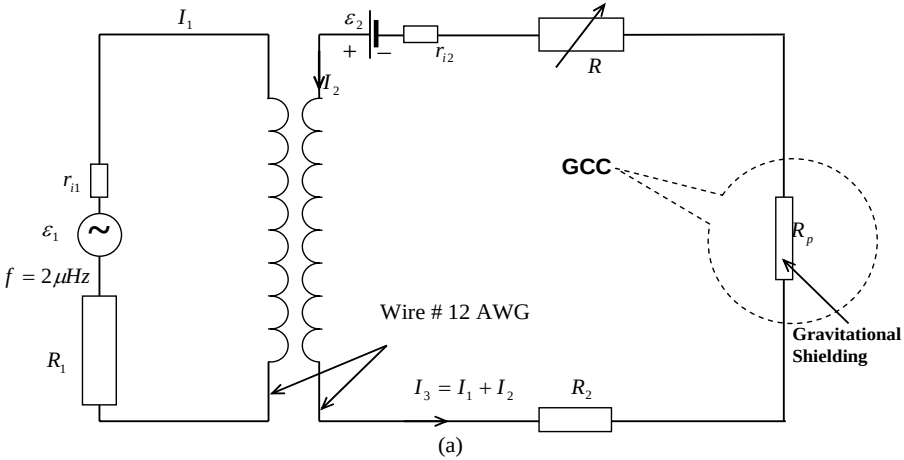

(a)

ε_1 = Function Generator HP3325A(*Option* 002 High Voltage Output)

$r_{i1} < 2\Omega$; $R_1 = 500\Omega - 2\ W$; $\varepsilon_2 = 12V\ DC$; $r_{i2} < 0.1\Omega\ (Battery)$;

$R_2 = 4\Omega - 40W$; $R_p = 2.5\times10^{-3}\Omega$; $Reostat = 0 \le R \le 10\Omega - 90W$

$I_1^{\max} = 56mA\ (rms)$; $I_2^{\max} = 3A$; $I_3^{\max} \cong 3A\ (rms)$

Coupling Transformer to isolate the *Function Generator* from the Battery

• Air core 10 - mm diameter; wire #12 AWG; $N_1 = N_2 = 20; l = 42mm$

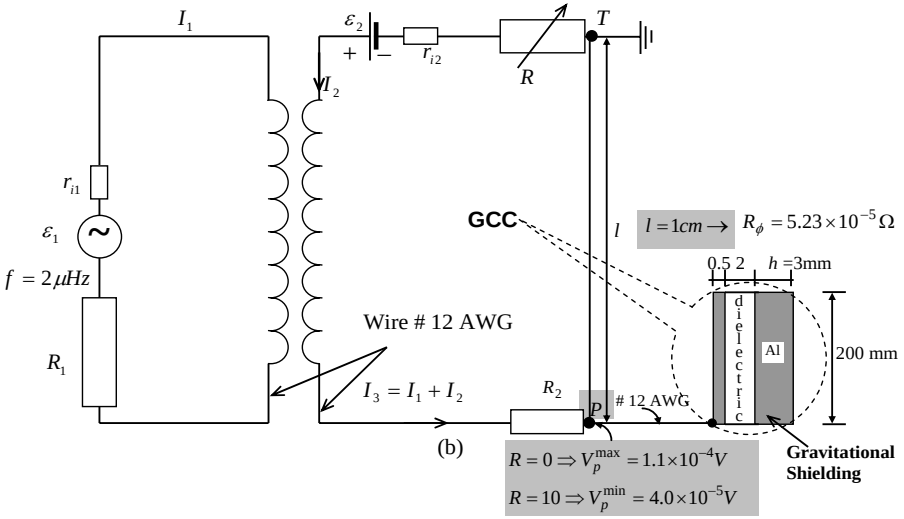

(b)

Fig. A4 – Equivalent Electric Circuits

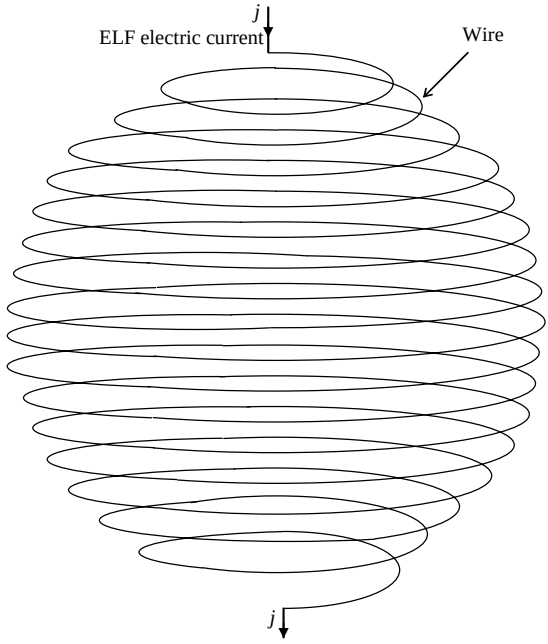

$$m_g = \left\{1 - 2\left[\sqrt{1 + 1.758\times10^{-27}\,\frac{\mu_r j^4}{\sigma\rho^2 f^3}} - 1\right]\right\} m_{i0}$$

Figure A5 – An ELF electric current through a wire, that makes a spherical form as shown above, reduces the gravitational mass of the wire and the gravity inside sphere at the same proportion $\chi = m_g / m_{i0}$ (Gravitational Shielding Effect). Note that this spherical form can be transformed into an ellipsoidal form or a disc in order to coat, for example, a Gravitational Spacecraft**.** It is also possible to coat with a wire several forms, such as cylinders, cones, cubes, etc. The characteristics of the wire are expressed by: μ_r, σ, ρ; j is the electric current density and f is the frequency.

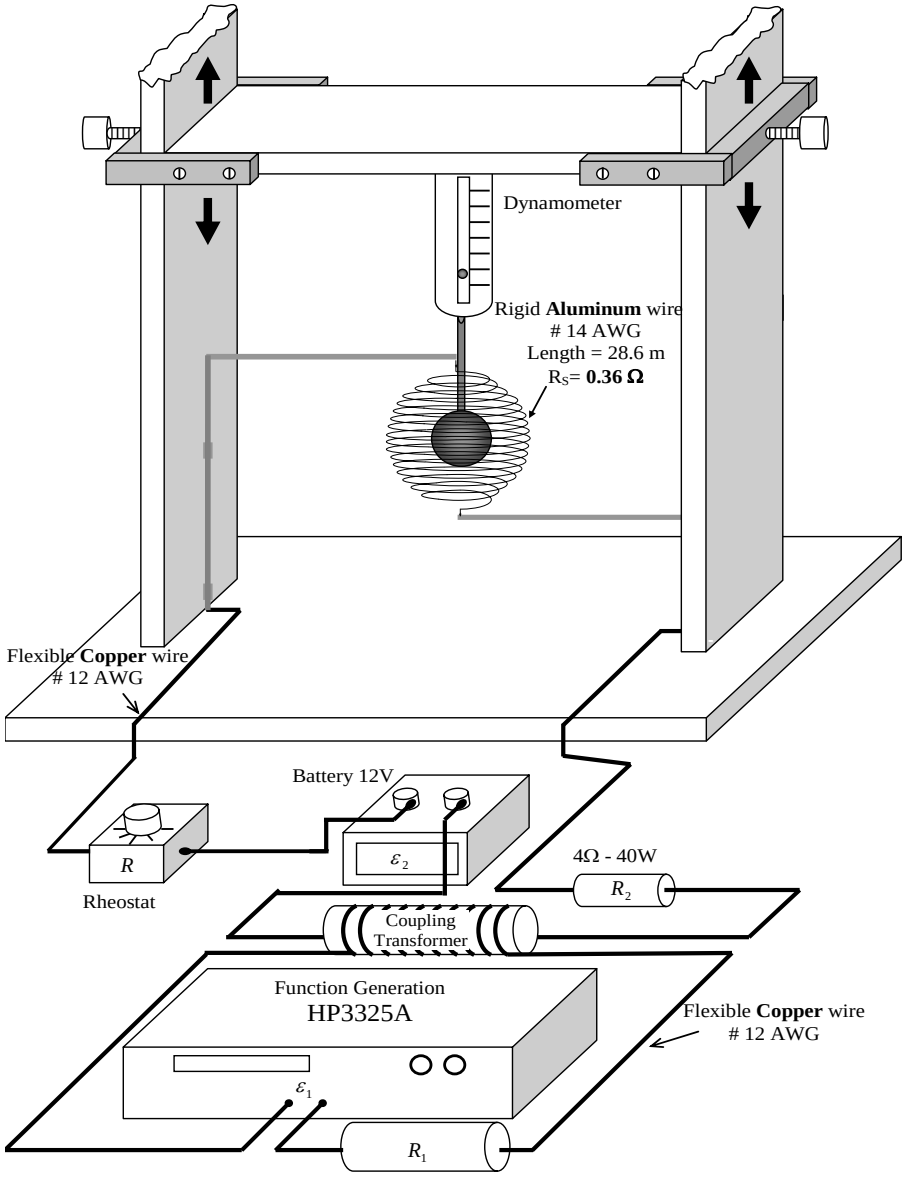

Figure A6 – Experimental set-up 2.

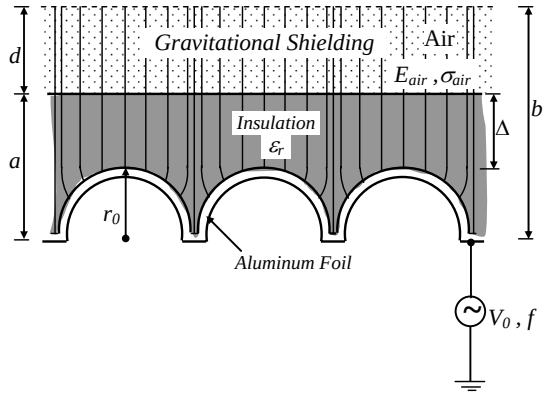

Figure A7 – *Gravitational shielding produced by semi-spheres stamped on the Aluminum foil* - By simply changing the geometry of the surface *of* the Aluminum foil it is possible to increase the working frequency f up to more than *1Hz*.

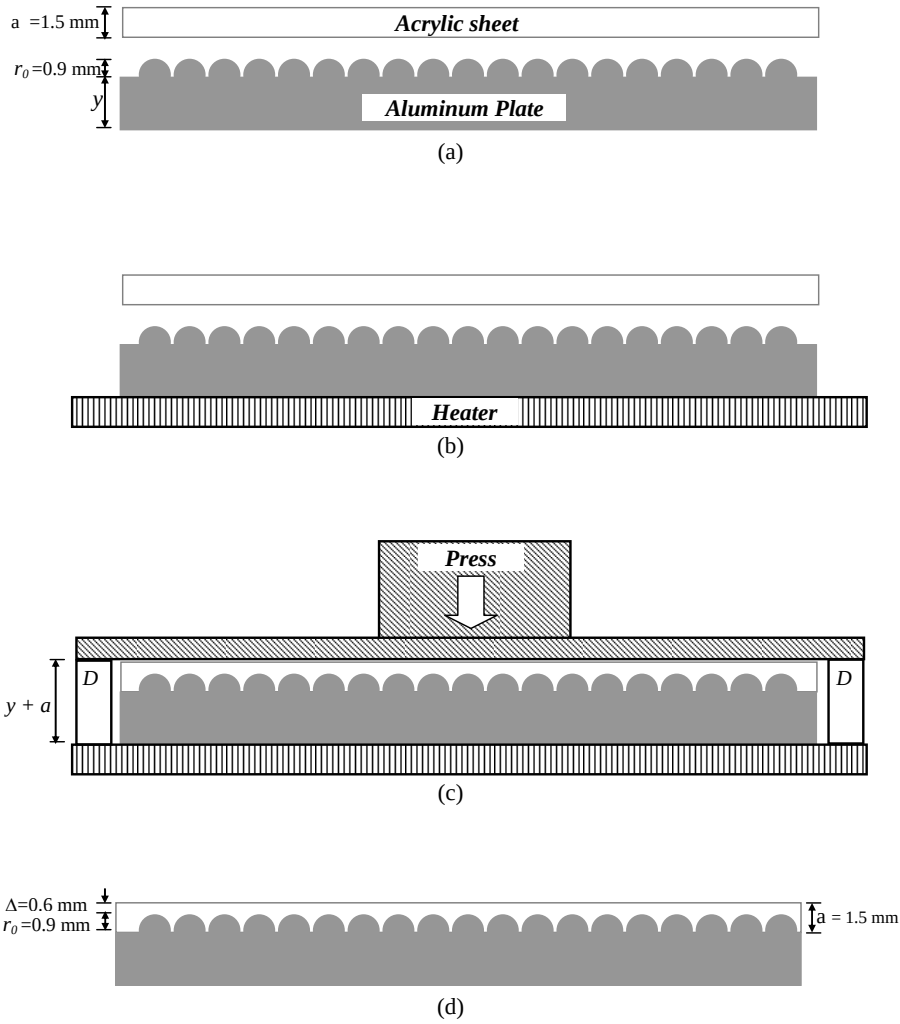

Figure A8 – *Method to coat the Aluminum semi-spheres with acrylic* $(\Delta = a - r_0 = 0.6mm)$. (a)Acrylic sheet (A4 format) with 1.5mm thickness and an Aluminum plate (A4) with several semi-spheres (radius $r_0 = 0.9\ mm$) stamped on its surface. (b)A heater is placed below the Aluminum plate in order to heat the Aluminum. (c)When the Aluminum is sufficiently heated up, the acrylic sheet and the Aluminum plate are pressed, one against the other (The two D devices shown in this figure are used in order to impede that the press compresses the acrylic and the aluminum besides distance $y + a$). (d)After some seconds, the press and the heater are removed, and the device is ready to be used.

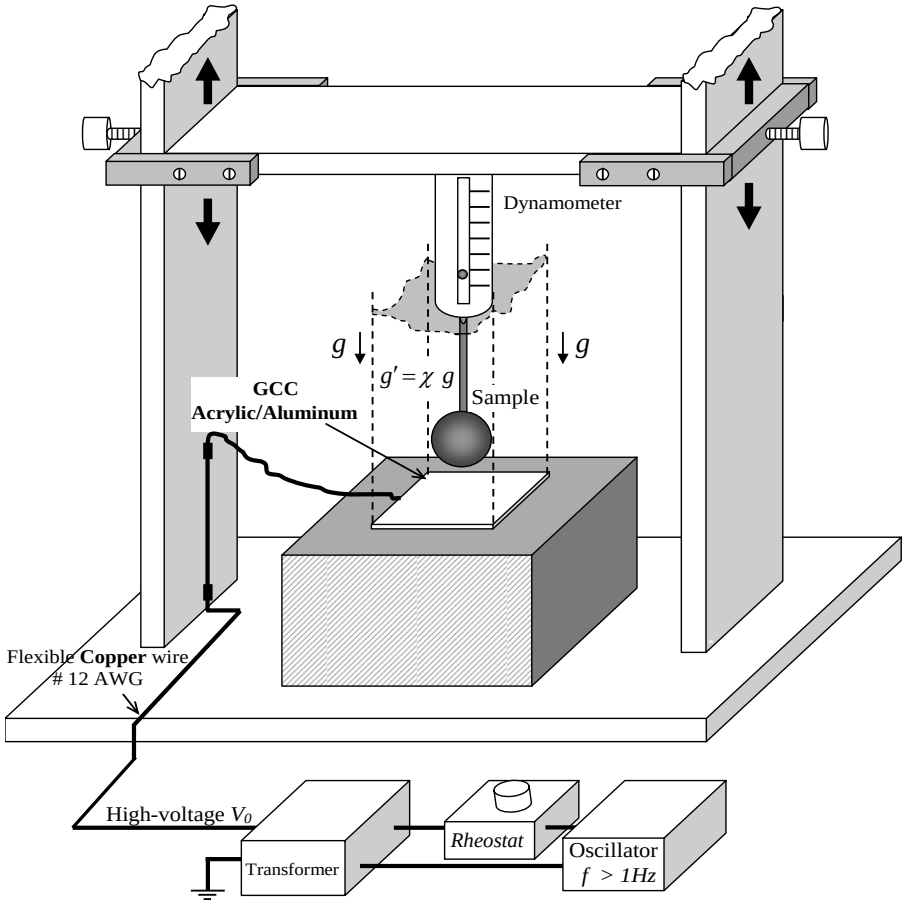

Figure A9 – *Experimental Set-up using a GCC subjected to high-voltage* V_0 *with frequency* $f > 1Hz$. Note that in this case, the pan balance is not necessary because the substance of the Gravitational Shielding is an *air layer* with thickness d *above* the acrylic sheet. This is therefore, more a type of Gravity Control Cell (GCC) with *external gravitational shielding.*

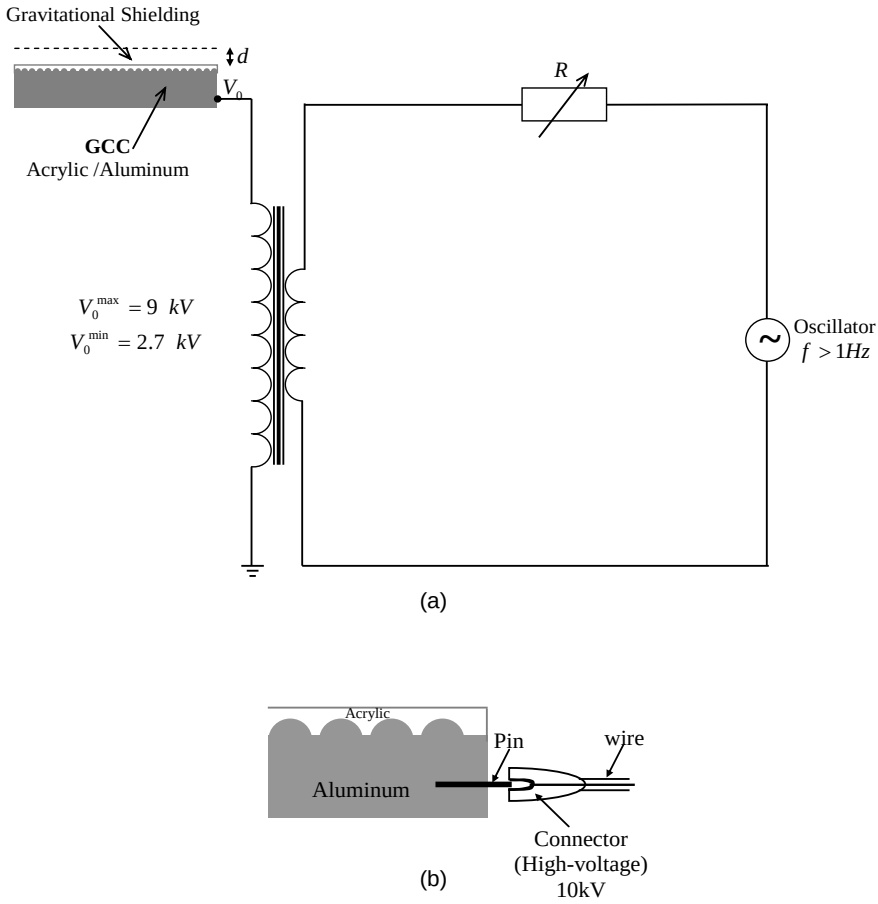

Figure A10 – (a) *Equivalent Electric Circuit.* (b) Details of the electrical connection with the Aluminum plate. Note that others connection modes (by the top of the device) can produce destructible interference on the electric lines of the E_{air} field.

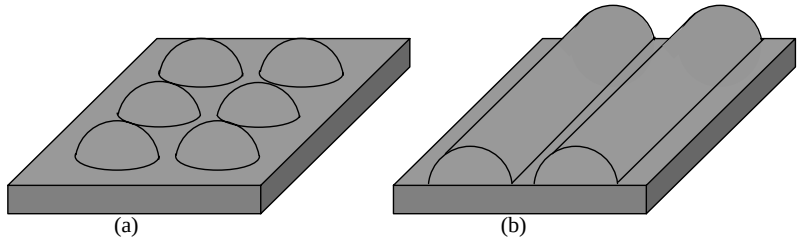

(a) (b)

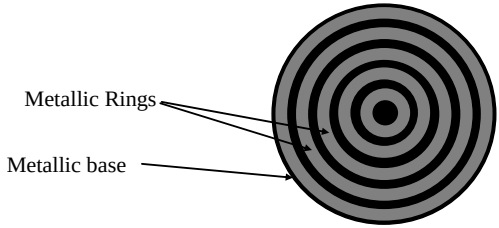

(c)

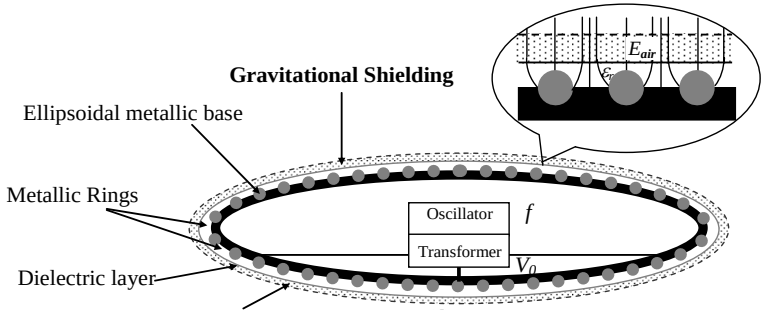

(d)

Figure A11 – *Geometrical forms with similar effects as those produced by the semi-spherical form* – (a) shows the semi-spherical form stamped on the metallic surface; (b) shows the *semi-cylindrical* form (an obvious evolution from the semi-spherical form); (c) shows *concentric metallic rings* stamped on the metallic surface, an evolution from semi-cylindrical form. These geometrical forms produce the same effect as that of the semi-spherical form, shown in Fig.A11 (a). By using concentric metallic rings, it is possible to build *Gravitational Shieldings* around bodies or spacecrafts with several formats (spheres, ellipsoids, etc); (d) shows a Gravitational Shielding around a Spacecraft with *ellipsoidal form.*

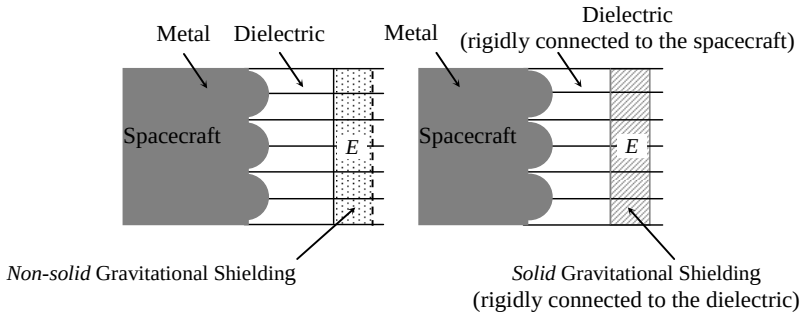

Figure A12 – *Non-solid and Solid Gravitational Shieldings* - In the case of the Gravitational Shielding produced on a *solid substance* (b), when its molecules go to the *imaginary* space-time, *the electric field that produces the effect also goes to the imaginary space-time together with them*, because in this case, the substance of the Gravitational Shielding is *rigidly connected (by means of the dielectric) to the metal* that produces the electric field. This does not occur in the case of *Air* Gravitational Shielding.

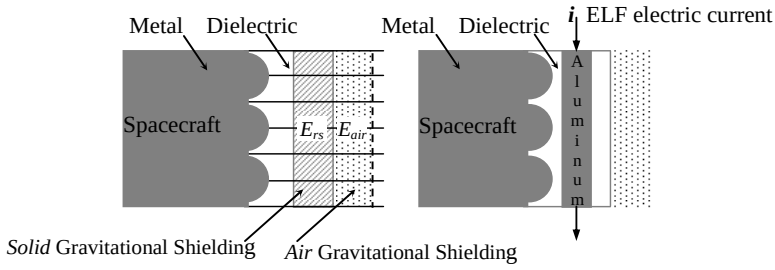

(a)

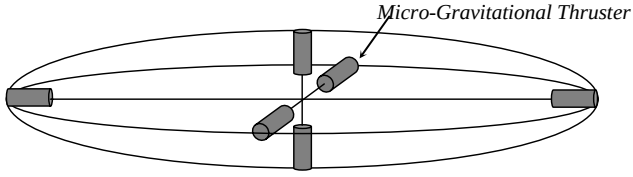

(b)

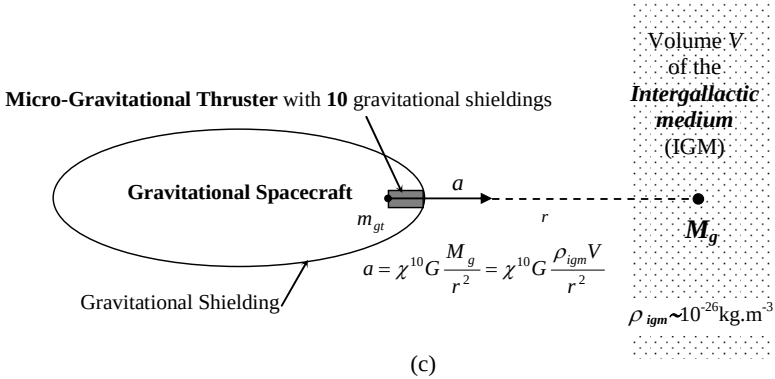

(c)

Figure A13 – *Double Gravitational Shielding and Micro-thrusters* – (a) Shows a double gravitational shielding that makes possible to decrease the *inertial effects* upon the spacecraft when it is traveling both in the *imaginary* space-time and in the *real* space-time. The *solid* Gravitational Shielding also can be obtained by means of *an ELF electric current through a metallic lamina* placed *between the semi-spheres and the Gravitational Shielding of Air* as shown above. (b) Shows 6 *micro-thrusters* placed inside a Gravitational Spacecraft, in order to propel the spacecraft in the directions x, y and z. Note that the Gravitational Thrusters in the spacecraft must have a very small diameter (of the order of *millimeters*) because the hole through the Gravitational Shielding of the spacecraft cannot be large. Thus, these thrusters are in fact *Micro-thrusters*. (c) Shows a micro-thruster inside a spacecraft, and in front of a volume *V* of the intergalactic medium (IGM). Under these conditions, the spacecraft acquires an acceleration *a* in the direction of the volume *V*.

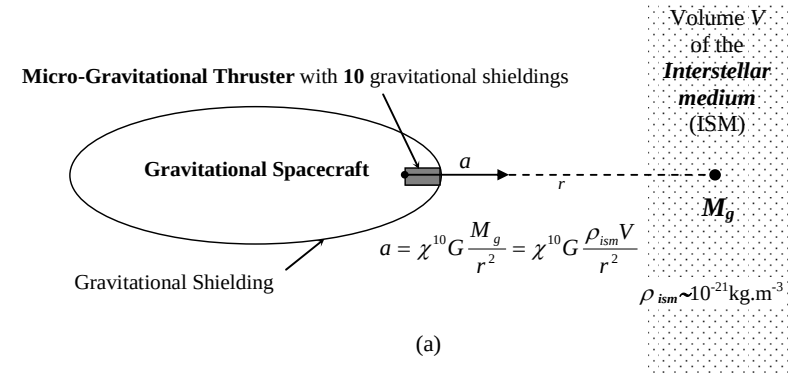

(a)

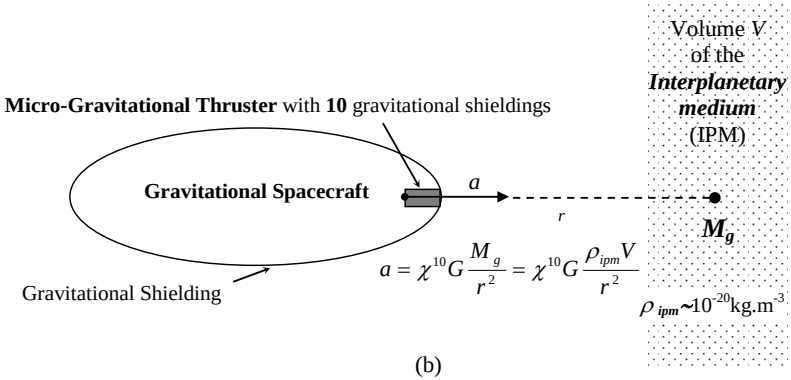

(b)

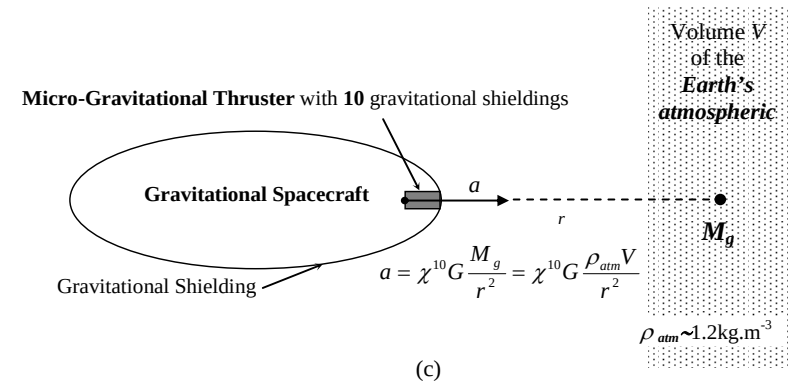

(c)

Figure A14 – *Gravitational Propulsion using Micro-Gravitational Thruster* – (a) Gravitational acceleration produced by a gravitational mass M_g of the *Interstellar Medium*. The density of the Interstellar Medium is about 10^5 times greater than the density of the *Intergalactic Medium* (b) Gravitational acceleration produced in the *Interplanetary Medium*. (c) Gravitational acceleration produced in the *Earth's atmosphere*. Note that, in this case, ρ_{atm} (*near to the Earth's surface*)is about 10^{26} times greater than the density of the *Intergalactic Medium.*

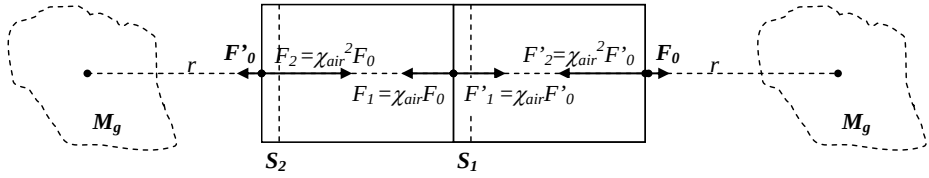

$F'_0 = F_0 \quad \Rightarrow \quad R = (F'_0 - F_2) + (F_1 - F'_1) + (F'_2 - F_0) = 0$

(a)

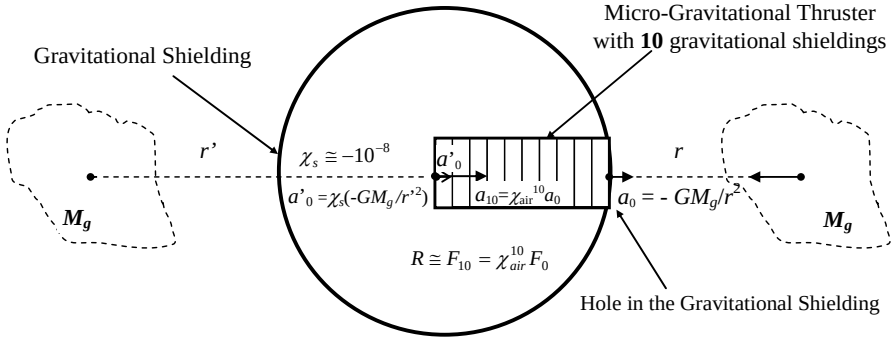

(b)

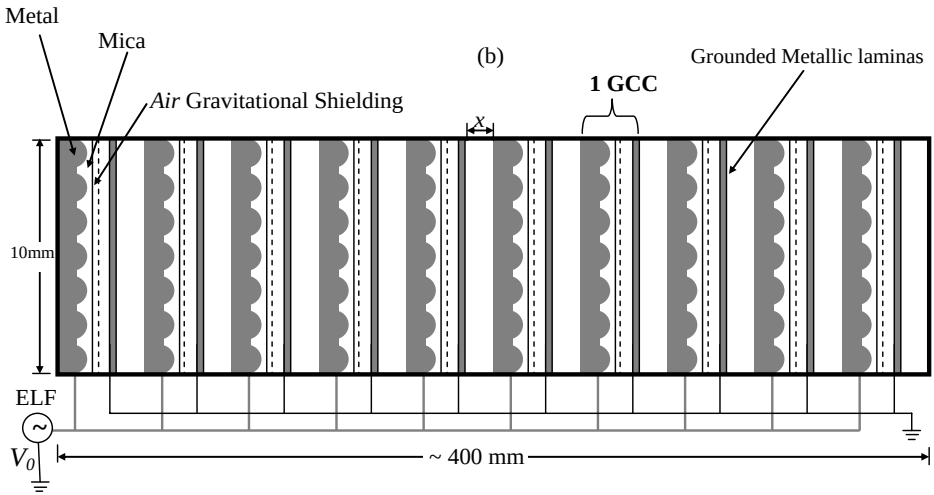

(c)

Figure A15 – *Dynamics and Structure of the Micro-Gravitational Thrusters* - (a) The Micro-Gravitational Thrusters do not work *outside* the Gravitational Shielding, because, in this case, *the resultant upon the thruster is null* due to the symmetry. (b) The Gravitational Shielding $\left(\chi_s \cong 10^{-8}\right)$ reduces strongly the intensities of the gravitational forces acting on the micro-gravitational thruster, except obviously, through the hole in the gravitational shielding. (c) Micro-Gravitational Thruster with *10 Air Gravitational Shieldings* (10GCCs). The grounded metallic laminas are placed so as to retain the electric field produced by metallic surface behind the semi-spheres.

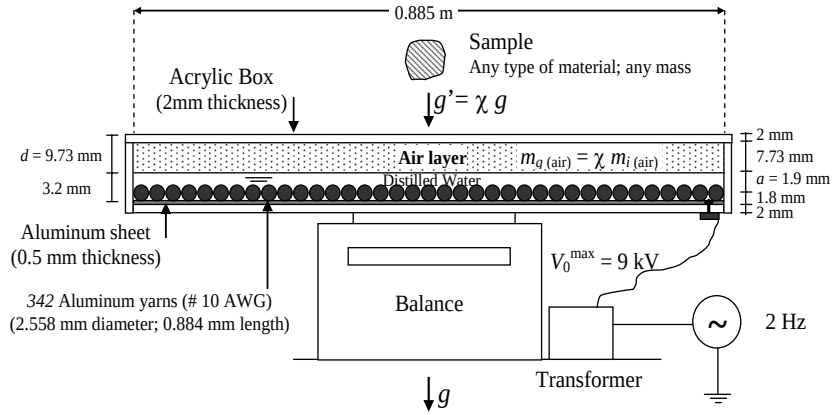

GCC Cross-section Front view

(a)

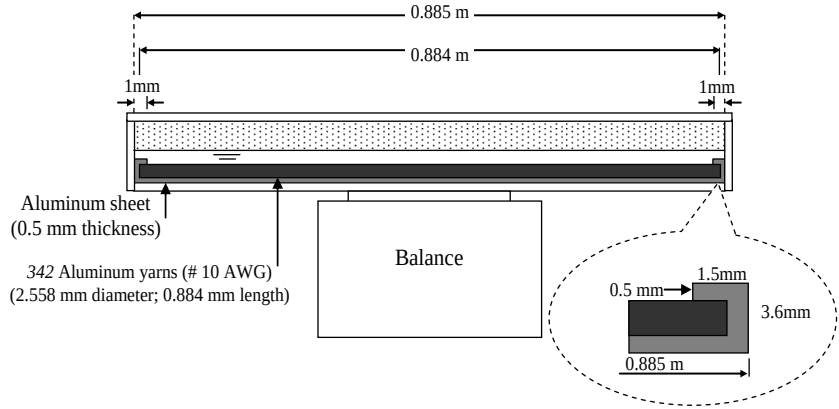

GCC Cross-section Side View

(b)

Fig. A16 – *A GCC using distilled Water*.

In total this GCC weighs about 6kg; the air layer 7.3 grams. The balance has the following characteristics: Range 0 – 6kg; readability 0.1g. The yarns are inserted side by side on the Aluminum sheet. Note the detail of fixing of the yarns on the Aluminum sheet.

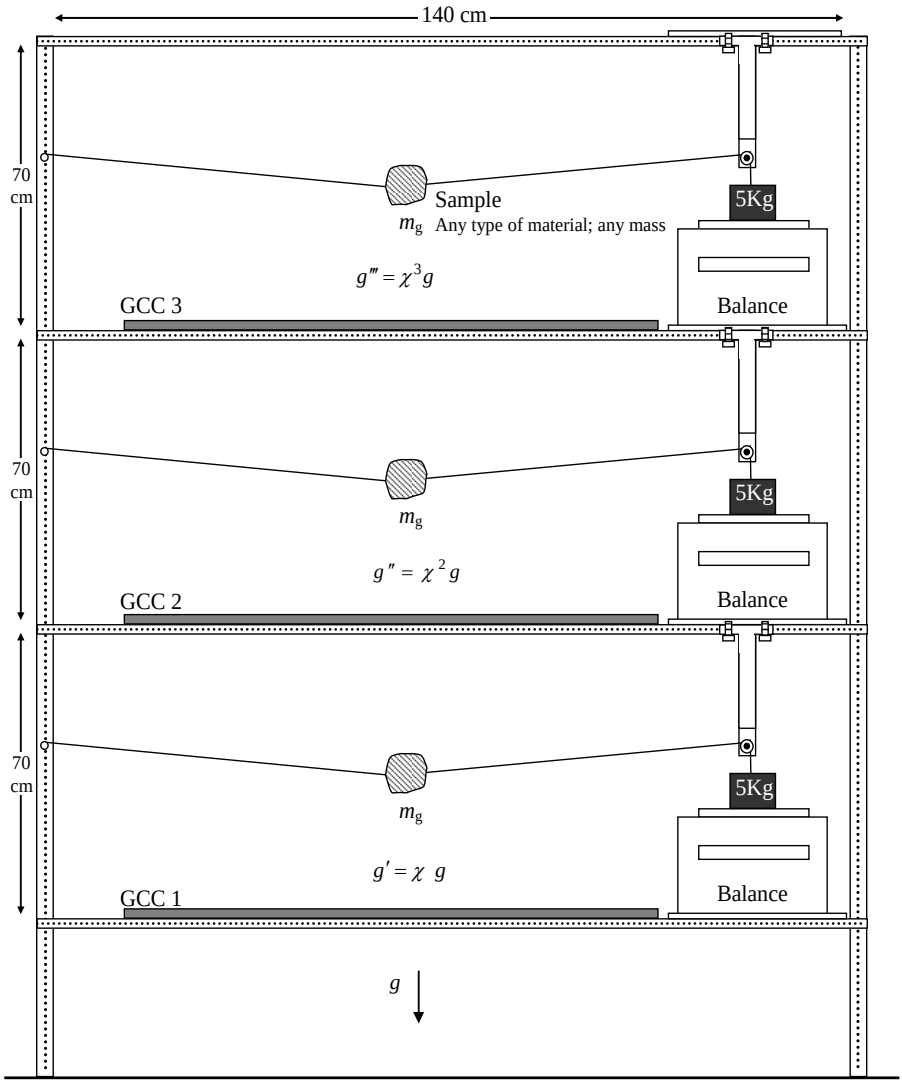

Fig. A17 – *Experimental set-up.* In order to prove *the exponential effect* produced by the superposition of the Gravitational Shieldings, we can take three similar GCCs and put them one above the other, in such way that above the GCC 1 the gravity acceleration will be $g' = \chi\, g$; above the GCC2 $g'' = \chi^2 g$, and above the GCC3 $g''' = \chi^3 g$. Where χ is given by Eq. (A47). The arrangement above has been designed for values of $m_g < 13g$ and χ up to -9 or $m_g < 1kg$ and χ up to -2 .

APPENDIX B: A DIDACTIC *GCC* USING A BATTERY OF CAPACITORS

Let us now show a new type of GCC - easy to be built with materials and equipments that also can be obtained with easiness.

Consider a battery of n parallel plate capacitors with capacitances $C_1, C_2, C_3, ..., C_n$, connected in parallel. The voltage applied is V; A is the area of each plate of the capacitors and d is the distance between the plates; $\varepsilon_{r(water)}$ is the relative permittivity of the dielectric (water). Then the electric charge q on the plates of the capacitors is given by

$$q = (C_1 + C_2 + C_3 + ... + C_n)V = n(\varepsilon_{r(water)}\varepsilon_0)\frac{A}{d}V \qquad (B1)$$

In Fig. I we show a GCC with *two* capacitors connected in parallel. It is easy to see that the electric charge density σ_0 on each area $A_0 = az$ of the edges B of the thin laminas (*z* is the thickness of the edges B and *a* is the length of them, see Fig.B2) is given by

$$\sigma_0 = \frac{q}{A_0} = n(\varepsilon_{r(water)}\varepsilon_0)\frac{A}{azd}V \qquad (B2)$$

Thus, the electric field E between the edges B is

$$E = \frac{2\sigma_0}{\varepsilon_{r(air)}\varepsilon_0} = 2n\left(\frac{\varepsilon_{r(water)}}{\varepsilon_{r(air)}}\right)\frac{A}{azd}V \qquad (B3)$$

Since $A = L_x L_y$, we can write that

$$E = 2n\left(\frac{\varepsilon_{r(water)}}{\varepsilon_{r(air)}}\right)\frac{L_x L_y}{azd}V \qquad (B4)$$

Assuming $\varepsilon_{r(water)} = 81$ [****] (bidistilled water); $\varepsilon_{r(air)} \cong 1$ (vacuum 10^{-4} Torr; 300K); $n = 2$; $L_x = L_y = 0.30m$; $a = 0.12m$; $z = 0.1mm$ and $d = 10mm$ we obtain

$$E = 2.43 \times 10^8 V$$

For $V_{max} = 220V$, the electric field is

$$E_{max} = 5.3 \times 10^{10} V / m$$

Therefore, if the frequency of the wave voltage is $f = 60Hz$, $(\omega = 2\pi f)$, we have that $\omega\varepsilon_{air} = 3.3 \times 10^{-9} S.m^{-1}$. It is known that the electric conductivity of the air, σ_{air}, at 10^{-4} Torr and 300K, is much smaller than this value, i.e.,

$$\sigma_{air} << \omega\varepsilon_{air}$$

Under this circumstance $(\sigma << \omega\varepsilon)$, we can substitute Eq. 15 and 34 into Eq. 7. Thus, we get

$$m_{g(air)} = \left\{1 - 2\left[\sqrt{1 + \frac{\mu_{air}\varepsilon_{air}^3}{c^2}\frac{E^4}{\rho_{air}^2}} - 1\right]\right\} m_{i0(air)}$$

$$= \left\{1 - 2\left[\sqrt{1 + 9.68 \times 10^{-57}\frac{E^4}{\rho_{air}^2}} - 1\right]\right\} m_{i0(air)} \qquad (B5)$$

The density of the air at 10^{-4} Torr and 300K is

$$\rho_{air} = 1.5 \times 10^{-7} kg.m^{-3}$$

Thus, we can write

$$\chi = \frac{m_{g(air)}}{m_{i(air)}} =$$

$$= \left\{1 - 2\left[\sqrt{1 + 4.3 \times 10^{-43} E^4} - 1\right]\right\} \qquad (B6)$$

Substitution of E for $E_{max} = 5.3 \times 10^{10} V/m$ into this equation gives

$$\chi_{max} \cong -1.2$$

This means that, in this case, the *gravitational shielding* produced in the vacuum between the edges B of the thin laminas can reduce the local gravitational acceleration g down to

$$g_1 \cong -1.2g$$

Under these circumstances, the weight, $P = +m_g g$, of any body just *above* the gravitational shielding becomes

$$P = m_g g_1 = -1.2 m_g g$$

[****] It is easy to see that by substituting the water for Barium Titanate ($BaTiO_3$) the dimensions L_x, L_y of the capacitors can be strongly reduced due to $\varepsilon_{r(BaTiO3)} = 1200$.

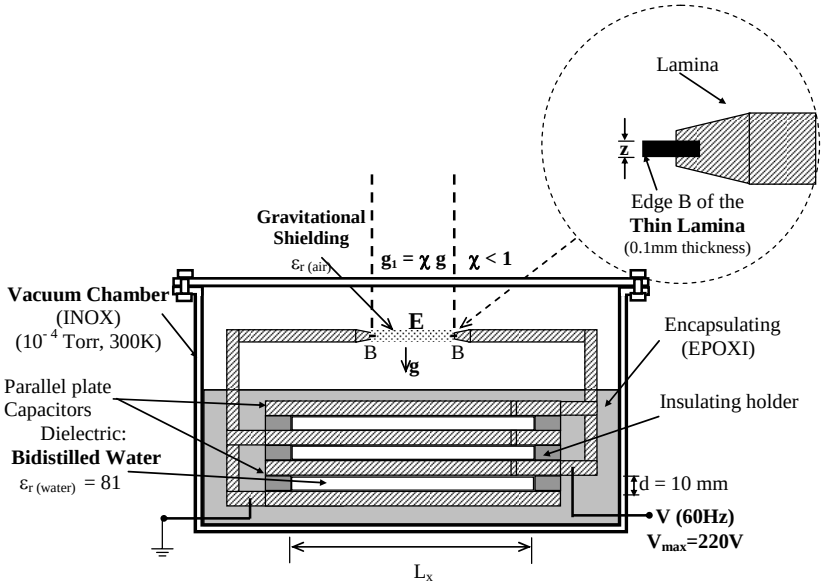

Vertical Cross Section

$$q = (C_1+C_2+...+C_n)\, V = \\ = n\, [\varepsilon_{r\,(water)} / \varepsilon_{r\,(air)}]\, [A/A_0]\, V / d$$

$$\varepsilon_{r\,(water)} = 81 \;;\; \varepsilon_{r\,(air)} \cong 1$$

$$\mathbf{E} = [q/A_0] / \varepsilon_{r\,(air)}\, \varepsilon_0 = n\, [\varepsilon_{r\,(water)} / \varepsilon_{r\,(air)}]\, [A/A_0]\, V / d$$

A is the area of the plates of the capacitors and A_0 the cross section area of the edges B of the thin laminas (z is the thickness of the edges).

Figure B1 – **Gravity Control Cell** (GCC) using a *battery of capacitors*. According to Eq. 7 , the electric field, **E**, through the air at 10^{-4} Torr; 300K, in the vacuum chamber, produces a gravitational shielding effect. The gravity acceleration above this gravitational shielding is reduced to $\chi\mathbf{g}$ where $\chi < 1$.

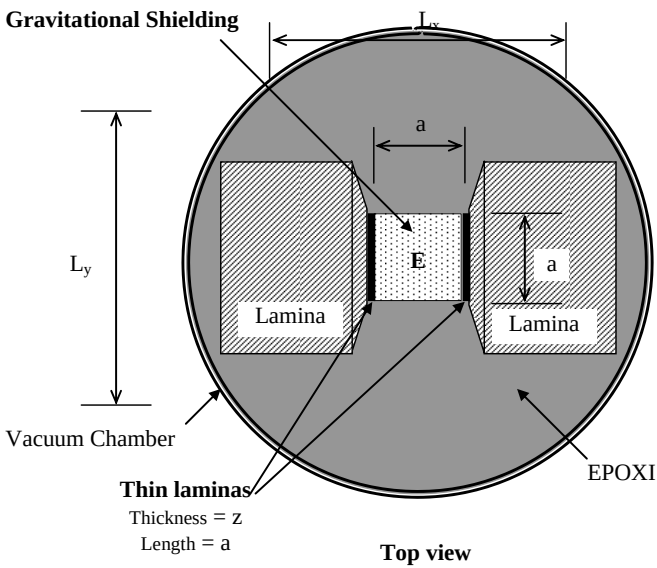

$A_0 = a\ z\ ;\quad A = L_x\ L_y$

Figure B2 – The gravitational shielding produced between the thin laminas.

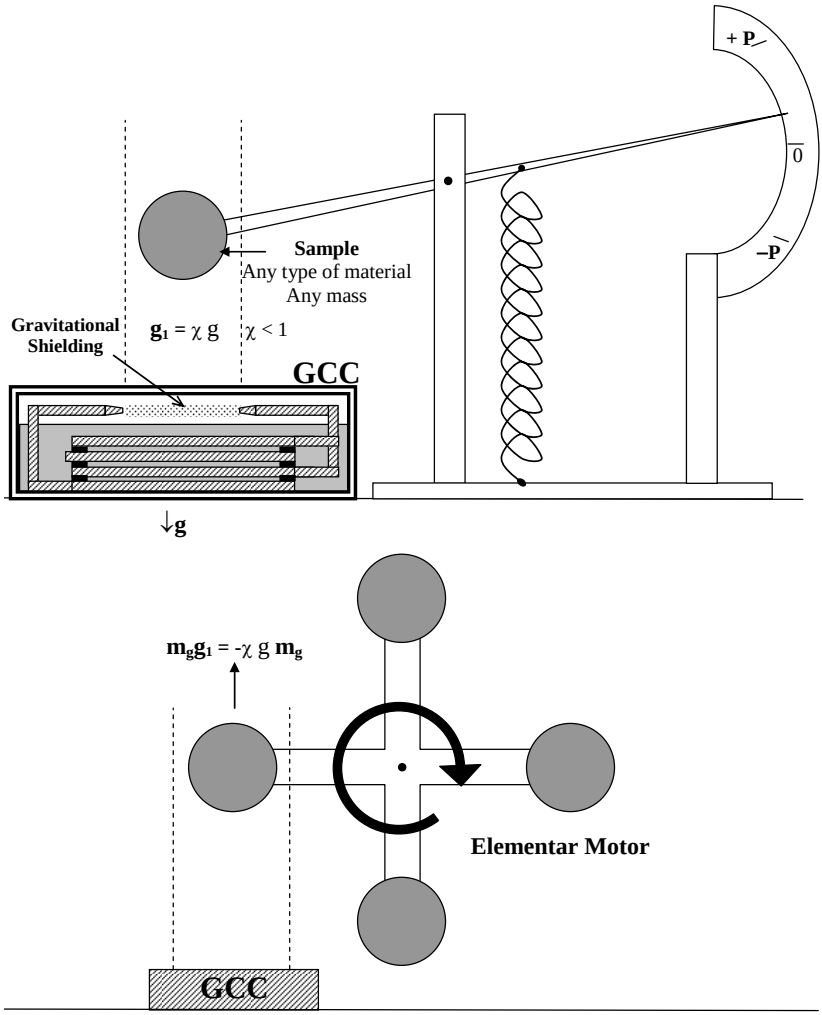

Figure B3 – Experimental arrangement with a GCC using battery of capacitors. By means of this set-up it is possible to check the weight of the sample even when it becomes *negative*.

REFERENCES

1. DeAquino, F. 2010. *Mathematical Foundations of the Relativistic Theory of Quantum Gravity*. Pacific Journal of Science and Technology. **11**(1), pp.173-232.

2. Freire, G. F. O and Diniz, A. B. (1973) *Ondas Eletromagnéticas*, Ed. USP,p.26.

3. Halliday, D. and Resnick, R. (1968) *Physics,* J. Willey & Sons, Portuguese Version, Ed. USP, p.1118.

4. Quevedo, C. P. (1977) *Eletromagnetismo*, McGraw-Hill, p.255 and 269.

5. GE Technical Publications (2007), 80044 – F20T12/C50/ECO, GE Ecolux ®T12.

6. Aplin, K. L. (2000) PhD thesis, The University of Reading, UK

7. Aplin K. L (2005) *Rev. Sci. Instrum.* **76**, 104501.

8. Beiser, A. (1967) *Concepts of Modern Physics*, McGraw-Hill,Portuguese version (1969) Ed. Polígono, S.Paulo, p.362-363.

9. Hayt, W. H. (1974), *Engineering Electromagnetics*, McGraw-Hill. Portuguese version (1978) Ed. Livros Técnicos e Científicos Editora S.A, RJ, Brasil. P.146.

10. Benjegerdes, R. et al.,(2001) *Proceedings of the 2001Particle Accelerator Conference*, Chicago. http://epaper.kek.jp/p01/PAPERS/TOAB009.PDF

11. Gourlay, S. et al., (2000) *Fabrication and Test of a 14T, Nb3Sn Superconducting Racetrack Dipole Magnetic*, IEE Trans on Applied Superconductivity, p.294.

12. BPE soft, *Extreme High Altitude Conditions Calculator*. http://bpesoft.com/s/wleizero/xhac/?M=p

13. Handbook of Chemistry and Physics, 77th ed.1996.

14. Halliday, D. and Resnick, R. (1968) *Physics,* J. Willey & Sons, Portuguese Version, Ed. USP, p.1118.

15. Zhan, G.D *et al.* (2003) *Appl. Phys. Lett.* **83,** 1228.

16. Davidson, K. & Smoot, G. (2008) *Wrinkles in Time*. N. Y: Avon, 158-163.

17. Silk, Joseph. (1977) *Big Bang*. N.Y, Freeman, 299.

18. Jafelice, L.C. and Opher, R. (1992). *The origin of intergalactic magnetic fields due to extragalactic jets*. RAS. http://adsabs.harvard.edu/cgi-bin/nph-bib query? Bib code = 1992 MNRAS. 257. 135J. Retrieved 2009-06-19.

19. Wadsley, J., et al. (2002). *The Universe in Hot Gas*. NASA. http://antwrp.gsfc.nasa.gov/apod/ap 020820. html. Retrieved 2009-06-19.

The Gravitational Mass at the Superconducting State

Fran De Aquino

Maranhao State University,
Physics Department,
65058-970 S.Luis/MA, Brazil.
E-mail: deaquino@elo.com.br

Abstract

It will be shown that the gravitational masses of the electrons of a superconducting material are strongly *negative*. Particularly, for an amount of mercury (*Hg*) at the transition temperature, $T_c = 4.15$ K , the negative gravitational masses of the electrons decrease the *total* gravitational mass of the *Hg* of approximately 0.1 percent. The weight reduction *increase* when the *Hg* is spinning inside a magnetic field or when it is placed into a strong oscillating EM field.

Introduction

We have shown in a previous paper[1] that the *gravitational mass* and the *inertial mass* are correlated by a dimensionless factor, which depends on the incident *radiation* upon the particle. It was shown that only in the absence of electromagnetic radiation this factor becomes equal to 1 and that, in specific electromagnetic conditions, it could be reduced, nullified or made negative.

The general expression of correlation between gravitational mass m_g and inertial mass m_i , is given by

$$m_g = m_i - 2\left\{\sqrt{1+\left\{\frac{q}{m_i c}\right\}^2} - 1\right\} m_i \qquad (1)$$

the *momentum* q is given by

$$q = N\hbar k = N\hbar\omega/(\omega/k) = U/(dz/dt) = \\ = U/v \qquad (2)$$

where U is the electromagnetic energy absorbed (or emitted) by the particle; v is the velocity of the incident(or emitted) radiation, which is

$$v = \frac{c}{\sqrt{\frac{\varepsilon_r \mu_r}{2}\left(\sqrt{1+(\sigma/\omega\varepsilon)^2}+1\right)}} \qquad (3)$$

where $\omega = 2\pi f$; f is the frequency of the radiation: ε ,μ and σ, are the electromagnetic characteristics of the outside medium around the particle in which the incident (or emitted) radiation is propagating ($\varepsilon = \varepsilon_r \varepsilon_0$; ε_r is the *relative electric permittivity* and $\varepsilon_0 = 8.854\times10^{-12}\, F/m$: $\mu = \mu_r \mu_0$; μ_r is the *relative magnetic permeability* and $\mu_0 = 4\pi\times10^{-7}\, H/m$).

The general expression of correlation between gravitational mass and inertial mass (Eq.(1)) was experimentally confirmed by an experiment using Extra-Low Frequency (ELF) radiation on ferromagnetic material.The experimental setup and the obtained results were presented in a previous paper[2] . Recently another experiment[3] using UV light on phosphorescent plastic have also confirmed the Eq.(1).

By the substitution of Eqs.(3) and (2) into Eq.(1), we obtain

$$m_g = m_i - 2\left\{\sqrt{1+\left\{\frac{U}{m_i c^2}\sqrt{\frac{\varepsilon_r\mu_r}{2}\left(\sqrt{1+(\sigma/\omega\varepsilon)^2}+1\right)}\right\}^2}-1\right\}m_i$$

$$= m_i - 2\left\{\sqrt{1+\left\{\frac{U}{m_i c^2}n_r\right\}^2}-1\right\}m_i \qquad (4)$$

In the equation above, n_r is the *refractive index* , which is given by:

$$n_r = \frac{c}{v} = \sqrt{\frac{\varepsilon_r\mu_r}{2}\left(\sqrt{1+(\sigma/\omega\varepsilon)^2}+1\right)} \qquad (5)$$

c is the speed in vacuum and v is the speed in medium.

It is important to note that the electromagnetic characteristics, ε ,μ and σ, do not refer to the particle, but to the outside medium around the particle in which the incident (or emitted) radiation is propagating. For an *electron* inside a body, the incident (or emitted)radiation on this electron will be propagating inside the body, and consequently, σ=σ_{body},ε=ε_{body}, μ=μ_{body}. Thus, according to the Eq.(4), the gravitational mass of the electron is given by

$$m_{ge} = m_e - 2\left\{\sqrt{1+\left\{\frac{U}{m_e c^2}n_{r(body)}\right\}^2}-1\right\}m_e \qquad (6)$$

where m_e is the *inertial* mass of the electron and $n_{r(body)}$ is the index of refraction of the body.

Based on the equation above, we will be show that the *gravitational masses* of the electrons of a superconducting material are strongly negative. Particularly, for an amount of mercury (*Hg*) at the transition temperature, the negative gravitational masses of the electrons decrease the *total gravitational mass* of the Hg of approximately 0.1%.

2. Superconductors

Usually, for *superconducting materials*, we have $\sigma >> \omega\varepsilon$. Thus, in that case, the index of refraction given by the Eq.(5), can be written

$$n_r = \sqrt{\frac{\mu\sigma c^2}{2\omega}} \qquad (7)$$

The equation above shows that the *refractive indices* of the superconducting materials are enormous. Consequently, in agreement with Eq.(6), the gravitational masses of their electrons can be significantly reduced even for U relatively small as, for example, in the case of *thermal radiation* emitted from a disk of superconducting material at the transition temperature T_c.

In the case of *thermal radiation*, it is common to relate the energy of photons to *temperature*, T, through the relation,

$$\langle hf \rangle \approx \kappa T$$

where κ = 1.38×10^{-23}J/K is the Boltzmann's constant. Thus, we can write

$$U = \eta\langle hf \rangle \approx \eta\kappa T .$$

Where η is a particle-dependent absorption (or emission) coefficient. Consequently, we can express Eq.(6) as follows:

$$m_{ge} = m_e - 2\left\{\sqrt{1+\left\{\frac{\eta_e}{m_e c}\sqrt{\frac{\mu\sigma\hbar\kappa T}{2}}\right\}^2}-1\right\}m_e \qquad (8)$$

For electrons[4] $\eta = \eta_e \cong 0.1$. Thus, for $T = T_c$ (Transition Temperature) the equation above can be written

$$m_{ge} = m_e - 2\left\{\sqrt{1+1.2\times10^{-22}\sigma T_c} - 1\right\}m_e \qquad (9)$$

From this equation we can conclude that *the gravitational masses* of the electrons of a superconducting material ($\sigma > 10^{22}\, S/m$) are strongly *negative*.

Let us now consider the Hg at the *transition temperature*[5], T_c = 4.15 K. At this temperature, the electric conductivity of the Hg is $\sigma \cong 10^{23}\, S/m$. Consequently, from the Eq.(9) we obtain

$$m_{ge} \cong -11.25 m_e$$

Thus the *total* gravitational mass of the Hg is

$$m_{g(Hg)} = \left[\frac{-11.25m_e + m_p + m_n}{m_e + m_p + m_n}\right] m_{i(Hg)} \cong 0.99 m_{i(Hg)}$$

This means that the negative gravitational masses of the electrons decrease the *total gravitational mass* of the Hg of *less than* 1% percent (approximately 0.1%).

This prediction can be verified in a very simple way, see Fig. 1. In addition, we suggest to check the weights of samples (of different masses and chemical compositions) hung above the Hg. Possibly the percentage of weight decrease will be *the same* of the Hg up to some meters upwards(due to shielding effect produced to the reduction of the gravitational mass of the Hg).

It is important to note that, if the Hg cylinder *rotates* at a strong

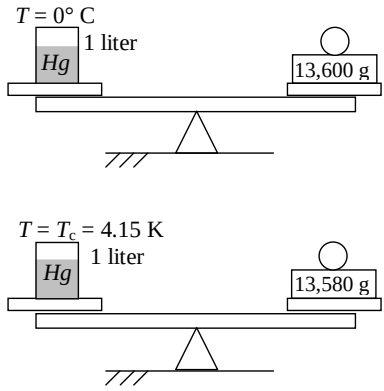

Fig.1 - The Gravitational Mass of the *Hg* at 0ºC and at 4.15K(Transition Temperature)

magnetic field B perpendicular to the cylinder, the weight reduction must *increase* due to the emission of radiation from the electrons rotating within the magnetic field. At this case, the radiation emitted from each electron has power P which, as we know, is given by[6]

$$P = \frac{\mu e^4 B^2 V^2}{6\pi m_e^2 c\left(1 - V^2/c^2\right)} \qquad (10)$$

Most of the emitted radiation has frequency f

$$f = f_0\left(1 - \frac{V^2}{c^2}\right)^{-3/2} \qquad (11)$$

where

$$f_0 = \frac{eB}{2\pi m_e}\sqrt{1 - V^2/c^2} \qquad (12)$$

is the named *cyclotron frequency*.

To simplify the calculations we can consider only the contribution of the emitted radiation with frequency f. Then we can put $U = nhf$ in Eq.(6), where n is the number of emitted

photons from the electron. Thus we can write

$$m_g = m_e - 2\left\{\sqrt{1+\left\{\frac{nhf}{m_e c^2}n_r\right\}^2} - 1\right\}m_e \qquad (13)$$

But $P = nhf/\Delta t = nhf^2$, thus we can write $n = P/hf^2$. Substitution of n into Eq.(13) gives

$$m_g = m_e - 2\left\{\sqrt{1+\left\{\frac{P}{m_e cvf}\right\}^2} - 1\right\}m_e \qquad (14)$$

For $\sigma >> \omega\varepsilon$ Eq.(3) reduces to

$$v = \sqrt{\frac{4\pi f}{\mu\sigma}} \qquad (15)$$

By the substitution of Eqs.(10) and Eq.(15) into Eq.(14) we obtain

$$m_g = m_e - 2\left\{\sqrt{1+\left\{\frac{e^4B^2V^2}{6\pi m_e^2c^2\left(1-V^2/c^2\right)}\sqrt{\frac{\mu^3\sigma}{4\pi f^3}}\right\}^2} - 1\right\}m_e \qquad (16)$$

Note that the *momentum* q in Eq.(1) can be also produced by an Electric and/or Magnetic field *if the particle has an electric charge* Q.

In that case, combination of *Lorentz's Equation* $\vec{F} = Q\vec{E}_0 + Q\vec{V}\times\vec{B}$ and $\vec{F} = m_g\vec{a}$ (see reference 1, p.78-Eq.(2.05)) gives

$$q' = m_g V = m_g\frac{Q\left(E_0 + \vec{V}\times\vec{B}\right)}{m_g}\Delta t \qquad (17)$$

In the particular case of an oscillating EM field (frequency f_{osc}, $\Delta t = 1/f_{osc}$) we have

$$q' = \frac{Q\left(E_{osc} + \vec{V}\times\vec{B}_{osc}\right)}{f_{osc}} \qquad (18)$$

Thus, the general expression of q in Eq.(1) will be

$$q = \frac{U}{v} + q' = \frac{U}{c}n_r + \frac{Q\left(E_{osc} + \vec{V}\times\vec{B}_{osc}\right)}{f_{osc}} \qquad (19)$$

Consequently, if the Hg cylinder *rotates* at an *oscillating* magnetic field B_{osc} of frequency f_{osc}, perpendicular to the cylinder, then the *total* value of q for the electrons of the Hg, according to Eq.(19), will be given by

$$q = \frac{U}{c}n_r + \frac{e\left(E_{osc} + \vec{V}\times\vec{B}_{osc}\right)}{f_{osc}} \qquad (20)$$

where $\frac{U}{c}\eta_r$, according to Eq.(16), is given by

$$\frac{U}{c}\eta_r = \frac{e^4B^2V^2}{6\pi m_e^2 c\left(1-V^2/c^2\right)}\sqrt{\frac{\mu^3\sigma}{4\pi f^3}}$$

where

$$\vec{V} = \vec{V}_{\omega_c} + \vec{V}_{osc}$$

In the equation above $V_{\omega_c} = \omega_c R$ and V_{osc} can be calculated by means of the well-known equations of the *Ohm's vectorial Law* : $\vec{J} = \sigma\vec{E}$ and $\vec{J} = \rho_m\vec{V}$ (J is the current density, in $\mathrm{A/m^2}$; ρ_m and V are respectively, the density ($\mathrm{C/m^3}$) and the velocity of charge carriers). Thus we can write

$$V_{osc} = \left(\frac{\sigma}{\rho_m}\right)E_{osc} = \left(\frac{\sigma}{\rho_m}\right)vB_{osc} = \\ = \left(\frac{\sigma}{\rho_m}\right)B_{osc}\sqrt{\frac{2\omega_{osc}}{\mu\sigma}} = B_{osc}\sqrt{\frac{4\pi f_{osc}\sigma}{\mu\rho_m^2}} \qquad (21)$$

Thus the Eq.(20) can be rewritten in the following form:

$$q=\frac{e^4B_{osc}^2V_{osc}^2}{6\pi m_e^3c^2\left(1-V_{osc}^2/c^2\right)}\sqrt{\frac{\mu^3\sigma}{4\pi f^3}}+ \\ +\frac{e\left(E_{osc}+\omega_c RB_{osc}+V_{osc}B_{osc}\right)}{f_{osc}} \qquad (22)$$

Where $E_{osc}=vB_{osc}$ (v given by the Eq.(3), $v=\sqrt{\frac{2\omega_{osc}}{\mu\sigma}}$).

By the substitution of Eq.(22) into Eq.(1), we obtain

$$m_{ge}=m_e-2\left\{\sqrt{1+\left[X+\frac{e\left(E_{osc}+\omega_c RB_{osc}+V_{osc}B_{osc}\right)}{\left(m_ecf_{osc}\right)}\right]^2}-1\right\}m_e \qquad (23)$$

where

$$X=\frac{e^4B_{osc}^2V_{osc}^2}{6\pi m_e^3c^2\left(1-V_{osc}^2/c^2\right)}\sqrt{\frac{\mu^3\sigma}{4\pi f^3}}$$

For H_g at the superconducting state we can take $\mu\cong\mu_0$; $\sigma\cong10^{23}S/m$ and $\rho_m\cong10^{13}C/m^3$. Thus, when the Hg cylinder is rotating at angular frequency $\omega_c\cong5000rpm$, within a magnetic field $B_{osc}\cong0.1T$ of frequency $f_{osc}\cong10Mhz$, a point at distance $R=10cm$ (*average* radius of the cylinder) from the rotating axis has tangential velocity $V_{\omega_c}=\omega_cR\cong52m/s$, and consequently the gravitational masses of the electrons at this distance are then

$$m_{ge}\cong-160.70m_e$$

We can assume this value as the *average* gravitational mass of the electrons. Thus, the *total average* gravitational mass can be written as follows

$$m_{g(Hg)}=\left[\frac{-160.70m_e+m_p+m_n}{m_e+m_p+m_n}\right]m_{i(Hg)}\cong \\ \cong0.96m_{i(Hg)}$$

This means that the *total gravitational mass* of the Hg decreases of approximately 4% percent.

In our opinion, this way *Podkletnov's effect*[7] may be understood.

When the Hg cylinder isn't rotating ($\omega_c=0$) the Eq.(23) reduces to

$$m_{ge}=m_e-2\left\{\sqrt{1+\left[\frac{e}{m_ec}\left(\frac{E_{osc}}{f_{osc}}+\frac{V_{osc}B_{osc}}{f_{osc}}\right)\right]^2}-1\right\}m_e \\ =m_e-2\left\{\sqrt{1+\left[\frac{eB_{osc}}{m_ec}\left(\sqrt{\frac{4\pi}{\mu\sigma f_{osc}}}+\frac{V_{osc}}{f_{osc}}\right)\right]^2}-1\right\}m_e \qquad (24)$$

By the substitution of Eq.(21) into Eq.(24) we obtain

$$m_{ge}=m_e-2\left\{\sqrt{1+\left[\frac{eB_{osc}}{m_ec}\left(\sqrt{\frac{4\pi}{\mu\sigma f_{osc}}}+B_{osc}\sqrt{\frac{4\pi\sigma}{\mu\rho_m^2f_{osc}}}\right)\right]^2}-1\right\}m_e \qquad (25)$$

Then, if $B_{osc}\cong10T$; $f_{osc}\cong10MHz$, Eq.(25) gives

$$m_{ge}\cong-3700m_e$$

Thus, the *total average* gravitational mass of the H_g is

$$m_{g(Hg)}=\left[\frac{-3700m_e+m_p+m_n}{m_e+m_p+m_n}\right]m_{i(Hg)}\cong-0.01m_{i(Hg)}$$

Again we suggest to check the weights of samples (of different masses and chemical compositions) above the Hg. Possibly the samples

will *float* above the Hg (the gravitational masses of the samples will be *slightly negative*, due to the *negative* gravitational mass of the Hg).

Let us now consider a *static* ($\omega_c = 0$) *parallel-plate capacitor*, where d is the distance between the plates; ΔV_{AC} is the applied voltage; $E_{osc} = \Delta V_{AC} / d$ is the external electric field. Inside the dielectric the electric field is $E = \sigma_m / \varepsilon = E_{osc} / \varepsilon_r$ where σ_m (in C/m^2) is the density of electric charge and $\varepsilon = \varepsilon_r \varepsilon_0$.

Thus the charge Q on each surface of the dielectric is given by $Q = \sigma_m S$ (S is the area of the surface). Then we have

$$Q = \sigma_m S = (E_{osc} \varepsilon_0) S \qquad (26)$$

Within the oscillating field E_{osc} the charge Q (or "charge layer") acquire a *momentum* q , according to Eq.(19), given by

$$q = \frac{U}{c} n_r + \frac{Q(E_{osc} + \vec{V}_{osc} \times \vec{B}_{osc})}{f_{osc}} = \\ = \frac{U}{c} n_r + \frac{Q(2E_{osc})}{f_{osc}} \qquad (27)$$

If $U = 0$ then Eq.(27) reduces to

$$q = \frac{2QE_{osc}}{f_{osc}} = \frac{2E_{osc}^2 \varepsilon_0 S}{f_{osc}} = \frac{2(\Delta V_{AC}/d)^2 \varepsilon_0 S}{f_{osc}} \qquad (28)$$

Assuming that in the dielectric of the capacitor there are N^* *layers of dipoles* with thickness ξ approximately equal to the diameter of the atoms ,i.e., $N^* = d/\xi \cong 10^{10} d$ then, according to Eq.(1), for $q >> m_i c$, the gravitational mass m_g^* of each *dipole layer* is

$$m_g^* \cong -2\left(\frac{q}{m_i c}\right) m_i \cong -\frac{2q}{c} \cong \\ \cong -4\left(\frac{\Delta V_{AC}}{d}\right)^2 \frac{\varepsilon_0 S}{f_{osc} c} \qquad (29)$$

Thus, the total gravitational mass m_g of the dielectric may be written in the following form

$$m_g = N^* m_g^* \cong -4 \times 10^{10} \left(\frac{\varepsilon_0 S}{f_{osc} c d}\right) \Delta V_{AC}^2 \qquad (30)$$

For example, if we have $\Delta V_{AC} = 50KV; S = 0.01m^2; f_{osc} \cong 10^2 Hz$ *and* $d = 1mm$

Eq.(30) gives $m_g \cong -0.3kg$

The result above can also be reach by means of the calculation of the gravitational masses of the electrons of the dielectric of the capacitor. Note that the acceleration upon the *electrons* (due to the field E_{osc}) is obviously equal to acceleration upon the *electric dipoles* of the dielectric. Consequently, the momentum q for the *electrons* (q_e) and for the *electric dipoles* (q_{dip}) are respectively, $q_e = m_e V$ and $q_{dip} = m_{dip} V$. Thus, $q_e = q_{dip}\left(\frac{m_e}{m_{dip}}\right)$.

From Eq.(27), for $U = 0$, we can write

$$q_{dip} = \frac{2Q_{dip} E_{osc}}{f_{osc}} \qquad (31)$$

where Q_{dip} is the *dipole electric charge*. Consequently,

$$q_e = \frac{2Q_{dip} E_{osc}}{f_{osc}} \left(\frac{m_e}{m_{dip}}\right) \qquad (32)$$

and

$$\frac{q_e}{m_e c} = \frac{2Q_{dip}E_{osc}}{m_e c f_{osc}}\left(\frac{m_e}{m_{dip}}\right) = \frac{2Q_{dip}E_{osc}}{m_{dip}cf_{osc}} \qquad (33)$$

By the substitution of Eq.(33) into Eq.(1), we obtain

$$m_{ge} = m_e - 2\left\{\sqrt{1+\left\{\frac{2Q_{dip}E_{osc}}{m_{dip}cf_{osc}}\right\}^2} - 1\right\}m_e \qquad (34)$$

Assuming $Q_{dip} \cong 2\times10^{-19}C; m_{dip} \cong 1\times10^{-26}kg$ and $\Delta V_{AC} = 50KV; d = 1mm; f_{osc} \cong 10^2 Hz$ then Eq.(34) gives

$$m_{ge} \cong -133000m_e$$

Then the total gravitational mass of the dielectric is

$$m_g = \left[\frac{-133000m_e + m_p + m_n}{m_e + m_p + m_n}\right]m_{i(Hg)} \cong -35m_i$$

But $m_i = \rho V = \rho Sd \cong 10^{-2}kg$ then

$$m_g \cong -0.3kg$$

Possibly this is the explanation for the *Biefeld-Brown Effect*.

References

1. De Aquino, F.(2000)"*Gravitation and Electromagnetism:Correlation and Grand Unification*", Journal of New Energy , vol.**5**, no2 , pp.76-84. Los Alamos National Laboratory preprint no.gr-qc/9910036.
2. De Aquino, F. (2000) "*Possibility of Control of the Gravitational Mass by Means of Extra-Low Frequencies Radiation*", Los Alamos National Laboratory preprint no.gr-qc/0005107.
3. Hardeman, C. (2001) " *The Aquino /Hardeman Photo-gravity effect*", in http://www.icnet.net/users/chrish/Photo-gravity.htm
4. De Aquino, F.(2000)"*Gravitation and Electromagnetism:Correlation and Grand Unification*", Journal of New Energy , vol.**5**, no2 , p78.
5. Lynton.E.A.(1962)"*Superconductivity*", John Wiley&Sons, New York.
6. Landau,L. and Lifchitz, E. (1969) *Theorie du Champ*, Ed. MIR, Moscow, Portuguese version (1974) Ed. Hemus, S.Paulo, p.264.
7. Podkletnov, E. and Nieminen, R. (1992) *Physica* C 203,441.

A Gravitational Shielding Based on *ZnS:Ag* Phosphor

Fran De Aquino

Maranhao State University,
Physics Department,
65058-970 S.Luis/MA, Brazil.
E-mail: deaquino@elo.com.br

Abstract

It was shown that there is a practical possibility of gravity control on *electroluminescent* (EL) materials (physics/0109060). We present here a type Gravitational Shielding based on an EL *phosphor* namely zinc sulfide doped with silver (ZnS:Ag) which can reduce the cost of the *Gravitational Motor* previously presented.

Introduction

A recent experiment[1] using UV light on a *phosphorescent* material has detected a small reduction in the gravitational mass of the material. In a previous paper [2] we have explained the reported effect and presented a complete theory for the alterations of the gravitational field in *luminescent* (photo, electro, thermo and tribo) materials. We have obtained the following expressions of correlation between gravitational mass m_g and inertial mass m_i for particles under incident (or emitted) radiation (*fluorescent* or *phosphorescent* radiation):

$$m_g = m_i - 2\left\{\sqrt{1+\left\{\left(\frac{8\pi V}{c^3}\right)f^2 n_r^3\right\}^2} - 1\right\}m_i \qquad (1)$$

and,

$$m_g = m_i - 2\left\{\sqrt{1+\left\{\left(\frac{8\pi V}{c^3}\right)f^2 n_r^4\right\}^2} - 1\right\}m_i \qquad (2)$$

The Eq. (1) if the EL material is a *dielectric* (its electric conductivity σ is such that $\sigma << \omega\varepsilon$, where $\omega = 2\pi f$; f is the frequency of the light emitted from the EL material and ε its electric permittivity). And Eq. (2) if the EL material is a *conductor* ($\sigma >> \omega\varepsilon$).

In Eqs. (1) and (2), V is the *volume* of the particle($m_i = \rho V$ where ρ is matter density of the particle).

We see that the *index of refraction* n_r of the EL material is a highly important factor in both equations, particularly in Eq. (2) where it appears with exponent 4.

In this paper we present a gravitational shielding based on an EL *phosphor* (*ZnS:Ag*) namely zinc sulfide doped with silver whose *index of refraction* is equal to 2.36.

The typical EL devices are consisted of light emitting ***phosphor*** sandwiched between two conductive electrodes. When an AC voltage is applied to the electrodes, the electric

field causes the phosphor to rapidly charge and discharge, resulting in the emission of light during each cycle. The number of light pulses are determined by the magnitude of applied voltage, so, the brightness and color of the light emitted from the EL material will vary subject to the change of the operating voltage and frequency. For example, increasing the voltage increases brightness, whereas increasing the frequency of applied voltage will increase brightness and the *frequency* f of the emitted light.

1. Gravitational Shielding

Let us consider a thin phosphor layer with chemical composition *ZnS:Ag*, index of refraction 2.36, and thickness ξ on a metallic spherical shell with outer radius R.

When a specific alternating voltage V_{AC} with frequency f_{AC} is applied to the metallic spherical shell, the electric field causes the phosphor to rapidly charge and discharge, resulting in the emission of *blue* light ($f = 6.5\times10^{14}\,Hz$). Inside the phosphor this fluorescent radiation will fall upon the atoms. It can be shown that the probability of this radiation to reach the *nucleons* (protons and neutrons) of the atoms is practically null, thus we can assume that the radiation fall only upon the electrons, consequently changing, their gravitational masses. Under these circumstances the gravitational masses of the *electrons*, according to Eq. (2), will be given by:

$$m_{ge} = m_e - 2\left\{\sqrt{1+\left\{1.53\times10^{8} R^2\xi\right\}^2} - 1\right\}m_e \quad (3)$$

and *the gravitational mass of the phosphor layer* will be

$$\begin{aligned} M_g &= n_1 Z_1\left(m_{ge}+m_{gn}+m_{gp}\right)+ \\ &\quad +n_2 Z_2\left(m_{ge}+m_{gn}+m_{gp}\right)+ \\ &\quad \cdots\cdots\cdots\cdots\cdots\cdots\cdots\cdots \\ &\quad +n_n Z_n\left(m_{ge}+m_{gn}+m_{gp}\right)= \\ &= \left(n_1 Z_1+n_2 Z_2+\ldots+n_n Z_n\right)\left(m_{ge}+m_{gn}+m_{gp}\right)= \\ &= N\left(m_{ge}+m_{gn}+m_{gp}\right)= \\ &= N\left\{m_e - 2\left\{\sqrt{1+\left\{1.53\times10^{8} R^2\xi\right\}^2} - 1\right\}m_e + m_n + m_p\right\} \quad (4) \end{aligned}$$

n_1 is the number of atoms with atomic number Z_1 inside the phosphor layer, n_2 is the number of atoms with atomic number Z_2, etc.

When $M_g = 0$ the *phosphor coating* works as a *gravitational shielding*. This occurs if

$$m_e - 2\left\{\sqrt{1+\left\{1.53\times10^{8} R^2\xi\right\}^2} - 1\right\}m_e + m_n + m_p = 0$$

i.e., if $R^2\xi = 1.19\times10^{-5} m^3$. For example if $\xi = 0.1mm$ then the external radius R of the metallic spherical crust must be $R = 0.35m$.

It is important to note that we can vary the frequency f of the emitted light to adjust the exact value of M_g. But, in the previous case where $R^2\xi = 1.19\times10^{-5} m^3$, if $f > 6.5\times10^{14}\,Hz$ the gravitational mass of the layer will be *negative*. This means that the weight of the phosphor layer will be *inverted*.

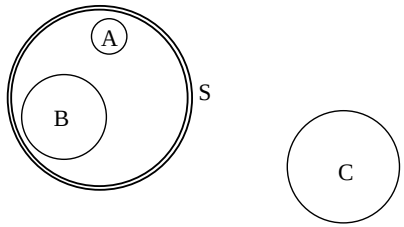

If the gravitational mass of the spherical shell S is equal to ZERO ($M_{gS}=0$) then the gravitational forces between the bodies A,B,C and S are the following:

$$\vec{F}_{AB} = -\vec{F}_{BA} = -G\frac{m_A m_B}{r^2}\hat{\mu}$$

$\vec{F}_{AC} = -\vec{F}_{CA} = 0$
$\vec{F}_{BC} = -\vec{F}_{CB} = 0$ } The interchange of gravitons between A and C, B and C is blockaded by S.

$\vec{F}_{BS} = -\vec{F}_{SB} = 0$
$\vec{F}_{CS} = -\vec{F}_{SC} = 0$ } $M_{gS}=0$

Fig.1-The Concept of Gravitational Shielding.

2. Gravitational Motor

From the technical point of view, the cost of the *Gravitational Motor* presented in recent papers[2,3] can be strongly reduced by means of the gravitational shielding above mentioned.

Let us consider the schematic diagram for the Gravitational Motor in Fig.2. Basically, it is similar to the previous design[2]. But the quantity of EL material in this model is very less than in the previous one. Consequently it will have a very smaller cost.

Now the idea isn't to invert the weight of the cylinders of EL material on the left side of the rotor but to *annul* the weight of *spheres of lead* by means of the gravitational shielding which coat them (see Fig.2).

In this design of the Gravitational Motor, the *average* mechanical *power* P of the motor is given by:

$$P = T\omega = (2P_s\bar{r})\omega = (2M_{gs}g)\bar{r}\left(\frac{g}{\bar{r}}\right)^{\frac{1}{2}} =$$

$$= 2M_{is}\sqrt{g^3\bar{r}} \qquad (5)$$

where $\bar{r} = r - (R_0 + \Delta r)$; $R_0 = R + \xi$, (see Fig.2a) and M_{is} is the *inertial mass* of *one* sphere.

Thus, if the radius of the rotor is $r = 0.35m$ *and* $R = 0.12m; \xi = 0.8mm;$ $\Delta r = 0.03m; M_{is} = 45kg$ we obtain

$$P \cong 1.2kw \cong 1.6HP$$

This is the power produced by *each group* of 6 spheres as shown in Fig.2a. Obviously additional similar groups can increase the total power.

An electric generator coupled at this motor can produce for one month an amount of electric energy W given by

$$W = P.\Delta t = (1200w)(2.59\times10^6 s) =$$

$$= 3.1\times10^9\ j \cong 861Kwh$$

We recall that the monthly residential consumption of electric energy of more than 99.7% of the Earth's residences is less than 800kwh.

3. Gravitational Spacecraft

In a previous paper[4] (Appendix B) we have presented a new concept of spacecraft and aerospace flight.

The new spacecraft, namely Gravitational Spacecraft, works by means of the gravity control.

The conception of the Gravitational Spacecraft is based on

the fact that it is possible to make negative the gravitational mass of a body. Thus, we can imagine a spacecraft with *positive* M_g^+ and *negative* M_g^- gravitational masses in such manner that its total gravitational mass M_g is given by $M_g = M_g^+ + M_g^-$. The *negative* masse can be supplied by means of a system-G [4] (Appendix A) or by means of an EL material as the phosphor (*ZnS:Ag*), in agreement with we have seen in the §1 of this paper.

In that case, to understand how it works, let us imagine an aircraft, which is totally coated with a layer of *ZnS:Ag*. When a appropriated voltage V_{AC} with frequency f_{AC} is applied on the metallic surface of the aircraft, the phosphor emits a fluorescent radiation (blue light ; $f = 6.5\times10^{14} Hz$) and consequently, as we have seen, inside the phosphor this fluorescent radiation will fall upon the electrons, consequently changing, their gravitational masses. Under these circumstances the gravitational masses of the *electrons*, according to Eq. (2), will be given by:

$$m_{ge} = m_e - 2\left\{\sqrt{1+\left\{\left(\frac{8\pi V}{c^3}\right)f^2 n_r^4\right\}^2} - 1\right\}m_e = \\ = m_e - Km_e \qquad (6)$$

where V is the volume of the phosphor layer upon the aircraft.

If $K>>1$ the gravitational masses of the electrons will be given by

$$m_{ge} \cong -Km_e \qquad (7)$$

Consequently, from the Eq. (4) we can write the gravitational mass of the phosphor layer M_{gs}

$$M_{gs} = -NKm_e + N(m_p + m_n) \cong \\ \cong \frac{-N(Km_e) + N(m_p + m_n)}{m_{is}} m_{is} \cong \\ \cong \frac{-N(Km_e) + N(m_p + m_n)}{N(m_e + m_p + m_n)} m_{is} \qquad (8)$$

where m_{is} is the *inertial* mass of the phosphor layer.

If $Km_e >> (m_p + m_n)$ the equation (8) reduces to

$$M_{gs} \cong \frac{-Km_e}{(m_e + m_p + m_n)} m_{is} \qquad (9)$$

Thus we can write the total gravitational mass M_{ga} of the aircraft i.e.,

$$M_{ga} = M_{ga}^+ + M_{gs} \cong \\ \cong M_{ga}^+ - \frac{Km_e}{(m_e + m_p + m_n)} m_{is} \qquad (10)$$

M_{ga}^+ is the *positive* gravitational mass of the aircraft.

Consequently we can decrease the gravitational mass of the aircraft increasing the value of *K*. In practice will be possible to reduce the value of M_{ga} up to some milligrams.

On the other hand, considering *the new expression for the inertial forces*, i.e., $\vec{F} = |M_g|\vec{a}$ deduced in a previous paper[4] , we can conclude that the aircraft can acquires an enormous acceleration $\vec{a} = \frac{\vec{F}}{|M_{ga}|}$ simply reducing its gravitational mass. In addition it is easy to see that the *inertial effects* on the aircraft will be strongly reduced due to the reduction of its gravitational mass. This is fundamentally a new concept of aerospace flight .

References

1. Hardeman, C. (2001) " *The Aquino /Hardeman Photo-gravity effect*", in http://www.icnet.net/users/chrish/Photo-gravity.htm
2. De Aquino, F. (2001) "*A Possibility of Gravity Control in Electroluminescent Materials"*, Los Alamos National Laboratory preprint no.physics/0109060.
3. De Aquino, F. (2000) " *How to Extract Energy Directly from a Gravitational Field"*, Los Alamos National Laboratory preprint no.gr-qc/0007069.

4. De Aquino, F.(2000)"*Gravitation and Electromagnetism:Correlation and Grand Unification*", Journal of New Energy , vol.**5**, no2 , pp.76-84. Los Alamos National Laboratory preprint no.gr-qc/9910036.

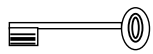

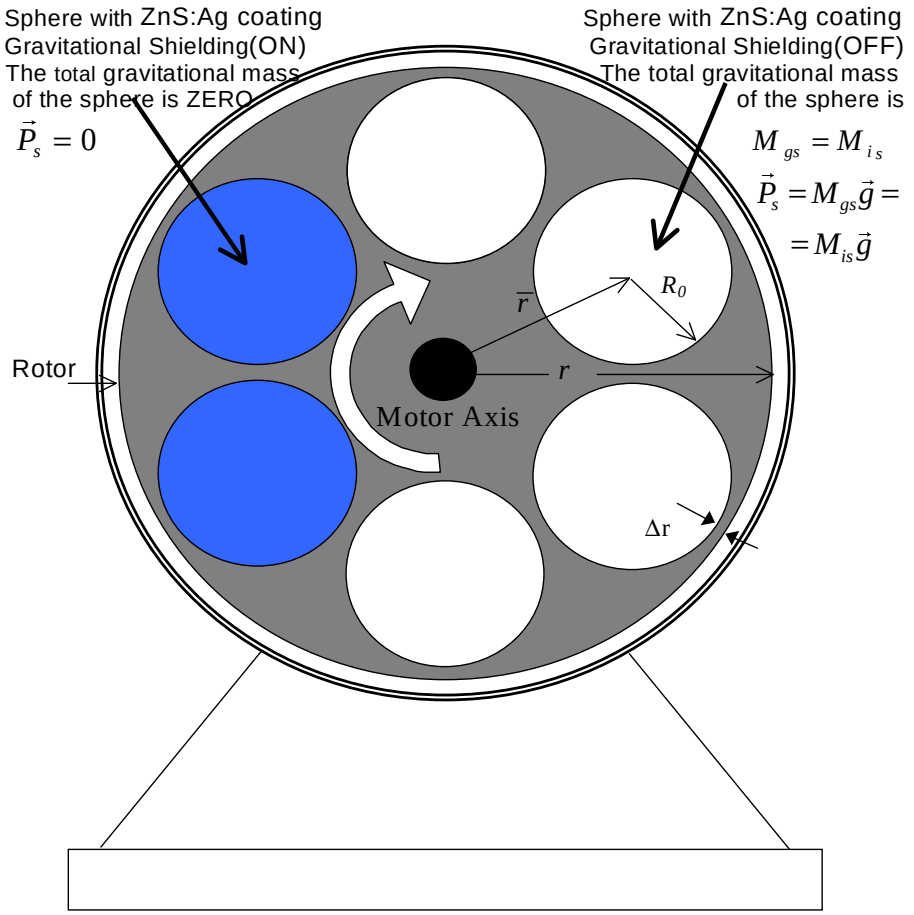

(a) Cross-section of the Motor

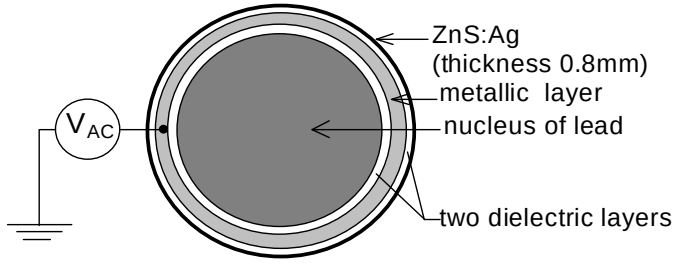

(b) Cross-section of the spheres

Fig.2 – The Gravitational Motor

A Possibility of Gravity Control in Luminescent Materials

Fran De Aquino

Maranhao State University,
Physics Department,
65058-970 S.Luis/MA, Brazil.
E-mail: deaquino@elo.com.br

Abstract

It was demonstrated (gr-qc/9910036) that the gravitational and inertial masses are correlated by an adimensional factor, which depends on the incident (or emitted)radiation upon the particle. There is a direct correlation between the radiation absorbed(or radiated) by the particle and its gravitational mass, independently of the inertial mass. Only in the absence of electromagnetic radiation the mentioned factor becomes equal to *one*. On the other hand, in specific electromagnetic conditions, it can be reduced, nullified or made negative. This means that there is the possibility of the gravitational masses can be reduced, nullified or made negative by means of electromagnetic radiation. This unexpected theoretical result was confirmed by an experiment using Extra-Low Frequency(ELF) radiation on ferromagnetic material (gr-qc/0005107). Recently another experiment using UV light on phosphorescent plastic have confirmed the phenomenon. We present a complete explanation for the alterations of the gravitational field in luminescent materials. This work indicates that the alterations of the gravitational field can be sufficiently strong to invert the gravity on *luminescent materials*.

Introduction

It is known that the physical property of mass has two distinct aspects, *gravitational mass* m_g and *inertial mass* m_i . Gravitational mass produces and responds to gravitational fields. It supplies the mass factors in Newton's famous inverse-square law of gravity($F_{12}=Gm_{g1}m_{g2}/r_{12}^2$). Inertial mass is the mass factor in Newton's 2nd Law of Motion ($F=m_i a$).

In a previous paper[1] we have shown that the *gravitational mass* and the *inertial mass* are correlated by an adimensional factor, which depends on the incident radiation upon the particle. It was shown that only in the absence of electromagnetic radiation this factor becomes equal to 1 and that, in specific electromagnetic conditions, it can be reduced, nullified or made negative.

The general expression of correlation between gravitational mass m_g and inertial mass m_i , is given by

$$m_g = m_i - 2\left\{\sqrt{1+\left\{\frac{q}{m_i c}\right\}^2} - 1\right\}m_i \qquad (1)$$

where the *momentum* q , according to the Quantum Mechanics, is given by

$$q = N\hbar k = N\hbar\omega/(\omega/k) = U/(dz/dt) =$$

$$= U/v \qquad (2)$$

where U is the electromagnetic energy absorbed (or emitted) by the particle; v is the velocity of the incident(or emitted) radiation. It can be shown that

$$v = \frac{c}{\sqrt{\frac{\varepsilon_r \mu_r}{2}\left(\sqrt{1+(\sigma/\omega\varepsilon)^2}+1\right)}} \qquad (3)$$

where ; ε ,μ and σ, are the electromagnetic characteristics of the outside medium around the particle in which the incident radiation is propagating ($\varepsilon = \varepsilon_r \varepsilon_0$ where ε_r is the *relative electric permittivity* and $\varepsilon_0 = 8.854\times10^{-12} F/m$; $\mu = \mu_r \mu_0$ where μ_r is the *relative magnetic permeability* and $\mu_0 = 4\pi\times10^{-7} H/m$). For an *atom* inside a body , the incident(or emitted) radiation on this atom will be propagating inside the body , and consequently , $\sigma = \sigma_{body}$, $\varepsilon = \varepsilon_{body}$, $\mu = \mu_{body}$.

By substitution of Eqs.(2) and (3) into Eq.(1), we obtain

$$m_g = m_i - 2\left\{\sqrt{1+\left\{\frac{U}{m_i c^2}\sqrt{\frac{\varepsilon_r\mu_r}{2}\left(\sqrt{1+(\sigma/\omega\varepsilon)^2}+1\right)}\right\}^2}-1\right\}m_i$$

$$= m_i - 2\left\{\sqrt{1+\left\{\frac{U}{m_i c^2}n_r\right\}^2}-1\right\}m_i \qquad (4)$$

In the equation above n_r is the *refractive index* , which is given by:

$$n_r = \frac{c}{v} = \sqrt{\frac{\varepsilon_r\mu_r}{2}\left(\sqrt{1+(\sigma/\omega\varepsilon)^2}+1\right)} \qquad (5)$$

c is the speed in vacuum and v is the speed in medium.

If the incident(or emitted) radiation is *monochromatic* and has frequency f , we can put $U = nhf$ in Equation(4), where n is the number of incident (or radiated) photons on the particle of mass m_i. Thus we obtain

$$m_g = m_i - 2\left\{\sqrt{1+\left\{\frac{nhf}{m_i c^2}n_r\right\}^2}-1\right\}m_i \qquad (6)$$

In that case, according to the *Statistical Mechanics*, the calculation of n can be made based on the well-known method of *Distribution Probability* . If all the particles inside the body have the same mass m_i, the result is

$$n = \frac{N}{A}a \qquad (7)$$

where N/A is the average density of incident (or emitted) photons on the body; a is the area of the surface of a particle of mass m_i from the body.

Obviously the power P of the incident radiation must be $P = Nhf/\Delta t = Nhf^2$, thus we can write $N = P/hf^2$. Substitution of N into Eq.(7) gives

$$n = \frac{a}{hf^2}\left(\frac{P}{A}\right) = \frac{a}{hf^2}D \qquad (8)$$

where D is the *power density* of the incident(or emitted) radiation. Thus Eq.(6) can be rewritten in the following form:

$$m_g = m_i - 2\left\{\sqrt{1+\left\{\frac{aD}{m_i cvf}\right\}^2}-1\right\}m_i \qquad (9)$$

For $\sigma >> \omega\varepsilon$ Eq.(3) reduces to

$$v = \sqrt{\frac{4\pi f}{\mu\sigma}} \qquad (10)$$

By substitution of Eq.(10) into Eq.(9) we obtain

$$m_g = m_i - 2\left\{\sqrt{1+\left\{\frac{aD}{m_i c}\sqrt{\frac{\mu\sigma}{4\pi f^3}}\right\}^2} - 1\right\} m_i \quad (11)$$

This equation shows clearly that, *atoms* (or *molecules*) can have their *gravitational masses* strongly reduced by means of Extra-Low Frequency (ELF) radiation.

We have built a system (called System G) to verify the effects of the ELF radiation on the gravitational mass of a body . In the system G, a 60Hz frequency radiation was produced by an ELF antenna. A thin layer of *annealed pure iron* around the antenna (toroid form) have absorbed all the ELF radiation.

In this annealed iron toroid $\mu_r = 25000$ ($\mu = 25000\mu_0$) and $\sigma = 1.03\times10^7 S/m$.The power density D of the incident ELF radiation reach approximately 10Kw/m^2 . By substitution of these values into Eq.11) it is easy to conclude the obtained results.

The experimental setup and the obtained results were presented in a paper[2] .

The experiment above mentioned have confirmed that the general expression of correlation between gravitational mass and inertial mass (Eq.4) is correct. In practice, this means that the gravitational forces can be reduced, nullified and *inverted* by means of electromagnetic radiation.

Recently another experiment using UV light on *phosphorescent* materials have confirmed the phenomenon[3].

In this paper we present a complete explanation for the alterations of the gravitational field in *luminescent* (photo, electro, thermo and tribo)materials. It was shown that the alterations of the gravitational field can be sufficiently strong to invert the gravity on *luminescent* materials .

1.Theory

When the material is *luminescent*, the radiated photons number n, radiated from the electrons, cannot be calculated by the Eq.(7), because, according to the quantum *statistical mechanics*, they are *undistinguishable* photons of varying frequencies and consequently follow the *Einstein-Bose statistics*. In that case, as we know, the number n (n is the number of photons with frequency between f and $f+\Delta f$) will be given by

$$n = \left(\frac{8\pi V f^2}{v^3}\right)\frac{1}{e^{E/m_i c^2}-1}\int_f^{f+\Delta f} df \cong$$

$$\cong \left(\frac{8\pi V}{v^3}\right)\frac{1}{e^{E/m_i c^2}-1} f^2 \Delta f$$

Thus, assuming $\Delta f \cong 1Hz$ (*quasi*-mono chromatic) we obtain

$$n \cong \left(\frac{8\pi V f^2}{v^3}\right)\frac{1}{e^{E/m_i c^2}-1} \cong \left(\frac{8\pi V f^2}{v^3}\right)\frac{1}{e^{q/m_i c}-1} \cong$$

$$\cong \left(\frac{8\pi V}{v\lambda^2}\right)\frac{1}{e^{\lambda_c/\lambda}-1} \qquad (12)$$

where $\lambda_c = h/m_i c$ is the *Compton wavelength* for the particle of mass m_i and λ is the *average* wavelength of the light emitted from the particle ; V is the volume of the body which contains the particle .

By substitution of Eq.(12) into Eq.(6) we obtain

$$m_g = m_i - 2\left\{\sqrt{1+\left\{\left(\frac{8\pi V}{v\lambda^2}\right)\frac{\lambda_c/\lambda}{e^{\lambda_c/\lambda}-1}\right\}^2} - 1\right\} m_i \quad (13)$$

For $\sigma << \omega\varepsilon$ the Eq.(3) reduces to

$$v = \frac{c}{\sqrt{\varepsilon_r \mu_r}} \qquad and \qquad \lambda = \frac{c}{f\sqrt{\varepsilon_r \mu_r}}$$

Consequently Eq.(13) can be rewritten In the following form

$$m_g = m_i - 2\left\{\sqrt{1+\left\{\left(\frac{8\pi V}{c^3}\right)f^2 n_r^3 \frac{\lambda_c/\lambda}{e^{\lambda_c/\lambda}-1}\right\}^2}-1\right\}m_i \quad (14)$$

For *electrons* $m_i = m_e = 9.11\times10^{-31} kg$ and $\lambda_{c(electrons)} = 2.42\times10^{-12} m$ .For atoms $\lambda_{c(atoms)} << \lambda_{c(electrons)}$. On the other hand, if

$$\lambda >> \lambda_c \Rightarrow \frac{\lambda_c/\lambda}{e^{\lambda_c/\lambda}-1} \approx 1$$

Then Eq.(14) reduces to

$$m_g = m_i - 2\left\{\sqrt{1+\left\{\left(\frac{8\pi V}{c^3}\right)f^2 n_r^3\right\}^2}-1\right\}m_i \quad (15)$$

In the *Hardeman* experiment [3]

$$\left(\frac{8\pi V}{c^3}\right)f^2 n_r^3 \approx 0.658$$

Consequently, from Eq.(15) we obtain for the electrons of the *luminescent* material:

$$m_{g_{(electrons)}} \approx 0.605 m_{i(electons)}$$

This means a 39.5% reduction in gravitational masses of the electrons of the atoms of the *phosphorescent* material. Thus, the *total* reduction in gravitational mass of the *phosphorescent* material will be given by

$$\frac{m_e - 0.605\, m_e}{m_e + m_p + m_n}\times 100\,\% \approx -0.011\,\%$$

Exactly the value obtained in the *Hardeman* experiment.

Now we will calculate the power of UV radiation, necessary to produce the reduction of weight, detected by Hardeman in the phosphorescent material.

According to the Quantum *Statistical Mechanics* the *gas of photons* inside a *luminescent material* has a *average* number of photons N , where

$$N = \frac{1}{e^{E/m_i c^2}} = \frac{1}{e^{\lambda_c/\lambda}-1} \quad (16)$$

This means that the UV *power* P should have the following value

$$P = Nhf^2 = \frac{hc^2}{\lambda^2(e^{\lambda_c/\lambda}-1)} \quad (17)$$

For $\lambda = 365\ nm$ (*UV light*).The equation above gives

$$P \approx 68\ W$$

From the Electrodynamics we know that a radiation with frequency f propagating within a material with electromagnetic characteristics ε, μ and σ has the amplitudes of its waves decreased of e^{-1}=0.37 (37%) when it penetrates a distance z, given by

$$z = \frac{1}{\omega\sqrt{\tfrac{1}{2}\varepsilon\mu\left(\sqrt{1+(\sigma/\omega\varepsilon)^2}-1\right)}} \quad (18)$$

The radiation is totally absorbed if it penetrates a distance $\delta \cong 5z$.

Thus, if we put under UV radiation (λ=365nm , > 68w) a sheet of phosphorescent plastic with $\sigma << 1$S/m and $\varepsilon > \varepsilon_0$; $\mu > \mu_0$, the Eq. above tell us that $z >>$ 5mm. Consequently, we can assume that the UV radiation at 365nm has a good penetration within the plastic sheet above (thickness = 2mm).

On the other hand, if we assume that the sheet has an index of refraction n_r~1, thus , according to Eq.(15), for f~6×10^{14}Hz (green light radiated from the sheet), the gravitational mass of the *electrons* of the sheet will be NEGATIVE and given by

$$m_g = m_e - 2\left\{\sqrt{1+\left\{\left(\frac{8\pi V}{c^3}\right)f^2 n_r^3\right\}^2} - 1\right\}m_e \cong$$

$$\cong -335.1 m_e \qquad (19)$$

Thus, the *total* reduction in **gravitational mass of the sheet of *phosphorescent* material** will be given by

$$\frac{m_e - 335.1 m_e}{m_e + m_p + m_n} \times 100\% \approx -9.1\%$$

If V=2m×1.36m×0.002m=0.00544m^3 we will have a reduction of approximately **100%.**

2.The Gravitational Motor

For $\sigma >> \omega\varepsilon$, as we have seen , Eq.(3) reduces to Eq.(10),i.e.,

$$v = \sqrt{\frac{4\pi f}{\mu\sigma}}$$

Consequently Eq.(13), for $\lambda >> \lambda_c$, can be rewritten in the following form,

$$m_g = m_i - 2\left\{\sqrt{1+\left\{\left(\frac{8\pi V}{c^3}\right)f^2 n_r^4\right\}^2} - 1\right\}m_i \qquad (20)$$

The difference between Eq.(20) and Eq.(15) is in exponent of the *index of refraction* n_r.

Both Eq.(15) and Eq.(20) tell us that *luminescent materials* with *high refractive indices* can be very efficients in gravity control technology .

In the particular case of the Gravitational Motor (presented in a previous paper[4]) these materials can simplify its construction.

Let us consider figure 1 where we present a new design for the Gravitational Motor based on *electroluminescent* materials.

The *average* mechanical *power* P of the motor is

$$P = T\omega = (F\bar{r})\omega = (m_g g)\bar{r}\left(\frac{g}{\bar{r}}\right)^{\frac{1}{2}} =$$

$$= m_g\sqrt{g^3\bar{r}} \qquad (21)$$

where $\bar{r} = R - (R_0 + \Delta r)$, (see Fig.1-a) and m_g is the *gravitational mass* of the *electroluminescent* material inside the left-half of the rotor (when NEGATIVE, obviously) (see rotor in Fig.1). It is easy to show that m_g may be written in the form

$$m_g \cong -\left[\frac{N(Km_e)}{N(m_e + m_p + m_n)}\right]m_i \qquad (22)$$

$$for \quad Km_e > m_e + m_p + m_n; K > 3666.3$$

where $m_p = m_n = 1.67\times10^{-27} kg$ are the masses of the proton and neutron respectively and K, in agreement with Eq.(20), is given by

$$K \approx 2\left[\frac{8\pi V f^2}{c^3} n_r^4\right] \qquad (23)$$

By substitution of Eq.(23) into Eq.(22) we obtain

$$m_g \cong -\left\{2\left[\frac{8\pi V f^2}{c^3} n_r^4\right]\frac{m_e}{m_e + m_p + m_n}\right\}m_i \qquad (24)$$

But the *electroluminescent* (EL) *material* of the rotor is divided in disks to reduce the gravitational pressure on them(see Fig.1-b). These disks(organic luminescent material) are between electrodes and submitted to suitable alternating voltage ΔV to emit *blue* light(frequency $f = 6.5\times10^{14} hz$). Thus, according to Eq.(24), the gravitational mass m_g^1 of *one* EL *disk,* (with volume $V = \pi R_0^2 \xi$ where

R_0, ξ are respectively, the radius and the thickness of the EL disk), is given by

$$m_g^1 \cong -\left\{\left[\frac{16\pi\left(\pi R_0^2 \xi\right)^2 f^2}{c^3} n_r^4\right]\frac{m_e}{m_e + m_p + m_n}\right\}\rho \quad (25)$$

$$K \approx 2\left[\frac{8\pi V f^2}{c^3} n_r^4\right] = \frac{16\pi\left(\pi R_0^2 \xi\right) f^2}{c^3} n_r^4$$

For example, if the rotor has $R = 627mm; L = 1350mm$ and the EL disks:

$R_0 = 190mm; \rho \cong 800kg/m^3; \xi = 45mm;$

$\chi = 0.2mm \quad and \quad n_r \cong 1$

then the *gravitational mass* of each EL disk (ON) is

$$m_g^1 \cong -4.4kg \quad ; \quad K \cong 4014$$

If the left-half of the rotor has $N_l = 2\frac{L-\chi}{\xi+\chi} = 60$ EL disks(ON), then the *total* gravitational mass m_g is

$$m_g = N_l\, m_g^1 = 264kg$$

Thus, according to Eq.(21) the power of the motor is

$$P = (264)\sqrt{(9.8)^3(0.627 - (0.190 + 0.002)} \cong$$

$$\cong 5.3Kw \cong 7HP$$

A electric generator coupled at this motor can produce for one month an amount of electric energy W given by

$$W = P.\Delta t = (5300w)(2.59 \times 10^6 s) =$$

$$= 1.4 \times 10^{10}\, j \cong 3800Kwh$$

It is important to note that if $n_r \cong 2$ the power of the motor increases to approximately 112 HP!

3. Conclusion

We have studied the possibility to control the gravity on luminescent materials and have concluded that *eletroluminescent materials with high refractive indices* are a new and efficient solution for the gravity control technology . Particularly in the case of the gravitational motors.

References

1. De Aquino, F.(2000)"*Gravitation and Electromagnetism:Correlation and Grand Unification*", Journal of New Energy , vol.**5**, no2 , pp.76-84. Los Alamos National Laboratory preprint no.gr-qc/9910036.
2. De Aquino, F. (2000) "*Possibility of Control of the Gravitational Mass by Means of Extra-Low Frequencies Radiation*", Los Alamos National Laboratory preprint no.gr-qc/0005107.
3. Hardeman, C. (2001) " *The Aquino /Hardeman Photo-gravity effect*", in http://www.icnet.net/users/chrish/Photo-gravity.htm
4. De Aquino, F. (2000) " *How to Extract Energy Directly from a Gravitational Field*", Los Alamos National Laboratory preprint no.gr-qc/0007069.

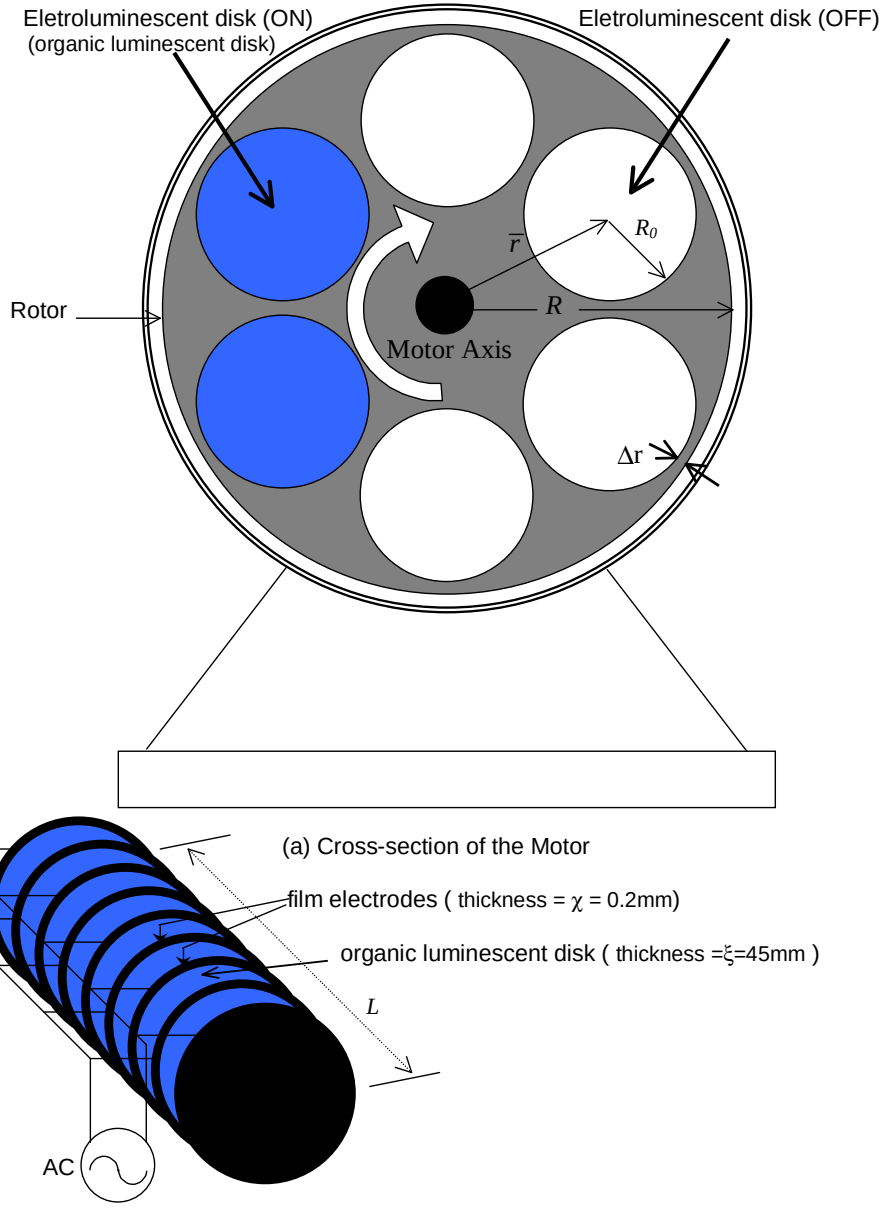

Fig.1 – The Gravitational Motor

APPENDIX A

It is important to note that the *momentum* q in Eq.(1) can be also produced by an Electric and/or Magnetic field if the particle has an electric charge Q.

In that case, combination of *Lorentz's Equation* $\vec{F} = Q\vec{E}_0 + Q\vec{V}\times\vec{B}$ and $\vec{F} = m_g\vec{a}$ (see reference 1, p.78-Eq.(2.05)) gives

$$q = m_g V = m_g \frac{Q\left(E_0 + \vec{V}\times\vec{B}\right)}{m_g}\Delta t \qquad (A1)$$

In the particular case of an oscillating particle(frequency $f, \Delta t = 1/f$) we have

$$q = \frac{Q\left(E_0 + \vec{V}\times\vec{B}\right)}{f} \qquad (A2)$$

Let us consider a *parallel-plate capacitor* where d is the distance between the plates; ΔV is the applied voltage; $E_0 = \Delta V/d$ is the external electric field. Inside the dielectric the electric field is $E = \sigma/\varepsilon = E_0/\varepsilon_r$ where σ (in C/m^2) is the density of electric charge and $\varepsilon = \varepsilon_r\varepsilon_0$.

Thus the charge Q on each surface of the dielectric is given by $Q = \sigma S$ (S is the area of the surface). Then we have

$$Q = \sigma S = (E\varepsilon)S = (E\varepsilon_r\varepsilon_0)S = E_0\varepsilon_0 S \quad (A3)$$

Within the field E_0 ,the charge Q (or "charge layer") acquire a *momentum* q , according to Eq.(A2), given by

$$q = \frac{QE_0}{f} = \frac{E_0^2\varepsilon_0 S}{f} = \frac{(\Delta V/d)^2\varepsilon_0 S}{f} \qquad (A4)$$

Assuming that in the dielectric of the capacitor there is N^* *layers of dipoles* with thickness ξ approximately equal to the diameter of the atoms ,i.e., $N^* = d/\xi \cong 10^{10}\,d$ then, according to Eq.(1), for $q >> m_i c$, the gravitational mass m_g^* of each *dipole layer* is

$$m_g^* \cong -2\left(\frac{q}{m_i c}\right)m_i \cong -\frac{2q}{c} \cong$$

$$\cong -2\left(\frac{\Delta V}{d}\right)^2\frac{\varepsilon_0 S}{fc} \qquad (A5)$$

Thus, the total gravitational mass m_g of the dielectric may be written in the form

$$m_g = N^* m_g^* \cong -2\times 10^{10}\left(\frac{\varepsilon_0 S}{fcd}\right)\Delta V^2 \qquad (A6)$$

For example, if we have $\Delta V = 50KV; S = 0.01m^2; f \cong 10^2 Hz; d = 1mm$ Eq.(A6) gives

$$m_g \cong -0.15kg$$

Possibly this is the explanation for the *Biefeld-Brown Effect*.

POSSIBILITY OF CONTROL OF THE GRAVITATIONAL MASS BY MEANS OF EXTRA-LOW FREQUENCIES RADIATION

Fran De Aquino*
Physics Department, Maranhao State University, S.Luis/ MA, Brazil.

According to the *weak* form of Einstein's general relativity *equivalence principle*, the gravitational and inertial masses are equivalent. However recent calculations have revealed that they are correlated by an adimensional factor, which is equal to one in absence of radiation only. We have built an experimental system to check this unexpected theoretical result. It verifies the effects of the extra-low frequency (ELF) radiation on the *gravitational mass* of a body. We show that there is a direct correlation between the radiation absorbed by the body and its gravitational mass, independently of the inertial mass.

Introduction

The physical property of mass has two distinct aspects, *gravitational mass* m_g and *inertial mass* m_i . Gravitational mass produces and responds to gravitational fields. It supplies the mass factors in Newton's famous inverse-square law of gravity($F_{12}=Gm_{g1}m_{g2}/r_{12}^2$). Inertial mass is the mass factor in Newton's 2nd Law of Motion ($F=m_i a$**)**. One of the deep mysteries of physics is the correlation between these two aspects of mass. Several experiments[1-6] have been carried out since the century XIX to try to verify the correlation between gravitational mass m_g and inertial mass m_i.

In a recent paper[7] we have shown that the *gravitational mass* and the *inertial mass* are correlated by an adimensional factor, which depends on the incident radiation upon the particle. It was shown that only in the absence of electromagnetic radiation this factor becomes equal to 1 and that, in specific electromagnetic conditions, it can be reduced, nullified or made negative. This means that there is the possibility of control of the gravitational mass by means of the incident radiation.

The general expression of correlation between gravitational mass m_g and inertial mass m_i , is given by

$$m_g = m_i - 2\left\{\sqrt{1+\left\{\frac{U}{m_i c^2}\sqrt{\frac{\varepsilon_r\mu_r}{2}\left(\sqrt{1+(\sigma/\omega\varepsilon)^2}+1\right)}\right\}^2}-1\right\}m_i \quad (1)$$

The electromagnetic characteristics, ε ,μ and σ do not refer to the particle, but to the outside medium around the particle in which the incident radiation is propagating. For an *atom* inside a body , the incident radiation on this atom will be propagating inside the body , and consequently , $\sigma = \sigma_{body}$, $\varepsilon = \varepsilon_{body}$, $\mu = \mu_{body}$. So, if $\omega << \sigma_{body}/\varepsilon_{body}$, equation above reduces to

$$m_g = m_a - 2\left\{\sqrt{1+\left\{\frac{U}{m_a c^2}\sqrt{\frac{c^2\mu_{body}\sigma_{body}}{4\pi f}}\right\}^2}-1\right\}m_a \quad (2)$$

where m_a is the *inertial* mass of the atom .

Thus we see that, *atoms* (or *molecules*)can have their *gravitational masses* strongly reduced by means of extra-low frequency (ELF) radiation.

We have built a system to verify the effects of the ELF radiation on the gravitational mass of a body . In this work we present the experimental set-up and the results obtained.

Experimental

Let us consider the apparatus in figure 1 . The Transformer has the following characteristics:

- Frequency : 60 Hz

* Permanent Address: R.Silva Jardim, 521-centro, 65020-560 S. Luis/MA, Brazil.(E-mail: deaquino@uema.br).

- Power : 11.5kVA
- Number of turns of coil : $n_1 = 12$, $n_2 = 2$
- Coil 1 : copper wire 6 AWG
- Coil 2 : ½ inch diameter copper rod (with insulation paint).
- Core area:502.4cm^2 ;ϕ=10 inch (Steel)
- Maximum input voltage : V_1^{max} = 220 V
- Input impedance : $Z_1 = 4.2\ \Omega$
- Output impedance : $Z_2 < 1\text{m}\ \Omega$ (ELF antenna impedance : 116 mΩ)
- Maximum output voltage with coupled antenna : 34.8V
- Maximum output current with coupled antenna : 300 A

In the system-G the *annealed pure iron* has an electric conductivity $\sigma_i = 1.03\times10^7$S/m, magnetic permeability $\mu_i = 25000\mu_0$ [8],thickness 0.6 mm (to absorb the ELF radiation produced by the antenna).The *iron powder* which encapsulates the ELF antenna has $\sigma_p \approx 10$ S/m ;$\mu_p \approx 75\mu_0$ [9]. The antenna physical length is z_0 = 12 m, see Fig.1c.The power radiated by the antenna can be calculated by the well-known *general* expression, for $z_0 << \lambda$:

$$P = (I_0\,\omega z_0)^2/\ 3\pi\varepsilon v^3\ \{[1+(\sigma/\omega\varepsilon)^2]^{½}+1\} \quad (3)$$

where I_0 is the antenna current amplitude ; $\omega = 2\pi f$; f =60Hz ; $\varepsilon = \varepsilon_p$; $\sigma = \sigma_p$ and v is the wave phase velocity in the *iron powder* (given by Equation1.02 , in reference [1]). The radiation efficiency e = P / P+P_{ohmic} is nearly 100%.

Each atom of the annealed iron toroid absorbs an ELFenergy $U=\eta P_a /f$, where η is a particle-dependent absorption coefficient (the maxima η values occurs, as we know, for the frequencies of the atom's *absorption spectrum*) and P_a is the incident radiation power on the atom ; $P_a=DS_a$ where S_a is the atom's *geometric* cross section and $D=P/S$ the radiation power density on the iron atom (P is the power radiated by the antenna and S is the area of the annealed iron toroid (S = 0.374 m^2,see Fig.1b) . So, we can write :

$$U = \eta S_a(I_0 z_0)^2\omega/3S\varepsilon_i v^3\{[1+(\sigma_i/\omega\varepsilon_i)^2]^{½}+1\} \quad (4)$$

Consequently, according to Eq.(1) , for $\omega << \sigma_i/\varepsilon_i$, the gravitational masses of these iron atoms, under these conditions, will be given by :

$$m_g = m_a - 2\{[1+4.4\times10^{-9}\ I_0^4]^{½}-1\}m_a \quad (5)$$

Equation above shows that the *gravitational masses* (m_g) of the atoms of the annealed pure iron toroid can be *nullified* for I_0 = 129.83A. Above this critical value the gravitational masses becomes negatives (antigravity).

Results and Discussion

Figure 2 presents the results of m_g calculated by means of Eq.5, plotted as a function of current I_0 , for $\mu_i = 25000\mu_0$; $\sigma_i = 1.03\times10^7$ S/m ; $\sigma_p \approx 10$ S/m ; $\mu_p \approx 75\mu_0$; z_0 = 12 m.

The experimental results obtained (see Table1) are plotted on said figure to be compared with those supplied by the theory.

It is important to note that, in practice, when I_0 = 130.01A the gravitational mass of system-G reduces to 5.80kg ; exactly equal to the mass of the *steel toroid* (see fig.1). This occurs due to gravitational mass of the annealed pure iron toroid to become null when I_0 =130.01A (Exactly as predicted by the theory. i.e., the gravitational masses of the atoms of the annealed iron toroid become *null* for I_0 = 129.83A).

Under these circumstances, the toroid doesn't interact gravitationally with the Universe, and consequently , there can be no gravitational interaction between the matter inside the toroid and the rest of the Universe. Therefore, the gravitational mass of system-G reduces to the mass of the *steel toroid* , which is outside the annealed iron toroid.

Conclusion

This experiment (carried out by the author on January 27, 2000)

provides a strong evidence that the general expression of correlation between gravitational mass and inertial mass (Eq.1) is true. So, we can easily conclude that the gravitational forces can be reduced, nullified and inverted by means of electromagnetic radiation .

References

1. Eötvos, R. v. (1890), *Math. Natur. Ber. Ungarn*, **8**,65.
2. Zeeman, P. (1917), *Proc. Ned. Akad. Wet.*, **20**,542.
3. Eötvos, R. v., Pékar, D., Fekete, E. (1922) *Ann. Phys.*, **68**,11.
4. Dicke, R.H. (1963) *Experimental Relativity in "Relativity, Groups and Topology" (Les Houches Lectures)*, p. 185.
5. Roppl, P.G et. al. (1964) *Ann. Phys* (N.Y), **26**,442.
6. Braginskii,V.B, Panov, V.I (1971) *Zh. Eksp. Teor. Fiz*, **61**,873.
7. De Aquino, F.(1999)"Gravitation and Electromagnetism: Correlation and Grand Unification", Los Alamos National Laboratory preprint no.gr-qc/9910036.
8. *Reference Data for Radio Engineers* ,ITT Howard ,W. Sams Co.,1983, p.4-33,Table21,ISB0-672-21218-8.
9. *Standard Handbook for Electrical Engineers*, McGraw-Hill Co, D.G. Fink,H.W.Beaty,1987,p4110,Table 4-50, ISBN 0-07-020975-8 .

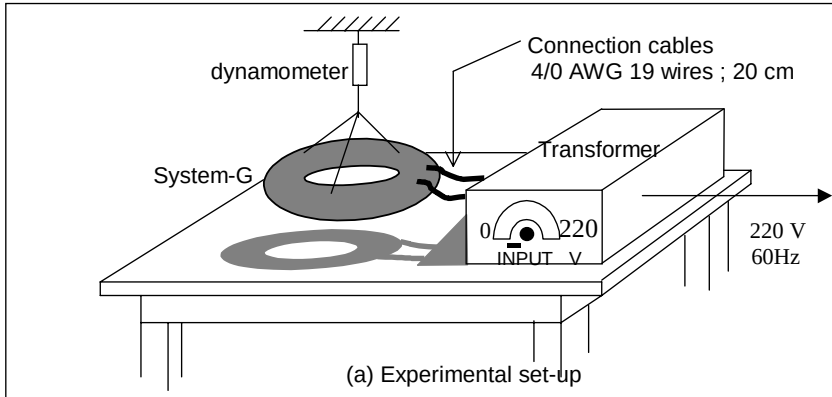

(a) Experimental set-up

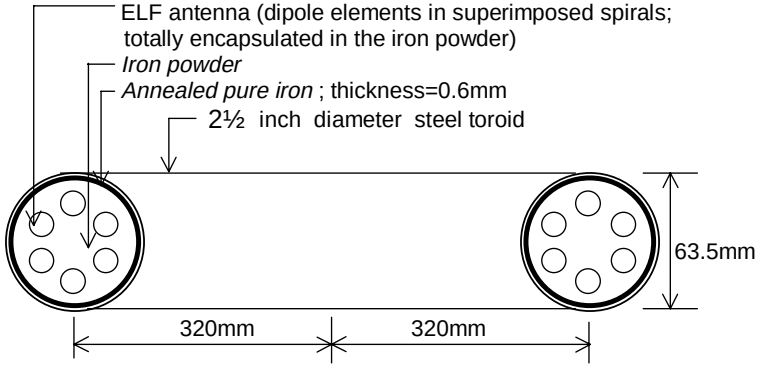

(b) Cross section of the System - G

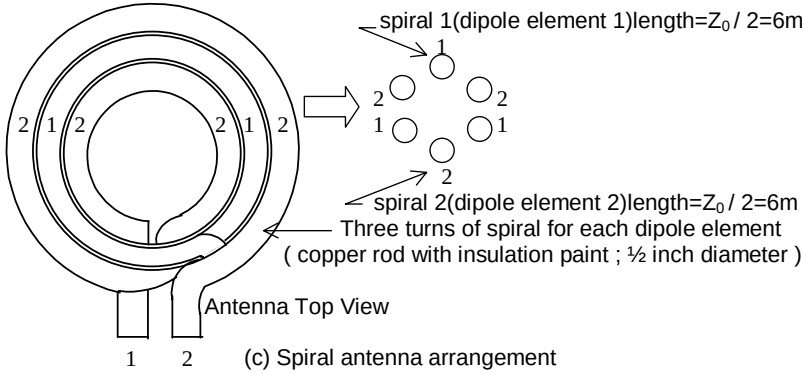

(c) Spiral antenna arrangement

Fig. 1 – Schematic View of the Experimental Apparatus

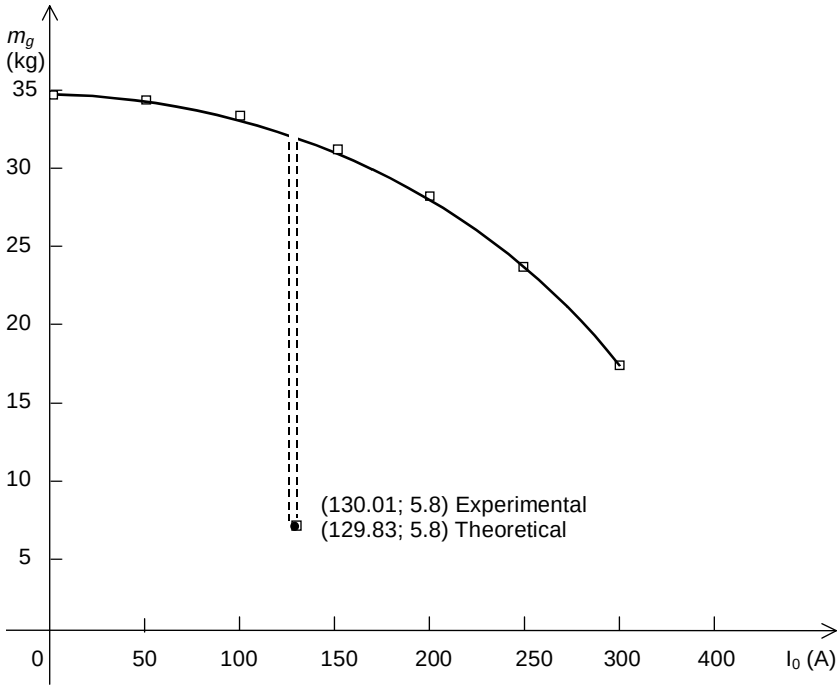

Fig.2 – Comparison between experimental data(□) and theory (solid line).

I_0 (A)	m_g (kg)	
	Theory	Exper.
0	34.85	34.85
50	34.80	34.83
100	34.17	34.26
130.01	5.80	5.80
150	32.14	32.25
200	28.61	28.68
250	23.75	23.80
300	17.68	17.69

Table 1

Repulsive Gravitational Force Field

Fran De Aquino

A method is proposed in this paper to generate a repulsive gravitational force field, which can strongly repel material particles, while creating a gravitational shielding that can nullify the *momentum* of incident particles (including photons). By nullifying the *momentum* of the *particles* and *photons*, including in the *infrared* range, this force field can work as a *perfect thermal insulation*. This means that, a spacecraft with this force field around it, cannot be affected by any external temperature and, in this way, *it can even penetrate (and to exit) the Sun* without be damaged or to cause the death of the crew. The repulsive force field can also work as a *friction reducer with the atmosphere* (between an aeronave and the atmosphere), which allows traveling with very high velocities through the atmosphere without overheating the aeronave. The generation of this force field is based on the reversion and intensification of gravity by electromagnetic means.

Key words: Quantum Gravity, Gravitation, Gravity Control, Repulsive Force Field.

1. Introduction

The Higgs field equations are [1]:

$$\nabla_\mu \nabla^\mu \varphi_a + \tfrac{1}{2}\left(m_0^2 - f^2 \varphi_b \varphi_b\right)\varphi_a = 0 \qquad (1)$$

Assuming that mass m_0 is the gravitational mass m_g, then we can say that in Higgs field the term $m_g^2 < 0$ arises from a product of positive and negative gravitational masses $(m_g)(-m_g) = -m_g^2$, however it is not an imaginary particle. Thus, when the Higgs field is decomposed, the positive gravitational mass is called *particle*, and spontaneous gives origin to the *mass*; the *negative* gravitational mass is called "dark matter". The corresponding Goldstone boson is $(+m_g)+(-m_g)=0$, which is a symmetry, while the Higgs mechanism is spontaneously broken symmetry. Thus, the existence of the Higgs bosons [2] implies in the existence of *positive gravitational mass* and *negative gravitational mass*.

On the other hand, the existence of negative gravitational mass implies in the existence of *repulsive gravitational force*. Both in the Newton theory of gravitation and in the General Theory of Relativity the gravitational force is exclusively attractive one. However, the *quantization of gravity* shows that the gravitational forces can also be *repulsive* [3].

Based on this discovery, here we describe a method to generate a *repulsive gravitational force field* that can strongly repel material particles and photons of any frequency. It was developed starting from a process *patented* in July, 31 2008 (BR Patent Number: PI0805046-5) [4].

2. Theory

In a previous paper [5] it was shown that, if the *weight* of a particle in a side of a lamina is $\vec{P} = m_g \vec{g}$ ($\vec{g}$ perpendicular to the lamina) then the weight of the same particle, in the other side of the lamina is $\vec{P}' = \chi m_g \vec{g}$, where $\chi = m_g / m_{i0}$ (m_g and m_{i0} are respectively, the gravitational mass and the inertial mass of the lamina). Only when $\chi = 1$, the weight is equal in both sides of the lamina. The lamina works as a Gravitational Shielding. This is the *Gravitational Shielding* effect. Since $P' = \chi P = (\chi m_g) g = m_g (\chi g)$, we can consider that $m_g' = \chi m_g$ or that $g' = \chi g$.

If we take two parallel gravitational shieldings, with χ_1 and χ_2 respectively, then the gravitational masses become: $m_{g1} = \chi_1 m_g$, $m_{g2} = \chi_2 m_{g1} = \chi_1 \chi_2 m_g$, and the gravity will be given by $g_1 = \chi_1 g$, $g_2 = \chi_2 g_1 = \chi_1 \chi_2 g$. In the case of multiples gravitational shieldings, with $\chi_1, \chi_2, ..., \chi_n$, we can write that, after the n^{th} gravitational shielding the gravitational mass, m_{gn}, and the gravity, g_n, will be given by

$$m_{gn} = \chi_1 \chi_2 \chi_3 ... \chi_n m_g, \quad g_n = \chi_1 \chi_2 \chi_3 ... \chi_n g \qquad (2)$$

This means that, n superposed gravitational shieldings with different $\chi_1, \chi_2, \chi_3, ..., \chi_n$ are equivalent to a single gravitational shielding with $\chi = \chi_1 \chi_2 \chi_3 ... \chi_n$.

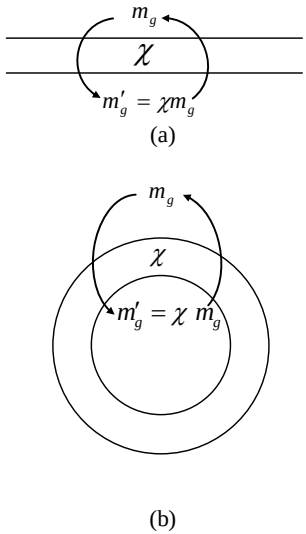

Fig. 1 – *Plane* and *Spherical* Gravitational Shieldings. When the radius of the gravitational shielding (b) is very small, any particle inside the spherical crust will have its gravitational mass given by $m'_g = \chi\, m_g$, where m_g is its gravitational mass out of the crust.

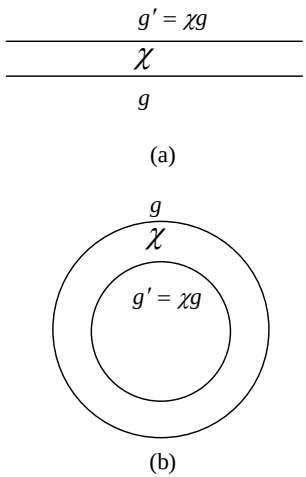

Fig. 2 – The gravity acceleration in both sides of the gravitational shielding.

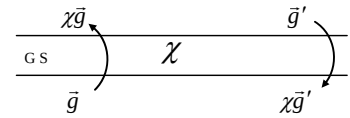

Fig. 3 – *Gravitational Shielding* (GS). If the *gravity* at a side of the GS is $\vec{g}$ ($\vec{g}$ perpendicular to the lamina) then the gravity at the other side of the GS is $\chi\vec{g}$. Thus, in the case of $\vec{g}$ and $\vec{g}'$ (see figure above) the resultant gravity at each side is $\vec{g} + \chi\vec{g}'$ and $\vec{g}' + \chi\vec{g}$, respectively.

The extension of the shielding effect, i.e., the distance at which the gravitational shielding effect reach, beyond the gravitational shielding, depends basically of the magnitude of the shielding's surface. Experiments show that, when the shielding's surface is large (a disk with radius a) the action of the gravitational shielding extends up to a distance $d \cong 20a$ [6]. When the shielding's surface is *very small* the extension of the shielding effect becomes experimentally undetectable .

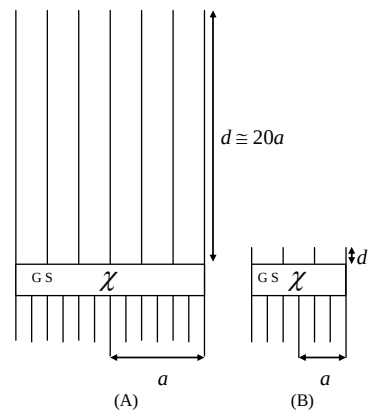

Fig. 4 - When the shielding's surface is large the action of the gravitational shielding extends up to a distance $d \cong 20a$ (A).When the shielding's surface is *very small* the extension of the shielding effect becomes experimentally undetectable (B).

The quantization of gravity shows that the *gravitational mass* m_g and *inertial mass* m_i are correlated by means of the following factor [3]:

$$\chi = \frac{m_g}{m_{i0}} = \left\{1 - 2\left[\sqrt{1 + \left(\frac{\Delta p}{m_{i0} c}\right)^2} - 1\right]\right\} \qquad (3)$$

where m_{i0} is the *rest* inertial mass of the particle and Δp is the variation in the particle's *kinetic momentum*; c is the speed of light.

In general, the *momentum* variation Δp is expressed by $\Delta p = F \Delta t$ where F is the applied force during a time interval Δt. Note that there is no restriction concerning the *nature* of the force F, i.e., it can be mechanical, electromagnetic, etc.

For example, we can look on the *momentum* variation Δp as due to absorption or emission of *electromagnetic energy*. In this case, substitution of $\Delta p = \Delta E / v = \Delta E / v(c/c)(v/v) = \Delta E \eta / c$ into Eq. (1), gives

$$\chi = \frac{m_g}{m_{i0}} = \left\{1 - 2\left[\sqrt{1 + \left(\frac{\Delta E}{m_{i0} c^2} n_r\right)^2} - 1\right]\right\} \qquad (4)$$

By dividing ΔE and m_{i0} in Eq. (4) by the volume V of the particle, and remembering that, $\Delta E / V = W$, we obtain

$$\chi = \frac{m_g}{m_{i0}} = \left\{1 - 2\left[\sqrt{1 + \left(\frac{W}{\rho\, c^2} n_r\right)^2} - 1\right]\right\} \qquad (5)$$

where ρ is the matter density $\left(kg/m^3\right)$.

Based on this possibility, we have developed a method to generate a *repulsive gravitational force field* that can strongly repel material particles.

In order to describe this method we start considering figure 5, which shows a set of n spherical gravitational shieldings, with $\chi_1, \chi_2, \ldots, \chi_n$, respectively. When these gravitational shielding are *deactivated*, the gravity generated is $g = -Gm_{gs}/r^2 \cong -Gm_{i0s}/r^2$, where m_{i0s} is the total inertial mass of the n spherical gravitational shieldings. When the system is *actived*, the gravitational mass becomes $m_{gs} = (\chi_1 \chi_2 \ldots \chi_n) m_{i0s}$, and the gravity is given by

$$g' = (\chi_1 \chi_2 \ldots \chi_n) g = -(\chi_1 \chi_2 \ldots \chi_n) G m_{i0s} / r^2 \qquad (6)$$

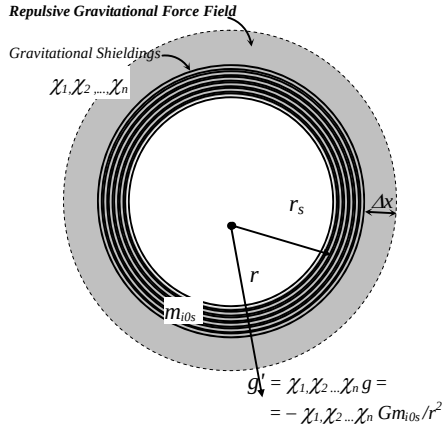

Fig. 5 – *Repulsive Gravitational Field Force* produced by the Spherical Gravitational Shieldings (*1, 2,…, n*).

If we make $(\chi_1 \chi_2 \ldots \chi_n)$ *negative* (n odd) the gravity g' becomes *repulsive*, producing a pressure p upon the matter around the sphere. This pressure can be expressed by means of the following equation

$$p = \frac{F}{S} = \frac{m_{i0(matter)} g'}{S} = \frac{\rho_{i(matter)} S \Delta x g'}{S} =$$

$$= \rho_{i(matter)} \Delta x g' \qquad (7)$$

Substitution of Eq. (6) into Eq. (7), gives

$$p = -(\chi_1 \chi_2 \ldots \chi_n) \rho_{i(matter)} \Delta x \left(G m_{i0s} / r^2\right) \qquad (8)$$

If the matter around the sphere is only the atmospheric air ($p_a = 1.013 \times 10^5 N.m^{-2}$), then, in order to expel all the atmospheric air from the inside the belt with Δx - thickness (See Fig. 5), we must have $p > p_a$. This requires that

$$(\chi_1 \chi_2 \ldots \chi_n) > \frac{p_a r^2}{\rho_{i(matter)} \Delta x G m_{i0s}} \qquad (9)$$

Satisfied this condition, *all* the matter is expelled from this region, except the

Continuous Universal Fluid (CUF), which density is $\rho_{CUF} \cong 10^{-27}\, kg.m^{-3}$ [7].

The density of the Universal Quantum Fluid is clearly *not uniform* along the Universe. At *supercompressed* state, it gives *origin* to the *known matter* (quarks, electrons, protons, neutrons, etc). Thus, the *gravitational mass* arises with the supercompression state. At the normal state (free space, far from matter), the local *inertial mass* of Universal Quantum Fluid does not generate gravitational mass, i.e., $\chi = 0$. However, if some bodies are placed in the neighborhoods, then this value will become greater than zero, due to *proximity effect*, and the gravitational mass will have a non-null value. This is the case of the region with Δx - thickness, i.e., in spite of *all* the matter be expelled from the region, remaining in place just the Universal Quantum Fluid, the proximity of neighboring matter makes non-null the gravitational mass of this region, but extremely close to zero, in such way that, the value of $\chi = m_g / m_{i0}$ is also extremely close to zero (m_{i0} is the inertial mass of the Universal Quantum Fluid in the mentioned region).

Another important equations obtained in the quantization theory of gravity is the new expression for the *momentum* q and *gravitational energy* of a particle with gravitational mass M_g and velocity v, which is given by [3]

$$\vec{q} = M_g \vec{v} \qquad (10)$$

$$E_g = M_g c^2 \qquad (11)$$

where $M_g = m_g \Big/ \sqrt{1 - v^2/c^2}$; m_g is given by Eq.(1), i.e., $m_g = \chi\, m_i$. Thus, we can write

$$M_g = \frac{\chi\ m_i}{\sqrt{1 - v^2/c^2}} = \chi M_i \qquad (12)$$

Substitution of Eq. (12) into Eq. (11) and Eq. (10) gives

$$E_g = \chi\ M_i c^2 \qquad (13)$$

$$\vec{q} = \chi M_i \vec{v} = \frac{\vec{v}}{c} \chi \frac{h}{\lambda} \qquad (14)$$

For $v = c$, the *momentum* and the energy of the particle become infinite. This means that a particle with non-null mass cannot travel with the light speed. However, in Relativistic Mechanics there are particles with *null mass* that travel with the light speed. For these particles, Eq. (14) gives

$$q = \chi \frac{h}{\lambda} \qquad (15)$$

Note that only for $\chi = 1$ the Eq. (15) is reduced to the well=known expressions of DeBroglie $(q = h/\lambda)$.

Since the factor χ can be strongly reduced under certain circumstances (See Eq.(1)), then according to the Eqs. (13) and (14), the *gravitational energy* and the *momentum* of a particle can also be strongly *reduced*. In the case of the region with Δx - thickness, where χ is *extremely close to zero*, the *gravitational energy* and the *momentum* of the *material particles* and *photons* become practically *null*.

By nullifying the *gravitational energy* and the *momentum* of the *particles* and *photons*, including in the *infrared* range, this force field can work as a *perfect thermal insulation*. This means that, a spacecraft with this force field around it, cannot be affected by any external temperature and, in this way, *it can even penetrate (and to exit) the Sun* without be damaged or to cause the death of the crew. The repulsive force field can also work as a *friction reducer with the atmosphere* (between an aeronave and the atmosphere), which allows traveling with very high velocities through the atmosphere without overheating the aeronave.

Considering Eq. (8), for $p = p_a$ at $r = 6m$, we can write that

$$(\chi_1 \chi_2 \cdots \chi_n) = -\frac{36 p_a}{\Delta x \rho_{i(matter)} G M_{i0s}} \qquad (16)$$

The gravitational shieldings $(1,2,..,n)$ can be made very thin, in such way that the total inertial mass of them, for example in the case of $r_s \cong 4.9m$, can be assumed as $M_{i0s} \cong 5000kg$. Thus, for $\Delta x = 1m$ and $\rho_{i(matter)} = 1.2kg.m^{-3}$, Eq. (16) gives

$$(\chi_1 \chi_2 \cdots \chi_n) = -9.1 \times 10^{12}\, m \qquad (17)$$

By making $\chi_1 = \chi_2 = ... = \chi_n$, then, for $n = 7$, we obtain the following value

$$\chi_1 = \chi_2 = ... = \chi_7 = -71.00 \qquad (22)$$

It is relatively easy to build the set of spherical gravitational shieldings with these values. First we must choose a convenient material, with density ρ and refraction index n_r, in such way that, by applying an electromagnetic field E sufficient intense $\left(W = \varepsilon_0 E^2\right)$, we can obtain, according to Eq. (5), the values given by Eq. (22).

Since in the region with Δx - thickness, the value of χ is extremely close to zero, we can conclude that the gravitational mass of the spacecraft, which is given by $m_{gs} = \chi\left(\chi_1 \chi_2 ... \chi_n\right) m_{i0s}$, becomes very small. This makes possible to the spacecraft acquire strong accelerations, even when subjected to small thrusts $\left(a = F / m_{gs}\right)$[3]. On the other hand, with a small gravitational mass, the weight of the spacecraft will be also small.

Note that the Gravitational Repulsive Force Field aggregates new possibilities to the *Gravitational Spacecraft*, previously proposed [8], while showing that the performance of this spacecraft goes much beyond the conventional spacecrafts.

References

[1] Higgs, P. W. (1966) *Phys. Rev.* 145, 1156.

[2] CERN (2012) *Observation of a new boson at a mass of 125 GeV with the CMS experiment at the LHC*, Phys. Lett. B 716 (2012) 30.

[3] De Aquino, F. (2010) *Mathematical Foundations of the Relativistic Theory of Quantum Gravity*, Pacific Journal of Science and Technology, **11** (1), pp. 173-232.

[4] De Aquino, F. (2008) *Process and Device for Controlling the Locally the Gravitational Mass and the Gravity Acceleration*, BR Patent Number: PI0805046-5, July 31, 2008.

[5] De Aquino, F. (2010) *Gravity Control by means of Electromagnetic Field through Gas at Ultra-Low Pressure*, Pacific Journal of Science and Technology, **11**(2) November 2010, pp.178-247, Physics/0701091.

[6] Modanese, G., (1996), *Updating the Theoretical Analysis of the Weak Gravitational Shielding Experiment*, supr-con/9601001v2.

[7] De Aquino, F. (2011) *The Universal Quantum Fluid*, http://vixra.org/abs/1202.0041

[8] De Aquino, F. (1998) *The Gravitational Spacecraft*, Electric Spacecraft Journal (USA) Volume 27, December 1998 (First Version), pp. 6-13. http://arXiv.org/abs/physics/9904018

Gravitational Holographic Teleportation

Fran De Aquino

A process of teleportation is here studied. It involves holography and reduction of the gravitational mass of the bodies to be transported. We show that if a holographic three-dimensional image of a body is created and sent to another site *and* the gravitational mass of the body is reduced to a specific range, then the body will disappear and posteriorly will reappear exactly where its holographic three-dimensional image was sent.

Key words: Modified theories of gravity, Experimental studies of gravity, Holography.
PACS: 04.50.Kd, 04.80.-y, 42.40.-i.

.

1. Introduction

During long time evidences have been shown that *spacetime is holographic*. A holographic principle has been conjectured to apply not just to black holes, but to *any spacetime* [1, 2, 3, 4]. Covariant holographic entropy bounds generalize to other spacetimes [5, 6]. Fully holographic theories have now been demonstrated, in which a system of quantum fields and dynamical gravity in N dimensions is dual to a system of quantum fields in N − 1 classical dimensions [7, 8, 9, 10, 11].

Recently, scientists from University of Arizona led by Nasser Peyghambarian have invented a system that creates *holographic, three-dimensional images that may be viewed at another site* [12]. Peyghambarian says the machine could potentially transport a person's image over vast distances.

Here, we show that if a holographic three-dimensional image of a body is created and sent to another site *and* the gravitational mass of the body is reduced to a specific range, then the body will disappear and posteriorly will reappear exactly where its holographic three-dimensional image was sent.

2. Theory

From the quantization of gravity it follows that the *gravitational mass* m_g and the *inertial mass* m_i are correlated by means of the following factor [13]:

$$\chi = \frac{m_g}{m_{i0}} = \left\{1 - 2\left[\sqrt{1+\left(\frac{\Delta p}{m_{i0}c}\right)^2} - 1\right]\right\} \qquad (1)$$

where m_{i0} is the *rest* inertial mass of the particle and Δp is the variation in the particle's *kinetic momentum*; c is the speed of light.

This equation shows that only for $\Delta p = 0$ the gravitational mass is equal to the inertial mass.

In general, the *momentum* variation Δp is expressed by $\Delta p = F\Delta t$ where F is the applied force during a time interval Δt. Note that there is no restriction concerning the *nature* of the force F, i.e., it can be mechanical, electromagnetic, etc.

Equation (1) tells us that the *gravitational mass* can be *negative*. This fact is highly relevant because shows that the well-known *action integral* for a free-particle: $S = -m\,c\int_a^b ds$, $m > 0$, must be generalized for the following form (where m_g can be *positive* or *negative*):

$$S = -m_g c\int_a^b ds \qquad (2)$$

or

$$S = -\int_{t_1}^{t_2} m_g c^2\sqrt{1 - V^2/c^2}\,dt \qquad (3)$$

where the Lagrange's function is

$$L = -m_g c^2\sqrt{1 - V^2/c^2}. \qquad (4)$$

The integral $S = \int_{t_1}^{t_2} m_g c^2\sqrt{1 - V^2/c^2}\,dt$, preceded by the *plus* sign, cannot have a *minimum*. Thus, the integrand of Eq.(3) must be *always positive*. Therefore, if $m_g > 0$, then necessarily $t > 0$; if $m_g < 0$, then $t < 0$. The possibility of $t < 0$ is based on the well-known equation $t = \pm t_0/\sqrt{1 - V^2/c^2}$ of Einstein's Theory.

Thus if the *gravitational mass* of a particle is *positive,* then t is also *positive* and, therefore, given by $t=+t_0/\sqrt{1-V^2/c^2}$. This leads to the well-known relativistic prediction that the particle goes to the *future,* if $V \to c$. However, if the *gravitational mass* of the particle is *negative,* then t is *negative* and given by $t=-t_0/\sqrt{1-V^2/c^2}$. In this case, the prediction is that the particle goes to the *past,* if $V \to c$. Consequently, $m_g < 0$ *is the necessary condition for the particle to go to the past.*

The Lorentz's transforms follow the same rule for $m_g > 0$ and $m_g < 0$, i.e., the sign before $\sqrt{1-V^2/c^2}$ will be $(+)$ when $m_g > 0$ and $(-)$ if $m_g < 0$.

The *momentum*, as we know, is the vector $\vec{p}=\partial L/\partial \vec{V}$. Thus, from Eq.(4) we obtain

$$\vec{p} = \frac{m_g \vec{V}}{\pm\sqrt{1-V^2/c^2}} = M_g \vec{V} \qquad (5)$$

The $(+)$ sign in the equation above will be used when $m_g > 0$ and the $(-)$ sign if $m_g < 0$. Consequently, we can express the momentum $\vec{p}$ in the following form

$$\vec{p} = \frac{m_g \vec{V}}{\sqrt{1-V^2/c^2}} = M_g \vec{V} \qquad (6)$$

whence we get a new relativistic expression for the gravitational mass, i.e.,

$$M_g = \frac{m_g}{\sqrt{1-V^2/c^2}} \qquad (7)$$

Note that m_g *is not the gravitational mass at rest*, which is obtained making $\Delta p = 0$ in Eq. (1), i.e., $m_{g0} = m_{i0}$. In this case, the equation above reduces to the well-known Einstein's equation:

$$M_i = \frac{m_{i0}}{\sqrt{1-V^2/c^2}}$$

Substitution of Eq. (1) into Eq. (7) leads to the following equation

$$M_g = \frac{m_g}{\sqrt{1-V^2/c^2}} = \frac{\chi\ m_{i0}}{\sqrt{1-V^2/c^2}} = \chi M_i \qquad (8)$$

It is known that the *uncertainty principle* can also be written as a function of ΔE (uncertainty in the energy) and Δt (uncertainty in the time), i.e.,

$$\Delta E.\Delta t \geq \hbar \qquad (9)$$

This expression shows that a variation of energy ΔE, during a time interval Δt, can only be detected if $\Delta t \geq \hbar/\Delta E$. Consequently, a variation of energy ΔE, during a time interval $\Delta t < \hbar/\Delta E$, cannot be experimentally detected. This is a limitation imposed by Nature and not by our equipments.

Thus, a *quantum* of energy $\Delta E = hf$ that varies during a time interval $\Delta t = 1/f = \lambda/c < \hbar/\Delta E$ (wave period) cannot be experimentally detected. This is an *imaginary* photon or a "*virtual*" photon.

Now, consider a particle with energy $M_g c^2$. The DeBroglie's gravitational and inertial wavelengths are respectively $\lambda_g = h/M_g c$ and $\lambda_i = h/M_i c$. In Quantum Mechanics, particles of matter and quanta of radiation are described by means of *wave packet* (DeBroglie's waves) with average wavelength λ_i. Therefore, we can say that during a time interval $\Delta t = \lambda_i/c$, a *quantum* of energy $\Delta E = M_g c^2$ varies. According to the uncertainty principle, the particle will be detected if $\Delta t \geq \hbar/\Delta E$, i.e., if $\lambda_i/c \geq \hbar/M_g c^2$ or $\lambda_i \geq \lambda_g/2\pi$. This condition is usually satisfied when $M_g = M_i$. In this case, $\lambda_g = \lambda_i$ and obviously, $\lambda_i > \lambda_i/2\pi$. However, when M_g decreases λ_g increases and $\lambda_g/2\pi$ can become bigger than λ_i, making the particle *non-detectable* or *imaginary*.

Since the condition to make the particle *imaginary* is

$$\lambda_i < \frac{\lambda_g}{2\pi}$$

and

$$\frac{\lambda_g}{2\pi} = \frac{\hbar}{M_g c} = \frac{\hbar}{\chi M_i c} = \frac{\lambda_i}{2\pi\chi}$$

Then we get

$$\chi < \frac{1}{2\pi} = 0.159$$

However, χ can be positive or negative ($\chi < +0.159$ or $\chi > -0.159$). This means that when

$$-0.159 < \chi < +0.159 \qquad (10)$$

the particle becomes *imaginary*. Consequently, it leaves our *Real* Universe, i.e., it performs a transition to the *Imaginary* Universe, which contains our *Real* Universe. The terms real and imaginary are borrowed from mathematics (real and imaginary numbers).

All these conclusions were originally deduced in a previous article [13].

Quantum Mechanics tells us that if an experiment involves a large number of identical particles, all described by the same wave function Ψ , *real* density of mass ρ of these particles in x, y, z, t is proportional to the corresponding value Ψ^2 (Ψ^2 is known as *density of probability*. If Ψ is *imaginary* then $\Psi^2 = \Psi\Psi^*$. Thus, $\rho \propto \Psi^2 = \Psi.\Psi^*$). Similarly, in the case of imaginary particles, the *density of imaginary gravitational mass*, $\rho_{g(imaginary)}$, in x, y, z, will be expressed by $\rho_{g(imaginary)} \propto \Psi^2 = \Psi\Psi^*$. Since Ψ^2 is always *real* and *positive* and $\rho_{g(imaginary)} = m_{g(imaginary)}/V$ is an *imaginary* quantity then, in order to transform the proportionality above into an equation, we can write

$$\Psi^2 = k\left|\rho_{g(imaginary)}\right| \qquad (11)$$

Since the *modulus* of an imaginary number is always real and positive; k is a *proportionality constant* (real and positive) to be determined.

The *Mutual Affinity* is a dimensionless quantity with which we are familiarized and of which we have perfect understanding as to its meaning. It is revealed in the molecular formation, where atoms with strong mutual affinity combine to form molecules. It is the case, for example of the water molecules, in which two Hydrogen atoms join an Oxygen atom. It is the so-called *Chemical Affinity*.

The degree of *Mutual Affinity*, A, in the case of imaginary particles , respectively described by the wave functions Ψ_1 and Ψ_2, might be correlated to Ψ_1^2 and Ψ_2^2. Only a simple algebraic form fills the requirements of interchange of the indices, the product

$$\Psi_1^2.\Psi_2^2 = \Psi_2^2.\Psi_1^2 = \\ = \left|A_{1,2}\right| = \left|A_{2,1}\right| = \left|A\right| \qquad (12)$$

In the above expression, $|A|$ is due to the product $\Psi_1^2.\Psi_2^2$ will be always positive. From equations (11) and (12) we get

$$\left|A\right| = \Psi_1^2.\Psi_2^2 = k^2\left|\rho_{1g(imaginary)}\right|\left|\rho_{2g(imaginary}\right| = \\ = k^2\frac{\left|m_{1g(imaginary)}\right|}{V_1}\frac{\left|m_{2g(imaginary)}\right|}{V_2} \qquad (13)$$

Since *imaginary* gravitational masses are equivalent to *real* gravitational masses then the equations of the *Real Gravitational Interaction* are also applied to the *Imaginary Gravitational Interaction*. However, due to imaginary gravitational mass, $m_{g(imaginary)}$, to be an *imaginary* quantity, it is necessary to put $\left|m_{g(imaginary)}\right|$ into the mentioned equations in order to homogenize them, because as we know, the module of an imaginary number is always real and positive.

Thus, based on gravity theory, we can write the equation of the *imaginary gravitational field* in *nonrelativistic* Mechanics.

$$\Delta\Phi = 4\pi G\left|\rho_{g(imaginary)}\right| \qquad (14)$$

It is similar to the equation of the real gravitational field, with the difference that now instead of the density of real gravitational mass we have the density of *imaginary gravitational mass*. Then, we can write the general solution of Eq. (14), in the following form:

$$\Phi = -G\int\frac{\left|\rho_{g(imaginary}\right|dV}{r^2} \qquad (15)$$

This equation expresses, with nonrelativistic approximation, the potential of the imaginary

gravitational field of any distribution of imaginary gravitational mass.

Particularly, for the potential of the field of only one particle with imaginary gravitational mass $m_{g(imaginary)}$, we get:

$$\Phi = -\frac{G\left|m_{g\,(imaginary\ )}\right|}{r} \qquad (16)$$

Then the force produced by this field upon another particle with imaginary gravitational mass $m'_{g(imaginary)}$ is

$$\left|\vec{F}_{g(imaginary)}\right| = \left|-\vec{F}'_{g(imaginary)}\right| = -\left|m'_{g(imaginary}\right|\frac{\partial\Phi}{\partial r} = \\ = -G\frac{\left|m_{g(imaginary}\right|\left|m'_{g(imaginary}\right|}{r^2} \qquad (17)$$

By comparing equations (17) and (13) we obtain

$$\left|\vec{F}_{12}\right| = \left|-\vec{F}_{21}\right| = -G\left|A\right|\frac{V_1V_2}{k^2r^2} \qquad (18)$$

In the *vectorial* form the above equation is written as follows

$$\vec{F}_{12} = -\vec{F}_{21} = -GA\frac{V_1V_2}{k^2r^2}\hat{\mu} \qquad (19)$$

V*ersor* $\hat{\mu}$ has the direction of the line connecting the mass centers (imaginary masses) of both particles and oriented from 1 to 2.

In general, we may distinguish and quantify two types of mutual affinity: *positive* and *negative*. The occurrence of the first type is synonym of *attraction*, (as in the case of the atoms in the water molecule) while the aversion is synonym of *repulsion*. In fact, Eq. (19) shows that the forces $\vec{F}_{12}$ and $\vec{F}_{21}$ are attractive, if A is *positive* (expressing *positive* mutual affinity between the two *imaginary particles*), and *repulsive* if A is *negative* (expressing *negative* mutual affinity between the two *imaginary particles*).

Now, after this theoretical background, we can explain the *Gravitational Holographic Teleportation*.

Initially, is created a holographic three-dimensional image of the bodies and sent to another site. The technology for this is already known [12]. Next, the gravitational masses of the bodies are reduced to a range $-0.159m_{i0} < m_g < +0.159m_{i0}$. When this occur the gravitational masses becomes *imaginaries* and the bodies perform transitions to the *Imaginary* Universe (leaving the Real Universe) (See Eq. (10)). However, the physical phenomenon that caused the reduction of the gravitational masses of the bodies stays at the Real Universe. *Consequently, the bodies return immediately to the Real Universe* for the same positions they were before the transition to the Imaginary Universe. This is due to the Imaginary Gravitational Interaction between the imaginary gravitational masses of the bodies and the imaginary gravitational masses of the forms shaped by the bodies in the imaginary spacetime[1] before the transition to the Imaginary Universe. These imaginary forms initially shaped by the bodies are preserved in the imaginary spacetime by *quantum coherence effects* [14, 15, 16, 17].

Since spacetime is holographic then an imaginary form shaped in imaginary spacetime by the holographic three-dimensional image of a body has much more *similarity* with the body than the imaginary form shaped in the imaginary spacetime by the real body.

Mutual affinity is directly related to *similarity*. This means that the *degree of mutual affinity*, A, between the imaginary bodies (which were sent to the Imaginary Universe) and the imaginary forms *shaped by their holographic images* is far greater than the degree of mutual affinity between the imaginary bodies and the imaginary forms shaped in the imaginary spacetime by the real bodies before the transition to the Imaginary Universe. Thus, according to Eq. (19), the bodies are strongly attracted to the holographic three-dimensional image placed in the far site. Consequently, the bodies do not return for the positions they were before the transition, they reappear as real bodies exactly where their holographic three-dimensional images were sent. Thus, is carried out the teleportation of the bodies to the far site. Since the process combines holography and gravitation, we have called this process of *Gravitational Holographic Teleportation*.

[1] The *real spacetime* is contained in the *imaginary spacetime*. Such as the set of real numbers is contained in the set of imaginary numbers.

References

[1] G. 't Hooft (1993) *Dimensional Reduction in Quantum Gravity*, arXiv: gr-qc/9310026.

[2] Susskind, L. (1995) *J. Math. Phys*. 36, 6377.

[3] G.'t Hooft (2000) *The Holographic Principle*, arXiv: hep-th/0003004.

[4] Bigatti, D., and Susskind, L. (2000) *TASI lectures on the Holographic Principle*. arXiv: hep-th/0002044.

[5] Bousso, R. (2002) *Rev. Mod. Phys*. 74, 825.

[6] Padmanabhan, T. (2007) arXiv: 0706.1654 [gr-qc].

[7] Maldacena, J.M., (1998) *Adv. Theor. Math. Phys*. 2, 231 [(1999) Int. J. Theor. Phys. 38, 1113]

[8] Witten, E., (1998) *Adv. Theor. Math. Phys*. 2, 505.

[9] Aharony, O. et al., (2000) Phys. Rept. 323, 183.

[10] Alishahiha, M. Et al., (2005) JHEP 0506, 028.

[11] Horowitz G. T. and Polchinski, J., (2006) arXiv :gr-qc/0602037.

[12] Peyghambarian, N. et al., (4 November 2010) *Nature*, **468**, 1-128, p. 80.

[13] De Aquino, F. (2010) *Mathematical Foundations of the Relativistic Theory of Quantum Gravity*, Pacific Journal of Science and Technology, **11** (1), pp. 173-232.

[14] Preparata, G. (1995) QED Coherence in matter (Singapore: World Scientific)

[15] Arani R, Bono I, Del Giudice E, Preparata G (1995) Int. J. Mod. Phys. B9 1813–1841.

[16] Del Giudice E, Preparata G and Vitiello G (1988) Phys. Rev. Lett.61, 1085–1088.

[17] Del Giudice E and Vitiello G (2006) Phys. Rev. A,74, 022105

Bose-Einstein Condensate and Gravitational Shielding

Fran De Aquino

In this work we show that when possible transform some types of substance into a Bose-Einstein condensate at room temperature, which exists long enough to be used in practice then will be possible to use these substances in order to create efficient Gravitational Shieldings.

Key words: Quantum Gravity, Gravitation, Gravitational Shielding, Bose-Einstein Condensate.

The quantization of gravity shows that the *gravitational mass* m_g and *inertial mass* m_i are correlated by means of the following factor [1]:

$$\chi = \frac{m_g}{m_{i0}} = \left\{1 - 2\left[\sqrt{1+\left(\frac{\Delta p}{m_{i0}c}\right)^2} - 1\right]\right\} \qquad (1)$$

where m_{i0} is the *rest* inertial mass of the particle and Δp is the variation in the particle's *kinetic momentum*; c is the speed of light.

In general, the *momentum* variation Δp is expressed by $\Delta p = F\Delta t$ where F is the applied force during a time interval Δt. Note that there is no restriction concerning the *nature* of the force F, i.e., it can be mechanical, electromagnetic, etc.

For example, we can look on the *momentum* variation Δp as due to absorption or emission of *electromagnetic energy*. In this case, we can write that

$$\Delta p = n\hbar k_r = n\hbar\omega/(\omega/k_r) = \Delta E/(dz/dt) =$$
$$= \Delta E/v = \Delta E/v(c/c) = \Delta E n_r/c \qquad (2)$$

where k_r is the real part of the *propagation vector* $\vec{k}$; $k = |\vec{k}| = k_r + ik_i$; ΔE is *the electromagnetic energy absorbed or emitted by the particle;* n_r is the index of refraction of the medium and v is the *phase* velocity of the electromagnetic waves, given by:

$$v = \frac{dz}{dt} = \frac{\omega}{\kappa_r} = \frac{c}{\sqrt{\frac{\varepsilon_r\mu_r}{2}\left(\sqrt{1+(\sigma/\omega\varepsilon)^2}+1\right)}} \qquad (3)$$

ε, μ and σ, are the electromagnetic characteristics of the particle ($\varepsilon = \varepsilon_r\varepsilon_0$ where ε_r is the *relative electric permittivity* and $\varepsilon_0 = 8.854\times10^{-12}\,F/m$; $\mu = \mu_r\mu_0$ where μ_r is the *relative magnetic permeability* and $\mu_0 = 4\pi\times10^{-7}\,H/m$).

Thus, substitution of Eq. (2) into Eq. (1), gives

$$\chi = \frac{m_g}{m_{i0}} = \left\{1 - 2\left[\sqrt{1+\left(\frac{\Delta E}{m_{i0}c^2}n_r\right)^2} - 1\right]\right\} \qquad (4)$$

By dividing ΔE and m_{i0} in Eq. (4) by the volume V of the particle, and remembering that, $\Delta E/V = W$, we obtain

$$\chi = \frac{m_g}{m_{i0}} = \left\{1 - 2\left[\sqrt{1+\left(\frac{W}{\rho\, c^2}n_r\right)^2} - 1\right]\right\} \qquad (5)$$

where ρ is the matter density (kg/m^3).

Equation (2) tells us that $F = d(\Delta p)/dt = (1/v)d(\Delta E)/dt$. Since $W \equiv pressure$ then we can write that $W = F/A = (1/v)d(\Delta E)/dt/A = Dv$, where D is the power density of the absorbed (or emitted) radiation. Substitution of $W = D/v$ into Eq. (5) yields

$$\chi = \frac{m_g}{m_{i0}} = \left\{1 - 2\left[\sqrt{1+\left(\frac{D}{\rho\, c^3}n_r^2\right)^2} - 1\right]\right\} =$$
$$= \left\{1 - 2\left[\sqrt{1+\left(\frac{D}{\rho\, cv^2}\right)^2} - 1\right]\right\} \qquad (6)$$

In a previous paper [2] it was shown that, if the *weight* of a particle in a side of a lamina is $\vec{P} = m_g\vec{g}$ ($\vec{g}$ perpendicular to the lamina) then the weight of the same particle, in the other side of the lamina is $\vec{P}' = \chi m_g\vec{g}$, where $\chi = m_g/m_{i0}$ (m_g and m_{i0} are respectively, the gravitational mass and the inertial mass of the lamina). Only when $\chi = 1$, the weight is equal in both sides of the lamina. The lamina works as a Gravitational Shielding. This is the *Gravitational Shielding* effect. Since $P' = \chi P = (\chi m_g)g = m_g(\chi g)$, we can consider that $m_g' = \chi m_g$ or that $g' = \chi g$.

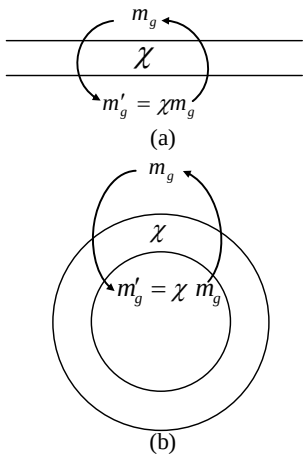

Fig. 1 – *Plane* and *Spherical* Gravitational Shieldings. When the radius of the gravitational shielding (b) is very small, any particle inside the spherical crust will have its gravitational mass given by $m'_g = \chi\, m_g$, where m_g is its gravitational mass out of the crust.

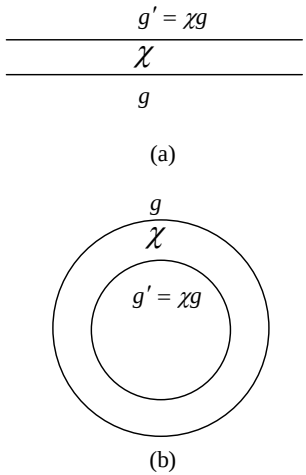

Fig. 2 – The gravity acceleration in both sides of the gravitational shielding.

In 1999, Danish physicist Lene Hau et al., by passing a light beam through a Bose-Einstein condensate (BEC) of sodium atoms at *nK*, succeeded in slowing a beam of light to about 17 meters per second [3]. In this case, the enormous index of refraction $(n_r = c/v)$ of the BEC is equal to 17.6 million. Even higher refractive indices are expected (light speed as low as *micrometer/sec*).

According to Eq. (6), this strong decreasing of v, shows that the values of χ in a BEC can be strongly reduced with small values of D. This can be very useful to create Gravitational Shieldings.

The Hau's experiment requires temperatures near absolute zero. However, at the beginning of 2013, Ayan Das and colleagues [4] have used *nanowires* to produce an excitation known as a *polariton*[1]. These polaritons formed a Bose-Einstein condensate *at room temperature*, potentially opening up a new way for studying systems that otherwise require expensive cooling and trapping. Instead of atoms, condensation was achieved using *quasiparticles*.

At the end of 2013 researchers at IBM's Binning and Rohrer Nano Center have been able to achieve the BEC at room temperature by placing a thin polymer film[2]—only 35 nanometers thick—between two mirrors and then shining a laser into the configuration [5]. The photons of the laser interact with *excitions*[3] [6] leading to the onset of a new *quasi-particle* that exhibits properties of light and matter - *Polaritons*. Because polaritonic quasiparticles have extraordinarily light masses and *they are bosons*, they can condense together in a single quantum state. This makes for extremely unusual emitters, as well as new solid-state devices *exhibiting Bose-Einstein condensation at room temperature*. Unfortunately, this BEC state of matter only lasts for a few picoseconds.

When possible transform some types of substance into a Bose-Einstein condensate at room temperature, which exists long enough to be used in practice then will be possible to use these substances in order to create efficient *Gravitational Shieldings*, according to (6).

---

[1] *Polaritons* are quasiparticles resulting from strong coupling of electromagnetic waves with an electric or magnetic dipole-carrying excitation.

[2] The luminescent plastic film is similar to that used in many smart phones for their light-emitting displays.

[3] An *exciton* is a bound state of an electron and an electron hole which are attracted to each other by the electrostatic Coulomb force. It is an electrically neutral quasiparticle that exists in insulators, semiconductors and in some liquids. The exciton is regarded as an elementary excitation of condensed matter that can transport energy without transporting net electric charge [6].

References

[1] De Aquino, F. (2010) *Mathematical Foundations of the Relativistic Theory of Quantum Gravity*, Pacific Journal of Science and Technology, **11** (1), pp. 173-232.

[2] De Aquino, F. (2010) *Gravity Control by means of Electromagnetic Field through Gas at Ultra-Low Pressure*, Pacific Journal of Science and Technology, **11**(2) November 2010, pp.178-247, Physics/0701091.

[3] Hau, L.V, et al., (1999) *Light Speed Reduction to 17 Meters per Second in an Ultracold Atomic Gas*, Nature 397, 594-598.

[4] Ayan Das, et al., (2013) *Polariton Bose–Einstein condensate at room temperature in an Al(Ga)N nanowire–dielectric microcavity with a spatial potential trap*, PNAS *2013; published ahead of print February 4, 2013, doi:10.1073/pnas.1210842110*

[5] J. D. Plumhof et al., (2013) *Room-temperature Bose–Einstein condensation of cavity exciton–polaritons in a* ***polymer*****,** Nature Materials, Letters, 1476-4660. Published online 08 December 2013.

[6] Liang, W.Y (1970) *Excitons*, *Physics Education* **5** (4): 226.

Gravitational Shockwave Weapons

Fran De Aquino
Maranhao State University, Physics Department, S.Luis/MA, Brazil.

Detonation velocities, greater than that generated by high explosives (~10^4m/s), can be achieved by using the gravitational technology recently discovered. This possibility leads to the conception of powerful shockwave weapons. Here, we show the design of a portable gravitational shockwave weapon, which can produce detonation velocities greater than 10^5m/s, and detonation pressures greater than 10^{10}N/m^2 .

Key words: Modified theories of gravity, Detonation waves, Shockwaves, Nozzle flow.
PACS: 04.50.Kd, 47.40.Rs, 47.40.-x, 47.60.Kz.

1. Introduction

The most important single property of an explosive is the *detonation velocity*. It is the speed at which the detonation wave travels through the explosive. Typical detonation velocities in solid explosives often range beyond 3,000 m/s to 10,300 m/s [1].

At the front of the detonation zone, an energy pulse or "shockwave" is generated and transmitted to the adjacent region. The shockwave travels outward as a compression wave, moving at or near detonation velocity. When the intensity of the shockwave exceeds the compression strength of the materials they are destroyed. If the mass of the body is too large the wave energy is simply absorbed by the body [2].

The pressure produced in the explosion zone is called *Detonation Pressure*. It expresses the intensity of the generated shockwave. A high detonation pressure is necessary when blasting hard, dense bodies. Detonation pressures of high explosives are in the range from 10^6N/m^2 to over 10^7 N/m^2 [3].

Here, we show the design of a portable shockwave weapon, which uses the *Gravitational Shielding Effect* (BR Patent Number: PI0805046-5, July 31, 2008) *in order to produce detonations velocities greater than 100,000m/s*, and detonation pressures greater than 10^{10}N/m^2. It is important to remember that an aluminum-nitrate truck bomb has a relatively low detonation velocity of 3,500 m/s (sound speed is 343.2m/s)[*]. High explosives such as TNT has a detonation velocity of 6,900m/s; Military explosives used to destroy strong concrete and steel structures have a detonation velocity of 7,000 to 8,000 m/s [3].

2. Theory

The contemporary greatest challenge of the Theoretical Physics was to prove that, Gravity is a *quantum* phenomenon. The quantization of gravity showed that the *gravitational mass* m_g and *inertial mass* m_i are correlated by means of the following factor [4]:

$$\chi = \frac{m_g}{m_{i0}} = \left\{1 - 2\left[\sqrt{1+\left(\frac{\Delta p}{m_{i0}c}\right)^2} - 1\right]\right\} \qquad (1)$$

where m_{i0} is the *rest* inertial mass of the particle and Δp is the variation in the particle's *kinetic momentum*; c is the speed of light.

When Δp is produced by the absorption of a photon with wavelength λ, it is expressed by $\Delta p = h/\lambda$. In this case, Eq. (1) becomes

$$\frac{m_g}{m_{i0}} = \left\{1 - 2\left[\sqrt{1+\left(\frac{h/m_{i0}c}{\lambda}\right)^2} - 1\right]\right\} = \left\{1 - 2\left[\sqrt{1+\left(\frac{\lambda_0}{\lambda}\right)^2} - 1\right]\right\} \qquad (2)$$

[*] When a shockwave is created by high explosives it will always travel at high supersonic velocity from its point of origin.

where $\lambda_0 = h/m_{i0}c$ is the *De Broglie wavelength* for the particle with *rest* inertial mass m_{i0}.

It was shown that there is an additional effect - *Gravitational Shielding* effect - produced by a substance whose gravitational mass was reduced or made negative [5]. The effect extends beyond substance (gravitational shielding) , up to a certain distance from it (along the central axis of gravitational shielding). This effect shows that in this region the gravity acceleration, g_1, is reduced at the same proportion, i.e., $g_1 = \chi_1 g$ where $\chi_1 = m_g/m_{i0}$ and g is the gravity acceleration *before* the gravitational shielding). Consequently, *after a second gravitational shielding*, the gravity will be given by $g_2 = \chi_2 g_1 = \chi_1 \chi_2 g$, where χ_2 is the value of the ratio m_g/m_{i0} for the *second* gravitational shielding. In a generalized way, we can write that after the *nth* gravitational shielding the gravity, g_n, will be given by

$$g_n = \chi_1 \chi_2 \chi_3 \cdots \chi_n g \qquad (3)$$

This possibility shows that, by means of a battery of gravitational shieldings, we can make particles acquire enormous accelerations. In practice, this can lead to the conception of powerful particles accelerators, kinetic weapons or weapons of shockwaves.

From Electrodynamics we know that when an electromagnetic wave with frequency f and velocity c incides on a material with relative permittivity ε_r, relative magnetic permeability μ_r and electrical conductivity σ, its *velocity is reduced* to $v = c/n_r$ where n_r is the index of refraction of the material, given by [6]

$$n_r = \frac{c}{v} = \sqrt{\frac{\varepsilon_r \mu_r}{2}\left(\sqrt{1+(\sigma/\omega\varepsilon)^2}+1\right)} \qquad (4)$$

If $\sigma >> \omega\varepsilon$, $\omega = 2\pi f$, Eq. (4) reduces to

$$n_r = \sqrt{\frac{\mu_r \sigma}{4\pi\varepsilon_0 f}} \qquad (5)$$

Thus, the wavelength of the incident radiation (See Fig. 1) becomes

$$\lambda_{\text{mod}} = \frac{v}{f} = \frac{c/f}{n_r} = \frac{\lambda}{n_r} = \sqrt{\frac{4\pi}{\mu f \sigma}} \qquad (6)$$

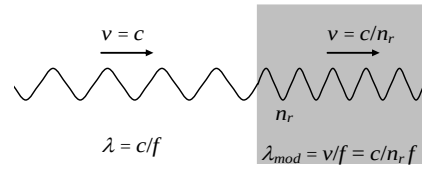

Fig. 1 – *Modified Electromagnetic Wave*. The wavelength of the electromagnetic wave can be strongly reduced, but its frequency remains the same.

If a lamina with thickness equal to ξ contains n molecules/m^3, then the number of molecules per area unit is $n\xi$. Thus, if the electromagnetic radiation with frequency f incides on an area S of the lamina it reaches $nS\xi$ molecules. If it incides on the *total area of the lamina*, S_f, then the total number of molecules reached by the radiation is $N = nS_f\xi$. The number of molecules per unit of volume, n, is given by

$$n = \frac{N_0 \rho}{A} \qquad (7)$$

where $N_0 = 6.02\times10^{26}\, molecules/kmole$ is the Avogadro's number; ρ is the matter density of the lamina (in kg/m^3) and A is the molar mass.

When an electromagnetic wave incides on the lamina, it strikes on N_f front molecules, where $N_f \cong (nS_f)/\phi_m$, ϕ_m is the "diameter" of the molecule. Thus, the electromagnetic wave incides effectively on an area $S = N_f S_m$, where $S_m = \frac{1}{4}\pi\phi_m^2$ is the cross section area of one molecule. After these collisions, it carries out $n_{collisions}$ with the other molecules (See Fig.2).

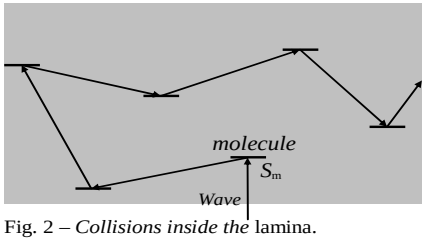

Fig. 2 – *Collisions inside the* lamina.

Thus, the total number of collisions in the volume $S\xi$ is

$$N_{collisions} = N_f + n_{collisions} = nS\phi_m + (nS\xi - n_m S\phi_m) = n_m S\xi \quad (8)$$

The power density, D, of the radiation on the lamina can be expressed by

$$D = \frac{P}{S} = \frac{P}{N_f S_m} \quad (9)$$

We can express the *total mean number of collisions in each molecule*, n_1, by means of the following equation

$$n_1 = \frac{n_{total\ \ photons} N_{collisions}}{N} \quad (10)$$

Since in each collision a *momentum* h/λ is transferred to the molecule, then the *total momentum* transferred to the lamina will be $\Delta p = (n_1 N)h/\lambda$. Therefore, in accordance with Eq. (1), we can write that

$$\frac{m_{g(l)}}{m_{i0(l)}} = \left\{1 - 2\left[\sqrt{1 + \left[(n_1 N)\frac{\lambda_0}{\lambda}\right]^2} - 1\right]\right\} = \left\{1 - 2\left[\sqrt{1 + \left[n_{total\ photons} N_{collisions}\frac{\lambda_0}{\lambda}\right]^2} - 1\right]\right\} \quad (11)$$

Since Eq. (8) gives $N_{collisions} = n\ S\xi$, we get

$$n_{total\ \ photons} N_{collisions} = \left(\frac{P}{hf^2}\right)(n\ S\xi) \quad (12)$$

Substitution of Eq. (12) into Eq. (11) yields

$$\frac{m_{g(l)}}{m_{i0(l)}} = \left\{1 - 2\left[\sqrt{1 + \left[\left(\frac{P}{hf^2}\right)(n\ S\xi)\frac{\lambda_0}{\lambda}\right]^2} - 1\right]\right\} \quad (13)$$

Substitution of P given by Eq. (9) into Eq. (13) gives

$$\frac{m_{g(l)}}{m_{i0(l)}} = \left\{1 - 2\left[\sqrt{1 + \left[\left(\frac{N_f S_m D}{f^2}\right)\left(\frac{n\ S\xi}{m_{i0(l)} c}\right)\frac{1}{\lambda}\right]^2} - 1\right]\right\} \quad (14)$$

Substitution of $N_f \cong (n\ S_f)\phi_m$ and $S = N_f S_m$ into Eq. (14) results

$$\frac{m_{g(l)}}{m_{i0(l)}} = \left\{1 - 2\left[\sqrt{1 + \left[\left(\frac{n^3 S_f^2 S_m^2 \phi_m^2 \xi D}{m_{i0(l)} c f^2}\right)\frac{1}{\lambda}\right]^2} - 1\right]\right\} \quad (15)$$

where $m_{i0(l)} = \rho_{(l)} V_{(l)}$.

Now, considering that the lamina is inside a ELF electromagnetic field with E and B, then we can write that [7]

$$D = \frac{n_{r(l)} E^2}{2\mu_0 c} \quad (16)$$

Substitution of Eq. (16) into Eq. (15) gives

$$\frac{m_{g(l)}}{m_{i0(l)}} = \left\{1 - 2\left[\sqrt{1 + \left[\left(\frac{n_{r(l)} n^3 S_f^2 S_m^2 \phi_m^2 \xi E^2}{2\mu_0 m_{i0(l)} c^2 f^2}\right)\frac{1}{\lambda}\right]^2} - 1\right]\right\} \quad (17)$$

Now assuming that the lamina is a *cylindrical air lamina* (diameter = α ; thickness = ξ) where $n = N_0 \rho_{(l)}/A = 2.6 \times 10^{25}$ *molecules* $/ m^3$; $\phi_m = 1.55 \times 10^{-10} m$; $S_m = \pi\phi_m^2/4 = 1.88 \times 10^{-20} m^2$, then, Eq. (17) reduces to

$$\frac{m_{g(l)}}{m_{i0(l)}}=\left\{1-2\left[\sqrt{1+\left[6.6\times10^{5}\left(\frac{n_{r(l)}S_f^2\xi}{m_{i0(l)}f^2}\right)\frac{E^2}{\lambda}\right]^2}-1\right]\right\} \quad (18)$$

An *atomized water spray* is created by forcing the water through an orifice. The energy required to overcome the pressure drop is supplied by the *spraying pressure* at each detonation. Spraying pressure depends on feed characteristics and desired *particle size*. If *atomizing water* is injected into the air lamina, then the area S_f to be considered is the *surface area* of the *atomizing water*, which can be obtained by multiplying the *specific surface area*(SSA) *of the atomizing water* (which is given by $SSA=A/\rho_w V=3/\rho_w r_d$) *by the total mass of the atomizing water* ($m_{i0(w)}=\rho_w V_{water\ droplets}N_d$). Assuming that the *atomizing water* is composed of monodisperse particles with $10\mu m$ radius$\left(r_d=1\times10^{-5}m\right)$, and that the *atomizing water* has $N_p\approx10^8 droplets/m^3$ [8] then we obtain $SSA=3/\rho_w r_d=300m^2/kg$ and $m_{i0(w)}=\rho_w V_{water\ droplets}N_d\approx10^{-5}kg$. Thus, we get

$$S_f=(SSA)m_{i0(w)}\approx10^{-3}m^2 \quad (18)$$

Substitution of $S_f\approx10^{-3}m^2$ and $m_{i0(l)}=\rho_{air}S_\alpha\xi=1.2S_\alpha\xi$ into Eq. (18) gives

$$\frac{m_{g(l)}}{m_{i0(l)}}=\left\{1-2\left[\sqrt{1+\sim\frac{n_{r(l)}^2E^4}{S_\alpha^2f^4\lambda^2}}-1\right]\right\} \quad (19)$$

The injection of atomized water increases the electrical conductivity of the mean, making it greater than the conductivity of water $(\sigma>>0.005S/m)$. Under these conditions, the value of λ, given by Eq. (6), becomes

$$\lambda=\lambda_{\mathrm{mod}}=\sqrt{\frac{4\pi}{\mu_0 f\sigma}} \quad (20)$$

where f is the frequency of the ELF electromagnetic field.

Substitution of Eq. (20) into Eq. (19) yields

$$\chi=\frac{m_{g(l)}}{m_{i0(l)}}=\left\{1-2\left[\sqrt{1+\sim10^{-7}\frac{n_{r(l)}^2\sigma E^4}{S_\alpha^2f^3}}-1\right]\right\} \quad (21)$$

where $n_{r(l)}^2=\mu_r\sigma/4\pi\varepsilon_0 f$

Note that $E=E_m\sin\omega t$ .The average value for E^2 is equal to $\frac{1}{2}E_m^2$ because E varies sinusoidaly (E_m is the maximum value for E). On the other hand, $E_{rms}=E_m/\sqrt{2}$. Consequently we can change E^4 by E_{rms}^4, and the equation above can be rewritten as follows

$$\chi=\frac{m_{g(l)}}{m_{i0(l)}}=\left\{1-2\left[\sqrt{1+\sim10^{-7}\frac{n_{r(l)}\sigma E_{rms}^4}{S_\alpha^2f^3}}-1\right]\right\} \quad (22)$$

Now consider the weapon showed in Fig. 3 $(\alpha=12.7mm)$. When an ELF electromagnetic field with frequency $f=10Hz$ is activated, an electric field E_{rms} passes through the 7 cylindrical air laminas. Then, according to Eq. (22) the value of χ (for $\sigma>>0.005S/m$) at each lamina is

$$\chi>>\left\{1-2\left[\sqrt{1+\sim10^{-3}E_{rms}^4}-1\right]\right\} \quad (23)$$

For example, if $E_{rms}\cong125.93V/m$ we get

$$\chi>>-10^3 \quad (24)$$

Therefore, according to Eq. (3) the gravitational acceleration produced by the gravitational mass $M_g=4.23kg$, just after

the 7^{th} cylindrical air lamina $(r_7 = 150mm)$, will be given by

$$g_7 = \chi^7 g = -\chi^7 \frac{GM_g}{r_7^2} >> +10^{13} m/s^2 \qquad (25)$$

This is the acceleration acquired by the air molecules that are just after the 7^{th} cylindrical air lamina. Obviously, this produces enormous pressure in the air after the 7^{th} cylindrical air lamina, in a similar way that pressure produced by a detonation. The detonation velocity after the 7^{th} cylindrical air lamina is

$$v_d = \sqrt{2g_7(\Delta r)} >> 10^5 m/s \qquad (26)$$

Consequently, the detonation pressure is

$$p = 2\rho_{air} v_d^2 >> 10^{10} N/m^2 \qquad (27)$$

These values show how powerful can be the gravitational shockwaves weapons. The maxima resistance of the most resistant steels is of the order of 10^{11}N/m^2 (*Graphene* ~10^{12}N/m^2). Since the gravitational shockwave weapons can be designed to produce detonation pressures of these magnitudes, we can conclude that it can destroy anything.

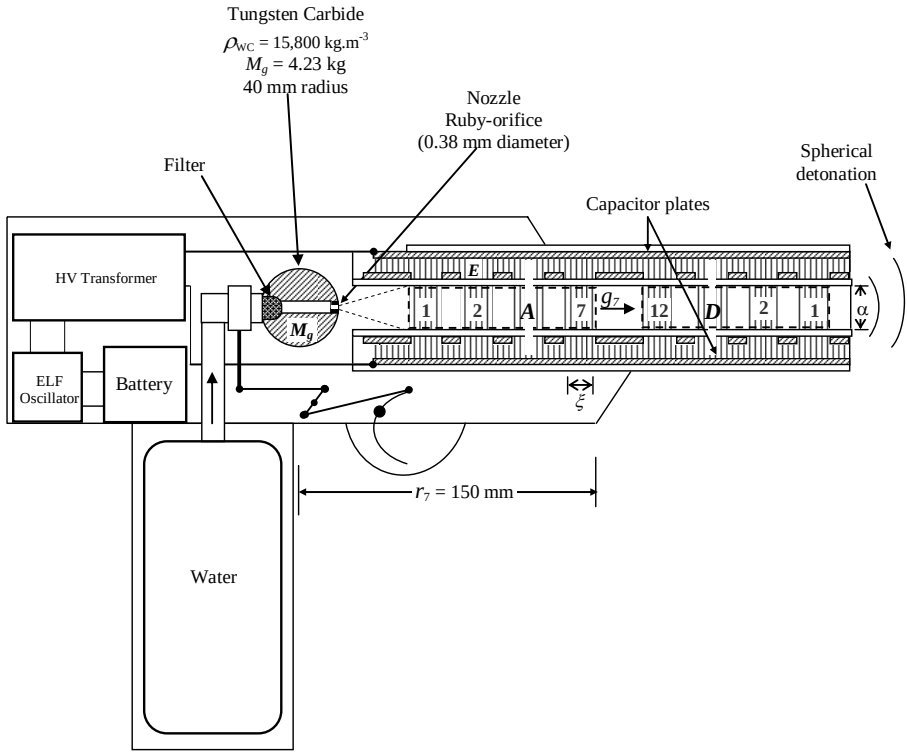

Fig. 3 – *Portable Weapon of Gravitational Shockwaves*. Note that there are two sets of Gravitational Shieldings (GS): the set ***A*** (accelerator) with 7 GS and the set ***D*** (decelerator) with 12 GS. The objective of the set ***D***, with 12 GCC, is to reduce strongly the value of the *external* gravity along the axis of the tube (in the opposite direction of the acceleration g_7). In this case, the value of the external gravity, g_{ext}, is reduced by the factor $\chi_d^{12} g_{ext}$, where $\chi_d = 10^{-2}$. For example, if the opening of the tube (α) of the weapon is positioned on the Earth surface then $g_{ext} = 9.81 m/s^2$ is reduced to $\chi_d^{12} g_{ext}$ and, after in the set ***A***, it is increased by χ^7. Without the set ***D***, the back of the weapon can explode.

References

[1] Cooper, P. W.(1996) *Explosives Engineering*, New York: Wiley-VCH.

[2] Lee, J.H.(1984)*"Dynamic parameters of gaseous detonations"* ,Ann. Rev. Fluid Mech., 16

[3] Fickett, W. and Davis, W.C. (1979)*"Detonation"*, University of California Press, Berkeley.

[4] De Aquino, F. (2010) *Mathematical Foundations of the Relativistic Theory of Quantum Gravity*, Pacific Journal of Science and Technology, **11** (1), pp. 173-232.

[5] De Aquino, F. (2010) *Gravity Control by means of Electromagnetic Field through Gas at Ultra-Low Pressure*, Pacific Journal of Science and Technology, **11**(2) November 2010, pp.178-247, Physics/0701091.

[6] Quevedo, C. P. (1977) *Eletromagnetismo*, McGraw-Hill, p. 270.

[7] Halliday, D. and Resnick, R. (1968) *Physics*, J. Willey & Sons, Portuguese Version, Ed. USP, p.1124.

[8] Yashiro, H., et al., (2010) *Measurement of Number Density of Water Droplets in Aerosol by Laser-Induced Breakdown*, Applied Physics Express 3, 036601.

Negative Gravitational Mass in a Superfluid Bose-Einstein Condensate

Fran De Aquino
Professor Emeritus of Physics, Maranhao State University, UEMA.
Titular Researcher (R) of National Institute for Space Research, INPE

Newton's 2nd law of motion tells us that objects accelerate in the same direction as the applied force. However, recently it was shown experimentally that a Superfluid Bose-Einstein Condensate (BEC) accelerates in the *opposite direction* of the applied force, due to the inertial mass of the BEC becoming *negative* at the specifics conditions of the mentioned experiment. Here we show that is not the inertial mass but the *gravitational mass* of the BEC that becomes *negative*, due to the electromagnetic energy absorbed from the trap and the Raman beams used in the experimental set-up. This finding can be highly relevant to the gravitation theory.

Key words: Negative Gravitational Mass, Bose-Einstein Condensates, Superfluids.

1. Introduction

A recent paper described an experiment that shows a Superfluid Bose-Einstein Condensate (BEC) with *negative* mass, and accelerating in the *opposite direction* of an applied force [1]. The experiment starts with a BEC of approximately 10^5 ^{87}Rb atoms confined in a cigar-shaped trap oriented along the x-axis of a far-detuned crossed dipole trap. Using an adiabatic loading procedure, the BEC is initially prepared such that it occupies the lowest minimum of the lower spin-orbit coupled (SOC) BEC. By suddenly switching off one of the two dipole *trap beams*, the condensate is allowed to spread out along the x-axis. Then, the BEC is imaged in-situ for expansion times of 0, 10 and 14 ms. In the negative x-direction, the BEC encounters an essentially parabolic dispersion, while in the positive x-direction, it enters a *negative mass* region. This leads to a marked asymmetry in the expansion.

Obviously, *negative mass* does not mean *anti-matter*. Anti-matter is simply matter which has the opposite electric charge from normal matter, whereas negative mass means more exactly *negative gravitational mass*. If one particle had ordinary positive gravitational mass, and one had *negative* gravitational mass, then the gravitational force between the masses would be *repulsive* differently of in the case of two positive gravitational masses where the force would be of attraction.

In this article, we show that is not the inertial mass but the *gravitational mass* of the BEC that becomes *negative*, due to the electromagnetic energy absorbed from the trap and the Raman beams used in the experimental set-up. The consequences of this finding can be highly relevant to the gravitation theory.

2. Theory

Some years ago I wrote a paper [2] where a correlation between gravitational mass and inertial mass was obtained. In the paper I pointed out that the relationship between gravitational mass, m_g, and *rest* inertial mass, m_{i0}, is given by

$$\chi = \frac{m_g}{m_{i0}} = \left\{1 - 2\left[\sqrt{1+\left(\frac{Un_r}{m_{i0}c^2}\right)^2} - 1\right]\right\} \qquad (1)$$

where U is *the electromagnetic energy absorbed or emitted by the particle;* $n_r = c/v$ is the index of refraction of the particle; c is the speed of light.

Equation (1) can be rewritten as follows

$$\chi = \frac{m_g}{m_{i0}} = \left\{1 - 2\left[\sqrt{1+\left(\frac{W}{\rho c\ v}\right)^2} - 1\right]\right\} \qquad (2)$$

where ρ is the matter density, v is the velocity of radiation through the particle, and W is the density of absorbed electromagnetic energy. Substitution of the well-known relation $W = 4D/v$ into Eq. (2) yields

$$\chi = \frac{m_g}{m_{i0}} = \left\{1 - 2\left[\sqrt{1+\left(\frac{4D}{\rho c v^2}\right)^2} - 1\right]\right\} \qquad (3)$$

where D is the power density of the radiation *absorbed* by the particle.

In order to apply the Eq. (3) to the BEC previously mentioned, we start calculating the *rest* inertial mass of the BEC, which is given by

$$m_{i0(BEC)} \cong 1\times10^5\left(86.909187\times1.66\times10^{-27}\,kg\right) =$$

$$= 1.4\times10^{-20}\,kg$$

Assuming that the average radius of the BEC is approximately 40 μm (See reference [1]), then we can calculate the density of the BEC, i.e.,

$$\rho_{BEC} = \frac{m_{i0(BEC)}}{V_{BEC}} = \frac{1.4\times10^{-20}kg}{\frac{4}{3}\pi\left(40\times10^{-6}m\right)^3} \cong 5.2\times10^{-8}\,kg.m^{-3}$$

Substitution of the values of ρ_{BEC} into Eq. (3) gives

$$\chi_{BEC} = \frac{m_{g(BEC)}}{m_{i0(BEC)}} = \left\{1 - 2\left[\sqrt{1+0.065\frac{D^2}{v_{BEC}^4}} - 1\right]\right\} \qquad (4)$$

The variable D, in Eq. (4), refers now to the total power density of the radiation *absorbed* by the BEC (from t*he trap and the Raman beams*, used in the experimental set-up of reference [1]). According to the authors of the experiment the power of the Raman beams are of approximately 3mW (2.9 *m*W in one of the two beams,3.3 *m*W in the other), focused to a beam waist of 120 microns ($60\mu m$ radius); the absorption coefficient is $1E_R/2.5E_R = 0.4$. Thus, we can write that

$$D = \frac{P_{abs}}{S_{BEC}} = \frac{0.4P_{beams}}{4\pi\left(60\times10^{-6}m\right)^2} =$$

$$= \frac{0.4\times\left(2.9mW + 3.3mW\right)}{4\pi\left(60\times10^{-6}m\right)^2} \cong 5.4\times10^4\,W.m^{-2} \qquad (5)$$

Substitution of this value into Eq. (4) gives

$$m_{g(BEC)} = \left\{1 - 2\left[\sqrt{1+\frac{1.8\times10^8}{v_{BEC}^4}} - 1\right]\right\} m_{i0(BEC)} \qquad (6)$$

Note that, for $v_{BEC} < 109.5m.s^{-1}$ the *gravitational mass* of the BEC ($m_{g(BEC)}$) becomes *negative*. Lene Hau et al., [3] showed that light speed through a BEC reduces to values much smaller than $100m.s^{-1}$.

Consequently, we can conclude that it is the *gravitational mass* of the BEC of ^{87}Rb atoms that becomes *negative* and not its inertial mass.

Also it was deduced in the reference [2] a generalized expression for the Newton's 2nd law of motion, which shows that the expression for *inertial forces* is given by

$$\vec{F} = m_g\vec{a} \qquad (7)$$

The presence of m_g in this equation shows that the inertial forces have origin in the *gravitational interaction* between the particle and the others particles of the Universe, just as *Mach's principle* predicts. In this way, the new equation expresses the incorporation of the Mach's principle into Gravitation Theory, and reveals that the inertial effects upon a body can be strongly reduced by means of the decreasing of its gravitational mass. Note that only when m_g reduces to m_{i0} is that we have the well-know expression ($\vec{F} = m_i\vec{a}$) of the Newton's law.

Taking Eq. (6) for an arbitrary value of $v_{BEC} < 109.5m.s^{-1}$, we obtain $m_{g(BEC)} = -Km_{i0(BEC)}$, where K is a positive number. Substitution of this equation into Eq. (7) yields

$$\vec{F}_{BEC} = -Km_{i0(BEC)}\vec{a} \qquad (8)$$

The sign $(-)$ in this expression reveals clearly why the BEC accelerates in the *opposite direction* of the *applied force*, i.e.,

$$\vec{F}_{BEC} = -\vec{F}_{BEC} = Km_{i0(BEC)}\vec{a} \qquad (9)$$

Recently it was created a BEC with 2.506×10^{17} ^{23}**Na** atoms [4]. The inertial mass of this BEC is

$$m_{i0(BEC)} = 2.506\times10^{17}(23)\left(1.66\times10^{-27}\right) = 3.8\times10^{-9}\,kg$$

The number of atoms/cm^3, as showed in reference [4], is $n_0 = 2.742\times10^{6}\,cm^{-3} = 2.742\times10^{22}\,m^{-3}$. Thus, the density of the BEC is given by

$$\rho = (23)\left(1.66\times10^{-27}\right)2.742\times10^{22} = 1.04\times10^{-3}\,kg.m^{-3}$$

Substitution of these values into Eq. (3) gives

$$m_{g(BEC)} = \left\{1-2\left[\sqrt{1+1.6\times10^{-10}\frac{D^2}{v_{BEC}^4}}-1\right]\right\}m_{i0(BEC)} \quad (10)$$

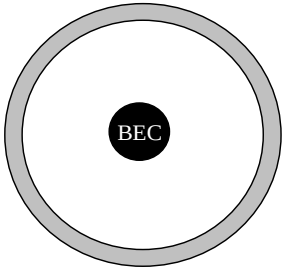

Fig. 1 – A BEC inside a hollow sphere.

Now consider the system showed in Fig.1. Inside the hollow sphere, whose *gravitational* mass is $m_{g(sphere)} \cong m_{i0(sphere)}$, there is a BEC whose *gravitational* mass is given by Eq. (10). Thus, the *total gravitational* mass of the system, $m_{g(SYS)}$, is given by

$$m_{g(SYS)} = m_{g(sphere)} + m_{g(BEC)} =$$

$$\cong m_{i0(sphere)} + \left\{1-2\left[\sqrt{1+1.6\times10^{-10}\frac{D^2}{v_{BEC}^4}}-1\right]\right\}m_{i0(BEC)} \quad (11)$$

In 2001 Lene Hau et al., have shown that the light speed through a BEC could have values very close to *zero*. Therefore, v_{BEC} with these magnitudes are not unusual. This shows that the value of $m_{g(SYS)}$, given Eq. (11), can be strongly reduced even the value of D be small, for example, of the order of $1W/m^2$.

Then, consider a system in which the inertial mass of the hollow sphere is $m_{i0(sphere)} = 10{,}000\,kg$; $m_{i0(BEC)} = 3.8\times10^{-9}\,kg$; $D \cong 1W/m^2$ and $v_{BEC} = 10^{-9}\,m.s^{-1}$ *, then the gravitational mass of the system will have the following value:

$$m_{g(SYS)} = m_{i0(sphere)} - 2.5\times10^{13}\,m_{i0(BEC)} =$$

$$= -8.5\times10^{4}\,kg \quad (12)$$

Thus, if this system is subjected to a gravity acceleration $\vec{g} = 9.8\,m.s^{-1}$, as shown in Fig.2, then its weight force will be given by $\vec{P} = \left|m_{g(SYS)}\right|\vec{g} = 8.5\times10^{4}\,\vec{g}$, $\left(P = 8.3\times10^{5}\,N\right)$. This value is greater than the thrust of the fighter aircraft F-22 Raptor (fifth-generation), which reaches 160,000N.

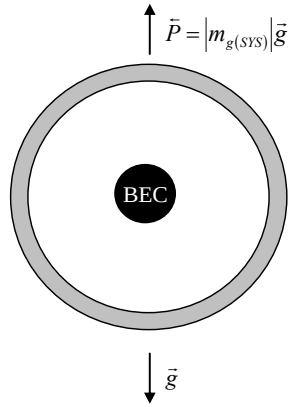

Fig. 2 – The system sphere-BEC, with *negative* gravitational mass ($m_{g(SYS)} < 0$), in a gravitational field.

It is important to note that, in spite the light speed reach values very close to zero through the BEC in the Lene Hau experiments, the number of atoms in the BEC, in this case is very small $\left(10^5 - 10^6\,atoms\right)$ in comparison with the 2.506×10^{17} atoms of the BEC of ^{23}**Na,** here mentioned. Consequently, the weight force, acting on the BEC in the case of the Lene Hau experiments is approximately 10^{-12} times smaller than in the case of the BEC of Na atoms.

* With this velocity the light beam would travel about $0.1mm$ in a day.

References

[1] M.A. Khamehchi *et al*. (2017). *Negative-Mass Hydrodynamics in a Spin-Orbit–Coupled Bose-Einstein Condensate. Phys. Rev. Lett*. 118 (15): 155301; doi: 10.1103/PhysRevLett.118.155301
Available at: https://arxiv.org/abs/1612.04055

[2] De Aquino, F. (2010) *Mathematical Foundations of the Relativistic Theory of Quantum Gravity*, Pacific Journal of Science and Technology, **11** (1), pp. 173-232.
Available at: https://hal.archives-ouvertes.fr/hal-01128520

[3] Hau, L.V, et al., (1999) *Light Speed Reduction to 17 Meters per Second in an Ultracold Atomic Gas*, Nature 397, 594-598.

[4] Pei-Lin You (2016) *Bose–Einstein condensation in a vapor of sodium atoms in an electric field*, Physica B, **491**, 84-92.

Controlling the Gravitational Mass of a Metallic Lamina, and the Gravity Acceleration above it.

Fran De Aquino
Professor Emeritus of Physics, Maranhao State University, UEMA.
Titular Researcher (R) of National Institute for Space Research, INPE

It is proposed a very simple device for controlling the gravitational mass of a metallic lamina, and the gravity acceleration above it. These effects are obtained when a specific extra-low frequency current passes through a specially designed metallic lamina.

Key words: Gravitational Interaction, Gravitational Mass, Gravitational Force Control.

1. Introduction

In a previous paper [1] we shown that there is a correlation between the gravitational mass, m_g, and the rest inertial mass m_{i0}, which is given by

$$\chi = \frac{m_g}{m_{i0}} = \left\{1-2\left[\sqrt{1+\left(\frac{\Delta p}{m_{i0}c}\right)^2}-1\right]\right\} = \left\{1-2\left[\sqrt{1+\left(\frac{Un_r}{m_{i0}c^2}\right)^2}-1\right]\right\} = \left\{1-2\left[\sqrt{1+\left(\frac{Wn_r}{\rho c^2}\right)^2}-1\right]\right\} \quad (1)$$

where Δp is the variation in the particle's *kinetic momentum*; U is *the electromagnetic energy absorbed or emitted by the particle;* n_r is the index of refraction of the particle; W is the density of energy on the particle (J/kg); ρ is the matter density (kg/m^3) and c is the speed of light.

The *instantaneous values* of the density of electromagnetic energy in an *electromagnetic* field can be deduced from Maxwell's equations and has the following expression

$$W = \tfrac{1}{2}\varepsilon E^2 + \tfrac{1}{2}\mu H^2 \quad (2)$$

where $E = E_m \sin\omega t$ and $H = H\sin\omega t$ are the *instantaneous values* of the electric field and the magnetic field respectively.

It is known that $B = \mu H$, $E/B = \omega/k_r$ [2] and

$$v = \frac{dz}{dt} = \frac{\omega}{\kappa_r} = \frac{c}{\sqrt{\frac{\varepsilon_r\mu_r}{2}\left(\sqrt{1+(\sigma/\omega\varepsilon)^2}+1\right)}} \quad (3)$$

where k_r is the real part of the *propagation vector* $\vec{k}$ (also called *phase constant*); $k = |\vec{k}| = k_r + ik_i$; ε , μ and σ, are the electromagnetic characteristics of the medium in which the incident (or emitted) radiation is propagating ($\varepsilon = \varepsilon_r\varepsilon_0$; $\varepsilon_0 = 8.854\times10^{-12} F/m$; $\mu = \mu_r\mu_0$ where $\mu_0 = 4\pi\times10^{-7} H/m$). From Eq. (3), we see that the *index of refraction* $n_r = c/v$ is given by

$$n_r = \frac{c}{v} = \sqrt{\frac{\varepsilon_r\mu_r}{2}\left(\sqrt{1+(\sigma/\omega\varepsilon)^2}+1\right)} \quad (4)$$

Equation (3) shows that $\omega/\kappa_r = v$. Thus, $E/B = \omega/k_r = v$, i.e.,

$$E = vB = v\mu H$$

Then, Eq. (2) can be rewritten as follows

$$W = \tfrac{1}{2}\varepsilon E^2 + \tfrac{1}{2}\mu\left(\frac{E}{v\mu}\right)^2 = \tfrac{1}{2}\varepsilon E^2 + \tfrac{1}{2}\left(\frac{1}{v^2\mu}\right)E^2 = \tfrac{1}{2}\left(\frac{1}{v^2\mu}\right)E^2 + \tfrac{1}{2}\left(\frac{1}{v^2\mu}\right)E^2 = \left(\frac{1}{v^2\mu}\right)E^2 = \left(\frac{c^2}{v^2\mu c^2}\right)E^2 = \left(\frac{n_r^2}{\mu c^2}\right)E^2 \quad (5)$$

For $\sigma >> \omega\varepsilon$, Eq. (3) gives

$$n_r^2 = \frac{c^2}{v^2} = \frac{\mu\sigma}{2\omega}c^2 \quad (6)$$

Substitution of Eq. (6) into Eq. (5) gives

$$W = (\sigma/2\omega)E^2 \quad (7)$$

Substitution of Eq. (7) into Eq. (1), yields

$$m_g = \left\{1-2\left[\sqrt{1+\frac{\mu}{c^2}\left(\frac{\sigma}{4\pi f}\right)^3\frac{E^4}{\rho^2}}-1\right]\right\}m_{i0} = \left\{1-2\left[\sqrt{1+\left(\frac{\mu_0}{64\pi^3c^2}\right)\left(\frac{\mu_r\sigma^3}{\rho^2 f^3}\right)E^4}-1\right]\right\}m_{i0} = \left\{1-2\left[\sqrt{1+7.032\times10^{-27}\left(\frac{\mu_r\sigma^3}{\rho^2 f^3}\right)E^4}-1\right]\right\}m_{i0} \quad (8)$$

Note that if $E = E_m \sin\omega t$ .Then, the average value for E^2 is equal to $\frac{1}{2}E_m^2$ because

E varies sinusoidaly (E_m is the maximum value for E). On the other hand, we have $E_{rms}=E_m/\sqrt{2}$. Consequently, we can change E^4 by E_{rms}^4, and the Eq. (8) can be rewritten as follows

$$m_g=\left\{1-2\left[\sqrt{1+7.032\times10^{-27}\left(\frac{\mu_r\sigma^3}{\rho^2 f^3}\right)E_{rms}^4}-1\right]\right\}m_{i0} \quad (9)$$

The *Ohm's vectorial Law* tells us that $j_{rms}=\sigma E_{rms}$. Thus, we can write Eq. (9) in the following form:

$$m_g=\left\{1-2\left[\sqrt{1+7.032\times10^{-27}\,\frac{\mu_r j_{rms}^4}{\sigma\rho^2 f^3}}-1\right]\right\}m_{i0} \quad (10)$$

where $j_{rms}=j/\sqrt{2}$ [3]. Since

$$j=\frac{i}{S}=\frac{V/R}{S}=\frac{V}{RS}=\frac{V}{(L/\sigma S)S}=\sigma\left(\frac{V}{L}\right) \quad (11)$$

Then, we can write that

$$j_{rms}=\frac{\sigma}{\sqrt{2}}\left(\frac{V}{L}\right) \quad (12)$$

By substitution of Eq. (12) into Eq.(10), we get

$$\chi=\frac{m_g}{m_{i0}}=\left\{1-2\left[\sqrt{1+1.758\times10^{-27}\left(\frac{\mu_r\sigma^3}{\rho^2}\right)\frac{(V/L)^4}{f^3}}-1\right]\right\} \quad (13)$$

Also, it was shown in the above mentioned paper [1] that, if the *weight* of a particle in a side of a lamina is $\vec{P}=m_g\vec{g}$ ($\vec{g}$ perpendicular to the lamina) then the weight of the same particle, in the other side of the lamina is $\vec{P}'=\chi m_g\vec{g}$, where $\chi=m_g^l/m_{i0}^l$ (m_g^l and m_{i0}^l are respectively, the gravitational mass and the rest inertial mass *of the lamina*). Only when $\chi=1$, is that the weight is equal in both sides of the lamina. Thus, the lamina can control the gravity acceleration above it, and in this way, it can work as a *Gravity Controller Device*.

Since the gravitational mass of a body above the lamina is $m_g=m_{i0}$, then we can conclude that $P'=m_{i0}(\chi g)$. Therefore, this means that the gravity acceleration above the lamina is $g'=\chi g$.

Here, we describe a very simple device, which works as the mentioned lamina. This device is easy to build, and can be used in order to test the correlation between gravitational mass and inertial mass previously mentioned (Eq. (1)), and also the modification of the gravity acceleration above the lamina (χg).

2. The Device

Consider the device shown in Fig.1 (a). It is basically a thin Aluminum strip attached to an electrical insulating plate. This strip has been designed over an Aluminum lamina, in order to an electrical current $(j_{rms};f)$ to pass through it, producing the decreasing of its gravitational mass $m_{g(strip)}$, according to Eq. (10). The Aluminum of this strip has the following characteristics: 99.9% Aluminum; $\mu_r=1$; ρ = 2700 kg/m^{-3}; σ = 3.5x10^{7}S/m. The Aluminum strip has the following dimensions; Length, L=3528 mm; Width: l = 5mm; Thickness: Δx =3μm. The Resistance of the Aluminum strip is: $R=L/\sigma S=L/\sigma(\Delta x l)=6.7\Omega$ and the maximum current density, according to Eq. (12), is:

$$j_{\max(rms)}=\frac{\sigma}{\sqrt{2}}(V/L)_{\max}=3.5\times10^6 A/m^2=3.5A/mm^2;$$

the maximum current is $i_{\max(rms)}=j_{\max(rms)}S=0.05A$ [*]; the Maximum Dissipated Power is: $P_{\max}=Ri_{\max(rms)}^2=0.017watts$.

By substuting the values of μ_r, σ, ρ and L into Eq. (13), we obtain.

$$\chi=\frac{m_{g(strip)}}{m_{i0(strip)}}=\left\{1-2\left[\sqrt{1+6.67\times10^{-14}\frac{V^4}{f^3}}\right]-1\right\} \quad (14)$$

Consequently, the gravity acceleration *above the Aluminum strip* is given by

$$g'=\chi g=\left\{1-2\left[\sqrt{1+6.67\times10^{-14}\frac{V^4}{f^3}}\right]-1\right\}g \quad (15)$$

The calculated results starting from Eqs.(14) and (15) for $f=5\mu Hz$; $f=10\mu Hz$; $f=15\mu Hz$, in the voltage range $0.1V-0.5V$ are plotted in Table 1.

Figure 1(b) shows an experimental set up in order to control the decreasing of the *Gravitational Mass* of the Aluminum strip. Figure 1(c) shows an experimental set up in order to control the decreasing of the *gravity acceleration above the Aluminum strip*.

[*] The *maximum out put current* of the HP 3325 Function Generator (option 002 High Voltage out put) is 0.08A$_{pp}$,(0.056A$_{rms}$). Voltage range 4.0mV to 40.0V$_{pp}$; sine 1 μHz to 20MHz.

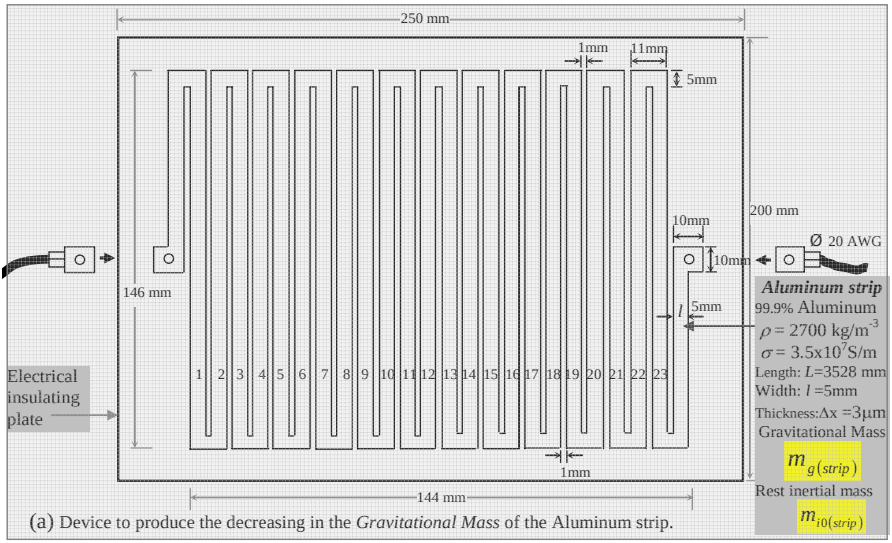

(a) Device to produce the decreasing in the *Gravitational Mass* of the Aluminum strip.

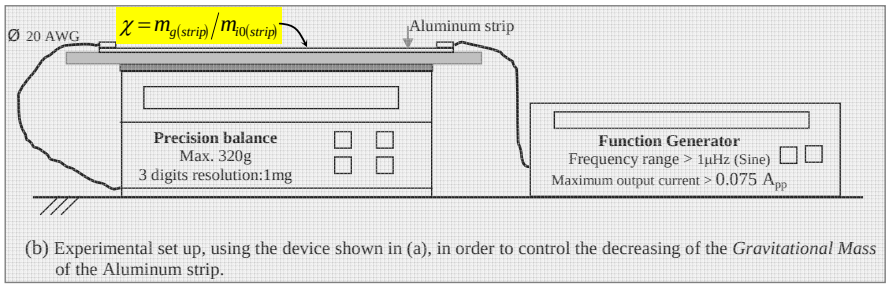

(b) Experimental set up, using the device shown in (a), in order to control the decreasing of the *Gravitational Mass* of the Aluminum strip.

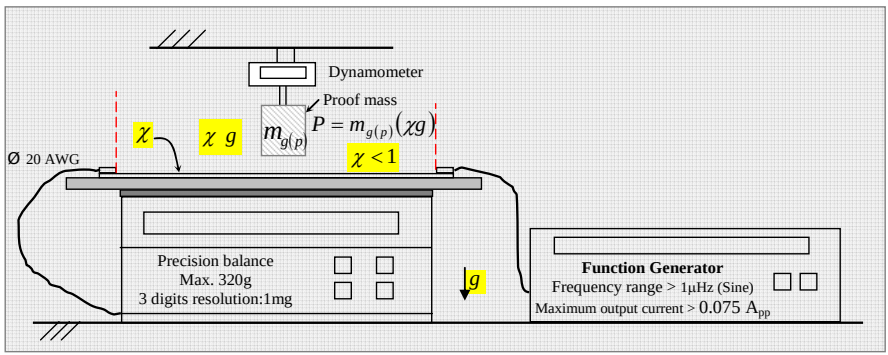

(c) Experimental set up, using the device shown in (a), in order to control the decreasing of the Local *Gravity* (g) *above the Aluminum strip* (*Gravity Controller Device*).

Fig. 1 – Experimental set ups for controlling the *Gravitational Mass* of the Aluminum strip, and the *Gravity* acceleration above it.

$$\chi = \frac{m_{g(strip)}}{m_{i0(strip)}} = \left\{1 - 2\left[\sqrt{1 + 1.758\times10^{-27}\left(\frac{\mu_r \sigma^3}{L^4\rho^2}\right)\frac{V^4}{f^3}}\right] - 1\right\} = \left\{1 - 2\left[\sqrt{1 + 6.67\times10^{-14}\,\frac{V^4}{f^3}}\right] - 1\right\}$$

$\sigma = 3.5\times10^7\, S/m;\ \rho = 2700\, kg/m^3;\ L = 3.528\, m;\ \mu_r = 1;$
$m_{i0(strip)} = \rho(\Delta x l L) = 1.428\times10^{-4}\, kg = 0.1428\, grams$

f = 5 μHz

V (volts)	$m_{i0(strip)}$ (gr)	$m_{g(strip)}$ (gr)	χ	χg (m/s^2)
0.1	0.1428	0.1352	0.9473	9.2930
0.2	0.1428	0.0395	02769	2.6771
0.3	0.1428	-0.2304	-1.6139	-15.8323
0.4	0.1428	-0.6651	-4.6577	-45.6922
0.5	0.1428	-1.2454	-8.7217	-85.5598

g =9.81 m/s^2

f = 10 μHz

V (volts)	$m_{i0(strip)}$ (gr)	$m_{g(strip)}$ (gr)	χ	χg (m/s^2)
0.1	0.1428	0.1418	0.9933	9.7442
0.2	0.1428	0.1279	0.8959	8.7887
0.3	0.1428	0.0794	0.5178	5.0796
0.4	0.1428	-0.0415	-0.2909	-2.8537
0.5	0.1428	-0.2209	-1.5469	-15.1750

g =9.81 m/s^2

f = 15 μHz

V (volts)	$m_{i0(strip)}$ (gr)	$m_{g(strip)}$ (gr)	χ	χg (m/s^2)
0.1	0.1428	0.1425	0.9980	9.7903
0.2	0.1428	0.1383	0.9686	9.5019
0.3	0.1428	0.1207	0.8458	8.2972
0.4	0.1428	0.0779	0.5456	5.3523
0.5	0.1428	0.0014	0.0098	0.0961

g =9.81 m/s^2

Tab. 1 – Calculated results for the *Gravitational Mass* of the Aluminum strip $m_{g(strip)}$, and for the *Gravity* acceleration above the Aluminum strip (χg).

Next, we will show that by reducing the thickness of the Aluminum strip to $3nm$ [†] it is possible to design a similar device for working with *frequency* up to $f = 2mHz$. In this case the period T of the wave is $T = 500s \cong 8.3\min$ [‡].

Let us then consider an Aluminum strip with $3nm$ thickness, $5mm$ width and $3{,}528mm$ length as shown in Fig.2. If the *maximum* applied voltage is $V_{\max} = 22.2volts$ then, according to Eq. (13), we have

$$\chi = \frac{m_{g(strip)}}{m_{i0(strip)}} =$$

$$= \left\{1 - 2\left[\sqrt{1 + 1.758\times10^{-27}\left(\frac{\mu_r \sigma^3}{\rho^2}\right)\frac{(V_{\max}/L)^4}{f^3}} - 1\right]\right\} =$$

$$= \left\{1 - 2\left[\sqrt{1 + \frac{1.6\times10^{-8}}{f^3}} - 1\right]\right\} \qquad (16)$$

For $f = 2mHz$, Eq. (16) gives

$$\chi = \frac{m_{g(strip)}}{m_{i0(strip)}} = -0.46 \qquad (17)$$

Through the Aluminum strip, the maximum intensity of the electrical current is given by

$$i_{\max} = j_{\max} S = \sigma (V_{\max}/L) S =$$

$$= (3.5\times10^7 S/m)(22.2/3.528)[(3\times10^{-9})(5\times10^{-3})] =$$

$$= 3.3mA$$

The electrical resistance of the Aluminum strip is

$$R_{strip} = \frac{L}{\sigma S} =$$

$$= \frac{3.528}{(3.5\times10^7)[(3\times10^{-9})(5\times10^{-3})]} = 6720\Omega$$

Therefore, the *maximum dissipated power* by the strip has now the following value

$$P_{strip}^{\max} = R_{strip} i_{\max}^2 = 73.2mW$$

Note that this power is almost the double of the power in the first device (37.7*mW*).

Let us now verify if the area of the surface of the Aluminum strip (area of the surface of thermal transfer ; 5mm x 3,528mm) is sufficient to transfer to the surrounding air *all the heat* produced by the strip (in order to avoid the fusion of the strip).

The coefficient of heat transfer, h, can be expressed by the following equation [4, 5,6]

$$h = \frac{(\Delta Q/\Delta t)}{A_n \Delta T} \qquad (18)$$

where $\Delta Q/\Delta t$ (in *W*) is the dissipated power ; A_n (in m^2) is the necessary area of the surface of thermal transfer and ΔT the difference of temperature between the area of the solid surface and the surrounding fluid (*K*).

When the surrounding fluid is the *air* , the heat transfer coefficient, h, varies from 10 up to $100W/m^2.°K$ [7]. Assuming $h = 10W/m^2.°K$, and $\Delta T = 1°K$, then for $P_{strip}^{\max} = 73.2mW$, Eq. (18) gives

$$A_n = \frac{(\Delta Q/\Delta t)}{h\Delta T} = 7.32\times10^{-3} m^2 \qquad (19)$$

Since the area of the surface of the Aluminum strip is

$$A_{strip} = 5mm \times 3{,}528mm = 17.6\times10^{-3} m^2 >> A_n$$

Then, we can conclude that *the area of the Aluminum strip is sufficient to transfer to the surrounding air all the heat produced by it.* The same is valid in the case of the first device, where the dissipated power by the Aluminum strip is even smaller than in the second device.

[†] Ultra Thin Aluminum Nanofoils (foils with *nanometers* thicknesses) are manufactured, for example by *American Elements - The Advanced Materials Manufacturer* (See the available nanofoils at: https://www.americanelements.com/ultra-thin-aluminum-nanofoil-7429-90-5).

[‡] In the case of the first device the frequency it were $f = 10\mu Hz$ and the period $T = 10^5 s \cong 27.77hours$.

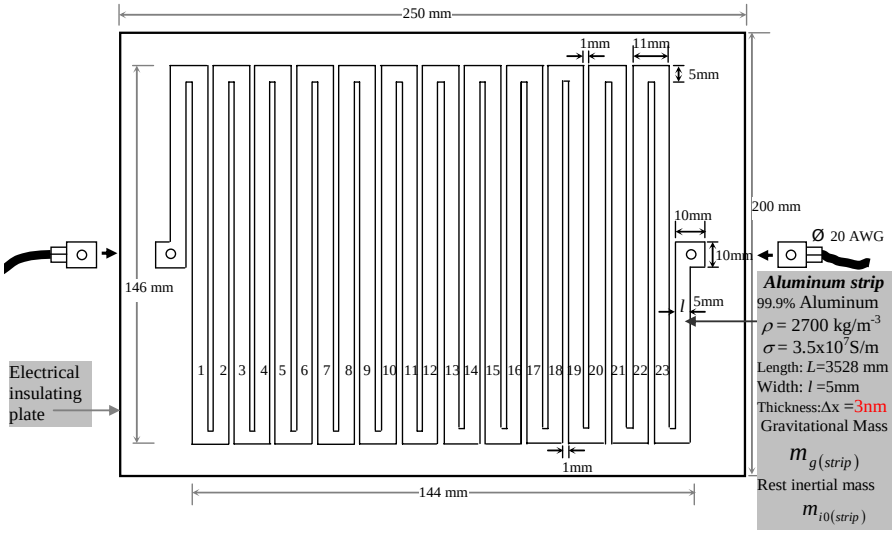

Fig. 2 – Device using Aluminum strip with $3nm$ thickness.

References

[1] De Aquino, F. (2010) *Mathematical Foundations of the Relativistic Theory of Quantum Gravity*, Pacific Journal of Science and Technology,**11** (1), pp. 173-232.
Available at https://hal.archives-ouvertes.fr/hal-01128520

[2] Halliday, D. and Resnick, R. (1968) *Physics*, J. Willey & Sons, Portuguese Version, Ed. USP, p.1118.

[3] Halliday, D. and Resnick, R. (1968) *Physics*, J. Willey & Sons, Portuguese Version, Ed. USP, p.1410.

[4] Halliday, D., Resnick, R., Walker, J., (1996) *Fundamentos de Física 2* - São Paulo: Livros Técnicos e Científicos Editora, 4a Edição, 1996.

[5] Sears, F. W. E Zemansky, M. W. – *Física* - vol. 2, cap. 15, Ed. Universidade de Brasília, Rio de Janeiro – 1973.

[6] *Heat transfer coefficient*. Available at: https://en.wikipedia.org/wiki/Heat_transfer_coefficient

[7] *Overall heat transfer coefficient.* Available at: https://en.wikipedia.org/wiki/Heat_transfer_coefficient

Quantum Controller of Gravity

Fran De Aquino
Professor Emeritus of Physics, Maranhao State University, UEMA.
Titular Researcher (R) of National Institute for Space Research, INPE

A new type of device for controlling gravity is here proposed. This is a quantum device because results from the behaviour of the matter and energy at subatomic length scale (10^{-20}m). From the technical point of view this device is easy to build, and can be used to develop several devices for controlling gravity.

Key words: Gravitation, Gravitational Mass, Inertial Mass, Gravity, Quantum Device.

Introduction

Some years ago I wrote a paper [1] where a correlation between gravitational mass and inertial mass was obtained. In the paper I pointed out that the relationship between gravitational mass, m_g, and *rest* inertial mass, m_{i0}, is given by

$$\chi = \frac{m_g}{m_{i0}} = \left\{1 - 2\left[\sqrt{1+\left(\frac{\Delta p}{m_{i0}c}\right)^2} - 1\right]\right\} =$$

$$= \left\{1 - 2\left[\sqrt{1+\left(\frac{Un_r}{m_{i0}c^2}\right)^2} - 1\right]\right\} =$$

$$= \left\{1 - 2\left[\sqrt{1+\left(\frac{Wn_r}{\rho c^2}\right)^2} - 1\right]\right\} \qquad (1)$$

where Δp is the variation in the particle's *kinetic momentum*; U is *the electromagnetic energy absorbed or emitted by the particle;* n_r is the index of refraction of the particle; W is the density of energy on the particle (J/kg); ρ is the matter density (kg/m^3) and c is the speed of light.

Also it was shown that, if the *weight* of a particle in a side of a lamina is $\vec{P} = m_g\vec{g}$ ($\vec{g}$ perpendicular to the lamina) then the weight of the same particle, in the other side of the lamina is $\vec{P}' = \chi m_g \vec{g}$, where $\chi = m_g^l / m_{i0}^l$ (m_g^l and m_{i0}^l are respectively, the gravitational mass and the inertial mass *of the lamina*). Only when $\chi = 1$, the weight is equal in both sides of the lamina. The lamina works as a *Gravity Controller*. Since $P' = \chi P = (\chi m_g)g = m_g(\chi g)$, we can consider that

$$m_g' = \chi m_g \text{ or that } g' = \chi g$$

In the last years, based on these concepts, I have proposed some types of devices for controlling gravity. Here, I describe a device, which acts controlling the *electric field* in the Matter at *subatomic level* $(\Delta x \cong 10^{-20}\, m)$. This *Quantum Controller of Gravity* is easy to build and can be used in order to test the correlation between gravitational mass and inertial mass previously mentioned.

2. The Device

Consider a *spherical capacitor*, as shown in Fig.1. The *external* radius of the inner spherical shell is r_a, and the *internal* radius of the outer spherical shell is r_b. Between the inner shell and the outer shell there is a dielectric with electric permittivity $\varepsilon = \varepsilon_r \varepsilon_0$. The inner shell works as an *inductor*, in such way that, when it is charged with an electric charge $+q$, and the outer shell is connected to the ground, then the outer shell acquires a electric charge $-q$, which is uniformly distributed at the *external surface of the outer shell*, while the electric charge $+q$ is uniformly distributed at the external surface of the inner shell (See Halliday, D. and Resnick, R., *Physics*, Vol. II, Chapter 28 (*Gauss law*), *Paragraph* 28.4).

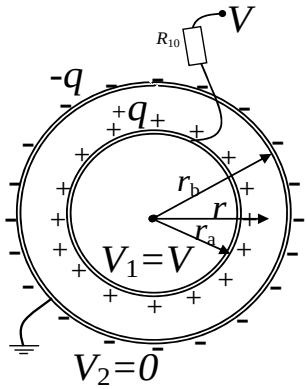

Fig.1 – *Spherical Capacitor* - A Device for Controlling Gravity developed starting from a Spherical Capacitor.

Under these conditions, the electric field between the shells is given by the vectorial sum of the electric fields $\vec{E}_a$ and $\vec{E}_b$, respectively produced by the inner shell and the outer shell. Since they have the same direction in this region, then one can easily show that the resultant intensity of the electric field for $r_a < r < r_b$ is $E_R = E_a + E_b = q/4\pi\varepsilon_r\varepsilon_0 r^2$. In the nucleus of the capacitor and out of it, the *resultant electric field* is *null* because $\vec{E}_a$ and $\vec{E}_b$ have *opposite* directions (See Fig. 2(a)).

Note that the electrostatic force, $\vec{F}$, between $-q$ and $+q$ will move the *negative electric charges* in the direction of the positive electric charges. This causes a displacement, Δx, of the electric field, $\vec{E}_b$, *into the outer shell* (See Fig. 2 (b)). Thus, in the region with thickness Δx the intensity of the electric field *is not null* but equal to E_b.

The negative electric charges are accelerated with an acceleration, $\vec{a}$, in the direction of the positive charges, in such way that they acquire a velocity, given by $v = \sqrt{2a\Delta x}$ (drift velocity).

The drift velocity is given by [2]

$$v = \frac{i}{nSe} = \frac{V/Z}{nSe} = \frac{V/\sqrt{R^2 + X_C^2}}{nSe} \qquad (2)$$

where V is the *positive* potential applied on the inner shell (See Fig. 1); $X_C = 1/2\pi fC$ is the capacitive reactance; f is the frequency; $C = 4\pi\varepsilon(r_a r_b / r_b - r_a)$ is the capacitance of the spherical capacitor; R is the total electrical resistance of the external shell, given by $R = (\Delta z/\sigma S) + R_{10}$, where $\Delta z/\sigma S$ is the electrical resistance of the shell ($\Delta z = 5mm$ is its thickness; σ is its conductivity and S is its surface area), and R_{10} is a 10gigaohms resistor. Since $R_{10} >> \Delta z/\sigma S$, we can write that $R \cong R_{10} = 1\times10^{10}\,\Omega$.

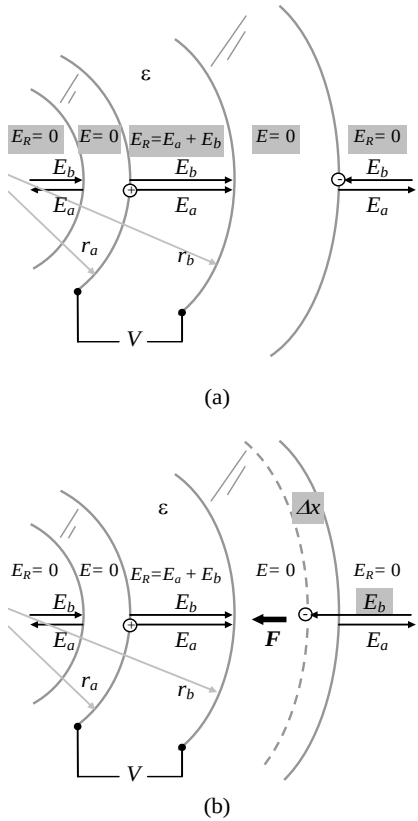

Fig.2 - The displacement, Δx, of the electric field, E_b, *into the outer shell*. Thus, in the region with thickness Δx the intensity of the electric field *is not null* but equal to E_b.

If the shells are made with *Aluminum*, with the following characteristics: $\rho = 2700 kg.m^{-3}$, $A = 27 kg/kmol, n = N_0 \rho / A \cong 6 \times 10^{28} m^{-3}$ (N_0 is the Avogadro's number $N_0 = 6.02 \times 10^{26} kmol^{-1}$), and $r_a = 0.1m; r_b = 0.105m; S = 4\pi (r_b + \Delta z)^2 \cong 0.152 m^2$; $r_b - r_a = 5 \times 10^{-3} m$, then $R >> X_C = (6.8 \times 10^8 / f)$ *ohms*, ($f > 1Hz$), and Eq. (2) can be rewritten in the following form:

$$v = \frac{i}{nSe} \cong \frac{V/R_{10}}{nSe} = 6.8 \times 10^{-20} V \qquad (3)$$

The *maximum size of an electron* has been estimated by several authors [3, 4, 5]. The conclusion is that the electron must have a physical radius smaller than 10^{-22} m*.

Assuming that, under the action of the force $\vec{F}$ (produced by a pulsed voltage waveform, V), the electrons would fluctuate about their initial positions with the *amplitude* of $\Delta x \cong 1 \times 10^{-20} m$ (See Fig.3), then we get

$$\Delta t = \sqrt{\frac{2\Delta x}{a}} = \frac{2\Delta x}{v} \cong \frac{0.294}{V} \qquad (4)$$

However, we have that $f = 1/\Delta T = 1/2\Delta t$. Thus, we get

$$f = 1.7V \qquad (5)$$

Now consider Eq. (1). The *instantaneous values* of the density of electromagnetic energy in an *electromagnetic* field can be deduced from Maxwell's equations and has the following expression

$$W = \tfrac{1}{2} \varepsilon E^2 + \tfrac{1}{2} \mu H^2 \qquad (6)$$

where $E = E_m \sin \omega t$ and $H = H \sin \omega t$ are the *instantaneous values* of the electric field and the magnetic field respectively.

It is known that $B = \mu H$, $E/B = \omega / k_r$ [6] and

$$v = \frac{dz}{dt} = \frac{\omega}{\kappa_r} = \frac{c}{\sqrt{\frac{\varepsilon_r \mu_r}{2}\left(\sqrt{1 + (\sigma/\omega\varepsilon)^2} + 1\right)}} \qquad (7)$$

where k_r is the real part of the *propagation vector* $\vec{k}$ (also called *phase constant*); $k = |\vec{k}| = k_r + ik_i$; ε, μ and σ, are the electromagnetic characteristics of the medium in which the incident (or emitted) radiation is propagating ($\varepsilon = \varepsilon_r \varepsilon_0$; $\varepsilon_0 = 8.854 \times 10^{-12} F/m$; $\mu = \mu_r \mu_0$ where $\mu_0 = 4\pi \times 10^{-7} H/m$). It is known that for *free-space* $\sigma = 0$ and $\varepsilon_r = \mu_r = 1$. Then Eq. (7) gives

$$v = c$$

From Eq. (7), we see that the *index of refraction* $n_r = c/v$ is given by

$$n_r = \frac{c}{v} = \sqrt{\frac{\varepsilon_r \mu_r}{2}\left(\sqrt{1 + (\sigma/\omega\varepsilon)^2} + 1\right)} \qquad (8)$$

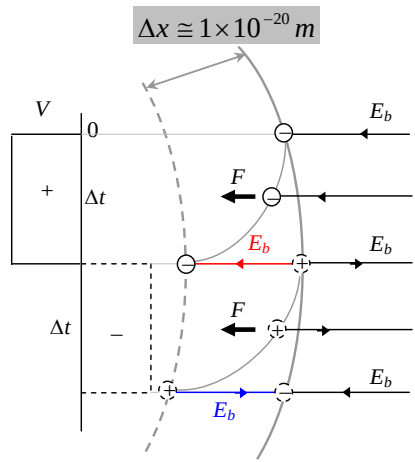

Fig.3 - Controlling the Electric Field in the Matter at *subatomic level* ($\Delta x \cong 10^{-20} m$).

Equation (7) shows that $\omega/\kappa_r = v$. Thus, $E/B = \omega/k_r = v$, i.e.,

* Inside of the matter.

$$E = vB = v\mu H$$

Then, Eq. (6) can be rewritten in the following form:

$$W = \tfrac{1}{2}\left(\varepsilon v^2 \mu\right)\mu H^2 + \tfrac{1}{2}\mu H^2 \qquad (9)$$

For $\sigma << \omega\varepsilon$, Eq. (7) reduces to

$$v = \frac{c}{\sqrt{\varepsilon_r \mu_r}}$$

Then, Eq. (9) gives

$$W = \tfrac{1}{2}\left[\varepsilon\left(\frac{c^2}{\varepsilon_r \mu_r}\right)\mu\right]\mu H^2 + \tfrac{1}{2}\mu H^2 = \mu H^2$$

This equation can be rewritten in the following forms:

$$W = \frac{B^2}{\mu} \qquad (10)$$

or

$$W = \varepsilon\ E^2 \qquad (11)$$

For $\sigma >> \omega\varepsilon$, Eq. (7) gives

$$v = \sqrt{\frac{2\omega}{\mu\sigma}} \qquad (12)$$

Then, from Eq. (9) we get

$$W = \tfrac{1}{2}\left[\varepsilon\left(\frac{2\omega}{\mu\sigma}\right)\mu\right]\mu H^2 + \tfrac{1}{2}\mu H^2 = \left(\frac{\omega\varepsilon}{\sigma}\right)\mu H^2 + \tfrac{1}{2}\mu H^2 \cong$$

$$\cong \tfrac{1}{2}\mu H^2 \qquad (13)$$

Since $E = vB = v\mu H$, we can rewrite (13) in the following forms:

$$W \cong \frac{B^2}{2\mu} \qquad (14)$$

or

$$W \cong \left(\frac{\sigma}{4\omega}\right)E^2 \qquad (15)$$

Substitution of Eq. (15) into Eq. (2), gives

$$m_g = \left\{1 - 2\left[\sqrt{1 + \frac{\mu}{4c^2}\left(\frac{\sigma}{4\pi f}\right)^3 \frac{E^4}{\rho^2}} - 1\right]\right\} m_{i0} =$$

$$= \left\{1 - 2\left[\sqrt{1 + \left(\frac{\mu_0}{256\pi^3 c^2}\right)\left(\frac{\mu_r \sigma^3}{\rho^2 f^3}\right)E^4} - 1\right]\right\} m_{i0} =$$

$$= \left\{1 - 2\left[\sqrt{1 + 1.758\times10^{-27}\left(\frac{\mu_r \sigma^3}{\rho^2 f^3}\right)E^4} - 1\right]\right\} m_{i0} \qquad (16)$$

Using this equation we can then calculate the gravitational mass, $m_{g(\Delta x)}$, of the region with thickness Δx, in the outer shell. We have already seen that the electric field in this region is $\vec{E}_b$, whose intensity is given by $E_b = q/4\pi\varepsilon(r_b + \Delta z)^2$. Thus, we can write that

$$E_b \cong \frac{q}{4\pi\varepsilon r_b^2} = \frac{CV}{4\pi\varepsilon r_b^2} \qquad (17)$$

where $C = 4\pi\varepsilon\left(r_a r_b / r_b - r_a\right)$ is the capacitance of the spherical capacitor; V is the potential applied on the inner shell (See Fig. 1 and 3). Thus, Eq. (17) can be rewritten as follows

$$E_b = \frac{r_a V}{r_b\left(r_b - r_a\right)} \cong 1.9\times10^2 V \qquad (18)$$

Substitution of $\rho = 2700 kg.m^{-3}$, $\sigma = 3.5\times10^7 S/m$, $\mu_r \cong 1$ (Aluminum) and $E = E_b \cong 1.9\times10^2 V$ into Eq. (16) yields

$$m_{g(\Delta x)} = \left\{1 - 2\left[\sqrt{1 + \frac{1.3\times10^{-2} V^4}{f^3}} - 1\right]\right\} m_{i0(\Delta x)} \qquad (19)$$

Equation (5) shows that there is a correlation between V and f to be obeyed, i.e., $f = 1.7V$. By substituting this expression into Eq. (19), we get

$$\chi = \frac{m_{g(\Delta x)}}{m_{i0(\Delta x)}} = \left\{1 - 2\left[\sqrt{1 + 2.64\times10^{-3} V} - 1\right]\right\} \qquad (20)$$

For $V = 35.29\ Volts\ \ (f = 1.7V = 60Hz)$[†], Eq. (20) gives

$$\chi = \frac{m_{g(\Delta x)}}{m_{I0(\Delta x)}} \cong 0.91 \qquad (21)$$

For $V = 450\ Volts\ \ (f = 1.7V = 765Hz)$, Eq. (20) gives

$$\chi = \frac{m_{g(\Delta x)}}{m_{I0(\Delta x)}} \cong 0.04 \qquad (22)$$

For $V = 1200\ Volts\ \ (f = 1.7V = 2040Hz)$, Eq. (20) gives

$$\chi = \frac{m_{g(\Delta x)}}{m_{I0(\Delta x)}} \cong -1.1 \qquad (23)$$

In this last case, the weight of the shell with thickness Δx will be $\vec{P}_{\Delta x} \cong -1.1 m_{i0(\Delta x)} \vec{g}$; the sign (-) shows that it becomes *repulsive* in respect to Earth's gravity. Besides this it is also *intensified* 1.1 times in respect to its initial value.

It was shown that, if the *weight* of a particle in a side of a lamina is $\vec{P} = m_g \vec{g}$ ($\vec{g}$ perpendicular to the lamina) then the weight of the same particle, in the other side of the lamina is $\vec{P}' = \chi m_g \vec{g}$, where $\chi = m_g^I / m_{i0}^I$ (m_g^I and m_{i0}^I are respectively, the gravitational mass and the inertial mass *of the lamina*) [1]. Only when $\chi = 1$, the weight is equal in both sides of the lamina. The lamina works as a *Gravity Controller*. Since $P' = \chi P = (\chi m_g) g = m_g (\chi g)$, we can consider that

$$m_g' = \chi m_g \text{ or that } g' = \chi g$$

Now consider the Spherical Capacitor previously mentioned. If the gravity below the capacitor is g, then *above the first* hemispherical shell with thickness Δx (See Fig.4) it will become χg, and above the second hemispherical shell with thickness Δx, the gravity will be $\chi^2 g$.

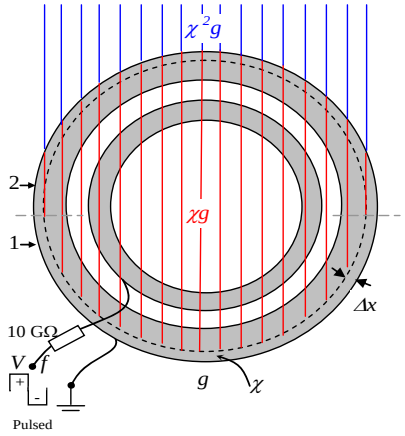

Fig.4 – The shell with thickness Δx works as a *Quantum Controller of Gravity*.

Since the voltage V is correlated to the frequency f by means of the expression $f = 1.7V$ (Eq. (5)), then it is necessary to put a *synchronizer* before the pulse generator (See Fig.5), in order to synchronize V with f. Thus, when we increase the voltage, the frequency is simultaneously increased at the same proportion, according to Eq. (5).

[†] Note that the frequency f must be greater than 1Hz (See text above Eq. (3)).

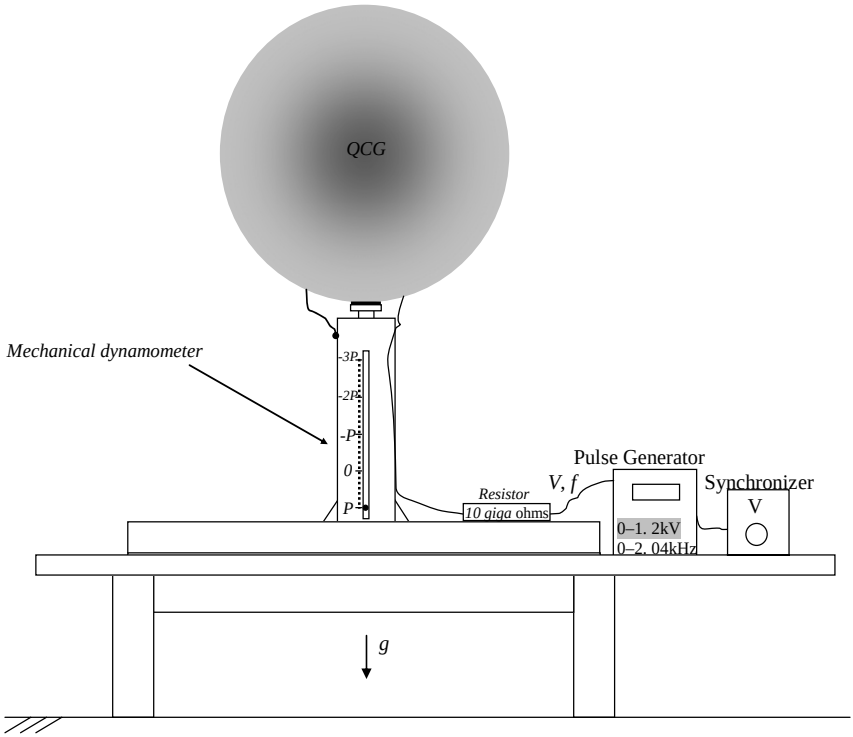

Fig.4 – Experimental Set-up using a Quantum Controller of Gravity (QCG).

References

[1] De Aquino, F. (2010) *Mathematical Foundations of the Relativistic Theory of Quantum Gravity*, Pacific Journal of Science and Technology, **11** (1), pp. 173-232.
Available at https://hal.archives-ouvertes.fr/hal-01128520

[2] Griffiths, D., (1999). *Introduction to Electrodynamics* (3 Ed.). Upper Saddle River, NJ: Prentice-Hall, p. 289.

[3] Dehmelt, H.: (1988). *A Single Atomic Particle Forever Floating at Rest in Free Space: New Value for Electron Radius*. Physica Scripta **T22**, 102.

[4] Dehmelt, H.: (1990). Science 4942 539-545.

[5] Macken, J. A. *Spacetime Based Foundation of Quantum Mechanics and General Relativity*. Available at http://onlyspacetime.com/QM-Foundation.pdf

[6] Halliday, D. and Resnick, R. (1968) *Physics*, J. Willey & Sons, Portuguese Version, Ed. USP, p.1118.

Quantum Gravitational Shielding

Fran De Aquino
Professor Emeritus of Physics, Maranhao State University, UEMA.
Titular Researcher (R) of National Institute for Space Research, INPE

We propose here a new type of Gravitational Shielding. This is a quantum device because results from the behaviour of the matter and energy on the subatomic length scale. From the technical point of view this Gravitational Shielding can be produced in laminas with positive electric charge, subjected to a magnetic field sufficiently intense. It is easy to build, and can be used to develop several devices for gravity control.

Key words: Gravitation, Gravitational Mass, Inertial Mass, Gravitational Shielding, Quantum Device.

1. Introduction

Some years ago [1] I wrote a paper where a correlation between gravitational mass and inertial mass was obtained. In the paper I pointed out that the relationship between gravitational mass, m_g, and *rest* inertial mass, m_{i0}, is given by

$$\chi = \frac{m_g}{m_{i0}} = \left\{1-2\left[\sqrt{1+\left(\frac{\Delta p}{m_{i0}c}\right)^2}-1\right]\right\} =$$

$$= \left\{1-2\left[\sqrt{1+\left(\frac{Un_r}{m_{i0}c^2}\right)^2}-1\right]\right\} =$$

$$= \left\{1-2\left[\sqrt{1+\left(\frac{Wn_r}{\rho c^2}\right)^2}-1\right]\right\} \qquad (1)$$

where Δp is the variation in the particle's *kinetic momentum*; U is *the electromagnetic energy absorbed or emitted by the particle;* n_r is the index of refraction of the particle; W is the density of energy on the particle (J/kg); ρ is the matter density (kg/m^3) and c is the speed of light.

Also it was shown that, if the *weight* of a particle in a side of a lamina is $\vec{P} = m_g\vec{g}$ ($\vec{g}$ perpendicular to the lamina) then the weight of the same particle, in the other side of the lamina is $\vec{P}' = \chi m_g\vec{g}$, where $\chi = m_g/m_{i0}$ (m_g and m_{i0} are respectively, the gravitational mass and the inertial mass of the lamina). Only when $\chi = 1$, the weight is equal in both sides of the lamina. The lamina works as a Gravitational Shielding. This is the *Gravitational Shielding effect.* Since $P' = \chi P = (\chi m_g)g = m_g(\chi g)$, we can consider that $m_g' = \chi m_g$ or that $g' = \chi g$.

In the last years I have proposed several types of Gravitational Shieldings. Here, I describe the Quantum Gravitational Shielding. This quantum device is easy to build and can be used in order to test the correlation between gravitational mass and inertial mass previously obtained.

2. Theory

Consider a conducting spherical shell with outer radius r. From the subatomic viewpoint the region with thickness of ϕ_e (diameter of an electron) in the border of the spherical shell (See Fig.1 (a)) contains an amount, N_e, of electrons. Since the number of atoms per m^3, n_a, in the spherical shell is given by

$$n_a = \frac{N_0\rho_S}{A_S} \qquad (2)$$

where $N_0 = 6.02214129\times10^{26}\, atoms/kmole$, is the Avogadro's number; ρ_S is the matter density of the spherical shell (in kg/m^3) and A_S is the molar mass ($kg.kmole^{-1}$). Then, at a volume ϕS of the spherical shell, there are N_a atoms per m^3, where

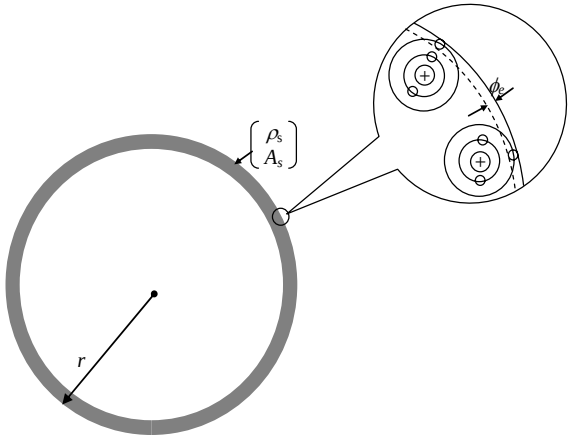

(a)

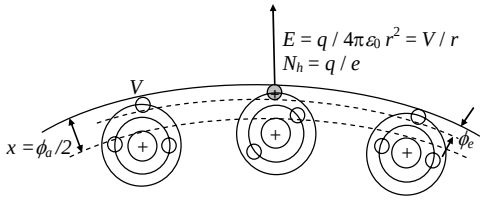

(b)

Fig.1 – Subatomic view of the border of the conducting spherical shell.

$$N_a = n_a \phi S \qquad (3)$$

Similarly, if there are n_e electrons per m^3 in the same volume ϕS, then we can write that

$$N_e = n_e \phi S \qquad (4)$$

By dividing both sides of Eq. (3) by N_e, given by Eq. (4), we get

$$n_e = n_a \left(\frac{N_e}{N_a} \right) \qquad (5)$$

Then, the amount of electrons, in the border of the spherical shell, at the region with thickness of ϕ_e is

$$N_e(\phi_e) = n_e \phi_e S = \frac{N_0 \rho_S}{A_S} \left(\frac{N_e}{N_a} \right) \phi_e S \qquad (6)$$

Assuming that in the border of the spherical shell, at the region with thickness of $x \cong \phi_a / 2$ (See Fig.1 (b)), *each atom* contributes with approximately $Z/2$ electrons (Z is the atomic number). Thus, the total number of electrons, *in this region*, is $N_e(x) = (Z/2) N_{\acute{e}}(\phi_e)$. Thus, we can write that

$$N_e(x) = \left(\frac{Z}{2} \right) N_e(\phi_e) = \left(\frac{Z}{2} \right) \frac{N_0 \rho_S}{A_S} \left(\frac{N_e}{N_a} \right)_x \phi_e S \qquad (7)$$

where $(N_e / N_a)_x \cong Z/2$.

Now, if a potential V is applied on the spherical shell an amount of electrons, N_h, is removed from the mentioned region. Since $N_h = q/e$ and $E = q/4\pi\varepsilon_r \varepsilon_0 r^2$, then we obtain

$$N_h = \frac{\left(4\pi r^2\right) \varepsilon_r \varepsilon_0 E}{e} = \frac{S \varepsilon_r \varepsilon_0 E}{e} \qquad (8)$$

Thus, we can express the matter density, ρ, in the border of the spherical shell, at the region with thickness of $x \cong \phi_a / 2$, by means of the following equation

$$\rho = \frac{\left(N_e(x) - N_h\right) m_{e0}}{Sx} = \frac{\left(N_e(x) - N_h\right) 2 m_{e0}}{S \phi_a} =$$

$$= \left[\left(\frac{Z}{2} \right)^2 \frac{N_0 \rho_S}{A_S} \left(\frac{\phi_e}{\phi_a} \right) - \frac{\varepsilon_r \varepsilon_0 E}{e \phi_a} \right] 2 m_{e0}$$

or

$$\rho = \left[\left(\frac{Z}{2} \right)^2 \frac{N_0 \rho_S}{A_S} \left(\frac{\phi_e}{\phi_a} \right) - \frac{\varepsilon_r \varepsilon_0 V}{r e \phi_a} \right] 2 m_{e0} \qquad (9)$$

since $E = V/r$.

If the spherical shell is made of *Lithium* ($Z = 3$, $\rho_S = 534 kg.m^{-3}$, $A_S = 6.941 kg/kmole$, $\phi_a = 3.04 \times 10^{-10} m$ and outer radius $r = 0.10 m$) and covered with a thin layer ($20 \mu m$) of Barium titanate* ($BaTiO_3$), whose relative permittivity at 20°C is $\varepsilon_r = 1250$, then Eq. (9) gives

$$\rho = \left(3.4310685 \times 10^{38} \phi_e - 2.2725033 \times 10^{21} V \right) 2 m_{e0} \qquad (10)$$

Assuming that the electron is a sphere with radius r_e and surface charge $-e$, and that *at an atomic orbit* its total energy $E \cong m_{e0} c^2$ is equal to the potential electrostatic energy of the surface charge, $E_{pot} = e^2 / 8\pi\varepsilon_0 r$ [2], then these conditions determine the radius $r \equiv r_e$: $r_e = e^2 / 2.4\pi\varepsilon_0 m_{e0} c^2 \cong 1.4 \times 10^{-15} m$ †, which is equal to the radii of the protons and neutrons. Thus, we can conclude that *in the atom*, electrons, protons and neutrons have the same radius. Thus, substitution of $\phi_e = 2r_e = 2.8 \times 10^{-15} m$ into Eq. (10) gives

$$\rho = \left(9.6069918 \times 10^{23} - 2.2725033 \times 10^{21} V \right) 2 m_{e0} \qquad (11)$$

For $V = 422.7493$ *volts*, Eq. (11) gives

$$\rho = \left(6.8 \times 10^{14} \right) 2 m_{e0} = 1.2 \times 10^{-15} kg.m^{-3} \qquad (12)$$

Note that the voltage $V = 422.7493$ *volts* is only a theoretical value resulting from inaccurate values of the constants present in the Eq. (11), and that leads to the *critical value* 6.8×10^{14} shown in Eq. (12), which is fundamental to obtain a low density, ρ. However, if for example, $V = 422.7$ *volts*, then the critical value increases to 1.1×10^{20} (more than 100,000 times the initial value) and, therefore the system shown in

---

* Dielectric Strength: $6 kV/mm$, density: 6,020kg/m^3.

† The radius of the electron depends on the circumstances (energy, interaction, etc) in which it is measured. This is because its structure is easily deformable. For example, the radius of a *free electron* is of the order of $10^{-13} m$ [3], when accelerated to 1GeV total energy it has a radius of $0.9 \times 10^{-16} m$ [4].

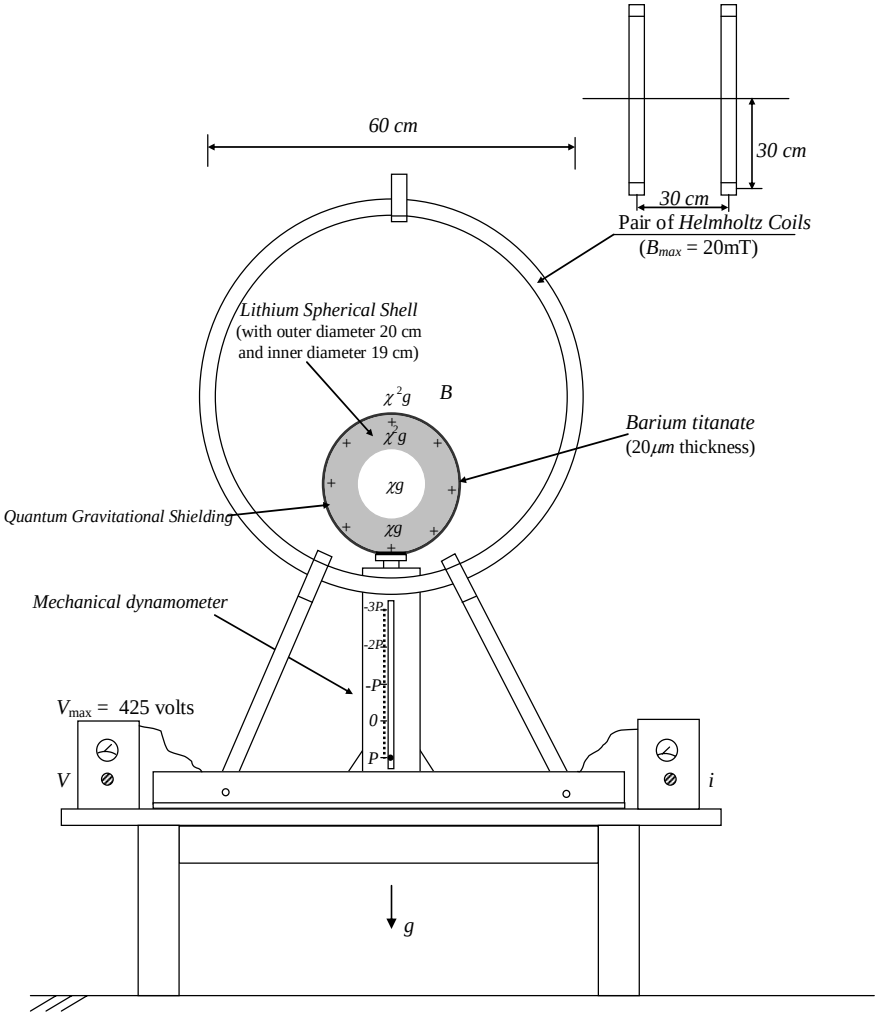

Fig.2 – *Quantum Gravitational Shielding* produced in the border of a *Lithium Spherical Shell* with positive electric charge, subjected to a magnetic field *B*.

Fig.2 will require a magnetic field 402 times more intense. In practice, the value of V, which should lead to the critical value 6.8×10^{14} or *a close value*, must be found by using a *very accurate voltage source* in order to apply accurate voltages around the value $V = 4227493$ *volts* at ambient temperature of 20°C.

Substitution of the value of ρ (*density in the border of the Lithium Spherical Shell, at the region with thickness of* $x \cong \phi_a/2$), given by Eq. (12), into Eq. (1) yields

$$\chi = \left\{1 - 2\left[\sqrt{1+\left(9.3\times10^{-3}W\right)^2} - 1\right]\right\} \qquad (13)$$

Substitution of

$$W = \tfrac{1}{2}\varepsilon_0 E^2 + \tfrac{1}{2}\mu_0 H^2 = \tfrac{1}{2}\varepsilon_0 c^2 E^2 + \tfrac{1}{2}\left(B^2/\mu_0\right) = B^2/\mu_0$$

into Eq. (13) gives

$$\chi = \left\{1 - 2\left[\sqrt{1+5.4\times10^{7}\,B^4} - 1\right]\right\} \qquad (14)$$

Therefore, if a magnetic field $B = 0.020T$ passes through the spherical shell (See Fig. (2)) it produces a Gravitational Shielding (*in the border of the Lithium Spherical Shell, at the region with thickness of* $x \cong \phi_a/2$) with a value of χ, given by

$$\chi \cong -3 \qquad (15)$$

Also, it is possible to build a *Flat Gravitational Shielding*, as shown in Fig. 3. Consider a cylindrical or hexagonal container, and a parallel plate capacitor, as shown in Fig. 3(a). When the capacitor is inserted into the container the *positive* charges of the plate of the capacitor are transferred *to the external surface of the container* (Gauss law), as shown in Fig. 3(b). Thus, in the border of the container, at the region with thickness of $x \cong \phi_a/2$ the density, ρ, will be given by Eq. (9), i.e.,

$$\rho = \left[\left(\frac{Z}{2}\right)^2 \frac{N_0\rho_S}{A_S}\left(\frac{\phi_e}{\phi_a}\right) - \frac{\varepsilon_r\varepsilon_0 E}{e\phi_a}\right]2m_{e0}$$

where

$$E = \sigma/\varepsilon_r\,\varepsilon_0 = q/\varepsilon_r\,\varepsilon_0 S = CV/\varepsilon_r\,\varepsilon_0 S =$$

$$= \varepsilon_{r(c)} AV/\varepsilon_r\, Sd \qquad (16)$$

Thus, we obtain

$$\rho = \left[\left(\frac{Z}{2}\right)^2 \frac{N_0\rho_S}{A_S}\left(\frac{\phi_e}{\phi_a}\right) - \frac{\varepsilon_{r(c)}\varepsilon_0 AV}{e\phi_a Sd}\right]2m_{e0} \qquad (17)$$

Therefore, if the container is made of *Lithium* ($Z = 3$, $\rho_S = 534kg.m^{-3}$, $A_S = 6.941kg/kmole$, $\phi_a = 3.04\times10^{-10}\,m$) and, if the dielectric of the capacitor is Barium titanate ($BaTiO_3$), whose relative permittivity at 20°C is $\varepsilon_r = 1250$, and the area of the capacitor is $A = S$, and $d = 1mm$, then Eq. (17) gives

$$\rho = \left(9.6069918\times10^{23} - 2.2725033\times10^{23}V\right)2m_{e0} \qquad (18)$$

For $V = 4.227493$ *volts*, Eq. (18) gives

$$\rho = \left(6.8\times10^{14}\right)2m_{e0} = 1.2\times10^{-15}kg.m^{-3} \qquad (19)$$

Substitution of this value into Eq. (1) gives

$$\chi = \left\{1 - 2\left[\sqrt{1+\left(9.3\times10^{-3}W\right)^2} - 1\right]\right\}$$

This is exactly the Eq. (13), which leads to

$$\chi = \left\{1 - 2\left[\sqrt{1+5.4\times10^{7}\,B^4} - 1\right]\right\}$$

Therefore, if a magnetic field $B = 0.020T$ passes through the Lithium container, it produces a Quantum Gravitational Shielding (*in the border of the container, at the region with thickness of* $x \cong \phi_a/2$) with a value of χ, given by

$$\chi \cong -3$$

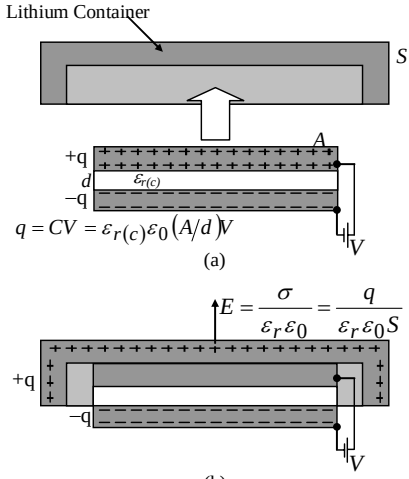

Fig. 3 – *Flat Gravitational Shielding* or *Flat Gravity Control Cell* (GCC).

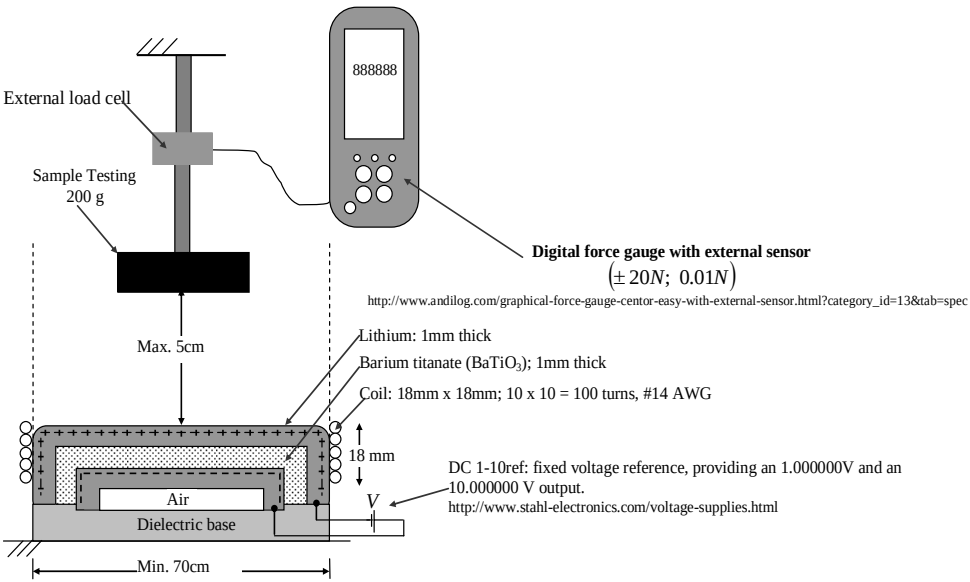

Fig. 4 – *Flat Gravity Control Cell* - Experimental Set-up. (BR Patent Number: PI0805046-5, July 31, 2008).

References

[1] De Aquino, F. (2010) *Mathematical Foundations of the Relativistic Theory of Quantum Gravity*, Pacific Journal of Science and Technology, **11** (1), pp. 173-232.

[2] Alonso, M., and Finn, E., (1967) *Foundations of University Physics*. Portuguese version (1977), Vol. II, Ed. Blucher, SP, p.149.

[3] Mac Gregor, M. H., (1992) *The Enigmatic Electron*, Boston, Klurer Academic; Bergman, D. L., (2004) *Foundations of Science*, (7) 12.

[4] Caesar, C., (2009) *Model for Understanding the Substructure of the Electron*, Nature Physics 13 (7).

New Gravitational Effects from Rotating Masses

Fran De Aquino

Two gravitational effects related to rotating masses are described. The first is the *decreasing of the gravitational mass* when the rotational kinetic energy is increased. In the case of ferromagnetic materials, the effect is strongly increased and the gravitational mass can even become negative. The second is the *gravitational shielding effect* produced by the decreasing of the gravitational mass of the rotating mass.

Key words: Modified theories of gravity, Gravitational Effects of Rotating Masses, Experimental studies of gravity, New topics in Superconductivity.
PACS: 04.50.Kd, 04.90.+e, 04.80.-y, 74.90.+n.

.

1. Introduction

In 1918, H. Thirring [1] showed that a rotating mass shell has a weak dragging effect on the inertial frames within it. In today's literature these results are known as *Lense-Thirring effects*.

Recently, the Lense-Thirring effect has received new interest because it becomes now possible to directly measure this tiny effect [2]. In the years 1959-1960 it was discovered by G. E. Pugh [3] and Leonard Schiff [4,5] that the mentioned dragging phenomenon leads to another effect - called the *Schiff effect* - which might be suited for experimental confirmation: The rotation axis of a gyroscope, inside a satellite orbiting the Earth, in a height of 650 km, suffers a precession of 42 milliarcseconds per year, due to the Earth's rotation [6].

Here, we show new gravitational effects related to rotating gravitational masses, including superconducting masses.

2. Theory

From the quantization of gravity it follows that the *gravitational mass* m_g and the *inertial mass* m_i are correlated by means of the following factor [7]:

$$\chi = \frac{m_g}{m_{i0}} = \left\{1 - 2\left[\sqrt{1+\left(\frac{\Delta p}{m_{i0}c}\right)^2} - 1\right]\right\} \qquad (1)$$

where m_{i0} is the *rest* inertial mass of the particle and Δp is the variation in the particle's *kinetic momentum*; c is the speed of light.

That equation shows that only for $\Delta p = 0$ the gravitational mass is equal to the inertial mass.

In general, the *momentum* variation Δp is expressed by $\Delta p = F\Delta t$ where F is the applied force during a time interval Δt. Note that there is no restriction concerning the *nature* of the force F, i.e., it can be mechanical, electromagnetic, etc.

For example, we can look on the *momentum* variation Δp as due to absorption or emission of *electromagnetic energy* by the particle.

In this case Δp can be obtained as follows: It is known that the *radiation pressure*, dP, upon an area $dA = dxdy$ of a volume $dV = dxdydz$ of a particle (the incident radiation normal to the surface dA) is equal to the energy dU absorbed (or emitted) per unit volume (dU/dV).i.e.,

$$dP = \frac{dU}{dV} = \frac{dU}{dxdydz} = \frac{dU}{dAdz} \qquad (2)$$

Substitution of $dz = vdt$ (v is the speed of radiation) into the equation above gives

$$dP = \frac{dU}{dV} = \frac{(dU/dAdt)}{v} = \frac{dD}{v} \qquad (3)$$

Since $dPdA = dF$ we can write:

$$dFdt = \frac{dU}{v} \qquad (4)$$

However we know that $dF = dp/dt$, then

$$dp = \frac{dU}{v} \qquad (5)$$

From this equation it follows that

$$\Delta p = \frac{U}{v}\left(\frac{c}{c}\right) = \frac{U}{c} n_r \qquad (6)$$

where n_r is the index of refraction.

Substitution of Eq.(6) into Eq. (1) yields

$$m_g = \left\{1 - 2\left[\sqrt{1+\left(\frac{U}{m_{i0}c^2} n_r\right)^2} - 1\right]\right\} m_{i0} \qquad (7)$$

In the case of absorption of a single photon with wavelength λ and frequency f, Eq. (7) becomes

$$\frac{m_g}{m_{i0}} = \left\{1 - 2\left[\sqrt{1+\left(\frac{hf}{m_{i0}c^2} n_r\right)^2} - 1\right]\right\} =$$

$$= \left\{1 - 2\left[\sqrt{1+\left(\frac{\lambda_0}{\lambda} n_r\right)^2} - 1\right]\right\} \qquad (8)$$

where $\lambda_0 = h/m_{i0}c$ is the *De Broglie wavelength* for the particle with *rest* inertial mass m_{i0}.

From Electrodynamics we know that when an electromagnetic wave with frequency f and velocity c incides on a material with relative permittivity ε_r, relative magnetic permeability μ_r and electrical conductivity σ, its *velocity is reduced* to $v = c/n_r$ where n_r is the index of refraction of the material, given by [8]

$$n_r = \frac{c}{v} = \sqrt{\frac{\varepsilon_r \mu_r}{2}\left(\sqrt{1+(\sigma/\omega\varepsilon)^2} + 1\right)} \qquad (9)$$

If $\sigma >> \omega\varepsilon$, $\omega = 2\pi f$, Eq. (9) reduces to

$$n_r = \sqrt{\frac{\mu_r \sigma}{4\pi\varepsilon_0 f}} \qquad (10)$$

Thus, the wavelength of the incident radiation (See Fig. 1) becomes

$$\lambda_{\text{mod}} = \frac{v}{f} = \frac{c/f}{n_r} = \frac{\lambda}{n_r} = \sqrt{\frac{4\pi}{\mu f \sigma}} \qquad (11)$$

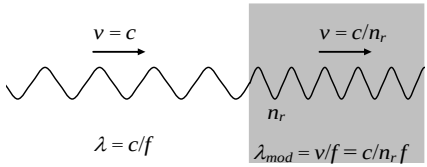

Fig. 1 – *Modified Electromagnetic Wave*. The wavelength of the electromagnetic wave can be strongly reduced, but its frequency remains the same.

If a lamina with thickness equal to ξ contains n atoms/m^3, then the number of atoms per area unit is $n\xi$. Thus, if the electromagnetic radiation with frequency f incides on an area S of the lamina it reaches $nS\xi$ atoms. If it incides on the *total area of the lamina*, S_f, then the total number of atoms reached by the radiation is $N = nS_f\xi$. The number of atoms per unit of volume, n, is given by

$$n = \frac{N_0 \rho}{A} \qquad (12)$$

where $N_0 = 6.02 \times 10^{26}\, atoms/kmole$ is the Avogadro's number; ρ is the matter density of the lamina (in *kg/m*^{3}) and A is the molar mass(*kg/kmole*).

When an electromagnetic wave incides on the lamina, it strikes N_f front atoms, where $N_f \cong (nS_f)\phi_m$, ϕ_m is the "diameter" of the atom. Thus, the electromagnetic wave incides effectively on an area $S = N_f S_m$, where $S_m = \frac{1}{4}\pi\phi_m^2$ is the cross section area of one atom. After these collisions, it carries out $n_{collisions}$ with the other atoms (See Fig.2).

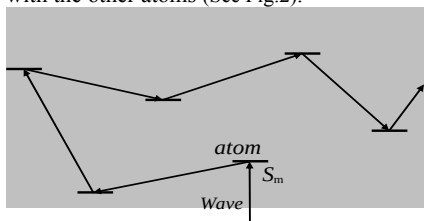

Fig. 2 – *Collisions inside the* lamina.

Thus, the *total number of collisions* in the volume $S\xi$ is

$$N_{collisions}=N_f+n_{collisions}=n_l S\phi_m+(n_l S\xi-n_m S\phi_m)= =n_l S\xi \quad (13)$$

The power density, D, of the radiation on the lamina can be expressed by

$$D=\frac{P}{S}=\frac{P}{N_f S_m} \quad (14)$$

We can express the *total mean number of collisions in each atom*, n_1, by means of the following equation

$$n_1=\frac{n_{total\ \ photons}\,N_{collisions}}{N} \quad (15)$$

Since in each collision a *momentum* h/λ is transferred to the atom, then the *total momentum* transferred to the lamina will be $\Delta p=(n_1 N)h/\lambda$. Therefore, in accordance with Eq. (8), we can write that

$$\frac{m_{g(l)}}{m_{i0(l)}}=\left\{1-2\left[\sqrt{1+\left[(n_1 N)\frac{\lambda_0}{\lambda}n_r\right]^2}-1\right]\right\}= =\left\{1-2\left[\sqrt{1+\left[n_{total\ photons}N_{collisions}\frac{\lambda_0}{\lambda}n_r\right]^2}-1\right]\right\} \quad (16)$$

Since Eq. (13) gives $N_{collisions}=n_l S\xi$, we get

$$n_{total\ \ photons}\,N_{collisions}=\left(\frac{P}{hf^2}\right)(n_l S\xi) \quad (17)$$

Substitution of Eq. (17) into Eq. (16) yields

$$\frac{m_{g(l)}}{m_{i0(l)}}=\left\{1-2\left[\sqrt{1+\left[\left(\frac{P}{hf^2}\right)(n_l S\xi)\frac{\lambda_0}{\lambda}n_r\right]^2}-1\right]\right\} \quad (18)$$

Substitution of P given by Eq. (14) into Eq. (18) gives

$$\frac{m_{g(l)}}{m_{i0(l)}}=\left\{1-2\left[\sqrt{1+\left[\left(\frac{N_f S_m D}{f^2}\right)\left(\frac{n_l S\xi}{m_{i0(l)}c}\right)\frac{n_r}{\lambda}\right]^2}-1\right]\right\} \quad (19)$$

Substitution of $N_f\cong(n_l S_f)\phi_m$ and $S=N_f S_m$ into Eq. (19) results

$$\frac{m_{g(l)}}{m_{i0(l)}}=\left\{1-2\left[\sqrt{1+\left[\left(\frac{n_l^3 S_f^2 S_m^2\phi_m^2\xi D}{m_{i0(l)}cf^2}\right)\frac{n_r}{\lambda}\right]^2}-1\right]\right\} \quad (20)$$

where $m_{i0(l)}=\rho_{(l)}V_{(l)}$.

In the case in which the area S_f is just the *area of the cross-section of the lamina* (S_α), we obtain from Eq. (20), considering that $m_{i0(l)}=\rho_{(l)}S_\alpha\xi$, the following expression

$$\frac{m_{g(l)}}{m_{i0(l)}}=\left\{1-2\left[\sqrt{1+\left[\left(\frac{n_l^3 S_\alpha S_m^2\phi_m^2 D}{\rho_l cf^2}\right)\frac{n_r}{\lambda}\right]^2}-1\right]\right\} \quad (21)$$

If the electrical conductivity of the lamina, $\sigma_{(l)}$, is such that $\sigma_{(l)}>>\omega\varepsilon$, then Eq. (9) reduces to

$$n_r=\sqrt{\frac{\mu_r\sigma}{4\pi\varepsilon_0 f}} \quad (22)$$

Substitution of Eq. (22) into Eq. (21) gives

$$\frac{m_{g(l)}}{m_{i0(l)}}=\left\{1-2\left[\sqrt{1+\frac{n_l^6 S_\alpha^2 S_m^4\phi_m^4\mu\sigma D^2}{4\pi\rho_l^2 c^2 f^3}}-1\right]\right\} \quad (23)$$

This is therefore the expression of correlation between gravitational mass and inertial mass in the particular case of *incident radiation on ordinary matter* (non-coherent matter) *at rest*.

If the body is *also* rotating, with an angular speed ω around its central axis, then it acquires an additional energy equal to its rotational energy $\left(E_k=\tfrac{1}{2}I\omega^2\right)$. Since this is an increase in the internal energy of the body, and this energy is basically electromagnetic, we can assume that E_k, such as U, corresponds to an amount of electromagnetic energy absorbed by the body. Thus, we can consider E_k as an increase $\Delta U=E_k$ in the electromagnetic energy U absorbed by the body. Consequently, in this case, we must replace U in Eq. (7) for $(U+\Delta U)$, i.e.,

$$m_g=\left\{1-2\left[\sqrt{1+\left(\frac{U+\Delta U}{m_{i0}c^2}n_r\right)^2}-1\right]\right\}m_{i0} \quad (24)$$

Note that the variable U can refer to both the electromagnetic energy of a radiation as *the electromagnetic energy of the electromagnetic field due to an electric current through the rotating gravitational mass*.

Thus, Eq. (24) can be rewritten as

$$m_g = \left\{1-2\left[\sqrt{1+\left(\frac{(U_m+E_k)\sin 2\pi ft}{m_{i0}c^2}n_r\right)^2}-1\right]\right\}m_{i0} \qquad (25)$$

Note that E_k is not an amplitude of a wave such as U_m, $(U = U_m \sin 2\pi ft)$. Therefore, E_k and $\sin 2\pi ft$ are independent parameters. Consequently, there is no sense to talk about average value for $E_k \sin 2\pi ft$, such as in the case of $U_m \sin 2\pi ft$, where the average value for U^2 is equal to $\frac{1}{2}U_m^2$ because U varies sinusoidaly (U_m is the maximum value for U).

Then, if $U_m << E_k$, the Eq. (25) reduces to

$$m_g \cong \left\{1-2\left[\sqrt{1+\left(\frac{I\omega^2 n_r \sin 2\pi ft}{2m_{i0}c^2}\right)^2}-1\right]\right\}m_{i0} \qquad (26)$$

For $\sigma >> \omega\varepsilon$, Eq.(9) shows that and $n_r = \sqrt{\mu\sigma c^2/4\pi f}$. In this case, Eq. (26) gives

$$m_g \cong \left\{1-2\left[\sqrt{1+\frac{\mu\sigma\omega^4 I^2 \sin^2 2\pi ft}{16\pi f m_{i0}^2 c^2}}-1\right]\right\}m_{i0} \qquad (27)$$

Note that the effect of the electromagnetic field applied upon the mass is highly relevant, because in the absence of this radiation the index of refraction, present in Eq. (26), becomes equal to 1. Under these circumstances, the possibility of reducing the gravitational mass is null. On the other hand, the equation above shows that, in practice, the decreasing of the gravitational mass can become relevant in the particular case of *ferromagnetic materials* subjected to electromagnetic fields with *extremely low frequencies* (ELF).

Figure 3 shows a schematic diagram of a *Mumetal disk* ($\mu_r = 105{,}000\ at\ 100\ gauss$; $\sigma = 2.1\times10^6\ S.m^{-1}$) with radius $R = 0.10m$ $\left(I = \frac{1}{2}m_{i0}R^2\right)$ rotating with an angular velocity $\omega = 2.09\times10^4\ rad/s\ (\sim 200{,}000\ rpm)$. Thus, if an ELF radiation or an electrical current with extremely low frequency e.g., $f = 0.1Hz$ is applied on the Mumetal disk, then according to Eq.(27), the gravitational mass of the disk will oscillate between $m_g = m_{i0}$ and

$$m_g \cong -0.96m_{i0} \qquad (28)$$

It has been shown that there is an additional effect - *Gravitational Shielding* effect - produced by a substance whose gravitational mass was reduced or made negative [9]. The effect extends beyond substance (gravitational shielding), up to a certain distance from it (along the central axis of gravitational shielding). This effect shows that in this region the gravity acceleration, g_1, is reduced at the same proportion, i.e., $g_1 = \chi_1 g$ where $\chi_1 = m_g/m_{i0}$ and g is the gravity acceleration *before* the gravitational shielding. Here, according to Eq.(28), we have $-0.96 \le \chi_1 \le 1$. Thus, the gravity acceleration *above* the Mumetal disk will vary in the range $-0.96g \le g_1 \le g$ since the gravity before (below) the gravitational shielding is g.

Let us now consider the case in which the rotating mass is a *superconducting material*.

The most famous characteristic of superconductivity is zero resistance. However, the superconductors are not the same as a perfect conductor. The observed *surface resistance*, R_s, of most superconductors to *alternating currents* shows that the resistivity can be extremely small *at the internal region close to the surface of the superconductor*. The thickness of this region is known as *London penetration depth*, λ_L [10]. According to BCS theory $R_s = (1/\lambda_L)\left(\sigma/\sigma^2 + \sigma_s^2\right)$ where σ is the normal-state conductivity and σ_s is the conductivity of the mentioned region, which is given by [11]:

$$\sigma_s = \frac{1}{2\pi\mu\ \lambda_L^2 f} \qquad (29)$$

It is important to note that Eq. (16) refers to the case of *ordinary matter* (*non-coherent matter*). In the case of superconductors the radiation is absorbed by the *Cooper-pairs fluid* (coherent part of the superconductors) and there is no scattering of the incident radiation. Consequently, $N_{collisions} = 1$ (the *total number of collisions*). Therefore, in the case of superconductors Eq. (16) reduces to

$$\begin{aligned}\frac{m_{g(l)}}{m_{i0(l)}} &= \left\{1-2\left[\sqrt{1+\left[n_{total\ photons}\frac{\lambda_0}{\lambda}n_r\right]^2}-1\right]\right\} \\ &= \left\{1-2\left[\sqrt{1+\left[n_{total\ photons}\frac{hf}{m_{i0}c^2}n_r\right]^2}-1\right]\right\} \\ &= \left\{1-2\left[\sqrt{1+\left[\frac{U}{m_{i0}c^2}n_r\right]^2}-1\right]\right\}\end{aligned} \qquad (30)$$

which is exactly the equation (7). Thus, we conclude that *Eq.* (7) *is general for all types of matter (coherent and non-coherent).*

Since $U = U_m \sin 2\pi ft$, the average value for U^2 is equal to $\frac{1}{2}U_m^2$ because U varies sinusoidaly (U_m is the maximum value for U). On the other hand, $U_{rms} = U_m / \sqrt{2}$. Consequently we can change U^2 by U_{rms}^2 in the Eq. (7).

Alternatively, we may put this equation as a function of the radiation power density, D_{rms}, since $U_{rms} = VD_{rms}/v$ (See Eq. (3)). Thus, we obtain

$$\frac{m_{g(l)}}{m_{i0(l)}} = \left\{1 - 2\left[\sqrt{1 + \left(\frac{D_{rms} n_r^2}{\rho c^3}\right)^2} - 1\right]\right\} \qquad (31)$$

where $\rho = m_{i0}/V$.

. For $\sigma >> \omega\varepsilon$, Eq.(9) shows that and $n_r = \sqrt{\mu\sigma c^2 / 4\pi f}$. In this case, equation above becomes

$$\frac{m_{g(l)}}{m_{i0(l)}} = \left\{1 - 2\left[\sqrt{1 + \left(\frac{\mu\sigma D_{rms}}{4\pi\rho c f}\right)^2} - 1\right]\right\} \qquad (32)$$

Now consider a superconducting disk (YBCO) on the Earth's atmosphere. It is known that the *Schumann resonances* [12] are global electromagnetic resonances (a set of spectrum peaks in the extremely low frequency ELF), excited by lightning discharges in the *spherical resonant cavity* formed by the Earth's surface and the inner edge of the ionosphere (60km from the Earth's surface). The Earth–ionosphere waveguide behaves like a resonator at ELF frequencies and amplifies the spectral signals from lightning at the resonance frequencies. In the normal mode descriptions of Schumann resonances, the fundamental mode $(n = 1)$ is a standing wave in the Earth–ionosphere cavity with a wavelength equal to the circumference of the Earth. This lowest-frequency (and highest-intensity) mode of the Schumann resonance occurs at a frequency $f_1 = 7.83Hz$ [13].

It was experimentally observed that ELF radiation escapes from the *Earth–ionosphere waveguide* and reaches the Van Allen belts [14-17]. In the ionospheric spherical cavity, the ELF radiation power density, D, is related to the energy density inside the cavity, W, by means of the well-known expression:

$$D = \frac{c}{4} W \qquad (33)$$

where c is the speed of light, and $W = \frac{1}{2}\varepsilon_0 E^2$. The electric field E, is given by

$$E = \frac{q}{4\pi\varepsilon_0 r_\oplus^2} \qquad (34)$$

where $q = 500{,}000C$ [16] and $r_\oplus = 6.371 \times 10^6 m$. Therefore, we get

$$\begin{aligned} E &= 1107 V/m, \\ W &= 5.4 \times 10^{-8} J/m^3, \\ D_{rms} &\cong 4.1\ W/m^2 \end{aligned} \qquad (35)$$

In the case of YBCO $\lambda_L \cong 140nm$ [18,19]. Then, substitution of this value into Eq.(29) gives

$$\mu\sigma_s = \frac{1}{2\pi\lambda_L^2 f} = \frac{8.12 \times 10^{12}}{f} \qquad (36)$$

The variable σ in Eq. (32) is σ_s, and the density of the YBCO is $\rho = 6300 kg.m^{-3}$ [20,21]. Thus, we can rewrite Eq. (32) as follows

$$\frac{m_{g(l)}}{m_{i0(l)}} = \left\{1 - 2\left[\sqrt{1 + \left(\frac{0.34 D_{rms}}{f^2}\right)^2} - 1\right]\right\} \qquad (37)$$

Since the superconducting disk is inside the Earth's atmosphere then it is subjected to *Schumann resonances*. Thus, the values of f and D_{rms} are given respectively by $f = f_1 = 7.83Hz$ and $D_m = 4.1\ W/m^2$ (Eq. (35)). Therefore the value of χ given by Eq. (37) is

$$\chi = \frac{m_{g(l)}}{m_{i0(l)}} = 0.9995 \qquad (38)$$

Since the weight of the disk is $\chi\, m_{i0} g$ then $m_{i0} g - \chi\, m_{i0} g = 5 \times 10^{-4} m_{i0} g$ is the decrease in the weight of the disk. Therefore the disk 0.05% of its weight (without any rotation). Due to the *Gravitational Shielding effect*, these variations are the same for a sample above the disk .

When the disk acquires an angular velocity ω, then the additional value χ_a, due to the rotation, can be obtained making $U_m = 0$ in Eq.(25), i.e.,

$$\chi_a \cong \left\{1 - 2\left[\sqrt{1 + \frac{\mu\sigma\omega^4 I^2 \sin^2 2\pi f}{16\pi f m_{i0}^2 c^2}} - 1\right]\right\} \quad (39)$$

In the Podkletnov experiment, the YBCO disk is a rectangular toroid with radius $R_{outer} = 275mm$, R_{inner}=80mm, 10 mm-thickness, with an angular velocity $\omega = 523.6 rad/s$ (5,000 rpm) [22,23]. Considering these values and the value of $\mu\sigma_s$ given by Eq. (36), then Eq. (39) shows that χ_a, in this case, is given by

$$\chi_a \cong -1$$

Note that this value corresponds to the region of the disk with thickness λ_L. Thus, we can write that

$$m_{g(disk)} = \chi m_{i0(disk)} + \chi_a m_{i0(\lambda_L)} =$$

$$= \chi m_{i0(disk)} + \chi_a \left(\frac{m_{i0(\lambda_L)}}{m_{i0(disk)}}\right) m_{i0(disk)} \quad (40)$$

where

$m_{i0(\lambda_L)} = \rho_{YBCO} V_{(\lambda_L)}$ and $m_{i0(disk)} = \rho_{YBCO} V_{(disk)}$

Thus, we get

$$\frac{m_{i0(\lambda_L)}}{m_{i0(disk)}} = \frac{V_{(\lambda_L)}}{V_{(disk)}} = \frac{2\lambda_L}{10mm} \cong 200\lambda_L \quad (41)$$

Substitution of Eq. (41) into Eq. (40) gives

$$m_{g(disk)} = \chi m_{i0(disk)} + 200\lambda_L \chi_a m_{i0(disk)} =$$

$$= \chi m_{i0(disk)} - 2.9\times10^{-5} m_{i0(disk)} \quad (42)$$

In this case the disk loses *more* 2.9×10^{-3}% of its weight due to its rotation. This corresponds to a *decrease* of about 5.8% on the initial value of 0.05% that the disk loses *without any rotation*. Due to the Gravitational Shielding effect, a sample above the disk will have its weight decreased of the same percentage (5.8% on the initial value of 0.05% that the sample loses).

Thus, when $\sin\omega t = 0$ Eq. (39) shows that $\chi_a = 1$, i.e., the *decreases of gravitational mass vanish*, this corresponds to an *increase* in the weight of the sample of about 5.8% on the initial value of 0.05% that the sample lost *more* a portion due to the *increase* of the weight of the *air column* above the sample. Due to the gravitational shielding effect, the gravity acting on the air column above the sample (height~12R_{outer} [24]) is reduced in the same proportion that is reduced the gravitational mass of the disk (gravitational shielding). Thus, there is also an *increase* in the weight of the sample of 5.8% *on the weight of the air column above the sample*. Considering that 5.8% on the weight of the air column is equivalent to x% on the initial value of 0.05% that the sample lost, i.e.,

$$5.8\% m_{g(air)} g' = x\% of\ 0.05\% m_{g(sample)} g'$$

Then, we get

$$x\% = \frac{5.8\%}{0.05\%}\left(\frac{m_{g(air)}}{m_{g(sample)}}\right) =$$

$$= \frac{5.8\%}{0.05\%}\left(\frac{\rho_{(air)} V_{air}}{\rho_{(sample)} V_{sample}}\right) \cong 2\%$$

Since $\rho_{air} = 1.2 kg.m^{-3}$, $\rho_{sample} = 1400 kg.m^{-3}$ and $V_{air}/V_{sample} = \sim 12R_{outer}/150mm \cong 80R_{outer} \cong 22$.

Under these circumstances, the balance measures an *increase* correspondent to 5.8% on the initial value of 0.05% *more* 2%on the initial value of 0.05%, i.e., a total *increase* of about 7.8% on the initial value of 0.05%.

Consequently, the weight of the sample becomes unstable with fluctuations from −5.8% to +7.8% of the initial value of 0.05%. This means that the total variation of the weight of the sample oscillates in the range

0.047% *to* 0.053%

of its weight.

In the Podkletnov's experiment the findings were −2.5% to +5.5% of the initial value of 0.05% [22,23]. This means that the total variation of the weight of the sample oscillates in the range

0.048% *to* 0.052%

of its weight.

Note that, according to Eq. (39) and Eq. (42), for $\omega = 2.09\times10^4 rad/s$ (200,000 rpm) the sample weight decrease can reach about 17%. This very smaller than the 96% in the case of the Mumetal disk (Eq. (28)).

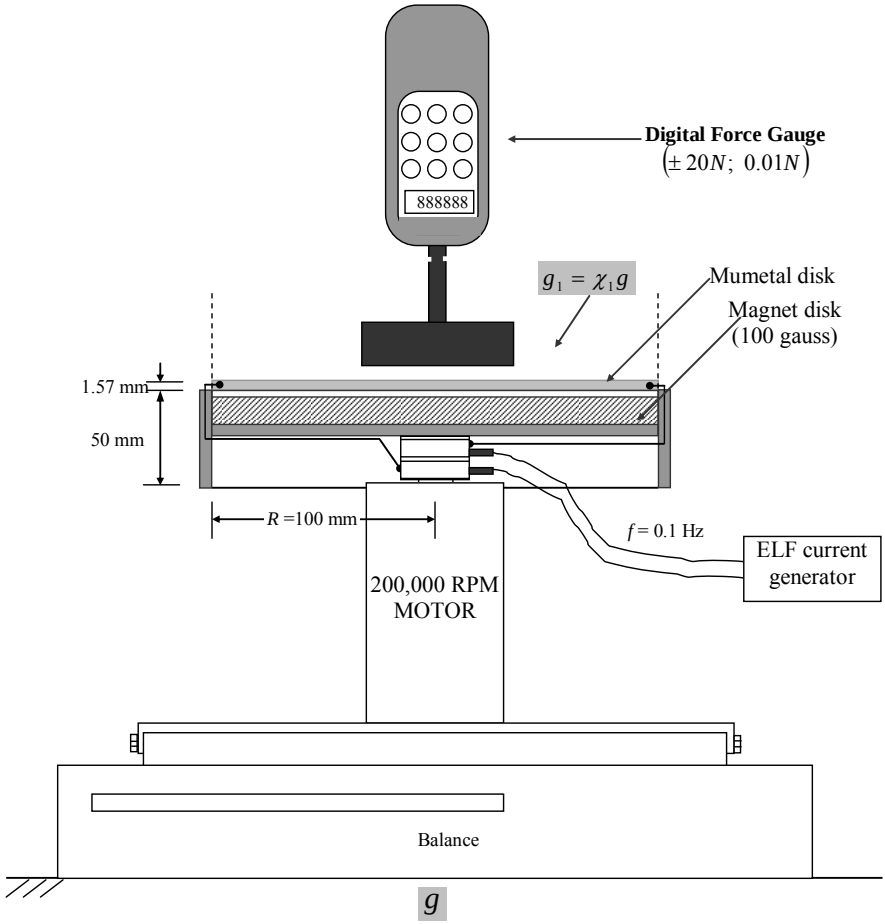

Fig.3 – Schematic diagram of an experimental set-up to measure the decrease of the gravitational mass of the Mumetal disk and the gravitational shielding effect produced by the rotating disk.

References

[1] Thirring, H (1918) Uber *die Wirkung rotierender ferner Massen in der Einsteinschen Gravitationstheorie*. Phys. ZS. **19**, 33.

[2] Ciufolini, I., and Pavlis,E.C. (2004). *A confirmation of the general relativistic prediction of the Lense-Thirring effect*. Nature, 431, 958-960.

[3] Pugh, G.E. (1959). *Proposal for a satellite test of the Coriolis prediction of general relativity*. WSEG Research Memorandum No.11. Washington, DC: The Pentagon.

[4] Schiff, L.I. (1960). *Possible new experimental test of general relativity theory*. Physical Review Letters, 4, 215-217.

[5] Schiff,L.I. (1960). *Motion of a gyroscope according to Einstein's theory of gravitation.* Proceedings of the National Academy of Sciences of the USA, 46, 871-882.

[6] Ciufolini,I, and Wheeler, J. A. (1995). *Gravitation and Inertia*. Princeton: Princeton University Press.

[7] De Aquino, F. (2010) *Mathematical Foundations of the Relativistic Theory of Quantum Gravity*, Pacific Journal of Science and Technology, **11** (1), pp. 173-232.

[8] Quevedo, C. P. (1977) *Eletromagnetismo*, McGraw-Hill, p. 270.

[9] De Aquino, F. (2010) *Gravity Control by means of Electromagnetic Field through Gas at Ultra-Low Pressure*, Pacific Journal of Science and Technology, **11**(2) November 2010, pp.178-247, Physics/0701091.

[10] F. London and H. London (1935) Proc. Roy. Soc. (London) **A149** 71.

[11] Bardeen, J.; Cooper, L. N., Schrieffer, J. R.(1957)*Microscopic Theory of Superconductivity*, Physical Review **106** (1): 162–164.

[12] Schumann W. O. (1952). "Über die strahlungslosen Eigenschwingungen einer leitenden Kugel, die von einer Luftschicht und einer Ionosphärenhülle umgeben ist". *Zeitschrift und Naturfirschung* **7a**: 149–154

[13] Volland, H. (1995), *Handbook of Atmospheric Electrodynamics*, CRC Press, vol.I, Chapter11.

[14] Carpenter, D. L., and T. R. Miller (1976), *Ducted magnetospheric propagation of signals from the Siple, Antarctica, VLF transmitter*, J. Geophys. Res., 81(16), 2692– 2700.

[15] Helliwell, R. A., D. L. Carpenter, and T. R. Miller (1980), *Power threshold for growth of coherent VLF signals in the magnetosphere*, J. Geophys. Res., 85(A7), 3360– 3366.

[16] Cohen, M. B., (2009), *ELF/VLF Phased array generation via frequency-matched steering of a continuous HF ionospheric heating beam*, PHD thesis, p.13.

[17] Golkowski, M. et al., (2008), *Magnetospheric amplification and emission triggering by ELF/VLF waves injected by the 3.6 MW HAARP ionospheric heater*, J. Geophys. Res., 113 (A10201), doi:10.1029/2008JA013, 157.

[18] Jiang, H., et al., (1993) Measurements of anisotropic characteristic lengths in YBCO films at microwave frequencies, Journal of Applied Physics, 73(10)5865.

[19] Kieft, R.F., et al., (2010) Direct measurement of the London penetration depth in YBCO using low energy muSR, Physical Review B, 81(18):180502.

[20] Knizhnik, A (2003) "Interrelation of preparation conditions, morphology, chemical reactivity and homogeneity of ceramic YBCO". *Physica C: Superconductivity* **400**: 25.

[21] Grekhov, I (1999)"Growth mode study of ultrathin HTSC YBCO films on YBaCuNbO buffer". *Physica C: Superconductivity* **324**: 39.

[22] Rabounski, D. and Borissova, L. (2007) *A Theory of the Podkletnov Effect Based on General Relativity*, Progress in Physics, **3**, p.57.

[23] Podkletnov, E., and Nieminen, R., (1992) *Physica C* 203, 441. Podkletnov, E., (1997) *cond-mat/* 9701074.

[24] Modanese, G., (1996) *On the Theoretical interpretation of E. Podkletnov's experiment*, gr-qc/9612022.

The Bipolar Linear *Momentum* transported by the Electromagnetic Waves: Origin of the Gravitational Interaction

Fran De Aquino

Besides energy, the electromagnetic waves transport linear *momentum*. Then, if this momentum is absorbed by a surface, pressure is exerted on the surface. This is the so-called Radiation Pressure. Here we show that this pressure has a *negative* component (opposite to the direction of propagation of the radiation) due to the existence of the negative linear *momentum* transported by the electromagnetic waves. This fact leads to an important theoretical discovery: the velocity of the electromagnetic waves in free space is not a constant. In addition, *a generalized equation* of the Newton's law of Gravitation, is deduced starting from the concept of *negative* radiation pressure applied on the Gravitational Interaction.

Key words: Gravity, Gravitation, Electromagnetic Waves, Radiation Pressure.

1. Introduction

Electromagnetic waves transport energy as well as linear *momentum*. Then, if this *momentum* is absorbed by a surface, pressure is exerted on the surface. Maxwell showed that, if the incident energy U is totally absorbed by the surface during a time t, then the total *momentum* q transferred to the surface is $q = U/v$ [1]. Then, the pressure, p (defined as force F per unit area A), exerted on the surface, is given by

$$p = \frac{F}{A} = \frac{1}{A}\frac{dq}{dt} = \frac{1}{A}\frac{d}{dt}\left(\frac{U}{v}\right) = \frac{1}{v}\frac{(dU/dt)}{A} \qquad (1)$$

whence we recognize the term $(dU/dt)/A$ as the radiation *power density*, D, (in *watts/m*^{2}) arriving at the surface[1]. Thus, if $v = c$ the *radiation pressure* exerted on the surface is

$$p = \frac{D}{c} \qquad (2)$$

Here we show that this pressure has a *negative* component (*opposite to the direction of propagation of the photons*) due to the existence of the negative linear *momentum* transported by the photons. This fact leads to an important theoretical discovery: the velocity of the electromagnetic waves in free space is not a constant. In addition, *a generalized equation* of the Newton's law of Gravitation is deduced starting from the concept of *negative* radiation pressure applied on the Gravitational Interaction.

.2. Theory

The energy of a harmonic oscillator is quantized in multiples of hf, and given by

$$E_n = \left(n + \tfrac{1}{2}\right)hf \qquad n = 0,1,2,... \qquad (3)$$

where f is the classical frequency of oscillation, and h is the Planck's constant [2]. When $n = 0$, Eq. (3) shows that $E_0 = \frac{1}{2}hf$. This value is called *energy of the zero point*. Thus, the energy of the harmonic oscillator, at equilibrium with the surrounding medium, does not tend to zero when temperature approaches to absolute zero, but stays equal to E_0.

In the particular case of *massless oscillators* (photons, for example), E_0 does not correspond to the lowest value of the energy, which the oscillator can have, because, when temperature approaches to absolute zero the oscillator frequency becomes dependent of the temperature T, as show the well-known expression of the *thermal De Broglie wavelength* (Λ) for *massless particles* [3, 4], which is given by

$$\Lambda = \frac{ch}{2\pi^{\frac{1}{3}}kT} \qquad \Rightarrow \qquad \tfrac{1}{2}hf = \pi^{\frac{1}{3}}kT \qquad (4)$$

Then, *the lowest value of the energy* $\frac{1}{2}hf$, in the case of the *photon*, for example, will be a *fraction* of the value $\frac{1}{2}hf$ correspondent to a critical temperature T_c very close to absolute zero. The mentioned *fraction* must be only related to the frequency f, and a frequency limit, f_g, whose value must be extremely large. Just a simple algebraic form, the quotient f/f_g, can express satisfactorily the mentioned fraction. Thus, according to Eq. (4), we can write that

[1] This value is also called of *Poynting vector*.

$$\tfrac{1}{2}hf\left(\frac{f}{f_g}\right)=\pi^{\frac{1}{3}}kT \qquad (5)$$

Above T_c, the photon absorbs energy from the surrounding medium[2] [5], and its energy becomes equal to hf. Therefore, the energy absorbed by the photon is

$$U=hf-\tfrac{1}{2}hf\left(\frac{f}{f_g}\right) \qquad (6)$$

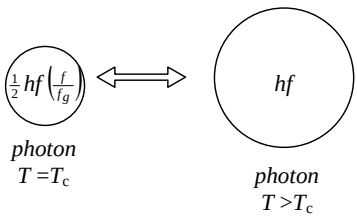

Fig. 1 – Above T_c, the photon absorbs energy from the surrounding medium, and its energy becomes equal to hf.

The *absorbed energy is that thrust the photon* and gives to it its velocity $\vec{v}$. Consequently, the *momentum* q transported by the photon with velocity $\vec{v}$ will be expressed by

$$\vec{q}=\frac{U}{\vec{v}}=\frac{hf-\frac{1}{2}hf\left(\frac{f}{f_g}\right)}{\vec{v}}=\left(1-\frac{1}{2}\frac{f}{f_g}\right)\frac{hf}{\vec{v}}=$$

$$=\left(1-\frac{1}{2}\frac{f}{f_g}\right)\frac{hf}{\vec{v}}\left(\frac{c}{c}\right)=\left(1-\frac{1}{2}\frac{f}{f_g}\right)\frac{hf}{c}\left(\frac{c}{\vec{v}}\right)=$$

$$=\left(1-\frac{1}{2}\frac{f}{f_g}\right)\frac{hf}{c}\vec{n}_r \qquad (7)$$

Equation above shows the existence of a *bipolar linear momentum* transported by the electromagnetic waves. For $f<2f_g$ the resultant *momentum* transported by the photon is *positive*, i.e., If this *momentum* is absorbed by a surface, pressure is exerted on the surface, in the same direction of propagation of the photon. These photons are well-known. However, Eq. (7) point to a new type of photons when $f=2f_g$. In this case $q=0$, i.e., *this type of photon does not exert pressure when it incides on a surface*. What means that it does not interact with matter. Obviously, this corresponds to a special type of photon, which we will call of *neutral photon*. Finally, if $f>2f_g$ the resultant *momentum* transported by the photon is *negative*. If this *momentum* is absorbed by a surface, pressure is exerted on the surface, in the *opposite direction of propagation of the photon*. This special type of photon will be denominated of *attractive photon*.

The quantization of gravity shows that the *gravitational mass* m_g and *inertial mass* m_i are correlated by means of the following factor [6]:

$$\chi=\frac{m_g}{m_{i0}}=\left\{1-2\left[\sqrt{1+\left(\frac{\Delta p}{m_{i0}c}\right)^2}-1\right]\right\} \qquad (8)$$

where m_{i0} is the *rest* inertial mass of the particle and Δp is the variation in the particle's *kinetic momentum*.

Another important equation obtained in the quantization theory of gravity is the new expression for the *momentum* q of a particle with gravitational mass M_g and velocity v, which is given by

$$\vec{q}=M_g\vec{v} \qquad (9)$$

where $M_g=m_g/\sqrt{1-v^2/c^2}$; m_g is given by Eq.(8), i.e., $m_g=\chi\, m_i$.

By comparing Eq. (9) with (7) we obtain

$$v=c\sqrt{\frac{hf}{M_gc^2}\left(1-\frac{f}{2f_g}\right)} \qquad (10)$$

M*ass–energy equivalence principle* states that anything having mass has *an equivalent* amount of energy and vice versa. In the particular case of photons, the energy of the photons, $E=hf$, has a corresponding equivalent mass, M_g, given by its energy *E divided* by the speed of light squared *c*², i.e.,

$$M_g\equiv E/c^2 \qquad (11)$$

or

[2] In order to provide the equilibrium the harmonic oscillator absorbs energy from the surrounding medium.

$$M_g c^2 \equiv hf \qquad (12)$$

Considering this expression, Eq. (10) can be rewritten as follows

$$v = c\sqrt{\left(1-\frac{f}{2f_g}\right)} \qquad (13)$$

Equation (13) shows that the speed of the electromagnetic waves in free space *is not a constant*. Thus, also the speed of light is not a constant.

Theories proposing a varying speed of light have recently been widely proposed under the claim that they offer a solution to cosmological puzzles [7 , 8].

It is known that the interactions are communicated by means of the changing of "virtual" *quanta*. The maximum velocity of these *quanta* is a *constant* called maximum velocity of propagation of the interactions. Currently, it is assumed that this velocity is equal to the velocity of the electromagnetic waves in free space (c). This is the reason of the constant c to appear in the relativistic factor (Eq. (10)). However, Eq. (13) shows that the velocity of the electromagnetic waves in free space is not a constant. In addition, Eq. (13) shows that for $f > 2f_g$ the velocity of the photon is *imaginary*. This means that the *attractive* photons are *virtual* photons.

Now we will apply the concept of *negative* radiation pressure, here developed, to the Gravitational Interaction.

According to Eq. (7), the resultant *momentum* transported by the photons with frequency $f > 2f_g$ is *negative*. If this *momentum* is absorbed by a surface, pressure is exerted on the surface, in the *opposite direction of propagation of the photon*.

Now consider two particles A and B with *gravitational* masses m_A and m_B, respectively. If both particles emit att*ractive radiation* ($f > 2f_g$), then the powers P_A and P_B emitted from A and B, according to Eq. (6), are respectively given by

$$P_A = N_A hf\left(1-\frac{f}{2f_g}\right)f \qquad (14)$$

$$P_B = N_B hf\left(1-\frac{f}{2f_g}\right)f \qquad (15)$$

where N_A and N_B are respectively, the number of attractive photons emitted from A and B, during the time interval $\Delta t = 1/f$.

Equations (14) and (15) can be rewritten as follows

$$P_A \cong \left[N_A hf\left(1-\frac{f}{2f_g}\right)\right]f = E_{g(A)}f =$$

$$\cong \left(\frac{1}{\sqrt{1-\frac{V_A^2}{c^2}}}\right)M_{g(A)}c^2 f \qquad (16)$$

$$P_B \cong \left[N_B hf\left(1-\frac{f}{2f_g}\right)\right]f = E_{g(B)}f =$$

$$\cong \left(\frac{1}{\sqrt{1-\frac{V_B^2}{c^2}}}\right)M_{g(B)}c^2 f \qquad (17)$$

where $E_{g(A)}$ and $E_{g(B)}$ are respectively the *total energies* of the particles A and B, given respectively by: $E_{g(A)} = M_{g(A)}c^2 = m_A c^2 \Big/ \sqrt{1-V_A^2/c^2}$ and $E_{g(B)} = M_{g(B)}c^2 = m_B c^2 \Big/ \sqrt{1-V_B^2/c^2}$ [6]; V_A is the velocity of the particle A in respect to the particle B and V_B is the velocity of the particle B in respect to the particle A. Obviously, $V_A = V_B$.

Thus, if r is the distance between the mentioned particles, then the power densities of the *attractive* radiation in A and B are respectively, given by

$$D_A = \frac{P_A}{4\pi r^2} = \left(\frac{1}{\sqrt{1-\frac{V^2}{c^2}}}\right)\frac{M_{g(A)}c^2 f}{4\pi r^2} = \left(\frac{1}{\sqrt{1-\frac{V^2}{c^2}}}\right)\xi_0\frac{M_{g(A)}}{r^2} \qquad (18)$$

$$D_B = \frac{P_B}{4\pi r^2} = \left(\frac{1}{\sqrt{1-\frac{V^2}{c^2}}}\right)\frac{M_{g(B)}c^2 f}{4\pi r^2} = \left(\frac{1}{\sqrt{1-\frac{V^2}{c^2}}}\right)\xi_0\frac{M_{g(B)}}{r^2} \qquad (19)$$

where $V = V_A = V_B$; ξ_0 is expressed by

$$\xi_0 = \frac{c^2 f}{4\pi} \qquad (20)$$

Let us now show that the *gravitational attraction* between two particles A and B is generated by the interchange of *attractive*

photons $\left(virtual\ photons\ with\ f > 2f_g\right)$, emitted reciprocally by the two particles.

It is known that the *electric force* on an electric charge A, due to another electric charge B is related to the product of the charge of A $\left(q_A\right)$ by the flux density on A, due to the charge of B, $\left(D_B = q_B/4\pi r^2\right)$, i.e., $\vec{F}_{BA} \propto \vec{D}_B q_A$. By analogy, the charge A exerts an opposite electric force on the charge B, which is related to the product of the charge of B $\left(q_B\right)$ by the flux density on B, due to the charge of A, $\left(D_A = q_A/4\pi r^2\right)$, i.e., $\vec{F}_{AB} = -\vec{F}_{AB}$, $\vec{F}_{AB} \propto \vec{D}_A q_B$. These proportionalities are usually written by means of the following equations:

$$\vec{F}_{AB} = -\vec{F}_{BA} = \frac{\vec{D}_A q_B}{\varepsilon_0} = -\frac{\vec{D}_B q_A}{\varepsilon_0} = \frac{q_A q_B}{4\pi\varepsilon_0 r^2}\hat{\mu} \qquad (21)$$

where ε_0 is the so-called *permissivity constant* for free space $\left(\varepsilon_0 = 8.854\times10^{-12} F/m\right)$.

Similarly, the *magnetic force* that a magnetic pole B exerts on another magnetic pole A is related to the product of the pole intensity p_A of the pole A by the flux density on A, due to the pole intensity p_B of the pole B, $\left(D_B = p_B/4\pi r^2\right)$, i.e., $\vec{F}_{BA} \propto \vec{D}_B p_A$. By analogy, the pole A exerts an opposite magnetic force on the pole B, which is related to the product of the pole intensity p_B of the pole B by the flux density on B, due to the pole intensity p_A of the pole A, $\left(D_A = p_A/4\pi r^2\right)$, i.e., $\vec{F}_{AB} = -\vec{F}_{AB}$, $\vec{F}_{AB} \propto \vec{D}_A q_B$. Usually these proportionalities are expressed by means of the following equations:

$$\vec{F}_{AB} = -\vec{F}_{BA} = \frac{\vec{D}_A p_B}{\mu_0} = -\frac{\vec{D}_B p_A}{\mu_0} = \frac{p_A p_B}{4\pi\mu_0 r^2}\hat{\mu} \qquad (22)$$

where μ_0 is the so-called *permeability constant* for free space $\left(\mu_0 = 4\pi\times10^{-7} H/m\right)$.

In the case of the forces produced by the action of *attractive photons* emitted reciprocally from the particles A and B, their expressions can be deduced by using the same argument previously shown in order to obtain the expressions of the electric forces and magnetic forces. That is, the force exerted on the particle A (whose gravitational mass is $M_{g(A)}$), by another particle B (whose gravitational mass is $M_{g(B)}$) is related to the product of $M_{g(A)}$ by the flux density (*power density*) on A, due to the mass $M_{g(B)}$, $\left(D_B = P_B/4\pi r^2.\ See\ Eq.(19)\right)$, i.e., $\vec{F}_{BA} \propto \vec{D}_B M_{g(A)}$. By analogy, the particle A exerts an opposite force on the particle B, which is related to the product of the mass $M_{g(A)}$ by the flux density (*power density*) on B, due to the mass $M_{g(A)}$ of the particle A, $\left(D_A = P_A/4\pi r^2.\ See\ Eq.(18)\right)$,i.e., $\vec{F}_{AB} = -\vec{F}_{AB}$, $\vec{F}_{AB} \propto \vec{D}_A M_{g(B)}$. Thus, we can write that

$$\vec{F}_{AB} = -\vec{F}_{BA} = \frac{\vec{D}_A M_{g(A)}}{k_0}\hat{\mu} = -\frac{\vec{D}_B M_{b(B)}}{k_0}\hat{\mu} \qquad (23)$$

Substitution of Eqs. (18) and (19) into Eq. (23) we get

$$\vec{F}_{AB} = -\vec{F}_{BA} = \left(\frac{1}{\sqrt{1-\frac{v^2}{c^2}}}\right)\left(\frac{\xi_0}{k_0}\right)\frac{M_{g(A)}M_{g(B)}}{r^2}\hat{\mu} \qquad (24)$$

For $V = 0$ Eq. (24) reduces to

$$\vec{F}_{AB} = -\vec{F}_{BA} = \left(\frac{\xi_0}{k_0}\right)\frac{m_A m_B}{r^2}\hat{\mu} =$$

$$= G\frac{m_A m_B}{r^2}\hat{\mu} \qquad (25)$$

where $G = 6.67\times10^{-11} N.m^2.kg^{-2}$ is the Universal constant of Gravitation.

Equation (25) tells us that

$$\xi_0/k_0 = G \qquad (26)$$

By substituting ξ_0 given by Eq. (20) into this expression, we obtain

$$k_0 = \frac{\xi_0}{G} = \frac{c^2 f}{4\pi G} \qquad (27)$$

From the above exposed, we can then conclude that the *gravitational interaction* is caused by the interchange of *virtual* photons with frequencies $f > 2f_g$ (attractive photons). In this way, the called *graviton* must have spin 1 and not 2. Consequently, the gravitational forces are also *gauge* forces because they are yielded by the exchange of *virtual quanta* of spin 1, such as the electromagnetic forces and the weak and strong nuclear forces.

Now consider the emission of N attractive photons with frequency $f > 2f_g$ (*gravitons*)

from a particle with mass m_{i0}. According to Eq. (8) , and considering that $q = U/v$, we get

$$\chi = \frac{m_g}{m_{i0}} = \left\{1-2\left[\sqrt{1+\left(\frac{U}{m_{i0}cv}\right)^2}-1\right]\right\} \qquad (28)$$

Substitution of Eq. (6) and (13) into Eq. (28) gives

$$\frac{m_g}{m_{i0}} = \left\{1-2\left[\sqrt{1+\left(\frac{Nhf}{m_{i0}c^2}\sqrt{1-\frac{f}{2f_g}}\right)^2}-1\right]\right\} \qquad (29)$$

In case of *protons*, for example, the number of *attractive photons* emitted from a proton, N_p, can be expressed by means of the following relation: $N_p = N\left(m_{p0}/m_{i0}\right)$, where N is the number of attractive photons emitted from the particle with mass m_{i0}; m_{p0} is the rest inertial mass of the proton. In this case, the equation (29) will be rewritten as follows:

$$\frac{m_{gp}}{m_{p0}} = \left\{1-2\left[\sqrt{1+\left(\frac{N_p hf}{m_{p0}c^2}\sqrt{1-\frac{f}{2f_g}}\right)^2}-1\right]\right\} = \left\{1-2\left[\sqrt{1+\left(\frac{N\,hf}{m_{i0}c^2}\sqrt{1-\frac{f}{2f_g}}\right)^2}-1\right]\right\} \qquad (30)$$

In the case of, *electrons*, for example, the number of attractive photons emitted from an electron N_e, can be expressed by means of the following relation: $N_e = N\left(m_{e0}/m_{i0}\right)$, where m_{e0} is the rest inertial mass of the electron. In this case, the equation (29) will be rewritten as

$$\frac{m_{ge}}{m_{e0}} = \left\{1-2\left[\sqrt{1+\left(\frac{N_e hf}{m_{e0}c^2}\sqrt{1-\frac{f}{2f_g}}\right)^2}-1\right]\right\} = \left\{1-2\left[\sqrt{1+\left(\frac{N\,hf}{m_{i0}c^2}\sqrt{1-\frac{f}{2f_g}}\right)^2}-1\right]\right\} \qquad (31)$$

This is *exactly the same expression* for the *proton* (Eq. (30).

In the case of, *neutrinos*, for example, the number of attractive photons, N_n, emitted from a neutrino can be expressed by means of the following relation: $N_n = N\left(m_{n0}/m_{i0}\right)$, where m_{n0} is the rest inertial mass of the neutrino. In this case, the equation (29) will be rewritten as follows:

$$\frac{m_{gn}}{m_{n0}} = \left\{1-2\left[\sqrt{1+\left(\frac{N_n hf}{m_{n0}c^2}\sqrt{1-\frac{f}{2f_g}}\right)^2}-1\right]\right\} = \left\{1-2\left[\sqrt{1+\left(\frac{N\,hf}{m_{i0}c^2}\sqrt{1-\frac{f}{2f_g}}\right)^2}-1\right]\right\} \qquad (32)$$

Also, in this case, the obtained expression is *exactly the same expression* for the *proton* and the *electron* (the term N/m_{i0} is a *constant*). In short, the result *is the same for any particle with non-null mass*.

By solving equation below

$$\left\{1-2\left[\sqrt{1+\left(\frac{N\,hf}{m_{i0}c^2}\sqrt{1-\frac{f}{2f_g}}\right)^2}-1\right]\right\} = \left\{1-2\left[\sqrt{1+\underbrace{\left(\frac{N\,h}{m_{i0}c^2}\right)^2}_{constant} f^2\left(1-\frac{f}{2f_g}\right)}-1\right]\right\} = \chi \qquad (33)$$

we get:

$$f^2\left(1-\frac{f}{2f_g}\right) = \frac{m_{i0}^2c^4}{N^2h^2}\left(\frac{\chi^2-6\chi+5}{4}\right) \qquad (34)$$

Note that, for $N = N_{\max}$, the value of f in Eq. (34) becomes equal to $f_{\min}$. But, the minimum frequency of the gravific photons is very close to $2f_g$, then we can write that $f = f_{\min} \cong 2f_g$. Under these circumstances, Eq. (33) shows that we have that $\chi = \chi_{\min} \cong 1$. Consequently, both terms of the Eq. (34) become approximately equal to *zero*. On the other hand, for $N = N_{\min} = 1$ (one gravific photon) the value of f in Eq. (34) becomes equal to $f_{\max}$ (the *maximum* frequency of the gravific photons) and Eq. (33) shows that, in this case, $\chi = \chi_{\max}$, i.e.,

$$\left\{1-2\left[\sqrt{1+\underbrace{\left(\frac{N\,h}{m_{i0}c^2}\right)^2}_{constant} f_{\max}^2\left(1-\frac{f_{\max}}{2f_g}\right)}-1\right]\right\} = \chi_{\max} \qquad (35)$$

By solving this equation, we obtain:

$$f_{\max}^2\left(1-\frac{f_{\max}}{2f_g}\right)=\frac{m_{i0}^2c^4}{h^2}\left(\frac{\chi_{\max}^2-6\chi_{\max}+5}{4}\right) \quad (36)$$

The energy density D at a distance r from the *mentioned particle* can be expressed by:

$$D=\frac{U/\Delta t}{S}=\frac{hf\left(1-f/2f_g\right)(f)}{4\pi r^2} \quad (37)$$

Substitution of Eq.(36) into Eq. (37) yields

$$D=\left(\frac{m_{i0}c^4}{4\pi h}\right)\left(\frac{\chi_{\max}^2-6\chi_{\max}+5}{4}\right)\frac{m_{i0}}{r^2} \quad (38)$$

By comparing Eq. (38) with equations (18) and (19), we can conclude that

$$\left(\frac{m_{i0}c^4}{4\pi h}\right)\left(\frac{\chi_{\max}^2-6\chi_{\max}+5}{4}\right)=\xi_0 \quad (39)$$

By comparing this equation with Eq.(20), we obtain

$$f_{\max}=\left(\frac{\chi_{\max}^2-6\chi_{\max}+5}{4}\right)\frac{m_{i0}c^2}{h} \quad (40)$$

Now, taking Eq. (8), where the term $\Delta p/m_{i0}c$ is putted in the following form: $\Delta p/m_{i0}c=(v/c)\left(1-v^2/c^2\right)^{-\frac{1}{2}}$ [6], we get

$$\chi=\frac{m_g}{m_{i0}}=\left\{1-2\left[\sqrt{1+\left(\frac{v/c}{\sqrt{1-v^2/c^2}}\right)^2}-1\right]\right\} \quad (41)$$

In practice, how close c the velocity v can approach? At the *Large Hadron Collider* (LHC) the protons each have energy of 6.5 TeV, giving total collision energy of 13 TeV. At this energy the protons move with velocity $v=0.999999990c$. Possibly this value will can be increased up to $v=0.999999999999c$, in the next experiments at the LHC. In this case, Eq. (41) gives $\chi\cong-10^7$. Since $\chi_{\max}$ is obviously, *very greater than* this value, then we can conclude that the term $\left(\chi_{\max}^2-6\chi_{\max}+5/4\right)$ in Eq. (40) is *very greater than* 10^{14}; showing, therefore, that the maximum frequency f of the *gravific* photons (See Eq. (40)) is *very greater than* $10^{14}\left(m_{i0}c^2/h\right)\cong10^{64}m_{i0}$. Thus, we can define the *frequency spectrum of the gravific photons* by means of the following expression:

$$f_{\min}\cong 2f_g\le\ f\ \le f_{\max}>>10^{64}m_{i0} \quad (42)$$

This expression shows then that *the frequency spectrum of the gravific photons must be above the spectrum of the gamma rays* (*neutrino* mass: $m_{i0}\cong10^{-37}kg$ [9]). Thus, considering that the *highest* energy of gamma ray detected is approximately $3\times10^{13}eV$ [10] [3], in terms of frequency $f_{\gamma\max}\approx10^{28}Hz$, then we can assume that *the characteristic value,* $2f_g$, in the Eq.(34), in spite to be greater than $f_{\gamma\max}$, it should be very close it, because the spectrum of the attractive photons should make limit with the gamma rays spectrum (See Fig.2). Thus, we can write that

$$2f_g\gtrsim f_{\gamma\max}\approx10^{28}Hz \quad (43)$$

It is very unlikely that there are gamma rays in the Nature with frequency much greater than the aforementioned value, but if they exist, they would only show that the value of $2f_g$ would be situated above the value indicated by Eq (43).

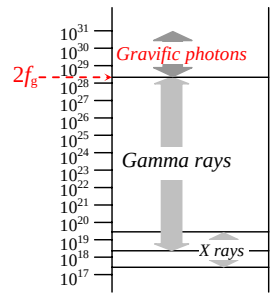

Fig. 2 – The *Gravific Photons* Spectrum (above $2f_g\approx10^{28}Hz$).

[3] The largest air shower detected is from a particle of around $4\times10^{20}eV$ but this is thought to be from a cosmic ray *particle* rather than photon.

References

[1] Henry, G. E., (1957) *Radiation Pressure*, Scientific American, p.99.

[2] Beiser, A. (1963) *Concepts of Modern Physics*, Portuguese version, Ed. Polígono, S.Paulo (1969), p. 165-166.

[3] Kittel, C., and Kroemer, H., (1980) *Thermal Physics* (2 ed), W.H. Freeman, p.73.

[4] Yan, Z., (2000) *Eur. J. Phys.*, 21, 625-631.

[5] Beiser, A. (1963) *Concepts of Modern Physics*, Portuguese version, Ed. Polígono, S.Paulo (1969), p. 166.

[6] De Aquino, F. (2010) *Mathematical Foundations of the Relativistic Theory of Quantum Gravity*, Pacific Journal of Science and Technology, **11** (1), pp. 173-232.

[7] Albrecht, A. and Magueijo, J. (1999) j. Phys. Rev. D 59 043516, [astro-ph/9811018].

[8] Barrow, J.D. and Magueijo, J. (1998) J. Phys. Lett. B 443 , 104, [astro-ph/9811072].

[9] Mertens, S. (2016). *Direct Neutrino Mass Experiments*. Journal of Physics: Conference Series. **718**: 022013. *ArXiv: 1605.01579.*

[10] http://er.jsc.nasa.gov/seh/gamray.html

Gravity Control by means of *Electromagnetic Field* through *Gas* or *Plasma* at Ultra-Low Pressure

Fran De Aquino
Maranhao State University, Physics Department, S.Luis/MA, Brazil.

It is shown that the gravity acceleration just above a chamber filled with *gas* or *plasma* at ultra-low pressure can be strongly reduced by applying an Extra Low-Frequency (ELF) electromagnetic field across the gas or the plasma. This Gravitational Shielding Effect is related to recent discovery of *quantum correlation* between gravitational mass and inertial mass. According to the theory samples hung above the gas or the plasma should exhibit a weight decrease when the frequency of the electromagnetic field is decreased or when the intensity of the electromagnetic field is increased. This Gravitational Shielding Effect is unprecedented in the literature and can not be understood in the framework of the General Relativity. From the technical point of view, there are several applications for this discovery; possibly it will change the paradigms of *energy* generation, *transportation* and *telecommunications*.

Key words: Phenomenology of quantum gravity, Experimental Tests of Gravitational Theories, Vacuum Chambers, Plasmas devices. **PACs**: 04.60.Bc, 04.80.Cc, 07.30.Kf, 52.75.-d.

CONTENTS

I. INTRODUCTION

It will be shown that the local gravity acceleration can be controlled by means of a device called Gravity Control Cell (GCC) which is basically a recipient filled with gas or plasma where is applied an *electromagnetic field*. According to the theory samples hung above the gas or plasma should exhibit a weight decrease when the frequency of the electromagnetic field is decreased or when the intensity of the electromagnetic field is increased. The electrical *conductivity* and the *density* of the gas or plasma are also highly relevant in this process.

With a GCC it is possible to convert the gravitational energy into rotational mechanical energy by means of the *Gravitational Motor*. In addition, a new concept of spacecraft (the *Gravitational Spacecraft*) and aerospace flight is presented here based on the possibility of gravity control. We will also see that the gravity control will be very important to *Telecommunication*.

II. THEORY

It was shown [1] that the relativistic *gravitational mass* $M_g = m_g \Big/ \sqrt{1-V^2/c^2}$ and the relativistic *inertial mass* $M_i = m_{i0} \Big/ \sqrt{1-V^2/c^2}$ are *quantized*, and given by $M_g = n_g^2 m_{i0(min)}$, $M_i = n_i^2 m_{i0(min)}$ where n_g and n_i are respectively, the *gravitational quantum number* and the *inertial quantum number* ; $m_{i0(min)} = \pm 3.9 \times 10^{-73} kg$ is the elementary *quantum* of inertial mass. The masses m_g and m_{i0} are correlated by means of the following expression:

$$m_g = m_{i0} - 2\left[\sqrt{1+\left(\frac{\Delta p}{m_i c}\right)^2} - 1\right] m_{i0}. \qquad (1)$$

Where Δp is the *momentum* variation on the particle and m_{i0} is the inertial mass at rest.

In general, the *momentum* variation Δp is expressed by $\Delta p = F\Delta t$ where F is the applied force during a time interval Δt. Note that there is no restriction concerning the *nature* of the force F, i.e., it can be mechanical, electromagnetic, etc.

For example, we can look on the *momentum* variation Δp as due to absorption or emission of *electromagnetic energy* by the particle.

In the case of radiation, Δp can be obtained as follows: It is known that the *radiation pressure*, dP, upon an area $dA = dxdy$ of a volume $dV = dxdydz$ of a particle (the incident radiation normal to the surface dA)is equal to the energy dU absorbed per unit volume (dU/dV).i.e.,

$$dP = \frac{dU}{dV} = \frac{dU}{dxdydz} = \frac{dU}{dAdz} \qquad (2)$$

Substitution of $dz = vdt$ (v is the speed of radiation) into the equation above gives

$$dP = \frac{dU}{dV} = \frac{(dU/dAdt)}{v} = \frac{dD}{v} \qquad (3)$$

Since $dPdA = dF$ we can write:

$$dFdt = \frac{dU}{v} \qquad (4)$$

However we know that $dF = dp/dt$, then

$$dp = \frac{dU}{v} \qquad (5)$$

From this equation it follows that

$$\Delta p = \frac{U}{v}\left(\frac{c}{c}\right) = \frac{U}{c} n_r$$

Substitution into Eq. (1) yields

$$m_g = \left\{1 - 2\left[\sqrt{1+\left(\frac{U}{m_{i0}c^2} n_r\right)^2} - 1\right]\right\} m_{i0} \qquad (6)$$

Where U, is the electromagnetic energy absorbed by the particle; n_r is the index of refraction.

Equation (6) can be rewritten in the following form

$$m_g = \left\{1 - 2\left[\sqrt{1+\left(\frac{W}{\rho\, c^2} n_r\right)^2} - 1\right]\right\} m_{i0} \qquad (7)$$

Where $W = U/V$ is the *density of electromagnetic energy* and $\rho = m_{i0}/\mathrm{V}$ is the density of inertial mass.

The Eq. (7) is the expression of the *quantum correlation* between the *gravitational mass* and the *inertial mass* as a function of the *density of electromagnetic energy*. This is also the expression of correlation between gravitation and electromagnetism.

The density of electromagnetic energy in an *electromagnetic* field can be deduced from Maxwell's equations [2] and has the following expression

$$W = \tfrac{1}{2}\varepsilon\, E^2 + \tfrac{1}{2}\mu H^2 \qquad (8)$$

It is known that $B = \mu H$, $E/B = \omega/k_r$ [3] and

$$v = \frac{dz}{dt} = \frac{\omega}{\kappa_r} = \frac{c}{\sqrt{\frac{\varepsilon_r \mu_r}{2}\left(\sqrt{1+(\sigma/\omega\varepsilon)^2}+1\right)}} \qquad (9)$$

Where k_r is the real part of the *propagation vector* $\vec{k}$ (also called *phase constant* [4]); $k = \left|\vec{k}\right| = k_r + ik_i$; ε, μ and σ, are the electromagnetic characteristics of the medium in which the incident (or emitted) radiation is propagating ($\varepsilon = \varepsilon_r \varepsilon_0$ where ε_r is the *relative dielectric permittivity* and $\varepsilon_0 = 8.854\times10^{-12} F/m$; $\mu = \mu_r \mu_0$ where μ_r is the *relative magnetic permeability* and $\mu_0 = 4\pi\times10^{-7} H/m$; σ is the *electrical conductivity*). It is known that for *free-space* $\sigma = 0$ and $\varepsilon_r = \mu_r = 1$ then Eq. (9) gives

$$v = c \qquad (10)$$

From (9) we see that the *index of refraction* $n_r = c/v$ will be given by

$$n_r = \frac{c}{v} = \sqrt{\frac{\varepsilon_r \mu_r}{2}\left(\sqrt{1+(\sigma/\omega\varepsilon)^2}+1\right)} \qquad (11)$$

Equation (9) shows that $\omega/\kappa_r = v$. Thus, $E/B = \omega/k_r = v$, i.e., $E = vB = v\mu H$. Then, Eq. (8) can be rewritten in the following form:

$$W = \tfrac{1}{2}\left(\varepsilon v^2 \mu\right)\mu H^2 + \tfrac{1}{2}\mu H^2 \qquad (12)$$

For $\sigma << \omega\varepsilon$, Eq. (9) reduces to

$$v = \frac{c}{\sqrt{\varepsilon_r \mu_r}}$$

Then, Eq. (12) gives

$$W = \tfrac{1}{2}\left[\varepsilon\left(\frac{c^2}{\varepsilon_r \mu_r}\right)\mu\right]\mu H^2 + \tfrac{1}{2}\mu H^2 = \mu H^2 \qquad (13)$$

This equation can be rewritten in the following forms:

$$W = \frac{B^2}{\mu} \qquad (14)$$

or

$$W = \varepsilon\, E^2 \qquad (15)$$

For $\sigma >> \omega\varepsilon$, Eq. (9) gives

$$v = \sqrt{\frac{2\omega}{\mu\sigma}} \qquad (16)$$

Then, from Eq. (12) we get

$$W = \tfrac{1}{2}\left[\varepsilon\left(\frac{2\omega}{\mu\sigma}\right)\mu\right]\mu H^2 + \tfrac{1}{2}\mu H^2 = \left(\frac{\omega\varepsilon}{\sigma}\right)\mu H^2 + \tfrac{1}{2}\mu H^2 \cong$$

$$\cong \tfrac{1}{2}\mu H^2 \qquad (17)$$

Since $E = vB = v\mu H$, we can rewrite (17) in the following forms:

$$W \cong \frac{B^2}{2\mu} \qquad (18)$$

or

$$W \cong \left(\frac{\sigma}{4\omega}\right)E^2 \qquad (19)$$

By comparing equations (14) (15) (18) and (19) we see that Eq. (19) shows that the better way to obtain a strong value of W *in practice* is by applying an *Extra Low-Frequency* (ELF) *electric field* $\left(w = 2\pi f << 1Hz\right)$ through a *mean with high electrical conductivity*.

Substitution of Eq. (19) into Eq. (7), gives

$$m_g = \left\{1 - 2\left[\sqrt{1+\frac{\mu}{4c^2}\left(\frac{\sigma}{4\pi f}\right)^3 \frac{E^4}{\rho^2}} - 1\right]\right\} m_{i0} \qquad (20)$$

This equation shows clearly that if an

electrical *conductor mean* has $\rho << 1\ Kg.m^{-3}$ and $\sigma >> 1$, then it is possible obtain strong changes in its gravitational mass, with a relatively small ELF *electric field*. An electrical *conductor mean* with $\rho << 1\ Kg.m^{-3}$ is obviously a *plasma*.

There is a very simple way to test Eq. (20). It is known that inside a fluorescent lamp *lit* there is *low-pressure Mercury plasma.* Consider a 20W T-12 *fluorescent lamp* (80044–F20T12/C50/ECO GE, Ecolux® T12), whose characteristics and dimensions are well-known [5]. At around $T \cong 318.15^0 K$, an optimum mercury vapor pressure of $P = 6\times10^{-3} Torr = 0.8 N.m^{-2}$ is obtained, which is required for maintenance of high luminous efficacy throughout life. Under these conditions, the mass density of the Hg plasma can be calculated by means of the well-known *Equation of State*

$$\rho = \frac{PM_0}{ZRT} \qquad (21)$$

Where $M_0 = 0.2006 kg.mol^{-1}$ is the molecular mass of the Hg; $Z \cong 1$ is the *compressibility factor* for the Hg plasma; $R = 8.314\ joule.mol^{-1}.^0K^{-1}$ is the *gases universal constant*. Thus we get

$$\rho_{Hg\ \ plasma} \cong 6.067\times10^{-5} kg.m^{-3} \qquad (22)$$

The electrical conductivity of the Hg plasma can be deduced from the *continuum form of Ohm's Law* $\vec{j} = \sigma\vec{E}$, since the *operating current* through the lamp and the *current density* are well-known and respectively given by $i = 0.35A$ [5] and $j_{lamp} = i/S = i/\frac{\pi}{4}\phi_{int}^2$, where $\phi_{int} = 36.1mm$ is the inner diameter of the lamp. The voltage drop across the electrodes of the lamp is $57V$ [5] and the distance between them $l = 570mm$. Then the electrical field *along* the lamp E_{lamp} is given by $E_{lamp} = 57V/0.570m = 100\ V.m^{-1}$. Thus, we have

$$\sigma_{Hg\ \ plasma} = \frac{j_{lamp}}{E_{lamp}} = 3.419\ \ S.m^{-1} \qquad (23)$$

Substitution of (22) and (23) into (20) yields

$$\frac{m_{g(Hg\ plasma)}}{m_{i(Hg\ plasma)}} = \left\{1 - 2\left[\sqrt{1 + 1.909\times10^{-17}\frac{E^4}{f^3}} - 1\right]\right\} \qquad (24)$$

Thus, if an *Extra Low-Frequency electric field* E_{ELF} with the following characteristics: $E_{ELF} \approx 100V.m^{-1}$ and $f < 1mHZ$ is applied through the Mercury plasma then a strong *decrease in the gravitational mass of the Hg plasma* will be produced.

It was shown [1] that there is an additional effect of *gravitational shielding* produced by a substance under these conditions. Above the substance the gravity acceleration g_1 is reduced at the same ratio $\chi = m_g/m_{i0}$, i.e., $g_1 = \chi\ g$, (g is the gravity acceleration *under* the *substance*). Therefore, due to the *gravitational shielding effect* produced by the decrease of $m_{g(Hg\ plasma)}$ *in the region where the ELF electric field* E_{ELF} *is applied*, the gravity acceleration just *above* this region will be given by

$$g_1 = \chi_{(Hg\ plasma)} g = \frac{m_{g(Hg\ plasma)}}{m_{i(Hg\ plasma)}} g =$$

$$= \left\{1 - 2\left[\sqrt{1 + 1.909\times10^{-17}\frac{E_{ELF}^4}{f_{ELF}^3}} - 1\right]\right\} g \qquad (25)$$

The trajectories of the electrons/ions through the lamp are determined by the electric field E_{lamp} *along* the lamp. If the ELF electric field *across* the lamp E_{ELF} is much greater than E_{lamp}, the current through the lamp can be interrupted. However, if $E_{ELF} << E_{lamp}$, these trajectories will be only slightly modified. Since here $E_{lamp} = 100\ V.m^{-1}$, then we can arbitrarily choose $E_{ELF}^{max} \cong 33\ V.m^{-1}$. This means that the *maximum* voltage drop, which can be applied across the metallic

plates, placed at distance d, is equal to the outer diameter (max *) of the bulb ϕ_{lamp}^{max} of the 20W T-12 Fluorescent lamp, is given by

$$V_{max} = E_{ELF}^{max}\phi_{lamp}^{max} \cong 1.5\ V$$

Since $\phi_{lamp}^{max} = 40.3mm$ [5].

Substitution of $E_{ELF}^{max} \cong 33\ V.m^{-1}$ into (25) yields

$$g_1 = \chi_{(Hg\ plasma)}g = \frac{m_{g(Hg\ plasma)}}{m_{i(Hg\ plasma)}}g =$$

$$= \left\{1-2\left[\sqrt{1+\frac{2.264\times10^{-11}}{f_{ELF}^3}}-1\right]\right\}g \qquad (26)$$

Note that, for $f < 1mHz = 10^{-3}Hz$, the gravity acceleration can be strongly reduced. These conclusions show that the ELF Voltage Source of the set-up shown in Fig.1 should have the following characteristics:

- Voltage range: 0 – 1.5 V
- Frequency range: 10^{-4}Hz – 10^{-3}Hz

In the experimental arrangement shown in Fig.1, an ELF electric field with intensity $E_{ELF} = V/d$ crosses the fluorescent lamp; V is the voltage drop across the metallic plates of the capacitor and $d = \phi_{lamp}^{max} = 40.3mm$. When the ELF electric field is applied, the gravity acceleration just above the lamp (inside the dotted box) decreases according to (25) and the changes can be measured by means of the system balance/sphere presented on the top of Figure 1.

In Fig. 2 is presented an experimental arrangement with *two* fluorescent lamps in order to test the gravity acceleration above the *second* lamp. Since gravity acceleration above the *first* lamp is given by $\vec{g}_1 = \chi_{1(Hg\ plasma)}\vec{g}$, where

$$\chi_{1(Hg\ plasma)} = \frac{m_{g1(Hg\ plasma)}}{m_{i1(Hg\ plasma)}} =$$

$$= \left\{1-2\left[\sqrt{1+1.909\times10^{-17}\frac{E_{ELF(1)}^4}{f_{ELF(1)}^3}}-1\right]\right\} \qquad (27)$$

Then, above the *second* lamp, the gravity acceleration becomes

$$\vec{g}_2 = \chi_{2(Hg\ plasma)}\vec{g}_1 = \chi_{2(Hg\ plasma)}\chi_{1(Hg\ plasma)}\vec{g} \qquad (28)$$

where

$$\chi_{2(Hg\ plasma)} = \frac{m_{g2(Hg\ plasma)}}{m_{i2(Hg\ plasma)}} =$$

$$= \left\{1-2\left[\sqrt{1+1.909\times10^{-17}\frac{E_{ELF(2)}^4}{f_{ELF(2)}^3}}-1\right]\right\} \qquad (29)$$

Then, results

$$\frac{g_2}{g} = \left\{1-2\left[\sqrt{1+1.909\times10^{-17}\frac{E_{ELF(1)}^4}{f_{ELF(1)}^3}}-1\right]\right\}\times$$

$$\times\left\{1-2\left[\sqrt{1+1.909\times10^{-17}\frac{E_{ELF(2)}^4}{f_{ELF(2)}^3}}-1\right]\right\} \qquad (30)$$

From Eq. (28), we then conclude that if $\chi_{1(Hg\ plasma)} < 0$ and also $\chi_{2(Hg\ plasma)} < 0$, then g_2 will have the *same direction* of g. This way it is possible to intensify several times the gravity in the direction of $\vec{g}$. On the other hand, if $\chi_{1(Hg\ plasma)} < 0$ and $\chi_{2(Hg\ plasma)} > 0$ the direction of $\vec{g}_2$ will be contrary to direction of $\vec{g}$. In this case will be possible to *intensify* and become $\vec{g}_2$ *repulsive* in respect to $\vec{g}$.

If we put a lamp above the *second* lamp, the gravity acceleration above the *third* lamp becomes

$$\vec{g}_3 = \chi_{3(Hg\ plasma)}\vec{g}_2 =$$

$$= \chi_{3(Hg\ plasma)}\chi_{2(Hg\ plasma)}\chi_{1(Hg\ plasma)}\vec{g} \qquad (31)$$

or

* After heating.

$$\frac{g_3}{g}=\left\{1-2\left[\sqrt{1+1.909\times10^{-17}\frac{E_{ELF(1)}^4}{f_{ELF(1)}^3}}-1\right]\right\}\times$$
$$\times\left\{1-2\left[\sqrt{1+1.909\times10^{-17}\frac{E_{ELF(2)}^4}{f_{ELF(2)}^3}}-1\right]\right\}\times$$
$$\times\left\{1-2\left[\sqrt{1+1.909\times10^{-17}\frac{E_{ELF(3)}^4}{f_{ELF(3)}^3}}-1\right]\right\} \qquad (32)$$

If $f_{ELF(1)}=f_{ELF(2)}=f_{ELF(3)}=f$ and

$$E_{ELF(1)}=E_{ELF(2)}=E_{ELF(3)}=V/\phi=$$
$$=V_0\sin\omega t/40.3mm=$$
$$=24.814V_0\sin 2\pi ft.$$

Then, for $t=T/4$ we get

$$E_{ELF(1)}=E_{ELF(2)}=E_{ELF(3)}=24.814V_0.$$

Thus, Eq. (32) gives

$$\frac{g_3}{g}=\left\{1-2\left[\sqrt{1+7.237\times10^{-12}\frac{V_0^4}{f^3}}-1\right]\right\}^3 \qquad (33)$$

For $V_0=1.5V$ and $f=0.2mHz$ $\left(t=T/4=1250s=20.83\text{min}\right)$ the gravity acceleration $\vec{g}_3$ above the *third* lamp will be given by

$$\vec{g}_3=-5.126\vec{g}$$

Above the *second* lamp, the gravity acceleration given by (30), is

$$\vec{g}_2=+2.972\vec{g} \quad .$$

According to (27) the gravity acceleration above the *first* lamp is

$$\vec{g}_1=-1{,}724\vec{g}$$

Note that, by this process an acceleration $\vec{g}$ can be increased several times in the direction of $\vec{g}$ or in the opposite direction.

In the experiment proposed in Fig. 1, we can start with ELF voltage sinusoidal wave of amplitude $V_0=1.0V$ and frequency $1mHz$. Next, the frequency will be progressively decreased down to $0.8mHz$, $0.6mHz$, $0.4mHz$ and $0.2mHz$. Afterwards, the amplitude of the voltage wave must be increased to $V_0=1.5V$ and the frequency decreased in the above mentioned sequence.

Table1 presents the *theoretical* values for g_1 and g_2, calculated respectively by means of (25) and (30).They are also plotted on Figures 5, 6 and 7 as a function of the frequency f_{ELF}.

Now consider a chamber filled with *Air* at $3\times10^{-12}torr$ and 300K as shown in Figure 8 (a). Under these circumstances, the mass density of the *air* inside the chamber, according to Eq. (21) is $\rho_{air}\cong4.94\times10^{-15}kg.m^{-3}$.

If the frequency of the *magnetic* field, B, through the *air* is $f=60Hz$ then $\omega\varepsilon=2\pi f\varepsilon\cong3\times10^{-9}S/m$. Assuming that the electric conductivity of the *air* inside the chamber, $\sigma_{(air)}$ is much less than $\omega\varepsilon$, i.e., $\sigma_{(air)}<<\omega\varepsilon$ (The atmospheric air conductivity is of the order of $2-100\times10^{-15}S.m^{-1}$ [6, 7]) then we can rewritten the Eq. (11) as follows

$$n_{r(air)}\cong\sqrt{\varepsilon_r\mu_r}\cong1 \qquad (34)$$

From Eqs. (7), (14) and (34) we thus obtain

$$m_{g(air)}=\left\{1-2\left[\sqrt{1+\left(\frac{B^2}{\mu_{air}\rho_{air}c^2}n_{r(air)}\right)^2}-1\right]\right\}m_{i(air)}=$$
$$=\left\{1-2\left[\sqrt{1+3.2\times10^6B^4}-1\right]\right\}m_{i(air)} \qquad (35)$$

Therefore, due to the *gravitational shielding effect* produced by the decreasing of $m_{g(air)}$, the gravity acceleration *above* the *air* inside the chamber will be given by

$$g'=\chi_{air}\,g=\frac{m_{g(air)}}{m_{i(air)}}g=$$
$$=\left\{1-2\left[\sqrt{1+3.2\times10^6B^4}-1\right]\right\}g$$

Note that the gravity acceleration above the *air* becomes *negative* for $B>2.5\times10^{-2}T$.

For $B = 0.1T$ the gravity acceleration above the air becomes

$$g' \cong -32.8g$$

Therefore the ultra-low pressure air inside the chamber, such as the Hg plasma inside the fluorescent lamp, works like a Gravitational Shield that in practice, may be used to build *Gravity Control Cells* (GCC) for several practical applications.

Consider for example the GCCs of Plasma presented in Fig.3. The ionization of the plasma can be made of several manners. For example, by means of an electric field between the electrodes (Fig. 3(a)) or by means of a RF signal (Fig. 3(b)). In the first case the ELF electric field and the ionizing electric field can be the same.

Figure 3(c) shows a GCC filled with *air* (at ambient temperature and 1 atm) strongly ionized by means of alpha particles emitted from 36 radioactive ions sources (a very small quantity of *Americium* 241[†]). The radioactive element Americium has a half-life of 432 years, and emits *alpha particles* and low energy gamma rays $(\approx 60KeV)$. In order to shield the *alpha* particles and *gamma* rays emitted from the Americium 241 it is sufficient to encapsulate the GCC with *epoxy*. The alpha particles generated by the americium ionize the oxygen and nitrogen atoms of the air in the *ionization chamber* (See Fig. 3(c)) increasing the *electrical conductivity* of the air inside the chamber. The high-speed alpha particles hit molecules in the air and knock off electrons to form ions, according to the following expressions

$$O_2 + H_e^{++} \rightarrow O_2^+ + e^- + H_e^{++}$$
$$N_2 + H_e^{++} \rightarrow N_2^+ + e^- + H_e^{++}$$

It is known that the electrical conductivity is proportional to both the concentration and the mobility of the *ions* and the *free electrons*, and is expressed by

$$\sigma = \rho_e \mu_e + \rho_i \mu_i$$

Where ρ_e and ρ_i express respectively the concentrations (C/m^3) of electrons and ions; μ_e and μ_i are respectively the mobilities of the electrons and the ions.

In order to calculate the electrical conductivity of the air inside the ionization chamber, we first need to calculate the concentrations ρ_e and ρ_i. We start calculating the *disintegration constant*, λ, for the Am 241 :

$$\lambda = \frac{0.693}{T^{\frac{1}{2}}} = \frac{0.693}{432(3.15 \times 10^7\, s)} = 5.1 \times 10^{-11} s^{-1}$$

Where $T^{\frac{1}{2}} = 432 years$ is the *half-life* of the Am 241.

One *kmole* of an isotope has mass equal to atomic mass of the isotope expressed in kilograms. Therefore, $1g$ of Am 241 has

$$\frac{10^{-3} kg}{241\ \ kg/kmole} = 4.15 \times 10^{-6} kmoles$$

One *kmole* of any isotope contains the Avogadro's number of atoms. Therefore $1g$ of Am 241 has

$$N = 4.15 \times 10^{-6} kmoles \times$$
$$\times 6.025 \times 10^{26}\ atoms/kmole = 2.50 \times 10^{21} atoms$$

Thus, the *activity* [8] of the sample is

[†] The radioactive element *Americium* (Am-241) is widely used in *ionization smoke detectors*. This type of smoke detector is more common because it is inexpensive and better at detecting the smaller amounts of smoke produced by flaming fires. Inside an ionization detector there is a small amount (perhaps 1/5000th of a gram) of americium-241. The Americium is present in oxide form (AmO_2) in the detector. The cost of the AmO_2 is US$ 1,500 per gram. The amount of radiation in a smoke detector is extremely small. It is also predominantly alpha radiation. Alpha radiation cannot penetrate a sheet of paper, and it is blocked by several centimeters of air. The americium in the smoke detector could only pose a danger if inhaled.

$R = \lambda N = 1.3 \times 10^{11}$ disintegrations/s.

However, we will use 36 ionization sources each one with 1/5000th of a gram of Am 241. Therefore we will only use $7.2 \times 10^{-3}\, g$ of Am 241. Thus, R reduces to:

$$R = \lambda N \cong 10^{9} \text{ disintegrations/s}$$

This means that at *one* second, about $10^{9}\, \alpha\ particles$ hit molecules in the air and knock off electrons to form ions O_2^+ and N_2^+ inside the ionization chamber. Assuming that *each* alpha particle yields *one* ion at each $1/10^{9}$ second then the total number of ions produced in one second will be $N_i \cong 10^{18} ions.$ This corresponds to an ions concentration

$$\rho_i = eN_i / V \approx 0.1 / V \quad \left(C/m^3\right)$$

Where V is the volume of the ionization chamber. Obviously, the concentration of electrons will be the same, i.e., $\rho_e = \rho_i$. For $d = 2cm$ and $\phi = 20cm$ (See Fig.3(c)) we obtain

$V = \frac{\pi}{4}(0.20)^2\left(2 \times 10^{-2}\right) = 6.28 \times 10^{-4} m^3$ The n we get:

$$\rho_e = \rho_i \approx 10^{2}\ C/m^3$$

This corresponds to the *minimum* concentration level in the case of *conducting materials*. For these materials, at temperature of 300K, the mobilities μ_e and μ_i vary from 10 up to $100\ m^2V^{-1}s^{-1}$ [9]. Then we can assume that $\mu_e = \mu_i \approx 10\ m^2V^{-1}s^{-1}$. (*minimum* mobility level for conducting materials). Under these conditions, the electrical conductivity of the air inside the ionization chamber is

$$\sigma_{air} = \rho_e\mu_e + \rho_i\mu_i \approx 10^{3} S.m^{-1}$$

At temperature of 300K, the air *density* inside the GCC, is $\rho_{air} = 1.1452 kg.m^{-3}$. Thus, for $d = 2cm$, $\sigma_{air} \approx 10^{3} S.m^{-1}$ and $f = 60Hz$ Eq. (20) gives

$$\chi_{air} = \frac{m_{g(air)}}{m_{i(air)}} =$$

$$= \left\{1 - 2\left[\sqrt{1 + \frac{\mu}{4c^2}\left(\frac{\sigma_{air}}{4\pi f}\right)^3 \frac{V_{rms}^4}{d^4\rho_{air}^2}} - 1\right]\right\} =$$

$$= \left\{1 - 2\left[\sqrt{1 + 3.10 \times 10^{-16} V_{rms}^4} - 1\right]\right\}$$

Note that, for $V_{rms} \cong 7.96KV$, we obtain: $\chi_{(air)} \cong 0$. Therefore, if the voltages range of this GCC is: $0 - 10KV$ then it is possible to reach $\chi_{air} \cong -1$ when $V_{rms} \cong 10KV$.

It is interesting to note that σ_{air} can be strongly increased by increasing the amount of Am 241. For example, by using $0.1g$ of Am 241 the value of R increases to:

$$R = \lambda N \cong 10^{10} \text{ disintegrations/s}$$

This means $N_i \cong 10^{20} ions$ that yield

$$\rho_i = eN_i / V \approx 10 / V \quad \left(C/m^3\right)$$

Then, by reducing, d and ϕ respectively, to 5mm and to 11.5cm, the volume of the ionization chamber reduces to:

$V = \frac{\pi}{4}(0.115)^2\left(5 \times 10^{-3}\right) = 5.19 \times 10^{-5} m^3$

Consequently, we get:

$$\rho_e = \rho_i \approx 10^{5}\ C/m^3$$

Assuming that $\mu_e = \mu_i \approx 10\ m^2V^{-1}s^{-1}$, then the electrical conductivity of the air inside the ionization chamber becomes

$$\sigma_{air} = \rho_e\mu_e + \rho_i\mu_i \approx 10^{6} S.m^{-1}$$

This reduces for $V_{rms} \cong 18.8V$ the voltage necessary to yield $\chi_{(air)} \cong 0$ and reduces

to $V_{rms} \cong 23.5V$ the voltage necessary to reach $\chi_{air} \cong -1$.

If the outer surface of a metallic sphere with radius a is covered with a radioactive element (for example Am 241), then the electrical conductivity of the air (very close to the sphere) can be strongly increased (for example up to $\sigma_{air} \cong 10^6 s.m^{-1}$). By applying a low-frequency electrical potential V_{rms} to the sphere, in order to produce an electric field E_{rms} starting from the outer surface of the sphere, then very close to the sphere the low-frequency electromagnetic field is $E_{rms} = V_{rms}/a$, and according to Eq. (20), the *gravitational mass* of the air in this region expressed by

$$m_{g(air)} = \left\{1-2\left[\sqrt{1+\frac{\mu_0}{4c^2}\left(\frac{\sigma_{air}}{4\pi f}\right)^3 \frac{V_{rms}^4}{a^4\rho_{air}^2}} -1\right]\right\} m_{i0(air)},$$

can be easily reduced, making possible to produce a controlled *Gravitational Shielding* (similar to a GCC) surround the sphere.

This becomes possible to build a spacecraft to work with a gravitational shielding as shown in Fig. 4.

The *gravity accelerations* on the spacecraft (due to the rest of the Universe. See Fig.4) is given by

$$g_i' = \chi_{air} g_i \qquad i = 1, 2, 3 \ldots n$$

Where $\chi_{air} = m_{g(air)}/m_{i0(air)}$. Thus, the *gravitational forces* acting on the spacecraft are given by

$$F_{is} = M_g g_i' = M_g\left(\chi_{air} g_i\right)$$

By reducing the value of χ_{air}, these forces can be reduced.

According to the *Mach's principle*;

"The *local inertial forces* are determined by the *gravitational interactions* of the local system with the distribution of the cosmic masses".

Thus, the local inertia is just the gravitational influence of the rest of matter existing in the Universe. Consequently, if we reduce the gravitational interactions between a spacecraft and the rest of the Universe, then *the inertial properties of the spacecraft* will be also reduced. This effect leads to a new concept of spacecraft and space flight.

Since χ_{air} is given by

$$\chi_{air} = \frac{m_{g(air)}}{m_{i0(air)}} = \left\{1-2\left[\sqrt{1+\frac{\mu_0}{4c^2}\left(\frac{\sigma_{air}}{4\pi f}\right)^3 \frac{V_{rms}^4}{a^4\rho_{air}^2}} -1\right]\right\}$$

Then, for $\sigma_{air} \cong 10^6 s.m^{-1}$, $f = 6Hz$, $a = 5m$, $\rho_{air} \cong 1Kg.m^{-3}$ and $V_{rms} = 3.35KV$ we get

$$\chi_{air} \cong 0$$

Under these conditions, the gravitational forces upon the spacecraft become approximately nulls and consequently, the spacecraft practically *loses its inertial properties.*

Out of the terrestrial atmosphere, the gravity acceleration upon the spacecraft is negligible and therefore the gravitational shielding is not necessary. However, if the spacecraft is in the outer space and we want to use the gravitational shielding then, χ_{air} must be replaced by χ_{vac} where

$$\chi_{vac} = \frac{m_{g(vac)}}{m_{i0(vac)}} = \left\{1-2\left[\sqrt{1+\frac{\mu_0}{4c^2}\left(\frac{\sigma_{vac}}{4\pi f}\right)^3 \frac{V_{rms}^4}{a^4\rho_{vac}^2}} -1\right]\right\}$$

The electrical conductivity of the ionized outer space (very close to the spacecraft) is small; however, its density is remarkably small $\left(<< 10^{-16} Kg.m^{-3}\right)$, in such a manner that the smaller value of the factor $\sigma_{vac}^3/\rho_{vac}^2$ can be easily compensated by the increase of V_{rms}.

It was shown that, when the gravitational mass of a particle is reduced to ranging between $+0.159M_i$ to $-0.159M_i$, it becomes *imaginary* [1], i.e., the gravitational and the inertial masses of the particle become *imaginary*. Consequently, the particle disappears from our ordinary space-time. However, the factor $\chi = M_{g(imaginary)}/M_{i(imaginary)}$ remains *real* because

$$\chi = \frac{M_{g(imaginary)}}{M_{i(imaginary)}} = \frac{M_g i}{M_i i} = \frac{M_g}{M_i} = real$$

Thus, if the gravitational mass of the particle is reduced by means of absorption of an amount of electromagnetic energy U, for example, we have

$$\chi = \frac{M_g}{M_i} = \left\{1 - 2\left[\sqrt{1+\left(U/m_{i0}c^2\right)^2} - 1\right]\right\}$$

This shows that the energy U of the electromagnetic field *remains acting on* the imaginary particle. In practice, this means that *electromagnetic fields act on imaginary particles*. Therefore, the electromagnetic field of a GCC remains acting on the particles inside the GCC even when their gravitational masses reach the gravitational mass ranging between $+0.159M_i$ to $-0.159M_i$ and they become imaginary particles. This is very important because it means that the GCCs of a gravitational spacecraft keep on working when the spacecraft becomes imaginary.

Under these conditions, the gravity accelerations on the *imaginary* spacecraft particle (due to the rest of the imaginary Universe) are given by

$$g'_j = \chi\ g_j \qquad j = 1,2,3,\ldots,n.$$

Where $\chi = M_{g(imaginary)}/M_{i(imaginary)}$ and $g_j = -Gm_{gj(imaginary)}/r_j^2$. Thus, the gravitational forces acting on the spacecraft are given by

$$\begin{aligned} F_{gj} &= M_{g(imaginary)} g'_j = \\ &= M_{g(imaginary)}\left(-\chi G m_{gj(imaginary)}/r_j^2\right) = \\ &= M_g i\left(-\chi G m_{gj} i/r_j^2\right) = +\chi G M_g m_{gj}/r_j^2 . \end{aligned}$$

Note that these forces are *real*. Remind that, the Mach's principle says that the *inertial effects* upon a particle are consequence of the gravitational interaction of the particle with the rest of the Universe. Then we can conclude that the *inertial forces* upon an *imaginary* spacecraft are also *real*. Consequently, it can travel in the imaginary space-time using its thrusters.

It was shown that, *imaginary particles* can have *infinite speed* in the *imaginary space-time* [1] . Therefore, this is also the speed upper limit for the spacecraft in the imaginary space-time.

Since the gravitational spacecraft can use its thrusters after to becoming an imaginary body, then if the thrusters produce a total thrust $F = 1000kN$ and the gravitational mass of the spacecraft is reduced from $M_g = M_i = 10^5 kg$ down to $M_g \cong 10^{-6} kg$, the acceleration of the spacecraft will be, $a = F/M_g \cong 10^{12} m.s^{-2}$. With this acceleration the spacecraft crosses the "visible" Universe ($diameter = d \approx 10^{26} m$) in a time interval $\Delta t = \sqrt{2d/a} \cong 1.4 \times 10^7 m.s^{-1} \cong 5.5\ months$

Since the inertial effects upon the spacecraft are reduced by $M_g/M_i \cong 10^{-11}$ then, in spite of the effective spacecraft acceleration be $a = 10^{12} m.s^{-1}$, the effects for the crew and for the spacecraft will be equivalent to an acceleration a' given by

$$a' = \frac{M_g}{M_i} a \approx 10 m.s^{-1}$$

This is the order of magnitude of the acceleration upon of a commercial jet aircraft.

On the other hand, the travel in the *imaginary* space-time can be very safe, because there won't any material body along the trajectory of the spacecraft.

Now consider the GCCs presented in Fig. 8 (a). Note that below and above the *air* are the bottom and the top of the chamber. Therefore the choice of the material of the chamber is highly relevant. If the chamber is made of steel, for example, and the gravity acceleration below the chamber is g then at the bottom of the chamber, the gravity becomes $g' = \chi_{steel}\, g$; in the air, the gravity is $g'' = \chi_{air} g' = \chi_{air}\chi_{steel} g$. At the top of the chamber, $g''' = \chi_{steel} g'' = (\chi_{steel})^2 \chi_{air} g$. Thus, out of the chamber (close to the top) the gravity acceleration becomes g'''. (See Fig. 8 (a)). However, for the steel at $B < 300T$ and $f = 1\times 10^{-6} Hz$, we have

$$\chi_{steel} = \frac{m_{g(steel)}}{m_{i(steel)}} = \left\{1 - 2\left[\sqrt{1 + \frac{\sigma_{(steel)} B^4}{4\pi f \mu \rho^2_{(steel)} c^2}} - 1\right]\right\} \cong 1$$

Since $\rho_{steel} = 1.1\times 10^6 S.m^{-1}$, $\mu_r = 300$ and $\rho_{(steel)} = 7800 k.m^{-3}$.

Thus, due to $\chi_{steel} \cong 1$ it follows that

$$g''' \cong g'' = \chi_{air}\, g' \cong \chi_{air}\, g$$

If instead of one GCC we have *three* GCC, all with steel box (Fig. 8(b)), then the gravity acceleration above the *second* GCC, g_2 will be given by

$$g_2 \cong \chi_{air} g_1 \cong \chi_{air}\chi_{air} g$$

and the gravity acceleration above the *third* GCC, g_3 will be expressed by

$$g_3 \cong \chi_{air} g'' \cong \chi_{air}{}^3 g$$

III. CONSEQUENCES

These results point to the possibility to convert gravitational energy into rotational mechanical energy. Consider for example the system presented in Fig. 9. Basically it is a motor with massive iron rotor and a box filled with gas or plasma at ultra-low pressure (Gravity Control Cell-GCC) as shown in Fig. 9. The GCC is placed below the rotor in order to become *negative* the acceleration of gravity inside *half* of the rotor $\left(g' = (\chi_{steel})^2 \chi_{air}\, g \cong \chi_{air}\, g = -ng\right)$. Obviously this causes a torque $T = (-F' + F)r$ and the rotor spins with angular velocity ω. The average power, P, of the motor is given by

$$P = T\omega = [(-F' + F)r]\omega \qquad (36)$$

Where

$$F' = \tfrac{1}{2} m_g g' \qquad F = \tfrac{1}{2} m_g g$$

and $m_g \cong m_i$ (mass of the rotor). Thus, Eq. (36) gives

$$P = (n+1)\frac{m_i g \omega\, r}{2} \qquad (37)$$

On the other hand, we have that

$$-g' + g = \omega^2 r \qquad (38)$$

Therefore the angular speed of the rotor is given by

$$\omega = \sqrt{\frac{(n+1)g}{r}} \qquad (39)$$

By substituting (39) into (37) we obtain the expression of the average power of the *gravitational motor*, i.e.,

$$P = \tfrac{1}{2} m_i \sqrt{(n+1)^3 g^3 r} \qquad (40)$$

Now consider an electric generator coupling to the gravitational motor in order to produce electric energy.

Since $\omega = 2\pi f$ then for $f = 60Hz$ we have $\omega = 120\pi rad.s^{-1} = 3600\, rpm$.

Therefore for $\omega = 120\pi rad.s^{-1}$ and $n = 788$ $(B \cong 0.22T)$ the Eq. (40) tell us that we must have

$$r = \frac{(n+1)g}{\omega^2} = 0.0545m$$

Since $r = R/3$ and $m_i = \rho\pi R^2 h$ where ρ, R and h are respectively the mass density, the radius and the height of the rotor then for $h = 0.5m$ and $\rho = 7800 Kg.m^{-3}$ (iron) we obtain

$$m_i = 327.05kg$$

Then Eq. (40) gives

$$P \cong 2.19\times10^{5}\, watts \cong 219\ KW \cong 294 HP \qquad (41)$$

This shows that the *gravitational motor* can be used to yield electric energy at large scale.

The possibility of gravity control leads to a new concept of spacecraft which is presented in Fig. 10. Due to the *Meissner effect*, the magnetic field *B* is expelled from the *superconducting shell*. The Eq. (35) shows that a magnetic field, B, through the *aluminum shell* of the spacecraft reduces its gravitational mass according to the following expression:

$$m_{g(Al)} = \left\{1-2\left[\sqrt{1+\left(\frac{B^2}{\mu c^2 \rho_{(Al)}} n_{r(Al)}\right)^2}-1\right]\right\} m_{i(Al)} \qquad (42)$$

If the frequency of the magnetic field is $f = 10^{-4} Hz$ then we have that $\sigma_{(Al)} >> \omega\varepsilon$ since the electric conductivity of the aluminum is $\sigma_{(Al)} = 3.82\times10^{7}\, S.m^{-1}$. In this case, the Eq. (11) tell us that

$$n_{r(Al)} = \sqrt{\frac{\mu c^2 \sigma_{(Al)}}{4\pi f}} \qquad (43)$$

Substitution of (43) into (42) yields

$$m_{g(Al)} = \left\{1-2\left[\sqrt{1+\frac{\sigma_{(Al)} B^4}{4\pi f \mu \rho_{(Al)}^2 c^2}}-1\right]\right\} m_{i(Al)} \qquad (44)$$

Since the mass density of the Aluminum is $\rho_{(Al)} = 2700\, kg.m^{-3}$ then the Eq. (44) can be rewritten in the following form:

$$\chi_{Al} = \frac{m_{g(Al)}}{m_{i(Al)}} = \left\{1-2\left[\sqrt{1+3.68\times10^{-8} B^4}-1\right]\right\} \qquad (45)$$

In practice it is possible to adjust B in order to become, for example, $\chi_{Al} \cong 10^{-9}$. This occurs to $B \cong 76.3T$. (Novel superconducting magnets are able to produce up to $14.7T$ [10, 11]).

Then the gravity acceleration in any direction *inside* the spacecraft, g_l', will be reduced and given by

$$g_l' = \frac{m_{g(Al)}}{m_{i(Al)}} g_l = \chi_{Al} g_l \cong -10^{-9} g_l \quad l = 1,2,..,n$$

Where g_l is the *externa*l gravity in the direction l. We thus conclude that the gravity acceleration inside the spacecraft becomes negligible if $g_l << 10^{9}\, m.s^{-2}$. This means that the aluminum shell, under these conditions, works like a gravity shielding.

Consequently, the gravitational forces between anyone point inside the spacecraft with gravitational mass, m_{gj}, and another external to the spacecraft (gravitational mass m_{gk}) are given by

$$\vec{F}_j = -\vec{F}_k = -G\frac{m_{gj} m_{gk}}{r_{jk}^2}\hat{\mu}$$

where $m_{gk} \cong m_{ik}$ and $m_{gj} = \chi_{Al} m_{ij}$. Therefore we can rewrite equation above in the following form

$$\vec{F}_j = -\vec{F}_k = -\chi_{Al} G\frac{m_{ij} m_{ik}}{r_{jk}^2}\hat{\mu}$$

Note that when $B = 0$ the *initial gravitational forces* are

$$\vec{F}_j = -\vec{F}_k = -G\frac{m_{ij} m_{ik}}{r_{jk}^2}\hat{\mu}$$

Thus, if $\chi_{Al} \cong -10^{-9}$ then the initial gravitational forces are reduced from 10^9 times and become repulsives.

According to the new expression for the *inertial forces* [1], $\vec{F} = m_g \vec{a}$, we see that these forces have origin in the *gravitational interaction* between a particle and the others of the Universe, just as *Mach's principle* predicts. Hence mentioned expression incorporates the Mach's principle into Gravitation Theory, and furthermore reveals that the inertial effects upon a body can be strongly reduced by means of the decreasing of its gravitational mass.

Consequently, we conclude that if the *gravitational forces* upon the spacecraft are reduced from 10^9 times then also the *inertial forces* upon the

spacecraft will be reduced from 10^9 times when $\chi_{Al} \cong -10^{-9}$. Under these conditions, the inertial effects on the crew would be strongly decreased. Obviously this leads to a new concept of aerospace flight.

Inside the spacecraft the gravitational forces between the dielectric with gravitational mass, M_g and the man (gravitational mass, m_g), when $B = 0$ are

$$\vec{F}_m = -\vec{F}_M = -G\frac{M_g m_g}{r^2}\hat{\mu} \qquad (46)$$

or

$$\vec{F}_m = -G\frac{M_g}{r^2} m_g \hat{\mu} = -m_g g_M \hat{\mu} \qquad (47)$$

$$\vec{F}_M = +G\frac{m_g}{r^2} M_g \hat{\mu} = +M_g g_m \hat{\mu} \qquad (48)$$

If the *superconducting box* under M_g (Fig. 10) is filled with *air* at ultra-low pressure (3×10^{-12} torr, 300K for example) then, when $B \neq 0$, the gravitational mass of the *air* will be reduced according to (35). Consequently, we have

$$g'_M = (\chi_{steel})^2 \chi_{air} g_M \cong \chi_{air} g_M \qquad (49)$$

$$g'_m = (\chi_{steel})^2 \chi_{air} g_m \cong \chi_{air} g_m \qquad (50)$$

Then the forces $\vec{F}_m$ and $\vec{F}_M$ become

$$\vec{F}_m = -m_g(\chi_{air} g_M)\hat{\mu} \qquad (51)$$

$$\vec{F}_M = +M_g(\chi_{air} g_m)\hat{\mu} \qquad (52)$$

Therefore if $\chi_{air} = -n$ we will have

$$\vec{F}_m = +n m_g g_M \hat{\mu} \qquad (53)$$

$$\vec{F}_M = -n M_g g_m \hat{\mu} \qquad (54)$$

Thus, $\vec{F}_m$ and $\vec{F}_M$ become *repulsive*. Consequently, the man inside the spacecraft is subjected to a gravity acceleration given by

$$\vec{a}_{man} = n g_M \hat{\mu} = -\chi_{air} G\frac{M_g}{r^2}\hat{\mu} \qquad (55)$$

Inside the GCC we have,

$$\chi_{air} = \frac{m_{g(air)}}{m_{i(air)}} = \left\{1 - 2\left[\sqrt{1 + \frac{\sigma_{(air)} B^4}{4\pi f \mu \rho^2_{(air)} c^2}} - 1\right]\right\} \qquad (56)$$

By ionizing the air inside the GCC (Fig. 10), for example, by means of a *radioactive* material, it is possible to increase the *air conductivity* inside the GCC up to $\sigma_{(air)} \cong 10^6 S.m^{-1}$. Then for $f = 10\ Hz$; $\rho_{(air)} = 4.94\times10^{-15} kg.m^{-3}$ (Air at 3×10^{-12} torr, 300K) and we obtain

$$\chi_{air} = \left\{2\left[\sqrt{1 + 2.8\times10^{21} B^4} - 1\right] - 1\right\} \qquad (57)$$

For $B = B_{GCC} = 0.1T$ (note that, due to the *Meissner effect*, the magnetic field B_{GCC} stay confined inside the *superconducting box*) the Eq. (57) yields

$$\chi_{air} \cong -10^9$$

Since there is no magnetic field through the *dielectric* presented in Fig.10 then, $M_g \cong M_i$. Therefore if $M_g \cong M_i = 100Kg$ and $r = r_0 \cong 1m$ the gravity acceleration upon the man, according to Eq. (55), is

$$a_{man} \cong 10 m.s^{-1}$$

Consequently it is easy to see that this system is ideal to yield artificial gravity inside the spacecraft in the case of *inter-stellar travel*, when the gravity acceleration out of the spacecraft - due to the Universe - becomes negligible.

The *vertical* displacement of the spacecraft can be produced by means of *Gravitational Thrusters*. A schematic diagram of a Gravitational Thruster is shown in Fig.11. The Gravitational Thrusters can also provide the *horizontal* displacement of the spacecraft.

The concept of Gravitational Thruster results from the theory of the *Gravity Control Battery*, showed in Fig. 8 (b). Note that the number of GCC increases the thrust of the thruster. For example, if the thruster has *three* GCCs then the gravity acceleration upon the gas sprayed inside the thruster will be *repulsive* in respect to M_g (See Fig. 11(a)) and given by

$$a_{gas} = (\chi_{air})^3 (\chi_{steel})^4 g \cong -(\chi_{air})^3 G\frac{M_g}{r_0^2}$$

Thus, if inside the GCCs, $\chi_{air} \cong -10^9$

(See Eq. 56 and 57) then the equation above gives

$$a_{gas} \cong +10^{27} G \frac{M_i}{r_0^2}$$

For $M_i \cong 10kg$, $r_0 \cong 1m$ and $m_{gas} \cong 10^{-12} kg$ the thrust is

$$F = m_{gas} a_{gas} \cong 10^5 N$$

Thus, the Gravitational Thrusters are able to produce strong thrusts.

Note that in the case of very strong χ_{air}, for example $\chi_{air} \cong -10^9$, the gravity accelerations upon the boxes of the second and third GCCs become very strong (Fig.11 (a)). Obviously, the walls of the mentioned boxes cannot to stand the enormous pressures. However, it is possible to build a similar system with 3 or more GCCs, *without material boxes*. Consider for example, a surface with several radioactive sources (Am-241, for example). The *alpha* particles emitted from the Am-241 cannot reach besides 10cm of air. Due to the trajectory of the alpha particles, three or more successive layers of air, with different electrical conductivities σ_1, σ_2 and σ_3, will be established in the ionized region (See Fig.11 (b)). It is easy to see that the gravitational shielding effect produced by these three layers is similar to the effect produced by the 3 GCCs shown in Fig. 11 (a).

It is important to note that if F is force produced by a thruster then the spacecraft acquires acceleration $a_{spacecraft}$ given by [1]

$$a_{spacecraft} = \frac{F}{M_{g(spacecraft)}} = \frac{F}{\chi_{Al} M_{i(inside)} + m_{i(Al)}}$$

Therefore if $\chi_{Al} \cong 10^{-9}$; $M_{i(inside)} = 10^4 Kg$ and $m_{i(Al)} = 100 Kg$ (inertial mass of the aluminum shell) then it will be necessary $F = 10kN$ to produce

$$a_{spacecraft} = 100 m.s^{-2}$$

Note that the concept of Gravitational Thrusters leads directly to the *Gravitational Turbo Motor* concept (See Fig. 12).

Let us now calculate the gravitational forces between two very close *thin* layers of the *air* around the spacecraft. (See Fig. 13).

The gravitational force dF_{12} that dm_{g1} exerts upon dm_{g2}, and the gravitational force dF_{21} that dm_{g2} exerts upon dm_{g1} are given by

$$d\vec{F}_{12} = d\vec{F}_{21} = -G \frac{dm_{g2} dm_{g1}}{r^2} \hat{\mu} \qquad (58)$$

Thus, the gravitational forces between the *air layer* 1, gravitational mass m_{g1}, and the *air layer* 2, gravitational mass m_{g2}, around the spacecraft are

$$\vec{F}_{12} = -\vec{F}_{21} = -\frac{G}{r^2} \int_0^{m_{g1}} \int_0^{m_{g2}} dm_{g1} dm_{g2} \hat{\mu} =$$

$$= -G \frac{m_{g1} m_{g2}}{r^2} \hat{\mu} = -\chi_{air} \chi_{air} G \frac{m_{i1} m_{i2}}{r^2} \hat{\mu} \qquad (59)$$

At 100km altitude the air pressure is $5.691 \times 10^{-3} torr$ and $\rho_{(air)} = 5.998 \times 10^{-6} kg.m^{-3}$ [12]. By ionizing the air surround the spacecraft, for example, by means of an oscillating electric field, E_{osc}, starting from the surface of the spacecraft (See Fig. 13) it is possible to increase the *air conductivity* near the spacecraft up to $\sigma_{(air)} \cong 10^6 S.m^{-1}$. Since $f = 1Hz$ and, in this case $\sigma_{(air)} >> \omega\varepsilon$, then, according to Eq. (11), $n_r = \sqrt{\mu \sigma_{(air)} c^2 / 4\pi f}$. From Eq.(56) we thus obtain

$$\chi_{air} = \frac{m_{g(air)}}{m_{i(air)}} = \left\{ 1 - 2 \left[\sqrt{1 + \frac{\sigma_{(air)} B^4}{4\pi f \mu_0 \rho_{(air)}^2 c^2}} - 1 \right] \right\} \qquad (60)$$

Then for $B = 763T$ the Eq. (60) gives

$$\chi_{air} = \left\{ 1 - 2 \left[\sqrt{1 + \sim 10^4 B^4} - 1 \right] \right\} \cong -10^8 \qquad (61)$$

By substitution of $\chi_{air} \cong -10^8$ into Eq., (59) we get

$$\vec{F}_{12} = -\vec{F}_{21} = -10^{16} G \frac{m_{i1} m_{i2}}{r^2} \hat{\mu} \qquad (62)$$

If $m_{i1} \cong m_{i2} = \rho_{air} \boldsymbol{V}_1 \cong \rho_{air} \boldsymbol{V}_2 \cong 10^{-8} kg$, and $r = 10^{-3} m$ we obtain

$$\vec{F}_{12} = -\vec{F}_{21} \cong -10^{-4} N \qquad (63)$$

These forces are much more intense than the *inter-atomic forces* (the forces which maintain joined atoms, and molecules that make the solids and liquids) whose intensities, according to the Coulomb's law, is of the order of 1-1000×10^{-8}N.

Consequently, the air around the spacecraft will be strongly compressed upon their surface, making an "*air shell*" that will accompany the spacecraft during its displacement and will protect the *aluminum shell* of the direct attrition with the Earth's atmosphere.

In this way, during the flight, the attrition would occur just between the "air shell" and the atmospheric air around her. Thus, the spacecraft would stay free of the thermal effects that would be produced by the direct attrition of the aluminum shell with the Earth's atmosphere.

Another interesting effect produced by the magnetic field B of the spacecraft is the possibility of to lift a body from the surface of the Earth to the spacecraft as shown in Fig. 14. By ionizing the air surround the spacecraft, by means of an oscillating electric field, E_{osc}, the *air conductivity* near the spacecraft can reach, for example, $\sigma_{(air)} \cong 10^6 S.m^{-1}$. Then for $f = 1Hz$; $B = 40.8T$ and $\rho_{(air)} \cong 1.2kg.m^{-3}$ (300K and 1 atm) the Eq. (56) yields

$$\chi_{air} = \left\{1 - 2\left[\sqrt{1 + 4.9 \times 10^{-7} B^4} - 1\right]\right\} \cong -0.1$$

Thus, the weight of the body becomes

$$P_{body} = m_{g(body)} g = \chi_{air} m_{i(body)} g = m_{i(body)} g'$$

Consequently, the body will be lifted on the direction of the spacecraft with acceleration

$$g' = \chi_{air} g \cong +0.98 m.s^{-1}$$

Let us now consider an important aspect of the flight dynamics of a Gravitational Spacecraft.

Before starting the flight, the *gravitational mass of the spacecraft*, M_g, must be strongly reduced, by means of a gravity control system, in order to produce – with a weak thrust $\vec{F}$, a strong acceleration, $\vec{a}$, given by [1]

$$\vec{a} = \frac{\vec{F}}{M_g}$$

In this way, the spacecraft could be strongly accelerated and quickly to reach very high speeds near speed of light.

If the gravity control system of the spacecraft is *suddenly* turned off, the *gravitational mass* of the spacecraft becomes immediately equal to its *inertial mass*, M_i, $\left(M'_g = M_i\right)$ and the velocity $\vec{V}$ becomes equal to $\vec{V}'$. According to the *Momentum* Conservation Principle, we have that

$$M_g V = M'_g V'$$

Supposing that the spacecraft was traveling in space with speed $V \approx c$, and that its gravitational mass it was $M_g = 1Kg$ and $M_i = 10^4 Kg$ then the velocity of the spacecraft is reduced to

$$V' = \frac{M_g}{M'_g} V = \frac{M_g}{M_i} V \approx 10^{-4} c$$

Initially, when the velocity of the spacecraft is $\vec{V}$, its kinetic energy is $E_k = \left(M_g - m_g\right)c^2$. Where $M_g = m_g \Big/ \sqrt{1 - V^2/c^2}$. At the instant in which the gravity control system of the spacecraft is turned off, the kinetic energy becomes $E'_k = \left(M'_g - m'_g\right)c^2$. Where $M'_g = m'_g \Big/ \sqrt{1 - V'^2/c^2}$.

We can rewritten the expressions of E_k and E'_k in the following form

$$E_k = \left(M_g V - m_g V\right)\frac{c^2}{V}$$

$$E'_k = \left(M'_g V' - m'_g V'\right)\frac{c^2}{V'}$$

Substitution of $M_g V = M'_g V' = p$,

$m_g V = p\sqrt{1-V^2/c^2}$ and $m'_g V' = p\sqrt{1-V'^2/c^2}$ into the equations of E_k and E'_k gives

$$E_k = \left(1-\sqrt{1-V^2/c^2}\right)\frac{pc^2}{V}$$

$$E'_k = \left(1-\sqrt{1-V'^2/c^2}\right)\frac{pc^2}{V'}$$

Since $V \approx c$ then follows that

$$E_k \approx pc$$

On the other hand, since $V' << c$ we get

$$E'_k = \left(1-\sqrt{1-V'^2/c^2}\right)\frac{pc^2}{V'} =$$

$$\cong \left(1-\frac{1}{1+\frac{V'^2}{2c^2}+\ldots}\right)\frac{pc^2}{V'} \cong \left(\frac{V'}{2c}\right)pc$$

Therefore we conclude that $E_k >> E'_k$. Consequently, when the gravity control system of the spacecraft is turned off, occurs an *abrupt* decrease in the kinetic energy of the spacecraft, ΔE_k, given by

$$\Delta E_k = E_k - E'_k \approx pc \approx M_g c^2 \approx 10^{17}\,J$$

By comparing the energy ΔE_k with the *inertial energy* of the spacecraft, $E_i = M_i c^2$, we conclude that

$$\Delta E_k \approx \frac{M_g}{M_i} E_i \approx 10^{-4} M_i c^2$$

The energy ΔE_k (several *megatons*) must be released in very short time interval. It is approximately the same amount of energy that would be released in the case of collision of the spacecraft[‡]. However, the situation is very different of a collision (M_g just becomes suddenly equal to M_i), and possibly the energy ΔE_k is converted into a *High Power Electromagnetic Pulse*.

[‡] In this case, the collision of the spacecraft would release $\approx 10^{17}$J (several megatons) and it would be similar to a powerful *kinetic weapon*.

Obviously this electromagnetic pulse (EMP) will induce heavy currents in all electronic equipment that mainly contains semiconducting and conducting materials. This produces immense heat that melts the circuitry inside. As such, *while not being directly responsible for the loss of lives*, these EMP are capable of disabling electric/electronic systems. Therefore, we possibly have a new type of *electromagnetic bomb*. An *electromagnetic bomb* or *E-bomb* is a well-known weapon designed to disable electric/electronic systems on a wide scale with an intense electromagnetic pulse.

Based on the theory of the GCC it is also possible to build a *Gravitational Press* of *ultra-high* pressure as shown in Fig.15.

The chamber 1 and 2 are GCCs with air at 1×10^{-4}torr, 300K $\left(\sigma_{(air)} \approx 10^6\, S.m^{-1};\ \rho_{(air)} = 5\times10^{-8}\, kg.m^{-3}\right)$. Thus, for $f = 10Hz$ and $B = 0.107T$ we have

$$\chi_{air} = \left\{1-2\left[\sqrt{1+\frac{\sigma_{(air)}B^4}{4\pi f\mu_0\rho^2_{(air)}c^2}}-1\right]\right\} \cong -118$$

The gravity acceleration above the air of the chamber 1 is

$$\vec{g}_1 = \chi_{stell}\chi_{air} g\hat{\mu} \cong +1.15\times10^3\,\hat{\mu} \qquad (64)$$

Since, in this case, $\chi_{steel} \cong 1$; $\hat{\mu}$ is an *unitary vector* in the opposite direction of $\vec{g}$.

Above the air of the chamber 2 the gravity acceleration becomes

$$\vec{g}_2 = (\chi_{stell})^2(\chi_{air})^2 g\hat{\mu} \cong -1.4\times10^5\,\hat{\mu} \qquad (65)$$

Therefore the *resultant* force $\vec{R}$ acting on m_2, m_1 and m is

$$\vec{R} = \vec{F}_2 + \vec{F}_1 + \vec{F} = m_2\vec{g}_2 + m_1\vec{g}_1 + m\vec{g} =$$
$$= -1.4\times10^5 m_2\hat{\mu} + 1.15\times10^3 m_1\hat{\mu} - 9.81m\hat{\mu} =$$
$$\cong -1.4\times10^5 m_2\hat{\mu} \qquad (66)$$

where

$$m_2 = \rho_{steel}V_{disk\,2} = \rho_{steel}\left(\frac{\pi}{4}\phi_{inn}^2 H\right) \qquad (67)$$

Thus, for $\rho_{steel} \cong 10^4\, kg.m^{-3}$ we can write that

$$F_2 \cong 10^9\phi_{inn}^2 H$$

For the steel $\tau \cong 10^5\, kg.cm^{-2} = 10^9\, kg.m^{-2}$ consequently we must have $F_2/S_\tau < 10^9\, kg.m^{-2}$ ($S_\tau = \pi\phi_{inn}H$ see Fig.15). This means that

$$\frac{10^9\phi_{inn}^2 H}{\pi\phi_{inn}H} < 10^9\, kg.m^{-2}$$

Then we conclude that

$$\phi_{inn} < 3.1m$$

For $\phi_{inn} = 2m$ and $H = 1m$ the Eq. (67) gives

$$m_2 \cong 3\times10^4\, kg$$

Therefore from the Eq. (66) we obtain

$$R \cong 10^{10}\, N$$

Consequently, in the area $S = 10^{-4}m^2$ of the Gravitational Press, the pressure is

$$p = \frac{R}{S} \cong 10^{14}\, N.m^{-2}$$

This enormous pressure is much greater than the pressure in the center of the Earth ($3.617\times10^{11}\, N.m^{-2}$) [13]. It is near of the gas pressure in the *center of the sun* ($2\times10^{16}\, N.m^{-2}$). Under the action of such intensities new states of matter are created and astrophysical phenomena may be simulated in the lab for the first time, e.g. supernova explosions. Controlled thermonuclear fusion by inertial confinement, fast nuclear ignition for energy gain, novel collective acceleration schemes of particles and the numerous variants of material processing constitute examples of progressive applications of such *Gravitational Press* of ultra-high pressure.

The GCCs can also be applied on generation and detection of *Gravitational Radiation*.

Consider a cylindrical GCC (GCC antenna) as shown in Fig.16 (a). The *gravitational mass* of the *air* inside the GCC is

$$m_{g(air)} = \left\{1 - 2\left[\sqrt{1 + \frac{\sigma_{(air)}B^4}{4\pi f\mu\rho_{(air)}^2 c^2}} - 1\right]\right\} m_{i(air)} \qquad (68)$$

By varying B one can varies $m_{g(air)}$ and consequently to vary the gravitational field generated by $m_{g(air)}$, producing then gravitational radiation. Then a GCC can work like a *Gravitational Antenna*.

Apparently, Newton's theory of gravity had no gravitational waves because, if a gravitational field changed in some way, that change took place *instantaneously* everywhere in space, and one can think that there is not a wave in this case. However, we have already seen that the gravitational interaction can be repulsive, besides attractive. Thus, as with electromagnetic interaction, the gravitational interaction must be produced by the exchange of "virtual" *quanta of* spin 1 and mass null, i.e., the *gravitationa*l "virtual" *quanta* (*graviphoton*) must have spin 1 and not 2. Consequently, the fact of a change in a gravitational field reach *instantaneously* everywhere in space occurs simply due to the speed of the *graviphoton* to be *infinite*. It is known that there is no speed limit for "*virtual*" photons. On the contrary, the *electromagnetic quanta* ("virtual" photons) could not communicate the *electromagnetic interaction* an infinite distance.

Thus, there are *two types* of gravitational radiation: the *real* and *virtual*, which is constituted of graviphotons; the *real* gravitational waves are ripples in the space-time generated by *gravitational field* changes. According to Einstein's theory of gravity the velocity of propagation of these waves is equal to the speed of light (c).

Unlike the electromagnetic waves the *real* gravitational waves have low interaction with matter and consequently low scattering. Therefore *real* gravitational waves are suitable as a means of transmitting information. However, when the distance between transmitter and receiver is too large, for example of the order of magnitude of several light-years, the transmission of information by means of gravitational waves becomes impracticable due to the long time necessary to receive the information. On the other hand, there is no delay during the transmissions by means of *virtual* gravitational radiation. In addition the scattering of this radiation is null. Therefore the *virtual* gravitational radiation is very suitable as a means of transmitting information at any distances including astronomical distances.

As concerns detection of the *virtual* gravitational radiation from GCC antenna, there are many options. Due to *Resonance Principle* a similar GCC antenna (receiver) *tuned at the same frequency* can absorb energy from an incident *virtual* gravitational radiation (See Fig.16 (b)). Consequently, the gravitational mass of the air inside the GCC receiver will vary such as the gravitational mass of the air inside the GCC transmitter. This will induce a magnetic field similar to the magnetic field of the GCC transmitter and therefore the current through the coil inside the GCC receiver will have the same characteristics of the current through the coil inside the GCC transmitter. However, the *volume* and *pressure* of the air inside the two GCCs must be exactly the same; also the *type* and the *quantity of atoms* in the air inside the two GCCs must be exactly the same. Thus, the GCC antennas are simple but they are not easy to build.

Note that a GCC antenna radiates *graviphotons* and *gravitational waves* simultaneously (Fig. 16 (a)). Thus, it is not only a gravitational antenna: it is a *Quantum Gravitational Antenna* because it can also emit and detect gravitational "virtual" *quanta* (graviphotons), which, in turn, can transmit information *instantaneously* from any distance in the Universe *without* scattering.

Due to the difficulty to build two similar GCC antennas and, considering that the electric current in the receiver antenna can be detectable even if the gravitational mass of the nuclei of the antennas are not *strongly* reduced, then we propose to replace the gas at the nuclei of the antennas by a thin *dielectric lamina*. The dielectric lamina with exactly 10^8 atoms (10^3atoms $\times$ 10^3atoms $\times$ 10^2atoms) is placed between the plates (electrodes) as shown in Fig. 17. When the *virtual* gravitational radiation strikes upon the dielectric lamina, its gravitational mass varies similarly to the gravitational mass of the dielectric lamina of the transmitter antenna, inducing an electromagnetic field (E, B) similar to the transmitter antenna. Thus, the electric current in the receiver antenna will have the same characteristics of the current in the transmitter antenna. In this way, it is then possible to build two similar antennas whose nuclei have the same volumes and the same types and quantities of atoms.

Note that the Quantum Gravitational Antennas can also be used to transmit *electric power*. It is easy to see that the Transmitter and Receiver (Fig. 17(a)) can work with strong voltages and electric currents. This means that strong electric power can be transmitted among Quantum Gravitational Antennas. This obviously solves the problem of *wireless* electric power transmission.

The existence of *imaginary masses* has been predicted in a previous work [1]. Here we will propose a method and a device using GCCs for obtaining *images* of *imaginary bodies*.

It was shown that the *inertial* imaginary mass associated to an *electron* is given by

$$m_{ie(ima)} = \frac{2}{\sqrt{3}}\left(\frac{hf}{c^2}\right)i = \frac{2}{\sqrt{3}}m_{ie(real)}\, i \qquad (69)$$

Assuming that the correlation between the gravitational mass and the inertial mass (Eq.6) is the same for both imaginary and real masses then follows that the *gravitational* imaginary mass associated to an *electron* can be written in the following form:

$$m_{ge(ima)} = \left\{1-2\left[\sqrt{1+\left(\frac{U}{m_i c^2}n_r\right)^2}-1\right]\right\}m_{ie(ima)} \qquad (70)$$

Thus, the gravitational *imaginary* mass *associated to matter* can be *reduced*, made

negative and *increased,* just as the gravitational *real* mass.

It was shown that also *photons* have imaginary mass. Therefore, the imaginary mass can be associated or *not* to the matter.

In a general way, the gravitational forces between two gravitational imaginary masses are then given by

$$\vec{F} = -\vec{F} = -G\frac{(iM_g)(im_g)}{r^2}\hat{\mu} = +G\frac{M_g m_g}{r^2}\hat{\mu} \qquad (71)$$

Note that these forces are *real* and *repulsive*.

Now consider a gravitational imaginary mass, $m_{g(ima)} = im_g$, *not associated with matter* (like the gravitational imaginary mass associated to the photons) and another gravitational imaginary mass $M_{g(ima)} = iM_g$ *associated to* a *material* body.

*Any material body has an imaginary mass associated to it, d*ue to the existence of imaginary masses associated to the electrons. We will choose a *quartz crystal* (for the material body with gravitational imaginary mass $M_{g(ima)} = iM_g$) because quartz crystals are widely used to detect forces (piezoelectric effect).

By using GCCs as shown in Fig. 18(b) and Fig.18(c), we can increase the gravitational acceleration, $\vec{a}$, produced by the imaginary mass im_g upon the crystals. Then it becomes

$$a = -\chi_{air}^3 G\frac{m_g}{r^2} \qquad (72)$$

As we have seen, the value of χ_{air} can be increased up to $\chi_{air} \cong -10^9$ (See Eq.57). Note that in this case, the gravitational forces become *attractive*. In addition, if m_g is not small, the gravitational forces between the imaginary body of mass im_g and the crystals can become sufficiently intense to be easily detectable.

Due to the piezoelectric effect, the gravitational force acting on the crystal will produce a voltage proportional to its intensity. Then consider a board with hundreds micro-crystals behind a set of GCCs, as shown in Fig.18(c). By amplifying the voltages generated in each micro-crystal and sending to an appropriated data acquisition system, it will be thus possible to obtain an image of the imaginary body of mass $m_{g(ima)}$ placed in front of the board.

In order to decrease strongly the gravitational effects produced by bodies placed behind the imaginary body of mass im_g, one can put five GCCs making a *Gravitational Shielding* as shown in Fig.18(c). If the GCCs are filled with air at 300K and $3\times10^{-12} torr$. Then $\rho_{air} = 4.94\times10^{-15} kg.m^{-3}$ and $\sigma_{air} \cong 1\times10^{-14} S.m^{-1}$. Thus, for $f = 60Hz$ and $B \cong 0.7T$ the Eq. (56) gives

$$\chi_{air} = \frac{m_{g(air)}}{m_{i(air)}} = \left\{1 - 2\left[\sqrt{1+5B^4} - 1\right]\right\} \cong -10^{-2} \qquad (73)$$

For $\chi_{air} \cong 10^{-2}$ the gravitational shielding presented in Fig.18(c) will reduce any value of g to $\chi_{air}^5 g \cong 10^{-10} g$. This will be sufficiently to reduce strongly the gravitational effects proceeding from both sides of the gravitational shielding.

Another important consequence of the correlation between gravitational mass and inertial mass expressed by Eq. (1) is the possibility of building *Energy Shieldings* around objects in order to protect them from *high-energy particles* and *ultra-intense fluxes of radiation*.

In order to explain that possibility, we start from the new expression [1] for the *momentum* q of a particle with gravitational mass M_g and velocity V, which is given by

$$q = M_g V \qquad (74)$$

where $M_g = m_g \Big/ \sqrt{1 - V^2/c^2}$ and $m_g = \chi\, m_i$ [1]. Thus, we can write

$$\frac{m_g}{\sqrt{1 - V^2/c^2}} = \frac{\chi\ m_i}{\sqrt{1 - V^2/c^2}} \qquad (75)$$

Therefore, we get

$$M_g = \chi M_i \qquad (76)$$

It is known from the Relativistic Mechanics that

$$q = \frac{UV}{c^2} \qquad (77)$$

where U is the *total* energy of the particle. This expression is valid for *any* velocity V of the particle, including $V = c$.

By comparing Eq. (77) with Eq. (74) we obtain

$$U = M_g c^2 \qquad (78)$$

It is a well-known experimental fact that

$$M_i c^2 = hf \qquad (79)$$

Therefore, by substituting Eq. (79) and Eq. (76) into Eq. (74), gives

$$q = \frac{V}{c}\chi\frac{h}{\lambda} \qquad (80)$$

Note that this expression is valid for *any* velocity V of the particle. In the particular case of $V = c$, it reduces to

$$q = \chi\frac{h}{\lambda} \qquad (81)$$

By comparing Eq. (80) with Eq. (77), we obtain

$$U = \chi hf \qquad (82)$$

Note that only for $\chi = 1$ the Eq. (81) and Eq. (82) are reduced to the well=known expressions of DeBroglie $(q = h/\lambda)$ and Einstein $(U = hf)$.

Equations (80) and (82) show for example, that *any* real particle (material particles, real photons, etc) that penetrates a region (with density ρ and electrical conductivity σ), where there is an ELF electric field E, will have its *momentum* q and its energy U reduced by the factor χ, given by

$$\chi = \frac{m_g}{m_i} = \left\{1 - 2\left[\sqrt{1 + \frac{\mu}{4c^2}\left(\frac{\sigma}{4\pi f}\right)^3\frac{E^4}{\rho^2}} - 1\right]\right\} \qquad (83)$$

The remaining amount of *momentum* and *energy*, respectively given by $(1-\chi)\left(\frac{V}{c}\right)\frac{h}{\lambda}$ and $(1-\chi)\,hf$, are *transferred to* the *imaginary* particle associated to the *real* particle[§] (material particles or real photons) that penetrated the mentioned region.

It was previously shown that, when the *gravitational mass* of a particle is reduced to ranging between $+0.159M_i$ to $-0.159M_i$, i.e., when $\chi < 0.159$, it becomes *imaginary* [1], i.e., the gravitational and the inertial masses of the particle become *imaginary*. Consequently, the particle disappears from our ordinary space-time. It goes to the Imaginary Universe. On the other hand, when the gravitational mass of the particle becomes greater than $+0.159M_i$, or less than $-0.159M_i$, i.e., when $\chi > 0.159$, the particle return to our Universe.

Figure 19 (a) clarifies the phenomenon of reduction of the *momentum* for $\chi > 0.159$, and Figure 19 (b) shows the effect in the case of $\chi < 0.159$. In this case, the particles become imaginary and consequently, they go to the *imaginary space-time* when they penetrate the electric field E. However, the electric field E stays at the *real* space-time. Consequently, the particles return immediately to the real space-time in order to return soon after to the *imaginary* space-time, due to the action of the electric field E. Since the particles are moving at a direction, they *appear* and *disappear* while they are crossing the region, up to collide with the plate (See Fig.19) with a *momentum,* $q_m = \chi\left(\frac{V}{c}\right)\frac{h}{\lambda}$, in the case of the *material particle*, and $q_r = \chi\frac{h}{\lambda}$ in the case of the *photon*. Note that by making $\chi \cong 0$, it is possible to block high-energy particles and ultra-intense fluxes of radiation. These *Energy Shieldings* can be built around objects in order to protect them from such particles and radiation.

It is also important to note that the gravity control process described here points to the possibility of obtaining *Controlled Nuclear Fusion* by means of increasing of the intensity of the gravitational interaction between the nuclei. When the gravitational forces $F_G = Gm_g m'_g/r^2$ become greater than the electrical forces $F_E = qq'/4\pi\varepsilon_0 r^2$ between the nuclei, then nuclear fusion reactions can occur.

Note that, according to Eq. (83), the gravitational mass can be strongly increased. Thus, if $E = E_m \sin\omega t$, then the average value for E^2 is equal to $\frac{1}{2}E_m^2$, because E varies sinusoidaly (E_m is the maximum value for E). On the other hand, $E_{rms} = E_m/\sqrt{2}$. Consequently, we can replace

[§] As previously shown, there are *imaginary particles* associated to each *real particle* [1].

E^4 for E_{rms}^4. In addition, as $j = \sigma E$ (*Ohm's vectorial Law*), then Eq. (83) can be rewritten as follows

$$\chi = \frac{m_g}{m_{i0}} = \left\{1 - 2\left[\sqrt{1 + K\frac{\mu_r j_{rms}^4}{\sigma\rho^2 f^3}} - 1\right]\right\} \qquad (84)$$

where $K = 1.758\times10^{-27}$ and $j_{rms} = j/\sqrt{2}$.

Thus, the gravitational force equation can be expressed by

$$F_G = Gm_g m_g'/r^2 = \chi^2 Gm_{i0}m_{i0}'/r^2 =$$
$$= \left\{1 - 2\left[\sqrt{1 + K\frac{\mu_r j_{rms}^4}{\sigma\rho^2 f^3}} - 1\right]\right\}^2 Gm_{i0}m_{i0}'/r^2 \qquad (85)$$

In order to obtain $F_G > F_E$ we must have

$$\left\{1 - 2\left[\sqrt{1 + K\frac{\mu_r j_{rms}^4}{\sigma\rho^2 f^3}} - 1\right]\right\} > \sqrt{\frac{qq'/4\pi\varepsilon_0}{Gm_{i0}m_{i0}'}} \qquad (86)$$

The *carbon fusion* is a set of nuclear fusion reactions that take place in massive stars (at least $8M_{sun}$ at birth). It requires high temperatures ($>5\times10^8 K$) and densities ($>3\times10^9\, kg.m^{-3}$). The principal reactions are:

$$^{12}\mathrm{C} + {}^{12}\mathrm{C} \rightarrow \begin{cases} {}^{23}\mathrm{Na} + \mathrm{p} + 2.24\ \mathrm{MeV} \\ {}^{20}\mathrm{Ne} + \alpha + 4.62\ \mathrm{MeV} \\ {}^{24}\mathrm{Mg} + \gamma + 13.93\ \mathrm{MeV} \end{cases}$$

In the case of Carbon nuclei (^{12}C) of a *thin carbon wire* ($\sigma \cong 4\times10^4 S.m^{-1}$; $\rho = 2.2\times10^3 S.m^{-1}$) Eq. (86) becomes

$$\left\{1 - 2\left[\sqrt{1 + 9.08\times10^{-39}\frac{j_{rms}^4}{f^3}} - 1\right]\right\} > \sqrt{\frac{e^2}{16\pi\varepsilon_0 G m_p^2}}$$

whence we conclude that the condition for the ^{12}C + ^{12}C fusion reactions occur is

$$j_{rms} > 1.7\times10^{18} f^{\frac{3}{4}} \qquad (87)$$

If the electric current through the carbon wire has Extremely-Low Frequency (ELF), for example, if $f = 1\mu Hz$, then the current density, j_{rms}, must have the following value:

$$j_{rms} > 5.4\times10^{13} A.m^{-2} \qquad (88)$$

Since $j_{rms} = i_{rms}/S$ where $S = \pi\phi^2/4$ is the area of the cross section of the wire, we can conclude that, for an *ultra-thin carbon* wire with $10\mu m$-diameter, it is necessary that the current through the wire, i_{rms}, have the following intensity

$$i_{rms} > 4.24\ kA$$

Obviously, this current will *explode* the carbon wire. However, this explosion becomes negligible in comparison with the very strong *gravitational implosion*, which occurs simultaneously due to the enormous increase in intensities of the gravitational forces among the carbon nuclei produced by means of the ELF current through the carbon wire as predicted by Eq. (85). Since, in this case, the gravitational forces among the carbon nuclei become greater than the repulsive electric forces among them the result is the production of ^{12}C + ^{12}C fusion reactions.

Similar reactions can occur by using a *lithium* wire. In addition, it is important to note that j_{rms} is directly proportional to $f^{\frac{3}{4}}$ (Eq. 87). Thus, for example, if $f = 10^{-8} Hz$, the current necessary to produce the nuclear reactions will be $i_{rms} = 130A$.

IV.CONCLUSION

The process described here is clearly the better way in order to control the gravity. This is because the *Gravity Control Cell* in this case is very easy to be built, the cost is low and it works at ambient temperature. The Gravity Control is the starting point for the generation of and detection of *Virtual Gravitational Radiation* (Quantum Gravitational *Transceiver*) also for the construction of the *Gravitational Motor* and the *Gravitational Spacecraft* which includes the system for generation of *artificial gravity* presented in Fig.10 and the *Gravitational Thruster* (Fig.11). While the *Gravitational Transceiver* leads to a new concept in *Telecommunication*, the Gravitational Motor changes the paradigm of *energy conversion* and the Gravitational Spacecraft points to a new concept in *aerospace flight*.

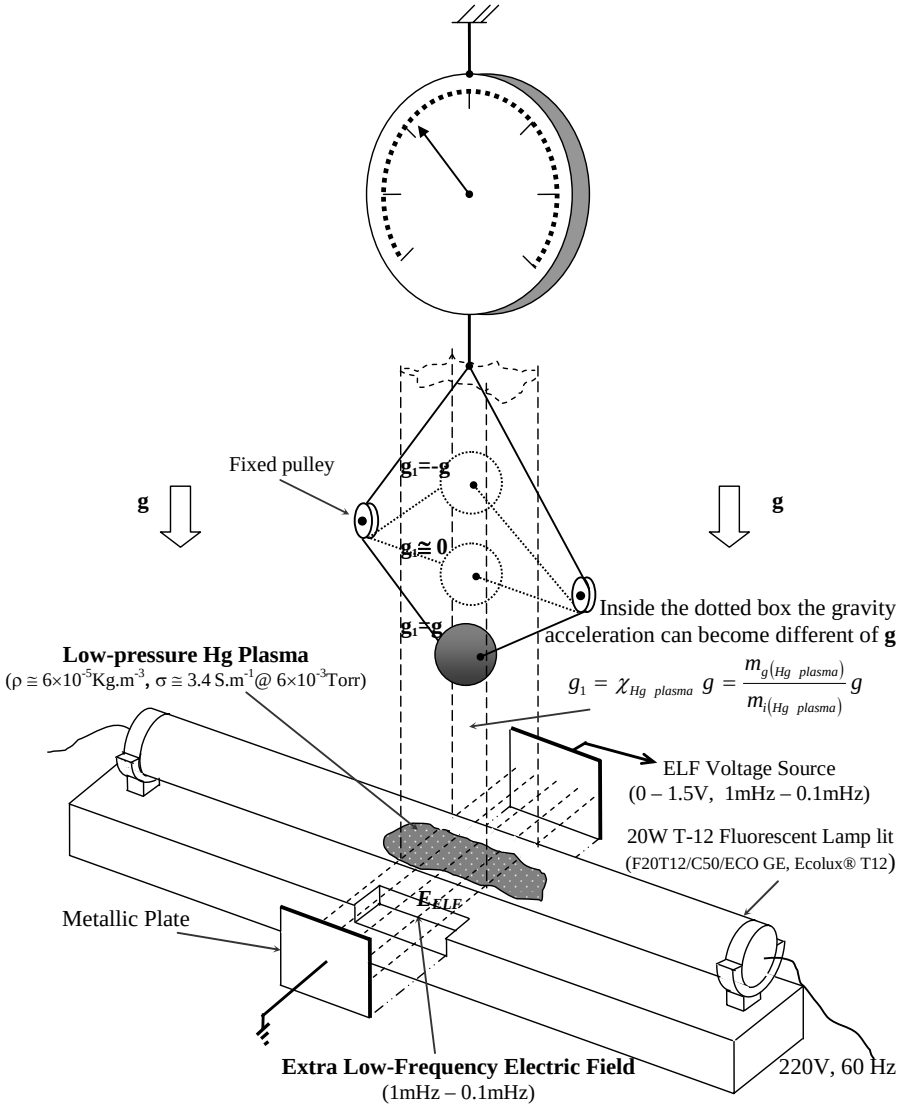

Fig. 1 – Gravitational Shielding Effect by means of an ELF electric field through low- pressure Hg Plasma.

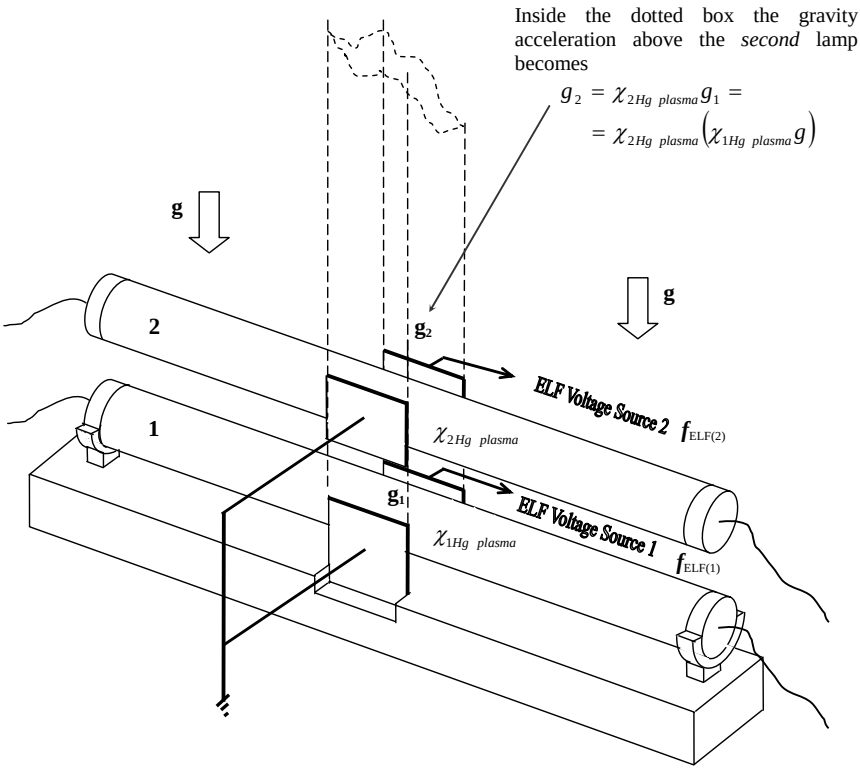

Fig. 2 – Gravity acceleration above a *second* fluorescent lamp.

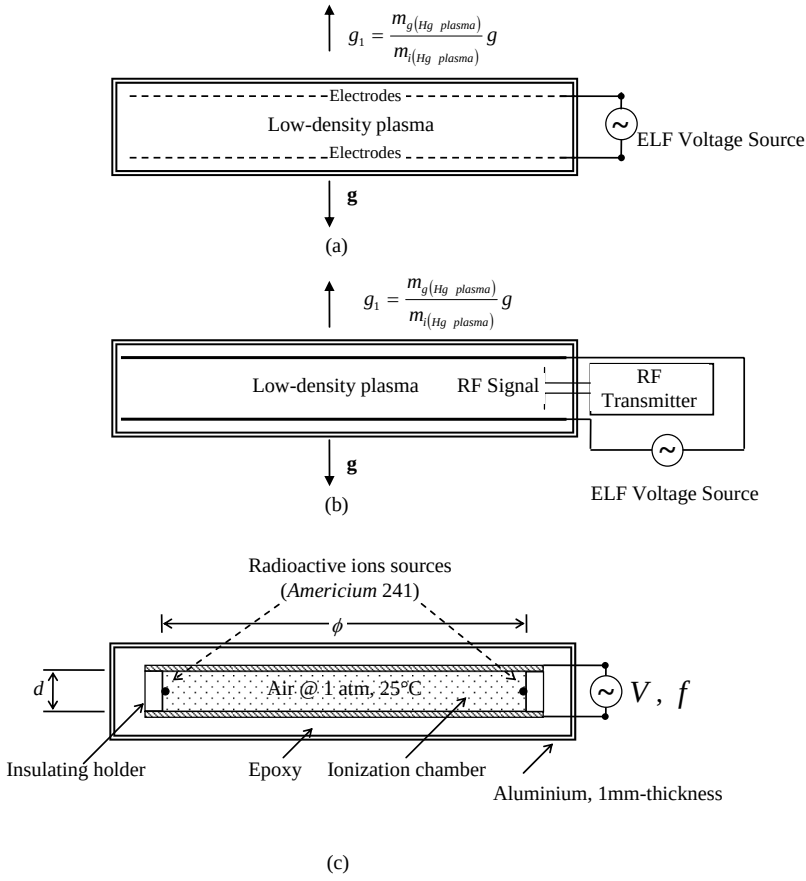

Fig. 3 – *Schematic diagram of Gravity Control Cells (GCCs).*
(a) GCC where the ELF electric field and the ionizing electric field can be the same. (b) GCC where the plasma is ionized by means of a RF signal. (c) GCC filled with *air* (at ambient temperature and 1 atm) strongly ionized by means of alpha particles emitted from radioactive ions sources (Am 241, *half-life* 432 years). Since the electrical conductivity of the ionized air depends on the amount of ions then it can be strongly increased by increasing the amount of Am 241 in the GCC. This GCC has 36 radioactive ions sources each one with $1/5000^{th}$ of gram of Am 241, conveniently positioned around the ionization chamber, in order to obtain $\sigma_{air} \cong 10^3 S.m^{-1}$.

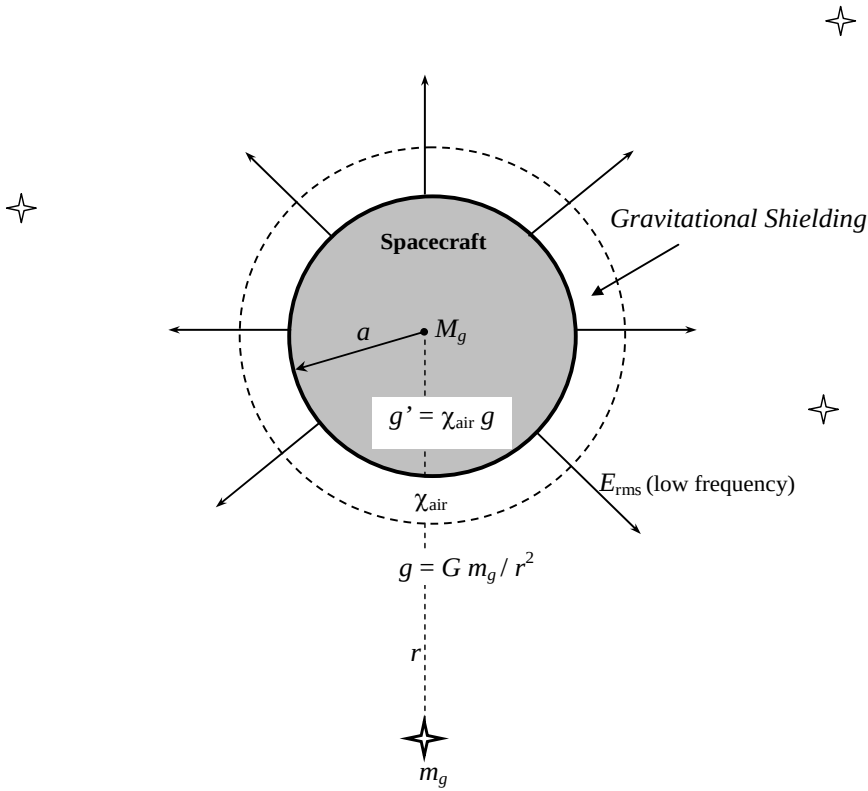

The *gravity accelerations* on the spacecraft (due to the rest of the Universe) can be controlled by means of the *gravitational shielding*, i.e.,

$$g'_i = \chi_{air}\, g_i \qquad i = 1, 2, 3 \ldots n$$

Thus,

$$F_{is} = F_{si} = M_g\, g'_i = M_g\, (\chi_{air}\, g_i)$$

Then the inertial forces acting on the spacecraft (s) can be strongly reduced. According to the *Mach's principle* this effect can reduce *the inertial properties of the spacecraft* and consequently, leads to a new concept of spacecraft and aerospace flight.

Fig. 4 – Gravitational Shielding surround a Spherical Spacecraft.

$V = V_0$ (Volts)	t = T /4		$E_{ELF\,(1)}$ (V/m)	$f_{ELF\,(1)}$ (mHz)	g_1/g		$E_{ELF\,(2)}$ (V/m)	$f_{ELF\,(2)}$ (mHz)	g_2/g	
	(s)	(min)			Exp.	Teo.			Exp.	Teo.
1.0 V	250	**4.17**	24.81	1	-	**0.993**	24.81	1	-	**0.986**
	312.5	**5.21**	24.81	0.8	-	**0.986**	24.81	0.8	-	**0.972**
	416.6	**6.94**	24.81	0.6	-	**0.967**	24.81	0.6	-	**0.935**
	625	**10.42**	24.81	0.4	-	**0.890**	24.81	0.4	-	**0.792**
	1250	**20.83**	24.81	0.2	-	**0.240**	24.81	0.2	-	**0.058**
1.5V	250	**4.17**	37.22	1	-	**0.964**	37.22	1	-	**0.929**
	312.5	**5.21**	37.22	0.8	-	**0.930**	37.22	0.8	-	**0.865**
	416.6	**6.94**	37.22	0.6	-	**0.837**	37.22	0.6	-	**0.700**
	625	**10.42**	37.22	0.4	-	**0,492**	37.22	0.4	-	**0.242**
	1250	**20.83**	37.22	0.2	-	**-1,724**	37.22	0.2	-	**2.972**

Table 1 – Theoretical Results.

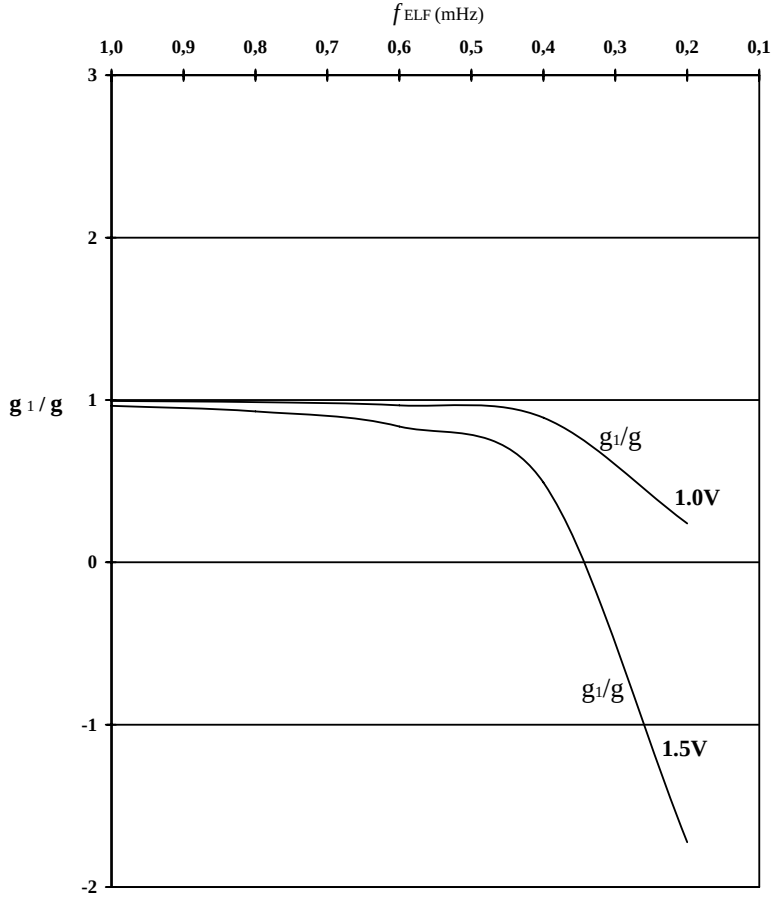

Fig. 5- Distribution of the correlation $\mathbf{g}_1/\mathbf{g}$ as a function of f_{ELF}

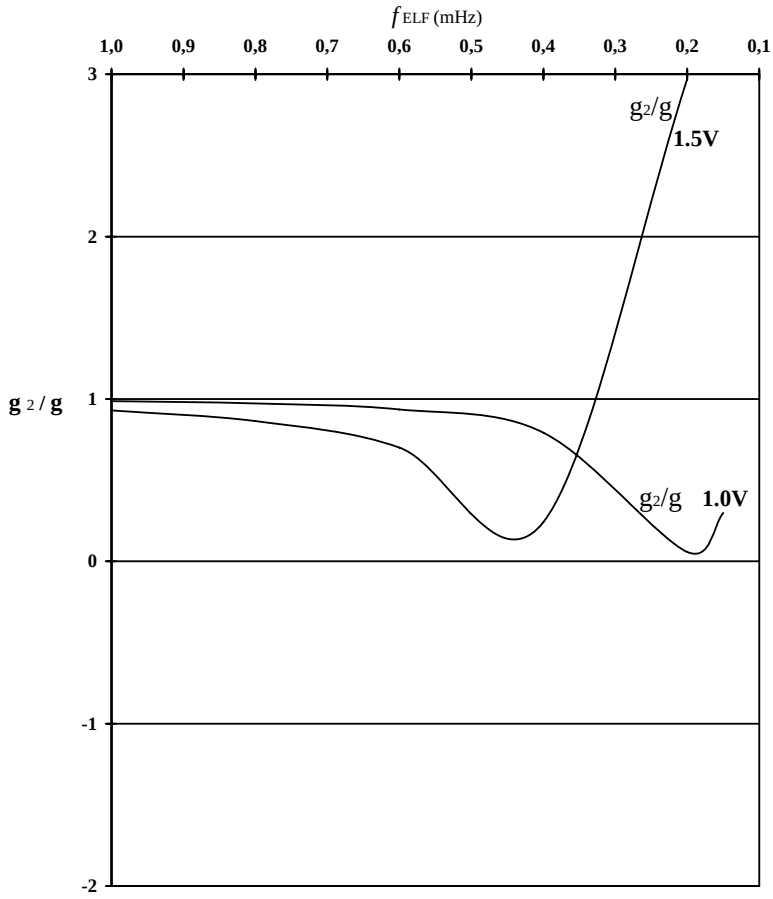

Fig. 6- Distribution of the correlation $\mathbf{g}_2 / \mathbf{g}$ as a function of f_{ELF}

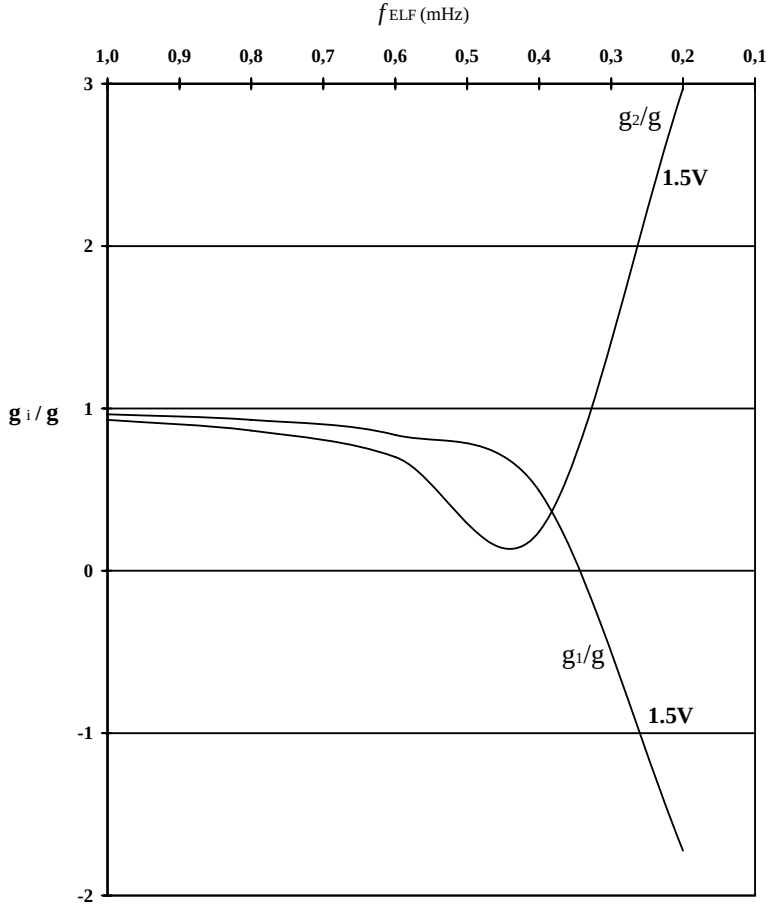

Fig. 7- Distribution of the correlations $\mathbf{g}_i / \mathbf{g}$ as a function of f_{ELF}

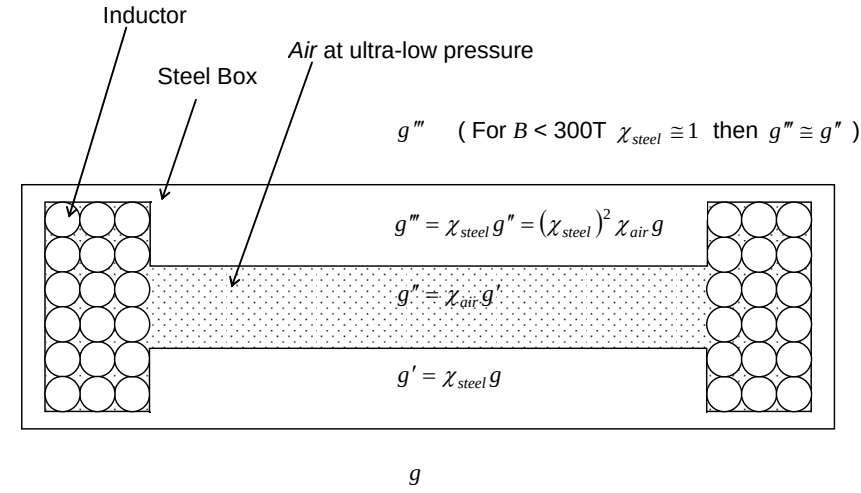

(a)

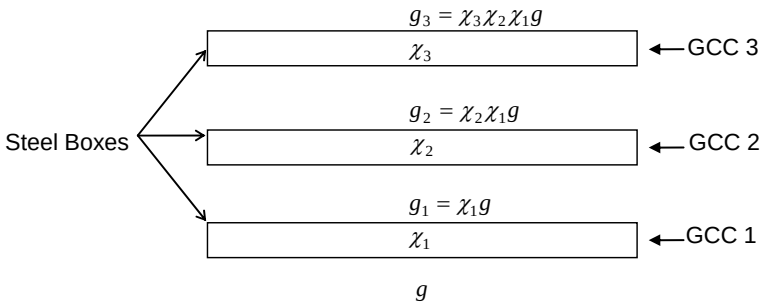

(b)

Fig. 8 – (a) Gravity Control Cell (GCC) filled with *air* at ultra-low pressure.
(b) Gravity Control Battery (Note that if $\chi_1 = \chi_2^{-1} = -1$ then $g'' = g$)

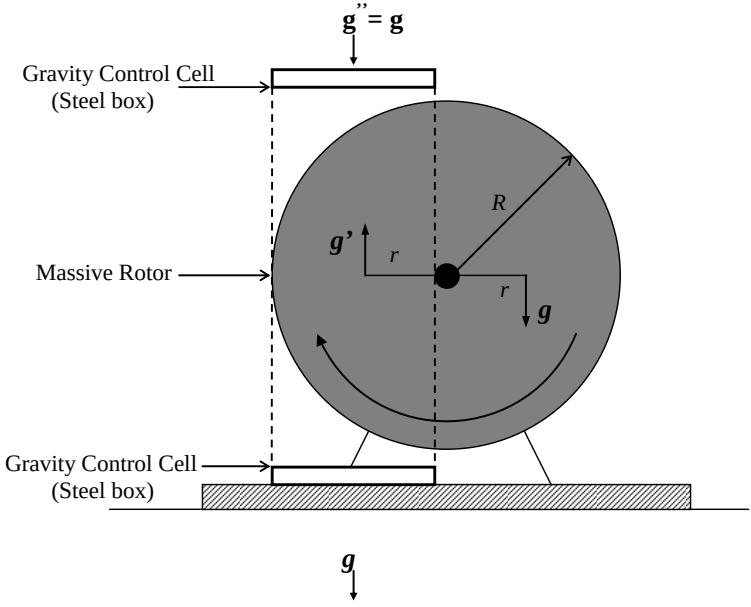

Note that $g' = (\chi_{steel})^2 \chi_{air} g$ and $g'' = (\chi_{steel})^4 (\chi_{air})^2 g$ therefore for $\chi_{steel} \cong 1$ and $\chi_{air(1)} = \chi^{-1}_{air(2)} = -n$ we get $g' \cong -ng$ and $g'' = g$

Fig. 9 – The Gravitational Motor

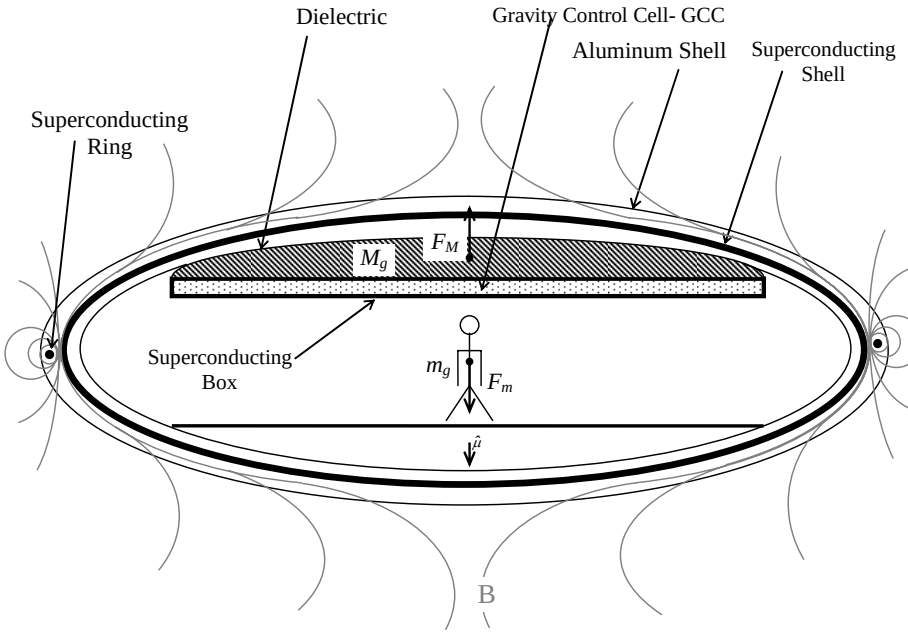

Fig. 10 – The Gravitational Spacecraft – Due to the *Meissner effect*, the magnetic field B is expelled from the *superconducting shell*. Similarly, the magnetic field B_{GCC}, of the GCC stay confined inside the *superconducting box*.

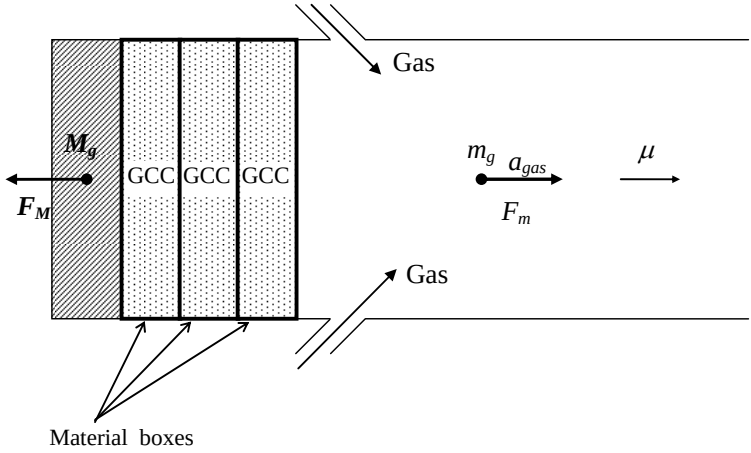

(a)

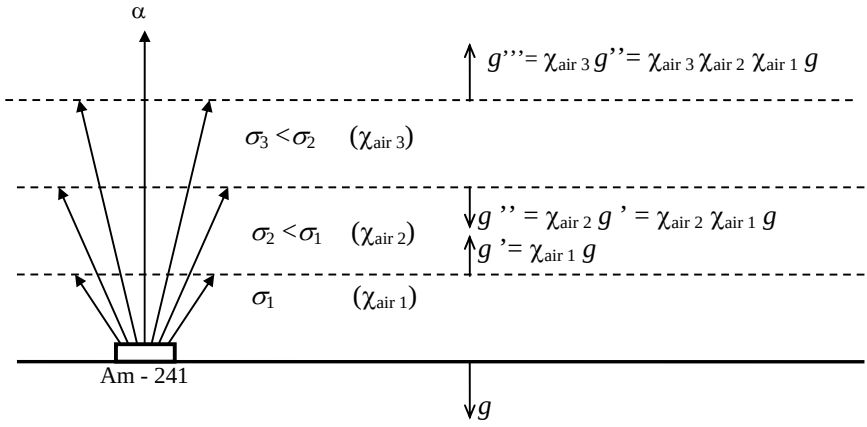

(b)

Fig. 11 – The Gravitational Thruster .
(a) Using material boxes. (b) Without material boxes

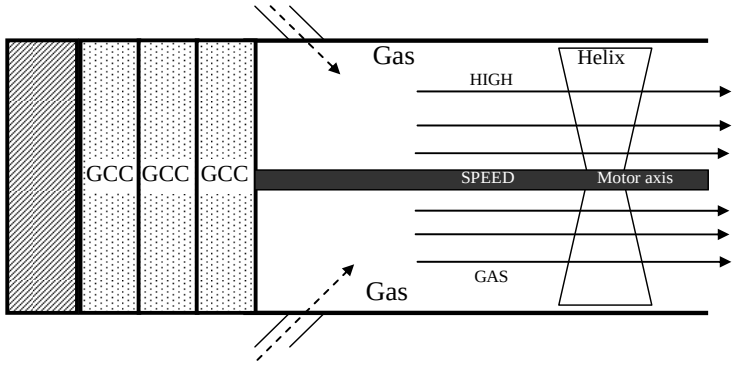

Fig. 12 - The Gravitational Turbo Motor – The gravitationally accelerated gas, by means of the GCCs, propels the helix which movies the motor axis.

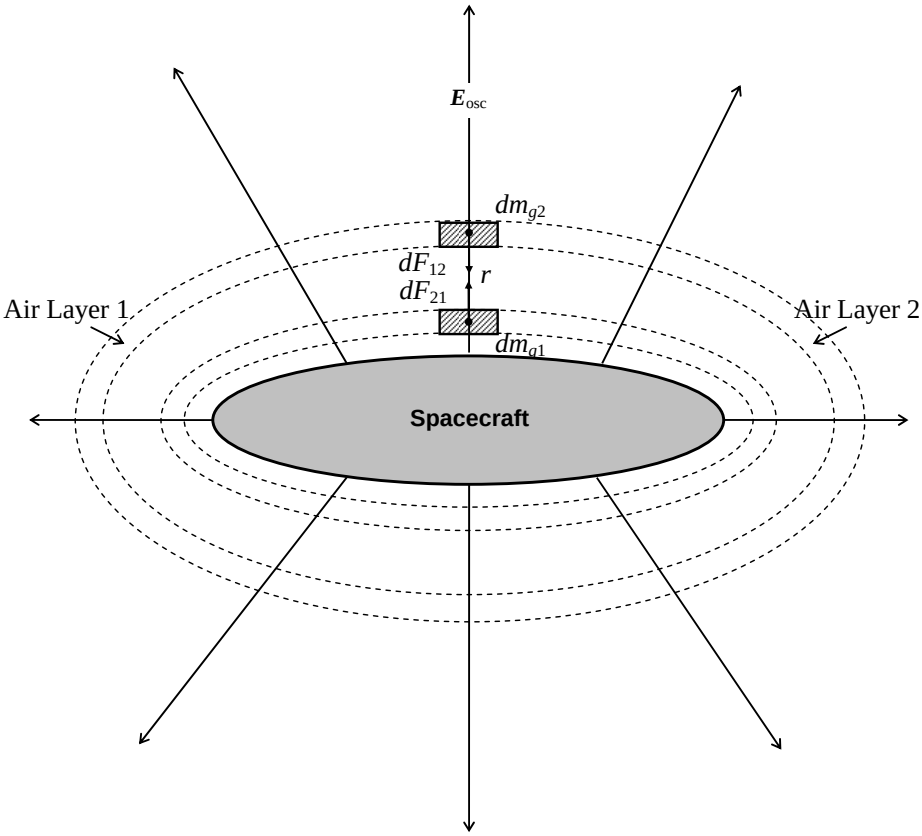

Fig. 13 – Gravitational forces between two layers of the "*air shell*". The electric field $\boldsymbol{E}_{osc}$ provides the *ionization* of the *air*.

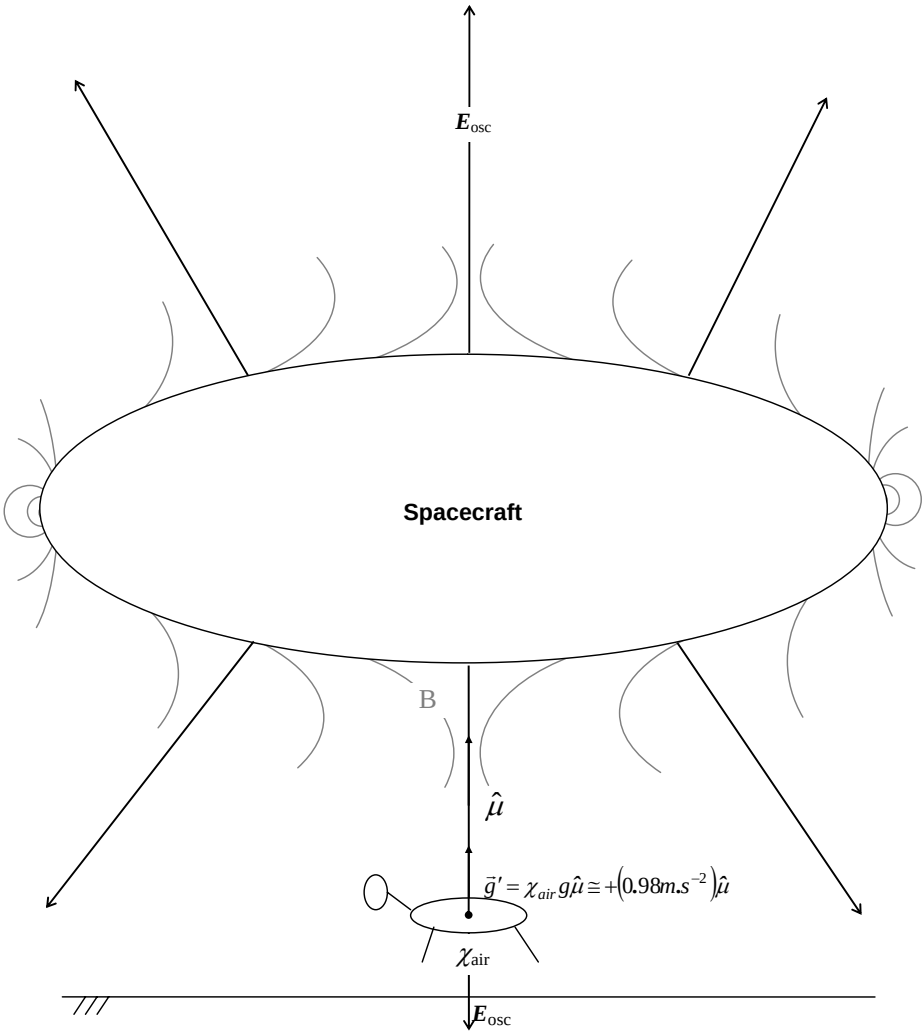

Fig. 14 – The Gravitational Lifter

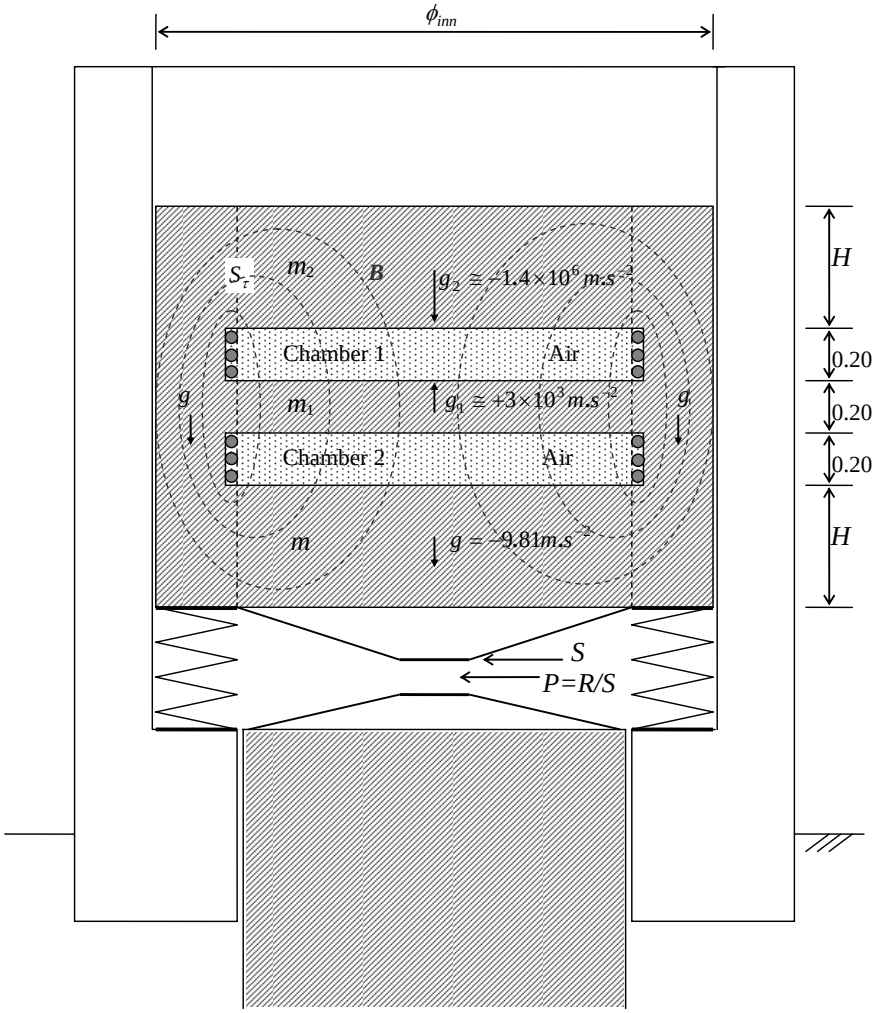

Fig. 15 – *Gravitational Press*

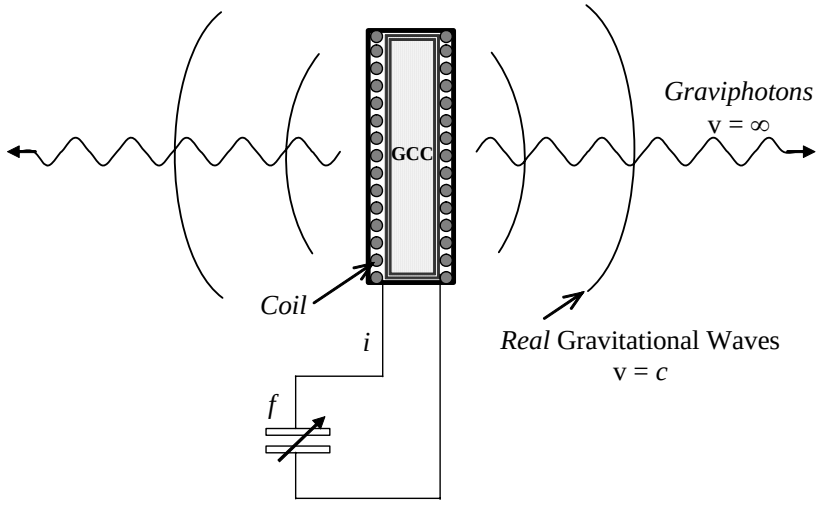

(a) GCC Antenna

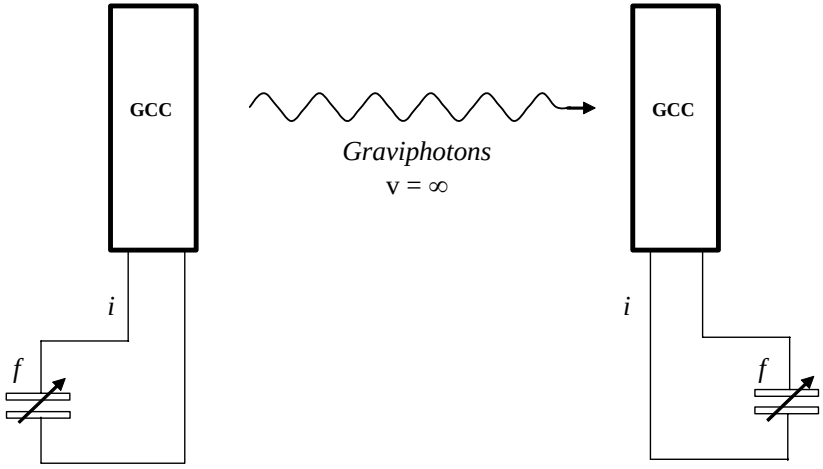

Fig. 16 - Transmitter and Receiver of *Virtual* Gravitational Radiation.

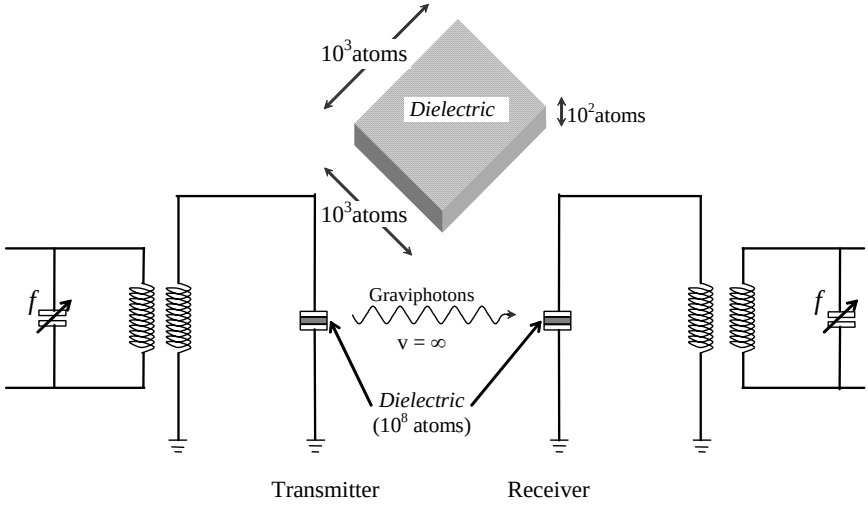

(a)

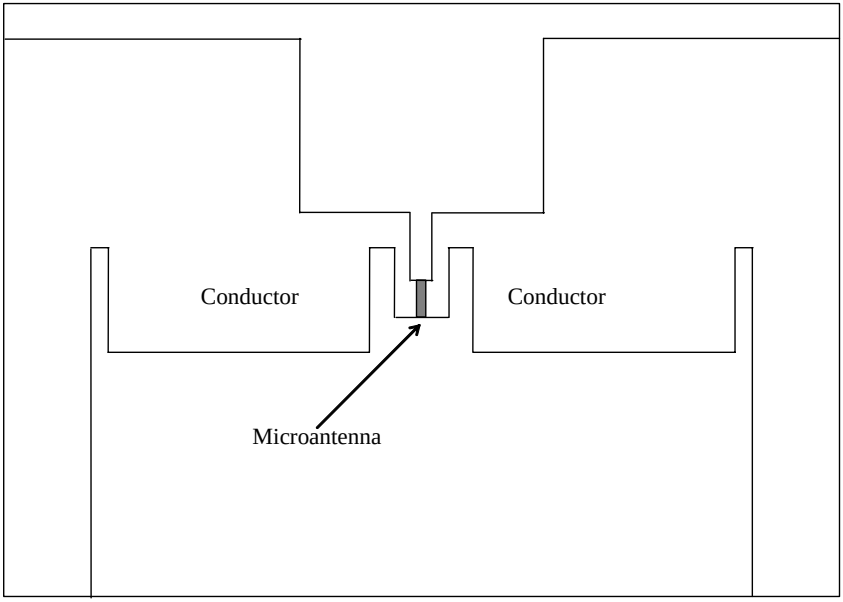

(b)

Fig. 17 – Quantum Gravitational Microantenna

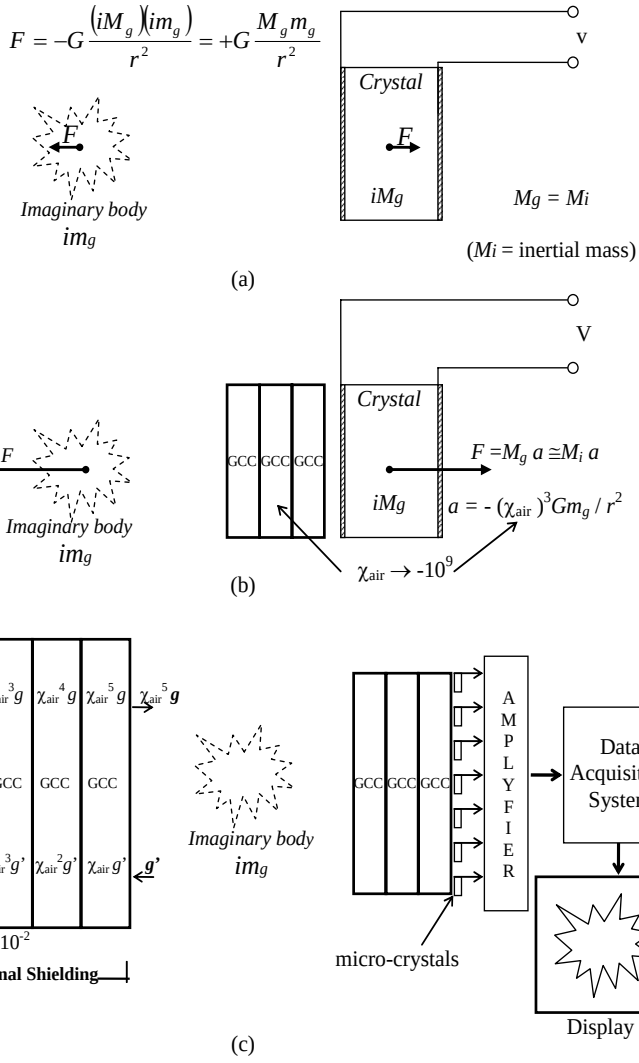

Fig.18 – Method and device using GCCs for obtaining *images* of *imaginary bodies*.

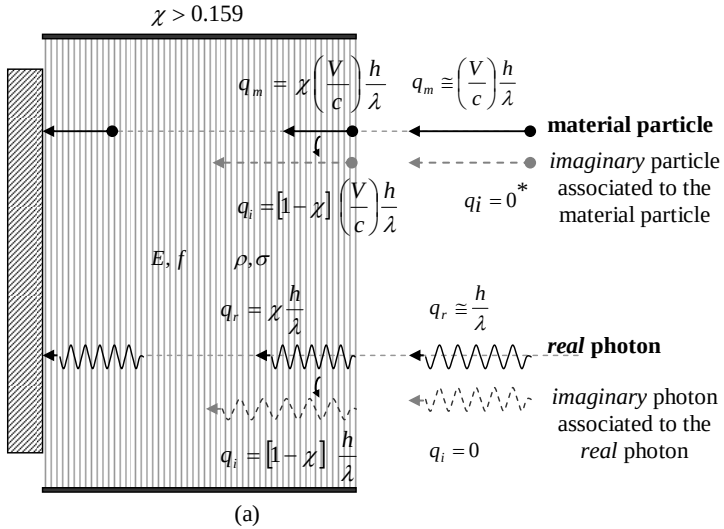

(a)

* There are a type of neutrino, called "ghost" neutrino, predicted by General Relativity, with *zero mass* and *zero momentum*. In spite its *momentum be zero*, it is known that there are wave functions that describe these neutrinos and that prove that really they exist.

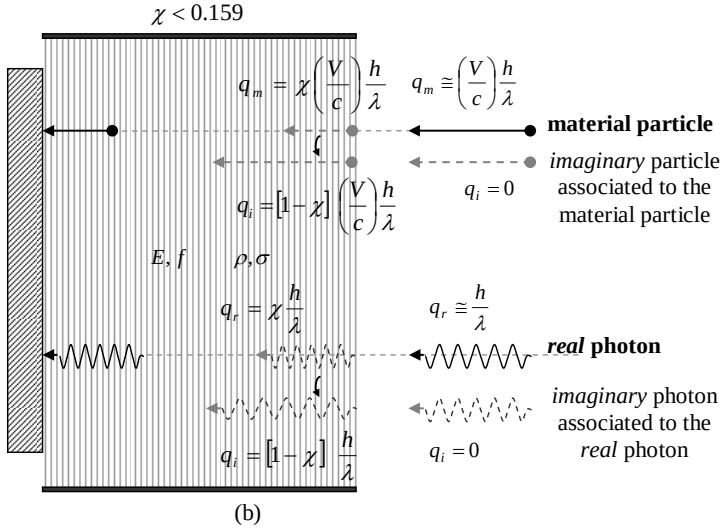

(b)

Fig. 19 – *The phenomenon of reduction of the momentum*. (a) Shows the reduction of *momentum* for $\chi > 0.159$. (b) Shows the effect when $\chi < 0.159$. Note that in both cases, the *material* particles collide with the cowl with the *momentum* $q_m = \chi(V/c)(h/\lambda)$, and the photons with $q_r = \chi\frac{h}{\lambda}$. Therefore, that by making $\chi \cong 0$, it is possible to block high-energy particles and ultra-intense fluxes of radiation.

APPENDIX A: THE SIMPLEST METHOD TO CONTROL THE GRAVITY

In this Appendix we show the simplest method to control the gravity.

Consider a body with mass density ρ and the following electric characteristics: $\mu_r, \varepsilon_r, \sigma$ (relative permeability, relative permittivity and electric conductivity, respectively). Through this body, passes an electric current I, which is the sum of a sinusoidal current $i_{osc} = i_0 \sin \omega t$ and the DC current I_{DC}, i.e., $I = I_{DC} + i_0 \sin \omega t$; $\omega = 2\pi f$. If $i_0 << I_{DC}$ then $I \cong I_{DC}$. Thus, the current I varies with the frequency f, but the variation of its intensity is quite small in comparison with I_{DC}, i.e., I will be practically constant (Fig. 1A). This is of fundamental importance for maintaining the value of the gravitational mass of the body, m_g, sufficiently stable during all the time.

The *gravitational mass* of the *body* is given by [1]

$$m_g = \left\{1 - 2\left[\sqrt{1 + \left(\frac{n_r U}{m_{i0} c^2}\right)^2} - 1\right]\right\} m_{i0} \qquad (A1)$$

where U, is the electromagnetic energy absorbed by the body and n_r is the index of refraction of the body.

Equation (A1) can also be rewritten in the following form

$$\frac{m_g}{m_{i0}} = \left\{1 - 2\left[\sqrt{1 + \left(\frac{n_r W}{\rho\, c^2}\right)^2} - 1\right]\right\} \qquad (A2)$$

where, $W = U/V$ is the *density of electromagnetic energy* and $\rho = m_{i0}/\mathrm{V}$ is the density of inertial mass.

The *instantaneous values* of the density of electromagnetic energy in an *electromagnetic* field can be deduced from Maxwell's equations and has the following expression

$$W = \tfrac{1}{2}\varepsilon E^2 + \tfrac{1}{2}\mu H^2 \qquad (A3)$$

where $E = E_m \sin \omega t$ and $H = H \sin \omega t$ are the *instantaneous values* of the electric field and the magnetic field respectively.

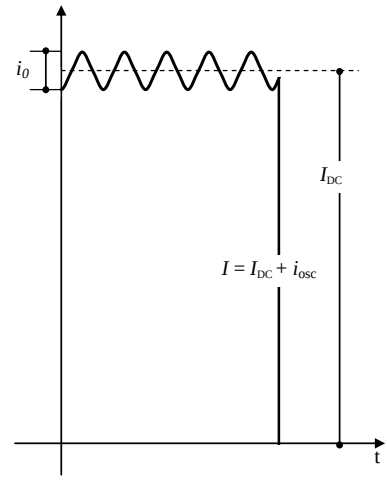

Fig. A1 - The electric current I varies with frequency f. But the variation of I is quite small in comparison with I_{DC} due to $i_o << I_{DC}$. In this way, we can consider $I \cong I_{DC}$.

It is known that $B = \mu H$, $E/B = \omega/k_r$ [11] and

$$v = \frac{dz}{dt} = \frac{\omega}{\kappa_r} = \frac{c}{\sqrt{\frac{\varepsilon_r \mu_r}{2}\left(\sqrt{1 + (\sigma/\omega\varepsilon)^2} + 1\right)}} \qquad (A4)$$

where k_r is the real part of the *propagation vector* $\vec{k}$ (also called *phase constant*); $k = |\vec{k}| = k_r + ik_i$; ε, μ and σ, are the electromagnetic characteristics of the medium in which the incident (or emitted) radiation is propagating($\varepsilon = \varepsilon_r \varepsilon_0$; $\varepsilon_0 = 8.854 \times 10^{-12} F/m$; $\mu = \mu_r \mu_0$ where $\mu_0 = 4\pi \times 10^{-7} H/m$). It is known that for *free-space* $\sigma = 0$ and $\varepsilon_r = \mu_r = 1$. Then Eq. (A4) gives

$$v = c$$

From (A4), we see that the *index of refraction* $n_r = c/v$ is given by

$$n_r = \frac{c}{v} = \sqrt{\frac{\varepsilon_r \mu_r}{2}\left(\sqrt{1 + (\sigma/\omega\varepsilon)^2} + 1\right)} \qquad (A5)$$

Equation (A4) shows that $\omega/\kappa_r = v$. Thus, $E/B = \omega/k_r = v$, i.e.,

$$E = vB = v\mu H \qquad (A6)$$

Then, Eq. (A3) can be rewritten in the following form:

$$W = \tfrac{1}{2}\left(\varepsilon v^2\mu\right)\mu H^2 + \tfrac{1}{2}\mu H^2 \qquad (A7)$$

For $\sigma << \omega\varepsilon$, Eq. (A4) reduces to

$$v = \frac{c}{\sqrt{\varepsilon_r \mu_r}}$$

Then, Eq. (A7) gives

$$W = \tfrac{1}{2}\left[\varepsilon\left(\frac{c^2}{\varepsilon_r\mu_r}\right)\mu\right]\mu H^2 + \tfrac{1}{2}\mu H^2 = \mu H^2$$

This equation can be rewritten in the following forms:

$$W = \frac{B^2}{\mu} \qquad (A8)$$

or

$$W = \varepsilon\ E^2 \qquad (A9)$$

For $\sigma >> \omega\varepsilon$, Eq. (A4) gives

$$v = \sqrt{\frac{2\omega}{\mu\sigma}} \qquad (A10)$$

Then, from Eq. (A7) we get

$$W = \tfrac{1}{2}\left[\varepsilon\left(\frac{2\omega}{\mu\sigma}\right)\mu\right]\mu H^2 + \tfrac{1}{2}\mu H^2 = \left(\frac{\omega\varepsilon}{\sigma}\right)\mu H^2 + \tfrac{1}{2}\mu H^2 \cong$$

$$\cong \tfrac{1}{2}\mu H^2 \qquad (A11)$$

Since $E = vB = v\mu H$, we can rewrite (A11) in the following forms:

$$W \cong \frac{B^2}{2\mu} \qquad (A12)$$

or

$$W \cong \left(\frac{\sigma}{4\omega}\right)E^2 \qquad (A13)$$

By comparing equations (A8) (A9) (A12) and (A13), we can see that Eq. (A13) shows that the best way to obtain a strong value of W *in practice* is by applying an *Extra Low-Frequency* (ELF) *electric field* $\left(w = 2\pi f << 1Hz\right)$ through a *medium with high electrical conductivity*.

Substitution of Eq. (A13) into Eq. (A2), gives

$$m_g = \left\{1 - 2\left[\sqrt{1 + \frac{\mu}{4c^2}\left(\frac{\sigma}{4\pi f}\right)^3\frac{E^4}{\rho^2}} - 1\right]\right\}m_{i0} =$$

$$= \left\{1 - 2\left[\sqrt{1 + \left(\frac{\mu_0}{256\pi^3 c^2}\right)\left(\frac{\mu_r\sigma^3}{\rho^2 f^3}\right)E^4} - 1\right]\right\}m_{i0} =$$

$$= \left\{1 - 2\left[\sqrt{1 + 1.758\times10^{-27}\left(\frac{\mu_r\sigma^3}{\rho^2 f^3}\right)E^4} - 1\right]\right\}m_{i0} \qquad (A14)$$

Note that $E = E_m \sin\omega t$. The average value for E^2 is equal to $\frac{1}{2}E_m^2$ because E varies sinusoidaly (E_m is the maximum value for E). On the other hand, $E_{rms} = E_m/\sqrt{2}$. Consequently, we can change E^4 by E_{rms}^4, and the equation above can be rewritten as follows

$$m_g = \left\{1 - 2\left[\sqrt{1 + 1.758\times10^{-27}\left(\frac{\mu_r\sigma^3}{\rho^2 f^3}\right)E_{rms}^4} - 1\right]\right\}m_{i0}$$

Substitution of the well-known equation of the *Ohm's vectorial Law*: $j = \sigma E$ into (A14), we get

$$m_g = \left\{1 - 2\left[\sqrt{1 + 1.758\times10^{-27}\frac{\mu_r j_{rms}^4}{\sigma\rho^2 f^3}} - 1\right]\right\}m_{i0} \qquad (A15)$$

where $j_{rms} = j/\sqrt{2}$.

Consider a 15 cm square *Aluminum thin foil* of *10.5 microns thickness* with the following characteristics: $\mu_r = 1$; $\sigma = 3.82\times10^7\ S.m^{-1}$; $\rho = 2700\ Kg.m^{-3}$. Then, (A15) gives

$$m_g = \left\{1 - 2\left[\sqrt{1 + 6.313\times10^{-42}\frac{j_{rms}^4}{f^3}} - 1\right]\right\}m_{i0} \qquad (A16)$$

Now, consider that the ELF electric current $I = I_{DC} + i_0 \sin\omega t$, $\left(i_0 << I_{DC}\right)$ passes through that Aluminum foil. Then, the current density is

$$j_{rms} = \frac{I_{rms}}{S} \cong \frac{I_{DC}}{S} \qquad (A17)$$

where

$$S = 0.15m\left(10.5\times10^{-6}\,m\right) = 1.57\times10^{-6}\,m^2$$

If the ELF electric current has frequency $f = 2\mu Hz = 2\times10^{-6}\,Hz$, then, the gravitational mass of the aluminum foil, given by (A16), is expressed by

$$m_g = \left\{1-2\left[\sqrt{1+7.89\times10^{-25}\,\frac{I_{DC}^4}{S^4}}-1\right]\right\}m_{i0} =$$

$$= \left\{1-2\left[\sqrt{1+0.13I_{DC}^4}-1\right]\right\}m_{i0} \qquad (A18)$$

Then,

$$\chi=\frac{m_g}{m_{i0}}\cong\left\{1-2\left[\sqrt{1+0.13I_{DC}^4}-1\right]\right\} \qquad (A19)$$

For $I_{DC}=2.2A$, the equation above gives

$$\chi=\left(\frac{m_g}{m_{i0}}\right)\cong-1 \qquad (A20)$$

This means that *the gravitational shielding* produced by the aluminum foil can change the gravity acceleration *above* the foil down to

$$g'=\chi\ g\cong-1g \qquad (A21)$$

Under these conditions, the Aluminum foil works basically as a Gravity Control Cell (GCC).

In order to check these theoretical predictions, we suggest an experimental set-up shown in Fig.A2.

A 15cm square Aluminum foil of *10.5 microns thickness* with the following composition: Al 98.02%; Fe 0.80%; Si 0.70%; Mn 0.10%; Cu 0.10%; Zn 0.10%; Ti 0.08%; Mg 0.05%; Cr 0.05%, and with the following characteristics: $\mu_t=1$; $\sigma=3.82\times10^7\,S.m^{-1}$; $\rho=2700Kg.m^{-3}$, is fixed on a 17 cm square *Foam Board* [**] plate of 6mm thickness as shown in Fig.A3. This device (the simplest Gravity Control Cell GCC) is placed on a pan balance shown in Fig.A2.

Above the Aluminum foil, a *sample* (any type of material, any mass) connected to a dynamometer will check the decrease of the *local gravity acceleration* upon the sample $\left(g'=\chi\ g\right)$, due to the gravitational shielding produced by the decreasing of gravitational mass of the Aluminum foil $\left(\chi=m_g/m_{i0}\right)$. Initially, the sample lies 5 cm above the Aluminum foil. As shown in Fig.A2, the board with the dynamometer can be displaced up to few meters in height. Thus, the initial distance between the Aluminum foil and the sample can be increased in order to check the reach of the gravitational shielding produced by the Aluminum foil.

In order to generate the ELF electric current of $f=2\mu Hz$, we can use the widely-known Function Generator HP3325A (Op.002 High Voltage Output) that can generate sinusoidal voltages with *extremely-low* frequencies down to $f=1\times10^{-6}Hz$ and amplitude up to 20V ($40V_{pp}$ into 500Ω load). The maximum output current is $0.08A_{pp}$; output impedance <2Ω at ELF.

Figure A4 shows the equivalent electric circuit for the experimental set-up. The electromotive forces are: ε_1 (HP3325A) and ε_2 (*12V* DC Battery).The values of the *resistors* are : $R_1=500\Omega-2W$; $r_{i1}<2\Omega$; $R_2=4\Omega-40W$; $r_{i2}<0.1\Omega$; $R_p=2.5\times10^{-3}\Omega$; *Rheostat* (0≤ *R* ≤10Ω - 90W). The *coupling transformer* has the following characteristics: air core with diameter $\phi=10mm$; area $S=\pi\phi^2/4=7.8\times10^{-5}m^2$; wire#12AWG; $N_1=N_2=N=20$; $l=42mm$; $L_1=L_2=L=\mu_0N^2(S/l)=9.3\times10^{-7}H$ .Thus, we get

$$Z_1=\sqrt{\left(R_1+r_{i1}\right)^2+\left(\omega L\right)^2}\cong501\Omega$$

and

$$Z_2=\sqrt{\left(R_2+r_{i2}+R_p+R\right)^2+\left(\omega L\right)^2}$$

For $R=0$ we get $Z_2=Z_2^{\min}\cong4\Omega$; for $R=10\Omega$ the result is $Z_2=Z_2^{\max}\cong14\Omega$. Thus,

$$Z_{1,total}^{\min}=Z_1+Z_{1,reflected}^{\min}=Z_1+Z_2^{\min}\left(\frac{N_1}{N_2}\right)^2\cong505\Omega$$

$$Z_{1,total}^{\max}=Z_1+Z_{1,reflected}^{\max}=Z_1+Z_2^{\max}\left(\frac{N_1}{N_2}\right)^2\cong515\Omega$$

The maxima *rms* currents have the following values:

$$I_1^{\max}=\tfrac{1}{\sqrt{2}}40V_{pp}\,/\,Z_{1,total}^{\min}=56mA$$

(The maximum output current of the Function Generator HP3325A (Op.002 High Voltage Output) is $80mA_{pp}\cong56.5mA_{rms}$);

$$I_2^{\max}=\frac{\varepsilon_2}{Z_2^{\min}}=3A$$

and

$$I_3^{\max}=I_2^{\max}+I_1^{\max}\cong3A$$

The new expression for the *inertial forces*, (Eq.5) $\vec{F}_i=M_g\vec{a}$, shows that the inertial forces are proportional to *gravitational mass*. Only in the particular case of $m_g=m_{i0}$, the expression above reduces to the well-known Newtonian expression $\vec{F}_i=m_{i0}\vec{a}$. The equivalence

[**] *Foam board* is a very strong, *lightweigh*t (density: 24.03 kg.m^{-3}) and easily cut material used for the mounting of photographic prints, as backing in picture framing, in 3D design, and in painting. It consists of three layers — an inner layer of polystyrene clad with outer facing of either white clay coated paper or brown Kraft paper.

between gravitational and inertial forces $\left(\vec{F}_i \equiv \vec{F}_g\right)$ [1] shows then that a balance measures the *gravitational mass* subjected to acceleration $a = g$. Here, the decrease in the *gravitational mass* of the Aluminum foil will be measured by a pan balance with the following characteristics: range 0-200g; readability 0.01g.

The mass of the Foam Board plate is: $\cong 4.17g$, the mass of the Aluminum foil is: $\cong 0.64g$, the total mass of the ends and the electric wires of connection is $\cong 5g$. Thus, *initially* the balance will show $\cong 9.81g$. According to (A18), when the electric current through the Aluminum foil (resistance $r_p^* = l/\sigma S = 2.5\times10^{-3}\Omega$) reaches the value: $I_3 \cong 2.2A$, we will get $m_{g(Al)} \cong -m_{i0(Al)}$. Under these circumstances, the balance will show:

$$9.81g - 0.64g - 0.64g \cong 8.53g$$

and the gravity acceleration g' *above* the Aluminum foil, becomes $g' = \chi\ g \cong -1g$.

It was shown [1] that, when the gravitational mass of a particle is reduced to the gravitational mass ranging between $+0.159M_i$ to $-0.159M_i$, it becomes *imaginary*, i.e., the gravitational and the inertial masses of the particle become *imaginary*. Consequently, the particle *disappears* from our ordinary space-time. This phenomenon can be observed in the proposed experiment, i.e., *the Aluminum foil will disappear* when its gravitational mass becomes smaller than $+0.159M_i$. It will become visible again, only when its gravitational mass becomes smaller than $-0.159M_i$, or when it becomes greater than $+0.159M_i$.

Equation (A18) shows that the gravitational mass of the Aluminum foil, $m_{g(Al)}$, goes *close to zero* when $I_3 \cong 1.76A$. Consequently, the gravity acceleration *above* the Aluminum foil also goes close to zero since $g' = \chi\ g = m_{g(Al)}/m_{i0(Al)}$. Under these circumstances, the Aluminum foil remains *invisible*.

Now consider a rigid Aluminum wire # 14 AWG. The area of its cross section is

$$S = \pi\left(1.628\times10^{-3}m\right)^2/4 = 2.08\times10^{-6}m^2$$

If an ELF electric current with frequency $f = 2\mu Hz = 2\times10^{-6}Hz$ passes through this wire, its gravitational mass, given by (A16), will be expressed by

$$m_g = \left\{1-2\left[\sqrt{1+6.313\times10^{-42}\frac{j_{rms}^4}{f^3}}-1\right]\right\}m_{i0} =$$

$$= \left\{1-2\left[\sqrt{1+7.89\times10^{-25}\frac{I_{DC}^4}{S^4}}-1\right]\right\}m_{i0} =$$

$$= \left\{1-2\left[\sqrt{1+0.13I_{DC}^4}-1\right]\right\}m_{i0} \qquad (A22)$$

For $I_{DC} \cong 3A$ the equation above gives

$$m_g \cong -3.8m_{i0}$$

Note that we can replace the Aluminum foil for this wire in the experimental set-up shown in Fig.A2. It is important also to note that an ELF electric current that passes through a wire - which makes a spherical form, as shown in Fig A5 - reduces the gravitational mass of the wire (Eq. A22), and the gravity *inside sphere* at the same proportion, $\chi = m_g/m_{i0}$, (Gravitational Shielding Effect). In this case, that effect can be checked by means of the Experimental set-up 2 (Fig.A6). Note that the spherical form can be transformed into an ellipsoidal form or a disc in order to coat, for example, a Gravitational Spacecraft. It is also possible to coat with a wire several forms, such as cylinders, cones, cubes, etc.

The circuit shown in Fig.A4 (a) can be modified in order to produce a new type of Gravitational Shielding, as shown in Fig.A4 (b). In this case, the Gravitational Shielding will be produced in the Aluminum plate, with thickness h, of the parallel plate capacitor connected in the point P of the circuit (See Fig.A4 (b)). Note that, in this circuit, the Aluminum foil (resistance R_p) (Fig.A4(a)) has been replaced by a Copper wire # 14 AWG with *1cm* length ($l = 1cm$) in order to produce a resistance $R_\phi = 5.21\times10^{-5}\Omega$. Thus, the voltage in the point P of the circuit will have the maximum value $V_p^{\max} = 1.1\times10^{-4}V$ when the resistance of the rheostat is null $(R = 0)$ and the minimum value $V_p^{\min} = 4.03\times10^{-5}V$ when $R = 10\Omega$. In this way, the voltage V_p (with frequency $f = 2\mu Hz$) applied on the capacitor will produce an electric field E_p with intensity $E_p = V_p/h$ through the Aluminum plate of thickness $h = 3mm$. It is important to note that *this plate cannot be connected to ground* (earth), in other words, cannot be grounded, because, in

this case, the electric field through it will be *null* [††].

According to Eq. A14, when $E_p^{\max}=V_p^{\max}/h=0.036\,V/m$, $f=2\mu Hz$ and $\sigma_{Al}=3.82\times10^{7}\,S/m$, $\rho_{Al}=2700kg/m^3$ (Aluminum), we get

$$\chi=\frac{m_{(Al)}}{m_{i(Al)}}\cong-0.9$$

Under these conditions, the maximum *current density* through the plate with thickness h will be given by $j^{\max}=\sigma_{Al}E_p^{\max}=1.4\times10^{6}A/m^2$ (It is well-known that the maximum current density supported by the Aluminum is $\approx10^{8}A/m^2$).

Since the area of the plate is $A=(0.2)^2=4\times10^{-2}m^2$, then the maximum current is $i^{\max}=j^{\max}A=56kA$. Despite this enormous current, the maximum dissipated power will be just $P^{\max}=\left(i^{\max}\right)^2R_{plate}=6.2W$, because the resistance of the plate is very small, i.e., $R_{plate}=h/\sigma_{Al}A\cong2\times10^{-9}\Omega$.

Note that the area A of the plate (where the Gravitational Shielding takes place) can have several geometrical configurations. For example, it can be the area of the external surface of an ellipsoid, sphere, etc. Thus, it can be the area of the external surface of a Gravitational Spacecraft. In this case, if $A\cong100m^2$, for example, the maximum dissipated power will be $P^{\max}\cong15.4kW$, i.e., approximately $154W/m^2$.

All of these systems work with Extra-Low Frequencies $\left(f<<10^{-3}Hz\right)$. Now, we show that, by simply changing *the geometry of the surface of the Aluminum foil*, it is possible to increase the working frequency f up to more than *1Hz*.

Consider the Aluminum foil, now with several semi-spheres stamped on its surface, as shown in Fig. A7 . The semi-spheres have radius $r_0=0.9\ mm$, and are joined one to another. The Aluminum foil is now coated by an insulation layer with relative permittivity ε_r and dielectric strength k. A voltage source is connected to the Aluminum foil in order to provide a voltage V_0 (rms) with frequency f. Thus, the electric potential V at a distance r, in the interval from r_0 to a, is given by

$$V=\frac{1}{4\pi\varepsilon_r\varepsilon_0}\frac{q}{r}\qquad(A23)$$

In the interval $a<r\le b$ the electric potential is

$$V=\frac{1}{4\pi\varepsilon_0}\frac{q}{r}\qquad(A24)$$

since for the air we have $\varepsilon_r\cong1$.

Thus, on the surface of the metallic spheres $\left(r=r_0\right)$ we get

$$V_0=\frac{1}{4\pi\varepsilon_r\varepsilon_0}\frac{q}{r_0}\qquad(A25)$$

Consequently, the electric field is

$$E_0=\frac{1}{4\pi\varepsilon_r\varepsilon_0}\frac{q}{r_0^2}\qquad(A26)$$

By comparing (A26) with (A25), we obtain

$$E_0=\frac{V_0}{r_0}\qquad(A27)$$

The electric potential V_b at $r=b$ is

$$V_b=\frac{1}{4\pi\varepsilon_0}\frac{q}{b}=\frac{\varepsilon_rV_0r_0}{b}\qquad(A28)$$

Consequently, the electric field E_b is given by

$$E_b=\frac{1}{4\pi\varepsilon_0}\frac{q}{b^2}=\frac{\varepsilon_rV_0r_0}{b^2}\qquad(A29)$$

From $r=r_0$ up to $r=b=a+d$ *the electric field is approximately constant* (See Fig. A7). Along the distance d it will be called E_{air}. For $r>a+d$, the electric field stops being constant. Thus, the intensity of the electric field at $r=b=a+d$ is approximately equal to E_0, i.e., $E_b\cong E_0$. Then, we can write that

$$\frac{\varepsilon_rV_0r_0}{b^2}\cong\frac{V_0}{r_0}\qquad(A30)$$

whence we get

$$b\cong r_0\sqrt{\varepsilon_r}\qquad(A31)$$

Since the intensity of the electric field through the air, E_{air}, is $E_{air}\cong E_b\cong E_0$, then, we can write that

$$E_{air}=\frac{1}{4\pi\varepsilon_0}\frac{q}{b^2}=\frac{\varepsilon_rV_0r_0}{b^2}\qquad(A32)$$

Note that ε_r refers to the *relative permittivity of*

[††] When the voltage V_p is applied on the capacitor, the charge distribution in the dielectric induces positive and negative charges, respectively on opposite sides of the Aluminum plate with thickness *h*. If the plate is not connected to the ground (Earth) this charge distribution produces an electric field $E_p=V_p/h$ through the plate. However, if the plate is connected to the ground, the negative charges (electrons) escapes for the ground and the positive charges are redistributed along the entire surface of the Aluminum plate making *null* the electric field through it.

the insulation layer, which is covering the Aluminum foil.

If the intensity of this field is greater than the dielectric strength of the air $\left(3\times10^{6}V/m\right)$ there will occur the well-known *Corona effect*. Here, this effect is necessary in order to increase the electric conductivity of the air at this region (layer with thickness *d*). Thus, we will assume

$$E_{air}^{\min}=\frac{\varepsilon_r V_0^{\min} r_0}{b^2}=\frac{V_0^{\min}}{r_0}=3\times10^{6}V/m$$

and

$$E_{air}^{\max}=\frac{\varepsilon_r V_0^{\max} r_0}{b^2}=\frac{V_0^{\max}}{r_0}=1\times10^{7}V/m \quad (A33)$$

The electric field $E_{air}^{\min}\le E_{air}\le E_{air}^{\max}$ will produce an *electrons flux* in a direction and an *ions flux* in an opposite direction. From the viewpoint of electric current, the ions flux can be considered as an "electrons" flux at the same direction of the real electrons flux. Thus, the current density through the air, j_{air}, will be the *double* of the current density expressed by the well-known equation of Langmuir-Child

$$j=\frac{4}{9}\varepsilon_r\varepsilon_0\sqrt{\frac{2e}{m_e}}\frac{V^{\frac{3}{2}}}{d^2}=\alpha\frac{V^{\frac{3}{2}}}{d^2}=2.33\times10^{-6}\frac{V^{\frac{3}{2}}}{d^2} \quad (A34)$$

where $\varepsilon_r\cong1$ for the *air*; $\alpha=2.33\times10^{-6}$ is the called *Child's constant*.

Thus, we have

$$j_{air}=2\alpha\frac{V^{\frac{3}{2}}}{d^2} \quad (A35)$$

where d, in this case, is the thickness of the air layer where the electric field is approximately constant and V is the voltage drop given by

$$V=V_a-V_b=\frac{1}{4\pi\varepsilon_0}\frac{q}{a}-\frac{1}{4\pi\varepsilon_0}\frac{q}{b}=$$

$$=V_0 r_0\varepsilon_r\left(\frac{b-a}{ab}\right)=\left(\frac{\varepsilon_r r_0 d}{ab}\right)V_0 \quad (A36)$$

By substituting (A36) into (A35), we get

$$j_{air}=\frac{2\alpha}{d^2}\left(\frac{\varepsilon_r r_0 d V_0}{ab}\right)^{\frac{3}{2}}=\frac{2\alpha}{d^{\frac{1}{2}}}\left(\frac{\varepsilon_r r_0 V_0}{b^2}\right)^{\frac{3}{2}}\left(\frac{b}{a}\right)^{\frac{3}{2}}=$$

$$=\frac{2\alpha}{d^{\frac{1}{2}}}E_{air}^{\frac{3}{2}}\left(\frac{b}{a}\right)^{\frac{3}{2}} \quad (A37)$$

According to the equation of the *Ohm's vectorial Law*: $j=\sigma E$, we can write that

$$\sigma_{air}=\frac{j_{air}}{E_{air}} \quad (A38)$$

Substitution of (A37) into (A38) yields

$$\sigma_{air}=2\alpha\left(\frac{E_{air}}{d}\right)^{\frac{1}{2}}\left(\frac{b}{a}\right)^{\frac{3}{2}} \quad (A39)$$

If the insulation layer has thickness $\Delta=0.6\ mm$, $\varepsilon_r\cong3.5$ (1- 60Hz), $k=17kV/mm$ (Acrylic sheet 1.5mm thickness), and the semi-spheres stamped on the metallic surface have $r_0=0.9\ mm$ (See Fig.A7) then $a=r_0+\Delta=1.5\ mm$. Thus, we obtain from Eq. (A33) that

$$V_0^{\min}=2.7kV$$

$$V_0^{\max}=9kV \quad (A40)$$

From equation (A31), we obtain the following value for b:

$$b=r_0\sqrt{\varepsilon_r}=1.68\times10^{-3}m \quad (A41)$$

Since $b=a+d$ we get

$$d=1.8\times10^{-4}m$$

Substitution of a, b, d and A(32) into (A39) produces

$$\sigma_{air}=4.117\times10^{-4}E_{air}^{\frac{1}{2}}=1.375\times10^{-2}V_0^{\frac{1}{2}}$$

Substitution of σ_{air}, $E_{air}(rms)$ and $\rho_{air}=1.2\ kg.m^{-3}$ into (A14) gives

$$\frac{m_{g(air)}}{m_{i0(air)}}=\left\{1-2\left[\sqrt{1+1.758\times10^{-27}\frac{\sigma_{air}^3E_{air}^4}{\rho_{air}^2f^3}}-1\right]\right\}=$$

$$=\left\{1-2\left[\sqrt{1+4.923\times10^{-21}\frac{V_0^{5.5}}{f^3}}-1\right]\right\} \quad (A42)$$

For $V_0=V_0^{\max}=9kV$ and $f=2Hz$, the result is

$$\frac{m_{g(air)}}{m_{i0(air)}}\cong-1.2$$

Note that, by increasing V_0, the values of E_{air} and σ_{air} are increased. Thus, as show (A42), there are two ways for decrease the value of $m_{g(air)}$: increasing the value of V_0 or decreasing the value of f.

Since $E_0^{\max}=10^7V/m=10kV/mm$ and $\Delta=0.6\ mm$ then the dielectric strength of the insulation must be $\ge16.7kV/mm$. As mentioned above, the dielectric strength of the acrylic is $17kV/mm$.

It is important to note that, due to the strong value of E_{air} (Eq. A37) the *drift velocity* v_d, $\left(v_d=j_{air}/ne=\sigma_{air}E_{air}/ne\right)$ of the free charges inside the ionized air put them at a

distance $x = v_d / t = 2 f v_d \cong 0.4m$, which is much greater than the distance $d = 1.8 \times 10^{-4} m$. Consequently, the number n of free charges decreases strongly inside the air layer of thickness d [‡‡], except, obviously, in a thin layer, very close to the dielectric, where the number of free charges remains sufficiently increased, to maintain the air conductivity with $\sigma_{air} \cong 1.1 S/m$ (Eq. A39).

The thickness h of this thin air layer close to the dielectric can be easily evaluated starting from the charge distribution in the neighborhood of the dielectric, and of the repulsion forces established among them. The result is $h = \sqrt{0.06e / 4\pi\varepsilon_0 E} \cong 4 \times 10^{-9} m$. This is, therefore, the thickness of the *Air* Gravitational Shielding. If the area of this Gravitational Shielding is equal to the area of a format A4 sheet of paper, i.e., $A = 0.20 \times 0.291 = 0.0582 m^2$, we obtain the following value for the resistance R_{air} of the Gravitational Shielding: $R_{air} = h / \sigma_{air} A \cong 6 \times 10^{8} \Omega$. Since the maximum electrical current through this air layer is $i^{\max} = j^{\max} A \cong 400 kA$, then the maximum power radiated from the Gravitational Shielding is $P_{air}^{\max} = R_{air} \left(i_{air}^{\max} \right)^2 \cong 10 kW$. This means that a very strong light will be radiated from this type of Gravitational Shielding. Note that this device can also be used as a lamp, which will be much more efficient than conventional lamps.

Coating a ceiling with this lighting system enables the entire area of ceiling to produce light. This is a form of lighting very different from those usually known.

Note that the value $P_{air}^{\max} \cong 10 kW$, defines the power of the transformer shown in Fig.A10. Thus, the maximum current in the secondary is $i_s^{\max} = 9 kV / 10 kW = 0.9 A$.

Above the Gravitational Shielding, σ_{air} is reduced to the normal value of conductivity of the atmospheric air $\left(\approx 10^{-14} S/m \right)$. Thus, the power radiated from this region is

$$P_{air}^{\max} = (d - h) \left(i_{air}^{\max} \right)^2 / \sigma_{air} A =$$

$$= (d - h) A \sigma_{air} \left(E_{air}^{\max} \right)^2 \cong 10^{-4} W$$

Now, we will describe a method to coat the Aluminum semi-spheres with acrylic in the necessary dimensions $(\Delta = a - r_0)$, we propose the following method. First, take an Aluminum plate with $21cm \times 29.1cm$ (A4 format). By means of a convenient process, several semi-spheres can be stamped on its surface. The semi-spheres have radius $r_0 = 0.9\ mm$, and are joined one to another. Next, take an acrylic sheet (A4 format) with 1.5mm thickness (See Fig.A8 (a)). Put a heater below the Aluminum plate in order to heat the Aluminum (Fig.A8 (b)). When the Aluminum is sufficiently heated up, the acrylic sheet and the Aluminum plate are pressed, one against the other, as shown in Fig. A8 (c). The two D devices shown in this figure are used in order to impede that the press compresses the acrylic and the aluminum to a distance shorter than $y + a$. After some seconds, remove the press and the heater. The device is ready to be subjected to a voltage V_0 with frequency f, as shown in Fig.A9. Note that, in this case, the balance is not necessary, because *the substance that produces the gravitational shielding* is an *air layer* with thickness d *above* the acrylic sheet. This is, therefore, more a type of Gravity Control Cell (GCC) with *external gravitational shielding*.

It is important to note that this GCC can be made very thin and as flexible as a fabric. Thus, it can be used to produce *anti- gravity clothes*. These clothes can be extremely useful, for example, to walk on the surface of high gravity planets.

Figure A11 shows some geometrical forms that can be stamped on a metallic surface in order to produce a Gravitational Shielding effect, similar to the produced by the *semi-spherical form*.

An obvious evolution from the semi-spherical form is the *semi-cylindrical* form shown in Fig. A11 (b); Fig.A11(c) shows *concentric metallic rings* stamped on the metallic surface, an evolution from Fig.A11 (b). These geometrical forms produce the same effect as the semi-spherical form, shown in Fig.A11 (a). By using concentric metallic rings, it is possible to build *Gravitational Shieldings* around bodies or spacecrafts with several formats (spheres, ellipsoids, etc); Fig. A11 (d) shows a Gravitational Shielding around a Spacecraft with *ellipsoidal form*.

The previously mentioned Gravitational Shielding, produced on a thin layer of ionized air, has a *behavior different from* the Gravitational Shielding produced on a *rigid substance*. When the gravitational masses of the air molecules, inside the shielding, are reduced to within the range $+0.159 m_i < m_g < -0.159 m_i$, they go to the *imaginary space-time*, as previously shown in this article. However, the electric field E_{air} stays at the real space-time. Consequently, the molecules return immediately to the real space-

[‡‡] Reducing therefore, the conductivity σ_{air}, to the normal value of conductivity of the atmospheric air.

time in order to return soon after to the *imaginary* space-time, due to the action of the electric field E_{air}.

In the case of the Gravitational Shielding produced on a *solid substance*, when the molecules of the substance go to the *imaginary* space-time, *the electric field that produces the effect, also goes to the imaginary space-time together with them*, since in this case, the substance of the Gravitational Shielding is rigidly connected to the metal that produces the electric field. (See Fig. A12 (b)). This is the fundamental difference between the *non-solid* and *solid* Gravitational Shieldings.

Now, consider a Gravitational Spacecraft that is able to produce an *Air* Gravitational Shielding and also a *Solid* Gravitational Shielding, as shown in Fig. A13 (a) [§§]. Assuming that the intensity of the electric field, E_{air}, necessary to reduce the gravitational mass of the *air molecules* to within the range $+0.159m_i < m_g < -0.159m_i$, *is much smaller* than the intensity of the electric field, E_{rs}, necessary to reduce the gravitational mass of the *solid substance* to within the range $+0.159m_i < m_g < -0.159m_i$, then we conclude that the Gravitational Shielding made of ionized air goes to the imaginary space-time *before* the Gravitational Shielding made of *solid substance*. When this occurs the spacecraft does not go to the imaginary space-time together with the Gravitational Shielding of air, because the air molecules are not rigidly connected to the spacecraft. Thus, while the air molecules go into the imaginary space-time, the spacecraft stays in the *real space-time*, and remains subjected to the effects of the Gravitational Shielding around it, since the shielding does not stop to work, due to its extremely short permanence at the imaginary space-time. Under these circumstances, the gravitational mass of the Gravitational Shielding can be reduced to $m_g \cong 0$. For example, $m_g \cong 10^{-4} kg$. Thus, if the *inertial mass* of the Gravitational Shielding is $m_{i0} \cong 1kg$, then $\chi = m_g / m_{i0} \cong 10^{-4}$. As we have seen, this means that *the inertial effects on the spacecraft* will be reduced by $\chi \cong 10^{-4}$. Then, in spite of the effective acceleration of the spacecraft be, for example, $a = 10^5 m.s^{-2}$, the effects on the crew of the spacecraft will be equivalent to an acceleration of only

$$a' = \frac{m_g}{m_{i0}} a = \chi \ a \approx 10 m.s^{-1}$$

This is the magnitude of the acceleration upon the passengers in a contemporary commercial jet.

Then, it is noticed that Gravitational Spacecrafts can be subjected to enormous *accelerations* (or *decelerations*) without imposing any harmful impacts whatsoever on the spacecrafts or its crew.

Now, imagine that the intensity of the electric field that produces the Gravitational Shielding around the spacecraft is *increased* up to reaching the value E_{rs} that reduces the gravitational mass of the *solid* Gravitational Shielding to within the range $+0.159m_i < m_g < -0.159m_i$. Under these circumstances, the *solid* Gravitational Shielding goes to the imaginary space-time and, since it is rigidly connected to the spacecraft, also the spacecraft goes to the imaginary space-time together with the Gravitational Shielding. Thus, the spacecraft can travel within the imaginary space-time and make use of the Gravitational Shielding around it.

As we have already seen, the maximum velocity of propagation of the interactions in the imaginary space-time is *infinite* (in the real space-time this limit is equal to the light velocity c). This means that *there are no limits for the velocity of the spacecraft in the imaginary space-time*. Thus, the acceleration of the spacecraft can reach, for example, $a = 10^9 m.s^{-2}$, which leads the spacecraft to attain velocities $V \approx 10^{14} m.s^{-1}$ (about 1 million times the speed of light) after one day of trip. With this velocity, after 1 month of trip the spacecraft would have traveled about $10^{21} m$. In order to have idea of this distance, it is enough to remind that the diameter of our Universe (visible Universe) is of the order of $10^{26} m$.

[§§] The *solid* Gravitational Shielding can also be obtained by means of *an ELF electric current through a metallic lamina* placed *between the semi-spheres and the Gravitational Shielding of Air* (See Fig.A13 (a)). The gravitational mass of the solid Gravitational Shielding will be controlled just by means of the intensity of the ELF electric current. Recently, it was discovered that Carbon nanotubes (CNTs) can be added to *Alumina* (Al_2O_3) to convert it into a good electrical conductor. It was found that the electrical conductivity increased up to 3375 S/m at 77°C in samples that were 15% nanotubes by volume [12]. It is known that the density of α-Alumina is 3.98kg.m^{-3} and that it can withstand 10-20 KV/mm. Thus, these values show that the Alumina-CNT can be used to make a *solid* Gravitational Shielding. In this case, the electric field produced by means of the semi-spheres will be used to control the gravitational mass of the Alumina-CNT.

Due to the extremely low density of the *imaginary* bodies, the collision between them cannot have the same consequences of the collision between the real bodies.

Thus, *for a Gravitational Spacecraft in imaginary state, the problem of the collision in high-speed doesn't exist.* Consequently, the Gravitational Spacecraft can transit freely in the imaginary Universe and, in this way, reach easily any point of our real Universe once they can make the transition back to our Universe by only increasing the gravitational mass of the Gravitational Shielding of the spacecraft in such way that it leaves the range of $+0.159M_i$ to $-0.159M_i$.

The return trip would be done in similar way. That is to say, the spacecraft would transit in the imaginary Universe back to the departure place where would reappear in our Universe. Thus, trips through our Universe that would delay millions of years, at speeds close to the speed of light, could be done in just a few *months* in the imaginary Universe.

In order to produce the acceleration of $a \approx 10^9\, m.s^{-2}$ upon the spacecraft we propose a Gravitational Thruster with 10 GCCs (10 Gravitational Shieldings) of the type with several semi-spheres stamped on the metallic surface, as previously shown, or with the *semi-cylindrical* form shown in Figs. A11 (b) and (c). The 10 GCCs are filled with air at 1 atm and 300K. If the insulation layer is made with *Mica* $(\varepsilon_r \cong 5.4)$ and has thickness $\Delta = 0.1\ mm$, and the semi-spheres stamped on the metallic surface have $r_0 = 0.4\ mm$ (See Fig.A7) then $a = r_0 + \Delta = 0.5\ mm$. Thus, we get

$$b = r_0\sqrt{\varepsilon_r} = 9.295\times10^{-4} m$$

and

$$d = b - a = 4.295\times10^{-4} m$$

Then, from Eq. A42 we obtain

$$\chi_{air} = \frac{m_{g(air)}}{m_{i0(air)}} = \left\{1 - 2\left[\sqrt{1+1.758\times10^{-27}\frac{\sigma_{air}^3 E_{air}^4}{\rho_{air}^2 f^3}} - 1\right]\right\} =$$

$$= \left\{1 - 2\left[\sqrt{1+1.0\times10^{-18}\frac{V_0^{5.5}}{f^3}} - 1\right]\right\}$$

For $V_0 = V_0^{\max} = 15.6kV$ and $f = 0.12Hz$, the result is

$$\chi_{air} = \frac{m_{g(air)}}{m_{i0(air)}} \cong -1.6\times10^4$$

Since $E_0^{\max} = V_0^{\max} / r_0$ is now given by $E_0^{\max} = 15.6kV/0.9mm = 17.3kV/mm$ and $\Delta = 0.1\ mm$ then the dielectric strength of the insulation must be $\geq 173kV/mm$. As shown in the table below[***], *0.1mm - thickness of* Mica *can withstand 17.6 kV* (that is greater than $V_0^{\max} = 15.6kV$), in such way that the dielectric strength is *176 kV/mm*.

The Gravitational Thrusters are positioned at the spacecraft, as shown in Fig. A13 (b). Then, when the spacecraft is in the *intergalactic space*, the gravity acceleration upon the gravitational mass m_{gt} of the bottom of the thruster (See Fig.A13 (c)), is given by [2]

$$\vec{a} \cong (\chi_{air})^{10}\,\vec{g}_M \cong -(\chi_{air})^{10} G\frac{M_g}{r^2}\hat{\mu}$$

where M_g is the gravitational mass in front of the spacecraft.

For simplicity, let us consider just the effect of a hypothetical volume $V = 10\times10^3\times10^3 = 10^7 m^3$ of intergalactic matter in front of the spacecraft $(r \cong 30m)$. The average density of matter in the *intergalactic medium (IGM)* is $\rho_{ig} \approx 10^{-26} kg.m^{-3}$)[†††]. Thus, for $\chi_{air} \cong -1.6\times10^4$ we get

$$a = -\left(-1.6\times10^4\right)^{10}\left(6.67\times10^{-11}\right)\left(\frac{10^{-19}}{30^2}\right) =$$

$$= -10^9\, m.s^{-2}$$

In spite of this gigantic acceleration, the inertial effects for the crew of the spacecraft can be strongly reduced if, for example, the gravitational mass of the Gravitational Shielding is reduced

---

[***] The *dielectric strength* of some dielectrics can have different values in lower thicknesses. This is, for example, the case of the *Mica*.

Dielectric	*Thickness* (mm)	*Dielectric Strength* (kV/mm)
Mica	0.01 mm	200
Mica	**0.1 mm**	**176**
Mica	1 mm	61

[†††] Some theories put the average density of the Universe as the equivalent of *one hydrogen atom per cubic meter* [13,14]. The density of the universe, however, is clearly not uniform. Surrounding and stretching between galaxies, there is a rarefied plasma [15] that is thought to possess a cosmic filamentary structure [16] and that is slightly denser than the average density in the universe. This material is called the *intergalactic medium (IGM)* and is mostly ionized hydrogen; i.e. a plasma consisting of equal numbers of electrons and protons. The IGM is thought to exist at a density of 10 to 100 times the average density of the Universe (10 to 100 hydrogen atoms per cubic meter, i.e., $\approx 10^{-26}\, kg.m^{-3}$).

down to $m_g \cong 10^{-6} kg$ and its inertial mass is $m_{i0} \cong 100kg$. Then, we get $\chi = m_g / m_{i0} \cong 10^{-8}$. Therefore, *the inertial effects on the spacecraft* will be reduced by $\chi \cong 10^{-8}$, and consequently, the inertial effects on the crew of the spacecraft would be *equivalent to* an acceleration a' of only

$$a' = \frac{m_g}{m_{i0}} a = \left(10^{-8}\right)\left(10^{9}\right) \approx 10 m.s^{-2}$$

Note that the Gravitational Thrusters in the spacecraft must have a very small diameter (of the order of *millimeters*) since, obviously, the hole through the Gravitational Shielding cannot be large. Thus, these thrusters are in fact, *Micro-Gravitational Thrusters*. As shown in Fig. A13 (b), it is possible to place several micro-gravitational thrusters in the spacecraft. This gives to the Gravitational Spacecraft, several degrees of freedom and shows the enormous superiority of this spacecraft in relation to the contemporaries spacecrafts.

The density of matter in the *intergalactic medium (IGM)* is about *10 $^{-26}$ kg.m^{-3}* , which is very less than the density of matter in the *interstellar medium* (*~10^{-21} kg.m^{-3}*) that is less than the density of matter in the *interplanetary medium* (*~10^{-20} kg.m^{-3}*). The density of matter is enormously increased inside the Earth's atmosphere (*1.2kg.m^{-3}* near to Earth's surface). Figure A14 shows the gravitational acceleration acquired by a Gravitational Spacecraft, in these media, using Micro-Gravitational thrusters.

In relation to the *Interstellar* and *Interplanetary medium*, the *Intergalactic medium* requires the greatest value of χ_{air} (χ inside the *Micro-Gravitational Thrusters*), i.e., $\chi_{air} \cong -1.6 \times 10^4$. This value strongly decreases when the spacecraft is within the Earth's atmosphere. In this case, it is sufficient only[‡‡‡] $\chi_{air} \cong -10$ in order to obtain:

$$a = -\left(\chi_{air}\right)^{10} G \frac{\rho_{atm} V}{r^2} \cong$$

$$\cong -\left(-10\right)^{10} \left(6.67 \times 10^{-11}\right) \frac{1.2\left(10^7\right)}{\left(20\right)^2} \cong 10^4 m.s^{-2}$$

With this acceleration the Gravitational Spacecraft can reach about *50000 km/h* in a few seconds. Obviously, the Gravitational Shielding of the spacecraft will reduce strongly *the inertial effects upon the crew* of the spacecraft, in such way that the inertial effects of this strong acceleration will not be felt. In addition, the *artificial atmosphere*, which is possible to build around the spacecraft, by means of gravity control technologies shown in this article (See Fig.6) and [2], will protect it from the *heating* produced by the friction with the Earth's atmosphere. Also, the gravity can be controlled inside of the Gravitational Spacecraft in order to maintain a value close to the Earth's gravity as shown in Fig.3.

Finally, it is important to note that a Micro-Gravitational Thruster does not work *outside* a Gravitational Shielding, because, in this case, *the resultant upon the thruster is null* due to the symmetry (See Fig. A15 (a)). Figure A15 (b) shows a micro-gravitational thruster inside a Gravitational Shielding. This thruster has 10 Gravitational Shieldings, in such way that the gravitational acceleration upon the *bottom* of the thruster, due to a gravitational mass M_g *in front* of the thruster, is $a_{10} = \chi_{air}^{10} a_0$ where $a_0 = -G M_g / r^2$ is the gravitational acceleration acting on the front of the micro-gravitational thruster. *In the opposite direction*, the gravitational acceleration upon the bottom of the thruster, produced by a gravitational mass M_g, is

$$a_0' = \chi_s \left(-GM_g / r'^2\right) \cong 0$$

since $\chi_s \cong 0$ due to the Gravitational Shielding around the micro-thruster (See Fig. A15 (b)). Similarly, the acceleration in front of the thruster is

$$a_{10}' = \chi_{air}^{10} a_0' = \left[\chi_{air}^{10}\left(-GM_g / r'^2\right)\right] \chi_s$$

where $\left[\chi_{air}^{10}\left(-GM_g / r'^2\right)\right] < a_{10}$, since $r' > r$. Thus, for $a_{10} \cong 10^9 m.s^{-2}$ and $\chi_s \approx 10^{-8}$ we conclude that $a_{10}' < 10 m.s^{-2}$. This means that $a_{10}' << a_{10}$. Therefore, we can write that the resultant on the micro-thruster can be expressed by means of the following relation

$$R \cong F_{10} = \chi_{air}^{10} F_0$$

Figure A15 (c) shows a Micro-Gravitational Thruster with *10 Air Gravitational Shieldings* (10 GCCs). Thin Metallic laminas are placed after

[‡‡‡] This value is within the range of values of χ $\left(\chi < -10^{3}.\ See\ \ Eq.A15\right)$, which can be produced by means of *ELF electric currents* through metals as *Aluminum*, etc. This means that, in this case, if convenient, we can replace *air* inside the GCCs of the Gravitational Micro-thrusters by metal laminas with *ELF electric currents* through them.

each *Air* Gravitational Shielding in order to retain the electric field $E_b = V_0/x$, produced by metallic *surface behind* the semi-spheres. The laminas with semi-spheres stamped on its surfaces are connected to the ELF voltage source V_0 and the thin laminas in front of the Air Gravitational Shieldings are grounded. The air inside this Micro-Gravitational Thruster is at 300K, 1atm.

We have seen that the insulation layer of a GCC can be made up of Acrylic, Mica, etc. Now, we will design a GCC using *Water* (*distilled water*, $\varepsilon_{r(H_2O)} = 80$) and Aluminum *semi-cylinders* with radius $r_0 = 1.3mm$. Thus, for $\Delta = 0.6mm$, the new value of a is $a = 1.9mm$. Then, we get

$$b = r_0\sqrt{\varepsilon_{r(H_2O)}} = 11.63\times10^{-3}m \qquad (A43)$$

$$d = b - a = 9.73\times10^{-3}m \qquad (A44)$$

and

$$E_{air} = \frac{1}{4\pi\varepsilon_{r(air)}\varepsilon_0}\frac{q}{b^2} =$$

$$= \varepsilon_{r(H_2O)}\frac{V_0 r_0}{\varepsilon_{r(air)} b^2} =$$

$$= \frac{V_0/r_0}{\varepsilon_{r(air)}} \cong \frac{V_0}{r_0} = 11111\ V_0 \qquad (A45)$$

Note that

$$E_{(H_2O)} = \frac{V_0/r_0}{\varepsilon_{r(H_2O)}}$$

and

$$E_{(acrylic)} = \frac{V_0/r_0}{\varepsilon_{r(acrylic)}}$$

Therefore, $E_{(H_2O)}$ and $E_{(acrylic)}$ are much smaller than E_{air}. Note that for $V_0 \le 9kV$ the intensities of $E_{(H_2O)}$ and $E_{(acrylic)}$ are not sufficient to produce the ionization effect, which increases the electrical conductivity. Consequently, the conductivities of the water and the acrylic remain $<< 1\ S.m^{-1}$. In this way, with $E_{(H_2O)}$ and $E_{(acrylic)}$ much smaller than E_{air}, and $\sigma_{(H2O)} << 1$, $\sigma_{(acrylic)} << 1$, the decrease in both the gravitational mass of the acrylic and the gravitational mass of water, according to Eq.A14, is negligible. This means that only in the air layer the decrease in the gravitational mass will be relevant.

Equation A39 gives the electrical conductivity of the air layer, i.e.,

$$\sigma_{air} = 2\alpha\left(\frac{E_{air}}{d}\right)^{\frac{1}{2}}\left(\frac{b}{a}\right)^{\frac{3}{2}} = 0.029V_0^{\frac{1}{2}} \qquad (A46)$$

Note that $b = r_0\sqrt{\varepsilon_{r(H_2O)}}$. Therefore, here the value of b is larger than in the case of the acrylic. Consequently, *the electrical conductivity of the air layer will be larger here than in the case of acrylic.*

Substitution of $\sigma_{(air)}$, E_{air} (*rms*) and $\rho_{air} = 1.2kg.m^{-3}$ into Eq. A14, gives

$$\frac{m_{g(air)}}{m_{i0(air)}} = \left\{1 - 2\left[\sqrt{1 + 4.54\times10^{20}\frac{V_0^{5.5}}{f^3}} - 1\right]\right\} \qquad (A47)$$

For $V_0 = V_0^{\max} = 9kV$ and $f = 2Hz$, the result is

$$\frac{m_{g(air)}}{m_{i0(air)}} \cong -8.4$$

This shows that, by using *water* instead of acrylic, the result is much better.

In order to build the GCC based on the calculations above (See Fig. A16), take an Acrylic plate with *885mm* X *885m* and *2mm* thickness, then paste on it an Aluminum sheet with *895.2mm* X *885mm* and *0.5mm* thickness(note that two edges of the Aluminum sheet are bent as shown in Figure A16 (b)). Next, take *342* Aluminum yarns with *884mm* length and *2.588mm* diameter (wire # 10 AWG) and insert them side by side on the Aluminum sheet. See in Fig. A16 (b) the detail of fixing of the yarns on the Aluminum sheet. Now, paste acrylic strips (with *13.43mm* height and *2mm* thickness) around the Aluminum/Acrylic, making a box. Put *distilled water* (approximately *1 litter*) inside this box, up to a height of exactly *3.7mm* from the edge of the acrylic base. Afterwards, paste an Acrylic lid (*889mm* X *889mm* and *2mm* thickness) on the box. Note that above the water there is an *air* layer with *885mm* X *885mm* and *7.73mm* thickness (See Fig. A16). This thickness plus the acrylic lid thickness (*2mm*) is equal to $d = b - a = 9.73mm$ where $b = r_0\sqrt{\varepsilon_{r(H_2O)}} = 11.63mm$ and $a = r_0 + \Delta = 1.99mm$, since $r_0 = 1.3mm$, $\varepsilon_{r(H_2O)} = 80$ and $\Delta = 0.6mm$.

Note that the gravitational action of the electric field E_{air}, extends itself only up to the distance d, which, in this GCC, is given by the sum of the Air layer thickness (*7.73mm*) plus the thickness of the Acrylic lid (*2mm*).

Thus, it is ensured the gravitational effect on the air layer while it is practically nullified in

the acrylic sheet above the air layer, since $E_{(acrylic)} << E_{air}$ and $\sigma_{(acrylic)} << 1$.

With this GCC, we can carry out an experiment where the *gravitational mass of the air layer* is progressively reduced when the voltage applied to the GCC is increased (or when the frequency is decreased). A precision balance is placed below the GCC in order to measure the mentioned mass decrease for comparison with the values predicted by Eq. A(47). In total, this GCC weighs about *6kg*; the *air layer 7.3grams*. The balance has the following characteristics: *range 0-6kg; readability 0.1g*. Also, in order to prove the *Gravitational Shielding Effect*, we can put a *sample* (connected to a dynamometer) above the GCC in order to check the gravity acceleration in this region.

In order to prove *the exponential effect* produced by the superposition of the Gravitational Shieldings, we can take three similar GCCs and put them one above the other, in such way that above the GCC 1 the gravity acceleration will be $g' = \chi\, g$; above the GCC2 $g'' = \chi^2 g$, and above the GCC3 $g''' = \chi^3 g$. Where χ is given by Eq. (A47).

It is important to note that the intensity of the electric field through the air *below* the GCC is *much smaller* than the intensity of the electric field through the air layer inside the GCC. In addition, the electrical conductivity of the air below the GCC is much smaller than the conductivity of the air layer inside the GCC. Consequently, the decrease of the gravitational mass of the air below the GCC, according to Eq.A14, is negligible. This means that the GCC1, GCC2 and GCC3 can be simply overlaid, on the experiment proposed above. However, since it is necessary to put samples among them in order to measure the gravity above each GCC, we suggest a spacing of 30cm or more among them.

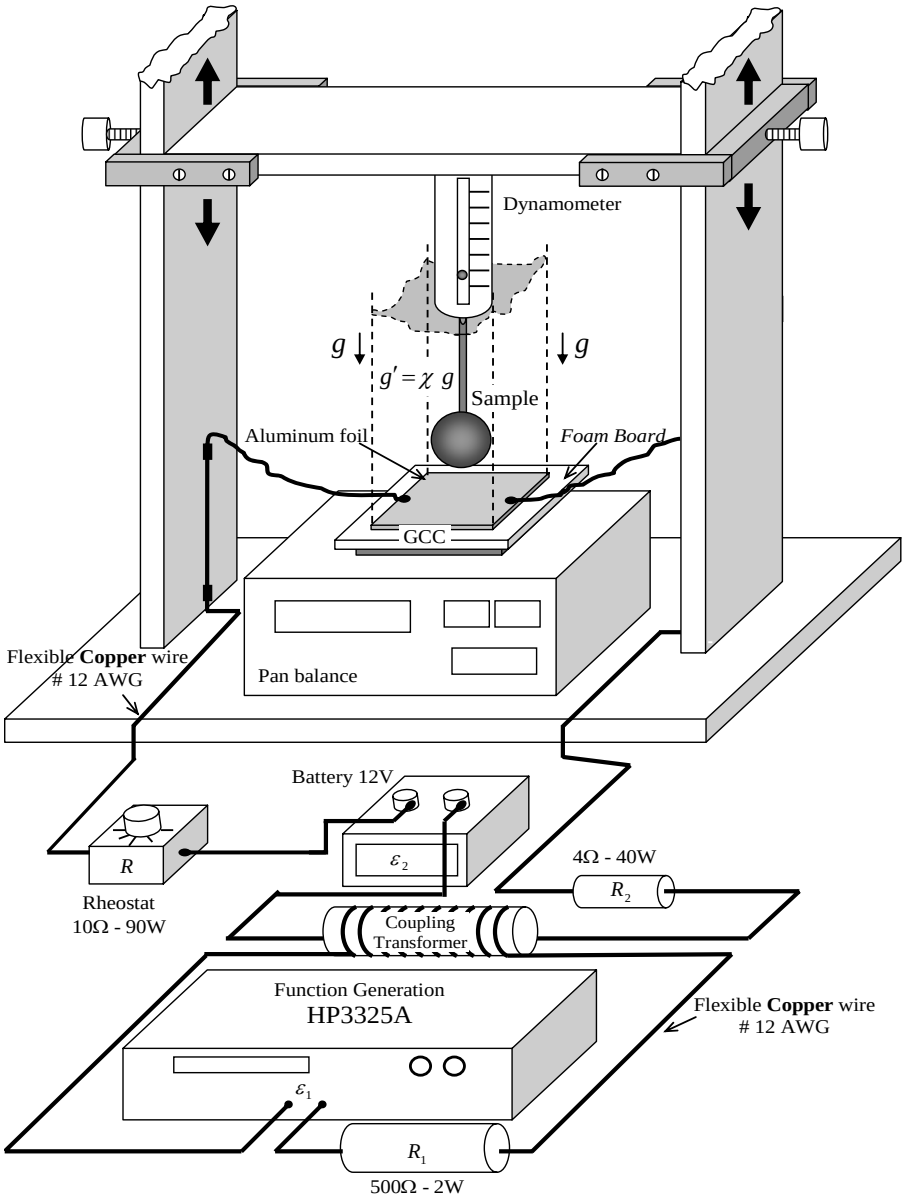

Figure A2 – Experimental Set-up 1.

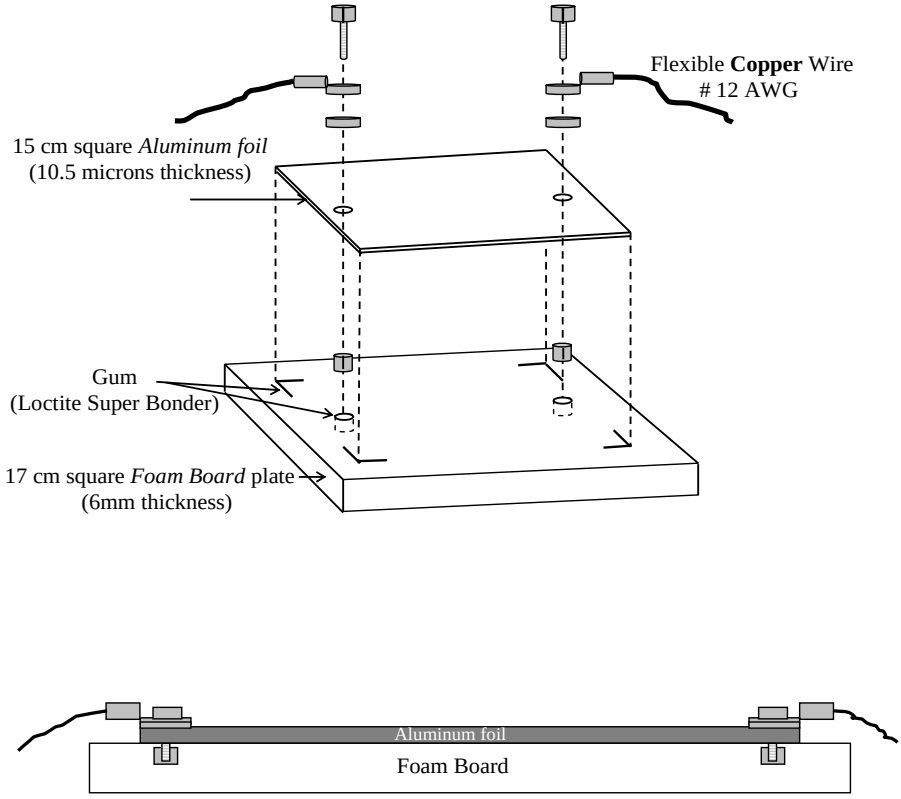

Figure A3 – The Simplest *Gravity Control Cell* (GCC).

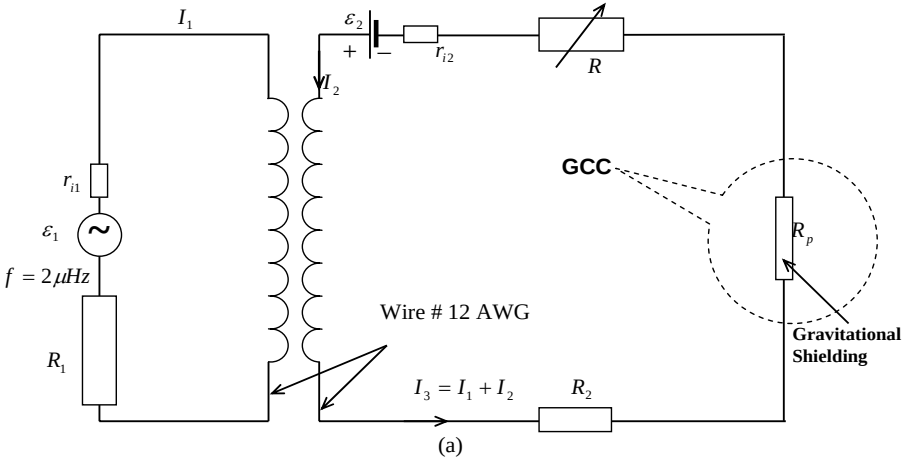

(a)

ε_1 = Function Generator HP3325A(*Option* 002 High Voltage Output)

$r_{i1} < 2\Omega$; $R_1 = 500\Omega - 2\ W$; $\varepsilon_2 = 12V\ DC$; $r_{i2} < 0.1\Omega\ (Battery)$;

$R_2 = 4\Omega - 40W$; $R_p = 2.5\times10^{-3}\Omega$; $Reostat = 0 \le R \le 10\Omega - 90W$

$I_1^{\max} = 56mA\ (rms)$; $I_2^{\max} = 3A$; $I_3^{\max} \cong 3A\ (rms)$

Coupling Transformer to isolate the *Function Generator* from the Battery

• Air core 10 - mm diameter; wire #12 AWG; $N_1 = N_2 = 20; l = 42mm$

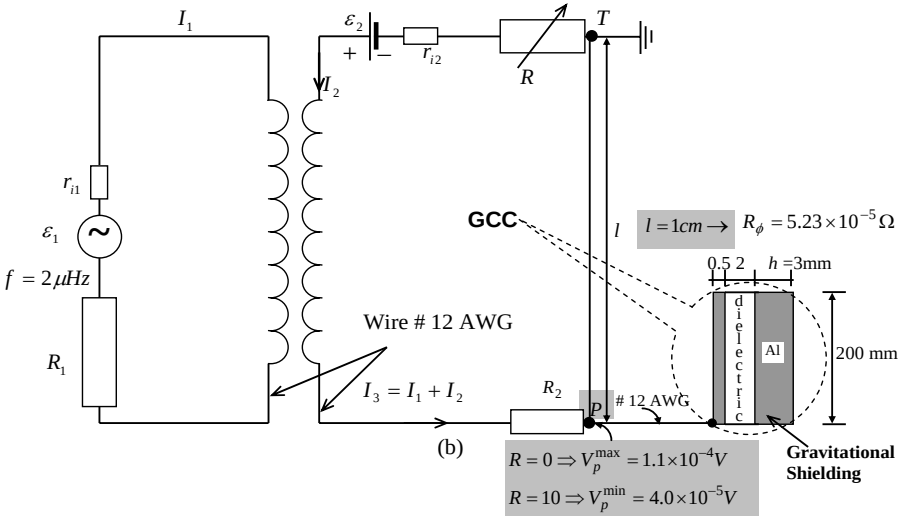

(b)

Fig. A4 – Equivalent Electric Circuits

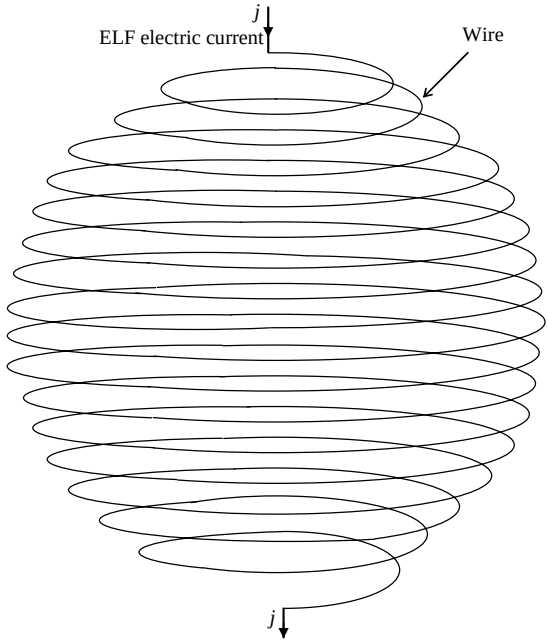

$$m_g = \left\{1 - 2\left[\sqrt{1 + 1.758\times10^{-27}\,\frac{\mu_r j^4}{\sigma\rho^2 f^3}} - 1\right]\right\} m_{i0}$$

Figure A5 – An ELF electric current through a wire, that makes a spherical form as shown above, reduces the gravitational mass of the wire and the gravity inside sphere at the same proportion $\chi = m_g / m_{i0}$ (Gravitational Shielding Effect). Note that this spherical form can be transformed into an ellipsoidal form or a disc in order to coat, for example, a Gravitational Spacecraft**.** It is also possible to coat with a wire several forms, such as cylinders, cones, cubes, etc. The characteristics of the wire are expressed by: μ_r, σ, ρ; j is the electric current density and f is the frequency.

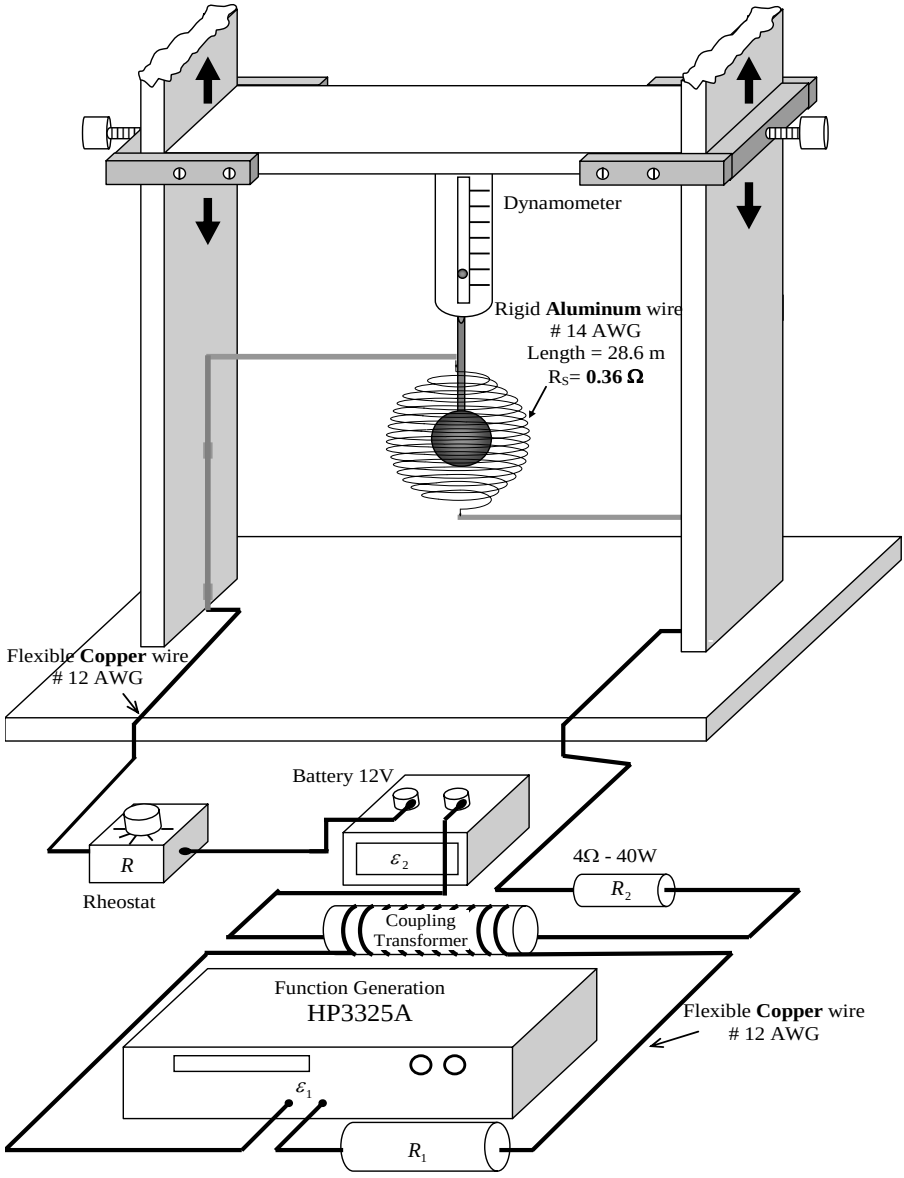

Figure A6 – Experimental set-up 2.

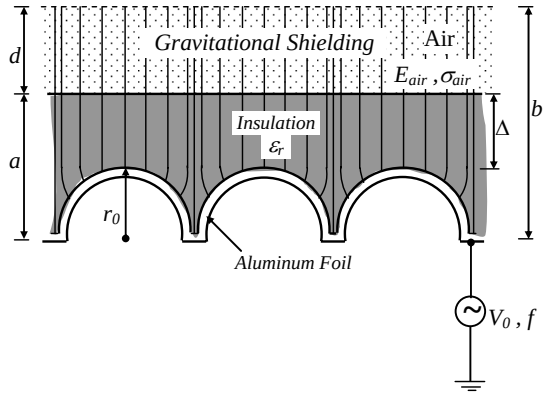

Figure A7 – *Gravitational shielding produced by semi-spheres stamped on the Aluminum foil* - By simply changing the geometry of the surface *of* the Aluminum foil it is possible to increase the working frequency f up to more than *1Hz*.

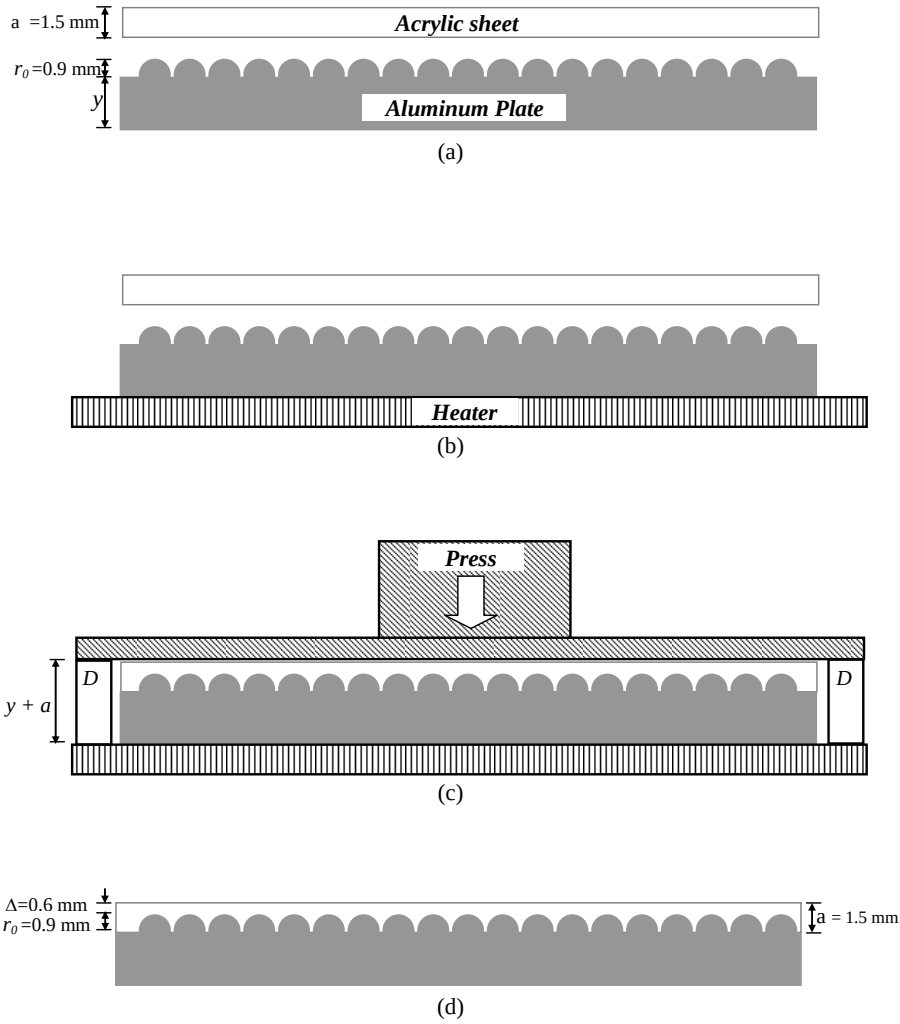

Figure A8 – *Method to coat the Aluminum semi-spheres with acrylic* $(\Delta = a - r_0 = 0.6mm)$. (a)Acrylic sheet (A4 format) with 1.5mm thickness and an Aluminum plate (A4) with several semi-spheres (radius $r_0 = 0.9\ mm$) stamped on its surface. (b)A heater is placed below the Aluminum plate in order to heat the Aluminum. (c)When the Aluminum is sufficiently heated up, the acrylic sheet and the Aluminum plate are pressed, one against the other (The two D devices shown in this figure are used in order to impede that the press compresses the acrylic and the aluminum besides distance $y + a$). (d)After some seconds, the press and the heater are removed, and the device is ready to be used.

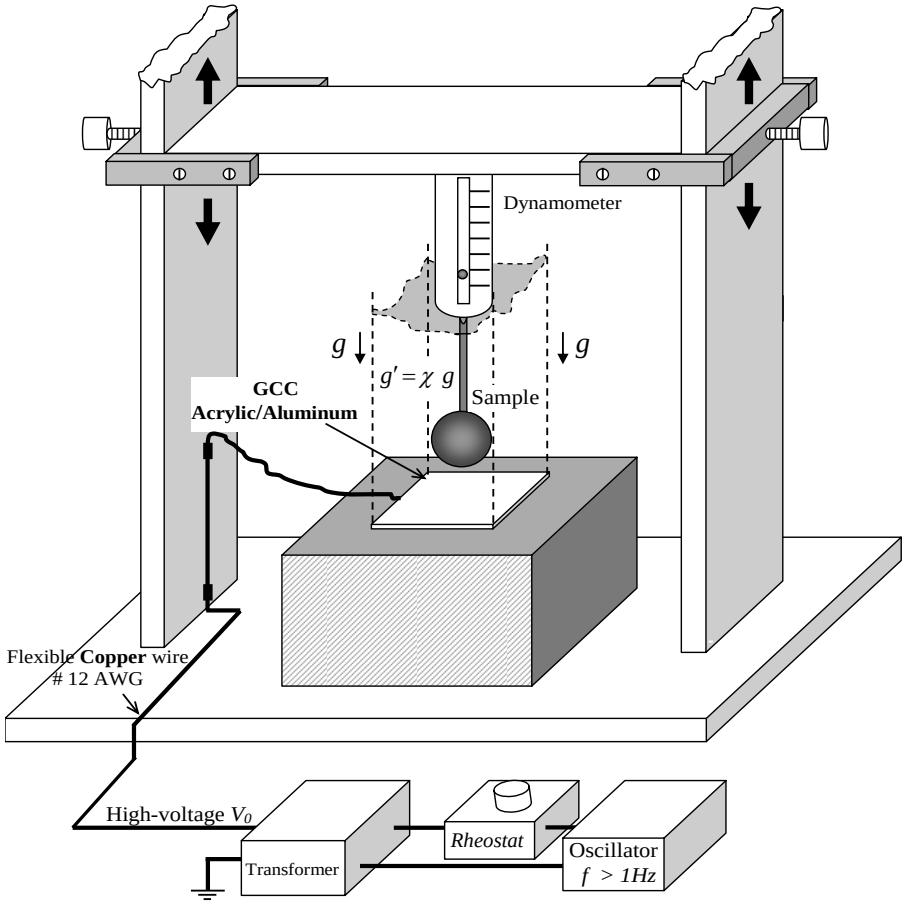

Figure A9 – *Experimental Set-up using a GCC subjected to high-voltage* V_0 *with frequency* $f > 1Hz$. Note that in this case, the pan balance is not necessary because the substance of the Gravitational Shielding is an *air layer* with thickness d *above* the acrylic sheet. This is therefore, more a type of Gravity Control Cell (GCC) with *external gravitational shielding.*

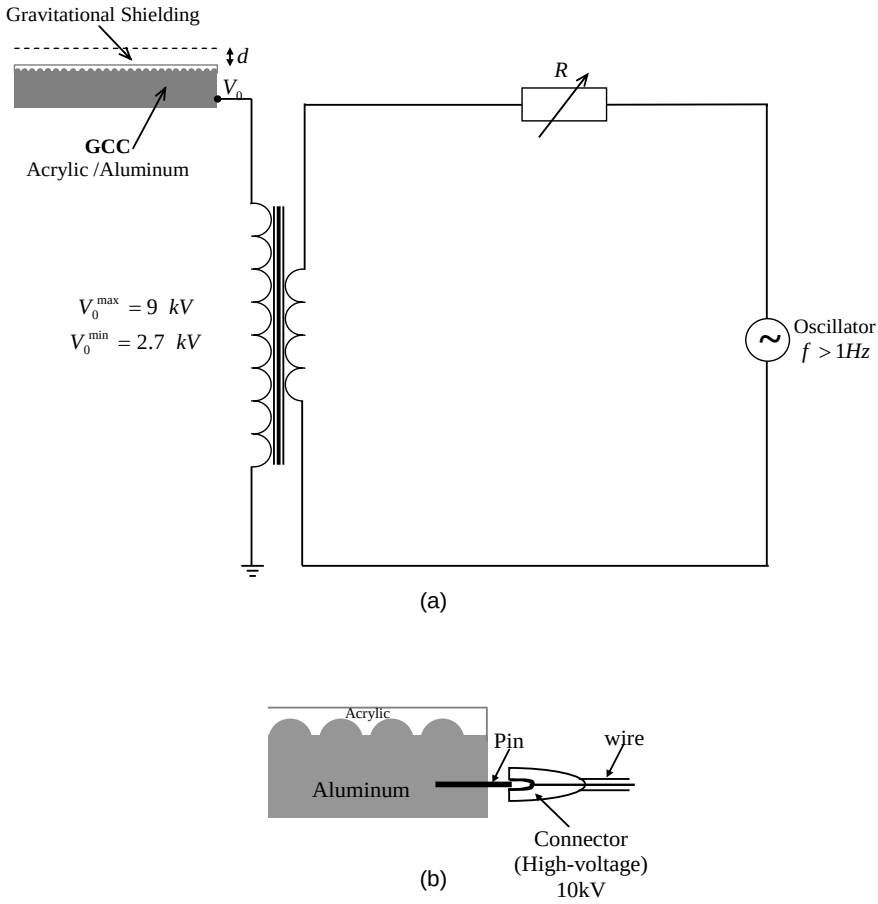

Figure A10 – (a) *Equivalent Electric Circuit.* (b) Details of the electrical connection with the Aluminum plate. Note that others connection modes (by the top of the device) can produce destructible interference on the electric lines of the E_{air} field.

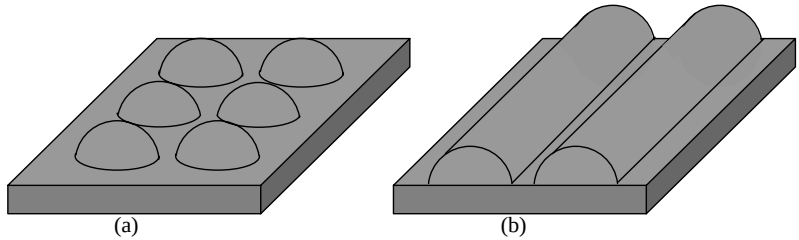

(a) (b)

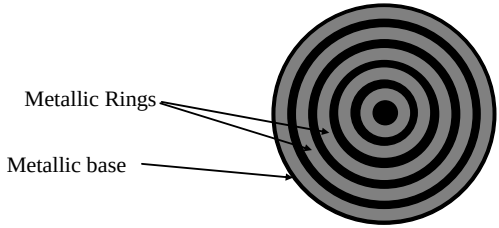

(c)

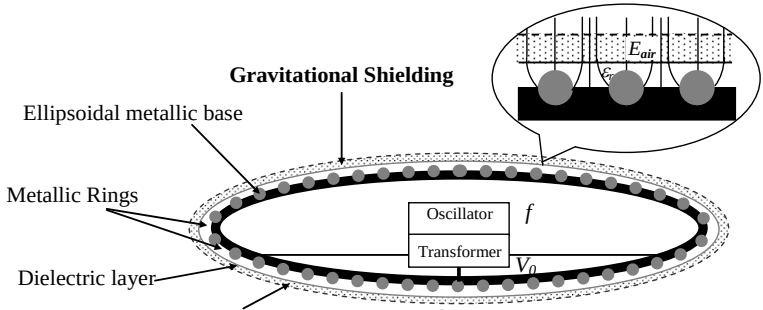

(d)

Figure A11 – *Geometrical forms with similar effects as those produced by the semi-spherical form* – (a) shows the semi-spherical form stamped on the metallic surface; (b) shows the *semi-cylindrical* form (an obvious evolution from the semi-spherical form); (c) shows *concentric metallic rings* stamped on the metallic surface, an evolution from semi-cylindrical form. These geometrical forms produce the same effect as that of the semi-spherical form, shown in Fig.A11 (a). By using concentric metallic rings, it is possible to build *Gravitational Shieldings* around bodies or spacecrafts with several formats (spheres, ellipsoids, etc); (d) shows a Gravitational Shielding around a Spacecraft with *ellipsoidal form.*

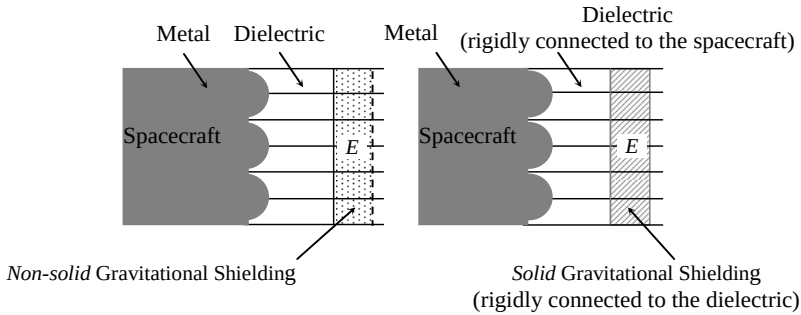

Figure A12 – *Non-solid and Solid Gravitational Shieldings* - In the case of the Gravitational Shielding produced on a *solid substance* (b), when its molecules go to the *imaginary* space-time, *the electric field that produces the effect also goes to the imaginary space-time together with them*, because in this case, the substance of the Gravitational Shielding is *rigidly connected (by means of the dielectric) to the metal* that produces the electric field. This does not occur in the case of *Air* Gravitational Shielding.

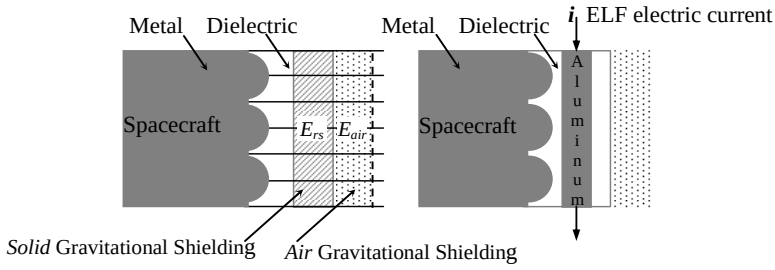

(a)

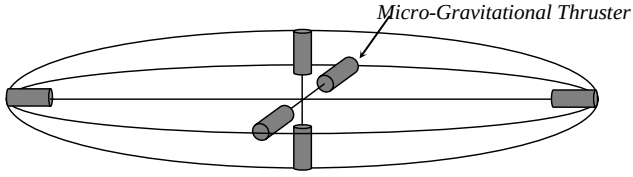

(b)

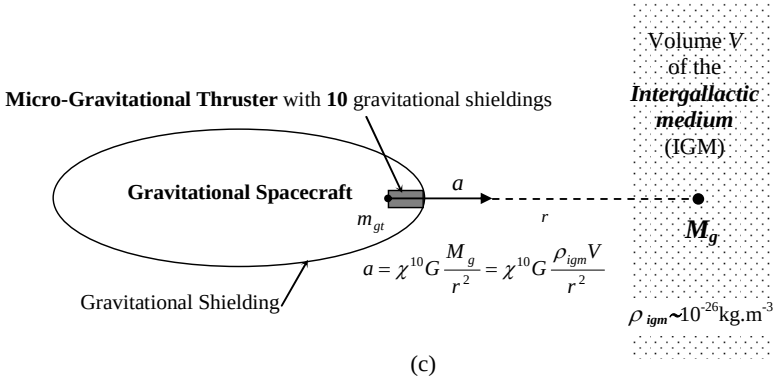

(c)

Figure A13 – *Double Gravitational Shielding and Micro-thrusters* – (a) Shows a double gravitational shielding that makes possible to decrease the *inertial effects* upon the spacecraft when it is traveling both in the *imaginary* space-time and in the *real* space-time. The *solid* Gravitational Shielding also can be obtained by means of *an ELF electric current through a metallic lamina* placed *between the semi-spheres and the Gravitational Shielding of Air* as shown above. (b) Shows 6 *micro-thrusters* placed inside a Gravitational Spacecraft, in order to propel the spacecraft in the directions x, y and z. Note that the Gravitational Thrusters in the spacecraft must have a very small diameter (of the order of *millimeters*) because the hole through the Gravitational Shielding of the spacecraft cannot be large. Thus, these thrusters are in fact *Micro-thrusters*. (c) Shows a micro-thruster inside a spacecraft, and in front of a volume *V* of the intergalactic medium (IGM). Under these conditions, the spacecraft acquires an acceleration *a* in the direction of the volume *V*.

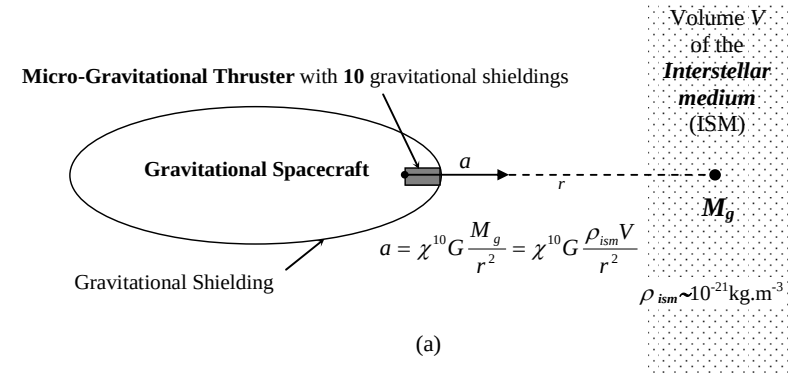

(a)

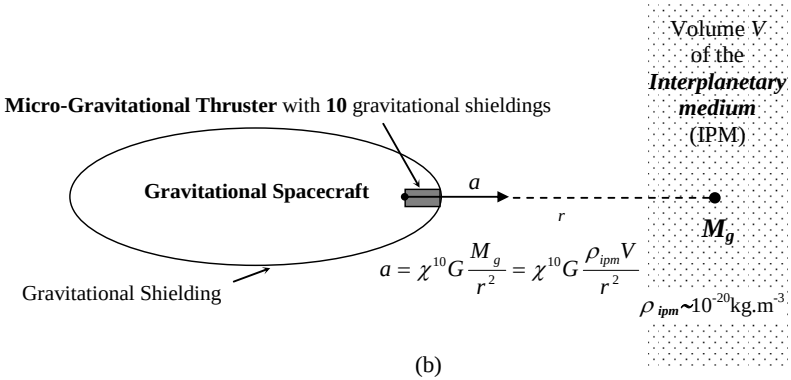

(b)

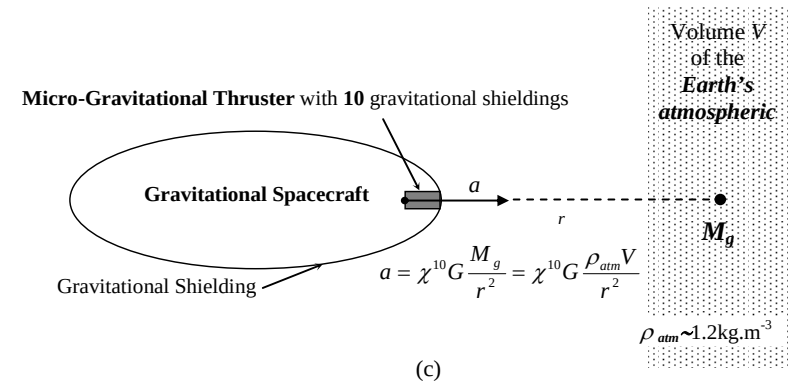

(c)

Figure A14 – *Gravitational Propulsion using Micro-Gravitational Thruster* – (a) Gravitational acceleration produced by a gravitational mass M_g of the *Interstellar Medium*. The density of the Interstellar Medium is about 10^5 times greater than the density of the *Intergalactic Medium* (b) Gravitational acceleration produced in the *Interplanetary Medium*. (c) Gravitational acceleration produced in the *Earth's atmosphere*. Note that, in this case, ρ_{atm} (*near to the Earth's surface*)is about 10^{26} times greater than the density of the *Intergalactic Medium.*

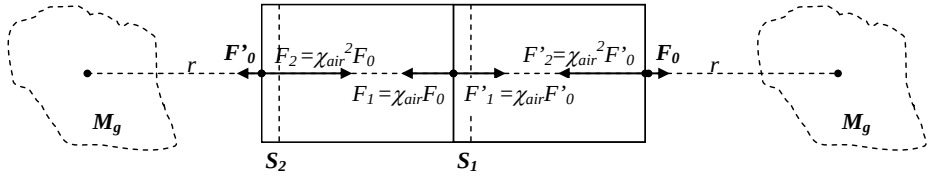

$F'_0 = F_0 \quad \Rightarrow \quad R = (F'_0 - F_2) + (F_1 - F'_1) + (F'_2 - F_0) = 0$

(a)

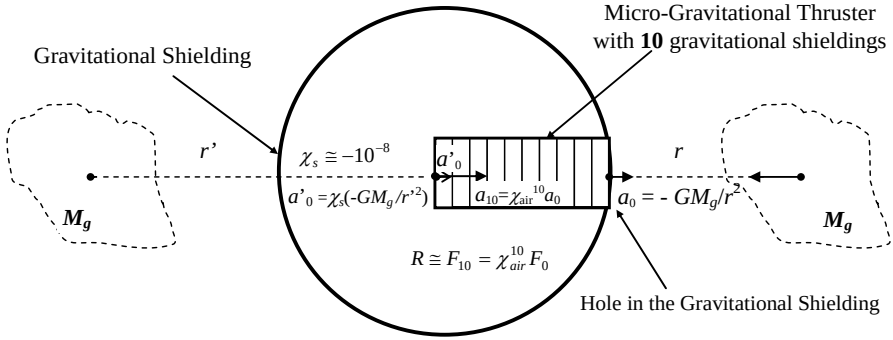

(b)

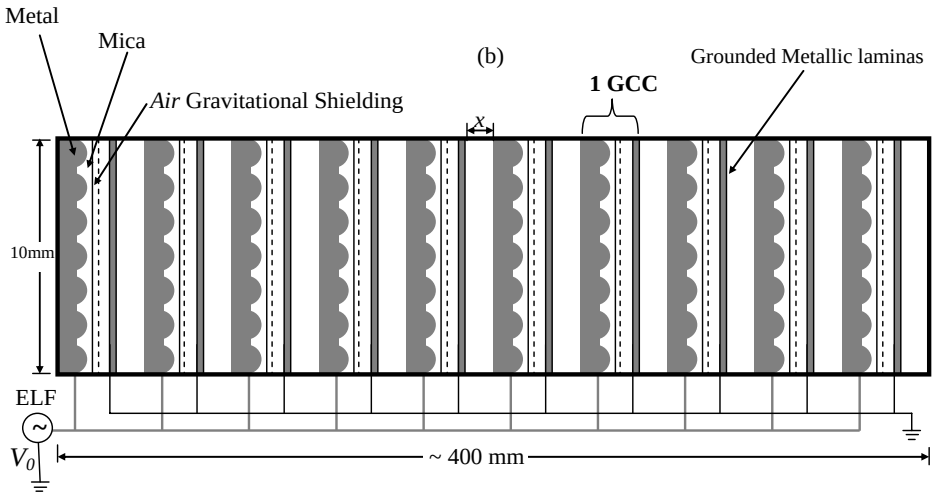

(c)

Figure A15 – *Dynamics and Structure of the Micro-Gravitational Thrusters* - (a) The Micro-Gravitational Thrusters do not work *outside* the Gravitational Shielding, because, in this case, *the resultant upon the thruster is null* due to the symmetry. (b) The Gravitational Shielding $\left(\chi_s \cong 10^{-8}\right)$ reduces strongly the intensities of the gravitational forces acting on the micro-gravitational thruster, except obviously, through the hole in the gravitational shielding. (c) Micro-Gravitational Thruster with *10 Air Gravitational Shieldings* (10GCCs). The grounded metallic laminas are placed so as to retain the electric field produced by metallic surface behind the semi-spheres.

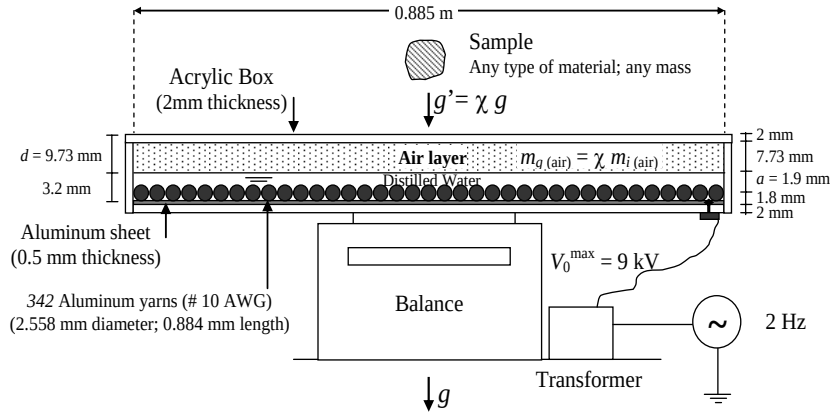

GCC Cross-section Front view

(a)

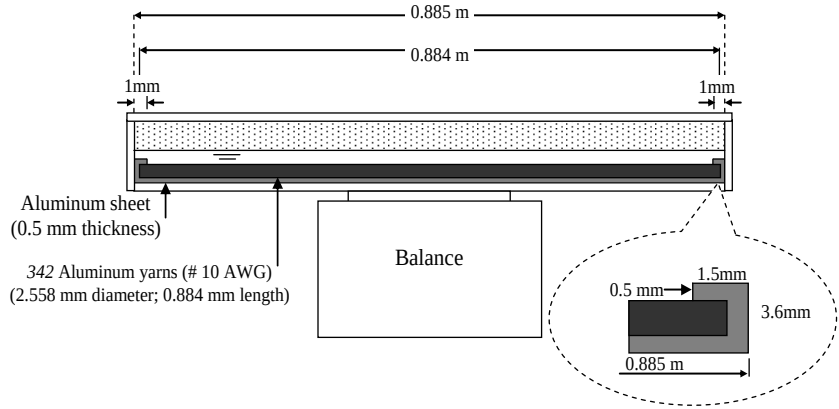

GCC Cross-section Side View

(b)

Fig. A16 – *A GCC using distilled Water*.

In total this GCC weighs about 6kg; the air layer 7.3 grams. The balance has the following characteristics: Range 0 – 6kg; readability 0.1g. The yarns are inserted side by side on the Aluminum sheet. Note the detail of fixing of the yarns on the Aluminum sheet.

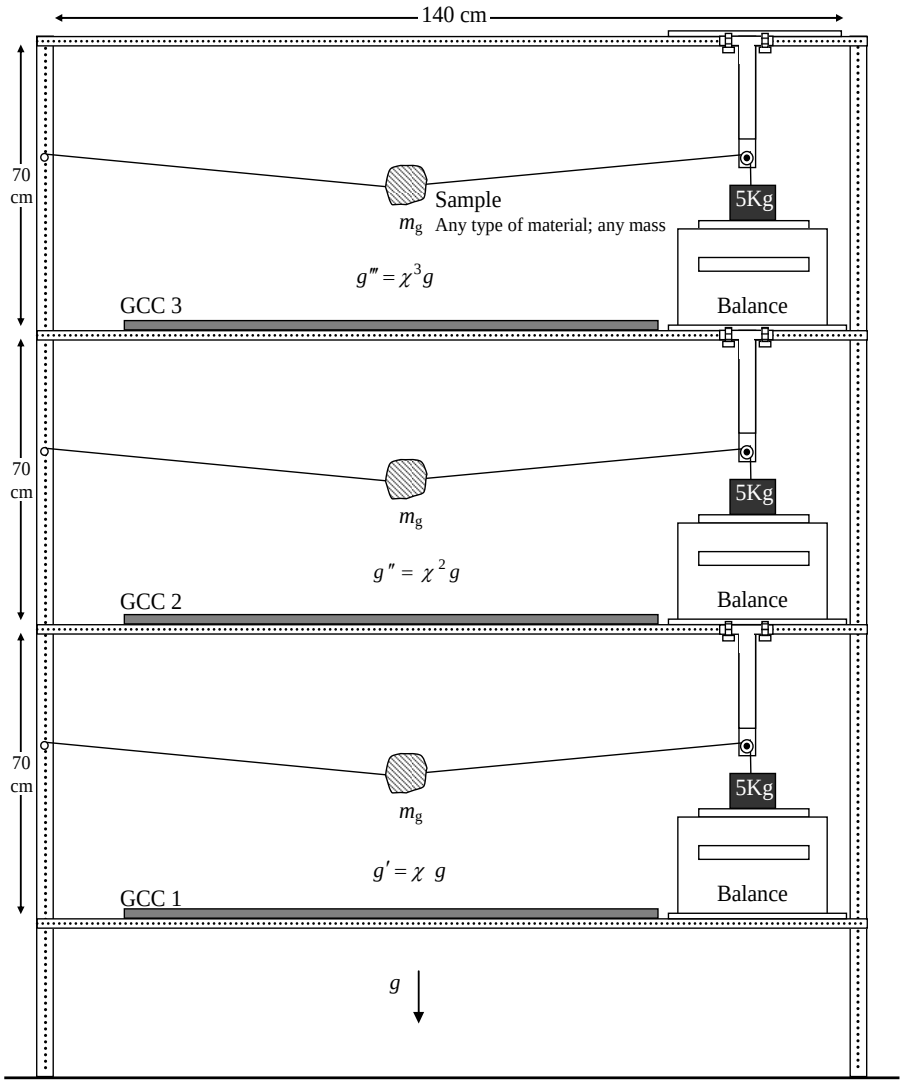

Fig. A17 – *Experimental set-up.* In order to prove *the exponential effect* produced by the superposition of the Gravitational Shieldings, we can take three similar GCCs and put them one above the other, in such way that above the GCC 1 the gravity acceleration will be $g' = \chi\, g$; above the GCC2 $g'' = \chi^2 g$, and above the GCC3 $g''' = \chi^3 g$. Where χ is given by Eq. (A47). The arrangement above has been designed for values of $m_g < 13g$ and χ up to -9 or $m_g < 1kg$ and χ up to -2 .

APPENDIX B: A DIDACTIC *GCC* USING A BATTERY OF CAPACITORS

Let us now show a new type of GCC - easy to be built with materials and equipments that also can be obtained with easiness.

Consider a battery of n parallel plate capacitors with capacitances $C_1, C_2, C_3, ..., C_n$, connected in parallel. The voltage applied is V; A is the area of each plate of the capacitors and d is the distance between the plates; $\varepsilon_{r(water)}$ is the relative permittivity of the dielectric (water). Then the electric charge q on the plates of the capacitors is given by

$$q = (C_1 + C_2 + C_3 + ... + C_n)V = n(\varepsilon_{r(water)}\varepsilon_0)\frac{A}{d}V \qquad (B1)$$

In Fig. I we show a GCC with *two* capacitors connected in parallel. It is easy to see that the electric charge density σ_0 on each area $A_0 = az$ of the edges B of the thin laminas (*z* is the thickness of the edges B and *a* is the length of them, see Fig.B2) is given by

$$\sigma_0 = \frac{q}{A_0} = n(\varepsilon_{r(water)}\varepsilon_0)\frac{A}{azd}V \qquad (B2)$$

Thus, the electric field E between the edges B is

$$E = \frac{2\sigma_0}{\varepsilon_{r(air)}\varepsilon_0} = 2n\left(\frac{\varepsilon_{r(water)}}{\varepsilon_{r(air)}}\right)\frac{A}{azd}V \qquad (B3)$$

Since $A = L_x L_y$, we can write that

$$E = 2n\left(\frac{\varepsilon_{r(water)}}{\varepsilon_{r(air)}}\right)\frac{L_x L_y}{azd}V \qquad (B4)$$

Assuming $\varepsilon_{r(water)} = 81$ [****] (bidistilled water); $\varepsilon_{r(air)} \cong 1$ (vacuum 10^{-4} Torr; 300K); $n = 2$; $L_x = L_y = 0.30m$; $a = 0.12m$; $z = 0.1mm$ and $d = 10mm$ we obtain

$$E = 2.43 \times 10^8 V$$

For $V_{max} = 220V$, the electric field is

$$E_{max} = 5.3 \times 10^{10} V / m$$

Therefore, if the frequency of the wave voltage is $f = 60Hz$, $(\omega = 2\pi f)$, we have that $\omega\varepsilon_{air} = 3.3 \times 10^{-9} S.m^{-1}$. It is known that the electric conductivity of the air, σ_{air}, at 10^{-4} Torr and 300K, is much smaller than this value, i.e.,

$$\sigma_{air} << \omega\varepsilon_{air}$$

Under this circumstance $(\sigma << \omega\varepsilon)$, we can substitute Eq. 15 and 34 into Eq. 7. Thus, we get

$$m_{g(air)} = \left\{1 - 2\left[\sqrt{1 + \frac{\mu_{air}\varepsilon_{air}^3}{c^2}\frac{E^4}{\rho_{air}^2}} - 1\right]\right\} m_{i0(air)}$$

$$= \left\{1 - 2\left[\sqrt{1 + 9.68 \times 10^{-57}\frac{E^4}{\rho_{air}^2}} - 1\right]\right\} m_{i0(air)} \qquad (B5)$$

The density of the air at 10^{-4} Torr and 300K is

$$\rho_{air} = 1.5 \times 10^{-7} kg.m^{-3}$$

Thus, we can write

$$\chi = \frac{m_{g(air)}}{m_{i(air)}} =$$

$$= \left\{1 - 2\left[\sqrt{1 + 4.3 \times 10^{-43} E^4} - 1\right]\right\} \qquad (B6)$$

Substitution of E for $E_{max} = 5.3 \times 10^{10} V/m$ into this equation gives

$$\chi_{max} \cong -1.2$$

This means that, in this case, the *gravitational shielding* produced in the vacuum between the edges B of the thin laminas can reduce the local gravitational acceleration g down to

$$g_1 \cong -1.2g$$

Under these circumstances, the weight, $P = +m_g g$, of any body just *above* the gravitational shielding becomes

$$P = m_g g_1 = -1.2 m_g g$$

[****] It is easy to see that by substituting the water for Barium Titanate ($BaTiO_3$) the dimensions L_x, L_y of the capacitors can be strongly reduced due to $\varepsilon_{r(BaTiO3)} = 1200$.

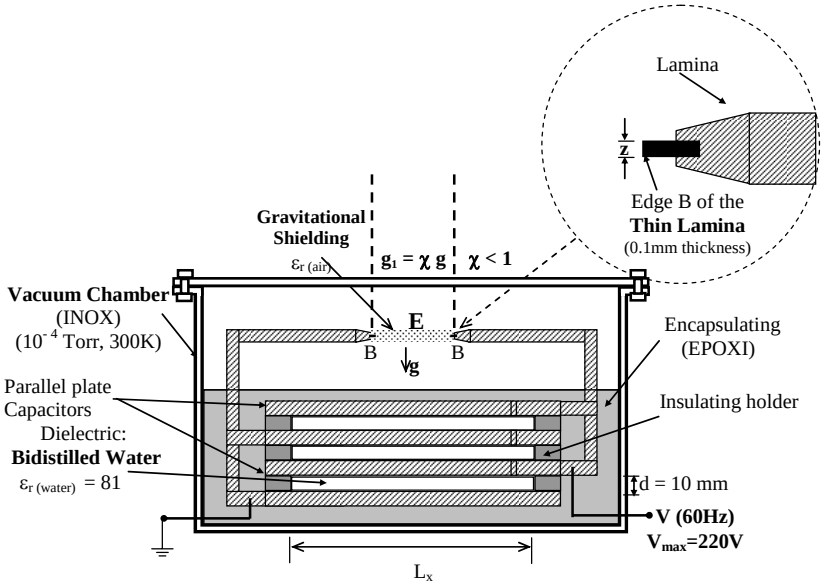

Vertical Cross Section

$$q = (C_1+C_2+...+C_n)\, V = \\ = n\, [\varepsilon_{r\,(water)} / \varepsilon_{r\,(air)}]\, [A/A_0]\, V / d$$

$$\varepsilon_{r\,(water)} = 81 \;;\; \varepsilon_{r\,(air)} \cong 1$$

$$\mathbf{E} = [q/A_0] / \varepsilon_{r\,(air)}\, \varepsilon_0 = n\, [\varepsilon_{r\,(water)} / \varepsilon_{r\,(air)}]\, [A/A_0]\, V / d$$

A is the area of the plates of the capacitors and A_0 the cross section area of the edges B of the thin laminas (z is the thickness of the edges).

Figure B1 – **Gravity Control Cell** (GCC) using a *battery of capacitors*. According to Eq. 7 , the electric field, **E**, through the air at 10^{-4} Torr; 300K, in the vacuum chamber, produces a gravitational shielding effect. The gravity acceleration above this gravitational shielding is reduced to $\chi\mathbf{g}$ where $\chi < 1$.

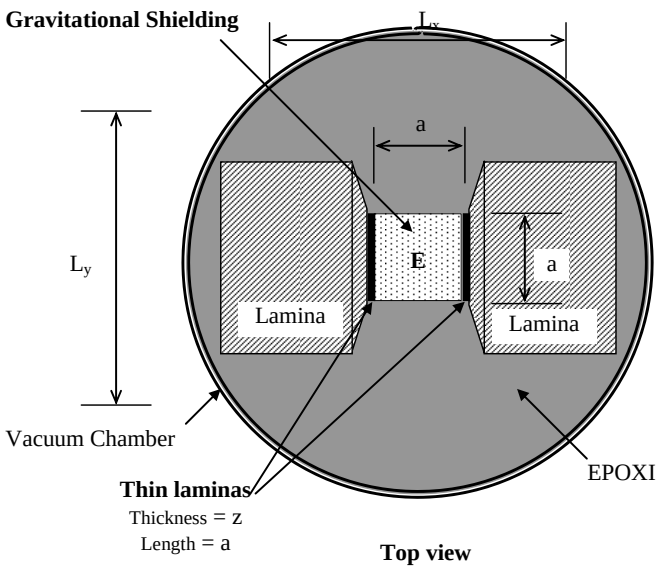

$A_0 = a\ z\ ;\quad A = L_x\ L_y$

Figure B2 – The gravitational shielding produced between the thin laminas.

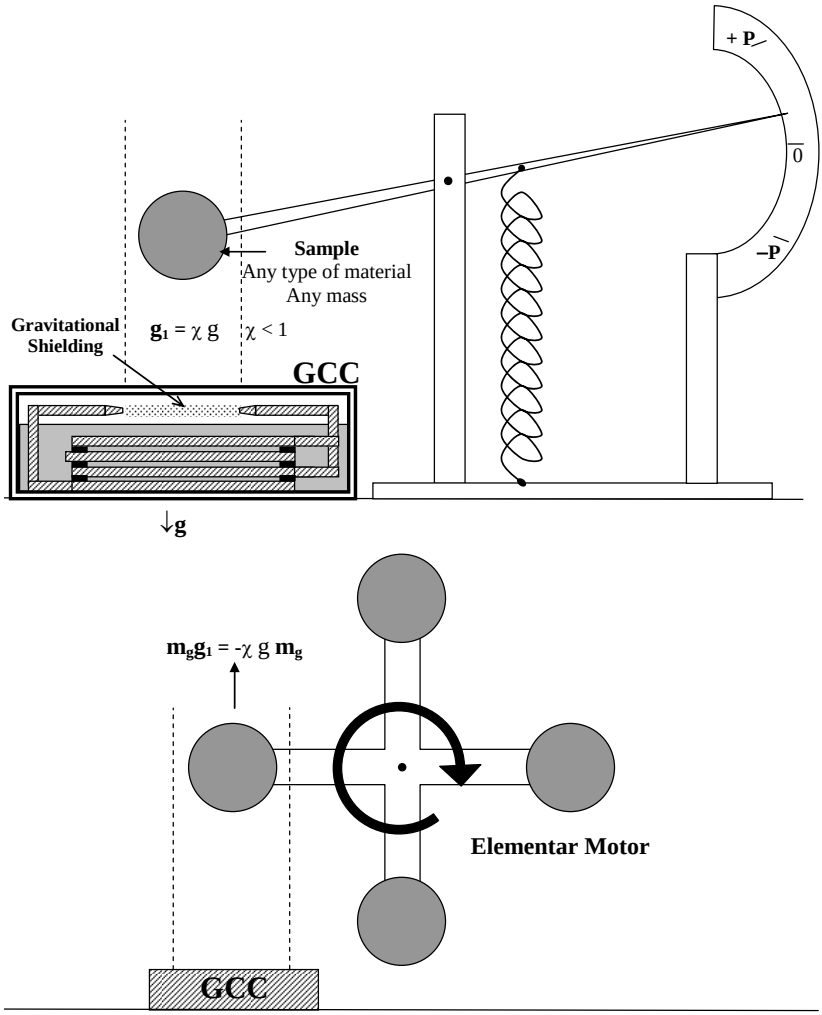

Figure B3 – Experimental arrangement with a GCC using battery of capacitors. By means of this set-up it is possible to check the weight of the sample even when it becomes *negative*.

REFERENCES

1. DeAquino, F. 2010. *Mathematical Foundations of the Relativistic Theory of Quantum Gravity*. Pacific Journal of Science and Technology. **11**(1), pp.173-232.

2. Freire, G. F. O and Diniz, A. B. (1973) *Ondas Eletromagnéticas*, Ed. USP,p.26.

3. Halliday, D. and Resnick, R. (1968) *Physics,* J. Willey & Sons, Portuguese Version, Ed. USP, p.1118.

4. Quevedo, C. P. (1977) *Eletromagnetismo*, McGraw-Hill, p.255 and 269.

5. GE Technical Publications (2007), 80044 – F20T12/C50/ECO, GE Ecolux ®T12.

6. Aplin, K. L. (2000) PhD thesis, The University of Reading, UK

7. Aplin K. L (2005) *Rev. Sci. Instrum.* **76**, 104501.

8. Beiser, A. (1967) *Concepts of Modern Physics*, McGraw-Hill,Portuguese version (1969) Ed. Polígono, S.Paulo, p.362-363.

9. Hayt, W. H. (1974), *Engineering Electromagnetics*, McGraw-Hill. Portuguese version (1978) Ed. Livros Técnicos e Científicos Editora S.A, RJ, Brasil. P.146.

10. Benjegerdes, R. et al.,(2001) *Proceedings of the 2001Particle Accelerator Conference*, Chicago. http://epaper.kek.jp/p01/PAPERS/TOAB009.PDF

11. Gourlay, S. et al., (2000) *Fabrication and Test of a 14T, Nb3Sn Superconducting Racetrack Dipole Magnetic*, IEE Trans on Applied Superconductivity, p.294.

12. BPE soft, *Extreme High Altitude Conditions Calculator*. http://bpesoft.com/s/wleizero/xhac/?M=p

13. Handbook of Chemistry and Physics, 77th ed.1996.

14. Halliday, D. and Resnick, R. (1968) *Physics,* J. Willey & Sons, Portuguese Version, Ed. USP, p.1118.

15. Zhan, G.D *et al.* (2003) *Appl. Phys. Lett.* **83,** 1228.

16. Davidson, K. & Smoot, G. (2008) *Wrinkles in Time*. N. Y: Avon, 158-163.

17. Silk, Joseph. (1977) *Big Bang*. N.Y, Freeman, 299.

18. Jafelice, L.C. and Opher, R. (1992). *The origin of intergalactic magnetic fields due to extragalactic jets*. RAS. http://adsabs.harvard.edu/cgi-bin/nph-bib query? Bib code = 1992 MNRAS. 257. 135J. Retrieved 2009-06-19.

19. Wadsley, J., et al. (2002). *The Universe in Hot Gas*. NASA. http://antwrp.gsfc.nasa.gov/apod/ap 020820. html. Retrieved 2009-06-19.

Further Readings

[1] F. de Aquino, *The Correlation Between Gravitation and Electromagnetism, Inertia and Unification.*

[https://arxiv.org/html/physics/9905003?]

[2] P.A. LaViolette, *Secrets of Antigravity Propulsion.*

[https://www.bibliotecapleyades.net/archivos_pdf/secrets-antigravprop.pdf]

[3] Nick Cook, *The Hunt for Zero Point: Inside the Classified World of Antigravity Technology.*

[https://www.bibliotecapleyades.net/archivos_pdf/hunt_zeropoint.pdf]

[4] Leonard G. Cramp, *UFOs and AntiGravity: Piece for A Jig-Saw.*

[https://www.bibliotecapleyades.net/archivos_pdf/UFOs-antigravity.pdf]

[5] Thomas Valone (ed.), *Electrogavitic Systems*

[https://www.bibliotecapleyades.net/archivos_pdf/electrogravitics_systems.pdf]

[6] David H. Childress, *The Anti-Gravity Handbook.*

[7] David H. Childress,*Anti-gravity & the Unified Field.*

[8] David H. Childress, *Anti-gravity & the World Grid.*

[9] David H. Childress & R. Vesco,*Man-Made UFOs: 1954-1994 - 50 years of suppression.*

[10] M. B. King, *Tapping the Zero Point Energy.*

[11] B. L. Cathie, *The Bridge to Infinity.*

[12] 803-Page Collection of Papers on Anti-Gravity Research.
[https://pt.scribd.com/document/109685653/803-Page-Collection-of-Papers-on-Anti-Gravity-Research]

Flying-Saucer Shaped Aircraft Patents

[1] Spacecraft for interplanetary/lunar travel (US20060163434)
[https://patentimages.storage.googleapis.com/13/a6/2c/ed10f3898eb30a/US20060163434A1.pdf]

[2] Method and means for creating artificial gravity in spacecraft (US3675879)
[https://patentimages.storage.googleapis.com/c3/ee/af/976dc80125916b/US3675879.pdf]

[3] Amusement Device (US2912244)
[https://patentimages.storage.googleapis.com/b6/6d/de/c35508e1321efe/US2912244.pdf]

[4] Saucer-shaped aircraft (US2801058)
[https://patentimages.storage.googleapis.com/b5/2b/95/f9771231f28c84/US2801058.pdf]

[6] High velocity high altitude v.t.o.l. aircraft (US3103324)
[https://patentimages.storage.googleapis.com/9e/2b/bd/3a5601f6dbe495/US3103324.pdf]

[7] Circular aircraft and control system therefor (US2772057)
[https://patentimages.storage.googleapis.com/9e/2b/bd/3a5601f6dbe495/US3103324.pdf]

[8] Circular wing aircraft with universally tiltable ducted power plant (US2876965)
[https://patentimages.storage.googleapis.com/00/46/a1/c13b572ce95a5c/US2876965.pdf]

[9] Aircraft propulsion and control (US3124323)
[https://patentimages.storage.googleapis.com/c9/30/9e/a933d771237933/US3124323.pdf]

[10] Rotating jet aircraft with lifting disc wing and centrifuging tanks (US2939648)
[https://patentimages.storage.googleapis.com/6c/0a/98/a7bb4f873a5a59/US2939648.pdf]

Institutes and Webpages

[1] American Antigravity.

[http://www.americanantigravity.com/]

[2] Institute of Gravity Research.

[http://www.goede-stiftung.org/en/institute-for-gravity-research/]

[3] To the Stars Academy of Arts and Science.

[https://dpo.tothestarsacademy.com/]

[4] Antigravity Technology.

[http://www.antigravitytechnology.net/]

[5] Gravity Research Foundation.

[https://www.gravityresearchfoundation.org/]

[6] Biblioteca Pleyades - Antigravity.

[https://www.bibliotecapleyades.net/ciencia/ciencia_gravity-antigravity.htm]

[7] Antigravity Power - Free Energy.

[http://antigravitypower.tripod.com/FreeEnergy/index.html]

[8] Antigravity Power - Bio-Gravitics

[http://antigravitypower.tripod.com/BioGravity/index.html]

[9] Mufon - Anti-Gravity.

[https://www.mufon.com/anti-gravity]

[10] Fran de Aquino's papers.

[http://vixra.org/author/fran_de_aquino]

Online Articles

[1] UFO Anti-Gravity.

[https://www.gaia.com/article/ufo-anti-gravity-technology-understood]

[2] Are these scientists about to SWITCH-OFF GRAVITY - and if they do what will happen?

[https://www.express.co.uk/news/science/899169/science-gravity-warp-Quantam-Entanglement-Jeremy-Rys-PHOENIX-techn

[3] NASA Is Spending Half A Million Dollars On Bizarre Anti-gravity Research.

[https://www.eurekalert.org/pub_releases/1999-02/NS-NISH-030299.php]

[4] AntiGravity: The Holy Grail of the 21st Century.

[http://www.aulis.com/manned-space-flight.htm]

[5] How to Build a UFO-like Anti Gravity Spaceship.

[https://www.greenoptimistic.com/build-ufo-anti-gravity-spaceship/#.W8dpiktKjIU]

[6] Boeing tries to defy gravity.

[http://news.bbc.co.uk/2/hi/science/nature/2157975.stm]

[7] Q&A: Boeing and anti-gravity.

[http://news.bbc.co.uk/2/hi/science/nature/2159487.stm]

[8] British probe anti-gravity device.

[http://news.bbc.co.uk/2/hi/europe/692544.stm]

Video Documentaries

[1] Anti Gravity & Zero Point Energy.

[https://www.youtube.com/watch?v=F6LdcLfYBGg]

[2] Anti-Gravity Machine.

[https://www.youtube.com/watch?v=Taj4VA1L_vw]

[3] The Futuristic Antigravity Technology that is Way Above Top Secret.

[https://www.youtube.com/watch?v=q2EaLi8rn1A]

[4] Stan Deyo- Anti-Gravity Technology.

[https://www.youtube.com/watch?v=CsagEYfxPgs]

[5] Antigravity Technology So Advanced You Wont See It For Another 50 Years .

[https://www.youtube.com/watch?v=1oWEIEtrYTI]

[6] Proof Faster than Light Black Budget Antigravity Technology is Real.

[https://www.youtube.com/watch?v=h9CAftwO1x8]

[7] Suppressed Antigravity Inventions That You Might Never Know About.

[https://www.youtube.com/watch?v=YxTIVqIIqvc]